UNIVERSITY OF NOVA GORICA
GRADUATE SCHOOL

NATURAL HYDROCHEMICAL BACKGROUND AND DYNAMICS OF GROUNDWATER IN SLOVENIA

DISSERTATION

Kim MEZGA

Mentors: Assist. Prof. Dr. Barbara Čenčur Curk
Dr. Janko Urbanc

Nova Gorica, 2014

Abstract

Title: Natural hydrochemical background and dynamics of groundwater in Slovenia

A 3-year (2009–2011) geochemical and isotopic study of Slovenian groundwaters has been conducted in the aquifers composed of the most representative lithological and lithostratigraphic units observed in Slovenia. Groundwater sampling network consists of 87 sampling locations, including springs, boreholes and wells, which are evenly distributed throughout the territory. For every sampling location its characteristics of recharge area were studied in detail.

Geochemical analyses of groundwater were conducted in order to determine the impact of lithological structure of aquifer, recharge area climatic characteristics and land use on the groundwater chemical and isotopic composition.

Sampled groundwater is mostly modern (recent) which has been verified by the ^{3}H activity in groundwater. Groundwater stable isotope composition (δ^{18}O and δ^2H) and d-*excess* values provided the information on recharge areas characteristics (altitude, mixing with surface waters) and source of precipitation recharge (prevailing Atlantic and Mediterranean air masses). Also three different groundwater isotopic altitude effects zones were defined, as well as the groundwater isotope continental effect.

Groundwater concentrations of Ca^{2+}, Mg^{2+}, and HCO_3^- are mostly of natural origin and depend on dissolution of carbonate rocks in relation with the altitude, soil temperature, partial pressure of CO_2 from the atmosphere and soil, amount of precipitation, and vegetation cover. The share of carbon contributions from dissolution of carbonate rocks, degradation of organic matter in aquifers, and the atmosphere on the groundwater, has been calculated with dissolved carbon concentration (DIC) and isotopic composition of carbon (δ^{13}C). Major product of silicate weathering in groundwater is Si and to a lesser extends Na^+ and K^+. Groundwater Na^+ and Cl^- can be linked to vicinity of the sea, and groundwater SO_4^{2-} to weathering of gypsum and sulphide minerals. Prevailing sources of groundwater Na^+, Cl^-, NO_3^-, K^+, and SO_4^{2-} in Slovenian groundwaters are mostly of anthropogenic origin. Use of salts for deicing roads during winter time contributes to groundwater Na^+ and Cl^-. Excessive use of fertilizers, application of manure and slurry on the fields, leakages from sewage systems, septic tanks, and waste waters, contribute to elevated concentrations of groundwater NO_3^-, K^+, SO_4^2, Na^+ and Cl^-**.**

The prevailing process influencing Slovenian groundwater chemical in isotopic composition is dissolution of carbonate rocks which are the most abundand rock type found in Slovenia. In more than 80 % of all water samples the concentrations of Ca^{2+}, Mg^{2+}, and HCO_3^- in groundwater are therefore increased. To lesser extent the dissolution of silicate minerals is observed in groundwater from NNE and NE part of Slovenia (Pohorje Mt. and Prekmurje region) where igneous and metamorphic rocks dominate (~14 % of all water samples). In the recharge areas with clays in the NNE part of Slovenia the processes of ion exchange reactions are observed (~1 % of all water samples). In the NE part of Slovenia in old groundwater from deep aquifers redox conditions are present (~2 % of all water samples). Groundwater chemical composition in lowland alluvial plains in central, E, and NE part of Slovenia reflects agricultural activities and fertilizers uses, because the soil and climate are favourable for agricultural harvest production. Additionally urban land use is reflected in groundwater geochemistry which might be a consequence of decrepit and improper sewage systems or septic tanks (~10 % of all water samples). Urban influence is also observed in groundwater in the central part of Slovenia which is the most densely populated city in Slovenia (~1 % of all water samples).

According to measured values of geochemical parameters in groundwater and their occurance the typical chemical and isotopic values were determined according to a certain prevailing lithological and lithostratigraphic units in the recharge areas of sampled groundwater. Additionally the groundwater natural background levels for selected chemical parameters, which sources are mostly anthropogenic, are determined. Results of spatial variations of studied parameters are illustrated as hydrochemical thematic maps.

Keywords: groundwater, Slovenia, chemical and isotopic composition, natural chemical background level.

Izvleček

Naslov: Naravna hidrokemijska ozadja in dinamika podzemnih vod Slovenije

V obdobju od 2009 do 2011 so potekale geokemijske in izotopske raziskave slovenskih podzemnih vod v vodonosnikih, katerih geološka zgradba vključuje najbolj reprezentativne litološke in litostratigrafske enote v Sloveniji. V vzorčno mrežo je bilo vključenih 87 vzorčnih mest (izviri, vrtine, vodnjaki), ki so bili enakomerno razporejeni po celotnem slovenskem ozemlju. Napajalno zaledje vseh vzorčnih mest je bilo podrobno preučeno.

Analiza geokemijskih parametrov v podzemni vodi je bila izvedena z namenom, da bi ugotovili v kolikšni meri vplivajo litološka zgradba vodonosnika, klimatske karakteristike napajalnega zaledja in raba tal na na kemijsko in izotopsko sestavo podzemne vode.
Preiskovana podzemna voda je večinoma mlada (recentna), kar je bilo potrjeno z meritvijo aktivnosti tritija (^3H) v vodi. S pomočjo izotopske sestave podzemne vode ($\delta^{18}O$ in δ^2H) in devterijevim presežkom so bile ugotovljene karakteristike napajalnega zaledja (nadmorska višina, mešanje vode s površinsko vodo) in izvor vode v padavinah, kjer so bile kot prevladujoče določene zračne mase iz severnega Atlantika in iz območja Sredozemlja. Prav tako so bili v podzemni vodi določeni trije višinski izotopski efekti in kontinentalni efekt.
Pojavljanje Ca^{2+}, Mg^{2+} in HCO_3^- v podzemni vodi je naravnega izvora, koncentracije pa so odvisne od raztapljanja karbonatnih kamnin glede na nadmorsko višino, temperaturo tal, parcialnega tlaka v atmosferi in v tleh, količine padavin ter vegetacijskega pokrova. S pomočjo raztopljenega anorganskega ogljika (DIC) in izotopske sestave ogljika ($\delta^{13}C$) v podzemnih vodah se je ocenil delež doprinosa ogljika iz procesov raztapljanja karbonatov, razgradnje organske snovi v vodonosniku in vpliva atmosfere na podzemno vodo. Glavni produkti raztapljanja silikatnih mineralov v podzemni vodi so Si in v manjši meri Na^+ in K^+. Povišane koncentracije Na^+ in Cl^- v podzemni vodi so lahko posledica neposredne bližine morja, ter vir SO_4^{2-} raztapljanje sadre in drugih sulfidnih mineralov. Na povišane koncentracije Na^+, Cl^-, NO_3^-, K^+ in SO_4^{2-} v slovenskih podzemnih vodah v veliki meri vplivajo antropogeni dejavniki. Uporaba soli za soljenje cest v zimskem času vpliva na povišano koncentracijo Na^+ in Cl^- v podzemni vodi. Prekomerna uporaba gnojil, nanašanje gnoja in gnojevke na polja, izpusti iz slabo tesnjenih kanalizacijskih sistemov in greznic ter odpadne vode, so lahko vzrok povišanih koncentracij NO_3^-, K^+, SO_4^2, Na^+ in Cl^- v podzemni vodi.
Glavni procesi, ki vplivajo na kemijsko in izotopsko sestavo slovenskih podzemnih vod so raztapljanje karbonatnih kamnin, ki so v Sloveniji najbolj razširjene. V več kot 80 % vzorcih podzemne vode je bila koncentracija Ca^{2+}, Mg^{2+} in HCO_3^- namreč povišana. V manjši meri vpliva na kemijsko sestavo podzemnih vod raztapljanje silikatnih mineralov v S-SV in SV delu države (Pohorje in Prekmurje), kjer v napajalnem zaledju prevladujejo magmatske in metamorfne kamnine (~14 % vzorcev podzemne vode). V S-SV delu Slovenije, kjer v napajalnem zaledju prevladujej glina, so opazni procesi ionske izmenjave (~1 % vzorcev podzemne vode). V »stari« vodi v globokih vodonosnikih, ki se nahajajo v SV delu Slovenije se najverjetneje pojavljajo redukcijski pogoji (~2 % vzorcev podzemne vode). Kemijska sestava podzemne vode v nižinskih aluvialnih ravnicah v centralnem, V in SV delu Slovenije odraža kmetijske dejavnosti ter uporabo gnojil, saj so tla in podnebje ugodni za pridelavo kmetijskih pridelkov. Nadalje se v podzemni vodi prav tako odraža urbana raba prostora, ki je posledica dotrajanih in neustreznih kanalizacijskih sistemov ali greznic (~10 % vzorcev podzemne vode). Prav tako se urbani vpliv na podzemno vodo odraža v centralnem delu Slovenije, ki je hkrati najbolj poseljeno (glavno) mesto (~1 % vzorcev podzemne vode).

Na osnovi merjenih vrednosti geokemijskih parametrov in vzrokov njihovega pojavljanja so bile določene tipične kemijske in izotopske vrednosti glede na prevladujočo litološko in litostratigrafsko enoto v zaledju analizirane podzemne vode. Določene so bile koncentracije naravnih ozadij za izbrane kemijske parametre, katerih izvor v podzemnih vodah je predvsem antropogen. Končen rezultat raziskave predstavljajo hidrokemijske tematske karte s podano prostorsko porazdelitev obravnavanih parametrov.

Ključne besede: podzemna voda, Slovenija, kemijska in izotopska sestava, naravna kemijska ozadja.

TABLE OF CONTENTS

ACKNOWLEDGEMENTS

LIST OF TABLES

LIST OF FIGURES

LIST OF APPENDICES

ABBREVIATIONS

A	coefficient of skewness (Section 2.4.)
A	cross sectional area (Section 3.5.)
a.s.l.	above sea level
CV	coefficient of variation
d-*excess*	deuterium excess
DIC	dissolved inorganic carbon
DO	dissolved oxygen
E	coefficient of kurtosis
EARS	Environmental Agency of the Republic of Slovenia
EC	electrolytic conductivity of water
GMWL	global meteoric water line
h_1, h_2	hydraulic heads
IAEA	Isotope Hydrology Section of the International Atomic Energy Agency
IAP	ion-activity product of the dissociated chemical species in solution
IRMS	isotope ratio mass spectrometry
LMWL	local meteoric water line
EMMWL	eastern Mediterranean meteoric water line
K	hydraulic conductivity or permeability
K_t	equilibrium solubility product of the chemical involved at the sample temperature
L	length in direction of flow
LOD	limit of detection
LOQ	limit of quantification
MAE	Ministry for Agriculture and the Environment
Max	maximum value
Md	median value
meq/L	milliequivalents per liter
MESP	Ministry of the Environment and Spatial Planning
mg/L	milligrams per liter
Min	minimum value
mmol/L	millimoles per liter
Mt.	mountain
Mts.	mountains
n	number of observations
NBL	natural background level
P_{CO2}	partial pressure of CO_2
ppm	parts per million
Q	flow rate
S	standard deviation
SCDL	seawater concentration-dilution line
SI	saturation index
SI_{cal}	calcite saturation index
SI_{dol}	dolomite saturation index
r_s	Spearman’s rank correlation coefficient
R^2	linear determination coefficient
T	temperature
TU	tritium unit
TV	threshold value
X	mean value
δ	delta, relative isotopic composition, value given in parts per thousand or per mil (‰)
δ^{13}C-DIC	isotopic composition of dissolved inorganic carbon
$\delta^{15}N_{tot}$	isotopic composition of total dissolved nitrogen
$\delta^{18}O$	isotopic composition of oxygen
$\delta^{2}H$	isotopic composition of hydrogen (deuterium)
µg/L	micrograms per liter

‰	per mil (parts per thousand)
^3H	tritium
WFD	Water Framework Directive
WHO	World Meteorological Organization

1. INTRODUCTION

1.1. The research problem

Groundwater is a globally important, valuable and renewable resource. It originates from the infiltration of rain and snow. Rain contains small amounts of dissolved solids and gases, and is accumulated through the soil below the earth's surface in a porous layer. During infiltration through the soil it reacts with soil and forms a solution which affects the rock material, thereby increasing the concentrations of chemical constituents of water. Generally groundwater flows slowly through geological formations and remains in contact with minerals often isolated from the atmosphere (Jordana and Batista, 2004). The groundwater geochemical and isotopic composition varies widely as a function of the many complex natural and anthropogenic factors during its flow, either with depth or geographic distances.

Prevailing natural factors influencing the groundwater chemical and isotopic composition are mainly lithological composition and climatic factors in the recharge area of sampled groundwater. Along with the lithological composition, also hydraulic type of the aquifer, thickness of saturated and unsaturated zone of the aquifer, groundwater flow and recharge rate play an important role. Further, recharge dynamics are also very important since it determine interaction time between groundwater and groundwater-bearing rocks, and also retention time of pollutant in the aquifer. Annual soil temperature and the amount of oxygen in the ground (aerobic/anaerobic conditions) are also very important, as well as other climatic conditions (temperature, and intensity and duration of precipitation), altitude, distribution and type of vegetation in the recharge area, thickness and soil type, and intensity of biological processes in soil. Finally, an important parameter is also partial pressure of CO_2 which determines carbonate equilibrium in the groundwater and associated mineralization of groundwater.

Groundwater quality and quantity are also affected by anthropogenic factors which can be assessed only if the natural background of the recharge area of the aquifer is known. These components could be evaluated as a difference between the total concentration of the chemical parameter (pollutant) and parameters natural background level. The most frequent anthropogenic sources influencing groundwater chemical composition are the agricultural land use (use of fertilizers and substances for plant protection) and urbanization. Discharges from sewerage systems can enter groundwater directly if the sewage pipes are old or broken, or if septic tanks are not properly maintained. Also municipal landfills, wastewater treatment, and industrial plants influence on groundwater chemical status (Appelo and Postma, 2005; Domenico and Schwartz, 1990; LAWA, 2001; Kunkel *et al.*, 2004; Wendland *et al.*, 2005; Kunkel *et al.*, 2007; Wendland *et al.*, 2008).

Groundwater chemical status significantly influences the use of groundwater as a source of drinking water, in food-processing industry, or in technological and recreational purposes. According to Morris *et al.* (2003) groundwater provides 25 to 40 % of the world's drinking water, 75 % in Europe (Sampat, 2000) and more than 97 % in Slovenia (Krajnc *et al.*, 2007).

The introduction of the European Union (EU) Water Framework Directive (WFD) (Directive 2000/60/EC) and its Daughter Groundwater Directive (2006/118/EC) on the protection of groundwater against pollution and deterioration of its chemical status has set out criteria (WFD, Article 17) for the assessment of the groundwater chemical status based on the existing European Community quality standards (nitrates, pesticides, and biocides) and on the requirement for Member States. The aim was to identify pollutants and threshold values (TVs) for groundwater bodies at risk in accordance with the analysis of pressures and impacts carried out under the WFD. In this context groundwater background levels (NBLs) are required as a reference to establish whether the groundwater is affected by contamination, and if, to what degree (Nieto *et al.*, 2005).

In Slovenia the hydrogeochemical map of Slovenian groundwaters is still not available, nor are the bases for determination of the reference state for the assessment of good chemical status of groundwater according to WFD (2000/60/EC) and it’s daughter directive (2006/118/EC) where both comprise the determination of NBLs as a basic information on the hydrochemical situation in aquifers.

1.2. Purpose, goals and main research hypothesis

Despite a large number of routine chemical and isotopic analyses on individual water sources in Slovenia, there has not yet been a comprehensive research on chemical or isotopic characteristics of groundwater, nor has any detailed interpretation of groundwater's isotopic composition, based on its origin, ever been made. Additionally, Slovenia so far does not yet have a hydrogeochemical map of Slovenia, like e.g. Austria (Kralik, 2005) and Germany (Birke *et al.*, 2009). The closest map ever made is a map of lithological and litogeochemical classification of aquifers in Slovenia (Bavec *et al.*, 2008) which has been made according to the lithostratigraphic units of Geological map of Slovenia (1:250.000) (Buser, 2010).

The purpose of this study is to present the spatial distribution of measured chemical parameters in groundwater, which sampling network contains 87 sampling locations and extended range of measured parameters. The working hypothesis is based on the presumption that by determining the recharge area of sampled groundwater, which includes the study of aquifer's hydrogeological and hydrodynamic characteristics, available data on climate and vegetation cover in the recharge area, and groundwater chemical and isotopic data, it would be possible to quantify the prevailing factors which determine the groundwater chemical and isotopic parameters, which provide the information on groundwater recharge, dynamics, and groundwater age.

Over the past three years (2009-2011) groundwater samples were taken from all the main geological formations with the focus on the representativeness of the groundwater sampling location natural recharge area. Groundwater samples have been analysed for major and minor ion concentrations, as well as trace element concentrations, and various groundwater isotopic composition. This dataset represents a unique collection of chemical and isotopic analysis by using the same laboratory techniques and procedures for individual parameters. The results therefore are directly comparable to each other and can be correlated to each other. The natural background levels (NBLs) of studied parameters were determined according to anthropogenic influence on the groundwater.

The hypotheses are based on the assumption that origin of groundwater chemical (and isotopic) composition depend on the mineralogical composition of rocks that groundwater has passed through. If the residence time between groundwater and aquifer host rocks is long enough, groundwater develops so called compositional fingerprint of the local geology.

The main hypotheses are:

→ the main natural factors controlling Slovenian groundwater chemical and isotopic composition are lithological composition of the aquifer recharge area and recharge area climatic conditions,

→ chemical composition of anthropogenically influenced groundwater mostly depends on the land use in the groundwater recharge areas.

The main goals of the study are:

→ to determine the optimal methodology for geochemical research of Slovenian groundwater regarding the sampling network density, data processing, interpretation of results, and data presentation,

→ to identify typical Slovenian groundwater chemical and isotopic composition in relation to lithological and lithostratigraphic units,

→ to identify and quantify the main factors controlling different chemical and isotope parameters in Slovenian groundwater and to interpret the role of each factor,

→ to develop the optimal methodology for evaluation of natural background levels (NBLs) in groundwater for selected chemical parameters according to specific Slovenian hydrogeological conditions,

→ to prepare various hydrochemical thematic maps of the main hydrochemical and isotope parameters for the whole Slovenian territory. Thematic maps display typical concentrations of studied hydrochemical parameters for individual sampling locations and whole groundwater bodies.

1.2.1. Significance of research

This research provides fundamental information about the relationship between the groundwater chemical composition and lithological composition of aquifer and its dynamics in the recharge area. Natural groundwater concentrations of the most important ions are evaluated which are not significantly or directly influenced by anthropogenic sources. By using the obtained data, it is possible to study the chemical interactions between groundwater and host rock, which appears to be the most important process that enables certain elements to enter the groundwater. Further on, data on stable isotopes composition of oxygen ($\delta^{18}O$) and hydrogen ($\delta^{2}H$) is used to identify the origin of infiltrated water, and radioactive isotope tritium (^{3}H) complements the data about the age and dynamics of groundwater. With this information it is possible to create a more complete picture of hydrochemical characteristics of groundwater in aquifers of different lithological, climatological, vegetation and other conditions in Slovenia.

1.2.2. Scientific contributions

In the last decades, there has been a major progress in research of the relations between natural and anthropogenic factors on groundwater recharge areas and its hydrochemical parameters. However, there is still a deficiency, especially for individual chemical compounds, stable and radioactive isotopes composition and trace elements, which are less used in regular practice of hydrogeology. Previous studies gathered a large data-set of historical data and used statistical approaches on determining the natural background level within comparable groundwater typologies. This study covers systematic research on hydrochemical composition and identification of processes controlling the geochemical evolution of groundwater, covering heterogeneous regions in their recharge areas.

Hydrochemical investigations worldwide regarding the discussed topic had their starting point in LAWA (2001) and BRIDGE (2005) methodology (Pauwels, 2007). The aim of this research was to assess the natural background levels based on the statistical analysis of basic chemical parameters and trace elements combined of past National groundwater monitoring network's results. In comparison, this research includes present (recent) groundwater data and different basic methodological approaches for evaluating the natural background level and spatial distribution of observed parameters. This study also considers land cover/use data and data on climate.

Further on, this research will also create an expert basis to complement the conceptual models of different groundwater bodies and aquifer systems, which were described by Prestor *et al.* (2003, 2006). Without reliable conceptual models, it is not possible to make hydraulic models that could predict the characteristics of the contaminant transport in groundwater. So far there are only conceptual models that often do not consider hydrochemical and isotopic characteristics of groundwater in Slovenia, which also contain virtually no measured data on the groundwater dynamics or their age.

1.2.3. Applicative contributions

From the application's point of view, the final results of this research are hydrochemical thematic maps which have different purposes: planning of utilization of water resources for drinking water and technological purposes (water mineralization, Fe and Mn concentration that are limiting the use of drinking and technological water, aggressiveness and toxicity of groundwater) and planning water resources protection (data on groundwater flow, velocity, age, and other purposes in context of environmental protection) and for assessment of water vulnerability and sustainable management with groundwater. These hydrochemical thematic maps, which have not yet been done for Slovenia, are a summary of statistical methods that have been applied to geochemical data. These maps could help to efficiently manage groundwater sources in Slovenia, as part of Water Framework Directive (2000/60/EC) and Daughter Groundwater Directive (2006/118/EC) which both comprise the determination of natural background levels, and will give the researches basic information on the hydrochemical situation in aquifers. Additionally the information provided by those maps is very useful for general population as well, due to practical aspects; e.g. in households (groundwater hardness map or groundwater pollution with nitrates).

2. THEORETICAL BACKGROUND

2.1. State of the art

Many studies have been conducted in the past decades considerning the chemical and isotopic composition in Slovenian groundwaters, but none of these studies covers the complete Slovenian territory with broad range of observed parameters. In Slovenia the first general and systematic study of hydrogeological characteristics of Slovenian territory has been made by Drobne *et al.* (1976). Pirc *et al.* (1998) studied general distribution of stable isotopes of carbon and oxygen in surface waters in Slovenia. Kukar *et al.* (2003) used statistical approaches on macro- and trace-elements in Slovenian springs in order to establish the distribution of their properties. Physico-chemical parameters in groundwater were studied by Vončina *et al.* (2007), where on the results various chemometrics methods were employed. Brenčič and Vreča (2006a, 2006b) studied general chemical and isotopic composition of bottled waters in Slovenia, as well as d-*excess* (Brenčič *et al.*, 2011). In Slovenian spring water also ^{3}H activity was investigated (Korun *et al.*, 2011; Vaupotič *et al.*, 2011) as well as some other radioisotopes (Kobal *et al.*, 1990; EARS, 2002; Vaupotič *et al.*, 2011; Korun and Kovačič, 2011; Benedik and Jeran, 2012). Stable isotope composition of dissolved inorganic carbon (δ^{13}C-DIC) in groundwater were frequently used in studies of tracing DIC sources and dynamics in water (Vogel *et al.*, 1975, Pezdič *et al.*, 1990; Urbanc, 1989, 1993; Pirc *et al.*, 1998; Brenčič, 1998; Lojen *et al.*, 2009; Cukrov *et al.*, 2012; Doctor *et al.* 2008, Kanduč *et al.*, 2013, Zavadlav *et al.*, 2013). Groundwater δ^{13}C-DIC in the recharge areas of silicate rocks was studied by Shin *et al.* (2011). Stable isotopic ratios of nitrogen in groundwater have been used to identify sources of nitrate by Zupanc *et al.* (2011), Urbanc and Jamnik (2007), Šturm and Lojen (2011), Šturm (2011), Pintar (1993, 2002), and Pintar *et al.* (1996, 2008).

Since 1987, regular systematic national groundwater quality monitoring has been carried out by the Environmental Agency of the Republic of Slovenia (EARS) within the Ministry of the Environment and Spatial Planning (MESP). The monitoring was established on the alluvial aquifers, which are important for drinking water supply, and the groundwater quality monitoring for karstic springs followed in 1990 (Krajnc *et al.*, 2007). Groundwater quality monitoring is carried out according to Regulation on the groundwater imission monitoring (2002, 42/02). The Slovene Environmental Protection Act (EPA, 1993) provides a legal basis for groundwater monitoring. Decree on groundwater quality standards (2005) defines the groundwater quality standards and methodology for chemical status assessment. Chemical status is additionally assessed by the monitoring results of drinking water abstracted from the groundwater resources. The results are assessed according to the Rules on drinking water (2004). In 2007, the national monitoring network included 206 monitoring sites. Although sampling network covered all 21 groundwater bodies the density of sampling sites is higher on alluvial aquifers than on fissure and karst porosity aquifers (Krajnc *et al.*, 2008). Two to four times a year about 160 different chemical and physical parameters are analysed (Krajnc *et al.*, 2007). The main aim of these monitorings is a report of the current chemical status of groundwater and trends of physico-chemical parameters according to current meteorological conditions and past results, and the assessment for each individual groundwater body. No detailed interpretation is provided on the source of origin or transport of measured parameters. Additional groundwater quality monitoring programmes are performed on the local level by the water supply managements and local authorities (Krajnc *et al.*, 2008).

In the last decade the introduction of the European Union (EU) Water Framework Directive (WFD) (2000/60/EC) and its Daughter Groundwater Directive (2006/118/EC) on the protection of groundwater against pollution and deterioration of its chemical status has set out criteria (Article 17 of the Water Framework Directive) for the assessment of the chemical status of groundwater based on the existing European Community quality standards (nitrates, pesticides and biocides) and on the requirement for Member States to identify pollutants and threshold values (TVs) for groundwater bodies at risk in accordance with the analysis of pressures and impacts carried out under the WFD. In this context groundwater background values (NBLs) are required as a reference to establish whether the groundwater is affected by contamination, and if, to what degree (Nieto *et al.*, 2005).

The actual value of natural groundwater background can be difficult to establish, because the concentrations of dissolved substances vary with time and space. Additionally, finding an environment in densely populated Europe that has not been affected by the anthropogenic influences is quite difficult. Therefore geochemical studies were performed to establish the natural background chemistry of groundwater. Two bigger projects were focused on the defining and determining the natural background value: cross border and EU-wide projects BaSeLiNe – Natural Baseline Quality in European Aquifers: a basis for aquifer managament Ref EVK-CT-1999-00006 (Edmunds and Shand, 2008), and later BRIDGE – Background cRiteria for the IDentification of Groundwater NBLs and TVs values (2005-2007) (Pauwels *et al.*, 2007). The criteria used in the BRIDGE project are the most relevant ones to explain the natural chemical signature of the aquifer (Quevauviller *et al.*, 2009). Detailed description of the methodology of the project is found in BRIDGE (2005). The applicability and validity of this approach is checked in 14 case studies at the level of aquifer typologies throughout Europe including Upper Rhine Valley as a transboundary case study (Wendland *et al.*, 2008), groundwater from Rhodope area (Thrace, Greece) (Gemitzi, 2011), groundwater from Campania region (southern Italy) (Ducci and Sellerino, 2012), and Western River Rhine (The Netherlands) (Griffioen *et al.*, 2008).

Prior to the BRIDGE, a Germany's Working Group of the Federal States on Water Problems (LAWA) (2002-2004) developed the procedure to define good chemical status (natural groundwater conditions) on existing data from regular groundwater monitoring network provided by the Federal States (LAWA, 2001). For the distribution pattern of a specific groundwater parameter, observed by a number of groundwater monitoring stations within comparable groundwater typologies (petrographical and hydrodynamical), two statistical distribution functions were used – the natural and the anthropogenic component. In order to separate those two influencing factors a statistical analysis of a large number of groundwater samples was considered, with condition that groundwater samples were taken from aquifers, which can be regarded as almost hydrochemically homogenous. Methodology is based on the statistical analysis with observation of the frequency distribution of the observed concentration of groundwater parameter. The lognormal distribution is expected of concentrations resulting from the redox reactions in the soil or the groundwater bearing rocks (natural component), whereas the concentration patterns originating from direct inputs from the soil are expected to be normal (anthropogenic component). The explicit shape of both distribution functions is determined by 3 parameters (amplitude, median and variance), which have to be fitted to the observed frequency distribution using standard algorithms. Natural groundwater concentrations are characterised by a concentration range defined by the confidence intervals (10 % and 90 % percentiles) of the concentration distribution of the natural component (Wendland *et al.*, 2005). Based on monitoring data from 7,920 groundwater monitoring stations, 15 different hydrochemical parameters were evaluated for each groundwater typology, and the range of natural groundwater concentrations has been identified. The applicability of the approach was established for 4 hydrochemically different groundwater typologies occurring through Germany (Wendland *et al.*, 2003; Voigt *et al.*, 2005). They use 2 statistical methods, the separation method, and the selection (ranking) method. Results of both methodologies are slightly different, but NBLs are comparable. NBLs from both projects have been used as a starting point to derive pollutant TVs values for the groundwater bodies.

As stated above, groundwater quality in aqifers is influenced by natural and anthropogenic sources among which is sometimes difficult to distinguish whether an observed groundwater parameters is influenced by pollution or is still natural (Wendland, 2008). Therefore various methods for assessing the natural background chemistry of groundwater were proceed, e.g. assessment of historical groundwater quality data, comparison of up-gradient and cross-gradient groundwater quality, comparison with similar geochemical environments, geochemical modelling, and statistical methods. They all have advantages and limitations (Shand *et al.*, 2007).

2.2. Isotopes in the global water cycle

2.2.1. Radioactive isotopes

Radioactive isotopes occurring in groundwater originate from cosmogenic nuclear reactions, and additionally from atmospheric nuclear testing. In groundwater studies they are used for determination of groundwater residence time (age) for estimating aquifer storage, as well as the rate of groundwater renewal and flow velocity (^{3}H, ^{14}C, ^{81}Kr, ^{36}Cl, uranium isotopes and ^{4}He).

2.2.1.1. *Radioactive isotope of hydrogen (tritium) (^{3}H)*

Tritium (^{3}H or T) is a short-lived radioisotope of hydrogen with a half-life of 12.43±0.02 years (Clark and Fritz, 1997; Kendall and McDonnell, 1998; Ravikumar and Somashekar, 2011). Tritium activity is expressed as absolute concentrations using tritium units (TU) (Clark and Fritz, 1997) which equals to the activity of 0.118 Bq/kg of water (Kazemi *et al.*, 2006). Small amount of tritium is produced naturally in the stratosphere by cosmic radiation on ^{14}N ($^{14}N + n \rightarrow {}^{15}N \rightarrow {}^{3}H + {}^{12}C$), or are of anthropogenic formation after atmospheric nuclear weapons tests throughout the 20th century (Clark and Fritz, 1997) which disturbed the natural levels of tritium. The natural concentration of tritium prior the nuclear bomb testing ranged from approx. 2 to 8 TU (Motzer, 2005), and at the peak in 1963 was about 5,000 TU in precipitation in the N hemisphere (Gat *et al.*, 2001). After cessation of nuclear tests the tritium concentrations dropped to between 12 and 15 TU (Motzer, 2005) and is still decreasing (Motzer, 2005; Gat *et al.*, 2001).

Tritium is mostly distributed in the environment as water so its concentration in precipitation is reflected in groundwater, and can therefore be used to date groundwater recharge. Since tritium activity varies spatially and temporally, to estimate groundwater recharge and a travel time, it is important to use, as a reference, the closest precipitation measurement site. Groundwater age estimation using tritium only provides semi-quantitative values (Motzer, 2005):

- < 0.8 TU indicates older water (prior to 1950's)
- 0.8 to 4 TU indicates a mixture between older and recent water
- 5 to 15 TU indicates recent water (< 5 to 10 years)
- 15 to 30 TU indicates some bomb tritium
- > 30 TU indicates the recharge in the 1960's to 1970's.

Tritium data provide an estimation of groundwater age, or time since groundwater was recharged (Clark and Fritz, 1997). But tritium data alone cannot provide the age of groundwater (U.S. Geological Survey, 1999). Namely groundwater dating is more complex and requires long time series data at particular sampling location, requires measurements of vertical tritium activity in object, as well as estimation of the initial tritium activity prior to recharge.

In the precipitation (atmosphere) long term tritium records show that tritium activity is continually decreasing after 1963 (Fig. 1), therefore any references used for the interpretation of groundwater tritium activity needs to consider the closest precipitation measurement location and a year of reference (Kazemi *et al.*, 2006). Therefore the presented groundwater age estimation guide values have changed during the last few years.

Groundwater age and residence time can be estimated on the basis of groundwater tritium activities modelled by the groundwater exponential model (Maloszewski and Zuber, 1982, 1996; Zuber *et al.*, 2001).

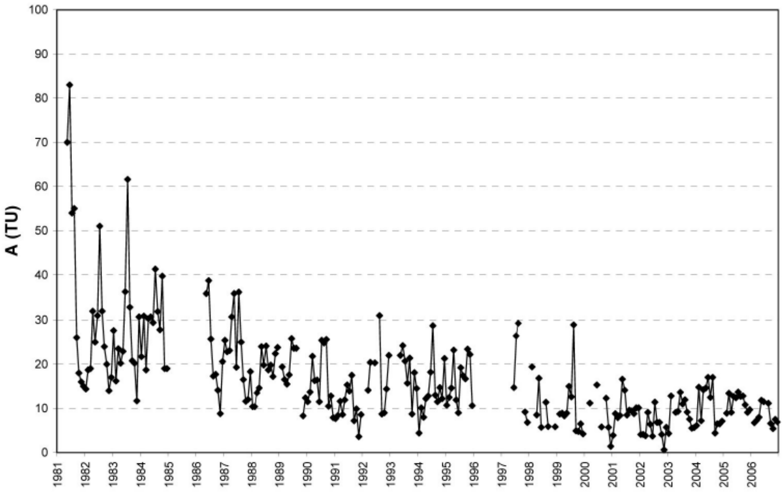

Figure 1: Monthly variation of ^{3}H activity (A) in precipitation in Ljubljana (1981-2006) (Vreča et al., 2008)

2.2.2. Stable isotopes

Stable isotopes can be used to investigate groundwater recharge (altitude and climatic conditions), groundwater dynamics, contamination, interaction (mixing) with other waters, and can help to identify the source of pollution, as well as other processes in the aquifer. Stable isotope analyses are generally reported as isotopic ratios of the particular element being analysed. By established convention, isotopic ratios are reported as delta (δ) in per mill (‰):

$$\delta_{(sample)}\ (‰) = [(R_{(sample)}/R_{(standard)}) - 1] \times 1000, \qquad (1)$$

where R represents the isotopic ratio (heavier to lighter isotope, e.g. $^{18}O/^{16}O$, $^2H/^1H$, $^{13}C/^{12}C$, $^{15}N/^{14}N$) of the sample and standard, respectively. A commonly used standard for $^{18}O/^{16}O$ and $^2H/^1H$ is Vienna Standard Mean Ocean Water (V-SMOW), for $^{13}C/^{12}C$ is Vienna Pee Dee Belemnite (VPDB), and for $^{15}N/^{14}N$ is the atmospheric air (Air).

Isotope fractionation is a process affecting the relative abundance of stable isotopes of the same element. Detail describtions of isotope fractionation is found in Zeebe and Wolf-Gladrow (2001), Clark and Fritz (1997), Hoefs (1997) and other textbooks on environmental isotopes.

An interpretation of meteoric water lines can help to determine the source of air masses, together with the deuterium excess (*d-excess*) which is calculated on the basis of the relationship (Craig, 1691; Dansgaard, 1964):

$$d\text{-}excess = \delta^2H - 8\delta^{18}O. \qquad (2)$$

The *d-excess* is believed to be related mainly to the meteorological conditions in the source region from which the sample is derived, i.e. the relative humidity in the atmosphere above the ocean, the wind regime, surface roughness of the ocean, as well as its temperature (Merlivat and Jouzel, 1979). In addition, *d-excess* reflects the prevailing conditions during the evolution and interaction of air masses mixing en route to the precipitation site (Fröhlich *et al.*, 2002). It is measured from the relative proportions of $\delta^{18}O$ and δ^2H contained in water and can be depicted visually as an index of deviation from the GMWL. Vapour generated over a closed basin with restricted communication such as the Mediterranean Sea is characterised by a higher *d-excess* value (~20‰) (Gat and Carmi, 1970; Gat and Dansgaard, 1972; Różański *et al.*, 1993), compared to Atlantic air masses with a lower *d-excess* value (~10‰) (Fröhlich *et al.*, 2002; Gat and Dansgaard, 1972; Różański *et al.*, 1993).

2.2.2.1. Stable isotope composition of oxygen and hydrogen ($\delta^{18}O$ and $\delta^{2}H$) in groundwater

Stable isotopes, as a result of their conservative behaviour in water and the large variability of their isotope ratios, are powerful tools for studying the global water cycle. The stable isotopes of oxygen and hydrogen (^{18}O and D) in water are applied for tracing water in its various stages of migration (Mook, 2006) and are used for identifying recharge areas (source and movement) of groundwater (Clark and Fritz, 1997) which reflects the stable isotope ratio of precipitation. Variations of $\delta^{18}O$ and $\delta^{2}H$ in atmospheric water vapour, which starts from isotope fractionation during evaporation from the ocean and condensates during the formation of rainfall, occur almost exclusively in the atmospheric and the Earth's surface part of the water cycle. During those phase changes, i.e. evaporation and condensation of water, the heavy water molecules ($H_2{}^{18}O$, $^{1}H^{2}H^{16}O$) remain preferentially in, or pass into, the liquid (solid) phase. During infiltration of precipitation below the unsaturated zone, the isotopic composition remains practically unchanged during subsurface movement and storage, except at higher temperatures (>60°C), where isotopic exchange of oxygen with the rock matrix can occur (Araguas-Araguas *et al.*, 2000; Gat *et al.*, 2010).

Hydrogen isotopes are fractionated proportionally to oxygen isotopes (Clark and Fritz, 1997), where the linear relation between $\delta^{18}O$ and $\delta^{2}H$ on the global scale is expressed as the global meteoric water line (GMWL) (Fig. 2), defined by Craig (1961) as:

$$\delta^{2}H=8\delta^{18}O+10\ (‰) \tag{3}$$

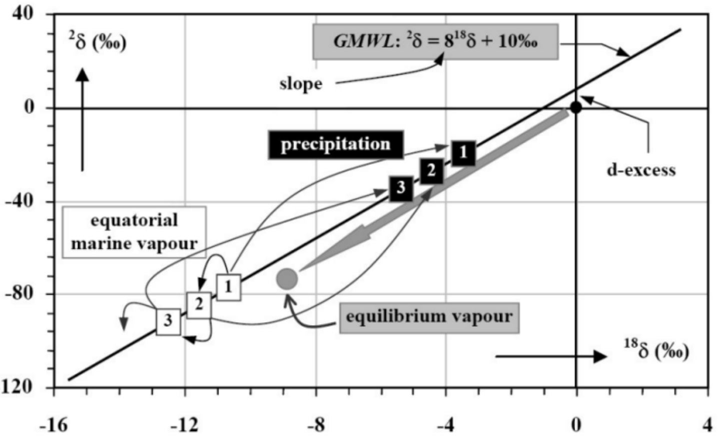

Figure 2: Global meteoric water line: relation between $\delta^{18}O$ and $\delta^{2}H$ of water vapour (source of precipitation) and resulting precipitation (IAEA, 2011)

Różański *et al.* (1993) and Gourcy *et al.* (2005) reported a refined empirical regression line for the long-term (1961–2000) annual weighted means of $\delta^{18}O$ and $\delta^{2}H$ values, collected in the Global Network of Isotopes in Precipitation (GNIP), as $\delta^{2}H=(8.07\pm0.02)\delta^{18}O+(9.9\pm0.01)$.

Dansgaard (1964) also observed the geographic distribution in the isotopic composition of precipitation in relation to many environmental parameters, e.g. latitude (latitude effect), altitude (altitude effect) (Figs. 3 and 4), distance from coast (continental effect), the amount of precipitation (amount effect) and surface air temperature (temperature effect). The altitude effect is caused by increasing elevation in mountain regions as a result of the continuous pseudo-adiabatical cooling of the air mass to below the dew point in an orographic precipitation system where heavier isotopes precipitate preferentially (Clark and Fritz, 1997; Dansgaard, 1964; Jouzel and Merlivat, 1984; Gat, 1996; Ingraham, 1998). Hydrological applications of isotopic measurements derive usually from the knowledge of the altitude effect, which is one of numerous applications of environmental isotope techniques in hydrology often used to calculate the mean altitude of the recharge area of aquifers (Longinelli and Selmo, 2003). The altitude effect is temperature-related, and values of ^{18}O mentioned in the literature vary between –0.1 and –0.6 ‰ $\delta^{18}O$/100 m (Clark and Fritz, 1997; Eriksson, 1983).

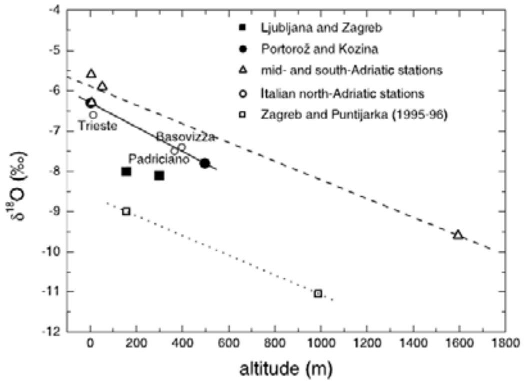

Figure 3: Relation between weighted mean δ^{18}O and the altitude of the sampling precipitation stations (Vreča et al., 2006a)

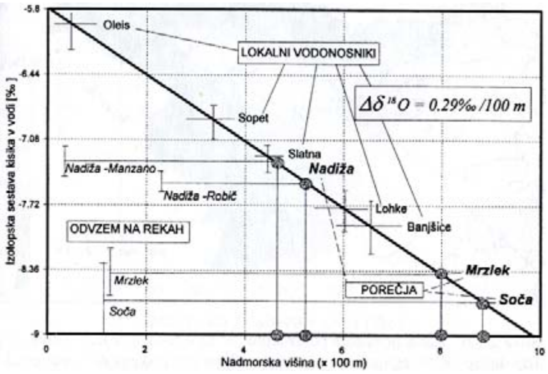

Figure 4: Altitude effect based on mean δ^{18}O in small aquifers in west Slovenia (In Pezdič, 1999)

The continental effect is present when sea water evaporates from the sea to the atmosphere (Fig. 5), and the vapour masses move inland. Isotopic fractionation occurs in moving air masses, resulting in the depletion of heavy isotopes (Ingraham, 1998). Coastal precipitation is isotopically enriched (Fig. 6) relative to colder, inner continental regions, which receive isotopically depleted precipitation with strong seasonal differences (Clark and Fritz, 1997; Ingraham, 1998). For example, in Irish precipitation over Europe, from the Irish coast to the Ural mountains, an average depletion of 7 ‰ in δ^{18}O is observed (Mook, 2006).

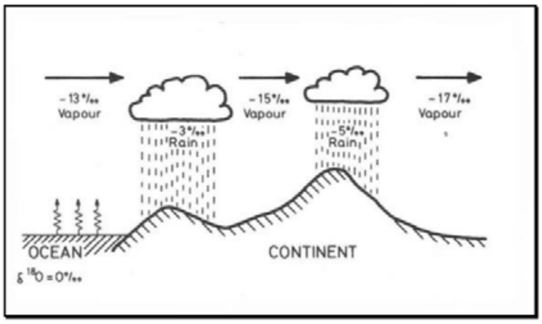

Figure 5: Altitude effect (Hoefs, 1997)

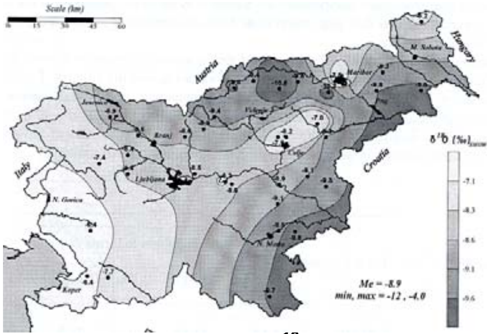

Figure 6: Distribution of δ^{18}O in stream waters in Slovenia (Pirc et al., 1998)

Depending on the region, differences in the amount of precipitation, temperature variations, distinct air mass sources, evaporation and fractionation processes occurring below the cloud base are characteristic at a local scale, which cause the relationship between stable isotopes of water δ^{18}O and δ^{2}H to vary from that of the GMWL also known as local meteoric water line (LMWL) (Hoefs, 1997). Vreča *et al.* (2010) calculated LMWLs for precipitation at 3 precipitation locations: Ljubljana, Portorož Airport, and Kozina (Tab. 1).

Table 1: Slovenian local meteoric water lines (Vreča et al., 2010)

Local meteoric water line	Time period
Ljubljana: δ^2H=(8.1±0.1)δ^{18}O+(9.8±0.7)	1981–2006
Portorož Airport: δ^2H=(8.05±0.22)δ^{18}O+(9.35±1.55)	2000–2006
Kozina: δ^2H=(7.7±0.3)δ^{18}O+(9.6±0.7)	2001–2003

The nearest LMWLs to Slovenia found in the literature are: Zagreb (Croatia) with δ^2H=7.8δ^{18}O+5.7 (Vreča *et al.*, 2006a); Northern Italy with δ^2H=7.74δ^{18}O+9.4; Central Italy with δ^2H=7.0δ^{18}O+5.6; Southern Italy with δ^2H=6.94δ^{18}O+7.31 (Longinelli and Selmo, 2003); and the eastern Mediterranean meteoric water line (EMMWL) with δ^2H=8δ^{18}O+22 (Gat and Carmi, 1970).

In Slovenia, the precipitation station at Ljubljana and occasionally a few other stations are included in the GNIP, organised jointly by the Isotope Hydrology Section of the International Atomic Energy Agency

(IAEA) and the World Meteorological Organization (WHO) (Gourcy *et al.*, 2005). The precipitation quantity monitoring programme is performed in the framework of the regular activities of the Slovenian Environmental Agency, but monitoring of the isotopic composition is not included in the regular monitoring. It has been performed by the Jožef Stefan Institute in Ljubljana at the Ljubljana meteorological station (since 1981), Portorož Airport (since 2000) and Kozina (2000–2003).

Stable isotope composition in precipitation in Slovenia was already the topic of many researchers like Krajcar-Bronić *et al.*, (2003, 2006), Vreča *et al.*, (2005, 2006ab, 2007, 2010,), Ogrinc *et al.* (2008), and others. The stable isotopic composition of oxygen and hydrogen has been implemented in groundwater studies as well by Pezdič (1997), Trček (2006), Doctor *et al.* (2000, 2006), Brenčič and Vreča (2006ab), Brenčič and Poltnig (2008), Ogrinc *et al.* (2008), Kanduč *et al.* (2012, 2013), Urbanc *et al.* (2012), Urbanc and Jamnik (1999), Mali and Urbanc (2006 and 2009) and others. Calculation of altitude and continental effects for Slovenia with mean values of δ^{18}O in surface water in Slovenia was conducted by Pirc *et al.* (1998).

2.2.2.2. Stable isotope composition of dissolved inorganic carbon (δ^{13}C-DIC) in groundwater

Rainwater equilibrates with atmospheric CO_2 which solubility is temperature dependent (Lower, 2010; Appelo and Postma, 2005). As rainwater seeps through the soil layer (Fig. 7) it equilibrates with soil CO_2, which is produced from dead plants and animal decay or root respiration, and increases the content of H_2CO_3 (Rastogi *et al.*, 2002). The weak acid (H_2CO_3) then dissolves limestone and dolomite allowing the water to pick up calcium, magnesium, and carbonate ions (Hem, 1963; Lower, 2010; Appelo and Postma, 2005; Faimon *et al.*, 2012).

$$CO_{2(g)} \rightarrow CO_{2(aq)} \tag{4}$$

$$CO_{2(aq)} + H_2O \rightarrow H_2CO_3 \tag{5}$$

$$H_2CO_3 \rightarrow H^+ + HCO_3^- \tag{6}$$

$$HCO_3^- \rightarrow H^+ + CO_3^{2-} \tag{7}$$

$$CaCO_3 \rightarrow Ca^{2+} + CO_3^{2-} \tag{8}$$

The total dissolved inorganic carbon (DIC) is generally a sum of H_2CO_3, $CO_{2(aq)}$, HCO_3^-, and CO_3^{2-} (Stumm and Morgan, 1996; Drever, 1997; Clark and Fritz, 1997; Kendall and Doctor, 2003; Redondo and Yélamos, 2005). DIC is produced by various reactions: (1) weathering of carbonate minerals by acidic rain originated by reaction between precipitation water and soil CO_2 (H_2CO_3), or other strong acids (H_2SO_4, HNO_3); (2) weathering of silicate minerals by H_2CO_3 produced by the dissolution of biogenic soil CO_2 by infiltrating rain water; and (3) weathering of carbonate minerals by H_2CO_3 (Kendall and Doctor, 2003).

δ^{13}C-DIC is a non-conservative tracer and depends on various sources of origin, where each of these sources contributes to the DIC of groundwater in diverse δ^{13}C ratios (Stumm and Morgan, 1996; Hoefs, 1997; Kendall and McDonnell, 1998). In general δ^{13}C-DIC is used to identify sources of carbon where it is particularly valuable for distinguishing between carbon derived from organic matter, transport of CO_2 gas from a soil atmosphere, and carbon derived from carbonate weathering (Clark and Fritz, 1997; Drever, 1997; Hoefs, 1997; Kendall and McDonnell, 1998).

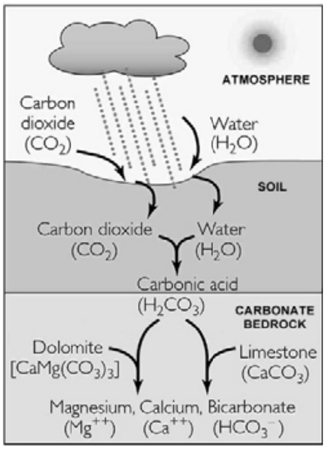

Figure 7: Carbonate dissolution (adapted after Sinkgole, 2013)

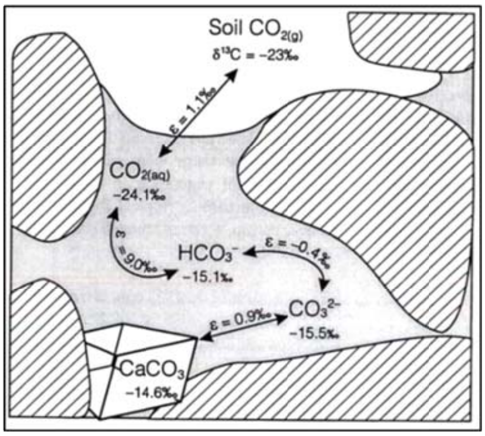

Figure 8: Fractionation factors of ^{13}C during equilibrium exchange of carbon between CO_2, DIC, and $CaCO_3$ (Clark and Fritz, 1997)

The evolution of DIC and $\delta^{13}C$-DIC begins with the atmospheric CO_2 with $\delta^{13}C$ ~ -7 ‰ (Clark and Fritz, 1997; Kendall and Doctor, 2003). $\delta^{13}C$-DIC of meteoric water is usually negative, but the specific values are variable (Drever, 1997). Dissolution of $CO_{2(g)}$ in water causes depletion in ^{13}C and results in a $\delta^{13}C$ of ~ -8 ‰ for $CO_{2(aq)}$ (Appelo and Postma, 2005; Deines *et al.*, 1974), depending on the temperature (Redondo and Yélamos, 2005). When meteoric water infiltrates through the soil into the aquifer it equilibrates with soil CO_2 ($\delta^{13}C$ ~ -25 ‰) which derives from root respiration and microbial decomposition of soil organic matter and causes depletion in ^{13}C of the soil CO_2 by about 20 ‰ (Appelo and Postma, 2005). Isotopic composition of soil CO_2 depends on the type of vegetation in the recharge area (Appelo and Postma, 2005; Drever, 1997) and fractionation processes during CO_2 transfer through the soil horizon of 4.4 ‰ (O'Leary, 1980; Cerling, 1991) (Fig. 8). During photosynthesis, the carbon that becomes fixed in plant tissue is significantly depleted in ^{13}C relative to the atmosphere (Kendall *et al.*, 1995). The extend of fractionation depends on the type of vegetation: C_3 vegetation (Calvin photosynthetic pathway), e.g. wheat, rice, pine, apple trees, barley, potatoes, and dandelions, is around -27 ‰, C_4 vegetation (Hatch-Slack photosynthetic pathway), e.g. maize, sugar cane, and millet around -12 ‰, (Deines, 1980) and as CAM Plants (Crassulacean acid metabolism), e.g. pineapple which has intermediate value of both C_3 and C_4 (Clark and Fritz, 1997). As vegetation debris accumulates in the soil, decay by aerobic bacteria converts it back to CO_2 (Kendall and Doctor, 2003; Clark and Fritz, 1997; Appelo and Postma, 2005). The $\delta^{13}C$ of CO_2 produced by respiration in the soil is approximately equivalent to $\delta^{13}C$ of the predominant organic matter, where exchanges with atmospheric CO_2, diffusion of CO_2 out of the soil, and decomposition of organic matter can enrich soil CO_2 in ^{13}C (Doctor *et al.*, 2008).

Dissolved soil CO_2 lowers the pH and increases the carbonate dissolution capacity of groundwater. The amount of CO_2 that can be dissolved depends on the temperature, pH of the water, the partial pressure of CO_2, and the weathering reactions in the soil of recharge area (Clark and Fritz, 1997). Also greater soil thickness enables accumulation of more soil CO_2, which results in more negative $\delta^{13}C$-DIC values (Kanduč *et al.*, 2013). Carbonate rocks typically have $\delta^{13}C$ value of 0±5 ‰ (Clark and Fritz, 1997; Kendall and Doctor, 2003). DIC produced by the equal shares of dissolution of calcite ($\delta^{13}C$ = 0 ‰) by carbonic acid ($\delta^{13}C$ = -22 ‰) has a $\delta^{13}C$ value of about -11 ‰ (Kendall and Doctor, 2003; Redondo and Yélamos, 2005), and the precipitation of calcite will result in an isotopically lighter CO_2 in solution (Redondo and Yélamos, 2005). The $\delta^{13}C$ of precipitated carbonate minerals is by around 15 ‰ higher than the DIC from the soil water. The low pH is buffered by mineral weathering in the soil and upper bedrock, with the calcite dissolution as the most common and effective buffering reaction: $CaCO_3 \rightarrow Ca^{2+} + CO_3^{2-}$. This reaction can be enhanced by carbonic acid from soil CO_2 to the net reaction:

$$CO_{2(g)} + H_2O + CaCO_3 \rightarrow Ca^{2+} + 2HCO_3^-. \tag{9}$$

The higher the CO_2 concentration in the soil atmosphere, the lower is the initial groundwater pH, the greater is the amount of dissolved calcite, and larger is the groundwater's DIC concentration. The dissolution of carbonate minerals depends on the characteristics of the system (open or closed system)

(Clark and Fritz, 1997; Deines *et al.*, 1974). In the open system, there is a constant inflow of CO_2 where gas and aqueous phases coexist in the unsaturated zone, and the calcite dissolution proceeds with a constant supply of soil CO_2. Due to continuous replenishment of CO_2, more calcite is dissolved, and the final equilibrium concentration of DIC will be high (Deines *et al.*, 1974; Clark and Fritz, 1997; Kendall and Doctor, 2003). Open system equilibration of DIC with CO_2 enriches DIC in ^{13}C by about 9 ‰ (Mook *et al.*, 1974). In the closed system the soil CO_2 is not replenished as carbonate dissolution proceeds and the amount of final DIC concentration is low. Dissolution of carbonate minerals provides an additional source of carbon to DIC which evolves to more enriched groundwater $\delta^{13}C$-DIC values (Clark and Fritz, 1997).

Weathering of silicate minerals has a different effect on the carbonate system. In this case the main source of DIC is derived from the soil CO_2 (Clark and Fritz, 1997; Shin *et al.*, 2011) consumed by the alteration of feldspars (albite, anortite, kaolinite) (Clark and Fritz, 1997). Chemical reactions in the aquifer produce a non-significant shift in DIC isotope composition (Redondo and Yélamos, 2005).

The worldwide $\delta^{13}C$-DIC in catchment waters is generally in the range of -25 ‰ to -5 ‰ (Clark and Fritz, 1997; Kendall and Doctor, 2003; Mills, 1988; Kendall *et al.*, 1995).

2.2.2.3. Stable isotope composition of nitrogen ($\delta^{15}N$) in groundwater

Nitrogen isotopes ($\delta^{15}N$) are widely used to identify the nitrogen sources, processes and migration of contaminant in the aquifer. The isotopic fingerprints of nitrogen are derived from the atmosphere, fertilizers, soils, or manure (Kendall and McDonnell, 1998).

The dominant source of nitrogen is the atmosphere ($\delta^{15}N_{Air}$=0 ‰) which is fixed by many plants and transported to soil. The $\delta^{15}N$ range in soil (-10 to +15 ‰) depends on whether they are cultivated, on the soil depth, vegetation, climate, and more. Most soils have $\delta^{15}N$ range of +2 to +5 ‰. Plants by fixing N_2 from the atmosphere have $\delta^{15}N$ between 0 to +2 ‰ which is close to $\delta^{15}N$ of atmospheric N_2. Artificial (inorganic) fertilizers produced by the fixation of atmospheric N_2 include the urea, ammonium nitrate and potassium nitrate, and are generally reflecting their atmospheric source (-4 to +4 ‰). Animal waste products are enriched in ^{15}N because of volatilisation of ^{15}N-depleted ammonia, and oxidation of residual waste material (+10 to +25 ‰) (Kendall and McDonnell, 1998). In Slovenia organic fertilizers have $\delta^{15}N$ values around 9.5±3.9 ‰ (mean 8 ‰) and synthetic fertilizers around 3.0±3.3 ‰ (mean 0.4 ‰) (Šturm and Lojen, 2011). Rocks contributions are almost always negligible (Kendall and McDonnell, 1998).

The $\delta^{15}N$ values can be significantly altered by fractionation processes such as volatilisation, nitrification, and denitrification. During denitrification the lighter isotope ^{14}N is preferentially utilized, leaving a larger fraction of the heavier isotope ^{15}N in the unreacted NO_3^-. In anoxic groundwater, denitrification results in an increase in $\delta^{15}N$ of dissolved nitrate and decreasing the total concentration of NO_3^- (Kendall and McDonnell, 1998).

2.3. Groundwater geochemical processes and groundwater chemistry

2.3.1. Physico-chemical parameters

2.3.1.1. Hydrogen ion activity (pH)

pH is the term used to express the intensity of the acidity of a solution and measurement of hydrogen ion (H^+) activity in a water sample, or acid-base equilibrium, respectively (Rail, 2000). At the typical groundwater temperature the pH less than 7 is considered as acidic, and with a pH greater than 7 as alkaline (Freeze and Cherry, 1979). The common range of pH in natural waters is between 5 and 8.5 (Hem, 1985). Groundwater pH depends on the type of rocks through which it passes; carbonate rocks neutralise acidic water and give them alkaline pH, whereas igneous rocks have a limited effect on the pH (Bradshaw, 1975). Natural rainwater is slightly acidic (Krauskopf and Bird, 1994) due to reaction with the atmospheric CO_2, forming H_2CO_3.

For drinking water purposes the water should not be aggressive, and the pH range is between 6.5 and 9.5 (Rules on drinking water, 2004).

2.3.1.2. *Electrical conductivity (EC)*

The EC in groundwater is temperature dependent (Moore *et al.*, 2008) and estimates the concentration of all dissolved constituents in water (Hem, 1970) which influence on the ability of that water to conduct an electrical current measured in µS/cm. Rainwater has low electrical conductivity, generally of several tens of µS/cm, and brines in deep sedimentary basins contain hundreds of thousands µS/cm (Freeze and Cherry, 1979). EC between 50 and 750 µS/cm indicates good water quality (Saulnier *et al.*, 2011). Additionally the EC can be also used as an indicator for anthropogenic pollution (Birke *et al.*, 2009). This parameter is a good estimator of total dissolved solids (TDS) and for that matter the mineral salt content of the groundwater (Hem, 1970; Freeze and Cherry, 1979).

The allowed maximum permitted level for drinking water purposes is 2500 µS/cm (20°C) in water (Rules on drinking water, 2004).

2.3.2. Major and secondary major ions chemistry

Major cations and major anions in groundwater are detected in concentrations generally ranging from 1 to 1,000 mg/L (Hounslow, 1995). The major cations include Ca^{2+}, Mg^{2+}, Na^{+}, K^{+}, Si, and the major anions HCO_3^-, Cl^-, NO_3^-, S and SO_4^{2-}. Secondary constituents in groundwater are detected in concentrations ranging generally from 0.01 to 10 mg/L (Hounslow, 1995). Those are B, Ba, Fe, NH_4^+, PO_4^{2-}, Sr, and Zn.

Groundwater chemical composition provides the information on the share of individual chemical parameter. This data is used to identify the sources and relations between the groundwater and the lithological composition of the aquifer (Hounslow, 1995). The geochemical processes in the aquifer which are responsible for the evolution of the chemical character of the groundwater are also being explained by the use of various chemical ratios, e.g. Ca^{2+}/Mg^{2+} molar ratio.

Groundwater chemistry is a subject of kinetics reaction rate which affects groundwater (dis)equilibrium and should be considered when modelling groundwater reaction processes. For example, in carbonate aquifers the soluble carbonate minerals react fast upon contact with water and equilibrium is attained very quickly compared to residence time of groundwater. Contrary slowly soluble silicate minerals react very sluggishly so that equilibrium at low temperatures is never attained and reaction kinetics needs to be considered (Appelo and Postma, 2005).

2.3.2.1. *General calcium (Ca^{2+}) geochemistry*

Calcium generally has a high mobility and can easily become a major ion of water (Jordana and Batista, 2004). Its natural source is found in rock minerals like calcite and aragonite ($CaCO_3$), dolomite $CaMg(CO_3)_2$, gypsum ($CaSO_4*2H_2O$), anhydrite ($CaSO_4$), fluorite (CaF_2), apatite, plagioclase (anortite), pyroxenes, amphiboles, feldspar and clay minerals (e.g. illite, chlorite, and Ca-montmorillonite) (Hounslow, 1995; Hem, 1985; Zupančič and Pirc, 1999). Less important calcium sources are of anthropogenic origin which include construction materials (e.g. cement, brick lime ($Ca(OH)_2$), and concrete), batteries, application in plasters ($CaSO_4 \times \frac{1}{2} H_2O$), fertilizers ($CaCl_2$ or $Ca(NO_3)_2$), and lime ($CaCO_3$) (Cardarelli, 2000; LennTech, 2013a; De Vos *et al.*, 2006). In natural waters and particularly groundwater the Ca^{2+} concentrations up to 100 mg/L (Hounslow, 1995; Hem, 1985) or higher (National Research Council, 1977) are very common. Groundwater Ca^{2+} concentration can be also influenced by cation-exchange reaction with clayey and ferric aquifer minerals where natural softening can occur, where calcium ion is replaced with sodium ion (Hounslow, 1995; Selinus *et al.* 2005).

There is no maximum permitted level for drinking water purposes for Ca^{2+} according to Rules on drinking water (2004).

2.3.2.2. General magnesium (Mg^{2+}) geochemistry

The major natural sources of magnesium are found in the carbonate rocks (dolomite and magnesite), ferromagnesian minerals (e.g. amphiboles, olivine, pyroxenes) and clay minerals (micas) which are found mostly in igneous rocks. In groundwater increased Mg^{2+} concentrations are possible due to interactions with seawater (mixing, intrusion) (Hounslow, 1995; Hem, 1985). Magnesium in the form of insoluble silicates breaks down into more soluble carbonates, clay minerals (cation exchange) and silica, depending on the presence of H_2CO_3 in the water (Karanth, 1987). The magnesium release rate from clays (e.g. chlorite, vermiculite, and montmorillonite) is generally slow (Mikkelsen, 2010). As anthropogenic source it can be found in plant nutrient, in fire protection devices, in fertilizers, cattle feed, in beer breweries ($MgSO_4$), in wastewater treatment plants ($Mg(OH)_2$), medicines, and as magnesium alloys in cars and other (LennTech, 2013b). Fertilization with other cations (e.g. K^+ and Ca^{2+}) frequently leads to enhanced magnesium solubility in the soil as they exchange on the clay sites and make magnesium more susceptible to leaching (Mikkelsen, 2010). In natural waters magnesium concentration is usually found from negligible to about 50 mg/l (Hounslow, 1995; Hem, 1985) and rarely above 100 mg/l, so calcium-based hardness usually predominates (National Research Council, 1977).

There is no maximum permitted level for drinking water purposes for Mg^{2+} according to Rules on drinking water (2004).

2.3.2.3. General calcium and magnesium (Ca^{2+}/Mg^{2+}) molar ratio geochemistry

Molar ratio between calcium and magnesium in groundwater indicates the relative proportion of the lithological composition of sampling location recharge area, and is equal to 1 if dissolution of dolomite prevails, whereas higher ratio indicates a greater contribution of calcite minerals dissolution (Mayo and Loucks, 1995). Higher Ca^{2+}/Mg^{2+} molar ratio (>2) indicates greater share of calcite according to dolomite, and is indicative also for the dissolution of silicate minerals, which contribute Ca^{2+}/Mg^{2+} ions to groundwater (Katz *et al.*, 1998). Based on the Ca^{2+}/Mg^{2+} molar ratio in groundwater it is possible to estimate the prevailing origin of rocks (limestone or dolomite) in the recharge area of sampled groundwater.

2.3.2.4. General bicarbonate (HCO_3^-) geochemistry

Carbonate-rich sedimentary rocks are by far the most common geogenic source of alkalinity in waters whereas igneous rocks present relatively insignificant sources of carbonate (Todd and Mays, 2005). The carbon in water arises from the reaction of CO_2 dissolved in soil water and groundwater with carbonate (calcite and dolomite) and silicate minerals (Ca-silicates, Mg-silicates, Na-silicates, K-silicates). During reaction of carbonate weathering (Equations 4-9) half of HCO_3^- is derived from soil CO_2. During the silicate weathering:

$$2CO_2 + 11H_2O + 2NaAlSi_3O_8 \rightarrow 2Ba^+ + 2HCO_3^- + Al_2Si_2O_5(OH)_4 + 4H_4SiO_4, \qquad (10)$$

all HCO_3^- is derived from soil CO_2 due to lack of carbonate minerals in the rocks (Berner and Berner, 2012). Anthropogenic sources of alkalinity include agricultural practices (lime application) on the fields, the effluent from wastewater treatment plants, wastewater from industry, and domestic uses in the cleaning agents and food residues (De Vos *et al.*, 2006). Usually less than 500 mg/L is found in the natural waters (Todd and Mays, 2005).

Three carbonate species (H_2CO_3, HCO_3^-, and CO_3^{2-}) contribute to total alkalinity and are pH and temperature depended (Fig. 9. At a pH of 6.3, the activities of HCO_3^- and H_2CO_3 are nearly equal. With pH > 6.3, HCO_3^- is the predominant species and at pH < 6.3 there is more $H_2CO_3^*$. The same relation for the CO_3^{2-} / HCO_3^- couple shows that the two species have equal activity at pH = 10.3. At a pH > 10.3, CO_3^{2-} becomes the predominant species while HCO_3^- is more abundant at pH < 10.3 (Appelo and Postma, 2005).

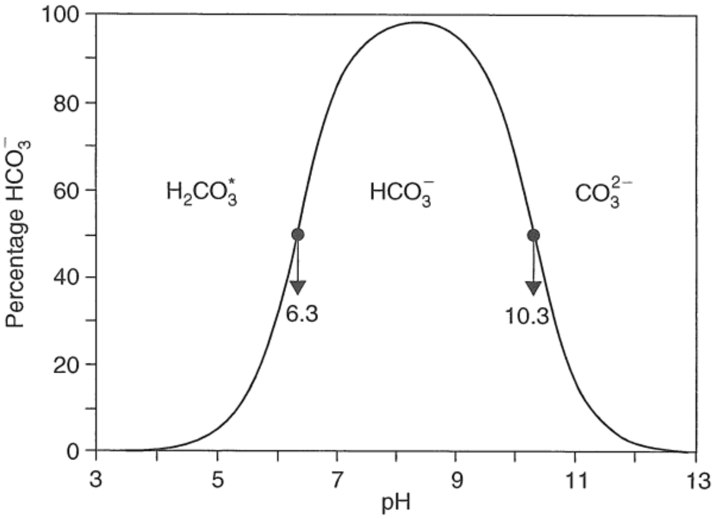

Figure 9: Percentage of HCO_3^- of total dissolved carbonate as function of pH (Appelo and Postma, 2005)

Alkalinity is a sum total of components in water that tend to elevate its pH above a value of 4.5 (McKee and Wolf, 1972). Alkalinity is the true measure of acid-neutralizing capacity which includes the bicarbonate (HCO_3^-), carbonate (CO_3^-) and hydroxide (OH^-) ions (Radtke *et al.*, 1998).

Formula for alkalinity in carbonate systems is (Stumm and Morgan, 1996):

$$[Alk] = [HCO_3^-] + 2[CO_3^{2-}] + [OH^-] - [H^+], \quad (11)$$

and formula for alkalinity in systems other than aqueous carbonate is (Stumm and Morgan, 1996):

$$[Alk] = [HCO_3^-] + 2[CO_3^{2-}] + [NH_3] + [HS^-] + 2[S^{2-}] + [H_3SiO_4^-] + 2[H_2SiO_4^{2-}] + [B(OH)_4^-] + [Org^-] + [HPO_4^{2-}] + 2[PO_4^{3-}] - [H_3PO_4] + [OH^-] - [H^+]. \quad (12)$$

2.3.2.5. *Practical aspects of groundwater mineralization ($CaCO_3$)*

Water hardness is caused mainly by the divalent ions of Ca^{2+} and Mg^{2+} which source is found mostly in carbonate rocks (limestone and dolomite) and other calcium-bearing minerals in soil and rock formations. The classification of waters regarding their hardness is arbitrary, with a number of classifications used: as concentration of $CaCO_3$ (mg/L or ppm, or mmol/L), as German degrees hardness (°dH), or as French degrees (°F) (Selinus *et al.*, 2005; Gray, 2008). Until recently, in Slovenia the German water hardness scale was used, but in order to make the scale of water hardness internationally comparable, in 2007 a new scale was introduced (Tab. 2) where molar concentration of $CaCO_3$ (mmol/L) is used as a unit for classification (WRMG, 2007). Since Ca^{2+} concentrations usually exceed the Mg^{2+} concentrations in water the calcium-based water hardness usually predominates (National Research Council, 1977). Hard waters are associated with the thick soil layer and limestone in the recharge areas, whereas soft waters occurs in the recharge areas of poorly permeable rocks in the recharge area (e.g. granite) (Gray, 2008), where the soil is sandy and/or thin, and where limestone formations are sparse or absent (Gray, 2008; Ritter, 2010).

Table 2: A new 3-point water hardness scale $CaCO_3$ (mmol/L) and its corresponding values in German degrees (°dH)

Water hardness	$CaCO_3$ (mmol/L)	German hardness (°dH)
soft	< 1.5	< 8.4
medium hard	1.5 – 2.5	8.4 - 14
hard	> 2.5	>14

Groundwater (total) hardness is calculated as (Freeze and Cherry, 1979):

$CaCO_3=2.5(Ca^{2+})+4.1(Mg^{2+})$ (13)

was calculated following the formulas below:

$M_{CaCO3}/M_{Ca}=100.1/40.1=2.5$ (14)

$M_{CaCO3}/M_{Mg}=100.1/24.3=4.1.$ (15)

Calculated $CaCO_3$ concentration was converted to mmol/L (divided by $CaCO_3$ molar mass) and °dH (divided by 17.8 mg/L).

Hard water can cause water pipes, kettles, boilers and washing machines to scale up, whereas soft water is more aggressive (corrosive) and increases the solubility of heavy metals such as Cu, Zn, Pb and Cd in water (Gray, 2008). Groundwater hardness varies locally depending on chemical and mining industry effluents, or excessive application of lime to the soil in agricultural areas (British Columbia of Canada, 2007; Gray, 2008).

2.3.2.6. *Soil CO_2 partial pressure (P_{CO2})*

The volume percent of CO_2 in the dry air is 0.03 % (Lower, 2010) ($10^{-3.5}$ or $3*10^{-4}$ atm) and rainwater in equilibrium with atmospheric CO_2 has a pH of 5.6 (Stumm and Morgan, 1996). Significantly higher P_{CO2} levels of 10^{-1} to 10^{-3} atm are observed in soil than in the atmosphere (Langmuir 1971; Stumm and Morgan, 1996; Drever, 1997; McPherson, 2009).

The pH in most groundwater is controlled in part by effects of dissolved CO_2 and the amount of gas dissolved affected by the temperature and pressure (Hem, 1963). The additional CO_2 from the soil increases the amount of $CaCO_3$ the water can dissolve (Drever, 1997) which increases the content of Ca^{2+} (Appelo and Postma, 2005). Lowering the pH causes more $CaCO_3$ to dissolve, and raising the pH causes precipitation of $CaCO_3$ (Appelo and Postma, 2005).

The distribution of DIC species can be calculated for two idealized cases: open and closed system of carbonate dissolution. In an open system (Fig. 10) the solution exchanges with either CO_2 gaseous phase or the solid ($CaCO_3$) (IAEA and UNESCO, 2000). The CO_2 partial pressure is constant and the CO_2 which has been consumed by dissolution of calcite is replaced with new so the dissolution of calcite is not limited until the water carbonate equilibria is reached (Appelo and Postma, 2005). Examples of open system are streams and shallow lakes, and the upper, wind-mixed regions of the oceans (Lower, 2010). In the closed system (Fig. 11) the transport of CO_2 between the atmosphere and the system is closed with respect to CO_2 (Appelo and Postma, 2005). P_{CO2} is changing in dependence of dissolved carbonate species distribution, as a function of pH. Examples of closed systems are deep regions of stratified bodies of water and the air component of soils (Appelo and Postma, 2005; Lower, 2010). If CO_2 is not replenished, the amount of calcite that water can dissolve is essentially limited by the amount of CO_2 present initially (Drever, 1997), so more calcite will dissolve under open system than in closed system conditions (Appelo and Postma, 2005).

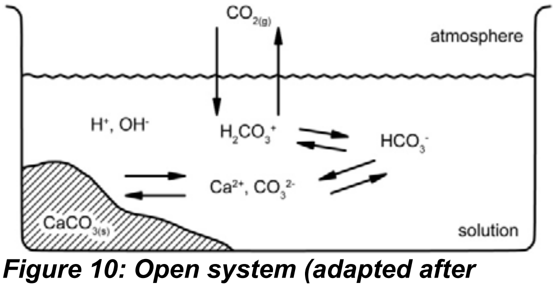

Figure 10: Open system (adapted after Snoeyink and Jenkins, 1980)

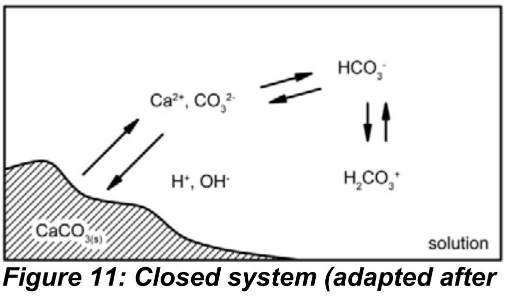

Figure 11: Closed system (adapted after Snoeyink and Jenkins, 1980)

The main difference between open and closed systems is that in the open system the concentration of carbonic acid (H_2CO_3) remains constant due to constant CO_2 supply, where concentrations of DIC varies with pH, whereas in the closed system the concentrations of DIC remain constant (Snoeyink and Jenkins, 1980).

2.3.2.7. General silicon (Si) geochemistry

Silicon in groundwater is mainly found in the form of silicon dioxide (SiO_2) and (ortho)silicic acid (H_4SiO_4). It is a major constituent of nearly all rocks with exceptions of carbonates. The simplest mineral form of Si is silica or quartz (SiO_2) which is an important component of detrital sedimentary rocks and felsic and intermediate igneous rocks (feldspar, ferromagnesium and clay minerals, amorphous silica, chert and opal). Silica in metamorphic rock types includes high silica rock types (gneiss, migmatite, and slate), and low silica rock types (eclogite and amphibolite). Quartz has very low solubility, and silica distribution is pH dependent, and its soluble form is the weak H_4SiO_4 (De Vos *et al.*, 2006). Groundwater SiO_2 content in geothermal waters are typically high due to higher solubility of quartz at higher temperatures (Singhal and Gupta, 2010). Weathering of minerals is the primary source of Si in water. Quartz, which is the commonest and the most stable form of SiO_2, has a lower solubility than other forms of SiO_2, e.g., opal or chalcedony (De Vos *et al.*, 2006).

Silicates and other “insoluble rocks” are also soluble to some degree under certain chemical conditions and yield the minor or trace constituents in groundwater (Tóth, 1999). Groundwater in recharge area of igneous rocks dissolved very little mineral matter due to relative insolubility of rock composition, where mostly silica is added to groundwater (Todd and Mays, 2005).

HCO_3^- derives mainly from the soil zone CO_2 at the time of weathering of minerals of the parent rocks. Soil zone contains elevated CO_2 pressure due to the decay of organic matter and root respiration, and forms with rainwater the H_2CO_3 (Subba Rao and Surya Rao, 2010):

$$\text{(cations)(silicates)} + H_2CO_3 \rightarrow H_4SiO_4 + HCO_3^- + \text{cations} + \text{clay minerals.} \qquad (16)$$

Concentrations of Si in fresh water range typically from 1 to 30 mg/L (Hem, 1970; Todd and Mays, 2005) and higher in groundwater from deeper aquifers due to longer residence time (Cox, 2003). Low silicate concentrations are observed in stream water (<3.5 mg/L) found over the central Alps, Slovenia and W Croatia (De Vos *et al.*, 2006). In groundwater silica concentration also strongly depends on adsorption of dissolved silica onto clay minerals as well as neoformation of (secondary) silicate minerals (mainly clay minerals).

There is no maximum permitted level for drinking water purposes for Si according to Rules on drinking water (2004).

2.3.2.8. General sodium (Na^+) geochemistry

Sodium is one of the alkali metals like Li, K, Rb, and Cs. The most common minerals containing sodium are evaporates (NaCl), silicate minerals (feldspars albite and nepheline), clay minerals (Na-mica), carbonates, sulphates and rarly phosphates, nitrates, and borates (De Vos *et al.*, 2006). Other natural sodium sources are maritime precipitation and sea spray, hot springs, and brines (Hounslow, 1995). In addition sodium commonly results from an ion exchange process, when groundwater flows through clay-bearing aquifer (usually montmorillonite). Ca^{2+} ions typically replace Na^+ from the surface of clay minerals which causes groundwater Ca^{2+} concentration to decrease, and Na^+ to increase (Drever, 1982; Hounslow, 1995):

$$2\text{Na-clay} + Ca^{2+} \rightarrow \text{Ca-clay} + Na^+. \qquad (17)$$

This exchange causes higher Na^+ concentrations and softer water (decreased Ca^{2+} and Mg^{2+} concentrations) (Hounslow, 1995) and is controlled naturally or anthropogenically (by applying gypsum). Reverse effect is less common (Hem, 1970). Anthropogenic sources of sodium include waste disposal and landfill sites (Hounslow, 1995; Hem, 1985; Todd and Mays, 2005), pumping of fresh water from coastal aquifers (intrusion of saline water), application of salts (NaCl) for deicing roads, and use of soaps (Alley, 1993; De Vos *et al.*, 2006).

Sodium in water is very soluble and mobile, and can have in natural waters a wide range of concentrations (Jordana and Batista, 2004). Generally less than 200 mg/L of Na^+ is found in natural waters (Hounslow, 1995; Hem, 1985; Todd and Mays, 2005). Rainwater contains about 1 mg/L and brines higher than 100 g/L of Na^+ (De Vos *et al.*, 2006).

The allowed maximum permitted level for drinking water purposes is 200 mg/L of Na^+ in water (Rules on drinking water, 2004).

2.3.2.9. General chloride (Cl^-) geochemistry

Chloride is very mobile and is not affected by the pH or redox conditions (Hem, 1970; De Vos *et al.*, 2006). Chloride does not form insoluble salts (except at extreme salinities) and is strongly adsorbed on mineral surfaces (Hem, 1970). Most chloride in groundwater is present as NaCl and KCl, and chloride concentration may exceed the sodium due to base-exchange phenomena. Calcium and magnesium chloride waters are rare (Karanth, 1987). Chloride salts are highly soluble and very mobile, and are widely used as tracers, because they do not react with minerals of aquifer rocks once they enter the solution. High salty water can cause corrosion of metals.

Chloride is present in various rock types in very low concentration. Chloride-bearing minerals are found in igneous rocks (sodalite and apatite), in metamorphic rocks, and in sedimentary rocks (evaporates) (Hem, 1970; De Vos *et al.*, 2006). Besides weathering of rocks, minerals and soil, the natural sources of chloride are associated with thermal water reservoirs, atmospheric deposition (sea spray and maritime precipitation), natural saline groundwater, and volcanic activity (Mullaney *et al.*, 2009). The common anthropogenic sources of chloride are use of salt for deicing paved surfaces, oil- and gas-field brines, leaching from municipal landfills, the treatment of drinking water and wastewater, discharge of wastewater from treatment facilities or septic systems (sewage), from animal feeds (and manure), use of agricultural products (pesticides and fertilizers), irrigation from deep groundwater sources (Mullaney *et al.*, 2009), improper drilling of wells between fresh and saline water aquifers (Richtef and Kreitler, 1992), and intensive pumping of fresh water near the coast (Richtef and Kreitler, 1992; De Vos *et al.*, 2006).

Common Cl^- concentrations in natural waters are less than 10 mg/L in humid regions, and higher in more arid areas (Hounslow, 1995; Hem, 1985; Todd and Mays, 2005). The allowed maximum permitted level for drinking water purposes is 250 mg/L of Cl^- in water (Rules on drinking water, 2004).

2.3.2.10. General nitrogen (NO_3^-) geochemistry

The natural sources of NO_3^- are found in the atmosphere, soil, rocks, legumes, and plant debris (Widory *et al.*, 2004). Nitrogen minerals are rarely found in the nature; in metamorphic and igneous rocks they occur as trace constituents in the form of NH_4^+, and in sediments and sedimentary rocks as NH_3^+ (Wedepohl, 1978). Because they are readily soluble, minerals with nitrogen as a major constituent are rare (De Vos *et al.*, 2006). Anthropogenic sources of nitrate are found in wastewater treatment effluent (municipal or industrial sludge), landfills, septic tank systems, animal manure (hog, cattle, and poultry), agrochemicals (nitrogen fertilizers: commercial or livestock waste) (Hounslow, 1995), nitrogen oxides emitted by the combustion of fossil fuels in power stations and also from vehicles (Hem, 1985).

In water nitrogen occurs as nitrate (NO_3^-), nitrite (NO_2^-), nitrogen gas (N_2), ammonium (NH_4^+), ammonia (NH_3), dissolved organic nitrogen (DON), and in particulate form, which is usually organic, but may contain inorganic nitrogen. These species depend on the pH, redox conditions, and temperature. Under aerobic (oxic) conditions NO_3^- dominates, and under redox (anoxic) conditions NH_4^+.

The primary source is nitrogen gas (N_2) which is converted to (organic nitrogen (NO_3^-) by some plant species (nitrogen fixation) Fig. 12). The decay of plant and animal material is decomposed from organic compounds to inorganic ammonium salts by microorganisms (ammonification) which transfers NH_4^+ to NO_2^- and NO_3^- (nitrification) (Hounslow, 1995). Because NO_3^- is highly mobile and is not strongly absorbed it freely moves through the aquifer and is highly susceptible to leaching through the soil; also if excess fertilizer nitrogen is present in the soil, or the soil is overirrigated (Alley, 1993). This is because NO_3^- is a negatively charges ion, and since soil particles are also negatively charged, there is very little adsorption, and NO_3^- is easily transported through the soil horizon by the infiltrating waste water and rain water. Once in groundwater NO_3^- continues to move unimpeded, generally migration concurrently in the direction and velocity of the groundwater itself (Taylor, 2003).

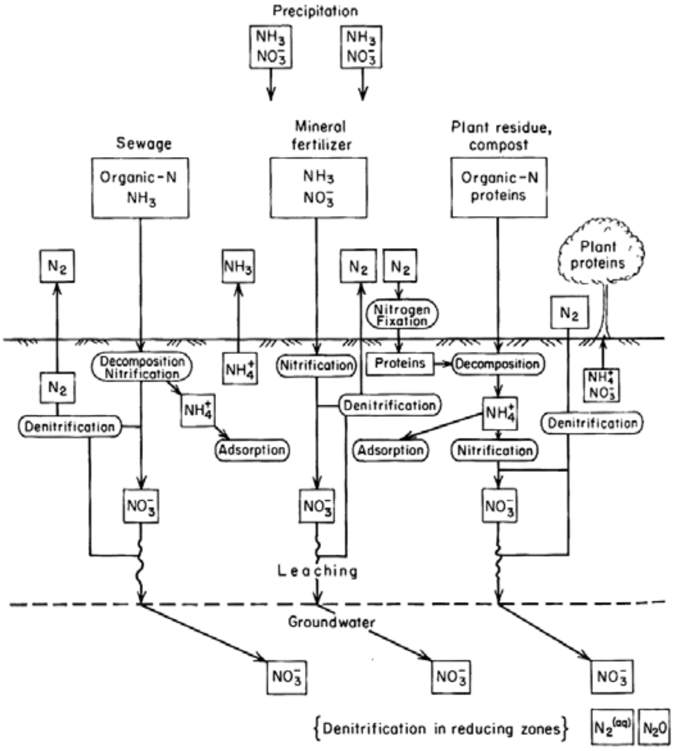

Figure 12: Sources and pathways of nitrogen from the atmosphere, biosphere, soil systems, and hydrosphere (Freeze and Cherry, 1979)

Denitrification is the reduction of NO_3^- to N_2 gas which is released to the atmosphere. This usually occurs under anaerobic conditions (closed aquifers), if organic carbon is available. Groundwater that is rich in oxygen and lacking in carbon is not likely to have any significant denitrification occurring. On the other hand, deeper anoxic groundwater zones or shallow groundwater entering organic rich riparian buffer zones may have substantial denitrification (Taylor, 2003). More details about the nitrogen cycle is found in Stumm and Morgan (1996) and others.

Natural NO_3^- concentrations in groundwater are generally up to 10 mg/L NO_3^- (Todd and Mays, 2005; Cushing *et al.*, 1973) with natural background of 0.1 mg/L (Nolan, 2003). In Ljubljana field aquifer the natural background was estimated between 1.7 to 5.6 mg/L NO_3^- (Bračič-Železnik, 2005). Higher natural concentrations (100—400 mg/L) are observed in groundwater from organic-rich shales in Canada and USA (Quevauviller *et al.*, 2009), or groundwater associated with leguminous vegetation (Edmunds and Gaye, 1997). In Slovenia no such high natural groundwater NO_3^- concentrations have been reported, and groundwater nitrate is washed from unfertilized vegetation cover into the aquifer, does not exceed the maximum allowable concentration for nitrate in the drinking water (50 mg/L) Pintar (1993). Increased NO_3^- concentrations may indicate contamination of anthropogenic origin (Hounslow, 1995; Hem, 1985), which is mostly due to use of artificial or natural fertilizers, leakage of sewage systems and cesspools, contamination from the surface water, traffic and the atmosphere.

The most common maximum concentration allowed in drinking water for NO_3^- is 50 mg/L (11.3 mg/L NO_3^--N), also in Slovenia (Rules on drinking water, 2004).

2.3.2.11. General ammonium (NH_4^+) geochemistry

Ammonium may occur naturally at low concentrations in many anaerobic groundwaters. High ammonium concentrations may be found in waters from ultrabasic rocks and thermal springs. The anthropogenic sources are found in application of inorganic fertilizers and manure, leakage from sewage or septic tanks, and landfills, which are associated with anaerobic conditions (Quevauviller *et al.*, 2009).

The maximum permitted level for drinking water purposes is 0.5 mg/L of NH_4^+ in water (Rules on drinking water, 2004).

2.3.2.12. General potassium (K^+) geochemistry

Potassium is one of alkali metals (together with Li, Na, Sc, and Rb) and a major constituent of many rock-forming minerals: silicate minerals (alkali feldspar (orthoclase and microcline), leucit, biotite, muscovite, phlogopice, and some amphiboles), phosphate, halide, sulphate minerals, and evaporate deposits (e.g. sylvite). Potassium is a major constituent in many igneous rocks, and argillaceous sediments and shales (illite shales). In carbonate rock potassium is present as detrital silicate material (clay) in the non-carbonate fraction. In the sand, sandstone, and non-detrital siliceous sediments potassium occurs as K-feldspar, K-mica, and glauconite. Potassium ion is very mobile but is readily incorporated into clay-mineral lattices, and is readily taken up by plants for growth (De Vos *et al.*, 2006). Potassium is also found in the sea water (Hem, 1970). Potash fertilizers (agrochemical or organic) are the main anthropogenic source of potassium (KCl, K_2SO_4, KNO_3) (De Vos *et al.*, 2006). Important source of potassium is also surface water used for irrigation (Ramesh and Jagadeeswari, 2012). Many potassium salts are important for chemical and medicinal applications (e.g. nitrate, carbonate, chloride, bromide, …) (De Vos *et al.*, 2006)

Generally less than 10 mg/L of potassium in natural waters is common (Hounslow, 1995; Hem, 1985; Todd and Mays, 2005; Jordana and Batista, 2004). Concentrations exceeding a few tens of mg/ L are unusual, except in water with high dissolved solids content, or water from hydrothermal systems; e.g. sea water contains on average 390 mg/L K^+ (Hem, 1985). There is no maximum permitted level for drinking water purposes for K^+ according to Rules on drinking water (2004).

2.3.2.13. General sulphate (SO_4^{2-}) geochemistry

The dominant sulphur species in most natural environments, which depend on the pH and redox conditions, are sulphate (SO_4^{2-}) and sulphide (S^{2-}). Natural sources of sulphate in groundwater are found in very soluble evaporate rocks (gypsum, anhydrite, and epsomite) (De Vos *et al.*, 2006), and less soluble barite and celestine (Hem, 1970). Major source of sulphate is also pyrite found in sulphide ore deposits, which is commonly associated with strongly reducing conditions from organic sulphur compounds (coal, petroleum). Sulphur is also found in the silicate minerals, e.g. feldspar, mica, pyroxene, and sodalite and non-silicate apatite (De Vos *et al.*, 2006). Sulphur may be also emitted by volcanoes, fumaroles and springs, and the solution of dust particles. Particles of sea salt are also an important source of atmospheric sulphate (Hem, 1970). High groundwater SO_4^{2-} concentrations can be associated with geothermal waters (Hounslow, 1995; Hem, 1970). Anthropogenic sources of SO_4^{2-} include mining and smelting operations, application of agrochemicals, coal processing activities (Quevauviller *et al.*, 2009), combustion of fuel (Hem, 1970), wastes from industries, and vulcanisation of rubber (De Vos *et al.*, 2006).

The natural concentration of SO_4^{2-} in waters less than 300 mg/L is common (Hounslow, 1995; Hem, 1985; Todd and Mays, 2005) and in rainfall up to 10 mg/L (Hem, 1970). The maximum permitted level for drinking water purposes is 250 mg/L of SO_4^{2-} in water (Rules on drinking water, 2004).

2.3.3. Trace constituents

Trace elements are generally present in small concentrations in natural water system. They are detectable in groundwater from 0.0001 to 0.1 mg/L (Al, As, Ba, Br, Cd, Cr, Co, Cu, Ge, I, Li, Mn, Mo, Ni, P, Pb, Rb, Sb, Se, Ti, U, V and Zn), or less than 0.001 mg/L (Ag, Au, Be, Bi, Ce, Cs, Ga, In, La, Nb, Pt, Ra, Ru, Sc, Tl, Th, Sn, W, Yb, Y, and Zr) (Harter, 2003).

2.3.3.1. Iron (Fe) in groundwater

Iron is found in igneous rocks (amphiboles, ferromagnesian micas, ferrous sulphide, ferric sulphide or iron pyrite, and magnetite), and in sandstone rocks (oxides, carbonates, and sulphides or iron clay minerals) (Todd and Mays, 2005). The solubility of iron is strongly redox and pH controlled. In reducing environments the oxygen content drops and increases the solubility of some elements (e.g. iron, manganese, sulphur) (Nelson, 2002). The causes for reducing reactions are from organic matter either as natural or anthropogenic sources. Low iron concentrations can be explained by the oxidation of Fe^{2+} under the oxygen conditions in aquifer followed by the precipitation as iron oxyhydroxides. The dissolution of iron from silicate minerals is a slow process normally, but shallow weathering of iron-bearing minerals may produce accumulation of ferric oxide or hydroxide (Hem, 1970). Anthropogenic sources of iron include the iron and steel industry, sewage and dust from iron mining (Reimann and de Caritat, 1998). Iron sulphate is also used as a fertiliser and herbicide (Reimann *et al.* 2003). Concentrations range generally less than 0.5 mg/L (in fully aerated water) and rarely as much as 50 mg/L ($pH < 8.0$) (Todd and Mays, 2005).

The maximum permitted level for drinking water purposes is 200 µg/L of Fe in water (Rules on drinking water, 2004).

2.3.3.2. Manganese (Mn) in groundwater

Iron is often accompanied by Mn which remains longer in solution under oxidising conditions, whereas iron oxidises and precipitates (Hem, 1970). Manganese is found in metamorphic and sedimentary rocks and mica biotite and amphibole hornblende minerals (Todd and Mays, 2005). Other natural atmospheric sources of manganese include ocean spray, forest fires, vegetation, and volcanic activity. The major anthropogenic sources of environmental manganese include municipal wastewater discharges, sewage sludge, mining and mineral processing, emissions from alloy, steel, and iron production, combustion of fossil fuels, and, to a much lesser extent, emissions from the combustion of fuel additives. Manganese depends on the pH and redox conditions (CIDAD, 2004). The concentration in natural water is usually less than 0.20 mg/L (rarely 10 mg/L) (Todd and Mays, 2005).

The maximum permitted level for drinking water purposes is 50 µg/L of Mn in water (Rules on drinking water, 2004).

2.3.3.3. Chromium (Cr) in groundwater

Chromium is found in minerals like chromite, magnetite, ilmenite, pyroxene, amphibole and mica. Chromium has a low mobility, especially under moderately oxidising and reducing conditions and near neutral pH. Its mobility in soil depends on the pH, Eh, and organic matter. Anthropogenic sources of chromium are found in industry production (steel production, leather tanning, and electroplating operations) (De Vos *et al.*, 2006).

Concentrations of Cr in uncontaminated natural water are typically less than 10 µg/L (Hem, 1985). The maximum permitted level for drinking water purposes for Cr is 50 µg/L (Rules on drinking water, 2004).

2.4. Data analysis techniques

2.4.1. Statistical methods

In order to understand the chemical and isotopic composition of sampled groundwater and their mutual correlations or dependences, the basic statistics/tables (BS), bivariate methods (e.g. correlations), and multivariate methods (i.g. factor and cluster analysis) were used. All statistical analyses were performed in the statistical software STATISTICA 6.1 (StatSoft, 2013).

2.4.1.1. Descriptive statistics and normality of distribution

Statistical normality of elemental distribution is estimated based on frequency tables and visually with the examination of shapes of histograms of either natural or transformed variables. This is performed by the observations of measures of location (comparison of mean, geometric mean, median, etc.), measures of spread (standard deviation) and measure of shape (tests of skewness and kurtosis, and the coefficient of variation) (Helsel and Hirsch, 1992).

The mean (X) is the arithmetic average defined as the sum of all observations divided by the number of observations. The geometric mean (X_G) is the n^{th} root of the product of the n observations and can be applied only to data of positive values. The median (Md) is the value midway in the frequency distribution. The standard deviation (S) is the square root of the variance. The standard error of mean (S_x) is the standard deviation of the sampling distribution of the sample mean and is given by the square root of the sample size (Davis, 2002).

The most commonly used statistic for summarizing the distribution symmetry is the coefficient of skewness (A). The distribution of the data set is symmetrical when it looks the same to the left and right of the center point. The normal distribution has skewness=0, negatively skewed to the left distribution has skewness <0, and positively skewed to the right has skewness >0. The coefficient of kurtosis (E) is a measure of peakedness/flatness in the variable distribution. If it is platykurtic, the distribution has a low degree of peakedness (kurtosis<0), if the distribution is mesokurtic, distribution is normal (kurtosis = 0), and leptokurtic distribution has a high degree of peakedness (kurtosis>0) (Helsel and Hirsch, 1992; MedCalc, 2013, StatSoft, 2013). The histogram is an effective graphical technique for showing both the skewness and kurtosis of data set (MedCalc, 2013; StatSoft, 2013). Coefficient of variation (C_v) is a normalized measure of dispersion of a probability distribution and is expressed as a function of mean $C_v=S/X$ (Davis *et al.*, 2002; MedCalc, 2013; StatSoft, 2013).

The Kolmogorov-Smirnov test (KS) is a non-parametric test that tries to determine if two datasets differ significantly by comparing their distribution. There are one-dimensional probability distributions that can be used to compare a sample with a reference probability distribution (one-sample K–S test), or to compare two samples (two-sample K–S test). The Kolmogorov–Smirnov test can be used to test the goodness of fit (Davis, 2002). Shapiro-Wilk test (W) is the preferred test of normality because of its good power properties as compared to a wide range of alternative tests (Shapiro, Wilk, and Chen, 1968; StatSoft, 2013). If the p value is less than or equal to 0.05 the test rejects the hypothesis of normality, and failing the normality test allows you to state with 95 % confidence the data does not fit the normal distribution. If the value is greater than 0.05, the test passes the normality test only allows you to state no significant departure from normality was found (Laerd Statistics, 2013). The Chi-Square test ($\chi 2$) is a statistical test commonly used to investigate the degree of fit between the frequency of occurrence of observations in an observed sample and the expected frequencies that are obtained from a hypothesized distribution (Huang *et al.*, 2008).

Data transformation

Many environmental variables are not normally distributed, therefore a data transformation (i.e. normalisation) is required. Common transformations are log or square root (Long *et al.*, 1997; Verbovšek, 2006, 2011b; Cukrov *et al.*, 2009).

2.4.1.2. *Multivariate statistical methods*

Multivariate analyses allow us to consider two or more variables at the same time, which enables us to study more complex interactions between observed variables (Davis, 2002). Three multivariate statistical methods were applied on the dataset to classify groundwater samples and to identify geochemical processes controlling groundwater geochemistry.

Bivariate statistical method (correlations)

Correlations refer to statistical relationship between two or more variables. Measure of the correlation between two variables is expressed by correlation coefficient. The most common is Pearson correlation coefficient (r) which is mainly sensitive to a linear relationship between two variables. If correlation r=+1, then the scatterplot will be a straight line with a positive slope; if r=-1, then the scatterplot will be a straight line with a negative slope. For |r|<1 the scatterplot appears as a cloud of points that becomes more diffuse as |r| decreases from 1 to 0 (Le Maitre, 1982; Bajpayee *et al.*, 2012). The Spearman rank correlation (r_s), which is used for ordinal data, is a nonparametric analogue to the standard correlation coefficient. Spearman's r is computed by replacing the individual values for each variable with their respective ranks and then computing a correlation coefficient (r) using the ranks, rather than the original data (Hensell and Hirsch, 1992; Davis, 2002; Gauthier, 2001).

Interpretation of the Spearman's rank order correlation coefficients used in this study is as follows: r_s=1 to 0.70 (strong association), r_s=0.69 to 0.50 (moderate association), and r_s=0.49 to 0.30 (weak association).

Factor analysis (FA)

Factor analysis (FA) is a method which is used to simplify the quantitative description of multivariate observations by determining the minimum number of new variables - factors (Le Maitre, 1982). The procedure reduces the original data matrix from one having n variables necessary to describe the N samples to a matrix with m factors (m<n) for each of the N samples (Davis, 2002; Johnston, 1980). Factor analysis is always done with standardized data so that individual variables have equal weight in their influence on the underlying variance-covariance structure (Glover *et al.*, 2005). High factor loadings are considered those above 0.75, medium ones those which lie between 0.50 and 0.75, and weak those between 0.40 and 0.50 (Panda *et al.*, 2006). The variables used in the analysis produce different variances called eigenvalues, which give a measure of the significance of the factor – the most significant factors are the one with the highest eigenvalues. Eigenvalues of 1.0 or greater are considered significant (Kim and Mueller, 1978). Each factor joins separate variables and finally correlates them directly or indirectly with a common process. Initial data is standardised in order to eliminate the influence of different units. Factor loadings are optimized with varimax rotation method which preserves the orthogonality of factor axes (Davis, 2002). Meaning that each original variable tends to be associated with one (or a small number) of factors, and each factor represents only a small number of variables (Abdi, 2003).

Cluster analysis (CA)

Cluster analysis is a technique designed to perform classification by assigning observations into relatively homogeneous groups or clusters. Variables within a cluster are similar to each other but different from those in other clusters. The result of clustering is a dendrogram which provides a visual summary of clustering process, and similarity levels at which groupings change. Known are several cluster techniques which are based on agglomeration of more elements according to their composition, giving different results: partitioning methods, arbitrary origin methods, mutual similarity procedures, and hierarchical clustering (Davis, 2002). The hierarchical clustering joins the most similar pair of variables and forms higher clusters step by step (Davis, 2002). One of the approaches is that the initial cluster is formed by linkage of two samples with the greatest similarity. Widely used linkage rule is Ward's method which uses an analysis of variance (ANOVA) approach to evaluate the distances between clusters, attempting to minimize the sum of squares at any two (hypothetical) clusters that can be formed at each step. The squared Euclidean distance usually gives the similarities between two samples and a distance can be represented by the "difference" between analytical values from both samples (Ramesh and Riyazuddin, 2008; StatSoft, Inc. 2006; Romesburg, 2004; Eriksson, 1985).

2.4.2. PHREEQC

In the programme PHREEQC a simulation of a variety of reactions and processes of aqueous geochemical calculations is performed. This programme is based on an ion-association aqueous model and has capabilities for speciation and saturation-index calculations, reaction-path and advective transport calculations involving specified irreversible reactions, mixing of solutions and more (Appelo and Postma, 2005; Parkhurst and Appelo, 1999).

2.4.3. AquaChem

The graphical and numerical analyses of geochemical data sets were performed in AquaChem®5.1. The programme features a powerful database that can be customized and configured to include an unlimited number of attributes per sample and a built-in database of inorganic chemicals that are commonly used for geochemical analyses, calculations and plotting (AquaChem, 2006).

In AquaChem the ion pattern was defined according to the concentration of the dominant dissolved species measured in groundwater. For the hydrogeochemical facies determination, definitions according to Back (1961) based on the hydrochemical trilinear Piper diagram (Piper, 1944) were used (Domenico and Schwartz, 1990). The diagram displays the relative concentrations of the major cations on the left triangular diagram (Ca^{2+}, Mg^{2+}, Na^{+} + K^{+}) and anions on the right triangular diagram (HCO_3^-, Cl^-, and SO_4^{2-}) on two separate trilinear plots, together with a central diamond plot, where the points from two trilinear plots are projected. The central diamond shaped plot is used to present the overall chemical character of the sampled water (Hill, 1940; Piper, 1944).

Additionally the saturation indices (SI) for calcite and dolomite in groundwater (Langmuir, 1997) were calculated in order to determine the saturation state of a mineral with respect to a given water composition. The saturation index is defined as:

$$SI = \log (IAP/K_t) \tag{18}$$

If the saturation index is less than zero, the mineral is unsaturated with respect to the solution and the mineral might dissolve very slowly or not at all, depending on the kinetics of the reaction. If the saturation index is greater than zero, the mineral might precipitate but cannot dissolve. If the saturation index is close to zero, the mineral may not be reacting at all or may be reacting reversibly, in which case the mineral could be dissolving or precipitating (Appelo and Postma, 2005). Since SI is the logarithmic quotient, a value of 1 signifies a ten-fold supersaturation and a value of -2 a hundred-fold undersaturation in relation to a certain mineral phase (Merkel and Friedrich, 2002).

2.4.4. ArcMap

Spatial data are analysed in ArcMap, which is the main component of Esri's ArcGIS (GIS – Geographical Information System) suite of geospatial processing programs, and is used primarily to view, edit, create, and analyze geospatial data. With ArcMap we explore data within a data set, symbolize features accordingly, and create hydrochemical maps of different parameters for the entire research area (spatial distribution) (Esri Inc., 2001).

3. MATERIALS AND METHODS

This section covers description of the study area and its natural caracteristics and land use. Additionally the emphasis is given on the selection of sampling locations as well as on the selection of hydrochemical parameters analysed in groundwater.

3.1. Description of the study area

The study area is Slovenia, covering around 20,273 km^2, with its very diverse geomorphologic, geological, pedological, hydrological and climatic characteristics.

3.1.1. Geographical description of study area

Slovenia is located at the junction of four major European relief units – the Alps, the Dinaric Alps, the Pannonian Basin and the Adriatic Sea basin (Appendix 1). Altitude changes from the sea level (0 m a.s.l.) and up to the altitude of 2,864 m (Mt. Triglav). Only 7 % of the surface of Slovenia lies below 200 m a.s.l., 45 % between 200 m and 500 m a.s.l., 36 % between 500 m and 1,000 m a.s.l., and 9 % between 1,000 m and 1,500 m a.s.l. Approx. 3 % of the territory is higher than 1,500 m (Frantar *et al.*, 2008). Several types of morphology can be found. Plains are formed by accumulation of sediments of major rivers with altitude ranging up to 400 m. In the hills (up to 1,000 m a.s.l) in eastern and central Slovenia erosion processes dominate. In the mountains of northern Slovenia, peaks and ridges reach up to and above the forest line (above 1,700 m a.s.l.) (Fridl *et al.*, 1998).

3.1.2. Geological description of study area

The Slovenian territory is a site of complex geological processes from the Paleozoic era to the present, with all main types of rocks present: sedimentary, metamorphic and igneous (Appendix 2). By far the most abundant are sedimentary rocks that make up the greatest part (around 93 %) of the Slovenian territory. Among the sedimentary rocks, Mesozoic to Paleocene carbonate rocks (limestone and dolomite) are characteristic, especially for the southern and north-western parts of the country (Julian Alps, Kamnik-Savinja Alps, Karavanke Mts., high Dinaric Karst, low Karst of Dolenjska, low karst plain of Bela krajina, and Kras) (Javornik *et al.*, 1989; Buser, 2010). Karst covers almost half of the Slovenian surface (Gams, 1974) where 35 % is on limestone and about 8 % on dolomite (Orožen Adamič, 2004). Permo-Carboniferous clastic sediments (shale, quartz sandstone and conglomerate) are found in the central part of the country (Posavje Hills), the Paleogene flysch rocks in south-western Slovenia (Istria and Gorica), and Neogene clastic sediments (sandstone, marl, and siltstone) in eastern and central parts of Slovenia). Quaternary clastic sediments (around 10 %), such as gravel and sand, cover river basins from the central part to the north-eastern territory of the country (e.g. the basins of tectonic origin such as Ljubljana and Celje basins and Krško-Brežice basin) (Javornik *et al.*, 1989; Buser, 2010). Along the Drava and Mura rivers in the north-western part of the country there are also wide valleys covered with gravel (Frantar *et al.*, 2008) of metamorphic rocks, clayey marl, and sandy sediments (Drobne *et al.*, 1976). On karstic fields and river basins (e.g. rivers Lendava, Ščavnica, Pesnica, Dravinja, Vipava) in less erosion-resistant rocks the fine-grained clay and silty sediments have developed (Bogataj *et al.*, 2012). Igneous rocks (around 3 %) make up smaller parts of Slovenia, mainly the north-eastern and northern parts (Pohorje Mt., Kozjak Mt., Karavanke Mts.), as well as a belt across the central part of the country and Goričko hills. The central part of Pohorje Mt. is built of a large granodiorite batholit where *cizlakite*, endemic Slovenian variety of gabbro, is found. This massif continues to north-west into dacite. Igneous rocks of Pohorje Mt. and Kozjak Mt. are of Oligocene to mid-Miocene age. Furthermore, Triassic granite, syenogranite, granite-porphyry and Oligocene tonalite are found in Karavanke Mts. Small areas of igneous rocks (volcanic and volcaniclastic) can also be found in the belt through central Slovenia (areas between Gornji Grad and Smrekovec; Dramlje and Rogaška Slatina; Jelovica, Idrija hills, and Škofja Loka hills; Kamniška Bistrica and Kokra valley) where mainly mid-Triassic porphyre, keratophyre, diabase and basalt prevail. The oldest, metamorphic, rocks are not abundant in Slovenia. Paleozoic (or perhaps even Precambrian) metamorphic rocks (around 4 %) are found in smaller areas of the north-eastern and northern parts of Slovenia (Pohorje Mt., Strojna, Karavanke Mts. and Kozjak Mt.) as gneiss, schist, amphibolite, eclogite, marble, and quartzite. Also low and medium grade metamorphic rocks from early Paleozoic (phyllite and mica schist) are found north of Drava River, while high temperature metamorphic rocks are found at Pohorje Mt. where mica schist and gneiss dominate (Javornik *et al.*, 1989; Buser, 2010).

3.1.3. Types of soil

Due to its lithological and climate diversity, and roughness of the terrain, the territory of Slovenia exhibits in a small area a variety of soil types (Appendix 3). The soils are strongly linked to the types of rocks. The most widespread soil types in Slovenia are Eutric Leptosols which prevail mostly in the mountains of Alpine regions and in Karst regions (Dinaric mountains), where they interweave with Eutric Cambisols. Dystric Cambisols develop on non-carbonate rocks of the hilly and mountainous regions (Pohorje Mt., Smrekovec Mt., the Posavje hills and Škofja Loka hills) and the non-carbonate flysch of the Brkini hills. The soils are characterized by increased acidity and low nutrient content. Highly fertile variety of Eutric Cambisols cover carbonate flysch in the Mediterranean and marl in Pannonian hills as well as the hills consisting of soft carbonate rocks. Eutric Cambisols interwoven with Rendzic Leptosols also cover gravel deposits and alluvial fans as well as glacial moraines of carbonate origin. Dystric Leptosols, shallow skeletic soils with increased acidity, developed on the non-carbonate gravel and sand (Dravsko polje, Dolinsko, Ravensko), and on the non-carbonate rocks of steep slopes. Sandy or silty loamy Fluvisols are common along rivers and larger creeks. On low permeable clayey deposits with shallow groundwater table Gleysols develop. In eastern parts of Slovenia Planosols and Stagnosols form on gentle slopes, while on the southern part of Ljubljana basin peat soils or Histosols are spread. Acidic Luvisols to very acidic Acrisols occur within the area of old gravel deposits of Gorenjska, and particularly on the leached residual of carbonates (infertile acric soil) in Bela krajina. Hyperskeletic Lithosols which develop on hard carbonate rocks and Regosols which develop on the soft carbonate rocks, are found on steep slopes of high mountain ridges or hilly areas (Vrščaj *et al.*, 2005; Bernard Vukadin *et al.*, 2008). In Karst area under the submediterranean climate conditions Chromic Cambisols commonly known as Terra Rossa develop (Vrščaj *et al.*, 2005; Repe, 2010). Detailed description of soil types is written in Repe (2004, 2010).

3.1.4. Meteorological conditions

The characteristics of the climate in Slovenia are affected by the country's position in the temperate zone, the proximity of the Mediterranean sea and the Eurasian continent, and by the diversity of the relief (Frantar *et al.*, 2008).

Four major air masses types influence the weather in Slovenia (Pučnik, 1980): (1) maritime polar air masses, which originate in the Northern Atlantic and North Sea; (2) maritime tropical air masses, which originate predominantly in the Azores area; (3) continental tropical air masses, originating in northern Africa and Asia Minor; and (4) continental polar air masses, which originate in Scandinavia, Finland, Russia, and also the Pannonian Plain.

Due to its specific geographic diversity, Slovenia is influenced by several climate types. There is a mixing of: a) continental climate, which influences the majority of the country; b) Alpine climate that prevails in the high mountains in the north-western part of the country; and c) the coastal sub-Mediterranean climate that influences the south-western part of the country (Rakovec and Vrhovec, 2007). In most parts of the country, except in mountains and along the coast, a moderate, warm, humid climate prevails. The warmest month on average is July and the coldest is January, with the exception of the high mountains where the coldest month is February and warmest is August. A mean temperature in January is around -3°C, and in July around 22°C. For the south-western part of the country, a sub-mediterranean climate is typical, with a mean temperature of the coldest month above 4°C and of the warmest above 22°C. In the mountains (Julian Alps, Karavanke Mts., Kamnik-Savinja Alps, Pohorje Mt. and Snežnik Mt.) a mean temperature in the coldest month is around -3°C, and around 10°C in the warmest month (above 2,000 m under 10°C) (Fridl *et al.*, 1998; EARS, 2006).

Most precipitation in Slovenia occurs in the Alpine-Dinaric barrier (Kredarica with 3,200 mm, Vojsko and Postojna), and the quantities diminish towards the NE and EW (Appendix 4). There is more than 1,500 mm of precipitation annually in the W part of the Slovenian interior. Usually, the least annual precipitation occurs in the NE part of the country (Murska Sobota), on average below 900 mm/y. On the coast, there is an average of around 1,100 mm/y of precipitation (Portorož).The areas affected by the sub-mediterranean climate receive the most precipitation in the autumn months (Portorož, Bilje, Kredarica, Vojsko and Postojna), while areas with a more pronounced continental climate receive the most precipitation in the summer (Šmartno pri Slovenj Gradcu, Murska Sobota, and Maribor) (Frantar *et al.*, 2008).

3.1.5. Hydrological characteristics

In Slovenia all types of surface water are present. Surface waters have created a dense river network with density of 1.33 km/km^2. Hydrological network is rare only on the karst surface due to the meteoric water draining below the surface. Here the river network is limited to karstic disappearing streams. The Karst has the role of a short-term water retention area. Most surface rivers are short; more than 100 km long are only Sava, Drava, Kolpa and Savinja rivers. Most rivers (81.5 %) drain to the Black Sea, the rest belongs to the Adriatic water catchment area. The largest lake is a disappearing karst Cerknica Lake. Most natural lakes are of glacial origin; the largest are Bohinj Lake and Bled Lake. Also many small mountain lakes are found here. Slovenia lies on the northern coast of the Adriatic Sea occupying one third of the Gulf of Trieste. The length of the Slovenian coast is 46.6 km (Fridl *et al.*, 1998).

Great part of Slovene territory is characterized with aquifers which are categorized on the basis of their porosity geometry as intergranular (19.8 %), fissured (14.2 %) and karstic aquifers (33.2 %) (Drobne *et al.*, 1976; Prestor *et al.*, 2002; Brenčič, 2009), the latter ones usually being combined in one category defined as karstic-fissured aquifers (Brenčič, 2009) (Appendix 5). Karst porosity is typical for the layers of limestone and partly dolomite, and fractured porosity is characteristics for dolomites (Uhan and Krajnc, 2003; Kranjc, 1995). Areas without important quantities of groundwater are rare and they are found in less permeable areas (flysch rocks, sandstones, marls, metamorphic schists) (Drobne *et al.*, 1976; Prestor *et al.*, 2001; Brenčič, 2009), and have usually fractured porosity (Uhan and Krajnc, 2003).

Groundwater in large intergranular aquifers on Quaternary and/or Pliocene alluvial plains is related to the balance and hydrodynamics of large rivers which are usually located inside larger pull-apart tectonic depressions. Along the rivers Drava and Mura we find the Pomurje aquifer system, the Drava River plain and Ptuj plain aquifer system, and along the rivers Savinja and Sava the lower Savinja valley aquifer, the Ljubljana plain aquifer system, the Krško-Brežice plain aquifer system, and along rivers Vipava and Soča the aquifer of Gorica. In the area of Goričko hills and the southern part of the Slovenske gorice hills, two other systems are present in the Tertiary sediments up to the lower part of the Quaternary intergranular aquifers. Those shallow alluvial aquifers are recharged mainly from precipitation and by infiltration of water into the ground from rivers and streams (Uhan and Krajnc, 2003). For an example, several intergranular Quaternary aquifers are connected by a water balance and cross groundwater flow with other aquifers (e.g. Pomurje and Krško-Brežice plain aquifer systems with lower-lying Tertiary sediments; Ljubljansko polje and Ljubljansko barje aquifer systems), are recharged with river water (Drava, Mura, Sava, Kokra, Savinja, Vipava, Soča rivers), and/or surface water from surrounding areas (e.g. Pohorje Mt., Krakovski gozd, Kamnik-Savinja Alps) (Brenčič, 2009). Quaternary intergranular aquifers are represented by high yield and high hydraulic conductivity, where the range of $5x10^{-3}$ m/s to $1x10^{-5}$ m/s is predominant (Prestor *et al.*, 2001). The amount of dynamic groundwater reserves in intergranular aquifers is appr. 18.3 m^3/s and presents about 36.8 % reserves (Kranjc, 1995). Since shallow intergranular aquifers in Slovenia are situated in flat river valleys, they are attracted to intense human activities, e.g. agriculture, industry, trade, traffic infrastructure, and high population density. Although the vadose zone of aquifer's intergranular porosity acts as filter for many pollutants, groundwater is still highly vulnerable and affected by those activities (Krajnc *et al.*, 2007).

Karstic-fissured aquifers are strongly anisotropic with mainly one direction emphasized. Hydraulic conductivities and transmissivities are distributed within several orders of magnitude. These aquifers are significant for the appearance of big karstic springs and are found in the central, southern and north-western parts of the country (regions of Suha krajina, Kočevski Rog, Dolenjska and Gorjanci). Large karstic-fissured aquifers are also present in mountainous regions (the Julian Alps, Kamnik-Savinja Alps and Karavanke Mts.) (Brenčič, 2009). The hydraulic conductivity coefficient ranges from 10^{-1} m/s for intensively karstified and fissured rocks to up to 10^{-11} m/s for massive limestones and dolomites (Prestor *et al.*, 2001). Dynamic groundwater reserves in karstic-fissured aquifers, which are related to the amount of precipitation (Uhan and Krajnc, 2003), are appr. 31 m^3/s and store around 62 % dynamics reserves of groundwater in Slovenia (Krajnc, 1995). In the recharge areas of aquifers with karstic and fractured porosity groundwater is naturally protected with forests, and human activities are less intense compared to river valleys. Still wide channels enable high groundwater flow and rapid long distance transport of pollutants (Krajnc *et al.*, 2007).

Slovenian groundwater serves as a drinking water to more than 97 % of population where around 60 % of drinking water originates from alluvial (intergranualr) aquifers while 40 % from aquifers with karstic and fractured porosity (Krajnc *et al.*, 2007).

For water management in accordance to the European legislation, the Slovenian territory is divided into 165 aquifer systems combined into 21 groundwater bodies (Mali, 2008; Prestor *et al.*, 2006).

3.1.6. Land cover and land use

Land use reflects a complex relation between natural and socio-economic factors. Among the most important are morphology, which is reflected in altitude, slopes and hill side insolation, and others are colonisation, economic conditions in the past and present, and land-possession relations (Fridl *et al.*, 1998). Forests cover more than half of Slovenia's territory and are found in the Dinaric region of S and SE Slovenia, and in the Alpine region of N and W Slovenia. Agricultural land prevails mostly in the Pannonian and Coastal region, where cultivated fields, orchards, and vineyards are very common (Bernard Vukadin *et al.*, 2008). Meadows are more common on the east compared to west side of the country, and pastures are found in Coastal and Alpine regions (Fridl *et al.*, 1998). Dispersed urbanization is characteristic of Slovenia where urban areas are found mostly at the bottoms of the basins. Less land is covered with water and irrigated areas (Bernard Vukadin *et al.*, 2008).

For the purposes of this study two land cover/use digital databases were used. First, CORINE (COoRdinating of INformation on the Environment) Land Cover (CLC) methodology by the Ministry of the Environment and Spatial Planning, Environmental Agency of the Republic of Slovenia, Surveying and Mapping, Authority of the Republic of Slovenia, European Environment Agency (2003) at the scale 1:100,000. This database was created on the basis of satellite photographs from year 2000 (Petek, 2004). Detailed description is found in Skumavec and Šabić (2005). Complete CORINE Land Cover map is not included because of its detailed data presentation. A legend is included in the Appendix 6.

Second, Actual agricultural and forest land usage map by the Ministry of Agriculture and the Environment (2011) at scale 1:1,000. The source were the digital orthophoto maps based on black-and-white aerial photographs (1996-2001), later also with the use of other records that improved the information on the type of the actual land use and through field visits and measurements. Map was developed in accordance to Rules on evidence of actual agricultural and forestal land use (2006). The interpretative keys (Ministry for Agriculture and the Environment, 2013ab) are used which contain coding of actual use, instructions for data entry, description of certain types of actual usage and minimum area of individual types of actual usage. Original database dates into 2002 with several updates by the Ministry of agriculture and forestry (Ministry of Agriculture and the Environment, 2012b). Complete Actual agricultural and forest land usage map is not included because of its detailed data presentation. A legend is included in the Appendix 7.

According to some users (Rikanovič, 2003) both databases have certain advantages as well as disadvantages, and the usage itself depends highly on the purpose and area of the study. The main advantage of the CLC database is that all the land use categories are presented equally, there are only few technical errors, and comparisons between different countries are possible. The main advantage of the Actual agricultural land use map is detailed information on agricultural land use.

3.2. Sampling design

Since the territory of Slovenia is very heterogeneous, composed of sedimentary, metamorphic and igneous rocks, diverse hydrological conditions in different types of aquifers are present, as well as very heterogeneous chemical and isotopic groundwater composition. Therefore the sampling network was created with methodology, which could provide objectivity and transparency, in a way that all the sampling locations were representative of the main aquifer porosity types, defined by the aquifer's most representative surface lithological and lithostratigraphic units found in Slovenia.

The priority was put on those sampling locations in which recharge areas of mainly one lithological/lithostratigraphic unit prevails (are mostly pure/homogenous). Some sampling locations were chosen based on their unique lithologies (flysch) which are representative for the country. Sampling network design consists of sampling locations which are quite evenly distributed throughout the whole Slovenian area, and include important water sources of particular regions (Rižana, Težka voda, Zadlaščica, Domžale water pumping station, Skorba pumping station). The sampling locations were also chosen based on conceptual models of individual groundwater bodies (Prestor *et al.*, 2006).

Three sampling campaigns were performed from year 2009 to 2011. The focus was mostly on the groundwater in the shallow aquifers and not on the thermal or mineral water from deep aquifers. Sampling locations represent springs, observation objects (boreholes, piezometers or wells), private wells and public water supply wells (pumping stations), water catchments and surface waters. The last ones were sampled where access to spring water was not possible.

Sampling was performed during hydrological conditions of base flow, which means the groundwater flow was permanent, and when it did not rain. The 3-year sampling covered three annual season cycles in the way that groundwater at each sampling location was sampled twice, in spring (March-July) and in autumn (August-November).

Water samples were collected from total 87 sampling locations (Appendix 8) from springs (51), piezometers or wells (5), private wells (4), public water supply wells (18), and surface waters (9).

In 2009, during second sampling period in autumn, the priority for sampling was on sampling locations in high mountains region in order to sample before fallen snow. Therefore, due to lack of time, the groundwater sampling for few sampling locations was postponed to the spring 2010. Water analysis from first sampling period for sampling location DEV-1 was not considered since it has been analysed in another laboratory. The results from Pasji rep and Potok pri dvorcu Visoko were sampled for the third time in 2011 to confirm the laboratory's mistake and missing values from previous samplings.

3.2.1. Collection of existing data

For each sampling location the data about the exact location and the ownership of the object needed to be found. Further, the lithological (lithological profile) and technical structure of the object (depth, diameter, position of filter tubes, depth of fixed pump if present and so on) needed to be collected, as well as past geochemical and isotopic analyses and groundwater levels. The data was collected from various hydrogeological databases, reports from archives of the Geological Survey of Slovenia (overview of a few thousand reports), topographical maps and available data from the internet.

3.2.2. Selection of hydrochemical parameters

The selection of the monitored hydrochemical parameters includes the most significant parameters that determine both the natural background of groundwater, as well as major pollutants that occur in groundwater due the anthropogenic factors. Following parameters in groundwater were chosen to be analyzed:

- physico-chemical parameters: T, pH, and EC
- major ions: Ca^{2+}, Mg^{2+}, Na^+, K^+, HCO_3^-, NO_3^-, Cl^-, SO_4^{2-}, S, and Si
- secondary major ions: B, Ba, Fe, NH_4^+, P, Sr, and Zn
- trace constituents: Ag, Al, As, Au, Be, Bi, Br, Cd, Ce, Co, Cr, Cs, Cu, Dy, Er, Eu, Ga, Gd, Ge, Hf, Hg, Ho, In, La, Li, Lu, Mn, Mo, Nb, Nd, Ni, Pb, Pd, Pr, Pt, Rb, Re, Rh, Ru, Sb, Sc, Se, Sm, Sn, Ta, Tb, Te, Th, Ti, Tl, Tm, U, V, W, Y, Yb, and Zr

- stable isotopic composition of oxygen ($^{18}O/^{16}O$), hydrogen ($^{2}H/^{1}H$), and carbon ($^{13}C/^{12}C$), and nitrogen ($^{15}N/^{14}N$)
- tritium (^{3}H)

3.2.3. Sampling protocols

Before the actual sampling it was necessary to check the current state of the object to see whether the actual sampling from the object could be performed. The exact locations of the sampling locations were determined by a portable GPS meter where X, Y and Z coordinates were measured. In the field the basic characteristics are observed: depth of the object, installed instruments, the access to object, potential sources of pollution in surrounding area and actual possibility to perform sampling. Additionally, the description of surrounding area and possible sources of pollution, accessibility to sampling points and possibility for water sampling needed to be examined prior sampling.

Since a lot of basic decisions depend on the assessment of the groundwater quality status, the data needs to be reliable and able to reflect the actual state of groundwater in the aquifer. Therefore, all the samples are prepared according to standard procedures and guidelines given by each laboratory. They provide the information about the procedure of sampling, storage and transport of water samples from collection site to the laboratory.

Standard procedures for sampling, transport and storage of groundwater samples are in accordance with the standards (SIST ISO 5667–11, 1996; SIST ISO 5667–06, 1996; SIST ISO 5667–03; 1996). A different sampling approach is required for each type of water analysis (Sundaram *et al.*, 2009). Sampling was always performed regarding the weather conditions (in case of rain, sampling was postponed for at least 3 days to sample from the base flow conditions). This was done in order to avoid direct sampling of meteoric water.

The groundwater samples from a well or piezometer (especially unused one) were taken after pumping a volume corresponding to three times that of the relevant well or borehole to get fresh groundwater. This was done with a pump Grundfos MP-1 made out of inert material and with pumping rate of 0.2 L/s. During pumping the field parameters were monitored and sampling was performed when measured values were stable. When sampling groundwater from springs it was necessary to sample water as near as possible to the point at which groundwater enters the surface in order to minimize the effects of atmospheric contamination and degassing.

3.2.4. Field measurements

Measurements of physical parameters like electrical conductivity (EC), pH and water temperature (T) of sampled water were carried out in situ with the portable WTW pH/Conductivity measuring instrument pH/Cond 340i SET (Fig. 13). The precision of physical parameters measurement is ± 0.01 for pH, ± 0.5 % for EC and ± 0.1 °C for temperature.

Before taking readings, pumping was carried out until the meter readings were stable for each parameter. The pH electrode was calibrated using 4.0, 7.0, and 10.0 buffer solution, and KCl solution of 200 and 500 µS/cm for EC.

In private wells and piezometers groundwater levels were measured by groundwater level measurement device on the site (Fig. 14).

Figure 13: Groundwater field parameters measurement

Figure 14: Groundwater level measurement

3.2.5. Field sampling

Water samples were taken for the chemical analysis of major and minor ions, stable and radioactive isotope analysis, and the trace elements analysis, according to laboratory guidelines for each type of analysis. Each water sample was sealed in a pre-cleaned polyethylene bottle which has been rinsed three times with sampled water prior sampling, filled to the rim with water and capped within seconds of collection to minimize exposure to the air (to avoid degassing of CO_2). Changes caused by escape of CO_2 from the water reflect on the pH, HCO_3^-, and other ions (Freeze and Cherry, 1979). For major ions and tritium analyses 1 L of water sample was required for each, 2 times per 1 L for $\delta^{14}N$ analyses, for stable isotopes of oxygen ($\delta^{18}O$) and deuterium (δ^2H) 0.1 L, and for stable isotope of dissolved inorganic carbon ($\delta^{13}C$-DIC) 3 times per 12 mL. For all trace elements 50 mL of water was required which first needed to be filtered on the site using hand-pump on site through a 0.45 µm cellulose membrane filter into pre-cleaned sample bottle, then immediately acidified with ultrapure nitric acid (HNO_3) to the pH<2 (Figs. 15-18). Water samples were then stored in a cooling box (<4°C) and later, transferred to different laboratories. During sampling also reserve and blank samples were taken to control accuracy of the analytical procedures.

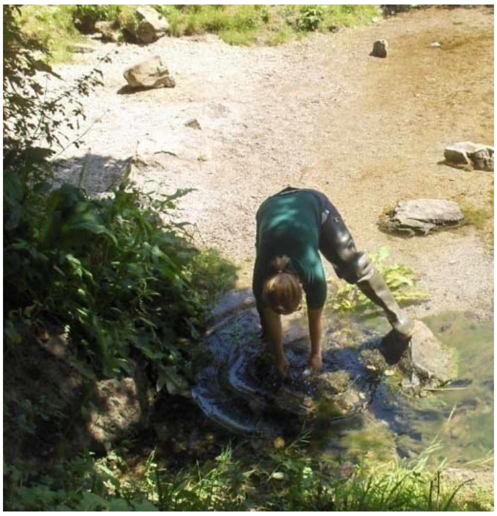

Figure 15: Sampling spring water

Figure 16: Water filtration

Figure 17: Groundwater samples from one sampling location

Figure 18: Required field equipment

3.3. Analytical methods

3.3.1. Chemical analyses of groundwater

Major cations and anions in sampled groundwater were analysed at the laboratory of Drinking water and Sewerage System Public Utility, Ljubljana, Slovenia. Table 3 presents the standards and equipment used for determining measured parameters in water.

Table 3: Standards and equipment used for determining measured parameters in water

Parameter	Standard	Laboratory instrument
pH	SIST ISO 10523, 2010	WTW inoLab pH/ION/Cond 750 instruments
electrical conductivity (at 20°C)	SIST EN 27888, 1998	WTW inoLab pH/ION/Cond 750 instruments
alkalinity (HCO_3^-)*	ASTM D1067-92, 1996 (Modified)	Buret and Erlenmeyer flask
ammonium (NH_4^+)	SIST ISO 7150-1, 1996	Spectrophotometer (Varian Cary 50 Bio)
calcium (Ca^{2+}), magnesium (Mg^{2+}), sodium (Na^+), potassium (K^+), chloride (Cl^-), nitrate (NO_3^-) sulphate (SO_4^{2-})	SIST EN ISO 14911, 2000	Ion chromatograph (IC) Metrohm
iron (Fe^{2+} and Fe^{3+})*	Ferrous Iron by Modified Method SM20 3500 Fe B, 1997	Varian Cary 50 UV-Vis Spectrophotometer

**parameters are not accredited*

The results for water samples which were not analyzed immediately the accreditation was provided outside the scope of accreditation (parameters HCO_3^- and Fe are not accredited). Each measurement for individual parameter in the water sample was carried out once, except for parameters HCO_3^-, Fe and NH_4^+ where sometimes second measurement was performed. In this case the final value was the mean value of both measurements. The uncertainty for pH is ±0.076, for electrical conductivity is ±1.12 μS/cm, for HCO_3^- is ±3 %, for NH_4^- is ±0.0016 mg/L, and for Fe is ±8 %. Anions and cations measurement uncertainty (coverage factor K=2, reliability 95 %) given by the analytical laboratory are calculated regarding the formula $U=2(0.08LOQ+0.02C_{vz})$, where C_{vz} is the measured concentration of analyte in sample (Drinking water and Sewerage System Public Utility Ljubljana, 2011; Sundaram *et al.*, 2009).

Limit of detection (LOD) is defined as the lowest concentration of an analyte in sample that can be determined to be statistically different from a blank (99 % confidence). Limit of quantitation (LOQ) is defined as the lowest concentration of an analyte in a sample that can be obtained with a specified degree of confidence (Wisconsin Department of Natural Resources Laboratory Certification Program, 1996). When the result for the measured parameter from the laboratory referred to lower value than the LOD or LOQ, it was replaced by its half value and was considered as the final result. This practice is also used by the Slovenian Environmental Agency in their reports (EARS, 2011c) according to Ministry of Environment and Spatial Planning (2009), and Decree on groundwater status (2009). A number of studies suggest what number to use as a substitute for LOD (Croghan and Egeghy, 2003; Verbovšek, 2011).

Analyses of 70 elements were performed ACME Labs - Analytical laboratories Ltd. in Vancouver, Canada (ACME Labs, 2007). Water samples were analysed as received directly by Inductively Coupled Plasma Mass Spectroscopy (ICP-MS) to determine trace to ultra-trace concentrations of elements. The uncertainty calculation has not been done, but for standard, most elements are running anywhere between 15 and 30 % at >10 times detection limit (LOD). The analytical precision and accuracy were determined as reasonable, which has been proven with random 9 blank and replicate water samples to the laboratory. Therefore the reliability of analytical procedures was considered adequate.

3.3.2. Groundwater isotope analyses

Isotopic analyses for $\delta^{18}O$ and $\delta^{2}H$ in groundwater samples were performed at the Hydroisotop GmbH laboratory in Schweitenkirchen, Germany, and stable isotope analysis for $\delta^{13}C$-DIC and ^{3}H in groundwater at the laboratory of Jožef Stefan Institute laboratories, Slovenia.

The oxygen isotopic composition ($\delta^{18}O$) in water was determined by the analysis of CO_2 equilibrated with sample water (Epstein and Mayeda, 1953), and the isotopic composition of hydrogen ($\delta^{2}H$) was determined using H_2 equilibrated with water sample using Pt-catalyst (Prosser and Scrimgeour, 1995). The equilibrated gases were measured with dual inlet method on a Finnigan MAT 250 and Finnigan MAT 251 isotope ratio mass spectrometers (IRMS). All samples were run at least twice where only one result is reported in general. Rarely a third measurement is done in order to control procedure, when e.g. another sample in the same run shows an unusual result or something happens during measurement. Maximum reported analytical uncertainty is ± 0.15 ‰ for $\delta^{18}O$ and ± 1.5 ‰, for $\delta^{2}H$, respectively. The accuracy of the instrument for ^{18}O is better than 0.03 ‰ and for D better than 1 ‰. All the measurements were carried out against laboratory standards that were periodically calibrated against the international isotope water standards recommended by IAEA. Values for d-*excess* were calculated by the laboratory from the $\delta^{18}O$ and $\delta^{2}H$ values in sampled water. Resulting errors of the d-*excess* and are in the order of ±1.5‰.

The stable isotope composition of dissolved inorganic carbon ($\delta^{13}C$-DIC) was determined in 5 mL water sample injected into He-flushed septum vials containing 100 % phosphoric acid (H_3PO_4) (Capasso *et al.*, 2003). The released CO_2 was analysed using a continuous flow Europa Scientific 20-20 IRMS (isotope ratio mass spectrometer) with an ANCA-TG trace gas separation module. Measurement reproducibility is better than 0.2 ‰ (Lojen *et al.*, 2009).

For the analysis of the total nitrogen isotope ratio ($^{15}N/^{14}N$ as denoted by the $\delta^{15}N_{tot}$), the water sample was first filtered through 0.45 µm membrane filters. The amount of the sample necessary for the analysis was calculated from the concentration of NO_3^- in water (determined by IRMS analysis). To isolate the nitrate, water was passed through the cation exchange resin (BIO-RAD AG 50W-X8, Hydrogen Form, USA) and anion exchange resin (BIO-RAD AG2-X8, Chloride Form, USA) according to the method of Silva *et al.* (2000) as modified by Fukada *et. al.* (2003). Nitrate was eluted from the anion exchange resin using 30 mL 3M HCl. The eluate was neutralized using Ag_2O in an ice-cooled water bath. During neutralization, Ag_2O reacted with eluted HNO_3 to produce $AgNO_3$, AgCl and water. Neutralization was completed when the pH of the slurry increased to > 5.5. The resulting AgCl precipitate was removed by vacuum filtration (Silva *et al.*, 2000), and the solution containing $AgNO_3$ was evaporated at 60°C in the dark (Fukada *et al.*, 2003). Aliquots of samples containing 100–200 µg of N were packed into silver capsules and analysed for ^{15}N using an Europa 20-20 IRMS connected to the ANCA-SL preparation module for solid and liquid samples (Europa Scientific Ltd, Crewe, UK). The standard uncertainty of the measurement is < ±0.2 ‰ (Šturm and Lojen, 2011).

Since the prevailing nitrogen ion in sampled groundwater was NO_3^- (majority of NH_4^+ concentrations were below LOD), determined recharge areas of sampled groundwater are not affected by the anthropogenic influences in a great share, and because the extractions of N in NO_3^- is expensive and time consuming, the isotopic analyses of groundwater $\delta^{15}N_{tot}$ are referred to total nitrogen N_{tot} instead of only NO_3^- .

The method used for tritium measurements is electrolytic enrichment which consists of primary distillation, electrolytic enrichment, and secondary distillation. Before any sample processing, pH and conductivity of the sample are measured. The sample is then distilled to remove any impurities that could interfere with tritium measurements. After that electrolytic enrichment of 500 mL of distilled samples using sodium peroxide (Na_2O_2) is performed and a second distillation with lead chloride ($PbCl_2$) is carried out in order to neutralise the sample. Final water samples, mixed with scintillation cocktail are measured in the liquid scintillation spectrometer (LSS) Quantulus (modified after Różański and Gröning, 2004). The minimum detectable activity (MDA) for tritium is about 0.40 TU. The standard uncertainty of the measurement is between ±3 and ±33 % and depends on several parameters. The average value of measurement uncertainties is ±12 % (Kožar Logar and Glavič-Cindro, 2009).

3.4. Data analysis techniques

3.4.1. Accuracy and precision

The first step of the water analysis is an assessment of the quality of the data, which is accomplished by calculating the ion balance (also known as reaction error). As an aqueous solution is always electrically neutral, the sum (in meq/L) of the anions and the cations should always balance. An anion is negatively charged group (HCO_3^-, Cl^-, NO_3^-, and SO_4^{2-}) and cation a positively charged group (Ca^{2+}, Mg^{2+}, Na^+, K^+). The level of error in the data is calculated by using the formula (Appelo, 1996; Murray and Wade, 1996):

$$EB\ (\%)=((\Sigma\text{cations}-\Sigma\text{anions})/(\Sigma\text{cations}+\Sigma\text{anions}))100. \qquad (19)$$

An error of up to ±5 % is tolerable (Appelo and Postma, 2005).

3.5. Determinations of recharge areas of sampling locations

For every sampling location its characteristics of recharge area were studied in detail. Recharge areas were determined for every sampling location according to the aquifer type and processed in ArcGIS Version 9.2 (Esri Inc., 2001) (Appendix 8). In the karstic and fissured aquifers (Fig. 19), the aquifer's lithological and hydrogeological structure, the topology of terrain, active water protection areas, past tracer tests results, past hydro-contours, orographic watersheds and borders of groundwater bodies and aquifer systems were examined in detail.

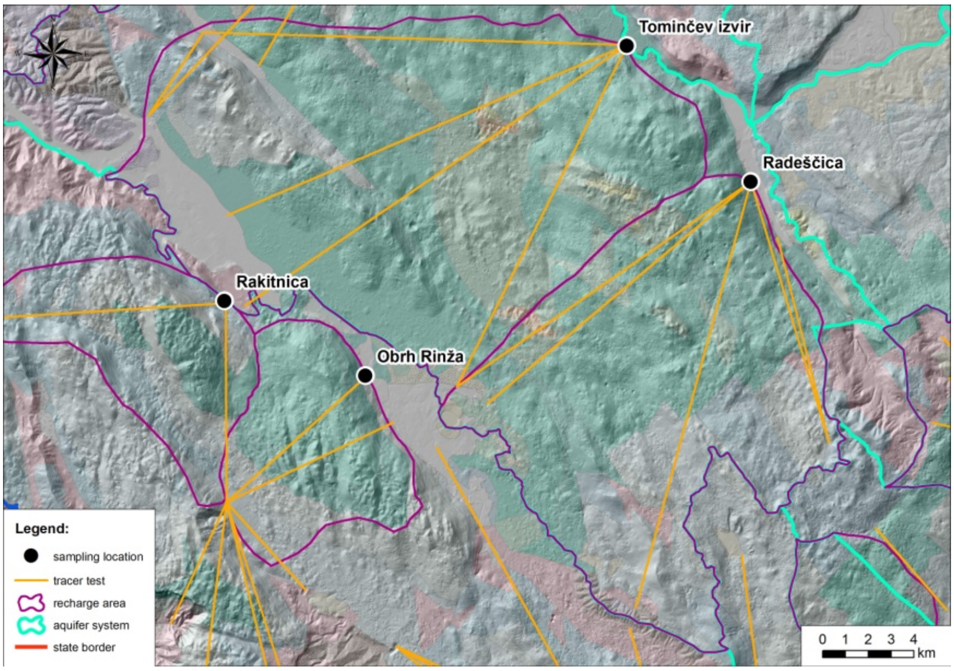

Figure 19: Recharge areas in karst-fissure aquifers (sampling locations Tominčev izvir and Radeščica)

Recharge areas of sampling locations in *intergranular aquifers* were determined regarding the hydrogeological characteristics of the aquifer: groundwater flow velocity and groundwater direction. Gradient of groundwater flow was assessed for each sampling location, and a permeability coefficient was used, based on past pumping experiments, and past results of hydrogeological modelling made for certain groundwater bodies. The groundwater flow was calculated according to Darcy (1856):

$$Q = - KA(h_1 - h_2)/L. \qquad (20)$$

Based on calculated groundwater flow velocity, the distance from the outer recharge area border and sampling location was determined perpendicular to hydro-contours within 1-year isochrones as the outer border of the recharge area (Fig. 20). At sampling locations where groundwater was constantly pumped, e.g. at pumping stations, the recharge area was limited with an angle of water-solute distribution due to processes of distribution in the aquifer; 45°angle because of greater influence on groundwater flow due to pumping and 30° angle at sampling locations where there was no previous pumping from the object, e.g. from piezometer, borehole or well. This value was taken as a rough approximation while in practice this angle is much smaller. Additional information was provided by hydrogeological modelling of some groundwater bodies which were done in the past (Rules on determining water bodies of groundwater, 2005; Prestor *et al.*, 2006).

The recharge areas of sampling locations in aquifers with minor groundwater reservoirs (Fig. 21), e.i. poorly permeable or impermeable rocks, were determined mostly according to the terrain topography.

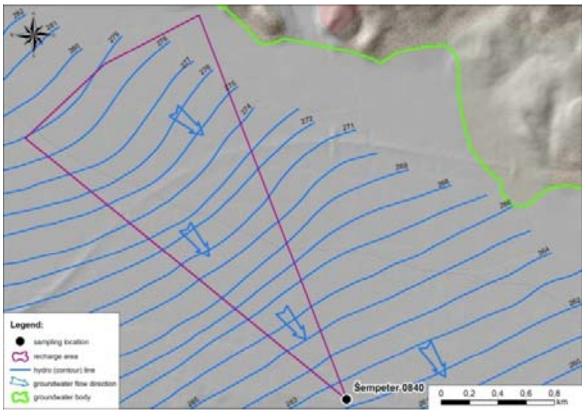

Figure 20: Recharge area in intergranular aquifer (sampling location Šempeter 0840)

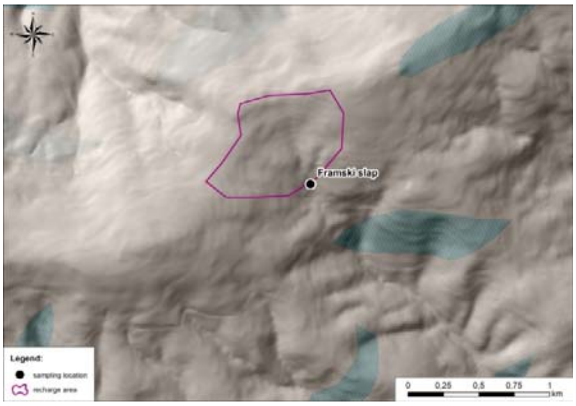

Figure 21: Recharge area in aquifers with minor groundwater reservoirs (sampling location Framski slap)

Detail information on recharge areas determination for particular sampling locations is found in Appendix 9.

3.6. Spatial analysis and generalizations

3.6.1. Spatial analysis

Spatial analysis of mean altitudes and climatic factors, like mean air temperature and mean amount of precipitation, were preceded for sampling locations recharge areas in ArcGIS.

Mean altitudes for sampling locations recharge areas were calculated in ArcGIS Version 9.2 as spatial analysis based on raster layer of Slovenian Digital Elevation Model of the cell size 12.5 x 12.5 m (GURS, 2005). Recharge area of sampling location DEV-1 Desenci could not be estimated and therefore spatial analysis was not made. For the mean altitude of recharge area the Z coordinate was considered.

For the mean air temperature of the recharge area the shape layer The average annual air temperature 1971-2000 with 1-2 km resolution was used (EARS, 2011a). The original layer has 8 classes (from -2°C to 14°C) where each class has a 2°C range, e.g. 2-4°C. In the shape attribute table a new column was added where we calculated the average temperature value from each class, e.g. if the class has 2-4°C we considered 3°C. In ArcGIS we did the spatial analysis of the temperatures regarding the surface share of recharge areas and calculated the share of each temperature class on recharge area, e.g. 8°C is 45 % of whole recharge area and 55 % has 9°C. Then this ratio was weighted to a single temperature.

For the mean amount of precipitation in the recharge area the shape layer The average annual precipitation corrected for 1971–2000 with 1-2 km resolution was used (EARS, 2011b). It has 13 classes (800 – 4000 mm) with different mutual ranges (at beginning 100 mm, later up to 800 mm). This analysis is preceded as the mean temperature of recharge area.

Distances from the seaside (Lucija Portorož) were calculated with the Euclidean distance in ArcGIS based on the raster layer of Slovenian Digital Elevation Model of the 12.5 x 12.5 m cell size (GURS, 2005), and was proceed as the calculation for the mean altitudes of recharge areas.

3.6.2. Generalizations

Lithological and lithostratigraphic units

The surface lithological and lithostratigraphic structure of the recharge areas was determined based on the digital geological map of Slovenia (Appendix 2) at the 1:250,000 scale (Buser, 2010). Due to consideravle geological diversity a simplification has been made. 114 lithological units (Appendix 2) were grouped into 14 lithological units (Tab. 4). Lithostratigraphic units were grouped based on the age of their formation and rock type into 28 lithostratigraphic subgroups.

Table 4: Simplified lithological classification of typical Slovenian rock types

Basic rock type classification	Lithological unit
Clastic sedimentary rocks	**flysch rocks***
	clay*
	gravel and sand*
	gravel, sand and clay*
	rubble and morena
	conglomerate and breccia
	marlstone
	shale and sandstone*
Carbonate rocks	**limestone prevailing***
	dolomite prevailing*
	carbonates with clastics*
	clastics with carbonates
Igneous and metamorphic rocks	**igneous rocks***
	metamorphic rocks*

Not all lithological and lithostratigraphic units are included in this study due to the chosen network pattern. Lithological (total 10) and lithostratographic units (total 14) marked with asterisk (Tabs. 4 and 5) are observed in the recharge areas of chosen sampling locations and are therefore solely used in the future tables and calculations.

Based on the new generalization and grouping the surface shares of individual lithological and lithostratographic units were calculated in ArcGIS, where the shares of the same lithological (and lithostratigraphic) units were combined in one for each recharge area. The surface areas (m^2) of recharge areas and all lithological (and lithostratigraphic) units within the polygon were calculated. In Excel the additional calculations were made where the prevailing share of one lithological (lithostratigraphic) unit was determined as the representative lithological (lithostratigraphic) unit of certain recharge area. In most cases the prevailing lithological (lithostratigraphic) unit was determined when prevailing lithological unit was above 75 %. Units marked with asterisk are observed in the recharge areas of sampling locations.

Table 5: Lithostratigraphic specification

	Period		Epoch	Lithostratigraphic unit
Cenozoic	**Quartenary**			**Quaternary clastics (medium- and coarse-grained)***
				Quaternaryclay (fine-grained)
	Tertiary	**Neogene**	**Pliocene**	**Pliocene clastics***
				Pliocene igneous rocks
			Miocene	**Miocene clastics***
				Lithothamnium limestone*
		Paleogene	**Oligocene**	**Oligocene clay “sivica”***
				Oligocene clastics
				Oligocene igneous rocks*
			Eocene	Eocene clastics
				Eocene flysch rocks*
				Eocene carbonates
			Paleocene	Paleocene flysch rocks
				Paleocene carbonates
Mesozoic				Mesozoic carbonates
	Cretaceous			Cretaceous clastic
				Cretaceous carbonates*
				Cretaceous flysch rocks
	Jurassic			**Jurassic carbonates***
				Jurassic clastics
	Triassic			**Triassic carbonates***
				Triassic clastics
			Middle	**Ladinian igneous rocks***
Paleozoic	**Permian**		**Middle**	**Val Gardena layers***
				Permian carbonates
				Carboniferous-Permian beds *
	Devonian			Devonian carbonates
				old Paleozoic rocks*

Aquifer porosity type

Based on the hydrogeological properties of the aquifer in which the groundwater was sampled and its recharge area, the aquifer porosity type has been classified into 5 groups (Tab. 6).

Table 6: Types of aquifer porosity

Type of porosity
intergranular porosity
fractured porosity
fractured and karstic porosity
karstic and fractured porosity
mixed porosity (karstic, fractured, intergranular)

Land cover/use

For the purposes of this study two land cover/use digital databases were used: CORINE Land Cover (GURS, 1998), and Actual agricultural and forest land usage (2011). Both land use data are used for specification of natural and anthropogenic influence on the recharge area of sampled groundwater. The focus regarding the natural influence is the type of vegetation in the recharge area, and regarding the anthropogenic influence the focus is on the urbanization and industry, waste landfill, sewage system leakage, areas where the use of fertilizers and pesticides could be present (fields, meadows, orchards, vineyards…) which could also provide the information of possible source of fertilizers or livestock.

The CORINE Land Cover Slovenia shape layer has been used in order to get the information about the type of land use on the individual recharge area. CORINE land cover units marked with asterisk (total 10 categories out of 33) (Tab. 7) are observed in the recharge areas of sampling locations and are therefore going solely to be used in the future tables and calculations. The share and the prevailing CORINE Land Cover use type within the recharge area has been determined and calculated in the same way as the previously described procedure for lithological and lithostratigraphic share.

Table 7: List of CORINE Land Cover use units

Description
Airports
Bare rocks*
Beaches, dunes, sands
Broad-leaved forest*
Complex cultivation patterns*
Coniferous forest*
Construction sites
Continuous urban fabric
Discontinuous urban fabric
Dump sites
Fruit trees and berry plantations
Glaciers and perpetual snow
Green urban areas
Industrial or commercial units*
Inland marshes
Land principally occupied by agriculture, with significant areas of natural vegetation*
Mineral extraction sites
Mixed forest*
Moors and heathland*
Natural grasslands*
Non-irrigated arable land*
Pastures
Port areas
Road and rail networks and associated land
Salines
Salt marshes
Sclerophyllous vegetation
Sparsely vegetated areas
Sport and leisure facilities
Transitional woodland-shrub
Vineyards
Water bodies
Water courses

Land use data presents a complex relation between natural and socio-economic factors. Spatial distribution on surface activities is presented as Actual agricultural and forest land usage Map 1:5,000 (MKGP) which is determined by Rules on evidence of actual agricultural and forestal land use (Official Gazette of RS 90/2006, 9/2008, 45/2008-ZKme-1, 122/2008). 25 classes were generalized into 12 categories (Tab. 8) and the share of individual groups was calculated within every recharge area. The share and the prevailing as Actual agricultural and forest land usage type within the recharge area has been determined and calculated in the same way as previously described procedure for lithological and lithistratiographic share.

Table 8: List of generalized Actual agricultural and forest land usage units

	Category	Land use type
Types of agricultural land use	1	Arable land, Hop fields, Other permanent crops on arable land
	2	Green houses, Vineyards, Nursery, Intensive Orchards, Extensive Orchards, Olive groves, Other permanent crops, Meadows and pastures, Swampy meadows
	3	Owergrown areas, Forest plantations, Riparian overgrowth and forest hedges, Forest trees on agricultural land
	4	Uncultivated agriculture land
Non-agricultural uses	5	Forest
	6	Built-up areas and related surfaces
	7	Swamps
	8	Reeds
	9	Other marshy areas
	10	Dried open areas with special vegetation
	11	Open areas with little or no vegetation
	12	Waters

Additional generalization has been made based on first grouping, where Actual agricultural and forest land usage types have been grouped into 4 subgroups (Tab. 9). The share and the prevailing land use type within the recharge area has been determined and calculated in the same way as previously described procedure for lithological share.

Table 9: List of additional generalized Actual agricultural and forest land usage units

No.	Actual source	Actual agricultural and forest land usage type	Category
1	anthropogenic	arable land, hop fields; other permanent crops on arable land	areas of intense use of nutrients and plant protection products
2	anthropogenic	green houses, vineyards, nursery, intensive orchards, extensive orchards, olive groves, other permanent crops, meadows and pastures, swampy meadows	areas of less intense use of nutrients and plant protection products
3	natural	owergrown areas, forest plantations, riparian owergrowth and forest hedges, forest trees on agricultural land; uncultivated agriculture land; forest; swamps; reeds; other marshy areas; dried open areas with special vegetation; open areas with little or no vegetation	forest
4	anthropogenic	built-up areas and related surfaces	urban areas

Detailed description on all 87 sampling locations according to hydrogeological, geological, CORINE Land cover, and Actual agricultural and forest land usage in their recharge areas is found in the Appendix 10.

3.6.3. Methodologies used for data evaluation and presentation

Methodology for determination of the typical groundwater value

From each sampling location groundwater was sampled two times, except at two sampling locations (Pasji rep and Potok pri dvorcu Visoko) it was sampled three times. The main purpose of repeating sampling twice at each sampling location was to obtain a more typical typical groundwater value of measured parameters at individual sampling location. This methodology has been verified on two samplings locations, where long term observations of $\delta^{18}O$ in groundwater were performed at the Krka spring (karstic aquifer) and LMV-1 (intergranular aquifer). Based on those graphs it is possible to conclude that two

samplings at a certain location can provide a quite representative (typical) mean of measured $\delta^{18}O$ in groundwater.
The focus of this study was not to monitor seasonal variations, but to obtain the most typical values of measured parameter in groundwater in the recharge areas of the most representative lithological and lithostratigraphic units found in Slovenia. Typical values of parameters were calculated as a mean value of two measurements.

Methodology for determination of groundwater natural background level (NBL)

The natural chemical background level (NBL) in groundwater was determined for the parameters which sources are mostly of anthropogenic origin. In order to determine the natural background level for observed groundwater parameter, the share of anthropogenic influence in the recharge areas of sampled groundwater were estimated. This has been provided by the generalization of the Actual agricultural and forest land usage (Table 9). The comparison between the shares of anthropogenic sources in the recharge areas of sampled groundwater, and the concentration of observed parameters, provides the information of the occurrence of parameter in the groundwater. The share of anthropogenic influence up to 20 % in the recharge areas was estimated as the natural recharge areas. Therefore the mean values of measured parameters in groundwater which have up to 20 % of anthropogenic influences in the recharge areas were considered as the natural chemical background level of observed parameter.

Hydrochemical thematic maps

For each observed parameter a hydrochemical thematic map was produced. The mean (typical) value of both (seasonal) samplings was considered for each sampling location. The mean value of a certain groundwater parameter for individual groundwater body was calculated on the basis of the obtained datasets for sampling locations included in a particular groundwater body. Mean concentrations of groundwater bodies do not present the actual concentrations for the whole groundwater body. Instead they serve as reference values which provide the information on possible trends in particular areas, and alert on the significant deviations between concentrations at sampling locations and groundwater body. The scales of the maps are determined by the frequency distributions of observed concentrations and personal choice.

System for result interpretation

The data from analyses were examined graphically and scrutinized for trends and clustering together with basic geologic and hydrologic data, and land-use information in order to indicate likely sources of observed parameter in sampled groundwater.
Presentation of results and the interpretation of studied groundwater parameters follow the similar pattern of description:

- descriptive statistics of the observed parameter
- typical groundwater values of observed parameter according to major rock type, lithological classification (Table 4) and lithostratigraphic classification (Table 5)
- typical groundwater values of observed parameter according to porosity type (Table 6)
- typical groundwater values of observed parameter according to land cover/use: CORINE Land Cover (Table 7) and Actual agricultural and forest land usage (Table 9)
- typical groundwater values of observed parameter according to the object type
- hydrochemical thematic map
- determination of natural background level (NBL) of the observed parameter

With respect to determination of typical groundwater values of observed parameters according to object type, the correlations with observed parameters are not statistically significant. They are apparent and not real. Instead they serve as possible indicators for climatic conditions, e.g. outgassing processes (CO_2) observed in waters samples as surface water.

All tables with exact values of concentrations from box and whisker plots for every observed parameter are found in Appendix 13 (13A-13S). For groundwater ^3H, $\delta^{18}O$, δ^2H, $\delta^{15}N_{tot}$, and d-*excess,* the plots for typical groundwater values according to some generalizations (geology or land use) are not presented because their isotopic composition (values) are not affected by it.

4. RESULTS AND DISCUSION

Interpretation of the occurrence and distribution of measured chemical and isotopic composition of groundwater has been carried out with the help of statistical data processing, and topographic, geological, and land use data. Interpretation has been upgraded with the existing geochemical and hydraulic data of aquifers, and by field observations.

4.1. Statistics and data analysis

4.1.1. Accuracy and precision

The charge balance calculations for all analyzed groundwater samples could not be calculated. Namely groundwater samples where the concentration of all major ions was above LOD the ion balance was within the error tolerance. Where at least one of measured major ion concentration in measured groundwater sample was below the LOD the ion balance could not be calculated, since its original value was replaced by the half of its LOD value. Additionally, during our 3-year sampling the laboratory changed in 2009 the limit of detection for K^+ and Cl^- concentrations.

4.1.2. Statistical methods

The dataset used for statistical analysis is a matrix of measured properties176 water samples taken from 87 sampling sites (Appendix 11). Groundwater at 85 sampling locations was sampled twice, and at 2 sampling locations it was sampled three times. Dataset includes analysis for 91 variables: physico-chemical parameters, major and secondary major ions, trace constituents, and isotopic composition of stable and radioactive isotopes.

A number of parameters have been eliminated from further analysis:
- concentration of measured parameters below LOD (Bi, Eu, Hf, In, Nb, Pd, Pt, Sm, Ta, Tb, Ti, Tm)
- in more than ⅓ of water samples the concentration of measured parameters was below LOD (NH_4^+, Ag, As, Au, B, Be, Cd, Ce, Co, Cr, Cs, Dy, Er, Fe, Ga, Gd, Ge, Hg, Ho, La, Lu, Mo, Nd, Ni, Pb, Pr, Re, Rh, Ru, Sb, Sc, Se, Sn, Te, Th, Tl, V, W, Yb, and Zr),
- were excluded from the laboratory analyses in 2010 (Ir and Os)

Finally, 176 groundwater samples and following parameters were considered for this study: T, pH, EC, $\delta^{18}O$, δ^2H, d-*exess*, $\delta^{13}C$-DIC, $\delta^{15}N_{tot}$, ^3H, Ca^{2+}, Mg^{2+}, Na^+, K^+, Cl^-, HCO_3^-, NO_3^-, SO_4^{2-}, Si, and Mn.

4.1.2.1. Descriptive statistics

Descriptive statistics are used to describe the basic information of studied dataset. The mean (X), geometric mean (X_G), median (Md), minimum (Min), maximum (Max), standard deviation (S), standard error of mean (S_X) and coefficient of variation (CV) were determined for observed variables. Various tests were performed in order to evaluate the normality of data distribution: Kolmogorov-Smirnov test (K-S), Shapiro-Wilk's test (W), and Chi-square test (χ^2) (Appendix 12).

Data transformation

Since the distribution of most observed variables is positively skewed and their frequency diagrams do not follow normal distribution the logarithmic transformation (log10(x+100)) was performed in order to achieve normality of observed data (Appenedix 12).

On the basis of the normality tests results and by visual inspection of histograms for all measured parameters in groundwater, the normal distribution (normality) was assumed for raw parameters of T, EC, $\delta^{18}O$, δ^2H, d-*excess*, Ca^{2+}, and HCO_3^-, as their curve is approaching normal distribution. For all other variables the logarithms of contents was considered normally distributed. Table 10 summarizes the descriptive statistics.

Table 10: Descriptive statistics of observed variables

Parameter	Dis	n	X	Md	XG	Min	Max	S	S_x	C_V	A	E	χ^2	d	p	W	p
T	N	174	10.7	10.6	10.3	5.2	18.2	2.9	0.2	27.4	0.26	-0.42	0.94	0.06	< 0.20	0.98	< 0.20
pH	Log	175	7.60	7.64	7.59	6.40	8.30	0.37	0.03	4.85	-0.91	1.13	7.78	0.09	< 0.10	0.95	< 0.01
EC	N	175	368	366	319	28	882	173	13	47	0.50	0.42	1.80	0.07	> 0.20	0.98	< 0.10
$\delta^{18}O$	N	174	-9.25	-9.23		-11.43	-6.49	0.94	0.07	-10.14	0.25	0.15	3.42	0.06	> 0.20	0.99	< 0.10
$\delta^{2}H$	N	174	-61.6	-62.5		-78.6	-40.6	7.5	0.6	-12.1	0.44	0.25	4.80	0.07	> 0.20	0.98	< 0.05
d-excess	N	174	12.4	12.4	12.2	6.0	21.4	2.0	0.2	16.4	0.53	2.33	0.75	0.06	> 0.20	0.97	< 0.10
$\delta^{13}C$-DIC	Log	173	-12.15	-12.92		-20.60	-0.70	3.71	0.28	-30.52	0.92	1.65	53.24	0.15	< 0.01	0.90	< 0.01
$\delta^{15}N_{tot}$	Log	133	4.24	3.65		-2.80	18.60	4.14	0.36	97.76	0.84	0.86	0.88	0.07	> 0.20	0.95	< 0.10
^{3}H	Log	172	6.14	6.01	5.80	0.48	11.77	1.69	0.13	27.51	-0.19	2.17	6.73	0.08	> 0.20	0.95	< 0.01
Ca^{2+}	N	175	60	58	49	2	152	30	2	50	0.52	0.65	2.76	0.07	> 0.20	0.97	< 0.05
Mg^{2+}	Log	175	13.0	9.5	9.0	1.0	42.0	10.1	0.8	78.2	0.91	-0.19	28.08	0.18	< 0.01	0.89	< 0.01
Na^{+}	Log	175	3.7	2.0	1.9	0.1	36.0	5.3	0.4	143.4	3.29	12.67	112.47	0.25	< 0.01	0.60	< 0.01
K^{+}	Log	175	0.82	0.44	0.41	0.04	12.00	1.60	0.12	194.99	5.07	28.09	268.45	0.31	< 0.01	0.41	< 0.01
HCO_3^-	N	175	235	234	201	19	575	110	8	47	0.16	-0.28	1.11	0.05	> 0.20	0.98	> 0.20
Cl^-	Log	175	5.00	2.34	2.35	0.12	36.70	7.10	0.54	142.08	2.55	6.40	90.44	0.27	< 0.01	0.64	< 0.01
NO_3^-	Log	175	9.56	4.47	4.94	0.33	92.56	15.87	1.20	165.92	3.51	12.96	283.67	0.34	< 0.01	0.51	< 0.01
SO_4^{2-}	Log	175	10.06	5.66	6.37	0.75	67.40	11.49	0.87	114.23	2.50	6.96	86.73	0.24	< 0.01	0.69	< 0.01
Si	Log	174	3.19	1.86	1.98	0.17	13.44	3.03	0.23	0.95	1.39	1.34	12.53	0.18	< 0.01	0.83	< 0.01
Mn	Log	174	0.82	0.23	0.26	0.03	22.11	2.55	0.19	309.02	5.89	38.49	369.22	0.39	< 0.01	0.29	< 0.01

Dis. – distribution (N – normal, Log – lognormal); Min – minimum; Max – maximum; Md – median; X – mean, S – standard deviation; S_x – standard error of mean; CV – coefficient of variation (%)

4.1.2.2. Multivariate statistical methods

Correlations

For estimating correlation between observed variables the nonparametric Spearman's rank correlation (Spearman’s rho) statistical test was used (Tab. 11). The correlation coefficients (r_s) are significant at $p<0.05$.

Strong correlation coefficients ($r_s>0.70$) were observed between $\delta^{18}O$ and δD ($r_s=0.96$), EC and Ca^{2+} ($r_s=0.89$), HCO_3^- and Ca^{2+} ($r_s=0.86$), EC and HCO_3^- ($r_s=0.82$), Na^+ and K^+ ($r_s=0.82$), Si and Na^+ ($r_s=0.81$), Na^+ and Cl^- ($r_s=0.81$), EC and Mg^{2+} ($r_s=0.79$), HCO_3^- and Mg^{2+} ($r_s=0.76$), mean amount of precipitation and Si ($r_s=-0.76$), NO_3^- and Cl^- ($r_s=0.76$), K^+ and $\delta^{15}N_{tot}$ ($r_s=0.73$), Br an Cl^- ($r_s=0.73$), Cl^- and $\delta^{15}N_{tot}$ ($r_s=0.72$), Si and K^+ ($r_s=0.71$), Br and Na^+ ($r_s=0.71$), and Cl^- and K^+ (0.71).

Table 11: Spearman rank order correlations (strong correlations are marked in bold and are underlined; marked in red correlations are significant at the 95 % confidence level)

	T	pH	EC	$\delta^{18}O$	$\delta^{2}H$	$\delta^{13}C$-DIC	$\delta^{15}N_{tot}$	^{3}H	Ca^{2+}	Mg^{2+}	Na^{+}	K^{+}	HCO_3^-	Cl^-	NO_3^-	SO_4^{2-}	Si	Br	Mn	Mean amount of precipitation
T	1.00																			
pH	-0.43	1.00																		
EC	0.54	-0.51	1.00																	
$\delta^{18}O$	0.30	-0.01	0.26	1.00																
$\delta^{2}H$	0.21	0.11	0.15	**0.96**	1.00															
$\delta^{13}C$-DIC	-0.30	0.58	-0.22	0.12	0.21	1.00														
$\delta^{15}N_{tot}$	0.68	-0.49	0.63	0.17	0.05	-0.39	1.00													
^{3}H	-0.09	-0.10	0.12	-0.26	-0.30	-0.08	0.11	1.00												
Ca^{2+}	0.44	-0.46	**0.89**	0.33	0.23	-0.21	0.48	0.12	1.00											
Mg^{2+}	0.44	-0.37	**0.79**	0.03	-0.06	-0.06	0.51	0.08	0.51	1.00										
Na^{+}	0.68	-0.52	0.41	0.32	0.20	-0.45	0.68	-0.05	0.35	0.21	1.00									
K^{+}	0.58	-0.47	0.47	0.21	0.10	-0.41	**0.73**	0.03	0.36	0.28	**0.82**	1.00								
HCO_3^-	0.45	-0.39	**0.92**	0.21	0.11	-0.17	0.50	0.10	**0.86**	**0.76**	0.26	0.34	1.00							
Cl^-	0.63	-0.46	0.69	0.45	0.33	-0.32	**0.72**	-0.03	0.62	0.46	**0.81**	**0.71**	0.55	1.00						
NO_3^-	0.39	-0.41	0.69	0.29	0.21	-0.30	0.57	0.13	0.60	0.47	0.51	0.58	0.54	**0.76**	1.00					
SO_4^{2-}	0.56	-0.35	0.58	0.27	0.19	-0.23	0.51	0.19	0.52	0.37	0.61	0.58	0.43	0.58	0.55	1.00				
Si	0.58	-0.61	0.28	0.02	-0.09	-0.57	0.60	0.07	0.20	0.14	**0.81**	**0.71**	0.14	0.49	0.32	0.56	1.00			
Br	0.56	-0.62	0.59	0.31	0.20	-0.42	0.60	0.06	0.49	0.38	**0.71**	0.61	0.43	**0.73**	0.61	0.54	0.64	1.00		
Mn	0.43	-0.22	0.19	0.28	0.23	-0.07	0.31	-0.04	0.10	0.15	0.44	0.41	0.10	0.38	0.12	0.29	0.37	0.37	1.00	
Mean amount of precipitation	-0.56	0.66	-0.57	0.13	0.26	0.52	-0.60	-0.28	-0.44	-0.49	-0.57	-0.59	-0.45	-0.50	-0.49	-0.64	**-0.76**	-0.64	-0.30	1.00

Moderate correlation coefficients ($0.7>r_s>0.5$) were observed between EC and Cl^- (r_s=0.69), EC and NO_3^- (r_s=0.69), T and $\delta^{15}N_{tot}$ (r_s=0.68), $\delta^{15}N_{tot}$ and Na^+ (r_s=0.68), T and Na^+ (r_s=0.68), Si and Br (r_s=0.64), mean amount of precipitation and Br (r_s=0.64), T and Cl^- (r_s=0.63), EC and $\delta^{15}N_{tot}$ and EC(r_s=0.63), Ca^{2+} and Cl^- (r_s=0.62), Na^+ and SO_4^{2-} (r_s=0.61), NO_3^- and Br (r_s=0.61), mean amount of precipitation and $\delta^{15}N_{tot}$ (r_s=0.60), $\delta^{15}N_{tot}$ and Si (r_s=0.60), $\delta^{15}N_{tot}$ and Br (r_s=0.60), and Ca^{2+} and NO_3^- (r_s=0.60).

Based on the knowledge from literature a few major groups could be extracted; e.g. a group that is linked to dissolution of carbonate rocks (EC, HCO_3^-, Ca^{2+}, and Mg^{2+}), a group that associates $\delta^{18}O$ and δ^2H, a group that is linked to silicate weathering (Si, Na^+ and K^+), and a group that might reflect the anthropogenic influence on the groundwater (Na^+, K^+, NO_3^-, Cl^-, and SO_4^{2-}), and others.
It needs to be pointed out that some correlations are not real (are apparent), and that their interpretation needs to be considered in aspects of geochemical reaction mechanisms.

Factor analysis (FA)

For factor analysis the data has been standardized to remove the effects of using different units in variables. The standardized values have a mean value of zero and standard deviation of unity. A total of 176 observations and 19 standardized variables were used for this analysis. With the factor analysis distribution is decreased to four factors (F1 to F4) after varimax orthogonal rotation. Four factors are connected regarding to geochemical similarities and they account for 76.25 % of total variance. The rotated loadings, eigenvalues, and percentage of variance are given in the Table 12. The total number of factors was chosen according to eigenvalues greater than 1 (scatterplot in the Appnedix 12), % of total variances explained (more than 75 %), and knowledge of geochemistry.

Table 12: Variables and factor loadings after varimax rotation

	F1	F2	F3	F4	Comm
Cl^-	**0.90**	0.17	0.24	0.03	95.87
Na^+	**0.89**	0.17	0.16	0.15	97.38
Br	**0.84**	0.24	0.25	0.17	87.38
K^+	**0.82**	0.03	0.10	0.00	90.43
SO_4^{2-}	**0.80**	0.09	0.23	-0.09	75.18
NO_3^-	**0.75**	0.02	0.30	-0.10	79.57
Si	**0.64**	-0.14	0.03	**0.65**	84.22
pH	**-0.62**	0.28	-0.17	-0.48	77.94
$\delta^{15}N_{tot}$	0.47	-0.03	0.45	0.26	58.39
EC	0.43	0.12	**0.86**	0.01	98.17
T	0.42	0.22	0.56	0.43	69.22
^3H	0.37	-0.40	0.05	**-0.62**	52.40
Ca^{2+}	0.36	0.25	**0.79**	-0.08	97.46
$\delta^{13}C$-DIC	-0.30	0.14	-0.42	-0.42	66.46
$\delta^{18}O$	0.21	**0.93**	0.12	0.06	96.25
δ^2H	0.12	**0.96**	0.01	0.01	96.13
HCO_3^-	0.07	0.10	**0.96**	-0.02	94.41
Mg^{2+}	0.07	-0.19	**0.80**	0.11	93.92
Mn	-0.02	0.04	0.03	**0.78**	51.08
eigen.	8.15	2.25	2.19	1.90	
Var.	42.92	11.82	11.51	9.99	76.25

F1…F4 – factor loadings; eigen – eigenvalue; Var - % total variance; Com – communalities in %.

Factor 1 (F1) is the strongest and accounts for 42.92 % of the total variance with eigenvalue of 7.61, and includes 6 variables Cl^-, Na^+, Br, K^+, SO_4^{2-}, NO_3^-, Si, and pH. Strong correlations between observed variables are most possibly due to anthropogenic land use (use of fertilizers, manure and slurry, leakage of waste water) in the recharge areas of sampled groundwater. Integration of variables Si and pH suggests the major anthropogenic input in the NE part of the study area.

Factor 2 (F2) is the second strongest factor and includes 11.82 % of entire variability with eigenvalue of 2.25. This factor associates $\delta^{18}O$ and $\delta^{2}H$.

Factor 3 (F3) associates HCO_3^-, EC, Ca^{2+}, and Mg^{2+} with strong mutual correlations. This factor explains 11.51 % of total variance with eigenvalue of 2.19. This group is linked to dissolution of carbonate minerals.

Factor 4 (F4) includes only 9.99 % of total variance, and has an eigenvalue of 1.90. This group associates Mn, Si, and ^3H, where in older groundwater (from deeper aquifers) the presence of Mn may indicate a reductive environment in the recharge areas of silicate clastics.

Figures 22 and 23 present the distribution of factor loadings F1 and F3 according to the variables, and factor scores according to sampling locations. Observed correlations are linked to a group of $\delta^{18}O$ and $\delta^{2}H$, and dissolution of carbonate minerals and cement (EC, HCO_3^-, Ca^{2+}, and Mg^{2+}) in the recharge areas of carbonate rocks, gravel, and sand. Further the anthropogenic influence (Na^+, K^+, NO_3^-, Cl^-, and SO_4^{2-}) on groundwater is observed mostly in the recharge areas of gravel and sand.

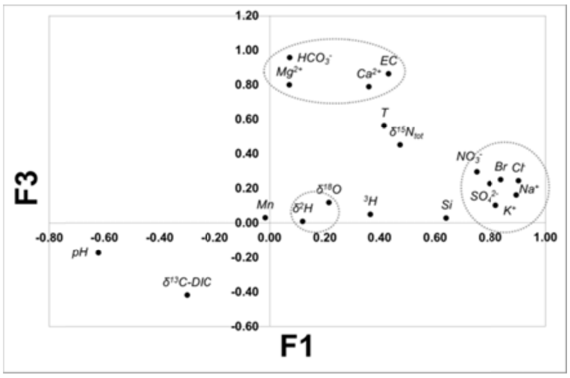

Figure 22: Factor loadings plot: F1 versus F3 according to variables

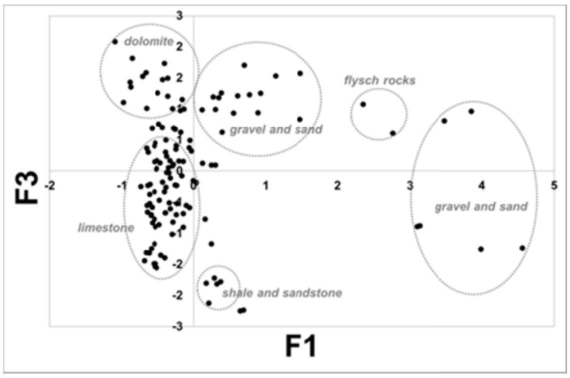

Figure 23: Factor scores plot: F1 versus F3 according to prevailing lithological unit in the recharge area

Cluster analysis (CA)

Cluster analysis (CA) was performed on the raw standardized dataset by Ward's method using squared Euclidean distance as similarity measure. The results of cluster analysis are shown in the form of hierarchical dendrogram (Fig. 24). The dendrogram consist of 17 variables: pH, $\delta^{13}C$-DIC, $\delta^{18}O$, $\delta^{2}H$, EC, Ca^{2+}, HCO_3^-, Mg^{2+}, $\delta^{15}N_{tot}$, Si, Mn, Na^+, Cl^-, Br, SO_4^{2-}, K^+, and NO_3^- of 176 water samples. Two variables were eliminated because they did not link to other variables on a bigger scale.

The first group links pH and $\delta^{13}C$-DIC suggesting enrichment in ^{13}C by increasing pH (and carbonate content) and co-variance of $\delta^{18}O$ and $\delta^{2}H$. Second group includes groundwater EC, Ca^{2+}, HCO_3^-, and Mg^{2+} which are linked to carbonate dissolution. Mg^{2+} is less correlated to HCO_3^- than Ca^{2+} since dissolution of limestone prevails in the recharge area of sampled water. Third group covers groundwater $\delta^{15}N_{tot}$, Si and Mn which are linked to reduction conditions in deeper aquifers. Fourth group links Na^+, K^+, Cl^-, Br, SO_4^{2-} and NO_3^-, suggesting anthropogenic influence on groundwater (fertilizers, manure, and waste water).

Subgroups in the second group join at about 50 %, and second and third group join on 70 %. Two major clusters are joined to each other at 100 %.

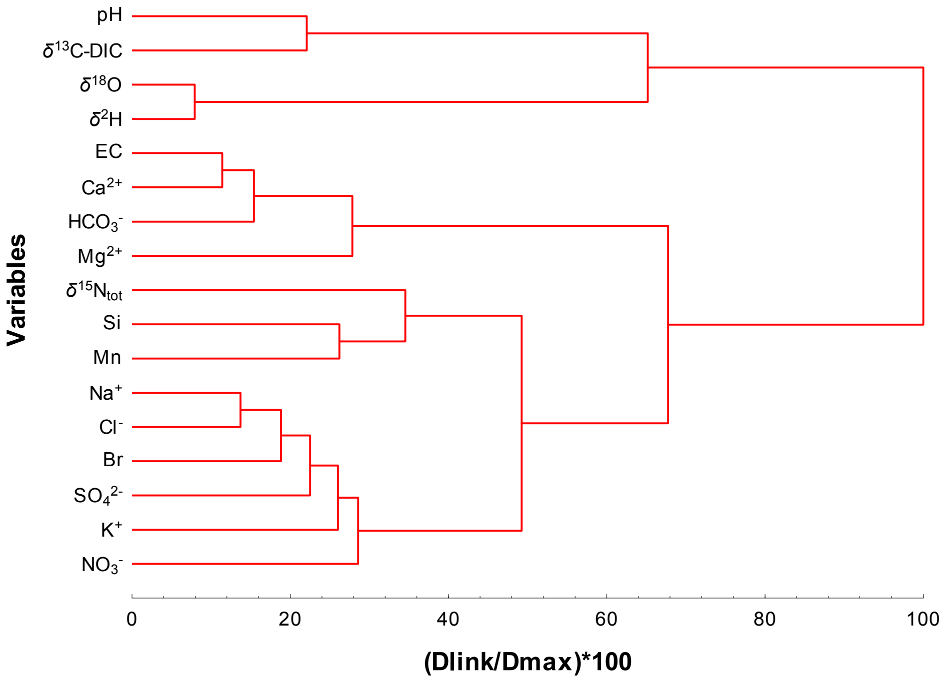

Figure 24: Cluster analysis dendrogram (n=176, 17 selected elements)

According to findings provided by the statistical data processing, occurrence and distribution in groundwater, the following section covers the interpretation of groundwater isotope ^{3}H, isotopic composition of $\delta^{18}O$, δD, $\delta^{13}C$-DIC, and $\delta^{15}N_{tot}$, physico-chemical parameters (pH and EC), major ions (Ca^{2+}, Mg^{2+}, Na^{+}, K^{+}, HCO_3^{-}, NO_3^{-}, Cl^{-}, SO_4^{2-}, and Si), secondary major ions (Fe and NH_4^{+}), and trace constituents (Br, Cr, and Mn). Chosen parameters have proven to be extremely important according to the interpretation of groundwater processes in the aquifers.

4.2. Age of Slovenian groundwaters

4.2.1. Tritium in Slovenian groundwaters

Descriptive statistics of groundwater ^{3}H

Groundwater ^{3}H activity varies between 0.45 TU and 11.77 TU, with mean value of 6.14 TU and median 6.01 TU (Tab. 13). Groundwater ^{3}H values are not normally distributed (Fig. 25) and values lower than 3.27 TU (VP-1 Prosenjakovci, Grad-1 Grad, DEV-1 Desenci, Ilirska Bistrica) and above 9.34 TU (Šumec, Mazej, Vt-1 Tinsko, Gradišče, Šumec, Trgovina Vurberk, TR-1 Trebelno) present outliers (Fig.26). The standard uncertainty of the measurement is between ±3 and ±33 %, and mean value of measurement uncertainties is ±12 % (Kožar Logar and Glavič-Cindro, 2009).

Table 13: Descriptive statistics of groundwater ^{3}H activity

Parameter	n	X	Md	Min	Max	S
^{3}H (TU)	172	6.14	6.01	0.48	11.77	1.69

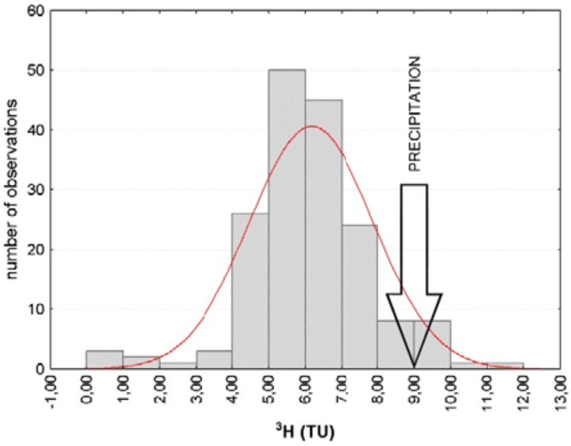

Figure 25: Histogram for groundwater ^{3}H activity (n=172)

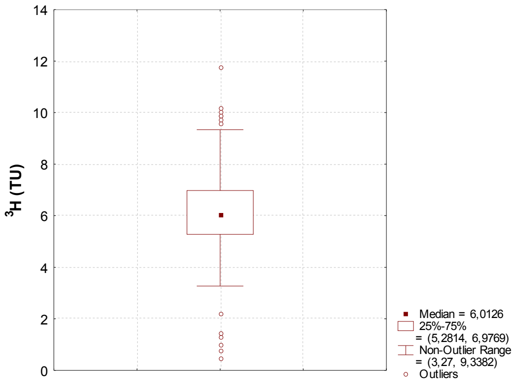

Figure 26: Box and whisker plot for groundwater ^{3}H activity (n=172)

Exponential model assumes exponential reduction of the ^{3}H in the groundwater with time. The input for model is the data on ^{3}H activities in precipitation measured since 1981 at Ljubljana precipitation station (GNIP database, 2013; Vreča *et al.*, 2008). In the model used ^{3}H activity in precipitation for each year were weighted by the precipitation volume shares, obtained by the exponential model (Urbanc, personal communication, 2013). The ^{3}H radioactive decay effect was also considered. The volume reduction with time is presented by a weighting function. Figure 27 presents the exponential model weighting functions for groundwater age of 10 years. Graph shows that at lower groundwater age the portion of ^{3}H from recent precipitation is higher, while the isotope signal decreases faster.

On the basis of weighted ^{3}H inputs from precipitation, ^{3}H activity in the groundwater was determined as a sum of yearly partial ^{3}H inputs. The results are presented on the graph (Fig. 28) showing the expected ^{3}H activity in the aquifer at various groundwater ages. In young groundwater (up to 5 years) ^{3}H activities occur in the range between 4.50 and 6.50 TU, and in the older waters higher ^{3}H activities are present due to nuclear tests in the sixties of 20th century (bomb tritium). For this groundwater the ^{3}H activities up to 8.00 TU are expected.

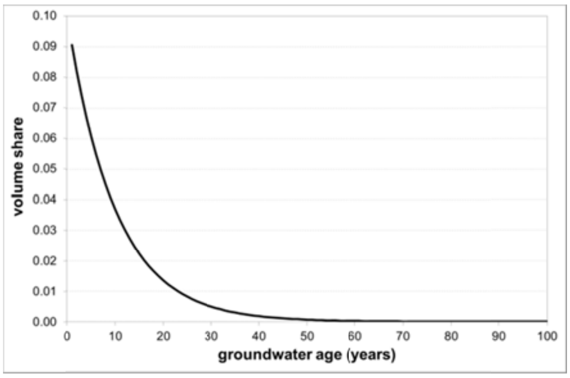

Figure 27: Exponential model weighting functions for groundwater age of 10 years

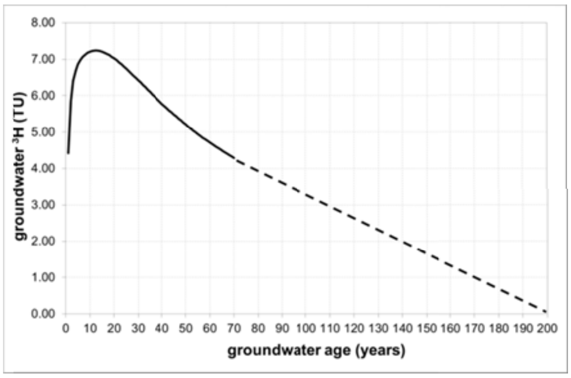

Figure 28: Exponential model for groundwater ^{3}H activity

It is evident from the graph that groundwater containing less than 2.00 TU is at least 140 years old, and the groundwater with ^{3}H activity below 1.00 TU at least 170 years old. Because of the specific characteristics of the tritium age curve, the exact tritium groundwater ages cannot be determined but it can provide the information to differ young groundwater from old groundwater. Similar approach was used also by other authors (Aston, 1985; Bradbury, 1991; Al-Charideh and Hasan, 2012).

Based on the ^{3}H activity in sampled groundwater it has been categorised as:

- old groundwater with natural pre-bomb tritium content (<2.00 TU),
- young (modern) groundwater (2.00 – 8.00 TU), which is up to 10 years old, and
- sub-modern groundwater (>8.00 TU) which is older water (sub-modern) (up to 50 years) and includes some "nuclear bomb tritium".

During sampling mostly groundwater which is closely related to recent precipitation events has been sampled (Tab. 14, Fig. 29). This has been verified by the ^{3}H activities of sampled groundwater and recent precipitation in Slovenia. ^{3}H activity of precipitation in Ljubljana (2002-2006) has a mean ^{3}H activity of about 9.0 TU (Fig. 25) (Vreča *et al.*, 2011) and is stil decreasing with more recent values of 5.0—8.0 TU (Logar Kožar, personal communication, 2013). Older groundwater (<0.5 TU) from deeper aquifers from NE part of the country is possibly younger than 1,000 years (Szőcs *et al.*, 2013). Since the ^{3}H activities in sampled groundwater (6.20 TU) are close to values measured in precipitation, it is expected that most of sampled groundwater is quite young.

Table 14: Groundwater age

Groundwater age	n	X	Md	Min	Max	S
modern groundwater (< 10 years)	165	6.24	6.04	2.21	10.14	1.37
old groundwater (50 to 1,000 years)	5	0.98	0.98	0.48	1.44	0.38
submodern groundwater with residence time up to 50 years	2	10.88	10.88	10.00	11.77	1.25

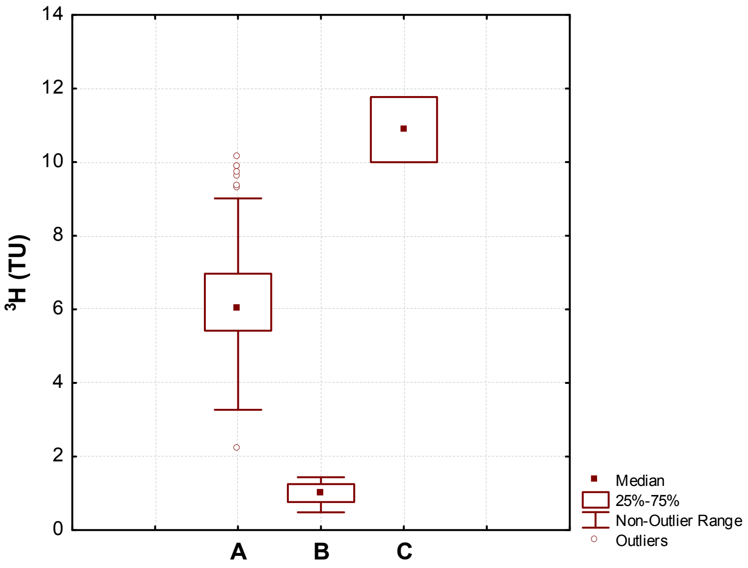

A = recent groundwater (n=165)
B = old groundwater (n=5)
C = groundwater up to 50 years old (n=2)

Figure 29: Box and whisker plots for groundwater ^{3}H activity according to groundwater age

Figure 30 presents the correlation between δ^{18}O and $\delta^2 H$ where older groundwater samples are plotted closely as they are depleted in ^{18}O and ^{2}H.

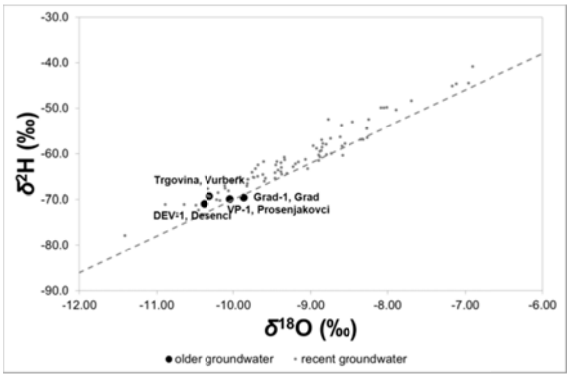

Figure 30: Correlation between groundwater $\delta^{18}O$ and δ^2H values

Additional description on ^3H activity in Slovenian groundwaters is found in Korun *et al.* (2011).

4.3. Isotopic composition of stable isotopes in Slovenian groundwaters

4.3.1. Groundwater oxygen isotopic composition ($\delta^{18}O$)

Descriptive statistics of groundwater $\delta^{18}O$

Groundwater $\delta^{18}O$ values vary between -11.43 ‰ and -6.49 ‰, with mean value of -9.25 ‰ and median value of -9.23 ‰ (Tab. 15). The isotope histogram (Fig. 31) shows that measured groundwater $\delta^{18}O$ is close to normally distributed, and variations of data in box and whisker plot (Fig. 32) show that outliers present groundwater enriched in ^{18}O (>7.07 ‰) at sampling locations Padiščak and P-1 Pliskovica which are close to the sea side.

Table 15: Descriptive statistics of groundwater $\delta^{18}O$

Parameter	n	X	Md	Min	Max	S
$\delta^{18}O$ (‰)	174	-9.25	-9.23	-11.43	-6.49	0.94

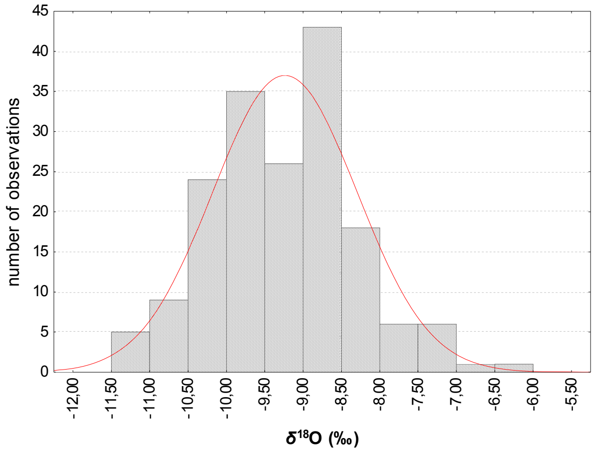

Figure 31: Histogram for groundwater $\delta^{18}O$ values (n=174)

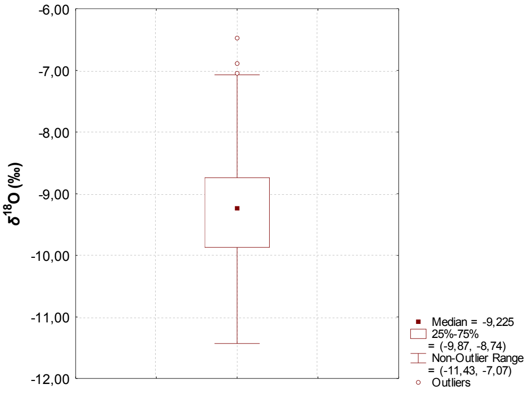

Figure 32: Box and whisker plot for groundwater $\delta^{18}O$ values (n=174)

Rock type

Groundwater is mostly depleted in ^{18}O in the recharge areas of igneous and metamorphic rocks (and in a few sampling locations in the carbonate rocks) (Fig. 33, Appendix 13A) which is significantly depleted in ^{18}O compared to groundwater in recharge areas of clastic sedimentary rocks and carbonates. Groundwater sampled in the high mountain regions receives isotopically depleted precipitation compared to groundwater in lowlands which recharge areas are in clastic sedimentary and carbonate rocks. Enriched in ^{18}O is groundwater sampled in clastic sedimentary rocks, located in vicinity of the seaside.

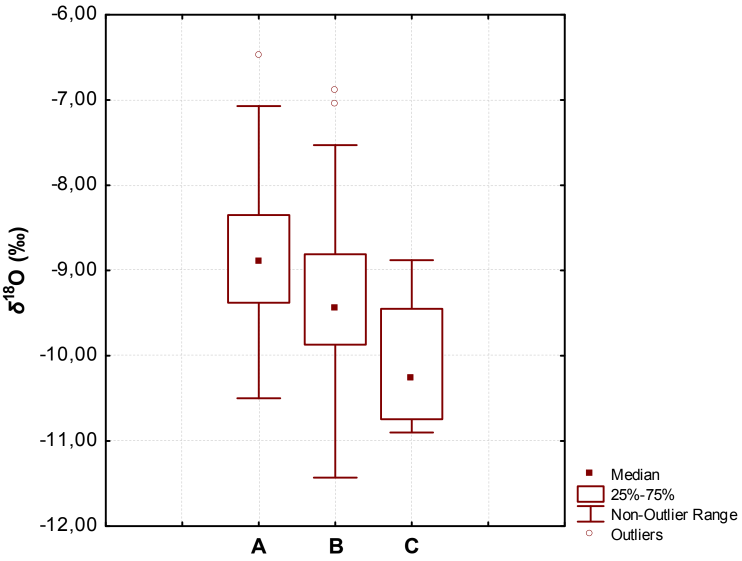

A = clastic sedimentary rocks (n=52)
B = carbonate rocks (n=110)
C = igneous and metamorphic rocks (n=12)

Figure 33: Box and whisker plots for groundwater δ^{18}O values in the recharge area of major rock types

Groundwater in the recharge areas with Eocene flysch rocks (Figs. 34 and 35, Appendix 13A) is significantly enriched ($p<0.05$) in ^{18}O compared to groundwater with recharge areas with Permian Val Gardena layers, Jurassic carbonates, Ladinian igneous rocks, Miocene Lithothamnium limestone, Oligocene igneous rocks, Pliocene clastics, Oligocene clay "sivica", old Paleozoic rocks, and Triassic carbonates. This is due to proximity of the Adriatic Sea and low elevation landscape. Groundwater sampled at higher altitudes (old Paleozoic rocks, and Triassic and Cretaceous carbonates) is depleted in ^{18}O due to receiving isotopically depleted precipitation. Groundwater with recharge areas in old Paleozoic metamorphic rocks is significantly depleted ($p<0.05$) in ^{18}O compared to groundwater with recharge areas with Cretaceous carbonates, Quaternary clastics (medium- and coarse-grained), Miocene clastics, and Carboniferous-Permian beds.

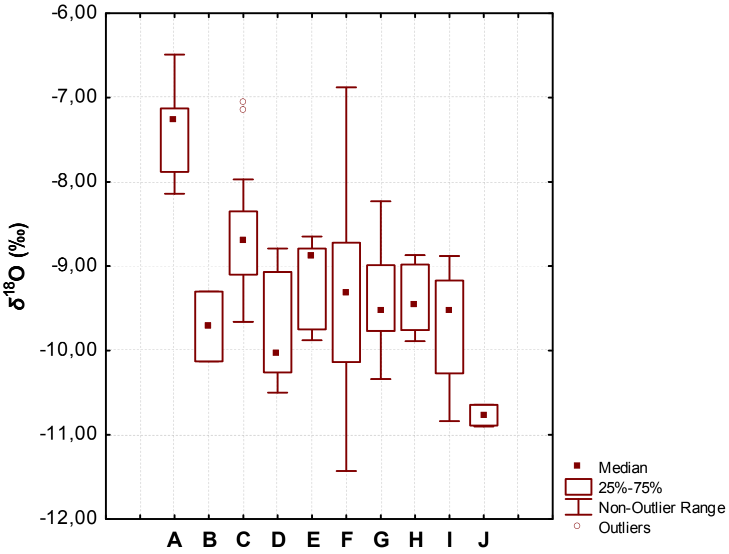

A = flysch rocks (n=6)
B = clay (n=2)
C = gravel and sand (n=26)
D = gravel, sand and clay (n=12)
E = shale and sandstone (n=6)
F = limestone prevailing (n=74)
G = dolomite prevailing (n=30)
H = carbonates with clastics (n=6)
I = igneous rocks (n=8)
J = metamorphic rocks (n=4)

Figure 34: Box and whisker plots for groundwater $\delta^{18}O$ values in the recharge area of prevailing lithological unit

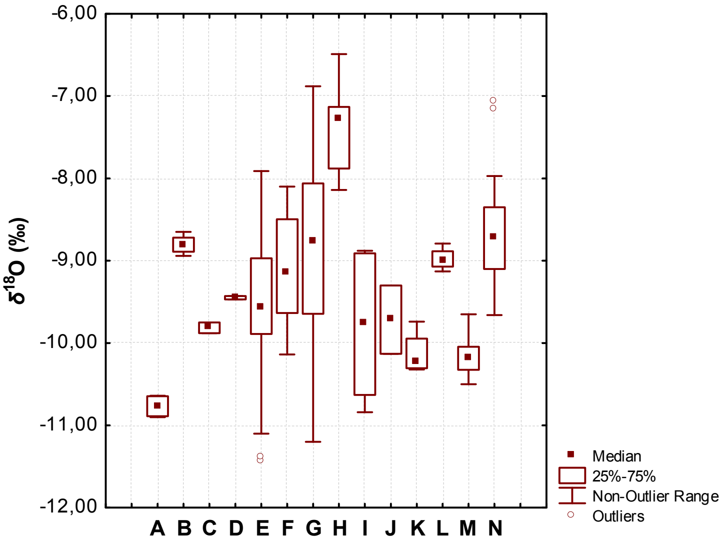

A = old Paleozoic rocks (n=4)
B = Carboniferous-Permian beds (n=4)
C = Permian Val Gardena layers (n=2)
D = Ladinian igneous rocks (n=2)
E = Triassic carbonates (n=70)
F = Jurassic carbonates (n=8)
G = Cretaceous carbonates (n=28)
H = Eocene flysch rocks (n=6)
I = Oligocene igneous rocks (n=6)
J = Oligocene clay "sivica" (n=2)
K = Miocene Lithothamnium limestone (n=4)
L = Miocene clastics (n=4)
M = Pliocene clastics (n=8)
N = Quaternary clastics (medium- and coarse-grained) (n=26)

Figure 35: Box and whisker plots for groundwater $\delta^{18}O$ values in the recharge area of prevailing lithostratigraphic unit

Since there is a relationship between the altitude and the mean air temperature, and groundwater ^{3}H activity confirmed the young groundwater age, a correlation between the groundwater isotopic composition and the mean air temperature is expected. For definition of the mean air temperature of the sampling location recharge area, a map of the spatial distribution of air temperatures with a resolution of 1–2 km was used (The average annual air temperature 1971–2000). The mean annual temperature of each sampling location has been estimated in ArcGIS according to its estimated recharge area. There is a positive correlation between $\delta^{18}O$ in groundwater and the mean annual temperature of the recharge area ($r_s = 0.56$, $p < 0.001$) (Fig. 36), as it has been reported by other authors (Wassenaar *et al.*, 2009). The mean groundwater $\delta^{18}O$ values from colder areas are more depleted in ^{18}O than those in lowlands as a consequence of the isotope altitude effect. The isotope temperature gradient is estimated at around 0.25 ‰ $\delta^{18}O$/°C, which coincides with estimated temperature gradients in precipitation of 0.11 ‰ $\delta^{18}O$/°C at the Portorož Airport station and 0.30 ‰ $\delta^{18}O$/°C at Ljubljana station (Vreča *et al.*, 2006a).

Good correlation between mean annual air temperature and mean altitude of recharge areas (Fig. 37) confirms their interdependence. At higher altitudes where mean temperatures are lower, the precipitation (and consequently groundwater) is isotopically depleted in ^{18}O (and ^{2}H).

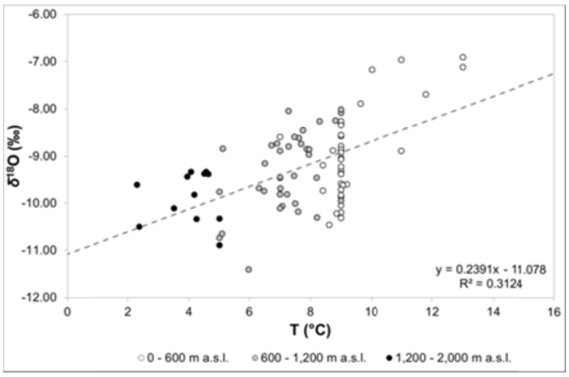

Figure 36: Groundwater $\delta^{18}O$ versus mean annual air temperature

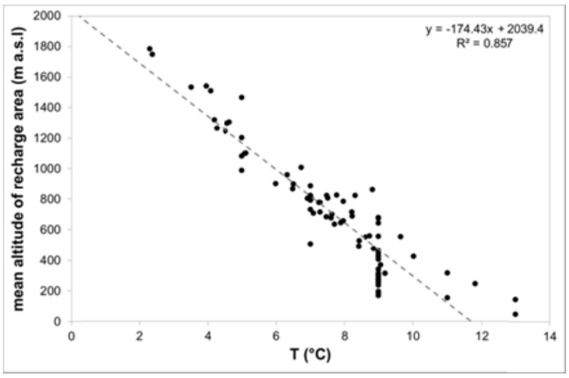

Figure 37: Mean annual air temperature versus mean altitude of recharge area

Aquifer porosity type

There are no significant differences between groundwater $\delta^{18}O$ and aquifer porosity type (Fig. 38, Appendix 13A).

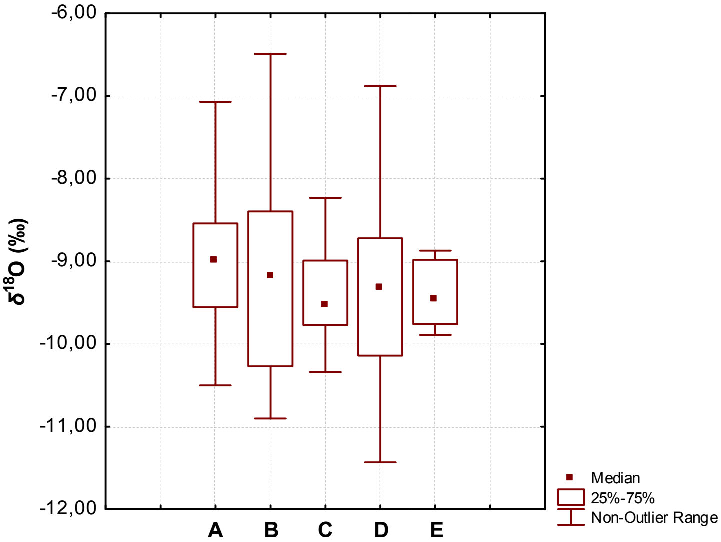

A = intergranular porosity (n=40)
B = fractured porosity (n=24)
C = fractured and karstic porosity (n=30)
D = karstic and fractured porosity (n=74)
E = mixed porosity (karstic, fractured, intergranular) (n=6)

Figure 38: Box and whisker plots for groundwater $\delta^{18}O$ values in the recharge area of the prevailing aquifer porosity type

Sampling object type

Groundwater is enriched in ^{18}O sampled from boreholes (Fig. 39, Appendix 13A) due to proximity of the seaside and recharge areas in lowlands. Depleted in ^{18}O is groundwater sampled from pumping stations (old groundwater) and in springs (high mountain regions).

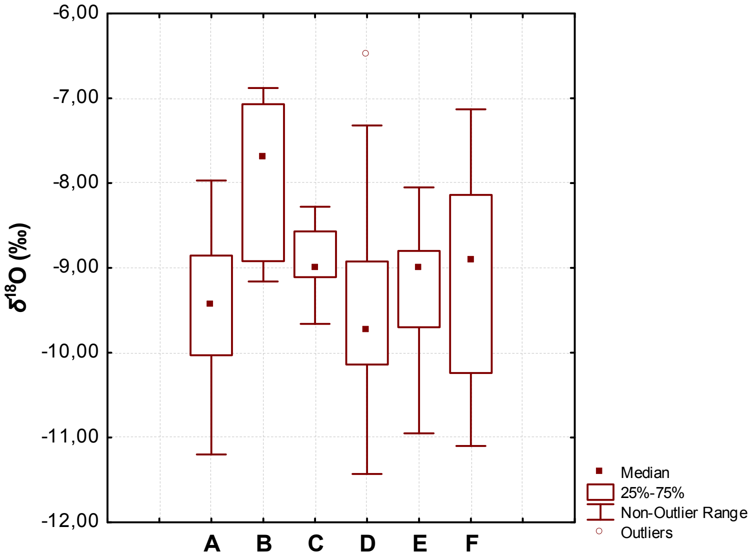

A = pumping station (n=36)
B = borehole (n=10)
C = private well (n=8)
D = spring capture (n=44)
E = spring (n=58)
F = surface water (n=18)

Figure 39: Box and whisker plots for groundwater δ^{18}O values according to sampling object type

Spatial distribution of groundwater δ^{18}O

The most enriched in ^{18}O is groundwater near the coast with low elevation in the recharge areas (Fig. 41, Appendix 11A). The inner continental waters receive ^{18}O depleted precipitation, as well as groundwater sampled at high elevations in the N-NW, N, and N-NE parts of the country (Karavanke Mts,. Alps region, and Pohorje Mt.).

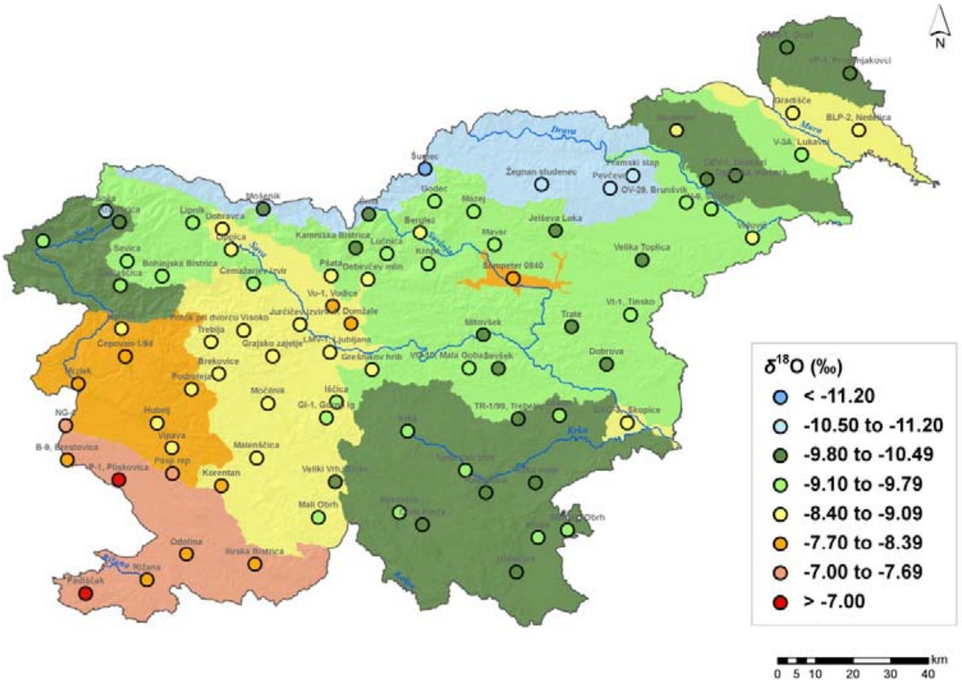

Figure 40: Spatial distribution of groundwater δ^{18}O

4.3.2. Groundwater deuterium isotopic composition (δ^2H)

Descriptive statistics of groundwater δ^2H

Groundwater δ^2H varies between -78.6‰ and -62.5‰, with mean value of -61.6‰ and median value of -62.5‰ (Tab. 16). Isotope histograms show that groundwater isotope data of δ^2H is close to normally distributed (Fig. 41), and variations of δ^2H values are shown in Figure 42. The outliers present groundwater enriched in ^{2}H (>44.0 ‰) at sampling locations Padiščak and Pasji rep which are close to the seaside.

Table 16: Descriptive statistics for groundwater δ^2H

Parameter	n	X	Md	Min	Max	S
δ^2H (‰)	174	-61.6	-62.5	-78.6	-40.6	7.5

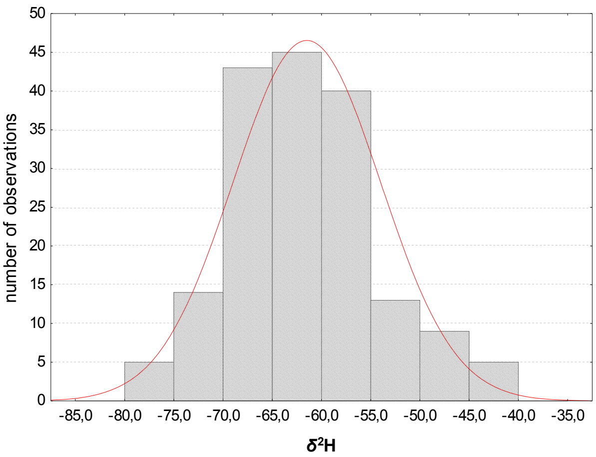

Figure 41: Histogram of groundwater δ^2H

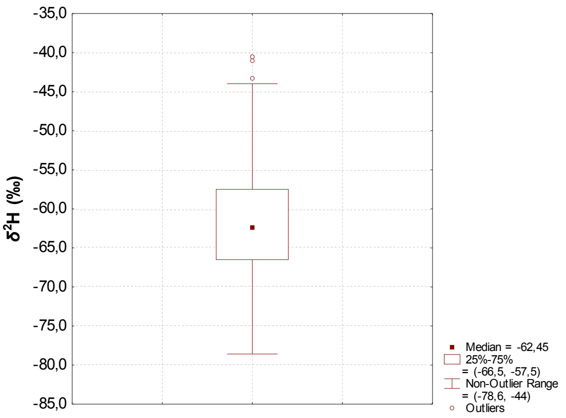

Figure 42: Box and whisker plot for groundwater δ^2H

Due to linear relationship between δ^{18}O and δ^2H which explains that isotopic fractionation factor of hydrogen is 8 times that of oxygen (Craig, 1961), the findings of groundwater δ^2H are similar to those observed with groundwater δ^{18}O.

Rock type

Mostly enriched in ^{2}H is groundwater in the recharge areas of clastic sedimentary rocks, located near the coastal side (Fig. 43, Appendix 13B). Groundwater is depleted in ^{18}O in the recharge area of igneous and metamorphic rocks (and in a few sampling locations in the carbonate rocks) which is significantly depleted in ^{18}O compared to groundwater in recharge areas of clastic sedimentary and carbonate rocks. This is because groundwater was sampled in the high mountain region which receives typically isotopically depleted ^{2}H precipitation.

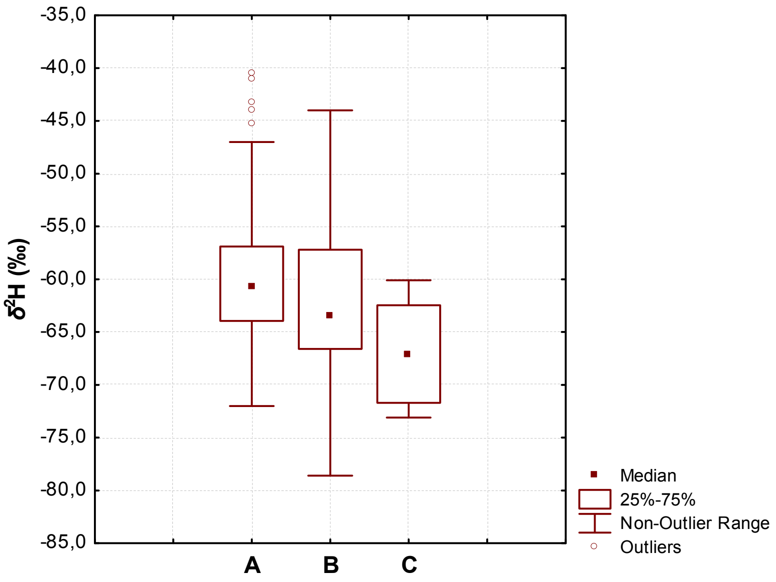

A = clastic sedimentary rocks (n=52)
B = carbonate rocks (n=110)
C = igneous and metamorphic rocks (n=12)

Figure 43: Box and whisker plots for groundwater δ^2H values in the recharge area of major rock types

Groundwater in the recharge areas of Eocene flysch rocks is the most enriched in ^{18}O (Figs. 44 and 45, Appendix 13B) and is significantly enriched ($p<0.05$) in ^{18}O compared to groundwater with recharge areas with Permian Val Gardena layers, Jurassic carbonates, Ladinian igneous rocks, Miocene clastics, Miocene Lithothamnium limestone, Oligocene igneous rocks, Pliocene clastics, Oligocene clay "sivica", old Paleozoic rocks, and Triassic carbonates. This is due to proximity of the Adriatic Sea and low elevated landscape. Groundwater sampled at higher altitudes (old Paleozoic rocks, and Triassic and Cretaceous carbonates) is depleted in ^{2}H due to receiving isotopically depleted precipitation.

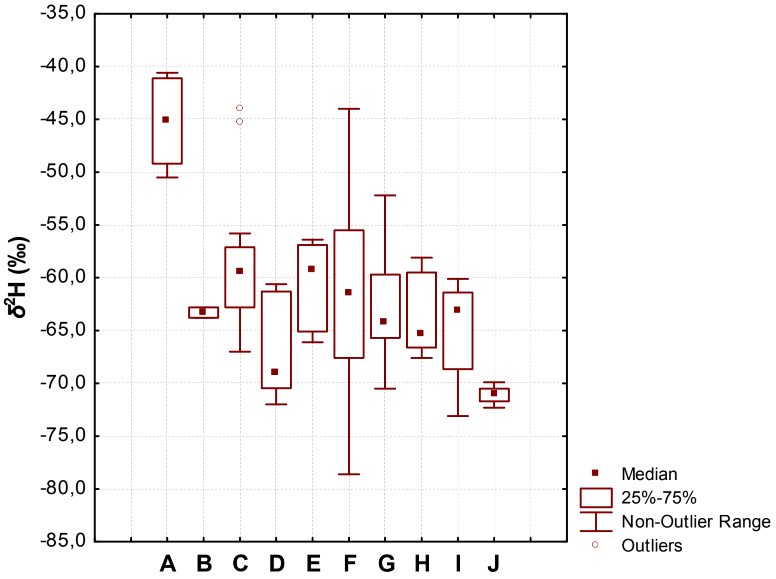

A = flysch rocks (n=6)
B = clay (n=2)
C = gravel and sand (n=26)
D = gravel, sand and clay (n=12)
E = shale and sandstone (n=6)
F = limestone prevailing (n=74)
G = dolomite prevailing (n=30)
H = carbonates with clastics (n=6)
I = igneous rocks (n=8)
J = metamorphic rocks (n=4)

Figure 44: Box and whisker plots for groundwater δ^2H values in the recharge area of prevailing lithological unit

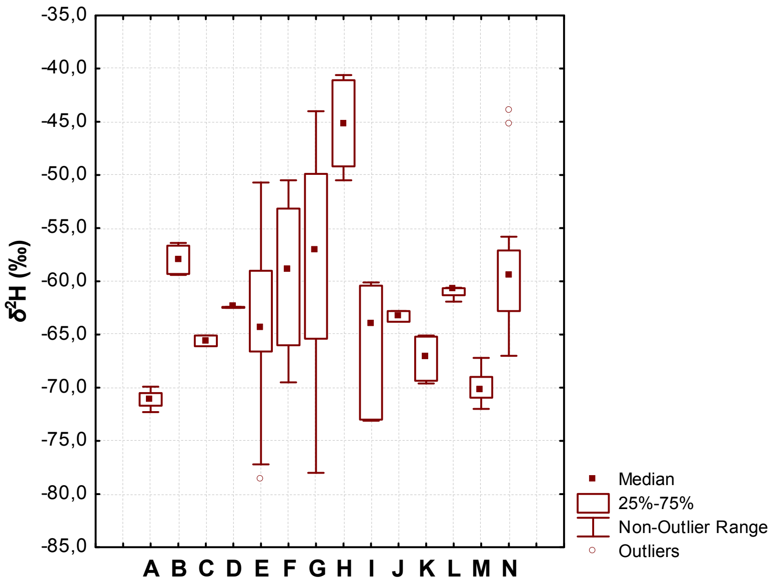

A = old Paleozoic rocks (n=4)
B = Carboniferous-Permian beds (n=4)
C = Permian Val Gardena layers (n=2)
D = Ladinian igneous rocks (n=2)
E = Triassic carbonates (n=70)
F = Jurassic carbonates (n=8)
G = Cretaceous carbonates (n=28)
H = Eocene flysch rocks (n=6)
I = Oligocene igneous rocks (n=6)
J = Oligocene clay “sivica” (n=2)
K = Miocene Lithothamnium limestone (n=4)
L = Miocene clastics (n=4)
M = Pliocene clastics (n=8)
N = Quaternary clastics(medium- and coarse-grained) (n=26)

Figure 45: Box and whisker plots for groundwater δ^{2}H values in the recharge area of prevailing lithostratigraphic unit

Aquifer porosity type

There are no significant dfifferences in groundwater δ^{2}H values and aquifer porosity type (Fig. 46, Appendix 13B) except of the large variance in distribution of groundwater δ^{2}H values in the aquifers with fractured, and karstic and fractured porosity. Both types of aquifers are observed near the coast and in the mountains.

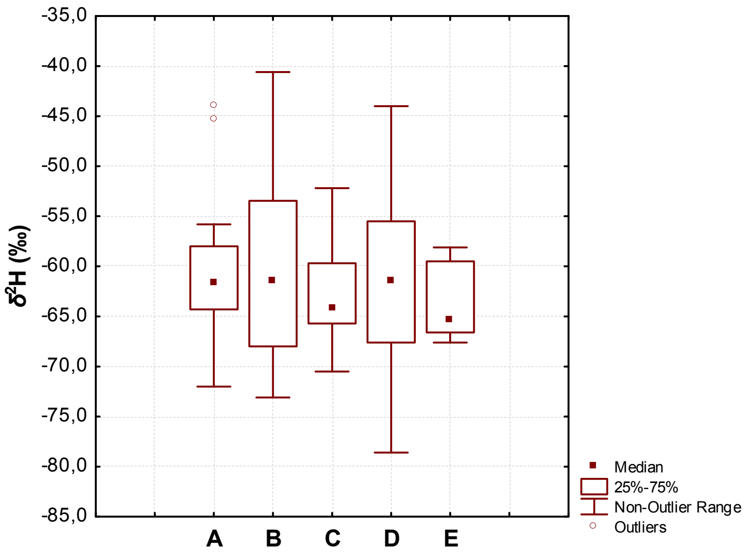

A = intergranular porosity (n=40)
B = fractured porosity (n=24)
C = fractured and karstic porosity (n=30)
D = karstic and fractured porosity (n=74)
E = mixed porosity (karstic, fractured, intergranular) (n=6)

Figure 46: Box and whisker plots for groundwater δ^{2}H values in the recharge area of prevailing aquifer porosity type

Sampling object type

Groundwater is enriched in ^{2}H sampled in boreholes (Fig. 47, Appendix 13B) due to proximity of the seaside and recharge areas in lowlands. Depleted in ^{2}H is groundwater sampled from pumping stations (old groundwater), and in springs (high mountain regions).

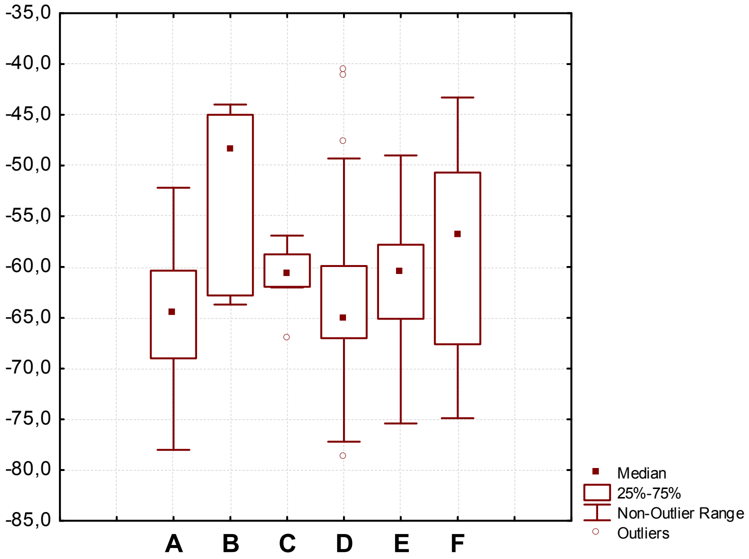

A = pumping station (n=36)
B = borehole (n=10)
C = private well (n=8)
D = spring capture (n=44)
E = spring (n=58)
F = surface water (n=18)

Figure 47 : Box and whisker plots for groundwater δ^2H values according to sampling object type

Spatial distribution of δ^2H in groundwater

Groundwater is enriched in ^{2}H in the SW part of the country near the coast (Fig. 48). The inner continental waters receive isotopically ^{2}H depleted precipitation, as well as groundwater sampled at high elevations in the N-NW, N, and N-NE part of the country (Karavanke Mts., Alps region, and Pohorje Mt.).

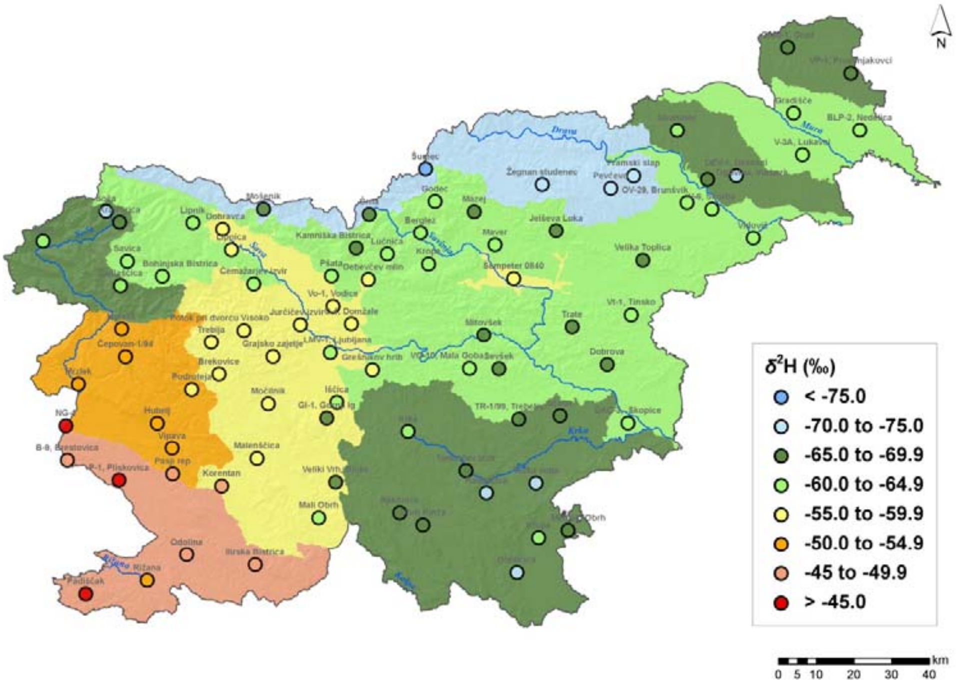

Figure 48: Spatial distribution of groundwater δ²H

4.3.3. Groundwater deuterium excess (d-*excess*)

Descriptive statistics of groundwater d-*excess*

Groundwater *d-excess* values vary between 6.0 ‰ and 21.4 ‰, with mean value of 12.4 ‰ and median 12.4 ‰ (Tab. 17). Histogram (Fig. 49) shows that groundwater *d-excess* is close to normally distributed (Fig. 50) and variations of d-*excess* are presented in Figure 50 with outliers (7.7<d-excess) observed at sampling location LMV-1 Ljubljana, and outliers (d-*excess*>17.1) at sampling locations Padiščak, Maver, and Hubelj.

Table 17: Descriptive statistics of groundwater d-excess

Parameter	n	X	Md	Min	Max	S
d-*excess* (‰)	174	12.4	12.4	6.0	21.4	2.0

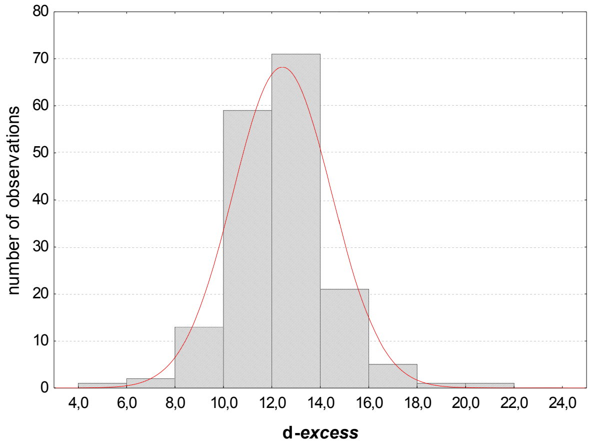

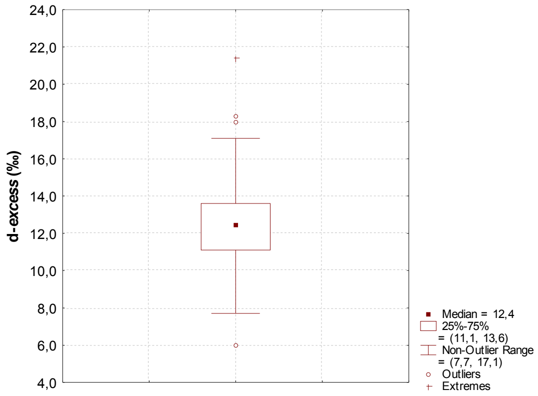

Figure 49: Histogram for groundwater d-excess (n=174)

Figure 50: Box and whisker plot for groundwater d-excess (n=174)

The d-*excess* in meteoric water depends on the elevation as well (Fig. 51, positive correlation). This suggests that precipitation which is recharging the aquifer could be influenced by site-specific secondary effects such as partial re-evaporation and isotope exchange of raindrops on their travel to the ground, due to the longer distance between the cloud base level and the ground, (high) relative humidity, and other factors described in more detail in Cruz-San *et al.* (1992), Peng *et al.* (2010) and others. Correlation between *d-excess* in groundwater and the altitude of the recharge area is positive and statistically significant ($r = 0.57$ and $p < 0.01$).

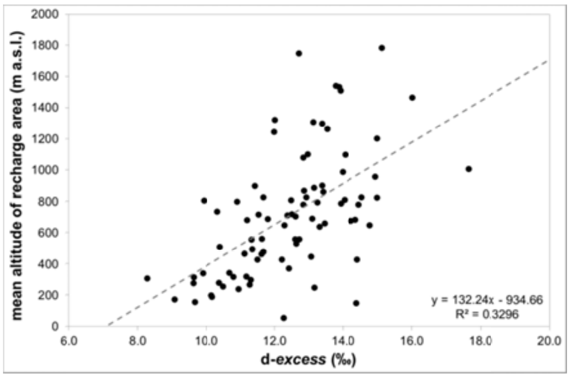

Figure 51: Mean d-excess values versus mean altitude of recharge areas for young groundwater

Spatial distribution of groundwater d-excess

The values of *d-excess* in groundwater suggest that the sampled groundwater is mainly recharged by Atlantic-derived precipitation (westerly circulation) while Mediterranean derived precipitation seems to be of minor importance as a precipitation source for the sampled groundwater (Fig. 52).

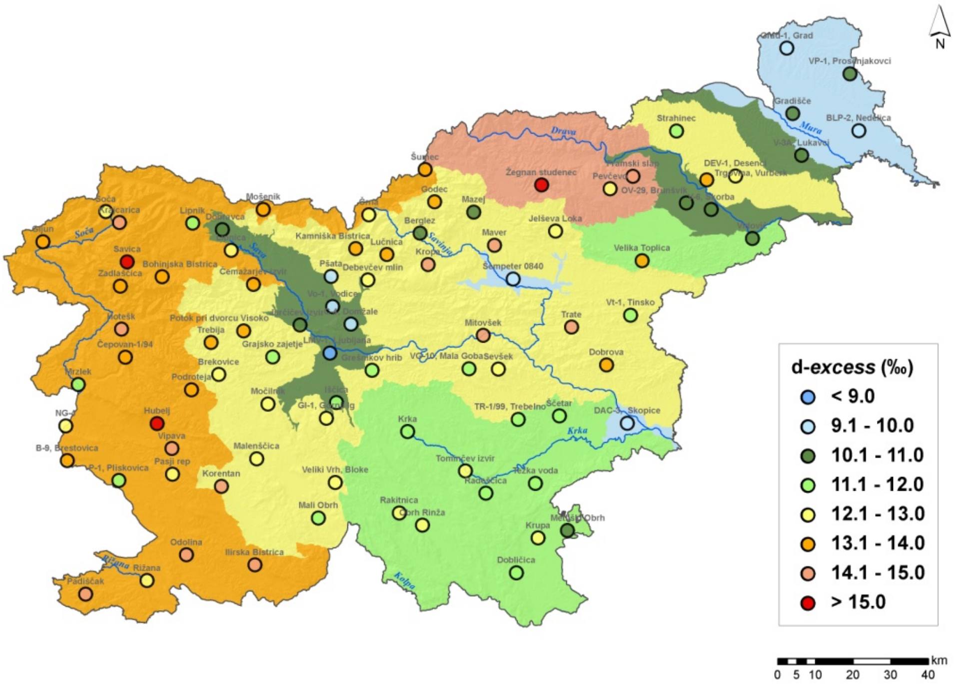

Figure 52: Spatial distribution of groundwater d-excess

Additional information on groundwater d-*excess* is found in the Appendix 13C.

4.3.4. Isotopic composition of Slovenian precipitation in comparison to groundwater

Comparison of isotopic composition in groundwater with precipitation

Groundwater samples were categorised based on ^{3}H activity into young and old groundwater (Tab. 18).

Table 18: Descriptive statistics of shallow (young) and deep (old) groundwater isotopic composition.

	shallow groundwater				deep groundwater			
	X	Min	Max	S	X	Min	Max	S
$\delta^{18}O$ (‰)	-9.21	-11.43	-6.49	0.94	-10.15	-10.5	-9.65	0.26
$\delta^{2}H$ (‰)	-61.2	-78.6	-40.6	7.4	-69.9	-72	-67.2	1.5
d-*excess* (‰)	12.44	6	21.4	2.03	11.29	8.6	14.8	1.84

The mean isotopic composition of oxygen (and hydrogen) in long-term measurements of precipitation at the meteorological stations at Ljubljana, Portorož Airport, and Kozina (Vreča *et al.*, 2010) was compared with isotopic composition measured in Slovenian groundwater (Tab. 19).

Table 19: Mean values of isotopic composition of Slovenian precipitation (meteorological stations Ljubljana, Portorož Airport, and Kozina) (Vreča et al., 2010) and groundwater.

	Precipitation			Groundwater
	Ljubljana	Portorož Airport	Kozina	Slovenia
$\delta^{18}O$ (‰)	-8.6	-6.3	-7.8	-9.21
$\delta^{2}H$ (‰)	-59	-40	-50	-61.2
d-*excess* (‰)	9.5	10.3	12.3	12.4

Groundwater isotopic composition of δ^{18}O and δ^{2}H are more depleted compared to values in precipitation. This is mostly because of altitude and continental effects (toward E), and lack of precipitation stations in the E part of the country. Additionally, the differences in isotopic composition are observed between groundwater and precipitation stations at the Portorož Airport and Kozina due to the proximity of the Adriatic Sea, where precipitation was more enriched in heavy oxygen (and hydrogen) isotopes comparing with the isotopic composition measured in the groundwater. The isotopic composition of the precipitation measured at the Portorož Airport and Kozina stations is more local and the time series of measurements is shorter than for the precipitation measured at the Ljubljana station, which is more representative due to its central location and the longer time series of measurements. Values of d-excess around 10 ‰ can be attributed to air masses coming mostly from the Atlantic (precipitation at Ljubljana and Portorož Airport), whereas higher values of d-*excess* suggest the additional greater influence of Mediterranean air masses (precipitation at Kozina and in Slovenian groundwater). Vreča *et al.* (2007) suggest that precipitation at the Kozina station is more complex to interpret due to its geographical position where there is a mixing of continental and Mediterranean air masses, and the presence of the strong northerly bora wind.

4.3.5. Groundwater isotope effects

The groundwater isotope altitude effect

Figure 53 presents the relation between groundwater δ^{18}O and the altitude of the recharge area for all corresponding sampling locations. The distribution of δ^{18}O values in groundwater decreases gradually with the increasing elevation of recharge area. Additionally, a grouping of sampling locations according to individual areas in Slovenia is observed.

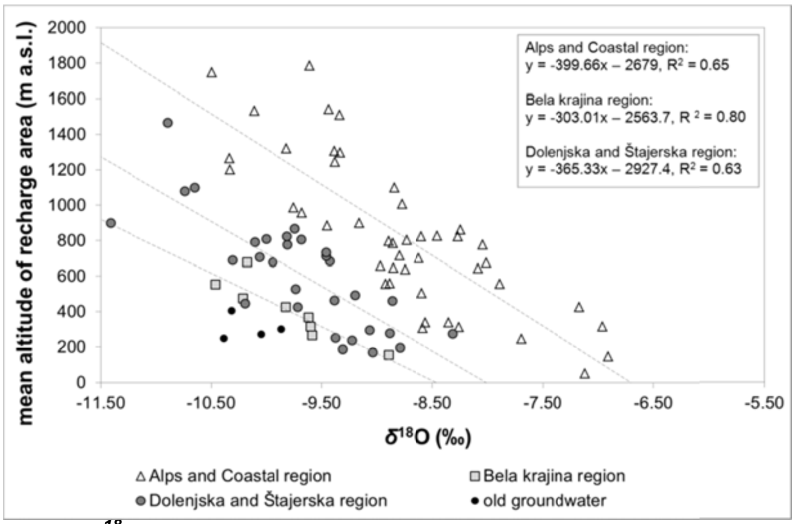

Figure 53: Groundwater δ^{18}O (V-SMOW) versus the altitude (altitude effect)

Comparison between groundwater δ^{18}O and the mean amount of precipitation (Fig. 54) shows that isotopically depleted in ^{18}O is groundwater in the high mountain regions (NE and N part). This area receives isotopically depleted precipitation (due to altitude effect) as well as greater amount of precipitation compared to other regions.

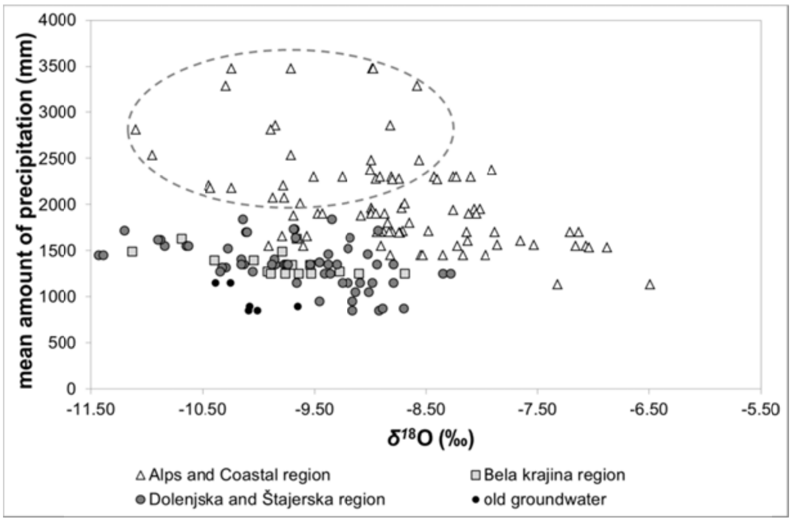

Figure 54: δ^{18}O (V-SMOW) versus mean amount of precipitation

The study area was divided into three regions (Fig. 55) with different groundwater isotope characteristics reflecting different precipitation formation history: (1) Alps and Coastal region, (2) Dolenjska and Štajerska region, and (3) Bela krajina region. Only young groundwater samples were included.

In the Figure 55 we can observe that the SW-NE direction of each group is generally in accordance with the prevailing precipitation trajectory. In Slovenia most of the important precipitation air masses that exceed a rain quantity of 50 L/m^2 generally come from the SW (Kegel, 2008). Statistical evaluation shows that 35 % of the intensive rain air masses come from the SW, 34 % from S-SW and 18 % from S.

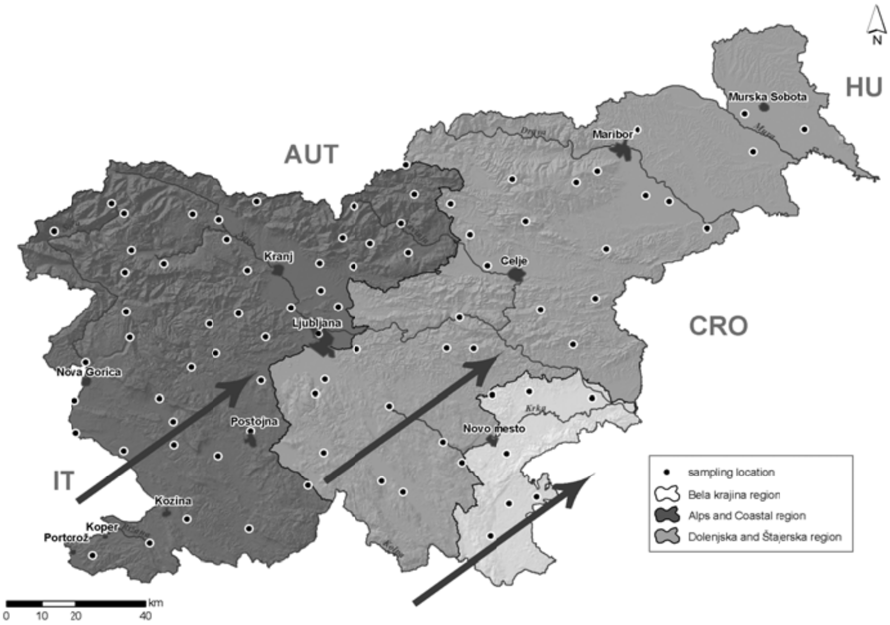

***Figure 55*: Spatial partition of studied area in three regions with prevailing precipitation trajectory directions**

A major role is also played by relief characteristics, which determine orographic precipitation formation processes, and are reflected further in the oxygen and hydrogen isotope composition in precipitation. In this frame, the orographic barriers of the Trnovo–Banjšice plateau on the west and the Dinaric Gorski Kotar massif on the east side of the study area play an important role, inducing strong orographic precipitation in SW wind situations (Rakovec *et al.*, 2003).

The radar pictures of a precipitation event in July 2009 and February 2013 (Figs. 56 and 57) show a prevailing precipitation direction and the meteorological situation where the SW parts of Slovenia (Alps and Coastal region) receive more rain than the SE part.

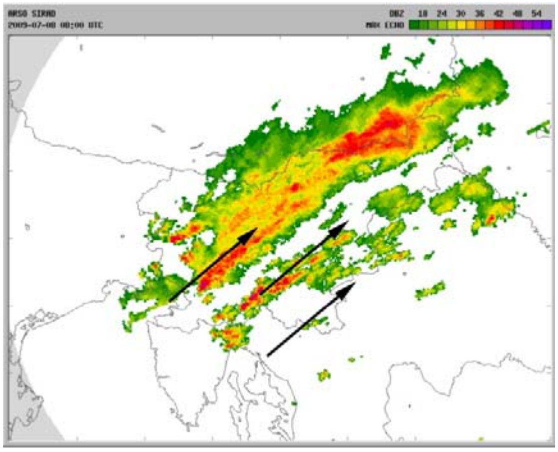

Figure 56: Radar picture showing a typical precipitation pathway (8 July 2009) (Report of the heavy rain from 6th to 10th July 2009)

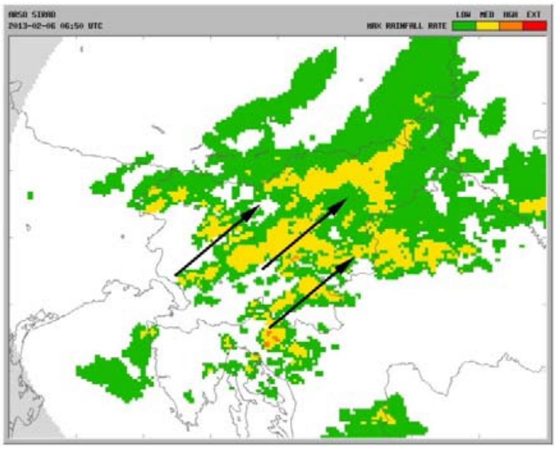

Figure 57: Radar picture showing a typical precipitation pathway (6 February 2013) (Radar precipitation measurement from 6th of February 2013)

For all three regions, the isotope altitude effect was calculated by adding the trend line on the scatter plot of mean altitudes of the recharge areas, compared with the mean values of δ^{18}O in the water. δ^{2}H variations in groundwater match equally well, as expected.

From the Fig. 53 it is observed that statistically significant correlation exists between δ^{18}O in groundwater and the mean altitude of the recharge area in the Alps and Coastal region. The altitude effect (total 45 sampling locations) is -0.25 ‰ δ^{18}O/100 m ($r=-0.81$, $p<0.001$) and -2.25 ‰ δ^{2}H/100 m ($r=-0.7$, $p<0.001$). Statistically significant correlation was observed also for the Štajerska and Dolenjska region. The altitude effect (total 30 sampling locations) is -0.27‰ δ^{18}O/100 m ($r=-0.79$, $p<0.001$) and -1.84‰ δ^{2}H/100 m ($r=-0.7$, $p<0.001$). The groundwater isotopic composition in Bela krajina region is more uniform within a limited area, and variations in isotopic values are small. The correlation is statistically significant, with an altitude effect (total 8 sampling locations) of -0.33 ‰ δ^{18}O/100 m ($r=-0.89$, $p<0.01$) and -2.40 ‰ δ^{2}H/100 m ($r=-0.89$, $p<0.01$) (Mezga *et al.*, 2014).

The calculated isotope altitude effects derived from groundwater samples are comparable to the estimated altitude effects in precipitation from the past researches in Slovenia and neighbouring countries. For example, for the Slovenian coastal part, the isotope altitude effect is -0.3 ‰ δ^{18}O/100 m (Vreča *et al.*, 2006a), for the central part of Slovenia -0.2 ‰ δ^{18}O/100 m (Brenčič and Poltnig, 2008), for Slovenia and Croatia -0.37 ‰ to -0.26 ‰ δ^{18}O/100 m (Horvatinčić *et al.*, 2005), in Austria -0.21 ‰ δ^{18}O/100 m (Kralik *et al.*, 2003) and in Italy close to -0.2 ‰ δ^{18}O/100 m (Longinelli and Selmo, 2003).

Isotopic composition of sampled water compared to meteoric water lines

Mean values of δ^{18}O and δ^{2}H in groundwater are plotted on a δ^{18}O-δ^{2}H graph (Fig. 58) compared with various precipitation' meteoric water lines; GMWL, EMMWL, and LMWLs for Ljubljana, Zagreb (Croatia), and Italy (Northern, Central, and Southern). As expected, a close linear relationship between δ^{18}O and $\delta^{2}H$ is seen where the slope between oxygen and hydrogen is approximately eight times greater for oxygen than hydrogen.

The comparison of δ^{18}O and δ^{2}H values in the sampled water shows that the majority of water samples fall between reference GMWL and EMMWL. Water samples from the Alps and Coastal regions lie between the GMWL and EMMWL lines, while LMWLs for Italy (North, Central and South) lie in between, suggesting some influence from the air masses coming from the Mediterranean Sea. Water from the Štajerska and Dolenjska region lies between the LMWL of Central Italy and Ljubljana, where the influence of the Mediterranean is less visible. A similar situation occurs in the case of waters from the Bela krajina region, where samples are plotted between the GMWL and LMWL of North Italy. Isotopic compositions that have been affected by evaporation are usually plotted below the GMWL (Kendall and McDonnell, 1998).

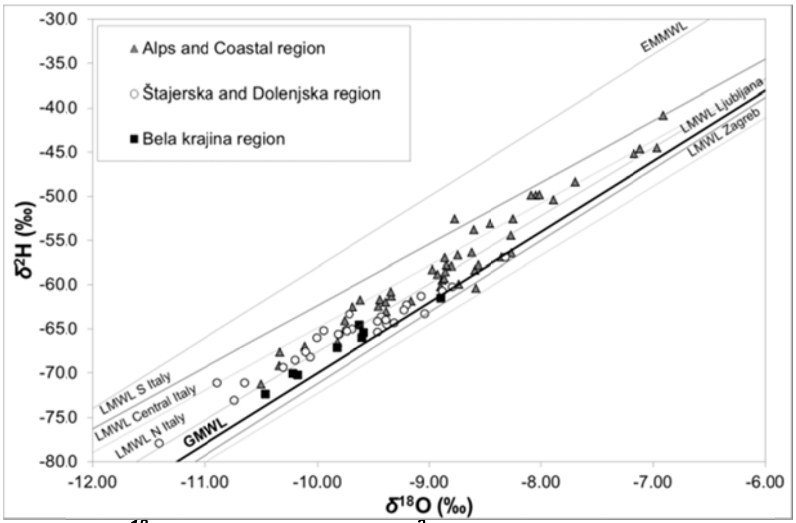

Figure 58: Mean values of δ^{18}O (V-SMOW) versus δ^{2}H (V-SMOW) for groundwater samples compared to GMWL, EMMWL and a few LMWLs

The groundwater isotope effect of distance from the sea (isotope continental effect)

In order to trace the variation change of δ^{18}O (and δ^{2}H) in precipitation during transit over the Slovenian territory in groundwater, we considered the main direction of the precipitation's progress. Because of the orographic influence of the Alps, the main precipitation pathway to the Slovenian territory passes from the Atlantic Ocean over the Mediterranean and onwards to the N-E. In order to evaluate this effect, the direct (air) distance from the south-west at the Coast (Adriatic Sea) to the north-east Prekmurje region was considered. Only 9 sampling locations, with a similar mean altitude of their recharge areas, were considered in this direction (Fig. 59). The calculated groundwater isotope effect of distance from the sea for Slovenian waters is approximately –0.83 ‰ δ^{18}O/100 km ($r = -0.89$, $p < 0.001$) (Mezga *et al.*, 2014).

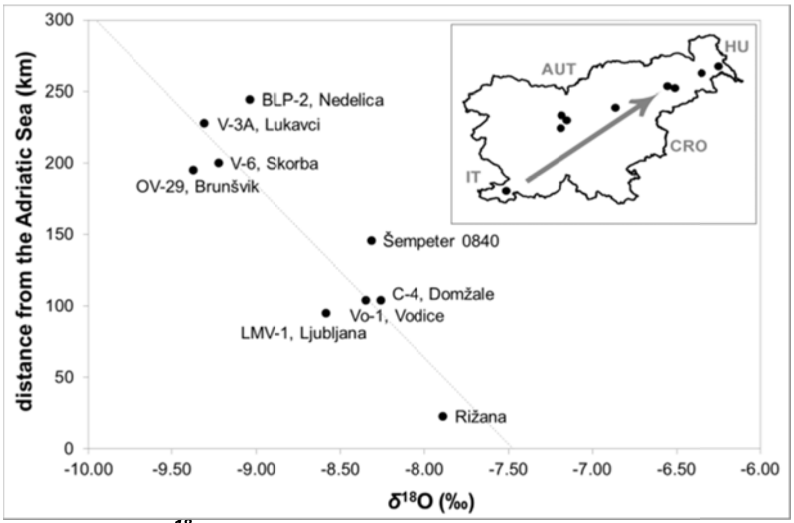

Figure 59: Mean groundwater $\delta^{18}O$ (V-SMOW) versus distance from the sea

Not much information is available about the precipitation values of the isotope continental effect in neighbouring countries. In present day European precipitation, the continental effect is around -2.0 ‰ $\delta^{18}O$/1000 km (Różański *et al.*, 1993) and in France -3.2 ‰ $\delta^{18}O$/1000 km (Millot *et al.*, 2010). We believe that the considerable isotope effect observed in Slovenia (-8.3 ‰ $\delta^{18}O$/1000 km) is a result of the specific relief conditions in Slovenia. Mountain barriers near the coastal area cause intensive precipitation, resulting in heavy depletion of heavy oxygen and deuterium from the air mass. The final result is a great continental isotope effect in the precipitation at a relatively short distance, which is reflected further in the groundwater isotope composition.

The most enriched in ^{18}O is groundwater at low elevations in the coastal areas, while groundwater at higher altitudes and in the inner part of the country (with increasing distance from the seaside) is isotopically depleted in ^{18}O. Similar observations are seen with $\delta^{2}H$ in sampled water. Based on the groundwater isotopic data and the geographic and climatic diversity of the study area, three different isotopic altitude effects zones were defined, following the precipitation intensity pattern with general direction of SW-NE. The isotope altitude effect for Alps and Coastal region is -0.25 ‰ $\delta^{18}O$/100 m, for the Štajerska and Dolenjska regions it is -0.27 ‰ $\delta^{18}O$/100 m, and for the Bela krajina region -0.33 ‰ $\delta^{18}O$/100 m. Furthermore, isotopic composition of groundwater is plotted mostly between GMWL and EMMWL suggesting groundwater reflects the isotopic composition of precipitation discharging mostly from Atlantic air masses, as well as from the Mediterranean basin, which has been indicated by higher d-*excess* values (> 10 ‰). Comparison between groundwater $\delta^{18}O$ and distance from the Adriatic Sea to Prekmurje region (SW-NE direction) indicates the presence of a strong ^{18}O isotope effect, with a value around -8.30 ‰ $\delta^{18}O$/1000 km. The magnitude of estimated effect is larger in comparison to precipitation isotope continental effects found in neighbouring countries. This could be due to Slovenian specific topography where air masses are influenced by relatively high altitude mountains not far from the coastal area. Additional comparison between mean annual air temperature of recharge area and groundwater isotopic composition has revealed, that groundwater from colder areas is isotopically depleted as compared to groundwater in lowlands. This is a consequence of the isotope altitude effect. The groundwater isotope temperature gradient was estimated and is around 0.25‰ $\delta^{18}O$/°C. Finally, groundwater in lowlands/valleys has lower d-*excess* values compared to groundwater in high mountain regions, which could be a result of isotopic fractionation during orographically uplifted air masses, or of other processes.

4.4. General geochemistry of Slovenian groundwaters

4.4.1. Ion pattern and hydrofacies

The descriptive statistics of major ion concentrations are given in Appendix 11. It is evident from the Fig. 60 that in sampled groundwater the dominant cation in groundwater is Ca^{2+} (range from 2-152 mg/L) and HCO_3^- by far the most dominant anion (19-575 mg/L).

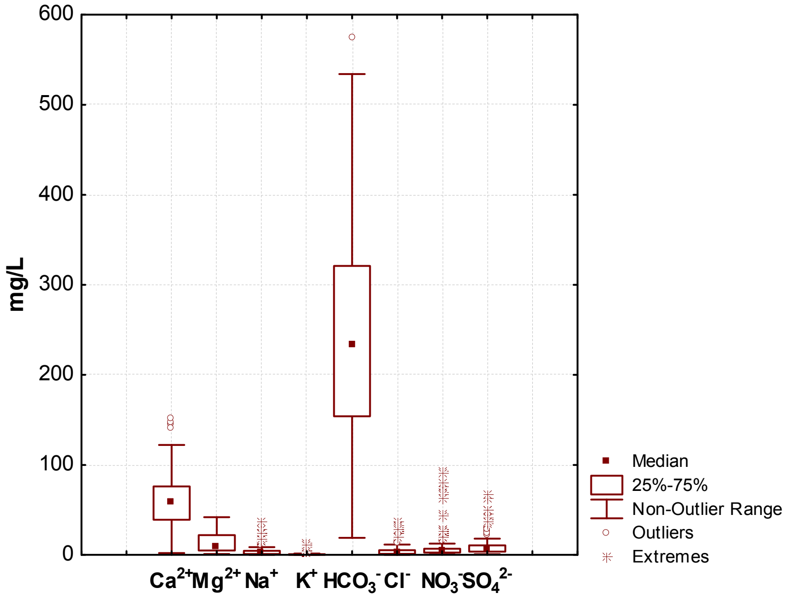

Figure 60: Box and whisker plots of major chemical ions in sampled groundwater

Ion pattern and hydrofacies characterisation showed that the majority of Slovenian groundwaters belong to calcium-magnesium rich waters characterized as Ca^{2+}-Mg^{2+}-HCO_3^- and Ca^{2+}-HCO_3^- waters (Table 19). Groundwater Ca^{2+}, Mg^{2+} and HCO_3^- contents result from dissolution of carbonate rocks prevailing in the recharge areas of sampled groundwater. This water is dominated by earth alkali elements and weak acids. Groundwater also has Na^+-Ca^{2+}-Mg^{2+}-HCO_3^- and Ca^{2+}-Na^+-HCO_3^- water types, which contain beside earth alkali elements and weak acidic anions also more alkali metals. The minority of water samples belongs to Ca^{2+}-Mg^{2+}-HCO_3^--NO_3^-, Ca^{2+}-HCO_3^--SO_4^{2-}, and Ca^{2+}-Mg^{2+}-HCO_3^--SO_4^{2-} water types, where water contains more strong acidic anions. It is believed that the source of NO_3^- in groundwater comes from leaching from the soil in agriculture and urban land uses. The source of SO_4^{2-} in groundwater in high mountain region is likely of natural origin from carbonate rocks containing gypsum (Brenčič and Polting, 2008; Vidrih, 2006).

The 7 sampling locations (Tab. 20) marked with asterisk in bold show different water types according to seasonal samplings. For instance, in one season the Ca^{2+}-HCO_3^- water is characteristic, whereas in other season the Ca^{2+}-Mg^{2+}-HCO_3^- water. This suggest that limestone as well as dolomite prevail in the recharge areas, what is also seen in the variations of groundwater Ca^{2+}/Mg^{2+} molar ratio.

Table 20: Water types according to sampling locations (sampling locations marked with asterisk have different water types between seasons)

Ca^{2+}-HCO_3^-	B-9 Brestovica, Berglez, Brekovice, Čemažarjev izvir, Debevčev mlin, Dobličica, Gljun, Godec, Gradišče, Hotešk, **Hubelj***, Ilirska Bistrica, **Kamniška Bistrica***, Korentan, **Krajcarica***, Kropa, Krupa, Lipnica, Lipnik, Malenščica, Mali Obrh, Metliški Obrh, Mitovšek, **Močilnik***, Mrzlek, NG-4, Obrh Rinža, Odolina, Padiščak, Pasji rep, Pšata, Radeščica, **Rakitnica***, Rižana, Savica, **Soča***, Težka voda, Tominčev izvir, Vidovič, Vipava, Vo-1 Vodice, Žegnani studenec
Ca^{2+}-HCO_3^--SO_4^{2-}	Grešnikov hrib
Ca^{2+}-Mg^{2+}-HCO_3^-	Bohinjska Bistrica, C-4 Domžale, Čepovan-1/94, Črna, DAC-3 Skopice, DEV-1 Desenci, Dobravca, Dobrova, GI-1 Gornji Ig, GRAD-1 Grad, Grajsko zajetje, **Hubelj*,** Iščica, Jelševa loka, Jurčičev izvir, **Kamniška Bistrica***, **Krajcarica***, Krka, LMV-1 Ljubljana, Lučnica, Mazej, **Močilnik***, **Mošenik***, OV-29 Brunšvik, P-1 Pliskovica, Podroteja, Potok pri dvorcu Visoko, **Rakitnica***, Sevšek, **Soča***, Strahinec, Ščetar, Šempeter 0840, Šumec, TR-1 Trebelno, Trate, Trebija, Trgovina Vurberk, V-3A Lukavci, V-6 Skorba, Velika Toplica, Veliki Vrh, Bloke, VG-10 Mala Goba, VP-1 Prosenjakovci, Vt-1 Tinsko, Zadlaščica
Ca^{2+}-Mg^{2+}-HCO_3^--NO_3^-	BLP-2 Nedelica
Ca^{2+}-Mg^{2+}-HCO_3^--SO_4^{2-}	**Mošenik***
Ca^{2+}-Na^+-HCO_3^-	Maver
Na^+-Ca^{2+}- Mg^{2+}-HCO_3^-	Framski slap, Pevčevo

Figure 66 presents the prevailing shares of various water types in sampled groundwater. Groundwater of Ca^{2+}-Mg^{2+}-HCO_3^- and Ca^{2+}-HCO_3^- water types prevailes which reflects the prevailing rock type (limestones, dolomites, and alluvial clastic sediments) in the recharge areas of sampled groundwater (Fig. 67).

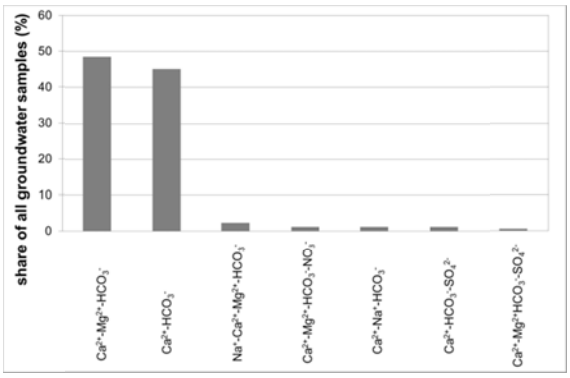

Figure 61: Shares of water types in groundwater

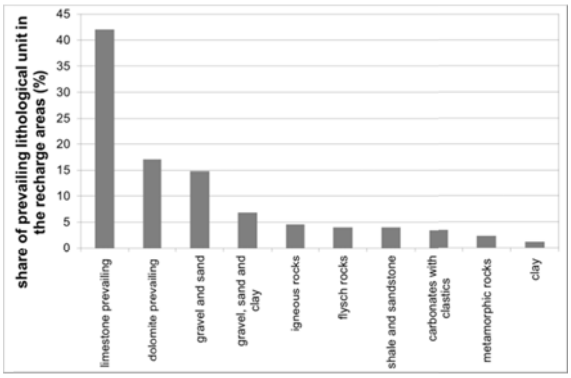

Figure 62: Shares of prevailing lithological units in observed recharge areas

Table 21 presents the types and number of sampled groundwater regarding the lithology and sampling location of recharge area (n=175). Ca^{2+}-HCO_3^- water type is observed in the recharge areas of flysch, gravel, sand (and clay), limestone, and dolomite.

Table 21: Water types according to prevailing lithological unit in the recharge areas (1 water sample excluded)

			Water type						
Rock type group	Geology	n	Ca^{2+}-HCO_3^-	Ca^{2+}-HCO_3^--SO_4^{2-}	Ca^{2+}-Mg^{2+}-HCO_3^-	Ca^{2+}-Mg^{2+}-HCO_3^--NO_3^-	Ca^{2+}-Mg^{2+}-HCO_3^--SO_4^{2-}	Ca^{2+}-Na^+-HCO_3^-	Na^+-Ca^{2+}-Mg^{2+}-HCO_3^-
Clastic sedimentary rocks	flysch rocks	7	7						
	clay	2						2	
	gravel, sand	26	6		18	2			
	gravel, sand and clay	11	2		9				
	shale and sandstone	7		2	5				
Carbonate rocks	limestone prevailing	74	52		21		1		
	dolomite prevailing	30	2		28				
	carbonates with clastics	6	2		4				
Igneous and metamorphic rocks	igneous rocks	8	6						2
	metamorphic rocks	4	2						2

Although Na^+ and Cl^- concentrations are generally low in most groundwater, their concentrations can be relatively high locally and the waters may tend toward the Na–K–Cl type. Water samples indicated by dashed circle (Fig. 63) belong to intergranular aquifers in north-eastern part of Slovenia where groundwater contains elevated concentrations of Cl^- and SO_4^{2-} and less HCO_3^-. The sources of both solutes in groundwater are likely anthropogenic. Water samples circled by the solid line have their recharge areas in metamorphic rocks and in clay, and contain more alkali metals. The observed trend could be a consequence of cation-exchange (natural water softening) in clay minerals, or a process of plagioclase mineral (albite) weathering.

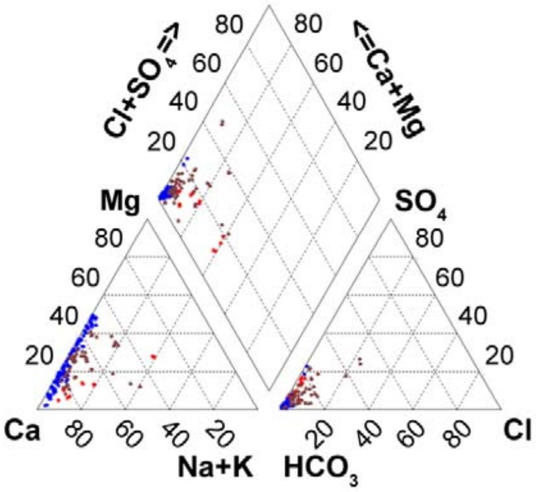

Figure 63: Piper diagram showing the composition of groundwater in the study area (**blue** ***– carbonate rocks: limestone prevailing, dolomite prevailing, carbonates with clastics;*** **brown** ***– clastic sedimentary rocks: flysch rocks, clay, gravel and sand, gravel, sand and clay, shale and sandstone;*** **red** ***- igneous and metamorphic rocks)***

4.4.2. Groundwater saturation indices (SI) of calcite (SI_{cal}) and dolomite (SI_{dol})

Most Slovenian groundwaters in the recharge areas of carbonate rocks and some clastic sedimentary rocks (Tab. 22) are supersaturated with respect to calcite and dolomite where SI_{cal} and SI_{dol} are mostly positive up to 1.

Table 22: **Groundwater SI with respect to calcite and dolomite**

major rock type	lithological unit	SI_{cal}	SI_{dol}
clastic sedimentary rocks	flysch rocks	**0.65**	**0.50**
	clay	**0.13**	*-0.26*
	gravel and sand	**0.03**	*-0.30*
	gravel, sand and clay	*-0.08*	*-0.41*
	shale and sandstone	*-0.89*	*-1.99*
carbonate rocks	limestone prevailing	**0.29**	*-0.04*
	dolomite prevailing	**0.32**	**0.52**
	carbonates with clastics	**0.25**	**0.08**
igneous and metamorphic rocks	igneous rocks	*-1.11*	*-2.80*
	metamorphic rocks	*-1.82*	*-4.15*

Groundwater is supersaturated with respect to calcite in 143 water samples and with respect to dolomite in 93 water samples. This groundwater was generally sampled in the recharge areas with carbonate rocks (limestone and dolomite), carbonates with clastics, and flysch rocks (Fig. 64). With respect to calcite groundwater is undersaturated in 31 (17.7 %) water samples and with respect to dolomite in 81 (46.3 %), which indicates the lack of carbonate minerals in the recharge areas. These groundwaters were sampled in the recharge areas of clastic sedimentary rocks, where calcite (and dolomite) minerals are mostly in silicate and carbonate rocks (and cement), and igneous and metamorphic rocks. Undersaturation of groundwater according to calcite possible arises due to the acidic pH of groundwater environment, low HCO_3^- concentration and low EC, short groundwater residence time. Water samples circled (Fig. 64) indicate groundwater Ca^{2+} and Mg^{2+} concentration below LOD. These calculations assume that dissolved species in groundwater are at chemical equilibrium.

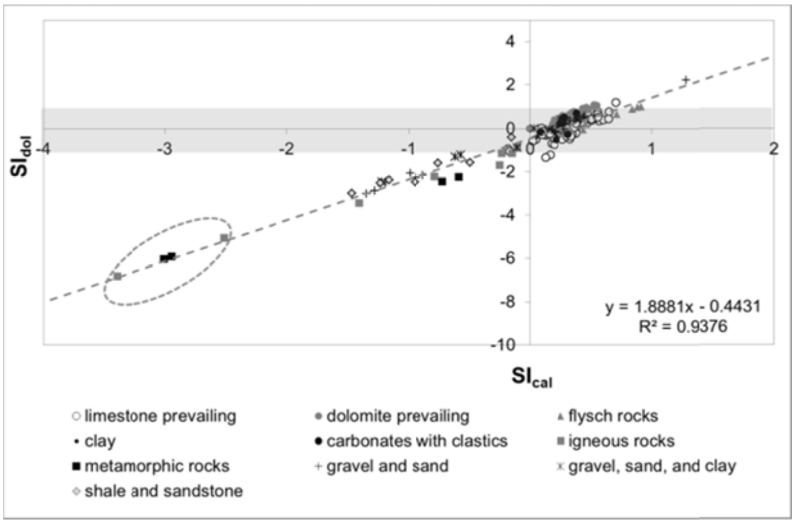

Figure 64: Scatter plot of groundwater SI_{cal} versus SI_{dol}

The concentration of groundwater HCO_3^- and pH increase with SI_{cal} and SI_{dol} (Figs. 65 and 66) where the lowest groundwater HCO_3^-, pH and SI (unsaturated groundwater) belong to groundwater which mostly have recharge areas in igneous and metamorphic rocks, and clastic sedimentary rocks. Very negative SI (<-1) were observed in groundwater samples in the recharge areas of igneous and metamorphic rocks because the concentrations of Ca^{2+} or Mg^{2+} were generally very low or below LOD.

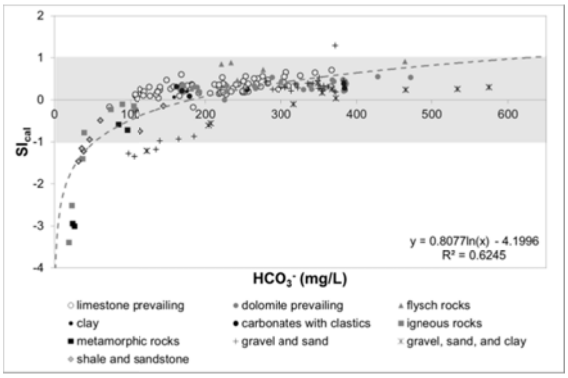

Figure 65: Groundwater SI_{cal} versus HCO_3^- concentrations

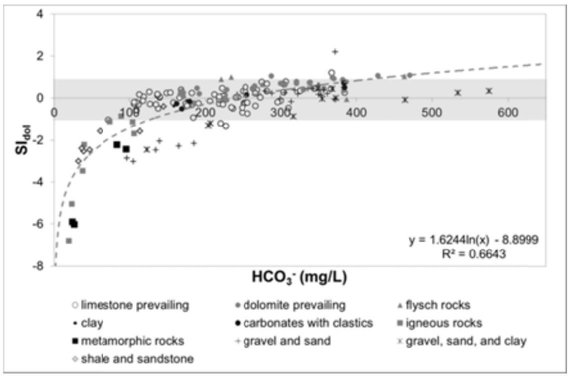

Figure 66: Groundwater SI_{dol} versus HCO_3^- concentrations

Groundwater is highly unsaturated with respect to calcite ($SI_{cal}<0$) and dolomite ($SI_{dol}<0$) where lower, more acidic, groundwater pH prevails (Figs. 67 and 68). This groundwater is mostly observed in the recharge areas with igneous and metamorphic rocks, and gravel, sand (and clay) in the NNE and NE part of study area.

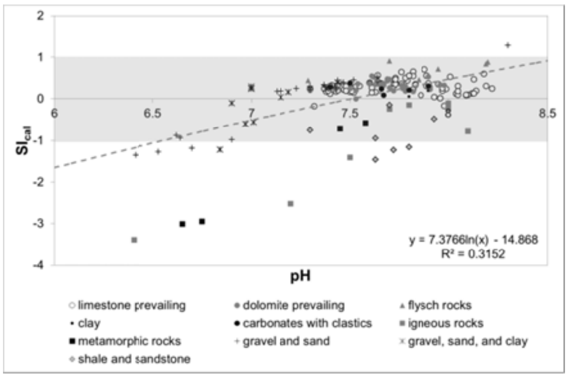

Figure 67: Scatter plot of groundwater SI_{cal} versus pH values

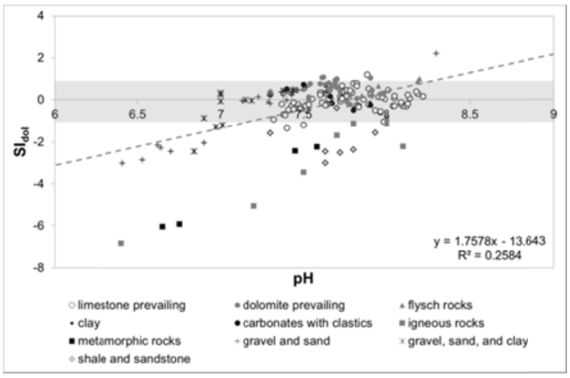

Figure 68: Scatter plot of groundwater SI_{dol} versus pH values

4.5. Physico-chemical parameters in Slovenian groundwaters

4.5.1 Groundwater pH

Descriptive statistics of groundwater pH

The groundwater pH values vary between 6.40 and 8.30, with mean of 7.60 and median 7.64 (Tab. 23), suggesting prevalence of slightly alkaline water. The histogram (Fig. 69) shows that values of pH are not normally distributed. Values below 6.8 (Fig. 70) present the outliers of moderately acidic groundwaters which are present at sampling locations Pevčevo, Framski slap, BLP-2 Nedelica, Gradišče, and V-3A Lukavci, located in the NE part of Slovenia. The precision of pH is ± 0.01.

Table 23: Descriptive statistics of groundwater pH

Parameter	n	X	Md	Min	Max	S
pH	175	7.60	7.64	6.40	8.30	0.37

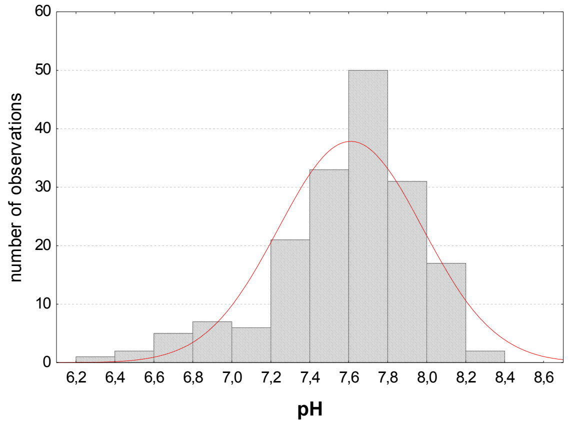

Figure 69: Histogram for groundwater pH values (n=175)

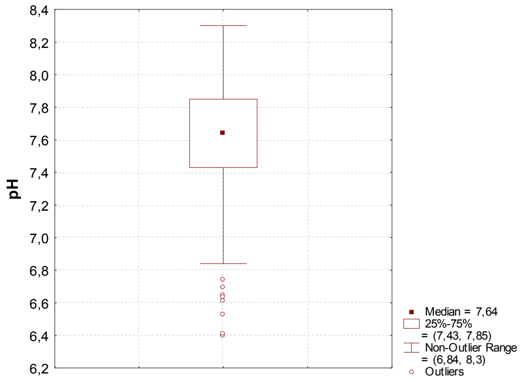

Figure 70: Box and whisker plot for groundwater pH values (n=175)

Rock type

Groundwater from recharge areas with carbonate rocks is significantly more alkaline ($p<0.05$) than groundwater from recharge areas of clastic sedimentary rocks, which is more acidic. In the recharge areas of clastic sedimentary, and igneous and metamorphic rocks (Fig. 71; Appendix 13D), groundwater could be influenced by the prevailing silicate rocks in the recharge areas of groundwater. This is indicated by the moderate correlation between groundwater Si and pH ($r_s=-0.61$, $p>0.05$). Additionally, the thickness of soil horizons and increased microbiological activities could also decrease soil pH as well as groundwater pH. In the recharge areas of carbonate rocks the range of pH is narrower, due to prevalence of carbonate minerals and thinner (or non-existent) soil horizon.

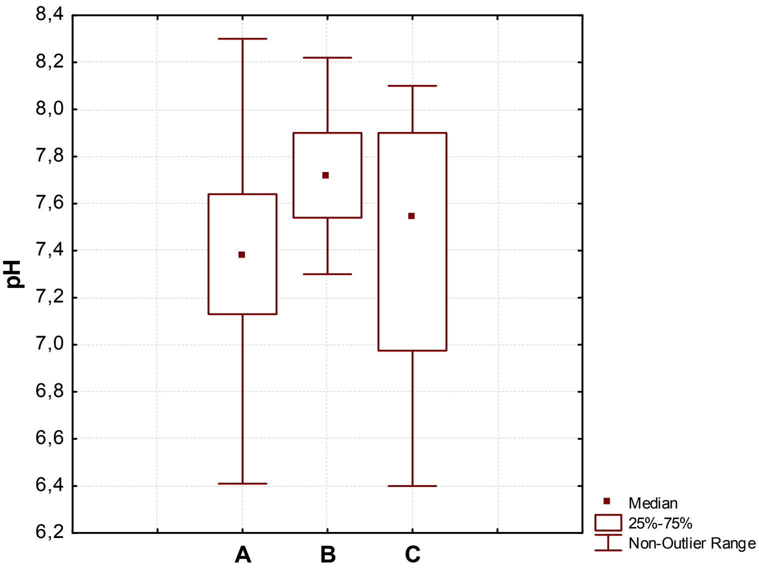

A = clastic sedimentary rocks (n=53)
B = carbonate rocks (n=110)
C = igneous and metamorphic rocks (n=12)

Figure 71: Box and whisker plots for groundwater pH values in the recharge area of major rock types

Groundwater with acidic character was found in the recharge areas of gravel, sand (and clay) (Miocene, Pliocene, and Quaternary clastics), and in Oligocene igneous rocks and old metamorphic Paleozoic rocks (Figs. 72 and 73; Appendix 13D). Groundwater pH values from recharge areas with gravel, sand and clay are significantly lower ($p<0.05$) compared groundwater from other recharge areas, except gravel and sand, and metamorphic rocks. According to lithological classification groundwater pH values from recharge areas with Pliocene clastitcs are significantly lower ($p<0.05$) pH compared to groundwater in recharge areas with Eocene flysch, Jurassic, Cretaceous, and Triassic carbonates, Ladinian igneous rocks, Miocene Lithothamnium limestone, Carboniferous-Permian beds, Oligocene clay “sivica”. This is a result of prevailing silicate minerals in the rocks, greater soil thickness and type and density of vegetation cover in the recharge areas. Alkaline groundwaters are observed in the areas where it is in contact with other lithological units where mostly carbonate minerals (and/or cement) dominate in the recharge areas.

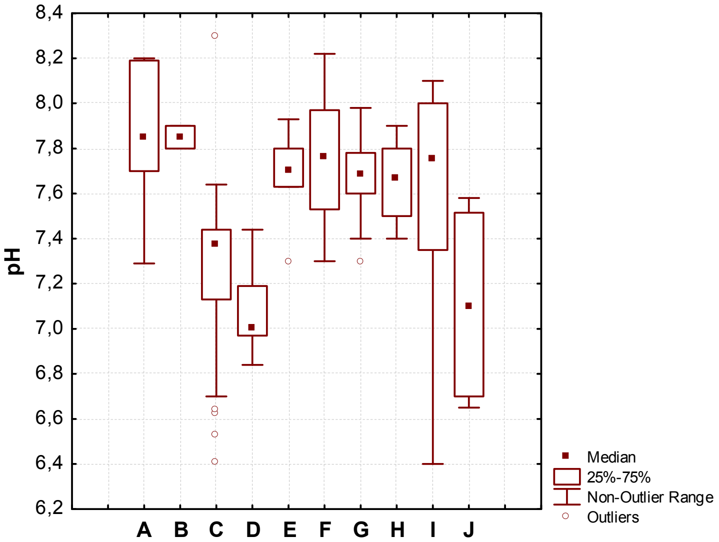

A = flysch rocks (n=7)
B = clay (n=2)
C = gravel and sand (n=26)
D = gravel, sand and clay (n=11)
E = shale and sandstone (n=7)
F = limestone prevailing (n=74)
G = dolomite prevailing (n=30)
H = carbonates with clastics (n=6)
I = igneous rocks (n=8)
J = metamorphic rocks (n=4)

Figure 72: Box and whisker plots for groundwater pH values in the recharge area of prevailing lithological unit

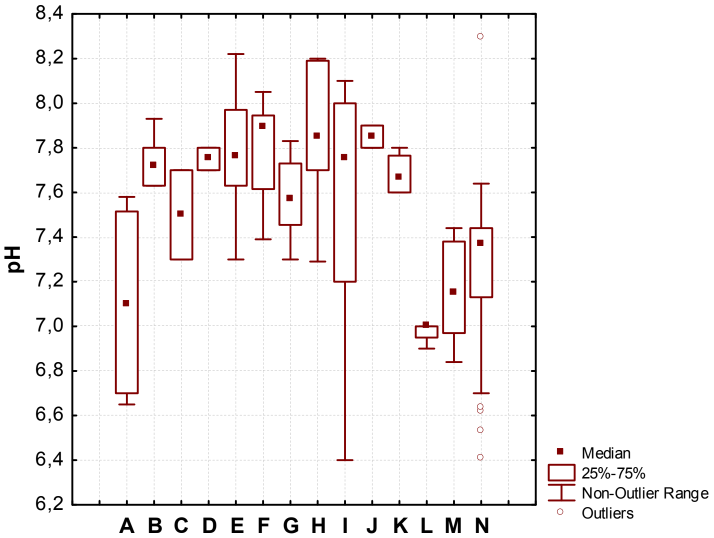

A = old Paleozoic rocks (n=4)
B = Carboniferous-Permian beds (n=5)
C = Permian Val Gardena layers (n=2)
D = Ladinian igneous rocks (n=2)
E = Triassic carbonates (n=70)
F = Jurassic carbonates (n=8)
G = Cretaceous carbonates (n=28)
H = Eocene flysch rocks (n=7)
I = Oligocene igneous rocks (n=6)
J = Oligocene clay “sivica” (n=2)
K = Miocene Lithothamnium limestone (n=4)
L = Miocene clastics (n=4)
M = Pliocene clastics (n=7)
N = Quaternary clastics (medium- and coarse-grained) (n=26)

Figure 73: Box and whisker plots for groundwater pH in the recharge area of prevailing lithostratigraphic unit

Aquifer porosity type

According to the aquifer porosity type the groundwater is mostly alkaline (Fig. 74, Appendix 13D), except for groundwater in the aquifers with intergranular porosity where acidic groundwater dominates it is significantly more acidic compared to groundwater from aquifers with karstic and fractured porosity, and fractured and karstic porosity. Acidic groundwater is observed in the alluvial plains of NE part of the study area, where Mura River deposits are mostly of silicate composition. Additonally, this part of Slovenia is known for intensive agricultural land uses, where leaching of nutrients, and influence of waste water and sewage decrease groundwater pH.

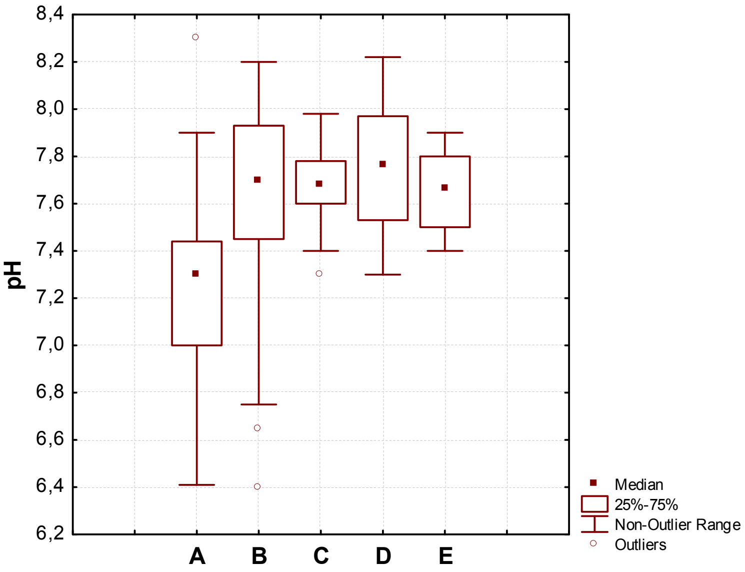

A = intergranular porosity (n=39)
B = fractured porosity (n=26)
C = fractured and karstic porosity (n=30)
D = karstic and fractured porosity (n=74)
E = mixed porosity (karstic, fractured, intergranular) (n=6)

Figure 74: Box and whisker plots for groundwater pH values in the recharge area of prevailing aquifer porosity type

Land cover/use

Alkaline groundwater is observed in the recharge areas with bare rocks, moors and heathland (Figs. 75 and 76; Appendix 13D) where urban and agricultural land uses are less dense. Acidic groundwater is observed mostly in the NE part of Slovenia in lowlands where in the recharge areas the thickness of soil layer is bigger, and intense agricultural activities are present on the arable lands (intense use of nutrients and plant protection products, applications of slurry and manure on the fields, leakage of sewage systems, septic tanks and waste water).
There are no significant differences between pH values according to both land cover/use classifications.

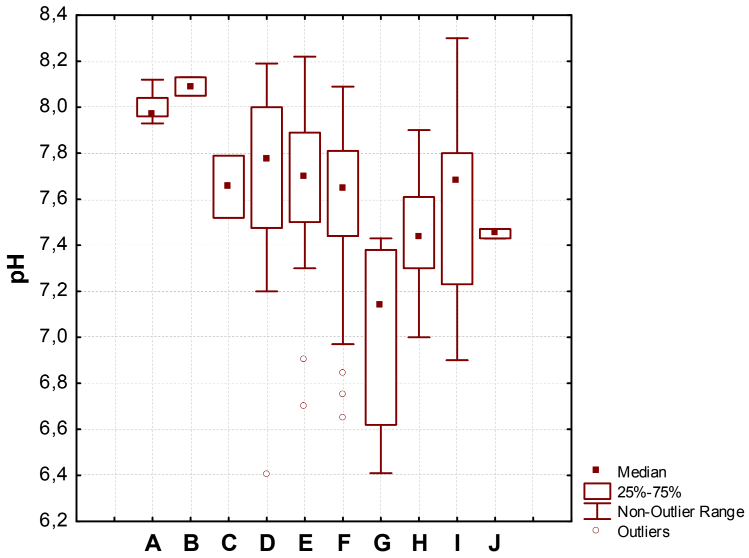

A = bare rocks (n=8)
B = moors and heathland (n=2)
C= natural grasslands (n=2)
D = coniferous forest (n=20)
E = broad-leaved forest (n=45)
F = mixed forest (n=56)
G = non-irrigated arable land (n=10)
H = complex cultivation patterns (n=18)
I = land principally occupied by agriculture, with significant areas of natural vegetation (n=10)
J =industrial or commercial units (n=2)

Figure 75: Box and whisker plots for groundwater pH values in the recharge area of prevailing land use type (CORINE Land Cover)

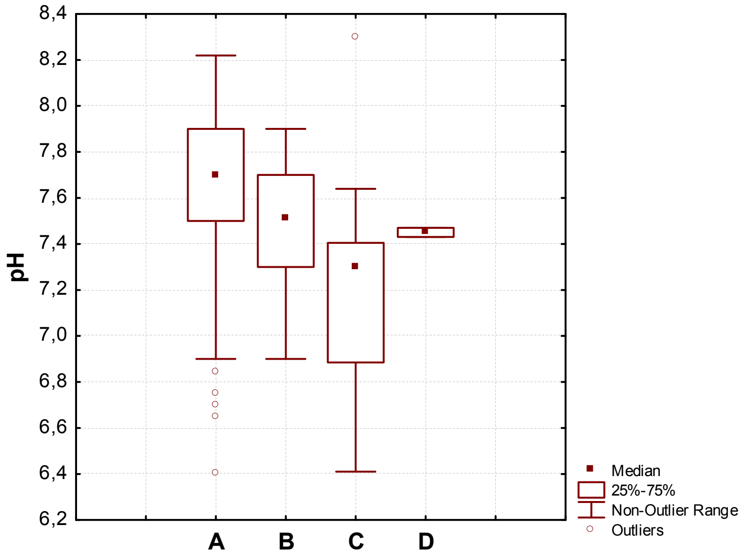

A = forest (n= 137)
B = areas of less intense use of nutrients and plant protection products (n=18)
C = areas of intense use of nutrients and plant protection products (n=16)
D = urban areas (n=2)

Figure 76: Box and whisker plots for groundwater pH values in the recharge area of prevailing land use type (Actual agricultural and forest land usage)

Along with mineralogical composition also the pollutants in the aquifer increas the groundwater acidity, as well as the EC (Fig. 77, circle) (r_s=0.51, $p<0.05$). Groundwater pH shows moderate correlation with Na$^+$ (r_s=-0.52, $p<0.05$) which, besides the silicate weathering, suggest the additional source of Na$^+$ in groundwater (Fig. 78, square).

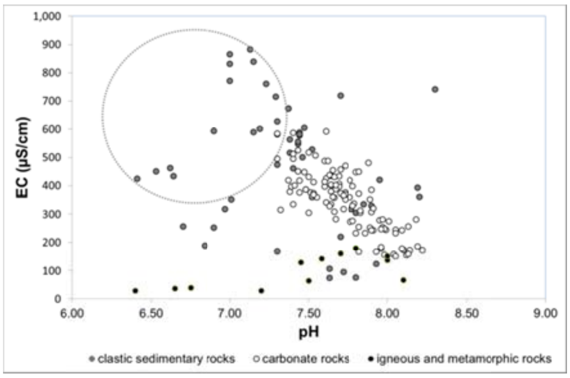

Figure 77: Groundwater pH values versus EC

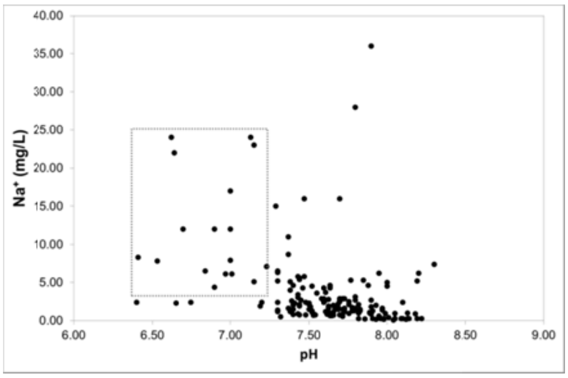

Figure 78: Groundwater pH values versus Na^+ concentration

Sampling object type

Alkaline groundwater is observed in the spring and surface water (Fig. 79, Appendix 13D), located in the recharge areas of carbonate rocks. The pH of surface water could be influenced by the degassing of CO_2 resulting in the increase of pH and consequently in $CaCO_3$ precipitation (Winter *et al.*, 1998). The lowest groundwater pH values were measured in groundwater from private wells which recharge areas are rich in silicate minerals and intense agricultural land use is present.

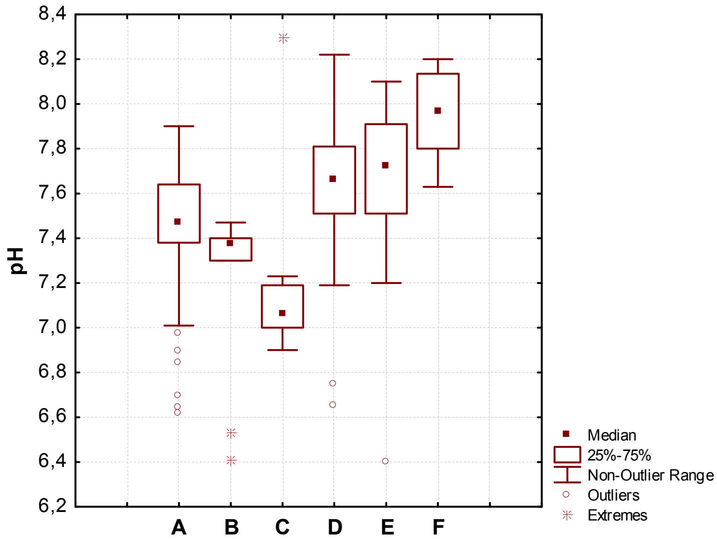

A = pumping station (n=35)
B = borehole (n=10)
C = private well (n=8)
D = spring capture (n=44)
E = spring (n=58)
F = surface water (n=20)

Figure 79: Box and whisker plots for groundwater pH values according to sampling object type

Spatial distribution of groundwater pH

Groundwater with more alkaline character (pH>7.75) is observed in the mountain regions (N, NW and W part of the country) where carbonate rocks are the prevailing rock type in the groundwater's recharge areas (Fig. 80). Groundwater pH in this area is governed by thinner (or non-existent) soil layer, limited microbiological activity as well as less dense vegetation, affecting the amount of the available CO_2 in the soil, especially when karstic aquifers are very open to the atmosphere. Alkaline groundwater is also observed in locations where groundwater was sampled as surface water, which could be the consequence of CO_2 degassing. Groundwater in this area is also affected by the greater precipitation rate and less intense human impact (less populated and less intensive agricultural land use) compared to other part of Slovenia. Contrary slightly acidic groundwater (pH<7.25) is observed in the NNE and NE parts of the country where in the recharge areas silicate mineral composition of igneous and metamorphic rocks, and Mura River deposits prevail. This suggests the weathering of silicate minerals in groundwater. Groundwater acidity could be additionally accelerated by various agricultural practices (plowing, excessive use of nutrients, and leakage of waste water) and by acid rain water. Like in the Podravje and Pomurje region (NE part of Slovenia), intense agricultural activity is present which in combination with silicate bedrock provides (very) acidic soil. Since intense crop production, acidic rain, leached bedrock cations (mostly Ca^{2+} and Mg^{2+} in soil), and acidic activity of most (mineral) fertilizers, destroy the favourable neutral soil pH for crop growth, the soil is neutralised by the application of limes CaO, $CaCO_3$, and $Ca(OH)_2$ (Mihelič *et al.*, 2010). Additionaly leaching from septic tanks or sewage systems could also affect groundwater pH character.

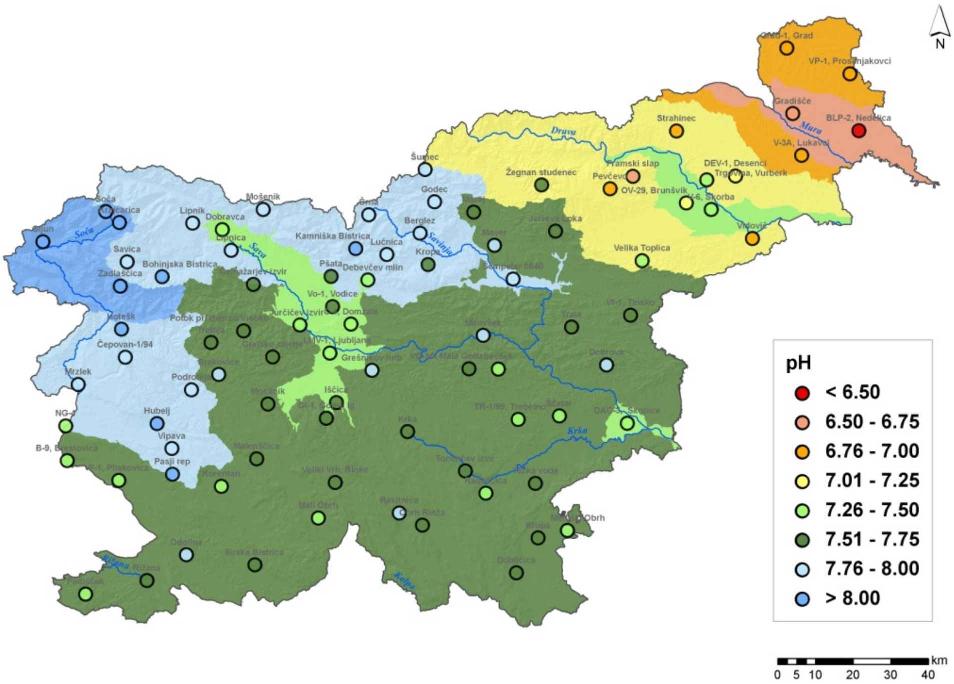

Figure 80: Spatial distribution of groundwater pH

In the recharge areas in the high mountain regions mostly with carbonate rocks in the NW and N part alkaline groundwater (pH>7.75) is observed. This is because of very thin (or non-existing) soil layers and consequently low microbiological activity as well as low vegetation density and high amount of precipitation (water dilution). Also karstic aquifers are known for their openness to the atmosphere. In these regions less human impact is observed. Slightly acidic groundwater (pH<7.25) is observed in the NE part of the country due to mostly prevailing silicate mineral composition of rocks in the recharge areas of igneous and metamorphic rocks, and clastics. In Podravje and Pomurje region (NE part) the soil acidity could be accelerated by various agricultural practices where farmers fertilize soil with slurry or manure, or the soil is being neutralized by lime application. Additionally possible leaching from septic tanks or sewage systems could also affect groundwater pH.

4.5.1.1. *Electrical conductivity (EC) in groundwater*

Descriptive statistics of groundwater EC

Groundwater EC varies between 28 µS/cm and 882 µS/cm, with mean value of 368 µS/cm, and median 366 µS/cm (Tab. 24). Histogram of EC (Fig. 81) in observed groundwater shows that data is normally distributed, and box and whisker plot for EC (Fig. 82) shows that there are some outliers

(EC >760 µS/cm), which are observed in the NE part of the study area (OV-29 Brunšvik, Šempeter 0840, Strahinec and Vidovič. The precision of EC is 0.5 %. None of water samples exceeds the allowed maximum level for drinking water (2500 µS/cm) according Rules on drinking water (2004).

Table 24: Descriptive statistics of groundwater EC

Parameter	n	X	Md	Min	Max	S
EC (µS/cm)	175	368	366	28	882	173

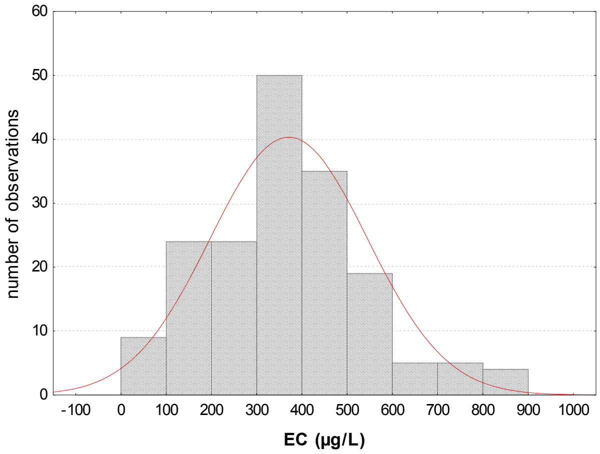

Figure 81: Histogram for groundwater EC (n=175)

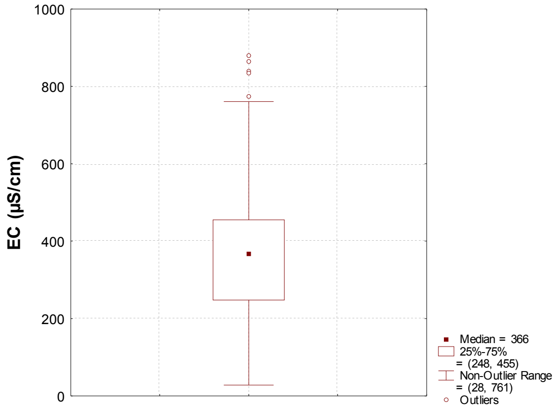

Figure 82: Box and whisker plot for groundwater EC (n=175)

Rock type

In the recharge areas of clastic sedimentary rocks the groundwater EC is the highest (Fig. 83, Appendix 13E) and is significantly higher ($p<0.05$) compared to groundwater in the recharge areas with igneous and metamorphic rocks. This suggests that increased concentrations of dissolved ions in groundwater are due to presence of soluble minerals. The lowest groundwater EC is measured in the recharge areas of igneous and metamorphic rocks which contain poorly soluble silicate minerals.

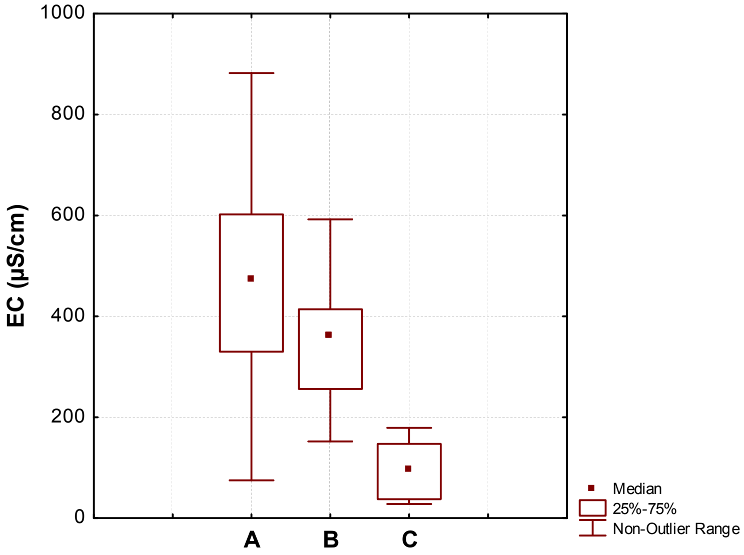

A = clastic sedimentary rocks (n=53)
B = carbonate rocks (n=110)
C = igneous and metamorphic rocks (n=12)

Figure 83: Box and whisker plots for groundwater EC in the recharge area of major rock types

Groundwater EC in recharge areas of gravel, sand (and clay) (Miocene and Quaternary clastics), and Eocene flysch rocks (Fig. 84 and 85, Appendix 13E) is the highest. In the recharge areas with Miocene clastics groundwater is significantly higher ($p<0.05$) compared to groundwater with recharge areas with all observed lithological units except with Quaternary clastics (medium- and coarse-grained).This is due to increased dissolved solids or salts in groundwater. Groundwater EC shows strong correlation with HCO_3^- (r_s = 0.92, $p<0.05$), Ca^{2+} (r_s=0.89, $p<0.05$), and Mg^{2+} (r_s=0.79, $p<0.05$) suggesting the majority of ions present in groundwater are due to dissolution of carbonate rocks. The lowest groundwater EC was observed in the recharge areas of poorly permeable rocks like shale and sandstone (Carboniferous-Permian beds), Oligocene igneous rocks and metamorphic rocks (old Paleozoic rocks). Groundwater with recharge areas in Oligocene igneous rocks, Permian Val Gardena layers, and old Paleozoic rocks is significantly lower ($p<0.05$) compared to recharge areas in Eocene flysch rocks, Cretaceous carbonates, Quaternary clastics (medium- and coarse-grained), Miocene Lithothamnium limestone, and Miocene clastics.

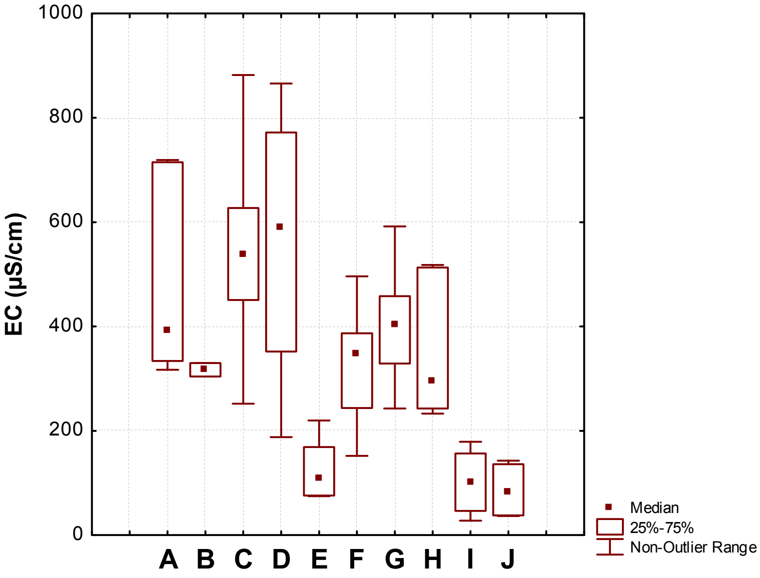

A = flysch rocks (n=7)
B = clay (n=2)
C = gravel and sand (n=26)
D = gravel, sand and clay (n=11)
E = shale and sandstone (n=7)
F = limestone prevailing (n=74)
G = dolomite prevailing (n=30)
H = carbonates with clastics (n=6)
I = igneous rocks (n=8)
J = metamorphic rocks (n=4)

Figure 84: Box and whisker plots for groundwater EC in the recharge areas of prevailing lithological unit

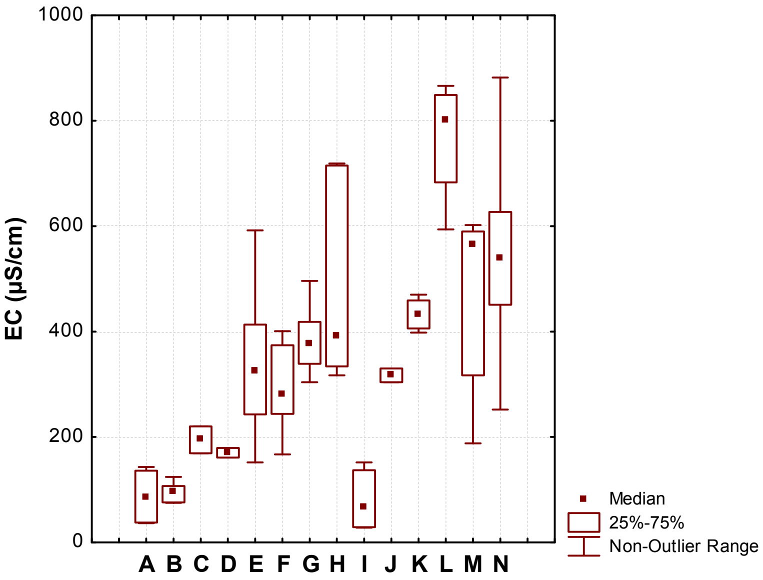

A = old Paleozoic rocks (n=4)
B = Carboniferous-Permian beds (n=5)
C = Permian Val Gardena layers (n=2)
D = Ladinian igneous rocks (n=2)
E = Triassic carbonates (n=70)
F = Jurassic carbonates (n=8)
G = Cretaceous carbonates (n=28)
H = Eocene flysch rocks (n=7)
I = Oligocene igneous rocks (n=6)
J = Oligocene clay “sivica” (n=2)
K = Miocene Lithothamnium limestone (n=4)
L = Miocene clastics (n=4)
M = Pliocene clastics (n=7)
N = Quaternary clastics (medium- and coarse-grained) (n=26)

Figure 85: Box and whisker plots for groundwater EC in the recharge area of prevailing lithostratigraphic unit

Aquifer porosity type

The highest groundwater EC is observed in aquifers with intergranular porosity (Fig. 86, Appendix 13E) which is significalnty higher ($p<0.05$) compared to groundwater from aquifers with fractured, karstic and fractured, and mixed porosity (karstic, fractured, intergranular). This is possible due to longer residence time, thicker soil layer, higher soil temperatures, and also influence of land use (urban and agricultural) in lowland alluvial aquifers. The lowest EC is observed in groundwater in aquifers with fractured porosity where groundwater usually has short residence time. Namelly fractured rock aquifers (dolomites, sandstones and igneous rocks) store and transmit water through crevices, joints, solution channels in otherwise impervious rocks (Sara, 2003).

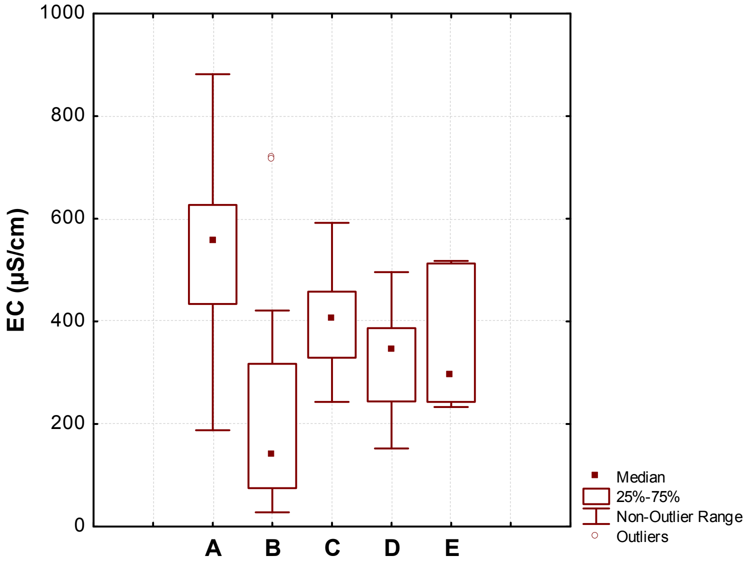

A = intergranular porosity (n=39)
B = fractured porosity (n=26)
C = fractured and karstic porosity (n=30)
D = karstic and fractured porosity (n=74)
E = mixed porosity (karstic, fractured, intergranular) (n=6)

Figure 86: Box and whisker plots for groundwater EC in the recharge area of prevailing aquifer porosity type

Land cover/use

Groundwater with higher EC (>500 µS/cm) is observed at locations which recharge areas that are influenced by various human activities (Figs. 87 and 88, Appendix 13E). This includes recharge areas of industrial or commercial units, complex cultivation patterns, non-irrigated arable land, and land principally occupied by agriculture, with significant areas of natural vegetation. Groundwater EC is significantly higher ($p<0.05$) compared to recharge areas with bare rocks, moors and heathland, and coniferous forest. The possible sources are the use of various fertilizers as well as manure and slurry, leakage from septic tanks and sewage systems, waste water, salt for deicing roads during winter, and landfill leachate. This has been verified by the moderate correlation between groundwater EC and NO_3^- ($r_s=0.69$, $p<0.05$), Cl^- ($r_s=0.69$, $p<0.05$), and SO_4^{2-} ($r_s=0.58$, $p<0.05$). The lowest groundwater EC is observed in the groundwater's recharge areas of bare rocks, moors and heathland, and forests at higher altitudes, due to absence of thick soil layer which could enhance carbonate dissolution by dissolved CO_2, and due to land use, which is not favourable for population as well as not for intensive agricultural activities.

According to Actual agricultural and forest land usage classification groundwater EC at areas of intense use of nutrients and plant protection products, and urban areas is significantly higher ($p<0.05$) compared to recharge areas under forest.

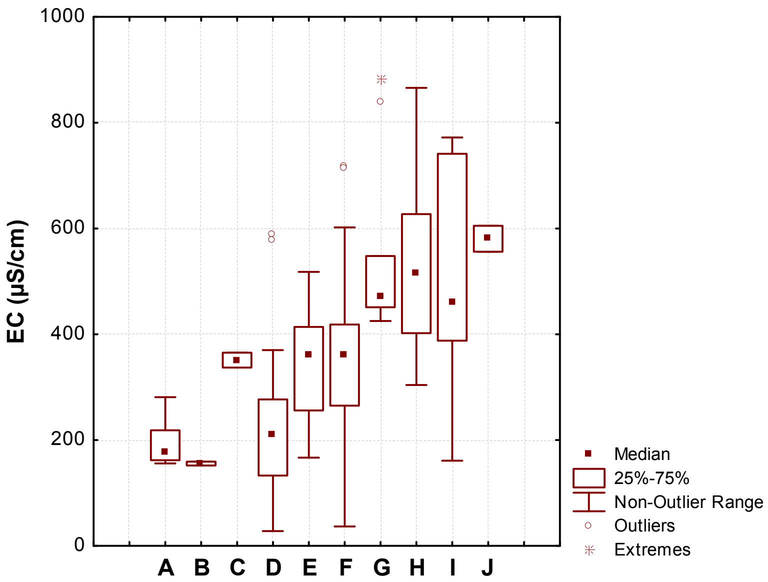

A = bare rocks (n=8)
B = moors and heathland (n=2)
C= natural grasslands (n=2)
D = coniferous forest (n=20)
E = broad-leaved forest (n=45)
F = mixed forest (n=56)
G = non-irrigated arable land (n=10)
H = complex cultivation patterns (n=18)
I = land principally occupied by agriculture, with significant areas of natural vegetation (n=10)
J = industrial or commercial units (n=2)

Figure 87: Box and whisker plots for groundwater EC in the recharge area of prevailing land use type (CORINE Land Cover)

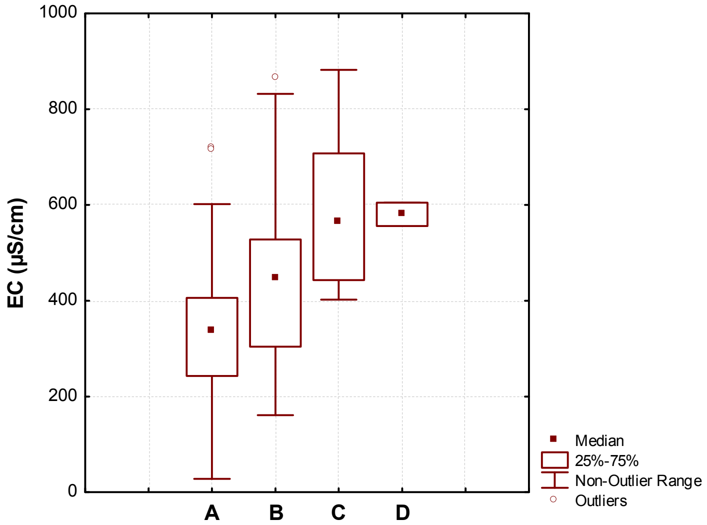

A = forest (n=137)
B = areas of less intense use of nutrients and plant protection products (n=18)
C = areas of intense use of nutrients and plant protection products (n=16)
D = urban areas (n=2)

Figure 88: Box and whisker plots for groundwater EC in the recharge area of prevailing land use type (Actual agricultural and forest land usage)

Sampling object type

The highest groundwater EC were observed in private wells (Figs. 89, Appendix 13E) because they are usually located in lowlands where the soil layer is thicker (soil CO_2 is enriched) and the soil temperature is higher. Additionally, private wells are usually located near the farms and arable land (fields), reflecting the use of nutrients as well as possible leakage from septic tanks or sewage systems. The lowest EC is measured in groundwater sampled as springs, and as as surface water. Springs are usually located in mountain regions, where steep slopes cause absence of (thick) soil layer and short groundwater residence time, and increased amount of precipitation causes dilution of groundwater. Surface water indicates either low HCO_3^- concentration, or low contents of dissolved salts in the water.

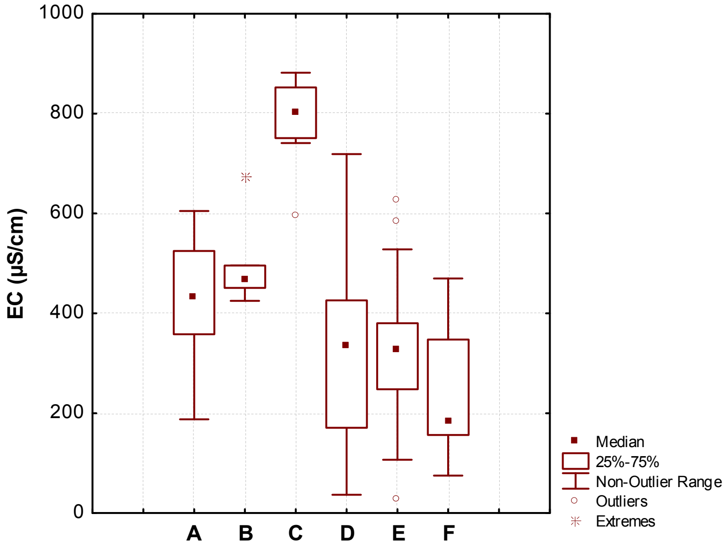

A = pumping station (n=35)
B = borehole (n=10)
C = private well (n=8)
D = spring capture (n=44)
E = spring (n=58)
F = surface water (n=20)

Figure 89: Box and whisker plots for groundwater EC according to sampling object type

Spatial distribution of groundwater EC

Increased groundwater EC (>500 µS/cm) (Fig. 90) is observed in alluvial plains in the central, E, and NE parts of Slovenia, and in the coastal part. Groundwater from alluvial plains is influenced mostly by the mineral composition of carbonate rocks, thick soil layer which enhaces dissolution of carbonate minerals, and higher soil temperatures present in lowlands. Additionally, intense agricultural land use (use of fertilizers, application of manure and slurry) and by direct human impact (leakage from septic tanks, sewage systems, waste water, use of salts for deicing roads during winter, and landfill leachate) also influence the groundwater EC. In the coastal part the proximity of the sea side could influence the groundwater composition in the form of precipitation or sea spray, or could be due to agricultural activity and use of fertilizers and pesticides.

The lowest groundwater EC (<200 µS/cm) is observed in the high mountain regions in the NW part, where in carbonate recharge areas due to steep slopes the soil layer is thin (or non-existent), and consequently, very little vegetation (low level of respiration of soil organisms and the decay of organic matter) are present, as well as low soil temperatures. In the recharge areas also low temperatures are observed, and consequently low $P_{CO2.}$ During intense precipitation of heavy rain and snow melting (r_s= -0.57, p<0.05) groundwater has short residence time, and is diluted. Most sampling locations in the high mountains are springs, which discharge responds primarily to heavy rainfalls, and also snowmelt runoff (fresh and soft water with low EC). Low groundwater EC is also observed in the recharge areas with igneous and metamorphic rocks which are poor in soluble carbonate minerals.

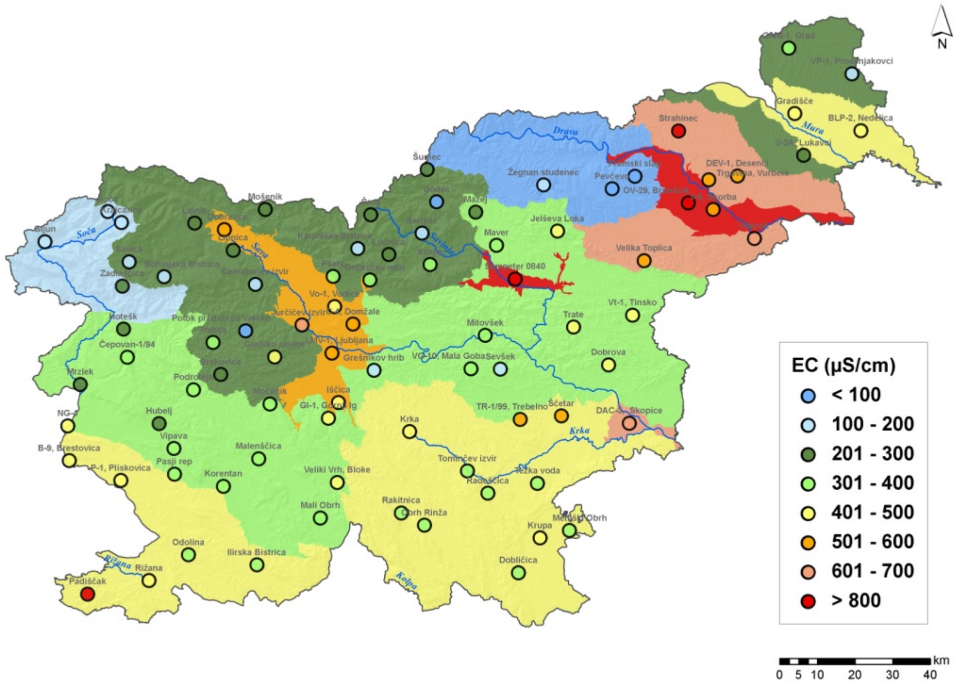

Figure 90: Spatial distribution of groundwater EC

4.6. Natural factors affecting Slovenian groundwater geochemistry

4.6.1. Carbonate geochemistry in Slovenian groundwaters

The main parameters that describe the carbonate dissolution in water are Ca^{2+}, Mg^{2+}, and their molar ratio (Ca^{2+}/Mg^{2+}), HCO_3^-, $CaCO_3$, P_{CO2}, and δ^{13}C-DIC.

4.6.1.1. Calcium (Ca^{2+}) in groundwater

Descriptive statistics of groundwater Ca^{2+}

Mean groundwater Ca^{2+} concentration is 60 mg/L, median 58 mg/L, maximum 152 mg/L, and minimum 2 mg/L (Tab. 25). Groundwater Ca^{2+} concentration is normally distributed (Fig. 91) and concentration greater than 122 mg/L present outliers (Fig. 92) which were measured at sampling locations Padiščak, Strahinec, and Vidovič. The analytical uncertainty for Ca^{2+} is between 4 and 14 % (n=171) and in 4 water samples the groundwater Ca^{2+} concentrations were below LOD (½ LOD=2 mg/L) measured at sampling locations Pevčevo and Framski slap.

Table 25: Descriptive statistics of groundwater Ca^{2+}

Parameter	n	X	Md	Min	Max	S
Ca^{2+} (mg/L)	175	60	58	2	152	30

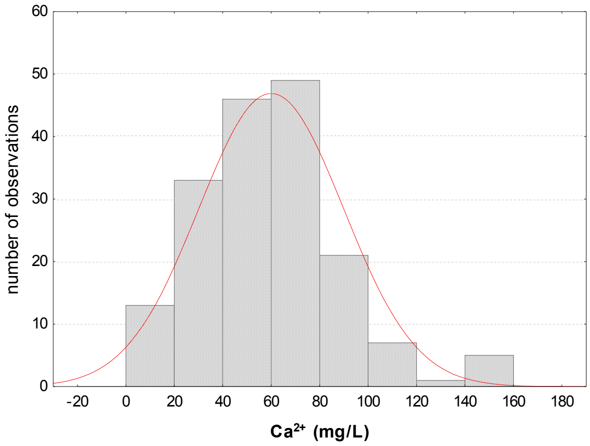

Figure 91: Histogram for groundwater Ca^{2+} concentration (n=175)

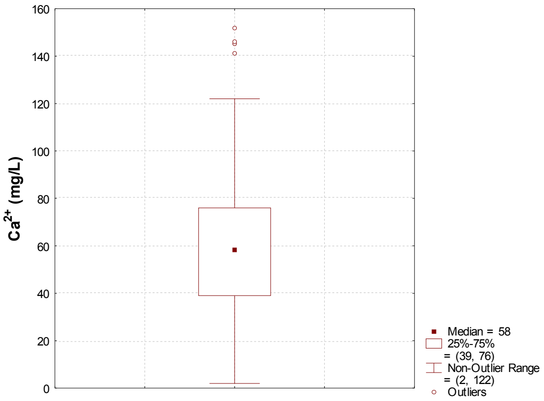

Figure 92: Box and whisker plot for groundwater Ca^{2+} concentration (n=175)

Rock type

The range of groundwater Ca^{2+} concentration is in the clastic sedimentary rocks (Fig. 93, Appendix 13F) varies very widely due to various origins of sediments (Ca-rich minerals in carbonate, igneous and metamorphic rock, and in carbonate cement) (Mioč and Žnidarčič, 1989). The lowest groundwater Ca^{2+} concentration is observed in igneous and metamorphic rocks which is significantlly lower ($p<0.05$) compared to groundwater with clastic sedimentary and carbonate rocks. These rocks are usually low in Ca-rich minerals, where silicate minerals weather slower compared to carbonate minerals (Appelo and Postma, 2005).

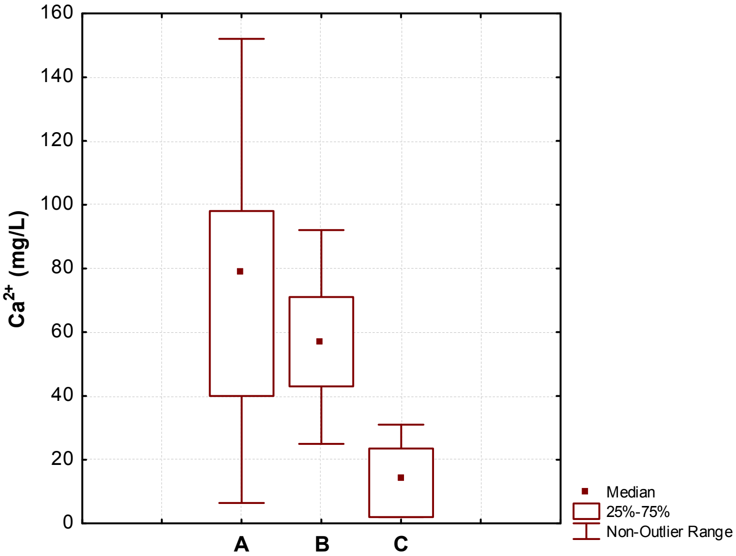

A = clastic sedimentary rocks (n=53)
B = carbonate rocks (n=110)
C = igneous and metamorphic rocks (n=12)

Figure 93: Box and whisker plots for groundwater Ca^{2+} concentration in the recharge area of major rock types

Increased groundwater Ca^{2+} concentrations are measured in the recharge area of gravel, sand (and clay), and flysch rocks (Figs. 94 and 95, Appendix 13F). The highest groundwater Ca^{2+} concentrations are measured in the recharge areas of Miocene clastics which are significantly higher ($p<0.05$) compared to recharge areas with other lithostratigraphic units. Thiese recharge areas contain pebbles of carbonate, igneous, metamorphic rocks, with sand-silt or carbonate cement (Mioč and Žnidarčič, 1989). The alluvial deposits mostly belong to Quaternary sediments of carbonate and silicate origin (Bavec and Pohar, 2009; EARS, 2009). In the sandstones the carbonate cement prevails, but micas in marls are also rich with calcium (Mioč and Žnidarčič, 1989). In Mura depression (NE part of Slovenia), the gravel is characterized by pebbles of quartz, igneous and metamorphic rocks, and to a lower extent, by pebbles of older sedimentary rocks originating from the Central Alps (Markič, 2009). In deep aquifers (NE part) the source of groundwater Ca^{2+} is in gravel, sand and clay in carbonates and phyllosilicates (Kralj, 2003). Similar mineralogical composition is also found in the recharge area of gravel and sand, where groundwater Ca^{2+} concentration is also high. The outlier in this group shows the absence of groundwater Ca^{2+} (and HCO_3^-) due to the mineralogical composition of alluvial deposits which have mostly quartz and silicate minerals in igneous and metamorphic rocks in their recharge area (Žlebnik, 1982; Mioč and Žnidarčič, 1989). In the recharge areas with igneous and metamorphic rocks (old Paleozoic rocks and Oligocene igneous rocks), and shale and sandstone (Carboniferous-Permian beds), groundwater Ca^{2+} concentrations are significantly lower ($p<0.05$) compared to groundwater with limestone or dolomite prevailing (Cretaceous and Jurassic carbonates), Eocene flysch rocks, carbonate with clastics, and gravel and sand (and clay) (Quaternary clastics(medium- and coarse-grained), Miocene Lithothamnium limestone, and Miocene clastics).

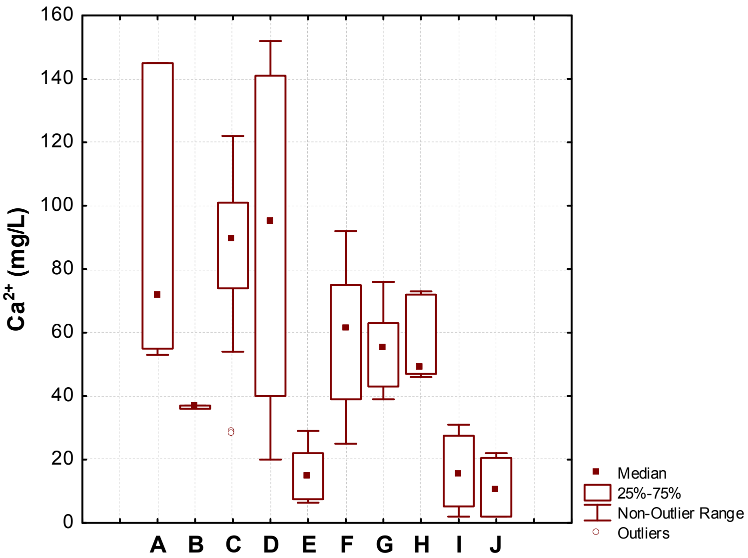

A = flysch rocks (n=7)
B = clay (n=2)
C = gravel and sand (n=26)
D = gravel, sand and clay (n=11)
E = shale and sandstone (n=7)
F = limestone prevailing (n=74)
G = dolomite prevailing (n=30)
H = carbonates with clastics (n=6)
I = igneous rocks (n=8)
J = metamorphic rocks (n=4)

Figure 94: Box and whisker plots for groundwater Ca^{2+} concentration in the recharge area of prevailing lithological unit

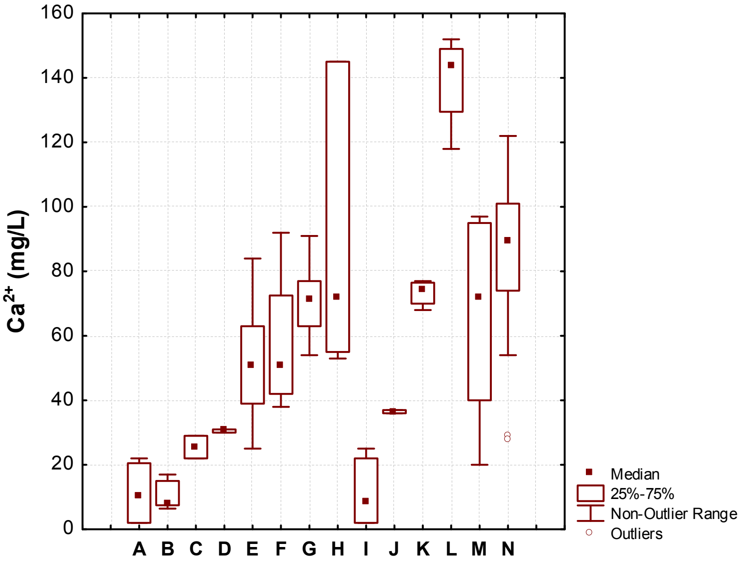

A = old Paleozoic rocks (n=4)
B = Carboniferous-Permian beds (n=5)
C = Permian Val Gardena layers (n=2)
D = Ladinian igneous rocks (n=2)
E = Triassic carbonates (n=70)
F = Jurassic carbonates (n=8)
G = Cretaceous carbonates (n=28)
H = Eocene flysch rocks (n=7)
I = Oligocene igneous rocks (n=6)
J = Oligocene clay “sivica” (n=2)
K = Miocene Lithothamnium limestone (n=4)
L = Miocene clastics (n=4)
M = Pliocene clastics (n=7)
N = Quaternary clastics(medium- and coarse-grained) (n=26)

Figure 95: Box and whisker plots for groundwater Ca^{2+} concentration in the recharge area of prevailing lithostratigraphic unit

Groundwater Ca^{2+} correlates strongly with EC (r_s=0.89, p<0.05), and with HCO_3^- (r_s=0.86, p<0.05) (Fig. 96) suggesting the carbonate dissolution. Encircled locations belong to sampling locations Padiščak, Strahinec, and Vidovič where increased concentrations are possible due to anthropogenic sources. Figure 97 presents only groundwater samples measured in the intergranular aquifers. Encircled sampling locations belong to groundwater sampled in mostly silicate alluvial deposits of Mura River (NE part), and deviate from other groundwater by their lower Ca^{2+} and HCO_3^- concentrations.

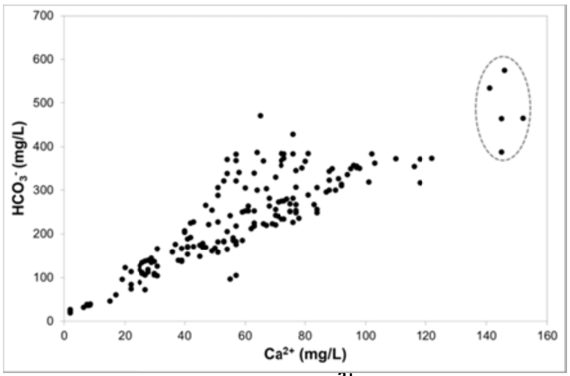

Figure 96: Groundwater Ca^{2+} versus HCO_3^- concentration

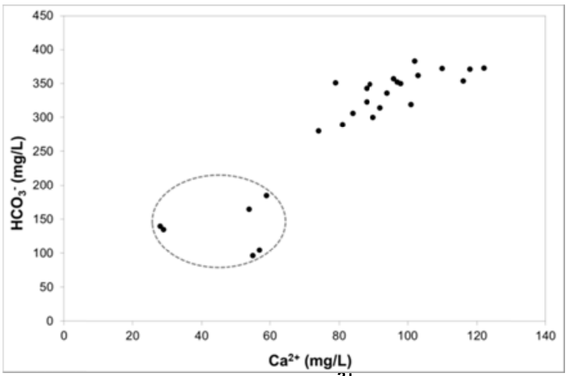

Figure 97: Groundwater Ca^{2+} versus HCO_3^- in intergranular aquifers

Figure 98 shows groundwater pH and Ca^{2+} concentrations where increased Ca^{2+} concentrations (I.) are observed in gravel, sand and clay (Miocene clastites), and lower Ca^{2+} concentrations in the recharge areas of gravel and sand (Quaternary sediments). The groundwater pH and Ca^{2+} concentrations are lower due to prevailing silicate minerals and less carbonate in the recharge area.

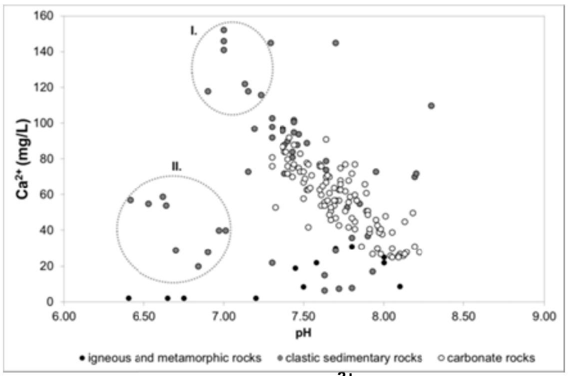

Figure 98: Groundwater Ca^{2+} concentrations versus pH

Groundwater Ca^{2+} concentration in the recharge area of Eocene flysch rocks is also high, because quartz grains in sandstone are bound by carbonate cement (Pavlovec, 1977, 1980; Zupančič and Pirc, 1999), and because calcite is found in calcarenites, marlstones, and separate grains and fossil skeletons in sandstones and calcarenites (Zupančič and Pirc, 1999). The range of groundwater Ca^{2+} concentration is wide due to higher Ca^{2+} concentrations measured in Istrian flysch rocks and lower in Brkini flysch rocks. This coincides with Zupančič and Pirc (1999) and Pretner (2013) where higher Ca^{2+} concentration in rocks was measured in Istrian flysch rocks and lower in Brkini flysch rocks.

Median concentration of groundwater Ca^{2+} is observed in the recharge areas of carbonate rocks. Groundwater Ca^{2+} concentration depends on the type of prevailing carbonate rocks in the recharge area (limestone or dolomite prevailing, and carbonates with clastics), on the presence of CO_2 in solution from the atmosphere and soil, and other climatic factors, which will be discussed later in detail.

Lower groundwater Ca^{2+} concentrations are measured in the recharge areas with clays, and shale and sandstone which are mostly impermeable for water. Marine clay termed *sivica* is composed of less soluble phyllosilicates (illite/muscovite, chlorite and montmorillonite) and soluble carbonates (Kralj and Mišič, 2003). Groundwater in the recharge area with clays suggests the decrease in groundwater Ca^{2+} cation-exchange with aquifer materials (see Piper diagram). In the recharge areas of shale and sandstone (Carboniferous-Permian beds) groundwater Ca^{2+} concentration is low due to mostly non-carbonate clastic sediments (Skaberne *et al.*, 2009). Low Ca^{2+} concentration in groundwater was also observed in the recharge area of Oligocene igneous and metamorphic rocks (old Paleozoic rocks), because minerals in igneous granodiorite, metamorphic biotite, and muscovite gneiss have a small proportion of Ca-bearing minerals and have low solubility rate. These rocks are also relatively impermeable for water so that precipitation runs off into surface streams and enters the aquifer in places where rocks are sufficiently fractured.

Aquifer porosity type

The highest groundwater Ca^{2+} concentrations are found in aquifers with intergranular porosity (Fig. 99, Appendix 13F), due to possible anthropogenic influence in the recharge area of groundwater where mostly agricultural activity is present in lowlands. Groundwater Ca^{2+} concentrations in those aquifers are significantly higher ($p<0.05$) compared to groundwater from recharge areas in aquifers with other porosity types. The lowest groundwater Ca^{2+} concentrations are observed in aquifers with fractured porosity where mostly non-carbonate minerals prevail.

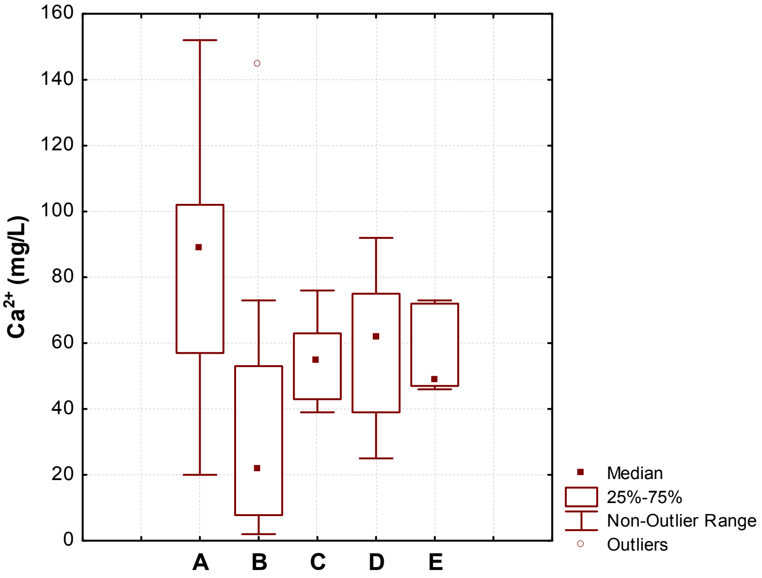

A = intergranular porosity (n=39)
B = fractured porosity (n=26)
C = fractured and karstic porosity (n=30)
D = karstic and fractured porosity (n=74)
E = mixed porosity (karstic, fractured, intergranular) (n=6)

Figure 99: Box and whisker plots for groundwater Ca^{2+} concentration in the recharge area of prevailing aquifer porosity type

Land cover/use

The highest groundwater Ca^{2+} concentration is observed in the recharge areas of non-irrigated arable land, complex cultivation patterns, land principally occupied by agriculture, with significant areas of natural vegetation (Figs. 100 and 101, Appendix 13F) where intense use of nutrients is present. Additionally, increased groundwater Ca^{2+} concentration was measured in groundwater in the recharge areas of industrial or commercial units, reflecting urban land use. Groundwater Ca^{2+} concentrations in the recharge areas of industrial or commercial units and complex cultivation patterns are significantly higher ($p<0.05$) compared to groundwater with bare rocks and moors and heathland. In the NE part of Slovenia the soil has due to natural and anthropogenic influences more acidic character which is not favourable for crops growth. When farmers apply lime and organic fertilizers on the fields, degradation of organic matter in soil is accelerated, leading to higher soil CO_2 and greater carbonate dissolution. Also the higher air and soil temperatures in lowlands contribute to greater soil CO_2 production. The lowest groundwater Ca^{2+} concentrations are observed in the recharge areas bare rocks, and marshes and heath, and forests, due to less intense use of nutrients and plant protection products, where agricultural and urban activities are less expressed. Groundwater Ca^{2+} concentrations are significantly lower ($p<0.05$) in the recharge areas with moors and heathland compared to recharge areas of land principally occupied by agriculture, with significant areas of natural vegetation, and non-irrigated arable land.

According to Actual agricultural and forest land usage classification groundwater Ca^{2+} concentrations are significantly higher ($p<0.05$) in the recharge areas of intense use of nutrients and plant protection products compared to forested recharge areas.

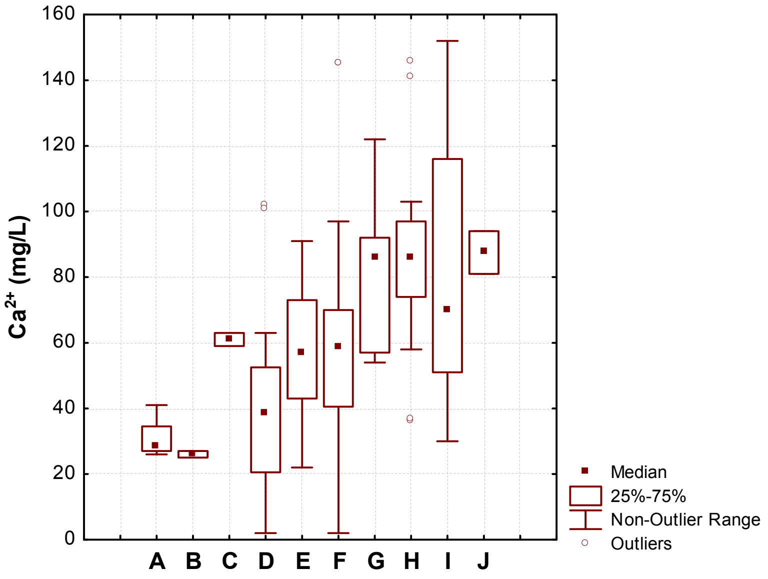

A = bare rocks (n=8)
B = moors and heathland (n=2)
C= natural grasslands (n=2)
D = coniferous forest (n=20)
E = broad-leaved forest (n=45)
F = mixed forest (n=56)
G = non-irrigated arable land (n=10)
H = complex cultivation patterns (n=18)
I = land principally occupied by agriculture, with significant areas of natural vegetation (n=10)
J = industrial or commercial units (n=2)

Figure 100: Box and whisker plots for groundwater Ca^{2+} concentration in the recharge areas of prevailing land use type (CORINE Land Cover)

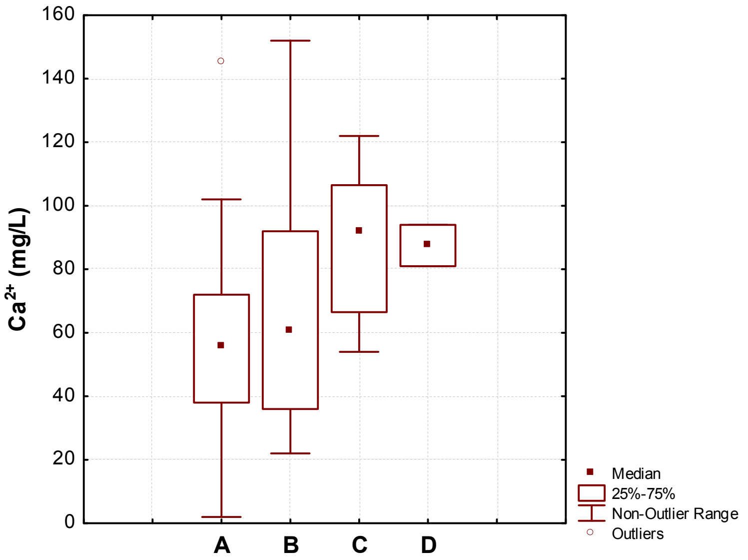

A = forest (n=137)
B = areas of less intense use of nutrients and plant protection products (n=18)
C = areas of intense use of nutrients and plant protection products (n=16)
D = urban areas (n=2)

Figure 101: Box and whisker plots for groundwater Ca^{2+} concentration in the recharge area of prevailing land use type (Actual agricultural and forest land usage)

Figures 102 and 103 suggest possible influence on increased groundwater Ca^{2+} concentrations due to anthropogenic influence on the groundwater, as a consequence of fertilizer use (sampling locations OV-29 Brunšvik, Šempeter 0840, Vidovič, Strahinec, Padiščak, Figs. 104-107) which has been verified with moderate correlation between Ca^{2+} and NO_3^- (r_s= 0.60, $p<0.05$), poor correlation between with K^+ (r_s= 0.36, $p<0.05$), moderate correlation with SO_4^{2-} (r_s= 0.52, $p<0.05$), and moderate correlation between Ca^{2+} and Cl^- (r_s= 0.62, $p<0.05$).

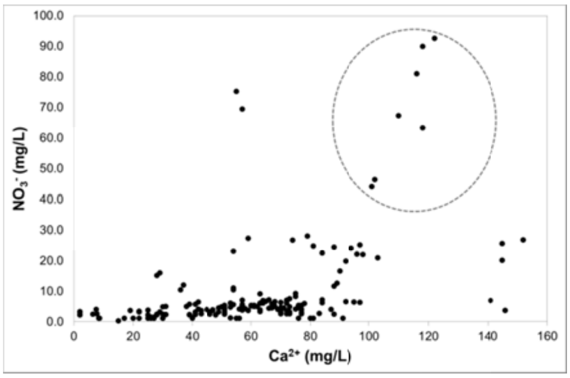

Figure 102: Groundwater Ca^{2+} versus NO_3^- concentration

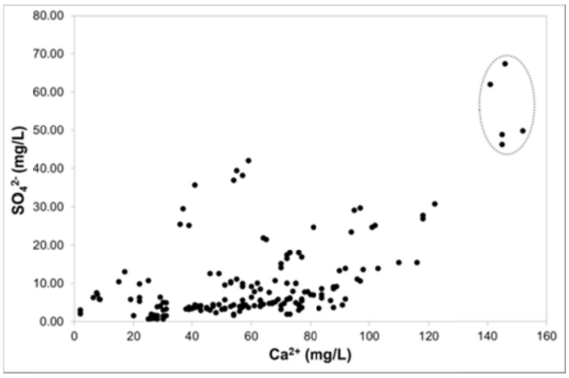

Figure 103: Groundwater Ca^{2+} versus SO_4^{2-} concentration

Figure 104: Sampling location Padiščak where construction material is present

Figure 105: Sampling location Vidovič where construction material is present (in the back)

Figure 106: Corn field in the recharge area of sampling location Strahinec

Figure 107: Field lime application in the area near sampling location Strahinec

Sampling object type

The highest groundwater Ca^{2+} concentrations are measured in private wells in lowlands where in recharge areas carbonate rocks rich in Ca-bearing minerals and cement dominate (Fig. 108, Appendix 13F). Possible additional source of groundwater Ca^{2+} is anthropogenic (fertilizers, construction material). The lowest groundwater Ca^{2+} concentrations are observed in surface waters where recharge areas are in high mountains or in poorly permeable rocks.

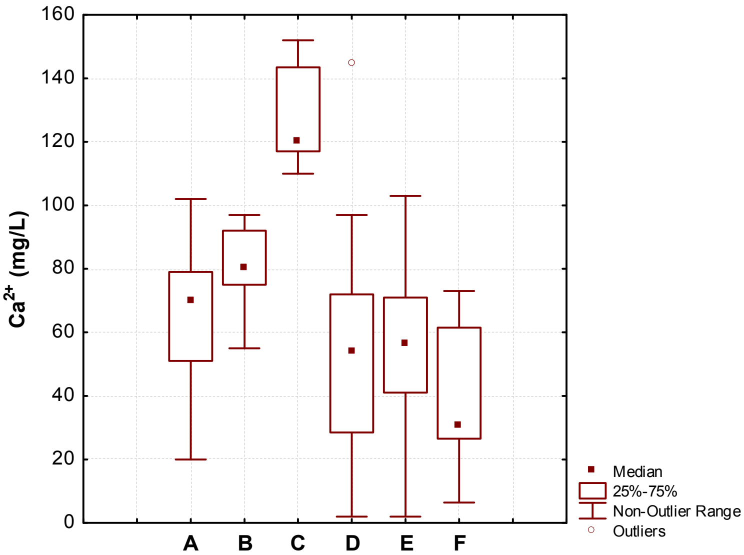

A = pumping station (n=35)
B = borehole (n=10)
C = private well (n=8)
D = spring capture (n=44)
E = spring (n=58)
F = surface water (n=20)

Figure 108: Box and whisker plots for groundwater Ca^{2+} concentration according to sampling object type

Spatial distribution of groundwater Ca^{2+}

The lowest groundwater Ca^{2+} concentrations were found in the NNE part (Pohorje Mt.), around central and north-eastern part of the country, where igneous and metamorphic rocks, shale and sandstone, and gravel, sand, and clay prevail in the recharge area of sampled groundwater. Plotted groundwater samples on the Piper diagram (Fig. 114) suggest a cation-exchange (natural water softening) in the recharge area of clays. Low groundwater Ca^{2+} values are also observed in the recharge area of high karst carbonate rocks most possibly due to low or non-existent soil layer and low atmospheric CO_2, alpine type of vegetation, low air temperatures, snow coverage (surface drainage when snow melting), groundwater dilution (increased precipitation rate by 1,500-3,200 mm of precipitation per year (EARS, 2006) causing fast underground drainage via channels or fractureds and surface drainage, or dolomite prevailing in the recharge areas. On the contrary, increased groundwater Ca^{2+} concentrations are observed mostly in all alluvial aquifers with the exception of alluvial plains in the NE and E part of the country, and coastal part. Groundwater Ca^{2+} concentration peaks are observed at sampling location Strahinec and Padiščak and are believed to be increased due to anthropogenic influence on groundwater.

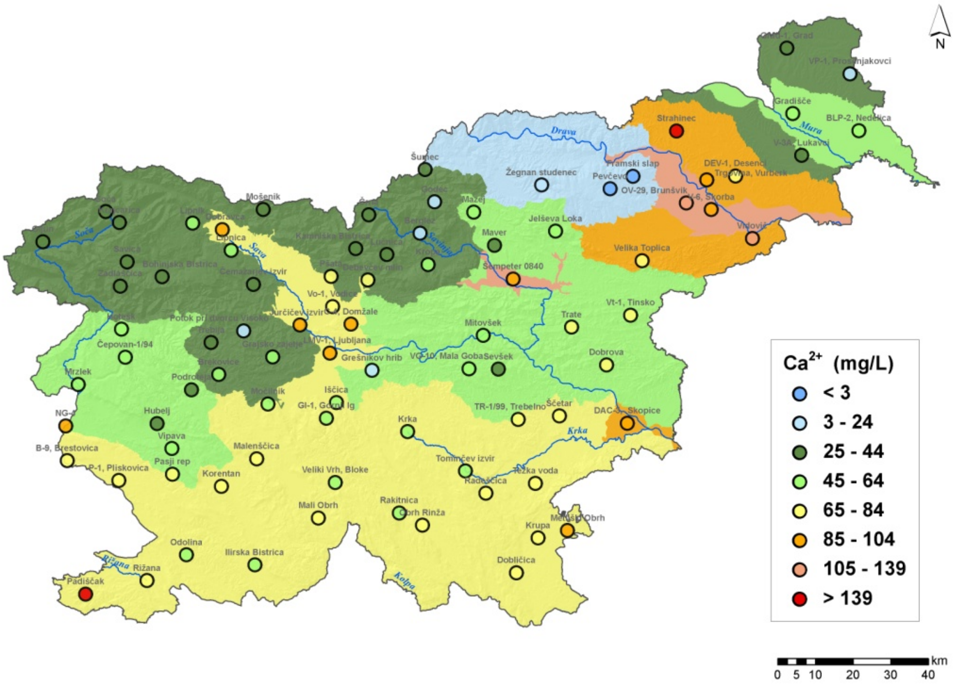

***Figure 109*: Spatial distribution of groundwater Ca^{2+}**

4.6.1.2. Magnesium (Mg^{2+}) in groundwater

Descriptive statistics of groundwater Mg^{2+}

The mean groundwater Mg^{2+} concentration is 13.0 mg/L, median 9.5 mg/L, maximum 42.0 mg/L, and minimum 1 mg/L (Tab. 26). Groundwater Mg^{2+} is not normally distributed (Fig. 110) and its concentration distribution is found in the Figure 111. The analytical uncertainty for Mg^{2+} is 4.5-19 % (n=164) and concentrations below LOD (½ LOD=1 mg/L) are found in 11 water samples (sampling locations Korentan, Čemažarjev izvir, Godec, Pevčevo, Framski slap, Žegnani studenec).

Table 26: Descriptive statistics of groundwater Mg^{2+}

Parameter	n	X	Md	Min	Max	S
Mg^{2+} (mg/L)	175	13.0	9.5	1.0	42.0	10.1

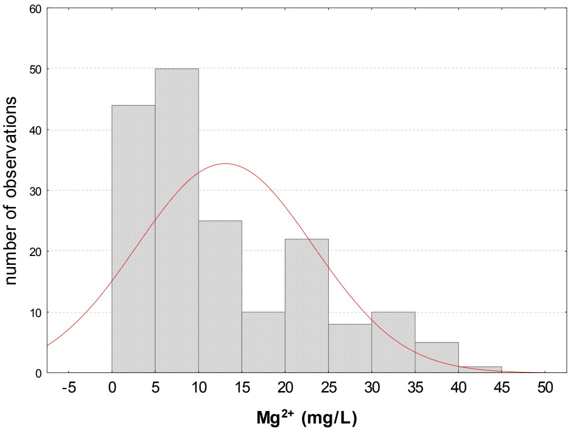

Figure 110: Histogram for groundwater Mg^{2+} concentration (n=175)

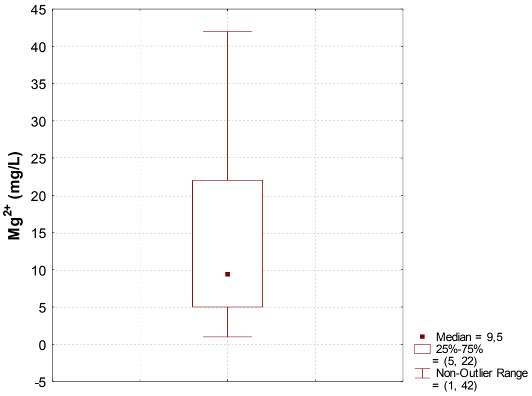

Figure 111: Box and whisker plot for groundwater Mg^{2+} concentration (n=175)

Rock type

Groundwater Mg^{2+} concentrations in clastic sedimentary and carbonate rocks is significantly higher ($p<0.05$) compared to concentrations measured in the recharge are of igneous and metamorphic rocks (Fig. 112, Appendix 13G). This is due to greater share of Mg-bearing minerals in the carbonate and clastis sedimentary rocks, solubility rate of minerals in aquifer's rocks, soil and atmospheric CO_2, groundwater dilution by precipitation, and also due to anthropogenic influence on groundwater mostly in the recharge area of clastic sedimentary rocks in the north-eastern part of the study area. In the recharge area of igneous and metamorphic rocks groundwater is depleted in Mg^{2+} content due to the lack of magnesium-rich minerals in silicate rocks, which are weathering slowly.

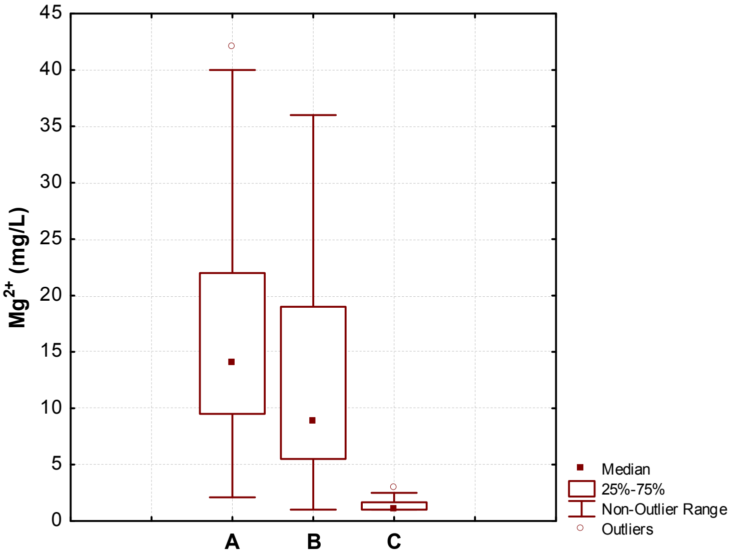

A = clastic sedimentary rocks (n=53)
B = carbonate rocks (n=110)
C = igneous and metamorphic rocks (n=12)

Figure 112: Box and whisker plots for groundwater Mg^{2+} concentration in the recharge area of major rock types

In the recharge areas of Pliocene, Quaternary, and Miocene clastics, the groundwater Mg^{2+} is the highest (Figs. 113 and 114, Appendix 11G). Medium groundwater Mg^{2+} values were found in the recharge area in Eocene flysch rocks, Oligocene clay "sivica", and carbonates. The lowest groundwater Mg^{2+} content was measured in the recharge area in igneous and metamorphic rocks. Groundwater Mg^{2+} concentrations in the recharge areas of Miocene clastics is significantly higher compared to recharge areas with Eocene flysch rocks, Jurassic and Cretaceous carbonates, Ladinian igneous rocks, Oligocene igneous rocks, Carboniferous-Permian beds, Oligocene clay “sivica”, and old Paleozoic rocks. Groundwater Mg^{2+} concentrations in the recharge areas of Pliocene clastics is significantly higher ($p<0.05$) compared to recharge areas with Ladinian igneous rocks, Oligocene igneous rocks, Carboniferous-Permian beds, and old Paleozoic rocks.

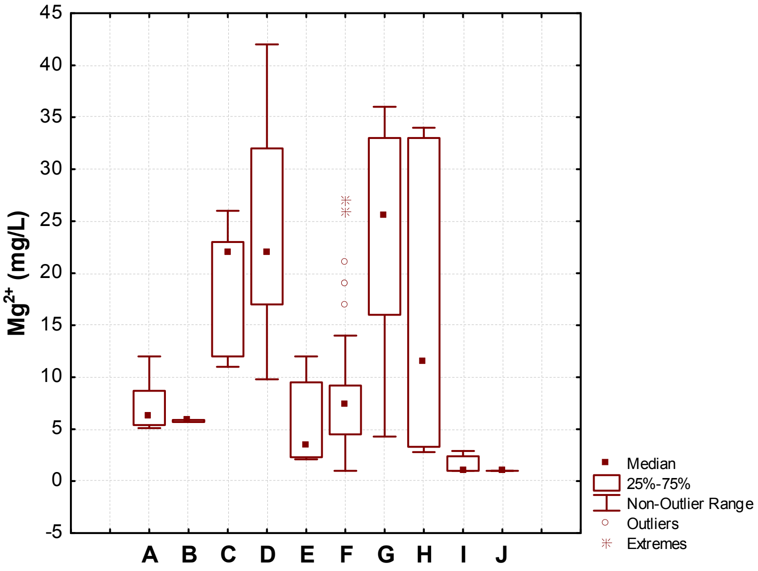

A = flysch rocks (n=7)
B = clay (n=2)
C = gravel and sand (n=26)
D = gravel, sand and clay (n=11)
E = shale and sandstone (n=7)
F = limestone prevailing (n=74)
G = dolomite prevailing (n=30)
H = carbonates with clastics (n=6)
I = igneous rocks (n=8)
J = metamorphic rocks (n=4)

Figure 113: Box and whisker plots for groundwater Mg^{2+} concentration in the recharge area of prevailing lithological unit

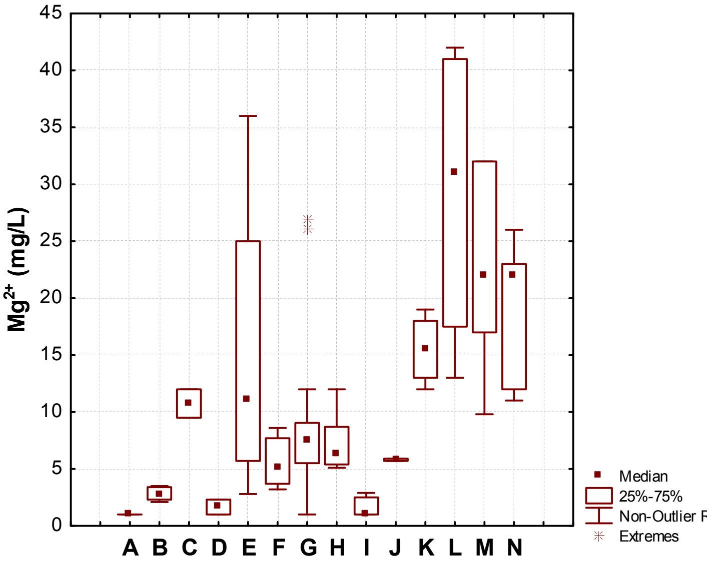

A = old Paleozoic rocks (n=4)
B = Carboniferous-Permian beds (n=5)
C = Permian Val Gardena layers (n=2)
D = Ladinian igneous rocks (n=2)
E = Triassic carbonates (n=70)
F = Jurassic carbonates (n=8)
G = Cretaceous carbonates (n=28)
H = Eocene flysch rocks (n=7)
I = Oligocene igneous rocks (n=6)
J = Oligocene clay “sivica” (n=2)
K = Miocene Lithothamnium limestone (n=4)
L = Miocene clastics (n=4)
M = Pliocene clastics (n=7)
N = Quaternary clastics (medium- and coarse-grained) (n=26)

Figure 114: Box and whisker plots for groundwater Mg^{2+} concentration in the recharge area of prevailing lithostratigraphic unit

High groundwater Mg^{2+} concentrations in the recharge areas with carbonate rocks (dolomite or limestone prevailing, and carbonates with clastics) are due to magnesium-rich minerals (dolomites) in carbonate rocks. This has been verified with strong correlations between Mg^{2+} and EC ($r_s=0.79$, $p<0.05$) and HCO_3^-

(r_s=0.76, $p<0.05$) (Fig. 115). In the recharge areas of limestone prevailing significant amounts of groundwater Mg^{2+} concentrations can occur because of mixing of dolomites and limestones in the recharge area). Outliers in the recharge area of limestone prevailing suggest prevailing dolomite over limestone. The wide range in groundwater Mg^{2+} in carbonates with clastics recharge area is due to heterogeneous lithologic structure of rock sequence. These rocks are mostly of carbonate origin and contain magnesium-rich minerals, which solubility depends on the presence of H_2CO_3 in the water. Increased groundwater Mg^{2+} values are also observed in the recharge area of gravel and sand, where the source of magnesium is mostly of carbonate origin of pebbles and sand grains except in north-eastern part of the country (Bavec and Pohar, 2009).

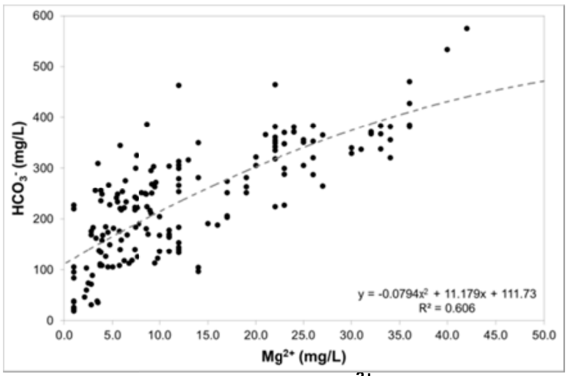

Figure 115: Groundwater Mg^{2+} versus HCO_3^- concentration

The source of magnesium in the recharge area of flysch rocks is in carbonate cement of sandstone and marl (Pavlovec, 1977, 1980), and possible anthropogenic influence (sampling location Padiščak). In the recharge area of gravel, sand and clay the sources of magnesium are magnesium-rich minerals (e.g. dolomites, amphiboles, and phyllosilicates) (Mioč and Žnidarčič, 1989; Kralj, 2003) found in the carbonate, metamorphic, and igneous rocks (Mioč and Žnidarčič, 1989; Kralj, 2003). The source of magnesium in Pliocene clastics (deep aquifers) is in the longer groundwater residence time and better geochemical equilibration with dolomite or magnesium silicates, or by ion exchange processes (Rman *et al.*, 2011). In the sampling location Strahinec (NE part) increased values of groundwater Mg^{2+} are observed most possibly due to anthropogenic origin (inorganic mineral fertilizers). Namely, in this particular sampling location groundwater also contains increased concentration of EC, Ca^{2+}, Mg^{2+}, HCO_3^-, SO_4^{2-}, K^+, B, Sr, Zn. It is believed that this is a consequence of fertilizer use above the aquifer's recharge area. Namely N, P, and K are considered as primary nutrients, S, Mg, Ca, Na as secondary, and B, Co, Cu, Fe, Mn, Mo and Zn as micronutrients (Ronen, 2007).

In Oligocene clay "sivica" the source of magnesium is found in carbonate minerals and phyllosilicates (illite/muscovite, chlorite and montmorillonite) (Kralj and Mišič, 2003). In the recharge area of shale and sandstone the groundwater Mg^{2+} content is low due to slow weathering rate, but the source for magnesium is in the carbonate mineralas and phyllosilicates (Skaberne *et al.*, 2009).

The lowest groundwater Mg^{2+} concentrations were measured in igneous and metamorphic rocks, where only 3 water samples had Mg^{2+} concentrations above the LOD, and 9 water samples below the LOD. These rocks are poor in Mg-rich minerals.

Groundwater Mg^{2+} concentrations in the recharge areas of gravel, sand, and clay are significantly higher ($p<0.05$) compared to groundwater with recharge areas with limestone prevailing, flysch rocks, clay, igneous and metamorphic rocks, and shale and sandstone. Similar is with groundwater in the recharge areas of gravel and sand which has Mg^{2+} concentrations significantly higher ($p<0.05$) compared to groundwater with recharge areas with clay, igneous and metamorphic rocks, and shale and sandstone. Groundwater Mg^{2+} concentrations in the recharge areas with dolomite prevailing is significantly higher ($p<0.05$) compared to groundwater in the recharge areas with limestone prevailing, flysch rocks, clay, igneous and metamorphic rocks, and shale and sandstone. Groundwater Mg^{2+} concentrations in the recharge areas of carbonates with clastics is significantly higher ($p<0.05$) compared to igneous and metamotphic rocks.

Increased groundwater Mg^{2+} concentration (>25 mg/L) is found in 14 sampling locations P-1 Pliskovica, Čepovan-1/94, GI-1 Gornji Ig, Grajsko zajetje, Ščetar, Velika Toplica, Veliki Vrh Bloke, VG-10 Mala Goba, Vt-1 Tinsko, TR-1 Trebelno, DAC-3 Skopice, Šempeter 0840, DEV-1 Desenci, and Strahinec which suggests that the prevailing lithological unit (or mineral) in the recharge area is dolomite (e.g. Čepovan-1/94, Grajsko zajetje; Velika Toplica, Vt-1 Tinsko). This has been verified by the molar ratio between Ca^{2+} and Mg^{2+} in groundwater. Higher molar ratios (>2) (Fig. 116) indicate dissolution of carbonate rocks (both dolomite and calcite), suggesting the dominant geochemical process is dissolution of carbonate minerals (calcite), followed by dissolution of dolomite and silicate minerals. Waters in grey are mostly of Ca^{2+}-Mg^{2+}-HCO_3^- water type, whereas waters with Ca^{2+}/Mg^{2+} molar ratio > 3 are mostly of Ca^{2+}-HCO_3^- water type.

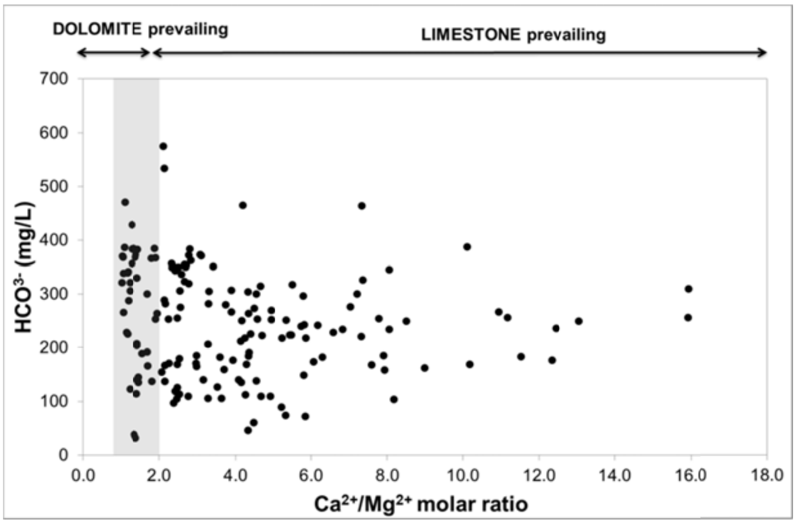

Figure 116: Groundwater Ca^{2+}/Mg^{2+} molar ratio versus HCO_3^- concentration

Figure 117 illustrates Ca^{2+} and Mg^{2+} molar concentrations and three lines (first $Ca^{2+}/Mg^{2+} = 1$, second $Ca^{2+}/Mg^{2+} = 2:1$, third $Ca^{2+}/Mg^{2+} = 10:1$) indicating the dissolution of dolomite, calcite, or both. All water samples having a ratio around 1 indicate the dissolution of dolomite, and higher ratios indicate dissolution of calcite, and other silicate minerals.

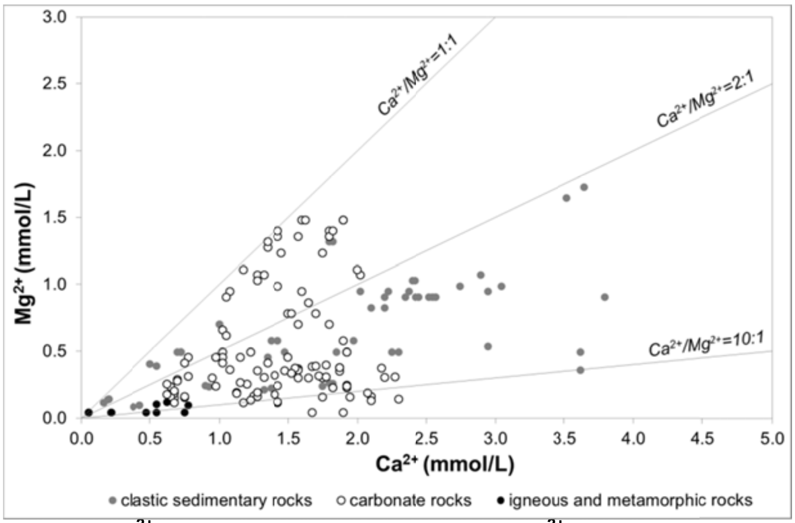

Figure 117: Groundwater Ca^{2+} molar concentration versus Mg^{2+} molar concentration

Sampled groundwater is dominated by the carbonate mineral dissolution, where water samples are plotted along the 2:1 line of HCO_3^- : Ca^{2+} + Mg^{2+}, 2:1 following the reactions:

calcite $CaCO_3+CO_{2(g)} + H_2O= Ca^{2+} + 2HCO_3^-$ (21)

dolomite $Ca_{0.5}Mg_{0.5}(CO3)+CO_2 + H_2O = 0.5\ Ca^{2+} + 0.5\ Mg^{2+} + 2HCO_3^-$ (22)

The half reaction for dolomite is used in order to put dolomite and calcite on an equal stoichiometric basis for the HCO_3^- produced during dissolution (Szramek *et al.*, 2007). Groundwater samples (Fig. 118) plotted on the $Ca^{2+}+Mg^{2+}$ line versus HCO_3^- = 1:2 indicate calcite and dolomite weathering of carbonate rocks in the recharge areas of sampling locations. Deviations of the line are probably due to weathering of other minerals, e.g. divalent cations in excess of carbonate dissolution (Szramek *et al.*, 2007), like e.g. groundwater from sampling location BLP-2 Nedelica suggesting the excess of Ca^{2+} and Mg^{2+} possibly due to lack of carbonate minerals in the recharge areas and possible lime application in the recharge areas of silicate minerals.

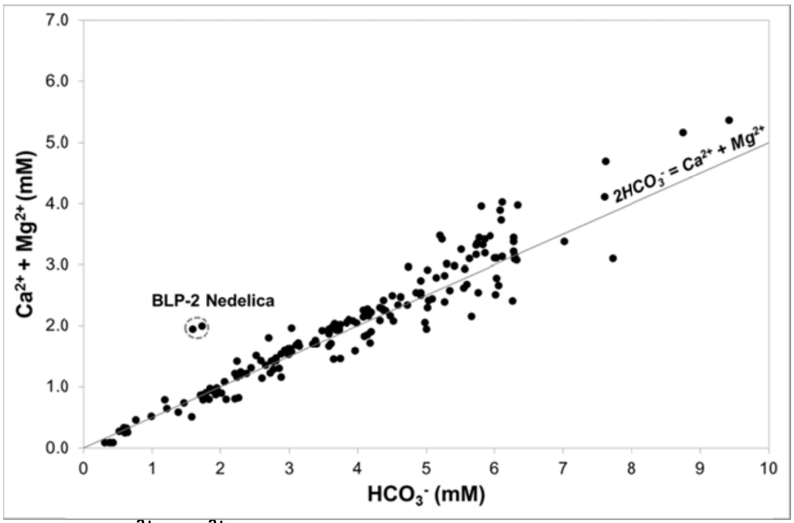

Figure 118: Groundwater $Ca^{2+}+Mg^{2+}$ versus HCO_3^- with line 1:2 indicating carbonate weathering

Aquifer porosity type

Groundwater from aquifers with intergranular, fractured and karstic, and mixed porosity (karstic, fractured, intergranular) has higher groundwater Mg^{2+} concentration compared to groundwater from fractured, and karstic and fractured porosity due to types and density of pores in the aquifer which induce groundwater flow through the network of pores, lower elevation of the recharge area, and other meteoric conditions (Fig. 119, Appendix 13G). Groundwater Mg^{2+} concentration is significantly lower ($p<0.05$) in aquifers with karstic and fractured porosity compared to intergranular, mixed (karstic, fractured, intergranular), and fractured and karstic porosity. Similar is groundwater with fractured porosity where groundwater has significantly lower ($p<0.05$) Mg^{2+} concentrations compared to groundwater with intergranular, mixed (karstic, fractured, intergranular), and fractured and karstic porosity.

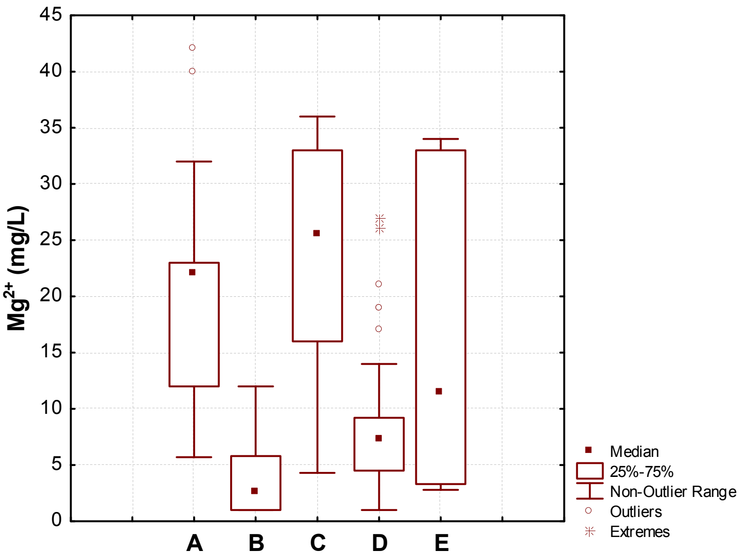

A = intergranular porosity (n=39)
B = fractured porosity (n=26)
C = fractured and karstic porosity (n=30)
D = karstic and fractured porosity (n=74)
E = mixed porosity (karstic, fractured, intergranular) (n=6)

Figure 119: Box and whisker plots for groundwater Mg^{2+} concentrations in the recharge area of prevailing aquifer porosity type

Land cover/use

The highest groundwater Mg^{2+} concentrations are observed in the recharge areas of land principally occupied by agriculture, with significant areas of natural vegetation, complex cultivation patterns, and industrial or commercial units (Figs. 120 and 121, Appendix 11G), suggesting possible anthropogenic source in groundwater (fertilizers). Increased groundwater Mg^{2+} values are also observed in few groundwater samples of the recharge area of deciduous forest. The lowest groundwater Mg^{2+} values are found in the recharge areas of bare rocks, marshes and heaths, and coniferous forest where the anthropogenic influence is less pronounced.

There are no significant differences in Mg^{2+} concentrations according to CORINE Land Cover classification and Actual agricultural and forest land usage classification.

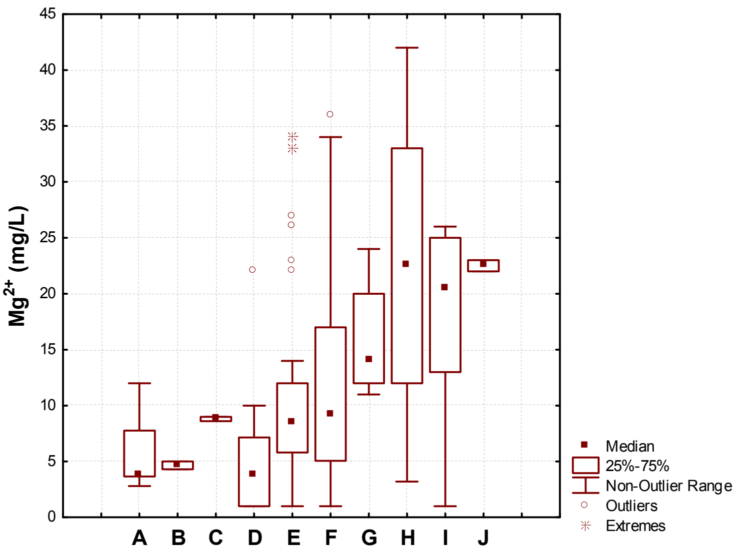

A = bare rocks (n=8)
B = moors and heathland (n=2)
C= natural grasslands (n=2)
D = coniferous forest (n=20)
E = broad-leaved forest (n=45)
F = mixed forest (n=56)
G = non-irrigated arable land (n=10)
H = complex cultivation patterns (n=18)
I = land principally occupied by agriculture, with significant areas of natural vegetation (n=10)
J = industrial or commercial units (n=2)

Figure 120: Box and whisker plots for groundwater Mg^{2+} concentration in the recharge area of prevailing land use type (CORINE Land Cover)

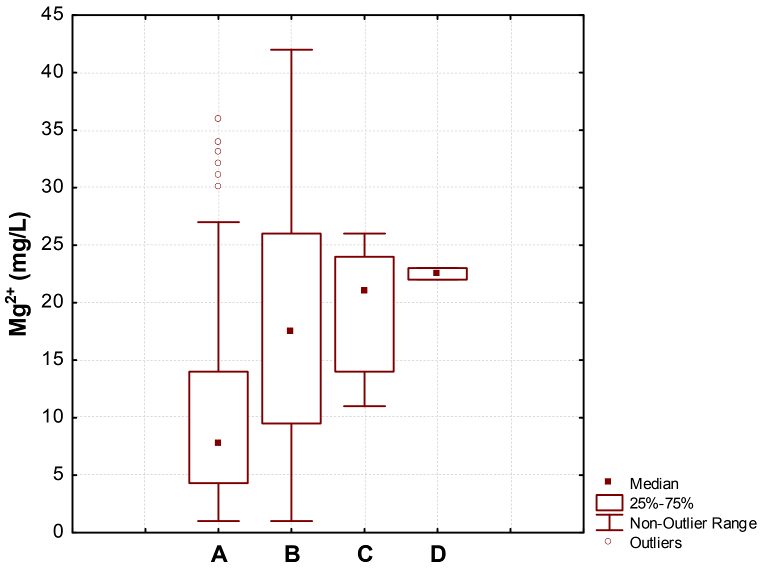

A = forest (n=137)
B = areas of less intense use of nutrients and plant protection products (n=18)
C = areas of intense use of nutrients and plant protection products (n=16)
D = urban areas (n=2)

Figure 121: Box and whisker plots for groundwater Mg^{2+} concentration in the recharge area of prevailing land use type (Actual agricultural and forest land usage)

Sampling object type

The highest groundwater Mg^{2+} concentrations are observed in private wells due to mineralogical composition of rocks in the recharge areas or possibly anthropogenic influence (Fig. 122, Appendix 13G). The lowest groundwater Mg^{2+} concentration was observed in springs and surface waters in high mountain regions, mostly due to rock type, and climatic conditions.

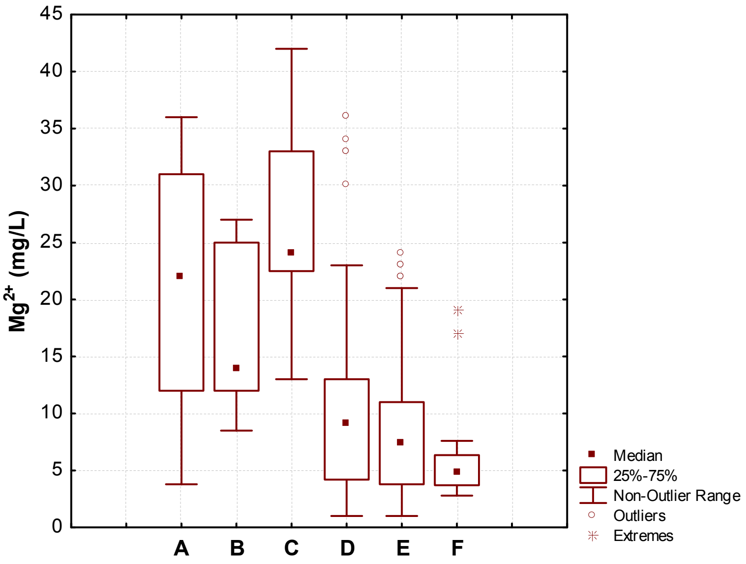

A = pumping station (n=35)
B = borehole (n=10)
C = private well (n=8)
D = spring capture (n=44)
E = spring (n=58)
F = surface water (n=20)

Figure 122: Box and whisker plots of groundwater Mg^{2+} concentrations according to sampling object type

Spatial distribution of groundwater Mg^{2+}

The lowest groundwater Mg^{2+} concentration is found in the NNE (Pohorje Mt.) and in the recharge area of igneous and metamorphic rocks (Fig. 123), where Mg-rich minerals are not so abundant (Hinterlechner-

Ravnik, 1973; Hinterlechner-Ravnik and Moine, 1977). The concentrations are also low due to elevated relief, which causes surface drainage and groundwater dilution by meteoric water of tributaries of various streams. Also low groundwater Mg^{2+} concentrations are found in the northern and north-western part of the country (Julian Alps and Kamnik-Savinja Alps) where more calcium enriched carbonate minerals prevail in the recharge area. Similar as groundwater Ca^{2+} concentrations the Mg^{2+} concentrations are low due to low CO_2 content in the soil and in the atmosphere, groundwater dilution causing fast underground drainage via channels or fractureds and surface drainage, and limestone prevailing in the recharge area.

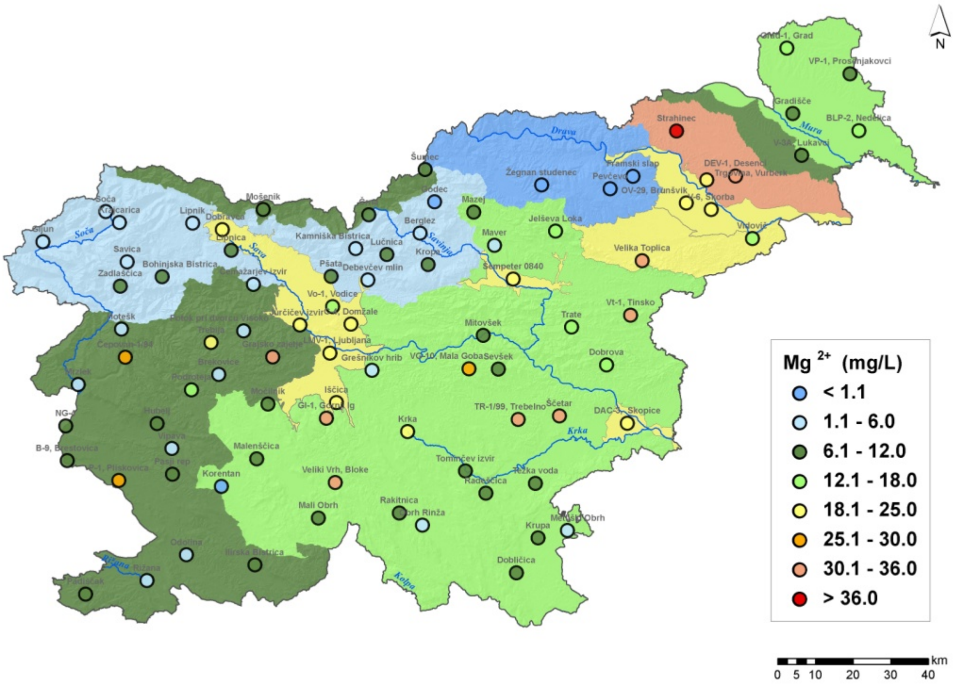

***Figure 123*: Spatial distribution of groundwater Mg^{2+}**

4.6.1.3. Molar ratio between calcium and magnesium (Ca^{2+}/Mg^{2+}) in groundwater

Descriptive statistics of groundwater Ca^{2+}/Mg^{2+} molar ratio

The mean Ca^{2+}/Mg^{2+} molar ratio is 4.0, median 3.1, minimum 1.0 and maximum 15.9 (Tab. 27). Groundwater samples where either Ca^{2+} or Mg^{2+} concentration was below LOD were excluded when calculating Ca^{2+}/Mg^{2+} molar ratios (sampling locations Pevčevo, Framski slap, Godec, Žegnani studenec, Korentan, and Čemažarjev izvir). Values of groundwater Ca^{2+}/Mg^{2+} molar ratio are not normally distributed (Fig. 124) and values above 10.2 present outliers (sampling locations Brekovice, Vipava, Metliški Obrh, Obrh Rinža, Debevčev mlin) (Fig. 125). None of water samples had the Ca^{2+}/Mg^{2+} molar ratio less than 1.

Table 27: Descriptive statistics of groundwater Ca^{2+}/Mg^{2+} molar ratio

Parameter	n	X	Md	Min	Max	S
Ca^{2+}/Mg^{2+} molar ratio	164	4.0	3.1	1.0	15.9	2.9

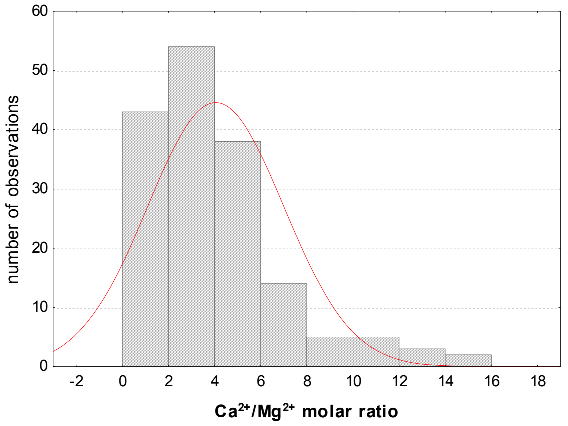

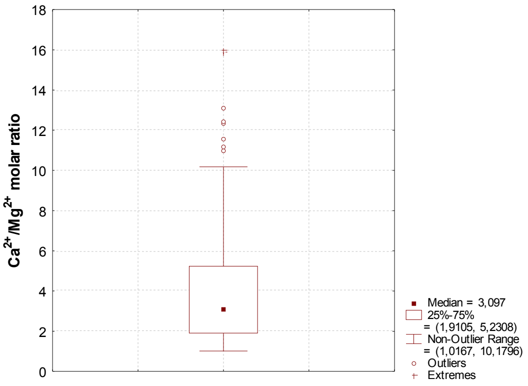

Figure 124: Histogram for groundwater Ca^{2+}/Mg^{2+} molar ratio (n=164)

Figure 125: Box and whisker plot for groundwater Ca^{2+}/Mg^{2+} molar ratio (n=164)

Rock type

The highest Ca^{2+}/Mg^{2+} molar ratio was found in the recharge ares of igneous and metamorphic rocks (Fig. 126, Appendix 13H) which suggest dissolution of silicate minerals (n=3) (sampling locations Brekovice and Čemažarjev izvir). There are no statistically significant differences ($p<0.05$) between observed groups. Extreme values of groundwater Ca^{2+}/Mg^{2+} molar ratios are observed in the recharge areas with carbonate rocks where Mg^{2+} concentration is very low. This suggests the prevalence of calcite over dolomite in the recharge area of limestones and in silicate rocks.

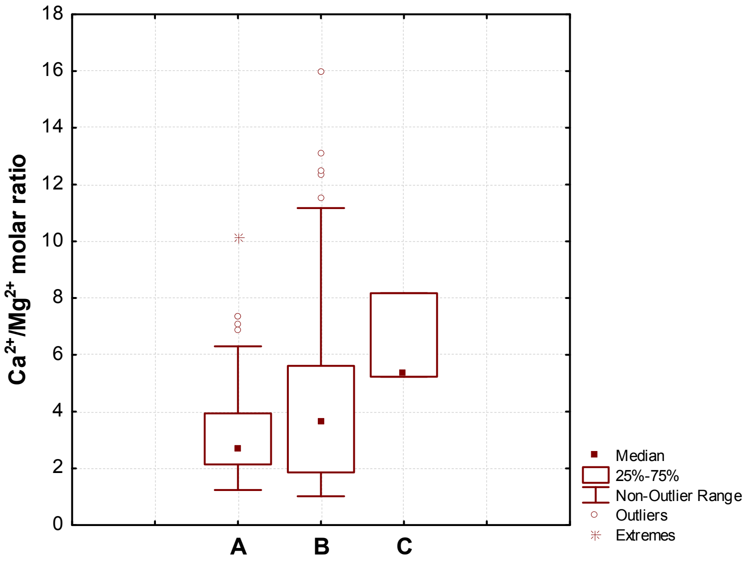

A = clastic sedimentary rocks (n=53)
B = carbonate rocks (n=108)
C = igneous and metamorphic rocks (n=3)

Figure 126: Box and whisker plots for groundwater Ca^{2+}/Mg^{2+} molar ratio in the recharge area of major rock types

The highest groundwater Ca^{2+}/Mg^{2+} molar ratio is observed in the recharge areas of flysch rocks (Figs. 127 and 128, 13H) which is significantly higher ($p<0.05$) compared to recharge areas with dolomite prevailing, gravel and sand (and clay), and shale and sandstone. Also high are Ca^{2+}/Mg^{2+} molar ratios in a few outliers in the recharge areas of limestone prevailing. The outliers in gravel and sand are observed at sampling location in the alluvial deposits (NE part) with lower carbonate content. Outlier with the highest molar ratio in gravel and sand was found in carbonate (limestone) recharge area of Soča River (north-western part). In the dolomite prevailing recharge area one sampling location appears as an outlier due to the highest molar ratio, suggesting the prevailing limestone over dolomite in the recharge area. The lowest molar ratios are observed in the recharge areas of shale and sandstone, and dolomite prevailing. Groundwater Ca^{2+}/Mg^{2+} molar ratio is significantly lower ($p<0.05$) in the recharge areas with Permian Val Gardena layers and Pliocene clastics compared to Eocene flysch rocks and Jurassic carbonates.

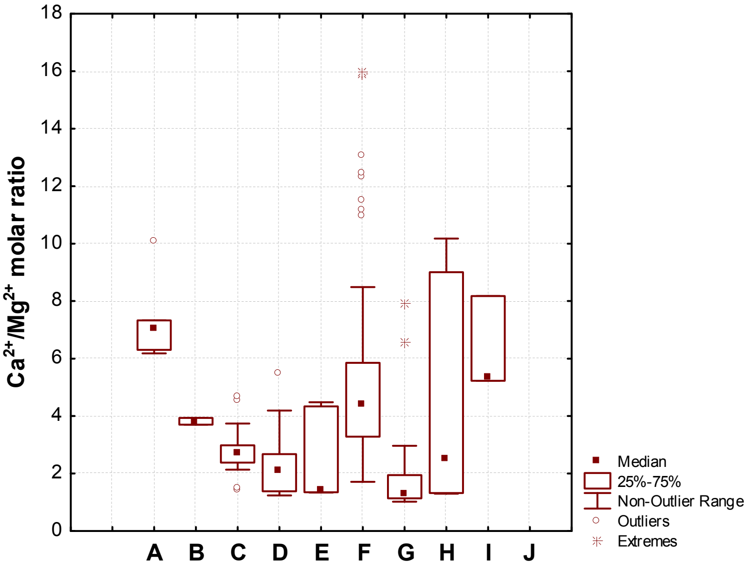

A = flysch rocks (n=7)
B = clay (n=2)
C = gravel and sand (n=26)
D = gravel, sand and clay (n=11)
E = shale and sandstone (n=7)
F = limestone prevailing (n=72)
G = dolomite prevailing (n=30)
H = carbonates with clastics (n=6)
I = igneous rocks (n=3)
J = metamorphic rocks (n=0)

***Figure 127: Box and whisker plots for groundwater* Ca^{2+}/Mg^{2+} molar ratio in the recharge area of prevailing lithological unit**

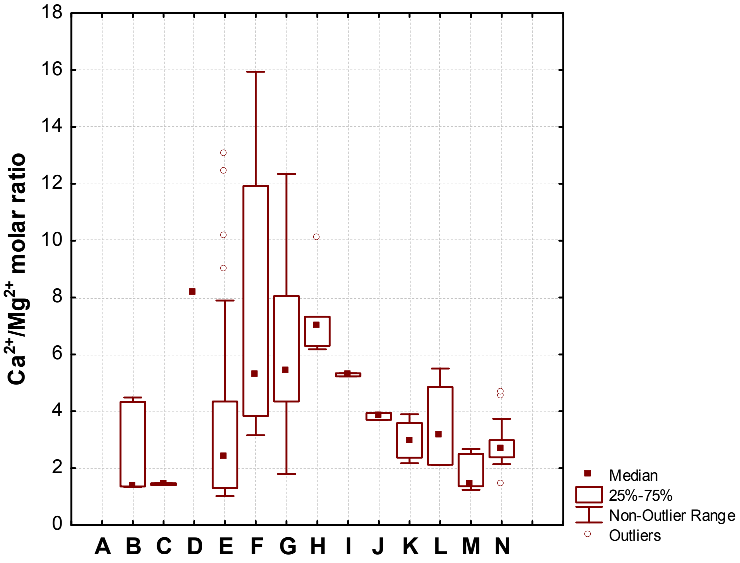

A = old Paleozoic rocks (n=0)
B = Carboniferous-Permian beds (n=5)
C = Permian Val Gardena layers (n=2)
D = Ladinian igneous rocks (n=1)
E = Triassic carbonates (n=70)
F = Jurassic carbonates (n=8)
G = Cretaceous carbonates (n=26)
H = Eocene flysch rocks (n=7)
I = Oligocene igneous rocks (n=2)
J = Oligocene clay “sivica” (n=2)
K = Miocene Lithothamnium limestone (n=4)
L = Miocene clastics (n=4)
M = Pliocene clastics (n=7)
N = Quaternary clastics (medium- and coarse-grained) (n=26)

Figure 128: Box and whisker plots for groundwater Ca^{2+}/Mg^{2+} concentration in the recharge areas of prevailing lithostratigraphic unit

Spatial distribution of groundwater Ca^{2+}/Mg^{2+} molar ratio

Groundwater Ca^{2+}/Mg^{2+} molar ratios (<2) indicate that recharge area of sampled groundwater is in dolomite and mixed dolomite with limestone, where the water types Ca^{2+}-Mg^{2+}-HCO_3^- and Na^+-Ca^{2+}-Mg^{2+}-HCO_3 prevail (Fig. 129). Groundwater with higher molar ratio (>2) has mostly Ca^{2+}-HCO_3^- water type indicating limestone prevalence in the recharge area of sampled groundwater. High molar ratios are observed in the recharge area of calcite prevailing over dolomite in the carbonate recharge area (Korentan) and in the recharge area of silicate rocks.

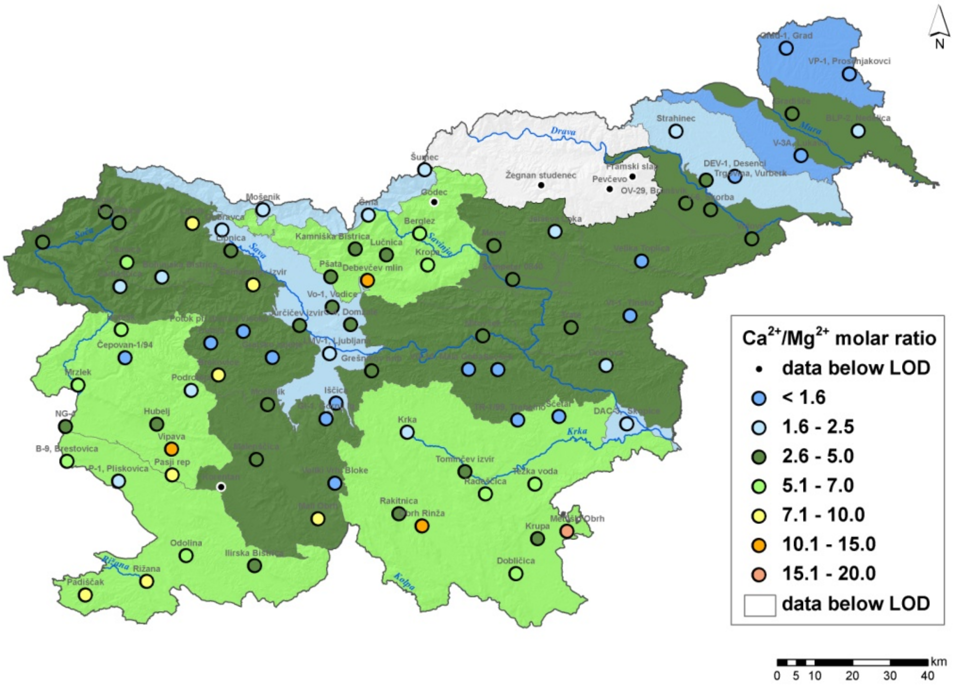

Figure 129: **Spatial distribution of groundwater Ca^{2+}/Mg^{2+} molar ratio**

4.6.1.4. *Bicarbonate (HCO_3^-) in groundwater*

Descriptive statistics of groundwater HCO_3^-

Descriptive statistics for groundwater HCO_3^- is present in the Table 28. Groundwater HCO_3^- concentration ranges between 19 mg/L and 575 mg/L, with mean value of 235 mg/L and median 234 mg/L. Groundwater HCO_3^- concentrations are normally distributed (Fig. 130) and values higher than 534 mg/L (Fig. 131) present outliers (sampling location Strahinec). The uncertainty for HCO_3^- is ± 3 % (n=175).

Table 28: Descriptive statistics of groundwater HCO_3^-

Parameter	n	X	Md	Min	Max	S
HCO_3^- (mg/L)	175	235	234	19	575	110

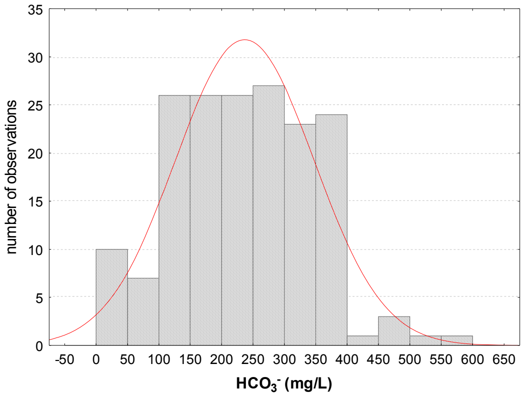

Figure 130: Histogram for groundwater HCO_3^- concentration (n=175)

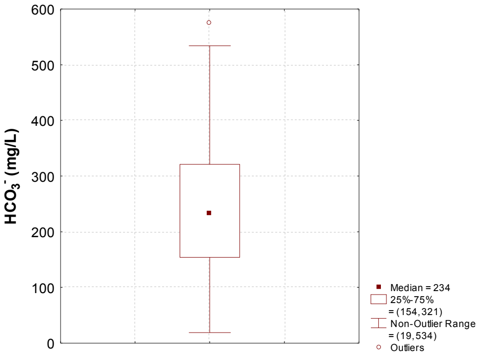

Figure 131: Box and whisker plot for groundwater HCO_3^- concentration (n=175)

Rock type

Groundwater HCO_3^- concentrations in the recharge areas of clastic sedimentary and carbonate rocks rocks are significantly higher ($p<0.05$) compared to recharge areas with igneous and metamorphic rocks. These rocks are rich in carbonate minerals and/or cement (Fig. 132, Appendix 13I). Since groundwater HCO_3^- concentrations in the recharge area of clastic sedimentary rocks exceed concentrations measured in some groundwater samples from recharge areas with carbonate rocks this may suggest the anthropogenic source in groundwater. Increased values (> 400 mg/L) are observed at sampling locations Strahinec, Vidovič, Padiščak, Vt-1 Tinsko, and Ščetar.

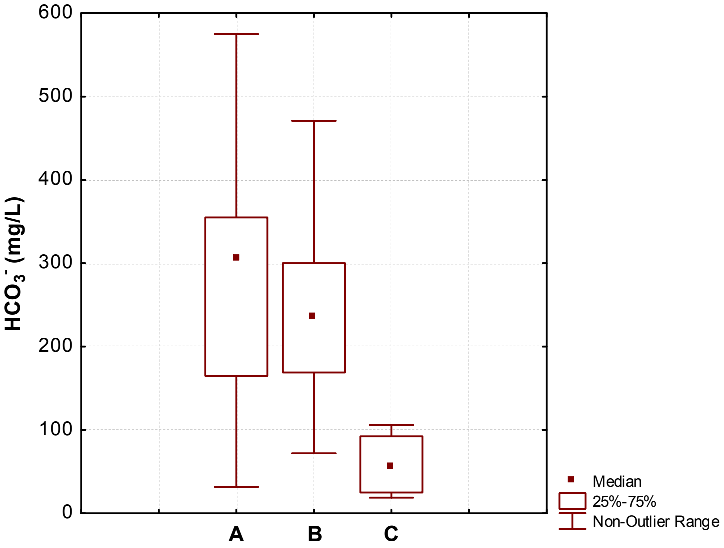

A = clastic sedimentary rocks (n=53)
B = carbonate rocks (n=110)
C = igneous and metamorphic rocks (n=12)

Figure 132: Box and whisker plots for groundwater HCO_3^- concentration in the recharge area of major rock types

The highest groundwater HCO_3^- concentrations are measured in the recharge areas with Miocene clastites which are significantly higher ($p<0.05$) compared to recharge areas with other lithostratigraphic units, except with Eocene flysch rocks, and Quaternary clastics (medium- and coarse-grained). This is due to dissolution of carbonate minerals and cement (Figs. 133 and 134, Appendix 13I). It is also believed that at sampling location Strahinec an anthropogenic influence is present (lime application). The lowest groundwater HCO_3^- concentrations are measured in poorly permeable old Paleozoic rocks, Carboniferous-Permian beds, and Oligocene igneous rocks. Groundwater HCO_3^- concentrations in the recharge areas with Oligocene igneous rocks, Carboniferous-Permian beds, and old Paleozoic rocks which are significantly lower ($p<0.05$) compared to recharge areas in Eocene flysch rocks, Cretaceous carbonates, Quaternary clastics (medium- and coarse-grained), Miocene Lithothamnium limestone, Miocene clastics, and Pliocene clastics.

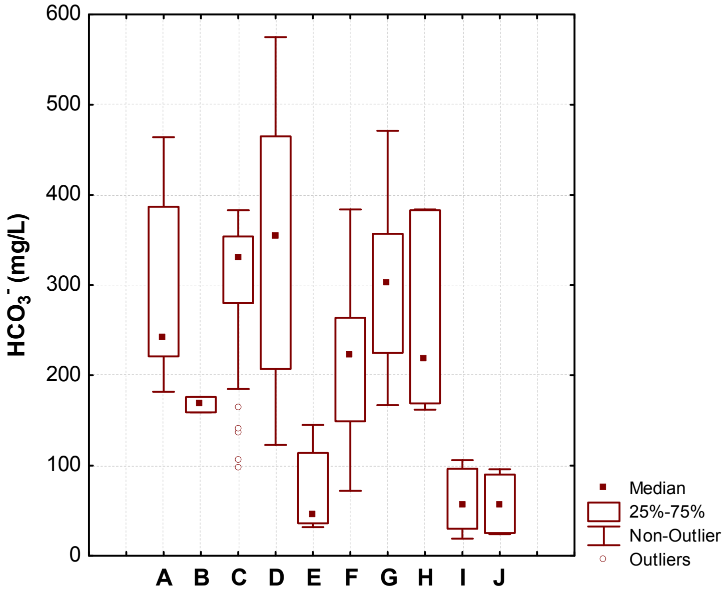

A = flysch rocks (n=7)
B = clay (n=2)
C = gravel and sand (n=26)
D = gravel, sand and clay (n=11)
E = shale and sandstone (n=7)
F = limestone prevailing (n=74)
G = dolomite prevailing (n=30)
H = carbonates with clastics (n=6)
I = igneous rocks (n=8)
J = metamorphic rocks (n=4)

Figure 133: Box and whisker plots for groundwater HCO_3^- concentration in the recharge areas of prevailing lithological unit

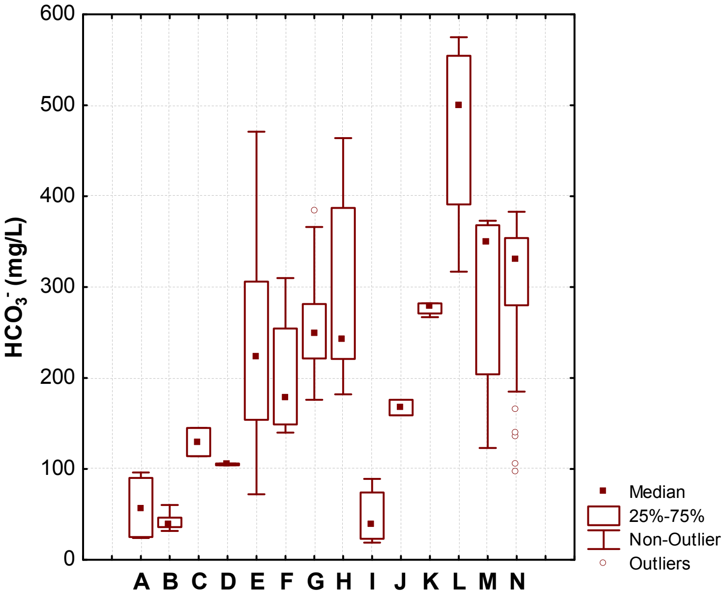

A = old Paleozoic rocks (n=4)
B = Carboniferous-Permian beds (n=5)
C = Permian Val Gardena layers (n=2)
D = Ladinian igneous rocks (n=2)
E = Triassic carbonates (n=70)
F = Jurassic carbonates (n=8)
G = Cretaceous carbonates (n=28)
H = Eocene flysch rocks (n=7)
I = Oligocene igneous rocks (n=6)
J = Oligocene clay “sivica” (n=2)
K = Miocene Lithothamnium limestone (n=4)
L = Miocene clastics (n=4)
M = Pliocene clastics (n=7)
N = Quaternary clastics (medium- and coarse-grained) (n=26)

Figure 134: Box and whisker plots for groundwater HCO_3^- concentration in the recharge area of prevailing lithostratigraphic unit

Dissolved groundwater Ca^{2+} and Mg^{2+} ions are supplied mostly by carbonate weathering and smaller contribution from the silicate weathering, as is indicated by low groundwater content of Si and relatively high HCO_3^- (Fig. 135).

Due to correlations with other parameters an anthropogenic influence on the groundwater is observed (use of lime, fertilizers, and construction material) at sampling locations Strahinec, Vidovič, and Padiščak. The origin of increased groundwater HCO_3^- from sampling locations Vt-1 Tinsko and Ščetar is geogenic, where mostly dolomites prevail in the recharge areas, and the soil type *rendzina*. This soil contains a great calcium carbonate reserve of parent material (Kolay, 2007). The graph below (Fig. 136) presents the correlations between the highest groundwater HCO_3^- and Ca^{2+} concentrations. Data suggest that groundwater influenced by the anthropogenic source (squares) (lime, fertilizers, construction material) could contain higher Ca^{2+} concentrations compared to geogenic source (circle).

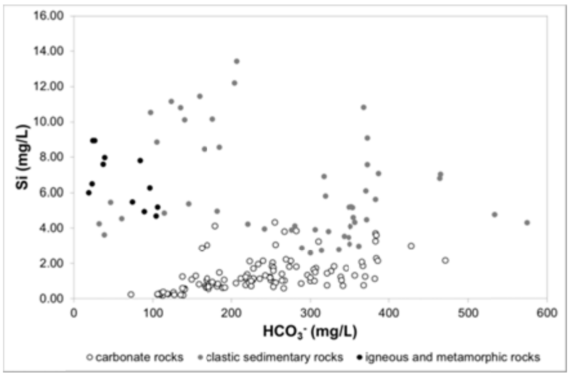

Figure 135: Groundwater HCO_3^- versus Si concentrations

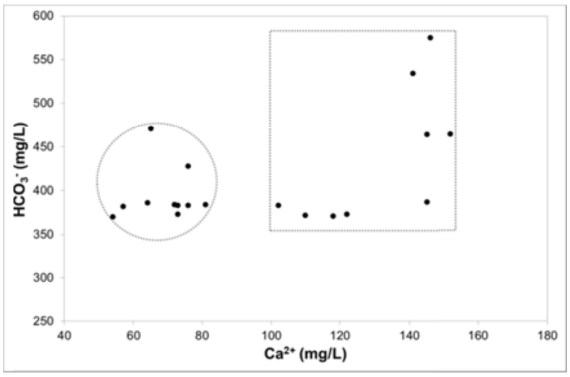

Figure 136: The highest groundwater HCO_3^- and Ca^{2+} concentrations

In the high mountain karst concentrations of groundwater HCO_3^- can be lower due to various reasons: due to the influence of fresh rainwater with low HCO_3^- concentration, which can flow long distances as surface waters (short residence time) before infiltrating into the aquifer, lower temperatures, thin (or non-existent) soil layer, and lower (initial) total CO_2. Lower groundwater HCO_3^- concentrations were measured in groundwater from the recharge area of poorly permeable rocks of silicate composition (igneous and metamorphic rocks) where concentrations are lower due to slow silicate weathering where cations like Ca^{2+}, Mg^{2+}, Na^+, and K^+, and clay minerals rich in alumosilicates are produced (Singhal and Gupta, 1999).

Figure 137 shows the correlation between groundwater HCO_3^- concentration and pH values. Groundwater samples from the recharge areas in some clastic sedimentary, igneous and metamorphic rocks deviate from the carbonate group, since groundwater contains less dissolved HCO_3^- at lower pH. Graph also indicates that the dominant anion in sampled groundwater is HCO_3^- which is also the prevalent component of DIC in the pH range. Figure 138 presents the relation between HCO_3^- concentration in groundwater and mean altitude of recharge areas. Groundwater at higher altitudes has less dissolved bicarbonate (HCO_3^-) compared to groundwater at lower altitudes. This is due to thinner (or non-existent) soil layer which is depleted in CO_2, low atmospheric CO_2 (P_{CO2}), and short residence time (surface runoff). Gams (1974) also studied the temperature dependence of water hardness of karstic springs in Slovenia. He observed that spring water at lower temperatures is softer than spring water at higher temperatures which is harder.

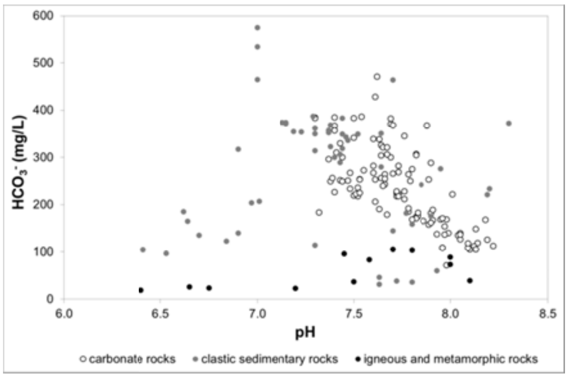

Figure 137: Scatter plot of groundwater HCO_3^- versus pH values

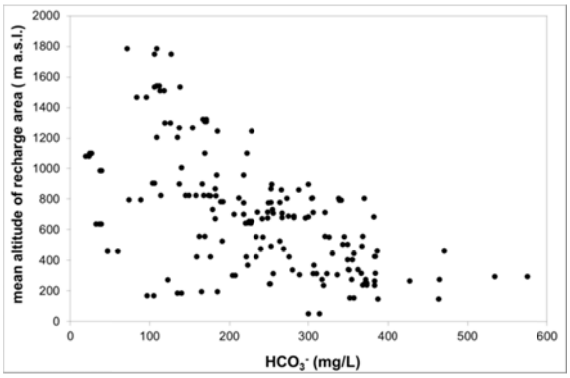

Figure 138: Scatter plot of groundwater HCO_3^- concentration versus mean altitude of recharge area

Groundwater correlation between HCO_3^- and EC is strong (r_s=0.92, $p<0.05$) (Fig. 139) which confirms that HCO_3^- is the major anion in Slovenian groundwaters. Association between groundwater HCO_3^- and calculated mean air temperature (Fig. 140) has been observed only between groundwater sampled in the recharge areas of carbonates (limestone prevailing, dolomite prevailing, and carbonates with clastics) where good positive correlation is observed ($y=0.183x^{0.6706}$, R=0.75). Lower groundwater HCO_3^- concentrations are observed at lower air temperatures due to elevated recharge area, low P_{CO2} and short residence time. High groundwater HCO_3^- concentrations are observed in the recharge areas with higher temperatures, thicker soil layer (increased bioproductivity), and lower altitudes, where mineral dissolution from the soil is more intense and the surface flow is slower. Groundwaters from sampling location B-9 Brestovica deviate from this line. Theoretically groundwater HCO_3^- concentration should be higher, but is lower due to high temperatures, small precipitation rate (summer drought) and thin soil layer with little vegetation cover left from the destruction from fire (destroyed forest vegetation like coppice, shrub lands with broadleaved species, and European black pine forests) (PGD Komen, 2003; Muhič, 2005; Košiček, 2005), which causes depletion in soil CO_2.

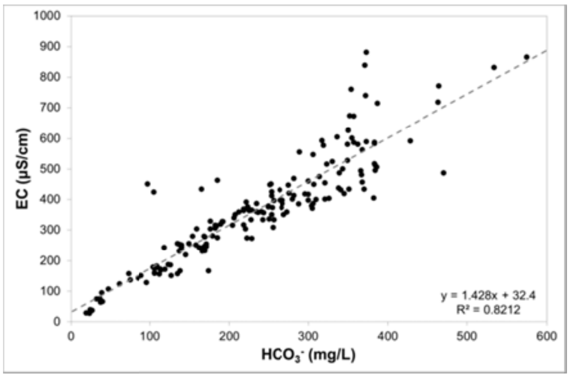

***Figure 139:* Scatter plot of groundwater HCO_3^- concentration versus EC**

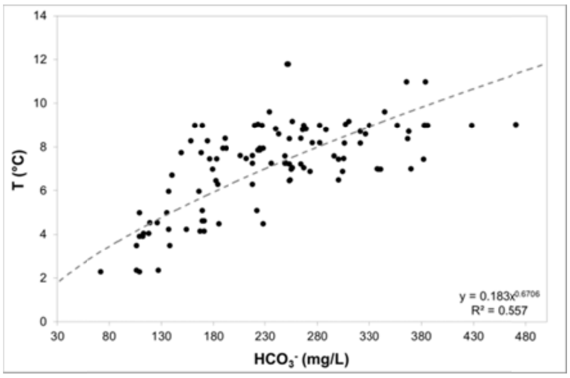

Figure 140: Groundwater HCO_3^- concentration versus mean air temperature of recharge area

Aquifer porosity type

Groundwater HCO_3^- concentrations Fig. 141, Appendix 13I) in the aquifers with fractured porosity are significantly lower ($p<0.05$) compared to aquifers with other porosity types. This is because less soluble minerals in the recharge areas of poorly permeable rocks are present, and also due to surface runoff of water.

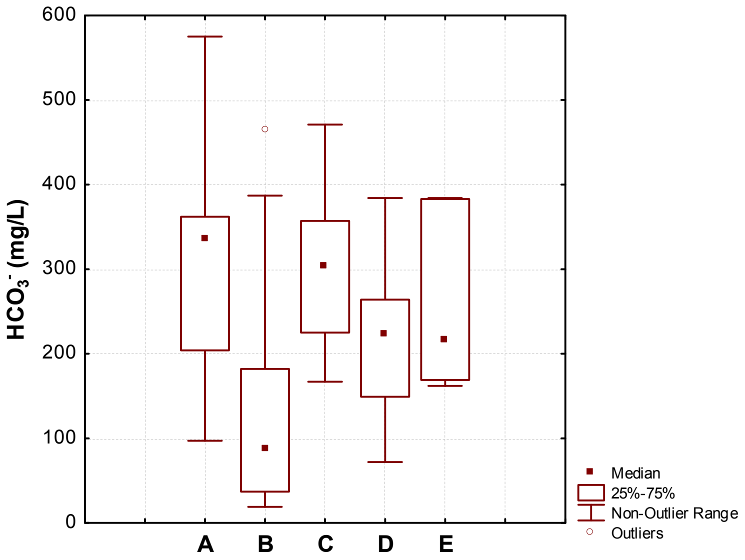

A = intergranular porosity (n=39)
B = fractured porosity (n=26)
C = fractured and karstic porosity (n=30)
D = karstic and fractured porosity (n=74)
E = mixed porosity (karstic, fractured, intergranular) (n=6)

Figure 141: Box and whisker plots for groundwater HCO_3^- concentration in the recharge area of prevailing aquifer porosity type

Land cover/use

The highest groundwater HCO_3^- concentrations are measured in the recharge areas of non-irrigated arable land, complex cultivation patterns, land principally occupied by agriculture, with significant areas of natural vegetation, and industrial or commercial units, which suggest possible anthropogenic influence (lime, fertilizers, construction material) on sampled groundwater (Figs. 142 and 143, Appendix 13I). Groundwater HCO_3^- concentrations in the recharge areas with industrial or commercial units and complex cultivation patterns are significantly higher ($p<0.05$) compared to recharge areas with bare rocks, moors and heathland, where the lowest HCO_3^- concentrations are measured.

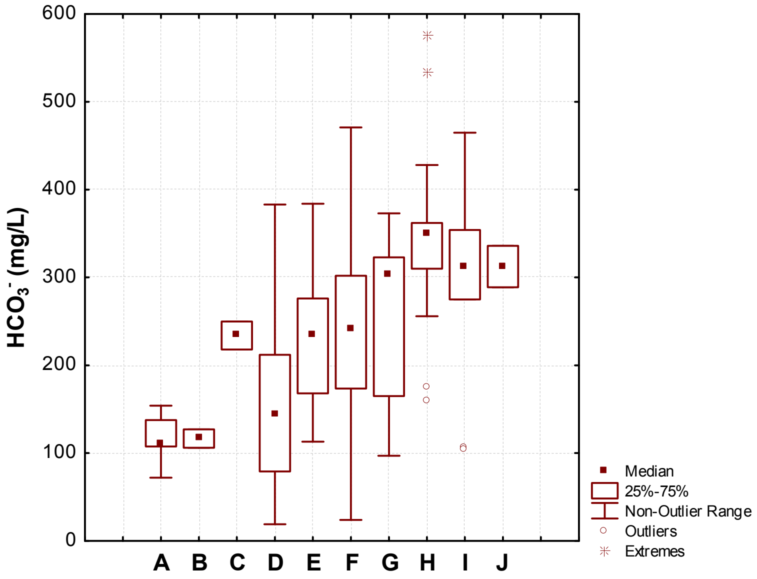

A = bare rocks (n=8)
B = moors and heathland(n=2)
C= natural grasslands (n=2)
D = coniferous forest (n=20)
E = broad-leaved forest (n=45)
F = mixed forest (n=56)
G = non-irrigated arable land (n=10)
H = complex cultivation patterns (n=18)
I = land principally occupied by agriculture, with significant areas of natural vegetation (n=10)
J = industrial or commercial units (n=2)

Figure 142: Box and whisker plots for groundwater HCO_3^- concentration in the recharge area of prevailing land use type (CORINE Land Cover)

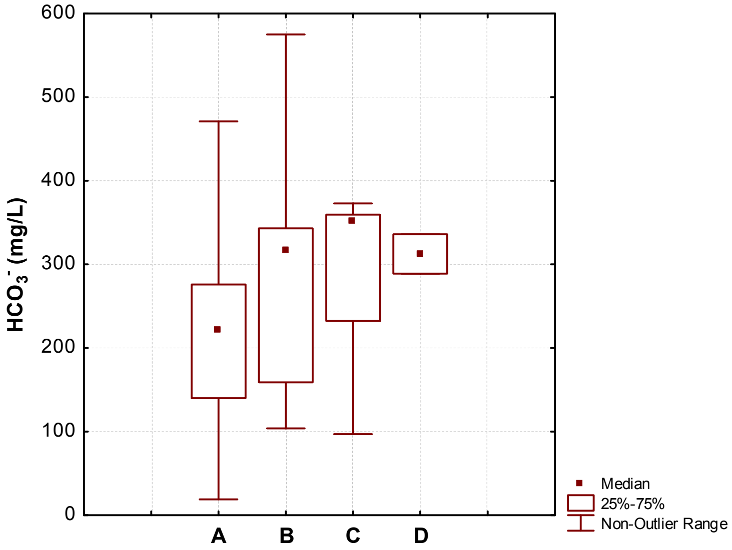

A = forest (n=137)
B = areas of less intense use of nutrients and plant protection products (n=18)
C = areas of intense use of nutrients and plant protection products (n=16)
D = urban areas (n=2)

Figure 143: Box and whisker plots for groundwater HCO_3^- concentration in the recharge area of prevailing land use type (Actual agricultural and forest land usage)

Sampling object type

The highest groundwater HCO_3^- concentrations are observed in water from private wells (Fig. 144, Appendix 13I) suggesting the carbonate origin of minerals in the recharge areas, high initial CO_2 (atmospheric and soil) content, and the influence of anthropogenic factors (due to vicinity of agricultural land) by lime application or other fertilizers. The lowest groundwater HCO_3^- concentrations are measured in the surface waters due to low level of dissolved constituents in groundwater in high mountain regions, and degassing of soil CO_2, which may be gradually released to the atmosphere as the water equilibrates with the atmospheric concentration of CO_2 (the outgassing effect) (De Vos *et al.*, 2006; Giesler *et al.*, 2013).

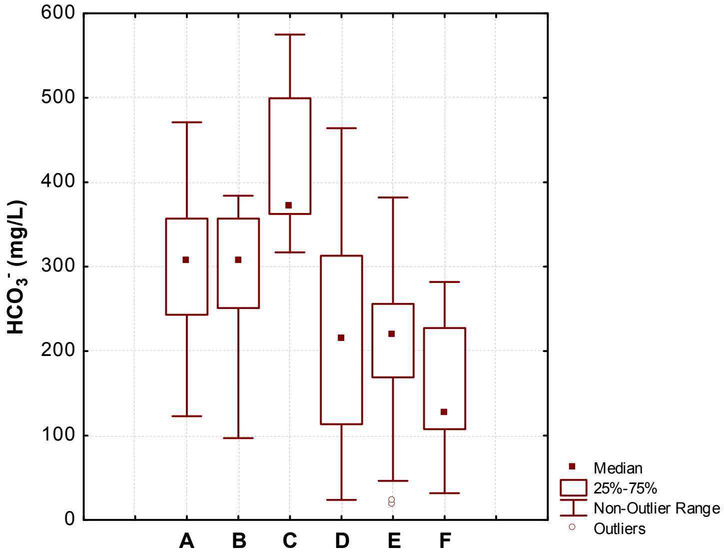

A = pumping station (n=36)
B = borehole (n=10)
C = private well (n=8)
D = spring capture (n=44)
E = spring (n=58)
F = surface water (n=18)

Figure 144: Box and whisker plots for groundwater HCO_3^- concentration according to sampling object type

Spatial distribution of groundwater HCO_3^-

High groundwater HCO_3^- concentrations are observed in the recharge areas of carbonates, and clastic sedimentary rocks in the NE, central, and SE part of the country (Fig. 145). In those recharge areas rock minerals or cement are rich in carbonates, and higher CO_2 partial pressures induced by higher mean air temperature, thicker soil layer, and more extensive vegetation cover influence greatly the mineral dissolution. Low groundwater HCO_3^- concentrations are observed in the northern band of the country extending from W-E part and have carbonate, metamorphic and igneous rocks, and clastics rocks in the recharge areas. Low groundwater HCO_3^- concentrations are also observed in deep aquifers in NE part of study area. Groundwater from the high mountain regions with mostly carbonate rocks in the recharge areas has low HCO_3^- concentrations. This is due to very thin (or non-existent) soil layer, very poor vegetation cover (low level of respiration of soil organisms and the decay of organic matter and therefore low soil CO_2), low temperatures and consequently low P_{CO2}, surface runoff during snow melting, and also because most sampling locations in high mountains are springs, which discharge responds primarily to snowmelt runoff. Snowfall is common for most of the country, with the exception of the lowlands in the coastal region. From late autumn to early spring it is frequent in interior low-lying areas, while during summer it is only present in isolated parts of mountains. Snow cover duration mostly depends on fresh snow accumulations, air temperature and sunshine (EARS, 2006), therefore snow coverage map is very similar to mean annual precipitation and temperature maps.

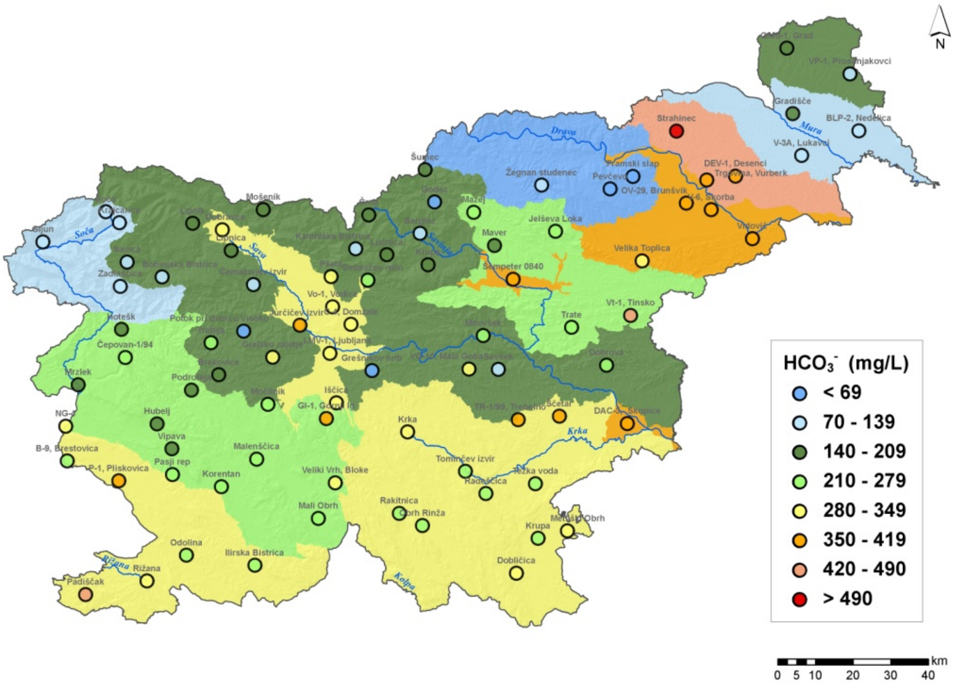

Figure 145: **Spatial distribution of groundwater** HCO_3^-

4.6.1.4.1. Water hardness ($CaCO_3$) in Slovenian groundwaters

Because alkalinity is reported in several ways the presented description of groundwater mineralization ($CaCO_3$) is not considered as individual paramaterer. Instead, $CaCO_3$ provides the general information on water hardness in Slovenian groundwaters.

Descriptive statistics of groundwater $CaCO_3$

Groundwater $CaCO_3$ varies between 0.1 and 5.4 mmol/L, with mean value of 2.0 mmol/L and median 2.0 mmol/L (Tab. 29). Based on the histogram (Fig. 146) the groundwater $CaCO_3$ concentration is not normally distributed, and values higher than 4.1 mmol/L presents the outliers (sampling locations Vidovič and Strahinec) (Fig. 147).

Table 29: Descriptive statistics of groundwater $CaCO_3$ (mmol/L)

Parameter	n	X	Md	Min	Max	S
$CaCO_3$ (mmol/L)	175	2.0	2.0	0.1	5.4	1.0

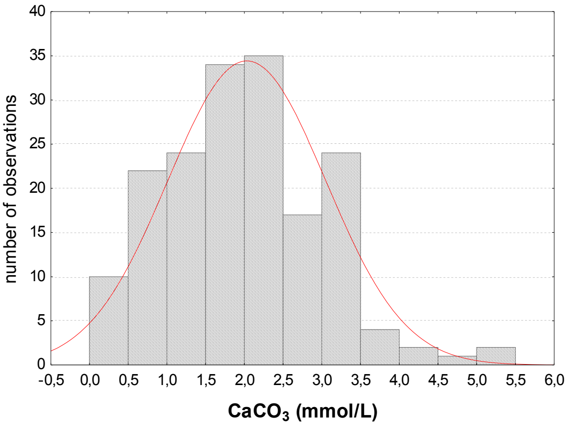

Figure 146: Histogram for groundwater $CaCO_3$ concentration (mmol/L) (n=175)

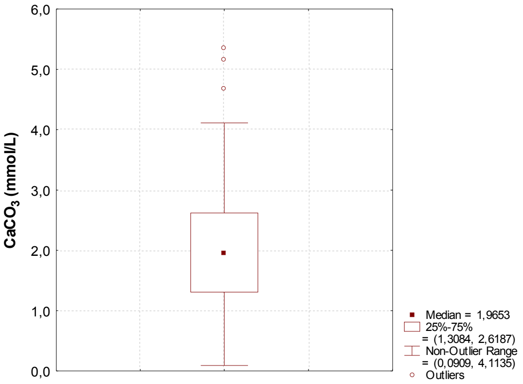

Figure 147: Box and whisker plot for groundwater $CaCO_3$ concentration (mmol/L) (n=175)

Rock type

Soft groundwater is observed mostly in the recharge areas of less permeable igneous and metamorphic rocks (Fig. 148, Appendix 13J), which is significantly softer ($p<0.05$) compared to medium hard groundwater in the recharge areas with carbonate rocks and hard groundwater in clastic sedimentary rocks.

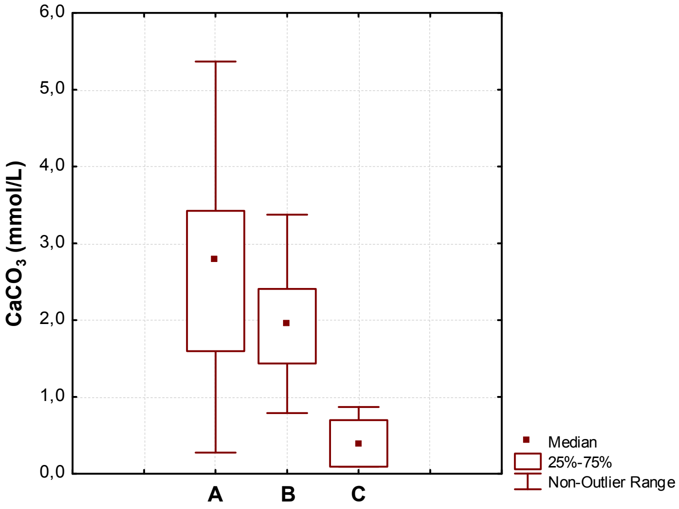

A = clastic sedimentary rocks (n=53)
B = carbonate rocks (n=110)
C = igneous and metamorphic rocks (n=12)

Figure 148: Box and whisker plots for groundwater $CaCO_3$ concentration in the recharge area of major rock types

Soft groundwater (Figs. 149 and 150, Appendix 13J) is observed in the recharge areas with less permeable rocks like igneous and metamorphic rocks where groundwater is significantly softer ($p<0.05$) compared to medium hard and hard groundwater observed in the recharge areas with limestone prevailing, dolomite prevailing, flysch rocks, carbonates with clastics, and gravel and sand (and clay). Additionally, soft groundwater in the recharge areas with shale and sandstone is significantly softer ($p<0.05$) compared to groundwater in the recharge areas with dolomite prevailing, flysch rocks, carbonates with clastics, and gravel and sand (and clay). Groundwater is soft due to the lack of carbonate minerals in their recharge areas. Namely, these rocks are poorly permeable, resistant to erosion, can generate surface runoff, and have therefore short water residence time (especially if located at higher altitudes). According to lithostratigraphic classification groundwater in recharge areas with Oligocene igneous rocks, Permian Val Gardena layers, and old Paleozoic rocks is significalnty softer ($p<0.05$) compared to recharge areas in Eocene flysch rocks, Cretaceous carbonates, Quaternary clastics (medium- and coarse-grained), Miocene Lithothamnium limestone, and Miocene clastics. Medium hard groundwater was sampled in the recharge area of Triassic carbonates, Cretaceous carbonates (outlier P-1 Pliskovica), and Eocene flysch rocks. Groundwater in carbonate recharge areas at higher altitudes is softer compared to groundwater sampled in Dinaric Karst. This is due to higher air temperatures at lower altitudes, and higher soil CO_2, and therefore increased dissolution of calcium- and magnesium-rich minerals in aquifers rocks. Hard groundwater was sampled in the recharge area of Lithothamnium limestone, Quaternary clastics (medium- and coarse-grained), Pliocene clastics, and Miocene clastics where groundwater hardness in the recharge areas with Miocene clastics is significantly harder ($p<0.05$) compared to recharge areas in other lithological units.

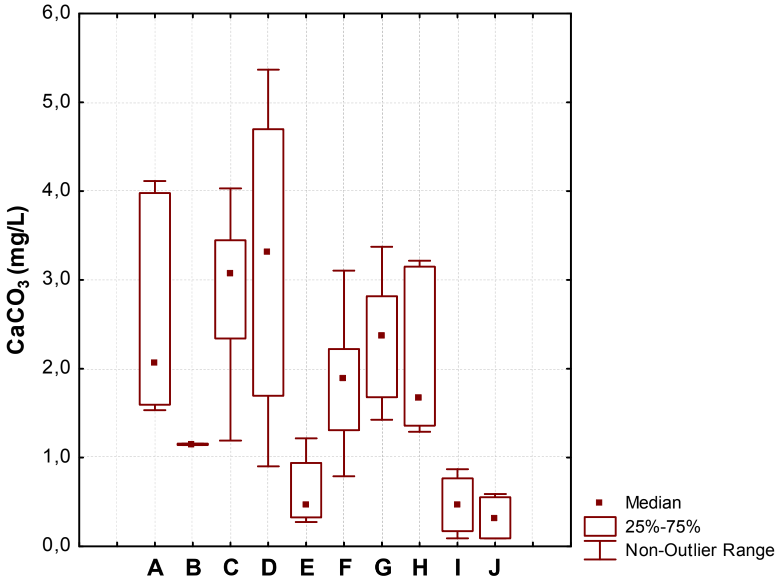

A = flysch rocks (n=7)
B = clay (n=2)
C = gravel and sand (n=26)
D = gravel, sand and clay (n=11)
E = shale and sandstone (n=7)
F = limestone prevailing (n=74)
G = dolomite prevailing (n=30)
H = carbonates with clastics (n=6)
I = igneous rocks (n=8)
J = metamorphic rocks (n=4)

Figure 149: Box and whisker plots for groundwater $CaCO_3$ concentration in the recharge area of prevailing lithological unit

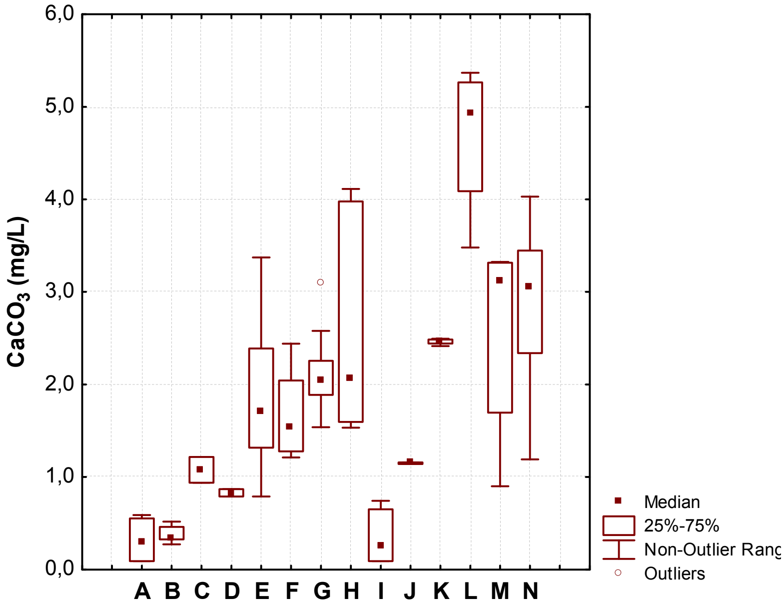

A = old Paleozoic rocks (n=4)
B = Carboniferous-Permian beds (n=5)
C = Permian Val Gardena layers (n=2)
D = Ladinian igneous rocks (n=2)
E = Triassic carbonates (n=70)
F = Jurassic carbonates (n=8)
G = Cretaceous carbonates (n=28)
H = Eocene flysch rocks (n=7)
I = Oligocene igneous rocks (n=6)
J = Oligocene clay “sivica” (n=2)
K = Miocene Lithothamnium limestone (n=4)
L = Miocene clastics (n=4)
M = Pliocene clastics (n=7)
N = Quaternary clastics (medium- and coarse-grained) (n=26)

Figure 150: Box and whisker plots for groundwater $CaCO_3$ concentration in the recharge area of prevailing lithostratigraphic unit

Aquifer porosity type

Soft groundwater is present in the aquifers with fractured porosity (Fig. 151, Appendix 13J) which is significantly softer ($p<0.05$) compared to groundwater with karstic and fractured porosity, mixed porosity (karstic, fractured, intergranular), and fractured and karstic porosity. An outlier (Padiščak) is located near the vicinity of the coast and is influenced by anthropogenic activity (lime application). Medium hard groundwater is observed in aquifers with both prevailing fractured or karstic porosity, and mixed porosity. Hard groundwater was sampled in aquifers with intergranular porosity where significantly harder ($p<0.05$) groundwater dominates compared to groundwater in aquifers with karstic and fractured porosity, mixed porosity (karstic, fractured, intergranular), and fractured porosity. As already mentioned, in Slovenian shallow alluvial intergranular aquifers carbonate pebbles and/or cement prevail and they are open to constant P_{CO2} supply.

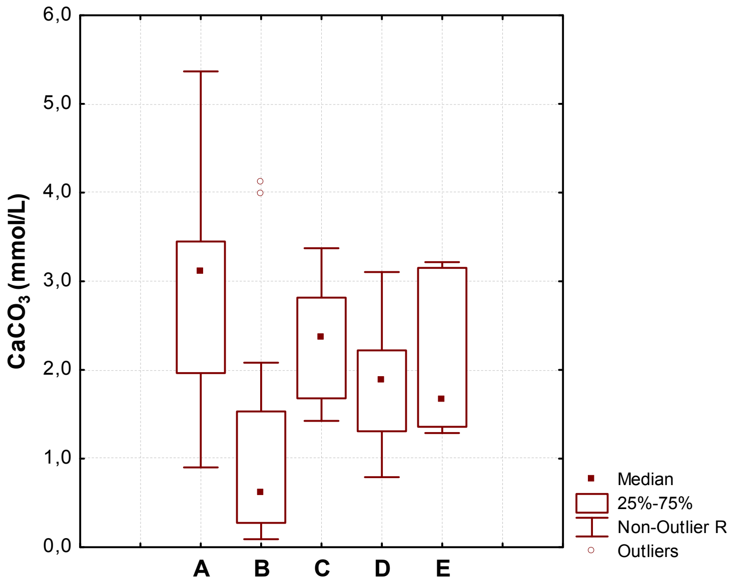

A = intergranular porosity (n=39)
B = fractured porosity (n=26)
C = fractured and karstic porosity (n=30)
D = karstic and fractured porosity (n=74)
E = mixed porosity (karstic, fractured, intergranular) (n=6)

Figure 151: Box and whisker plots for groundwater $CaCO_3$ concentration in the recharge area of the prevailing aquifer porosity type

Land cover/use

Soft groundwater is observed in the recharge areas with moors and heathland, bare rocks, and coniferous forest (Figs. 152 and 153, Appendix 13J). These areas are located at higher altitudes where there is a constant flow of fresh and soft rain water, the soil layer is very thin or non-existent and consequently, very little vegetation is present (low level of respiration of soil organisms and the decay of organic matter), low temperatures, and consequently low P_{CO2}, surface runoff during snow melting, and also because most sampling locations in high mountains are springs, which discharge responds primarily to snowmelt runoff. Medium hard groundwater is observed in the recharge areas with natural grasslands, mixed forest, and broad-leaved forest. Hard groundwater is observed mostly in the recharge area occupied by agriculture, with significant areas of natural vegetation, non-irrigated arable land, industrial or commercial units, and complex cultivation patterns. Groundwater in the recharge areas with industrial or commercial units, and complex cultivation patterns is significantly harder ($p<0.05$) compared to softer groundwater in the recharge areas with bare rocks, moors and heathland, and coniferous forest. Also hard is groundwater in the recharge areas with land principally occupied by agriculture, with significant areas of natural vegetation significantly higher ($p<0.05$) compared to bare rocks and moors and heathland. Medium hard and hard groundwater have mostly thicker soil layer in their recharge areas, and therefore increased microbiological activity and consequently greater P_{CO2}, which increases solubility of minerals, and prolongs the residence time compared to groundwater in high mountain regions.

According to Actual agricultural and forest land usage classification there are no significant differences in groundwater hardness.

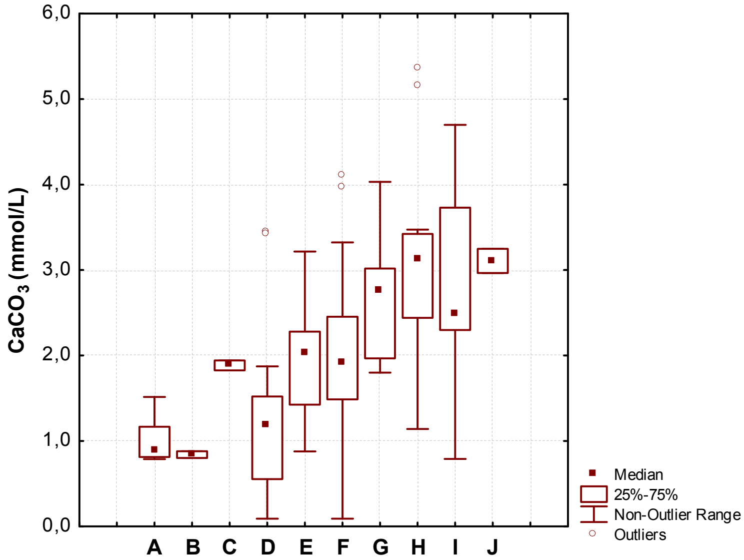

A = bare rocks (n=8)
B = moors and heathland (n=2)
C= natural grasslands (n=2)
D = coniferous forest (n=20)
E = broad-leaved forest (n=45)
F = mixed forest (n=56)
G = non-irrigated arable land (n=10)
H = complex cultivation patterns (n=18)
I = land principally occupied by agriculture, with significant areas of natural vegetation (n=10)
J = industrial or commercial units (n=2)

Figure 152: Box and whisker plots for groundwater $CaCO_3$ concentration in the recharge area of prevailing land use type (CORINE Land Cover)

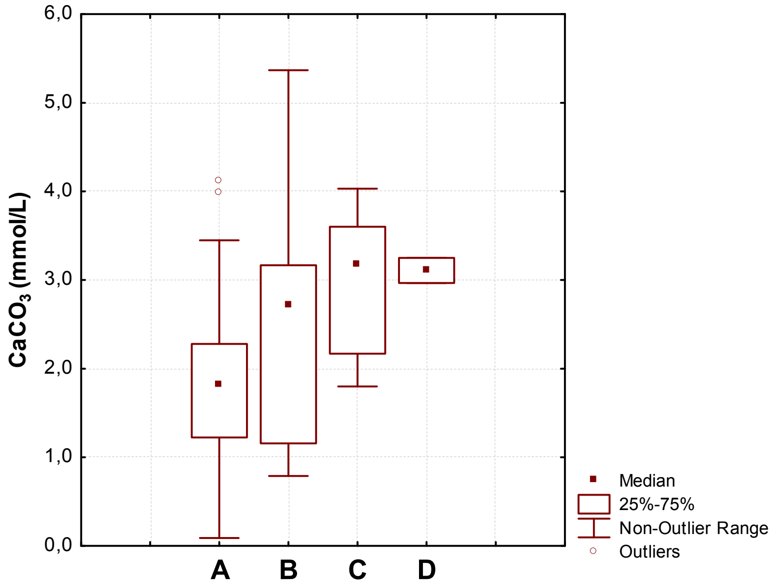

A = forest (n=137)
B = areas of less intense use of nutrients and plant protection products (n=18)
C = areas of intense use of nutrients and plant protection products (n=16)
D = urban areas (n=2)

Figure 153: Box and whisker plots for groundwater $CaCO_3$ concentration in the recharge area of prevailing land use type (Actual agricultural and forest land usage)

Spatial distribution of groundwater $CaCO_3$

In Slovenia medium hard groundwater prevails. Its hardness is presented as molar concentration and in German degrees (Fig. 154 and 155). Medium hard groundwater is found mostly across whole country except in high mountain regions, and hard groundwater in the recharge areas of carbonate rocks and clastics in carbonate alluvial deposits in the NE, central, and SW part (gravel, sand (clay), and flysch rocks). Medium hard and hard groundwater contain more Ca^{2+}, Mg^{2+} due to calcium- and magnesium-rich minerals in aquifers rocks, thick soil layer, increased microbiological activity and consequently greater P_{CO2}, higher air temperatures, and lower altitudes of recharge areas, which increase dissolution of rock minerals. Soft water is mostly observed in the N band extending from W to NNE part of the country in the recharge areas of carbonate rocks, metamorphic and igneous rocks, and clastics (including groundwater from deeper aquifers in NE). Groundwater from the high mountain regions (mostly carbonate rocks in recharge area) is softer due to very thin (or non-existent) soil layer and very little vegetation (low level of respiration of soil organisms and the decay of organic matter), low temperatures, and consequently low P_{CO2}. Soft groundwater in the recharge areas of igneous and metamorphic rocks is low in Ca- and Mg-rich minerals (Mezga and Urbanc, in press).

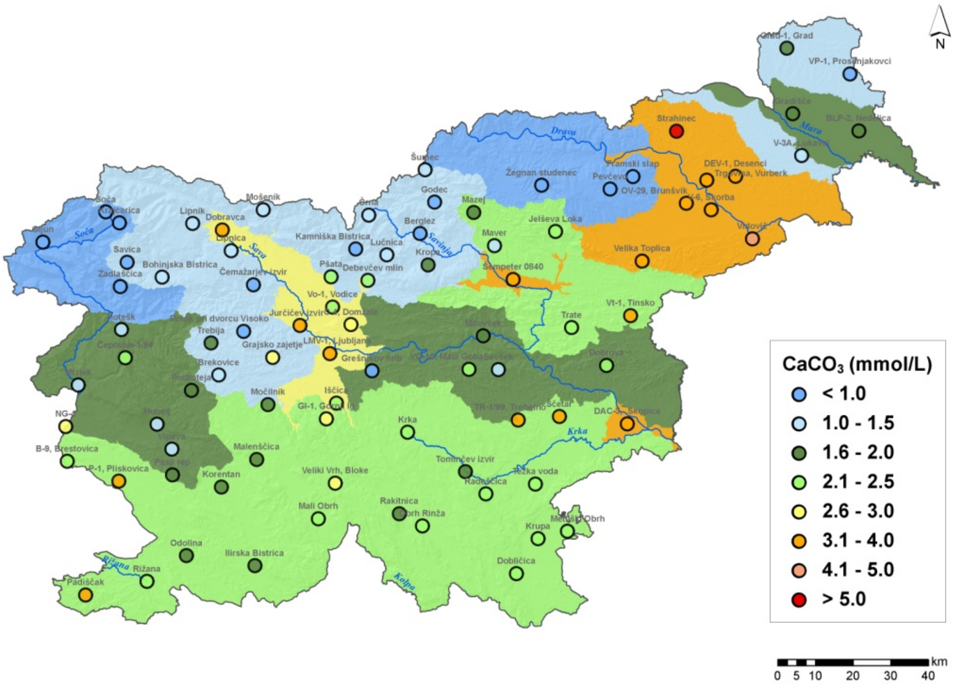

Figure 154: Spatial distribution of groundwater $CaCO_3$ (mmol/L)

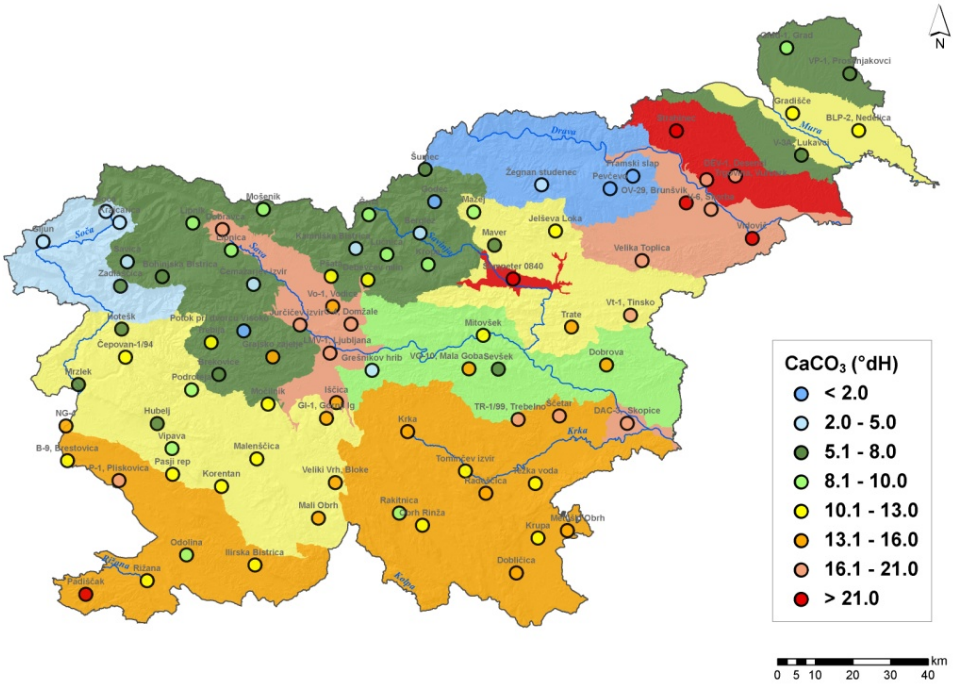

Figure 155: Spatial distribution of groundwater $CaCO_3$ (°dH)

4.6.1.5. Interpretation of initial soil CO_2 partial pressure on the basis of groundwater HCO_3^- concentration

The aim of this section was to calculate the hypothetical soil CO_2 partial pressure (P_{CO2}) for sampled groundwater and to identify the openness of the aquifer systems in Slovenia. In order to calculate the initial soil P_{CO2} in sampled groundwater only 55 sampling locations (Fig. 156) were considered in which recharge areas carbonate rocks prevail (in 37 sampling locations limestone prevails, in 15 sampling locations dolomite prevails, and in 3 sampling locations carbonates with clastics).

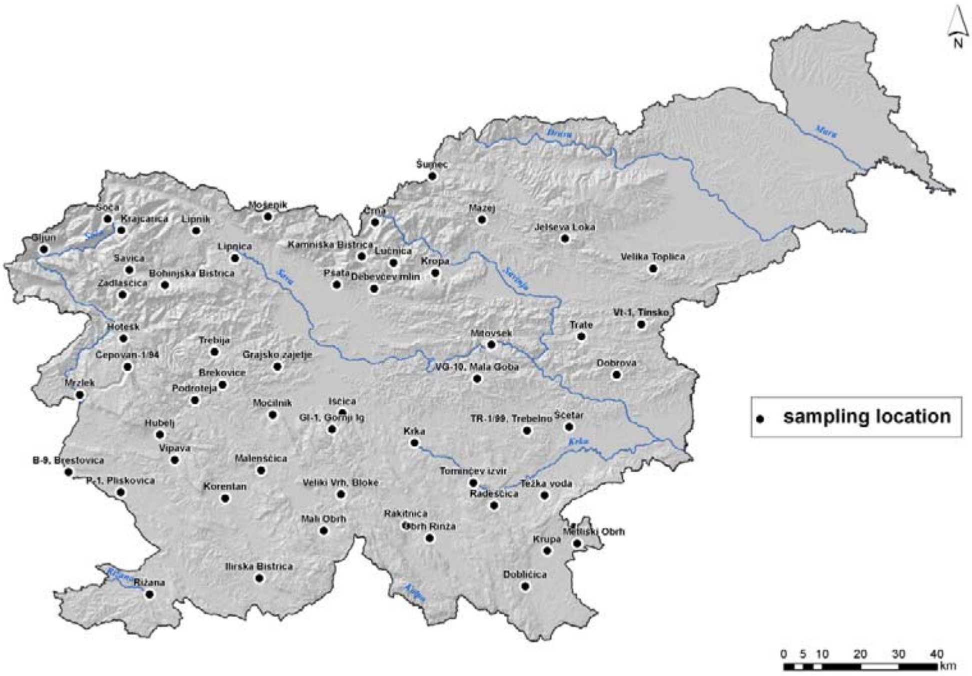

Figure 156: Spatial distribution of selected sampling locations

Due to prevailing carbonate rocks in the recharge areas in groundwater Ca^{2+} and Mg^{2+} are dominant cations and HCO_3^- is the most abundant anion. Groundwater samples have either Ca^{2+}-HCO_3^- water type (50.9 %) where limestone prevails in the recharge area, or Ca^{2+}-Mg^{2+}-HCO_3^- (48.2 %) water type where dolomite prevails or carbonates with clastics in the recharge area. One exception of Ca^{2+}-Mg^{2+}-HCO_3^--SO_4^{2-} water type was observed.

Schoeller diagram (Fig. 157) presents the major ion analyses (in meq/l) and different hydrochemical water types. The Piper diagram (Fig. 158) presents the distribution of sampled groundwaters. Groundwater from sampling location Mošenik deviates according to SO_4^{2-} concentration, and groundwater Ca^{2+} and Mg^{2+} concentration differ according to prevailing rock type in the recharge area, e.g. limestone or dolomite. In all water samples the dominant anion is HCO_3^- with its mean concentration of 273.8 mg/L, minimum 72 mg/L and maximum of 471 mg/L.

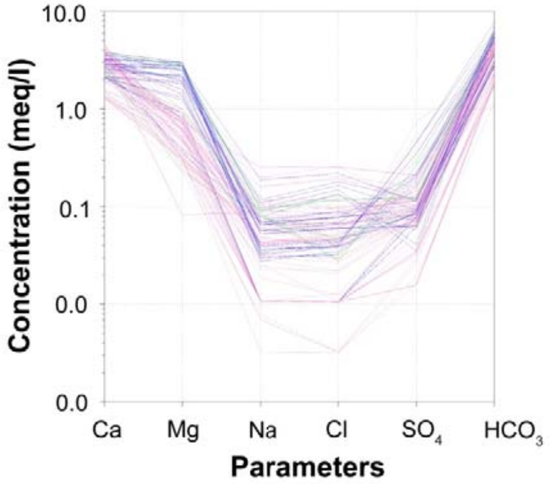

Figure 157: Schoeller diagram (blue – limestone prevailing, green – carbonates with clastics, and pink – dolomites prevailing)

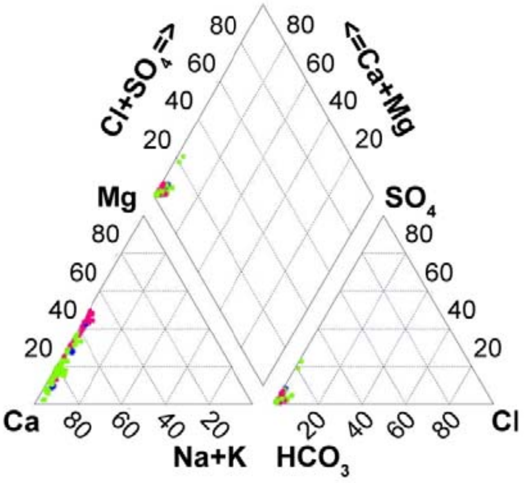

Figure 158: Piper diagram showing groundwater classification (green – limestone prevailing, blue – carbonates with clastics, and pink – dolomites prevailing)

Relation between Ca^{2+}+Mg^{2+} versus HCO_3^- (Fig. 159) indicates that groundwater is plotted along the 2:1 line indicating the carbonates dissolution. The minimum and maximum values for pH are 7.3 and 8.22 with mean value of 7.73. Comparison between groundwater pH and HCO_3^- concentration (Fig. 160) shows that based on the pH values (6.3 < pH < 10.3) the aqueous carbonate species HCO_3^- prevails. Good correlation exists between groundwater pH and HCO_3^- which is expected for groundwater in equilibrium with calcite under a wide range of P_{CO2} (Stumm and Morgan, 1996). Namely, higher initial P_{CO2} pressures can dissolve more carbonate minerals than water with low P_{CO2} which is observed in high mountain regions with low soil CO_2.

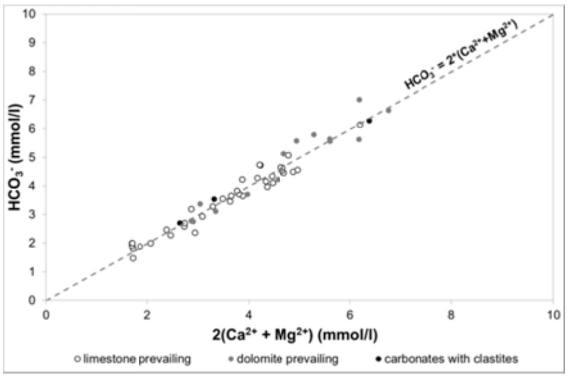

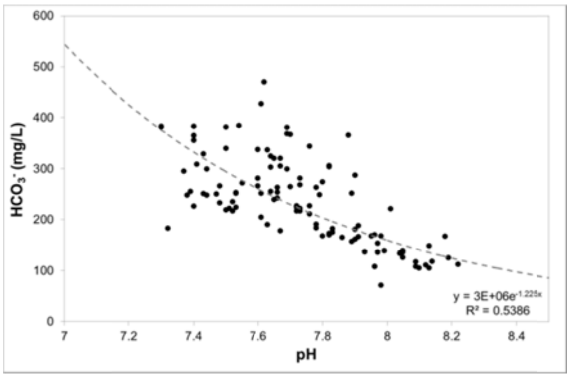

Figure 159: Scatter plot of groundwater HCO_3^- versus 2(Ca^{2+}+Mg^{2+}) concentration

Figure 160: Relation between groundwater pH and HCO_3^- concentration

Relation between groundwater EC and pH (Fig. 161) explains that groundwater with lower pH values has higher mineralization, where in the carbonate recharge areas the soil layer is thicker, altitudes are lower, and the temperatures are higher, compared to lower mineralized groundwater with higher pH, where the recharge areas are at higher altitudes, thinner soil layer and lower temperatures.

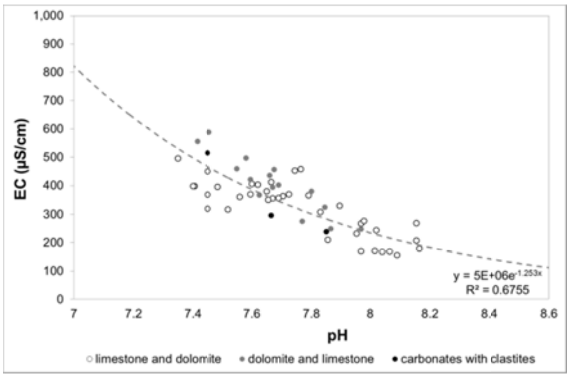

Figure 161: Groundwater pH values versus EC in the recharge areas with carbonate rocks

For modelling hypothetical soil P_{CO2} (in vol. %) the geochemical modelling code PHREEQC (Parkhurst and Appelo, 1999) was used. Final soil P_{CO2} was calculated based on measured groundwater HCO_3^- concentration. For the reference, the atmospheric soil $P_{CO2} = 10^{-3.5}$ atm was used.

For the input the typical rainwater composition was considered with a mean annual temperature of 10°C in the recharge area. In the calculation tables predicted shares of CO_2 (in %) were chosen, e.g. from 0.01 to 20 % of atmospheric CO_2 and its calculated logarithm. For additional calculation the concentration of calculated pH, total carbon (C_{tot}), HCO_3^-, Ca_{tot}, and Ca^{2+} were considered.

Open system

The following scenario was predicted for the open system, where rainwater is equilibrated with $CO_{2(g)}$ and calcite ($CaCO_3$) (Appendix 13K). Calculated values from PHREEQC were converted into mg/L and mmol/L according to their molecular weight for HCO_3^- and Ca^{2+}. Additionally, the total inorganic carbon (DIC) and atmospheric CO_2 were calculated. The graphs below (Figs. 162-165) suggest that in the open system higher soil P_{CO2} enhances the dissolution of carbonate (higher HCO_3^- and Ca^{2+}) and decreases the pH of solution. This means that in the carbonate recharge areas where the soil is thicker and consequently soil CO_2 is high, percolating groundwater dissolves more carbonate minerals as in recharge areas with thin (or non-existent) soil layer.

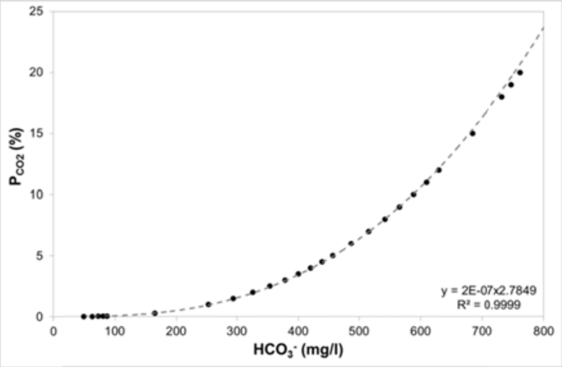

Figure 162: Groundwater HCO_3^- concentration versus soil P_{CO2}

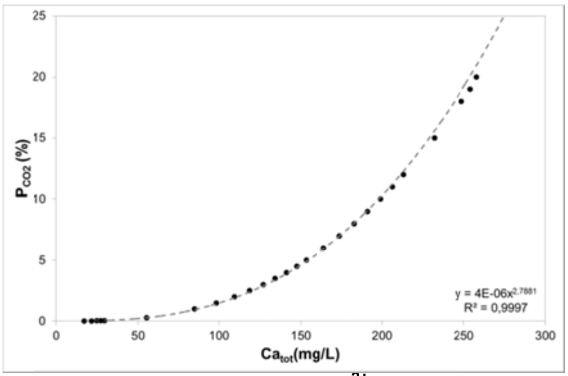

Figure 163: Groundwater Ca^{2+}_{tot} concentration versus P_{CO2}

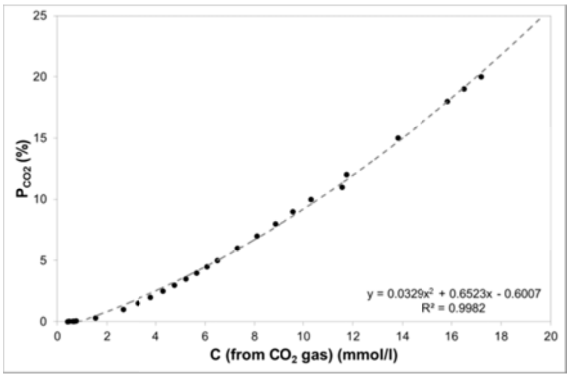

Figure 164: C (from CO_2) versus initial CO_2

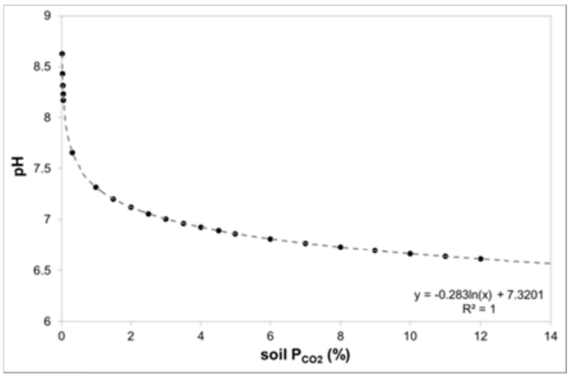

Figure 165: Soil P_{CO2} versus pH

Since calculation of HCO_3^- concentration considers both Ca^{2+} and Mg^{2+} ions combined, the equation for correlation of HCO_3^- (mg/L) versus soil P_{CO2} (%) was used on the real data to calculate the soil P_{CO2}:

$$y = 2*10^{-7}x^{2.7849} \text{ (R = 1)} \qquad (23)$$

Closed system

Closed system carbonate equilibria were calculated in 2 phases. In the first step water was equilibrated only with $CO_{2(g)}$ without the presence of calcite ($CaCO_3$), where the results of pH and gaseous CO_2 (mmol C/L, converted into mg C/L) from PHREEQC were considered (Appendix 13K). Second step considers the polynomial equation from the open system:

$$y = -0.002x^3 + 0.0826x^2 + 0.3418x – 0.2623 \qquad (24)$$

in order to calculate the equilibrating partial pressure of CO_2. For calculating the HCO_3^- concentrations the relation between soil P_{CO2} and HCO_3^- concentration for open system was used. The graphs (Figs. 166 and 167) suggest that higher soil P_{CO2} results in higher HCO_3^- and Ca^{2+} groundwater concentration.

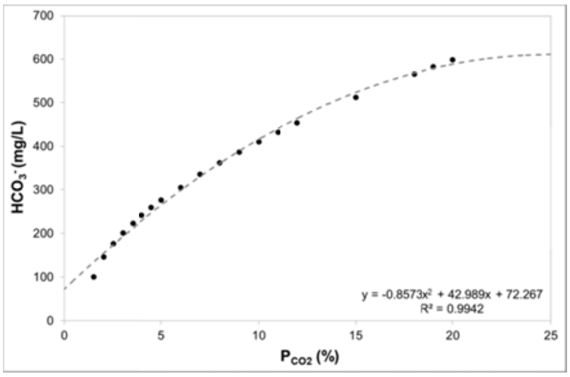

Figure 166: P_{CO2} versus HCO_3^- concentration for closed system

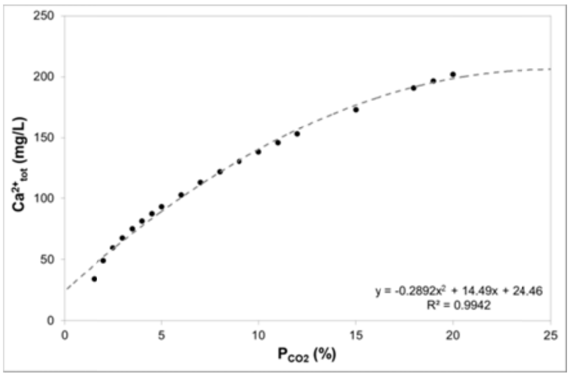

Figure 167: P_{CO2} versus Ca_{tot} concentration for closed system

Various graphs were produced, e.g. soil P_{CO2} (%) vs. CO_2 (equilibrated), HCO_3^- (mg/L) versus soil P_{CO2} (%), and Ca^{2+}_{tot} (mg/L) vs. P_{CO2} (%). Similarly as for open system was calculated the soil P_{CO2} (HCO_3^- versus soil P_{CO2}) for closed system with the equation:

$$y = 5*10^{-5}x^2 + 0.0012x + 0.7125 \text{ (R=1).} \qquad (25)$$

In the next step the calculation of the Ca^{2+} (mg/L) concentration based on the equation

$y = 86.647x^{0.3586}$ (R=1) (26)

from graph Ca^{2+}_{tot} versus soil P_{CO2} was calculated.

For the final CO_2 concentration the % of soil P_{CO2} was used and was considered as the logarithm of final calculated number: soil $P_{CO2}*10^{-3.5}*100$.

Parameters considered for calculation of soil P_{CO2} are HCO_3^- and Ca^{2+} concentration, but since HCO_3^- covers Ca^{2+} and Mg^{2+} ions combine, the calculations based only on Ca^{2+} were not evaluated.

Figure 168 presents the calculated soil P_{CO2} content for an open and closed system based on measured groundwater HCO_3^- concentrations, where the vertical line presents the mean groundwater HCO_3^- concentration of observed groundwaters (237 mg/L). The horizontal line presents the mean partial pressure of measured soil CO_2 in various sampling locations in Slovenia. Mean HCO_3^- concentration is crossing soil P_{CO2} data near the open system model calculation line, indicating prevalence of open system dissolution conditions in the Slovenian aquifers in carbonate recharge areas.

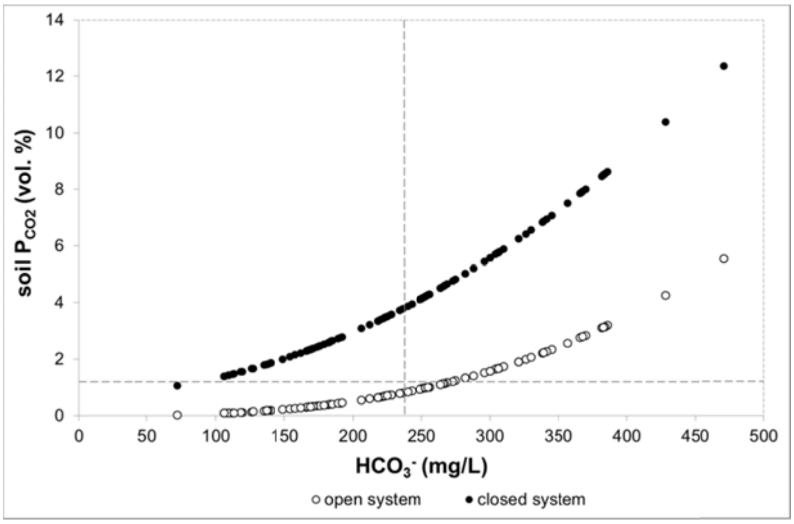

Figure 168: Calculated soil P_{CO2} concentration for open and closed systems

Figure 169 presents the histograms for calculated soil P_{CO2} concentration for open and closed systems and measured soil P_{CO2} concentration. Both calculated distribution lines are normal but open system distribution line is more leptokurtic compared to mesokurtic for closed system. Additionally open and closed systems calculated initial P_{CO2} concentration results are comparable to measured soil P_{CO2} concentration which has been measured on various locations around Slovenia.

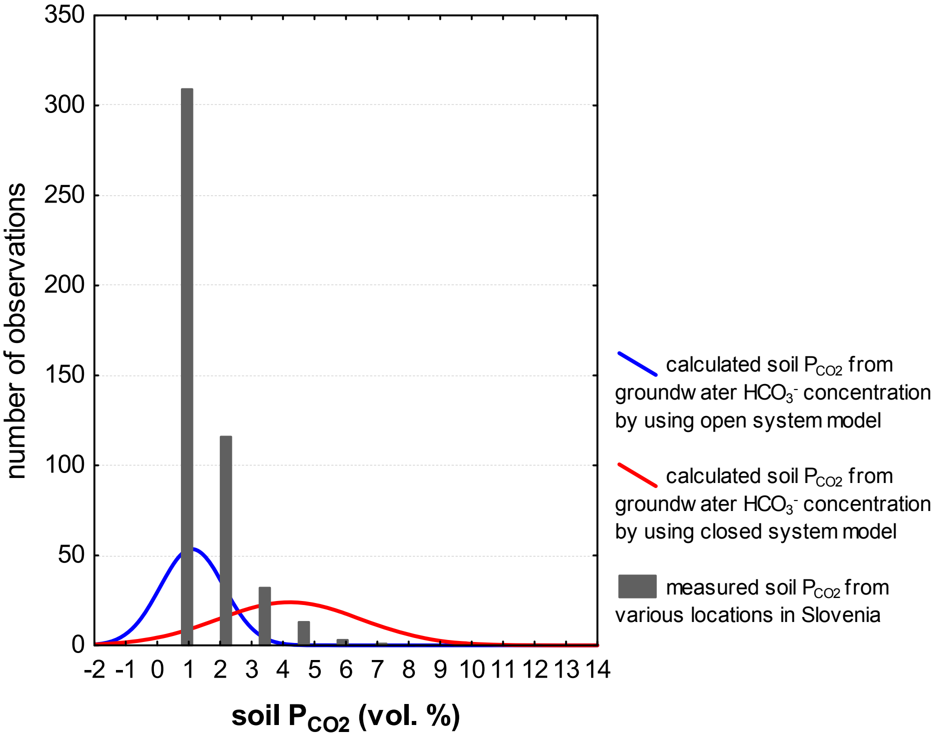

Figure 169: Distribution lines for open and closed systems, and measured data

Comparison between calculated data for soil P_{CO2} for open and closed systems and measured data from Slovenia (Fig. 170) shows that calculated data for soil P_{CO2} for open systems coinside with measured data from Slovenia. Additionaly calculated data for soil P_{CO2} for closed systems are significantly higher ($p<0.05$) compared to open system and measured data.

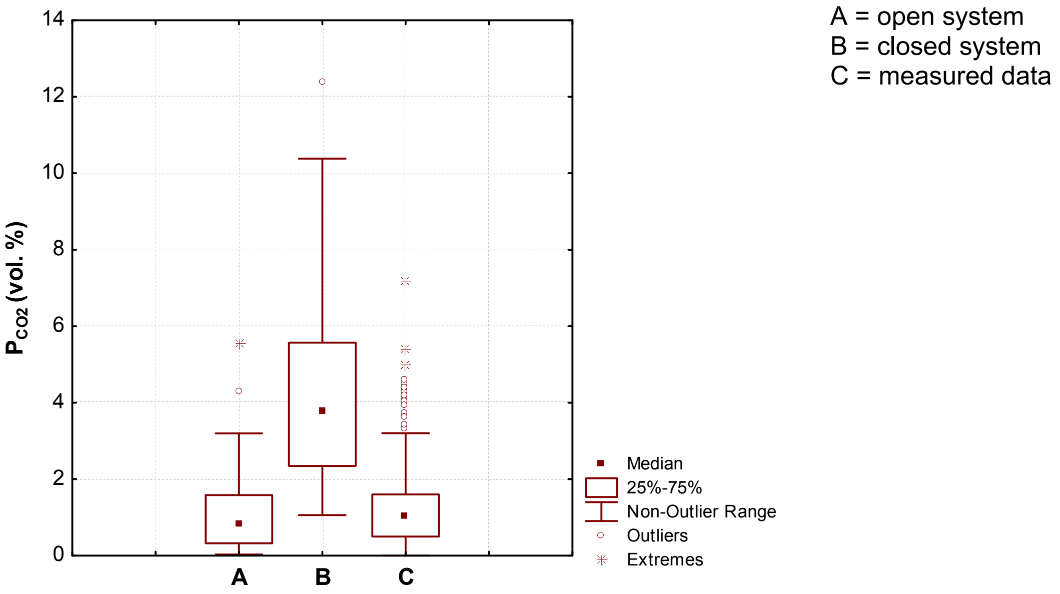

Figure 170: Box and whisker plots for soil P_{CO2} concentration for open and closed systems, and measured data

According to distribution of calculated and measured soil P_{CO2} concentrations it is assumed that in sampled groundwater dissolution of carbonates is performed according to open system dissolution model. For further data processing the soil P_{CO2} concentrations for open systems were used where the mean concentrations of calculated soil P_{CO2} is 1.09 vol. %, minimum value 0.03 vol. % and the maximum 5.56 vol. %. Calculated soil P_{CO2} concentrations are significantly higher than partial pressures of atmospheric CO_2, suggesting a higher production of CO_2 in the soil zone. This is caused mainly by biological activity in the soil (microbiological activity, respiration, decomposing of organic matter) although in some cases a minor influx of CO_2 from deeper strata (proximity of thermal springs) can't be excluded.

Fig. 171 presents the negative correlation between hypothetical soil P_{CO2} concentration and measured pH values in groundwater suggesting the lower soil P_{CO2} concentration is observed in waters with higher pH values, which is influenced mostly by the atmosphere. Contrary groundwater with higher soil P_{CO2} concentration has a lower pH. Further observation showed that groundwaters with lower EC (mineralization) have lower soil P_{CO2}, and waters with higher measured EC have higher soil P_{CO2} (Fig. 172).

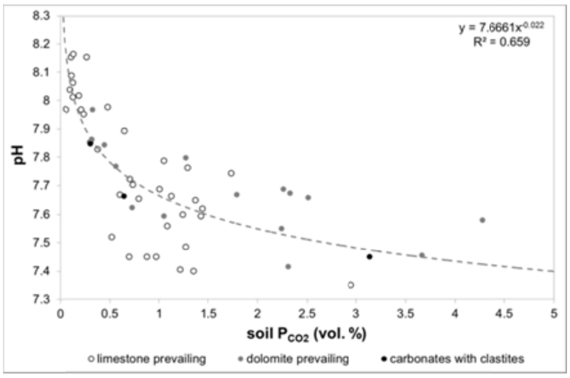

Figure 171: Relation between groundwater pH and calculated soil P_{CO2} concentration

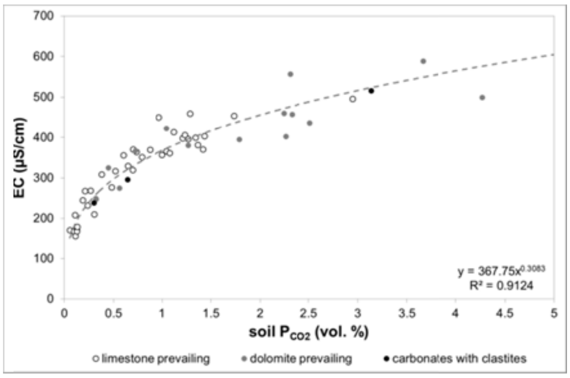

Figure 172: Relation between EC and soil P_{CO2} concentration

The sum of Ca^{2+} and Mg^{2+} ions in sampled groundwater was compared to calculated soil P_{CO2} concentration (Fig. 173). Concentration of soil P_{CO2} is lower in groundwater which is in contact with prevailing limestones and secondarily with dolomites. Higher soil P_{CO2} concentrations are mostly observed in groundwaters where dolomite prevails over limestones.

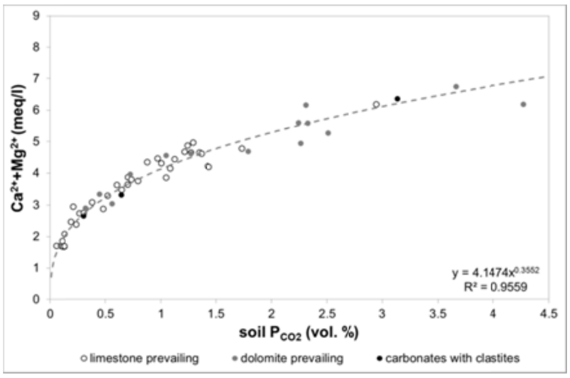

Figure 173: Relation between soil P_{CO2} concentration and the sum of groundwater Ca^{2+} and Mg^{2+} ions

Figure 174 presents spatial distribution of calculated hypothetical initial soil P_{CO2} concentration. The lowest soil P_{CO2} partial pressures are observed in high karstified mountains and low karst areas, where the recharge areas are mostly in bare rocks with thin layer of soil (lithosol) or overgrown with forests (e.g.

recharge areas of sampling locations Savica, Soča, Gljun, Zadlaščica, Kamniška Bistrica, and Mošenik). Groundwater in these areas has usually low initial soil CO_2 partial pressure most possible due to higher relative portion of atmospheric CO_2. High calculated initial soil P_{CO2} concentration (>3 vol. %) is observed in the E part of Slovenia at 3 sampling locations (Vt-1 Tinsko, TR-1 Trebelno, and Ščetar). Their recharge areas at lower altitudes are covered by thick soil layers of rendzina and brown soils which is developed on the carbonate rocks. These areas are mostly covered with deciduous or mixed forests. High concentrations of soil P_{CO2} are possible due to various reasons. The content of some measured groundwater ions (Mg^{2+} and SO_4^{2-}) from sampling location Vt-1 Tinsko is higher compared to other groundwater (increased mineralization). The pump in this pumping well is placed in the layer of crushed coal between sand with clay, organic clay, and silt clay is present. Due to increased groundwater SO_4^{2-} concentration the higher values of groundwater CO_2 could be derived from coal layer. Another possible explanation could also be due to the fact that those sampling locations are located near Podčetrtek, and Šmarješke toplice. Namely, eastern Slovenia is rich in mineral and thermal groundwater. On the E side of the study area, in the intersection of deep fault zones of the carbonate aquifers with fractured porosity, the low temperature thermal water can be found (Lapanje and Rman, 2009). It is possible that the CO_2 from deeper depths which mineralizes groundwater and increases the carbonate content, is also influencing groundwater in the shallow aquifers in those sampling sites.

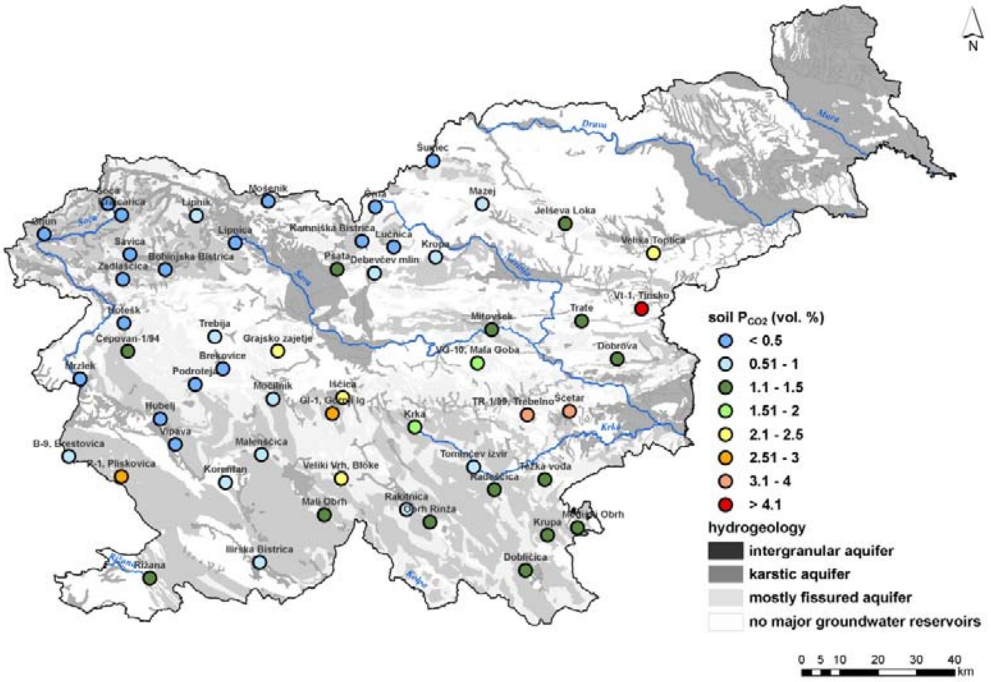

Figure 174: Spatial distribution of hypothetical soil P_{CO2} concentration in groundwater in the recharge areas with carbonate rocks

Figure 175 presents the relation between soil P_{CO2} concentration and mean altitude of recharge areas. The lowest soil P_{CO2} concentration is observed mostly in high mountain regions, and the high soil P_{CO2} concentration at lowland areas (plains) of the country. Additionally, the lowest soil P_{CO2} concentrations in groundwater were observed mostly in groundwater which is in contact with prevailing limestone, whereas the highest groundwater concentrations occurred where dolomites prevail.

Since the altitude and the mean air temperatures are closely related, correlation between the soil P_{CO2} concentration and mean temperature of recharge areas is expected (Fig. 176). The lowest soil P_{CO2} concentrations are observed in areas with lower temperature, which is mostly observed in the high mountain areas. The highest soil P_{CO2} concentrations are observed in areas where higher temperature prevails, e.g. lowland areas. The correlation between those two is exponential ($y=7.508x^{0.2408}$; $R^2 = 0{,}557$). Temperature is therefore the limiting factor for soil P_{CO2} production. Two sampling locations (P-1 Pliskovica and B-9 Brestovica) deviate from the trend line due to the fact that their recharge areas have been deforested and have thin soil layer, which consequently produces less biogenic CO_2. This area is also known as stripped karst.

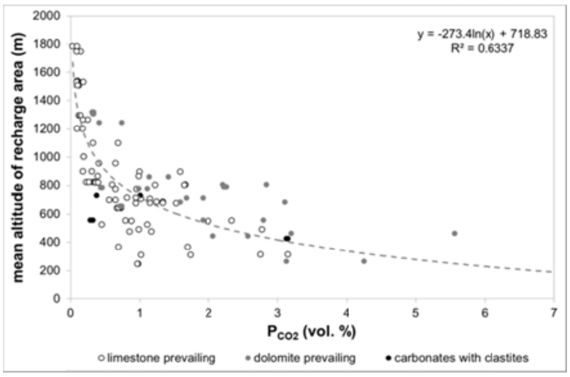

Figure 175: Correlation between soil P_{CO2} concentration and mean altitude of recharge area

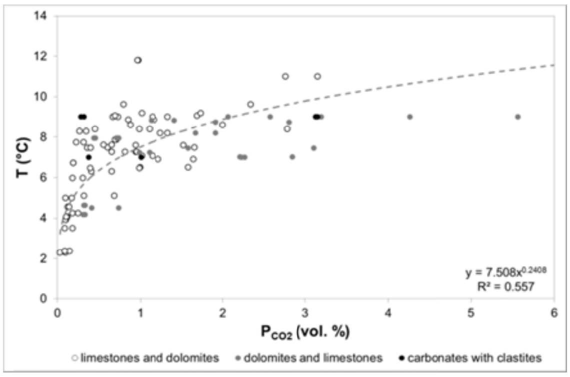

Figure 176: Correlation between soil P_{CO2} concentration and mean temperature of recharge area

4.6.1.6. Stable isotope composition of dissolved inorganic carbon (δ^{13}C-DIC) in groundwater

Descriptive statistics of groundwater δ^{13}C-DIC values

The δ^{13}C-DIC values in groundwater vary between -20.6 ‰ and -0.7 ‰, with mean value of -12.1 ‰ and median -12.9 ‰ (Tab. 30). Groundwater δ^{13}C-DIC values are not normally distributed (Fig. 177) and values above -7.5 ‰ and below -17.7 ‰ present outliers and extremes (Fig. 178).

Table 30: Descriptive statistics of δ^{13}C-DIC in groundwater

Parameter	n	X	Md	Min	Max	S
δ^{13}C (‰)	173	-12.1	-12.9	-20.6	-0.7	3.7

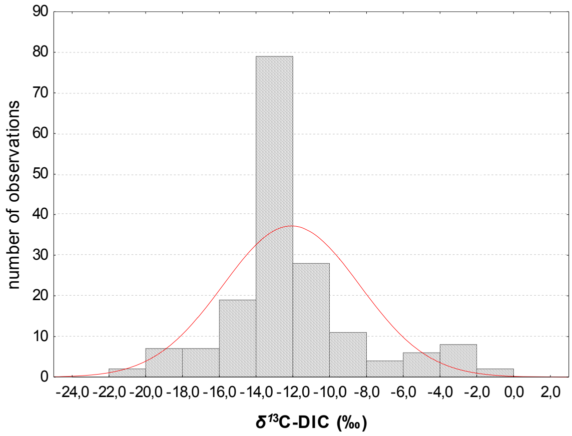

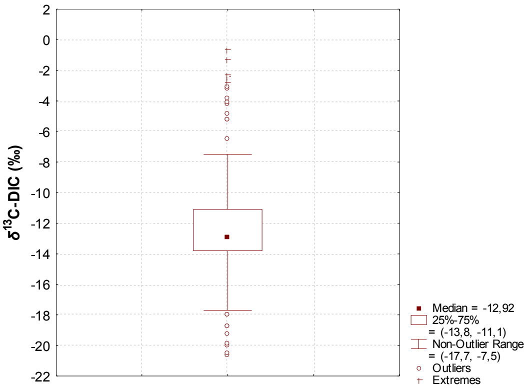

Figure 177: Histogram for groundwater δ^{13}C-DIC values (n=173)

Figure 178: Box and whisker plot for groundwater δ^{13}C-DIC values (n=173)

Rock type

Groundwater DIC is significantly depleted in ^{13}C ($p<0.05$) (δ^{13}C-DIC ~ -18.0 ‰) in the recharge areas of silicate igneous and metamorphic rocks (Fig. 179, Appendix 13L) compared to clastic sedimentary and carbonate rocks. The soil CO_2 contributes the largest share to groundwater DIC due to intense biochemical processes (organic matter degradation) in thick soil layers, as well as absence of carbonate minerals. Enriched in ^{13}C (δ^{13}C-DIC ~ > -12.0 ‰) is groundwater in the recharge areas of carbonate and clastic sedimentary rocks. Those groundwater δ^{13}C-DIC values suggest the dissolution of carbonate rocks in the reaction with biogenic CO_2 in soil.

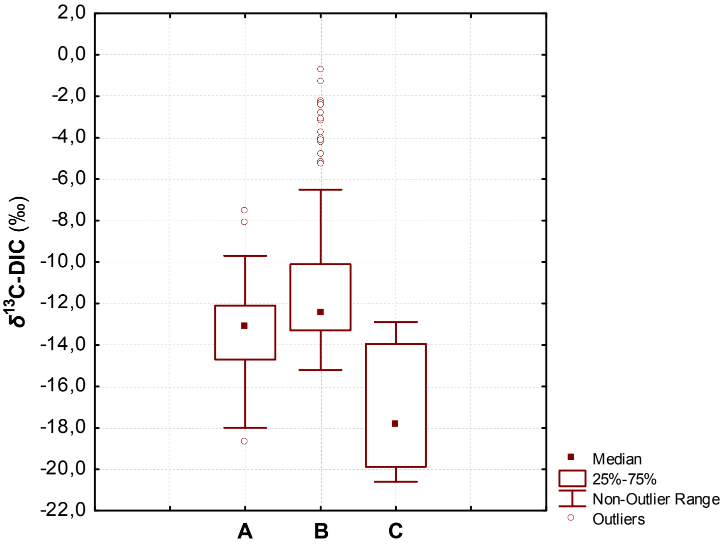

A = clastic sedimentary rocks (n=51)
B = carbonate rocks (n=110)
C = igneous and metamorphic rocks (n=12)

Figure 179: Box and whisker plots for groundwater δ^{13}C-DIC values in the recharge area of major rock types

Groundwater DIC is enriched with ^{13}C in the recharge areas with shale and sandstone and limestone prevailing (Figs. 180 and 181, Appendix 13L). This water is most probably under the influence of dissolution of carbonate rocks and atmospheric CO_2 (degassing), since groundwater was sampled as a surface water. According to groundwater in the recharge areas with carbonate rocks (Triassic, Jurassic, and Cretaceous carbonates, and Lithothamnium limestone) the most enriched in ^{13}C is groundwater with Triassic and Jurassic carbonates in the recharge areas. Groundwater in Triassic carbonates is more enriched due to recharge areas in higher altitudes (above the tree line), greater influence of dissolution of carbonates, higher share of atmospheric CO_2, and lesser share of organic CO_2 from soil. Important is also precipitation rate which dilutes the groundwater (Fig. 182) and lower contribution of biological CO_2 from the soil. Additionally, there is also a possibility for isotopic exchange with the atmospheric CO_2 due to openness of karstic channels. Groundwater is significantly depleted in ^{13}C-DIC ($p<0.05$) in the recharge area of poorly permeable rocks (old Paleozoic rocks, Permian Val Gardena layers, and Oligocene igneous rocks) compared to groundwater in the recharge areas with Carboniferous-Permian sands and sandstones. These rocks contain mostly silicate minerals and are poor in carbonate-rich minerals, so the majority of carbon is derived from soil CO_2 in thick horizon.

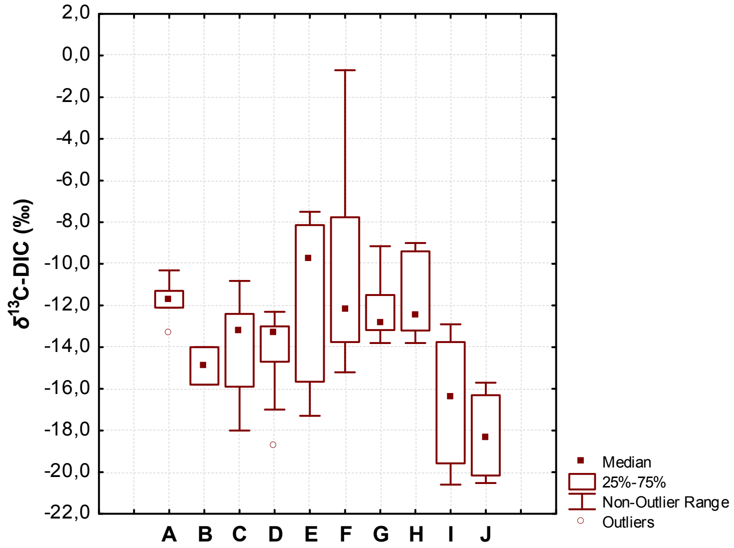

A = flysch rocks (n=6)
B = clay (n=2)
C = gravel and sand (n=26)
D = gravel, sand and clay (n=11)
E = shale and sandstone (n=6)
F = limestone prevailing (n=74)
G = dolomite prevailing (n=30)
H = carbonates with clastics (n=6)
I = igneous rocks (n=8)
J = metamorphic rocks (n=4)

Figure 180: Box and whisker plots for groundwater δ^{13}C-DIC values in the recharge area of prevailing lithological unit

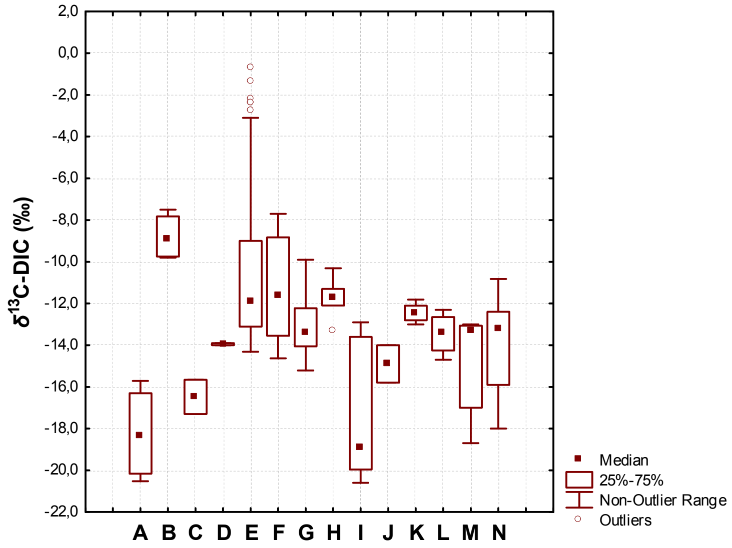

A = old Paleozoic rocks (n=4)
B = Carboniferous-Permian beds (n=5)
C = Permian Val Gardena layers (n=2)
D = Ladinian igneous rocks (n=2)
E = Triassic carbonates (n=70)
F = Jurassic carbonates (n=8)
G = Cretaceous carbonates (n=28)
H = Eocene flysch rocks (n=7)
I = Oligocene igneous rocks (n=6)
J = Oligocene clay “sivica” (n=2)
K = Miocene Lithothamnium limestone (n=4)
L = Miocene clastics (n=4)
M = Pliocene clastics (n=7)
N = Quaternary clastics (medium- and coarse-grained) (n=26)

Figure 181: Box and whisker plots for groundwater δ^{13}C-DIC values in the recharge area of prevailing lithostratigraphic unit

Moderate correlation is observed between mean amount of precipitation and groundwater δ^{13}C-DIC (r_s=0.52, $p<0.05$) (Fig. 182) where the amount of precipitation also influences the groundwater isotopic composition by groundwater dilution especially in the high mountain regions in the W part of the country where increased precipitation are typical. Figure 183 shows moderate correlation between groundwater Si and δ^{13}C-DIC (r_s=0.57, $p<0.05$) suggesting that groundwater is more enriched in ^{13}C-DIC in the recharge areas of carbonate rocks, whereas it is more depleted in ^{13}C-DIC in the recharge areas of prevailing silicate rocks. The reason is absence of soil thickness and vegetation density in the recharge areas of carbonate rocks in the high mountain recharge areas where greater atmospheric CO_2 is present, compared to groundwater in the recharge areas of silicate rocks with prevailing soil CO_2 from organic matter degradation and microbiological respiration.

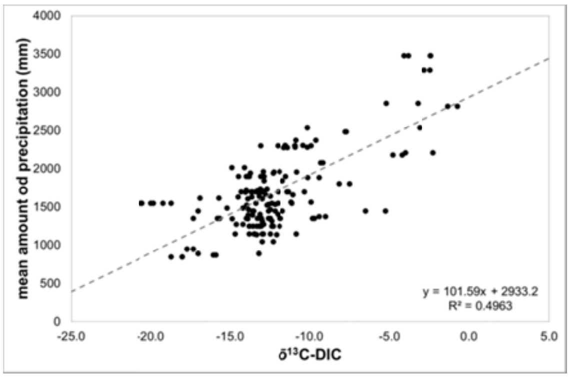

Figure 182: Mean amount of precipitation versus groundwater δ^{13}C-DIC values

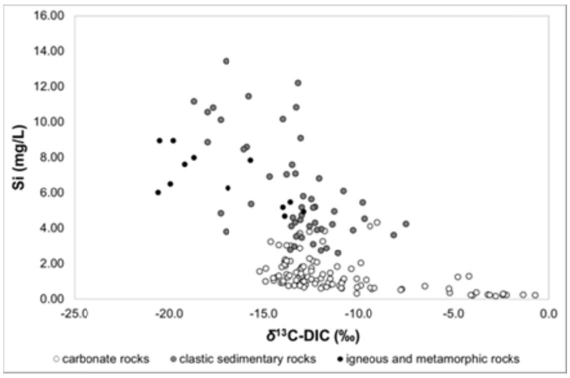

Figure 183: Groundwater Si concentration versus δ^{13}C-DIC values

A comparison between groundwater from sampling location Hubelj in the carbonate recharge area and Pevčevo in the silicate recharge area at similar mean altitudes and vegetation cover (forest) in their recharge areas (~1000 m a.s.l) has been made. The groundwater from Hubelj had groundwater δ^{13}C-DIC of -7.7 ‰ and groundwater from Pevčevo δ^{13}C-DIC of -20.3 ‰. This suggests that groundwater at Pevčevo is more influenced by the degradation of organic matter and leaching from soil layer while groundwater from Hubelj is influenced more by carbonate dissolution. Further a comparison between the δ^{13}C-DIC and the mean altitude of carbonate recharge area is presented in Figure 184. At higher altitudes the groundwater δ^{13}C-DIC values are less negative since more of its DIC is derived from atmospheric CO_2 (~–7.0 ‰) and dissolution of carbonate rocks (~0.0 ‰). Additionally, the soil layer is thin, and groundwater has consequently more positive δ^{13}C-DIC values. Contraty, groundwater in the recharge areas of carbonate rocks at lower altitudes is influenced by the greater share of soil CO_2 partial pressure because of thicker soil layers in lowlands as well as carbonate dissolution. Figure 185 shows the comparison between groundwater δ^{13}C-DIC values and temperature, where at lower temperatures (and higher altitude) δ^{13}C-DIC values are less negative, compared to lower altitudes (lowland) with higher temperatures which are very negative. Encircled is groundwater from sampling locations at higher altitudes, with poorly permeable minerals and thick soil layer in the recharge areas

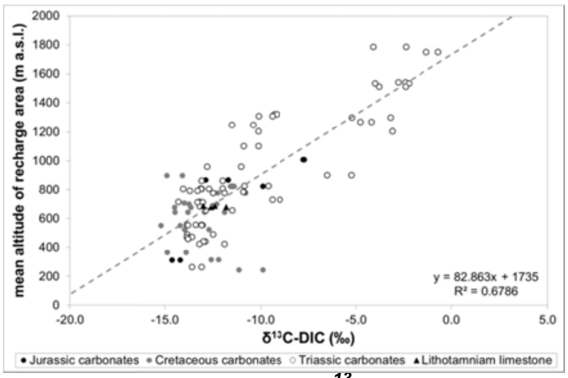

Figure 184: Groundwater δ^{13}C-DIC values versus to mean altitude of recharge areas

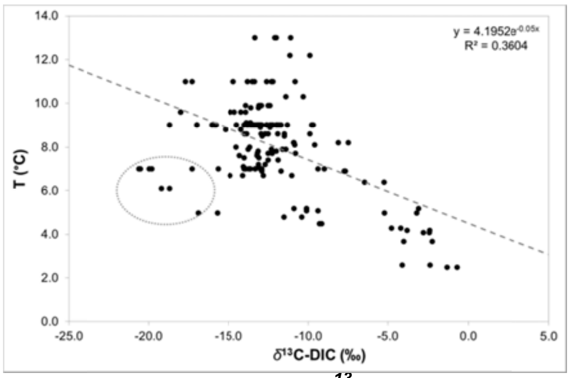

Figure 185: Groundwater δ^{13}C-DIC values versus the mean temperature in the recharge areas

Aquifer porosity type

Groundwater δ^{13}C-DIC values in aquifers with karstic and fractured porosity are significantly higher ($p<0.05$) compared to groundwater in the recharge areas with intergranular and fractured porosity (Fig. 186, Appendix 13L). In high mountain aquifers with karstic and fractured porosity groundwater is enriched in ^{13}C-DIC due to prevailing dissolution of carbonate rocks as the main contributor to DIC. In the aquifers with intergranular and fractured porosity groundwater DIC is depleted in ^{13}C due to prevailing influence of soil CO_2.

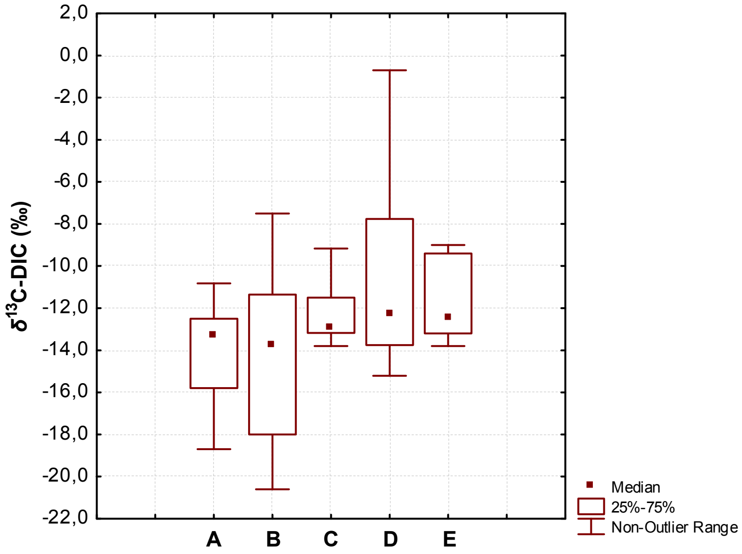

A = intergranular porosity (n=39)
B = fractured porosity (n=24)
C = fractured and karstic porosity (n=30)
D = karstic and fractured porosity (n=74)
E = mixed porosity (karstic, fractured, intergranular) (n=6)

Figure 186: Box and whisker plots for groundwater δ^{13}C-DIC values in the recharge area of prevailing aquifer porosity type

Isotopic mass balance calculations

A simple isotopic mass balance calculation (Katz, 1998) was performed in order to quantify different sources of DIC in sampled groundwater. The major inputs to the DIC in groundwater are following processes: the exchange with the atmospheric CO_2, soil CO_2 (degradation of organic matter), and dissolution of carbonate minerals. All calculations were performed by using the hydrogeochemical software PHREEQC v. 2 (Parkhurst and Appelo, 1999), using the wateqf4.dat database.

For input data a simple solution (rain water) was predicted which is (1) in equilibrium with atmospheric CO_2, and (2) in equilibrium with CO_2 which correspond the sampled groundwater's HCO_3^- concentration both considered as an open system. Detailed description is found in the Appendix 11L.

The molality of total carbon concentration (DIC_{tot}) was calculated which equals the DIC_{atm} concentration. As a references for further calculations the $\delta^{13}C_{CaCO3}$ of 0 ‰ (Pezdič, 1999; Appelo and Postma, 2005), $\delta^{13}C_{org}$ of -22.0 ‰ (Urbanc, 1993), and $\delta^{13}C_{atm}$ of -7.0 ‰ (Appelo and Postma, 2005) were considered. Selected references only serve to demonstrate a calculation of a simple isotopic mass balance calculation. Actual initial values can strongly deviate locally since they depend on the geology, altitude, soil thickness and many more. The aim was to assess the indicative share and ratio between DIC_{carb}, DIC_{atm}, and DIC_{org} in groundwater according to groundwater with recharge areas in high mountains and lowlands. Those values only serve as a rough approximation which can help to provide additional information on groundwater chemical and isotopic composition and processes.

$\delta^{13}C_{tot}$ = stable carbon isotope ratio of total dissolved inorganic carbon
DIC_{tot} = total dissolved carbon concentration
$\delta^{13}C_{carb}$ = stable carbon isotope ratio of carbonate rock
DIC_{carb} = dissolved inorganic carbon from dissolution of carbonate rocks
$\delta^{13}C_{org}$ = stable carbon isotope ratio of soil CO_2
DIC_{org} = dissolved inorganic carbon from organic matter
$\delta^{13}C_{atm}$ = stable carbon isotope ratio of atmosphere
DIC_{atm} = atmospheric concentration

In the second step the initial $CO_{2(g)}$ value was calculated from the measured alkalinity of HCO_3^- of groundwater samples (example for sampling location Soča). The dissolved inorganic carbon from organic matter (DIC_{org}) was calculated as:

$$f(DIC_{org}) = f(DIC_{tot}) – f(DIC_{carb}) - f(DIC_{atm}) \quad (27)$$

The overall equation is:

$$f(DIC_{tot}) = f(DIC_{carb}) + f(DIC_{org}) + f(DIC_{atm}) = 1 \quad (28)$$

$$f(\delta^{13}C\text{-}DIC^{*}DIC_{tot}) = f(\delta^{13}C\text{-}DIC_{carb}{}^{*}DIC_{carb}) + f(\delta^{13}DIC\text{-}DIC_{org}{}^{*}DIC_{org}) + f(\delta^{13}C\text{-}DIC_{atm}{}^{*}DIC_{atm}) \quad (29)$$

A share (%) of molar proportion between calculated contribution of dissolution of carbonates, degradation of organic matter, and the atmosphere in groundwater from sampling location Soča is approx. 49 : 50 : 1. Results for other sampling locations are found in Table 31.

Table 31: Calculated proportions of carbonate dissolution, organic matter, and the atmosphere for selected sampling locations

Sampling location	measured δ^{13}C-DIC (‰)	calculated δ^{13}C-DIC_{tot} (‰)	$f(DIC_{carb})$ (%)	$f(DIC_{org})$ (%)	$f(DIC_{atm})$ (%)
Soča	-1.0	-11.1	49	50	1
Krka	-13.2	-12.6	42	57	0
Kamniška Bistrica	-3.1	-11.2	49	51	1
B-9 Brestovica	-10.5	-12.2	45	56	0

The share of dissolution of carbonates and degradation of organic material are similar to shares calculated by Kanduč *et al.* (2013) for Kamniška Bistrica surface water, and Zavadlav *et al.* (2013) for Krka River surface water, taking into account their calculations are based on chemical and isotopic calculations of surface waters of those springs, where the outgassing of CO_2 was considered and the tributary inputs.

The comparison between measured and calculated groundwater total δ^{13}C-DIC values concerning groundwater from sampling locations Krka and B-9 Brestovica (recharge areas of lower altitudes) shows similar values. But measured groundwater total δ^{13}C-DIC values from sampling locations Kamniška Bistrica and Soča (recharge areas at higher altitudes) are much more positive compared to calculated values. It is believed that groundwater from those sampling locations is influenced by 2 additional isotopic effects because of recharge areas of higher altitudes (Fig. 187): (1) isotopic effect of initial organic CO_2, and (2) isotopic effect of exchanging carbon with the atmosphere. According to Urbanc (1993), soil CO_2 which is mostly derived from the atmosphere, is enriched in ^{13}C by decreasing the soil temperature and increasing the altitudes, respectively. A certain influence at higher altitudes could be also induced by the changes of vegetation cover with a greater proportion of grasses which have more positive δ^{13}C-DIC values. Based on those two mechanisms the soil CO_2 does not contain δ^{13}C -22.0 ‰ like it has been considered for modelling, but its initial isotopic composition of organic carbon is more positive. In high karstic regions the karstic channels are less filled with weathered debris. This means that greater possibilities of groundwater isotopic exchanges exist between carbon from HCO_3^- and carbon from the atmosphere during groundwater flow towards spring. Carbon isotope exchange between air and HCO_3^- can be also carried out at springs if groundwater acts as retention in ponds.

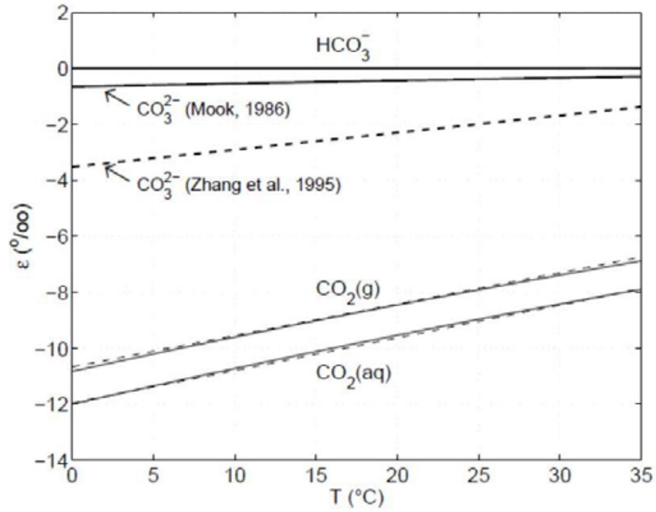

Figure 187: Carbon isotope fractionation between the species of the carbonate system as a function of temperature with respect to HCO_3^-. Values according to Mook (1986) and Zhang et al., (1995) are indicated by solid and dashed lines, respectively (Zeebe and Wolf-Gladrow, 2001).

Sources of DIC in groundwater

Groundwater δ^{13}C-DIC values can help to decipher the contributions of organic matter decomposition, carbonate mineral dissolution, and equilibration with atmospheric CO_2 to the DIC. Figure 197 shows δ^{13}C-DIC versus HCO_3^- and 4 lines which indicate the processes in groundwater. First (red) line indicates an open-system equilibration of DIC with soil CO_2 originating from degradation of organic matter with $\delta^{13}C_{org}$ (-25 ‰) which is enriched by 9 ‰ with corresponding value of -16 ‰ according to Mook *et al.* (1974). Non-equilibrium dissolution of carbonates with one part (50 %) of DIC originating from soil CO_2 (- 25 ‰), and the other (50 %) from carbonates with a mean value of $\delta^{13}C_{Ca}$ (0 ‰) produces an intermediate δ^{13}C-DIC value of -12.5 % (yellow line). Blue line indicates dissolution of carbonate rocks without considering any isotope fractionation. Given the isotopic composition of atmospheric CO_2 (-7 ‰) and the equilibration fractionation with DIC of +9 ‰, DIC in equilibrium with the atmosphere should have a $\delta^{13}C_{DIC}$ of about +2 ‰ (green line). Other fractionation factors were not considered in this study (e.g. exchange with the atmospheric CO_2, diffusion of CO_2 in the soil, carbonate dissolution, CO_2 outgassing in surface waters, and so on).

Groundwater δ^{13}C-DIC in the recharge area of high mountain carbonate rocks is mostly controlled by the geological composition (carbonate dissolution) and atmospheric CO_2 which is evident from more positive δ^{13}C-DIC values and lower alkalinity. In the lowland carbonate-bearing recharge area the alkalinity is higher and the groundwater is more influenced by the degradation of organic matter and leaching from soil layer, which is suggested by more negative δ^{13}C-DIC values. In the recharge areas of silicate and less permeable/impermeable rocks at higher altitudes the alkalinity is low and the biochemical process of degradation of organic matter and leaching from soil layer dominate (Pevčevo, Framski slap, and Godec), as it has been observed by Clark and Fritz (1997), Redondo and Yélamos (2005), Shin *et al.* (2011), and others. Igneous and metamorphic rocks make up two larger groups (Fig. 188). This could be due to soil CO_2, elevation differences, mineralogical composition of rocks in the recharge areas, or due to degassing or exchange with atmospheric CO_2 (when groundwater is sampled as surface water). In the recharge areas of shale and sandstone the alkalinity is low but groundwater is enriched in ^{13}C due to influence of surface water photosynthesis (Zavadlav *et al.*, 2013), or due to the outgassing of CO_2 (Kanduč *et al.*, 2007). In the NE part of Slovenia, where gravel, sand (and clay) prevail in the recharge area, the HCO_3^- concentration in higher, and the δ^{13}C-DIC in groundwater is higher which might be due to dissolution of small proportion of carbonate minerals. The alkalinity is increasing with increasing share of carbonates in the rocks in the recharge area.

Groundwater from deep aquifers (VP-1 Prosenjakovci, Grad-1 Grad, and DEV-1 Desenci) has $\delta^{13}C_{DIC}$ values between -18.7 to -13.06 ‰ with the most negative ones found in the groundwater from sampling location VP-1 Prosenjakovci. This suggests the influence from shallow/recent groundwater where the soil CO_2 makes a greatest contribution to groundwater DIC and dissolution of carbonate minerals a minor. Similar observations were found also by Szőcs *et al.* (2013).

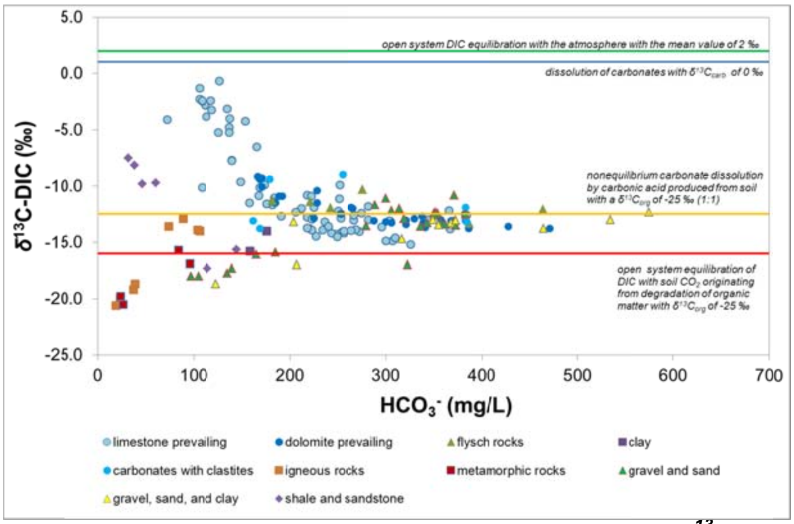

Figure 188: Comparison between groundwater HCO_3^- concentration and δ^{13}C-DIC values

Land cover/use

Enriched in ^{13}C is groundwater DIC in the recharge areas of bare rocks and marshes and heaths which is significantly enriched in ^{13}C ($p<0.05$) compared to recharge areas with other land use types according to CORINE Land Cover use classification. This occurs because the influence of soil CO_2 does not play an important role (Figs. 189 and 190, Appendix 13L). Depleted in ^{13}C is groundwater DIC in all other land use classes, particularly in non-irrigated areas and forests, which is rich in degraded organic material from plant litter and the soil layer is very thick, which causes an increased CO_2 concentration.

Interesting is the observation that groundwater in the recharge areas of different prevailing lithological rock type with the same type of vegetation cover has different δ^{13}C-DIC values. For instance, in the recharge areas coniferous forest on the bedrock of carbonate rocks groundwater has a mean δ^{13}C-DIC value of around -10 ‰, in the recharge areas of igneous rock around -7.5 ‰, and in the recharge areas of metamorphic rocks -16 ‰. In the recharge areas of broad-leaved forest vegetation the differences in groundwater are less obvious. In the recharge areas in the mixed forests and metamorphic rocks at sampling location Framski slap groundwater has a mean value of δ^{13}C-DIC of -20 ‰, suggesting that the major contributor to DIC is soil CO_2. At Pohorje Mt. the δ^{13}C of soil is around -27.3 ‰ and tree needles have -28.3 ‰.

There are no significant differences in groundwater δ^{13}C-DIC values according to Actual agricultural and forest land usage classification, except that in the recharge area of forest the scattering of measured data is very broad, suggesting the exchange in the prevailing sources of DIC (dissolution of carbonates, atmospheric CO_2 or soil CO_2).

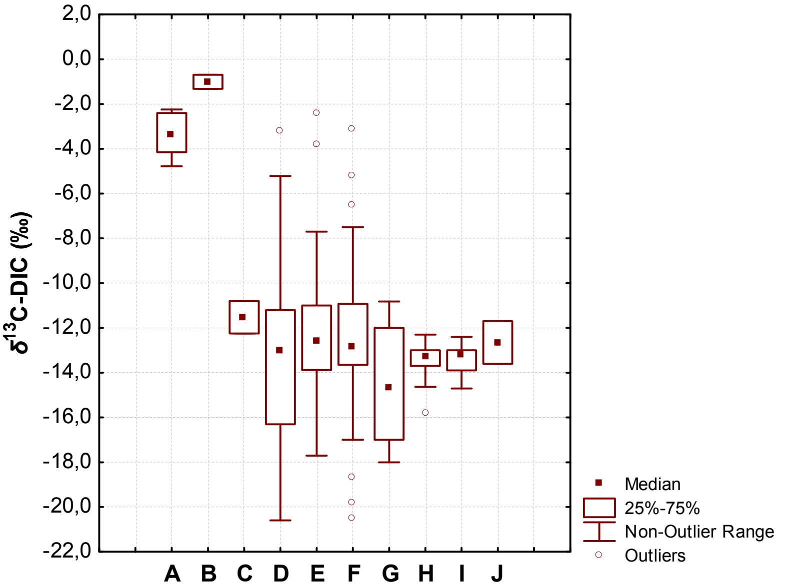

A = bare rocks (n=8)
B = moors and heathland (n=2)
C= natural grasslands (n=2)
D = coniferous forest (n=20)
E = broad-leaved forest (n=44)
F = mixed forest (n=55)
G = non-irrigated arable land (n=10)
H = complex cultivation patterns (n=18)
I = land principally occupied by agriculture, with significant areas of natural vegetation (n=10)
J = industrial or commercial units (n=10)

Figure 189: Box and whisker plots for groundwater δ^{13}C-DIC values according to prevailing land use type (CORINE Land Cover)

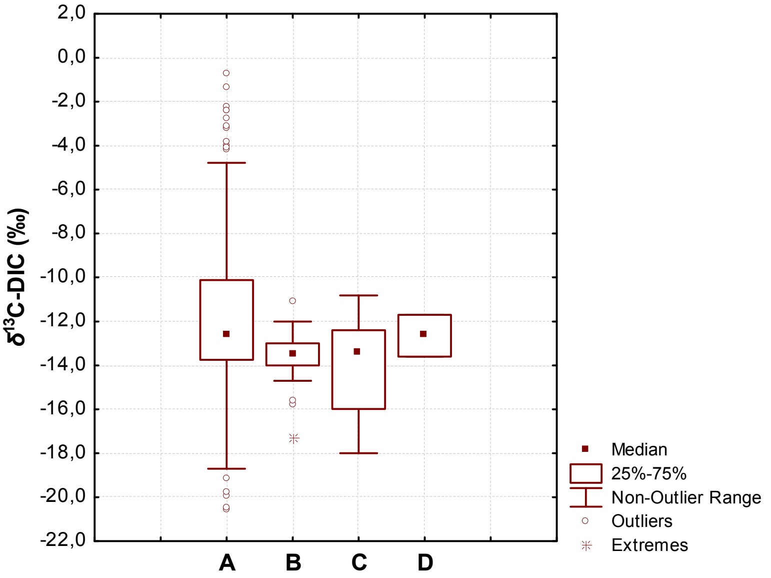

A = forest (n=135)
B = areas of less intense use of nutrients and plant protection products (n=18)
C = areas of intense use of nutrients and plant protection products (n=16)
D = urban areas (n=2)

Figure 190: Box and whisker plots for groundwater δ^{13}C-DIC values according to prevailing land use type (Actual agricultural and forest land usage)

Sampling object type

Water sampled as surface water (Fig. 191) is significantly enriched in ^{13}C-DIC ($p<0.05$) possible due to degassing of CO_2 from groundwater which causes loss of DIC (decrease in alkalinity) and enrichment of DIC in ^{13}C (Doctor *et al.*, 2008; Shin *et al.*, 2011). In surface water photosynthesis could be present which preferentially selects lighter isotope (^{12}C) leaving the remaining DIC enriched in ^{13}C (more positive values) (Shin *et al.*, 2011; Schulte *et al.*, 2011).

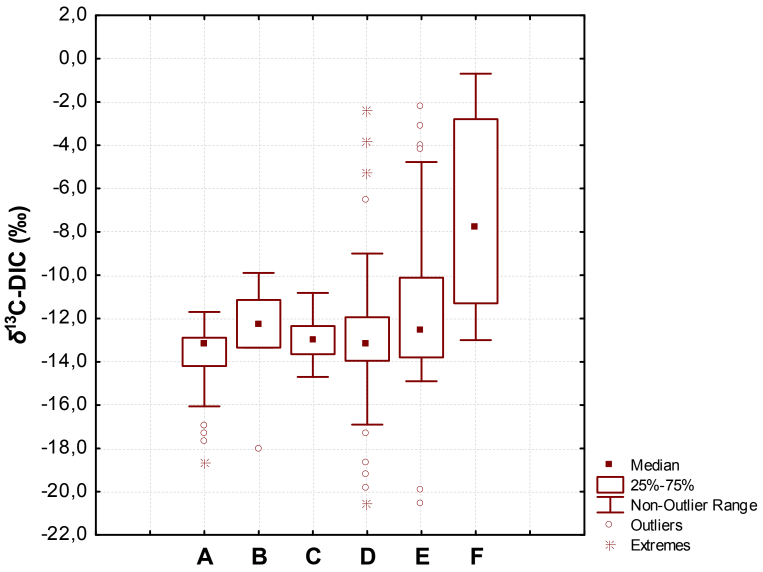

A = pumping station (n=35)
B = borehole (n=10)
C = private well (n=8)
D = spring capture (n=44)
E = spring (n=58)
F = surface water (n=18)

Figure 191: Box and whisker plots for groundwater δ^{13}C-DIC according to sampling object type

Spatial distribution of groundwater δ^{13}C-DIC

Spatial distribution of groundwater δ^{13}C-DIC values resembles the spatial distribution of groundwater carbonate equilibria parameters, like Ca^{2+}, HCO_3^-, P_{CO2}, and $CaCO_3$. Namely, the groundwater that originates in alpine karstic areas in high mountains (Julian Alps, Karavanke Mts., and Kamnik-Savinja Alps) is enriched in ^{13}C and is more alkaline (Fig. 192). This is due to the dissolution of carbonate rocks, greater relative contribution of atmospheric CO_2, thin (or non-existent) soil layer, and consequently low microbiological activities/organic matter degradation in the recharge areas. The soil horizon at the higher elevations in Slovenia can be very thin due to sloping surfaces and steep inclinations (Repe, 2004). This limits the biological activity and decreases the production of soil CO_2 where temperature and amount of precipitation play an important role (Leifeld and Fuhrer, 2005). At 2,500 m a.s.l. there is a reduction in pressure of almost 25 % compared to lowlands. Consequently, less CO_2 is available for dissolution in precipitation and surface runoff in high mountains (Bader and Kunz, 2000). At lower elevations the quantity of organic matter is increasing, and humus is being formed by the annual decay of plants roots and debris (Cocos, 1997). Namely, the tree roots contribute to the weathering of parent rock, and channels resulting from roots decay are improving the circulation of air and water within the soil (Cocos, 1997).

According to groundwater saturation indices of calcite (SI_{cal}), groundwater from high mountains recharge areas with carbonate rocks has SI_{cal} around 0 (Fig. 193, IV.), whereas groundwater from the recharge areas with igneous and metamorphic rocks (Fig. 193 I.), clastites from the NE part of Slovenia (Fig. 193, III.), and shale and sandstone (Fig. 193, II.) is undersaturated with respect to calcite.

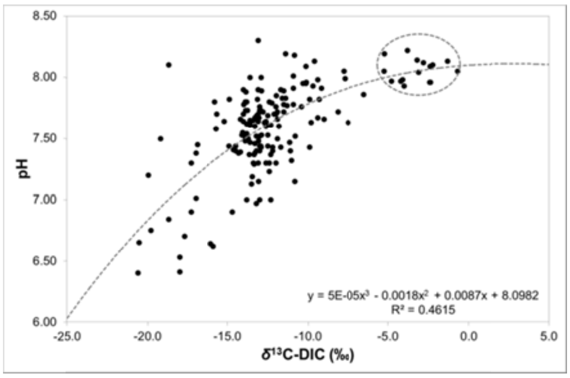

Figure 192: Groundwater pH versus δ^{13}C-DIC values

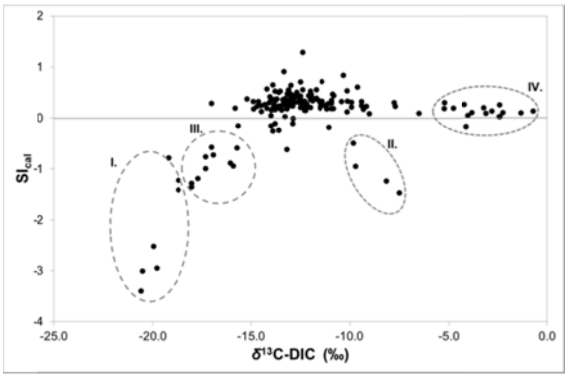

Figure 193: Groundwater SI_{cal} versus δ^{13}C-DIC values

The most depleted in ^{13}C is groundwater at Pohorje Mt. (Fig. 194) which consists of igneous and metamorphic rocks and has a thick soil layer under forest vegetation. The soil CO_2 contributes mostly to DIC, since the acidic and intermediate igneous rocks (granodiorite group) are rich in quartz, and relatively little CO_2 is consumed for feldspar weathering. Thick soil layer increases the organic matter degradation and root respiration in the soil. Soil that is formed under deciduous forests is very fertile because of the decomposing leaves at the soil surface. Soils formed under pine trees are usually more acidic and sandy. Also depleted in ^{13}C is groundwater in the north-eastern part of the country where groundwater samples reflect similar δ^{13}C depleted DIC values with respect to those of the soil CO_2. This is due to prevailing silicate rocks in the recharge area, where the soil CO_2 prevails over atmospheric CO_2 causing depletion of groundwater DIC in ^{13}C. The groundwater in the south and south-eastern part (Dolenjska region), the central part, and the north-eastern part (Štajerska region) of the country have the δ^{13}C values around -13 ‰ suggesting the influence from both, dissolution of carbonate minerals (of the carbonate bedrock or carbonate cement in clastic rocks) and influence from the soil CO_2.

Pirc *et al.*, 1998, studied the behaviour of δ^{13}C-DIC values in Slovenian streams which had a mean δ^{13}C-DIC value of -12 ‰ (-23 to -8.6 ‰). They also observed less negative values in the northern and north-western mountain parts, and more negative values in SE, and E part of the country. Variations of δ^{13}C-DIC are interpreted by varying climate conditions and vegetation cover characteristics.

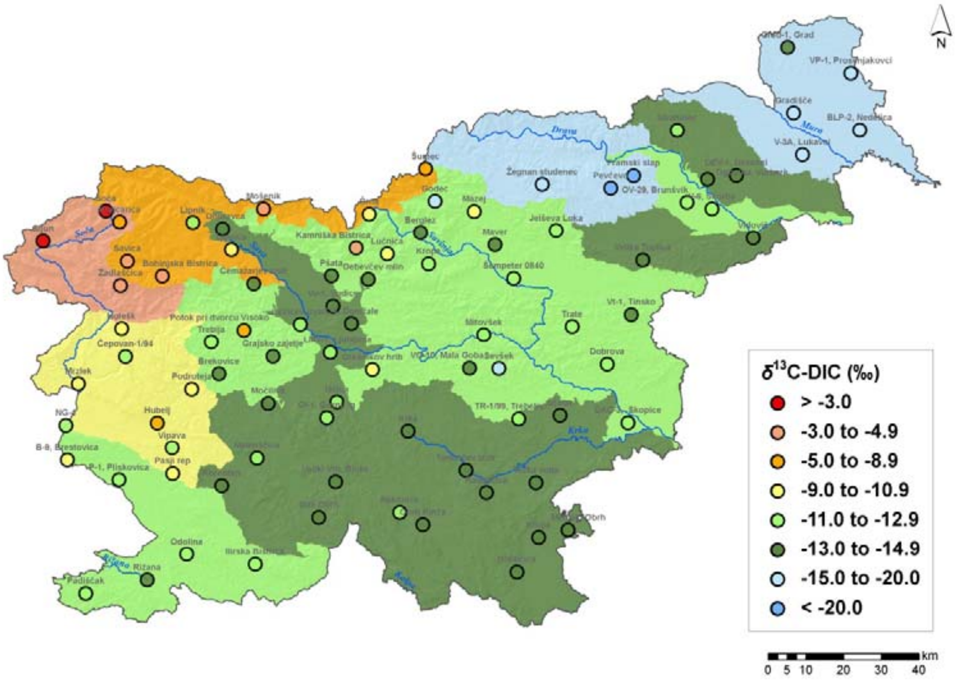

Figure 194: Spatial distribution of groundwater δ^{13}C-DIC values

4.6.2. Groundwater chemistry of silicate weathering

4.6.2.1. Silicon (Si) in Slovenian groundwaters

Descriptive statistics of groundwater Si

Mean groundwater Si concentration is 3.18 mg/L, median 1.85 mg/L, maximum 13.44 mg/L, and minimum 0.17 mg/L (Tab. 32). Groundwater Si is not normally distributed (Fig. 195) and concentrations higher than 9.07 mg/L present outliers (Fig. 196) which are found at sampling locations Maver, BLP-2 Nedelica, V-3A Lukavci, DEV-1 Desenci, GRAD-1 Grad, and VP-1 Prosenjakovi, all located in the NE part of Slovenia. The analytical uncertainty for groundwater Si is between 15 and 30 %.

Table 32: Descriptive statistics of groundwater Si concentration

Parameter	n	X	Md	Min	Max	S
Si (mg/L)	174	3.18	1.85	0.17	13.44	3.03

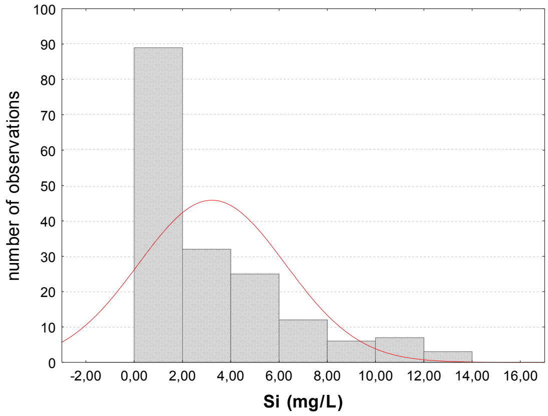

Figure 195: Histogram for groundwater Si concentration (n=174)

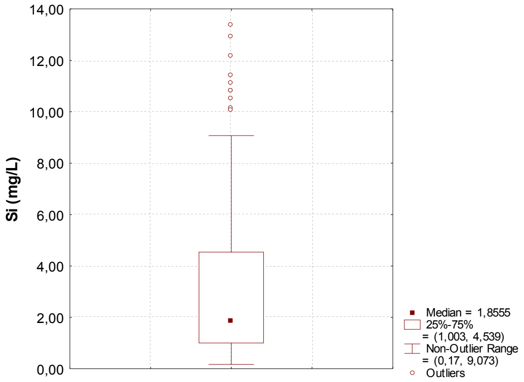

Figure 196: Box and whisker plot for groundwater Si concentration (n=174).

Rock type

Groundwater Si concentration is high in the recharge areas with clastic sedimentary and igneous and metamorphic rocks (Fig. 197, Appendix 13M) due to weathering of silicate minerals. Carbonate rocks are poor in silicate minerals, therefore the concentration of Si in this groundwater is significantly lower ($p<0.05$) compared to other two groups. Outliers in carbonate rocks are found at sampling locations Trate, Ščetar, Mazej, and TR-1 Trebelno.

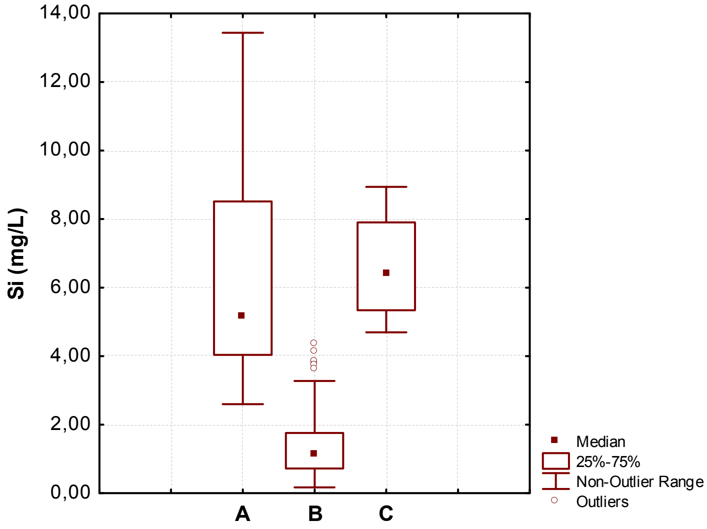

A = clastic sedimentary rocks (n=46)
B = carbonate rocks (n=110)
C = igneous and metamorphic rocks (n=12)

Figure 197: Box and whisker plots for groundwater Si concentration in the recharge area of major rock types

The highest groundwater Si concentration is observed in the recharge areas of Oligocene clay "sivica" (two groundwater samples) (Figs. 198 and 199, Appendix 11M) and Pliocene gravel, sand and clay where groundwater Si concentration is significanty higher ($p<0.05$) compared to recharge areas with all other lithostratigraphic units except old Paleozoic rocks. This is due to silicate weathering of phyllosilicates (illite/muscovite, chlorite and montmorillonite) (Kralj and Mišič, 2003) and longer residence time in deep aquifers (Kralj, 2003). Medium groundwater Si concentrations are observed in Eocene flysch rocks, Permian Val Gardena layers, shale and sandstone of Carboniferous-Permian beds, Miocene and Quaternary clastics, Ladinian and Oligocene igneous rocks, and metamorphic Paleozoic rocks which sources of Si are in silicate minerals. The lowest groundwater Si concentration measured in the recharge area of Jurassic, Cretaceous, and Triassic carbonates is significantly lower ($p<0.05$) compared to Eocene flysch rocks, Permian Val Gardena layers, Quaternary clastics (medium- and coarse-grained), Ladinian igneous rocks, Miocene clastics, Oligocene igneous rocks, Pliocene clastics, Oligocene clay "sivica", and and old Paleozoic rocks.

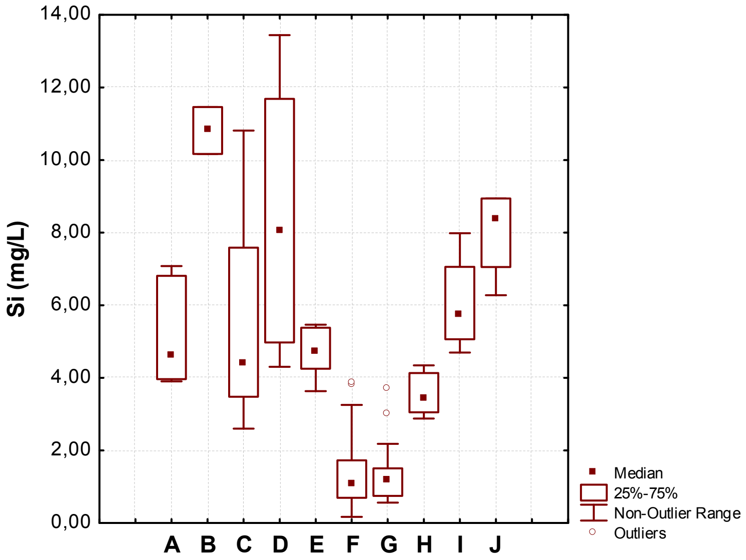

A = flysch rocks (n=7)
B = clay (n=2)
C = gravel and sand (n=26)
D = gravel, sand and clay (n=4)
E = shale and sandstone (n=7)
F = limestone prevailing (n=74)
G = dolomite prevailing (n=30)
H = carbonates with clastics (n=6)
I = igneous rocks (n=8)
J = metamorphic rocks (n=4)

Figure 198: Box and whisker plots for groundwater Si concentration in the recharge area of prevailing lithological unit

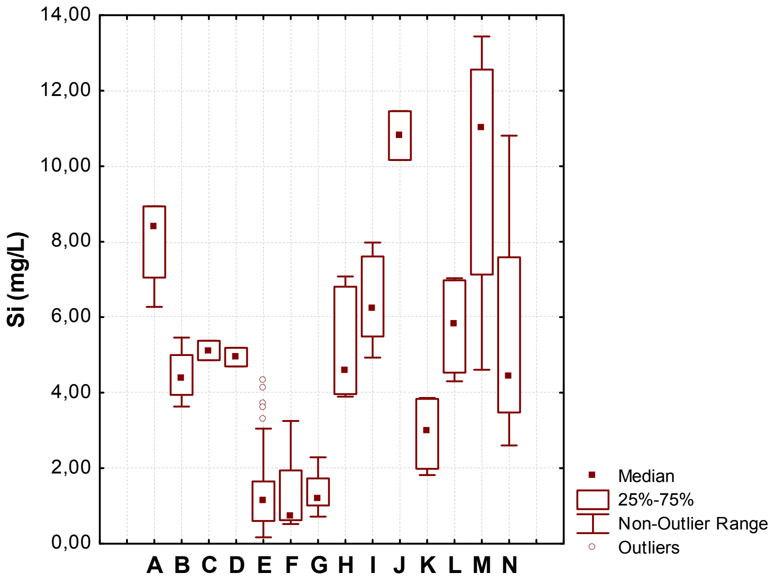

A = old Paleozoic rocks (n=4)
B = Carboniferous-Permian beds (n=4)
C = Permian Val Gardena layers (n=2)
D = Ladinian igneous rocks (n=2)
E = Triassic carbonates (n=70)
F = Jurassic carbonates (n=8)
G = Cretaceous carbonates (n=28)
H = Eocene flysch rocks (n=6)
I = Oligocene igneous rocks (n=6)
J = Oligocene clay "sivica" (n=2)
K = Miocene Lithothamnium limestone (n=4)
L = Miocene clastics (n=4)
M = Pliocene clastics (n=8)
N = Quaternary clastics (medium- and coarse-grained) (n=28)

Figure 199: Box and whisker plots for groundwater Si concentration in the recharge areas of prevailing lithostratigraphic unit

In the NE part of the country increased groundwater Si concentrations are observed not only in waters from from shallow aquifers (Mursko polje) but also from deep aquifers (Goričko). Also increased Si concentrations are observed on Pohorje Mt. and at sampling locations Maver and Godec, all located in the NNE part. Low groundwater Si concentrations are generally observed in all other parts of Slovenia, since the dominant minerals in recharge areas of sampled groundwater are calcite and dolomite. Figure 200 presents the correlation between groundwater Si and Na^+ concentration ($r_s=0.81$, $p<0.05$) which suggests, according to Rosen (2001), silicate weathering and ion exchange reactions within the aquifers at low groundwater temperatures (circled groundwater samples). Figure 201 presents the correlation between groundwater ^{3}H and Si concentration where increased groundwater Si dominates mostly the older groundwater (circle).

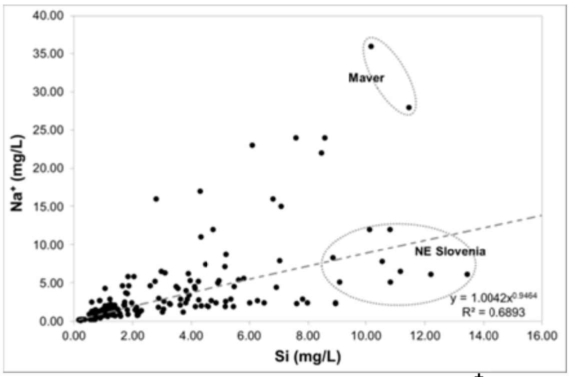

Figure 200: Groundwater Si versus Na$^+$ concentrations

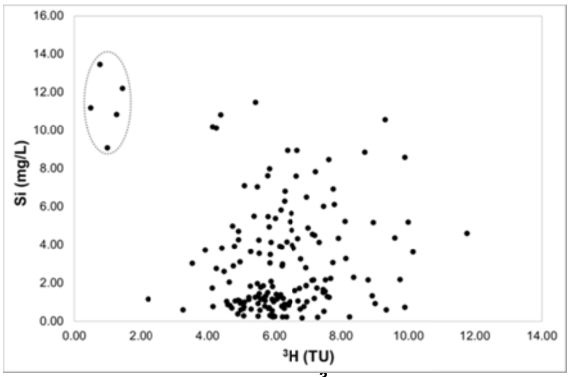

Figure 201: Groundwater ^{3}H versus Si concentration

In the recharge areas with clastic sedimentary, igneous, and metamorphic rocks, mostly located in the NE and W part, groundwater Si concentrations are high, and pH values are lower (Fig. 202) compared to groundwater from the recharge areas with carbonate rocks and other clastic sedimentary rocks with prevailing carbonate component.

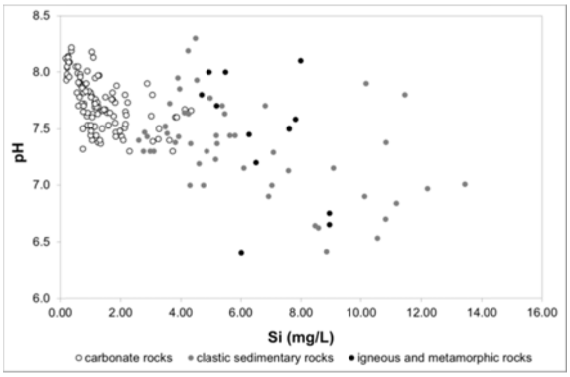

Figure 202: Groundwater Si concentration versus pH

Solubility and sources of groundwater Si

Since some sampling objects are drilled in deeper aquifers' layers where old groundwater is stored, the idea was to identify whether the source of silicon in groundwater is from deeper groundwater where the SiO_2 is temperature dependent, or is the source only from weathering of silica-containing rocks.

In the code PHREEQC various shares of CO_2 were used for calculation for pH and Si concentrations in the solution (Appendix 13M). With increasing groundwater pH also Si concentration is increasing (Fig. 203). On the contrary, groundwater Si concentration is decreasing by increasing the share of CO_2 (Fig. 204).

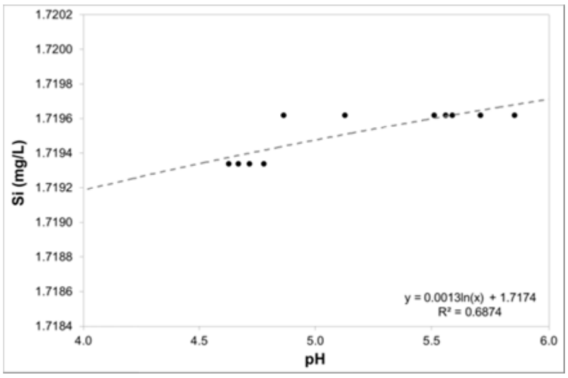

Figure 203: Groundwater pH versus Si concentration

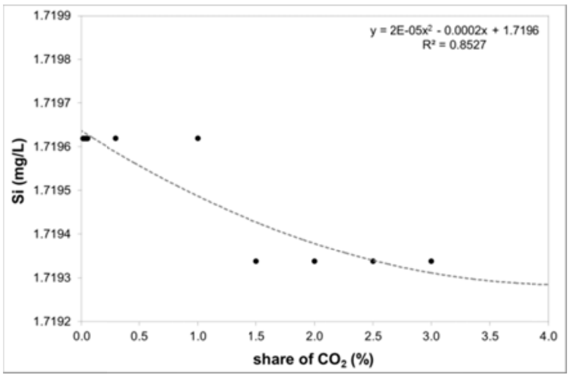

Figure 204: Correlation between the share of CO_2 and Si concentration

Solubility of quartz was calculated according to 5 different temperatures (0.01, 10, 25, 50, 75, and 100°C) (Tab. 33, Fig. 205). The line suggests that an increase in temperature substantially increases the solubility of Si (based on P_{CO2atm}). But due to slow dissolution kinetics of silicate minerals the concentration of Si increases very slowly.

Table 33: Solubility of Si according to various P_{CO2} and temperatures

	Temperature (°C)					
P_{CO2} (%)	0.01	10.00	25.00	50.00	75.00	100.00
0.035	2.49	3.67	6.28	13.72	26.82	47.90
1.000	2.49	3.67	6.28	13.72	26.81	47.89
10.000	2.49	3.67	6.28	13.72	26.81	47.88

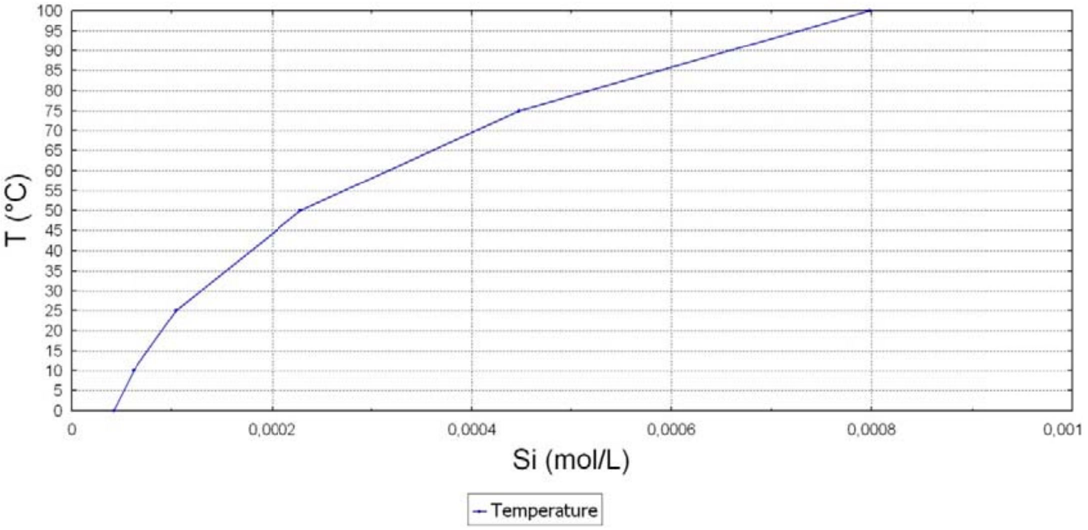

Figure 205: Solubility of Si as a function of temperature

Additionally, the solubility of several other silicate minerals which are most common in Slovenian silicate rocks (illite, Ca-montmorillonite, chlorite, and chalcedony) were calculated (Appendix 13M). Calculated concentrations of various ions (Ca^{2+}, Mg^{2+}, K^+, Fe, Al, and Si) of selected minerals were compared with concentrations measured in various groundwater samples. For an example, sources of Si in groundwater from sampling location Maver (clay in the recharge area, NNE part) could be from minerals kaolinite, K-mica, Ca-montmorillonite, chlorite, illite, phlogopite, quartz, anorthite, chalcedony, albite, and quartz, and possible sources of groundwater Si from sampling location Žegnani studenec (metamorphic rocks in the recharge area, NNE part) could be from quartz, chlorite, chalcedony, and albite.

This simplified approach only serves as a rough approximation to the range of Si concentration in groundwater. Although chemical reactions in silicate aquifers are very slow, the assumption was that in the time of contact between water and rock, the chemical equilibria were approximately established. Naturally, during further groundwater flow through the aquifer the groundwater could not be in chemical equilibrium with rock any more. In order to calculate the exact concentration of Si in groundwater dissolution of quartz and other silicate minerals other factors needed to be considered, e.g. incongruent dissolution, adsorption and neoformation of silicates, etc.

Aquifer porosity type

The highest groundwater Si concentration was measured in aquifers with intergranular and fractured porosity (Fig. 206, Appendix 13M), and median in aquifers with mixed porosity (karstic, fractured, intergranular), because of prevalence of silicate minerals in the aquifer. The lowest groundwater Si concentration was measured in aquifers with either prevailing fractured or karstic porosity which are significantly lower ($p<0.05$) compared to groundwater from aquifers with intergranular, mixed (karstic, fractured, intergranular), and fractured porosity because of prevailing carbonate rocks.

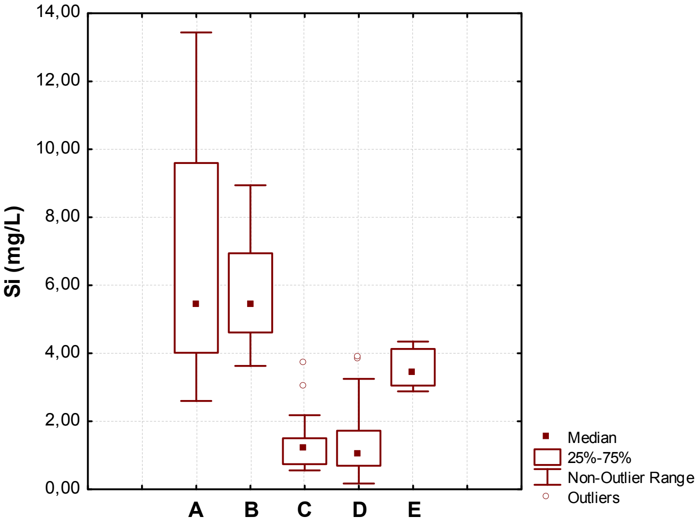

A = intergranular porosity (n=40)
B = fractured porosity (n=24)
C = fractured and karstic porosity (n=30)
D = karstic and fractured porosity (n=74)
E = mixed porosity (karstic, fractured, intergranular) (n=6)

Figure 206: Box and whisker plots for groundwater Si concentration in the recharge area of prevailing aquifer porosity type

Sampling object type

The highest groundwater Si concentrations are measured in private wells (Fig. 207, Appendix 13M), and median concentrations in groundwater from pumping stations, boreholes, and spring captures. Majority of those sampling locations are located in the NE part where silicate minerals prevail in the recharge areas. The lowest groundwater Si concentrations are observed in the springs and surface waters, since they were mostly sampled in the carbonate recharge areas.

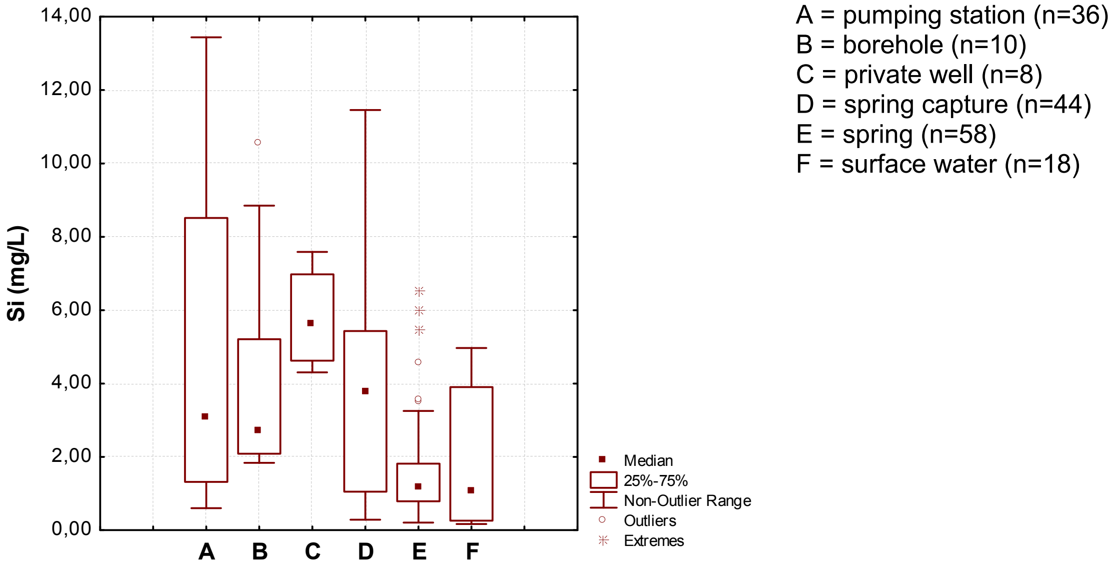

Figure 207: Box and whisker plots for groundwater Si concentration according to sampling object type

Spatial distribution of groundwater Si

Increased groundwater Si concentrations (>6.00 mg/L), as a result of silicate weathering, are observed in shallow and deep aquifers with clastic sedimentay rocks in the recharge areas (NNE part - Mursko polje and Goričko), igneous and metamorphic rocks (NNE part - Pohorje Mt.) and clay (NNE part), where mostly silicate minerals prevail in the recharge areas (Fig. 208). Low groundwater Si concentrations (<3.00 mg/L) are observed in other parts of Slovenia with carbonate rocks in the recharge areas.

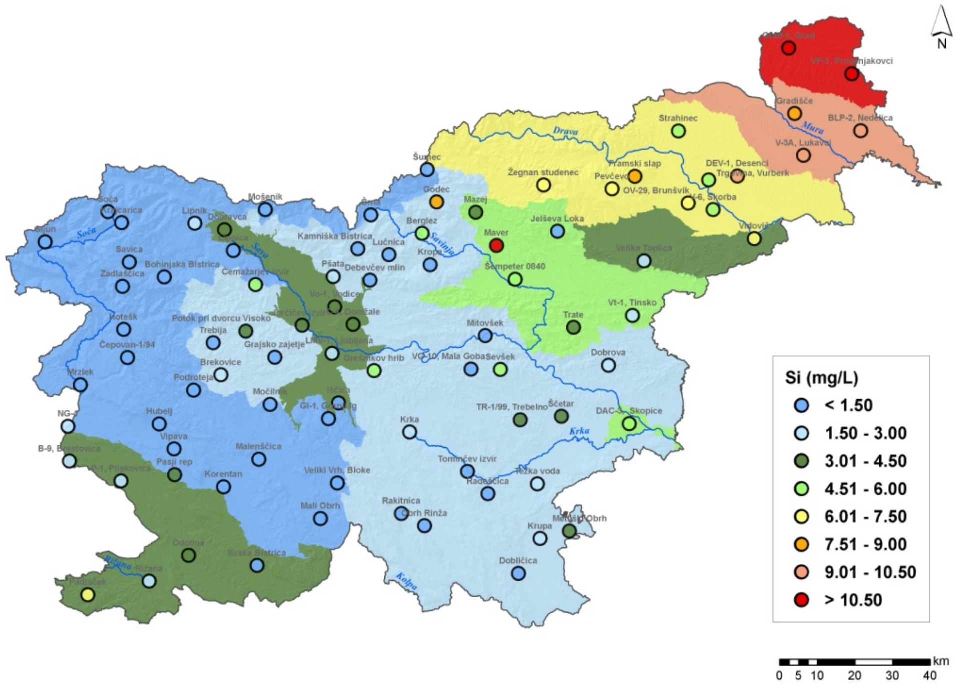

Figure 208: Spatial distribution of groundwater Si

4.7. Parameters affected mostly by anthropogenic influences

4.7.1. Sodium (Na^+) in groundwater

Descriptive statistics of groundwater Na^+

Groundwater Na^+ concentrations vary between 0.1 and 36.0 mg/L, with mean value 3.7 mg/L and median 2.0 mg/L (Table 34). Groundwater Na^+ concentration is not normally distributed (Fig. 209) and concentrations higher than 8.7 mg/L present outliers and extremes (sampling locations Padiščak (near the coast), Maver, Gradišče, LMV-1 Ljubljana, OV-29 Brunšvik, V-3A Lukavci, Strahinec (all located in the NE), and DAC-3 Skopice (E) (Fig. 210). The analytical uncertainty for Na^+ is between 4.2 and 22.6 % (n=155). In 20 groundwater samples Na^+ concentration is bellow LOD (½ LOD=0.25 mg/L) observed at sampling locations Bohinjska Bistrica, Gljun, Kamniška Bistrica, Krajcarica, Savica, Soča, Šumec, Zadlaščica, and Črna, all located in the NW and N part of the study area. None of water samples exceeds the allowed maximum level for drinking water (200 mg/L) according Rules on drinking water (2004).

Table 34: Descriptive statistics of groundwater Na^+ concentration

Parameter	n	X	Md	Min	Max	S
Na^+ (mg/L)	175	3.7	2.0	0.1	36.0	5.3

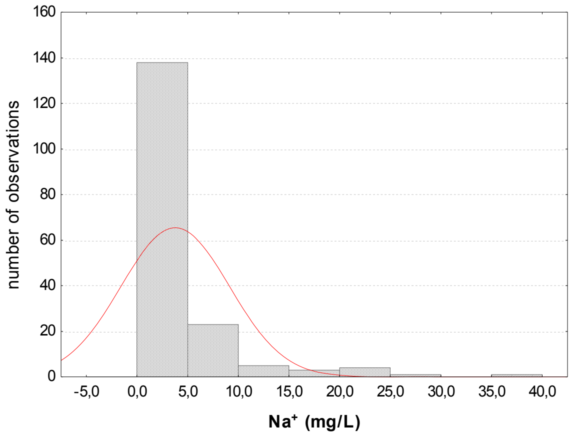

Figure 209: Histogram for groundwater Na^+ concentration (n=175)

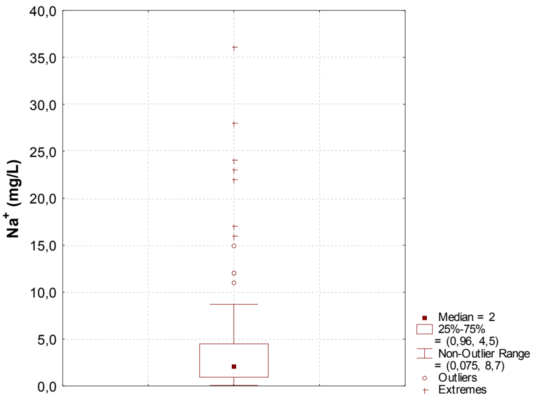

Figure 210: Box and whisker plot for groundwater Na^+ concentration (n=175)

Rock type

The highest groundwater Na^+ concentration is observed in the recharge areas with clastic sedimentary rocks (Fig. 211, Appendix 13N) where significantly higher concentrations ($p<0.05$) are measured compared to carbonate, igneous, and metamorphic rocks. Outliers are observed at sampling locations Maver, Gradišče, OV-29 Brunšnik, Strahinec, Padiščak, and LMV-1 Ljubljana, which are located in the NE, central, and coastal part of the country. Possible sources are weathering of silicate minerals, and proximity of the seaside. In the recharge areas of igneous and metamorphic rocks median groundwater Na^+ concentration are observed (n=2), possible due to silicate weathering of minerals. Sampling location Berglez is an outlier, since concentrations of Na^+ in those recharge areas were below LOD (n=6). The lowest groundwater Na^+ concentration is observed in the recharge areas with carbonate rocks (high mountain and Dinaric karst) which are deficient in Na-rich minerals.

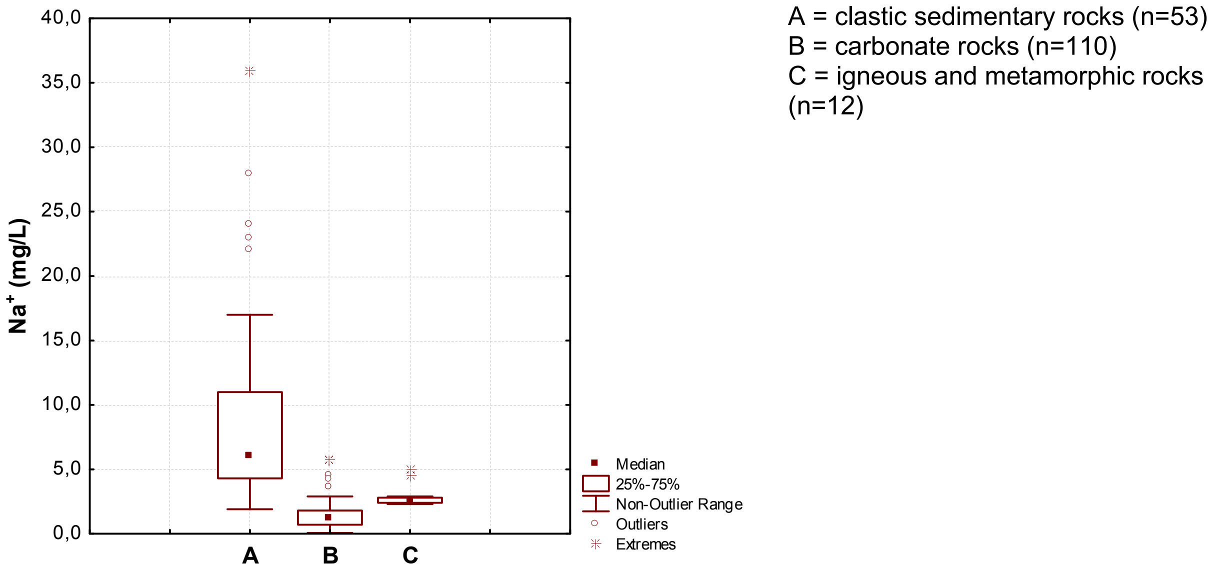

Figure 211: Box and whisker plots for groundwater Na^+ concentration in the recharge areas of major rock types

The highest groundwater Na^+ concentration is observed in the recharge areas with Oligocene clay “sivica” at sampling location Maver (Fig. 212 and 213, Appendix 13N) which is significantly higher ($p<0.05$) compared to other lithological and lithostratigraphic units, possibly due to cation exchange between Na^+ and Ca^{2+} (Fig. 214). Graph also shows that increased groundwater Na^+ concentrations are observed in hard groundwater in lowlands, possibly due to anthropogenic influences, e.g. roads deicing, use of fertilizers, leakage from sewage systems, or other. Increased Na^+ concentration is also observed in groundwater in contact with Eocene flysch rocks, Miocene clastics, and Quaternary clastics (medium- and coarse-grained) which are significantly higher ($p<0.05$) compared to Triassic and Jurassic carbonates. In the NE part the alluvial sediments were brought from high mountain regions from the N (Austria) and are composed of (Oligocene) tonalite and (Precambrian) quartz (sericite phyllite, phyllite schist, gneiss, amphibolite, chlorite, biotite – chlorite schist and marble) (Popit and Vaupotič, 2002). The lowest groundwater Na^+ concentration is observed in the recharge area of carbonate rocks (Fig. 215). Comparison between groundwater Na^+ and HCO_3^- concentration suggest on silicate weathering mechanism in some groundwater samples which have recharge areas with clastic sedimentary, igneous, and metamorphic rocks with prevailing silicate minerals. This groundwater has lower HCO_3^- concentration compared to groundwater in the recharge area of carbonate rocks. Most of these sampling locations have their recharge areas in silicate rocks, but this is not the major source of sodium in groundwater. In recharge areas wizh Triassic carbonates sampling locations Krka, Pšata, Veliki vrh Bloke are outliers, and in the recharge areas with Cretaceous carbonates sampling location B-9 Brestovica is an outlier. Possible natural source for increased groundwater Na^+ concentration is the sea spray or precipitation due to vicinity of the sea (Fig. 216).

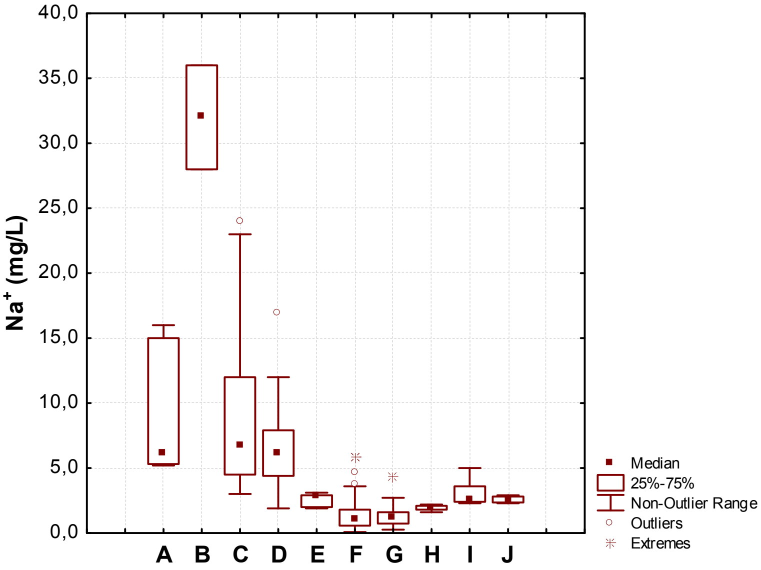

A = flysch rocks (n=7)
B = clay (n=2)
C = gravel and sand (n=26)
D = gravel, sand and clay (n=11)
E = shale and sandstone (n=7)
F = limestone prevailing (n=74)
G = dolomite prevailing (n=30)
H = carbonates with clastics (n=6)
I = igneous rocks (n=8)
J = metamorphic rocks (n=4)

Figure 212: Box and whisker plots for groundwater Na$^+$ concentration in the recharge area of prevailing lithological unit

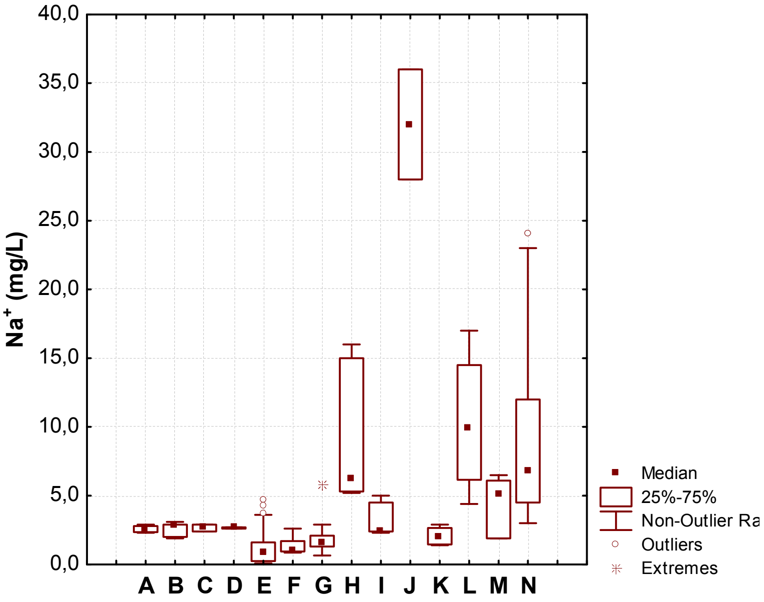

A = old Paleozoic rocks (n=4)
B = Carboniferous-Permian beds (n=5)
C = Permian Val Gardena layers (n=2)
D = Ladinian igneous rocks (n=2)
E = Triassic carbonates (n=70)
F = Jurassic carbonates (n=8)
G = Cretaceous carbonates (n=28)
H = Eocene flysch rocks (n=7)
I = Oligocene igneous rocks (n=6)
J = Oligocene clay “sivica” (n=2)
K = Miocene Lithothamnium limestone (n=4)
L = Miocene clastics (n=4)
M = Pliocene clastics (n=7)
N = Quaternary clastics (medium- and coarse-grained) (n=26)

Figure 213: Box and whisker plots for groundwater Na$^+$ concentration in the recharge area of prevailing lithostratigraphic unit

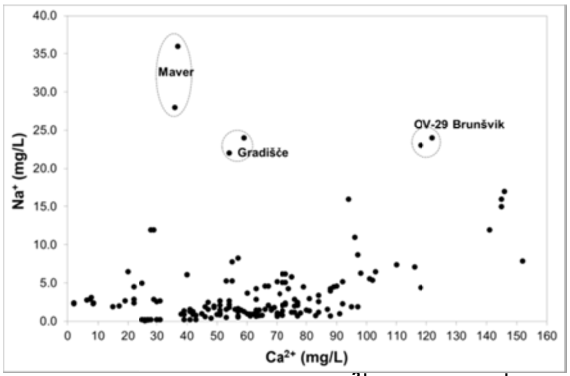

Figure 214: Groundwater Ca^{2+} versus Na^+ concentration

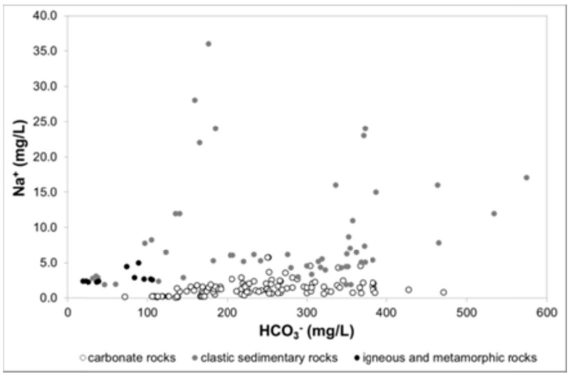

Figure 215: Groundwater HCO_3^- versus Na^+ concentrations

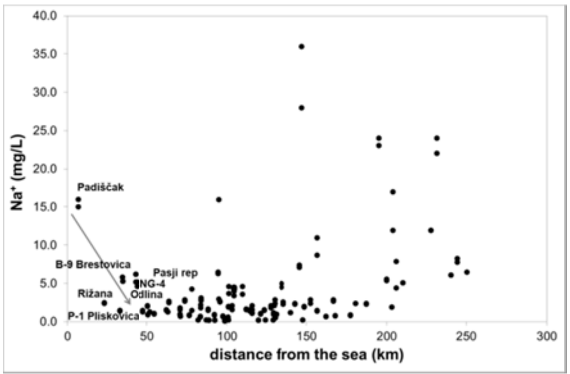

Figure 216: Groundwater Na^+ concentration versus the distance from the sea

Strong correlations exists between Cl^- and Na^+ ($r_s=0.81$, $p<0.05$). Groundwater samples are plotted on Na^+ versus Cl^- graph (Fig. 217) with majority of groundwater samples plotted along the halite dissolution line (Na^+:Cl^-=1:1, dashed line) suggesting the sources of Na^+ and Cl^- in most Slovenian groundwaters originate from dissolution of halite. A seawater concentration-dillution line (SCDL) (Hounslow, 1995; Stevens, 2010) presents the ratio in the sea water, where groundwater from sampling location is plotted. If the ratio is not equal it suggests beside halite dissolution of other minerals, e.g. silicate weathering (Meybeck, 1987). Groundwater samples from sampling locations Padiščak and B-9 Brestovica are plotted close the SCDL (solid line) suggesting the influence from the sea (Fig. 217) and groundwater from sampling location Maver suggests ion exchange. The lowest groundwater Na^+ concentration is observed in the recharge areas of carbonates (Triassic, Jurassic, Cretaceous carbonates, and Miocene Lithothamnium limestone) because of the lack of Na-rich minerals. Additionally the amount of precipitation in the Alps (NW and N part) is higher compared to other parts of Slovenia (NE), and the terrain is sloped. Therefore dilution of groundwater also influences the lower Na^+ concentration (Fig. 218).

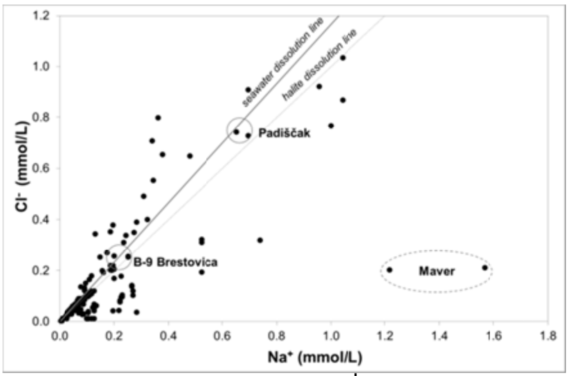

Figure 217: Groundwater Na^+ versus Cl^- molar concentration

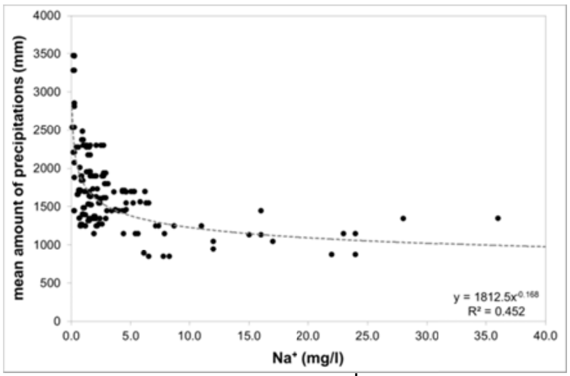

Figure 218: Groundwater Na^+ concentrations versus the mean amount of precipitation

According to lithological and lithostratigraphic classifications, it is believed that the main sources of Na^+ concentration in groundwater are not natural. Instead the anthropogenic activities above the aquifers, which include agricultural land use and urbanization in lowlands, could provide additional (main) sources of Na^+.

Aquifer porosity type

Groundwater Na^+ concentration is significantly higher in the aquifers with intergranular porosity (Fig. 219, Appendix 13N) compared to aquifers with other porosity types. In aquifers with intergranular porosity silicate minerals dominate and intense agricultural activity (use of fertilizers, manure and slurry) is present. Additionally, urban areas (leakages from septic tanks, sewage systems, and use of salts for deicing roads) are associated with dense road networks. Outliers are observed at sampling locations Maver and Gradišče (NNE and NE part). In other aquifers with various porosity types groundwater Na^+ concentration is low. Outliers in aquifers with fractured porosity are found at sampling location Padiščak, in in aquifers with fractured and karstic porosity at sampling location Veliki Vrh Bloke, and in aquifers with karstic and fractured porosity at sampling location B-9 Brestovica, Krka, and Pšata. In the karst region the anthropogenic influence on groundwater is less expressed due to less suitable conditions for farming and lower population number.

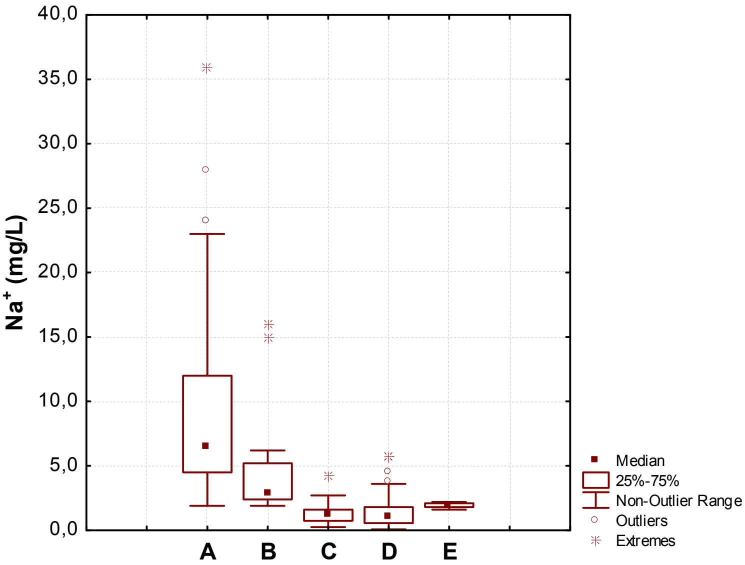

A = intergranular porosity (n=39)
B = fractured porosity (n=26)
C = fractured and karstic porosity (n=30)
D = karstic and fractured porosity (n=74)
E = mixed porosity (karstic, fractured, intergranular) (n=6)

Figure 219: Box and whisker plots for groundwater Na^+ concentration in the recharge area of the prevailing aquifer porosity type

Land cover/use

High groundwater Na$^+$ concentrations are observed in the recharge areas with non-irrigated arable land and industrial or commercial units (Figs. 220 and 221; Appendix 13N). Groundwater Na$^+$ concentration in the recharge areas with non-irrigated arable land is significantly higher ($p<0.05$) compared to recharge areas of all other land use types according to CORINE Land Cover except in the recharge areas with industrial or commercial units and complex cultivation patterns. In classical agricultural products often a variety of fertilizers and animal manure and slurry are used (also leakage from septic tanks), and in the recharge area of industrial or commercial units elevated Na$^+$ concentration is most likely from the use of salts for deicing roads (large seasonal fluctuations). Outliers in the recharge areas of complex cultivation patterns are observed at sampling location Maver. Strong correlations exists between groundwater Na$^+$ and K$^+$ (r_s=0.82, $p<0.05$; Fig. 222), Br (r_s=0.71, $p<0.05$; Fig. 223), and moderate with SO_4^{2-} (r_s=0.61, $p<0.05$; Fig. 224), and NO_3^- (r_s=0.51, $p<0.05$; Fig. 225) suggest the anthropogenic influence on groundwater, especially in the recharge area of silicate rocks in the NE part of the country. Low groundwater Na$^+$ concentrations are observed in all other classes. According to the type of forest (coniferous, broad-leaved, or mixed) in the recharge area of forests groundwater Na$^+$ concentrations are similar (outliers in coniferous forest: V-6 Skorba and Berglez; broad-leaved forest: V-3A Lukavci; and mixed forest: Padiščak, Grad-1 Grad, and VP-1 Prosenjakovci). Outliers are observed at sampling locations B-9 Brestovica, Odolina, Padiščak, and Pasji rep due to influence from the sea. At sampling locations V-3A Lukavci and V-6 Skorba due possible to agricultural activities (fertilizers, manure), leakage of septic tanks and sewage system, and use of road salt. The content of older groundwater Na$^+$ (sampling locations Grad-1 Grad and VP-1 Prosenjakovci) is possible due to longer groundwater residence time with silicate minerals in the recharge areas.

According to Actual agricultural and forest land usage classification (Fig. 221; Appendix 13N) groundwater Na$^+$ concentrations in the recharge areas with intense use of nutrients and plant protection products and urban areas are significantly higher ($p<0.05$) compared to recharge areas with forest and areas of less intense use of nutrients and plant protection products. In the recharge area of less intense use of nutrients and plant protection products the outliers are sampling locations OV-29 Brunšvik and Gradišče.

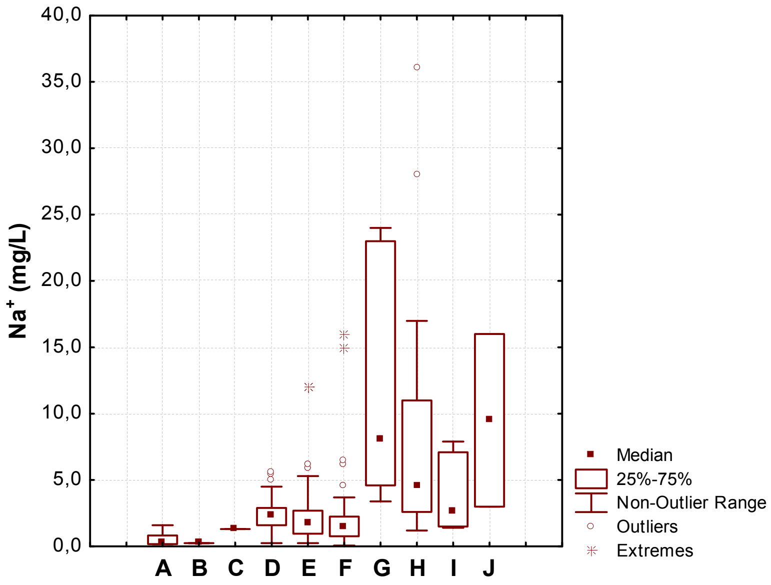

A = bare rocks (n=8)
B = moors and heathland (n=2)
C = natural grasslands (n=2)
D = coniferous forest (n=20)
E = broad-leaved forest (n=45)
F = mixed forest (n=56)
G = non-irrigated arable land (n=10)
H = complex cultivation patterns (n=18)
I = land principally occupied by agriculture, with significant areas of natural vegetation (n=10)
J = industrial or commercial units (n=2)

Figure 220: Box and whisker plots for groundwater Na$^+$ concentration in the recharge area of prevailing land use type (CORINE Land Cover)

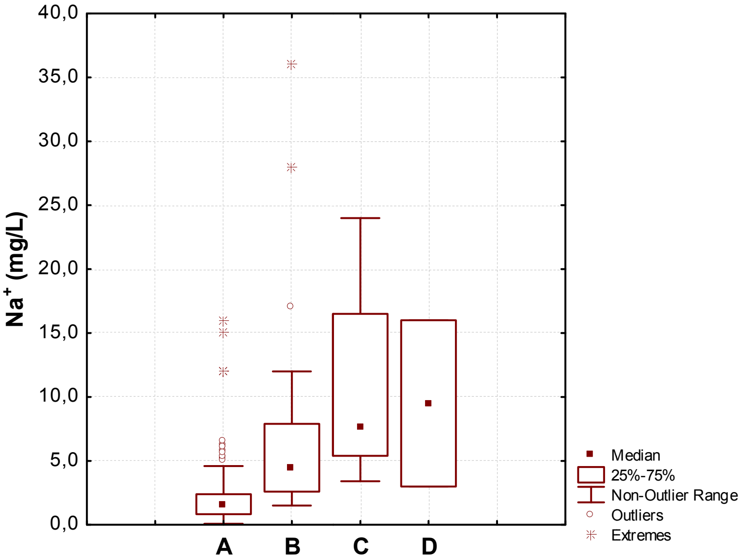

A = forest (n=137)
B = areas of less intense use of nutrients and plant protection products (n=18)
C = areas of intense use of nutrients and plant protection products (n=16)
D = urban areas (n=2)

Figure 221: Box and whisker plots for groundwater Na$^+$ concentration in the recharge area of prevailing land use type (Actual agricultural and forest land usage)

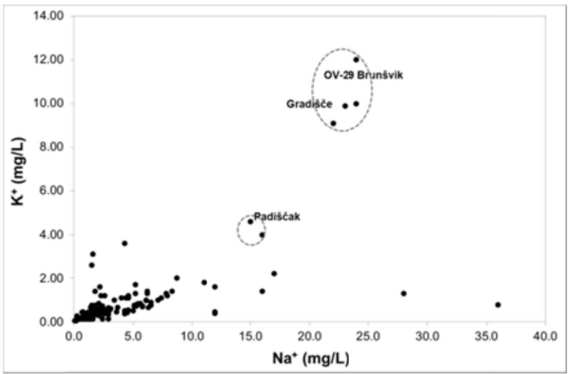

Figure 222: Groundwater Na$^+$ versus K$^+$ concentration

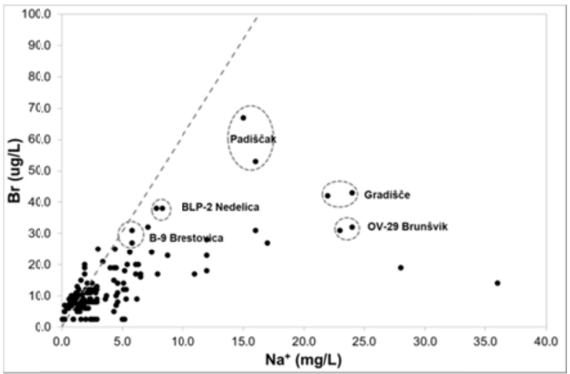

Figure 223: Groundwater Na$^+$ versus Br concentration

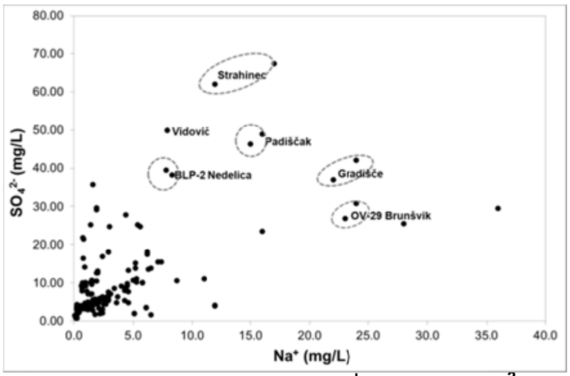

Figure 224: Groundwater Na$^+$ versus SO$_4^{2-}$ concentration

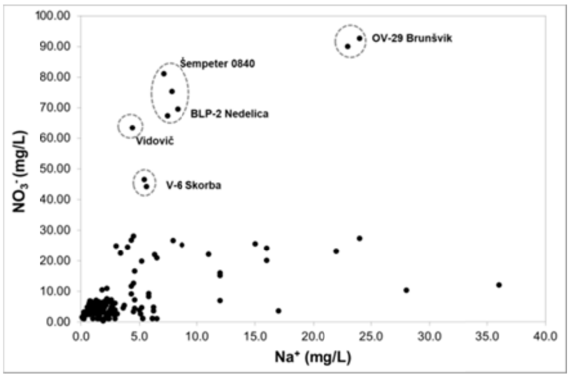

Figure 225: Groundwater Na$^+$ versus NO$_3^-$ concentration

Sampling object type

Groundwater from private wells contains the highest Na^+ concentration (Fig. 226, Appendix 13N), since they are located in the near vicinity of agricultural land use. The lowest groundwater Na^+ is found in water from springs and surface water which mostly originate at high mountain altitudes in carbonate recharge areas and are poor in Na-rich minerals and the human impact is less expressed. Outliers at pumping stations are found in LMV-1 Gradišče (salt from road deicing), in spring captures of Maver (cation exchange), Padiščak (vicinity of the seaside, use of fertilizers), and at spings Pšata, Krka, and Jurčičev izvir (anthropogenic influence).

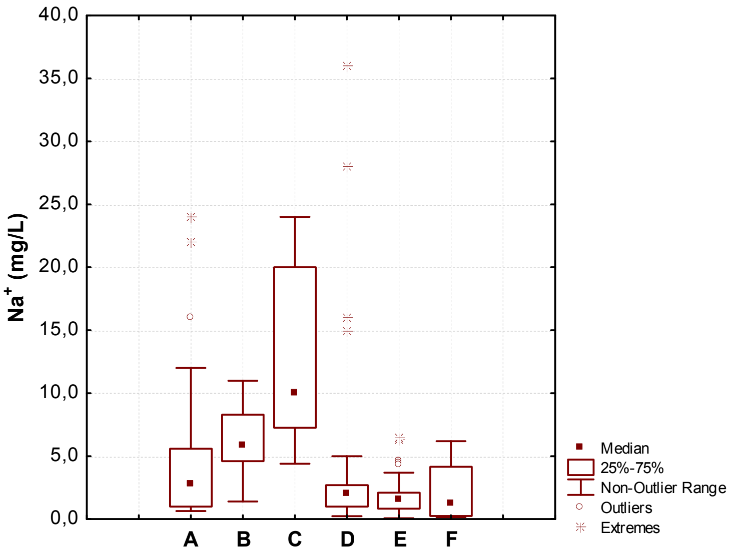

A = pumping station (n=35)
B = borehole (n=10)
C = private well (n=8)
D = spring capture (n=44)
E = spring (n=58)
F = surface water (n=20)

Figure 226: Box and whisker plots for groundwater Na^+ concentration according to sampling object type

Natural background level for Na^+

The natural background level for Na^+ in Slovenian groundwaters is 1.5 mg/L (n=91) (Fig. 227). There is no specified background concentration for Na^+ in groundwater according to available literature.

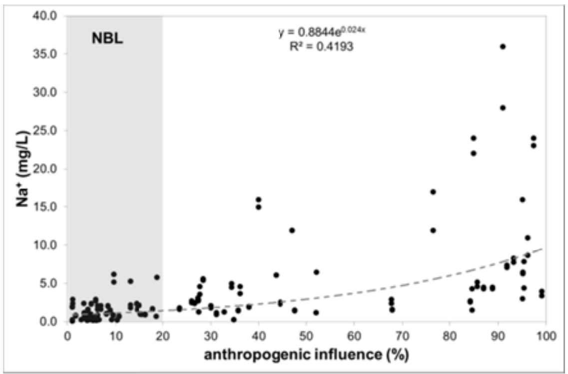

Figure 227: Groundwater Na^+ concentrations versus the share of anthropogenic influence

Spatial distribution of groundwater Na^+

The highest Na^+ concentration is measured at sampling location Maver (>30 mg/L) with clay in the recharge areas (Fig. 230). The excess of groundwater Na^+ concentration can be explained by the cation exchange with Ca^{2+}. Increased groundwater Na^+ concentrations (10-30 mg/L) are also observed in the NE part of the study area, where intense agricultural activities are present and in the recharge areas the silicate alluvial deposits prevail over carbonates. In the coastal part increased Na^+ concentrations suggest possible influence from the anthropogenic sources (fertilizers) or natural sources like the sea spray or maritime aerosols. Slightly increased Na^+ concentration are also observed in Krško-Brežice alluvial plain (E part) where gravel, sand, and clay of carbonate and silicate minerals mix, and aquifer is influenced by the surface water of Sava River (EARS, 2010). Lower groundwater Na^+ concentrations are observed in the NW and N part as well as in the karstic region of Dolenjska (SE). In these regions mostly carbonate rocks prevail in the recharge areas and the anthropogenic influences (agricultural and urban) are less pronounced than in the NE part of country.

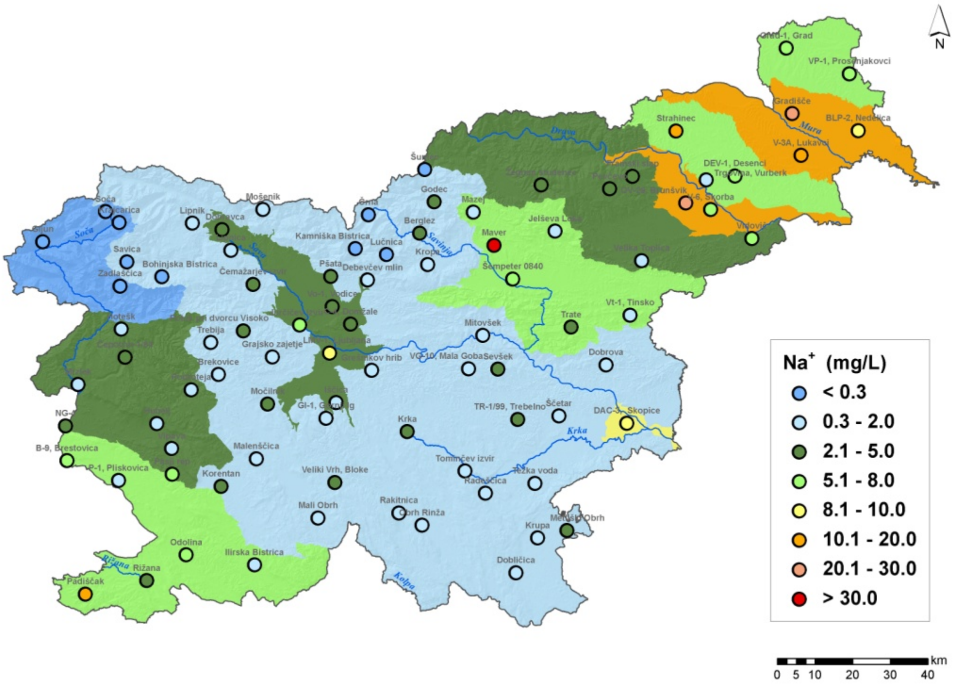

Figure 228: Spatial distribution of groundwater Na^+

4.7.2. Chloride (Cl^-) in groundwater

Descriptive statistics of groundwater Cl^-

Groundwater Cl^- concentrations range from 0.11 to 36.70 mg/L, with a mean value of 4.99 mg/L and median 2.34 mg/L (Tab. 35). Groundwater Cl^- is not normally distributed (Fig. 229) and concentrations higher than 12.00 mg/L present the outliers and extremes (sampling locations BLP-2 Nedelica, DAC-3 Skopice, Gradišče, Jurčičev izvir, LMV-1 Ljubljana, OV-29 Brunšvik, Padiščak, Šempeter 0840, V-6 Skorba, Vidovič, and Vo-1 Vodice) (Fig. 230). Those sampling locations are located in the NE, central and coastal part of study area. The analytical uncertainty for Cl^- is between 4.1 and 30.1 % (n=147). Groundwater Cl^- concentrations below LOD (1st ½ LOD=0.115 mg/L; 2nd ½ LOD=0.375 mg/L) were measured in 28 groundwater samples from sampling locations Gljun, Krajcarica, Kamniška Bistrica, Savica, Žegnani studenec, Kamniška Bitstrica, Lipnica, Savica, Šumec, Bohinjska Bistrica, Črna, Lučnica, Soča, Zadlaščica, Framski slap, Pevčevo, and Godec. None of water samples exceeds the allowed maximum level for drinking water (250 mg/L) according Rules on drinking water (2004).

Table 35: Descriptive statistics of groundwater Cl$^-$ concentration

Parameter	n	X	Md	Min	Max	S
Cl$^-$ (mg/L)	175	4.99	2.34	0.11	36.70	7.09

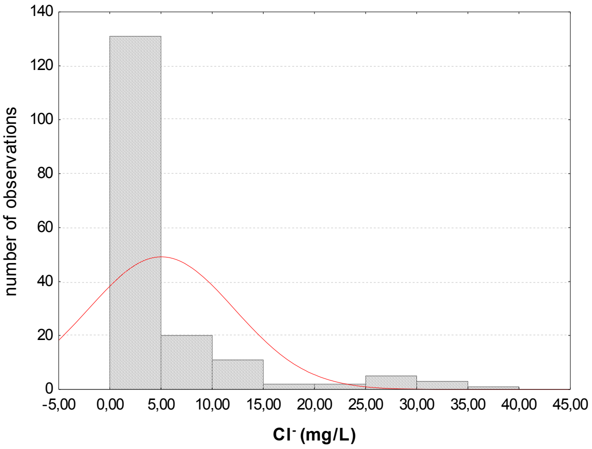

Figure 229: Histogram for groundwater Cl$^-$ concentration (n=175)

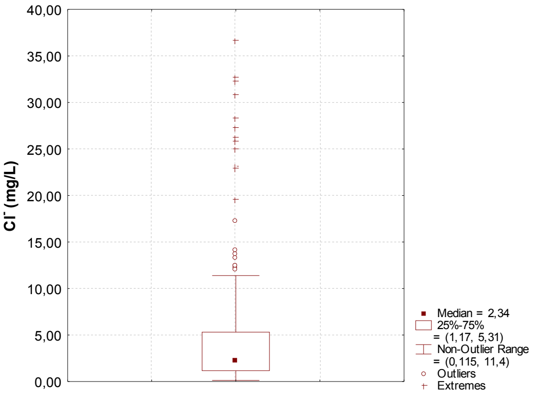

Figure 230: Box and whisker plot for groundwater Cl$^-$ concentration (n=175)

Rock type

Groundwater Cl$^-$ concentration in the recharge areas with clastic sedimentary rocks has the largest variance and the highest concentration (Fig. 231, Appendix 13O) and is significantly higher ($p<0.05$) compared to groundwater with carbonate, igneous, and metamorphic rocks. The outliers are observed in water samples from sampling locations Gradišče, OV-29 Brunšvik (NE part), and LMV-1 Ljubljana (central part). Although in NE part of Slovenia the concentration of carbonate minerals is lower, and silicate minerals dominate, their contribution to groundwater Cl$^-$ concentration has smaller impact. This has been verified with previous parameters – concentration of Si and Na$^+$. In the recharge areas with carbonate rock groundwater Cl$^-$ concentration is medium (outliers and extreme values at sampling locations B-9 Brestovica, Pšata, Čepovan-1/94, Krka, and Veliki Vrh). The lowest groundwater Cl$^-$ concentration is observed in the recharge areas with igneous and metamorphic rocks with outliers found at sampling location Čemažarjev izvir.

Groundwater Cl$^-$ concentration was in 8 water samples below LOD and only in 4 water samples above LOD. This suggests that silicate rocks weathering does not influence the groundwater Cl$^-$ concentration.

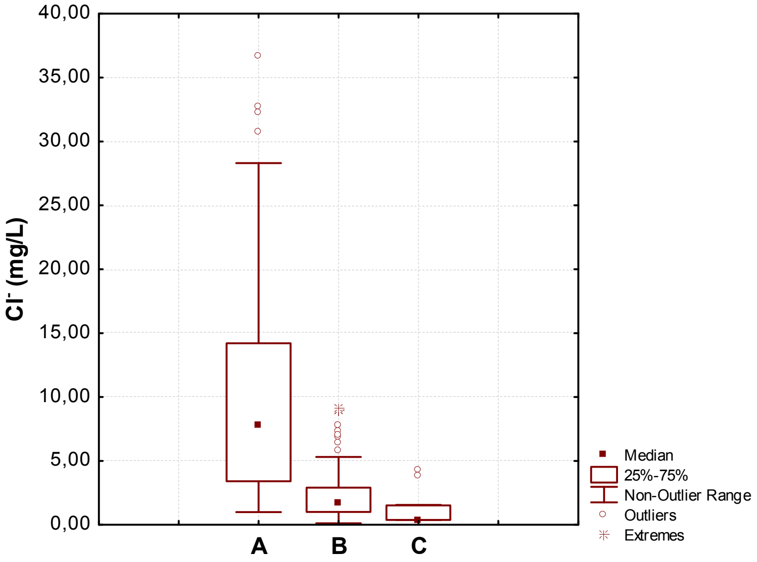

A = clastic sedimentary rocks (n=53)
B = carbonate rocks (n=110)
C = igneous and metamorphic rocks (n=12)

Figure 231: Box and whisker plots for groundwater Cl$^-$ concentration in the recharge area of major rock types

The widest range and the highest groundwater Cl$^-$ concentrations are observed in the recharge areas with Quaternary clastics (Figs. 232 and 233, Appendix 11O), which is significantly higher ($p<0.05$) compared to recharge areas with Permian Ladinian igneous rocks, Miocene Lithothamnium limestone, Cretaceous carbonates, Oligocene igneous rocks, Carboniferous-Permian beds, Pliocene clastics, Oligocene clay “sivica”, old Paleozoic rocks, and Triassic carbonates. Clastics (gravel and sand) in lowlands are usually suitable for agricultural land use, so the anthropogenic influence on groundwater is considered. Also, a wide range of Cl$^-$ concentrations is observed in groundwater with Eocene flysch rocks in the recharge areas. Groundwater Cl$^-$ concentration in the recharge areas with Brkini flysch rocks is lower compared to Istrian flysch, which suggest that groundwater is influenced by the sea water or by anthropogenic sources. Median groundwater Cl$^-$ values are observed in the recharge area of Miocene clastics (extreme values at sampling location Strahinec), and clay. Groundwater Cl$^-$ concentration in the recharge areas with Miocene clastics is significantly higher ($p<0.05$) compared to Miocene Lithothamnium limestone, Oligocene igneous rocks, Carboniferous-Permian beds, old Paleozoic rocks, and Triassic carbonates. In the recharge area of prevailing limestone the outliers are observed at sampling locations B-9 Brestovica, Pšata, and Krka, and extreme values in B-9 Brestovica and Pšata. In the recharge area of dolomite prevailing outliers are found at sampling locations Čepovan-1/94 and Veliki Vrh Bloke. The lowest groundwater Cl$^-$ concentrations are observed in igneous and metamorphic rocks.

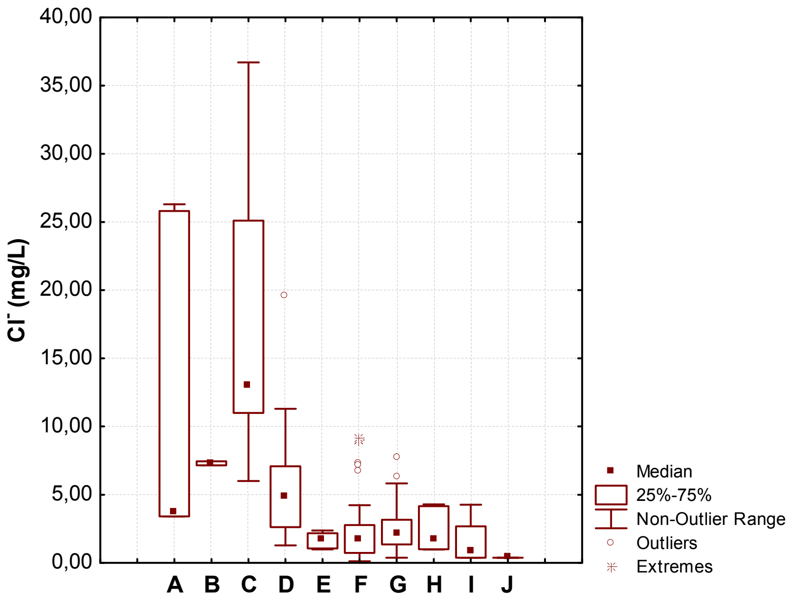

A = flysch rocks (n=7)
B = clay (n=2)
C = gravel and sand (n=26)
D = gravel, sand and clay (n=11)
E = shale and sandstone (n=7)
F = limestone prevailing (n=74)
G = dolomite prevailing (n=30)
H = carbonates with clastics (n=6)
I = igneous rocks (n=8)
J = metamorphic rocks (n=4)

Figure 232: Box and whisker plots for groundwater Cl^- concentration in the recharge area of prevailing lithological unit

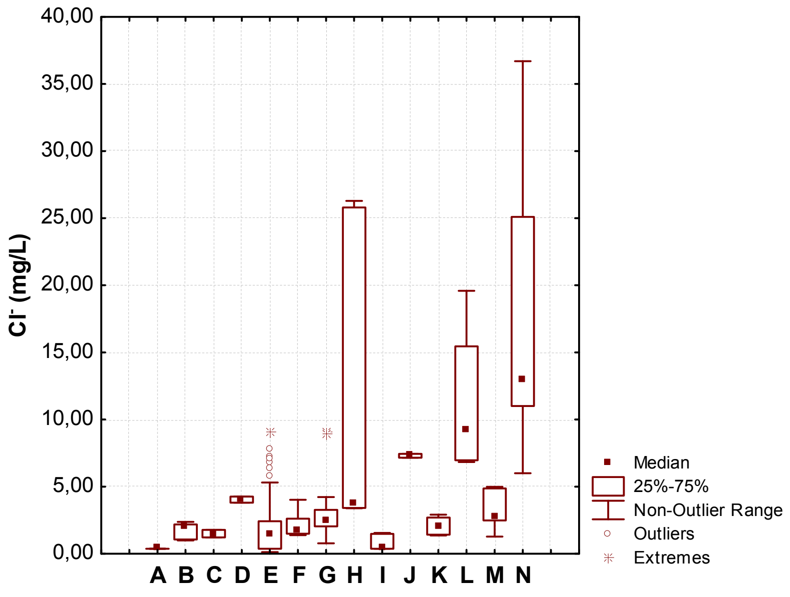

A = old Paleozoic rocks (n=4)
B = Carboniferous-Permian beds (n=5)
C = Val Gardena layers (n=2)
D = Permian Ladinian igneous rocks (n=2)
E = Triassic carbonates (n=70)
F = Jurassic carbonates (n=8)
G = Cretaceous carbonates (n=28)
H = Eocene flysch rocks (n=7)
I = Oligocene igneous rocks (n=6)
J = Oligocene clay “sivica” (n=2)
K = Miocene Lithothamnium limestone (n=4)
L = Miocene clastics (n=4)
M = Pliocene clastics (n=7)
N = Quaternary clastics (medium- and coarse-grained) (n=26)

Figure 233: Box and whisker plots for groundwater Cl^- concentration in the recharge area of prevailing lithostratigraphic unit

There is a link between groundwater Cl^- concentrations and the distance from coast (Fig. 234). Groundwater Cl^- concentration in rain water is usually less than 10 mg/L, and can increase in coastal areas due to influence of ocean spray (Davis *et al.* 1998; Karanth, 1987). In order to evaluate the possible influence from the sea on groundwater only 5 sampling locations were considered (B-9 Brestovica, P-1 Pliskovica, NG-4, Padiščak, and Rižana) which are possibly hydrologically connected to the sea, or are close to the sea (sea spray). As already mentioned, strong correlation between groundwater Cl^- and Na^+ as well as beween Cl^- and Br (r_s=0.73, $p<0.05$) is observed (Fig. 235). Bromide is found in various minerals (halides, oxides, and hydroxides), and seawater (Flury and Papritz, 1993), and since it forms highly soluble salts in sea water, it is also a good indicator for identifying the influence from the sea water in coastal areas (De Vos *et al.*, 2006; Hounslow, 1995). The anthropogenic sources are observed from mining, in scavengers in leaded fuel, and from use of fertilizers and pesticides in agriculture (Flury and Papritz, 1993). Figure 235 shows correlation between Cl$^-$ and Br concentration for only 8 water samples (B-9 Brestovica, P-1 Pliskovica, and Rižana) which are plotted close to SCDL. From the graph it is observed that groundwater from sampling location Padiščak has an additional source of Cl$^-$. Because Br concentrations in groundwater are very low, this could be due to analytical problem, because it is difficult to measure usually low Br concentration in natural water.

Groundwater from sampling location B-9 Brestovica could be due to its proximity to pumping station Klariči and the seaside in hydraulic contact with the sea. Since intense pumping could lead to salt water intrusion (Prestor *et al.*, 2006), it is being monitored for increased groundwater Cl$^-$ and Na$^+$ concentrations. It is possible, that this is due to aquifer's hydraulic contact with the sea, but not with intrusion of sea water in to the aquifer. Groundwater Cl$^-$ and Na$^+$ fluctuations are local due to pumping in Klariči pumping station (EARS, 2011c). Regarding the Cl$^-$ in groundwater Doctor *et al.* (2006) and Gemiti (2011) linked the source to anthropogenic components leaching into the local shallow vadose-zone circulation. Another explanation could also be the influence of the Adriatic seawater, either direct past or present influence of seawater on the karst aquifer (Gemiti, 2011), or indirectly due to sea spray transferred by stronger winds (Urbanc *et al.*, 2012).

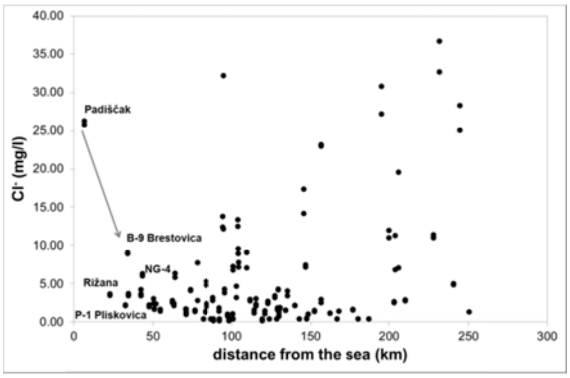

Figure 234: Groundwater Cl$^-$ concentration versus the distance from the sea

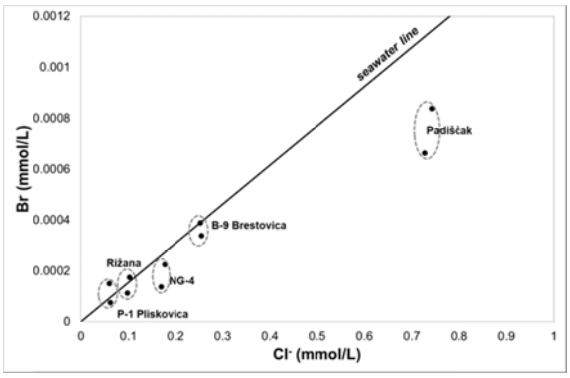

Figure 235: Groundwater Cl$^-$ versus Br concentration

Figure 236 presents 10 groundwater samples from 5 sampling locations which are the closest to the sea side. Water samples are plotted close to SCDL (solid black line) suggesting possible influence from the sea (P-1 Pliskovica, Rižana, B-9 Brestovica, Padiščak, and NG-4).

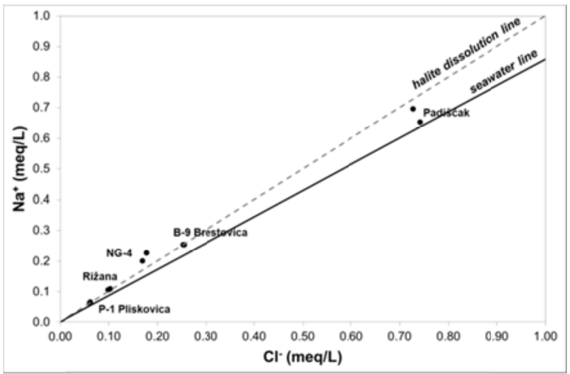

Figure 236: Groundwater Cl$^-$ versus Na$^+$ concentration

Aquifer porosity type

Groundwater Cl$^-$ concentration in aquifers with intergranular porosity has the widest range (Fig. 237, Appendix 13O), and is significantly higher ($p<0.05$) compared to other groups. In all other aquifer porosity types, mean concentrations of groundwater Cl$^-$ are similar. In aquifers with fractured porosity groundwater from Padiščak presents an extreme value, and in aquifers with fractured and karstic porosity the sampling locations Čepovan-1/94 and Veliki Vrh Bloke are outliers. In aquifer with karstic and fractured porosity the sampling location Pšata is an outlier, and B-9 Brestovica an extreme value.

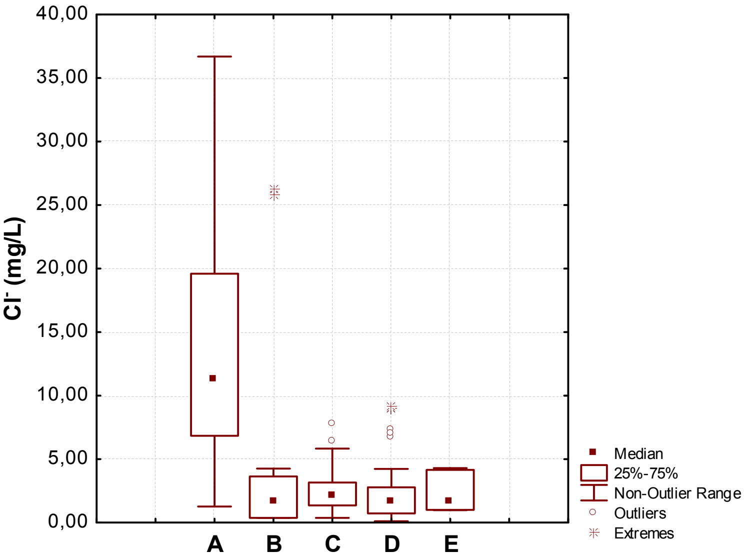

A = intergranular porosity (n=39)
B = fractured porosity (n=26)
C = fractured and karstic porosity (n=30)
D = karstic and fractured porosity (n=74)
E = mixed porosity (karstic, fractured, intergranular) (n=6)

Figure 237: Box and whisker plots for groundwater Cl$^-$ concentration in the recharge area of prevailing aquifer porosity type

Land cover/use

The largest variance and groundwater Cl$^-$ concentrations are observed in the recharge areas with non-irrigated arable land, and industrial or commercial units (Figs. 238 and 239, Appendix 13N), and are significantly higher ($p<0.05$) compared to all land use types according to CORINE Land Cover except in the recharge areas with land principally occupied by agriculture, with significant areas of natural vegetation. This is possible due to intensive use of fertilizers, application of manure and slurry, leakage from sewage systems or septic tanks, and salt from deicing roads during winter time (seasonal fluctuations). Median groundwater Cl$^-$ concentrations are observed in the recharge areas with complex cultivation patterns and land principally occupied by agriculture, with significant areas of natural vegetation. Low groundwater Cl$^-$ concentrations are found in the recharge areas of all other land use units. In the recharge area of coniferous forest outliers are observed at sampling location V-6 Skorba. In the recharge area of deciduous forest extreme values are observed at sampling location V-3A Lukavci and outliers in B-9 Brestovica. In the recharge area of mixed forest extreme values are observed at sampling location Padiščak and outliers in Krka and Pšata.

According to Actual agricultural and forest land usage classification groundwater Cl$^-$ concentrations in the recharge areas with areas of intense use of nutrients and plant protection products and urban areas is significantly higher ($p<0.05$) compared to recharge areas with forest areas of less intense use of nutrients and plant protection products.

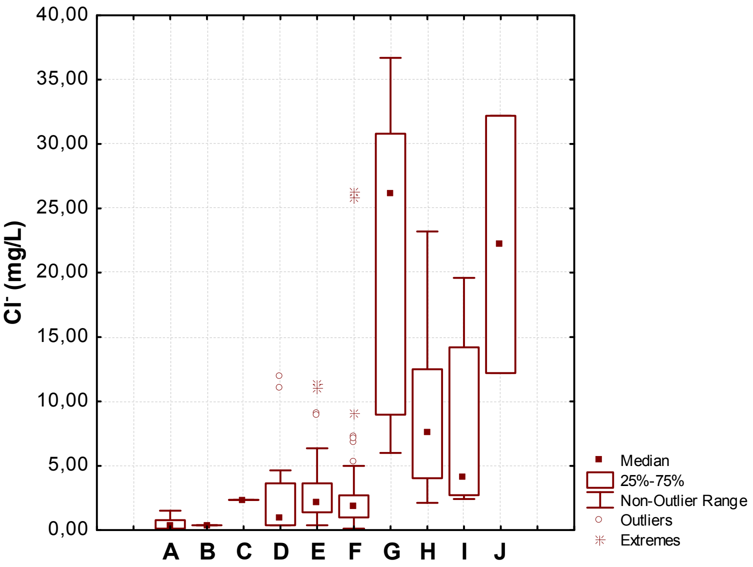

A = bare rocks (n=8)
B = moors and heathland (n=2)
C= natural grasslands (n=2)
D = coniferous forest (n=20)
E = broad-leaved forest (n=45)
F = mixed forest (n=56)
G = non-irrigated arable land (n=10)
H = complex cultivation patterns (n=18)
I = land principally occupied by agriculture, with significant areas of natural vegetation (n=10)
J = industrial or commercial units (n=2)

Figure 238: Box and whisker plots for groundwater Cl^- concentration the recharge area of prevailing land use type (CORINE Land Cover)

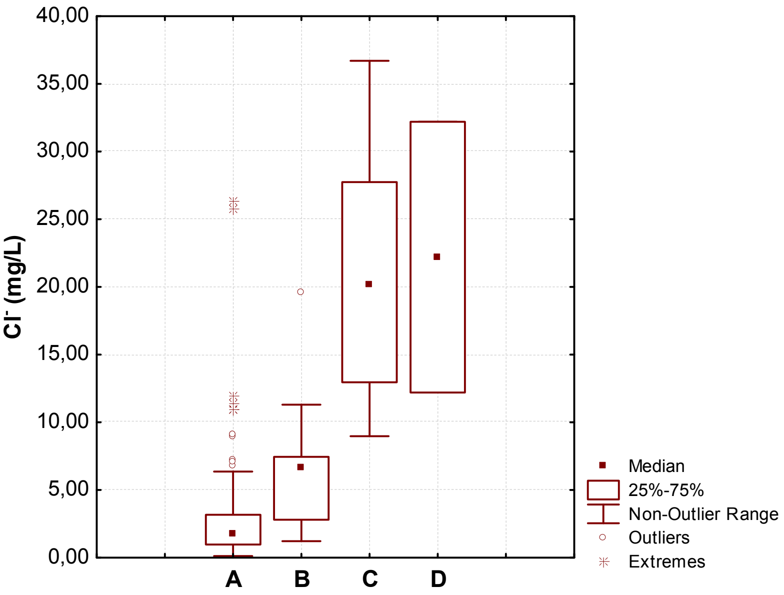

A = forest (n= 137)
B = areas of less intense use of nutrients and plant protection products (n=18)
C = areas of intense use of nutrients and plant protection products (n=16)
D = urban areas (n=2)

Figure 239: Box and whisker plots for groundwater Cl^- concentration in the recharge area of prevailing land use type (Actual agricultural and forest land usage)

Comparison between groundwater Cl^- concentration with EC, NO_3^-, K^+, and SO_4^{2-} values provides the information on agricultural and urban influences on groundwater. There is a moderate correlation between groundwater Cl^- and EC (r_s=0.69, $p<0.05$) (Fig. 240) suggesting that harder Slovenian groundwater in lowlands usually contains increased Cl^- concentrations due to anthropogenic activities (sampling locations OV-29 Brunšvik, LMV-1 Ljubljana, Gradišče, BLP-1 Nedelica, Padiščak, and DAC-3 Skopice). Strong correlation exists between Cl^- and NO_3^- (r_s=0.76, $p<0.05$) (Fig. 241) and K^+ and Cl^- (r_s=0.71, $p<0.05$) (Fig. 242) which suggests that groundwater is influenced by the (excessive) use of fertilizers or other waste water (OV-29 Brunšvik, BLP-2 Nedelica, and Šempeter 0840). Increased groundwater Cl^- and SO_4^{2-} (r_s=0.58, $p<0.05$) are observed at sampling locations Padiščak, BLP-2 Nedelica, Gradišče, OV-29

Brunšvik, and LMV-1 Ljubljana (Fig. 243) suggesting anthropogenic influence on groundwater from ferzilizers.

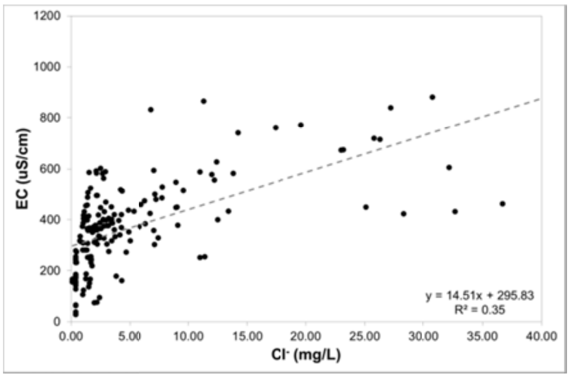

Figure 240: Groundwater Cl^- concentration versus EC

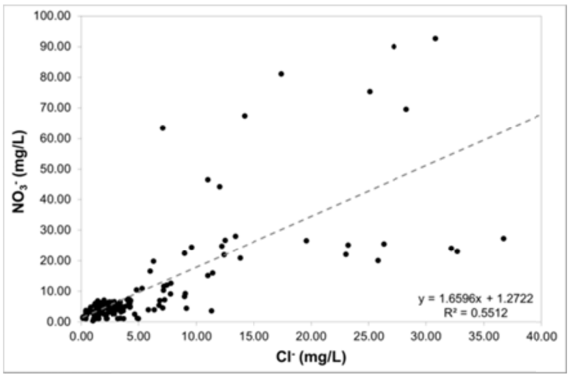

Figure 241: Groundwater Cl^- versus NO_3^- concentrations

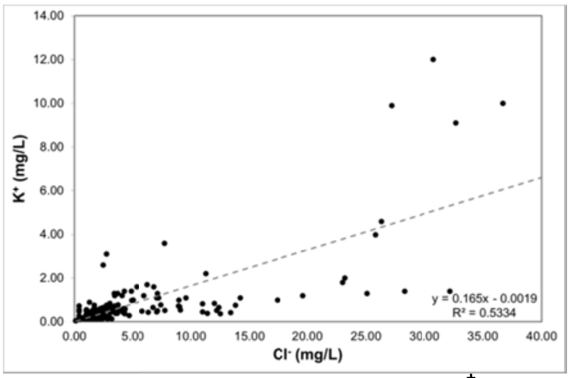

Figure 242: Groundwater Cl^- versus K^+ concentrations

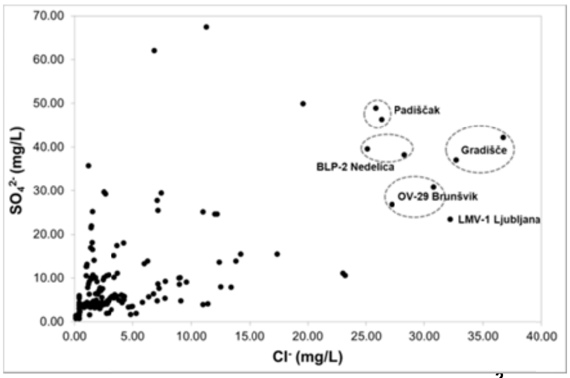

Figure 243: Groundwater Cl^- versus SO_4^{2-} concentrations

Practically the whole country with the exception of the coastal part (coast and Vipava valley) is during winter time covered with snow (EARS, 2006). Salinization occurs mostly in the vicinity of highways and main roads (Richtef and Kreitler, 1992) where tons of salt are applied on the roads in order to prevent icing (Strnad, 2009). Materials used for deicing roads are mostly NaCl and $CaCl_2$ or $MgCl_2$ (Urankar, 2007).

In order to observe the influence of surface deicing in groundwater only main public roads that are connecting cities and are most certainly de-iced during winter time were considered (road companies DARS and DRSC). Contamination from road salt vary seasonally or yearly, since groundwater Cl^- concentrations are higher in the spring time and are decreasing through the year, as well as due to chloride accumulation in soil and groundwater (Richtef and Kreitler, 1992). According to DRSC road types (Roads Act, 2010) few types of roads were excluded (forest, public, local, city, tourist, and cycling roads) due to great possibility they are not salted during winter time. Density of road network for every recharge area for DARS and DRSC was calculated individually and compared to measured groundwater Cl^- concentration.

The most dense road network is observed in the recharge area of LMV-1 Ljubljana, GI-1 Gornji Ig, Čepovan-1/94, Jurčičev izvir in the central part of the country, and Šempeter 0840 and VP-1 Prosenjakovi, in the NE part (Fig. 244). Potential impacts of dense road networks above the aquifers have been studied by Brenčič and Rikanovič (2002) and Brenčič (2003, 2006).

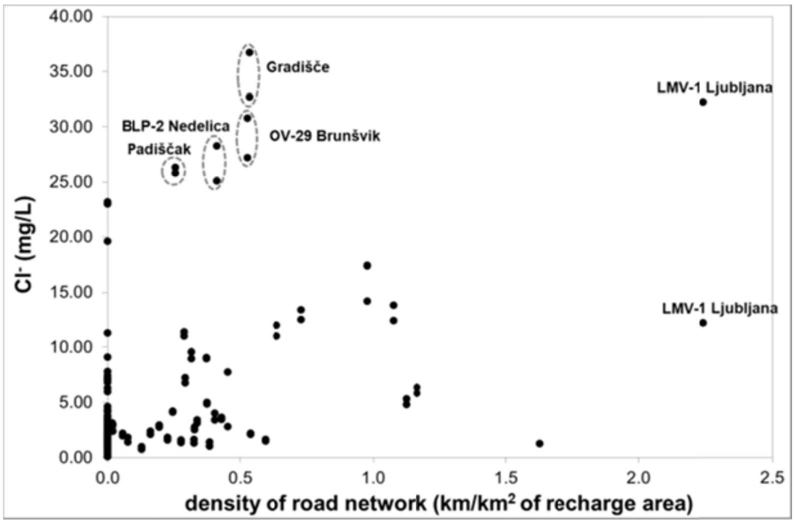

Figure 244: Groundwater Cl⁻ concentration versus density of road network

Based on length of the roads according to DARS and DRSC in each recharge area added salt was calculated where for DARS roads 29.02 t/km was considered, and for DRSC roads 6.87 t/km of salt (Lajevec, 2008). The graph (Fig. 246) shows that groundwater (LMV-1 Ljubljana, capital city) in intergranular aquifer where the road network is the most dense, receives the majority of salt most probably due to road salting (higher concentration in spring, and lower in autumn. The large seasonal variability in groundwater Cl⁻ concentration is probably due to chloride decreasing from spring to autumn. Another source of NaCl in groundwater is also leakage from sewage system. Groundwater Cl⁻ concentrations from sampling locations Šempeter 0840 and V-6 Skorba also suggest the influence from deicing roads, application of manure, and leakega from sewage system.

Sampling object type

The largest variances in groundwater Cl⁻ concentration are measured in boreholes and in private wells (Fig. 245, Appendix 13O) which are located in lowlands in the vicinity of fields (influence from fertilizers, manure, slurry, waste water). Median groundwater Cl⁻ concentrations were measured at pumping stations where in objects LMV-1 Ljubljana and Gradišče outliers are found. Lowest groundwater Cl⁻ concentrations are measured in springs (outliers Dobravca, Krka and Pšata; extreme value Jurčičev izvir), spring captures (Maver and Veliki Vrh Bloke as outliers, extreme values in Padiščak) and surface water due to minor impact from humans.

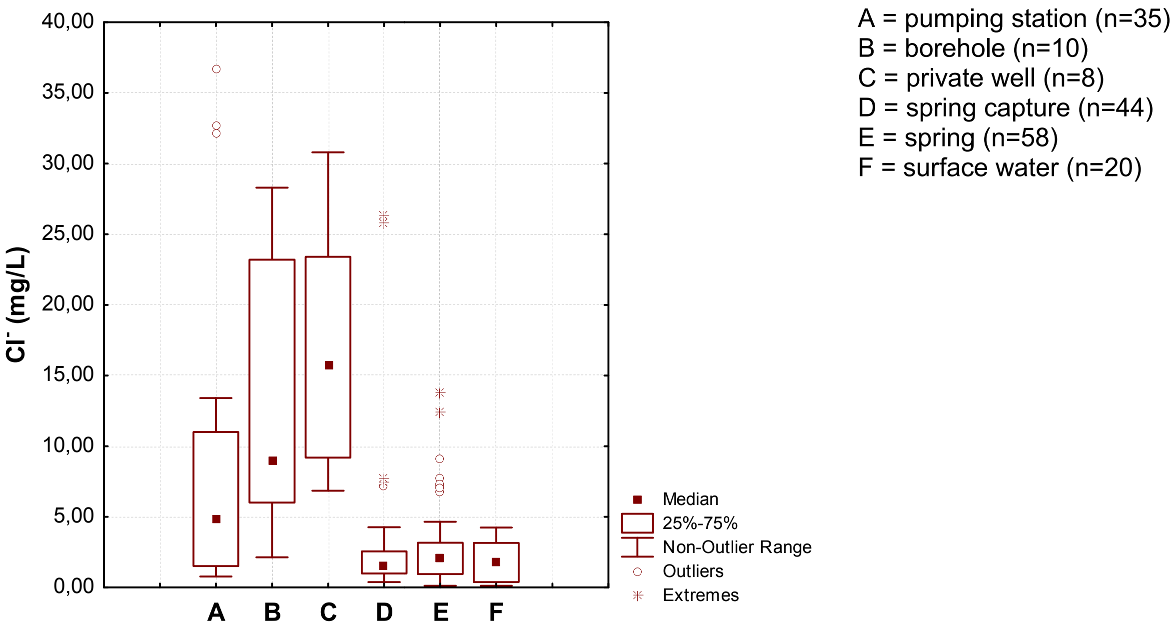

Figure 245: Box and whisker plots for groundwater Cl⁻ concentration according to sampling object type

Natural background level of Cl⁻

The natural background level for Cl⁻ in Slovenian groundwaters is 1.72 mg/L (n=91) (Fig. 246). Natural background levels for groundwater Cl⁻ concentrations were estimated by various authors worldwide. In the shallow unpolluted aquifers up to a few tens of mg/L (Edmunds, 1996; Herczeg and Edmunds 1999), in Germany ranging from 1.0 mg/L in Alpine limestones to 106 mg/L in unconsolidated Rhine Valley deposits (Kunkel *et al.* 2004), in coastal alluvial aquifer in Mersin (Turkey) about 40 mg/L (Demirel, 2004), in Chalk aquifer in Dorset (UK) of 21 mg/L Edmunds *et al.* (2002), and in groundwater older than 50 years in sand aquifers in the Netherlands about 26 mg/L (Meinardi *et al.*, 2003).

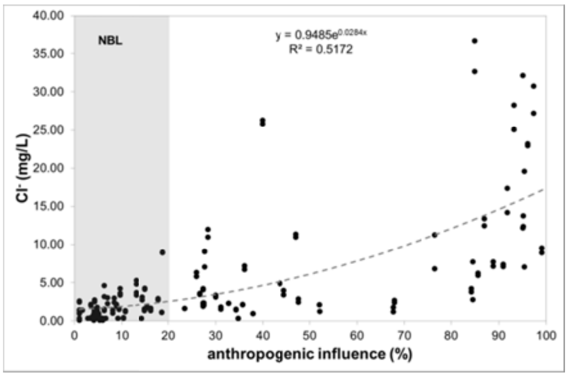

Figure 246: Groundwater Cl⁻ concentrations versus the share of anthropogenic influence

Spatial distribution of groundwater Cl⁻

Increased groundwater Cl⁻ concentrations (>10 mg/L) are observed mostly in the NE part of the country and in 5 alluvial plains (Sava basin aquifer, Savinja basin aquifer, Krško basin aquifer, Drava field aquifer, and Mura basin aquifer) (Fig. 247) which is a consequence of agricultural and urban land uses (intense use of fertilizers, leakage from sewer or septic tanks, slurry and/or manure on the fields, orchards, vineyards, and gardens, or from using salt for deicing roads). Also high groundwater Cl^- concentrations are observed near the coast suggesting the influence from fertilizers or waste water, or also from the sea (precipitations and seaspray). Lowest groundwater Cl^- concentrations (<2.00 mg/L) are observed in the NW, N, and NNE part along the Austrian border (high mountains) where agricultural activities are not so frequent and intense, urbanization is not so dense, and carbonate rocks prevail as well as groundwater dilution by heavy precipitation (increased in NW and N part of the country).

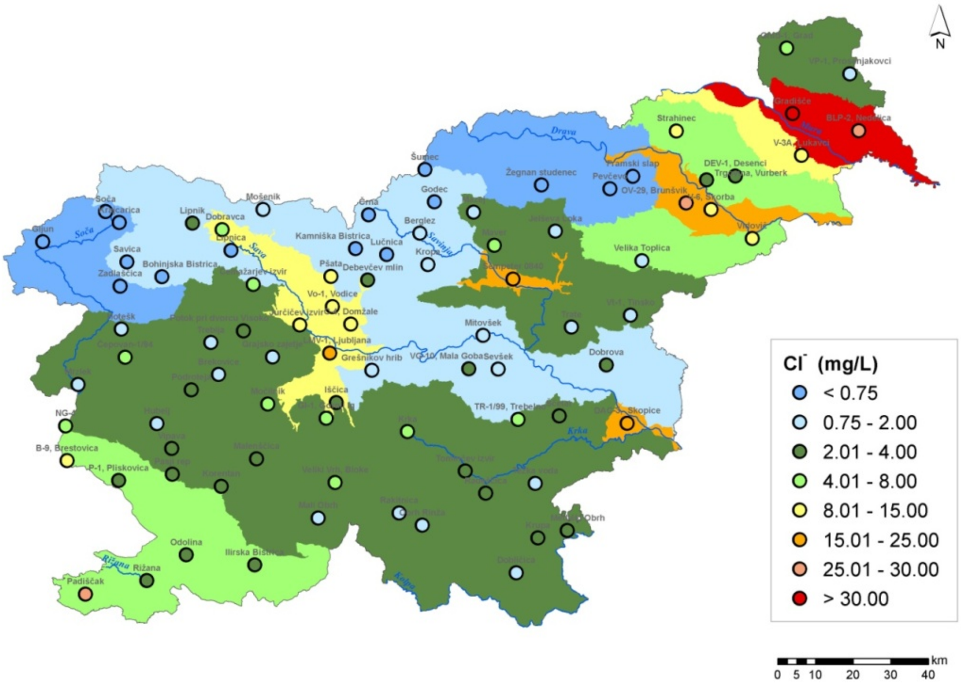

Figure 247: Spatial distribution in groundwater Cl⁻

4.7.3. Nitrate (NO_3^-) in groundwater

Descriptive statistics of groundwater NO_3^-

In Slovenian groundwaters NO_3^- concentration ranges between 0.33 and 92.56 mg/L, with mean value of 9.56 mg/L and median 4.47 mg/L (Tab. 36). Groundwater NO_3^- concentrations are not normally distributed (Fig. 248). Box and whisker plot for groundwater NO_3^- concentration (Fig. 249) shows concentrations higher than 12.57 mg/L present outliers and extremes. Most of these groundwaters were sampled from shallow intergranular aquifers (28) and fissured aquifers (2). The analytical uncertainty for groundwater NO_3^- is between 4.4 and 32.6 % (n=156). In 19 water samples the groundwater NO_3^- concentration is below LOD (½LOD=2.21 mg/L) which is observed in groundwater from sampling locations Dobličica, Gljun, Godec, GRAD-1 Grad, Grešnikov hrib, Kamniška Bistrica, Krajcarica, Lipnik, Odolina, P-1 Pliskovica, Savica, Soča, Trate, and VP-1, Prosenjakovci. Seven groundwater samples exceeded the quality standard for drinking water (>50 mg/L) according Rules on drinking water (2004) and were measured from sampling locations BLP-2 Nedelica, OV-29 Brunšvik, Šempeter 0840, and Vidovič.

One of determined water type is Ca^{2+}-Mg^{2+}-HCO_3^--NO_3^- where NO_3^- is one of the dominant anions in 2 water samples (sampling location BLP-2 Nedelca) sampled in intergranular aquifer with values ~70 mg/L of NO_3.

Table 36: Descriptive statistics of groundwater NO_3^- concentration

Parameter	n	X	Md	Min	Max	S
NO_3^- (mg/L)	175	9.56	4.47	0.33	92.56	15.87

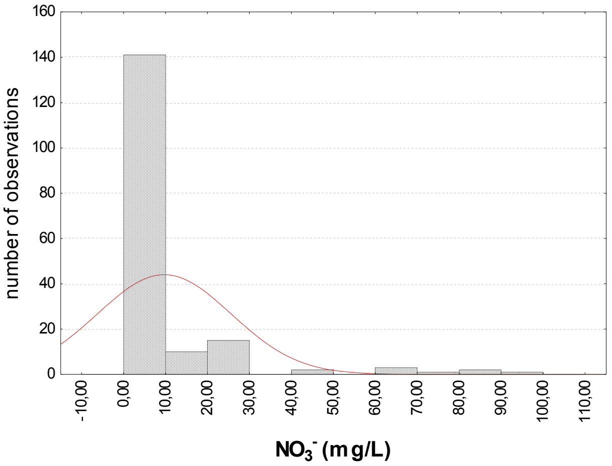

Figure 248: Histogram for groundwater NO_3^- concentration (n=175)

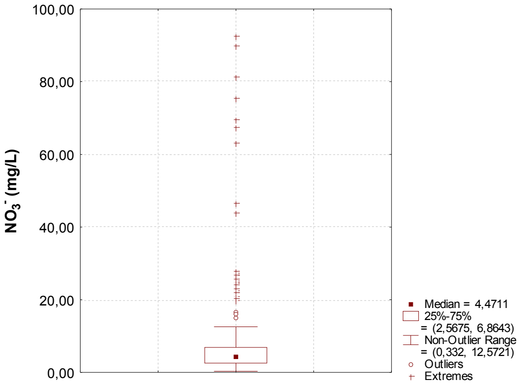

Figure 249: Box and whisker plot for groundwater NO_3^- concentration (n=175)

Rock type

The highest groundwater NO_3^- concentrations are observed in the recharge areas with clastic sedimentary rocks (Fig. 250, Appendix 13P) which are significantly higher ($p<0.05$) compared to groundwater in the recharge areas with carbonate and igneous and metamorphic rocks. Extremly high NO_3^- concentrations in groundwater were observed in the recharge areas with clastic sedimentary rocks from sampling locations Šempeter 0840, OV-29 Brunšvik, V-6 Skorba, BLP-2 Nedelica, and Vidovič (>60.00 mg/L). This is because in those recharge areas intensive agricultural and urban land uses are present. Medium high groundwater NO_3^- concentrations are observed in the recharge areas with carbonate rocks where groundwater from sampling location GI-1 Gornji Ig presents the outliers. It is believed that this sampling location is under the influence of contamination which occurs in approximate vicinity of urban and agricultural area land use. The lowest groundwater NO_3^- concentrations are observed in the recharge areas with igneous and metamorphic rocks due to absence of urban and agricultural land uses.

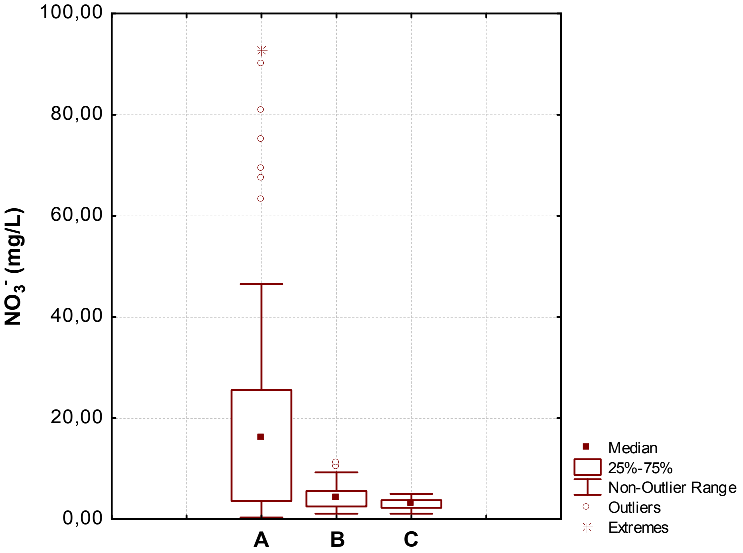

A = clastic sedimentary rocks (n=53)
B = carbonate rocks (n=110)
C = igneous and metamorphic rocks (n=12)

Figure 250: Box and whisker plots for groundwater NO_3^- concentration in the recharge areas of major rock types

The highest groundwater NO_3^- concentrations are observed in the recharge areas with gravel and sand (Fig. 251, Appendix 13P) which are significantly higher ($p<0.05$) compared to groundwater sampled from recharge areas with other lithological units. According to lithostratigraphic classification groundwater NO_3^- concentrations in the recharge areas with Quaternary clastics, Oligocene clay “sivica”, and Miocene clastics (Fig. 252, Appendix 13P) are significantly higher ($p<0.05$) compared to groundwater in the recharge areas with other lithostratigraphic units.

The highest peak (~90,00 mg/L) is measured in groundwater from sampling location OV-29 Brunšvik (NE part) due to intensive (excessive) use of fertilizers for production of vegetables and flowers in the immediate vicinity of sampling (Fig. 253). Concentration of groundwater NO_3^- in this group has a large variance due to various surface activities and land use above the aquifer. Medium high groundwater NO_3^- concentrations are observed in the recharge areas with flysch rocks and clay. In flysch rocks groundwater from sampling location Padiščak (SSW part) is influenced by the local contamination source. The lowest groundwater NO_3^- concentrations are observed in the recharge areas of shale and sandstone, limestone prevailing, dolomite prevailing, carbonates with clastics, and igneous and metamorphic rocks, due to less intensive agricultural and urban land use. In the recharge areas of prevailing limestone or dolomite the outliers at sampling locations B-9 Brestovica and GI-1 Gornji Ig are observed possibly due to point source contamination.

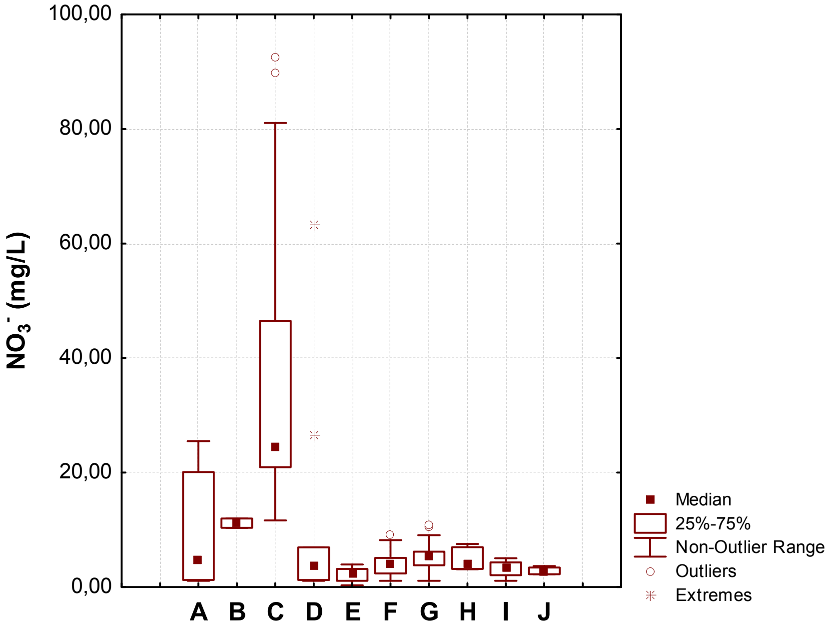

A = flysch rocks (n=7)
B = clay (n=2)
C = gravel and sand (n=26)
D = gravel, sand and clay (n=11)
E = shale and sandstone (n=7)
F = limestone prevailing (n=74)
G = dolomite prevailing (n=30)
H = carbonates with clastics (n=6)
I = igneous rocks (n=8)
J = metamorphic rocks (n=4)

Figure 251: Box and whisker plots for groundwater NO_3^- concentration in the recharge area of the prevailing lithological unit

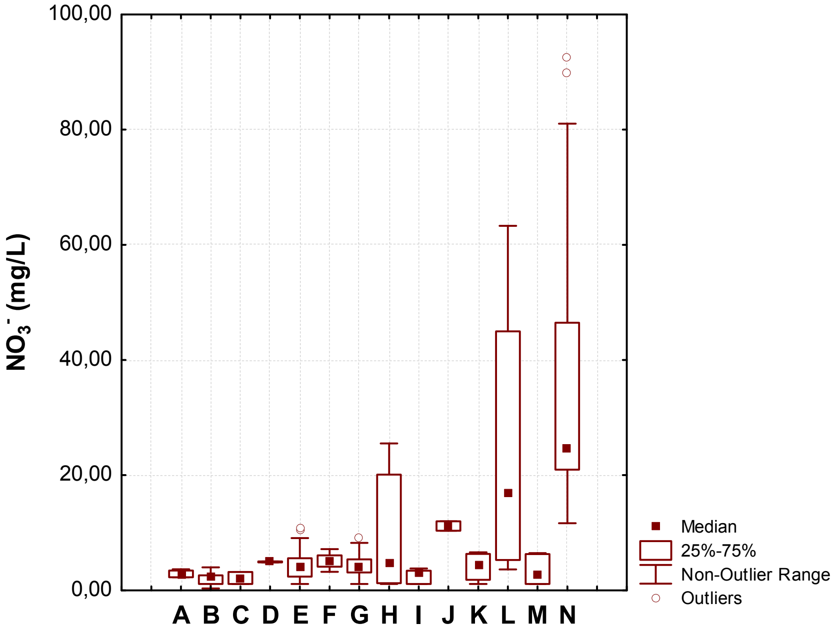

A = old Paleozoic rocks (n=4)
B = Carboniferous-Permian beds (n=5)
C = Permian Val Gardena layers (n=2)
D = Ladinian igneous rocks (n=2)
E = Triassic carbonates (n=70)
F = Jurassic carbonates (n=8)
G = Cretaceous carbonates (n=28)
H = Eocene flysch rocks (n=7)
I = Oligocene igneous rocks (n=6)
J = Oligocene clay “sivica” (n=2)
K = Miocene Lithothamnium limestone (n=4)
L = Miocene clastics (n=4)
M = Pliocene clastics (n=7)
N = Quaternary clastics (medium- and coarse-grained) (n=26)

Figure 252: Box and whisker plots for groundwater NO_3^- concentration in the recharge area of the prevailing lithostratigraphic unit

Figure 253: Plant cultivation at sampling location OV-29 Brunšvik

Aquifer porosity type

The highest groundwater NO_3^- concentrations are observed in the intergranular aquifers (Fig. 254, Appendix 13P) which are significantly higher ($p<0.05$) compared to groundwater in aquifers with other porosity types. Concentrations are high due to intense use of fertilizers and possible waste water leakage.

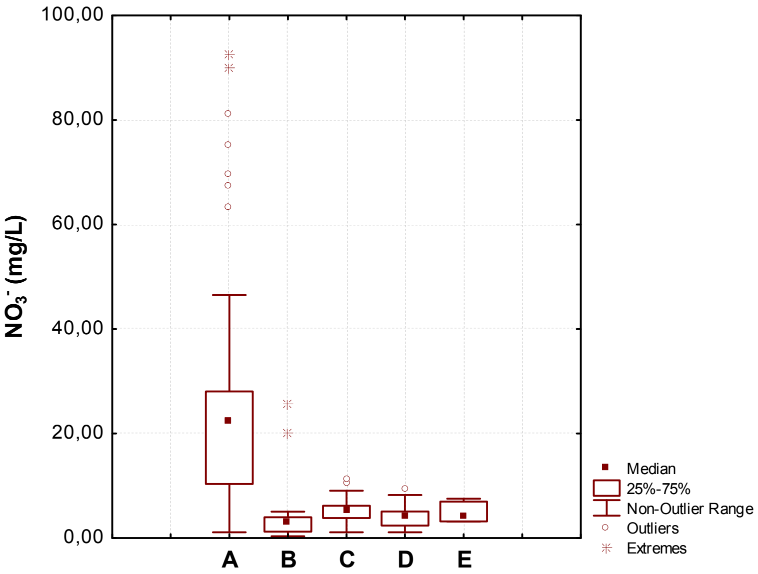

A = intergranular porosity (n=39)
B = fractured porosity (n=26)
C = fractured and karstic porosity (n=30)
D = karstic and fractured porosity (n=74)
E = mixed porosity (karstic, fractured, intergranular) (n=6)

Figure 254: Box and whisker plots for groundwater NO_3^- concentration in the recharge area of the prevailing aquifer porosity type

Land cover/use

The highest groundwater NO_3^- concentrations are observed in the recharge areas of non-irrigated arable land, land principally occupied by agriculture, with significant areas of natural vegetation, and industrial or commercial units, which are significantly higher ($p<0.05$) compared to other CORINE Land Cover classes. According to Actual agricultural and forest land usage classification (Fig. 255, Appendix 13P) the groundwater NO_3^- concentrations with areas of intense use of nutrients and plant protection products, and urban areas are significantly higher ($p<0.05$) compared to recharge areas with forest, and areas of less intense use of nutrients and plant protection products.

The highest measured groundwater NO_3^- concentrations are ~90 mg/L (Fig. 256, Appendix 13P). Those groundwater NO_3^- concentrations are most certainly derived from chemical fertilizers (Figs. 269 and 270) which are associated with the use of Cl^- ($r_s=0.76$, $p<0.05$), K^+ ($r_s=0.58$, $p<0.05$) and Na^+ ($r_s=0.51$, $p<0.05$), and SO_4^{2-} (r_s=0.55, p<0.05) observed at sampling locations OV-29 Brunšvik, BLP-2 Nedelica, Šempeter 0840, and V-6 Skorba (NE part). Medium high groundwater NO_3^- concentrations (< 30 mg/L) are observed in the recharge areas of agricultural surfaces of complex cultivation patterns. Industrial and urbanised areas can be a source of contamination due to possible septic tanks or sewage leaks (old and inefficient sewer system) (sampling location Gradišče), and to industrial waste water. Lower groundwater NO_3^- concentrations (< 6 mg/L) are observed in areas where mostly forest as a vegetation cover prevails, or where the use of fertilizers are not intense. Groundwater from the recharge areas of forest is expected to have lower NO_3^- concentrations, since it reflect mostly decomposing vegetation. Detailed observations of the surroundings of those sampling locations have shown that part of the recharge area of sampling location B-9 Brestovica is deforested (by fire destruction), or are contaminated a point source (sampling location Padiščak). Regarding groundwater in the recharge area with coniferous forest a sampling location with increased NO_3^- concentration was observed (~45 mg/L) at the pumping station IG-1 Gornji Ig.

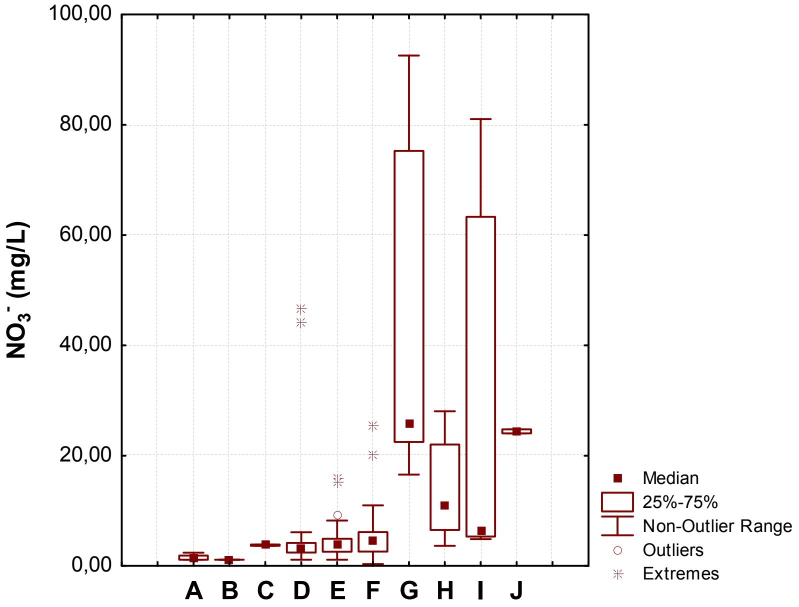

A = bare rocks (n=8)
B = moors and heathland (n=2)
C = natural grasslands (n=2)
D = coniferous forest (n=20)
E = broad-leaved forest (n=45)
F = mixed forest (n=56)
G = non-irrigated arable land (n=10)
H = complex cultivation patterns (n=18)
I = land principally occupied by agriculture, with significant areas of natural vegetation (n=10)
J = industrial or commercial units (n=10)

Figure 255: Box and whisker plots for groundwater NO_3^- concentration in the recharge area of the prevailing land use type (CORINE Land Cover)

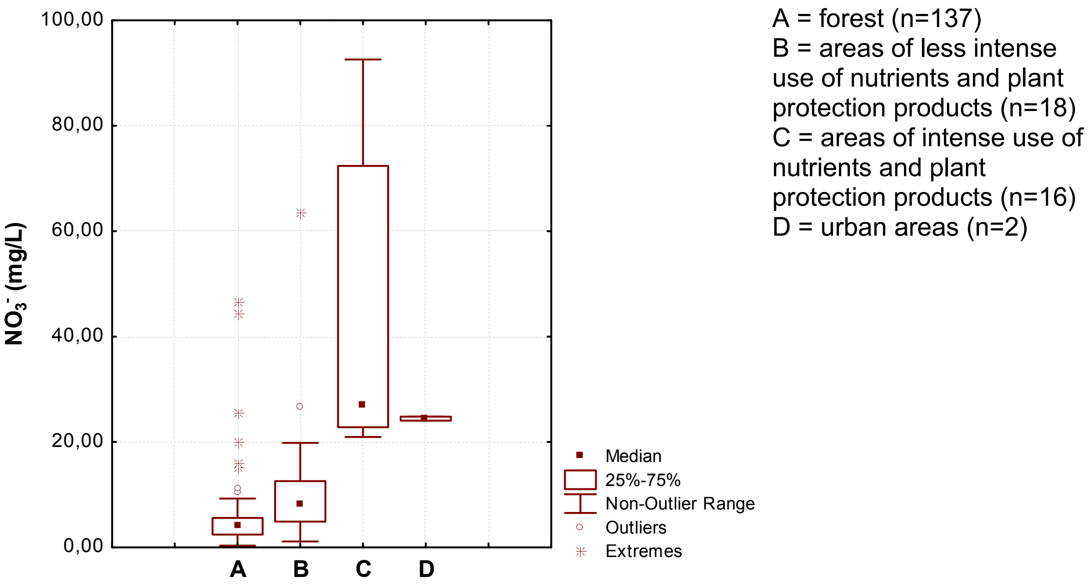

Figure 256: Box and whisker plots for groundwater NO_3^- concentration in the recharge area of the prevailing land use type (Actual agricultural and forest land use)

Grundwater Cl^- concentrations may provide additional evidence of supporting the observation of manure and/or slurry application, or leakage of sewage, in combination with NO_3^-, which is observed at sampling locations OV-29 Brunšvik, BLP-2 Nedelica, and Šempeter 0840.

Figure 257 illustrates the comparison between groundwater EC and NO_3^- which suggests that contaminated groundwater (>50.00 mg/L) is also more mineralised (harder) mostly observed in the NE part of the country, where intensive agricultural and urban land use are present. The source of groundwater contamination at sampling locations Gradišče and OV-29 Brunšvik is possible from a synthetic fertilizer potassium nitrate (KNO_3) (Fig. 258).

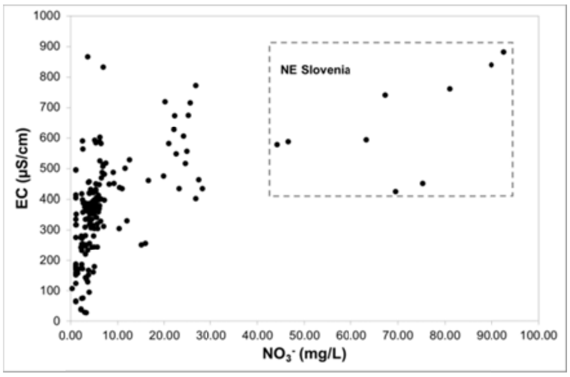

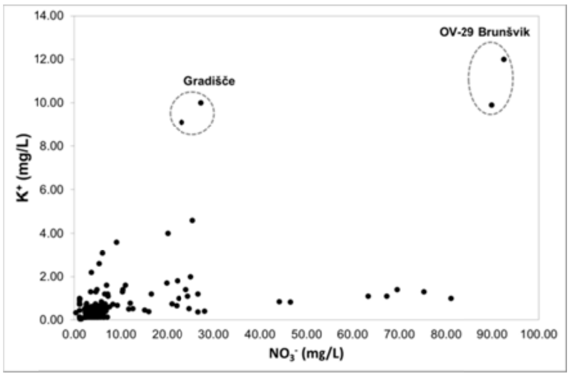

Figure 257: Groundwater EC versus NO_3^- concentration

Figure 258: Groundwater K^+ versus NO_3^- concentration

Sampling object type

The highest groundwater NO_3^- concentrations are observed in groundwaters sampled from private wells (Fig. 259, Appendix 13P). This is because private wells are located near the fields where intense agricultural activities are usually present.

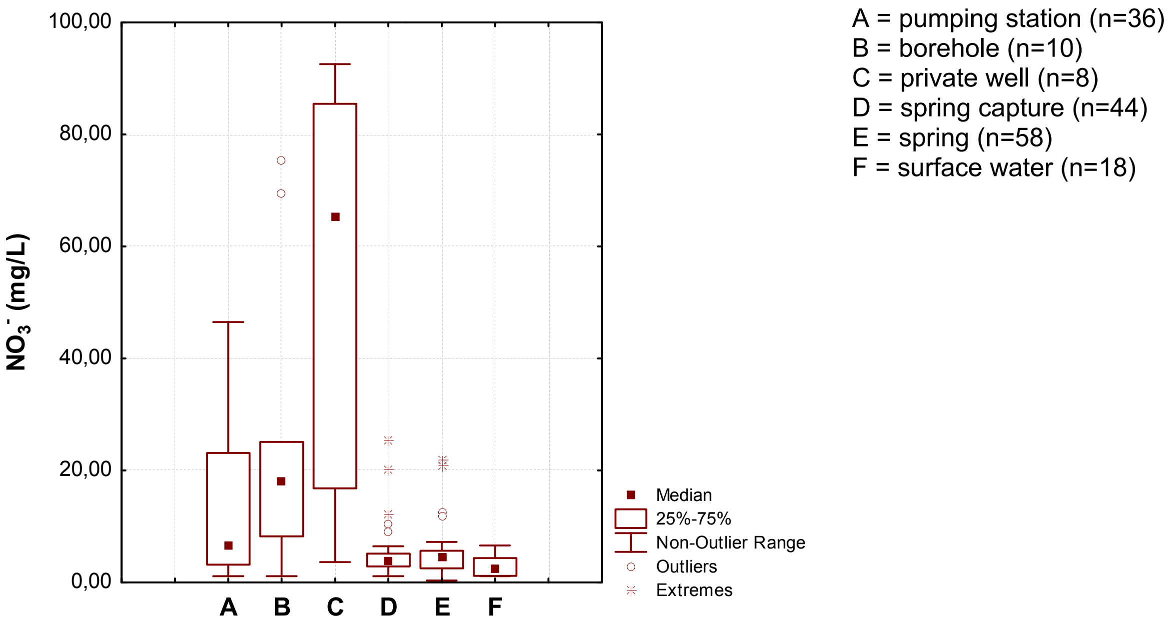

Figure 259: Box and whisker plots for groundwater NO_3^- concentration according to sampling object type

Natural background level for NO_3^-

In order to determine the natural background level for groundwater NO_3^- concentration (Fig. 260) only groundwater from shallow aquifers was considered (Fig. 261) because of recent contamination with NO_3^- which is evident by groundwater ^3H activity (Fig. 274). Circled groundwater NO_3^- concentrations are low and are measured in older groundwaters (NE part). The natural background level for NO_3^- concentration in the Slovenian groundwaters is 3.81 mg/L (n=91). Recent natural background concentrations of NO_3-N in groundwater from Illinois (USA) are estimated to be between 2.1 and 2.5 mg /L (Panno *et al.*, 2006), or less (Mueller and Helsel, 1996) which is ~10 mg/L NO_3^-. Voigt *et al.* (2005) estimated natural groundwater NO_3^- concentration in sands and gravel < 0.01 – 0.1 mg/L.

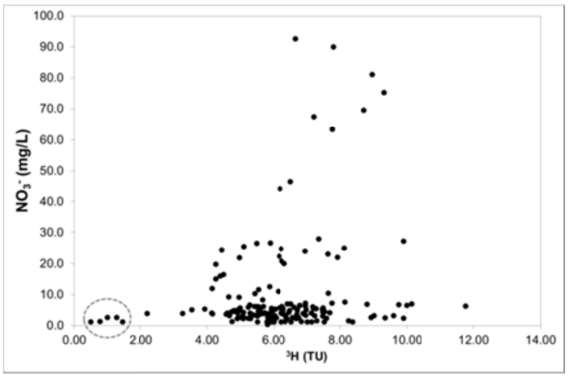

Figure 260: Groundwater NO_3^- concentration versus ^3H activity

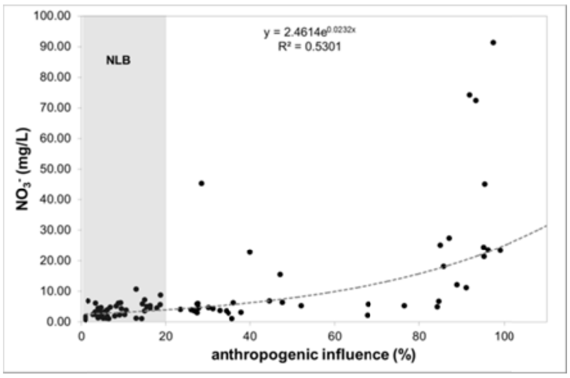

Figure 261: Groundwater NO_3^- concentrations versus the share of anthropogenic influence

Spatial distribution of groundwater NO_3^-

Low groundwater NO_3^- concentrations (< 1.11 mg/L) are mostly observed in the high mountain regions in the N and NW part of the country where agricultural activities and urban land use are not pronounced due to geomorphology of the surface of terrain, lack of soil thickness, and vegetation coverage. In the deeper aquifers (NE part) low groundwater NO_3^- concentrations are present most probably due to denitrification processes (Fig. 262) although the input NO_3^- concentrations with the percolation water were high. Increased groundwater NO_3^- concentrations are observed in the alluvial plains – Sava basin aquifer, Savinja basin aquifer, Krško basin aquifer, Drava field aquifer, and Mura basin aquifer, due to intensive land agricultural and urban land use. The highest groundwater NO_3^- concentration is observed in the Drava field aquifer due to excessive use of fertilizers.

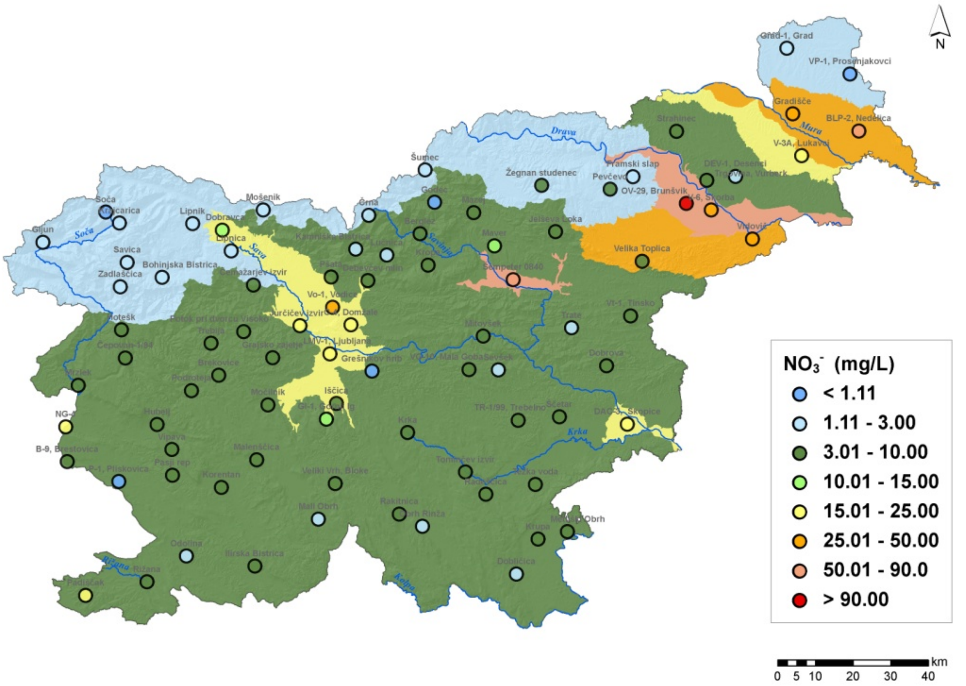

Figure 262: Spatial distribution of groundwater NO_3^-

Main sources of NO_3^- in groundwater are anthropogenic, e.g. (excessive) use of nitrogen fertilizers (organic and synthetic fertilizers), leakages from septic tanks and/or sewage systems, and waste water. Groundwater NO_3^- concentrations depend mostly on the type of land use in the recharge area, especially on the intensity of fertilizers usage. The natural background level for groundwater NO_3^- from shallow aquifers is 3.81 mg/L (n=91). Since agricultural activities are mostly present in lowlands, increased groundwater NO_3^- concentrations (> 50.00 mg/L) are observed in the intergranuar aquifers along larger rivers (central, E, and NE part). Groundwater NO_3^- concentrations in the NW, W, and NNE part are low (<3.00 mg/L) due to low intensity of agricultural and urban land use. Low groundwater NO_3^- concentrations are also observed in older groundwaters (<3.00 mg/L) (NE part) most possibly due to low initial NO_3^- concentration or due to denitrification processes in the groundwater recharge areas.

4.7.4. Ammonium (NH_4^+) in groundwater

Groundwater NH_4^+ concentration above LOD was detected in only one water sample from sampling location Vidovič (0.05 mg/L) located in the NE part of the country and is not exceeding the allowed maximum level for drinking water (0.5 mg/L) according Rules on drinking water (2004). This suggests that the prevailing nitrogen species in most Slovenian groundwaters is NO_3^-.

The reason for occurrence of NH_4^+ in groundwater is perhaps due to excessive use of inorganic or organic fertilizers (ammonium sulphate $(NH4)_2SO_4$, manure, slurry, leakage from septic tanks or sewage system) in the late summer which has been proven by the increased groundwater NO_3^- concentration (63.30 mg/L) in water sample from sampling location Vidovič. Rainwater (or increased irrigation on the surface) has transported NH_4^+ quickly into groundwater before it got transformed into NO_3^- and NO_2^-. This is confirmed by observation of reduced access of oxygen in to water in the presence of organic matter.

Although dissolved oxygen (DO) was not measured in the groundwater, other indicators for reductive environment were observed, e.g. Fe, Mn, As, and NH_4^+. Since their concentrations in groundwater are very low it is assumed that sampled groundwater is mostly oxidized.

4.7.5. Stable isotope composition of total nitrogen ($\delta^{15}N_{tot}$) in groundwater

Descriptive statistics of groundwater $\delta^{15}N_{tot}$

Based on the 133 groundwater samples the $\delta^{15}N_{tot}$ values vary between -2.8 ‰ and 18.6 ‰, with mean value of 4.2 ‰ and median 3.65 ‰ (Tab. 37). Measured groundwater $\delta^{15}N_{tot}$ values are not normally distributed (Fig. 263) and values above 15.10 ‰ present outliers observed at sampling locations Radeščica and DAC-3 Skopice (Fig. 264).

Table 37: Descriptive statistics of groundwater $\delta^{15}N_{tot}$ values

Parameter	n	X	Md	Min	Max	S
$\delta^{15}N_{tot}$ (‰)	133	4.24	3.6	-2.8	18.6	4.1

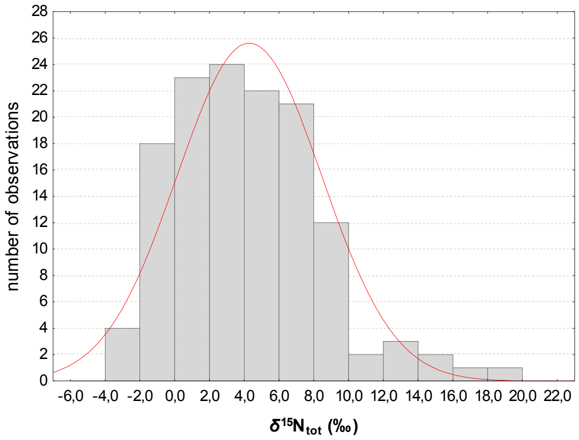

Figure 263: Histogram for groundwater $\delta^{15}N_{tot}$ values

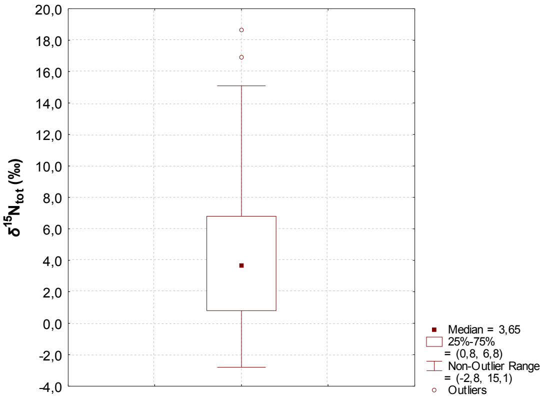

Figure 264: Box and whisker plot for groundwater $\delta^{15}N_{tot}$ values

Land cover/use

The most enriched in ^{15}N is groundwater sampled in the recharge areas of non-irrigated arable land (Fig. 265, Appendix 13Q) which suggests a mixture of organic and/or synthetic fertilizers (intense use of nutrients and plant protection products). By grouping groundwaters into 2 groups according to groundwater NO_3^- concentration — concentrations below the natural background level (>3.81 mg/L) and concentrations above the natural background level (<3.82 mg/L), it is observed that recharge areas from the first group are mostly vegetated by the natural vegetation, whereas in the second group the land is used for agricultural and urban purposes. This provides the information on the origin of groundwater $\delta^{15}N_{tot}$, where in the natural recharge areas groundwater $\delta^{15}N_{tot}$ values vary from -2.8 to 8.8 ‰ (mean 1.6 ‰), and in anthropogenically influenced recharge areas from -0.3 to 18.5 ‰ (mean 5.6 ‰). Groundwater which recharge areas are non-irrigated arable land is significantly enriched ($p<0.05$) in ^{15}N compared to groundwater with recharge areas with bare rocks, moors and heathland, natural grasslands, and coniferous forest. Also groundwater with recharge areas in complex cultivation patterns, and industrial or commercial units, which are significantly enriched in ^{15}N compared to groundwater with bare rocks and moors and heathland in its recharge areas, suggest the presence of both organic and synthetic fertilizers.

According to Actual agricultural and forest land usage classification (Fig. 266, Appendix 13Q) groundwater with forest in the recharge areas is significantly depleted in ^{15}N compared to groundwater in other classes. Groundwater in the recharge areas of forest (Fig. 280, Appendix 11Q) has $\delta^{15}N_{tot}$ values between 2 to 8 ‰ which refers to naturally occurring nitrate in soil horizons. Broad-leaved forests are slightly enriched in ^{15}N compared to coniferous forest because of more complete decomposition of leaves. The most depleted in ^{15}N is groundwater in the recharge areas of bare rocks, moors and heathland, and natural grasslands, where the dominant source of nitrogen is the atmosphere (precipitation) and soil horizon.

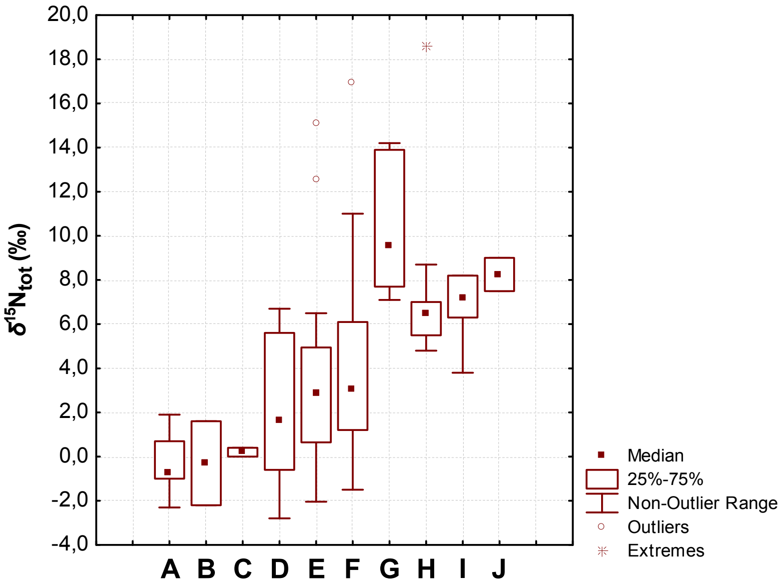

A = bare rocks
B = moors and heathland
C= natural grasslands
D = coniferous forest
E = broad-leaved forest
F = mixed forest
G = non-irrigated arable land
H = complex cultivation patterns
I = land principally occupied by agriculture, with significant areas of natural vegetation
J = industrial or commercial units

Figure 265: Box and whisker plots for groundwater $\delta^{15}N_{tot}$ values in the recharge area of the prevailing land use type (CORINE Land Cover)

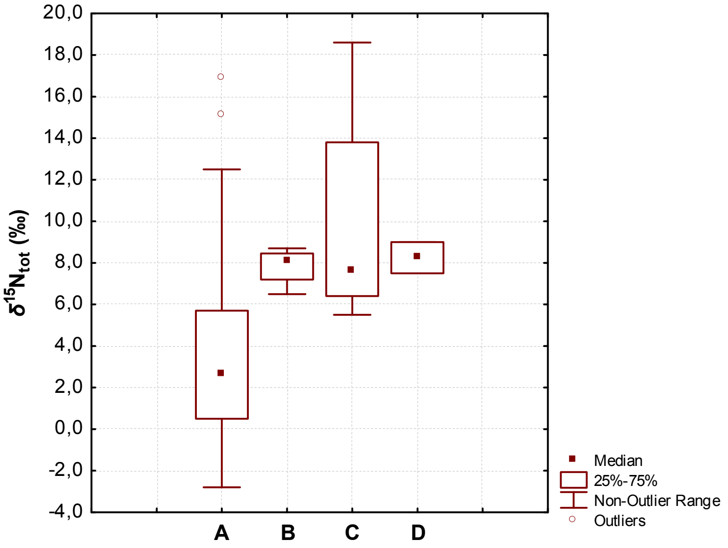

A = forest
B = areas of less intense use of nutrients and plant protection products
C = areas of intense use of nutrients and plant protection products
D = urban areas

Figure 266: Box and whisker plots of groundwater $\delta^{15}N_{tot}$ values in the recharge area of the prevailing land use type (Actual agricultural and forest land use)

Figure 267 shows the comparison between groundwater $\delta^{15}N_{tot}$ and the mean altitude of recharge area. At higher altitudes the naturally occurring nitrogen from the atmosphere (precipitation) and soil horizon dominates. With decreasing altitudes the share of organic nitrogen increases, and at lowlands the shares of organic and synthetic fertilizers dominate.

Figure 268 shows comparison between groundwater NO_3^- concentration and $\delta^{15}N_{tot\ values}$ (r_s=0.57, $p<0.05$). The highest groundwater NO_3^- concentrations were observed in the range of $\delta^{15}N_{tot}$ between ~ 5 and 12 ‰ which suggests the mixture of synthetic and organic fertilizers (grey squares). Groundwater enriched in ^{15}N (circle) has lower groundwater NO_3^- concentrations compared to previous group. This might suggest that in groundwater denitrification has occurred, or groundwater has been contaminated by e.g. septic tank effluent, feed lot discharges, or animal wastes. Black solid line illustrates the line between natural inorganic and organic soil source.

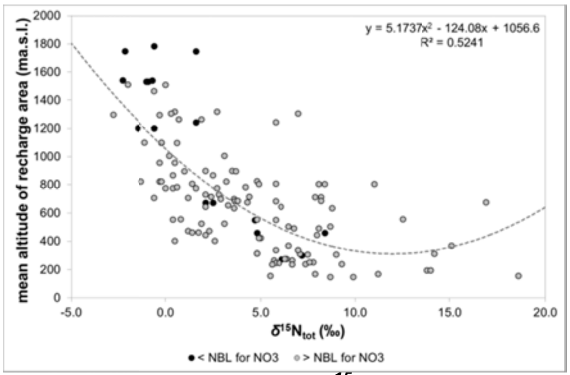

Figure 267: Groundwater $\delta^{15}N_{tot}$ values versus the altitude of recharge areas

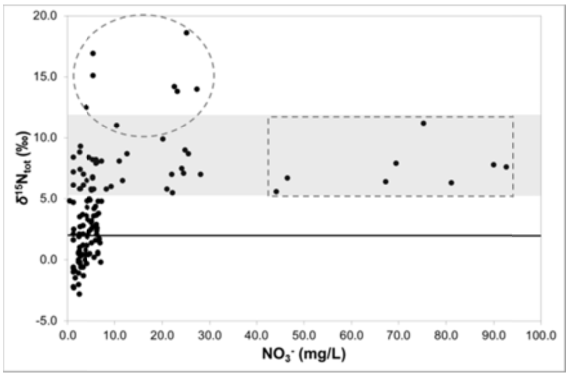

Figure 268: Groundwater NO_3^- concentration versus $\delta^{15}N_{tot}$ values

In order to determine the source of nitrogen more specifically, groundwater $\delta^{15}N_{tot}$ values have been compared to conservative traces of Cl^- (r_s=0.72, $p<0.05$) and Br (r_s=0.60, $p<0.05$). Figure 269 shows groundwater samples with increased NO_3^- and Br concentrations (black dots). This groundwater is also enriched in ^{15}N suggesting the source of nitrogen in organic (animal/human manure) or synthetic fertilizers. This has been verified by correlation of Cl^- and Br (Fig. 270) where groundwater samples in circles suggest that the origin of Cl^- is possible from organic fertilizers (manure, slurry), and/or salts of deicing streets (sampling locations LMV-1 Ljubljana, Gradišče, DAC-3 Skopice, C-4 Domžale). Groundwater $\delta^{15}N_{tot}$ also correlates moderately with Na^+ ($r_s=0.68$, $p<0.05$) and SO_4^{2-} ($r_s=0.51$, $p<0.05$) suggesting anthropogenic source from organic or synthetic fertilizers.

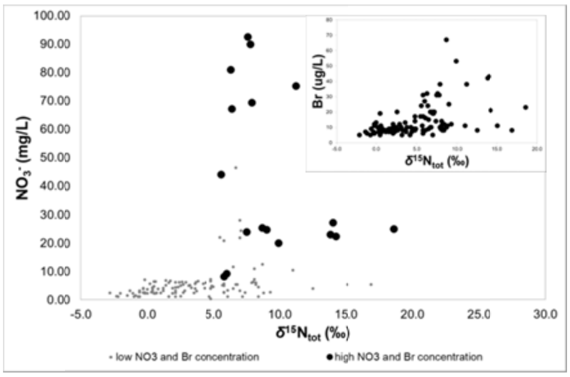

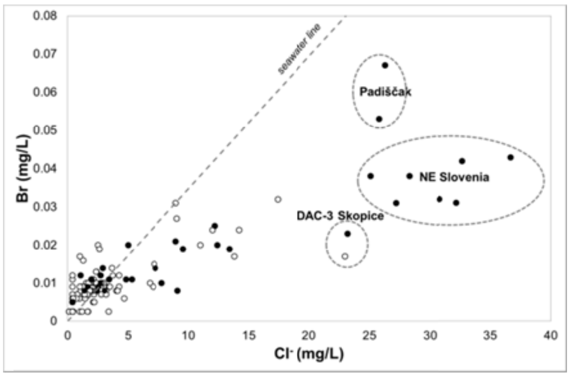

Figure 269: Groundwater $\delta^{15}N_{tot}$ versus NO_3^- and Br concentration

Figure 270: Groundwater Cl^- versus Br concentrations

Groundwater from sampling locations OV-29 Brunšvik and Gradišče suggest possible use of synthetic fertilizers, e.g. potassium nitrate (KNO_3) (Fig. 271). Strong correlation exists between groundwater $\delta^{15}N_{tot}$ and K^+ ($r_s=0.73$, $p<0.05$).

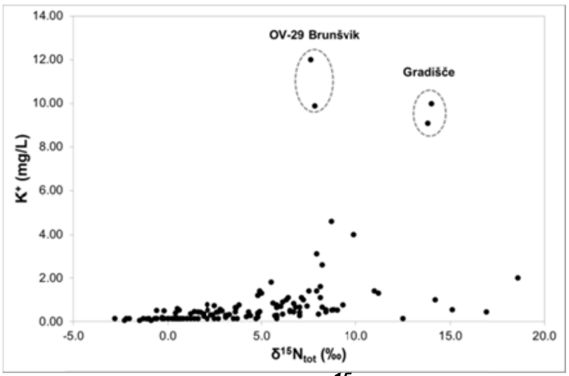

Figure 271: Groundwater $\delta^{15}N_{tot}$ values versus K^+ concentration.

Sampling object type

Groundwater from pumping stations, boreholes, and private wells (Fig. 272, Appendix 13Q) is more enriched in ^{15}N compared to groundwater sampled at spring and spring capture, and surface water, because of vicinity of fertilizers usage or other anthropogenic sources.

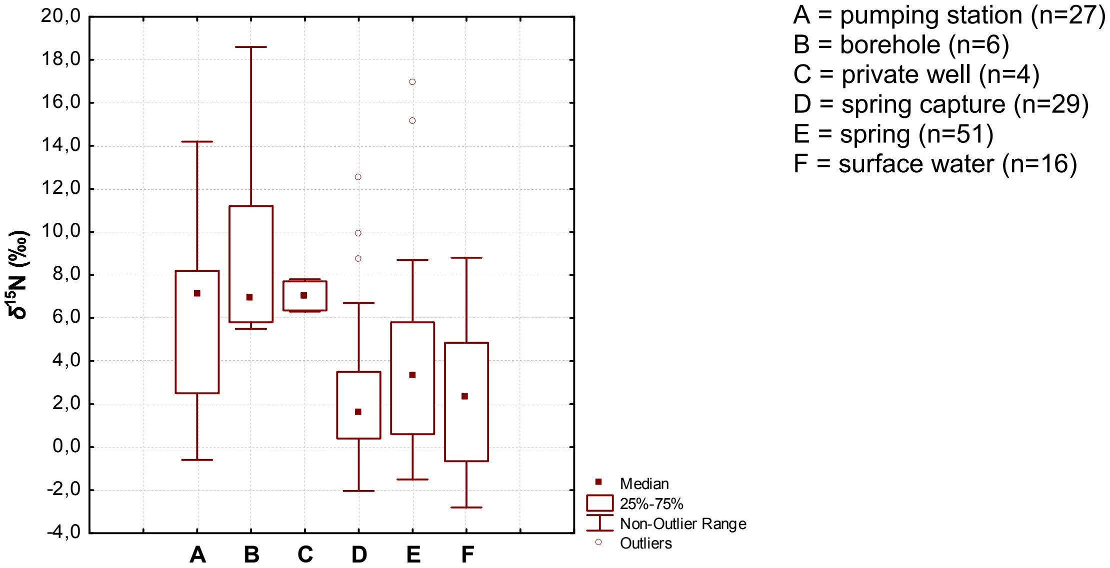

Figure 272: Box and whisker plots for groundwater $\delta^{15}N_{tot}$ values according to sampling object type

Spatial distribution of groundwater $\delta^{15}N_{tot}$

In the high mountain regions in the NE part of studied area (Julian Alps) groundwater is depleted in ^{15}N (< 0 ‰) (Fig. 273) suggesting naturally occurring nitrate in precipitation (and less from soil organic matter). Namely, groundwater from sampling locations Bohinjska Bistrica, Gljun, Krajcarica, Savica, Soča, and Zadlaščica (in the NW part) have very low (2.5 mg/L) mean groundwater NO_3^- concentration due to alpine vegetation, thin soil layer, and negligible influence from the agriculture and human land use. In the N part (Karavnke Mts., Kamnik-Savinja Alps) and NNE part of country (Pohorje Mt.) groundwater is enriched in ^{15}N due to mostly forest vegetation in the recharge area, thicker soil horizon and more organic matter in the soil (from leaves). Groundwater in some parts of N and NW could be influenced by grazing livestock which manure could enrich groundwater in ^{15}N. Groundwater enriched in ^{15}N (2.5 – 7.5 ‰) suggests possible use of synthetic fertilizers (-3 – 3 ‰) and organic fertilizers (3 – 7 ‰). The most enriched in ^{15}N (> 12.0 ‰) is groundwater stored in alluvial plains (Krško-Brežice and Pomurje) suggesting the source of $\delta^{15}N_{tot}$ is of organic fertilizers (animal manure or slurry from septic tanks) which are spilled on the fields, or perhaps due to leakage from septic tanks. Groundwater in deeper aquifers is probably denitrified because the concentration of NO_3^- is low and groundwater is enriched in ^{15}N (mean value 6.1 ‰; n=4).

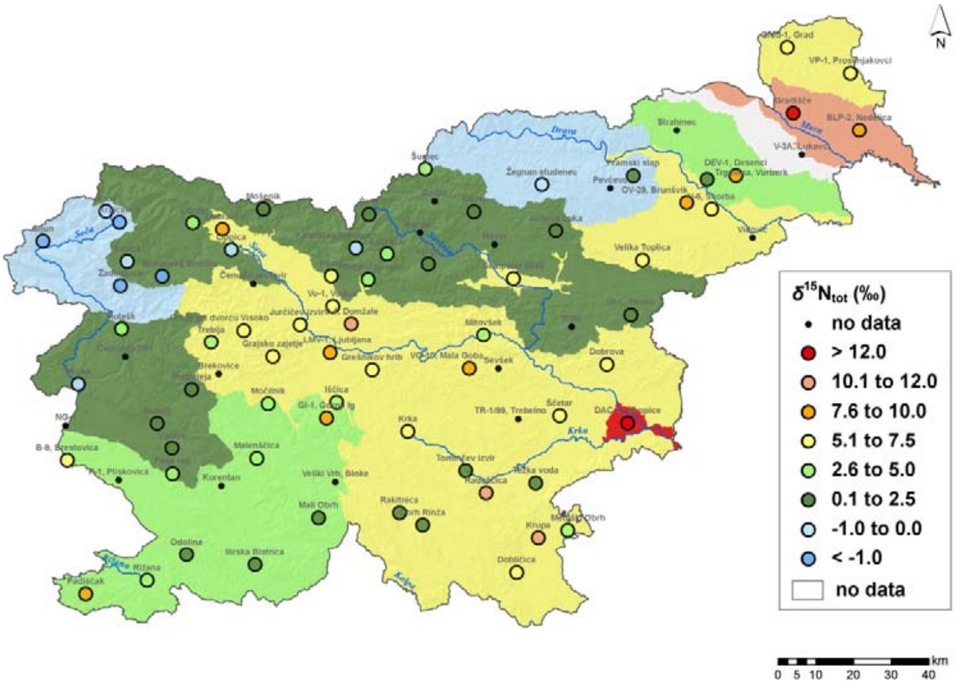

Figure 273: Spatial distribution of groundwater $\delta^{15}N_{tot}$

4.7.6. Potassium (K^+) in groundwater

Descriptive statistics of groundwater K^+

Groundwater K^+ concentration ranges between 0.04 and 12.00 mg/L, with mean value of 0.82 mg/L and median value of 0.44 mg/L (Tab. 38). Analytical uncertainty for groundwater K^+ concentration is between 4.1 and 18.8 %. In 47 groundwater samples K^+ concentration was below LOD (1st ½ LOD = 0.04 mg/L, 2nd ½ LOD = 0.125 mg/L) measured at sampling locations Gljun, Kamniška Bistrica, Krajcarica, Savica, Bohinjska Bistrica, Dobličica, Hotešk, Hubelj, Ilirska Bistrica, Kropa, Lipinica, Malenščica, Mali Obrh, Mitovšek, Mošenik, Mrzkel, Obrh Rinža, P-1 Pliskovica, Rakitnica, Soča, Šumec, Trate, Vipava, Zadlaščica, Črna, Grajsko zajetje, Kjarjcarica, Lipnik, Lučnica, Podroteja, Velika Toplica, Veliki vrh Bloke, and Sevšek. Distribution of groundwater K^+ concentration is not normal (Fig. 274) and values higher than 1.60 mg/L present outliers and extremes (Fig. 275). Those values were observed in groundwater from sampling locations NG-4 and Padiščak near the Coast, DAC-3 Skopice, Strahinec, Gradišče, OV-29 Brunšvik in alluvial plains, and VG-10 Mala Goba, Veliki Vrh Bloke in the central part of the country. There is no numerical Slovenian drinking water quality guideline for K^+ in water according to Rules on drinking water (2004).

Table 38: Descriptive statistics of groundwater K^+

Parameter	n	X	Md	Min	Max	S
K^+ (mg/L)	175	0.82	0.44	0.04	12.00	1.60

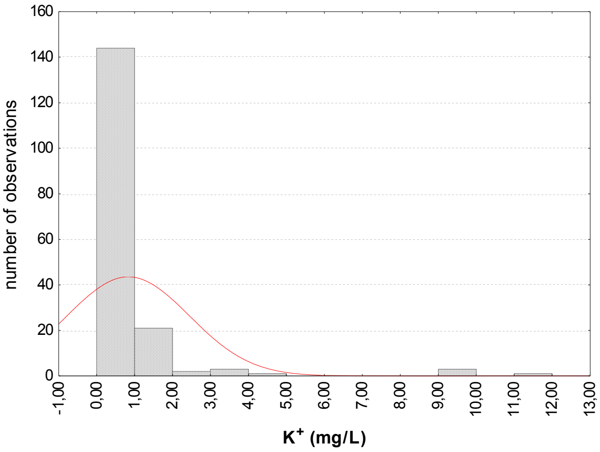

Figure 274: Histogram for groundwater K^+ concentration (n=175)

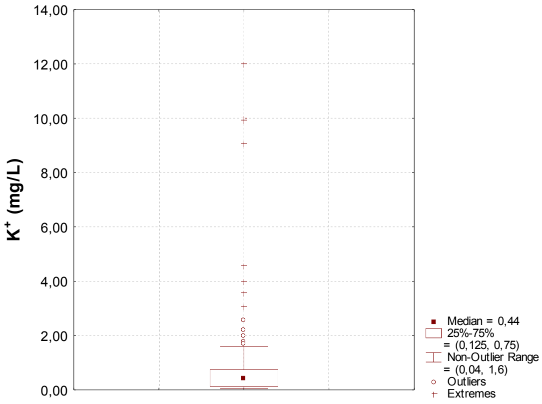

Figure 275: Box and whisker plot for groundwater K^+ concentration (n=175)

Rock type

Increased groundwater K^+ concentrations are observed in the recharge areas with clastic sedimentary rocks (Fig. 276, Appendix 13R) which are significantly higher compared to groundwater in the recharge areas with carbonate, igneous, and metamorphic rocks. Mineralogical composition of clastic silicate rocks could contribute to greater groundwater K^+ concentration. Medium groundwater K^+ concentration are observed in groundwater in the recharge areas with igneous and metamorphic rocks which also contain silicate minerals. The lowest groundwater K^+ concentration was observed in the recharge area of carbonate rocks due to lack of K-bearing minerals.

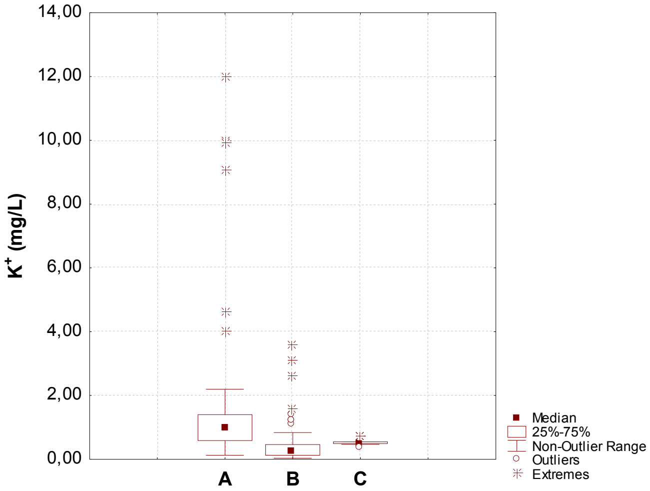

A = clastic sedimentary rocks (n=53)
B = carbonate rocks (n=110)
C = igneous and metamorphic rocks (n=12)

Figure 276: Box and whisker plots for groundwater K^+ concentration in the recharge area of major rock types

The highest groundwater K^+ concentrations are observed in the recharge areas with Quaternaryand Miocene clastics (gravel, sand, and clay), and flysch rocks (Figs. 277 and 278, Appendix 13R), where K-rich minerals could be found in the silicate rocks (phyllosilicates). The lowest groundwater K^+ concentrations are observed in the recharge areas of limestone prevailing. Most alluvial deposits in Slovenia belong to Quaternary sediments of carbonate and silicate origin (Bavec and Pohar, 2009; EARS, 2010), but alluvial deposits of Mura River (NE part) are mostly non-carbonate (Markič, 2009). The lowest groundwater K^+ concentrations are observed in the recharge areas of carbonate mineras due to lack of K-rich minerals. Groundwater K$^+$ concentrations between the groups (lithological and lithostratigraphic units) do not statistically differ.

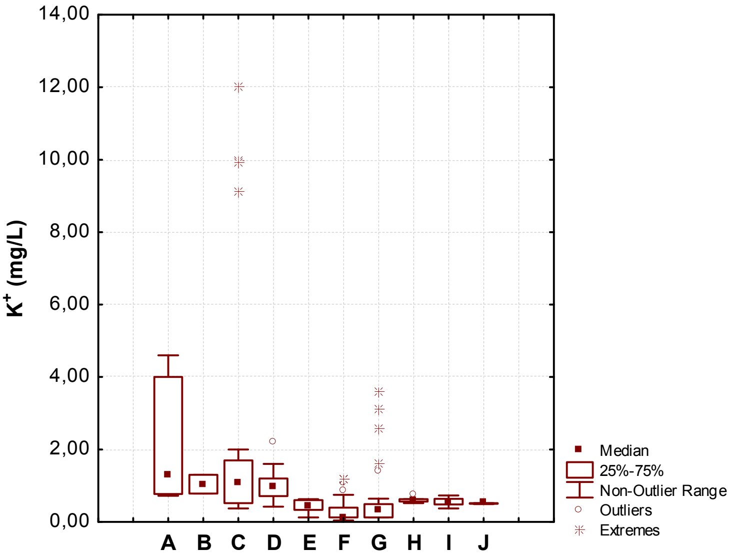

A = flysch rocks (n=7)
B = clay (n=2)
C = gravel and sand (n=26)
D = gravel, sand and clay (n=11)
E = shale and sandstone (n=7)
F = limestone prevailing (n=74)
G = dolomite prevailing (n=30)
H = carbonates with clastics (n=6)
I = igneous rocks (n=8)
J = metamorphic rocks (n=4)

Figure 277: Box and whisker plots for groundwater K$^+$ concentration in the recharge area of the prevailing lithological unit

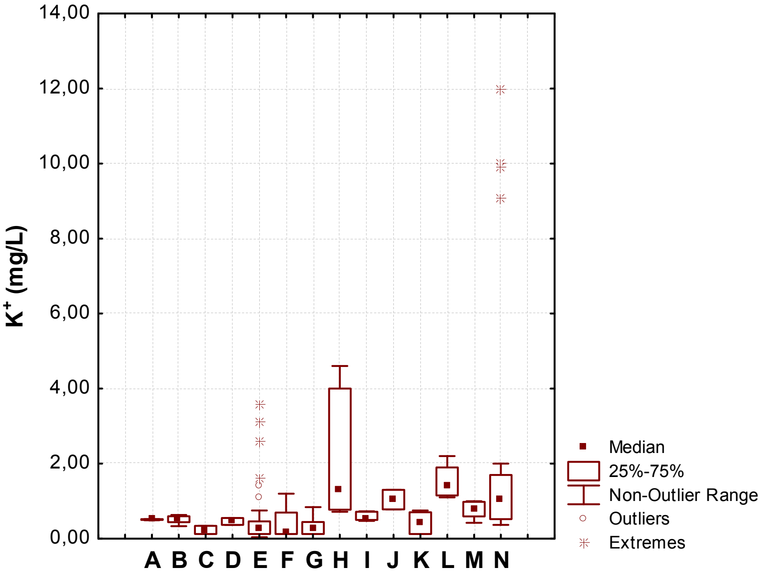

A = old Paleozoic rocks (n=4)
B = Carboniferous-Permian beds (n=5)
C = Permian Val Gardena layers (n=2)
D = Ladinian igneous rocks (n=2)
E = Triassic carbonates (n=70)
F = Jurassic carbonates (n=8)
G = Cretaceous carbonates (n=28)
H = Eocene flysch rocks (n=7)
I = Oligocene igneous rocks (n=6)
J = Oligocene clay “sivica” (n=2)
K = Miocene Lithothamnium limestone (n=4)
L = Miocene clastics (n=4)
M = Pliocene clastics (n=7)
N = Quaternary clastics (medium- and coarse-grained) (n=26)

Figure 278: Box and whisker plots for groundwater K$^+$ concentration in the recharge area of the prevailing lithostratigraphic unit

Aquifer porosity type

The highest groundwater K$^+$ concentrations are observed in aquifers with intergranular porosity (Fig. 279, Appendix 13R) which are due to their permeability and porosity, open to anthropogenic sources and therefore very vulnerable. Groundwater K$^+$ concentrations measured in aquifers with intergranular porosity are significantly higher ($p<0.05$) compared to aquifers with karstic and fractured porosity where the lowest groundwater K$^+$ concentrations are observed. This is because of absense ob anthropogenic and also urban activities in those areas, as well as the lack of K-bearing minerals in the host rocks.

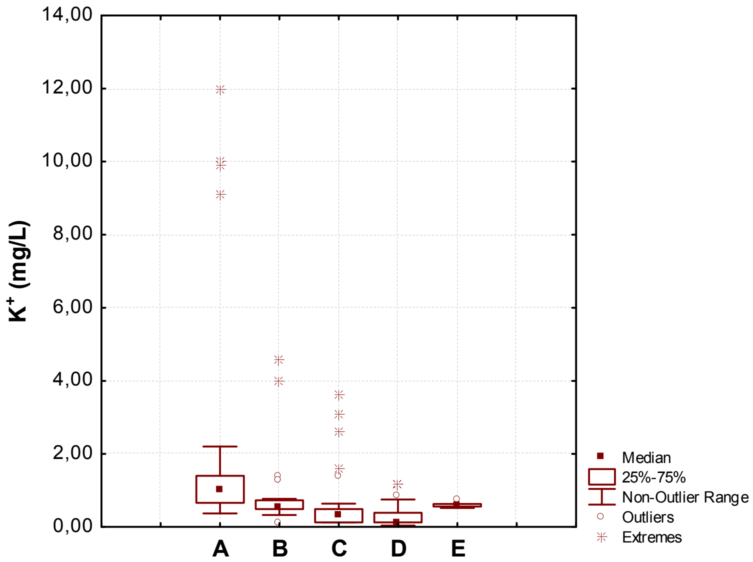

A = intergranular porosity (n=39)
B = fractured porosity (n=26)
C = fractured and karstic porosity (n=30)
D = karstic and fractured porosity (n=74)
E = mixed porosity (karstic, fractured, intergranular) (n=6)

Figure 279: Box and whisker plots for groundwater K^+ concentration in the recharge area of the prevailing aquifer porosity type

Land cover/use

The highest groundwater K^+ concentrations (Figs. 280 and 281, Appendix 13R) are measured in the recharge areas of non-irrigated areas which are significantly higher ($p<0.05$) compared to groundwater sampled from other recharge areas according to CORINE Land Cover use classes. In non-irrigated recharge areas the source of potassium is in the intense use of nutrients and plant protection products. The lowest groundwater K^+ concentrations are observed in the recharge area of bare rocks, marshes and heaths, and natural meadow and forests, where the human impact is less pronounced.
According to Actual agricultural and forest land usage classification groundwater K^+ concentrations in the recharge areas of intense use of nutrients and plant protection products are significantly higher ($p<0.05$) compared to other classes, suggesting major souces of potassium in the groundwater from fertilizers.

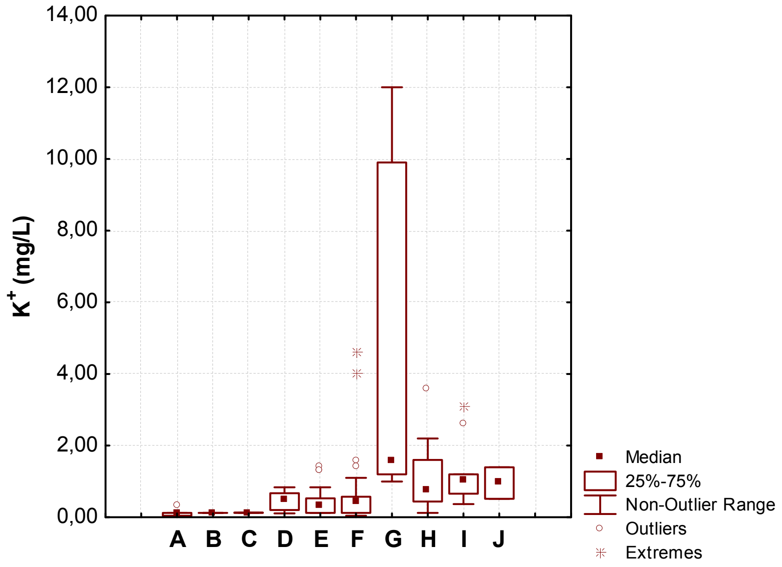

A = bare rocks (n=8)
B = marshes and heaths (n=2)
C= natural grassland (n=2)
D = coniferous forest (n=20)
E = broad-leaved forest (n=45)
F = mixed forest (n=56)
G = non-irrigated arable land (n=10)
H = Complex cultivation patterns (n=18)
I = land principally occupied by agriculture, with significant areas of natural vegetation (n=10)
J = industrial or commercial units (n=2)

Figure 280: Box and whisker plots for groundwater K^+ concentration in the recharge area of the prevailing land use type (CORINE Land Cover)

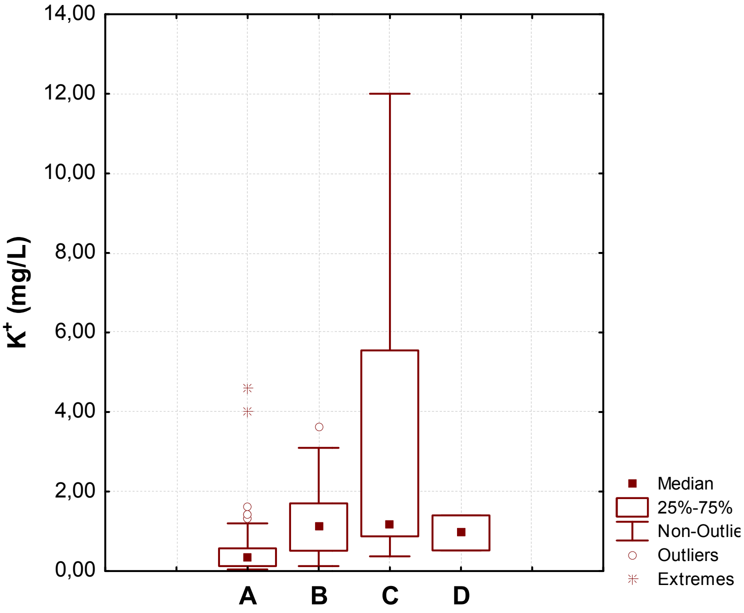

A = forest (n=137)
B = areas of less intense use of nutrients and plant protection products (n=18)
C = areas of intense use of nutrients and plant protection products (n=16)
D = urban areas (n=2)

Figure 281: Box and whisker plots for groundwater K^+ concentration in the recharge area of the prevailing land use type (Actual agricultural and forest land use)

Groundwater K^+ correlates strongly with Na^+ ($r_s=0.82$, $p<0.05$), Cl^- ($r_s=0.71$, $p<0.05$), Si ($r_s=0.71$, $p<0.05$), and moderately with NO_3^- ($r_s=0.58$, $p<0.05$), SO_4^{2-} ($r_s=0.58$, $p<0.05$), and Br ($r_s=0.61$, $p<0.05$) (Appendix 10). This suggests that groundwater is mostly influenced by anthropogenic factors. The anthropogenic sources could be linked to fertilizers (e.g., KCl and KNO_3). As already mentioned, near the sampling location OV-29 Brunšvik and Gradišče which have gravel and sand in their recharge areas, the land is used as arable land. Recharge areas of sampling location Padiščak in flysch rocks is used for orchards and olive groves.

Correlation between distance from the sea and groundwater K^+ concentration (Fig. 282) suggest the possible influence from the sea on the groundwater. Groundwater chemistry from sampling location Padiščak (closest to the sea) suggests mostly anthropogenic origin (fertilizers, wastewater) on groundwater. Increased groundwater Na^+ and Cl^- concentrations also suggest the influence from the sea spray or maritime precipitation.

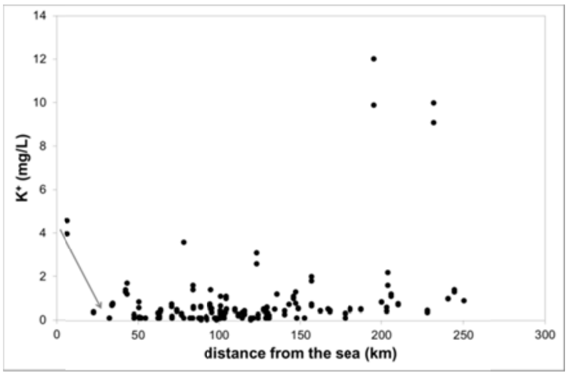

Figure 282: Groundwater K^+ concentration versus the distance from the sea

Sampling object type

The highest groundwater K$^+$ concentration was observed in private wells (Fig. 283, Appendix 13R) which are located in the vicinity of arable land and intense use of fertilizers. The lowest groundwater K$^+$ concentrations are observed in the spring water which is mostly located in high mountain regions of prevailing carbonate rocks and little anthropogenic influences fom man.

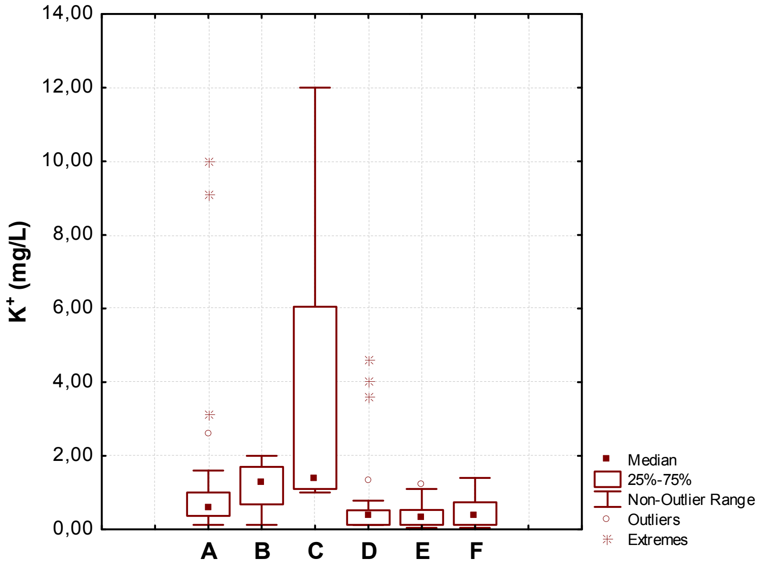

A = pumping station (n=35)
B=borehole (n=10)
C=private well (n=8)
D=spring capture (n=44)
E=spring (n=58)
F=surface water (n=20)

***Figure 283*: Box and whisker plots for groundwater *K$^+$ concentrations according to s*ampling object type**

Natural background level of K$^+$

The natural background level for K$^+$ concentrations in Slovenian groundwaters is 0.35 mg/L (n=91) (Fig. 284). Voigt *et al.*, (2005) estimated ranges for groundwater K$^+$ concentrations in the carbonate aquifers (0.3 – 2.1 mg/L) and sandstone 0.8 – 4.0 mg/L. Groundwater in Triassic Limestones and Loose Rock Sediments of the Saale Glaciation have K$^+$ concentrations ~ 2 mg/L (Wendland *et al.*, 2003).

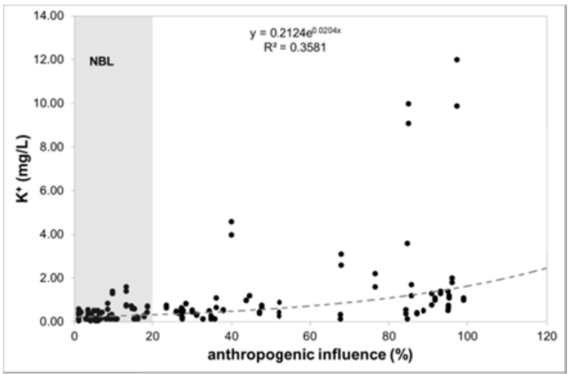

Figure 284: Groundwater K$^+$ concentrations versus the share of anthropogenic influence

Spatial distribution of groundwater K$^+$

Increased groundwater K$^+$ concentration (>5.00 mg/L) is observed in the NE part (Mursko polje and Dravsko polje aquifers) in the recharge areas with diverse mineralogical concentration (carbonate and silicate minerals) in clastic sedimentary rocks. Beside minor geogenic source from silicate weathering or from the sea, mostly intense agricultural activities and consequently excessive use of fertilizers in this area add its source to groundwater. Sampling location OV-29 Brunšvik, where in the vicinity intense horticulture takes place (arable land with ornamental plants and vegetables growth), at sampling location Padiščak (orchards and olive groves), and VG-10 Mala Goba (arable land and orchards), increased anthropogenic influence can be observed. High groundwater K^+ concentrations suggest strong impact of use of fertilizers containing potassium or waste water.

In more than ⅓ of sampling locations groundwater K^+ concentrations was below LOD (½ LOD = 0.125 mg/L). Low groundwater K^+ concentrations (<0.5 mg/L) are observed in the high mountain Karst and in classic Dinaric Karst where human impact is less pronounced as well as the lack of K-minerals in carbonate rocks (Fig. 285).

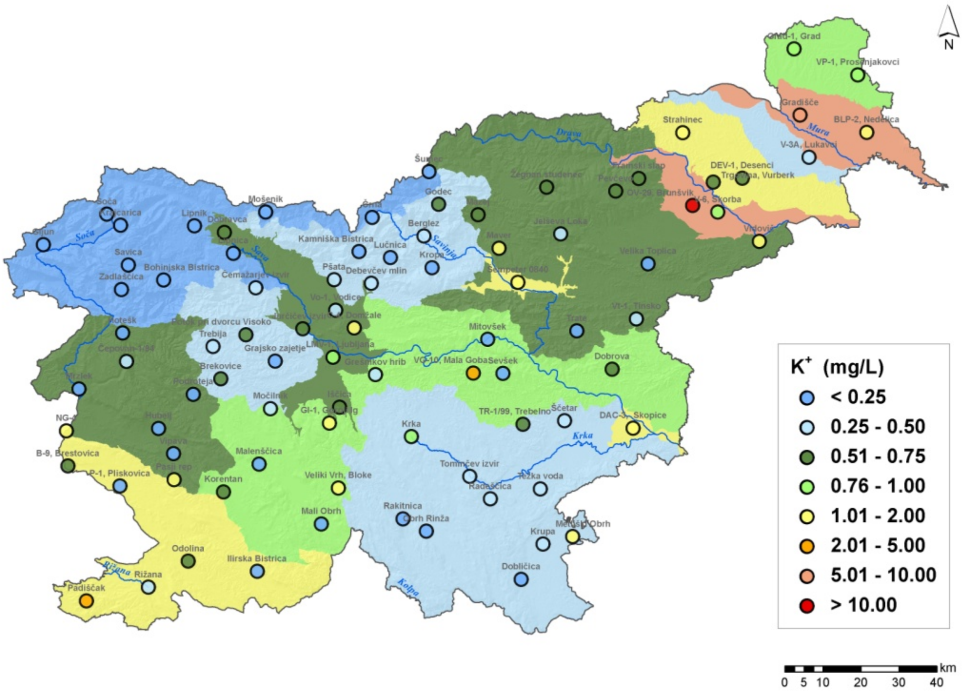

Figure 285*: Spatial distribution of groundwater *K^+

4.7.7. Sulphate (SO_4^{2-}) in groundwater

Descriptive statistics of groundwater SO_4^{2-}

Groundwater SO_4^{2-} concentration ranges between 0.75 and 67.40 mg/L, with mean value of 10.05 mg/L and median 5.66 mg/L (Tab. 39). Groundwater SO_4^{2-} concentration is not normally distributed (Fig. 286) and concentrations above 18.10 mg/L present outliers and extremes (Fig. 287). This groundwater was sampled at sampling locations Pasji rep, Trate, Vt-1 Tinsko, LMV-1, V-6 Skorba, Mošenik, Maver, OV-29 Brunšvik, Vidovič, Trgovina Vurberk, Mošenik, Gradišče, BLP-2 Nedelica, Padiščak, Vidovič, Strahinec, located throughout the Slovenian territory. Analytical uncertainty for groundwater SO_4^{2-} is between 4.4 and 45 % (n=171) and groundwater SO_4^{2-} concentration below LOD (½ LOD=0.375 mg/L) is observed in 4 groundwater samples from sampling locations Soča, Gljun, Zadlaščica, and Bohinjska Bistrica, all located in the NW part of the country. None of water samples exceeds the allowed maximum level for drinking water (250 mg/L) according Rules on drinking water (2004).

Table 39: Descriptive statistics of groundwater SO_4^{2-} concentration

Parameter	n	X	Md	Min	Max	S
SO_4^{2-} (mg/L)	175	10.05	5.66	0.75	67.40	11.49

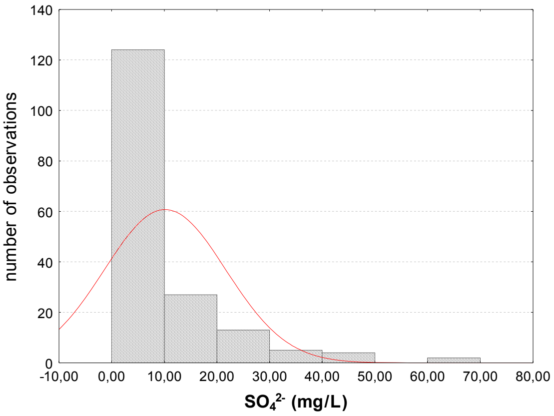

Figure 286: Histogram for groundwater SO_4^{2-} concentration (n=175).

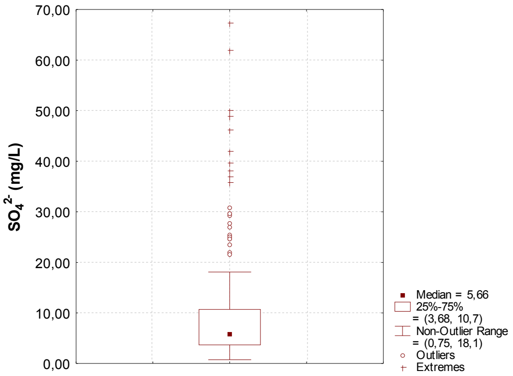

Figure 287: Box and whisker plot for groundwater SO_4^{2-} concentration (n=175).

None of groundwater samples (n=175) exceed the quality standard for drinking water (> 250 mg/L) (Rules on drinking water, 2004).

Rock type

The highest groundwater SO_4^{2-} concentrations and the highest variance in distribution of concentration is observed in the recharge areas with clastic sedimentary rocks (Fig. 288, Appendix 13S) which are significantly higher ($p<0.05$) compared to other recharge areas of other rock types. The source of groundwater SO_4^{2-} concentration is probably in the mineralogical composition of silicate and carbonate rocks (outliers at sampling location Strahinec). In the recharge areas of carbonate rocks the sources are possible evaporate minerals in limestones and dolomites where moderate correlation exists between SO_4^{2-} and EC ($r_s=0.58$, $p<0.05$) and SO_4^{2-} and Ca^{2+} ($r_s=0.52$, $p<0.05$). The outliers belong to sampling location Mazej, and extreme concentrations are observed at sampling locations Trate, Velika Toplica, Pasji rep, Vt-1 Tinsko, Maver and Mošenik. In the recharge areas of igneous and metamorphic rocks the possible source is in metal sulphides and silicate minerals (outlier at sampling location Berglez).

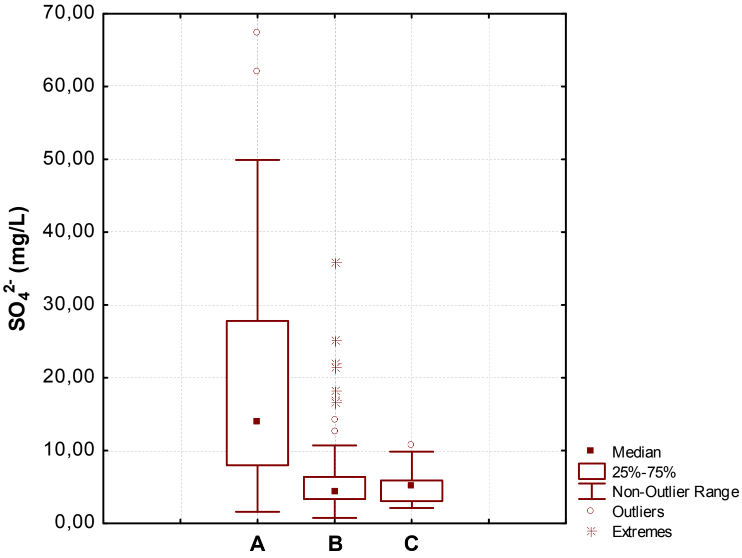

A = clastic sedimentary rocks (n=53)
B = carbonate rocks (n=110)
C = igneous and metamorphic rocks (n=12)

Figure 288: Box and whisker plots for groundwater SO_4^{2-} concentration in the recharge area of major rock types

The highest groundwater SO_4^{2-} concentrations are observed in the recharge area with Miocene clastics, Eocene flysch rocks, and Oligocene clay “sivica” which are significantly higher ($p<0.05$) compared to groundwater with recharge areas with Permian Val Gardena layers, Jurassic carbonates, Cretaceous carbonates, Ladinian igneous rocks, Miocene clastics, Oligocene igneous rocks, old Paleozoic rocks, and Triassic carbonates (Figs. 289 and 290, Appendix 13S). Increased groundwater SO_4^{2-} concentration in the recharge areas with Eocene flysch rocks is observed at sampling location Padiščak near the coast. Possible sources are from weathering of sulphide minerals — oxidation of pyrite in the zone of flysch weathering - sandstone (Košir *et al.*, 2013) which may not be homogeneously distributed in the aquifer. Similar increased SO_4^{2-} concentrations were obtained during investigations for the 2nd train rails Divača-Koper in the near vicinity (Divača – Črni kal) by Lapanje and Prestor (2011). Additionally, Zupan Hajna (2005) suggests that the sources of SO_4^{2-} concentration in Slovenian caves in the Eocene flysch sediments originate from impurities in limestone, from sulphide deposits, and volcanic rocks. It is also possible that groundwater in the recharge areas of Istrian flysch has naturally somewhat elevated groundwater SO_4^{2-} concentration compared to Brkini flysch. Namely mineralogical composition of Istrian flysch and Brkini flysch differs (Zupančič and Pirc, 1999), where in Istrian flysch carbonates dominate and in Brkini flysch silicates. Flysch rocks are mostly impermeable for water and flysch sequences are rich in carbonate and quartziferous minerals (Pavlovec, 1977; Knez and Slabe, 2009). Other possible natural sources, which could increase groundwater SO_4^{2-} concentration, are coal layers where boreholes are drilled, or the vicinity to the seaside. Low groundwater SO_4^{2-} concentrations are observed in the recharge of limestones, dolomites, carbonates with clastics, and igneous and metamorphic rocks. In the recharge areas with carbonate rocks several outliers and extremes are observed (Velika Toplica, Vt-1 Tinsko, Mošenik). It is belived the limestones and dolomite in the recharge areas of sampled groundwater could contain gypsum, like in the case of sampling location Mošenik near Karavanke tunel (Brenčič and Poltnig, 2008; Vidrih, 2006)

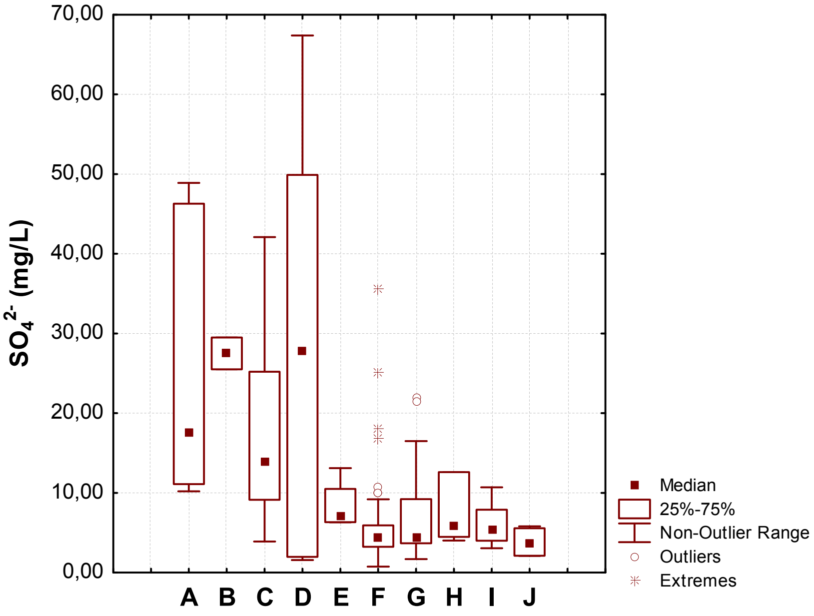

A = flysch rocks (n=7)
B = clay (n=2)
C = gravel and sand (n=26)
D = gravel, sand and clay (n=11)
E = shale and sandstone (n=7)
F = limestone prevailing (n=74)
G = dolomite prevailing (n=30)
H = carbonates with clastics (n=6)
I = igneous rocks (n=8)
J = metamorphic rocks (n=4)

Figure 289: Box and whisker plots for groundwater SO_4^{2-} concentration in the recharge area of the prevailing lithological unit

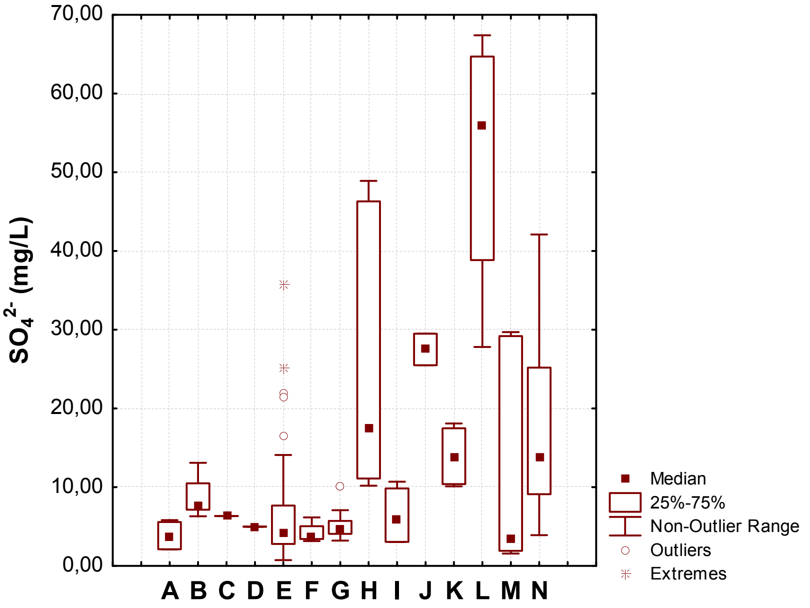

A = old Paleozoic rocks (n=4)
B = Carboniferous-Permian beds (n=5)
C = Permian Val Gardena layers (n=2)
D = Ladinian igneous rocks (n=2)
E = Triassic carbonates (n=70)
F = Jurassic carbonates (n=8)
G = Cretaceous carbonates (n=28)
H = Eocene flysch rocks (n=7)
I = Oligocene igneous rocks (n=6)
J = Oligocene clay “sivica” (n=2)
K = Miocene Lithothamnium limestone (n=4)
L = Miocene clastics (n=4)
M = Pliocene clastics (n=7)
N = Quaternary clastics (medium- and coarse-grained) (n=26)

Figure 290: Box and whisker plots for groundwater SO_4^{2-} concentration in the recharge area of the prevailing lithostratigraphic unit

Aquifer porosity type

Groundwater SO_4^{2-} concentrations in aquifers with intergranular porosity are significantly higher ($p<0.05$) compared to groundwater from aquifers with other porosity types (Fig. 291, Appendix 13S) which suggest anthropogenic influence on vulnerable alluvial aquifers.

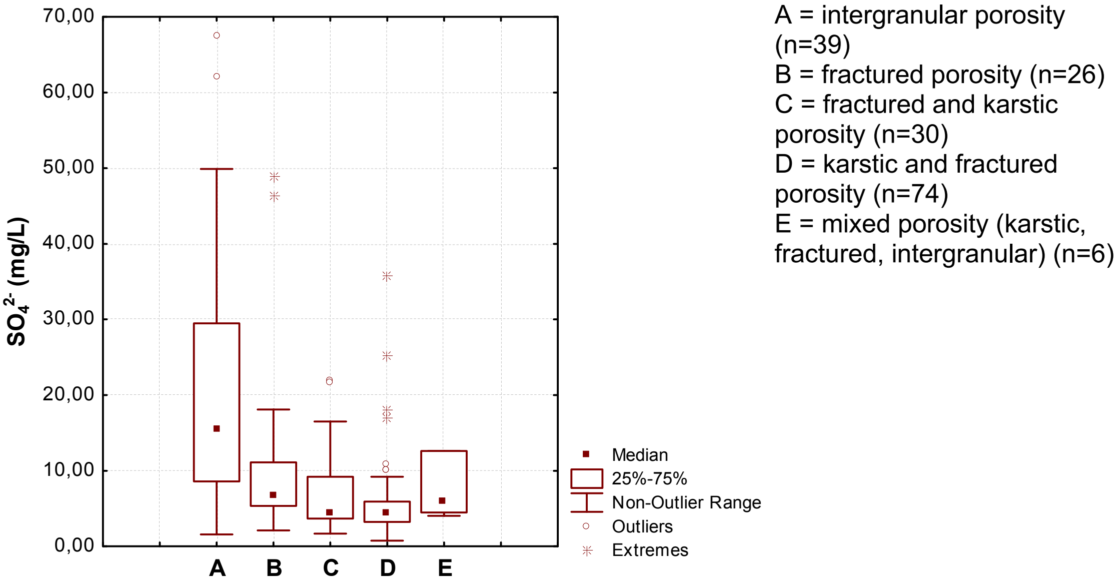

Figure 291: Box and whisker plots for groundwater SO_4^{2-} concentration in the recharge area of the prevailing aquifer porosity type

Land cover/use

Increased groundwater SO_4^{2-} concentrations are observed in the recharge areas of industrial and commercial units which are significantly higher ($p<0.05$) compared to groundwater in moors and heathland, and in the recharge areas with non-irrigated arable land which are signifinatly higher ($p<0.05$) compared to groundwater in natural grasslands (Figs. 292 and 293, Appendix 13S). This suggests that sources of SO_4^{2-} concentration in groundwater are mosty due to use of various fertilizers which is supported by moderate correlations between groundwater SO_4^{2-} and Na^+ ($r_s=0.61$, $p<0.05$; Fig. 294), K^+ ($r_s=0.58$, $p<0.05$; Fig. 295), Cl^- ($r_s=0.58$, $p<0.05$; Fig. 296), and NO_3^- ($r_s=0.55$, $p<0.05$; Fig. 297) observed at sampling locations Strahinec, Vidovič, Gradišče, BLP-2 Nedelica, C-4 Domžale, and OV-29 Brunšvik, all located in the NE part, and Padiščak located near the coast). In other lithological and lithostratigraphic classes groundwater SO_4^{2-} concentration is low. An outlier in recharge area of bare rocks is found at sampling location Mošenik, in the recharge area of coniferous forest the outlier is found in Berglez, and extreme values at sampling location V-6 Skorba. In the recharge area of broad-leaved forest the outlier is found at sampling location Trate and extreme values in Pasji rep and Trate, and outliers in the recharge area of mixed forest are found at sampling locations VT-1 Tinsko, and extremes in Trgovina Vurberk, and Padiščak.

According to recharge areas after Actual agricultural and forest land usage classification type groundwater with recharge areas of intense use of nutrients and plant protection products is significantly higher ($p<0.05$) compared to other classes.

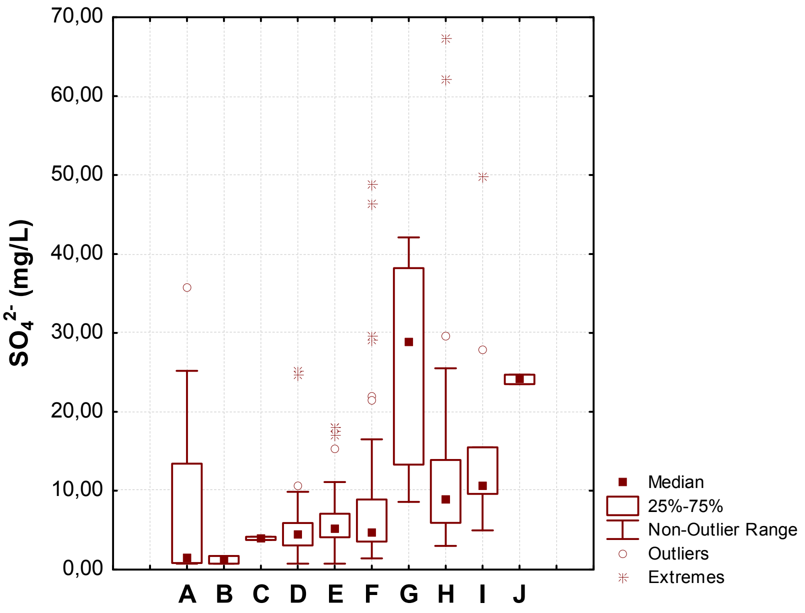

A = bare rocks (n=8)
B = moors and heathland (n=2)
C= natural grasslands (n=2)
D = coniferous forest (n=20)
E = broad-leaved forest (n=45)
F = mixed forest (n=56)
G = non-irrigated arable land (n=10)
H = complex cultivation patterns (n=18)
I = land principally occupied by agriculture, with significant areas of natural vegetation (n=10)
J = industrial or commercial units (n=2)

Figure 292: Box and whisker plots for groundwater SO_4^{2-} concentration in the recharge area of the prevailing land use type (CORINE Land Cover)

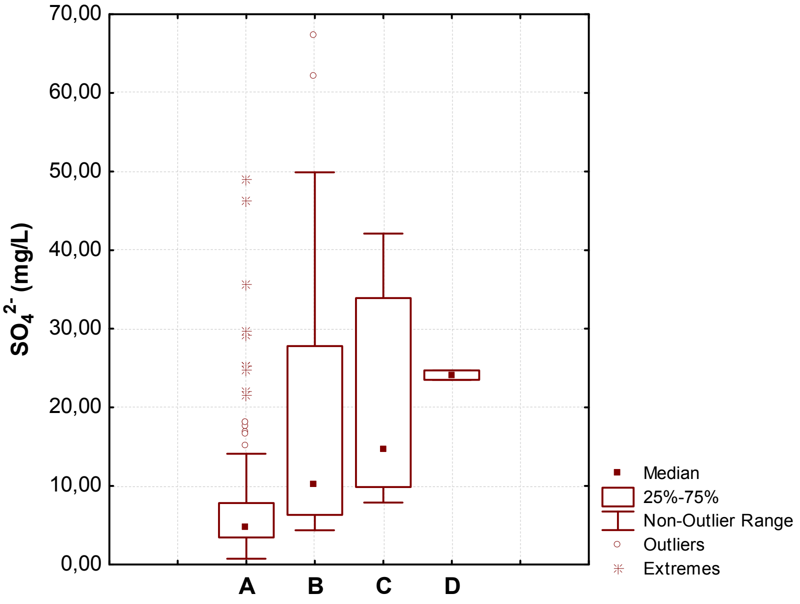

A = forest (n=137)
B = areas of less intense use of nutrients and plant protection products (n=18)
C = areas of intense use of nutrients and plant protection products (n=16)
D = urban areas (n=2)

Figure 293: Box and whisker plots for groundwater SO_4^{2-} concentration in the recharge area of the prevailing land use type (Actual agricultural and forest land use)

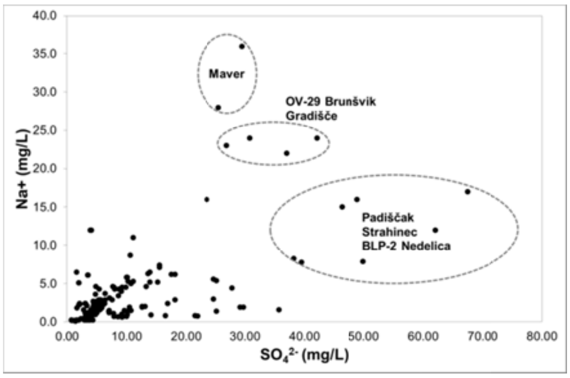

Figure 294: Groundwater SO_4^{2-} versus Na^+ concentrations

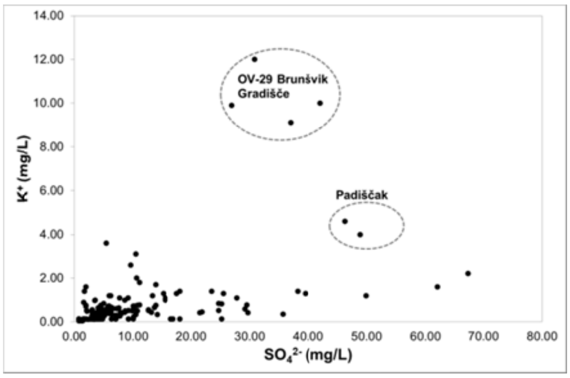

Figure 295: Groundwater SO_4^{2-} versus K^+ concentrations

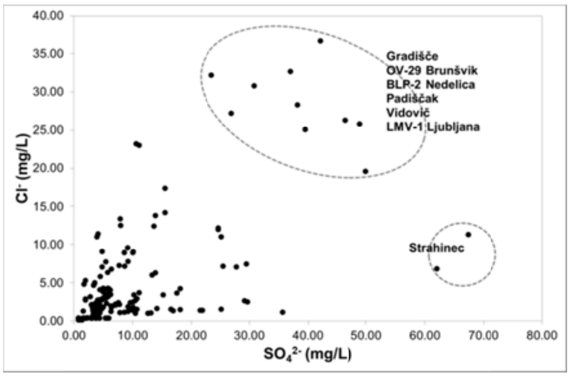

Figure 296: Groundwater SO_4^{2-} versus Cl^- concentrations

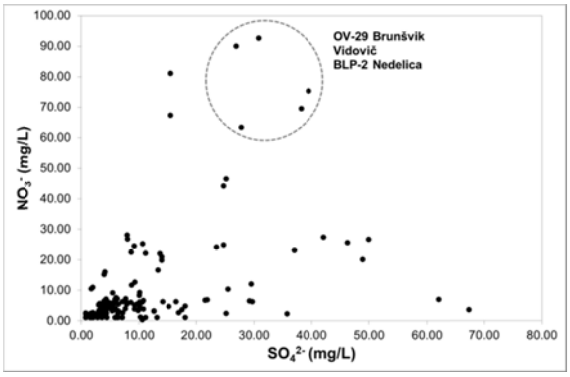

Figure 297: Groundwater SO_4^{2-} versus NO_3^- concentrations

Correlation between groundwater SO_4^{2-} concentration and number of people/km^2 (Fig. 298) estimated from the data of Records of house numbers (EHIS, 2013) suggest increased groundwater SO_4^{2-} concentration due to urban land use - SO_2 emission observed at sampling location LMV-1 Ljubljana located in the central part of the country.

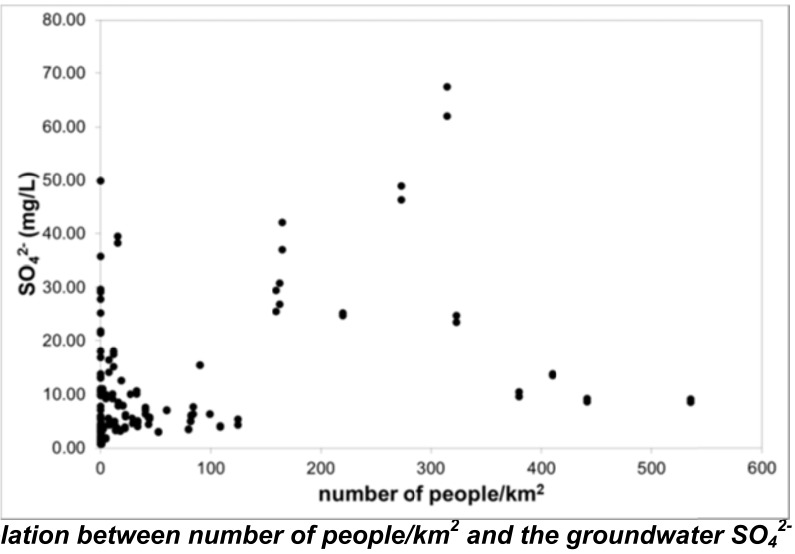

Figure 298: Correlation between number of people/km^2 and the groundwater SO_4^{2-} concentration

Sampling object type

The highest groundwater SO_4^{2-} concentrations are measured in the groundwater from private wells (Fig. 299, Appendix 13S) which are located near the fields, suggesting anthropogenic influence into the groundwater. Groundwater from other sampling objects has similar SO_4^{2-} concentrations.

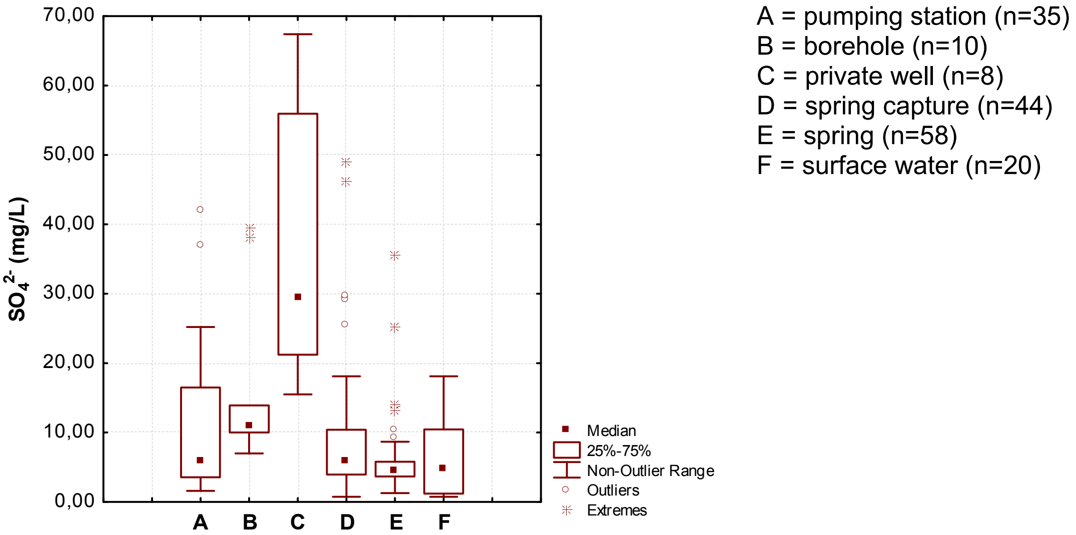

Figure 299: Box and whisker plots for groundwater SO_4^{2-} concentration according to sampling object type

Natural background level for SO_4^{2-}

Estimated natural background level for SO_4^{2-} in Slovenian groundwater is 6.93 mg/L (n=91) (Fig. 300). The natural (pre-industrial) background level for SO_4^{2-} concentration in the shallow East Midlands Triassic sandstone aquifer (UK) is below 10 mg/L, in deeper part of aquifer up to 365 mg/L due to anhydrite dissolution (Edmunds *et al.*, 1982). In Germany in the clastic sediments (sand and gravel, and Triassic sandstone) the range of groundwater SO_4^{2-} concentration is 4-68 mg/L, and in carbonate rocks (Jurassic and Triassic limestone) between 13 and 147 mg/L (Kunkel *et al.*, 2004; Voight *et al.*, 2005). In the older sandy aquifers in the Western River Rhine (The Netherlands) the groundwater SO_4^{2-} concentrations are 3.5-50 mg/L (Griffioen *et al.*, 2008), and in carbonate formations of Northern Apennines (Mt. Catria—Mt. Nerone ridge) (Italy) (Capaccioni *et al.*, 2001) observed SO_4^{2-} concentrations are up to 731 mg/L.

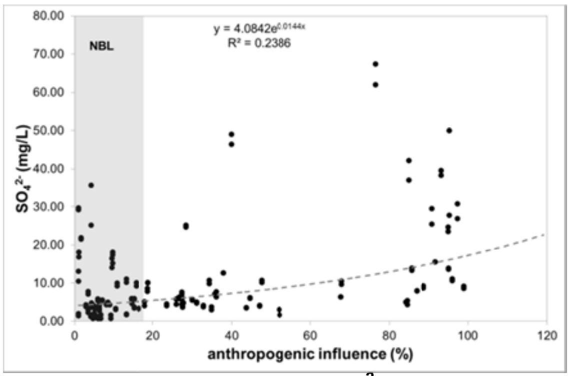

Figure 300: Groundwater SO_4^{2-} concentrations versus the share of anthropogenic influence

Spatial distribution of groundwater SO_4^{2-}

High groundwater SO_4^{2-} concentrations (>20.00 mg/L) are observed in the NE, E, and coastal part of the study area (Fig. 301) which are mostly associated with anthropogenic source due to intensive agricultural activities (use of fertilizers). Around bigger and densely populated cities like e.g. Ljubljana (central), Maribor (NE) and others, the additional source of groundwater SO_4^{2-} concentrations could be due to emission of SO_2. In the N part of Slovenia (Karavanke Mts.) the source of groundwater SO_4^{2-} concentrations is possible geogenic (dissolution of gypsum). Also in the coastal part the source is possible also geogenic, either from the seawater influences, or weathering of sulphide minerals.
Low groundwater SO_4^{2-} concentrations (<5.00 mg/L) are observed in the high mountains in NW part, and in low karst region in central and E part of the study area due to lack of intense agricultural and urban land uses in the recharge areas. Very low groundwater SO_4^{2-} concentrations are also observed in older groundwaters (NE), which is possible due to degradation through natural reduction reactions.

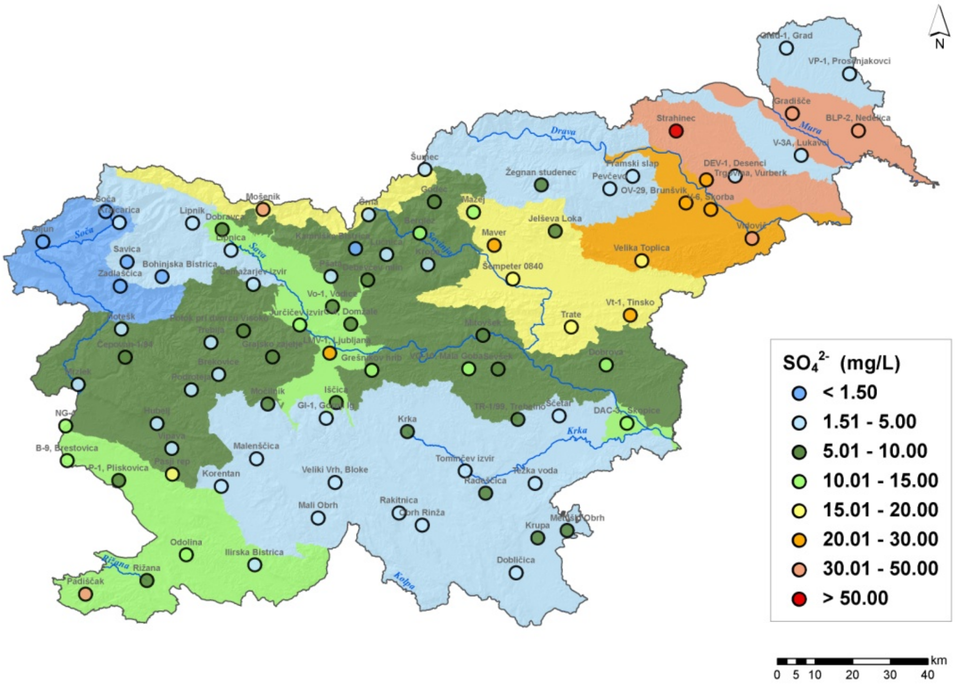

Figure 301: Spatial distribution of groundwater SO_4^{2-}

4.7.8. Trace constituents in groundwater

4.7.8.1. Iron (Fe) in groundwater

Groundwater Fe ranges between 10 and 132 µg/L with mean value of 36 µg/L and median 28 µg/L (Tab. 40). Groundwater Fe is not normally distributed (Fig. 302) and values above 94 µg/L present outliers and extremes (Fig. 303). In 123 groundwater samples the concentration of Fe was below LOD. None of water samples exceeds the allowed maximum level for drinking water (200 µg/L) according Rules on drinking water (2004).

Table 40: Descriptive statistics of groundwater Fe concentration

Parameter	n	X	Md	Min	Max	S
Fe (µg/L)	51	36	28	10	132	27

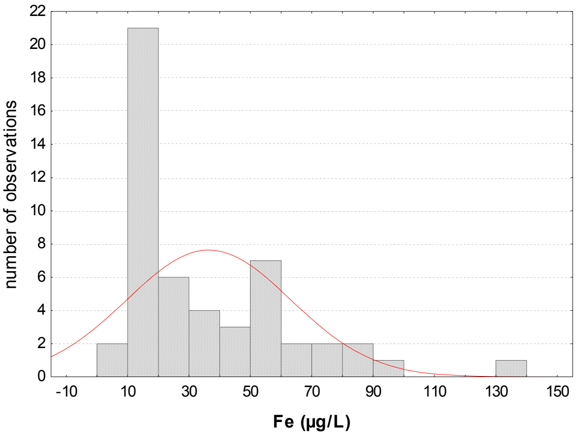

Figure 302: Histogram of groundwater Fe concentration (n=51)

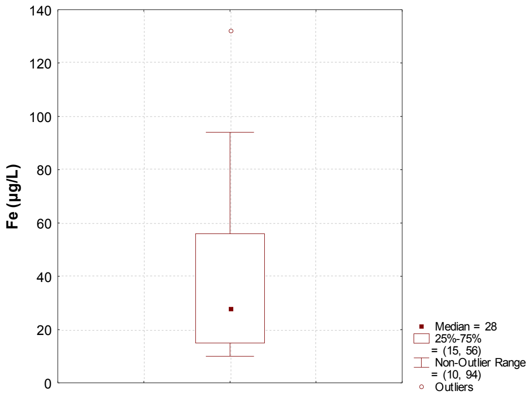

Figure 303: Box and whisker plot for groundwater Fe concentration (n=51)

The highest groundwater Fe concentrations (>70 μg/L) are observed at sampling locations B-9 Brestovica and NG-4 in the W part of the country (Fig. 304), which is possible due to type of material used for casing the borehole (steel). In this sampling location another additional possible source of iron could be due to limonite impregnation in carbonate rocks (Orehek, 1981). In deep aquifers (sampling locations GRAD-1 Grad and DEV-1 Desenci) in the NE part the source of Fe in (old) groundwater is probably due to reduction of Fe (>40 mg/L).
In other locations the level of Fe concentration is low due to prevailing oxidising conditions in observed aquifers.

Redox-sensitive solutes are e.g. As, Fe, Mn, NO_3^-, NH_4^+, SO_4^{2-}, therefore they are included in the interpretation for observations of redox conditions.

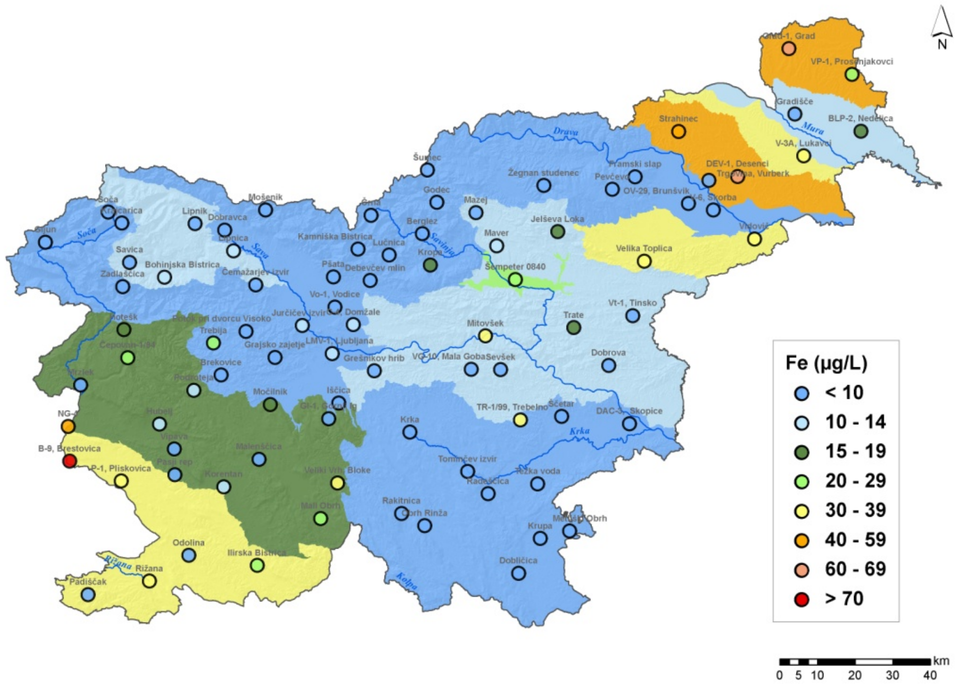

Figure 304: Spatial distribution of groundwater Fe

4.7.8.2. *Manganese (Mn) in groundwater*

Groundwater Mn ranges between 0.03 and 22.11 µg/L with mean value of 0.82 µg/L and median 0.23 µg/L (Tab. 41). Groundwater Mn is not normally distributed (Fig. 305), and values above 0.89 µg/L present outliers, and extremes (Fig. 306). In only 6 groundwater samples the conventration of Mn was belod LOD (½ LOD = 0.025 µg/L). None of water samples exceeds the allowed maximum level for drinking water (50 µg/L) according Rules on drinking water (2004).

Table 41: Descriptive statistics of groundwater Mn concentration

Parameter	n	X	Md	Min	Max	S
Mn (µg/L)	174	0.82	0.23	0.03	22.11	2.55

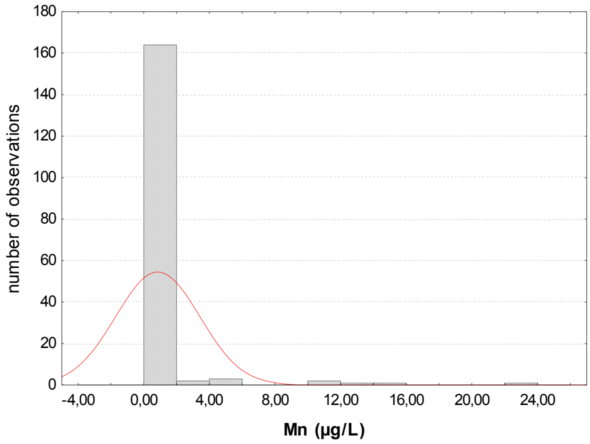

Figure 305: Histogram of groundwater Mn concentration (n=174)

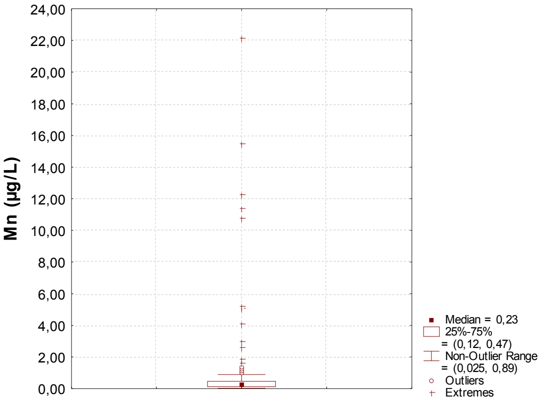

Figure 306: Box and whisker plot for groundwater Mn concentration (n=174)

Increased groundwater Mn concentrations (>1.00 µg/L) are observed in the NE part of the study area (Fig. 307), and near the coast. According to older groundwater from deeper aquifers (NE part) the highest Mn concentrations were measured at sampling location GRAD-1 Grad (As and NH_4^+ below LOD; Fe above LOD) and DEV-1 Desenci (As and Fe above LOD; NH_4^+ below LOD). It is believed that the source of Mn is increased due to strong reductive environment in deeper parts of aquifer. Lower groundwater Mn concentrations are observed in another old groundwater from sampling location VP-1 Prosenjakovci, which is younger, compared to GRAD-1 Grad and DEV-1 Desenci. This might be the reason for lower Mn concentration in groundwater. In the E side of the study area groundwater from sampling location Vidovič suggest the redox conditions in groundwater (NH_4^+ and Fe above LOD; As below LOD). At sampling location LMV-1 Ljubljana also enriched values of Mn are observed. Šajn *et al.* (1998) also observed elevated Mn concentrations in soil. Possible source is leakage from anaerobic layers where the soluble Mn^{2+} is present. Another possible source is due to use of fertilizers, or from sewage sludge.
In other groundwater samples Mn concentration was generaly low.

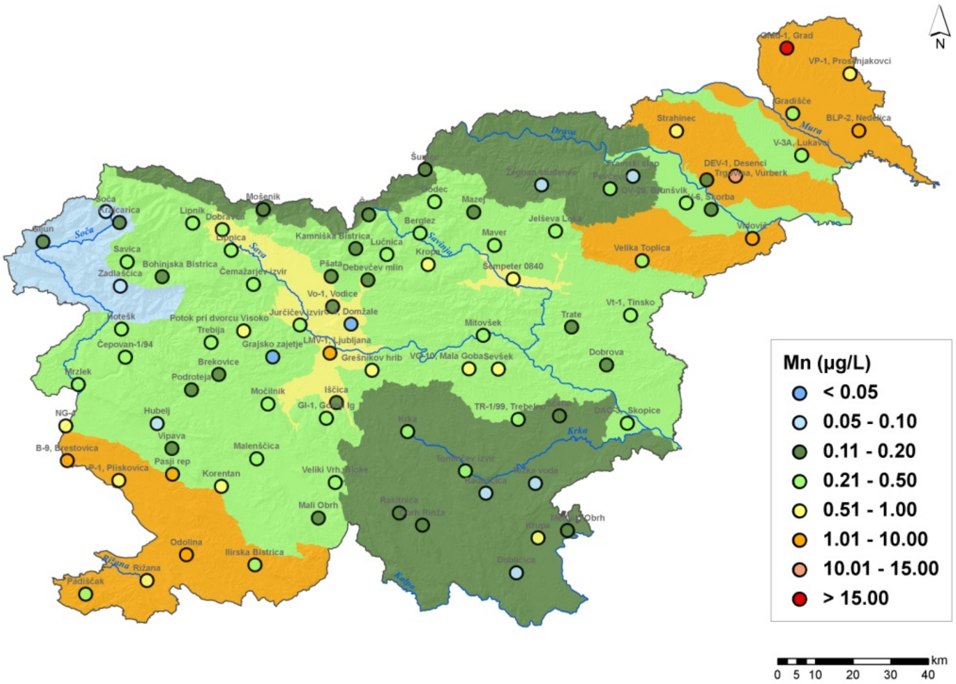

Figure 307: Spatial distribution of groundwater Mn

4.7.8.3. *Chromium (Cr) in groundwater*

Groundwater Cr concentration varies between 0.5 and 42.0 µg/L, with mean value of 1.7 µg/L and median 0.7 µg/L (Tab. 42). In 116 groundwater samples the concentration was below LOD (0.5 µg/L). Groundwater Cr concentration is not normally distributed (Fig. 308) and values above 1.3 µg/L present outliers and extermes (Fig. 309). In 97 groundwater samples the concentration of Cr was below LOD (½ LOD=0.025). None of water samples exceeds the allowed maximum level for drinking water (50 µg/L) according Rules on drinking water (2004).

Table 42: Descriptive statistics of groundwater Cr concentration

Parameter	n	X	Md	Min	Max	S
Cr (µg/L)	77	1.7	0.7	0.5	42.0	5.7

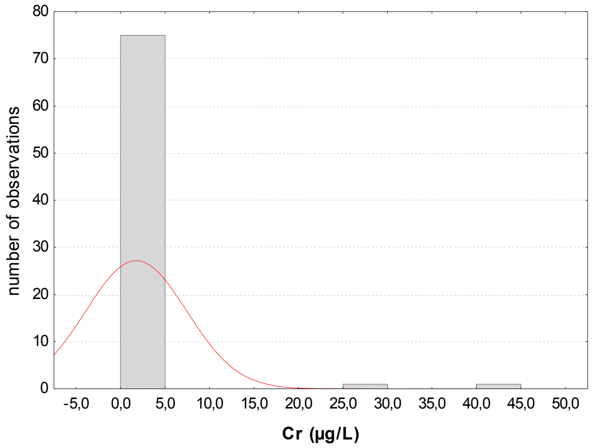

Figure 308: Histohram for groundwater Cr concentration (n=77)

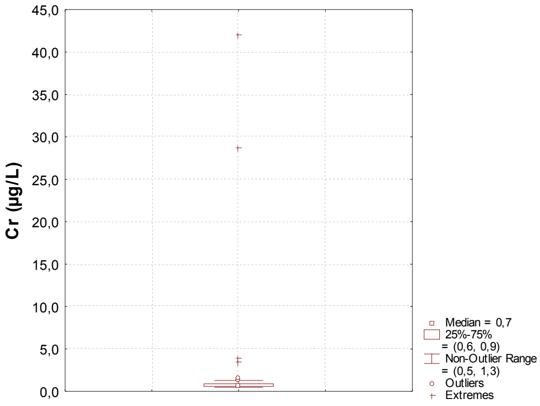

Figure 309: Box and whisker plot for groundwater Cr concentration (n=77)

Groundwater Cr concentrations 1 µg/L are found in groundwater from sampling locations: VP-1 Prosenjakovci, Framski slap, Grad-1 Grad, in the NE, NG-4 on the W, and C-4 Domžale and LMV-1 Ljubljana in the centre (Fig. 310). LMV-1 Ljubljana has the highest groundwater Cr concentrations (mean value is 35.3 µg/L). Ljubljana polje aquifer has been contaminated with Cr^{6+} in the past (1985), where the primary sources of pollution are emissions of galvanization plants at the pumping station where aggressive sewage has damaged the sewer systems and caused its spillage into the underground (Brilly *et al.*, 2003). Increased concentration of Cr^{6+} are gradually declining in Kleče pumping station, and are increasing in Hrastje pumping station (Rejec-Brancelj *et al.*, 2005). Increased Cr groundwater values at sampling location LMV have also been observed by others (Jazbinšek Seršen *et al.*, 2010; Urbanc *et al.*, 2010; Janža, 2013). Also from sampling location C-4 Domžale, the source is interpreted to be of anthropogenic origin. The source of Cr in groundwater from sampling location GRAD-1 Grad is possibly geogenic where Cr could origin from gravel, sand, and clay rocks, or organic matter (coal layers).

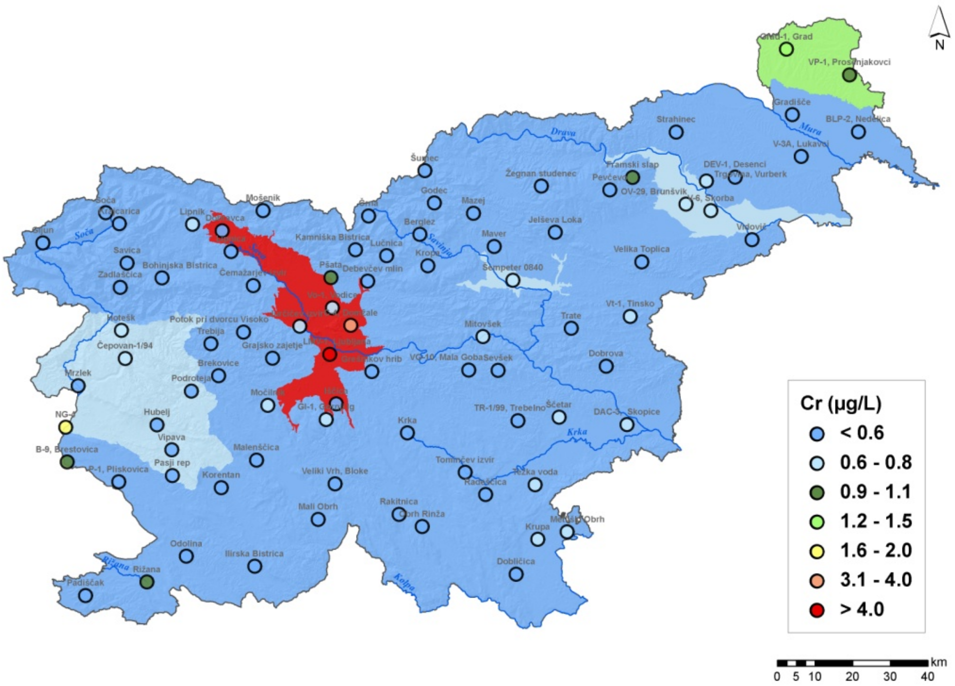

Figure 310: Spatial distribution of groundwater Cr

5. CONCLUSIONS

The main aim of the study was to identify, evaluate, and define the main factors controlling groundwater chemical and isotopic composition in Slovenian groundwaters. For this purpose groundwater was sampled at 87 sampling locations evenly distributed throughout the Slovenian territory, considering aquifers composed of the most representative lithological and lithostratigraphic units present in Slovenia.

For each sampling location its recharge area was determined according to aquifer type from which groundwater was sampled. The main factors considered were the aquifer's lithological and hydrogeological structure and its characteristics, the topology of terrain, active water protection areas, past tracer tests results, past hydro-contours, orographic watersheds and borders of groundwater bodies and aquifer systems. Based on determined sampling location's recharge areas several GIS based spatial analyses were preceded: mean altitudes, mean air temperature, mean amount of precipitation, distance from the sea, lithological and lithostratigraphic structure, and various types of land uses.

A thorough examination of results showed that chemical and isotopic parameters in groundwater vary according to geological or hydrogeological conditions in the recharge areas of aquifers. This has been proven with help of geostatistical, hydrogeochemical and hydrogeological data analysis. Statistical data analyses suggest that correlations between measured groundwater parameters are hydrochemically meaningful, describing the existing conditions of groundwater chemistry: carbonate and silicate dissolution, influence of organic matter in the soil layers, redox conditions in deeper aquifers, and anthropogenic influence.

Based on the groundwater ^{3}H activity, the sampled groundwater has been categorised as modern, submodern (up to 50 years), and old groundwater. The study is focused on groundwater sampled from shallow aquifers which has been confirmed by the ^{3}H activity measured in precipitation. Mean ^{3}H activity in recent precipitation in Ljubljana (2002—2006) is 9.0 TU, and has decreased in the last few years (5.0—9.0 TU). Similar ^{3}H activity is reflected in sampled groundwater with mean ^{3}H activity of 6.20 TU. Low ^{3}H activity (<2.00 TU) is observed in old groundwaters from deeper aquifers, and higher ^{3}H activities (>8.00 TU "nuclear bomb tritium") in sub-modern groundwater. Sub-modern groundwaters have somewhat longer residence time, most possible due to poorly permeable rocks in their recharge areas.

The most enriched in ^{18}O is groundwater at low elevations in the coastal areas while groundwater at higher altitudes and in the inner part of the country (with increasing distance from the seaside) is isotopically depleted in ^{18}O. Similar are observations of δ^2H in sampled water. Based on the groundwater isotopic data and the geographic and climatic diversity of the study area, three different isotopic altitude effects zones were defined, following the precipitation intensity pattern with general direction of SW-NE. The isotope altitude effect for Alps and Coastal region is -0.25 ‰ δ^{18}O/100 m, for the Štajerska and Dolenjska regions it is -0.27 ‰ δ^{18}O/100 m, and for the Bela krajina region -0.33 ‰ δ^{18}O/100 m. Furthermore the isotopic composition of groundwater is plotted mostly between GMWL and EMMWL suggesting the groundwater reflects the isotopic composition of precipitation discharging mostly from Atlantic air masses, as well as from the Mediterranean basin, which has been indicated by higher d-*excess* values (> 10 ‰). Comparison between groundwater δ^{18}O and distance from the Adriatic Sea to Prekmurje region (SW-NE direction) indicates the presence of a strong ^{18}O isotope effect, with a value around -8.30 ‰ δ^{18}O/1000 km. The magnitude of estimated effect is larger in comparison to precipitation isotope continental effects found in neighbouring countries. This could be due to Slovenian specific topography where air masses are influenced by relatively high altitude mountains not far from the coastal area. Additional comparison between mean annual air temperature of recharge area and groundwater isotopic composition has revealed, that groundwater from colder areas is isotopically depleted as compared to groundwater in lowlands. This is a consequence of the isotope altitude effect. The groundwater isotope temperature gradient was estimated and is around 0.25 ‰ δ^{18}O/°C. Finally, groundwater in lowlands/valleys has lower d-*excess* values compared to groundwater in high mountain regions, which could be a result of isotopic fractionation during orographically uplifted air masses, or of other processes.

Most of Slovenian groundwaters are of Ca^{2+}-Mg^{2+}-HCO_3^- and Ca^{2+}-HCO_3^- water type, dominated by earth alkali elements and weak acids. Few other water types are also observed, e.g. Na^+-Ca^{2+}-Mg^{2+}-HCO_3^-, Ca^{2+}-Mg^{2+}-HCO_3^--NO_3^-, Ca^{2+}-Na^+-HCO_3^-, Ca^{2+}-HCO_3^--SO_4^{2-}, and Ca^{2+}-Mg^{2+}- HCO_3^--SO_4^{2-}. Beside earth alkali elements and weak acidic anions, they also contain either alkali metals or strong acidic anions. In addition to ionic pattern and hydrogeochemical facies it can be concluded that sampled groundwater is predominantly controlled by the $CaCO_3$-CO_2-H_2O system where Ca^{2+}, Mg^{2+}, and HCO_3^- are the major components present in various combinations.

Groundwater in the recharge areas of carbonate rocks is generally supersaturated (SI>0) with respect to calcite and dolomite, and undersaturated (SI<0) with respect to both carbonate minerals in the recharge areas of silicate rocks (igneous and metamorphic rocks, and less permeable clastic sedimentary rocks).

Alkaline groundwater (pH>7.75) is observed in the high mountain regions dominated by carbonate rocks. Since the soil layers are usually very thin, also the microbiological activity is low. In the karstic mountain regions vegetation cover is low, but the amount of precipitation is usually high. Karstic aquifers are very open to the atmosphere. In these regions less human impact is observed. Slightly acidic groundwater (pH<7.25) is observed in the NE part of the country due to mostly prevailing silicate mineral composition of rocks in the recharge areas of igneous and metamorphic rocks, and clastics. In Podravje and Pomurje region (NE part) the soil acidity could be augmented by various agricultural practices where farmers fertilize soil with slurry or manure, or the soil is neutralized by application of lime. Additionaly, leaching from septic tanks or sewage systems can also affect groundwater pH.

Groundwater EC is increased in the alluvial plains towards NE and E, and in the coastal area (>800 µS/cm). Groundwater with increased EC occurs due to increased concentrations of soluble ions, which solution is also conditioned by the soil thickness and temperatures, and other climate factors. Additionally, EC could be influenced by the agricultural and urban land use. The lowest groundwater EC (<200 µS/cm) is observed in the high mountain regions due to thin (or non-existent) soil layer and consequently very little vegetation cover. The level of respiration of soil organisms and the decay of organic matter in the soil is low, therefore less H_2CO_3 needed for rock dissolution is formed. Also air temperatures and P_{CO2} are low, and frequent surface runoff during heavy rain or snowmelt is present.

Carbonate geochemistry (Ca^{2+}, Mg^{2+}, Ca^{2+}/Mg^{2+} molar ratio, HCO_3^- and $CaCO_3$, and P_{CO2}) depends mostly on the aquifer lithology with the carbonate mineralogical rock composition (calcite and dolomite) and carbonate cement as the main contributors to groundwater hardness. The lowest groundwater concentrations of Ca^{2+} (<24 mg/L), Mg^{2+} (<6.0 mg/L), and HCO_3^- (<140 mg/L) are observed in the NNE, NE, and central part of the country (recharge areas of shale and sandstone, gravel, sand, and clay, and igneous and metamorphic rocks). Groundwater Ca^{2+} and Mg^{2+} concentrations in high mountain karst (NW and N part) with the carbonate rocks in the recharge area are usually also low. This is a result of thin (or non-existent) soil layer and low atmospheric CO_2, which is one of the dominant drivers for carbonate dissolution. Additionally, low temperatures, and groundwater dilution by heavy precipitation water in high mountains influence the groundwater chemical and isotopic composition, together with elevated relief and tributaries of various streams. The rate of mineral weathering depends on the natural acidity of dissolved H_2CO_3 in the water which could be enhanced by the additional soil CO_2 (respiration and oxidation of organic matter), but is low due to thin soil thickness in the high mountain regions. The highest groundwater Ca^{2+} (>85 mg/L), Mg^{2+} (>25.0 mg/L), and HCO_3^- (>420 mg/L) concentrations are observed in the NE part of the country due to prevailing carbonate minerals and cement in the recharge areas, as well as thick soil layer and higher soil temperatures. In a few sampling locations the additional anthropogenic source is observed. Highly mineralized groundwater is observed in the recharge area of carbonate and clastic sedimentary rocks (NE, central, and SW part). Because Slovenia is rich in carbonate rocks, the medium hard water prevails in Slovenian groundwaters. Further high groundwater Ca^{2+}/Mg^{2+} molar ratios are observed in the recharge areas of calcium-rich rock, e.g. limestones, flysch rocks, carbonates with clastics, and clay. Low groundwater Ca^{2+}/Mg^{2+} molar ratios are found in the recharge areas of dolomite prevailing and shale and sandstone. Groundwater HCO_3^- from the carbonate recharge areas suggests good correlations with pH where higher P_{CO2} content dissolves more carbonate minerals than water with low P_{CO2} which is observed in high mountain regions with lower soil CO_2. Relation between groundwater HCO_3^- and mean altitude of recharge areas also suggests that lower groundwater HCO_3^- concentrations are measured at higher altitudes (colder air areas) and vice versa as a consequence of mineralogical composition, higher soil and atmospheric CO_2, vegetation cover, and other climatologic conditions in the recharge areas. Beside carbonate minerals also silicate minerals can contribute to groundwater Ca^{2+} and Mg^{2+} concentration, but are due to low and slow mineral weathering less significant. Groundwater Ca^{2+}, Mg^{2+}, and HCO_3^- concentration could be also influenced by the anthropogenic activities in the recharge area. The use of fertilizers, construction material, and lime can influence the rise of groundwater Ca^{2+}, Mg^{2+}, and HCO_3^- concentrations, mostly in the NE part of the country where the soil is more acidic and agricultural activities are intense.

Based on the measured groundwater HCO_3^- concentrations the initial soil CO_2 partial pressure was calculated. Calculated soil P_{CO2} content for closed system is much higher compared to content for open system. Calculated initial P_{CO2} for both, open and closed, systems were compared to soil P_{CO2} content measured on various locations around Slovenia. This reference soil P_{CO2} content coincides with calculated soil P_{CO2} content for open systems. Therefore dissolution of carbonates in sampled groundwater is assumed as an open system dissolution model. The lowest calculated initial soil P_{CO2} is observed in groundwater in high karstified mountains and low karst areas where in the recharge areas mostly bare rocks with thin layer of soil (lithosol) or forest cover are observed. Groundwater in this area has usually low initial soil CO_2 partial pressure most possible due to higher relative portion of atmospheric CO_2. High calculated initial soil P_{CO2} content (>3 vol. %) is observed in the E part of Slovenia. Recharge areas of those sampling locations are at lower altitudes, covered with thicker soil layer rendzina and brown soils type which developed on the carbonate rocks. High soil P_{CO2} contents are possible due to various reasons: the altitude and the air temperature of recharge areas, the content of measured groundwater ions (increased mineralization), and from CO_2 from deeper depths which make groundwater mineral and increases the carbonate content, and influences the groundwater in the shallow aquifers.

Groundwater DIC concentration in the high mountain regions (N and NW part) is enriched in ^{13}C (>-5 ‰) due to greater influence of atmospheric CO_2, thin (or non-existent) soil layer, carbonate rocks in the recharge area, and groundwater dilution by precipitation water. This groundwater usually contains low HCO_3^- concentration compared to groundwater in the lowland, which is rich in carbonate-bearing rocks with higher groundwater HCO_3^- concentrations. This is because this groundwater is more influenced by the degradation of organic matter and leaching of CO_2 from thicker soil layers. Most depleted in ^{13}C (<-15‰) is groundwater DIC in the recharge areas of less permeable silicate rocks located in higher altitudes. Soil CO_2 and the influence from the atmosphere mostly contribute to DIC concentration. Also depleted in ^{13}C is groundwater DIC in the NE part of Slovenia where the concentration of HCO_3^- is higher and the $\delta^{13}C$-DIC is less negative due to the dissolution of smaller proportion of carbonate minerals and carbonate cement. Groundwater $\delta^{13}C$-DIC values from deep aquifers suggests leaching of upper shallow groundwater into deeper aquifer, or the proportional share between soil CO_2 and minor share of carbonate component dissolution. In the karstic aquifers where water was sampled as surface water, it is enriched in ^{13}C due to possible degassing of CO_2 to the atmosphere and air-water isotopic exchange of carbon causing a loss of ^{13}C depleted DIC. In the S, SE, central, and NE parts of the studied area, the influence from both, dissolution of carbonate minerals and influence from the soil CO_2 is suggested. In Slovenian groundwaters the most important processes influencing groundwater according to DIC and $\delta^{13}C$-DIC in high mountains are dissolution of carbonate minerals which enrich groundwater DIC in ^{13}C, and and the partial pressure of atmospheric CO_2 which depends on the altitude air temperature. In groundwater recharge areas of lowlands dissolution of carbonates play an important role as well as soil partial pressure of CO_2 which depends on the altitude, air temperature, and vegetation cover.

The source of Si in groundwater is almost exclusively and unequivocally a result of water-rock interaction. This has been verified with a simple modelling which results suggest that the main source of Si in groundwater is silicate weathering. Increased groundwater Si concentrations (>6.00 mg/L) are observed in the NE part of the country in the shallow and deep aquifers, at Pohorje Mt., and in few other sampling locations where silicate minerals in the recharge areas of clastic sedimentary, igneous, and metamorphic rocks prevail. Low groundwater Si concentration (<3.00 mg/L) is observed in all other parts of Slovenia due to prevailing carbonate rocks in the recharge areas.

The main sources of Na^+ and Cl^- in Slovenian groundwaters are anthropogenic as a result of agricultural and urban land uses. Increased groundwater Na^+ (>10.0 mg/L) and Cl^- (>15.00 mg/L) can occur due to excessive use of fertilizers, slurry and/or manure on the fields, orchards, vineyards, and gardens. Additionally, increased groundwater Na^+ and Cl^- are also due to use of salts for deicing roads which are mostly dense in the big cities above highly vulnerable alluvial aquifers. Other important anthropogenic sources of groundwater Na^+ and Cl^- are also leakages from sewage systems or septic tanks (mostly in the NE part of the country). Natural sources of both ions are less pronounced but also important, like the influence from the seaside as precipitation or sea spray, and ion exchange for Na^+ in the recharge areas of clay. Sources of silicate rocks weathering are subordinate compared to anthropogenic influences. Lower groundwater Na^+ (<2.0 mg/L) and Cl^- (<2.00 mg/L) concentrations are observed in the recharge areas with carbonate rocks in the NW and N part of the country mostly due to prevailing carbonate minerals in the recharge areas, groundwater dilution by heavy precipitation (increased in NW and N part of the country), and lower level of urban and agricultural activities. In the lowlands in the SE and E parts with mostly carbonate rocks in the recharge areas the concentrations of both ions is slightly increased most possible due to anthropogenic influence. Natural background level for groundwater Na^+ is 1.5 mg/L and for Cl^- 1.72 mg/L.

Main groundwater NO_3^- sources are anthropogenic which include the (excessive) use of nitrogen (organic and synthetic) fertilizers, or leakages from septic tanks or sewage systems. Concentrations of NO_3^- in groundwater depend mostly on the type of land use in the recharge area, especially on the intensity of fertilizers usage. The natural background level for groundwater NO_3^- was estimated only for groundwater in shallow aquifers and is 3.81 mg/L. Since agricultural activities are mostly present in lowlands, increased groundwater NO_3^- concentrations (>50.00 mg/L) are observed in the intergranuar aquifers along larger rivers (central, E, and NE part). Groundwater NO_3^- concentration in the NW, W, and NNE part are low (<3.00 mg/L) because agricultural land use is not intense. Low groundwater NO_3^- concentrations are also observed in groundwater from deeper aquifers (<3.00 mg/L) most possibly due to low initial NO_3^- concentrations or due to denitrification processes in the groundwater recharge areas. In addition to NO_3^- the occurrence of NH_4^+ in groundwater is perhaps due to excessive use of inorganic or organic fertilizers (ammonium sulphate, manure or slurry), especially in the late summer together with increased groundwater NO_3^- concentration. The presence of NH_4^+ in groundwater is also possible because of reduced access of oxygen in to water (reductive environment).

Groundwater depletion in ^{15}N suggests the origin of nitrogen in groundwater is of naturally occurring nitrate in precipitation and soil organic matter observed mostly in the NW and NNE part of the study area. In the NW part groundwater is depleted in ^{15}N (<-1.0 ‰) because of alpine vegetation and thin soil layer, whereas in the recharge areas of forest vegetation in high mountains with thick soil layer the groundwater is slightly enriched in ^{15}N (<2.5 ‰) with prevailing natural nitrogen from soil. The most enriched in ^{15}N (>10.0 ‰) is groundwater in lowlands of alluvial plains in the NE and E part. Here intense agricultural activities are present, where the use of synthetic and organic fertilizers is observed. Application of manure on the fields or leakages in groundwater is possible. Groundwater in deeper aquifers is probably denitrified and enriched in ^{15}N (5.0 – 7.5 ‰).

Increased groundwater K^+ concentrations (> 5.00 mg/L) are observed in lowlands in the NE part (Mursko polje and Dravsko polje aquifers). The source of groundwater K^+ could be geogenic due to prevailing silicate rocks in the alluvial deposits in the recharge areas. But because of intense agricultural activities in this part of country and excessive use of nutrients and plant protection products, it is believed that silicate weathering is of minor importance as a source of K^+ in groundwater. Also near the coast the original geogenic footprint from the sea in groundwater is also smudged due to possible use of fertilizers or waste water. Groundwater K^+ concentrations are low (<0.50 mg/L) in the recharge area of carbonate rocks in the high mountain karst and in classic Dinaric (Dolenjska) karst due to lack of potassium-bearing minerals and minor impact of agricultural activities. The natural background level for K^+ in Slovenian groundwaters is 0.35 mg/L.

Sources of SO_4^{2-} in Slovenian groundwaters are mostly of anthropogenic origin where increased concentrations (>20.00 mg/L) are observed in the NE part of the study area due to use of fertilizers on agricultural land. Around densely populated regions the sources for increased groundwater SO_4^{2-} concentrations could be due to SO_2 emission. Geogenic sources of SO_4^{2-} in groundwater are observed in the N part of the country (Karavanke Mts.) as a consequence of dissolution of gypsum inclusions in the carbonate rocks, as well as near the coastal part because either from the seawater influences, or weathering of sulphide minerals. Low groundwater SO_4^{2-} concentrations (<5.00 mg/L) are observed in the high mountains in NW part, and in low karstic regions in central and SE part of the study area, due to lack of intense agricultural and urban land uses, and silicate minerals in the recharge areas. Low groundwater SO_4^{2-} concentrations are also observed in older groundwater which is possible due to degradation through natural reduction reactions. Natural background level for SO_4^{2-} in Slovenian groundwaters is 6.93 mg/L.

Although dissolved oxygen was not measured in the groundwater other observed parameters (Fe, Mn, As, and NH_4^+) suggest a reductive groundwater environment. Since their concentrations in groundwater are very low, it is assumed that sampled groundwater is mostly oxidized.
High groundwater Fe (>70 µg/L) is observed in the NW part because of type of material used for caving the borehole (steel), or due to limonite impregnation in carbonate rocks and rare brown limonite particles. In old groundwater from deep aquifers in the NE part of country the source of Fe (>40 mg/L) is probably the dissolution of Fe from rocks in the reducing chemical environment. In other locations Fe concentration is low (<10 µg/L) due to prevailing carbonate minerals in the recharge areas and oxidising conditions in the observed aquifers.
Increased groundwater Mn concentrations (>1.00 µg/L) are observed in the NE part of the study area, near the coast, and in the central part of the country. In old groundwater (NE) the source is possible due to strong reductive environment in deeper parts of aquifer, and in the location near the coast the source of Mn could be related to organic matter in the water. In the central part the possible source of Mn in groundwater is leakage from anaerobic layers where the soluble Mn^{2+} is present. Other possible sources are also use of fertilizers, or leakages from sewage sludge.

Increased groundwater Cr is observed in the central part of the country which is a consequence of groundwater contamination with Cr^{6+} in the past where the primary sources of pollution are emissions of galvanization plants, as well as other anthropogenic sources. In the NE part in groundwater from deeper aquifers the source of Cr is possibly of geogenic origin where Cr could be drived from gravel, sand, and clay rocks, or organic matter (coal layers).

Main factors controlling Slovenian groundwaters geochemical composition are summarized in the following table.

Table 43: Main factors controlling Slovenian groundwaters geochemical composition

SOURCE	Natural									Anthropogenic					
Factor	lithology mineralogical composition, cement)	climatic factors	morphology (altitude)	distance from the sea	soil thickness	type of vegetation cover	amount of precipitation	reductive environment	natural fertilization	deicing roads	fertilizers	lime application	leakage from sewage system, septic tanks, waste waster	casing material	air pollution
EC	X	X	X	X	X		X			X	X		X		
$\delta^{18}O$		X	X	X											
δD		X	X	X											
d-*excess*		X	X	X											
$\delta^{13}C$-DIC	X	X			X	X	X								
$\delta^{15}N_{tot}$						X		X	X		X		X		
^{3}H	X														
Ca^{2+}	X	X	X		X		X				X	X			
Mg^{2+}	X	X	X		X		X				X	X			
Na^{+}	X			X						X	X		X		
K^{+}	X			X							X		X		
NH_4^{+}								X	X		X		X		
HCO_3^{-}	X	X	X		X		X					X			
Cl^{-}	X			X						X	X		X		
NO_3^{-}									X		X		X		
SO_4^{2-}	X	X		X							X				X
Si	X	X					X								
As	X							X							
B	X										X		X		
Br	X			X									X		
Cr	X												X		
Fe	X							X						X	
Mn	X							X			X				

All above listed conclusions confirm the hypothesis, set at the begining of the research:

→ *the main natural factors controlling Slovenian groundwater chemical and isotopic composition are lithological composition of the aquifer recharge area and recharge area climatic conditions,*

Observations of chemical and isotopic composition in Slovenian groundwater in relation to lithostratigraphic composition and climatic conditions in groundwater recharge areas have confirmed the hypothesis, that natural groundwater geochemistry and isotopic composition are controlled in great extent by natural factors. Namely, groundwater Ca^{2+}, Mg^{2+}, HCO_3^-, and Si concentrations mostly depend on the mineralogical composition of rocks in the recharge areas, and various climate conditions as well as other natural factors, e.g., the altitude, air temperature, the amount of precipitation, thickness of soil horizon and vegetation cover of groundwater recharge areas, and also distance from the sea. Groundwater isotopic composition ($\delta^{18}O$, δD, d-*excess*, and ^3H) is being controlled by the direction of air masses, the amount of precipitation, altitude, air temperature, snow coverage, distance from the sea, and hydrogeological characteristics of the aquifer (permeability of rocks). Isotopic composition of groundwater $\delta^{13}C$-DIC depends on the thickness of soil horizon, mineralogical composition of rocks, and vegetation cover in groundwater recharge area. Groundwater $\delta^{15}N$ is mostly controlled by the type of vegetation cover in groundwater recharge area.

→ *chemical composition of anthropogenically influenced groundwater mostly depends on the land use in the groundwater recharge areas.*

Geochemistry of anthropogenically influenced groundwater has proven the hypothesis that the type of land use in the groundwater recharge areas influences the chemical composition of groundwater. In Slovenian groundwater the major anthropogenic factors influencing the groundwater chemical status are agricultural land use reflected in increased Na^+, K^+, NO_3^-, Cl^-, and SO_4^{2-} concentration, and urban land use reflected in increased Na^+, Cl^-, and SO_4^{2-} concentration.

With respect to objectives:

→ *to determine the optimal methodology for geochemical research of Slovenian groundwater regarding the sampling network density, data processing, interpretation of results, and data presentation,*

The methodology for geochemical research of Slovenian groundwater, based on the sampling network density, data processing, interpretation of results, and data presentation, has proven to be useful and economic. Groundwater was sampled in the recharge areas of the most typical lithological and lithostratigraphic units present in Slovenia. Additionally, the sampling locations were evenly distributed throughout Slovenian territory and are located in aquifers with various porosity types. Groundwater in each sampling location was sampled twice in order to get a more typical groundwater value of studied parameters. Further the obtained results of groundwater chemical and isotopic composition were statistically processed where the most important correlations between measured parameters and in correlation with climatic factors, as well as land use data, were observed and interpreted. Finally, the methodology used has provided the data on the typical groundwater values of observed parameters as well as the natural background levels for chosen parameters. Final products are also hydrochemical thematic maps which provide the information on spatial distribution of observed parameters in Slovenian groundwaters. Based on the available financial sources, sampling material, and time, it was possible to achieve predicted objectives.

→ *to identify typical Slovenian groundwater chemical and isotopic composition in relation to lithological and lithostratigraphic units,*

The study provides the information on typical groundwater (mean) values of observed groundwater chemical and isotopic parameters according to certain lithological and lithostratigraphic units, where the sources of natural and anthropogenic origin are combined due to land use. Each observed parameter was studied in detail, and its source was identified according to the lithological composition, climatic factors, and land use data in the groundwater recharge areas.

→ *to identify and quantify the main factors controlling different chemical and isotope parameters in Slovenian groundwater and to interpret the role of each factor,*

Groundwater chemical and isotopic composition of Slovenian groundwaters is controlled by natural and/or anthropogenic factors. Regarding the natural factors the lithological composition and climatic factors play the major role, whereas the agricultural activities and urban land use dominate as anthropogenic factors.
Based on the land use data it was possible to quantify the major anthropogenic sources in the groundwater. Observed parameters NO_3^-, Na^+, Cl^-, K^+, and SO_4^{2-} are typical constituents of many fertilizers, where its excess usage on arable lands is commonly reflected in groundwater chemical (and isotopic) composition. Leakages from septic tanks or sewage system, as well as use of animal manure and slurry also affect groundwater quality. In urban areas the use of salt for deicing roads has proven to be important as well.

→ *to develop the optimal methodology for evaluation of natural background levels (NBLs) in groundwater for selected chemical parameters according to specific Slovenian hydrogeological conditions,*

Methodology which has been developed for evaluation of natural background levels (NBL) in groundwater for chemical parameters according to Slovenian hydrogeological conditions has proven to be very applicable. In order to determine the natural background level for groundwater chemical parameters, the shares of anthropogenic influences in the recharge areas of sampled groundwaters was estimated and were correlated with the concentrations of observed parameters. The share of anthropogenic influence up to 20 % in the recharge areas was estimated as the natural recharge area. The natural background levels (NBLs) in Slovenian groundwater were determined only for selected chemical parameters (NO_3^-, Na^+, Cl^-, K^+, and SO_4^{2-}) because their anthropogenic sources overshadows the natural source (except for NO_3^-). This methodology provides the possibility for the evaluation of natural background levels (NBLs) of recent groundwater because the majority of groundwater was sampled in natural recharge areas with less significant anthropogenic influence, which could not be excluded in some sampling locations. Additionally, groundwater chemical and isotopic analyses were performed in the same laboratories during 2009-2011, and the results are therefore not only mutually comparable, but they also provide the most recent groundwater status in Slovenian groundwater. In comparison to other methodologies for determination of natural background levels (NBL) in groundwater this method requires less groundwater samples, which saves time and money.

→ *to prepare various hydrochemical thematic maps of the main hydrochemical and isotope parameters for the whole Slovenian territory. Thematic maps display typical concentrations of studied hydrochemical parameters for individual sampling locations and whole groundwater bodies.*

Hydrochemical thematic maps are the first ones of this kind ever made for Slovenian groundwater. They provide the information on the typical groundwater concentrations of studied hydrochemical and isotopic parameters in observed sampling locations, as well as for groundwater bodies. These hydrochemical thematic maps could be used for various purposes: planning of utilization of water resources for drinking water and technological purposes, water resources protection planning, for assessment of water vulnerability and sustainable management with groundwater, and in households. Finally, these maps could help to efficiently manage groundwater water bodies in Slovenia, as part of Water Frame Directive (2000/60/EC) and its Daughter Groundwater Directive (2006/118/EC) which both comprise the determination of natural background levels, and provide the basic information on the hydrochemical situation in aquifers.

6. SUMMARY

Groundwater is a globally important, valuable and renewable resource. Its chemical status significantly influences the use of groundwater for domestic uses, irrigation and agriculture, for livestock, in food-processing industry, for technological and recreational purposes. Despite numerous routine chemical and isotopic analyses on water sources in Slovenia a comprehensive research on chemical or isotopic characteristics of groundwater has not been conducted so far. Additionally, no comprehensive researches on the identification of the dominant parameters and mechanisms affecting chemical and isotopic composition of groundwater in Slovenia, as well as any detailed interpretation of groundwater's isotopic composition do exist. Additionally, hydrogeochemical map of Slovenia is still not available, and neither are the bases for determination of the reference state for the assessment of good chemical status of groundwater according to WFD (2000/60/EC) and Daughter Directive (2006/118/EC).

In order to provide expert basis for future work regarding mentioned issues, groundwater in Slovenia has been systematically sampled during past few years. The main purposes of the thesis were to identify whether the Slovenian groundwater chemical and isotopic composition is controlled by natural factors like lithological composition of the aquifer recharge area and recharge area climatic conditions. Additionally the aim was to declare to what extend and in which manner the groundwater chemical and isotopic composition depend on the land use in the groundwater recharge areas. The optimal methodology for geochemical research of Slovenian groundwater was identified according to sampling network density, data processing, interpretation of results, and data presentation. For evaluation of groundwater natural background levels for selected chemical parameters according to specific Slovenian hydrogeological conditions, another methodology was developed as well. Additionally this study also provides the typical values of measured hydrochemical parameters in groundwater for observed sampling locations and groundwater bodies.

The concept of sampling network was designed in such a way that groundwater was sampled in locations which recharge areas are in most representative lithological and lithostratigraphic units found in Slovenia. Additionally sampling locations were evenly distributed throughout Slovenian territory, and are located in aquifers with various porosity types. From each sampling location during the 3-year study (2009-2011) groundwater was sampled twice in order to get the typical groundwater values of observed parameters. Groundwater was sampled according to standard procedures for sampling where in the field the groundwater pH, T, and EC were measured, and groundwater was sampled for the following major ions: Ca^{2+}, Mg^{2+}, Na^{+}, K^{+}, HCO_3^{-}, NO_3^{-}, Cl^{-}, SO_4^{2-}, S and Si; major secondary ions: B, Ba, Fe, NH4+, P, Sr, and Zn; and trace constituents: Ag, Al, As, Au, Be, Bi, Br, Cd, Ce, Co, Cr, Cs, Cu, Dy, Er, Eu, Ga, Gd, Ge, Hf, Hg, Ho, In, La, Li, Lu, Mn, Mo, Nb, Nd, Ni, Pb, Pd, Pr, Pt, Rb, Re, Rh, Ru, Sb, Sc, Se, Sm, Sn, Ta, Tb, Te, Th, Ti, Tl, Tm, U, V, W, Y, Yb, and Zr; stable isotopic composition of oxygen ($^{18}O/^{16}O$), hydrogen ($^{2}H/^{1}H$), carbon ($^{13}C/^{12}C$) and nitrogen ($^{15}N/^{14}N$); and tritium (^{3}H). Groundwater samples were sent out to various laboratories for analyses.

For each sampling location its representative recharge area was determined according to the aquifer porosity type from which groundwater was sampled considering the aquifer's lithological and hydrogeological structure and its characteristics (openness, depth), the topology of terrain, active water protection areas, past tracer tests results, past hydro-contours, orographic watersheds and borders of groundwater bodies and aquifer systems. Based on determined recharge areas of sampling locations several spatial analyses were preceded: altitudes, air temperature, and amount of precipitation, distance from the sea, lithological and lithostratigraphic structure, and land use. These data was used for further comparison between groundwater chemical and isotopic composition.

Statistical analyses of data suggest that correlations between measured groundwater parameters are hydrochemically meaningful and are describing groundwater chemistry: dissolution of carbonate and silicate minerals, ion exchange reactions, redox conditions, and anthropogenic input.

According to ^{3}H activity in precipitation sampled groundwater was categorised as modern, submodern and old groundwater, with prevailing modern groundwater in shallow Slovenian aquifers. Stable isotopic composition of oxygen and deuterium provided the information on the mean altitude of recharge areas, and d-excess on the recent precipitation recharge from prevailing Atlantic and Mediterranean air masses. Based on the groundwater isotopic data as well as the geographic and climatic diversity of the study area, three different isotopic altitude effects zones were defined, following the precipitation intensity pattern: Alps and Coastal region (-0.25 ‰ δ^{18}O/100 m), Štajerska and Dolenjska regions (-0.27 ‰ δ^{18}O/100 m), and Bela krajina region (-0.33 ‰ δ^{18}O/100 m). The groundwater isotope continental effect is around 0.83‰ δ^{18}O/100 km. The groundwater isotope temperature gradient was estimated, and is around 0.25 ‰ δ^{18}O /°C.

The dominant water types in Slovenian groundwater are of Ca^{2+}-Mg^{2+}-HCO_3^- and Ca^{2+}-HCO_3^- water type, followed by Na^+-Ca^{2+}-Mg^{2+}-HCO_3^-, Ca^{2+}-Mg^{2+}-HCO_3^--NO_3^-, Ca^{2+}-Na^+-HCO_3^-, Ca^{2+}-HCO_3^--SO_4^{2-}, and Ca^{2+}-Mg^{2+}-HCO_3^--SO_4^{2-}. Groundwater concentrations of Ca^{2+}, Mg^{2+}, and HCO_3^- are of natural origin and depend on dissolution of carbonate rocks in relation with the altitude, air temperature, partial pressure of CO_2 from the atmosphere and soil, amount of precipitation, and vegetation cover. Based on the Ca^{2+}/Mg^{2+} molar ratios it was possible to determine the prevailing type of carbonate rock in the recharge areas (dolomite or limestone). Mostly dissolved carbonate minerals contribute to water hardness. Based on the groundwater HCO_3^- concentrations in the recharge areas of carbonate rocks the initial soil CO_2 partial pressures concentration was evaluated. The groundwater δ^{13}C-DIC values provided additional information on groundwater processes where the share of contribution to DIC for atmospheric and soil CO_2, and carbonate minerals, can be estimated. The source of Si in groundwater is almost exclusively and unequivocally a result of water-silicate rock interaction. Concentration of other major groundwater ions like Na^+ and Cl^- suggest the dominant origin from the NaCl used for deicing roads during winter, use of manure and slurry on the fields, fertilizers, and leakage from sewage systems or septic tanks. Natural sources are less pronounced but also important, like the influence from the sea by the precipitation or sea spray, and ion exchange in clay recharge areas for Na^+, and silicate weathering. Estimated natural background levels for Na^+ and Cl^- concentration in Slovenian groundwater are 1.5 mg/L and 1.70 mg/L, respectively. Main groundwater NO_3^- sources are of anthropogenic origin as nitrogen fertilizers (manure and slurry, and synthetic fertilizers), or a leakage of septic tanks or sewage systems. The natural background level for groundwater NO_3^- concentration is 3.81 mg/L. The occurrence of NH_4^+ in groundwater is perhaps due to excessive use of inorganic of organic fertilizers, or due to reduced access of oxygen into groundwater. Based on the groundwater $\delta^{15}N_{tot}$ values it was possible to identify the naturally occurring nitrate in precipitation and soil organic matter, or from anthropogenic sources (synthetic and organic fertilizers, manure or slurry, leakage from sewage or septic tanks). Groundwater in deeper aquifers is enriched in ^{15}N probably due to denitrification. Also important nutrient beside NO_3^- is K^+. Groundwater K^+ concentration suggest the prevailing anthropogenic origin by the excessive use of fertilizers or influence of waste waters. The natural background level for groundwater K^+ concentration is 0.35 mg/L. Sources of groundwater SO_4^{2-} in Slovenian groundwater are mostly anthropogenic (use of fertilizers and in SO_2 emissions), and to lesser extend natural (weathering of gypsum and sulphide minerals, proximity of sea side). Natural background level for SO_4^{2-} concentration in Slovenian groundwater is SO_4^{2-} 6.93 mg/L. Concentration of majority of trace elements analysed in groundwater were below LOD. The sources of groundwater Fe are due to type of material used for borehole casing, or due to limonite impregnation in carbonate rocks and rare brown limonite particles, or due to dissolution of Fe from rock in the geochemical reduction environment (deep aquifers). Reductive conditions are also identified by increased groundwater Mn (and As) concentrations in deeper aquifers, as well as in shallow groundwater possible due to presence of organic matter or leakage from anaerobic layers where soluble Mn^{2+} is present. The source of groundwater Cr is mostly of anthropogenic origin as a consequence of contamination Cr^{6+} in the past by the emissions of galvanization plants.

The final results also provide the information on typical groundwater concentrations of observed chemical and isotopic parameters according to certain lithological and lithostratigraphic units in the recharge areas as well as natural background levels for selected chemical parameters. Additionally hydrochemical thematic maps from which the spatial distribution of observed parameters is evident.

POVZETEK

Podzemna voda je izredno pomemben, cenjen in obnovljiv naravni vir. Kemijsko stanje podzemne vode bistveno vpliva na njeno uporabo, tako v gospodinjstvu, kmetijstvu in živilsko-predelovalni industriji, kot tudi za tehnološke in rekreacijske namene. Kljub temu, da je bilo na posameznih vodnih virih opravljenih veliko rutinskih kemijskih in izotopskih raziskav podzemne vode, v Sloveniji do sedaj še ne razpolagamo s celovitejšim pregledom analiz na celotnem območju Slovenije. Prav tako do sedaj še ni bila izdelana študija, v kateri bi bili podrobneje obravnavani parametri in procesi v podzemni vodi, ki vplivajo na njeno kemijsko in izotopsko sestavo. Za slovenske podzemne vode še niso bile izdelane tematske karte kemijske in izotopske sestave, prav tako še ne obstajajo osnove za določitev referenčnega stanja dobrega kemijskega stanja podzemne vode v skladu z vodno direktivo (2000/60/EC) in direktivo o varstvu podzemne vode pred onesnaževanjem in poslabšanjem (2006/118/EC).

Glede na omenjeno problematiko sem v sklopu predstavljene študije v preteklih letih sistematično vzorčila podzemno vodo z namenom, da bi ugotovila kateri faktorji vplivajo na kemijsko in izotopsko sestavo podzemne vode v Sloveniji. Predpostavila sem, da med naravnimi dejavniki najbolj vplivajo litološka zgradba vodonosnika in klimatski pogoji v napajalnem zaledju vodonosnika. Prav tako me je zanimalo v kakšni meri vplivajo na kemijsko in izotopsko sestavo podzemne vode antropogeni faktorji z rabo tal. V ta namen sem uporabila optimalno metodologijo za geokemijsko raziskovanje podzemnih vod v Sloveniji glede na gostoto vzorčne mreže, obdelavo, interpretacijo in predstavitev rezultatov. Glede na posebne hidrokemijske pogoje, ki prevladujejo v Sloveniji, sem za oceno naravnih kemijskih ozadij za izbrane parametre v podzemni vodi izdelala dodatno metodologijo. V predstavljeni študiji prav tako podajam tipične vrednosti merjenih geokemijskih parametrov v podzemni vodi na posameznih opazovanih vzorčnih mestih in vodnih telesih.

Mrežo vzorčnih mest sem izbrala tako, da so bila vzorčna mesta enakomerno razporejena po celotnem ozemlju Slovenije ter da so pokrivala tiste vodonosnike podzemne vode, ki so zgrajeni iz najpogosteje pojavljajočih se litoloških in litostratigrafskih enot v Sloveniji z različnimi tipi poroznosti. Na vsakem vzorčnem mestu sem med triletnim vzorčenjem (2009-2011) podzemno vodo vzorčila dvakrat v skladu s standardi SIST z namenom, da bi pridobila tipične vrednosti opazovanih parametrov v podzemni vodi. Na terenu sem izmerila fizikalno-kemijske parametre v podzemni vodi kot so pH, T in električna prevodnost (EC). Vzorce vode sem odvzela za sklop parametrov med katerimi so v laboratorijih vzorčili glavne ione (Ca^{2+}, Mg^{2+}, Na^{+}, K^{+}, HCO$_3^{-}$, NO$_3^{-}$, Cl^{-}, SO$_4^{2-}$, S in Si), drugotne glavne ione (B, Ba, Fe, NH$_4^{+}$, P, Sr, in Zn), sledne prvine (Ag, Al, As, Au, Be, Bi, Br, Cd, Ce, Co, Cr, Cs, Cu, Dy, Er, Eu, Ga, Gd, Ge, Hf, Hg, Ho, In, La, Li, Lu, Mn, Mo, Nb, Nd, Ni, Pb, Pd, Pr, Pt, Rb, Re, Rh, Ru, Sb, Sc, Se, Sm, Sn, Ta, Tb, Te, Th, Ti, Tl, Tm, U, V, W, Y, Yb, in Zr) ter izotopsko sestavo stabilnih izotopov (δ^{18}O, $\delta^{2}H$, δ^{13}C-DIC in δ^{15}N$_{tot}$) in radioaktivni izotop tritij (^{3}H).

Vsakemu vzorčnemu mestu sem določila napajalno zaledje glede na tip poroznosti vodonosnika, litološko sestavo, hidrogeološko strukturo in ostale karakteristike vodonosnika (odprtost, globina), morfologijo terena, aktivne vodovarstvene pasove, pretekle sledilne preizkuse, pretekle hidroizohipse, orografske razvodnice in meje z vodnimi telesi ter vodonosnimi sistemi. Na osnovi določenih zaledij sem izdelala prostorske analize za določitev srednje nadmorske višine, srednje temperature zraka, srednje količine padavin, oddaljenost vzorčnega mesta od morja, delež zastopanosti posameznih litoloških in litostratigrafskih enot ter delež posameznega tipa rabe tal. Rezultate prostorskih analiz sem uporabila za primerjavo s podatki kemijske in izotopske sestave podzemne vode, da bi ugotovila njihovo medsebojno odvisnost.

Statistična analiza podatkov je pokazala, da obstajajo statistično značilne hidrokemijske povezave med opazovanimi parametri v podzemni vodi, ki so posledica nekaterih glavnih geokemijskih procesov v podzemni vodi: raztapljanje karbonatnih in silikatnih mineralov, ionska izmenjava, prisotnost redoks pogojev in vpliv antropogenih dejavnikov.

Glede na koncentracijo ^{3}H v padavinski in podzemni vodi sem podzemne vode razvrstila v razrede in sicer v mlade, srednje mlade in stare podzemne vode. Analizirana podzemne vode je večinoma mlada (recentna) voda, ki predstavlja podzemno vodo iz plitvih vodonosnikov. Na osnovi izotopske sestave kisika in vodika v podzemni vodi sem pridobila informacijo o srednji nadmorski višini napajalnega zaledja in na podlagi devterijevega presežka informacijo o recentnem napajanju vodonosnikov s padavinsko vodo prevladujočih zračnih mas severnega Atlantika in območja Sredozemlja. Z izotopsko sestavo kisika in vodika v podzemni vodi in s podatki o geografski in klimatski raznolikosti slovenskega ozemlja sem določila 3 različne višinske izotopske efekte glede na intenziteto padavinskega vzorca (JZ-SV): Alpska in Primorska regija (-0,25 ‰ δ^{18}O/100 m), Štajerska in Dolenjska regija (-0,27 ‰ δ^{18}O/100 m) in Bela krajina (-0,33 ‰ δ^{18}O/100 m). Celinski izotopski efekt v podzemni vodi je bil ocenjen na okoli -0,83 ‰ δ^{18}O/100 km in izotopski temperaturni gradient okoli 0,25 ‰ δ^{18}O/°C.

V Slovenskih podzemnih vodah prevladuje Ca^{2+}-Mg^{2+}-HCO_3^- in Ca^{2+}-HCO_3^- tip vode, in v manjši meri Na^+-Ca^{2+}-Mg^{2+}-HCO_3^-, Ca^{2+}-Mg^{2+}-HCO_3^--NO_3^-, Ca^{2+}-Na^+-HCO_3^-, Ca^{2+}-HCO_3^--SO_4^{2-} in Ca^{2+}-Mg^{2+}-HCO_3^--SO_4^{2-} tip vode. Koncentracije ionov Ca^{2+}, Mg^{2+} in HCO_3^- v podzemni vodi so naravnega izvora in so odvisne od raztapljanja karbonatnih kamnin in nadmorske višine, temperature zraka, parcialnega tlaka CO_2 iz atmosfere in tal, količine padavin in vegetacijskega pokrova v napajalnem zaledju. Na podlagi molarnega razmerja med Ca^{2+} in Mg^{2+} v podzemni vodi sem ugotavljala prevladujoč tip karbonatnih kamnin v zaledju (dolomit ali apnenec). Prav tako sem na podlagi omenjenih ionov ugotavljala trdoto podzemne vode v Sloveniji. Ker na raztapljanje karbonatnih kamnin vpliva tudi parcialni tlak CO_2 v tleh, sem le-tega izračunala na podlagi izmerjene koncentracije HCO_3^- v podzemni vodi. Na osnovi izotopske sestave raztopljenega anorganskega ogljika (δ^{13}C-DIC) sem lahko ocenila delež doprinosa posameznih virov ogljika v podzemno vodo. Poleg raztapljanja karbonatnih mineralov se v slovenskih vodah prav tako odraža raztapljanje silikatnih mineralov, saj je vir silicija (Si) v podzemni vodi naravnega izvora. Kot glavni vir natrija (Na^+) in klora (Cl^-) v podzemni vodi sem določila soljenje cest v zimskem obdobju, uporabo gnoja in gnojevke na poljih, uporabo gnojil ter iztok kanalizacije ali greznic. Naravni viri natrija in klora so se izkazali za manj izrazite, ampak prav tako pomembne, kot je npr. vpliv morja (padavine in aerosoli), ionska izmenjava pri natriju in preperevanje silikatnih mineralov. Ocenjena meja naravnega ozadja za Na^+ je 1,5 mg/L in za Cl^- 1,70 mg/L. Glavni viri nitrata (NO_3^-) v podzemni vodi so antropogenega izvora v obliki dušikovih gnojil (gnoj in gnojevka ter sintetična gnojila) in iztok kanalizacije ali greznic. Ocenjena meja naravnega ozadja za NO_3^- je 3,81 mg/L. Možen razlog za pojavljanje amonijevega iona (NH_4^+) v podzemni vodi je prekomerna uporaba anorganskih in organskih gnojil ali omejen dostop kisika v podzemno vodo. S pomočjo izmerjenih vrednosti $\delta^{15}N_{tot}$ v podzemni vodi sem lahko opredelila naravne (v zraku, v tleh) in antropogene (naravna in sintetična gnojila) vire. Poleg NO_3^- je pomemben vir hranil tudi kalij (K^+). Vir kalija v podzemni vodi je večinoma antropogen in je posledica prekomerne uporabe gnojil, pride pa tudi iz odpadnih voda. Ocenjena meja naravnega ozadja za K^+ je 0,35 mg/L. Vir sulfata (SO_4^{2-}) v podzemni vodi je prav tako antropogen in sicer zaradi uporabe gnojil in emisij SO_2 iz zraka, ki so posledica izgorevanja fosilnih goriv. Drugotni naravni vir je preperevanje sadre in sulfidnih mineralov ter bližina morja (padavine in aerosoli). Ocenjena meja naravnega ozadja za SO_4^{2-} je 6,93 mg/L. Koncentracije večine slednih prvin v podzemni vodi je pod mejo zaznavnosti (LOD). Vir železa (Fe) v podzemni vodi je lahko v materialu, ki se je uporabil za cevitev objekta, limonitna impregnacija v karbonatnih kamninah ali raztapljanje mineralov pri redukcijskih pogojih. Slednje sem prav tako identificirala s pomočjo povišane koncentracije mangana (Mn) in arzena (As) v podzemni vodi v globokih vodonosnikih. Vir kroma (Cr) v podzemni vodi je posledica onesnaženja s Cr^{6+} v preteklosti zaradi bližine kovinskopredelovalne dejavnosti.

Končni rezultati raziskave tako podajajo informacijo o tipičnih koncentracijah opazovanih kemijskih in izotopskih parametrov v podzemni vodi glede na litološke in litostratigrafske enote v napajalnem zaledju ter naravno hidrokemijsko ozadje za izbrane kemijske parametre, katerih izvor je predvsem antropogen. Prav tako sem izdelala hidrokemijske tematske karte iz katerih je razvidna prostorska porazdelitev opazovanih parametrov.

7. REFERENCES

Abdi H. 2003. Factor rotations in factor analyses. In: The SAGE Encyclopedia of Social Science Research Methods. Lewis-Beck M., Bryman A., Futing T. (Eds.). Thousand Oaks, CA: 978-982

ACME Labs. 2007. Sample preparation & Disposal (Catalogue of services), 44 p. http://acmelab.com/pdfs/Acme_Price_Brochure.pdf (Dec 14 2008)

Alley W. M. (Ed.) 1993. Regional Ground-Water Quality. New York, Van Nostrand Reinhold: 634 p.

Al-Charideh. A, Hasan A. 2012. Use of isotopic tracers to characterize the interaction of water components and nitrate contamination in the arid Rasafeh area (Syria). Environmental Earth Sciences, 70, 1: 71-82

Appelo C.A.J., Postma D. 2005. Geochemistry, groundwater and pollution. 2nd Edition. Leiden: A.A. Balkema Publishers: 668 p.

Appelo C.A.J. 1996. Multicomponent ion exchange and chromatography in natural systems. In: Reactive Transport in Porous Media. Reviews in Mineralogy Vol. 34. Lichtner P.C., Steefel C. I., Oelkers E.H. (Eds). Mineralogical Society of America, Washington DC: 193-227

AquaChem. 2006. Water quality data analysis, plotting, and modeling (AquaChem v.5.1, Tutorial). Waterloo Hydrogeologic, Inc.: 76 p. http://www.aquagri.com/pdf/AQ_Demo_Guide.pdf (Jan 12 2011)

Araguas-Araguas L., Fröhlich K., Różański K. 2000. Deuterium and oxygen-18 isotope composition of precipitation and atmospheric moisture. Hydrological Processes, 14: 1341-1355

ASTM D1067-92. 1996: Standard Test Methods for Acidity or Alkalinity of Water: 8 p.

Aston T.R.C. 1985. Tritium Dating of Water Inflow at the Donkin-Morien Project, Nova Scotia. International Journal of Mine Water, 4, 2: 41-52

Bader S., Kunz P. 2000. Climate Risks - The Challenge for Alpine Regions: Final Scientific Report, No. 31. Zϋrich, Hochschulverlag AG: 291 p.

Bajpayee S., Das R., Ruj B., Adhikari K., Chatterjee P.K. 2012. Assessment by multivariate statistical analysis of ground water geochemical data of Bankura, India. International Journal of Environmental Sciences, 3, 2: 870-880

Bat. M., Dolinar M., Frantar P., Hrvatin M., Kobold M., Kurnik B., Nadbath M., Ožura V., Uhan J. and Ulaga F. 2008. Vodna bilanca Slovenije 1971–2000 = Water balance of Slovenia 1971–2000. Ministry for Environment and Spatial Planning – Environmental Agency of the Republic of Slovenia: 120 p.

Bavec M., Pohar V. 2009. Kvartar = Quaternary (Chapter 6.5). In: Geologija Slovenije = The geology of Slovenia. Ljubljana, Geological Survey of Slovenia: 441-464.

Bavec M., Meglič P., Prestor J. 2008. Litogeokemijska klasifikacija vodonosnikov v Sloveniji = Lithogeochemical classification of aquifers in Slovenia (in Slovene). Gelogical Survey of Slovenia, Archive number: K-II-30d/c-20/1394-š: 7 p.

Benedik L., Jeran Z. 2012. Radiological of natural and mineral drinking waters in Slovenia. Radiation protection dosimetry, 151, 2: 306-13

Bernard Vukadin B., Dolinar M., Kovač N., Kušar U., Plantan M., Polanec V., Vertačnik G., Vidrih R., Vrščaj B., Zupan N., Zupančič P., Žust A. 2008. Environment in the palm of your hand: Slovenia. Ministry of the Environment and Spatial Planning, Environmental Agency of the Republic of Slovenia, Ljubljana: 114 p.

Berner E.K., Berner. R. 2012. Global Environment: Water, Air and Geochemical Cycles. 2nd Edition. New Jersey, Princton University Press: 444 p.

Birke M., Rauch U., Siewers U., Kantor W., Wehner H. 2009. Geochemischer Atlas von Deutschland: 5 p. http://www.bgr.bund.de/EN/Themen/Sammlungen-Grundlagen/GG_geol_Info/Projekte/geochemical_atlas_of_germany/Geochemical_Atlas_of_Germany_pdf.pdf;jsessionid=1ADF762C9676FB74F349B9C8C42ABD21.1_cid334?__blob=publicationFile&v=2 (Sep 8 2013)

Bogataj J., Klemenc A., Komat A., Kos M., Krajčič D., Ogrin D., Plut D., Potočnik Slavič I. 2012. Enciklopedija: Veliki Atlas Slovenije. 1st edition. Ljubljana, Mladinska knjiga: 655 p.

Bračič-Železnik B. 2005. Can we manage the nitrate concentration in the Ljubljana Field aquifer (Slovenia)? In Nitrates in groundwater: selected papers from the European meeting of the International Association of Hydrogeologists. Razowska-Jaworek L., Sadurski A. (Eds.). Wisla, Poland, 4-7 June 2002: 235-245

Bradbury K.R. 1991. Tritium as an Indicator of Ground-Water Age in Centrai Wisconsin. Ground Water, 29, 3: 398–404

Bradshaw, P.M.D. 1975. Conceptual models in exploration geo-chemistry – the Canadian Cordillera and Canadian Shield. Amsterdam, Elsevier Scientific Pub. Co.: 223 p.

Brenčič M. 1998. Use of δ^{18}O for the hydrogeological mapping in the low permeability terrains = Uporaba δ^{18}O za hidrogeološko kartiranje v slabo prepustnih terenih. IV Isotope Workshop of the European Society for Isotope Research. Portorož, July 1-4: 224-225

Brenčič M. 2003. Past and present experiences of highways construction in Slovenia - groundwater and highways interaction. RMZ Materials and Geoenvironment, 50, 1: 61-64

Brenčič M. 2006. Groundwater and highways interaction: past and present experiences of highway construction in Slovenia. Environmental Geology, 49: 804–813

Brenčič M. 2009. Shallow groundwater (Chapter 9.1). In: Geologija = The geology of Slovenia. Pleničar M., Ogorelec B., Novak M. (Eds.). Ljubljana, Geological Survey of Slovenia: 543-553

Brenčič M., Rikanovič R. 2002. Groundwater and road network interractions - case study from Slovenia. Geologija, 45, 2, 325-330

Brenčič M., Poltnig W. 2008. Groundwaters of the Karavanke Mountains = Podzemne vode Karavank = Grundwasser der Karawanken (In German and Slovene). Ljubljana and Graz, Geological Survey of Slovenia & Joanneum Research Forschungsgesellschaft: 143 p.

Brenčič M., Vreča P. 2006a. General chemistry of bottled waters on the Slovene market. RMZ Materials and Geoenvironment, 52, 3: 549-560

Brenčič M., Vreča P. 2006b. Identification of sources and production processes of bottled waters by stable hydrogen and oxygen isotope ratios. Rapid Communications in Mass Spectrometry, 20, 21: 3205-3212

Brenčič M., Torkar A., Vreča P. 2011. Deuterium excess of waters in Slovenia. In: International Symposium on Isotopes in Hydrology, Marine Ecosystems, and Climate Change Studies, Monaco, 27 March-1 April 2011. Abstracts. Vienna: International Atomic Energy Agency, 96 p.

Brilly M., Jamnik B., Drobne D. 2003. Chromium contamination of the Ljubljansko polje aquifer. RMZ Materials and Geoenvironment, 50, 1: 71-74

BRIDGE. 2005. Proposal of the Methodology Framework. Research for Policy Support: 27 p. http://nfp-at.eionet.eu.int/Public/irc/eionet-circle/bridge/library?l=/deliverables (Jul 15 2012).

British Columbia of Canada. 2007. Hardness in groundwater fact sheet. The British Columbia groundwater association. 2 p. http://www.env.gov.bc.ca/wsd/plan_protect_sustain/groundwater/library/ground_fact_sheets/pdfs/hardness(020715)_fin2.pdf (Sep 8 2013)

Buser S. 2010. Geološka karta Slovenije v merilu 1:250.000 = Geological Map of Slovenia at scale 1:250,000 (in Slovene): Geological Survey of Slovenia, 1 sheet.

Capaccioni B., Didero M., Paletta C., Salvadori P. 2001. Hydrogeochemistry of groundwaters from carbonate formations with basal gypsiferous layers: an example from the Mt. Catria–Mt. Nerone ridge (Northern Apennines, Italy). Journal of Hydrology, 253: 14–26

Capasso G., Favara R., Grassa F., Inguaggiato S., Longo M. 2003. Automated technique for preparation and measuring stable carbon isotope of total dissolved inorganic carbon in samples (δ^{13}C-DIC). Programme & Abstract Book, 38. Katlenburg-Lindau, Germany, Copernicus GmbH. 7th International Conference on Gas Geochemistry , Freiberg, Germany, 22-26 September, ICGG 7 . 22-9-2003: 38 p.

Cardarelli F. 2000. Materials handbook. 2nd Edition. London, Springer: 1340 p.

Cerling T. 1991. Carbon dioxide in the atmosphere: evidence from Cenozoic and Mesozoic paleosols. American Journal of Science, 291:377–400

CICAD (Concise International Chemical Assessment Document). 2004. Manganese and its Compounds: Environmental Aspects. Concise international chemical assessment document 63. WHO, Geneva, Switzerland: 65 p. http://www.who.int/ipcs/publications/cicad/cicad63_rev_1.pdf (Feb 12 2013)

Clark I.D., Fritz P. 1997. Environmental Isotopes in Hydrogeology. Boca Raton, Florida, Lewis Publishers: 328 p.

Cocos O. 1997. Soil-Forming Factors and Their Impact on the Evolution of Soils in the Upper Semenic Mountains. Geographica Pannonica, 1: 11-12

Cox S.E. 2003. Estimates of Residence Time and Related Variations in Quality of Ground Water Beneath Submarine Base Bangor and Vicinity, Kitsap County, Washington. U.S. Geological Survey. Water-Resources Investigations Report 03-4058: 54 p.

Craig H. 1961. Isotopic Variations in Meteoric Waters. Science, 133, 3465: 1702-1703

Croghan C., Egeghy P. 2003. Methods of dealing with values below the limit of detection using SAS. Presented at SouthEast SAS User Group, September, 22-24., St. Petersburg, FL: 5 p. http://analytics.ncsu.edu/sesug/2003/SD08-Croghan.pdf (May 12 2012)

Cruz-San J., Araguas L., Różański K., Benavente J., Cardenal J., Hidalgo M. C., Garcia-Lopez S., Martinez-Garrido J. C., Moral F., Olias M. 1992. Sources of precipitation over South-Eastern Spain and groundwater recharge – an isotopic study. Tellus, 44B: 226–236

Cukrov N., Tepić N., Omanović D., Lojen S., Bura-Nakić E., Vojvodić V., Pižeta I. 2012. Qualitative interpretation of physico-chemical and isotopic parameters in the Krka River (Croatia) assessed by multivariate statistical analysis. International Journal of Environmental Analytical Chemistry, 92, 10: 1187-1199

Cukrov N., Tepić N., Omanović D., Lojen S., Bura-Nakić E., Vojvodić V., Pižeta I. 2009. Anhropogenic and natural influences on the Krka River (Croatia) Evaluated by Multivariate statistical analysis. Proceedings of the Information Technology Interfaces: 219-224

Cushing E.M., Kantrowitz I.H., Taylor K.R. 1973. Water Resources of the Delmarva Peninsula. Geological Survey Professional Paper 822. Washington DC: 58.

Dansgaard W. 1964. Stable isotopes in precipitation. Tellus, 16: 436-468

Darcy H. 1856. Les Fontaines Publiques de la Ville de Dijon. Dalmont, Paris. Dalmont, Paris: 647 p.

DARS. 2012. Cestninski sistem in ceste = The toll system and roads. http://www.dars.si/Dokumenti/Cestnina/Cestninski_sistem_in_ceste_35.aspx (May 15 2012)

Davis J.C. 2002. Statistics and Data analysis in Geology. John Wiley & Sons, New York: 656 p.

Davis S.N., Whittemore D.O., Fabryka-Martin J. 1998. Uses of chloride/bromide ratios in studies of potable water. Ground Water, 36, 2: 338-350

De Vos W., Tarvainen T., Salminen R., Reeder S., De Vivo B., Demetriades A., Pirc S., Batista M.J., Marsina K., Ottesen R.T., O'Connor P.J., Bidovec M., Lima A., Siewers U., Smith B., Taylor H., Shaw R., Salpeteur I., Gregorauskiene V., Halamic J., Slaninka I., Lax K., Gravesen P., Birke M., Breward N., Ander E.L., Jordan G., Duris M., Klein P., Locutura J., Bel-lan A., Pasieczna A., Lis J., Mazreku A., Gilucis A., Heitzmann P., Klaver G. , Petersell V. 2006. Geochemical Atlas of Europe. Part 2: Interpretation of Geochemical Maps, Additional Tables, Figures, Maps, and Related Publications. Geological Survey of Finland, Espoo: 692 p.

Decree on groundwater status. 2009. Official Gazette of the Republic of Slovenia, OJ RS, No. 25/2009, 68/2012. Date: Mar 26 2009.

Deines P. 1980. The isotopic composition of reduced organic carbon. In: Fritz P., Fontes J.C. (Ed.). Handbook of Environmental Isotope Geochemistry. Elsevier, Amsterdam: 329–406

Deines P., Langmuir D., Harmon R.S. 1974. Stable carbon isotope ratios and the existence of a gas phase in the evolution of carbonate groundwaters. Geochimica and Cosmochimica Acta 38: 1147-1164

Demirel Z. 2004. The history and evaluation of saltwater intrusion into a coastal aquifer in Mersin, Turkey. Journal of Environmental Management, 70: 275–282

Directive 2000/60/EC. Directive 2000/60/EC of the European Parliament and of the Council of 23 October 2000 establishing a framework for Community action in the field of water policy (Water framework directive). http://eur-lex.europa.eu/LexUriServ/LexUriServ.do?uri=CELEX:32000L0060:EN:NOT (Jan 17 2011)

Directive 2006/118/EC. Directive 2006/118/EC of the European Parliament and of the Council of 12 December 2006 on the protection of groundwater against pollution and deterioration (Daughter to 2000/60/EC). http://eur-lex.europa.eu/legal-content/EN/TXT/?qid=1396181964395&uri=CELEX:32006L0118 (Jan 17 2011)

Doctor D.H., Lojen S., Horvat M.. 2000. A stable isotope investigation of the Classical Karst aquifer: evaluating karst groundwater components for water quality preservation. Acta Carsologica, 29: 79–92

Doctor D.H., Alexander E.C. Jr., Petrič M., Kogovšek J., Urbanc J., Lojen S., Stichler W. 2006. Quantification of karst aquifer discharge components through end-member mixing analysis using natural chemistry and stable isotopes as tracers. Hydrogeology Journal, 14, 7: 1171-1191

Doctor D.H., Kendall C., Sebestyen S.D., Shanley J.B, Ohte N., Boyer E.W. 2008. Carbon isotope fractionation of dissolved inorganic carbon (DIC) due to outgassing of carbon dioxide from a headwater stream. Hydrological Processes, 22: 2410-2423

Domenico P.A., Schwartz F.W. 1990. Physical and Chemical Hydrogeology. New York, John Wiley & Sons: 824 p.

Drever J. 1982. Groundwater Chemistry. Background discussion. 9 p. http://www.deq.state.or.us/wq/groundwater/docs/lubgwma/hydrogeologyrpt/appx4a.pdf (Jun 1 2012)

Drever J. 1997. The geochemistry of natural waters. 3rd Edition. Prentice Hall Englewood Cliff. N.J., USA: 388 p.

Drinking water and Sewerage System Public Utility Ljubljana. 2011. Laboratory manual: 5 p.

Drobne F., Mencej Z. 1980. Letno poročilo. Podtalnica v Vrtojbenjskem polju. I. faza, leto 1979/80 (In Slovene): 18 p.

Drobne F. 1977. Podatki o gladini podtalne vode na območju "Aera" Doberteša vas pri Šempetru v Spodnje Savinjski dolini (In Slovene). Ljubljana, Geological Survey of Slovenia, Archive number: K-II-30d/b-4/3-c: 2 p.

Drobne F., Veselič M., Žlebnik L. 1976. Hidrogeološke značilnosti slovenskega ozemlja = Hydrogeological characteristics of the Slovenian territory (in Slovene). Zbornik referatov 8. jugoslovanskega geološkega kongresa. Ljubljana, 4th book: 59-70.

Ducci D., Sellerino M. 2012. Natural background levels for some ions in groundwater of the Campania region (southern Italy). Environmental Earth Sciences, 67, 3: 683-693

EARS (Environmental Agency of the Republic of Slovenia). 2002. Radioaktivnost v okolju = Radioactivity in the environment (in Slovene): 20 p. http://www.arso.gov.si/varstvo%20okolja/poro%C4%8Dila/poro%C4%8Dila%20o%20stanju%20okolja%20v%20Sloveniji/radioaktivnost.pdf (May 12 2011)

EARS (Environmental Agency of the Republic of Slovenia). 2006. Podnebne razmere v Sloveniji (obdobje 1971-2000) (in Slovene). Ljubljana: 28 p.

EARS (Environmental Agency of the Republic of Slovenia). 2009. Kakovost podzemne vode v Sloveniji v letih 2007 in 2008 (In Slovene): 233 p.

EARS (Environmental Agency of the Republic of Slovenia). 2010. Poročilo o kakovosti podzemne vode v Sloveniji v letu 2009 (in Slovene). Ljubljana: 114 p.

EARS (Environmental Agency of the Republic of Slovenia). 2011. Poročilo o kakovosti podzemne vode v Sloveniji v letu 2010 (In Slovene): 13 p.

EARS. 2011a. The annual air temperature 1971–2000. Resolution 1–2 km, vector form (shp). Ljubljana: Geoportal ARSO (Nov 23 2011) http://gis.arso.gov.si/wfs_web/faces/WFSLayerExportAttSingle.jspx?uuid=%7BD9EA365B-C202-43DF-A409-879DA57E9970%7D

EARS (Environmental Agency of the Republic of Slovenia). 2011b. The average annual precipitation corrected for 1971–2000 with 1-2 km resolution

EARS (Environmental Agency of the Republic of Slovenia) 2011c. Ocena kemijskega stanja podzemnih voda v Sloveniji v letu 2011 (In Slovene). Ljubljana: 73 p.

Edmunds W.M., Shand P. 2008. Natural Groundwater Quality. Blackwells, Oxford: 469 p.

Edmunds W.M., Doherty P., Griffiths K.J., Shand P., Peach D.W., Hargreaves R.L., Milodowski A.E., Newell A.J., Milne C.J. 2002. The Chalk of Dorset. Baseline Report Series 4. British Geological Survey Report CR/02/268N. British Geological Survey, National Groundwater and Contaminated Land Centre: 45 p.

Edmunds W.M., Gaye C.B. 1997. High nitrate baseline concentrations in groundwaters from the Sahel. Journal of Environmental Quality, 26: 1231-1239

Edmunds W.M. 1996. Bromide geochemistry in British groundwaters. Mineralogical Magazine, 60: 275-284

Edmunds W.M., Bath A. H., Miles D.L. 1982. Hydrochemical evolution of the East Midlands Triassic sandstone aquifer, England. Geochimica et Cosmochimica Acta, 46: 2069-2081

EHIS (Evidenca hišnih številk) 2013. Surveying and Mapping Authority of the Republic of Slovenia. Ljubljana. http://www.gu.gov.si/fileadmin/gu.gov.si/pageuploads/upravni_postopki/_novo_UP/EUR_UP_zen/evidentiranje_HS-info.doc (Nov 30 2007)

Environmental Agency of Slovenia. 2013: Environmental Atlas.

http://gis.arso.gov.si/atlasokolja/profile.aspx?id=Atlas_Okolja_AXL@Arso (Jan 14 2011)

EPA (The Slovene Environmental Protection Act = (ZVO-1) SOP-2004-01-1694). 1993.

Epstein S., Mayeda T. 1953. Variation of O^{18} content of waters from natural sources. Geochimica et Cosmochimica Acta, 4, 5: 213-224

Eriksson E. 1985. Principles and Application of Hydrochemistry. UK. Chapman & Hall, New York: 187 p.

Esri Inc. 2001. ArcGIS Desktop (Version 9.2). Redlands, California, USA: Environmental Systems Research Institute.
http://www.esri.com/software/arcgis/index.html (Feb 14 2011)

Faimon J., Ličbinská M., Zajíček P., Sracek O. 2012. Partial pressures of CO_2 in epikarstic zone deduced from hydrogeochemistry of permanent drips, the Moravian karst, Czech Republic. Acta Carsologica, 41, 1: 47-57

Ferrous Iron by Modified Method SM20 3500 Fe B. 1997.

Flury M., Papritz A. 1993. Bromide in the Natural Environment: Occurrence and toxicity. Journal of Environmental Quality, 22, 4, 747-758

Frantar P., Nadbath M., Ulaga F. 2008. Vplivni dejavniki na vodno bilanco = Water balance impact factors. In: Vodna bilanca Slovenije 1971-2000 = Water balance of Slovenia 1971-2000. Bat M. (Ed.). Ministry of the Environment and Spatial Planning; Environmental Agency of the Republic of Slovenia, Ljubljana: 14 p.

Freeze R.A., Cherry J.A. 1979. Groundwater. Prentice-Hall, Englewood Cliffs, New Jersey: 604 p.

Fridl J., Kladnik D., Orožen Adamič M., Perko D., Belec B., Drozg.V. 1998. Geografski atlas Slovenije: država v prostoru in času (In Slovene). DZS.d.d., Mladinska knjiga, Ljubljana: 360 p.

Fröhlich K., Gibson J.J. and Aggarwal P. 2002. Deuterium excess in precipitation and its climatological significance. Study of Environmental Change Using Isotope Techniques. C&S Papers Series 13/P, International Atomic Energy Agency, Vienna, Austria: 54–66

Fukada T., Hiscock K.M., Dennis P.F. 2004. A dual isotope approach to the nitrogen hydrochemistry of an urban aquifer. Applied Geochemistry, 19: 709-719

Gams I. 1974. Kras: Zgodovinski, naravoslovni in geografski oris (In Slovene). Ljubljana, Slovenska matica: 358 p.

Gat J.R. 2010. Isotope hydrology – A Study of the Water Cycle. Series on Environmental Science and Management. Imperial College Press, 6: 200 p.

Gat J.R., Mook, W.G., Meijer H.A.J. 2001. Environmental isotopes in the hydrological cycle - Principles and applications, Vol. 2. (Atmospheric water). International atomic energy agency and United Nations educational, scientific and cultural organization (reprinted with minor corrections): 235 p.

Gat J.R. 1996. Oxygen and hydrogen isotopes in the hydrologic cycle. Annual Review of Earth and Planetary Sciences, 24: 225–262

Gat J.R., Dansgaard W. 1972. Stable isotope survey of the freshwater occurrences in Israel and theJordan Rift Valley. Journal of Hydrology, 16: 177-211

Gauthier T.D. 2001. Detecting trends using Spearman's rank correlation coefficient. Environmental forensics, 2: 359-362

Geo Vrtina d.o.o., Hidrogeološko poročilo o izvedbi črpalnih poizkusov na zajetjih pitne vode v občini Tišina: 10-12

Gat J.R., Carmi I. 1970. Evolution of the isotopic composition of atmospheric waters in the Mediterranean Sea area. Journal of Geophysical Research, 75: 3039-3048

Gemiti F. 2011. Origine e bilancio dei cloruri nelle acque del Carso Classico. Atti e Memorie della Commissione Grotte »Eugenio Boegan«, 43: 117–149

Gemitzi A. 2011. Natural background levels and threshold values derivation in Rhodope area (Thrace, Greece). Proceedings of the 3rd International CEMEPE & SECOTOX Conference Skiathos, June 19-24 2011: 307 – 313

Giesler R., Lyon S.W., Mörth C.-M., Karlsson J., Jantze E.J., Destouni G., Humborg C. 2013. Biogeosciences discuss, 10: 7953-7988

Glover D. M., Jenkins W. J., Doney S.C. 2005. Modeling Methods for Marine Science. Woods Hole Oceanographic Institution: 529 p.

GNIP database. 2013. Precipitation: The GNIP database.
http://isohis.iaea.org (July 5 2013)

Gospodarič R., Habič P. 1976: Underground water tracing. ZRC, Postojna: 312 p.

Gourcy L.L., Groening P.K., Aggarwal P.K. 2005. Stable oxygen and hydrogen isotopes in precipitation. In: Isotopes in the water cycle: Past, present and future of a developing science. Aggarwal P.K., Gat J.R., Froehlich K. (Eds.) Dordrecht, Springer: 39–51.

Gray N. F. 2008. Hardness and total dissolved solids. Drinking Water Quality problems and solutions. 2nd Edition. John Wiley& Sons: 520 p.

Griffioen J., Passier H., Klei J. 2008. Comparison of selection methods to deduce natural background levels for groundwater units. Environmental science & technology, 42, 13: 4863-4869

GURS (Surveying and Mapping Authority of the Republic of Slovenia). 1998. CORINE Land Cover - Pokrovnost in raba prostora CORINE Land Cover Slovenija. http://kpv.arso.gov.si/kpv/Metadata_search/Metadata_report/report_metadata?DOC_ID=92&L1=302&L2=94&NODE_ID=92 (Jun 17 2011)

GURS. 2005, Digital elevation model – DMV 12.5, 1998–2005 (DEM with resolution 12.5x12.25 m), Surveying and Mapping Authority of the Republic of Slovenia.

Harter T. 2003. Groundwater quality and groundwater pollution. ANR Publication 8084 - Farm Water Quality Planning (FWQP), University of California. Division of Agriculture and Natural Resources, 5 p. http://groundwater.ucdavis.edu/files/136273.pdf (May 2 2011)

Helsel D.R. and Hirsch R.M. 1992. Statistical Methods in Water Resources. Elsevier: 522 p.

Hem J. D. 1985. Study and Interpretation of the Chemical Characteristics of Natural Water. 3rd edition. Alexandria, VA: Department of the Interior, U.S. Geological Survey, Water-Supply Paper 2254: 263 p.

Hem J.D. 1975. Study and Interpretation of the chemical characteristics of Natural water, Fluoride source and chemistry and fluoride, U.S. Geological Survey: 76-180

Hem J.D. 1970. Study and Interpretation of the Chemical Characteristics of Natural Water, 2nd Edition, PAPER, 1473: 363 p.

Hem J.D. 1963. Some Aspects of Chemical Equilibrium in Ground Water, Ground Water, 1: 30-34.

Herczeg A.L., Edmunds W.M. 1999. Inorganic ions as tracers. In Environmental tracers in subsurface hydrology. Cook P.G. and Herczeg A.L. (Eds). Boston, Kluwer Academic Publishers: 31-77

Herič J. 2005. Idejna zasnova in hidrogeološke strokovne osnove raziskovalno kaptažne vrtine LMV-1/05 v Ljubljanskih mlekarnah (In Slovene). Geological Survey of Slovenia, Ljubljana: K-II-30d/f-1/175: 11 p.

Hill R.A. 1940. Geochemical patterns in Coachella Valley, California. Eos, Transactions American Geophysical Union, 21: 46-49

Hinterlechner-Ravnik A., Moine B. 1977. Geochemical characteristics of the metamorphic rocks of the Pohorje mountains. Geologija, 20, 107-140

Hinterlechner-Ravnik A. 1973. The Metamorphic Rocks of Pohorje Mountains II. Geologija, 16: 245-270

Hoefs J. 1997. Stable isotopes geochemistry. 4th Edition. Berlin, Springer: 241 p.

Hoetzl M. 2012. Dodatek k predlogu strokovnih podlag za Občino Litija, Črpalna vrtina Mala Goba (MG-1/99) (In Slovene). Geological Survey of Slovenia, Ljubljana. Archive numer: K-II-30d/c-17/1596-p(I): 14 p.

Horvatinčić N., Krajcar Bronić I., Barešić J., Obelić B., Vidič S. 2005. Tritium and stable isotope distribution in the atmosphere at the coastal region of Croatia. Isotopic Composition of Precipitation in the Mediterranean Basin in Relation to Air Circulation Patterns and Climate. TECDOC Series No. 1453, IAEA, Vienna: 37–50

Hounslow A.W. 1995. Water quality data: Analysis and Interpretation. London, Boca Raton. Lewis Publishers: 397 p.

Huang Y.-P., Lee C.-H., Ting C.-S. 2008. Improved estimation of hydrologic data using the chi-square goodness-of-fit test. Journal of the Chinese Institute of Engineers, 31, 3: 515-521

IAEA/WMO (International atomic energy agency and united Nations educational, scientific and cultural organization), 2011. Environmental isotopes in the hydrological cycle: Principles and Applications, Vol. 2: 181-196

IAEA & UNESCO (International Atomic Energy Agency and United Nations Educational, Scientific and Cultural Organization). 2000. Environmental isotopes in the hydrological cycle - Principles and Applications, Water resources Programme (reprinted with minor corrections), 1: 185 p.

Ingraham N.L. 1998. Isotopic variations in precipitation. In: Isotope Tracers in Catchment Hydrology. Kendall C., McDonnell J.J. (Eds.). Elsevier: 87–118

Janža M. 2013. Matematični model za določitev možnega izvora onesnaženja s kromom (Cr VI) (In Slovene). Geological Survey of Slovenia. Archive number: K-II-30d/I-1/66: 8 p.

Jouzel J., Merlivat L. 1984. Deuterium and oxygen 18 in precipitation: Modeling of the isotopic effects during snow formation. Journal of Geophysical Research: Atmospheres, 89, D7: 11749–11757

Javornik M., Voglar D., Dermastia A., Pavlovec R., Resman B., Stergar J., Mlinar Z., Weiss P., Wraber T., Krbavčič A., Ferenc T., Torelli N. 1989. Enciklopedija Slovenije = Encyclopedia of Slovenia (In Slovene). Ljubljana, Mladinska knjiga: 416 p.

Jazbinšek Seršen N., Čermelj S., Jankovič M., Regina H., Strojin Božič Z., Piltaver A. 2010. Elektrotehnik MOL (In Slovene). Okolje v Mestni občini Ljubljana, Mestna občina Ljubljana, Oddelek za varstvo okolja: 104 p.

Johnston R. J. 1980. Multivariate Statistical Analysis in Geography: Longman, London, 280 p.

Jordana S. Batista E. 2004. Natural groundwater quality and health. Geologica Acta, 2, 2: 75-188

Kanduč T., Šturm M., and McIntosh J. 2013. Chemical Dynamics and Evaluation of Biogeochemical Processes in Alpine River Kamniška Bistrica, North Slovenia. Aquatic Geochemistry, 19, 4, 323-346

Kanduč T., Mori N., Kocman D., Stibilj V., Grassa F. 2012. Hydrogeochemistry of alpine springs from North Slovenia: Insights from stable isotopes. Chemical Geology, 300–301, 40–45

Karanth K.R. 1987. Groundwater assessment, development and management. New Delhi. New York: Tata McGraw-Hill Pub. Co.: 720 p.

Katz B.G. 1998. Using δ^{18}O and δD to quantify ground-water/surface-water interactions in karst systems of Florida. In: U.S. Environmental Protec-tion Agency (Eds.) Proceedings of the National Water Quality Monitoring Conference, Monitoring: Critical Foundations to Protect Our Waters, 7th–9th July 1998, Reno, Nevada. U.S. Environmental Protection Agency, Washington, D.C: 195–208

Kazemi G.A., Lehr J. H. Perrochet P. 2006. Groundwater Age. John Wiley & Sons, Inc.: 325 p.

Kegel L. Analiza razvrščanja padavinskih trajektorij ERA-40 (diplomsko delo) = Analysis of sorting precipitation trajectories ERA-40 (Graduation thesis). University of Ljubljana: 80 p.

Kendall C., Doctor D.H. 2003. Stable Isotope Applications in Hydrologic Studies. In: Treatise on Geochemistry. Holland H. D. and Turekian K.K. (Eds.). Elsevier, 5, Chapter 11: 319-364.

Kendall C., McDonnell J.J. 1998. Isotope Tracers in Catchment Hydrology. Amsterdam, Elsevier: 839 p.

Kendall C., Sklash M.G., Bullen T.D. 1995. Isotope Tracers of Water and Solute Sources in Catchments. In Solute Modelling in Catchment Systems. John Wiley & Sons, New York: 261- 303

Kim J. O., Mueller C. W. 1978. Introduction to Factor Analysis: What It Is and How To Do It. Sage University Paper Series on Quantitative Applications in the Social Sciences, 07-013, Beverly Hills, CA: Sage Publications: 79 p.

Knez M., Slabe T. 2009. Caves in breccia and flysch below mountain Nanos in the Vipava valley (Slovenia). ANNALES Series historia naturalis, 19, 1: 85-94

Kobal I., Vaupotič J., Mitić D., Kristan J., Ančik M., Jerančič S., Škofljanec M. 1990. Natural radioactivity of fresh waters in Slovenia, Yugoslavia. Environment International, 16, 141–154

Kolay A.K. 2007. Soil genesis, classification survey and evaluation. New Delhi, Atlantic Publishers & Distributors: 744 p.

Korun M., Kovačič K. 2011. Determination of the ^{238}U in ground-water samples using gamma-ray spectrometry. Applied Radiation and Isotopes, 69, 3: 636-640

Korun M., Kovačič K., Kožar Logar J. 2011. Concentration of tritium and members of the uranium and thorium decay chains in ground water in Slovenia and their implications for managing ground water resources. In: International Symposium on Isotopes in Hydrology, Marine Ecosystems, and Climate Change Studies, Monaco, 27 March-1 April 2011. Abstracts. Vienna: International Atomic Energy Agency: 110 p.

Košiček B. 2005. Fire at Sela na Krasu - a Forester‘s view. UJMA, 19: 108-113

Košir A., Andrea Martin Pérez, Popit T. 2013. Zakaj je slano blato slano? (In Slovene). 21. Posvetovanje slovenskih geologov: 75-77

Kožar Logar J., Glavič-Cindro D. 2009. Establishment of low-level tritium laboratory. In: Eikenberg J. (Ed.). LSC 2008, advances in liquid scintillation spectrometry: proceedings of the 2008 International Liquid Scintillation Conference, Davos, Switzerland, 25-30 May 2008. Tucson: Radiocarbon: 241-249

Krajnc M., Gacin M., Krsnik P., Sodja E., Kolenc A. 2007a. Groundwater quality in Slovenia assessed upon the results of national groundwater monitoring. European Water, 19/20: 37-46

Krajnc M., Gacin M., Dobnikar-Tehovnik M., Krsnik O. 2008. Groundwater chemical status assessment in Slovenia. International Symposium on Groundwater Flow and Transport Modelling: 29-38

Kranjc S. 1995. Stanje podzemnih voda v republiki Sloveniji = The balance of groundwater in Republic of Slovenia (Annual Report) (In Slovene). Institute of Geology, Geotechnics and Geophysics, Ljubljana, Slovenia: 31 p.

Kralj P. 2003. Geochemistry of Upper Pliocene silty and sandy sediments from the well Mt-7, Moravci Spa, North-Eastern Slovenia. Geologija 46, 1: 117-122

Kralj P., Mišič M. 2003. Chemical composition of Kiscellian silty sediment (sivica) from the Trobni Dol area, Eastern Slovenia. Geologija 46, 1: 113–116

Kralik M., Zieritz I., Grath J., Vincze G., Philippitsch R., Pavlik H. 2005. Hydrochemische Karte Österreich: Oberflächennaher Grundwasserkörper und Fließgewässern = Hydrochemical map of Austria, Mittelwerte von Wassergüteerhebungsdaten (WGEV-Daten) 1991 – 2001 (In German): 19 p. http://www.umweltbundesamt.at/fileadmin/site/publikationen/BE269.pdf (Jan 1 2011)

Krajcar-Bronić I., Horvatinčić N., Barešić J., Obelić B., Vreča P., Lojen S., Vidič S. 2003. Isotope composition of precipitation in Croatia and Slovenia: basic data for ground water studies. RMZ Materials and Geoenvironment, 50:173–176

Krajcar-Bronić I., Vreča P., Horvatinčić N., Barešić J., Obelić B. 2006. Distribution of hydrogen, oxygen and carbon isotopes in the atmosphere of Croatia and Slovenia. Archives of Industrial Hygiene and Toxicology, 57: 23-29

Krauskopf K.B., Bird D.K. 1994. Introduction to Geochemistry, 3rd Edition. McGraw-Hill, New York: 640 p.

Kukar N., Pirc S., Šajn R. 2003. Experimental geochemical mapping of Slovenia by spring water sampling. RMZ Materials and geoenvironment, 50, 1: 181-184

Kunkel R., Voigt H.-J., Wendland F., Hannappel S. 2004. Die natürliche, ubiquitär überprägte Grundwasserbeschaffenheit in Deutschland (In Greman). Schriften des Forschungszentrums Jülich, Reihe Umwelt/ Environment, Band 47, Forschungszentrum Jülich GmbH, Jülich, Germany: 204 p. http://juwel.fz-juelich.de:8080/dspace/bitstream/2128/350/1/Umwelt_47.pdf (Apr 7 2012)

Kunkel R., Wendland F., Hannappel S., Voigt. H.-J., Wolter R., 2007. The influence of diffuse pollution on groundwater content patterns for the groundwater bodies of Germany. Water Science and Technology, 55, 3: 97-105

Laerd Statistics, 2013. Testing for Normality using SPSS. https://statistics.laerd.com/spss-tutorials/testing-for-normality-using-spss-statistics.php

Lajevec D. 2008. Analiza vplivov onesnaženih voda s soljo iz cestišč na vodno okolje in čiščenje na komunalnih čistilnih napravah (diplomsko delo) = An analysis of the effects of deicing salts on water environment and wastewater treatment (Graduation Thesis) (In Slovene). University of Ljubljana, Faculty of Civil and Geodetic Engineering: 84 p.

Langmuir, D., 1997. Aqueous Environmental Geochemistry. Prentice-Hall, Englewood Cliffs, New Jersey: 600 p.

Langmuir D. 1971. The geochemistry of some carbonate ground waters in central, Pennsylvania. Geochimica et Cosmochimica Acta, 35, 10: 1023–1045

Lapanje A., Rman N. 2009. Therman and Thermomineral water (Chapter 9.2). In: Geologija = The geology of Slovenia. Pleničar M., Ogorelec B., Novak M. (Eds.). Ljubljana, Geological Survey of Slovenia: 553-560.

Lapanje A., Prestor J. 2001. Hidrogeološke raziskave za idejni projekt drugega železniškega tira Divača - Koper, varianta I/3 (Odsek od Črnega kala do Kopra) I. del: predori T3, T4 in T5 (In Slovene). Geological Survey of Slovenia. Archive number: K-II-30d/c-6/1002-e:19 p.

LAWA. 2001. German guidance for the implementation of the EC Water Framework Directive. Umweltbundesamt (UBA), Berlin, 148 p. http://www.lawa.de/documents/Arbeitshilfe_englisch_c40.pdf (Nov 15 2010)

Le Maitre R.W.1982. Numerical Petrology, Statistical interpretation of geochemical data. Elsevier, Amsterdam: 281 p.

Leifeld J., Fuhrer J. 2005. The temperature response of CO_2 production from bulk soils and soil fractions is related to soil organic matter quality. Biogeochemistry, 75: 433–453

LennTech-Water treatment solutions. 2013a. Calcium (Ca) and water. http://www.lenntech.com/periodic/water/calcium/calcium-and-water.htm (Nov 23 2013)

LennTech-Water treatment solutions. 2013b. Magnesium (Mg) and water. http://www.lenntech.com/periodic/water/magnesium/magnesium-and-water.htm (Oct 1 2013)

Lojen S., Trkov A., Ščančar J., Vázquez-Navarro J.A., Cukrov N. 2009. Continuous 60-year stable isotopic and earth-alkali element records in a modern laminated tufa (Jaruga, river Krka, Croatia): Implications for climate reconstruction. Chemical Geology, 258, 242–250

Long A.E., Brown J.G., Gellenbeck D.J. 1997. Statistical analysis of nitrate in ground water, west Salt River Valley, Arizona. U.S. Geological survey: 43 p.

Longinelli A., Selmo E. 2003 Isotopic composition of precipitation in Italy: a first overall map. Journal of Hydrology, 270: 75-88

Lower S.K. 2010. Carbonate equilibria in natural waters. Environmental Chemistry: 26 p. http://www.chem1.com/acad/pdf/c3carb.pdf (23.4.2011)

Mali N., Urbanc J. 2006. The use of environmental isotopes in groundwater flow study in the unsaturated zone of the Selniška Dobrava coarse gravel aquifer (Slovenia). Geologija, 49, 2: 371–381

Mali N., Urbanc J. 2009. Isotope Oxygen-18 as Natural Tracer of Water Movement in a Coarse Gravel Unsaturated Zone. Water, Air, & Soil Pollution, 203: 291-303

Mali N. 2008. Podzemna voda v Sloveniji = Groundwater in Slovenia. Novi glasnik Unesco = The New Unesco courier. 37, 75: 23-25

Maloszewski P., Zuber A. 1982. Determining the turnover time of groundwater systems with the aid of environmental tracers. I. Models and their applicability. Journal of Hydrology, 57: 207-231

Maloszewski P., Zuber A. 1996. Lumped parameter models for the interpretation of environmental tracer data. In: Manual on Mathematical Models in Isotope Hydrology, 9-58. IAEA-TECDOC-910, International Atomic Energy Agency, Vienna: 9-58.

Markič M. 2009. Pliocene and Plio-Quarternary (Chapter 6.4). In: Geologija Slovenije = The geology of Slovenia. Pleničar M., Ogorelec B., Novak M. (Eds.). Ljubljana, Geological Survey of Slovenia: 427-440.

Matoz T., Prestor J., Hoetzl M., Herič J., Rikanovič R., Pontelli N., 2002. Poročilo o izdelavi raziskovalno - kaptažne vrtine GRAD-1/02 v občini Grad s strokovnimi podlagami za varovanje vodnega vira (In Slovene). Geological Survey of Slovenia, Ljubljana. Archive number: K-II-30d/c-2/1132-a: 17 p.

Mayo A.L., Loucks M.D. 1995. Solute and isotopic geochemistry and groundwater flow in the Central Wasatch Range. Utah, Journal of Hydrology, 172: 31–59

McKee J.E., Wolf H.W. 1976. Water Quality Criteria. California State Water Quality Control Board, Publication No. 3-A. Sacramento CA: 533 p.

McPherson B.J. 2009. Looking Ahead: Research Agenda for the Study of Carbon Sequestration, Final Chapter in Carbon Sequestration and Its Role in the Global Carbon Cycle. McPherson B, Sundquist E (Eds.). Geophysical Monograph Series, Volume 183, American Geophysical Union, Washington, D.C.: 335-358

MedCalc, 2013. Skewness and Kurtosis. http://www.medcalc.org/manual/skewnesskurtosis.php (Oct 12 2012)

Meinardi C.R., Groot M.S.M., Prins H.F. 2003. Basiswaarden voor spoorelementen in het zoete grondwater van Nederland: gegevens uit de landelijke en provinciale meetnetten (LMG, PMG, LMB, sprengen Veluwe), Rijksinstituut voor Volksgezondheid en Milieu (RIVM): 43 p.

Mencej Z., Maurer J., Vehar S. 2002. Hidrogeološke razmere na območju občine Bloke. Osnove za izdelavo sanacijskih programov zajetij pitne vode za glavni vodovod in lokalne vodovode ter varstvena območja virov pitne vode. Hydroconsulting d.o.o., Dragomer: 41 p.

Mencej Z. 2000. Črpalni poskus na vodnjaku VO-I/98 v Vodicah v času hude suše (In Slovene). Hydroconsulting d.o.o., Dragomer: 4 p.

Mencej Z., Kmetec M. 1998. Strokovne podlage za zavarovanje Vitanjskih vodnih virov (In Slovene). Hydroconsulting d.o.o., Dragomer: 26 p.

Mencej Z., Kmetec M. 1997. Hidrogeološke razmere na območju občine Vodice in strokovne podlage za zavarovanje zajetij pitne vode in perspektivnih vodnih virov (In Slovene). Hidroconsulting d.o.o.: 12 p.

Merkel B.J., Friedrich B.P. 2002. Groundwater Geochemistry - A Practical Guide to Modeling of Natural and Contaminated Aquatic Systems. Nordstrom D.K. (Ed.), Springer, New York, USA: 200 p.

Merlivat L., Jouzel J. 1979. Global climatic interpretation of the deuterium-oxygen 18 relationship for precipitation. Journal of Geophysical Research, 84: 5029–5033

Meybeck M. 1987. Global chemical weathering of surficial rocks estimated from river dissolved loads. American Journal of Sciences, 287, 401–428

Mezga K., Urbanc J., Cerar S. 2014. The isotope altitude effect reflected in groundwater: a case study from Slovenia. Isotopes in Environmental and Health Studies, 50, 1: 33-51

Mezga K., Urbanc J. 2014. Groundwater calcium and magnesium content in various lithological types of aquifers in Slovenia. In: Calcium and Magnesium in Groundwater: Occurrence and Significance for Human Health (IAH - Selected Papers on Hydrogeology) CRC Press. Razowska-Jaworek L. (Ed.): 236 p. In Press.

Mihelič R., Čop J., Jakše M., Štampar F., Majer D., Tojnko S., Vršič S. 2010. Smernice za strokovno utemeljeno gnojenje (In Slovene). Ljubljana: Ministrstvo za kmetijstvo, gozdarstvo in prehrano: 182 p. http://www.mko.gov.si/fileadmin/mko.gov.si/pageuploads/publikacije/Program_razvoja_podezelja/smernice09_skupaj_april_2011.pdf (Jun 15 2012)

Mikkelsen R. 2010. Soil and fertilizer magnesium. Better Crops, 94, 2: 26-28

Millot R., Petelet-Giraud E., Guerrot C., Négre P. 2010. Multi-isotopic composition (δ^7Li-δ^{11}B-δD-δ^{18}O) of rainwaters in France: origin and spatio-temporal characterization. Applied Geochemistry, 25: 1510–1524

Mills A.L. 1988. Variations in the dC–13 of stream bicarbonate: Implications for sources of alkalinity (Master Thesis). Washington, D.C., George Washington University: 160 p.

Ministry of the Environment and Spatial planning, Environmental Agency of the Republic of Slovenia, Surveying and Mapping, Authority of the Republic of Slovenia, European Environment Agency, 2003. CORINE Land Cover 2006 in the scale 1:100,000 (Mar 12 2011)

Ministry of Environment and Spatial Planning. 2009. Metodologija za ugotavljanje stanja vodnih teles podzemne vode (In Slovene). 28 p. http://www.arhiv.mop.gov.si/fileadmin/mop.gov.si/pageuploads/zakonodaja/okolje/varstvo_okolja/voda/metodologija_podzemne_vode.pdf (Feb 12 2012)

Ministry for Agriculture and the Environment. 2013a. Interpretacijski ključ: Podroben opis metodologije zajema dejanske rabe kmetijskih in gozdnih zemljišč (In Slovene). 118 p. http://rkg.gov.si/GERK/documents/RABA_IntKljuc_20131009.pdf (Feb 12 2012)

Ministry for Agriculture and the Environment. 2013b. Obnova evidence dejanske rabe kmetijskih in gozdnih zemljišč v letu 2013 (In Slovene). 1 p. http://rkg.gov.si/GERK/documents/DOF_obnova_13.pdf (Jan 12 2012)

Ministry of Agriculture, Forestry and Food. 2011. Actual agricultural and forest land usage (Land use) 1:1000 (Raba tal) http://rkg.gov.si/GERK (Mar 12 2011)

Mioč P., Žnidarčič M. 1989. Osnovna geološka karta SFRJ. 1:100 000 (In Slovene). Tolmač za lista Maribor in Leibnitz: L 33-56, L 33-44. Beograd, Zvezni geološki zavod: 60 p.

Mook W.G. 2006. Introduction to Isotope Hydrology: Stable and Radioactive isotopes of Hydrogen, Oxygen and Carbon. London: Taylor & Francis: 226 p.

Mook W. G. 1986. ^{13}C in atmospheric CO_2. Netherlands Journal of Sea Research, 20: 211-23

Mook W.G., Bommerson J.C., Staverman W.H. 1974. Carbon isotope fractination between dissolved bicarbonate and gaseous carbon dioxide. Earth and Planetary Science Letters, 22: 169-176

Moore R.D., Story A., Richards G. 2008. Electrical conductivity as an indicator of water chemistry and hydrological processes. Streamline Watershed Management Bulletin, 11, 2: 25-29

Morris B.L., Lawrence A.R.L., Chilton P.J.C., Adams B., Calow R.C., Klinck B.A. 2003. Groundwater and its Susceptibility to Degradation: A Global Assessment of the Problem and Options for Management. United Nations Environment Programme. Kenya, DEWA: 128 p.

Motzer E.W. 2005. Age Dating Groundwater. 4 p. http://www.grac.org/agedatinggroundwater.pdf (May 29 2013)

Mueller D.K., Helsel D.R. 1996. Nutrients in the Nation's water - Too much of a good thing? U.S. Geological Survey Circular 1136: 24 p.

Muhič D. 2005. Fire at Sela na Krasu. UJMA, 19: 99-107

Mullaney J.R., Lorenz D.L., Arntson A.D. 2009. Chloride in Groundwater and Surface Water in Areas Underlain by the Glacial Aquifer System, Northern United States. National Water-Quality Assessment Program. Scientific Investigations Report 2009–5086: 54 p.

Murray K., Wade P. 1996. Checking anion-cation charge balance of water quality analyses: Limitations of the traditional method for non-potable waters. Water SA, 22, 1: 27-32

National Research Council. 1977. Drinking water and Health, Volume 1. Washington, D.C., The National Academies Press: 948 p.

Nelson D. 2002. Natural variations in the composition of groundwater. Drinking Water Program. Oregon Department of Human Services. Springfield, OR: 8 p.

http://public.health.oregon.gov/HealthyEnvironments/DrinkingWater/SourceWater/Documents/gw/chem.pdf (Jun 25 2012)

Nieto P., Custodio E., Manzano M. 2005. Baseline groundwater quality: A European approach. Environmental Science & Policy, 8: 399-409

Nolan B.T., Hitt K.J. 2003. Nutrients in Shallow Ground Waters Beneath Relatively Undeveloped Areas in the Conterminous United States. U.S. Geological Survey, Water-Resources Report 02-4289. Denver, Colorado.
http://pubs.usgs.gov/wri/wri024289/pdf/wri02-4289.pdf (Apr 5 2012)

Odlok o varstvu lokalnih virov pitne vode v Občini Medvode (In Slovene). 2001. Official Gazette of the Republic of Slovenia, OJ RS, No. 61/2001. Date: Jul 23 2001.

Odlok o zaščiti vodnih virov na območju Občine Škocjan (In Slovene). Official Gazette of the Republic of Slovenia, OJ RS, No. 34/2000. Date: Apr 17 2000.

Odlok o varstvu virov pitne vode na območju Občine Mislinja (In Slovene). Official Gazette of the Republic of Slovenia, OJ RS, No. 100/2000. Date: Oct 27 2000.

Odlok o varstvu virov pitne vode na območju Občine Laško (In Slovene). Official Gazette of the Republic of Slovenia, OJ RS, No. 38/1999. Date: May 21 1999.

Odlok o varstvu virov pitne vode v Občini Trebnje in ukrepih za zavarovanje kakovosti in količini vode (In Slovene). Official Gazette of the Republic of Slovenia, OJ RS, No. 75/1996. Date: Dec 20 1996.

Odlok o določitvi varstvenih območij in ukrepov za zavarovanje območja črpališča in vodozbirnega območja kaptažne vrtine v Dolu pri Čepovanu (In Slovene). Official Gazette of the Republic of Slovenia, OJ RS, No. 19/1996. Date: Dec 5 1996.

Odlok o dopolnitvi odloka o varstvu virov pitne vode (In Slovene). Official Gazette of the Republic of Slovenia, OJ RS, No. 20/1994. Date: Apr 15 1994.

Odlok o določitvi varstvenih pasov in ukrepov za zavarovanje vodnega zajetja Voje in zajetja Bistrica (Radovljica) (In Slovene). Official Gazette of the Republic of Slovenia, OJ RS, No. 21/1994. Date Apr 22 1994.

Odlok o spremembah in dopolnitvah odloka o varstvu virov pitne vode (In Slovene). Official Gazette of the Republic of Slovenia, OJ RS, No. 20/1991. Date 22. 4. 1991.

Odlok o varstvenih pasovih vodnih virov in termalnih vrelcev na območju občine Velenje (In Slovene). Official Gazette of the Republic of Slovenia 3/84. Date: 26. 4. 1986.

Odlok o spremembi in dopolnitvi odloka o varstvenih pasovih vodnih virov v Ljubljani in ukrepih za zavarovanje voda (In Slovene). Official Gazette of the Republic of Slovenia 15/1985. Date 26. 4. 1985.

Odlok o varstvenih pasovih vodnih virov "Podlipa" v Vipavi (In Slovene). Official Gazette of the Republic of Slovenia, OJ RS No. 14/1983. Date: 06.12.1983.

Ogrinc N., Kanduč T., Stichler W., Vreča P. 2005. Spatial and seasonal variations in δ^{18}O and δD values in the river Sava in Slovenia. Journal of Hydrology. 359: 303–312

Orehek S. 1981. Poročilo o petrografski preiskavi vzorcev iz vrtine B-9 Brestovica SW od Komna (In Slovene). Geological Survey of Slovenia, Ljubljana. Archive number: D-II-30d/o-1/107: 11 p.

Orožen Adamič M. (Ed.), Tuttle W., Strauss Fendi M. 2004. Slovenia: a geographical overview. Ljubljana: Association of the Geographical Societies of Slovenia. Založba ZRC: 159 p.

O'Leary M.H., Madhavan S., Paneth P. 1992. Physical and chemical basis of carbon isotope fractionation in plants. Plant, Cell and Environment 15: 1099-1104

Panda U.C., Sundaray S.K., Rath P., Nayak B.B., Bhatta D. 2006. Application of factor and cluster analysis for characterisation of river and estuearine water system – A case study: Mahanadi River (India). Journal of Hydrology, 331: 434-445

Panno S.V., Hackley K.C., Hwang H.H., Greenberg S., Krapac I.G., Landsberger S., O'Kelly D.J. 2006. Characterization and Identification of Na-Cl Sources in Groundwater, 44, 2: 176–187

Parkhurst D.L., Appelo C.A.J. 1999. User's guide to PHREEQC (version 2) - A computer program for speciation, batch-reaction, one-dimensional transport, and inverse geochemical calculations. U.S. Geological Survey Water-Resources Investigations Report, 99-4259: 312 p.

Pauwels H., Müller D., Griffioen J., Hinsby K., Melo T., Brower R. 2007. BRIDGE (BRIDGE - Background cRiteria for the IDentification of Groundwater thresholds). Publishable final activity report, 6th Framework Programme of European Commission: 37 p.

Pavlovec R. 1980. Preperevanje v flišnem peščenjaku (In Slovene). Ljubljana, Proteus, 43-3: 120 p.

Pavlovec R. 1977. Geološki sprehod po slovenski obali (In Slovene). Planinski vestnik 77-7. Ljubljana: 401-408

Peng T.R., Wang C.H., Huang C.C., Fei L.Y., Chen C.T.A., Hwong J.L. 2010. Stable isotopic characteristic of Taiwan's precipitation: a case study of western Pacific monsoon region. Earth and Planetary Science Letters, 289: 357-366.

Petauer D., Žlebnik L. 1993. Strokovne podlage za varovanje vodnega vira, zajetega s črpališčem Lukavci in predlog zaščite (In Slovene). GEOKO d.o.o.: 11 p.

Petek F. 2004. Land use in Slovenia. Slovenia: a geographical overview. Ljubljana, Association of the Geographical Societies of Slovenia. Založba ZRC: 105-108.

Petrič M., Šebela S. 2004. Vulnerability mapping in the recharge area of the Korentan spring, Slovenia. Acta Carsologica, 33, 2: 151-168

Pezdič J. 1999. Izotopi in geokemijski procesi (univerzitetni učbenik) = Isotopes and geochemical processes (University Book) (In Slovene). Faculty of Natural Sciences: Department of geology: 269 p.

Pezdič J. 1997. Recharge and Retention Time Study of a Partly Karstified Area of Boč (Eastern Slovenia) Using Hydrogen, Oxygen and Carbon Isotope Composition as Natural Tracers. Isotopes in Environmental and Health Studies, 33, 3: 293-306

Pezdič J., Novak D., Urbanc J., Dolenec T., Perko S., 1990. Isotopic investigations of springs and aquifers in Bela Krajina. In: Geološkite istražuvanja na mineralnite surovini vo uslovi na pazarnata ekonomija i nivinot pridones za razvoj na zemljata. Book 3, Rudni naogališta geohemija, metalogenija i ekonomska geologija / XII kongres na geolozi na Jugoslavija. Denkovski G. (Ed.). Ohrid: Geološko društvo na Makedonija; Beograd: Sojuz na geološkite društva na Jugoslavija: Sojuz na inžineri i tehničari od rudarska, geološka i metalurška struka na Jugoslavija: 182-202

PGD Komen. 2003. Poročilo o katastrofalnem požaru - Brestovica 2003 (In Slovene): 8 p. http://www.pgdkomen.si/dokumenti/Katastrofalni_pozar-BRESTOVICA_2003.pdf (Feb 9 2013)

Pintar M. 1993. Vpliv kmetijstva na pojavljanje nitrata in atrazine v vodah Apaškega polja (Master thesis) = The impact of agriculture on the occurrence of nitrate and atrazine in waters of Apače field (In Slovene). University of Ljubljana, Biotechnical faculty, Agronomy Department: 106 p.

Pintar M., Suhadolc M., Lobnik F., Hudnik V. 1996. Nitrate and atrazine transfer from rural catchment to water - a case study in the Apače valley, Slovenia. Fresenius Environmental Bulletin, 5, 11-12: 649-654

Pintar M. 2002. $^{15}N/^{14}N$ stable isotope ratios changes during nitrate reduction in a soil = Spremembe razmerja stabilnih izotopov $^{15}N/^{14}N$ pri redukciji nitrata v tleh. In: Zbornik Biotehniške fakultete Univerze v Ljubljani, Kmetijstvo = Research reports (of the) Biotechnical Faculty University of Ljubljana, Agricultural issue, 79, 1: 165-174

Pintar M., Velikonja Bolta Š., Lobnik F. 2008. Nitrogen isotope enrichment factor as an indicator of denitrification potential in top and subsoil in the Apače Valley, Slovenia. Australian Journal of Soil Research, 46, 8: 719-726

Piper A.M. 1944. A graphical procedure in the geochemistry interpretation of water analysis. Transactions, American Geophysical Union, 25, 6: 914-928

Pirc S., Brank M., Mattusch J., Pezdič J. 1998. Distribution of carbon and oxygen stable isotopes in stream waters in Slovenia. RMZ Materials and Geoenvirinment, 45, 1-2: 163-167

Popit A., Vaupotič J. 2002. The influence of geology on elevated radon concentrations in Slovene schools and kindergartens. Geologija, 45, 2: 499–504

Prestor J., Vidic S., Mali N., Krivic J., Rikanovič R., Mozetič S., Levičnik L. 2009. Končno poročilo za pripravo Uredbe o vodovarstvenem območju za vodno telo vodonosnikov za območje Postojne in Cerknice (In Slovene). Geological Survey of Slovenia, Ljubljana. Archive number: K-II-30d/c-11/1596-j: 16 p.

Prestor J., Janža M., Meglič P., Šinigoj J., Hribernik K., Komac M., Strojan M., Bizjak M., Feguš B., Brenčič M., Krivic J., Kumelj Š., Požar M., Hötzl M., Sušnik A., Benčina D., Krajnc M., Gacin M. 2006. Nacionalna baza hidrogeoloških podatkov za opredelitev teles podzemne vode v Republiki Sloveniji = National database of hydrogeological data for identification of groundwater bodies in the Republic of Slovenia (in Slovene). Ljubljana, Geological Survey of Slovenia, Archive number: K-II-30d/c-11/1113-j: 4 books.

Prestor J., Komac M., Janža M., Meglič P., Bavec M., Poljak M. 2004. Hydrogeological map of Slovenia 1:250.000 (IAH). Geological Survey of Slovenia, 1 sheet.

Prestor J., Rikanovič R., Janža M. 2002. Podzemne vode. nesreče in varstvo pred njimi (In Slovene). Ljubljana, Uprava RS za zaščito in reševanje Ministrstva za obrambo: 200-205.

Prestor J., Janža M., Rikanovič R., Strojan M. 2001. Dosegljivost, izkoristljivost in izkoriščenost podzemnih vodonosnikov = Accessibility, exploitability and utilization of underground aquifers (In Slovene). Ljubljana, Geological Survey of Slovenia: 44 p.

Pretner L. 2013. Lastnosti tal brkinskega in istrskega fliša = Soil characteristics of the Brkini and Istria flysch (Graduation thesis) (In Slovene). University of Ljubljana: 108 p.

Prosser S.J., Scrimgeour C.M. 1995. High-precision determination of $^2H/^1H$ in H_2 and H_2O by continuous-flow isotope ratio mass spectrometry. Analytical Chemistry, 67:1992–1997

Pučnik J. 1980. Velika knjiga o vremenu = Big book about the weather (In Slovene). Ljubljana: Cankarjeva založba

Quevauviller P.P., Fouillac A.M., Grath J., Ward R. (Eds.). 2009. Groundwater Monitoring (Water Quality Measurements). John Wiley & Sons Ltd., Chichester: 450 p.

Radar precipitation measurement from 6th of February 2013. Slovenian Environment Agency. Available from: http://www.arso.gov.si/vreme/napovedi%20in%20podatki/radar_animacija.html

Radtke D.B., Wilde F.D., Davis J.V., Popowski T.J. 1998. Alkalinity and acid neutralizing capacity. In: Wilde F.D., Radtke D.B. (Eds.). National Field Manuel for the Collection of Water Quality Data, U.S. Geological Survey TWRI Book 9, pp. ALK1–ALK33. USGS Office of Water Quality: Reston, Virginia http://water.usgs.gov/owq/FieldManual/Chapter6/Archive/Section6.6_4-98.pdf

Rail C.D. 2000. Groundwater Contamination: Contamination, Sources, & Hydrology, Vol. 1. Lancaster, Pennsylvania: Technomic Publishing Company, Inc.: 139 p.

Rakovec J., Vrhovec T. 2007. Osnove meteorologije za naravoslovce in tehnike (In Slovene). Ljubljana, DMFA: 313 p.

Rakovec J., Gregorič G., Vrhovec T., Gaberšek S. 2003. Terrain and precipitation patterns on southern side of the Alps in meso-beta scale. In: Publ. MeteoSwiss 66: International Conference on Alpine Meteorology and MAP-Meeting 2003. Extended Abstracts (Vol. A); 2003 May 19–23; ICAM and MAP Meeting Brig (CH): 4 p.

Ramesh K., Gowri V.S. 2012. Silicate or calcite weathering in wet-dry climate in lower Varahanadi basin, Tamilnadu, India – A determinant in warming. International Journal of Environmental Sciences, 2, 4: 2155-2166

Ramesh K., Jagadeeswari B.P. 2012. Hydrochemical Characteristics of Groundwater for Domestic and Irrigation Purposes in Periyakulam Taluk of Theni District, Tamil Nadu. International Research Journal of Environment Sciences, 1, 1: 19-27

Ramesh K.A., Riyazuddin P. 2008. Application of chemometric techniques in the assessment of groundwater pollution in a suburban area of Chennai city, India. Research articles: 11 p. http://www.currentscience.ac.in/Downloads/article_id_094_08_1012_1022_0.pdf (Nov 12 2012)

Rastogi M., Singh S., Pathak H. 2002. Emission of carbon dioxide from soil. Current science, 82, 5: 510-517

Ravikumar P., Somashekar R.K. 2011. Environmental Tritium (^3H) and hydrochemical investigations to evaluate groundwater in Varahi and Markandeya river basins, Karnataka, India. Journal of Environmental Radioactivity, 102, 2: 153-162

Redondo R., Yélamos J.G. 2005. Determination of CO_2 origin (natural or industrial) in sparkling bottled waters by $^{13}C/^{12}C$ isotope ratio analysis. Food Chemistry, 92: 507-514

Regulation on the groundwater imission monitoring = Pravilnik o imisijskem monitoringu podzemne vode. 2002. Official Gazette of Republic of Slovenia, OJ RS No. 42/02. (May 5 2002)

Reimann C., Siewers U., Tarvainen T., Bityukova L., Eriksson J., Giucis A., Gregorauskiene V., Lukashev V.K., Matinian N.N., Pasieczna A. 2003. Agricultural Soils in Northern Europe: A Geochemical Atlas. Geologisches Jahrbuch, Sonderhefte, Reihe D, Heft SD 5. Schweizerbart'sche Verlagsbuchhandlung, Stuttgart: 279 p.

Reimann C. de Caritat P. 1998. Chemical Elements in the Environment. Factsheets for the Geochemist and Environmental Scientist. Springer-Verlag, Berlin-Heidelberg: 398 p.

Rejec Brancelj I. (Ed.), Smrekar A. (Ed.), Kladnik D. (Ed.), Perko D. (Ed.), Andjelov M. 2005. Podtalnica Ljubljanskega polja, Geografija Slovenije, 10 (In Slovene). Ljubljana, Založba ZRC: 39-61

Repe B. 2004. Soils of Slovenia. In: Slovenia: a geographical overview. Orožen Adamič M (Ed.). Ljubljana: Association of the Geographical Societies of Slovenia: Založba ZRC: 51-56

Repe B. 2010. Prepoznavanje osnovnih prsti slovenske klasifikacije (In Slovene). Ljubljana, Oddelek za geografijo Filozofske fakultete, Razprave Dela: 143-166. http://www.dlib.si/details/URN:NBN:SI:DOC-AJEADGWL (Dec 4 2012)

Report of the heavy rain from 6th to 10th July 2009. Slovenian Environment Agency. Ljubljana, July 20th 2009. http://meteo.arso.gov.si/uploads/probase/www/climate/text/sl/weather_events/dezevje_jul09.pdf.

Richtef B.C., Kreitler C.W. 1992. Identification of Sources of Ground-Water Salinization Using Geochemical Techniques. U.S. Environmental Protection Agency: 1-6.

Rikanovič R. 2003. Digital land cover/use databases of Slovenia (In Slovene). Geologija, 47, 2: 283-290

Ritter J.A. 2010. Water quality (Principles and practices of water supply opreations). 4th edition. American Water Works Association: 213 p.

Rman N., Szőcs T. 2011. Hydrogeochemical conceptual model: Screening of the geothermal utilization, evaluation of the thermal groundwater bodies and preparation of the joint aquifer management plan in the Mura-Zala basin. Operational programme Slovenia-Hungary 2007-2013. 47 p. http://geo-portal.hu/static/tjam/En_pdf/EN_hydrogeochemical_model.pdf

Roads Act = Zakon o cestah/ZCes-1/. 2010. Official Gazette of the Republic of Slovenia 109/2010, OJ RS, No. 109/2010. Date Dec 30 2010.

Romesburg H. C. 2004. Cluster analysis for researchers. North Carolina, Lulu Press: 340 p.

Ronen E. 2007. Micro-elements in Agriculture. Practical Hydroponics & Greenhouses: 39-48 http://www.haifa-group.com/files/articles/micro_nutrients.pdf (Dec 1 2012)

Rosen M.R. 2001. Hydrochemistry of New Zealand's aquifers. In: Groundwaters of New Zealand. Rosen M.R., White P.A. The New Zealand Hydrological Society Inc., Wellington: 77-110

Różański K., Araguas-Araguas L., Gonfiantini R. 1993. Isotopic patterns in modern global precipitation. Geophysical Monograph, 78: 1-36

Różański K., Gröning M. 2004. Tritium assay in water samples using electrolytic enrichment and liquid scintillation spectrometry. In: Quantifying uncertainty in nuclear analytical measurements, International Atomic Energy Agency (IAEA). Vienna: 195-217

Rules on evidence of actual agricultural and forestal land use. 2006. Official Gazette of RS, OJ RS No. 90/06, 9/08, 45/08 - ZKme-1 in 122/08.

Rules on determining water bodies of groundwater. Official Gazette of the Republic of Slovenia, OJ RS No. 63/2005. Date Jul 4 2005.

Rules on drinking water. 2004 (In Slovene). Official Gazette of the Republic of Slovenia, OJ RS No. 19/2004, 35/2004, 26/2006, 92/2006, 25/2009. Date Feb 3 2004.

Sampat P. 2000. Deep Trouble: The Hidden Threat of Groundwater Pollution. Worldwatch Paper 154. Worldwatch Institute, Washington DC: 127 p.

Sara Martin N. 2003. Site Assessment and Remediation Handbook, 2nd Edition, CRC Press, Taylor & Francis Group: 1160 p.

Saulnier G. M., Castaings W., Hohenwallner D., Brancelj A., Bertoncelj I., Brenčič M., Brun A., Cadoux-Rivollet M., Cainelli O., Calvi C., De Bona A., Doering M., Defrancesco C., Dutto E., Freundl G., Harum T., Jamsek A., Klemenčič-Kosi S., Kopeinig C., Klug H., Komma J., Lachenal P., Lascours S., Leskosek T., Mezek T., Mignone N., Mori N., Mourembles C., Neuwirth J., Paccard P., Pascariello A., Pergher P., Poltnig W., Pusenjak M., Rampazzo R., Reszler C., Rikanovic R., Robinson C., Rollando A., Schlamberger J., Scussel R., Siligardi M., Suette G., Valentar V., Vercelli C., Wagner K., Zadravec D., Zalavari P., Zessar H. 2011. Monitoring and Modelling of Mountain Water Resources. A short guideline based on the results of Alp-Water-Scarce Alp-WAter-ScArce (Oct. 2008 – Oct. 2011). http://www.alpine-space.eu/fileadmin/media/Running_Projects/AlpWaterScarce/ALp_WaterScarce_results/Booklet_Monitoring_Modelling_web.pdf (Nov 11 2012)

Schulte P., Van Geldern R., Freitag H., Karim A., Négrel P., Petelet-Giraud E. Probst A., Probst J.-L., Telmer K., Veizer J., Barth J.,A.C. 2011. Applications of stable water and carbon isotopes in watershed research: Weathering, carbon cycling, and water balances. Earth-Science Reviews, 109, 1-2: 20-31

Selinus O. (Ed.). 2005. Essentials of Medical Geology, Elsevier: 812 p.

Shand P., Edmunds W.M., Lawrence A.R., Smedley P.L., Burke S. 2007. The natural (baseline) quality of groundwater in England and Wales (British Geological Survey Research Report RR/07/06). Environment Agency: 72 p.

Shapiro S.S., Wilk M.B., Chen H.J. 1968. A comparative study of various tests for normality. Journal of the American Statistical Association, 63: 1343-1372

Shin W.J., Chung G.S., Lee D., Lee K.S. 2011. Dissolved inorganic carbon export from carbonate and silicate catchments estimated from carbonate chemistry and $\delta^{13}C_{DIC}$. Hydrology and Earth System Sciences, 15: 2551-2560

Silva S.R., Kendall C., Wilkison D.H., Ziegler A.C., Chang C.C.Y., Avanzino R.J. 2000. A new method for collection of nitrate from fresh water and the analysis of nitrogen and oxygen isotope ratios. Journal of Hydrology, 228: 22-36

Singhal B.B.S., Gupta R.P. 2010. Applied Hydrogeology of Fractured Rocks. Dordrecht, Kluwer, 2nd Edition: 393 p.

Sinkhole. 2013. Learn About Sinkholes: Categories of Sinkholes.
http://www.sinkhole.org/facts3.php (Jul 15 2013)

SIST ISO 5667-11. 1996. Water quality, sampling part 11: guidance on sampling of groundwater. 10 p.

SIST ISO 5667-03. 1996. Water quality, sampling-part 3: instructions for storage and handling of samples.

SIST ISO 5667-6. 1996. Water quality, sampling-part 6: guidance on sampling of rivers and water courses.

SIST ISO 14911. 2000. Water quality-determination of dissolved Ca^{2+}, Mg^{2+}, Na^{+}, K^{+}, Cl^{-}, NO_3^{-}, SO_4^{2-} using ion chromatography-method for water and waste water.

SIST ISO 10523. 2010: Water quality- Determination of pH.

SIST EN 27888. 1998: Water quality - Determination of electrical conductivity (ISO 7888:1985). 6 p.

SIST ISO 7150-1. 1996: Water quality- Determination of NH_4^{+}. 7 p.

Skaberne D., Ramovš D., Ogorelec B. 2009. Middle and upper Permian (Chapter 4.5). In: Geologija Slovenije = The geology of Slovenia. Pleničar M., Ogorelec B., Novak M. (Eds.). Ljubljana, Geological Survey of Slovenia: 137-154

Skumavec D., Šabić D. 2005. Pokrovnost tal v Sloveniji 1993-2001 = Land cover in Slovenia 1993-2001, 68 p.
http://www.stat.si/doc/pub/rr-815-05.pdf (12 Nov 2013)

Snoeyink V.L., Jenkins D. 1980. Water Chemistry. Wiley: 480 p.

StatSoft.Inc. 2006. STATISTICA (Data Analysis Software System).Version 6.1 www.statsoft.com (Oct 28 2010)

StatSoft.Inc. 2013. StatSoft Electronics Textbook. Basic Statistics.
http://www.statsoft.com/Textbook/Basic-Statistics (Nov 2 2011)

Strnad J. 2009. O tem, zakaj solijo ceste in še o čem (In Slovene). Presek, list za mlade matematike, fizike, astronome in računarje: 9 p.
http://www.presek.si/8/472-Strnad.pdf (Dec 12 2011)

Stevens G.J. 2007. Groundwater Quality of Coastal Settlements, Golden Bay. Report EP07/06/02. Unpublished internal report, Tasman District Council: 1-10

Stumm W. Morgan J.J. 1996. Aquatic chemistry: Chemical equilibria and rates in natural waters. 3rd Edition. John Wiley & Sons, Inc., New York: 1022 p.

Subba Rao N., Surya Rao P. 2010. Major ion chemistry of groundwater in a river basin: a study from India. Environmental Earth Sciences, 61: 757-775

Sundaram B., Feitz A., Caritat P. de. Plazinska A., Brodie R., Coram J., Ransley T. 2009. Groundwater Sampling and Analysis – A Field Guide. Geoscience Australia, 27: 95 p.
http://www.ga.gov.au/image_cache/GA15501.pdf (Dec 1 2011)

Szőcs T., Rman N., Süveges M., Palcsu L., Tóth G., Lapanje A. 2013. The application of isotope and chemical analyses in managing transboundary groundwater resources. Applied Geochemistry, 32: 95-107

Szramek K., McIntosh J.C., Wiliams E.L., Kadunc T., Ogrinc N., Walter L.M. 2007. Relative weathering intensity of calcite versus dolomite in carbonate-bearing temperate zone watersheds: Carbonate geochemistry and fluxes from catchments within the St. Lawrence and Danube river basins. Geochemistry, Geophysicy, Geosystems, 8, 4: 26 p.

Šajn R., Bidovec M., Andjelov M., Pirc S., Gosar M. 1998. Geokemični atlas Ljubljane in okolice = Geochemical atlas of Ljubljana and environs. Ljubljana. Institute of Geology, Geotechnics and Geophysics, Ljubljana: 34 p.

Šturm M. 2011. Nitrate migration in plant-soil-groundwater system: The use of stable nitrogen isotopes in agricultural research. Paperback – August 26, 2011: 128 p.

Šturm M., Lojen S. 2011. Nitrogen isotopic signature of vegatables from the Slovenian market and its suitability as an indicator of organic production. Isotopes in Environmental and Health Studies, 47: 214-220

Taylor J.R. 2003. Evaluating Groundwater Nitrates from On-Lot Septic Systems, a Guidance Model for Land Planning in Pennsylvania. 12 p.
http://www.taylorgeoservices.com/papers/nitratereport.PDF (Jan 8 2013)

TIS/ICPVO - Infrastrukturni center za pedologijo in varstvo okolja, Biotehniška fakulteta, Univerza v Ljubljani, Ljubljana 1999-2014, 1 sheet.

Trček B. 2006. Isotopic investigations in the area of the Union brewery water body. Geologija, 49, 1: 103-112

Trček B. 2003. Epikarst zone and the karst aquifer behaviour: a case study of the Hubelj catchment, Slovenia. Geological Survey of Slovenia, Ljubljana: 100 p.

Todd D.K., Mays L.W. 2005. Groundwater Hydrology. 3rd Ed.John Wiley & Sons Inc. U.S.A: 636 p.

Tóth J. 1999. Groundwater as a geologic agent: An overview of the causes, processes and manifestation. Hydrogeology Journal, 7: 1-14

Uhan J., Krajnc M. 2003. Podzemna voda. In: Vodno bogastvo Slovenije = Water wealth in Slovenia (In Slovene). Ministry of the Environment and Spatial Planning; Environmental Agency of the Republic of Slovenia, Ljubljana: 54-67.

Urankar B. 2007. Zimsko vzdrževanje na državnih cestah Gorenjske regije (diplomsko delo) = Winter maintenance work on public motorways in Gorenjska region (graduate thesis) (In Slovene). B&B Višja strokovna šola, Kranj: 56 p.
http://www.bb.si/doc/diplome/Urankar_Bostjan-Zimsko_vzdrzevanje_cest.pdf (Sep 12 2013).

Urbanc J. 1989 Izotopska sestava ogljika v počasi iztekajočih kraških vodah (magisterij) = The isotopic composition of carbon in the karst waters with slow effluent (Master Thesis) (in Slovene). University of Ljubljana: 121 p.

Urbanc, J. 1993. Značilnosti izotopske sestave ogljika in kisika v vodah s karbonatnih kamnin (doktorska disertacija) = Characteristics of the isotopic composition of carbon and oxygen in the waters in carbonate rocks (Doctoral dissertation) (In Slovene). University of Ljubljana: 144 p.

Urbanc J., Jamnik B. 1999. Isotope investigations of groundwater from Ljubljansko polje (Slovenia). Geologija, 41: 355-364

Urbanc J., Jamnik B. 2007. Distribution and origin of nitrates in the groundwater of Ljubljansko polje. Geologija, 50, 2: 467-475

Urbanc J., Mali N., Jurkovšek B., Mezga K., Cerar S., Hoetzl M., Mozetič S., Levičnik L., Benčina D. 2010. Strokovne osnove za varovanje vodnih virov na območju kraškega vodonosnika Brestovica (In Slovene). Geological Survey of Slovenia, Ljubljana. Archive number: K-II-30d/c-20/1596-t: 64 p.

Urbanc J., Mezga K., Zini L. 2012. An assessment of capacity of Brestovica – Klariči karst water supply (Slovenia). Acta Carsologica, 41, 1: 89–100

U.S. Geological Survey. 1999. Tracing and Dating Young Ground Water. Fact sheet, 134, 99: 4 p. http://pubs.usgs.gov/fs/FS-134-99/pdf/fs-134-99.pdf (Nov 15 2011)

Vaupotič J., Ogrinc N., Brenčič M., Kobal I. 2011. Tritium mapping in spring waters in Slovenia. Geochemical Journal, 45: 505-512

Verbovšek T. 2006. Topographic setting, proximity to the rivers and technical factor influence on the well yield of the dolomite aquifers in Slovenia. RMZ Materials and Geoenvironment, 53, 4: 455-466

Verbovšek T. 2011. A comparison of parameters below the limit of detection in geochemical analyses by substitution methods. RMZ Materials and Geoenvironment, 58, 4: 393-404

Vidrih R. 2006. Minerali karavanškega predora = Karawanken tunnel minerals (In Slovene). Scopolia Supplement, 3: 125-127

Vogel J.C., Lerman J.C., Mook W.G. 1975. Natural isotopes in surface and groundwater from Argentina. Hydrological Sciences Bulletin, 2: 203-221

Voigt H.-J., Hannappel S., Kunkel R., Waendland F. 2005. Assessment of natural groundwater concentrations of hydrogeological structures in Germany. Geologija, 50: 35-47

Vončina E., Brodnjak Vončina D., Mirkovič N., Novič M. 2007. Chemometric characterisation of the quality of ground waters from different wells in Slovenia. Acta Chimica Slovenica, 54: 119-125

Vreča P., Kanduč T., Žigon S., Trkov Z. 2005. Isotopic composition of precipitation in the Mediterranean basin in relation to air circulation patterns and climate. Final report of a coordinated research project

---

2000–2004 (IAEATECDOC No.1453). Vienna, AU: IAEA, Isotopic composition of precipitation in Slovenia, p. 157–172.

Vreča P., Krajcar Bronić I., Horvatinčić N. 2006a. Isotopic characteristics of precipitation in Slovenia and Croatia: Comparison of continental and maritime stations. Journal of Hydrology, 330: 457-469

Vreča P., Leis A., Trkov Z., Žigon S., Lindbichler S. 2006b. Comparison of monthly and daily isotopic composition of precipitation in South-Western Slovenia. Paper presented at: Austrian Stable Isotope User Group Meeting. The 7th Group Meeting; 2006, Nov 24–25; Graz, AU: 43 -46

Vreča P., Brenčič M., Leis A., 2007. Comparison of monthly and daily isotopic composition of precipitation in the coastal area of Slovenia. Isotopes in Environmental and Health Studies, 43, 4: 307–321

Vreča P., Krajcar-Bronić I., Leis A., Brenčič M. 2008. Isotopic composition of precipitation in Ljubljana (Slovenia). Geologija, 52: 169–180

Vreča P., Brenčič M., Ogrinc N., Kocman D. 2010. Spatial and temporal variations of isotopic composition of precipitation in Slovenia. Paper presented at: The Commission internationale pour l'exploration scientifique de la Mer Méditeranée, CIESM (The Mediterranean Science Commission) 39th Congress; 2010 May 10–14; Venezia, Italy: 1 p.

Vreča P., Krajcar Bronić I., Leis A. 2011. Isotopic composition of precipitation in Portorož (Slovenia). Geologija, 54, 1: 129–138

Vrščaj B., Prus T., Lobnik F. 2005. Soil Information and Soil Data Use in Slovenia. In: Soil Resources of Europe. Jones, R.J.A., Houškova, B., Bullock, P., Montanarella, L. (Eds). 2nd Edition: 331-344 http://eusoils.jrc.ec.europa.eu/ESDB_Archive/eusoils_docs/esb_rr/n09_EUR20559.pdf (Jun 2 2012)

Wassenaar L.I., Van Wilgenburg S.L., Larson K., Hobson K.A. 2009. A groundwater isoscape (δD, δ^{18}O) for Mexico. Journal of Geochemical Exploration, 102: 123–136

Wedepohl K. H. 1978. Handbook of Geochemistry. Vol II/5. Springer-Verlag, New York: 90 p.

Wendland F., Hannappel S., Kunkel, R. Schenk R., Voigt H.-J., Wolter R. 2003. A Procedure to define natural groudwater conditions of groundwater bodies in Germany. Diffuse Pollution Conference Dublin. 7 p.

Wendland F., Hannappel S., Kunkel R., Schenk R., Voigt H.-J., Wolter R. 2005. A procedure to define natural groundwater conditions of groundwater bodies in Germany. Water Science and Technology 51, 3-4: 249-257

Wendland F., Bertholdb G., Blumc A., Elsass P., Fritscheb J.G., Kunkel R., Wolter R. 2008. Derivation of natural background levels and threshold values for groundwater bodies in the Upper Rhine Valley (France, Switzerland and Germany). Desalination, 226: 160-168

Widory D., Kloppmann W., Chery L., Bonnin J., Rochdi H., Guinamant J.L. 2004. Nitrate in groundwater: an isotopic multi-tracer approach. Journal of Contaminant Hydrology: 72, 1-4: 165-88

Winter T.C., Judson W.H., Lehn O.F., Alley W.M. 1998. Ground Water And Surface Water A Single Resource; U.S. Geological Survey Circular 1139; Denver, Colorado: 87 p.

Wisconsin Department of Natural Resources Laboratory Certification Program. 1996. Analytical Detection Limit Guidance & Laboratory Guide for Determining Method Detection Limits. 33 p. http://dnr.wi.gov/regulations/labcert/documents/guidance/-LODguide.pdf (Sep 25 2012)

WRMG (Wasch- und Reinigungsmittelgesetz). 2007. Gesetz über die Umweltverträglichkeit von Wasch- und Reinigungsmitteln. Ein Service des Bundesministeriums der Justiz in Zusammenarbeit mit der juris GmbH: 5 p. Available at: http://www.gesetze-im-internet.de/bundesrecht/wrmg/gesamt.pdf

Zavadlav S., Kanduč T., McIntosh J., Lojen S. 2013. Isotopic and chemical constraints on the biogeochemistry of dissolved inorganic carbon and chemical weathering in the karst watershed of Krka river (Slovenia). Aquatic geochemistry, 19, 3: 209-230

Zeebe R.E., Wolf-Gladrow D. 2001. CO_2 in Seawater: Equilibrium, Kinetics, Isotopes, 65. Oceanography Series. Elsevier, Amsterdam: 360 p.

Zhang J., Quay P.D., Walbur D.O. 1995. Carbon isotope fractionation during gas–water exchange and dissolution of CO_2. Geochimica et Cosmochimica Acta, 59, 1: 107–114

Zuber A., Michalczyk Z., Maloszewski P. 2001. Great tritium ages explain the occurrence of good-quality groundwater in a phreatic aquifer of an urban area, Lublin, Poland. Hydrogeology Journal, 9: 451-460

Zupan Hajna, N. 2005. Various types of gypsum crystals from Tajna jama, Slovenia. In: Final programme & Abstract book. Athens: Hellenic Speleological Society: Hellenic Federation of Speleology, 2005: 102. http://www.ese.edu.gr/media/lipes_dimosiefsis/14isc_proceedings/o/089.pdf (Jun 15 2012)

Zupanc V., Šturm B.M., Lojen S., Maršić-Kacjana N., Adu-Gyamfi J., Bračič-Železnik B., Urbanc J., Pintar M. 2011. Nitrate leaching under vegetable field above a shallow aquifer in Slovenia. Agriculture, Ecosystems & Environment, 144, 1: 167–174

Zupančič N., Pirc S. 1999. Calcium distibution in soil and stream sediments in Istria (Croatia) and the Slovenian littoral. Journal of Geochemical Exploration, 65: 205-218

Žlebnik L. 1982. Hidrogeološke razmere na Dravskem polju = Hydrogeology of Drava field Ljubljana (In Slovene), Geologija, 25, 1: 151-164

Žlebnik L. 1986. Poročilo o izvedbi vodnjakov V-5/86 in V-6/86 v Skorbi pri Ptuju in o poizkusnem črpanju (In Slovene). Ljubljana, Geological Survey of Slovenia. Archive number: K-II-30d/c-7/146-f: 11 p.

ACKNOWLEDGEMENTS

Doctoral dissertation was a part of the 3-year project »Natural hydrochemical background and dynamics of groundwater in Slovenia« which has been financially supported with state budget by the Ministry of the environment and spatial planning — Slovenian Research Agency (ARRS). The research has been implemented at the Department of Hydrogeology of Geological Survey of Slovenia.

I would like to thank my supervisors Assist. Prof.Dr. Barbara Čenčur Curk and Dr. Janko Urbanc for their help during formation of my doctoral dissertation.

Thanks to members of my thesis committee, Assoc.Prof.Dr. Sonja Lojen, Assist. Prof. Dr. Metka Petrič, and Prof.Dr. Martin Dietzel, for reviewing my research and for their constructive comments and suggestions which improved the final version.

I thank my colleagues from the Department of Groundwater - Hydrogeology at Geological Survey of Slovenia for their help, support and stimulation. Special thanks to Simon.

For useful discussions I would like to thank Sonja, Nina, Katarina, and Uroš.

My biggest thanks go to Tamara, for all the professional advices, discussions, and friendly talks.

To all my friends who encouraged me during my PhD study.

I dedicate this thesis to my parents. Thank you for all the support, understanding, and love!

APPENDICES

Appendix 1

Topographic map of Slovenia

GURS (2005)


N
W
E
S
Grad-1, Grad
VP-1, Prosenjakovci
Gradišče
Strahinec
BLP-2, Nedelica
V-3A, Lukavci
Šumec
Trgovina, Vurberk
DEV-1, Desenci
Žegnan studenec
Pevčevo
Godec
Mazej
V-6, Skorba
Mošenik
Soča
Črna
OV-29, Brunšvik
Krajcarica
Lipnik
Dobravca
Berglez
Jelševa loka
Gljun
Vidovič
Maver
Lipnica
Kamniška Bistrica
Savica
Lučnica
Kropa
Velika Toplica
Pšata
Šempeter 0840
Čemažarjev izvir
Debevčev mlin
Zadlaščica
Vo-1, Vodice
Vt-1, Tinsko
Jurčičev izvir
C-4, Domžale
Trate
Hotešk
Mitovšek
Trebija
Čepovan-1/94
Grajsko zajetje
Dobrova
Sevšek
Grešnikov hrib
Brekovice
LMV-1, Ljubljana
VG-10, Mala Goba
Mrzlek
Podroteja
Iščica
Močilnik
Ščetar
TR-1/99, Trebelno
GI-1, Gornji Ig
DAC-3, Skopice
NG-4
Hubelj
Krka
Vipava
B-9, Brestovica
Malenščica
Tominčev izvir
Pasji rep
Težka voda
P-1, Pliskovica
Korentan
Veliki Vrh, Bloke
Radeščica
Rakitnica
Mali Obrh
Obrh Rinža
Krupa
Metliški Obrh
Odolina
Ilirska Bistrica
Dobličica
Rižana
Padiščak
0
10
20
30
40
km

Appendix 2

Geological map of Slovenia

(Buser, 2010)

⬜ 1, Fluvial sediments (gravel, sand, silt and clay)
▨ 2, Recent marine deposits
▨ 3, Clay
▨ 4, Rubble
▨ 5, Alluvial fan (rubble, gravel and silt)
▨ 6, Deluvium (mostly clay with various rock fragments)
▨ 7, Mine waste deposits
▨ 8, Clay, peat (marsh deposits)
⬜ 9, Clay, silt and weathered peat (marsh and lacustrine deposits)
▨ 10, Gravel and sand
▨ 11, Clayey silt (loess)
▨ 12, Loose fluvial deposits; terraces (gravel, sand, silt and clay)
▨ 13, Coherent fluvial deposits; terraces (conglomerate with gravel intercalations)
▨ 14, Till; moraine
🟨 15, Brown clay, terra rossa, loam
▨ 16, Clay and soil with chert fragments
▨ 17, Clay, clayey silt with pebbles of quartz and siliceous rocks
▨ 18, Quartz gravel, sand and silt
▨ 19, Basaltic tuff and basalt
▨ 20, Gravel, sand and sandy clay
▨ 21, Sandy marl, clay and fine gravel
🟨 22, Clay, silt, sand and coal
▨ 23, Sand and clay
▨ 24, Clayey marl, sand, gravel and clay
▨ 25, Clayey marl and limestone
▨ 26, Marl, sand, gravel, sandstone and conglomerate
▨ 27, Lithothamnium limestone, marly limestone and marl
▨ 28, Marl
▨ 29, Lithothamnium limestone
▨ 30, Sand, silt, sandstone, siltstone and conglomerate
🟨 31, Sand, sandstone and marl
▨ 32, Conglomerate, sandstone and marl - Ivnik beds
▨ 33, Conglomerate (granodioritic, and metamorphic rocks pebbles) - Radlje beds
▨ 34, Lithothamnium-Lepidocyclina limestone, sand, silt and clay
▨ 35, Marly clay - Sivica
▨ 36, Alternation of andesitic tuff, tuffite and marlstone
🟧 37, Dacite, subordinately andesite
🟥 38, Granodiorite and quartz diorite

Figure: Geology legend (1/3)

▩ 39, Tonalite
▨ 40, Gravel, sand, marl, marly limestone, sandstone, clay and coal - "Psevdosocka beds"
▤ 41, Marlstone, sandstone, reef limestone - Gornji Grad beds
▒ 42, Limestone-dolomite conglomerate - Škofja Loka and Okonina Conglomerate
▒ 43, Marlstone, sandstone, claystone and coal - Socka beds
▒ 44, Alternation of marlstone, claystone and sandstone, intercalations of limestone breccia - flysch
▨ 45, Alveolina-nummulites limestone
■ 46, Alveolina-nummulites and miliolida limestone
▒ 47, Alternation of sandstone, marlstone and claystone, frequent intercalations of limestone breccia - flysch
▨ 48, Thick-bedded micritic limestone - Vreme and Kozina beds
■ 49, Reddish and greenish marlstone and marly limestone - Sabotin beds
▧ 50, Reddish and gray marly limestone and marlstone
▒ 51, Alternation of marlstone, claystone and sandstone - flysch
▒ 52, Coarse-grained limestone breccia with intercalations of flysch
■ 53, Platy Volče limestone with chert, red marly limestone and marlstone
■ 54, Rudist limestone and calcarenite - Lipica Formation
▨ 55, Platy limestone with chert - Dutovlje Formation
▧ 56, Platy limestone with chert in alternation with red marlstone - Krško beds
■ 57, Rudist and micritic limestone - Sežana Formation
▨ 58, Platy limestone with chert - Komen beds
■ 59, Thick-bedded micritic limestone and bituminous dolomite
▒ 60, Alternation of claystone and calcarenite, chert layers - flysch
■ 61, Alternation of limestone and dolomite (lower part), micritic limestone (upper part)
▒ 62, Alternation of marlstone, claystone and calcarenite - flysch
▧ 63, Platy Biancone limestone with chert
■ 64, Alternation of dolomite and limestone
▨ 65, Oolitic and micritic limestone
■ 66, Thick-bedded micritic and oolitic limestone
▨ 67, Reef limestone with corals, hydrozoans and sponges
■ 68, Reddish and grayish nodular limestone of Ammonitico Rosso type, limestone breccia, marlstone and claystone
▒ 69, Shale with chert, stripped marlstone and limestone
▧ 70, Massive crinoidal and oolitic limestone
■ 71, Micritic and oolitic limestone, bituminous dolomite
■ 72, Micritic and oolitic limestone, limestone breccia and bituminous dolomite
▒ 73, Platy micritic limestone and calcarenite with chert
■ 74, Limestone, dolomite, and limestone-dolomite breccia
▧ 75, Reef limestone with corals
■ 76, Thick-bedded Dachstein Limestone with transitions to dolomite

Figure: Geology legend (2/3)

🟥 77, Thick-bedded Main Dolomite
🟥 78, Platy Bača Dolomite with chert
🟥 79, Claystone, sandstone, tuff, tuffite, breccia, platy limestone, dolomite in alternation with marlstone, bauxite - Borovnica beds
▤ 80, Marly limestone, marlstone, dolomite, shale
▧ 81, Platy limestone and dolomite with chert, marlstone, marly limestone - Tamar Formation
▩ 82, Chert, platy limestone, claystone and siltstone - Kobla Formation
🟥 83, Alternation of claystone and sandstone, platy limestone in the upper part - Amphiclina beds
🟥 84, Massive coarse-crystalline dolomite and limestone
🟥 85, Massive Wetterstein Limestone and dolomite, thick-bedded limestone
🟥 86, Massive dolomite, subordinately limestone
🟥 87, Platy micritic limestone with chert nodules - Pokljuka Formation
🟥 88, Keratophyre, quartz keratophyre, porphyre, porphyrite and their tuffs
🟩 89, Diabase, spilitic diabase and their tuffs
🟪 90, Shale, siltstone, platy limestone with chert, marlstone, graywacke, sandstone, conglomerate, breccia, tuff
🟪 91, Thick-bedded and massive dolomite, subordinately limestone
🟪 92, Dolomite, micaceous siltstone, sandstone, claystone, oolitic limestone and dolomite, marlstone, marly limestone
🟧 93, Thick-bedded dolomite, subordinately limestone
🟫 94, Red and gray sandstone, shale and conglomerate - Val Gardena Formation, in the Karavanke Mts.Tarvis Breccia in the lower part
🟪 95, Porphyritic granite with diabase enclaves, granodiorite
🟫 96, Neoschwagerina reef limestone, limestone breccia
🟫 97, Light-gray to red limestone - Dovžanova soteska and Trogkofel Formations
🟫 98, Alternation of shale, quartz sandstone and conglomerate, limestone intercalations
⬜ 99, Alternation of shale and quartz sandstone, quartz conglomerate
⬜ 100, Alternation of shale, quartz sandstone and conglomerate, limestone intercalations
⬜ 101, Alternation of shale and graywacke, breccia, intercalations of laminated limestone
🟫 102, Thick-bedded limestone in the lower part, reef limestone in the middle part, thick-bedded micritic limestone in the upper part
🟩 103, Diabase and its tuff
🟩 104, Slate with intercalations of diabase and recrystallized limestone - Magdalensberg Formation
▨ 105, Serpentinite
⬜ 106, Quartz-sericite phyllite with marble and quartzite intercalations
🟩 107, Chlorite-amphibole and biotite-chlorite schist with amphibolite intercalations
🟧 108, Staurolite and almandine mica schist with transitions to gneiss
🟧 109, Fine-grained gneiss with transitions to mica schist
🟫 110, Diaphthorite
🟦 111, Marble
▨ 112, Amphibolites, lenses of eclogite
▨ 113, Biotite-muscovite mica schist with transitions to gneiss
🟧 114, Muscovite-biotite gneiss, kyanite flaser augen gneiss, veins of pegmatite gneiss

Figure: Geology legend (3/3)

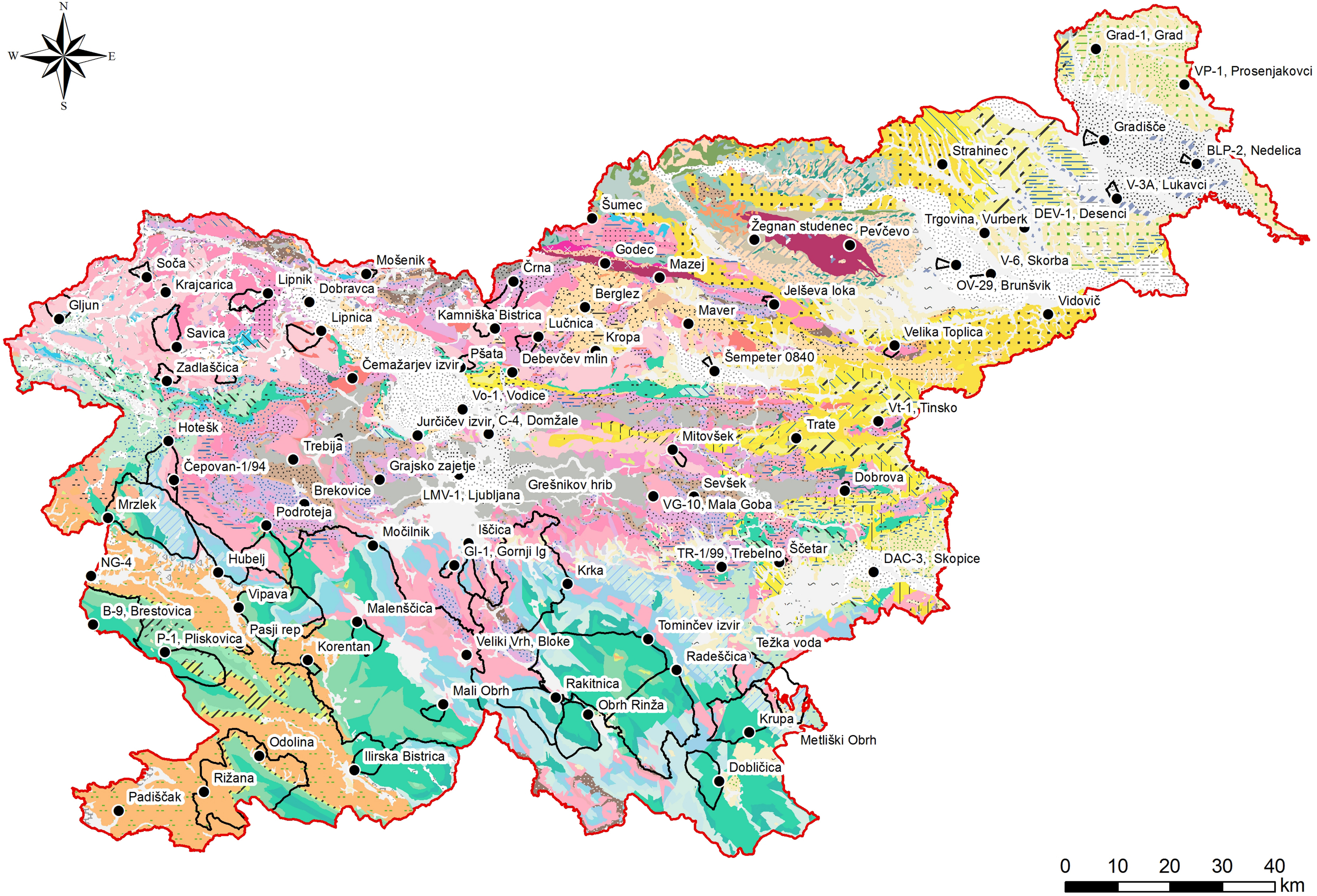
N
W
E
S
Grad-1, Grad
VP-1, Prosenjakovci
Gradišče
BLP-2, Nedelica
Strahinec
V-3A, Lukavci
Šumec
Trgovina, Vurberk
DEV-1, Desenci
Žegnan studenec
Pevčevo
Godec
Mazej
V-6, Skorba
Mošenik
Soča
Črna
OV-29, Brunšvik
Krajcarica
Lipnik
Dobravca
Berglez
Jelševa loka
Gljun
Vidovič
Lipnica
Kamniška Bistrica
Maver
Savica
Lučnica
Kropa
Velika Toplica
Pšata
Debevčev mlin
Šempeter 0840
Zadlaščica
Čemažarjev izvir
Vo-1, Vodice
Vt-1, Tinsko
Jurčičev izvir
C-4, Domžale
Trate
Hotešk
Mitovšek
Trebija
Čepovan-1/94
Grajsko zajetje
Dobrova
Brekovice
LMV-1, Ljubljana
Grešnikov hrib
Sevšek
Mrzlek
VG-10, Mala Goba
Podroteja
Močilnik
Iščica
NG-4
Hubelj
Gl-1, Gornji Ig
TR-1/99, Trebelno
Ščetar
DAC-3, Skopice
Krka
Vipava
B-9, Brestovica
Malenščica
Pasji rep
Tominčev izvir
P-1, Pliskovica
Korentan
Veliki Vrh, Bloke
Težka voda
Radeščica
Rakitnica
Mali Obrh
Obrh Rinža
Krupa
Metliški Obrh
Odolina
Ilirska Bistrica
Rižana
Dobličica
Padiščak
0
10
20
30
40
km

Appendix 3

Soil map of Slovenia

(TIS/ICPVO, 1999-2014)

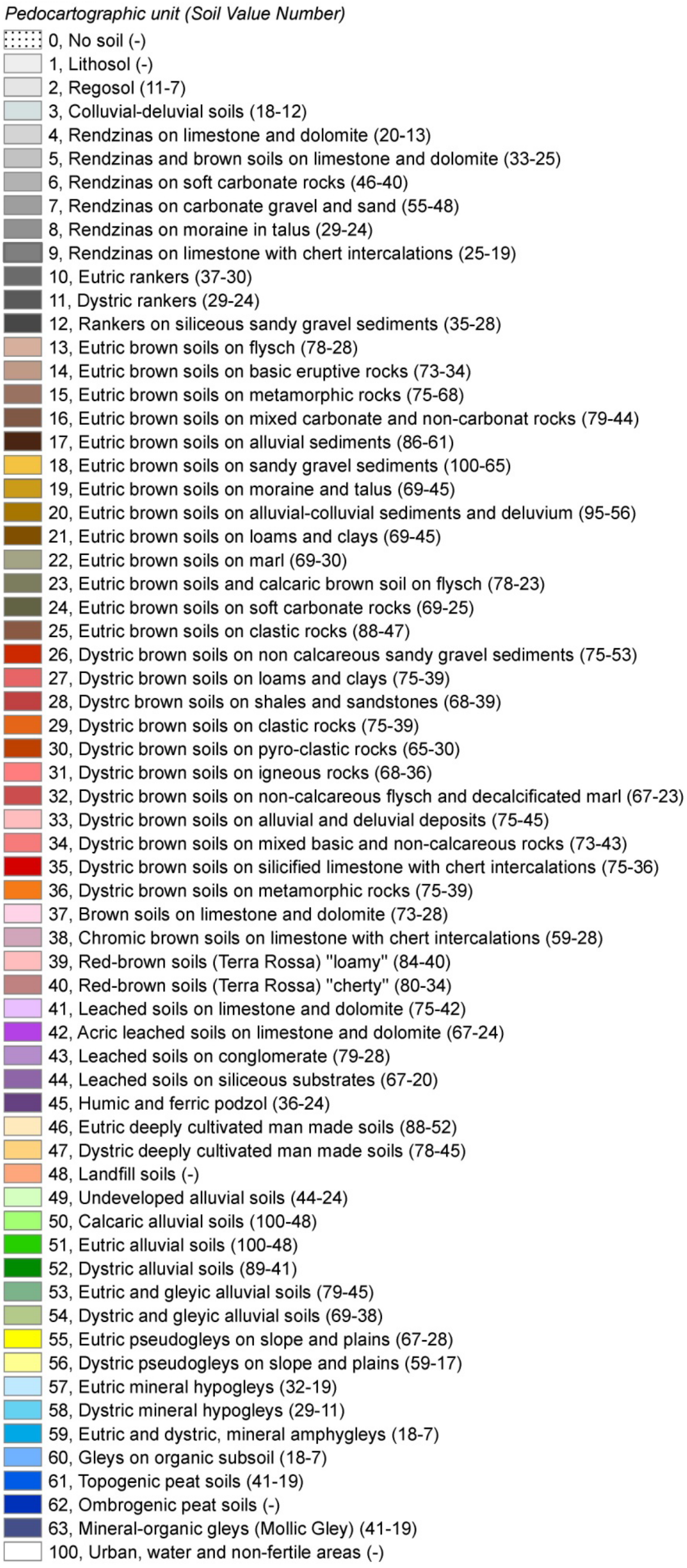

Pedocartographic unit (Soil Value Number)

0, No soil (-)
1, Lithosol (-)
2, Regosol (11-7)
3, Colluvial-deluvial soils (18-12)
4, Rendzinas on limestone and dolomite (20-13)
5, Rendzinas and brown soils on limestone and dolomite (33-25)
6, Rendzinas on soft carbonate rocks (46-40)
7, Rendzinas on carbonate gravel and sand (55-48)
8, Rendzinas on moraine in talus (29-24)
9, Rendzinas on limestone with chert intercalations (25-19)
10, Eutric rankers (37-30)
11, Dystric rankers (29-24)
12, Rankers on siliceous sandy gravel sediments (35-28)
13, Eutric brown soils on flysch (78-28)
14, Eutric brown soils on basic eruptive rocks (73-34)
15, Eutric brown soils on metamorphic rocks (75-68)
16, Eutric brown soils on mixed carbonate and non-carbonat rocks (79-44)
17, Eutric brown soils on alluvial sediments (86-61)
18, Eutric brown soils on sandy gravel sediments (100-65)
19, Eutric brown soils on moraine and talus (69-45)
20, Eutric brown soils on alluvial-colluvial sediments and deluvium (95-56)
21, Eutric brown soils on loams and clays (69-45)
22, Eutric brown soils on marl (69-30)
23, Eutric brown soils and calcaric brown soil on flysch (78-23)
24, Eutric brown soils on soft carbonate rocks (69-25)
25, Eutric brown soils on clastic rocks (88-47)
26, Dystric brown soils on non calcareous sandy gravel sediments (75-53)
27, Dystric brown soils on loams and clays (75-39)
28, Dystrc brown soils on shales and sandstones (68-39)
29, Dystric brown soils on clastic rocks (75-39)
30, Dystric brown soils on pyro-clastic rocks (65-30)
31, Dystric brown soils on igneous rocks (68-36)
32, Dystric brown soils on non-calcareous flysch and decalcificated marl (67-23)
33, Dystric brown soils on alluvial and deluvial deposits (75-45)
34, Dystric brown soils on mixed basic and non-calcareous rocks (73-43)
35, Dystric brown soils on silicified limestone with chert intercalations (75-36)
36, Dystric brown soils on metamorphic rocks (75-39)
37, Brown soils on limestone and dolomite (73-28)
38, Chromic brown soils on limestone with chert intercalations (59-28)
39, Red-brown soils (Terra Rossa) "loamy" (84-40)
40, Red-brown soils (Terra Rossa) "cherty" (80-34)
41, Leached soils on limestone and dolomite (75-42)
42, Acric leached soils on limestone and dolomite (67-24)
43, Leached soils on conglomerate (79-28)
44, Leached soils on siliceous substrates (67-20)
45, Humic and ferric podzol (36-24)
46, Eutric deeply cultivated man made soils (88-52)
47, Dystric deeply cultivated man made soils (78-45)
48, Landfill soils (-)
49, Undeveloped alluvial soils (44-24)
50, Calcaric alluvial soils (100-48)
51, Eutric alluvial soils (100-48)
52, Dystric alluvial soils (89-41)
53, Eutric and gleyic alluvial soils (79-45)
54, Dystric and gleyic alluvial soils (69-38)
55, Eutric pseudogleys on slope and plains (67-28)
56, Dystric pseudogleys on slope and plains (59-17)
57, Eutric mineral hypogleys (32-19)
58, Dystric mineral hypogleys (29-11)
59, Eutric and dystric, mineral amphygleys (18-7)
60, Gleys on organic subsoil (18-7)
61, Topogenic peat soils (41-19)
62, Ombrogenic peat soils (-)
63, Mineral-organic gleys (Mollic Gley) (41-19)
100, Urban, water and non-fertile areas (-)

Figure: Legend of Pedocartographic units

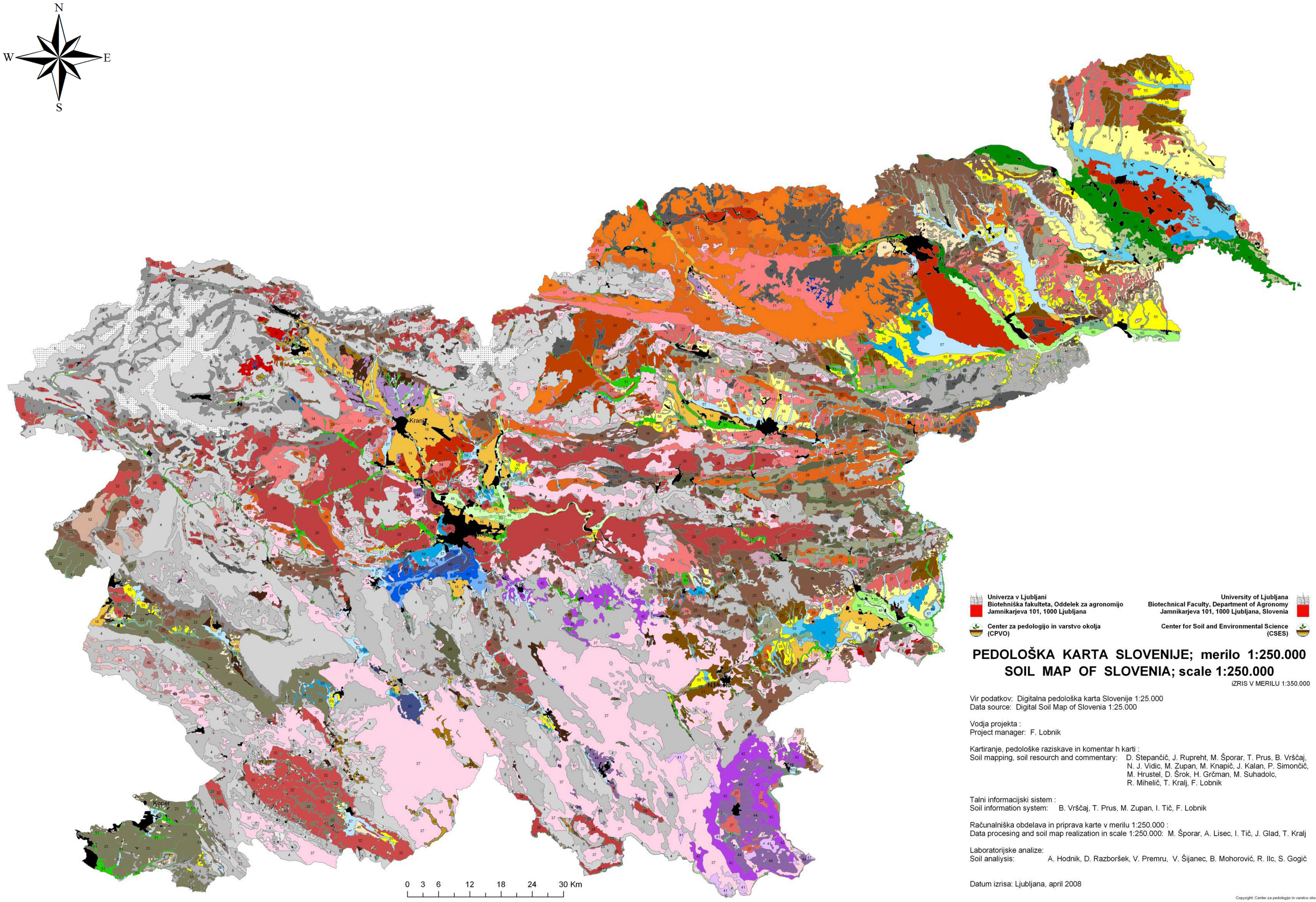

Univerza v Ljubljani
Biotehniška fakulteta, Oddelek za agronomijo
Jamnikarjeva 101, 1000 Ljubljana

University of Ljubljana
Biotechnical Faculty, Department of Agronomy
Jamnikarjeva 101, 1000 Ljubljana, Slovenia

Center za pedologijo in varstvo okolja
(CPVO)

Center for Soil and Environmental Science
(CSES)

PEDOLOŠKA KARTA SLOVENIJE; merilo 1:250.000
SOIL MAP OF SLOVENIA; scale 1:250.000

iZRIS V MERILU 1:350.000

Vir podatkov: Digitalna pedološka karta Slovenije 1:25.000
Data source: Digital Soil Map of Slovenia 1:25.000

Vodja projekta :
Project manager: F. Lobnik

Kartiranje, pedološke raziskave in komentar h karti :
Soil mapping, soil resourch and commentary: D. Stepančič, J. Rupreht, M. Šporar, T. Prus, B. Vrščaj,
N. J. Vidic, M. Zupan, M. Knapič, J. Kalan, P. Simončič,
M. Hrustel, D. Šrok, H. Grčman, M. Suhadolc,
R. Mihelič, T. Kralj, F. Lobnik

Talni informacijski sistem :
Soil information system: B. Vrščaj, T. Prus, M. Zupan, I. Tič, F. Lobnik

Računalniška obdelava in priprava karte v merilu 1:250.000 :
Data procesing and soil map realization in scale 1:250.000: M. Šporar, A. Lisec, I. Tič, J. Glad, T. Kralj

Laboratorijske analize:
Soil analiysis: A. Hodnik, D. Razboršek, V. Premru, V. Šijanec, B. Mohorović, R. Ilc, S. Gogić

Datum izrisa: Ljubljana, april 2008

Appendix 4

Mean annual precipitation in Slovenia (1971-2000)

(Bat *et al.* 2008)

KORIGIRANE PADAVINE (1971–2000)
CORRECTED PRECIPITATION (1971–2000)

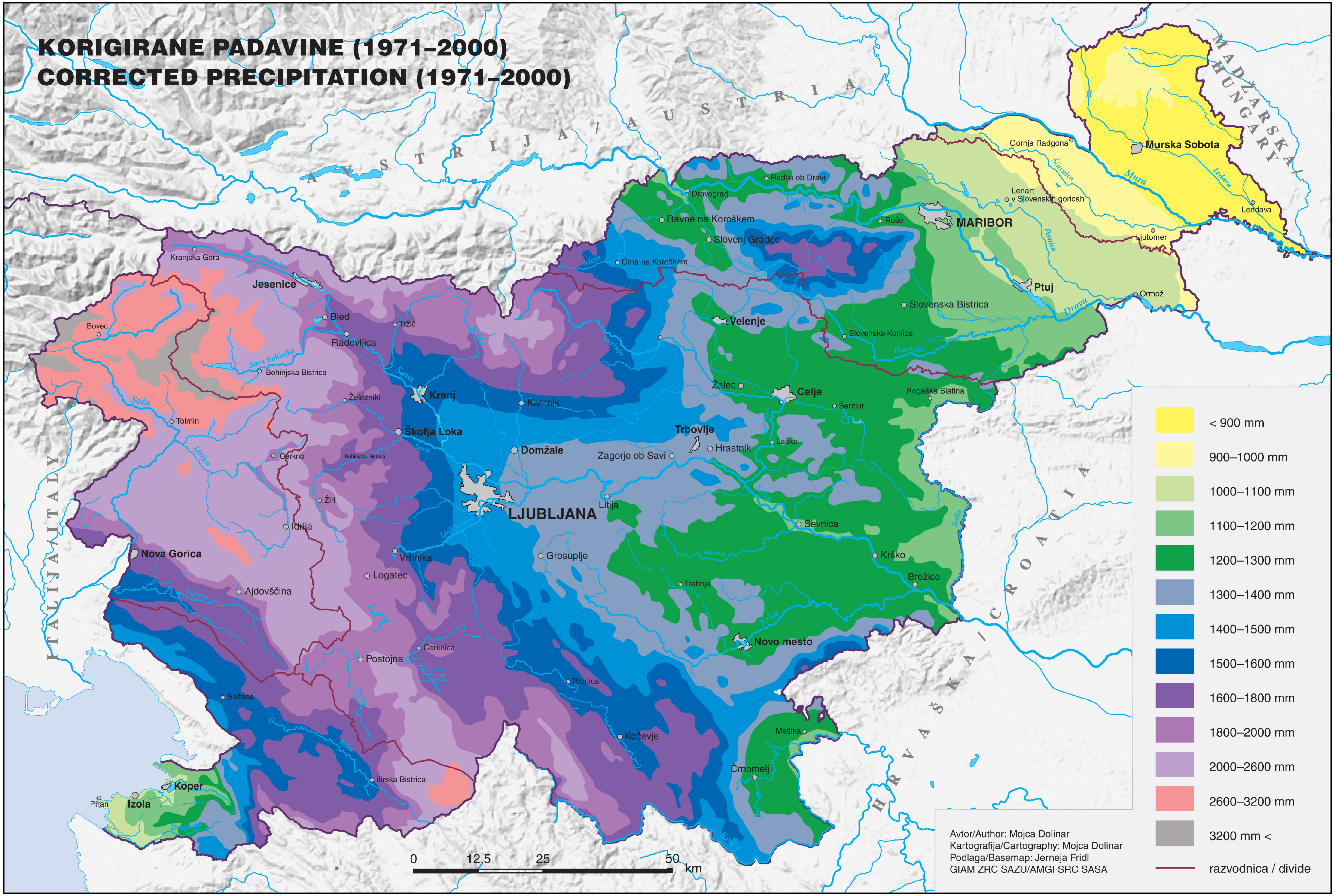

Avtor/Author: Mojca Dolinar
Kartografija/Cartography: Mojca Dolinar
Podlaga/Basemap: Jerneja Fridl
GIAM ZRC SAZU/AMGI SRC SASA

Appendix 5

Hydrogeological map of Slovenia (IAH)

(Prestor *et al.*, 2004)

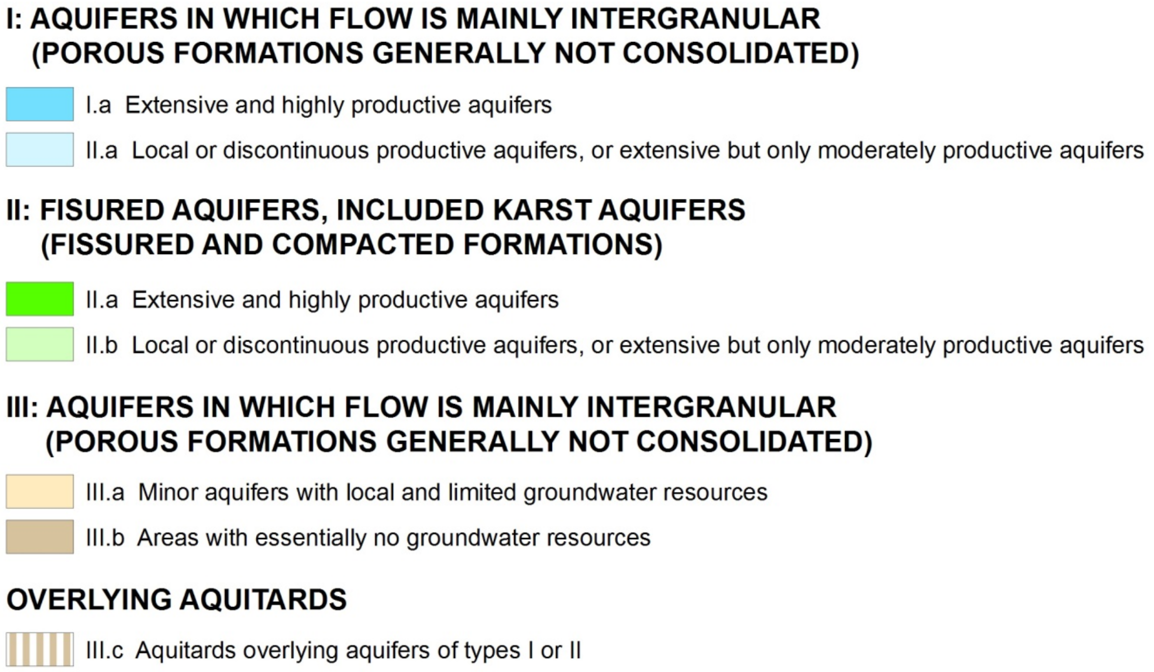

I: AQUIFERS IN WHICH FLOW IS MAINLY INTERGRANULAR
(POROUS FORMATIONS GENERALLY NOT CONSOLIDATED)

- 🟦 I.a Extensive and highly productive aquifers
- 🟦 II.a Local or discontinuous productive aquifers, or extensive but only moderately productive aquifers

II: FISURED AQUIFERS, INCLUDED KARST AQUIFERS
(FISSURED AND COMPACTED FORMATIONS)

- 🟩 II.a Extensive and highly productive aquifers
- 🟩 II.b Local or discontinuous productive aquifers, or extensive but only moderately productive aquifers

III: AQUIFERS IN WHICH FLOW IS MAINLY INTERGRANULAR
(POROUS FORMATIONS GENERALLY NOT CONSOLIDATED)

- 🟨 III.a Minor aquifers with local and limited groundwater resources
- 🟫 III.b Areas with essentially no groundwater resources

OVERLYING AQUITARDS

- ▥ III.c Aquitards overlying aquifers of types I or II

Figure: IAH legend

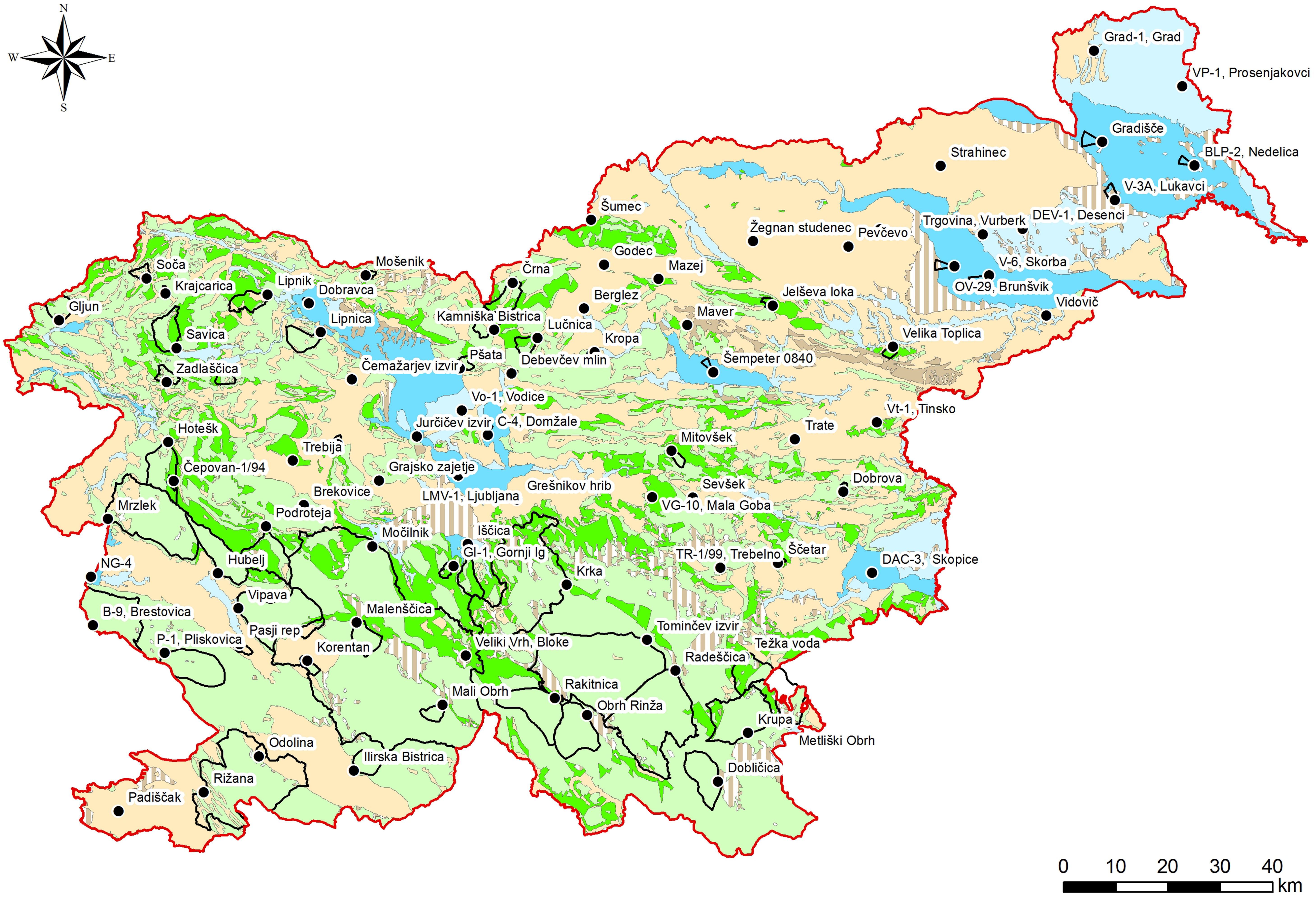
N
W
E
S
Grad-1, Grad
VP-1, Prosenjakovci
Gradišče
BLP-2, Nedelica
Strahinec
V-3A, Lukavci
Trgovina, Vurberk
DEV-1, Desenci
Šumec
Žegnan studenec
Pevčevo
Godec
Mazej
V-6, Skorba
OV-29, Brunšvik
Soča
Mošenik
Črna
Krajcarica
Lipnik
Dobravca
Berglez
Jelševa loka
Gljun
Lipnica
Maver
Vidovič
Savica
Kamniška Bistrica
Lučnica
Kropa
Velika Toplica
Pšata
Debevčev mlin
Šempeter 0840
Zadlaščica
Čemažarjev izvir
Vo-1, Vodice
Vt-1, Tinsko
Jurčičev izvir
C-4, Domžale
Trate
Hotešk
Mitovšek
Trebija
Čepovan-1/94
Grajsko zajetje
Dobrova
Sevšek
Grešnikov hrib
Brekovice
LMV-1, Ljubljana
VG-10, Mala Goba
Mrzlek
Podroteja
Močilnik
Iščica
Ščetar
TR-1/99, Trebelno
GI-1, Gornji Ig
DAC-3, Skopice
NG-4
Hubelj
Krka
Vipava
B-9, Brestovica
Malenščica
Pasji rep
Tominčev izvir
P-1, Pliskovica
Korentan
Veliki Vrh, Bloke
Težka voda
Radeščica
Rakitnica
Mali Obrh
Obrh Rinža
Krupa
Metliški Obrh
Odolina
Ilirska Bistrica
Rižana
Dobličica
Padiščak
0
10
20
30
40
km

Appendix 6

Legend: CORINE Land Cover

(Ministry of the Environment and Spatial planning, Environmental Agency of the Republic of Slovenia, Surveying and Mapping, Authority of the Republic of Slovenia, European Environment Agency, 2003).

- ⬜ Airports
- ⬜ Bare rocks
- ⬜ Beaches, dunes, sands
- 🟩 Broad-leaved forest
- 🟨 Complex cultivation patterns
- 🟩 Coniferous forest
- 🟪 Construction sites
- 🟥 Continuous urban fabric
- 🟥 Discontinuous urban fabric
- 🟫 Dump sites
- 🟧 Fruit trees and berry plantations
- 🟦 Glaciers and perpetual snow
- 🟪 Green urban areas
- 🟪 Industrial or commercial units
- 🟦 Inland marshes
- ⬜ Land principally occupied by agriculture, with significant areas of natural vegetation
- 🟪 Mineral extraction sites
- 🟩 Mixed forest
- 🟩 Moors and heathland
- 🟩 Natural grasslands
- 🟨 Non-irrigated arable land
- 🟨 Pastures
- ⬜ Port areas
- 🟥 Road and rail networks and associated land
- ⬜ Salines
- 🟦 Salt marshes
- 🟩 Sclerophyllous vegetation
- 🟩 Sparsely vegetated areas
- ⬜ Sport and leisure facilities
- 🟩 Transitional woodland-shrub
- 🟧 Vineyards
- 🟦 Water bodies
- 🟦 Water courses

Figure: CORINE Land Cover legend

Appendix 7

Legend: Actual agricultural and forest land usage

(Ministry for Agriculture and the Environment, 2012)

- 🟫 Arable land
- 🟪 Hop fields
- 🟧 Other permanent crops on arable land
- 🟫 Green houses
- 🟨 Vineyards
- 🟥 Nursery
- 🟧 Intensive Orchards
- 🟧 Ekstensive Orchards
- 🟨 Olive groves
- 🟧 Other permanent crops
- 🟩 Meadows and pastures
- 🟩 Swampy meadows
- 🟩 Owergrown areas
- 🟩 Forest plantations
- 🟩 Riparian owergrowth and forest hedges
- 🟩 Uncultivated agriculture land
- 🟩 Forest trees on agricultural land
- 🟩 Forest
- 🟥 Built-up areas and related surfaces
- 🟦 Swamps
- 🟦 Reeds
- 🟦 Other marshy areas
- ▨ Dried open areas with special vegetation
- ⬜ Open areas with little or no vegetation
- 🟦 Waters

Figure: Actual agricultural and forest land usage

Appendix 8

Sampling locations with determined recharge areas

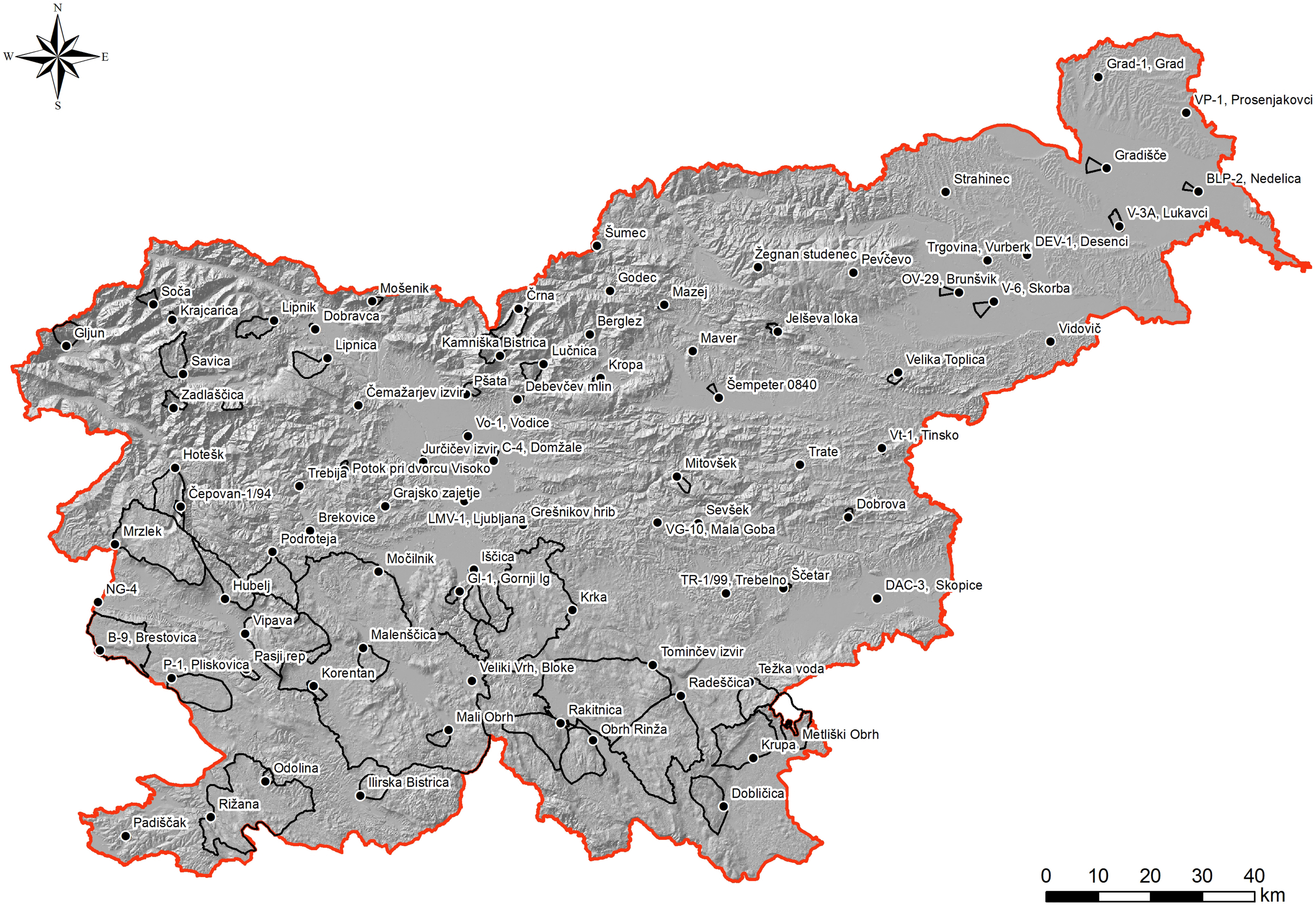
N
W
E
S
Grad-1, Grad
VP-1, Prosenjakovci
Gradišče
Strahinec
BLP-2, Nedelica
V-3A, Lukavci
Šumec
DEV-1, Desenci
Trgovina, Vurberk
Žegnan studenec
Pevčevo
Godec
OV-29, Brunšvik
V-6, Skorba
Mošenik
Soča
Črna
Mazej
Krajcarica
Lipnik
Dobravca
Berglez
Jelševa loka
Gljun
Kamniška Bistrica
Maver
Vidovič
Lipnica
Lučnica
Savica
Kropa
Velika Toplica
Pšata
Debevčev mlin
Šempeter 0840
Zadlaščica
Čemažarjev izvir
Vo-1, Vodice
Vt-1, Tinsko
Jurčičev izvir
C-4, Domžale
Hotešk
Trate
Mitovšek
Potok pri dvorcu Visoko
Trebija
Čepovan-1/94
Grajsko zajetje
Dobrova
Sevšek
Brekovice
Grešnikov hrib
LMV-1, Ljubljana
VG-10, Mala Goba
Mrzlek
Podroteja
Iščica
Močilnik
Ščetar
GI-1, Gornji Ig
TR-1/99, Trebelno
DAC-3, Skopice
NG-4
Hubelj
Krka
Vipava
B-9, Brestovica
Malenščica
Pasji rep
P-1, Pliskovica
Tominčev izvir
Korentan
Težka voda
Veliki Vrh, Bloke
Radeščica
Rakitnica
Mali Obrh
Obrh Rinža
Metliški Obrh
Krupa
Odolina
Ilirska Bistrica
Dobličica
Rižana
Padiščak
0
10
20
30
40
km

Appendix 9

Main keys for determination of groundwater recharge areas

Table: Main keys for determination of groundwater recharge areas (1/3)

Sampling location	Source	Reliability	area (km^2)	Reference
B-9, Brestovica	water protection zones	high	83.80	Urbanc *et al.*, 2010
Berglez	topology	high	0.29	
BLP-2, Nedelica	hydro-contour lines	medium	2.43	
Bohinjska Bistrica	water protection zones, tracer test, topology	medium	8.80	Odlok o določitvi varstvenih pasov in ukrepov za zavarovanje vodnega zajetja Voje in zajetja Bistrica (Official Gazette of the Republic of Slovenia 21/1994)
Brekovice	water protection zones (I.)	high	0.03	Odlok o spremembah in dopolnitvah odloka o varstvu virov pitne vode (Official Gazette of the Republic of Slovenia 20/1991)
Črna	tracer tests, aquifer system border	high	22.01	
Čemažarjev izvir	topology, watersheds	medium	0.05	
Čepovan-1/94	water protection zones	high	3.51	Odlok o določitvi varstvenih območij in ukrepov za zavarovanje območja črpališča in vodozbirnega območja kaptažne vrtine v Dolu pri Čepovanu (Official Gazette of the Republic of Slovenia 19/1996)
DAC-3, Skopice	conceptual model, hydro-contour lines	medium	0.04	Prestor *et al.*, 2006
Debevčev mlin	topology, tracer test	high	1.03	
Dobličica	topology, aquifer system border	high	45.63	
Dobravca	topology	medium	0.88	
Dobrova	topology	medium	1.84	
C-4, Domžale	water protection zones	high	1.38	
Framski slap	topology, watersheds	high	0.51	
GI-1, Gornji Ig	topology, watersheds	medium	5.93	
Gljun	article	low	18.53	Komac, 2001
Godec	topology, watersheds	medium	0.07	
Grad-1, Grad	water protection zones		0.70	Matoz *et al.*, 2002
Gradišče	hydro-contours lines, report	medium	6.01	Report (Geo Vrtina)
Grajsko zajetje	water protection zones	high	0.44	Odlok o spremembi in dopolnitvi odloka o varstvenih pasovih vodnih virov v Ljubljani in ukrepih za zavarovanje voda (Official Gazette of the Republic of Slovenia 15/1985)
Grešnikov hrib	topology	high	0.04	
Hotešk	topology, lithology, article	high	46.54	border with neighbouring recharge area
Hubelj	topology, lithology, aquifer system border, article	high	52.16	border with neighbouring recharge area; Trček *et al.* 2003, 2006
Ilirska Bistrica	topology	medium	19.22	
Iščica	tracer tests, topology, watersheds	high	23.78	
Jelševa Loka	water protection zones	high	2.41	Mencej and Kmetec, 1998
Jurčičev izvir	water protection zones	high	0.53	Odlok o varstvu lokalnih virov pitne vode v Občini Medvode (Official Gazette of the Republic of Slovenia 61/2001)
Kamniška Bistrica	topology	high	22.12	
Korentan	article	high	6.34	Petrič and Šebela, 2004
Krajcarica	topology	medium	0.87	

Table: Main keys for determination of groundwater recharge areas (2/3)

Sampling location	Source	Reliability	area (km^2)	Reference
Krka	topology, aquifer system border	high	261.30	
Kropa	topology		3.57	
Krupa	tracer tests, aquifer system border	high	85.69	
Lipnica	topology	low	21.26	
Lipnik	topology, watersheds, tracer tests	medium	20.39	
LMV-1, Ljubljana	report	high	1.28	Herič, 2005
Lucnica	tracer test, topology, aquifer system border	high	10.82	
V-3A, Lukavci	water protection zones	high	6.19	Petauer and Žlebnik, 1993
Malenščica	water protection zones	high	22.81	Prestor *et al.*, 2009
Mali Obrh	topology	medium	9.99	
Maver	topology	medium	0.11	
Mazej	water protection zones, topology	high	0.86	Odlok o varstvenih pasovih vodnih virov in termalnih vrelcev na območju občine Velenje (Official Gazette of the Republik of Slovenia 3/84)
Metliški Obrh	tracer test, aquifer system border	high	23.05	
Mitovšek	topology	medium	4.64	
Močilnik	aquifer body, literature (considering only Slovenia)	high	1054.00	Gospodarič and Habič, 1976
Mošenik	topology, lithology	high	2.11	
Mrzlek	topology, lithology, aquifer system	high	155.50	
NG-4	hydrocontours, report	medium	0.04	Drobne and Mencej, 1980
Obrh Rinža	topology, tracer test	high	61.00	
Odolina	topology	high	3.68	
OV-29, Brunšvik	conceptual model	medium	3.60	Prestor *et al.*, 2006
Padiščak	topology	high	0.51	
Pasji rep	topology, aquifer system border	high	4.23	topography, borders with aquifer systems
Pevčevo	topology	high	0.08	
P-1, Pliskovica	watershedes, topology S part, aquifer system, lithology	medium	60.94	
Podroteja	topology, aquifer system border	high	51.05	
Potok pri dvorcu Visoko	topology	high	1.64	topography
Pšata	topology	medium	5.67	
Radeščica	tracer test, topology, aquifer system border	high	194.50	
Rakitnica	topology, tracer test	high	65.65	
Rižana	tracer test	high	226.20	
Savica	topology, aquifer system border	low	30.28	topography, borders with aquifer systems
Ščetar	water protection zones	high	1.40	Odlok o zaščiti vodnih virov na območju Občine Škocjan (Official Gazette of the Republik of Slovenia 34/2000)
Šempeter 0840	hydrocountours	high	2.19	Drobne, 1977; Odlok o varstvu virov pitne vode na območju Občine Laško (Official Gazette of the Republik of Slovenia 38/1999); Uhan personal communication

Table: Main keys for determination of groundwater recharge areas (3/3)

Sampling location	Source	Reliability	area (km^2)	Reference
Sevšek	topology, watershed	medium	0.05	
V-6, Skorba	hydro-contours	high	5.97	Žlebnik, 1986
Soča	tracer tests, topology, aquifer system borders,	high	6.45	
Strahinec	topology, watersheds	medium	0.07	
Šumec	topology	high	0.91	
Težka voda	aquifer system border, topology, tracer test, watershed,	high	34.40	
Tominčev izvir	tracer tests, topology	high	278.20	
Trate	water protection zones	high	0.05	
TR-1/99, Trebelno	water protection zones	high	0.18	Odlok o varstvu virov pitne vode v Občini Trebnje in ukrepih za zavarovanje kakovosti in količini vode (Official Gazette of the Republik of Slovenia 75/1996)
Trebija	water protection zones	high	0.60	Odlok o dopolnitvi odloka o varstvu virov pitne vode (Official Gazette of the Republik of Slovenia 20/1994)
Trgovina, Vurberk	topology	medium	0.01	
Velika Toplica	topology, lithology	high	3.87	
Veliki Vrh, Bloke	water protection zones	high	0.47	Mencej *et al.*, 2002
VG-10, Mala Goba	water protection zones	high	0.05	Hoetzl, 2012
Vidovič	topology	medium	0.02	
Vipava	aquifer system border, topology, water protection zones, lithology	high	100.90	Lapajne, 2000; border with neighbouring recharge area; Odlok o varstvenih pasovih vodnih virov "Podlipa" v Vipavi (Official Gazette of the Republik of Slovenia 14/1983)
Vo-1, Vodice	water protection zones, report	high	0.45	Mencej and Kmetec, 1997; Mencej, 2000.
VP-1, Prosenjakovci	lithology of borehole	medium	0.37	
Vt-1, Tinsko	topology, water protection zones	high	0.45	Kutnjak, 1986.
Zadlaščica	watersheds, aquifer system border, topology	high	9.28	
Žegnani studenec	topology, water protection zones	high	0.12	Odlok o varstvu virov pitne vode na območju Občine Mislinja (Official Gazette of the Republic of Slovenia 100/2000).

Appendix 10

Listing of sampling locations in alphabetical order

- orthophoto picture of recharge area of sampling locations (Environmental Agency of Slovenia, 2013),

- photos of sampling locations (personal archive), and

- determined recharge areas of sampling locations according to:

    - Hydrogeological map (IAH) (Prestor *et al.*, 2004),
    - Geological map (Buser, 2010),
    - CORINE Land Cover (CLC) (Ministry of the Environment and Spatial planning *et al.*, 2003), and
    - Actual agricultural and forest land usage (Land use) (Ministry for Agriculture and the Environment, 2012).

Legends to figures are found in the Appendices 2, 5, 6 and 7.

B-9, Brestovica

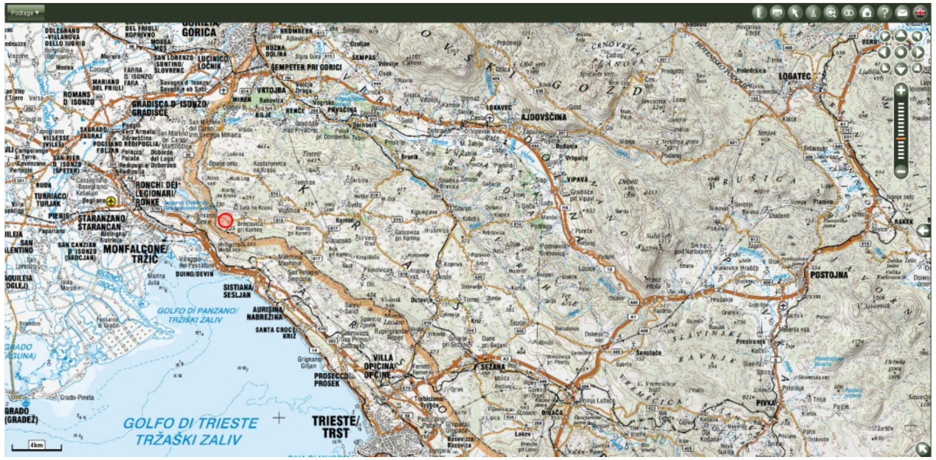

Sampling location B-9, Brestovica

Sampling location B-9, Brestovica

Sampling location B-9, Brestovica

Sampling location B-9, Brestovica

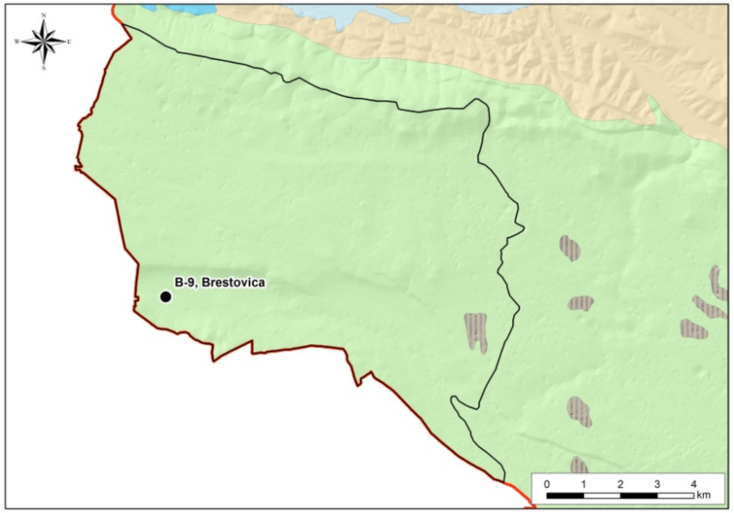

Sampling location B-9, Brestovica (IAH classification)

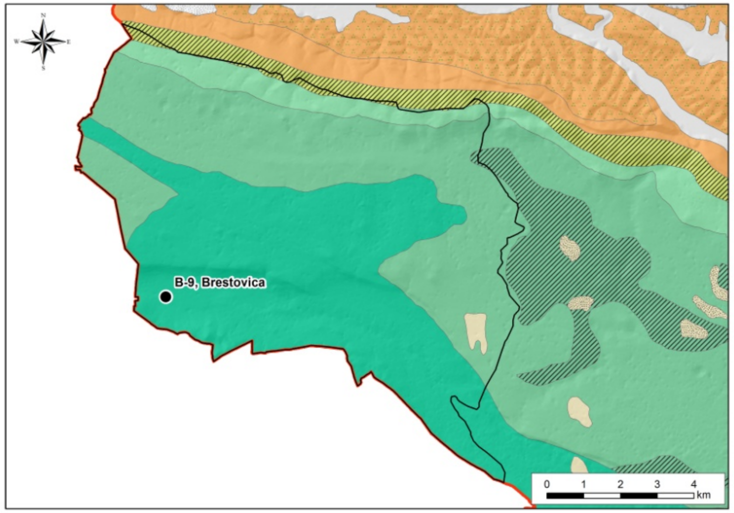

Sampling location B-9, Brestovica (Geological classification)

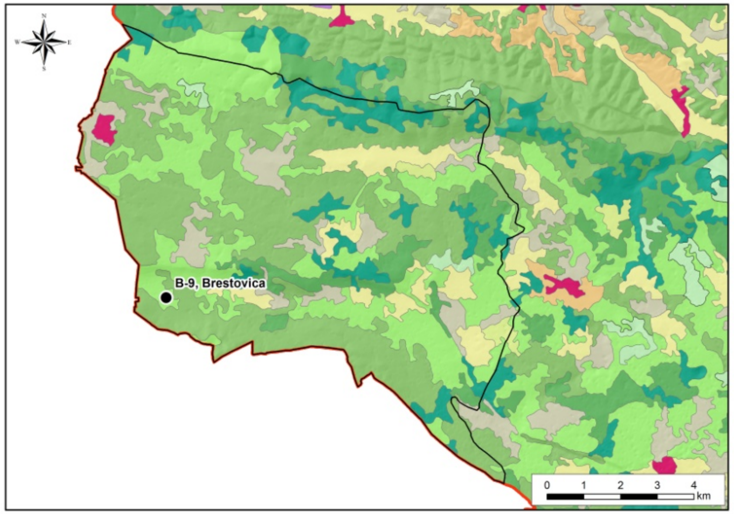

Sampling location B-9, Brestovica (CLC classification)

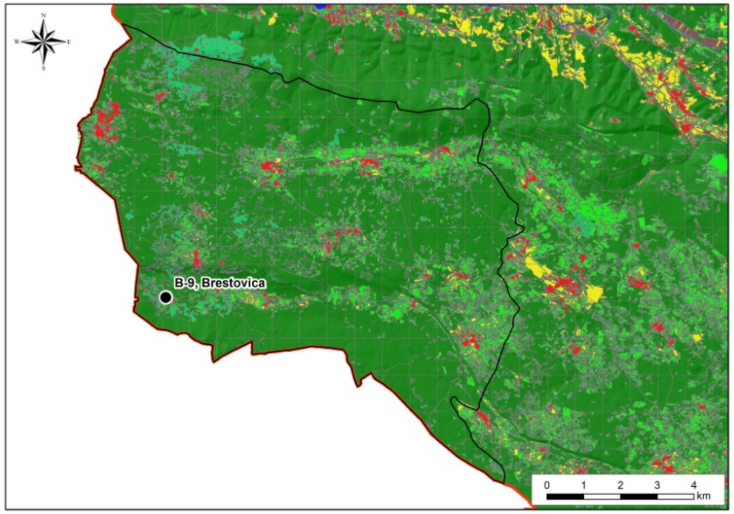

Sampling location B-9, Brestovica (Land use classification)

Berglez

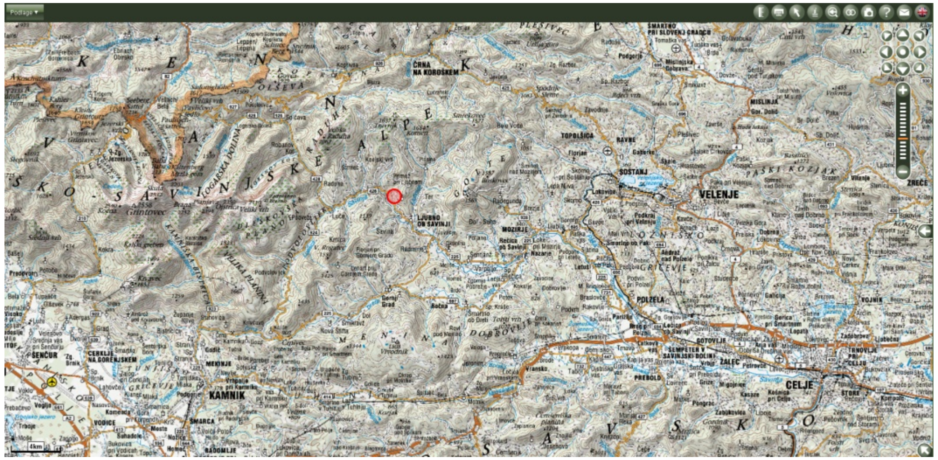

Sampling location Berglez

Sampling location Berglez

Sampling location Berglez

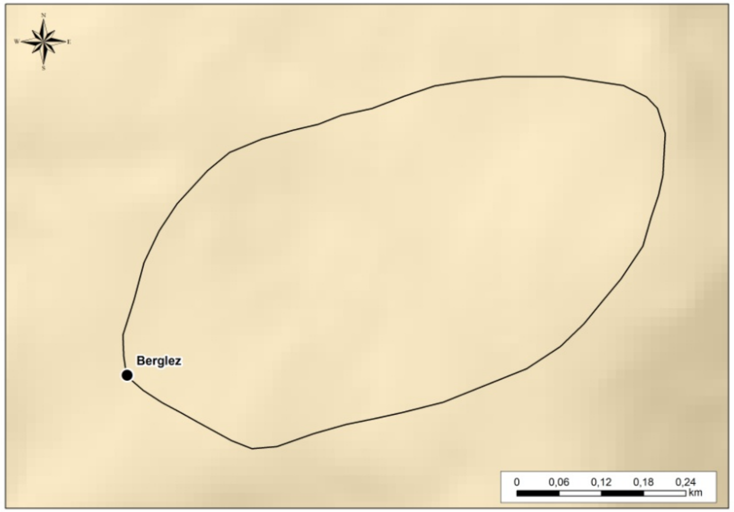

Sampling location Berglez (IAH classification)

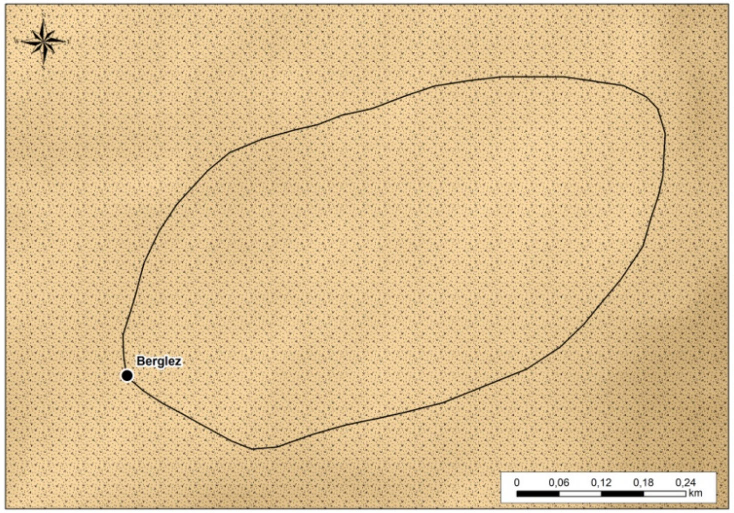

Sampling location Berglez (Geological classification)

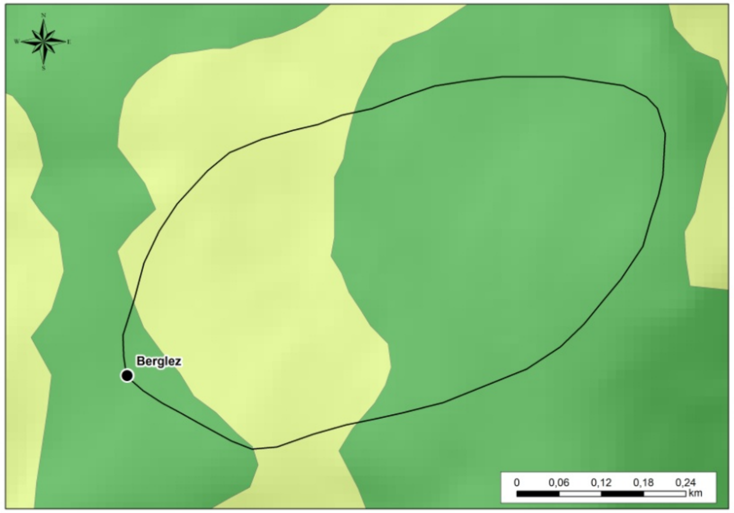

Sampling location Berglez (CLC classification)

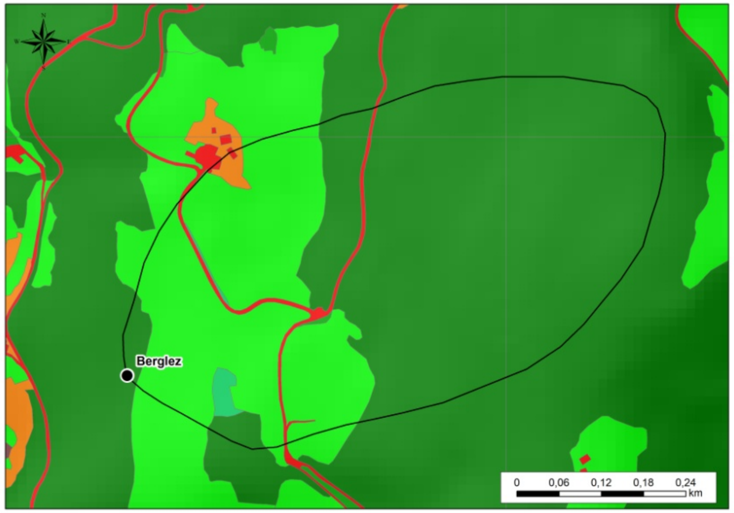

Sampling location Berglez (Land use classification)

BLP-2, Nedelica

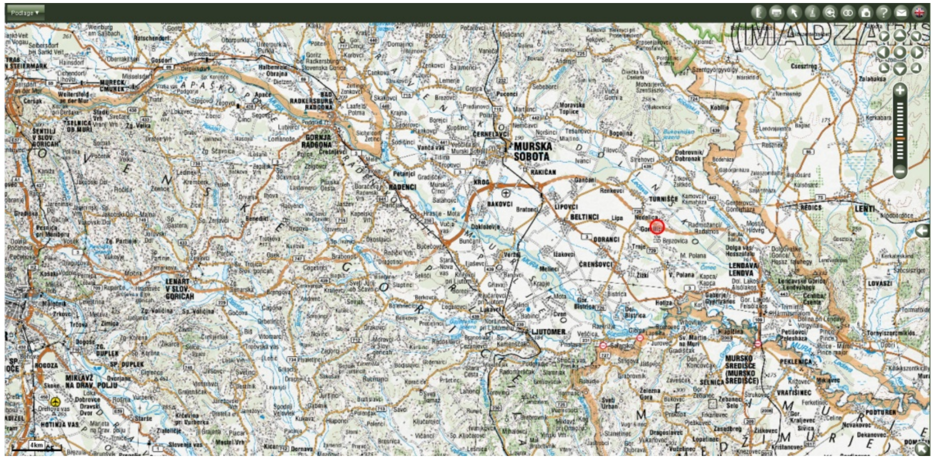

Sampling location BLP-2, Nedelica

Sampling location BLP-2, Nedelica

Sampling location BLP-2, Nedelica

Sampling location BLP-2, Nedelica

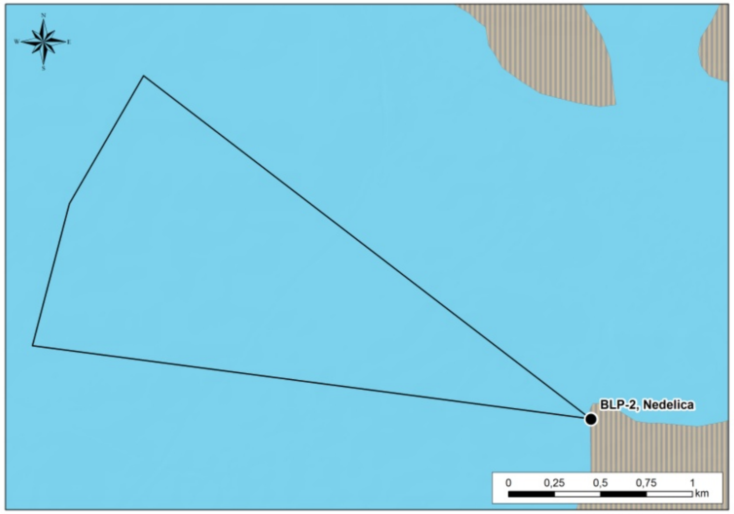

Sampling location BLP-2, Nedelica (IAH classification)

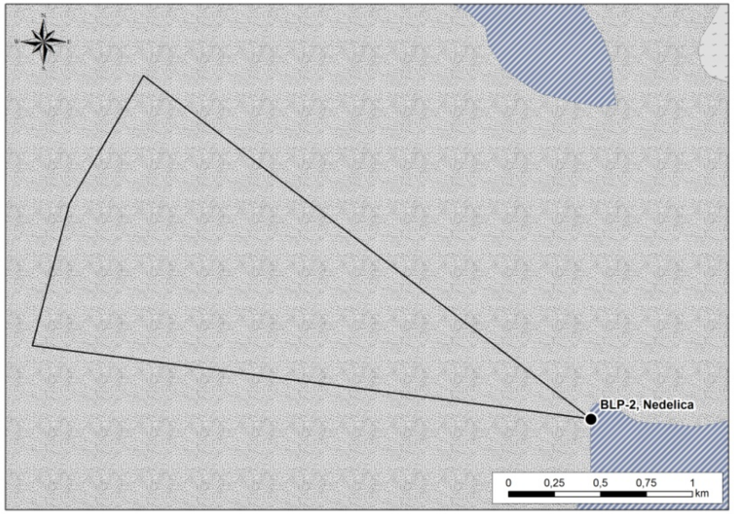

Sampling location BLP-2, Nedelica (Geological classification)

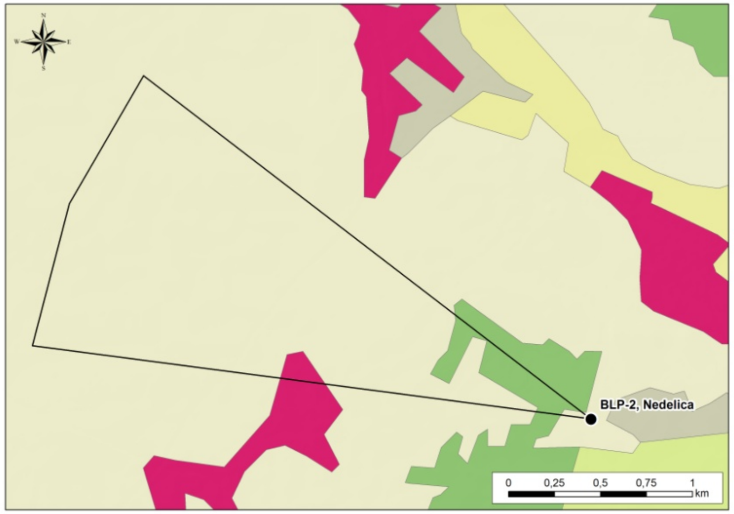

Sampling location BLP-2, Nedelica (CLC classification)

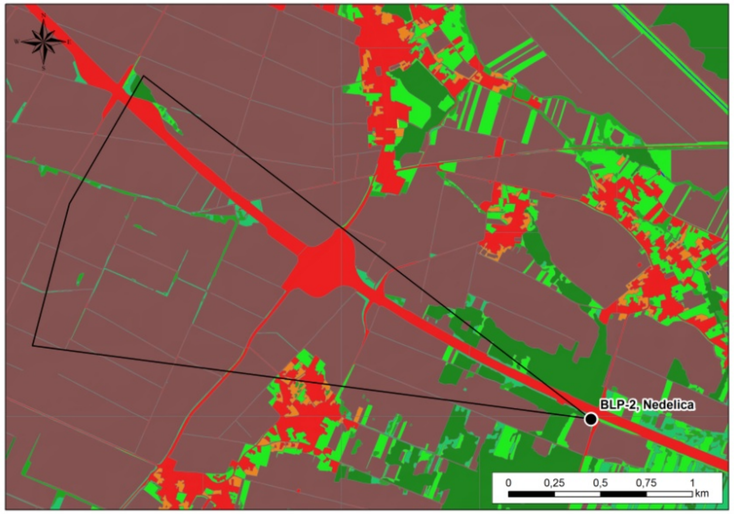

Sampling location BLP-2, Nedelica (Land use classification)

Bohinjska Bistrica

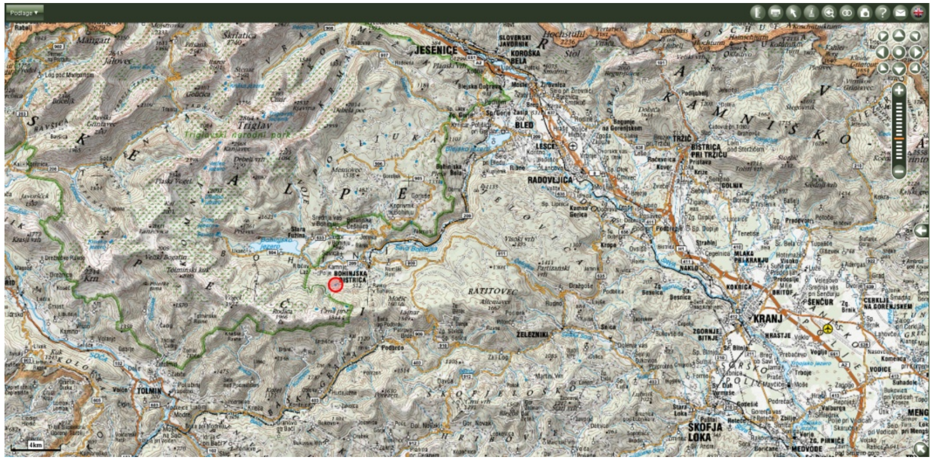

Sampling location Bohinjska Bistrica

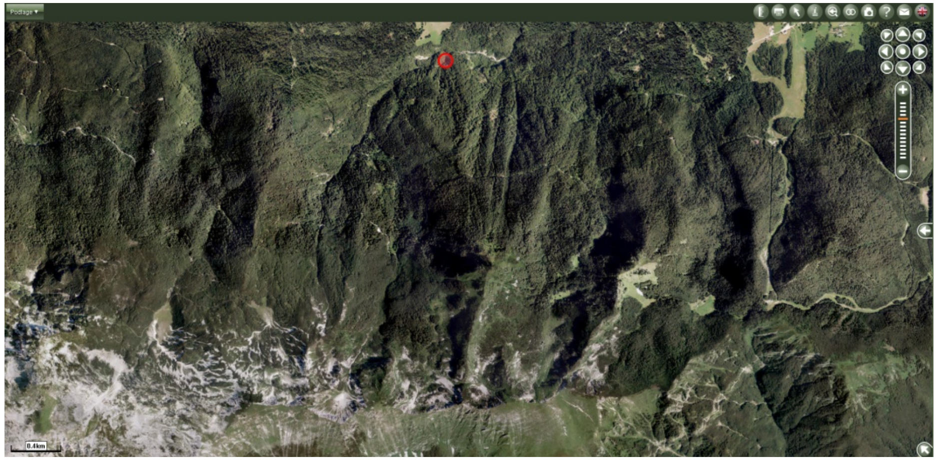

Sampling location Bohinjska Bistrica

Sampling location Bohinjska Bistrica

Sampling location Bohinjska Bistrica

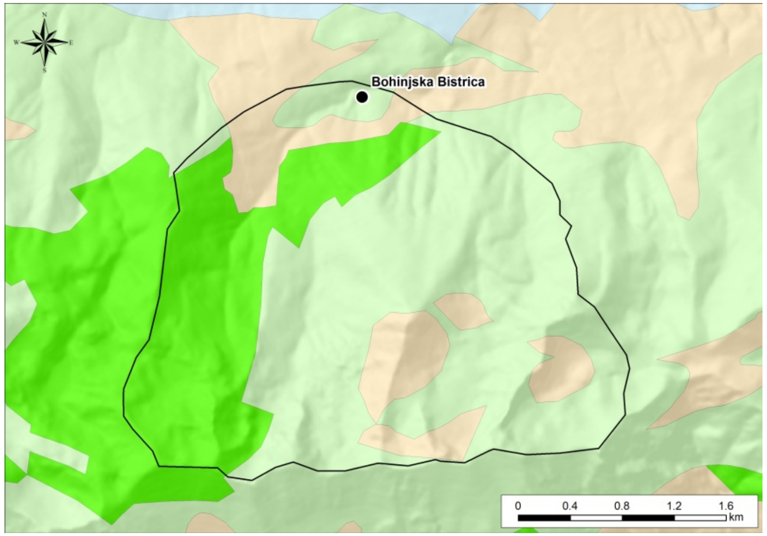

Sampling location Bohinjska Bistrica (IAH classification)

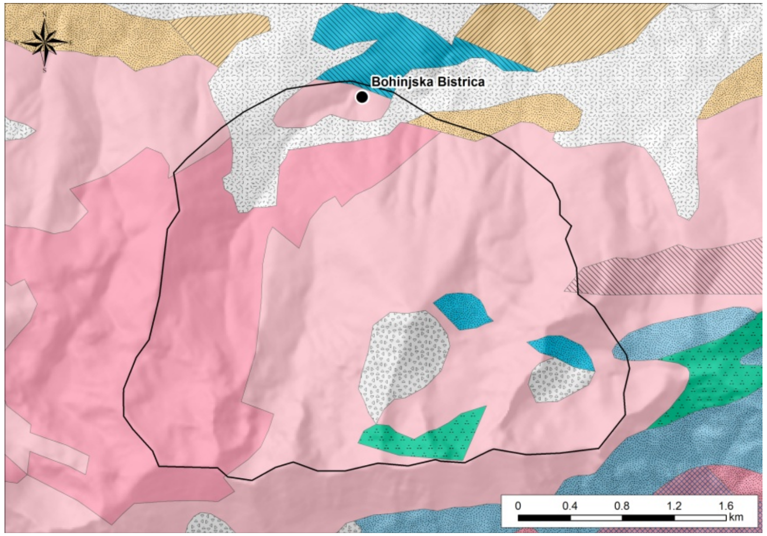

Sampling location Bohinjska Bistrica (Geological classification)

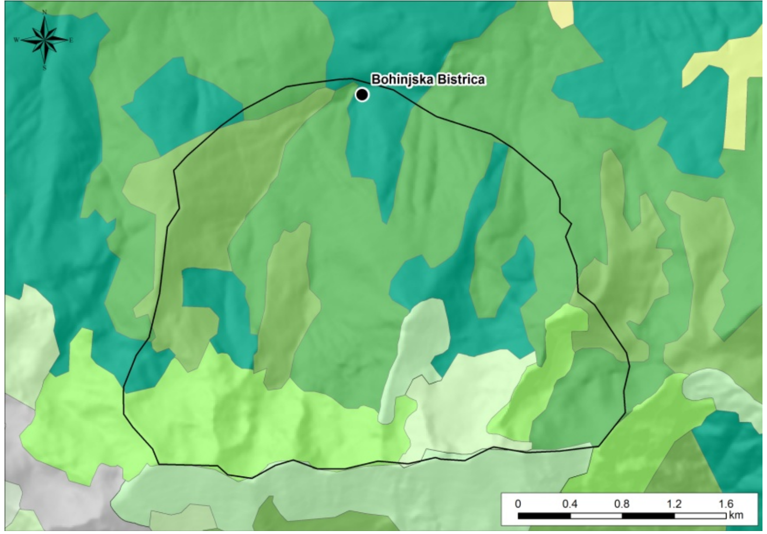

Sampling location Bohinjska Bistrica (CLC classification)

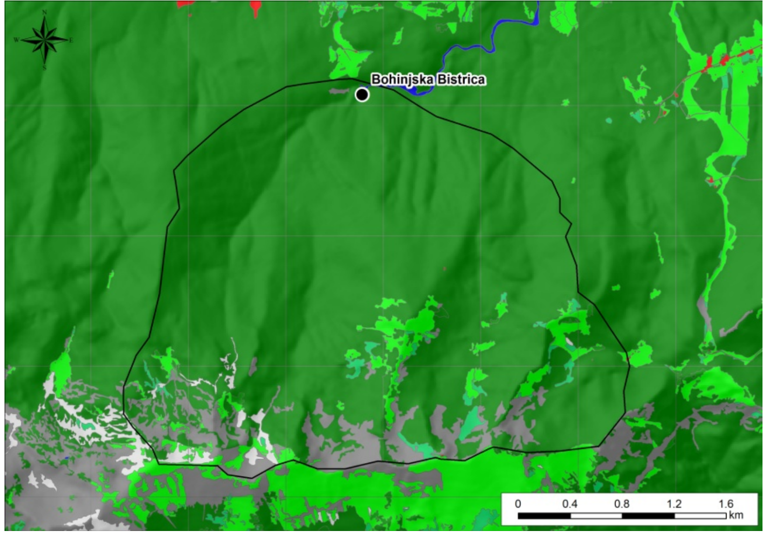

Sampling location Bohinjska Bistrica (Land use classification)

Brekovice

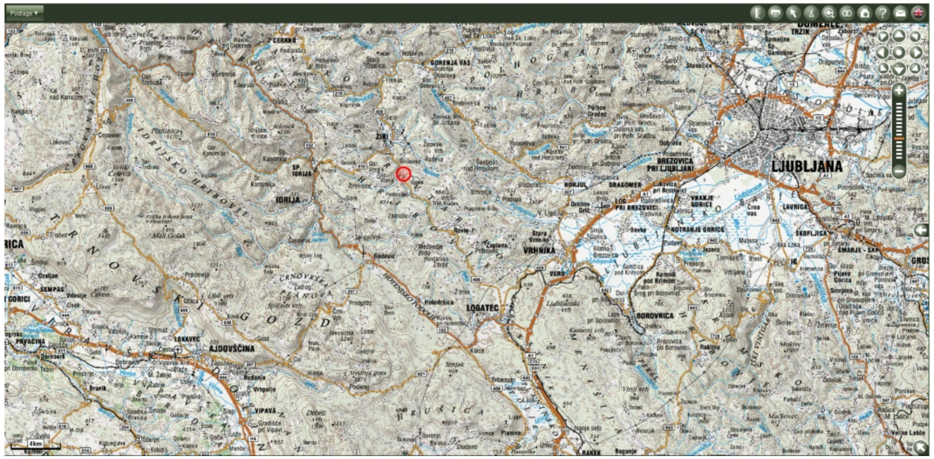

Sampling location Brekovice

Sampling location Brekovice

Sampling location Brekovice

Sampling location Brekovice

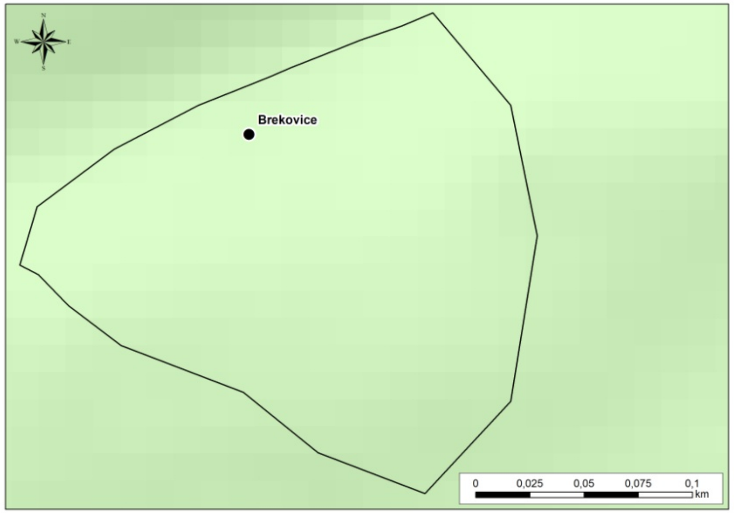

Sampling location Brekovice (IAH classification)

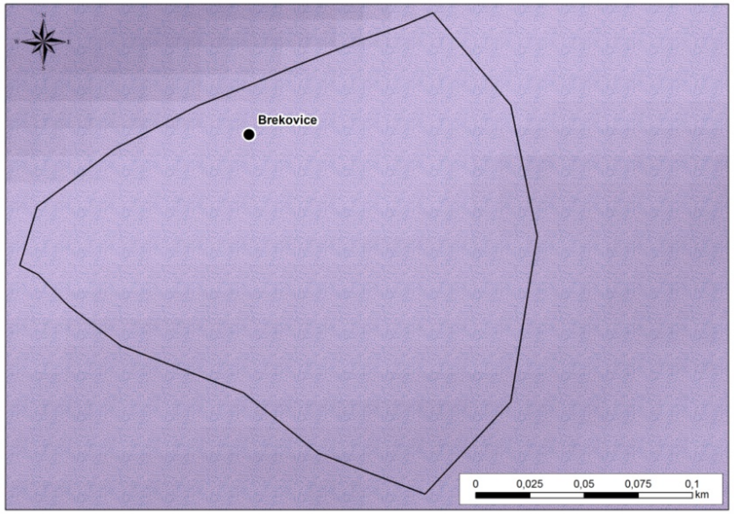

Sampling location Brekovice (Geological classification)

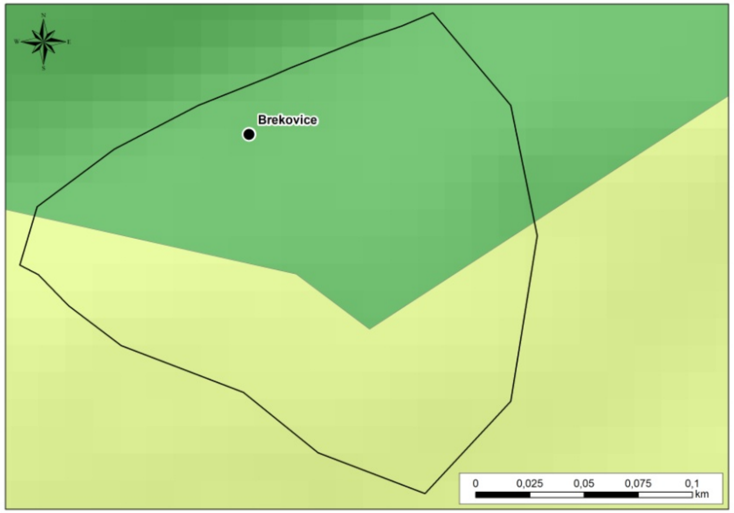

Sampling location Brekovice (CLC classification)

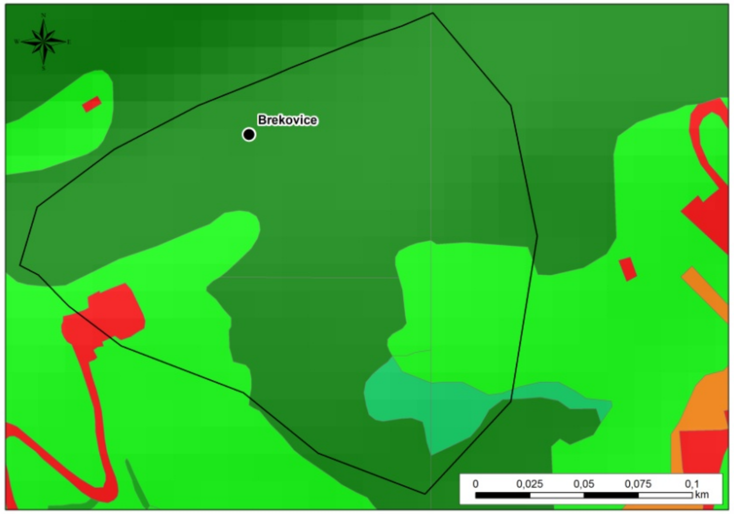

Sampling location Brekovice (Land use classification)

C-4, Domžale

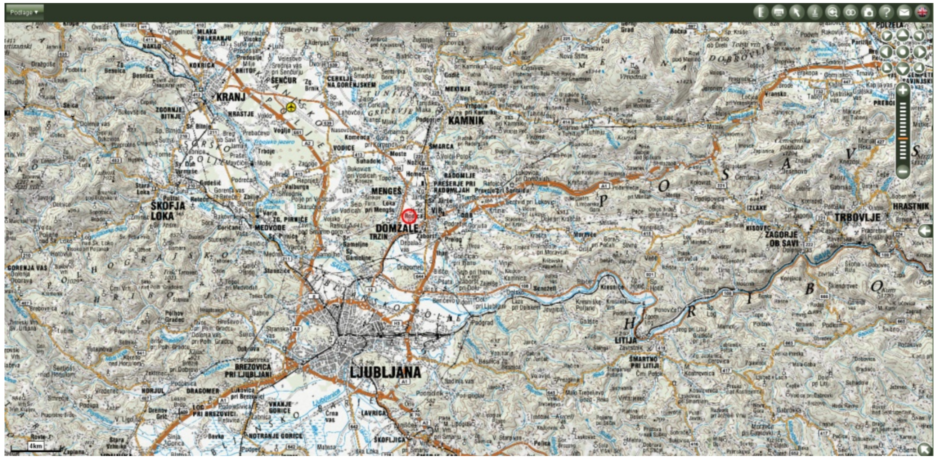

Sampling location C-4, Domžale

Sampling location C-4, Domžale

Sampling location C-4, Domžale

Sampling location C-4, Domžale

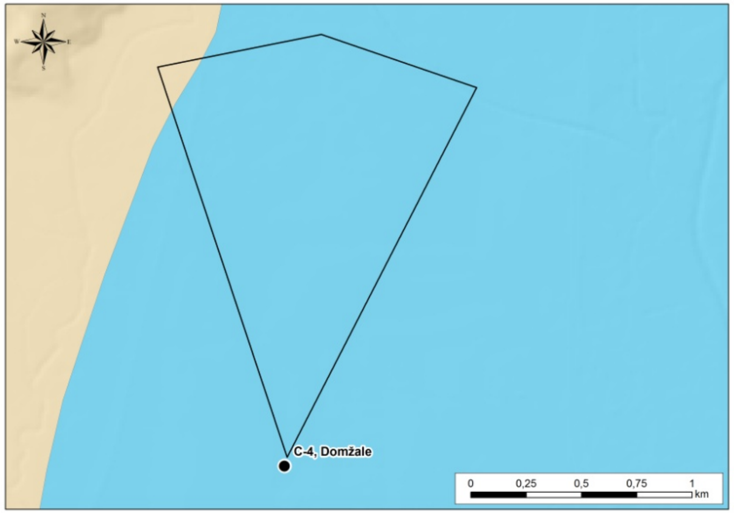

Sampling location C-4, Domžale (IAH classification)

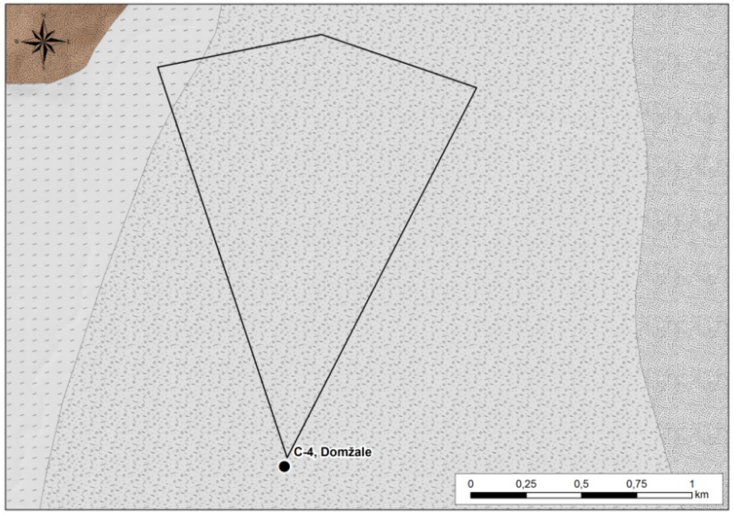

Sampling location C-4, Domžale (Geological classification)

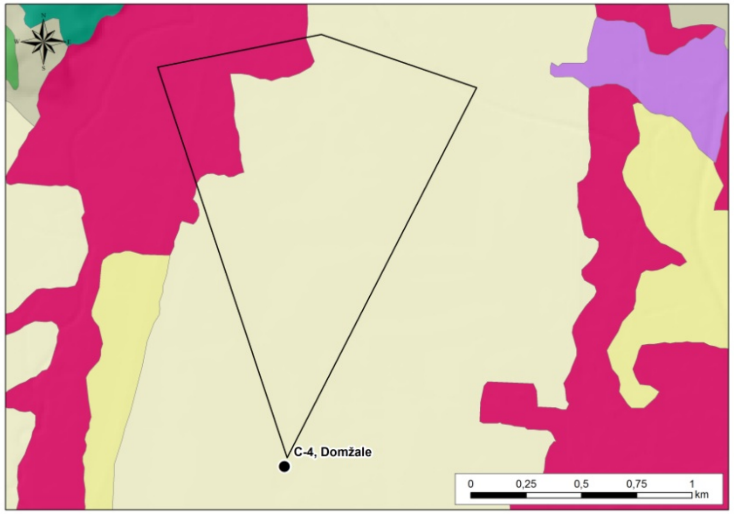

Sampling location C-4, Domžale (CLC classification)

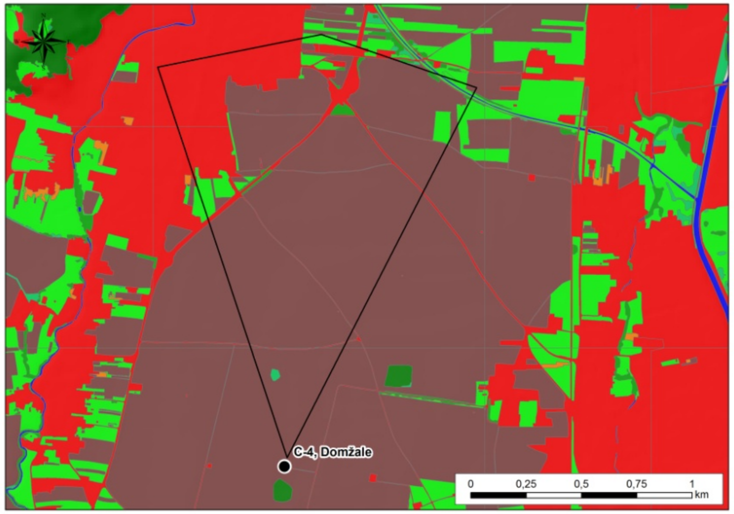

Sampling location C-4, Domžale (Land use classification)

Čemažarjev izvir

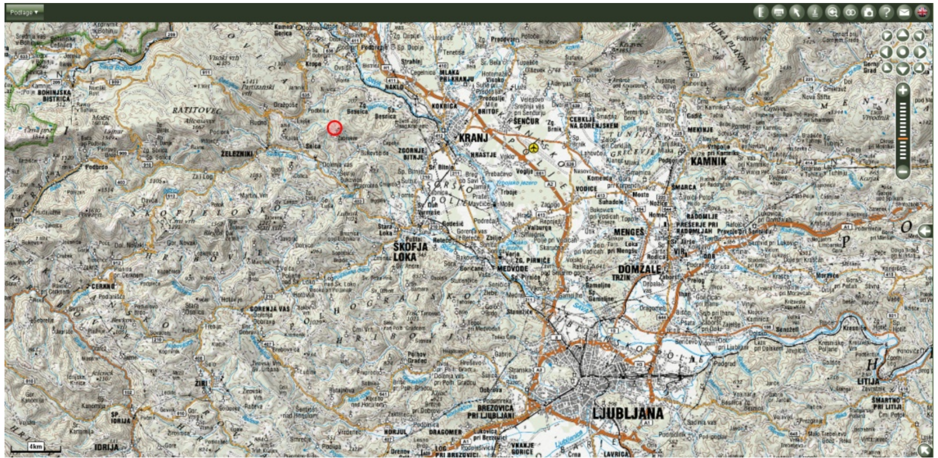

Sampling location Čemažarjev izvir

Sampling location Čemažarjev izvir

Sampling location Čemažarjev izvir

Sampling location Čemažarjev izvir

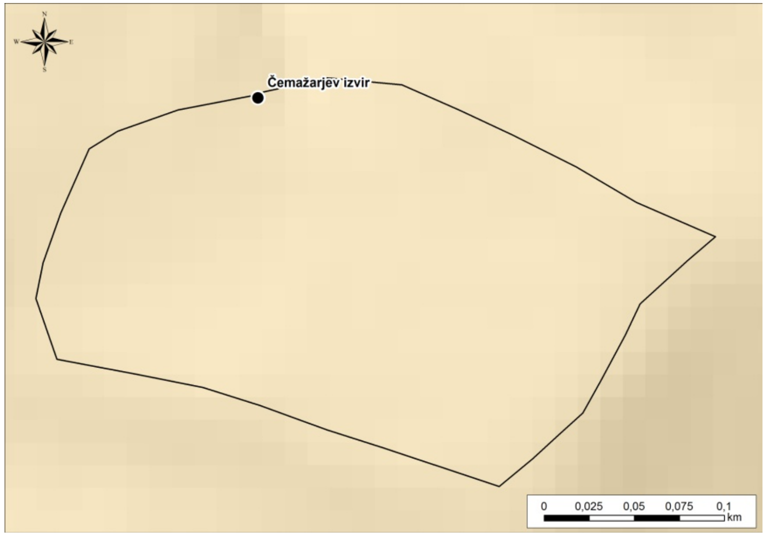

Sampling location Čemažarjev izvir (IAH classification)

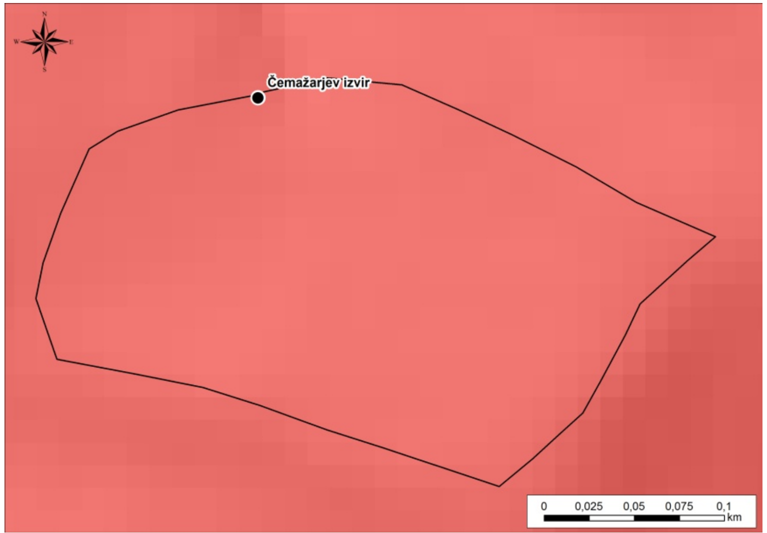

Sampling location Čemažarjev izvir (Geological classification)

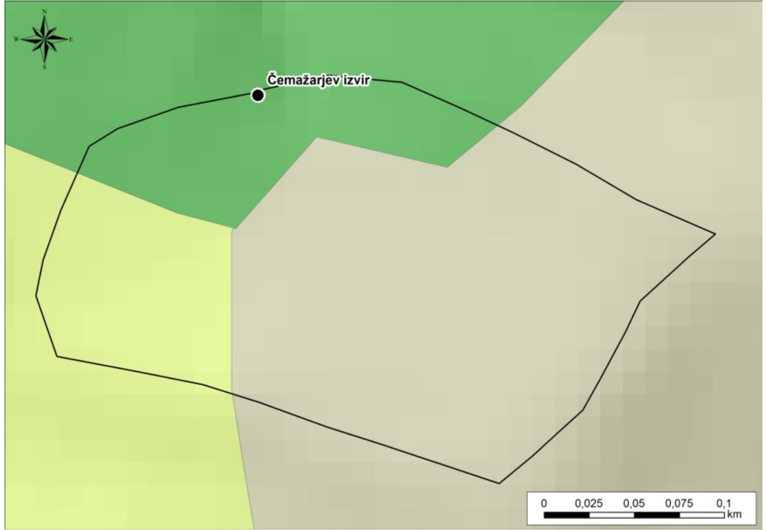

Sampling location Čemažarjev izvir (CLC classification)

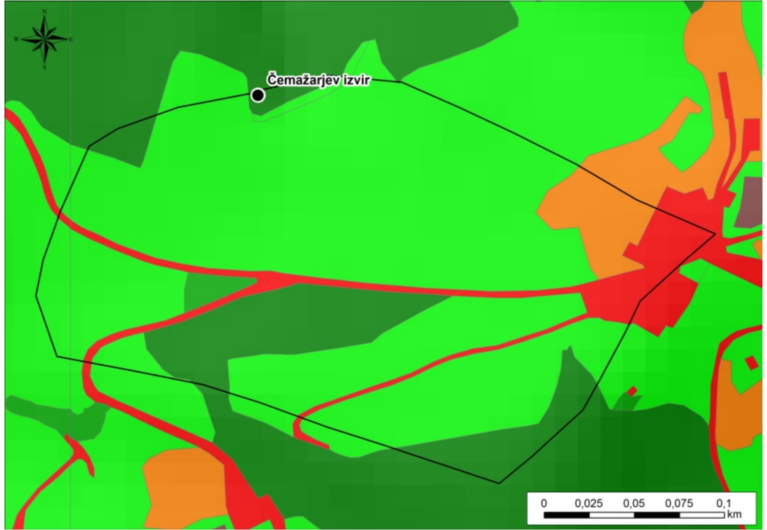

Sampling location Čemažarjev izvir (Land use classification)

Čepovan-1/94

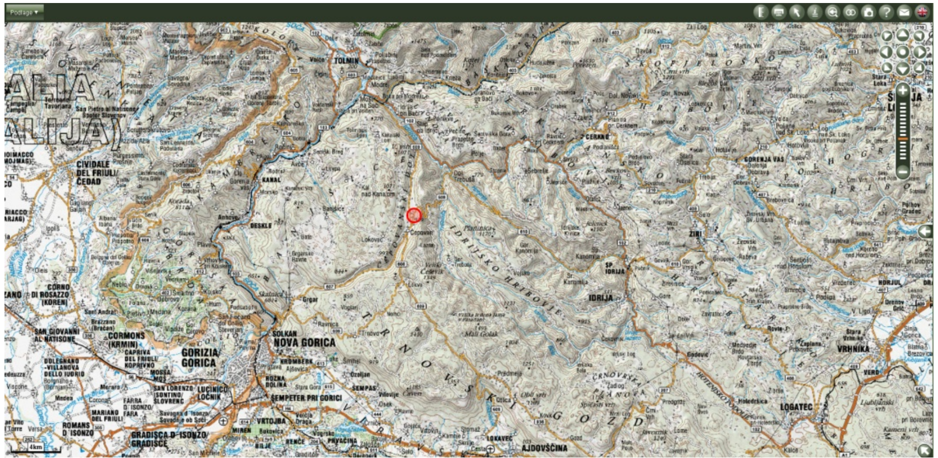

Sampling location Čepovan-1/94

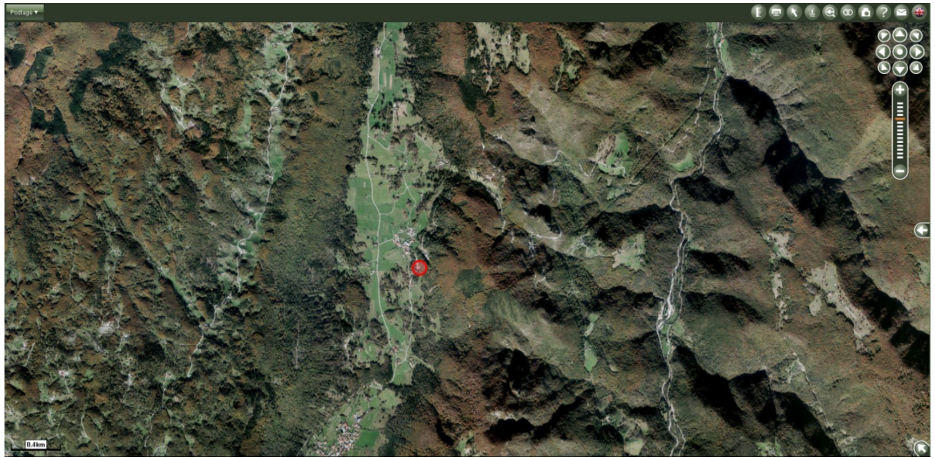

Sampling location Čepovan-1/94

Sampling location Čepovan-1/94

Sampling location Čepovan-1/94

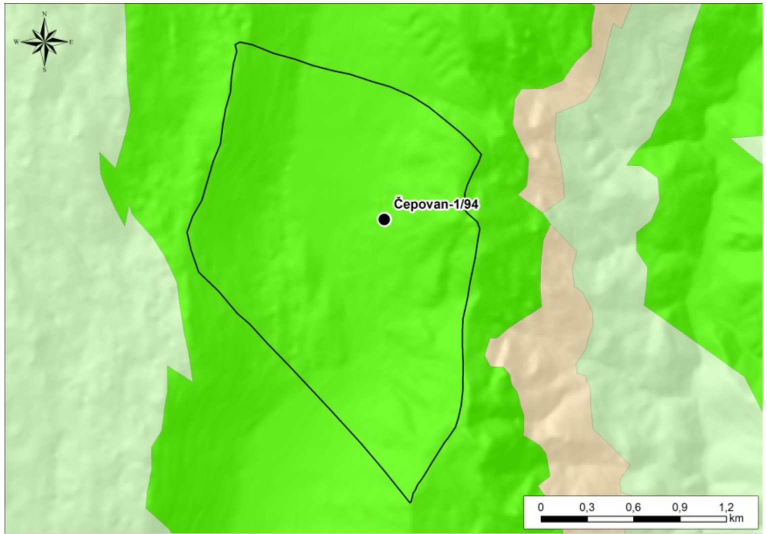

Sampling location Čepovan-1/94 (IAH classification)

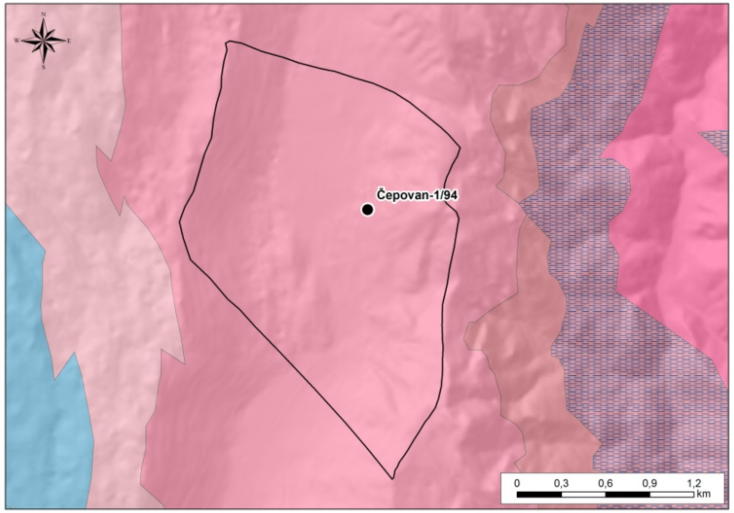

Sampling location Čepovan-1/94 (Geological classification)

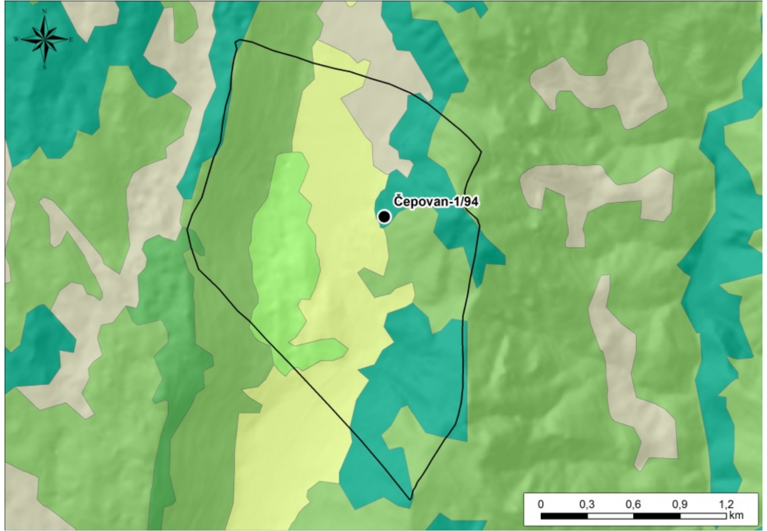

Sampling location Čepovan-1/94 (CLC classification)

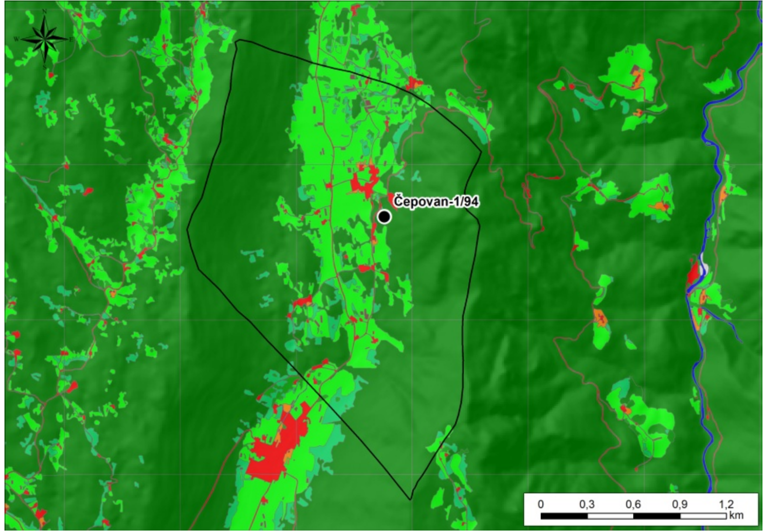

Sampling location Čepovan-1/94 (Land use classification)

Črna

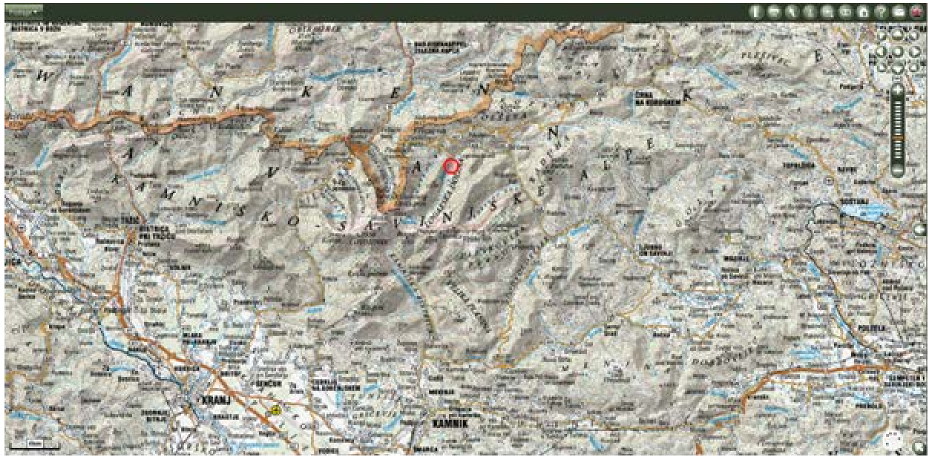

Sampling location Črna

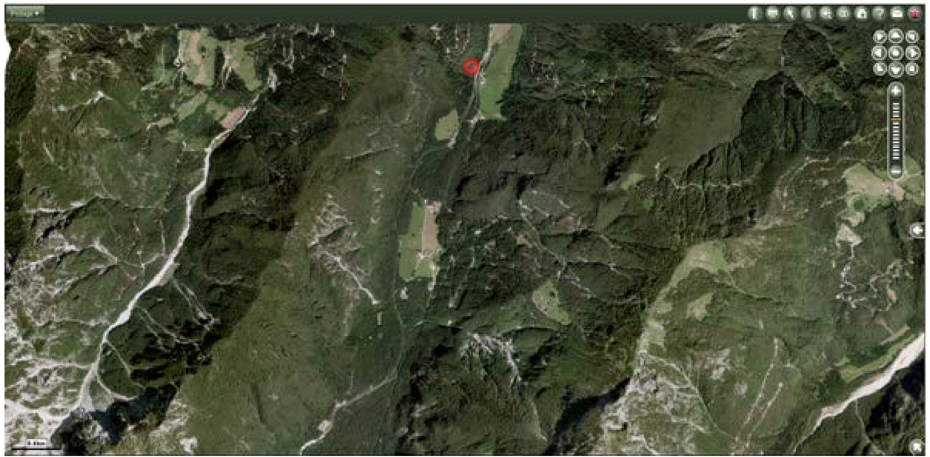

Sampling location Črna

Sampling location Črna

Sampling location Črna

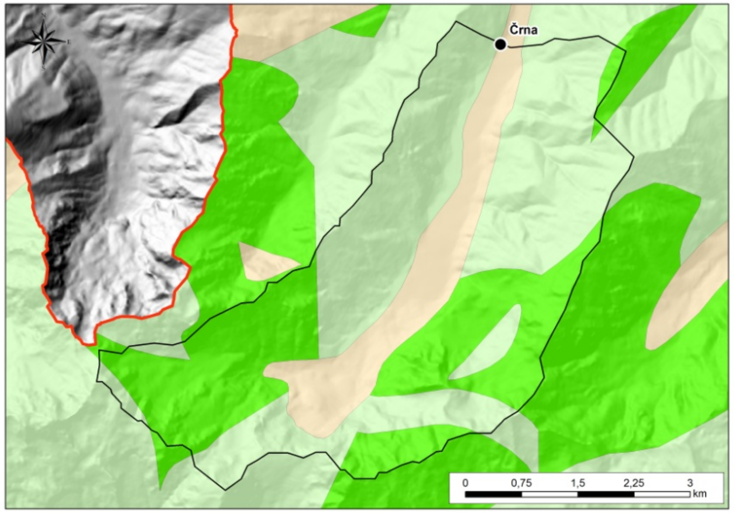

Sampling location Črna (IAH classification)

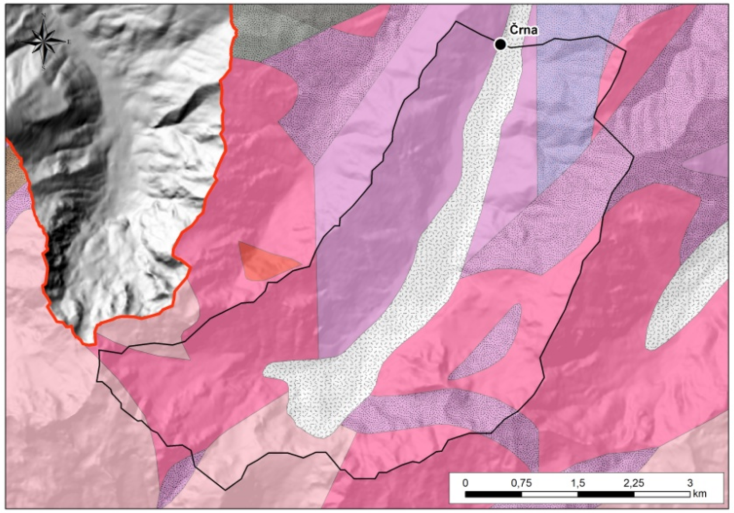

Sampling location Črna (Geological classification)

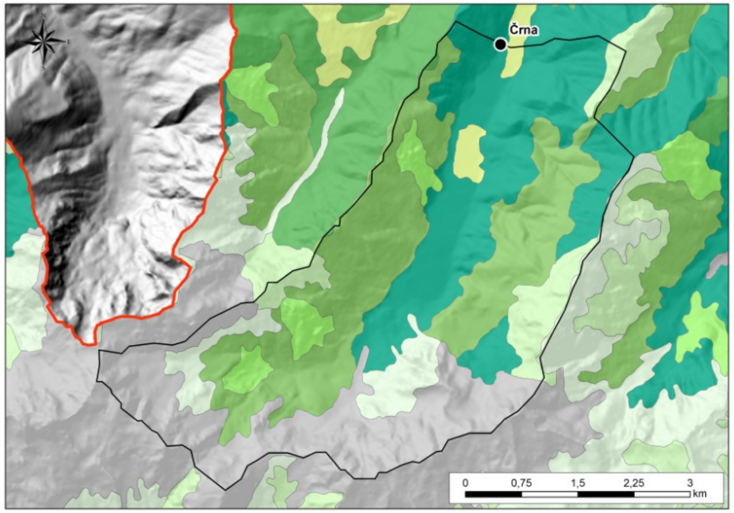

Sampling location Črna (CLC classification)

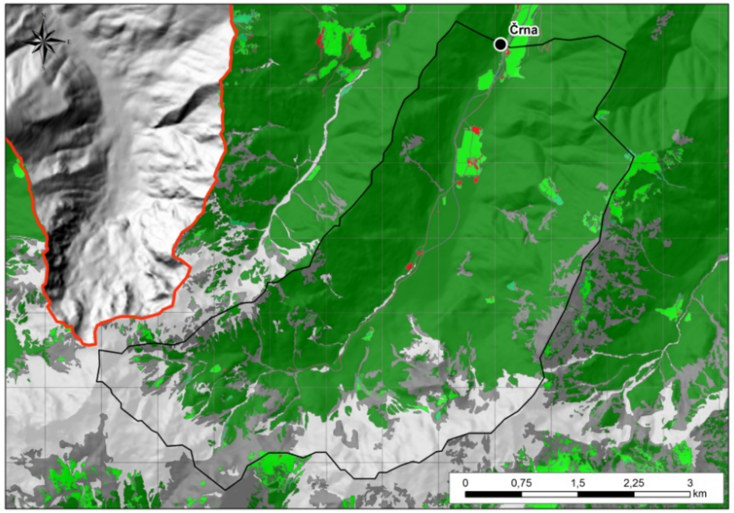

Sampling location Črna (Land use classification)

DAC-3, Skopice

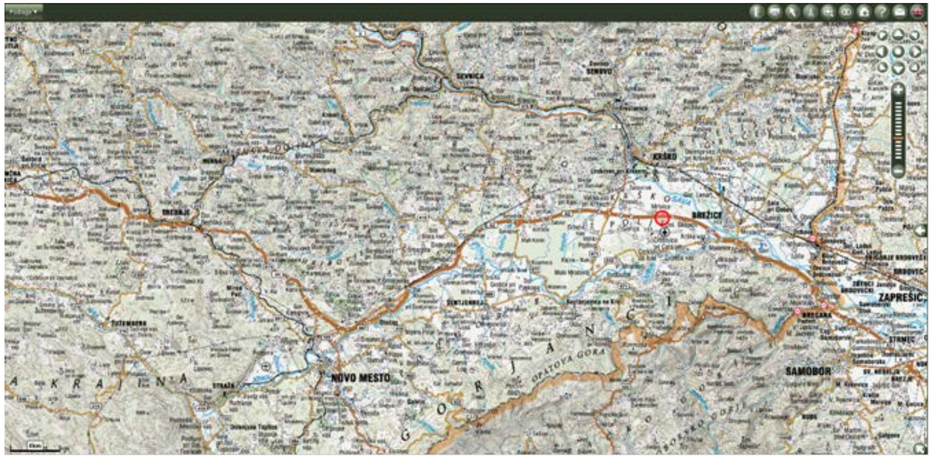

Sampling location DAC-3, Skopice

Sampling location DAC-3, Skopice

Sampling location DAC-3, Skopice

Sampling location DAC-3, Skopice

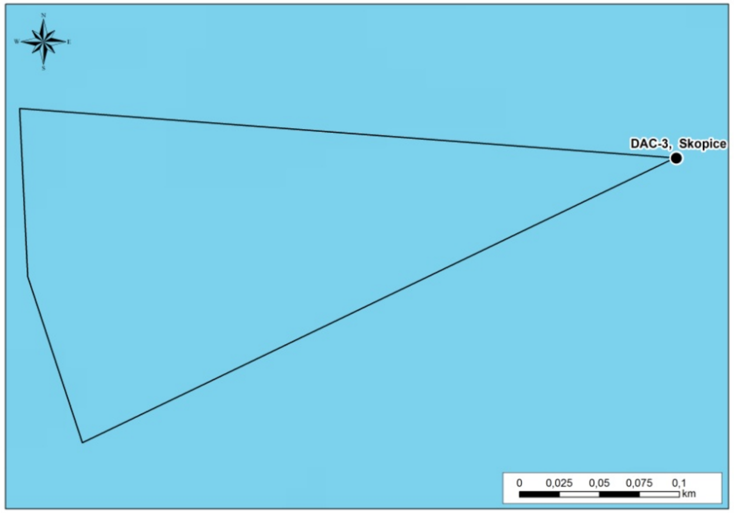

Sampling location DAC-3, Skopice (IAH classification)

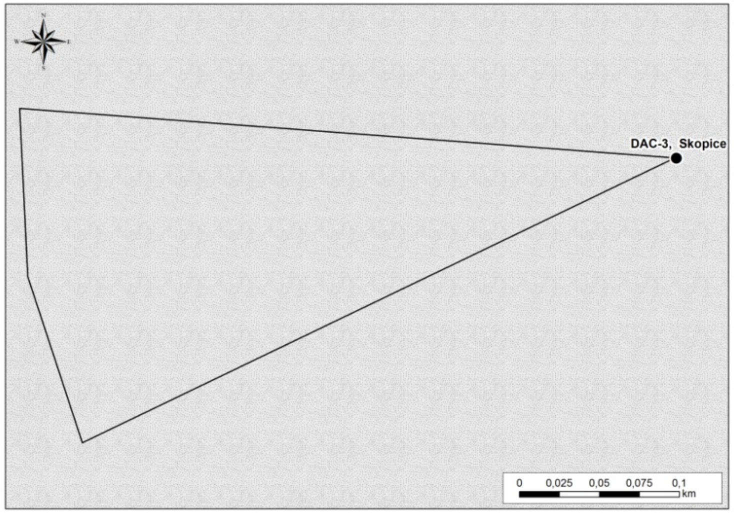

Sampling location DAC-3, Skopice (Geological classification)

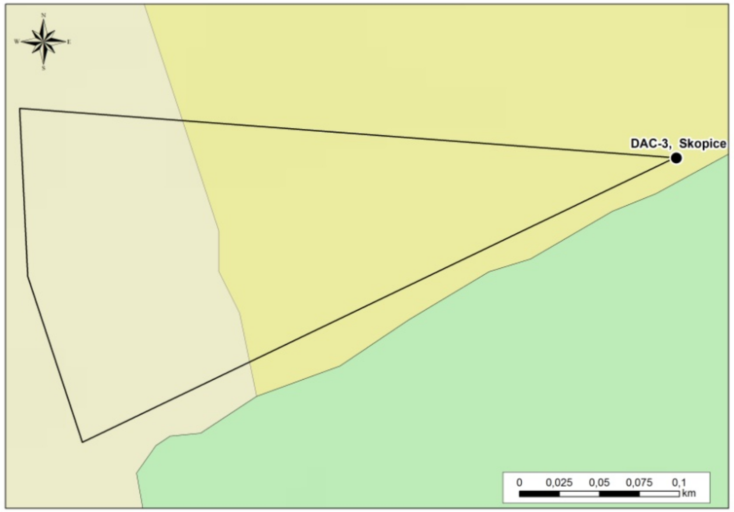

Sampling location DAC-3, Skopice (CLC classification)

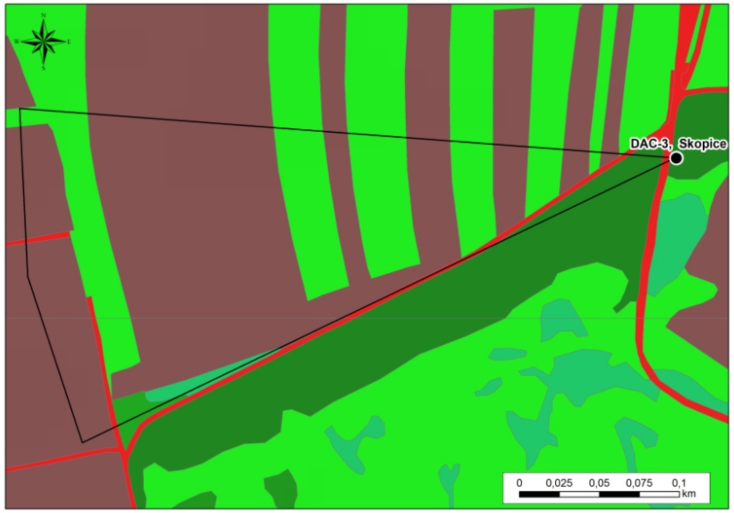

Sampling location DAC-3, Skopice (Land use classification)

Debevčev mlin

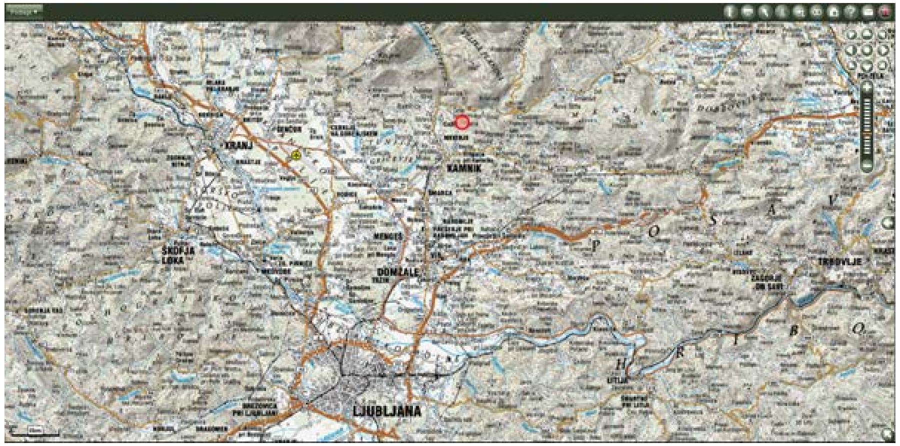

Sampling location Debevčev mlin

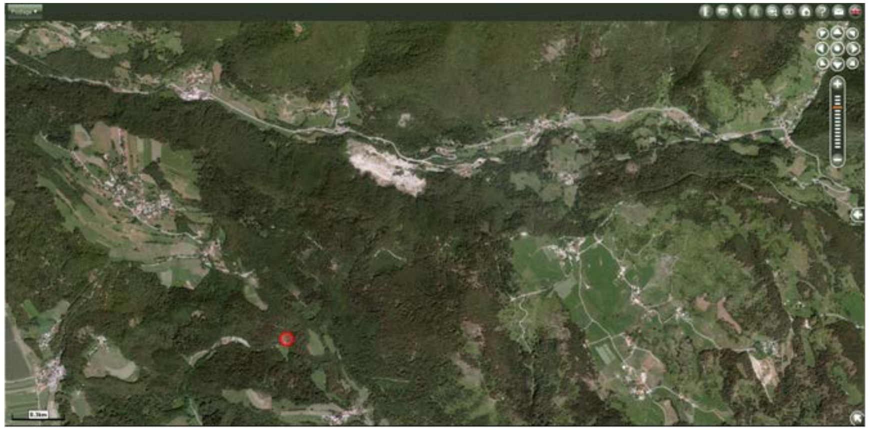

Sampling location Debevčev mlin

Sampling location Debevčev mlin

Sampling location Debevčev mlin

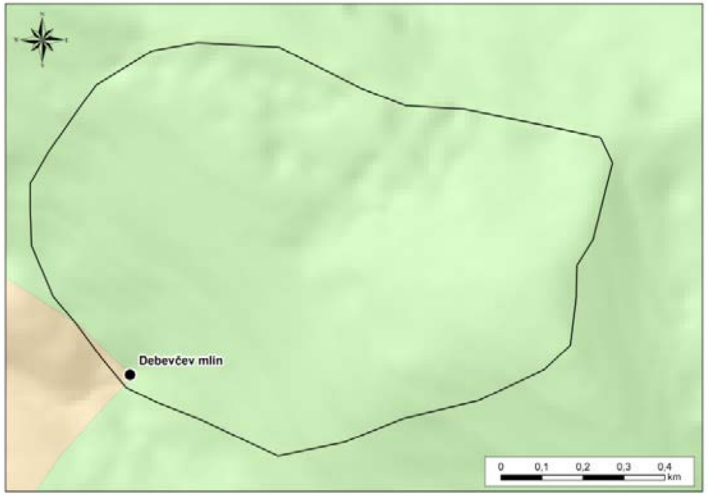

Sampling location Debevčev mlin (IAH classification)

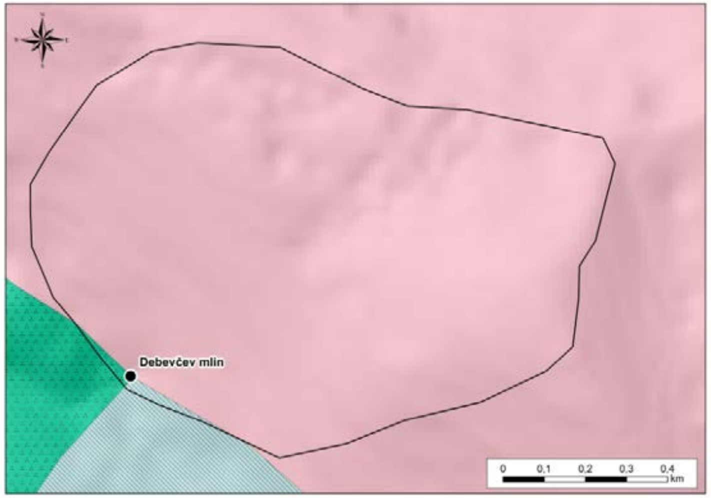

Sampling location Debevčev mlin (Geological classification)

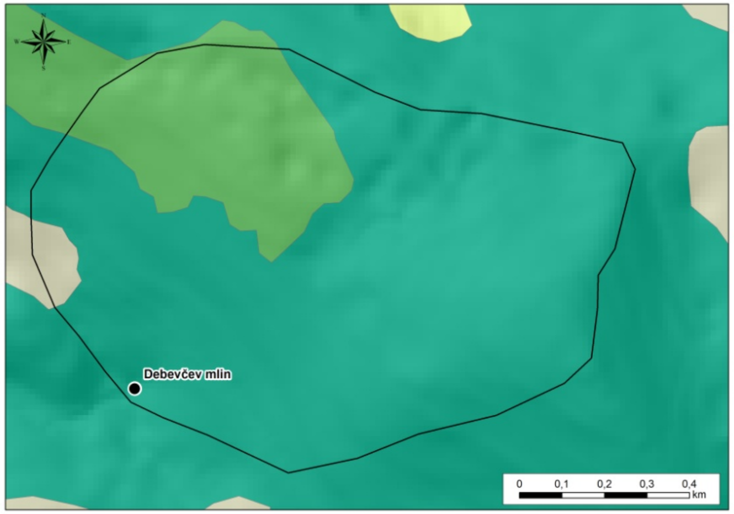

Sampling location Debevčev mlin (CLC classification)

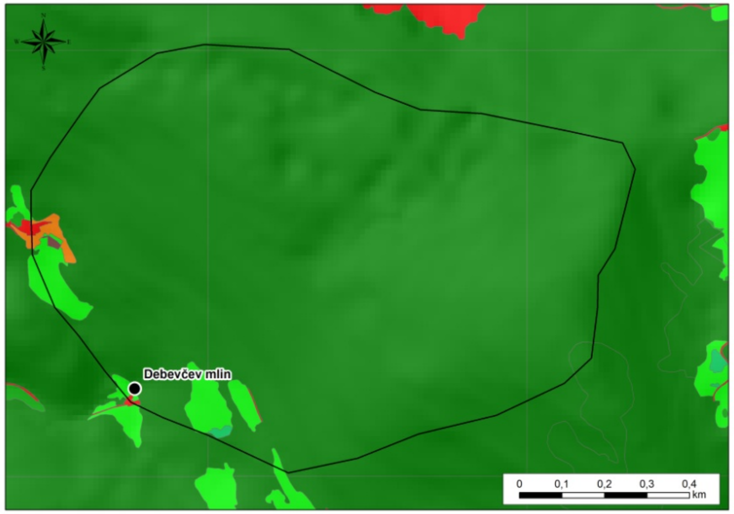

Sampling location Debevčev mlin (Land use classification)

DEV-1, Desenci

Sampling location DEV-1, Desenci

Sampling location DEV-1, Desenci

Sampling location DEV-1, Desenci

Sampling location DEV-1, Desenci

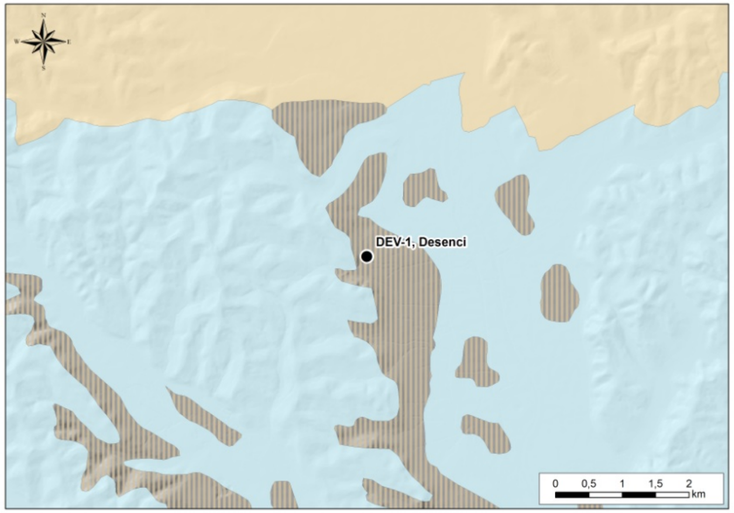

Sampling location DEV-1, Desenci (IAH classification)

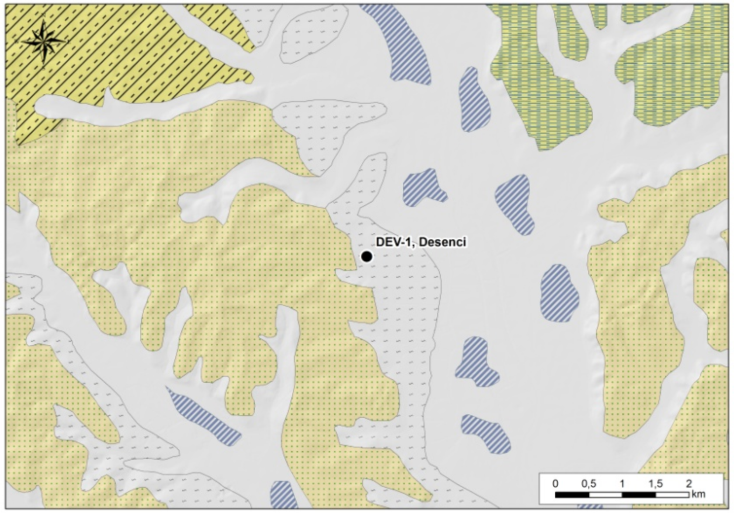

Sampling location DEV-1, Desenci (Geological classification)

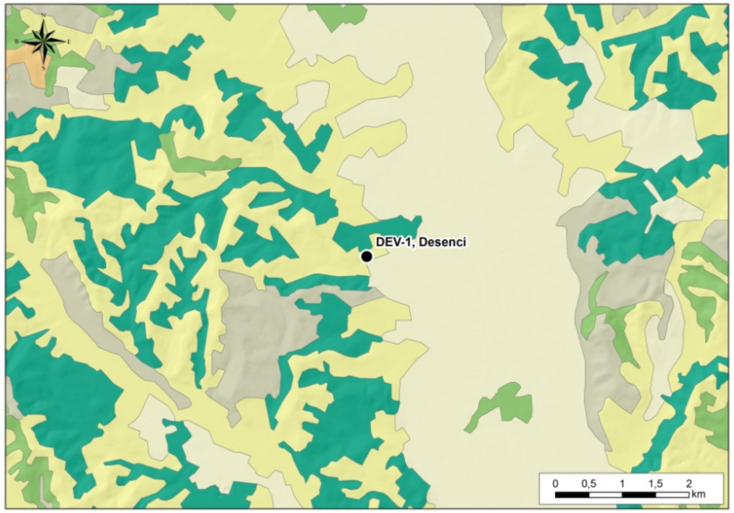

Sampling location DEV-1, Desenci (CLC classification)

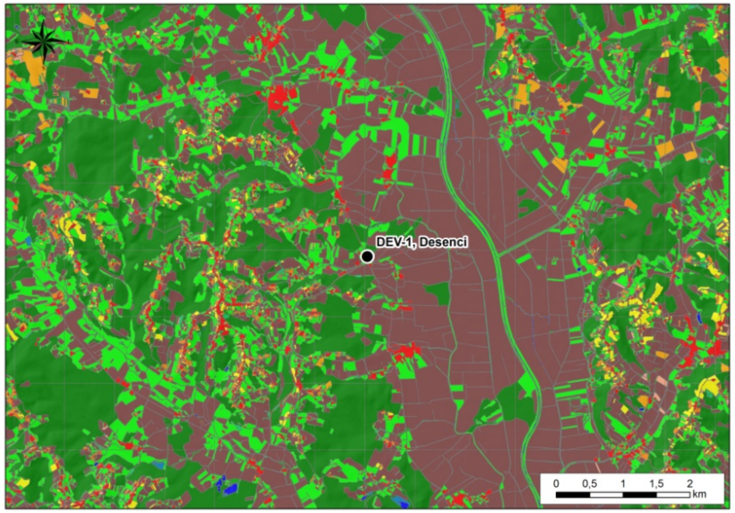

Sampling location DEV-1, Desenci (Land use classification)

Dobličica

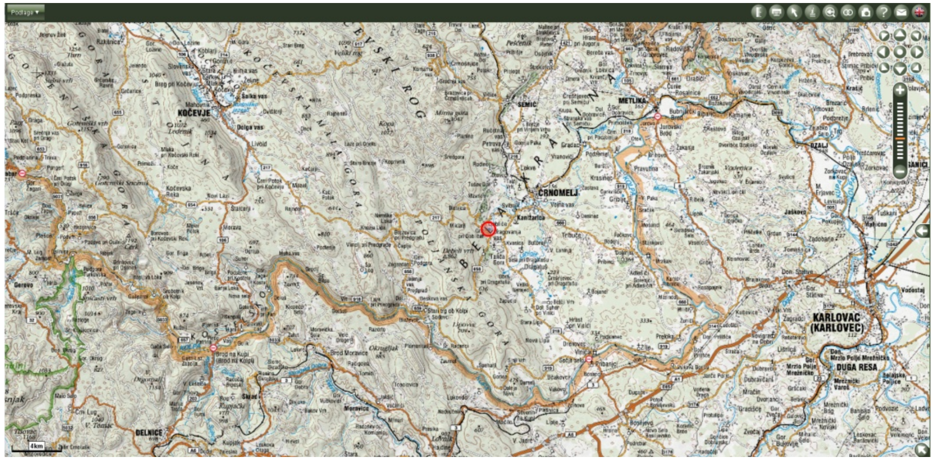

Sampling location Dobličica

Sampling location Dobličica

Sampling location Dobličica

Sampling location Dobličica

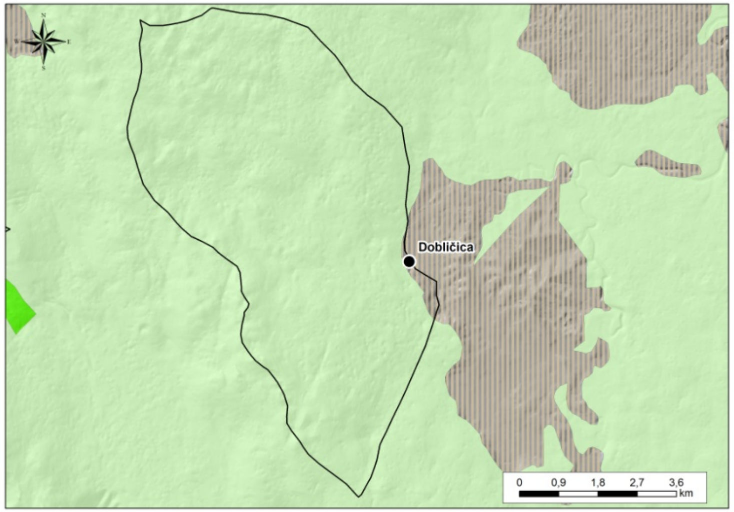

Sampling location Dobličica (IAH classification)

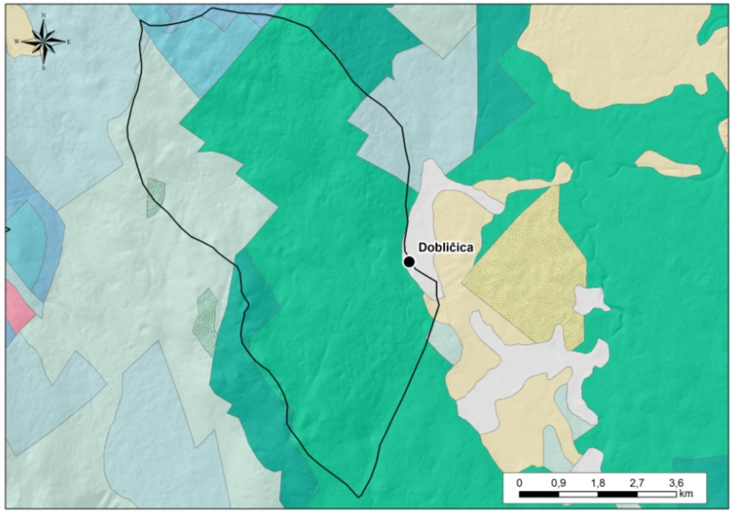

Sampling location Dobličica (Geological classification)

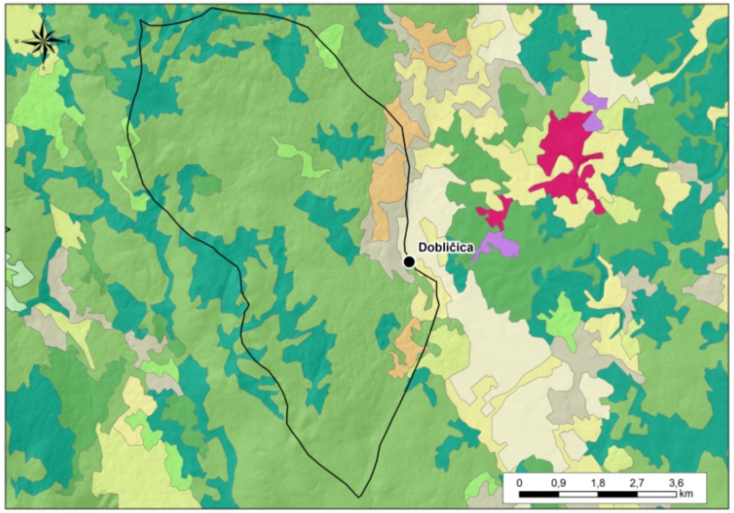

Sampling location Dobličica (CLC classification)

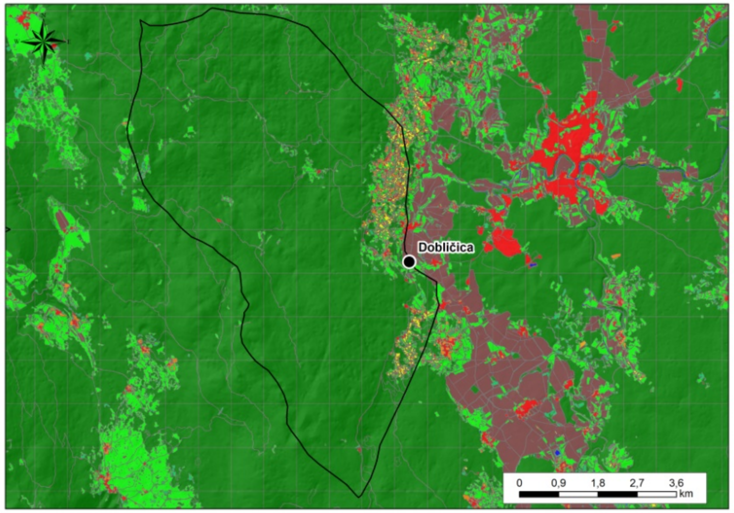

Sampling location Dobličica (Land use classification)

Dobravca

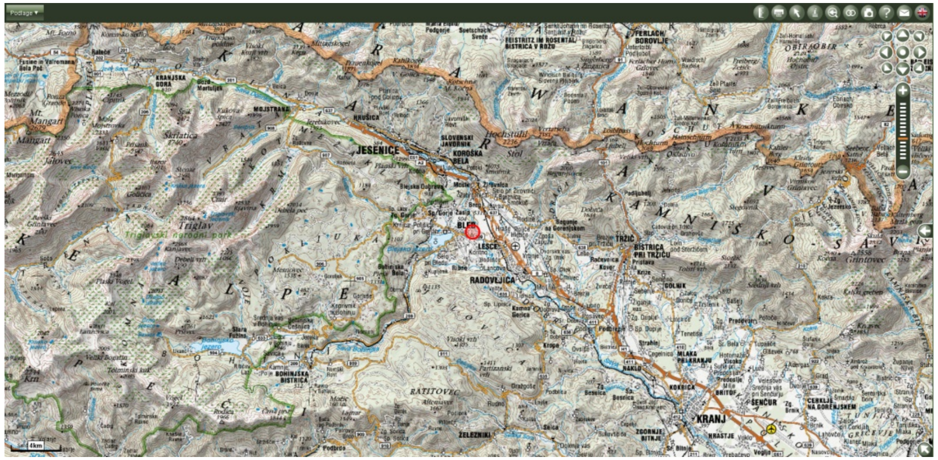

Sampling location Dobravca

Sampling location Dobravca

Sampling location Dobravca

Sampling location Dobravca

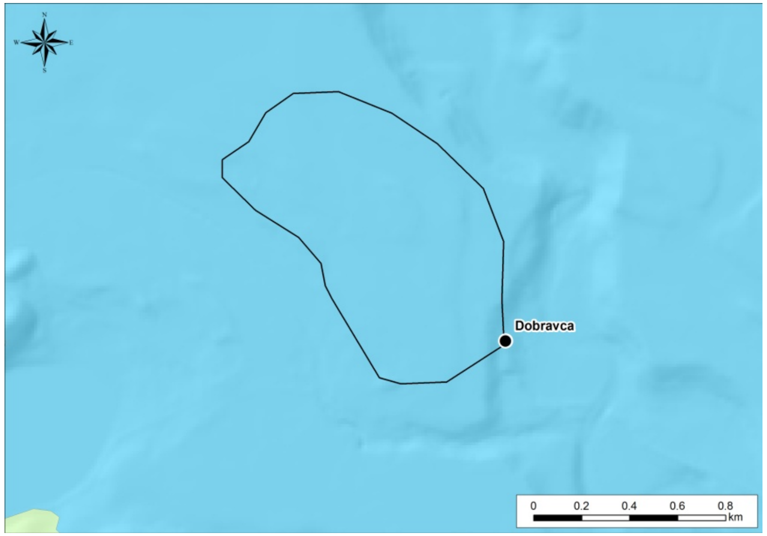

Sampling location Dobravca (IAH classification)

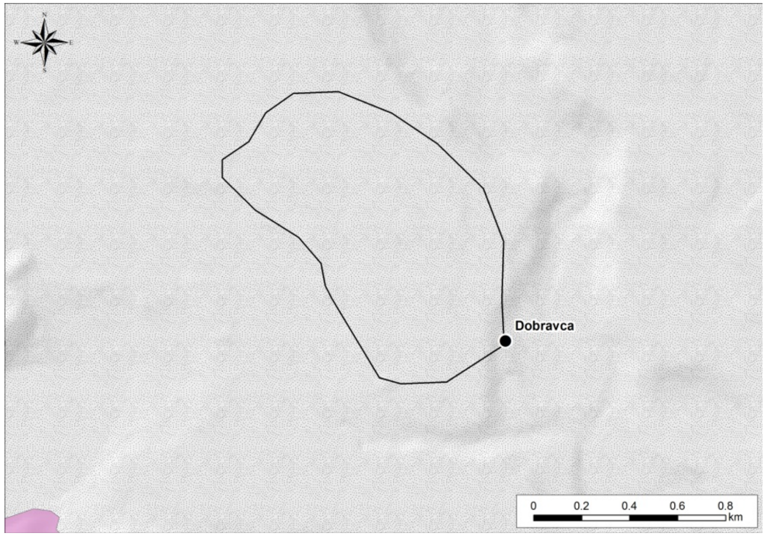

Sampling location Dobravca (Geological classification)

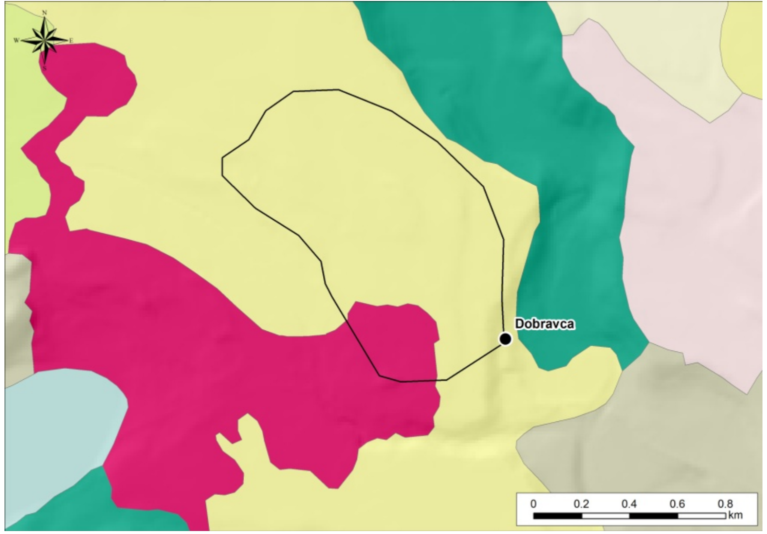

Sampling location Dobravca (CLC classification)

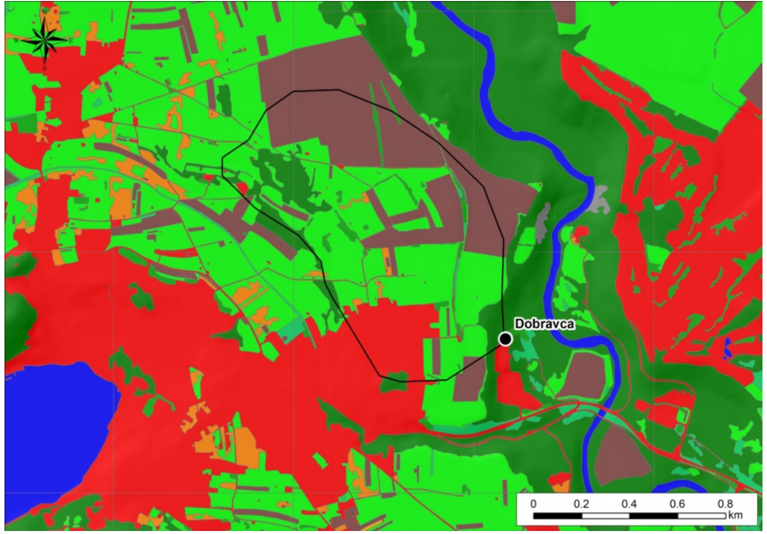

Sampling location Dobravca (Land use classification)

Dobrova

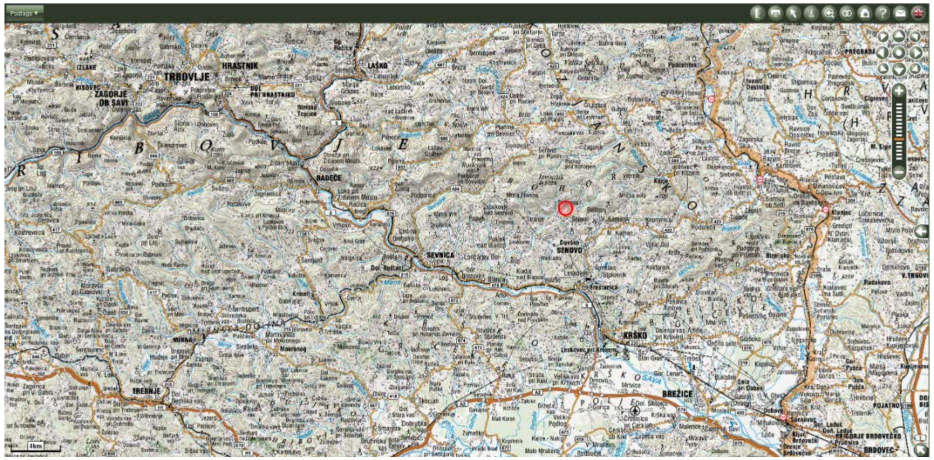

Sampling location Dobrova

Sampling location Dobrova

Sampling location Dobrova

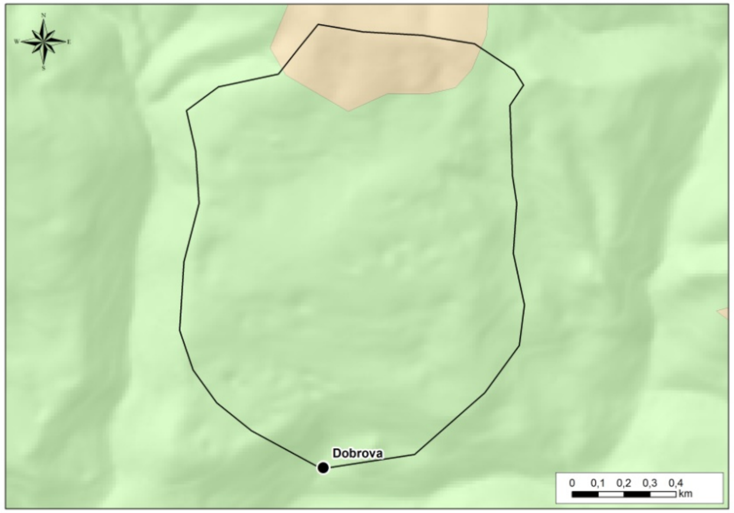

Sampling location Dobrova (IAH classification)

Sampling location Dobrova (Geological classification)

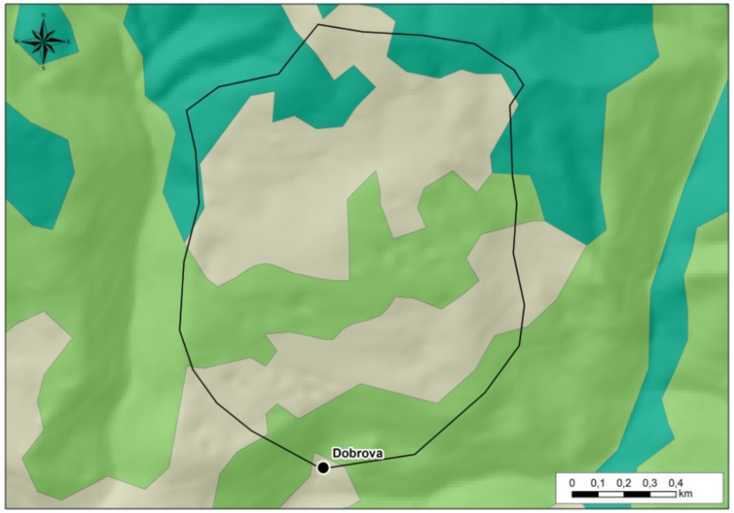

Sampling location Dobrova (CLC classification)

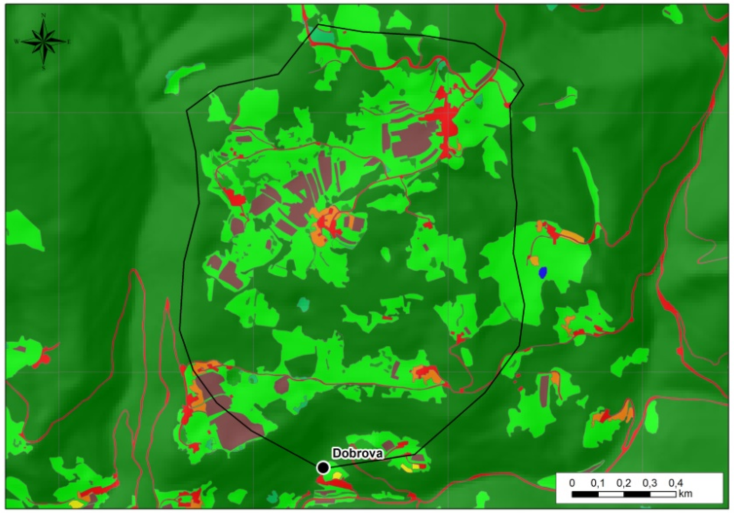

Sampling location Dobrova (Land use classification)

Framski slap

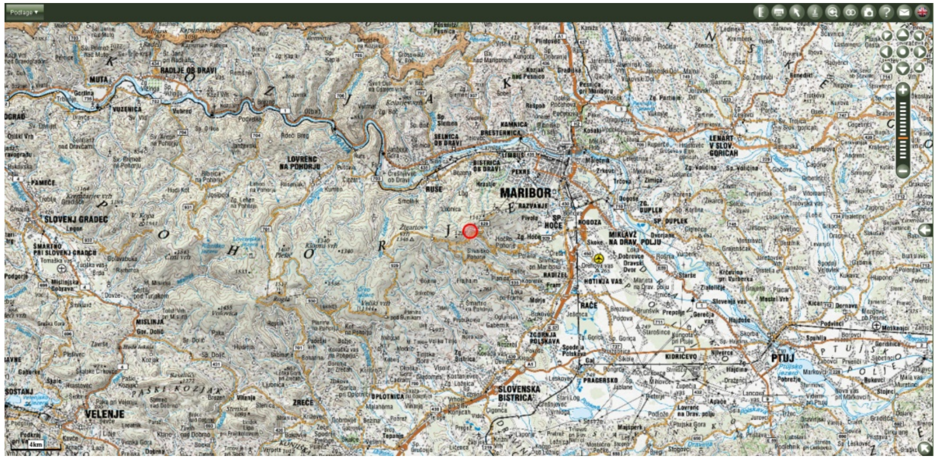

Sampling location Framski slap

Sampling location Framski slap

Sampling location Framski slap

Sampling location Framski slap

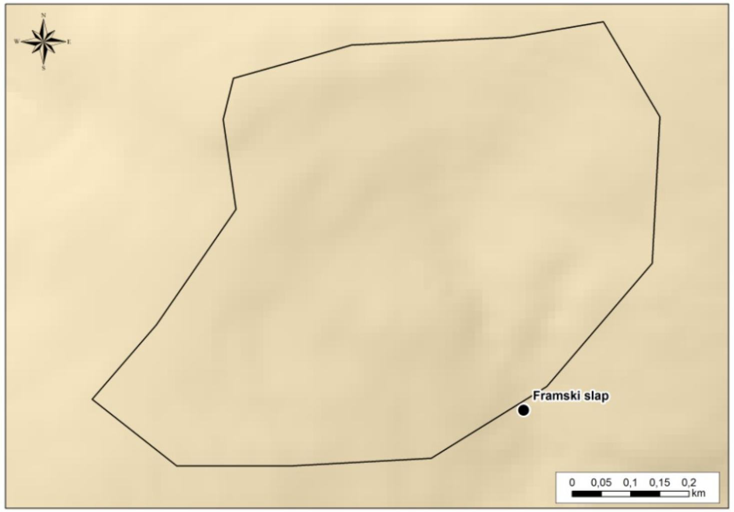

Sampling location Framski slap (IAH classification)

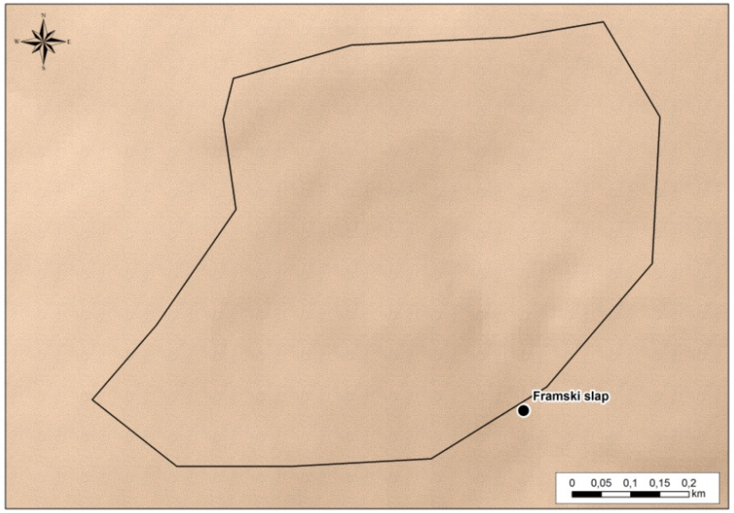

Sampling location Framski slap (Geological classification)

Sampling location Framski slap (CLC classification)

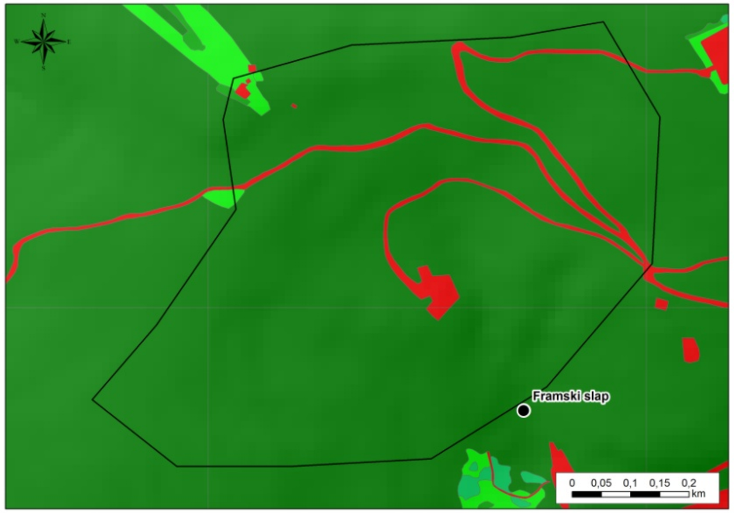

Sampling location Framski slap (Land use classification)

G-1, Gornji Ig

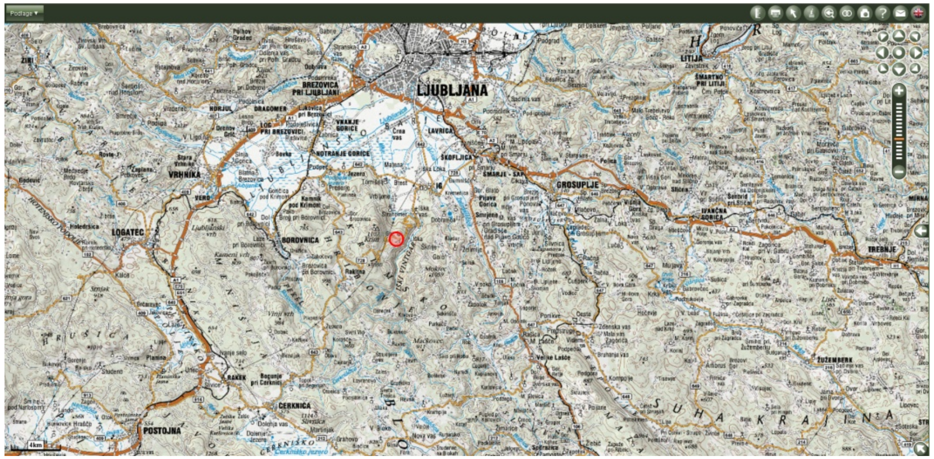

Sampling location G-1, Gornji Ig

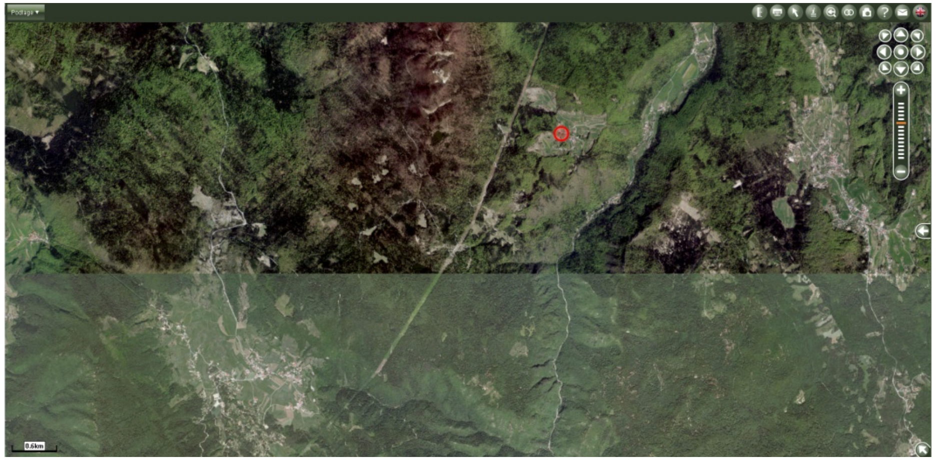

Sampling location G-1, Gornji Ig

Sampling location G-1, Gornji Ig

Sampling location G-1, Gornji Ig

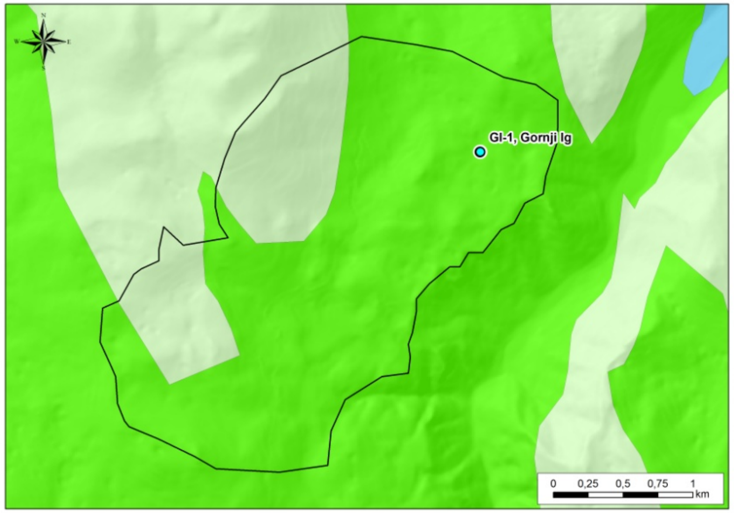

Sampling location GI-1, Gornji Ig (IAH classification)

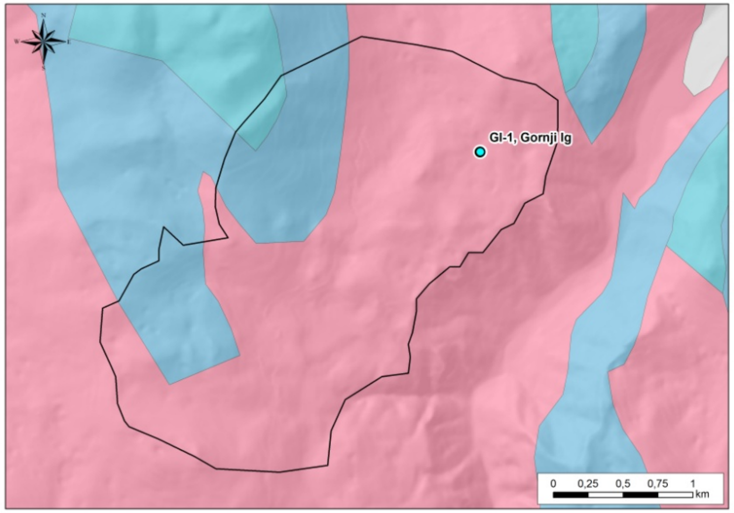

Sampling location GI-1, Gornji Ig (Geological classification)

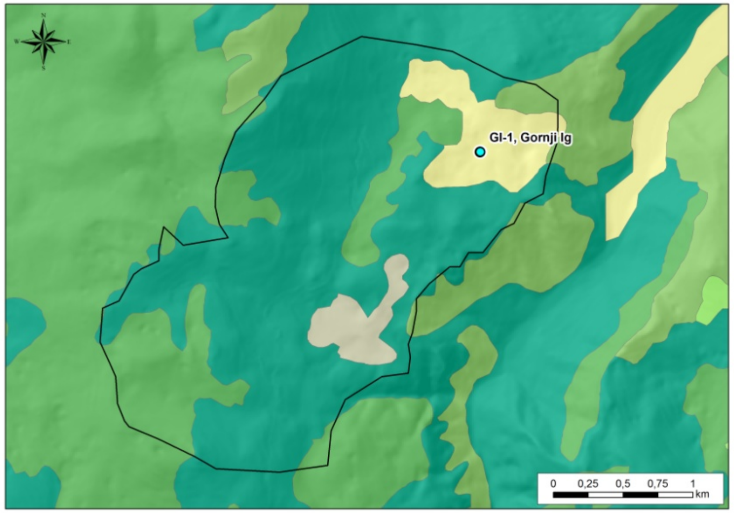

Sampling location GI-1, Gornji Ig (CLC classification)

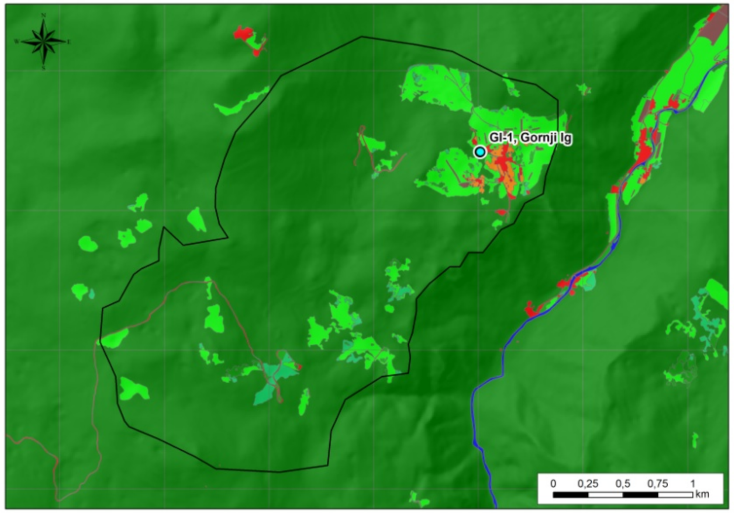

Sampling location GI-1, Gornji Ig (Land use classification)

Gljun

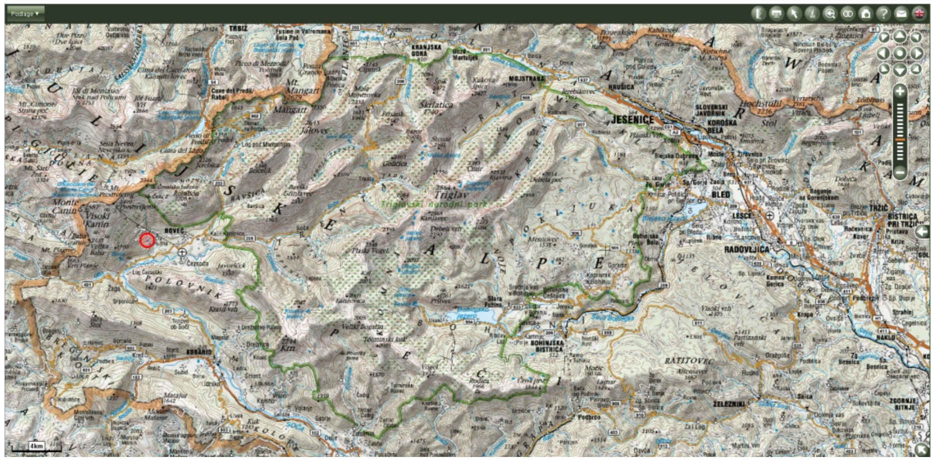

Sampling location Gljun

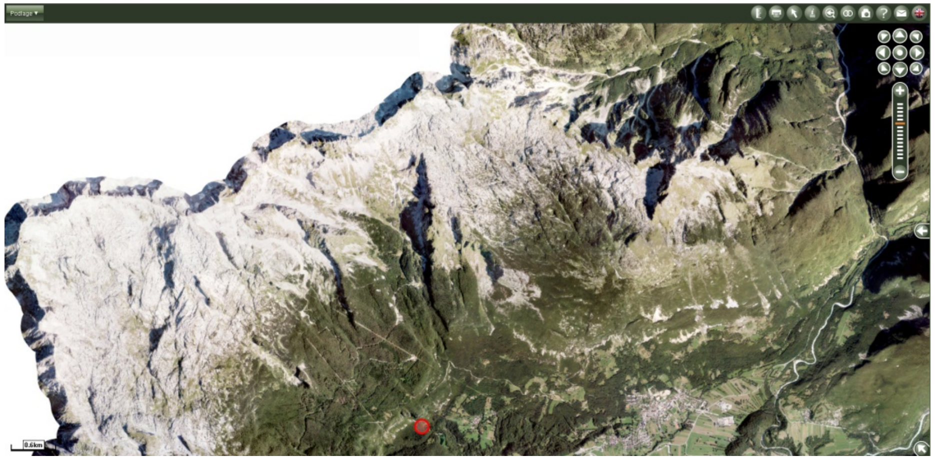

Sampling location Gljun

Sampling location Gljun

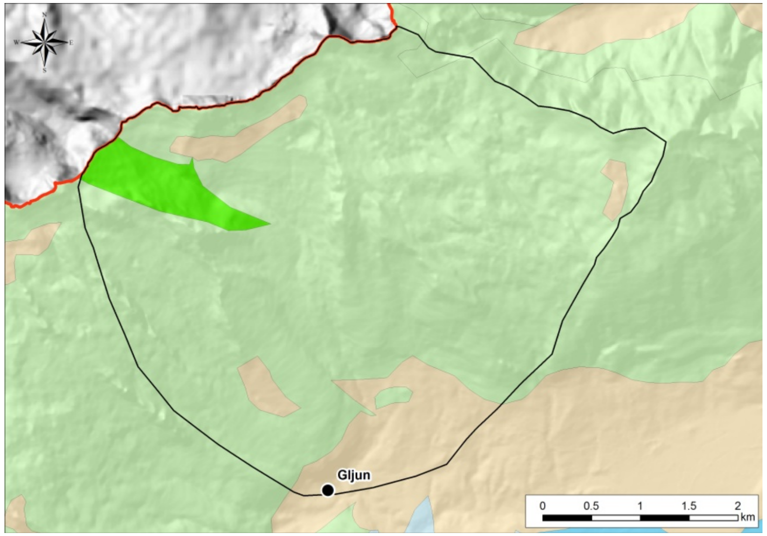

Sampling location Gljun (IAH classification)

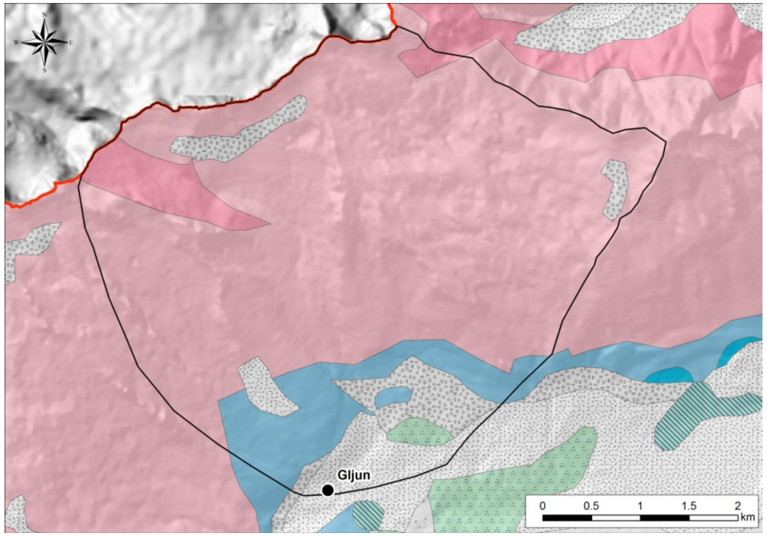

Sampling location Gljun (Geological classification)

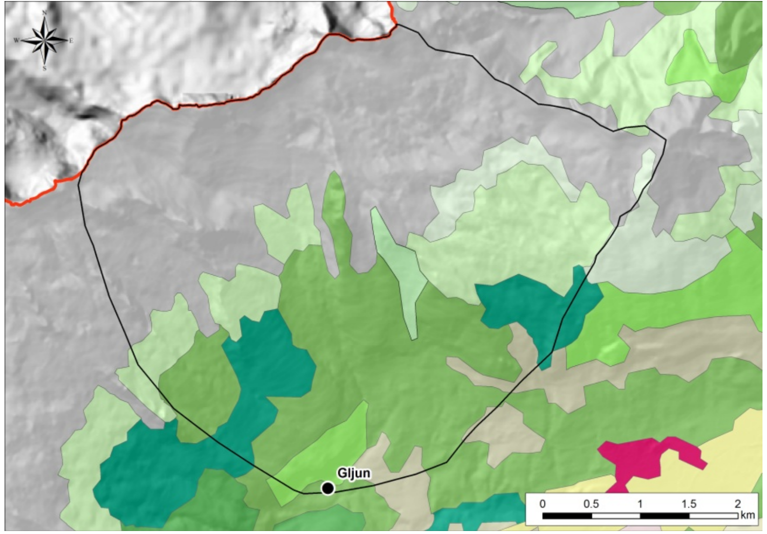

Sampling location Gljun (CLC classification)

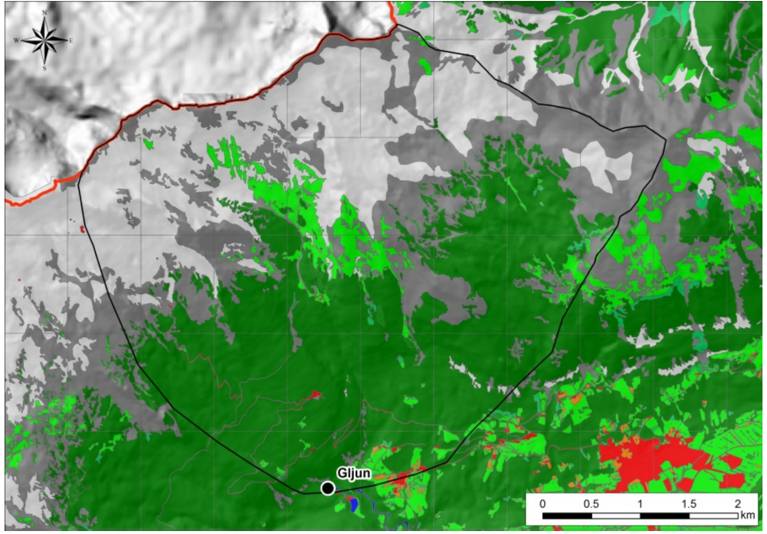

Sampling location Gljun (Land use classification)

Godec

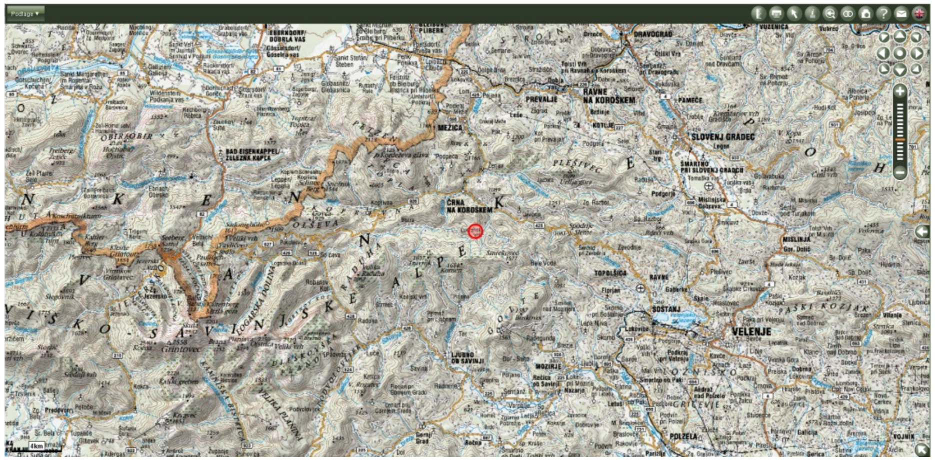
Sampling location Godec


Sampling location Godec


Sampling location Godec

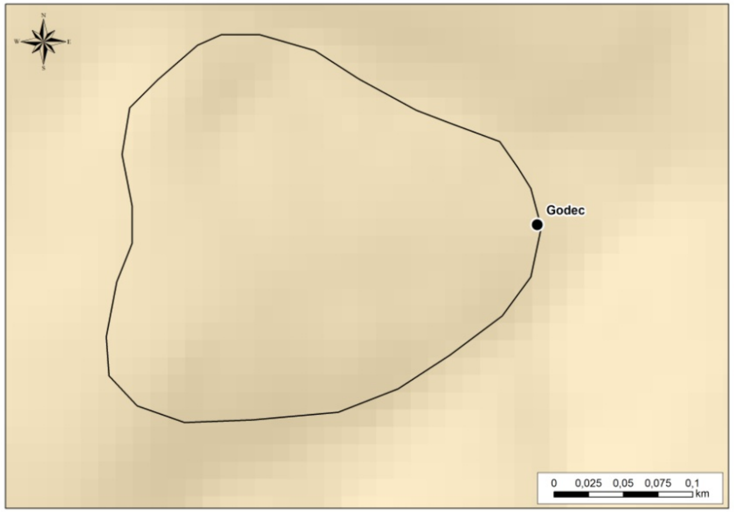

Sampling location Godec (IAH classification)

Sampling location Godec (Geological classification)

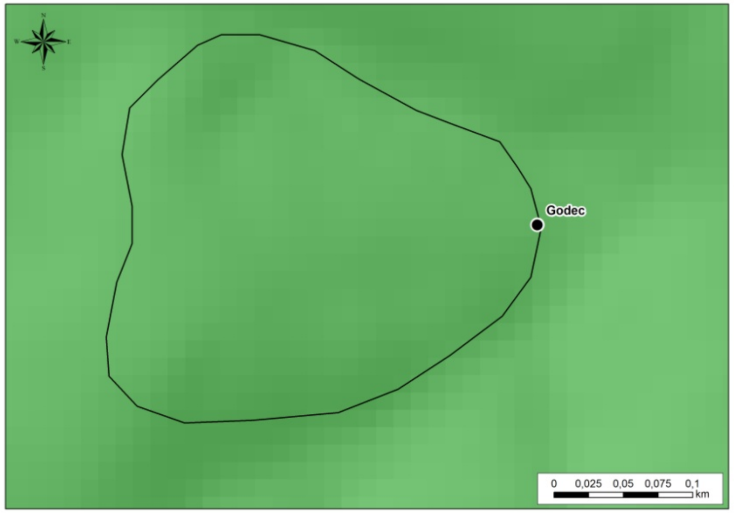

Sampling location Godec (CLC classification)

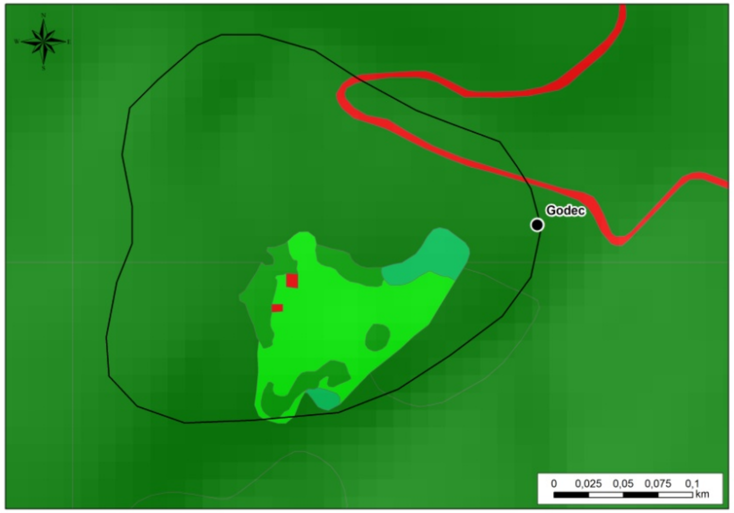

Sampling location Godec (Land use classification)

Grad-1, Grad

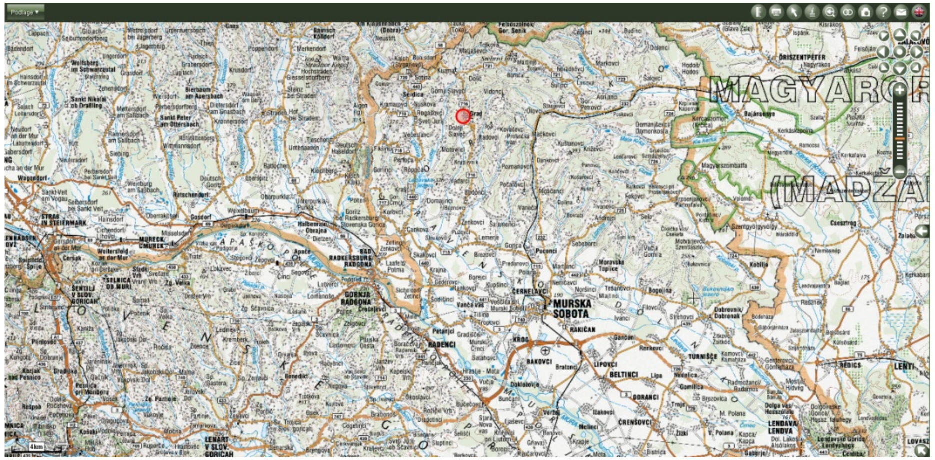

Sampling location Grad-1, Grad

Sampling location Grad-1, Grad

Sampling location Grad-1, Grad

Sampling location Grad-1, Grad

Sampling location Grad-1, Grad (IAH classification)

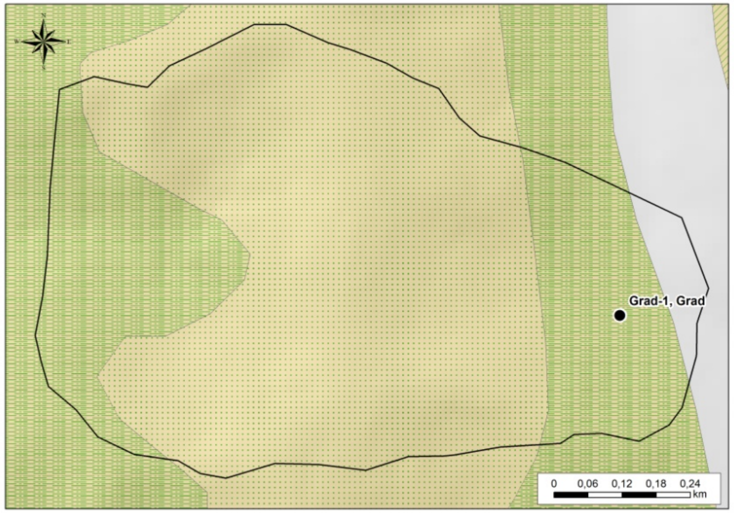

Sampling location Grad-1, Grad (Geological classification)

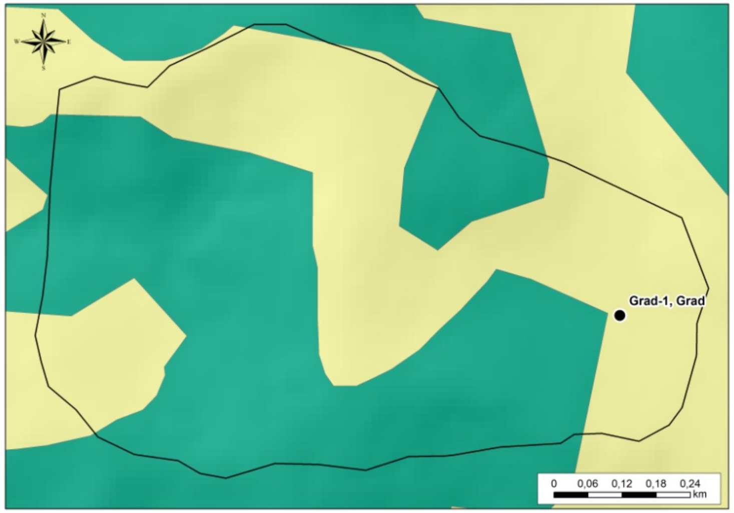

Sampling location Grad-1, Grad (CLC classification)

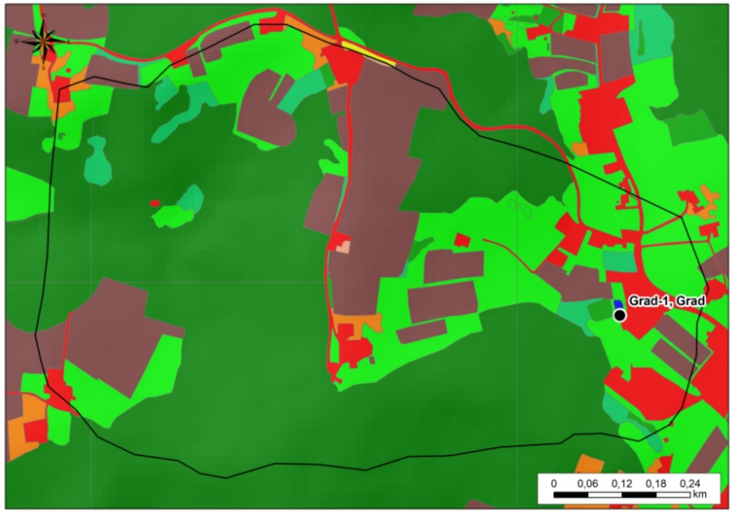

Sampling location Grad-1, Grad (Land use classification)

Gradišče

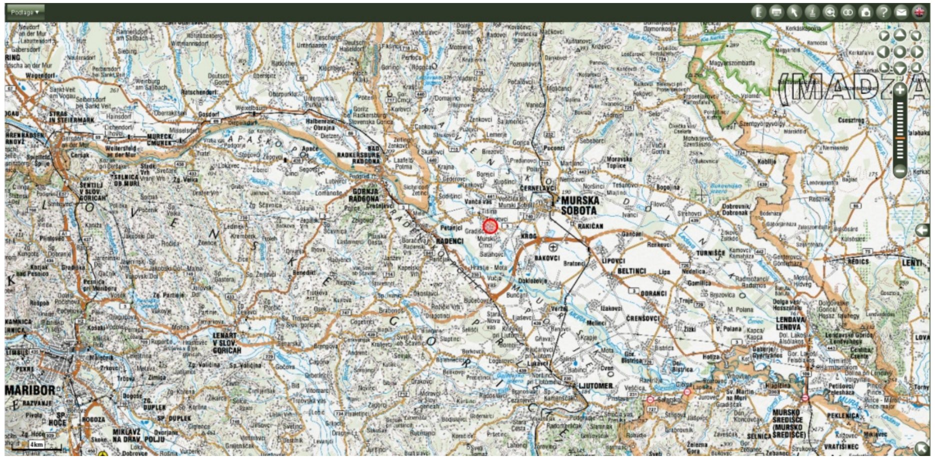

Sampling location Gradišče

Sampling location Gradišče

Sampling location Gradišče

Sampling location Gradišče

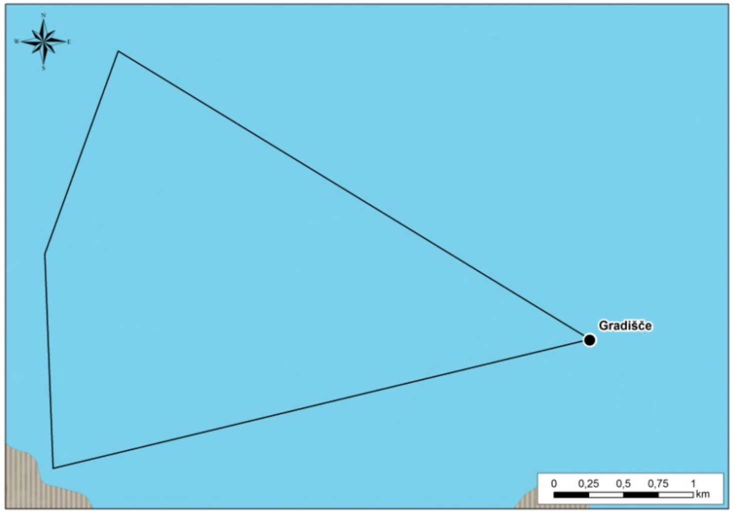

Sampling location Gradišče (IAH classification)

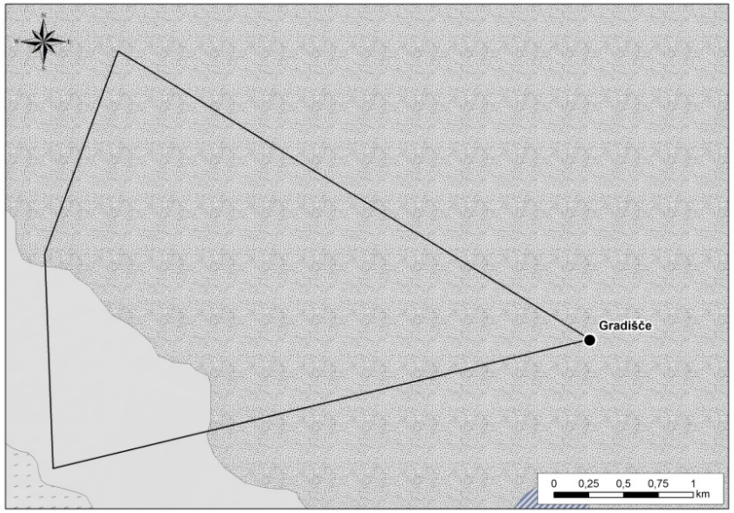

Sampling location Gradišče (Geological classification)

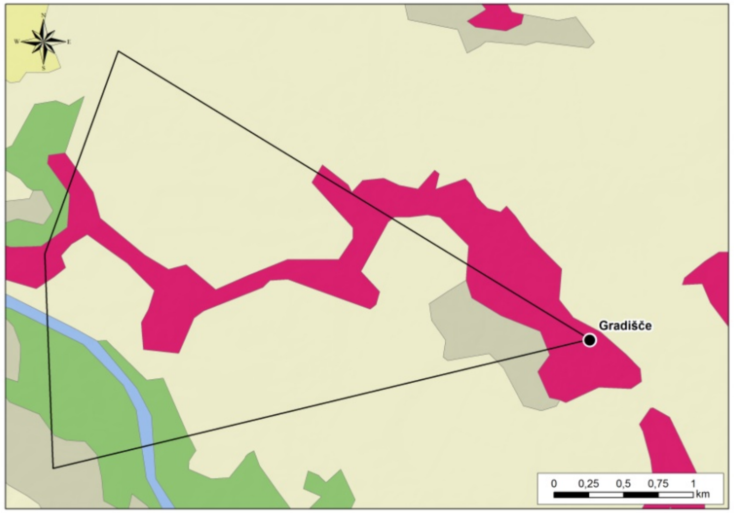

Sampling location Gradišče (CLC classification)

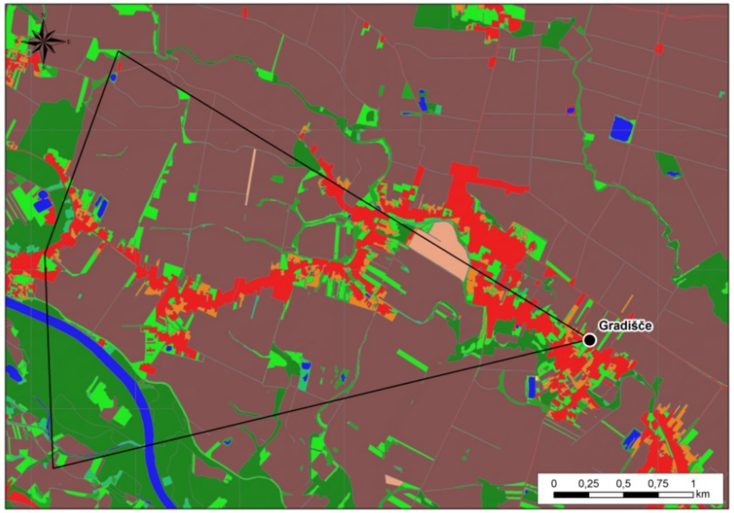

Sampling location Gradišče (Land use classification)

Grajsko zajetje

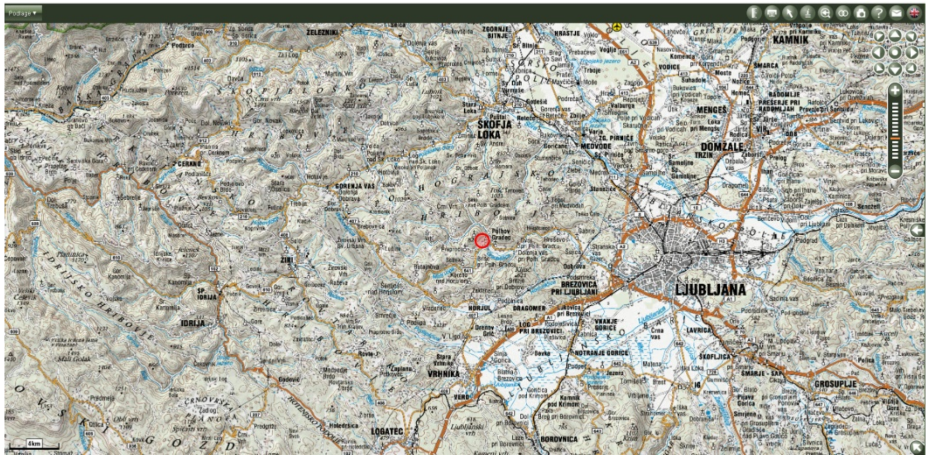

Sampling location Grajsko zajetje

Sampling location Grajsko zajetje

Sampling location Grajsko zajetje

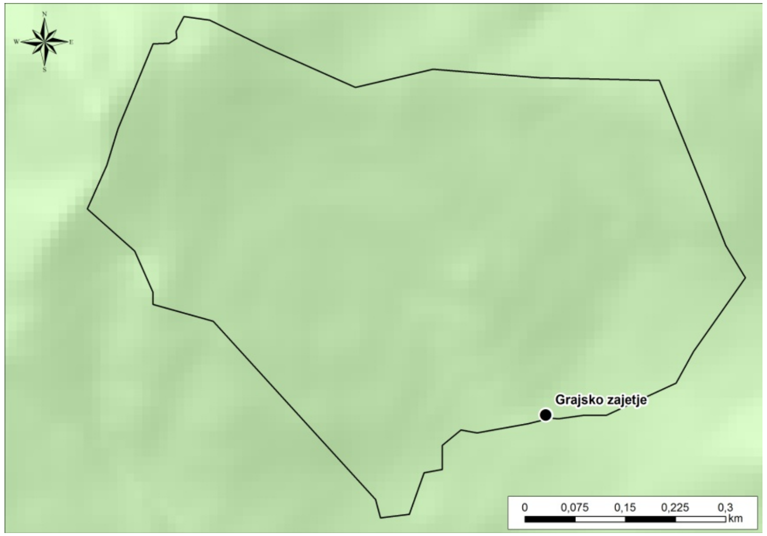

Sampling location Grajsko zajetje (IAH classification)

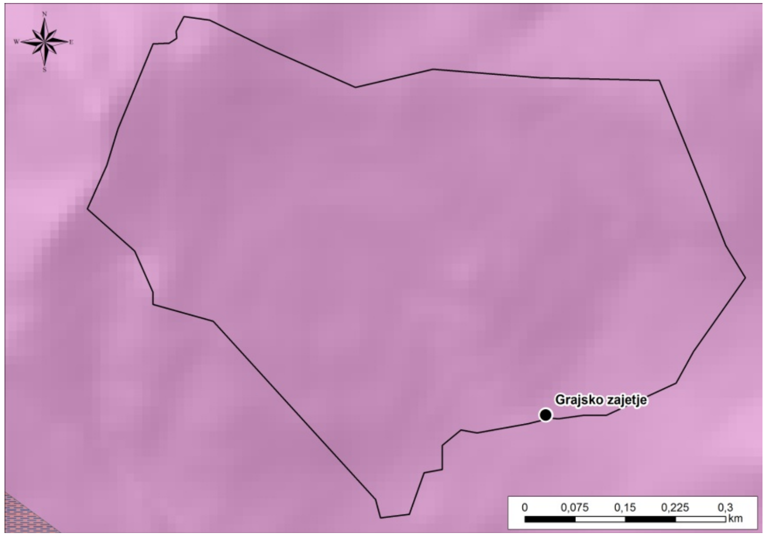

Sampling location Grajsko zajetje(Geological classification)

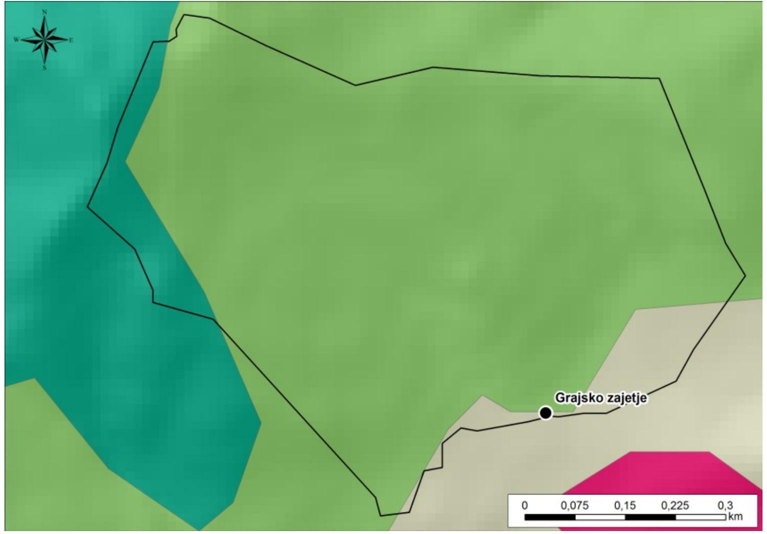

Sampling location Grajsko zajetje (CLC classification)

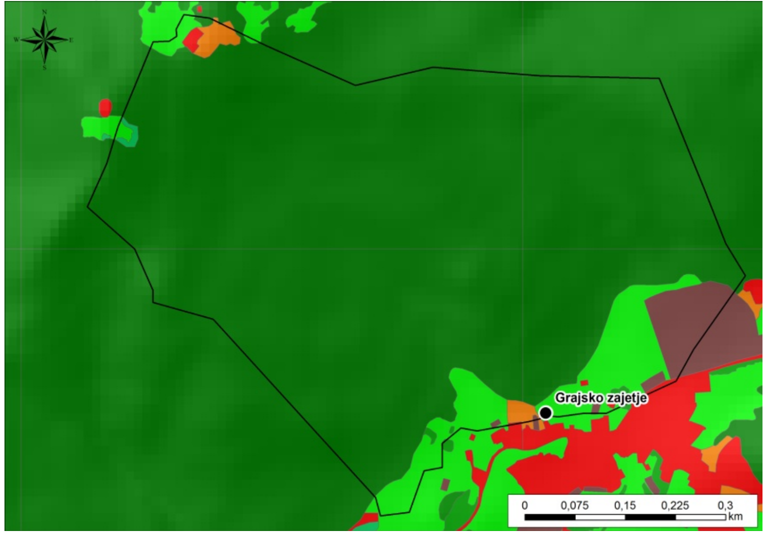

Sampling location Grajsko zajetje (Land use classification)

Grešnikov hrib

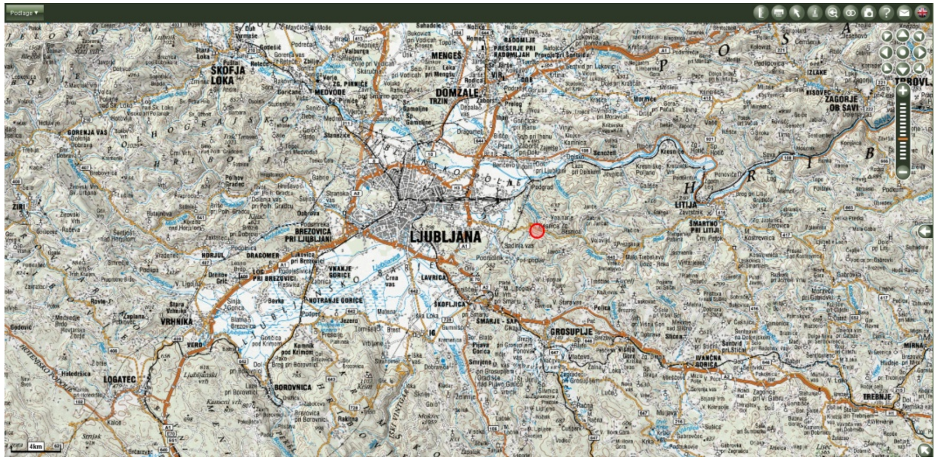

Sampling location Grešnikov hrib

Sampling location Grešnikov hrib

Sampling location Grešnikov hrib

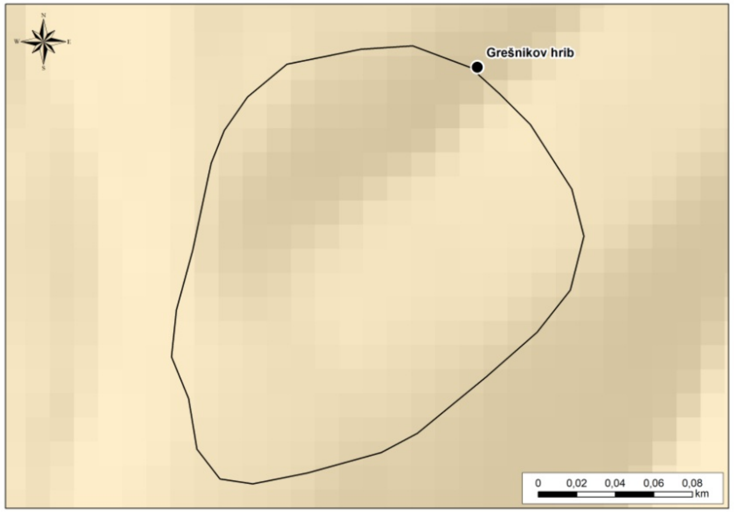

Sampling location Grešnikov hrib (IAH classification)

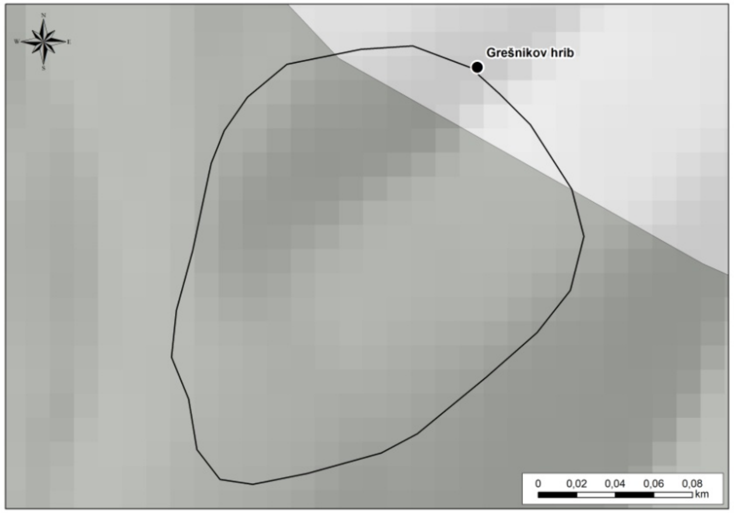

Sampling location Grešnikov hrib (Geological classification)

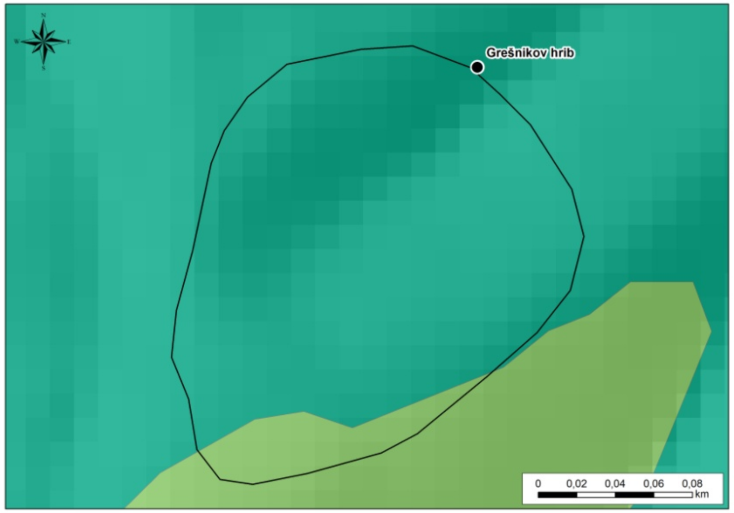

Sampling location Grešnikov hrib (CLC classification)

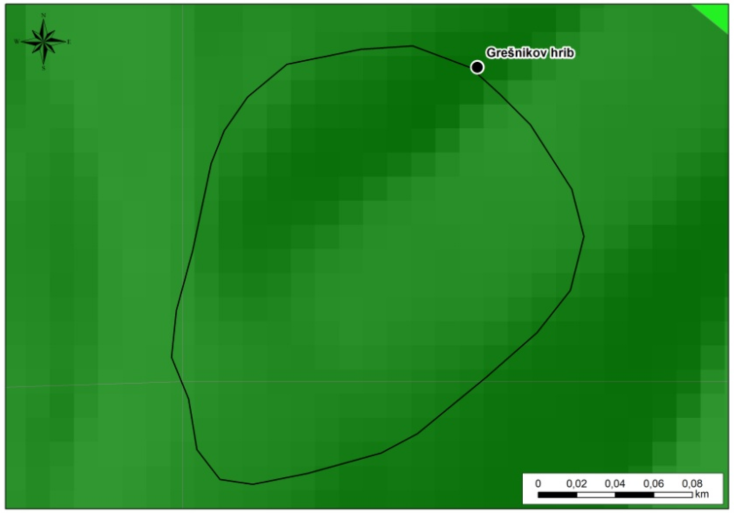

Sampling location Grešnikov hrib (Land use classification)

Hotešk

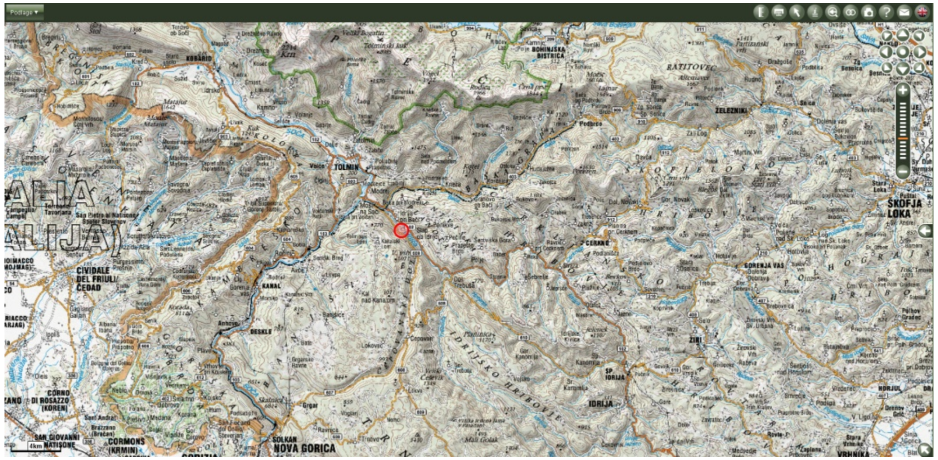

Sampling location Hotešk

Sampling location Hotešk

Sampling location Hotešk

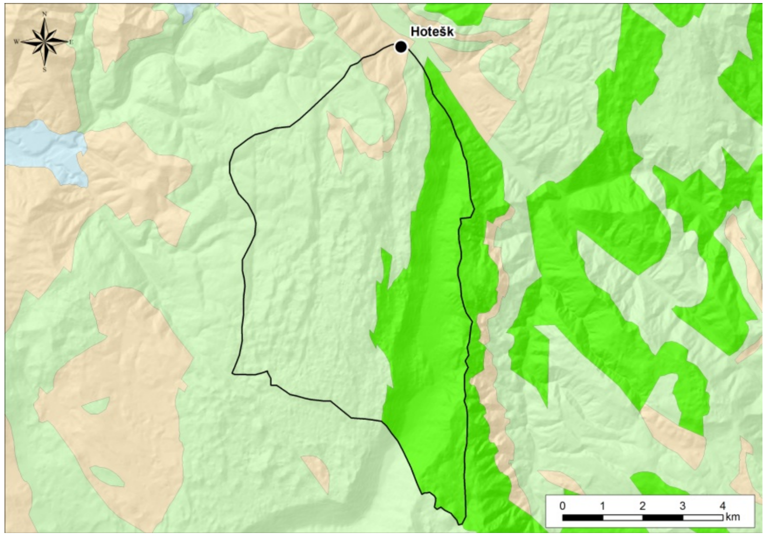

Sampling location Hotešk (IAH classification)

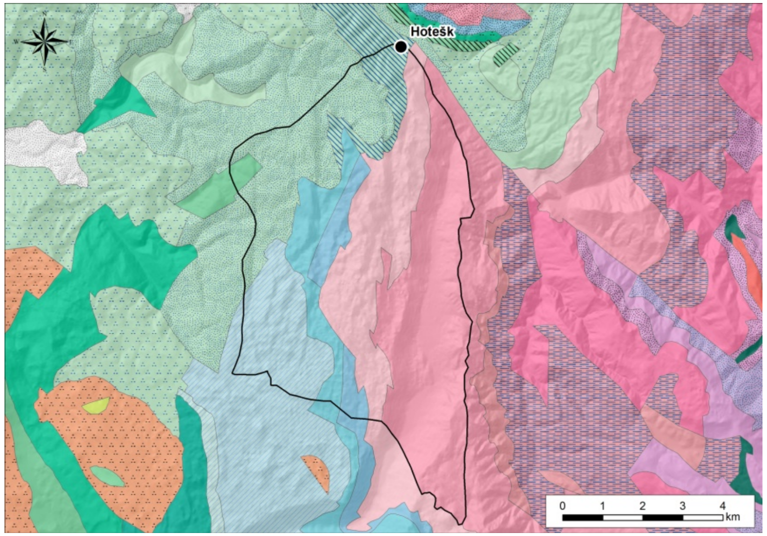

Sampling location Hotešk (Geological classification)

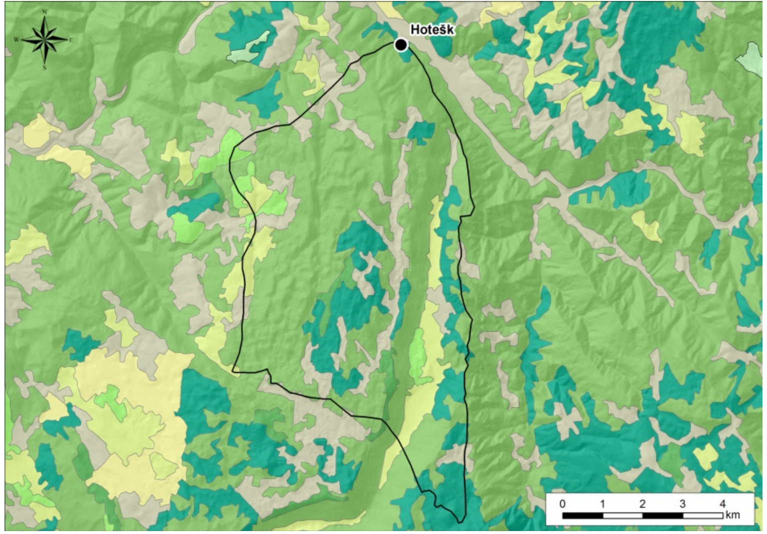

Sampling location Hotešk (CLC classification)

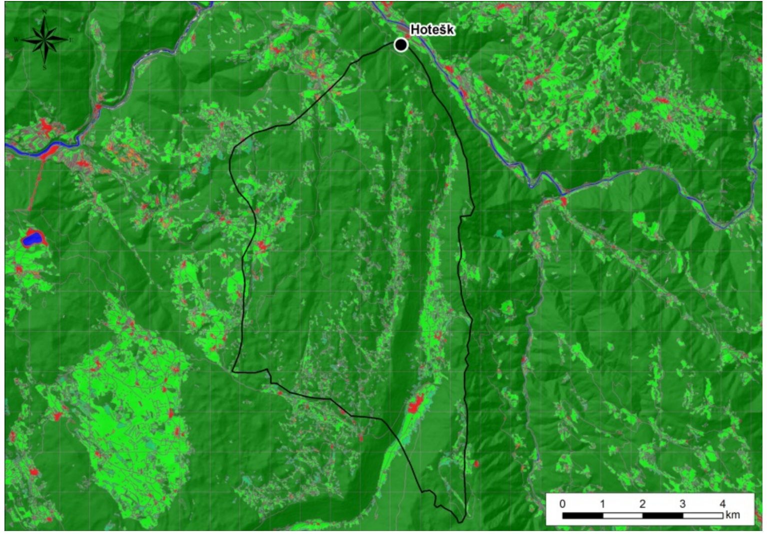

Sampling location Hotešk (Land use classification)

Hubelj

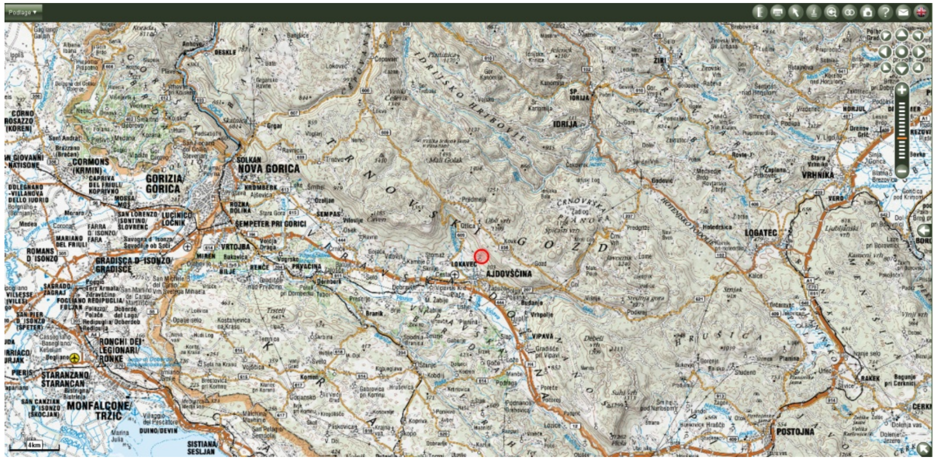

Sampling location Hubelj

Sampling location Hubelj

Sampling location Hubelj

Sampling location Hubelj

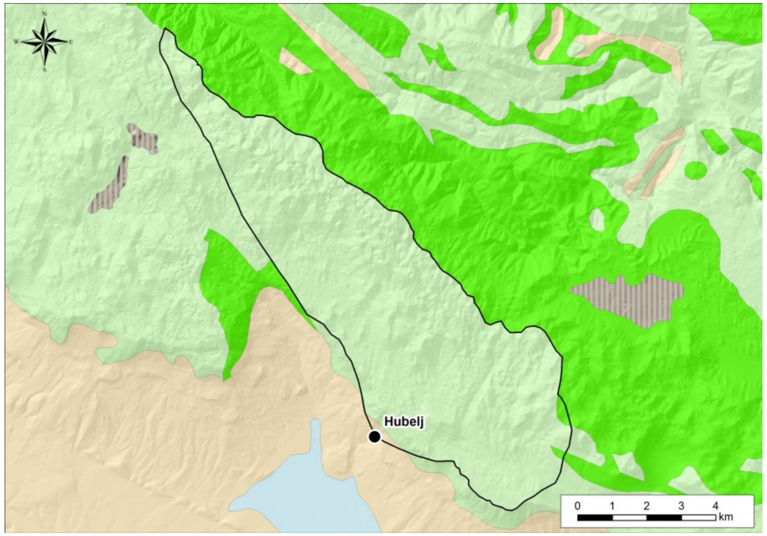

Sampling location Hubelj (IAH classification)

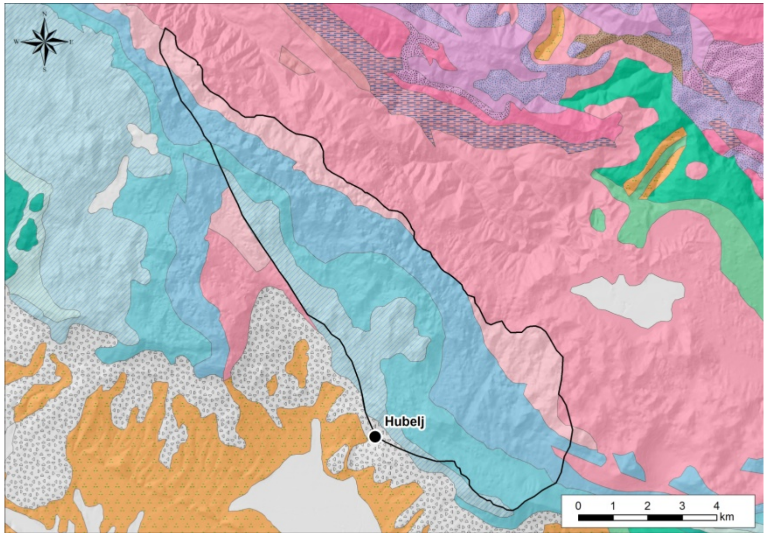

Sampling location Hubelj (Geological classification)

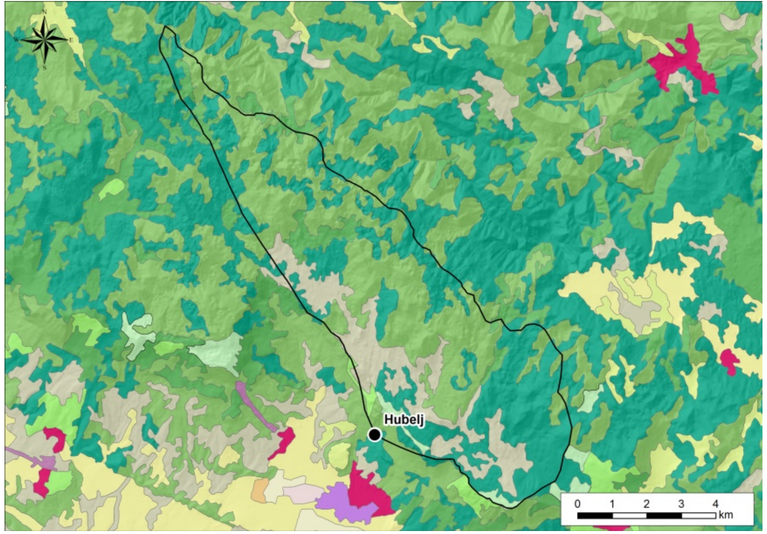

Sampling location Hubelj (CLC classification)

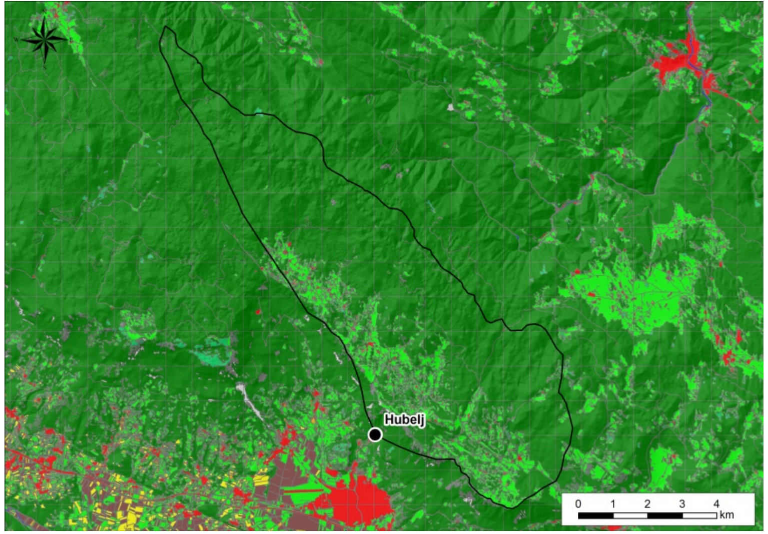

Sampling location Hubelj (Land use classification)

Ilirska Bistrica

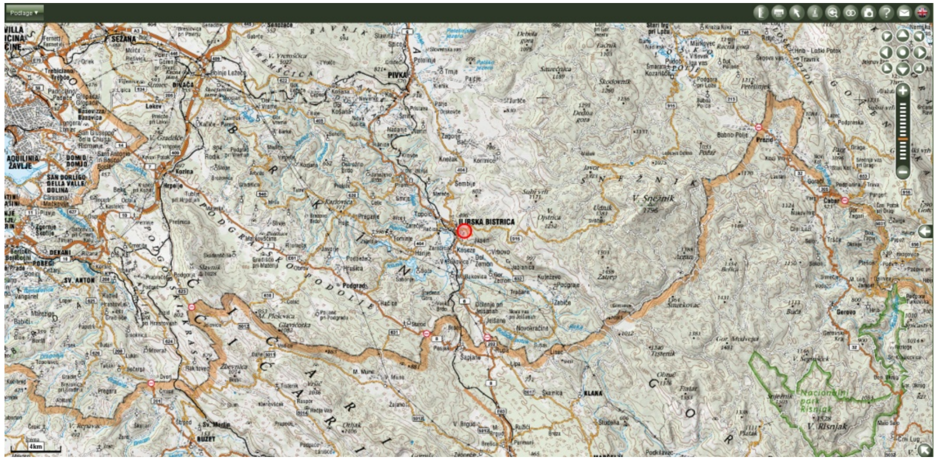

Sampling location Ilirska Bistrica

Sampling location Ilirska Bistrica

Sampling location Ilirska Bistrica

Sampling location Ilirska Bistrica

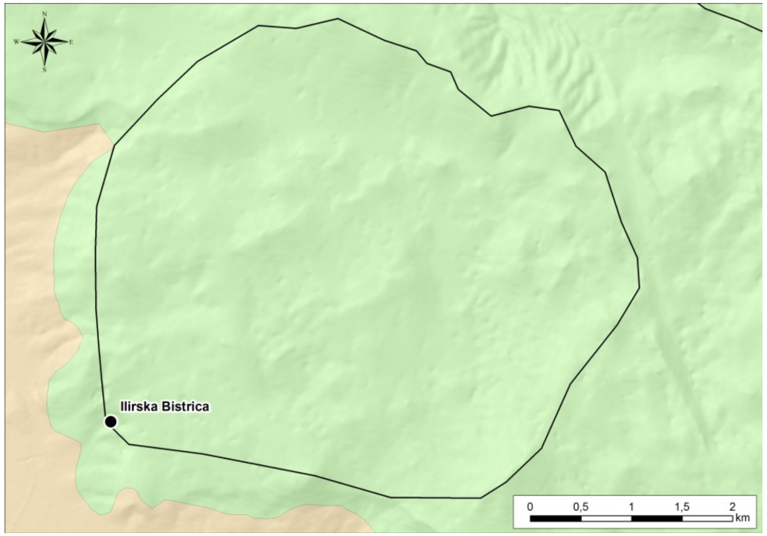

Sampling location Ilirska Bistrica (IAH classification)

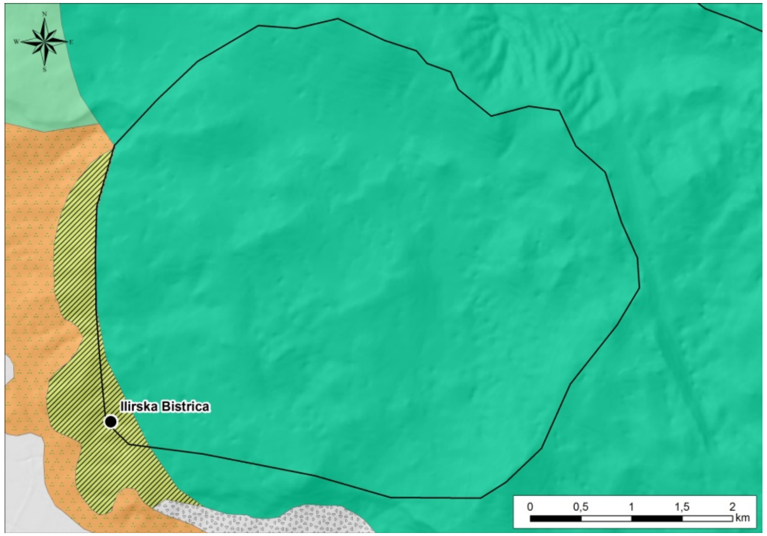

Sampling location Ilirska Bistrica (Geological classification)

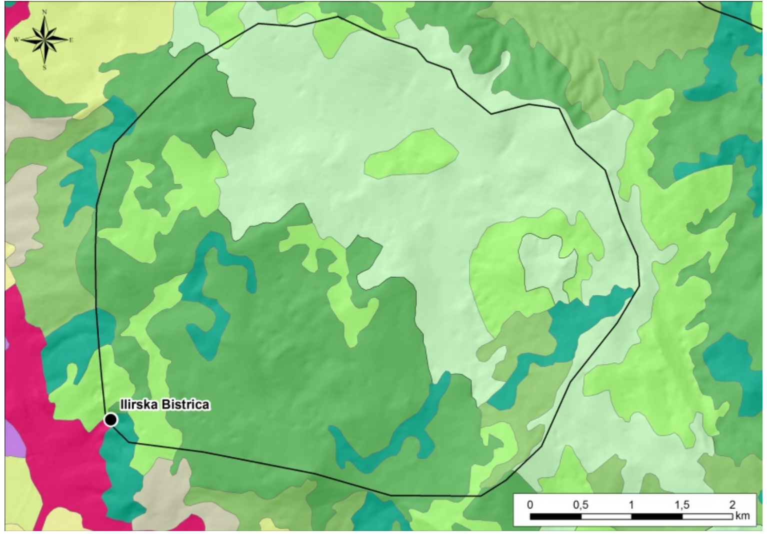

Sampling location Ilirska Bistrica (CLC classification)

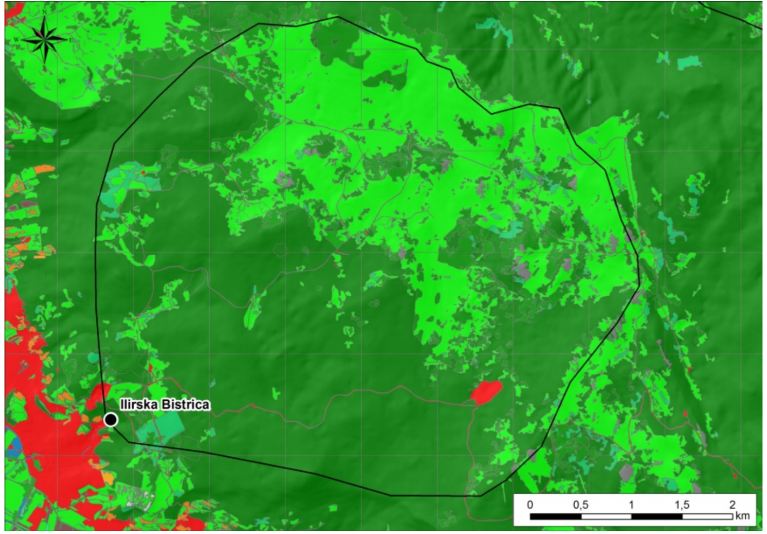

Sampling location Ilirska Bistrica (Land use classification)

Iščica

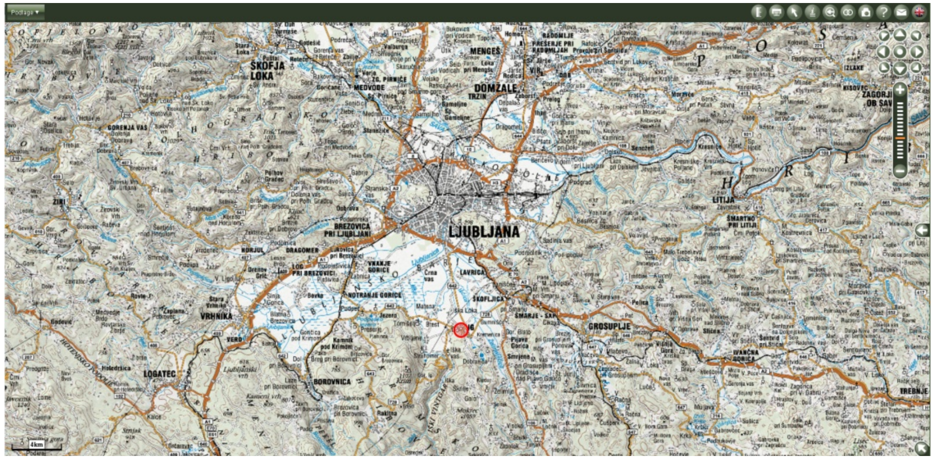

Sampling location Iščica

Sampling location Iščica

Sampling location Iščica

Sampling location Iščica

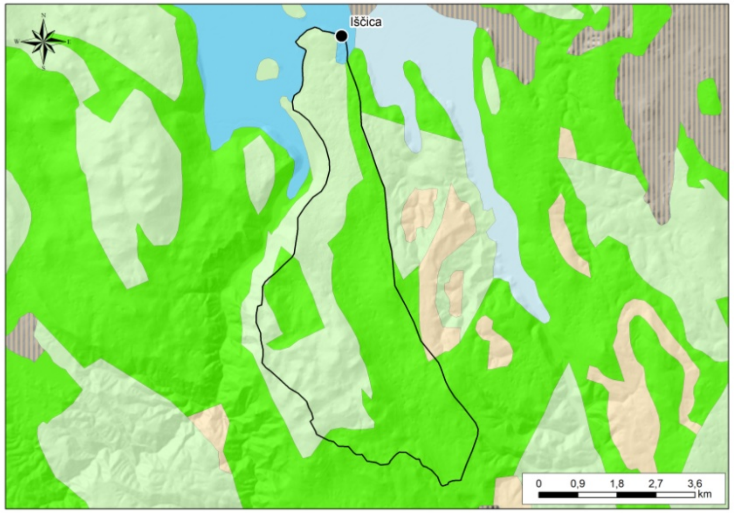

Sampling location Iščica (IAH classification)

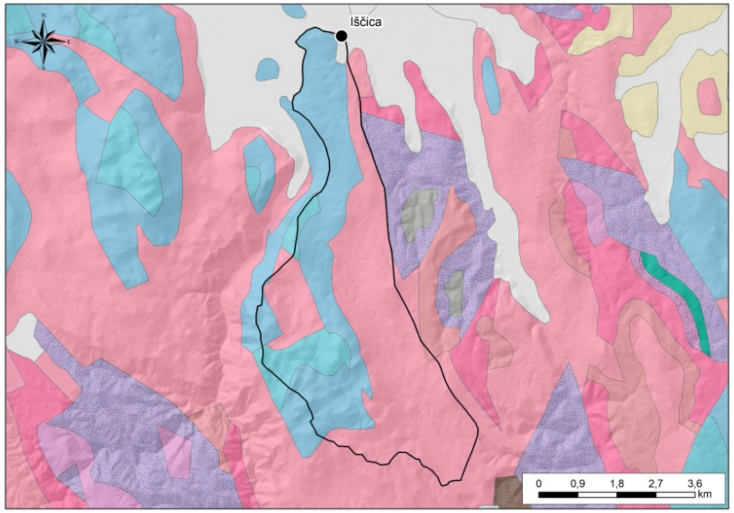

Sampling location Iščica (Geological classification)

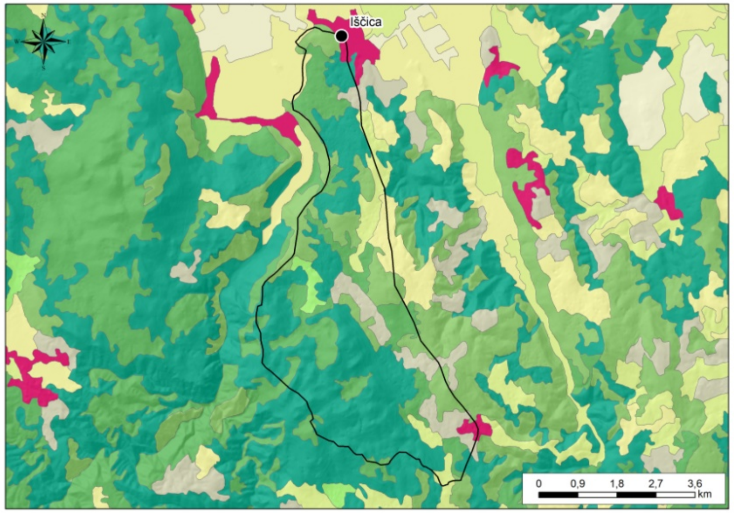

Sampling location Iščica (CLC classification)

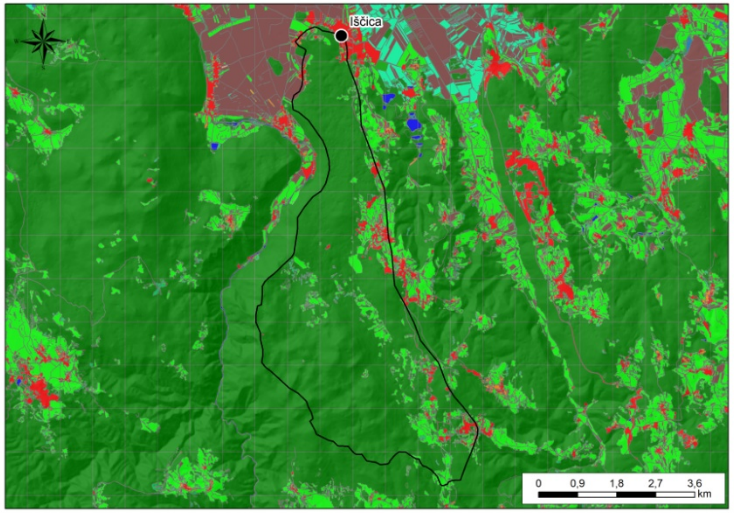

Sampling location Iščica (Land use classification)

Jelševa loka

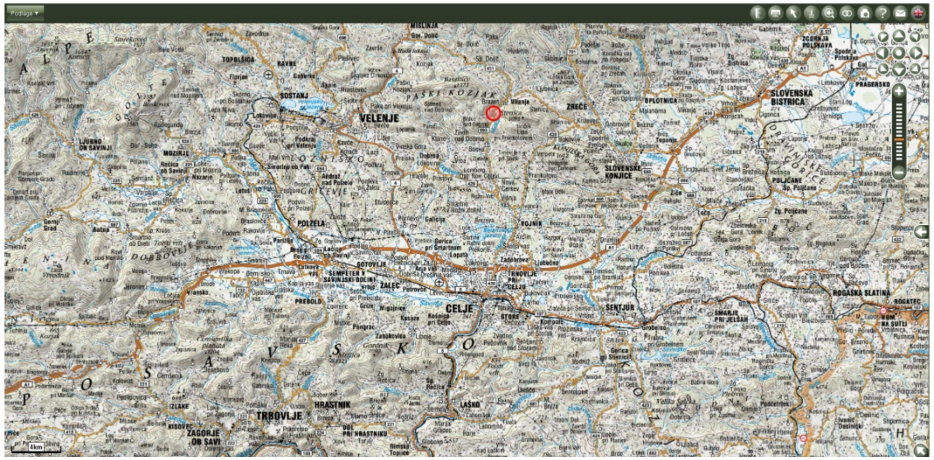

Sampling location Jelševa loka

Sampling location Jelševa loka

Sampling location Jelševa loka

Sampling location Jelševa loka

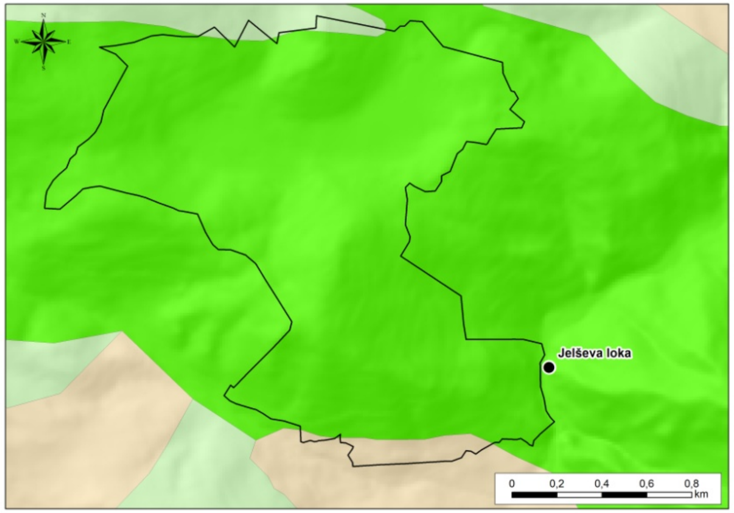

Sampling location Jelševa loka (IAH classification)

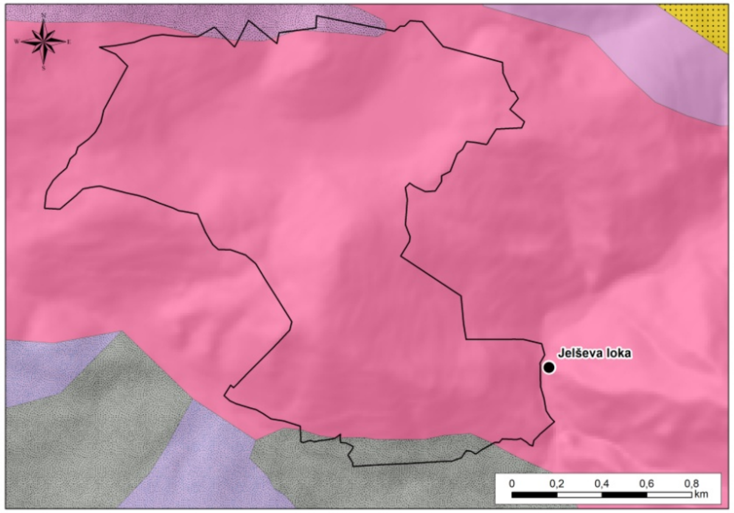

Sampling location Jelševa loka (Geological classification)

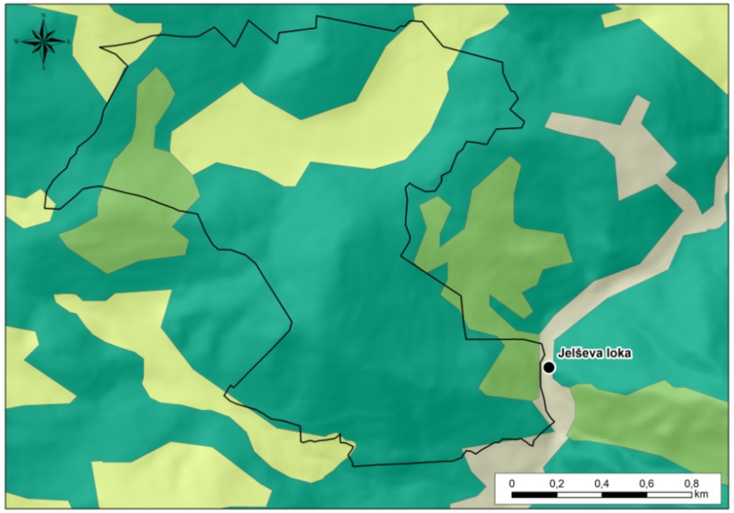

Sampling location Jelševa loka (CLC classification)

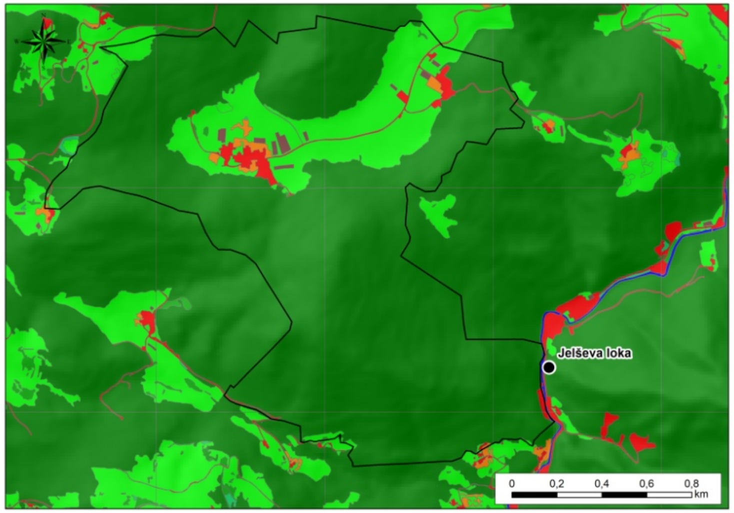

Sampling location Jelševa loka (Land use classification)

Jurčičev Izvir

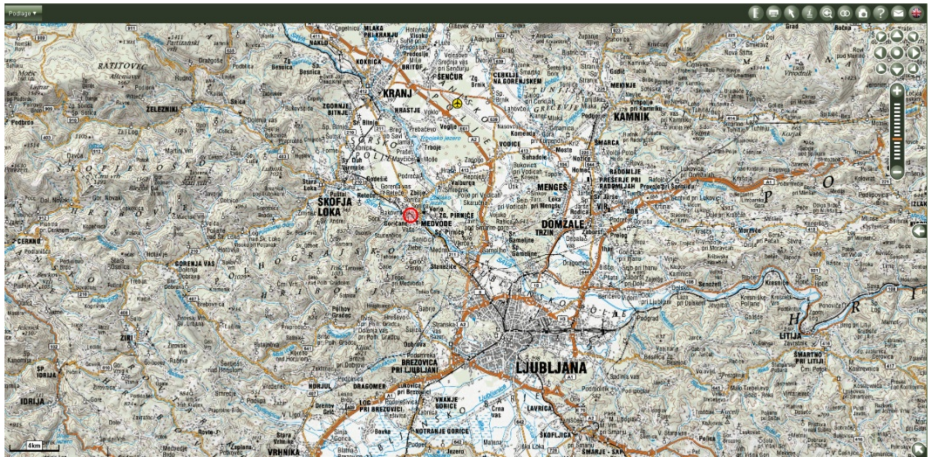

Sampling location Jurčičev izvir

Sampling location Jurčičev izvir

Sampling location Jurčičev izvir

Sampling location Jurčičev izvir

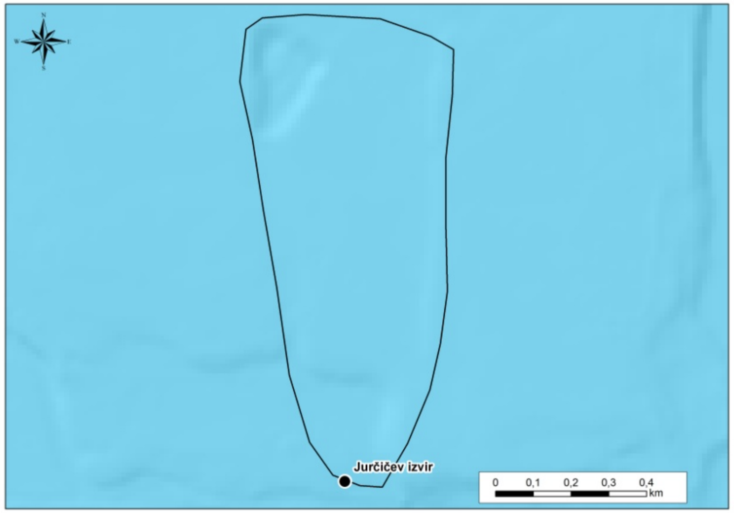

Sampling location Jurčičev izvir (IAH classification)

Sampling location Jurčičev izvir (Geological classification)

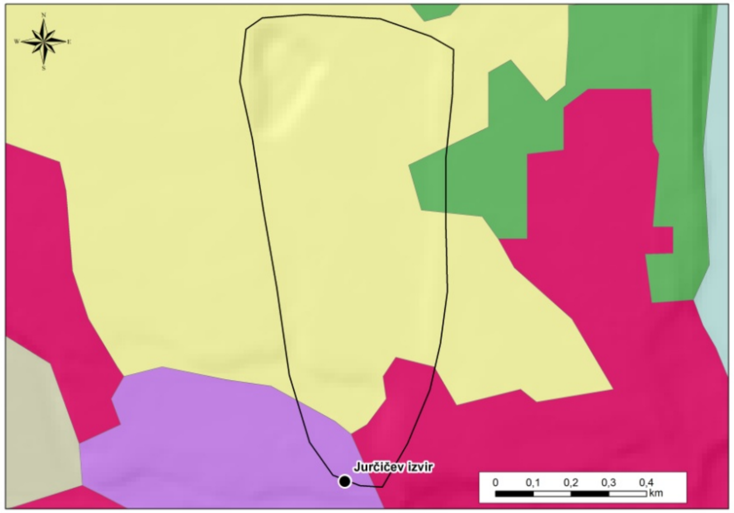

Sampling location Jurčičev izvir (CLC classification)

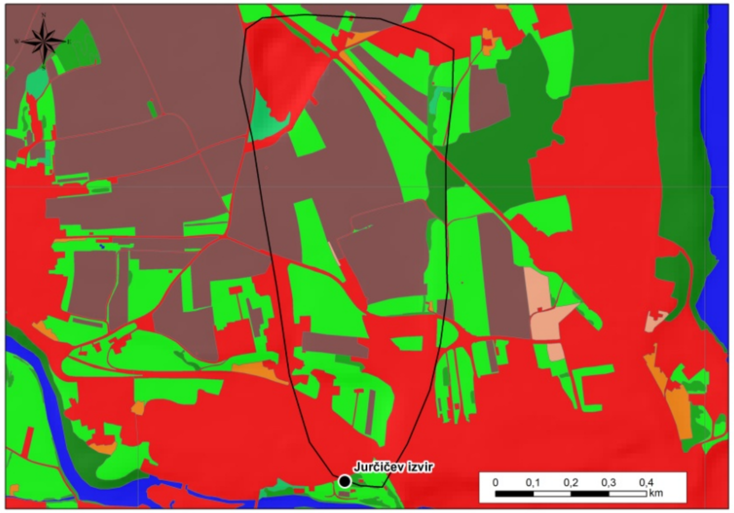

Sampling location Jurčičev izvir (Land use classification)

Kamniška Bistrica

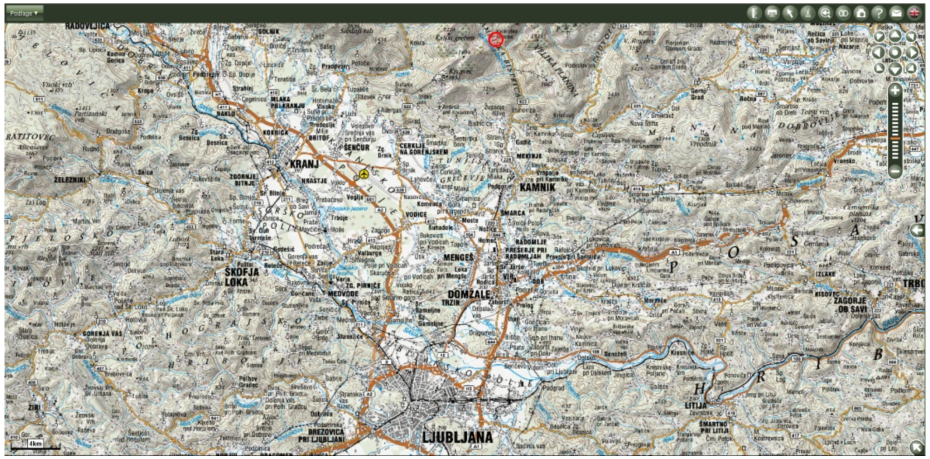

Sampling location Kamniška Bistrica

Sampling location Kamniška Bistrica

Sampling location Kamniška Bistrica

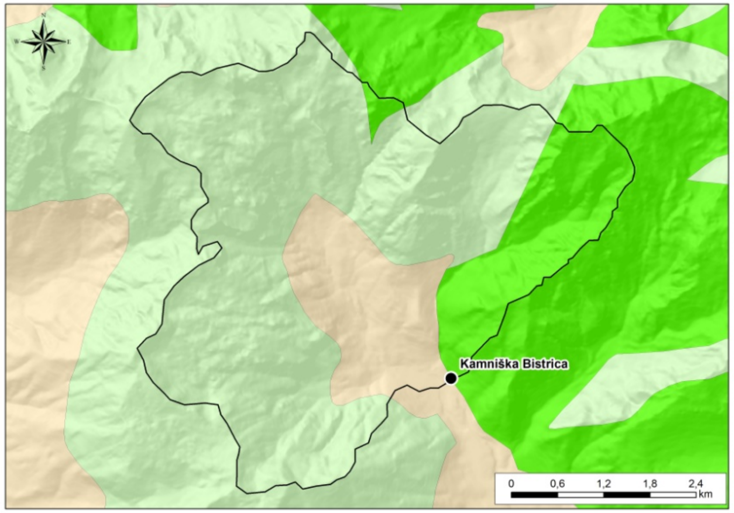

Sampling location Kamniška Bistrica (IAH classification)

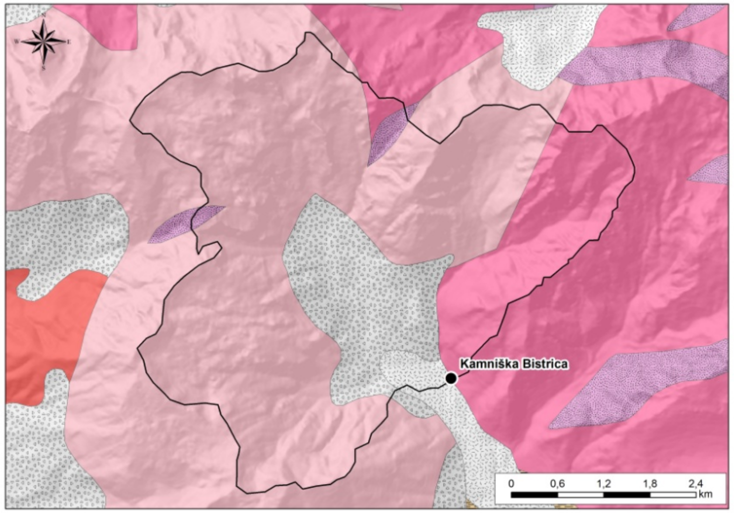

Sampling location Kamniška Bistrica (Geological classification)

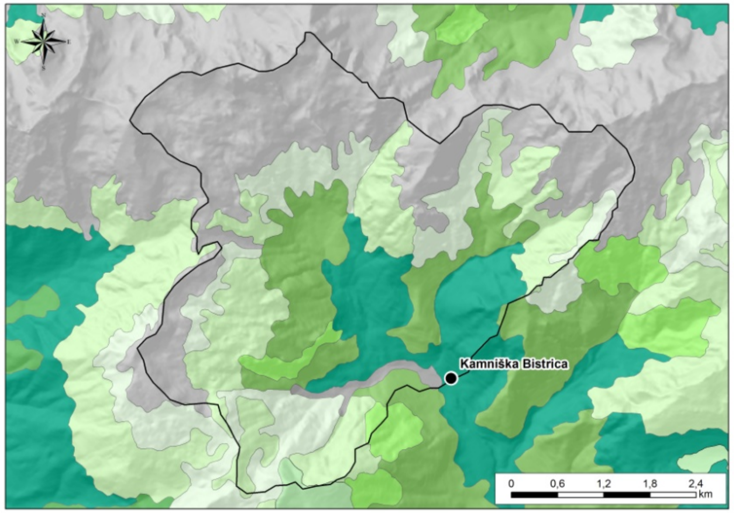

Sampling location Kamniška Bistrica (CLC classification)

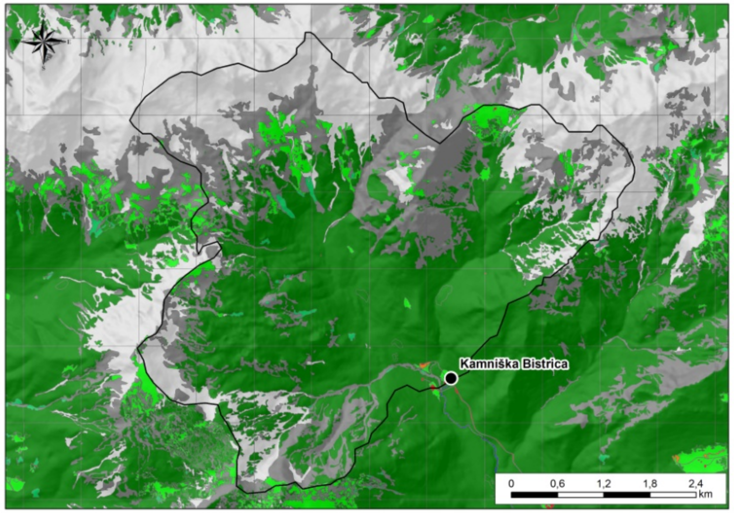

Sampling location Kamniška Bistrica (Land use classification)

Korentan

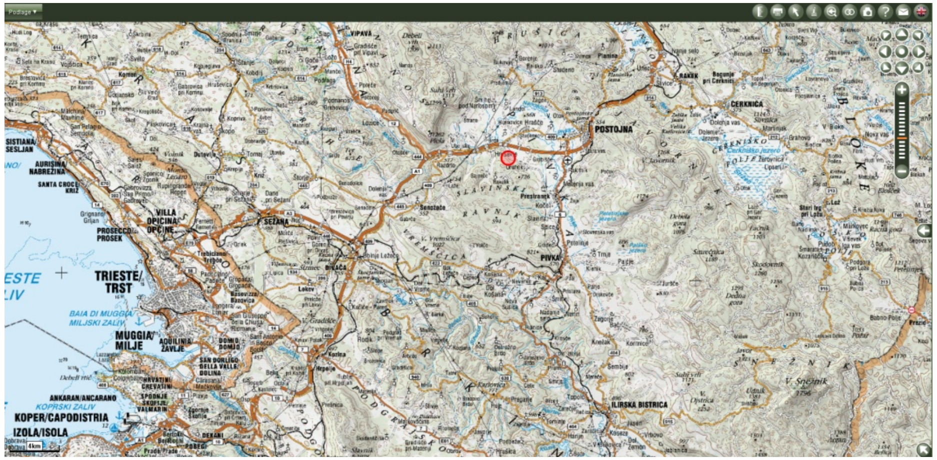

Sampling location Korentan

Sampling location Korentan

Sampling location Korentan

Sampling location Korentan

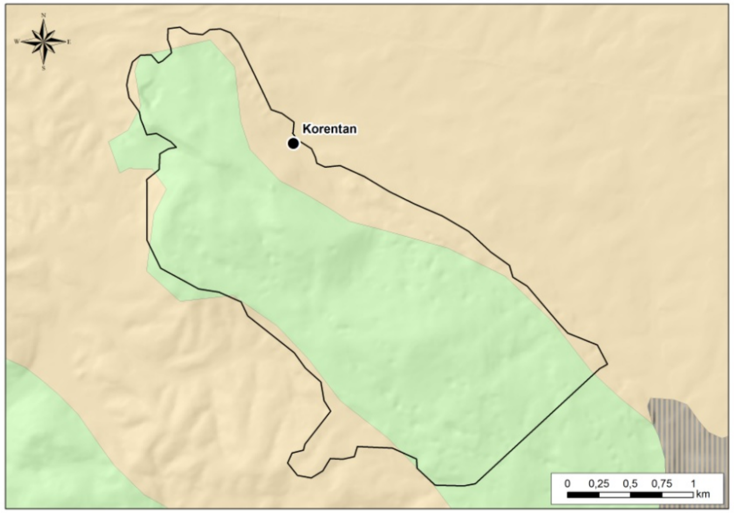

Sampling location Korentan (IAH classification)

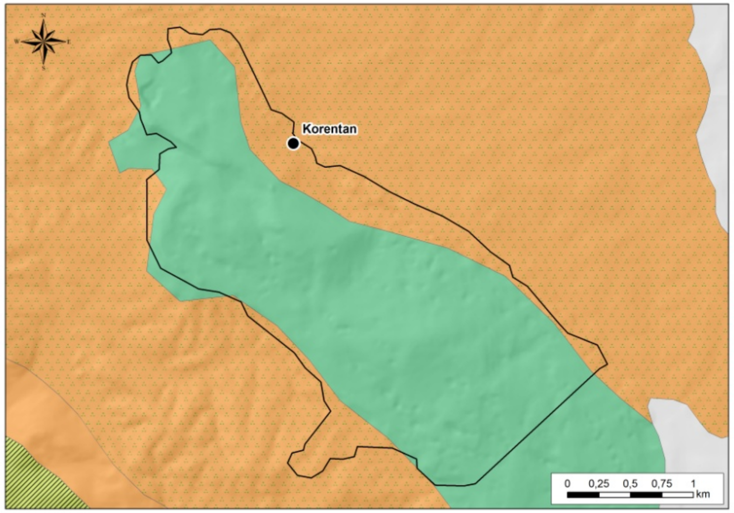

Sampling location Korentan (Geological classification)

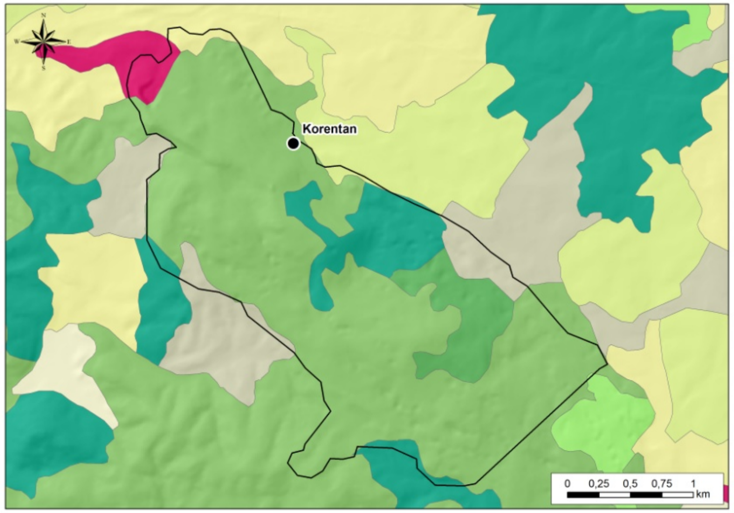

Sampling location Korentan (CLC classification)

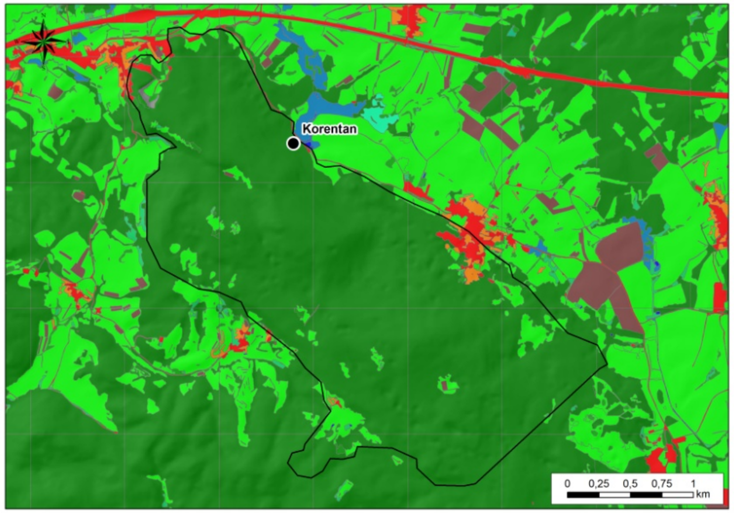

Sampling location Korentan (Land use classification)

Krajcarica

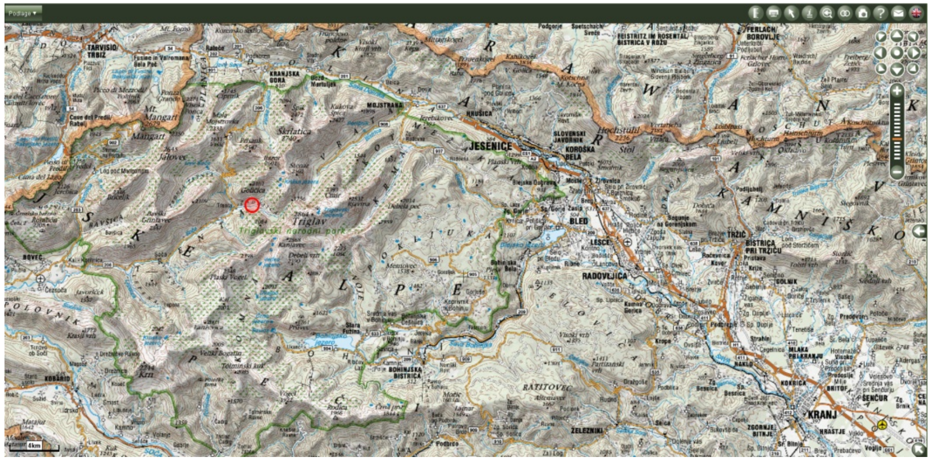

Sampling location Krajcarica

Sampling location Krajcarica

Sampling location Krajcarica

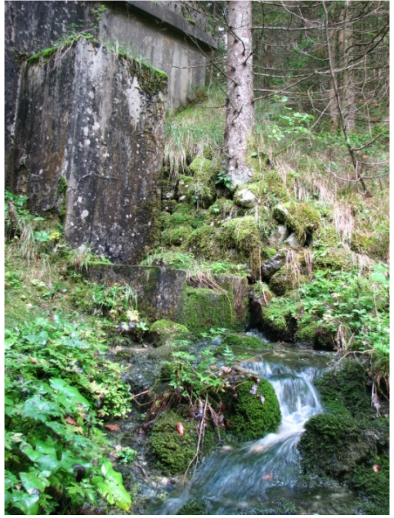

Sampling location Krajcarica

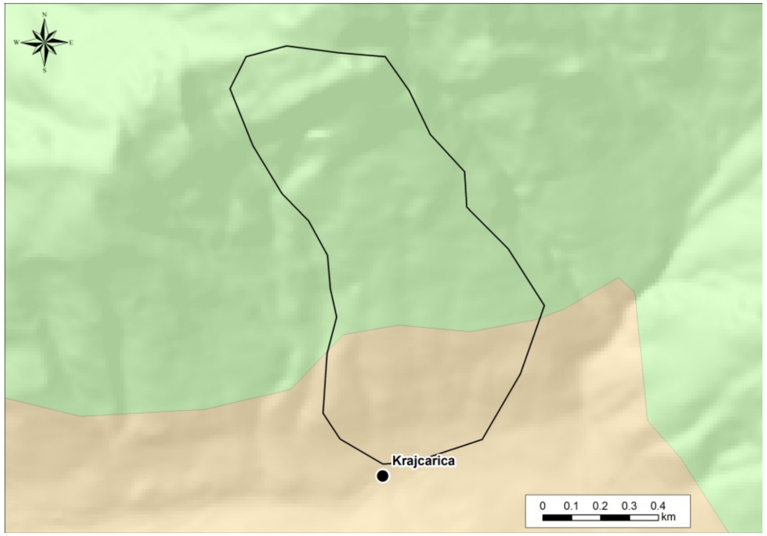

Sampling location Krajcarica (IAH classification)

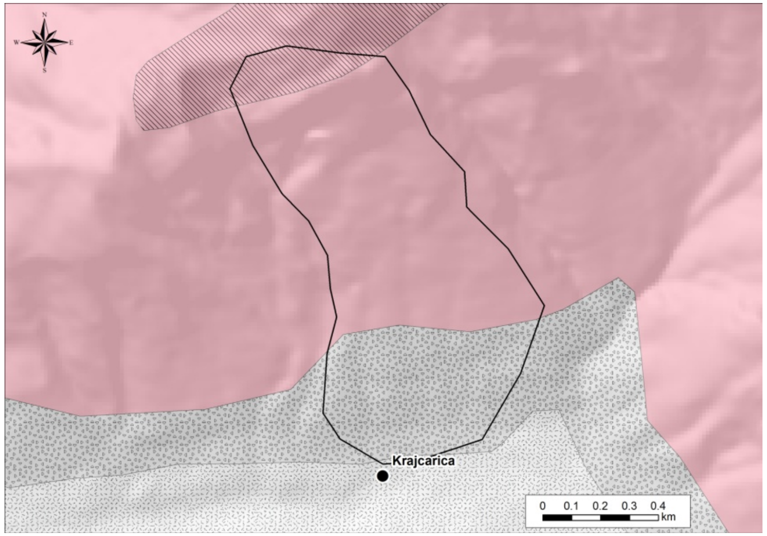

Sampling location Krajcarica (Geological classification)

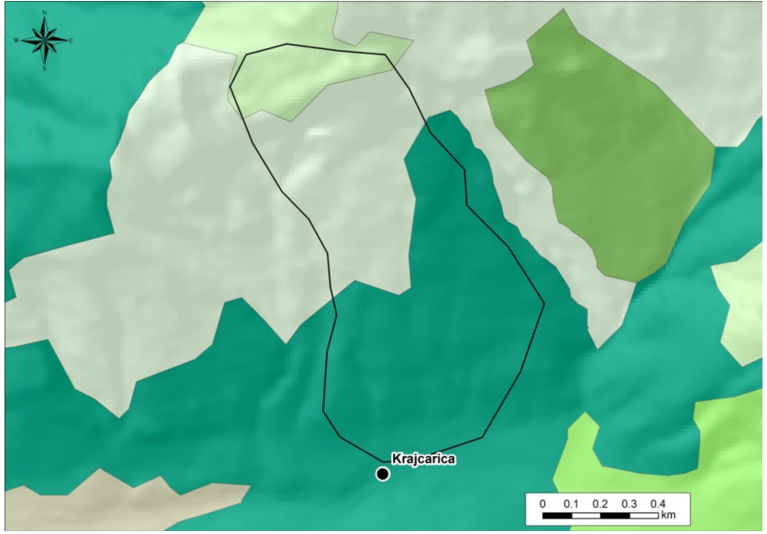

Sampling location Krajcarica (CLC classification)

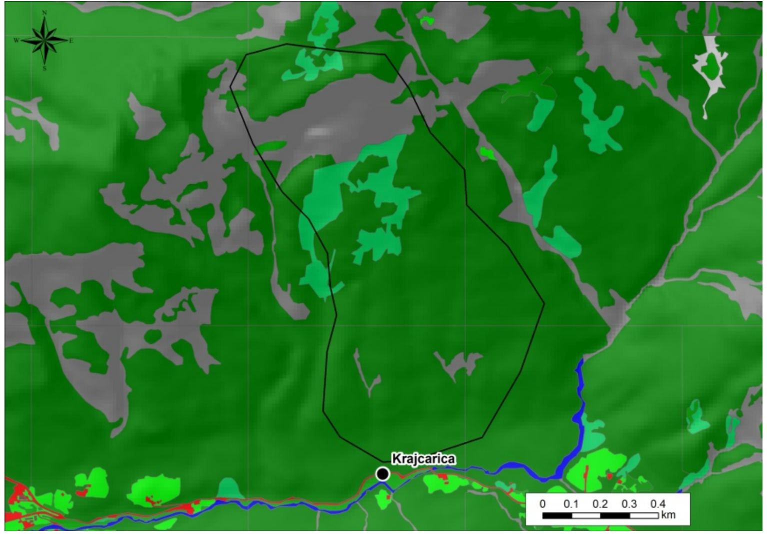

Sampling location Krajcarica (Land use classification)

Krka

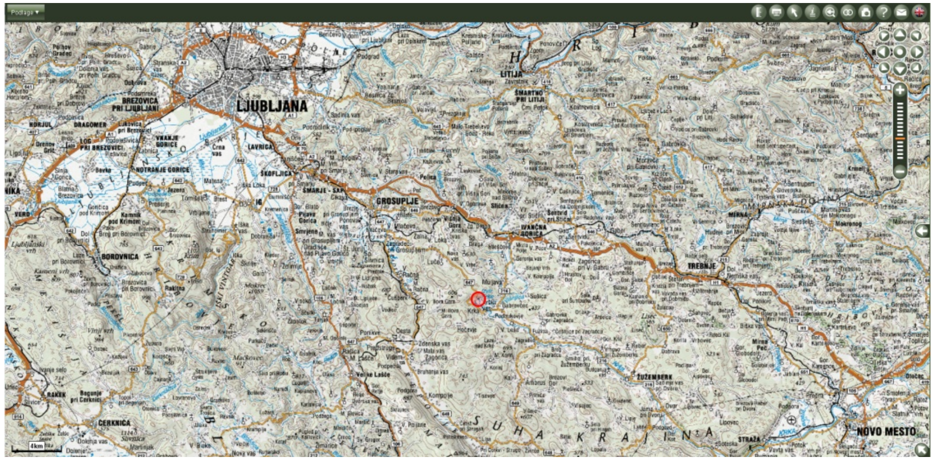

Sampling location Krka

Sampling location Krka

Sampling location Krka

Sampling location Krka

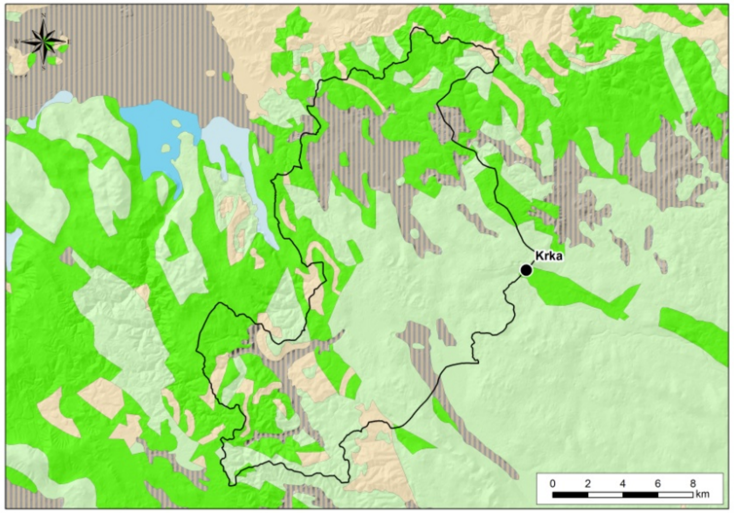

Sampling location Krka (IAH classification)

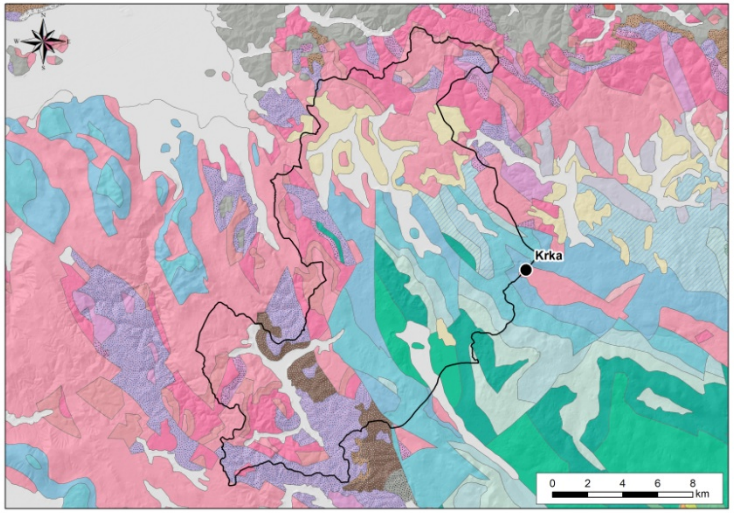

Sampling location Krka (Geological classification)

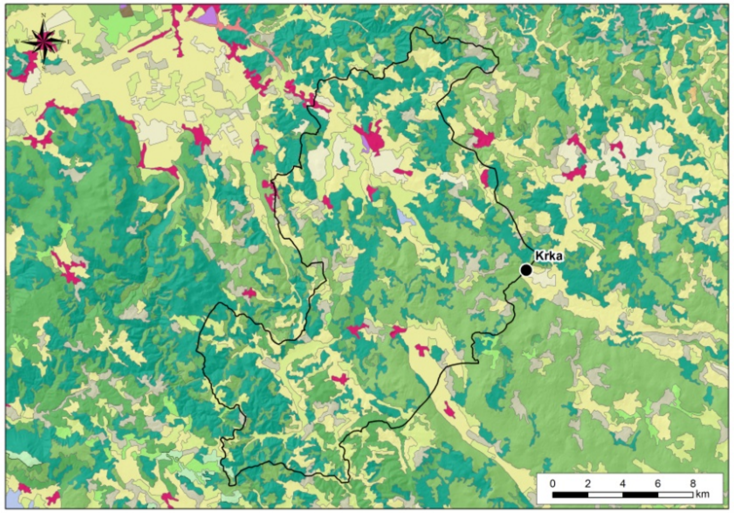

Sampling location Krka (CLC classification)

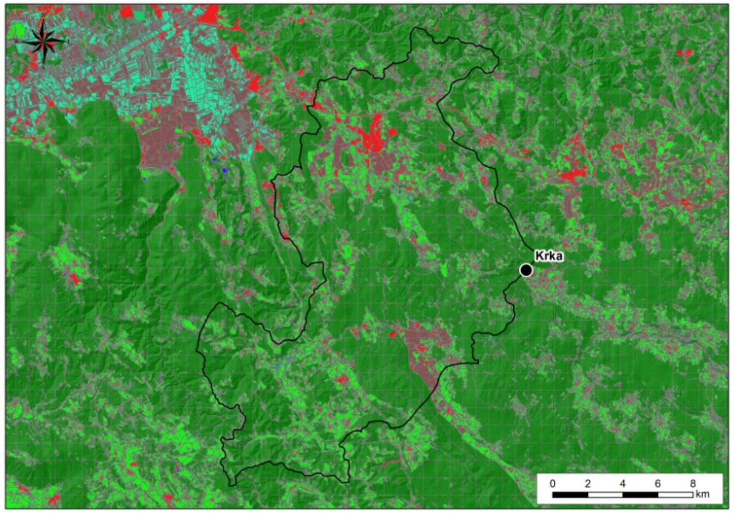

Sampling location Krka (Land use classification)

Kropa

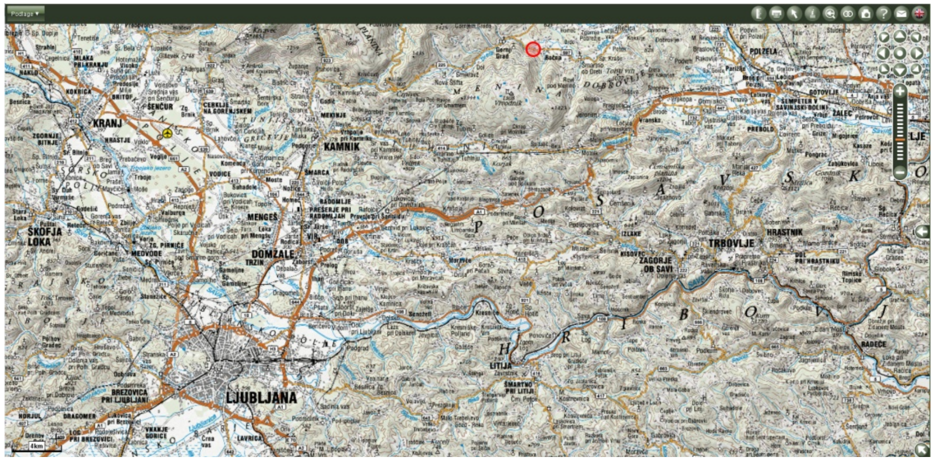

Sampling location Kropa

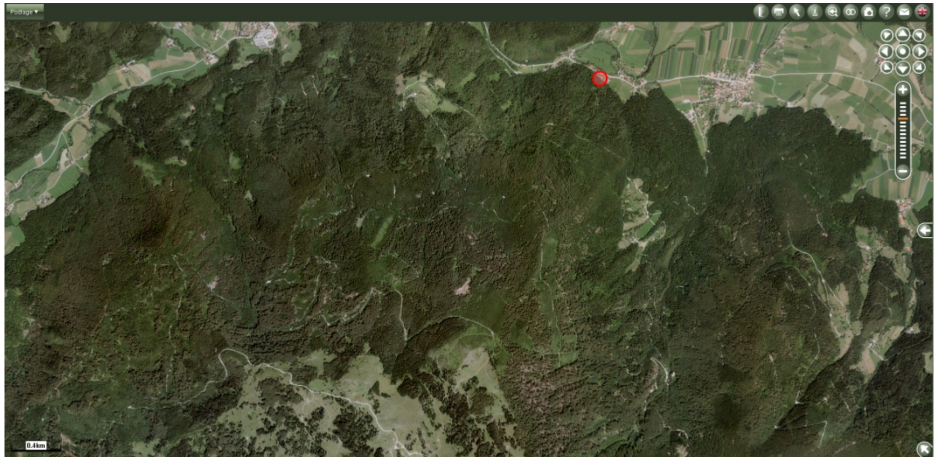

Sampling location Kropa

Sampling location Kropa

Sampling location Kropa

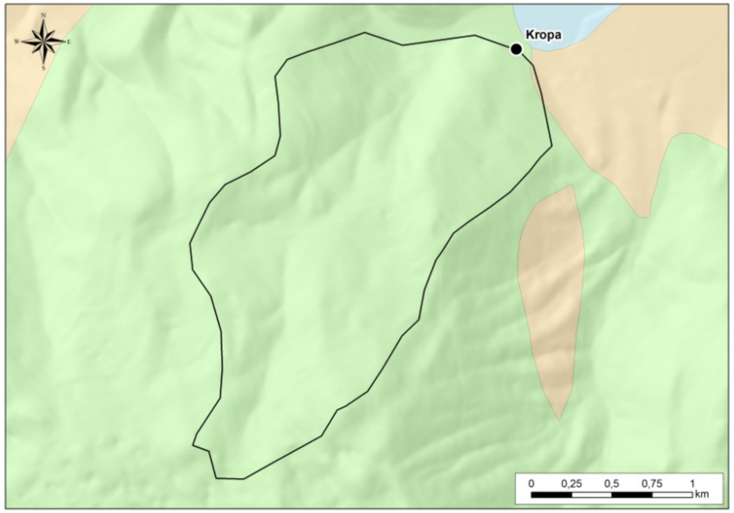

Sampling location Kropa (IAH classification)

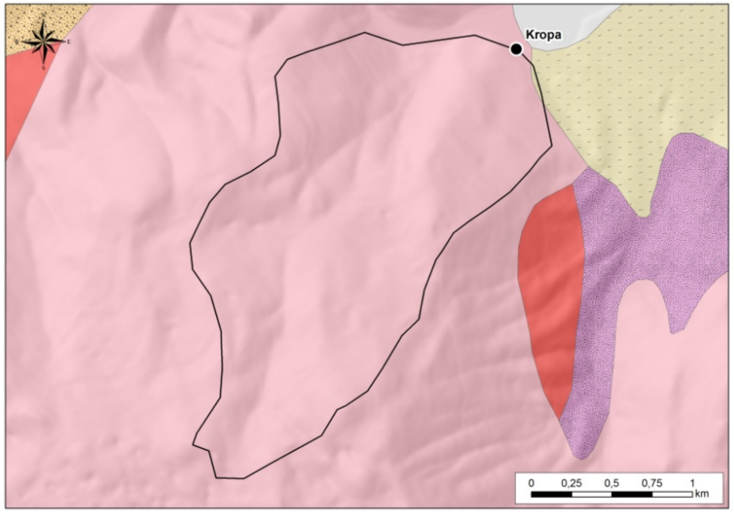

Sampling location Kropa (Geological classification)

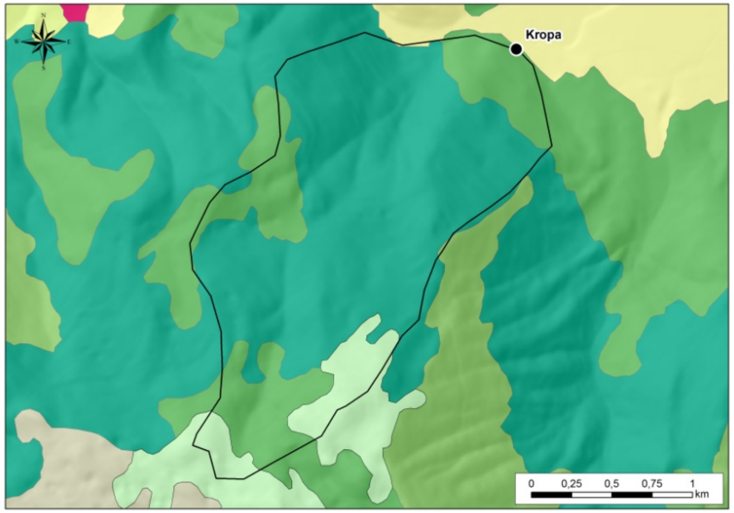

Sampling location Kropa (CLC classification)

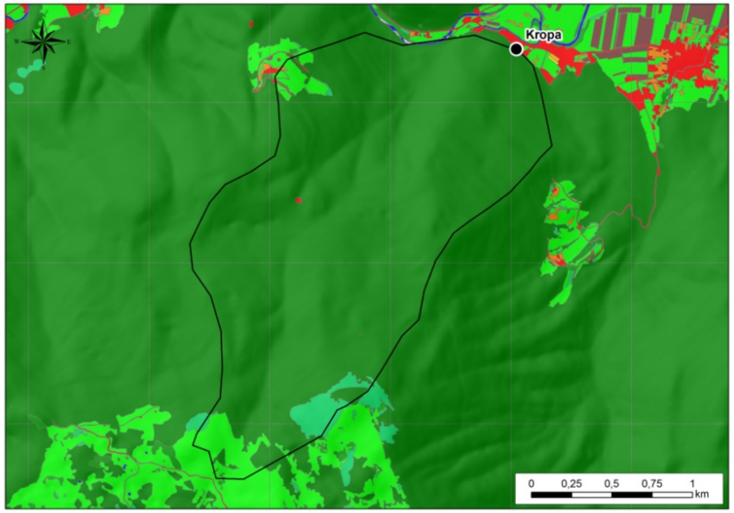

Sampling location Kropa (Land use classification)

Krupa

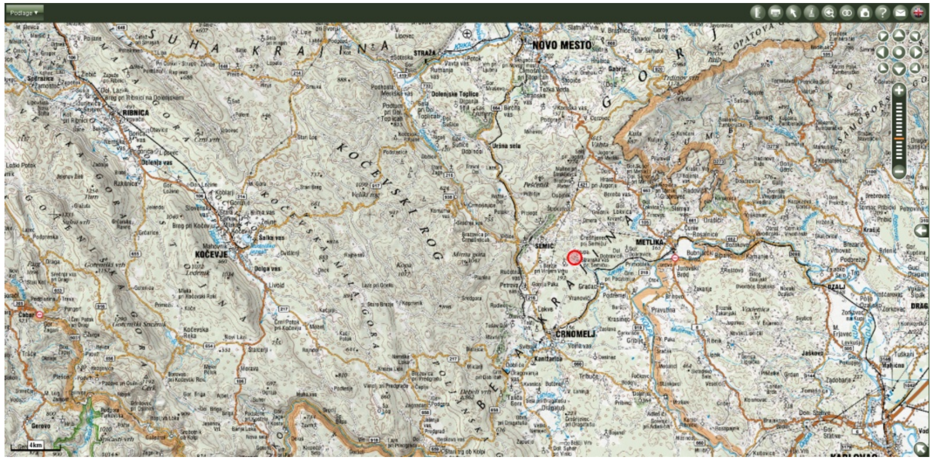

Sampling location Krupa

Sampling location Krupa

Sampling location Krupa

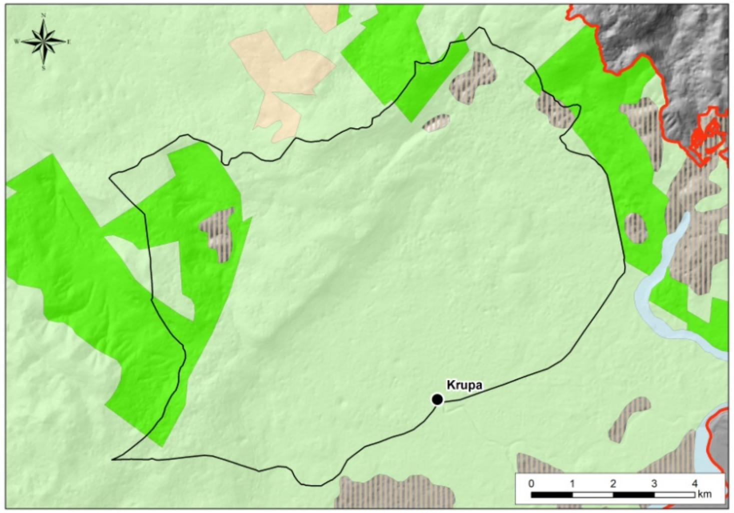

Sampling location Krupa (IAH classification)

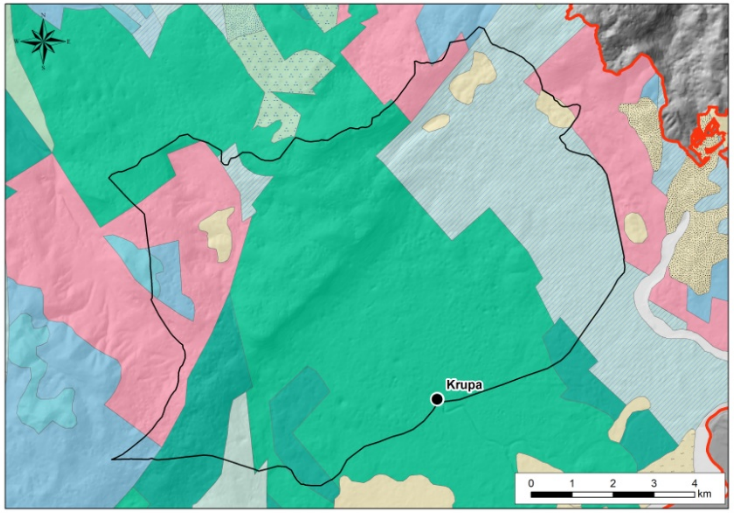

Sampling location Krupa (Geological classification)

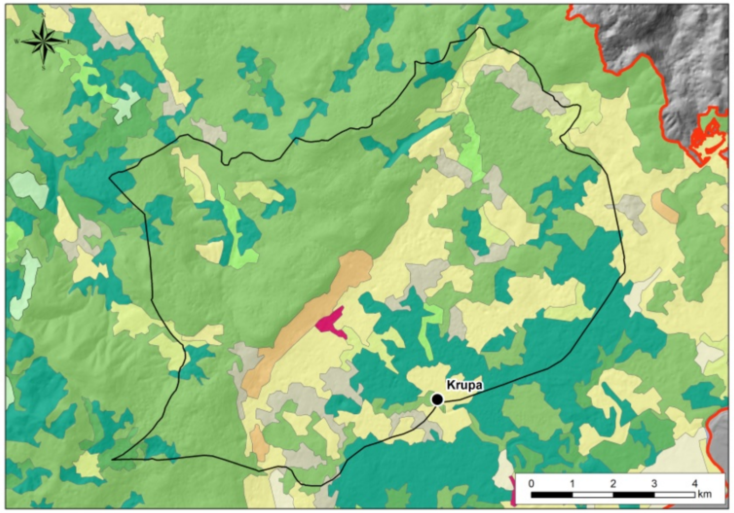

Sampling location Krupa (CLC classification)

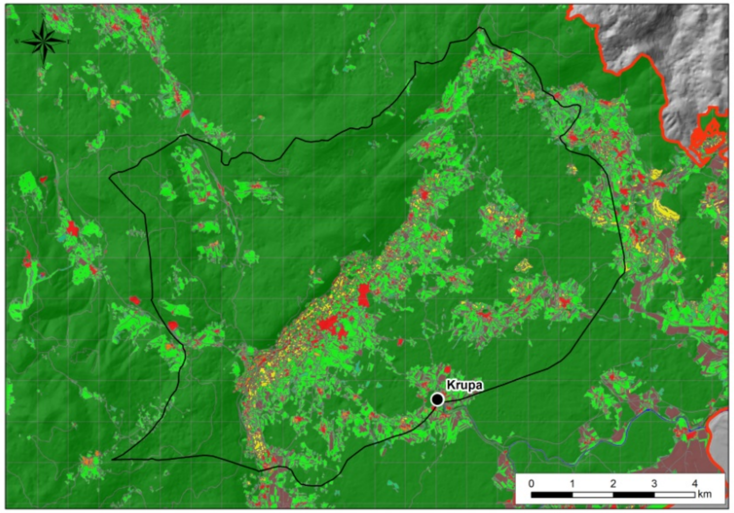

Sampling location Krupa (Land use classification)

Lipnica

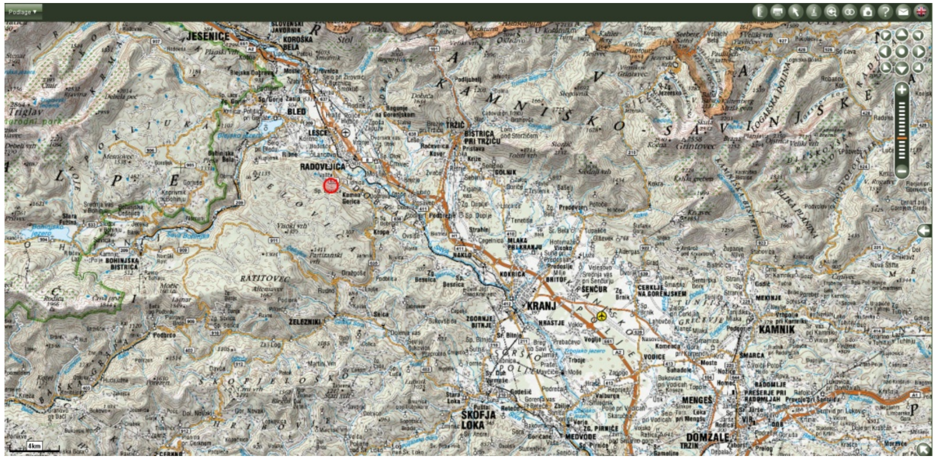

Sampling location Lipnica

Sampling location Lipnica

Sampling location Lipnica

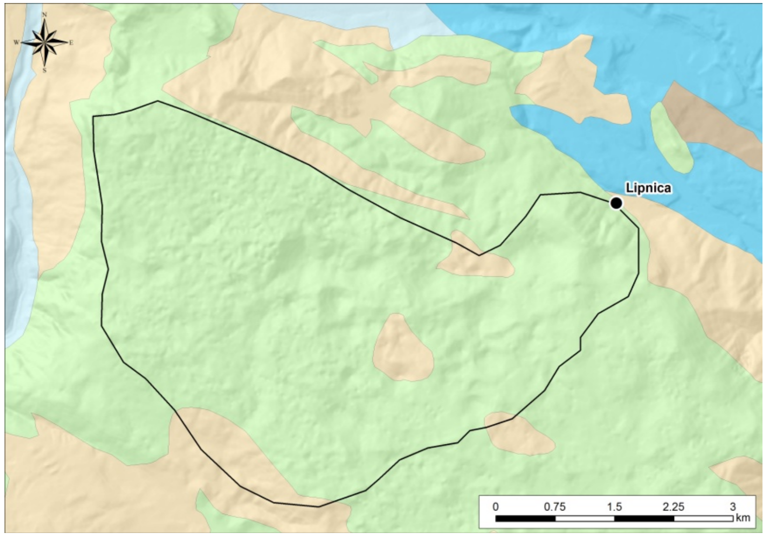

Sampling location Lipnica (IAH classification)

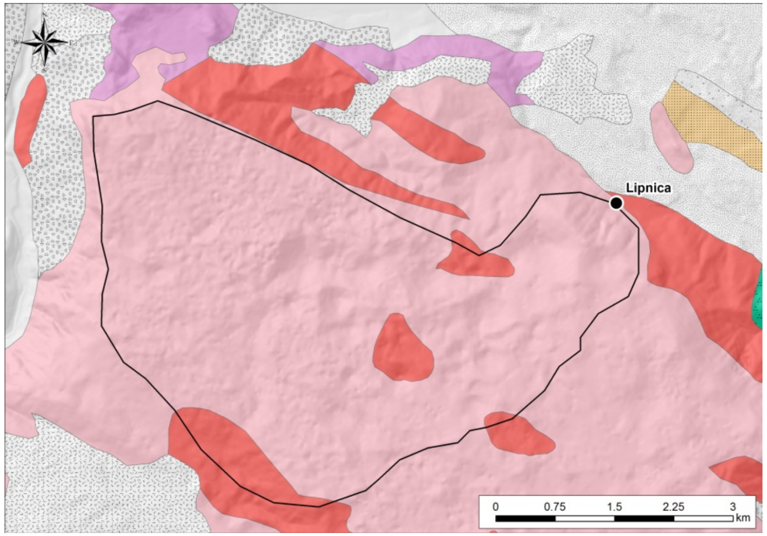

Sampling location Lipnica (Geological classification)

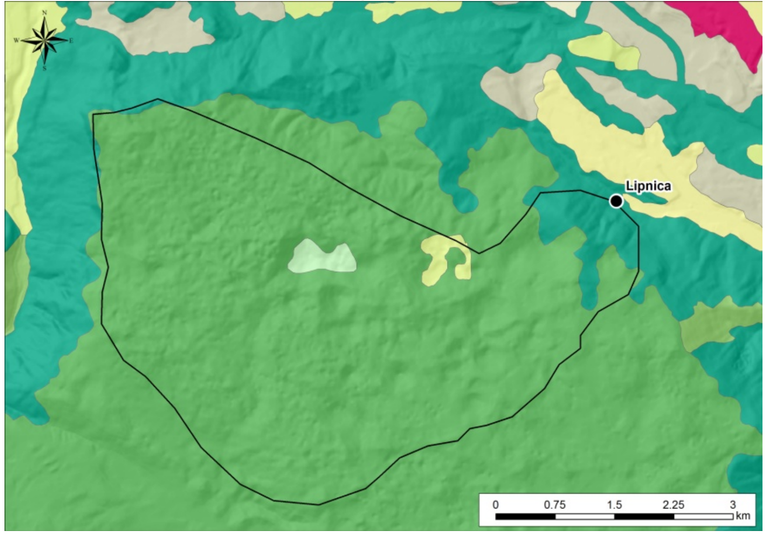

Sampling location Lipnica (CLC classification)

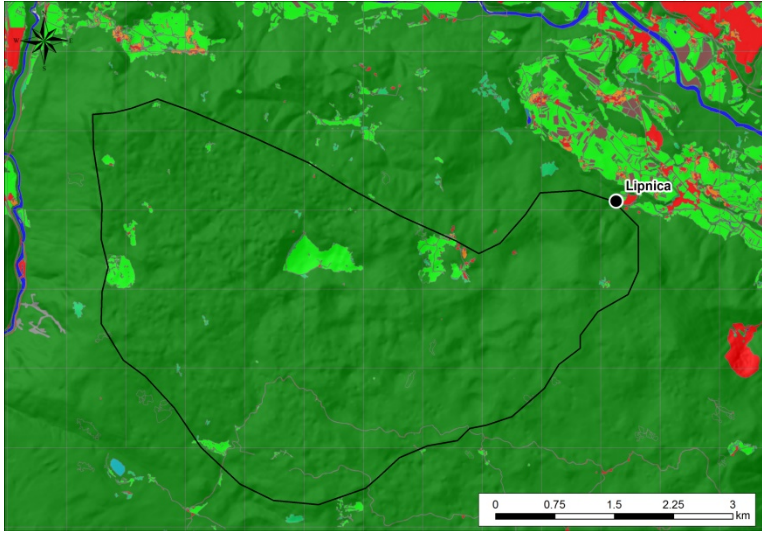

Sampling location Lipnica (Land use classification)

Lipnik

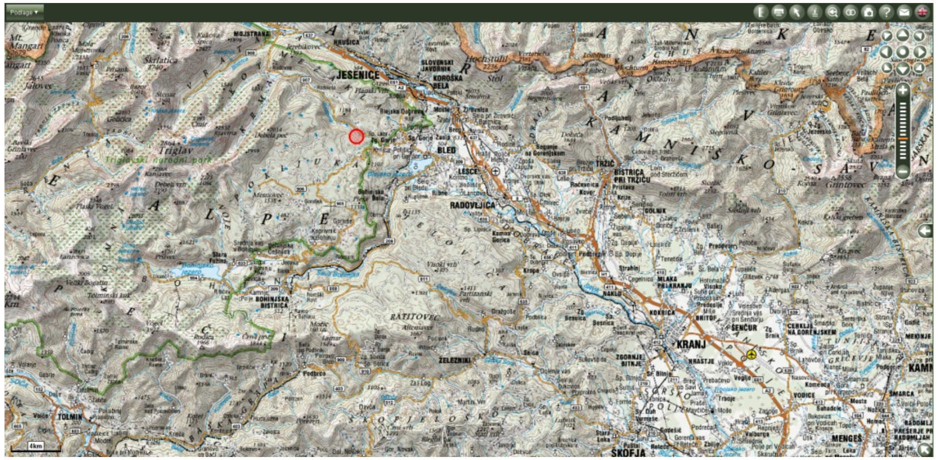

Sampling location Lipnik

Sampling location Lipnik

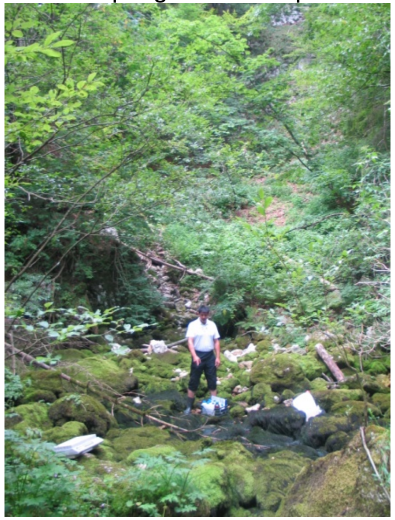

Sampling location Lipnik

Sampling location Lipnik

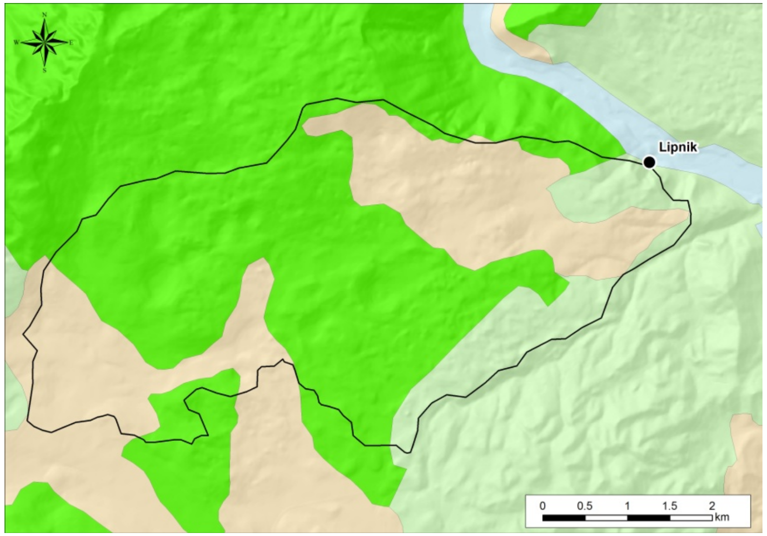

Sampling location Lipnik (IAH classification)

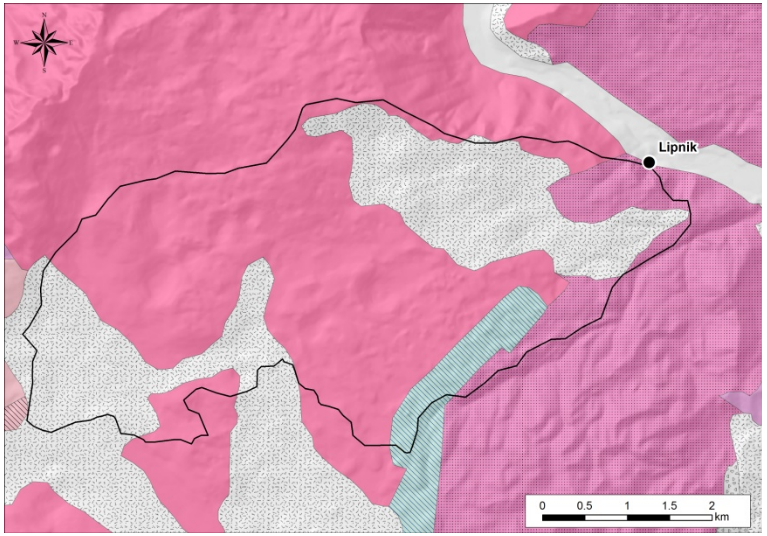

Sampling location Lipnik (Geological classification)

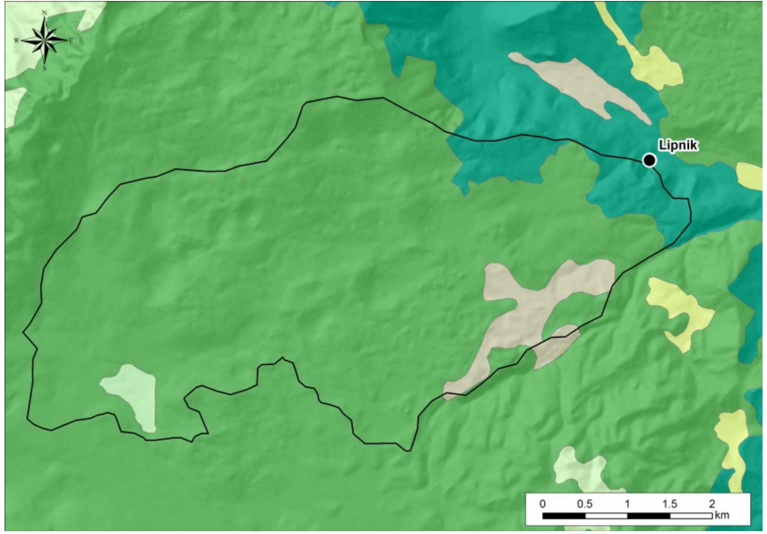

Sampling location Lipnik (CLC classification)

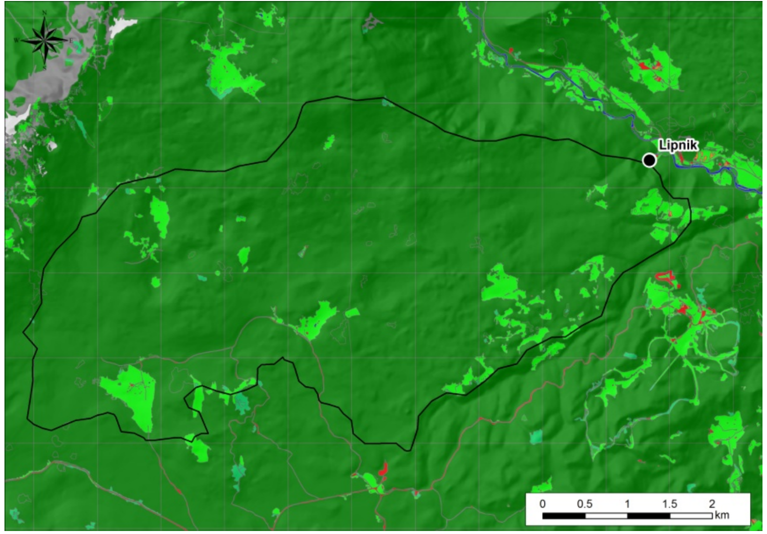

Sampling location Lipnik (Land use classification)

LMV-1, Ljubljana

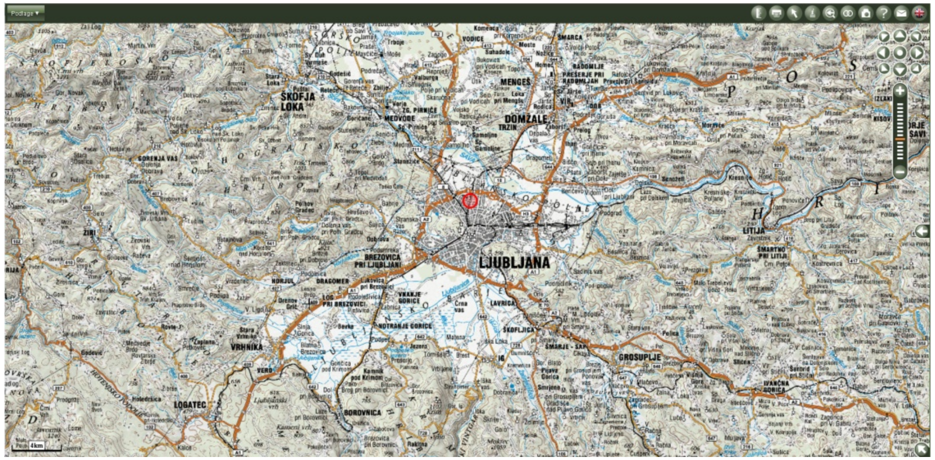

Sampling location LMV-1, Ljubljana

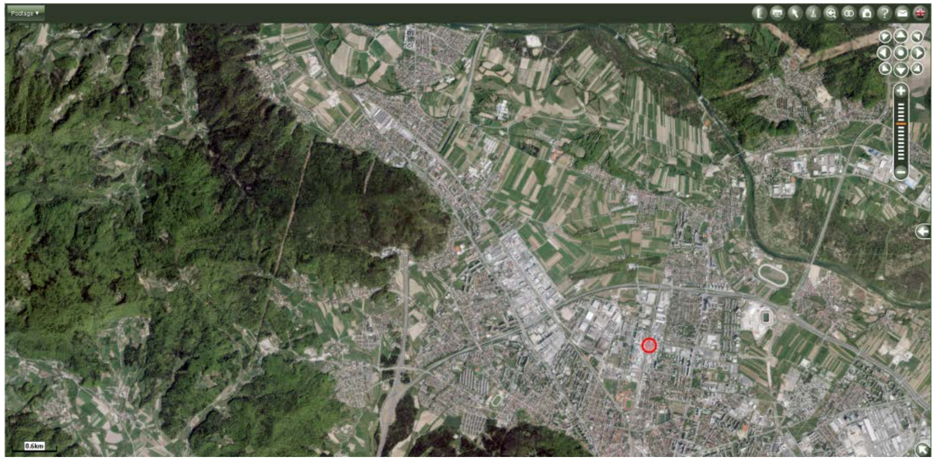

Sampling location LMV-1, Ljubljana

Sampling location LMV-1, Ljubljana

Sampling location LMV-1, Ljubljana

Sampling location LMV-1, Ljubljana (IAH classification)

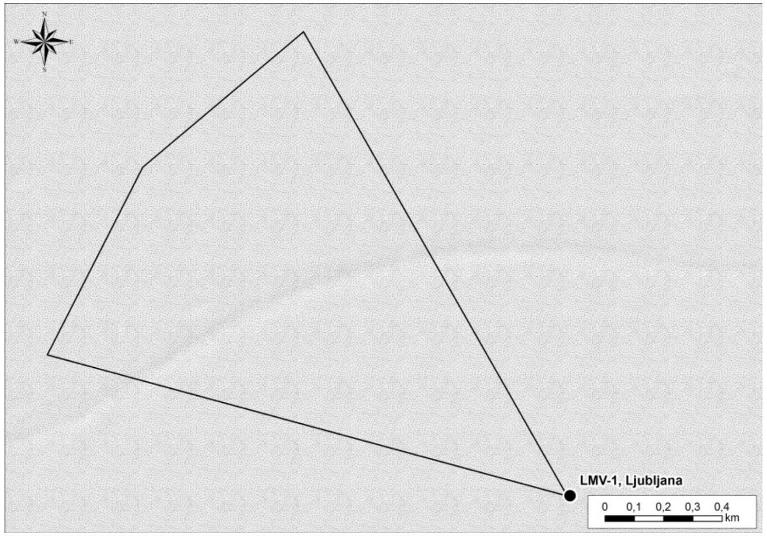

Sampling location LMV-1, Ljubljana (Geological classification)

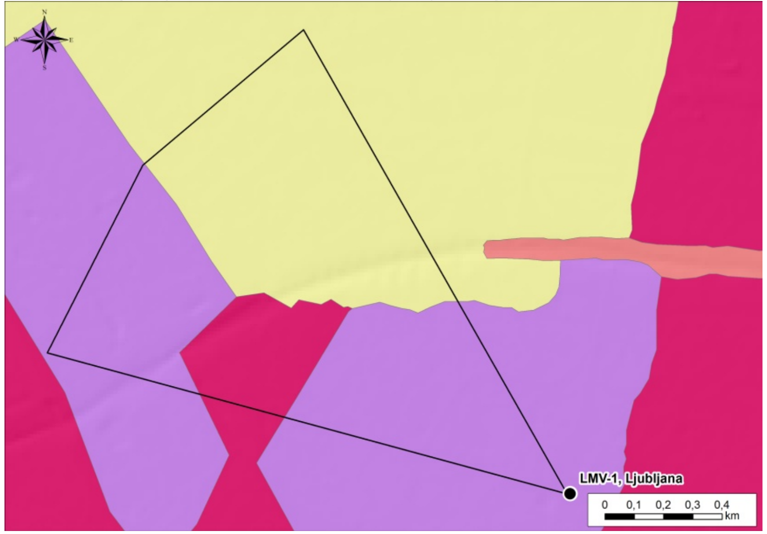

Sampling location LMV-1, Ljubljana (CLC classification)

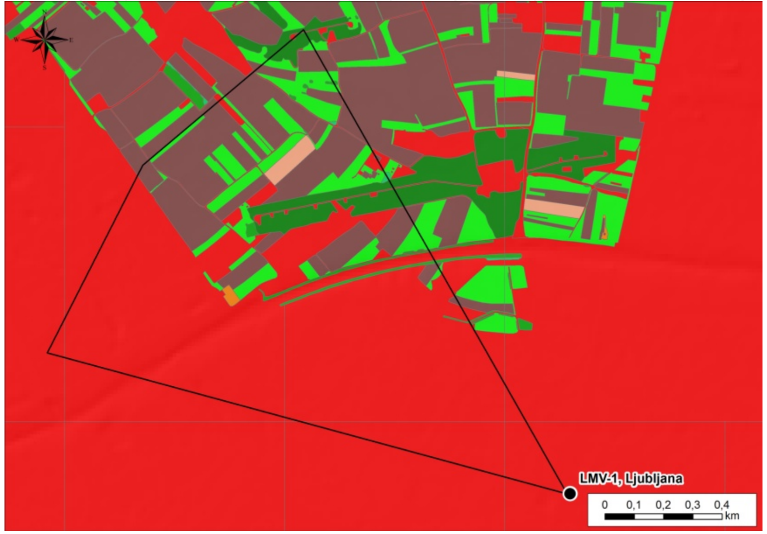

Sampling location LMV-1, Ljubljana (Land use classification)

Lučnica

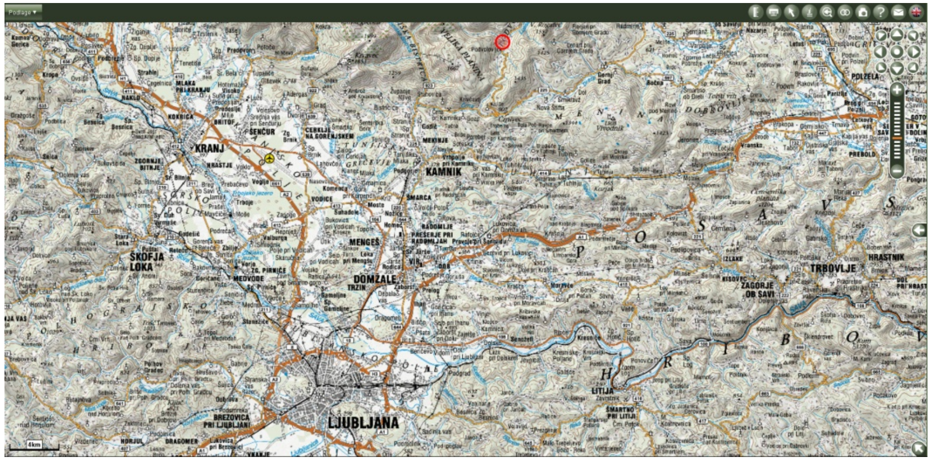

Sampling location Lučnica

Sampling location Lučnica

Sampling location Lučnica

Sampling location Lučnica

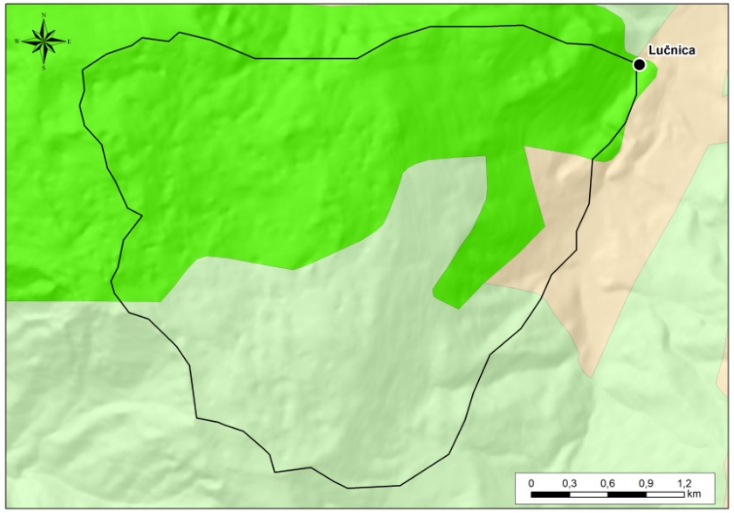

Sampling location Lučnica (IAH classification)

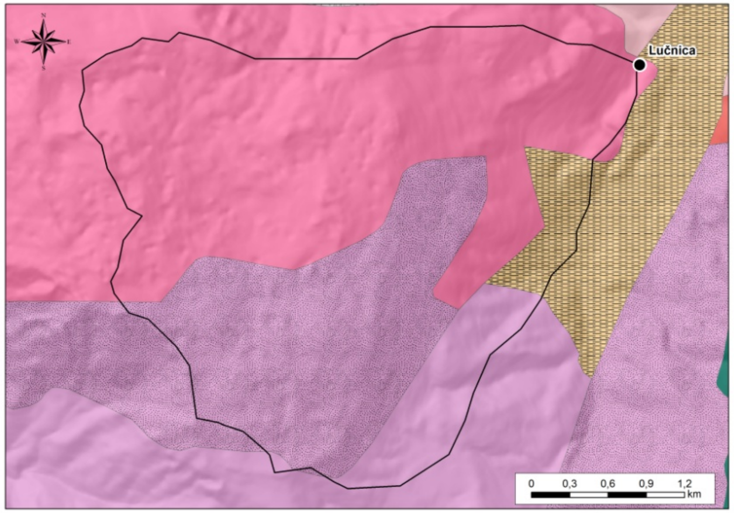

Sampling location Lučnica (Geological classification)

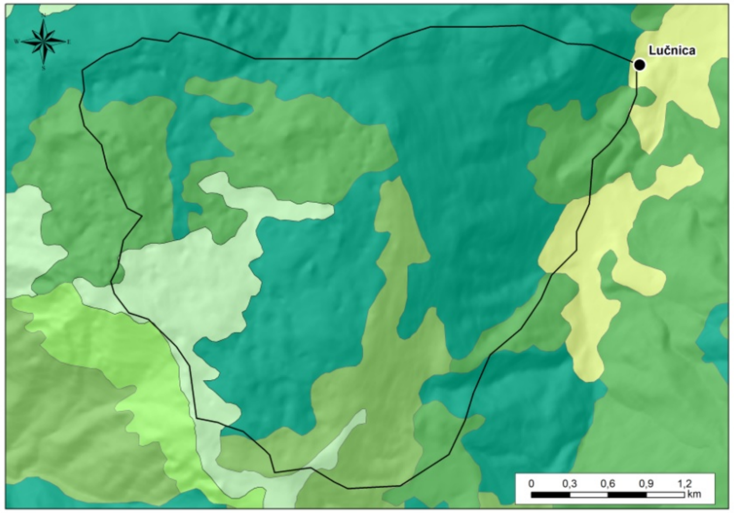

Sampling location Lučnica (CLC classification)

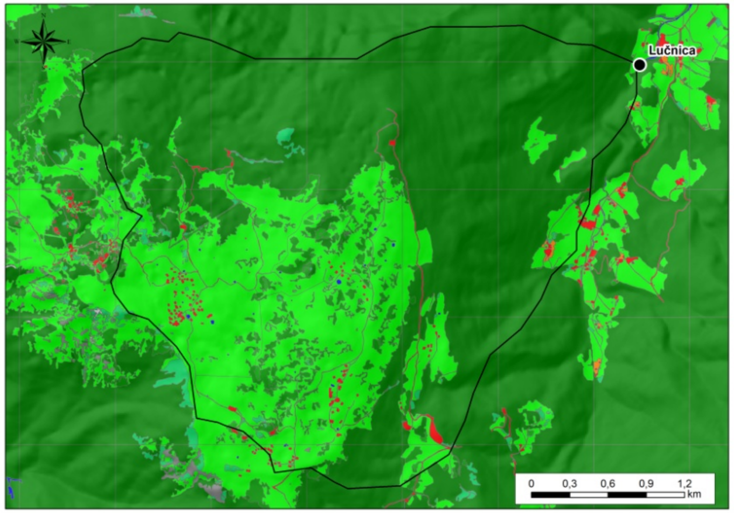

Sampling location Lučnica (Land use classification)

Malenščica

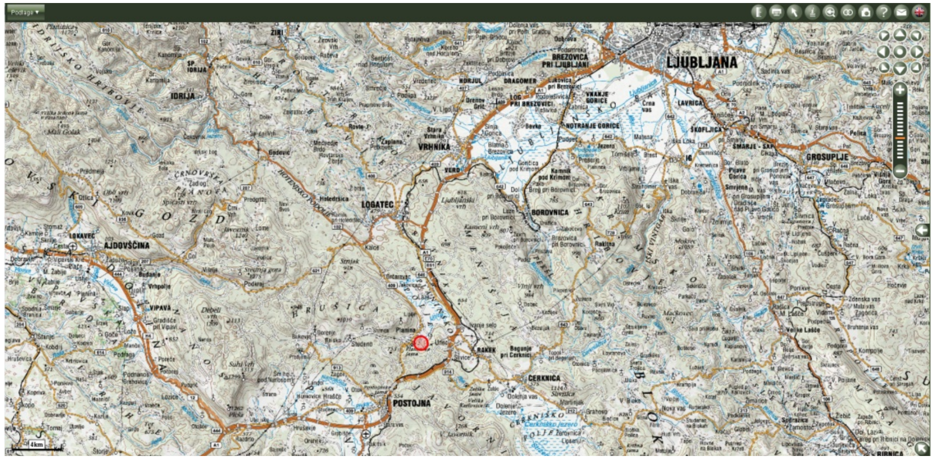

Sampling location Malenščica

Sampling location Malenščica

Sampling location Malenščica

Sampling location Malenščica

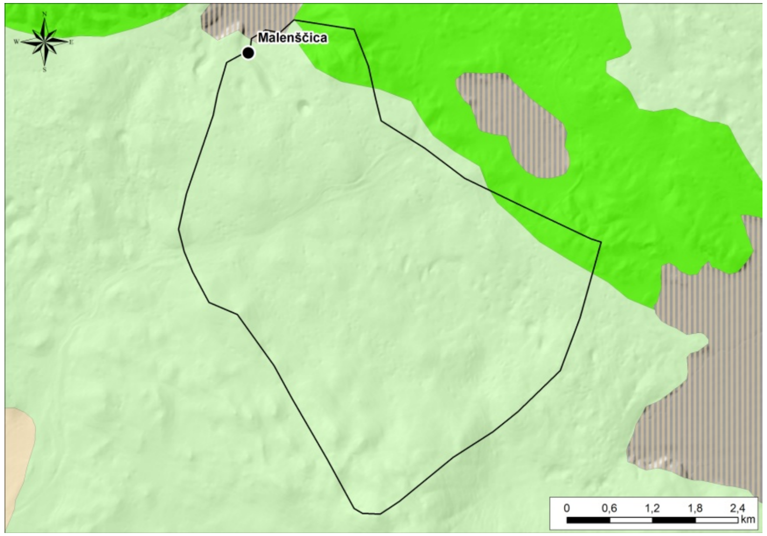

Sampling location Malenščica (IAH classification)

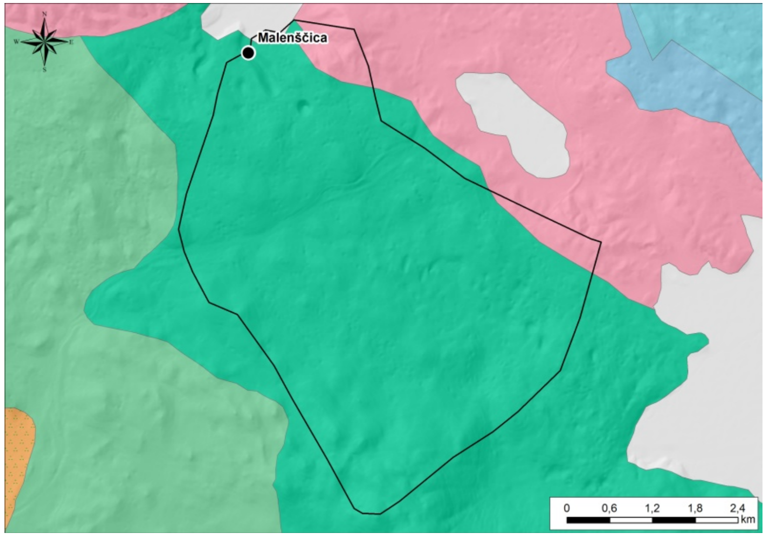

Sampling location Malenščica (Geological classification)

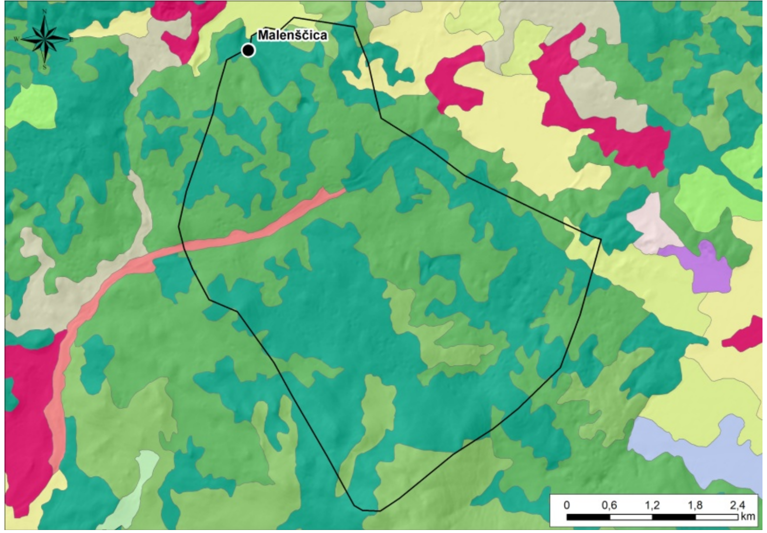

Sampling location Malenščica (CLC classification)

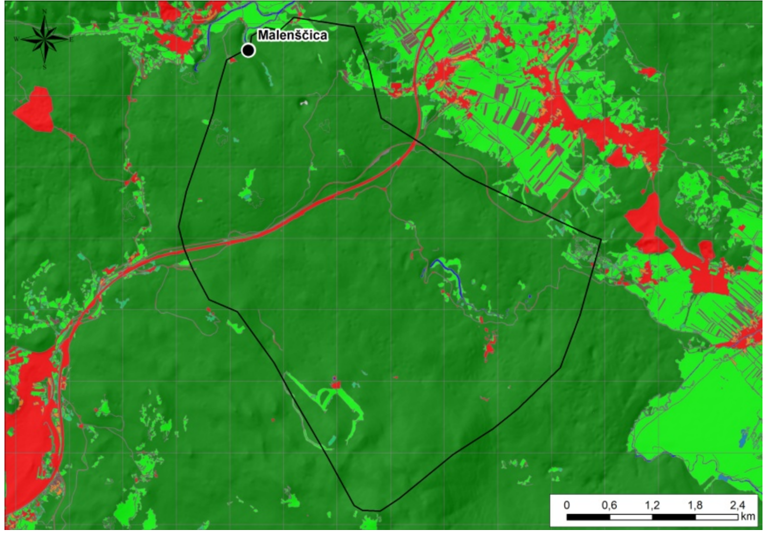

Sampling location Malenščica (Land use classification)

Mali Obrh

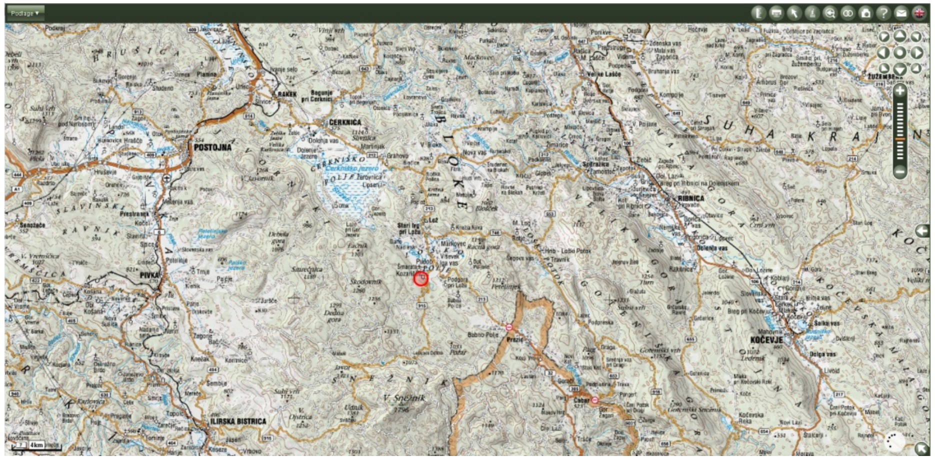

Sampling location Mali Obrh

Sampling location Mali Obrh

Sampling location Mali Obrh

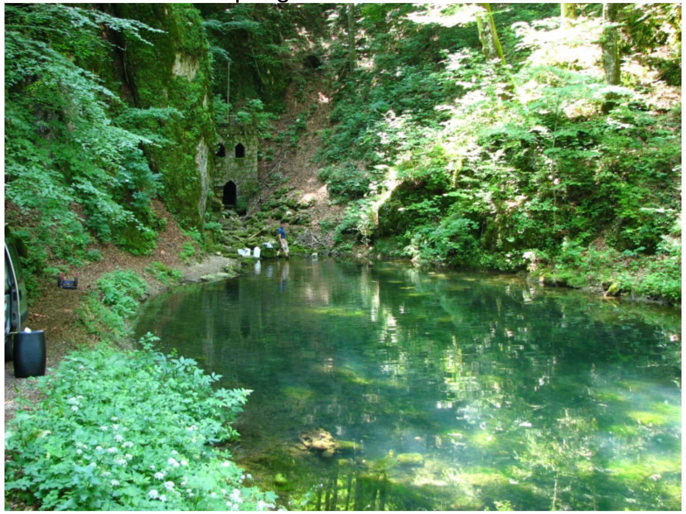

Sampling location Mali Obrh

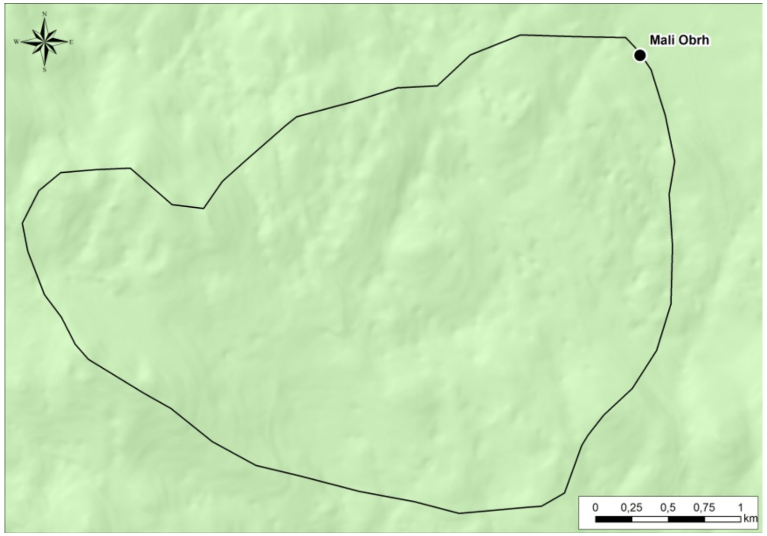

Sampling location Mali Obrh (IAH classification)

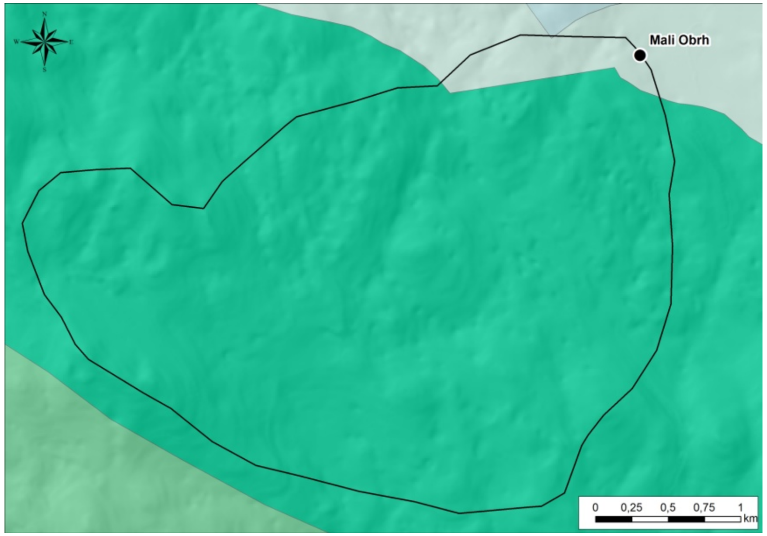

Sampling location Mali Obrh (Geological classification)

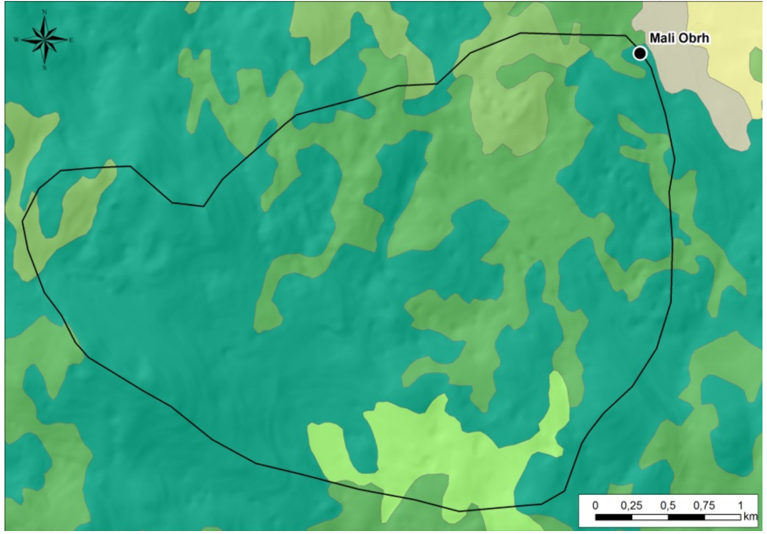

Sampling location Mali Obrh (CLC classification)

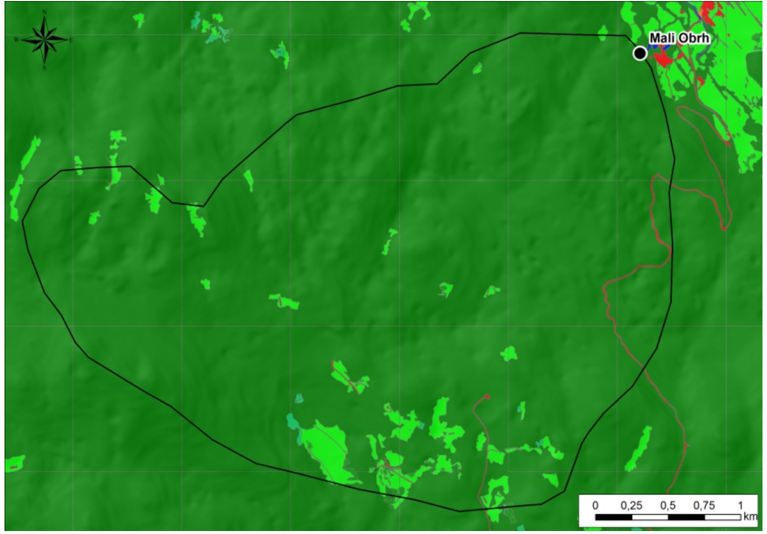

Sampling location Mali Obrh (Land use classification)

Maver

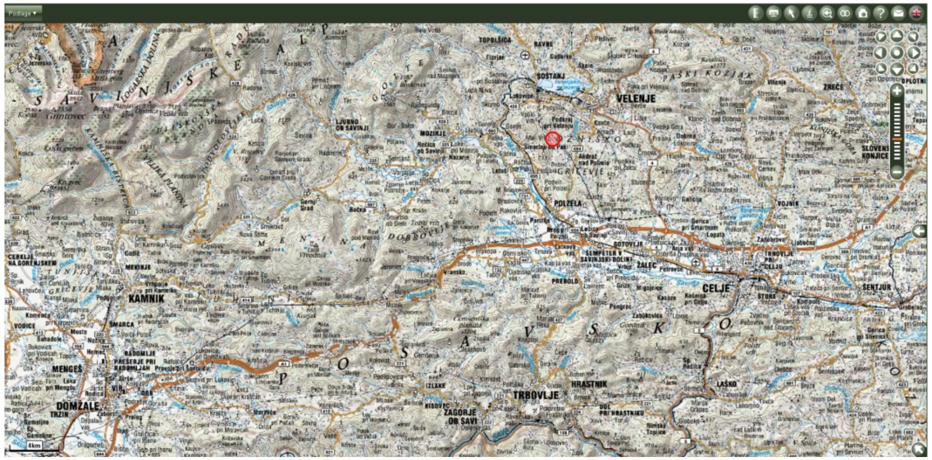

Sampling location Maver

Sampling location Maver

Sampling location Maver

Sampling location Maver

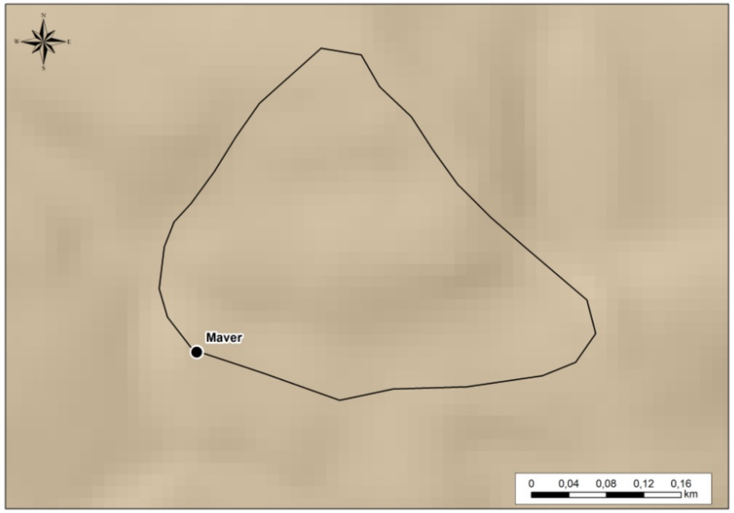

Sampling location Maver (IAH classification)

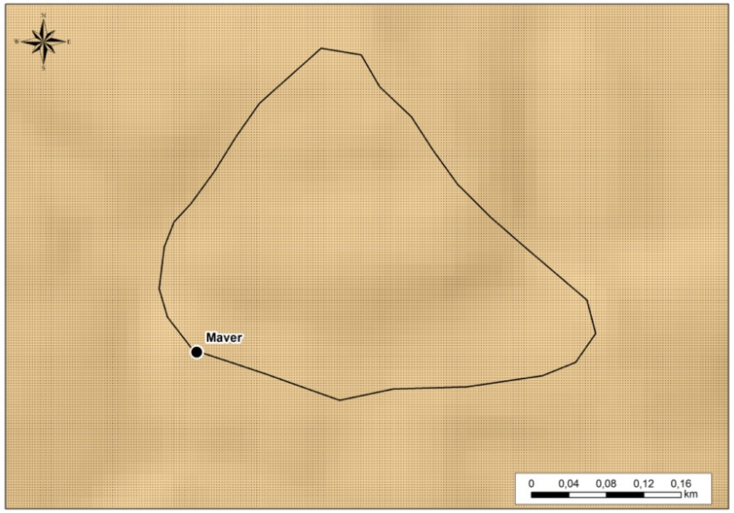

Sampling location Maver (Geological classification)

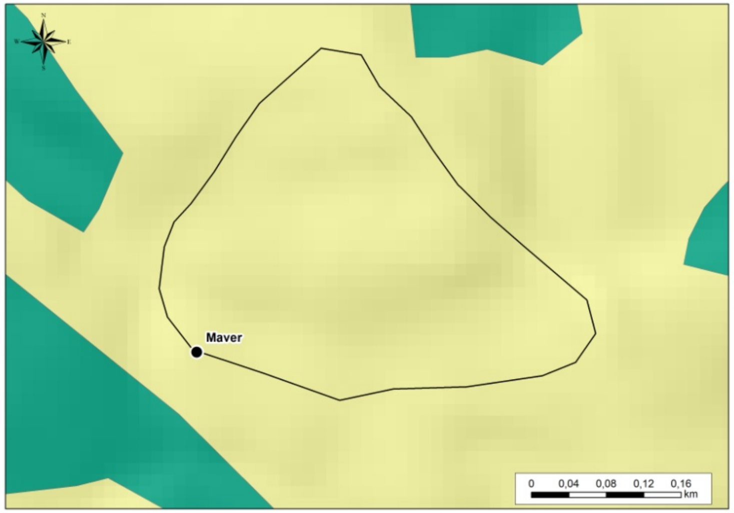

Sampling location Maver (CLC classification)

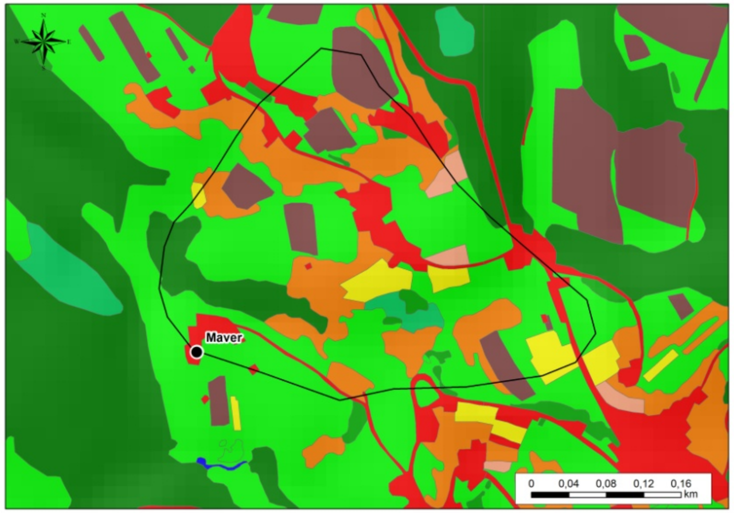

Sampling location Maver (Land use classification)

Mazej

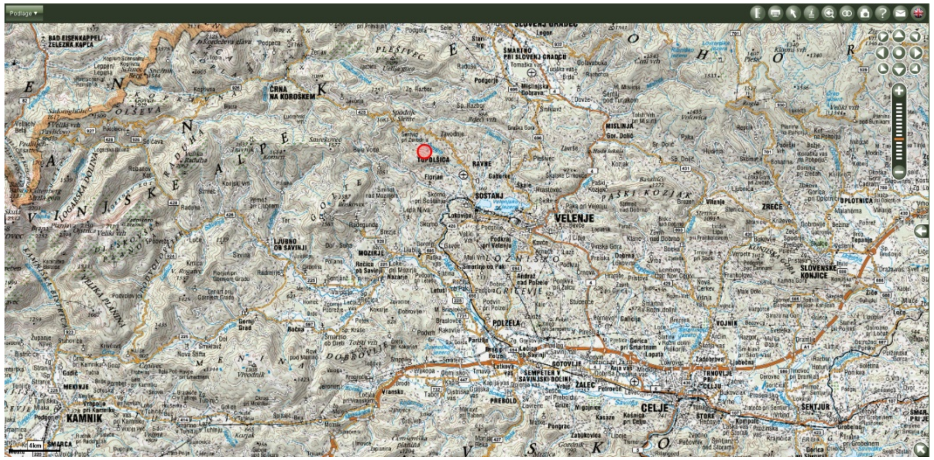

Sampling location Mazej

Sampling location Mazej

Sampling location Mazej

Sampling location Mazej

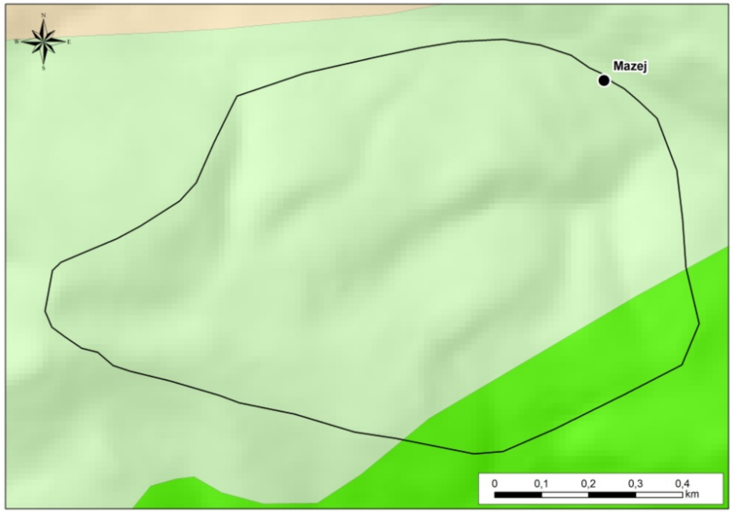

Sampling location Mazej (IAH classification)

Sampling location Mazej (Geological classification)

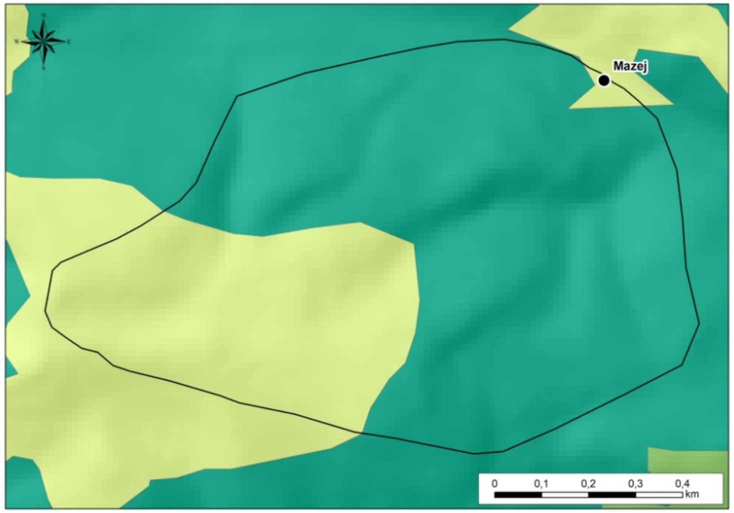

Sampling location Mazej (CLC classification)

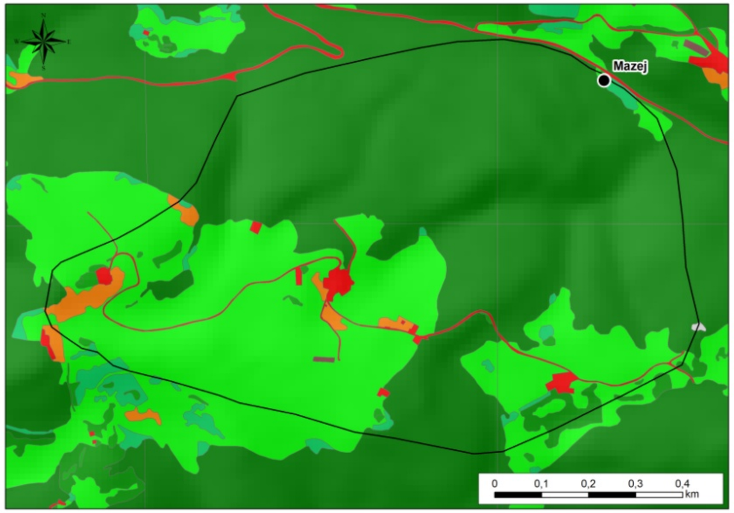

Sampling location Mazej (Land use classification)

Metliški Obrh

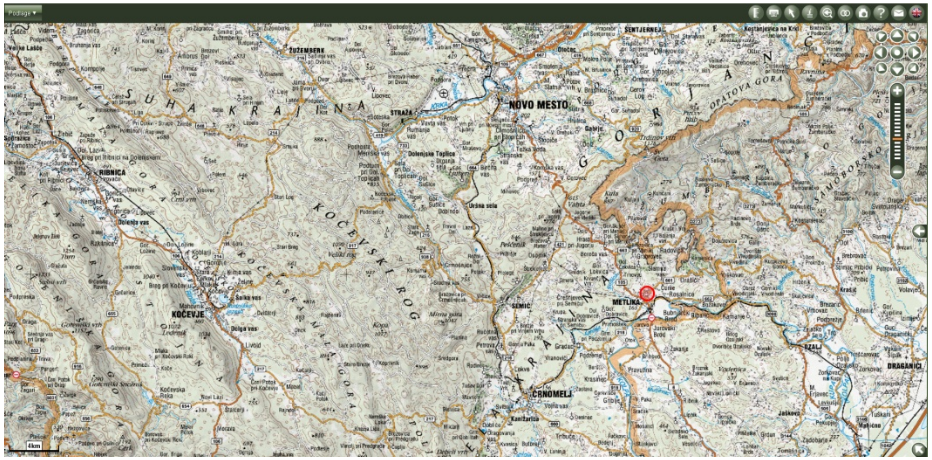

Sampling location Metliški Obrh

Sampling location Metliški Obrh

Sampling location Metliški Obrh

Sampling location Metliški Obrh

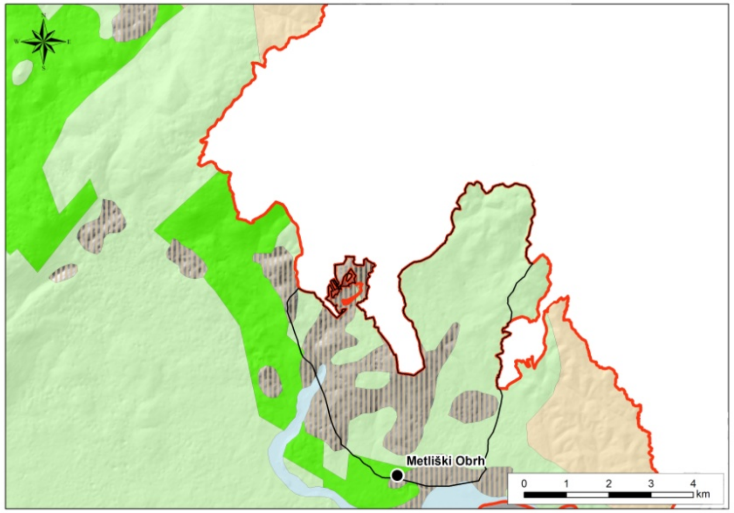

Sampling location Metliški Obrh (IAH classification)

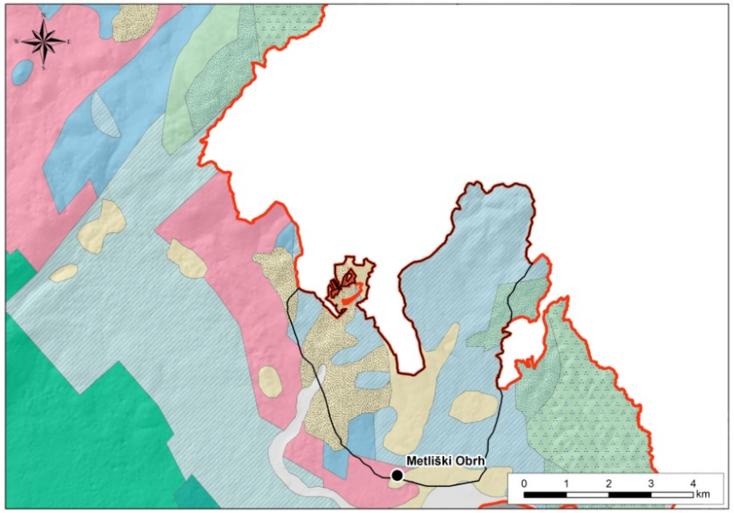

Sampling location Metliški Obrh (Geological classification)

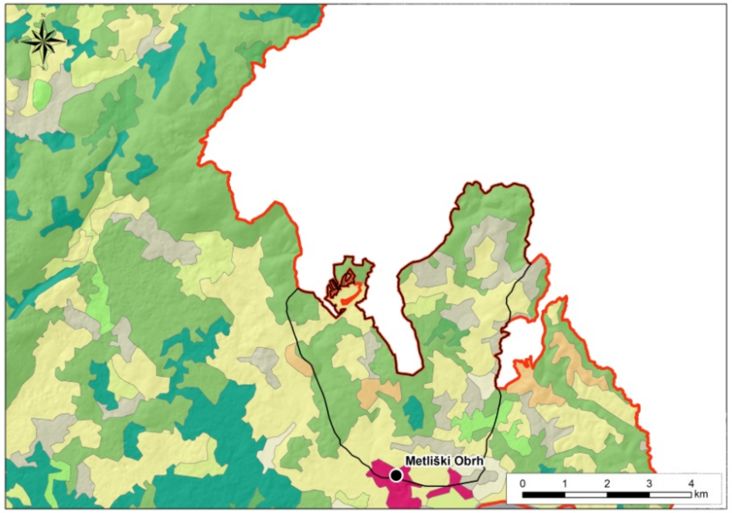

Sampling location Metliški Obrh (CLC classification)

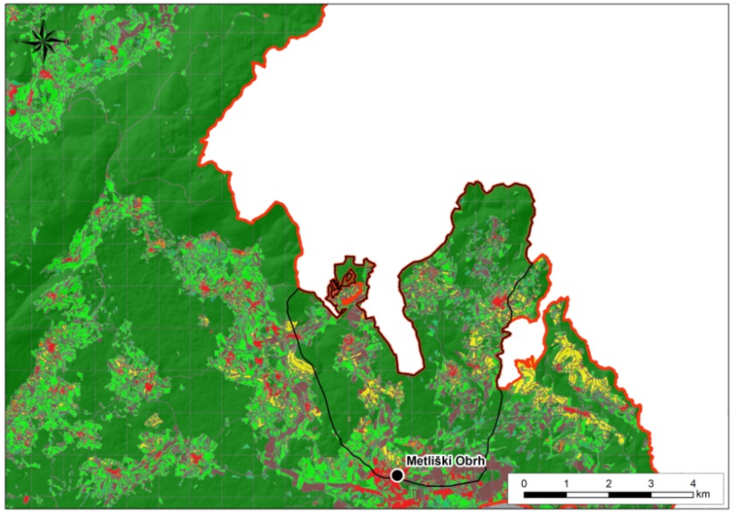

Sampling location Metliški Obrh (Land use classification)

Mitovšek

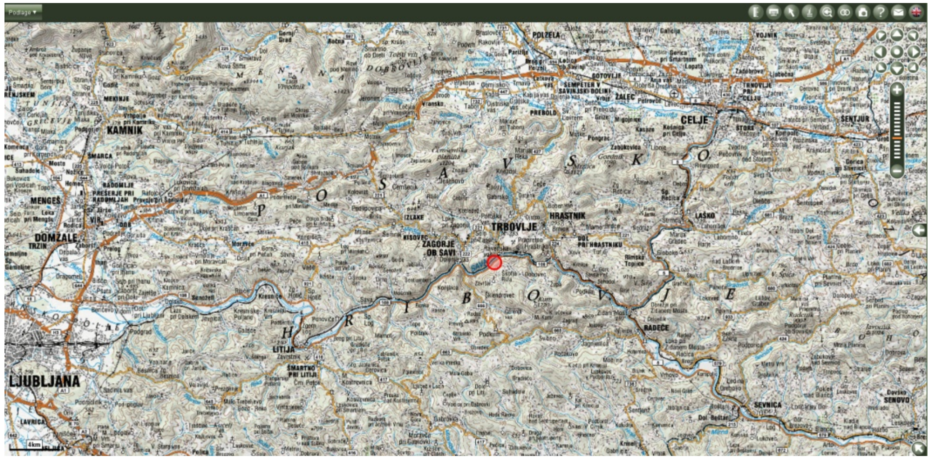

Sampling location Mitovšek

Sampling location Mitovšek

Sampling location Mitovšek

Sampling location Mitovšek

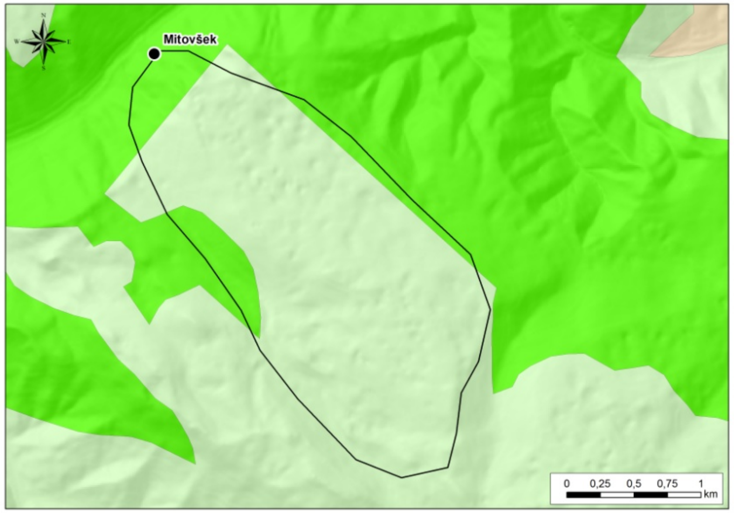

Sampling location Mitovšek (IAH classification)

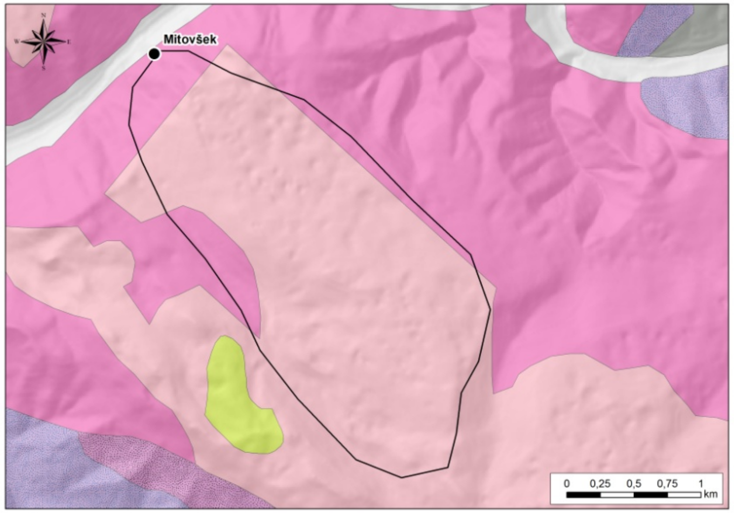

Sampling location Mitovšek (Geological classification)

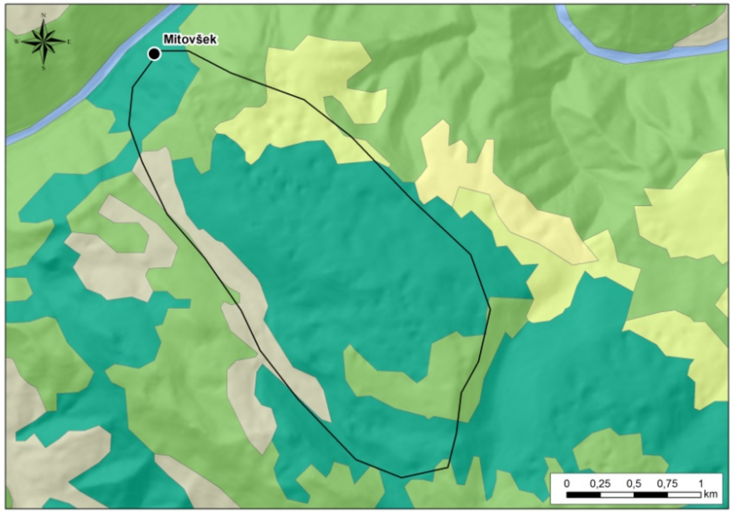

Sampling location Mitovšek (CLC classification)

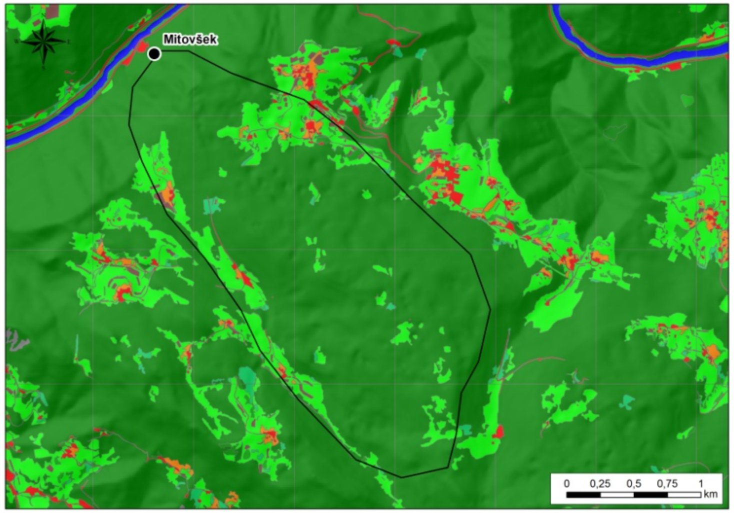

Sampling location Mitovšek (Land use classification)

Močilnik

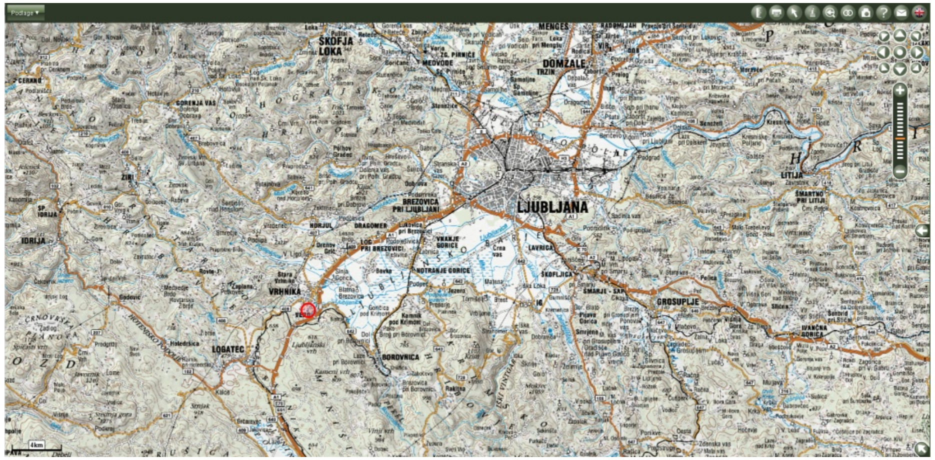

Sampling location Močilnik

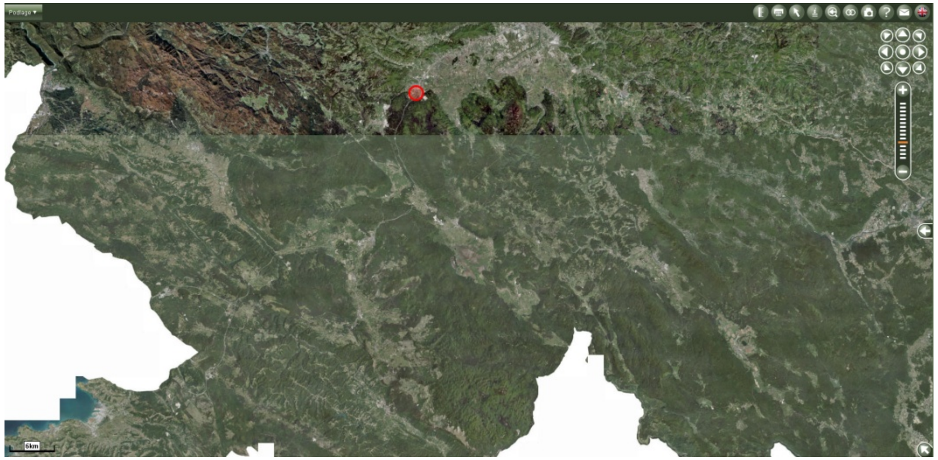

Sampling location Močilnik

Sampling location Močilnik

Sampling location Močilnik

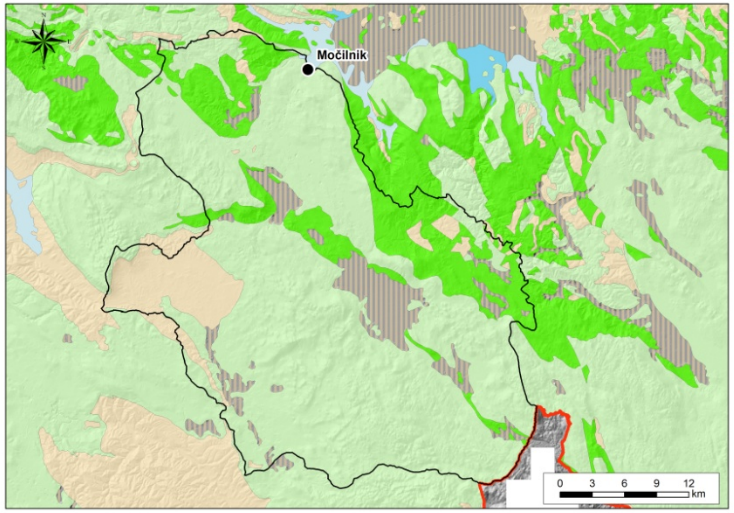

Sampling location Močilnik (IAH classification)

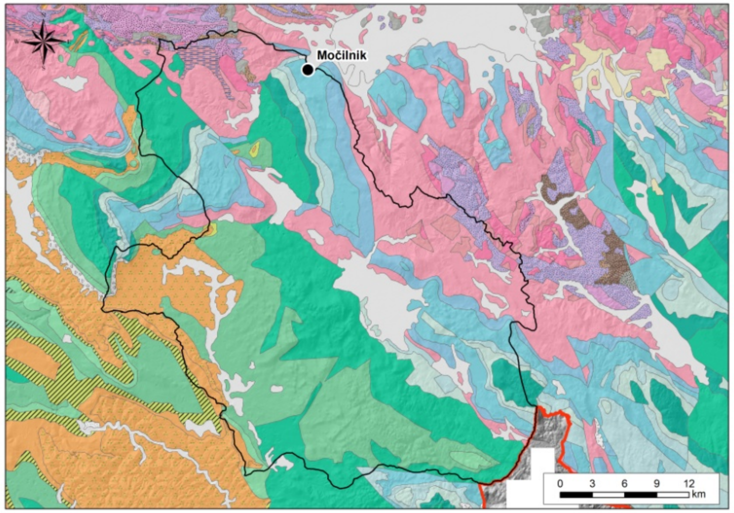

Sampling location Močilnik (Geological classification)

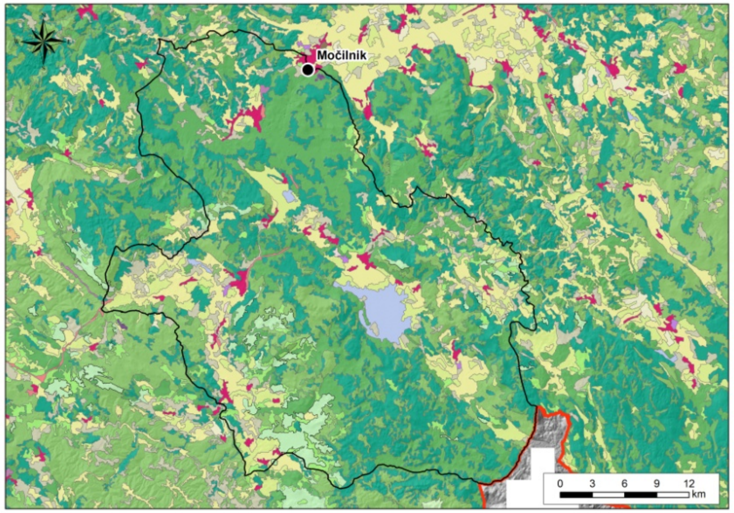

Sampling location Močilnik (CLC classification)

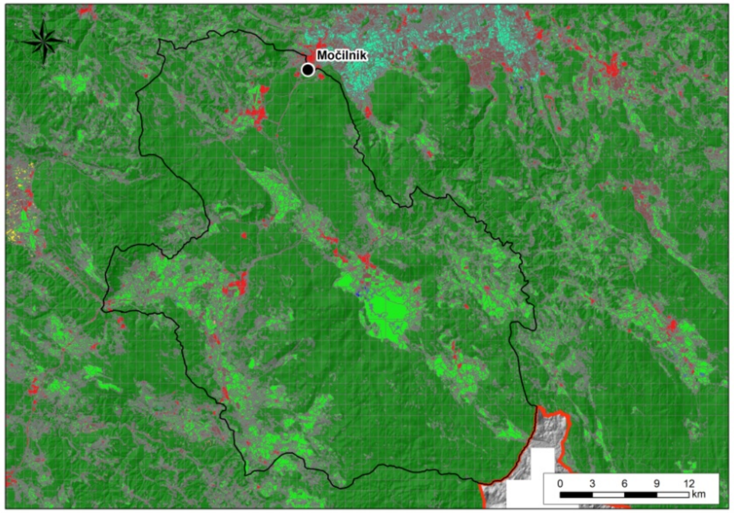

Sampling location Močilnik (Land use classification)

Mošenik

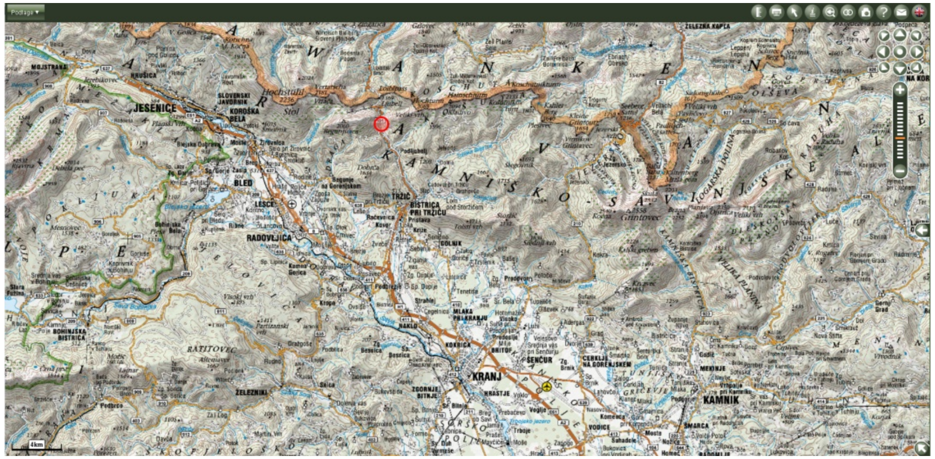

Sampling location Mošenik

Sampling location Mošenik

Sampling location Mošenik

Sampling location Mošenik

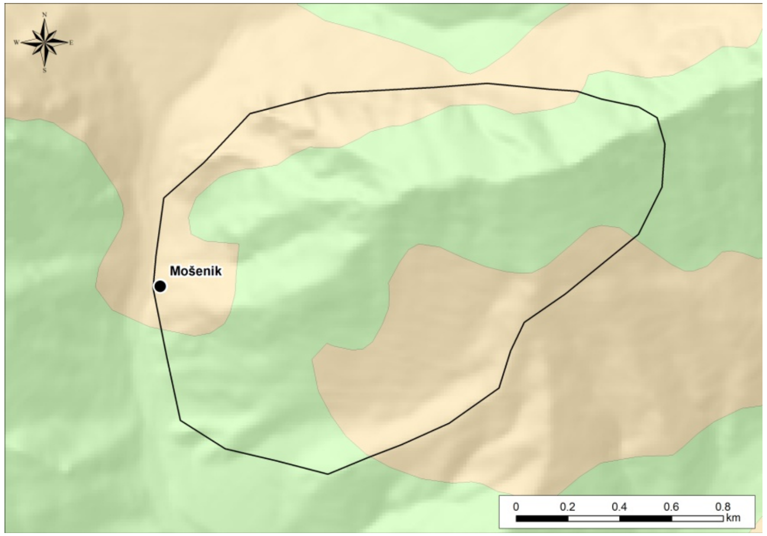

Sampling location Mošenik (IAH classification)

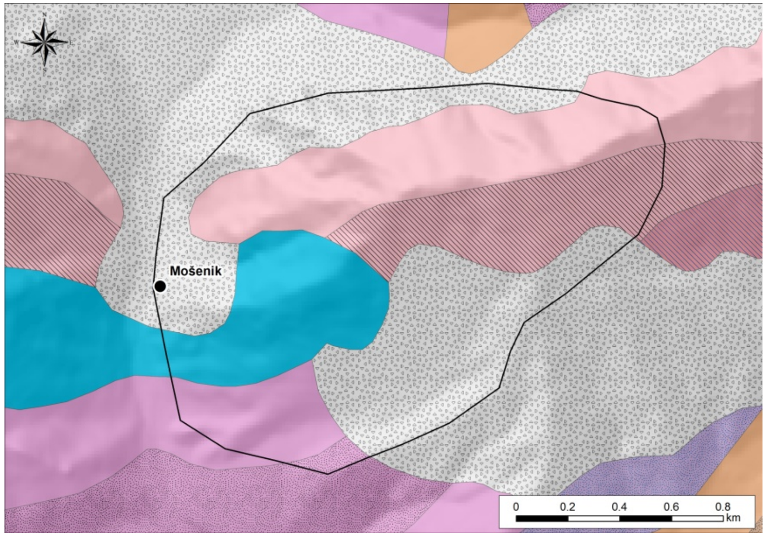

Sampling location Mošenik (Geological classification)

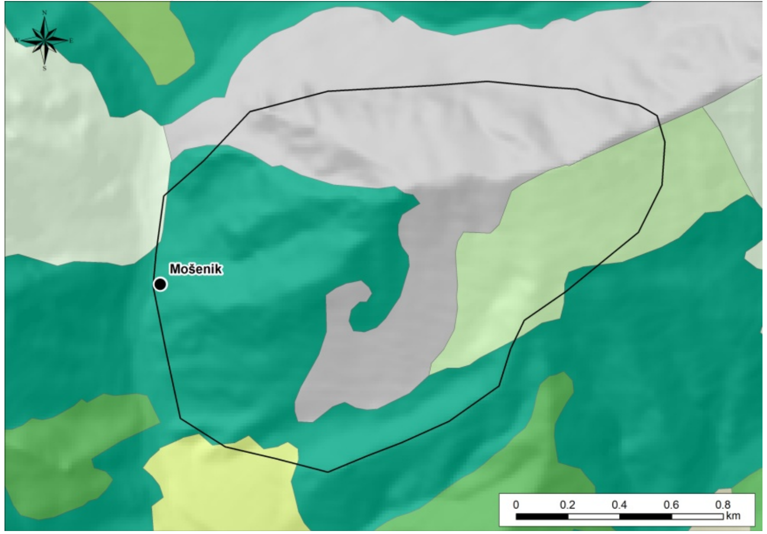

Sampling location Mošenik (CLC classification)

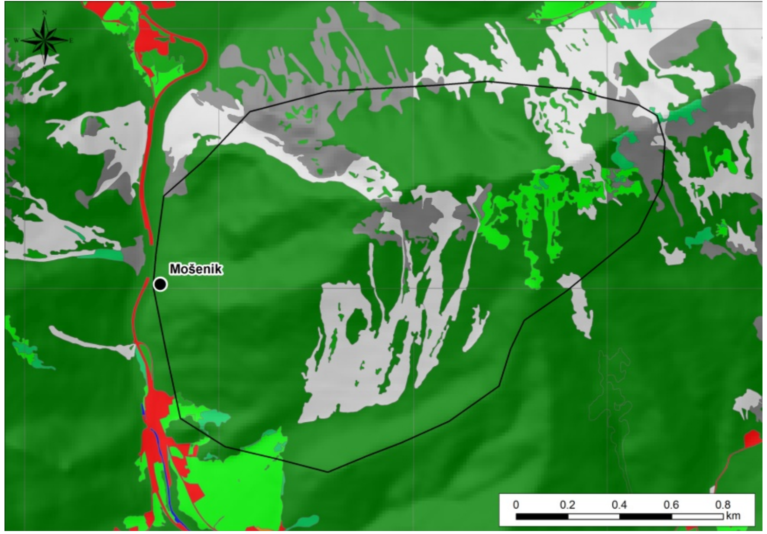

Sampling location Mošenik (Land use classification)

Mrzlek

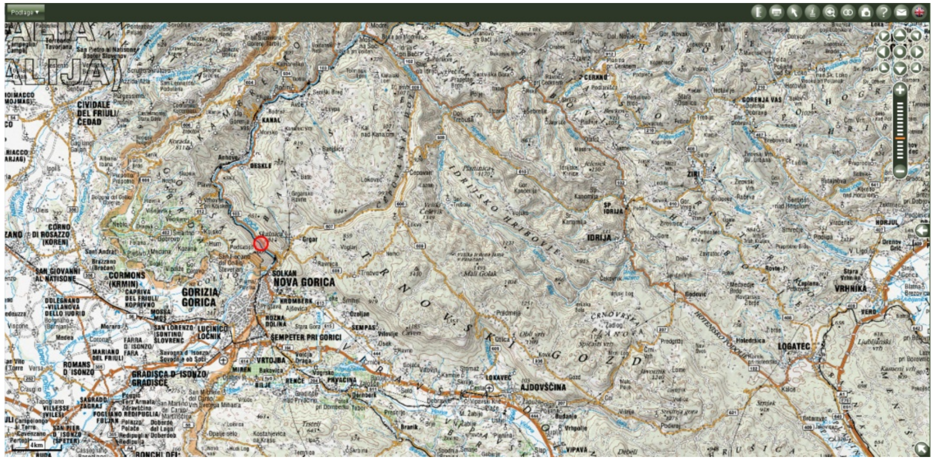

Sampling location Mrzlek

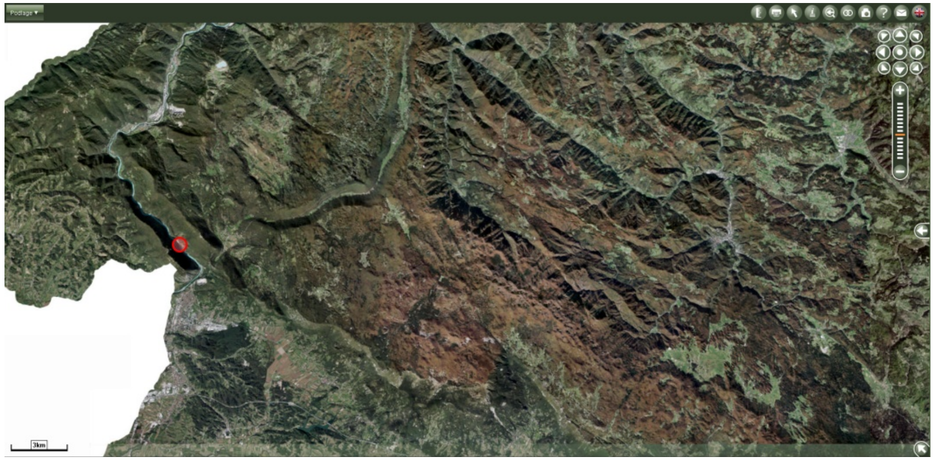

Sampling location Mrzlek

Sampling location Mrzlek

Sampling location Mrzlek

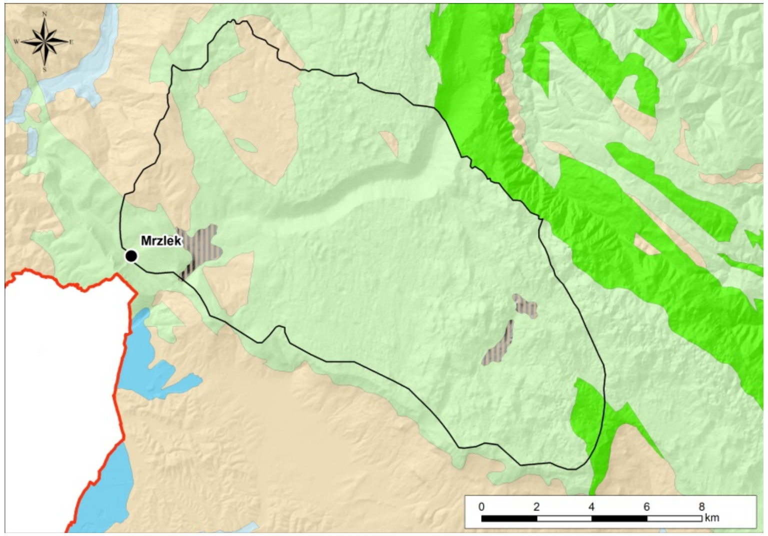

Sampling location Mrzlek (IAH classification)

P-1 ????

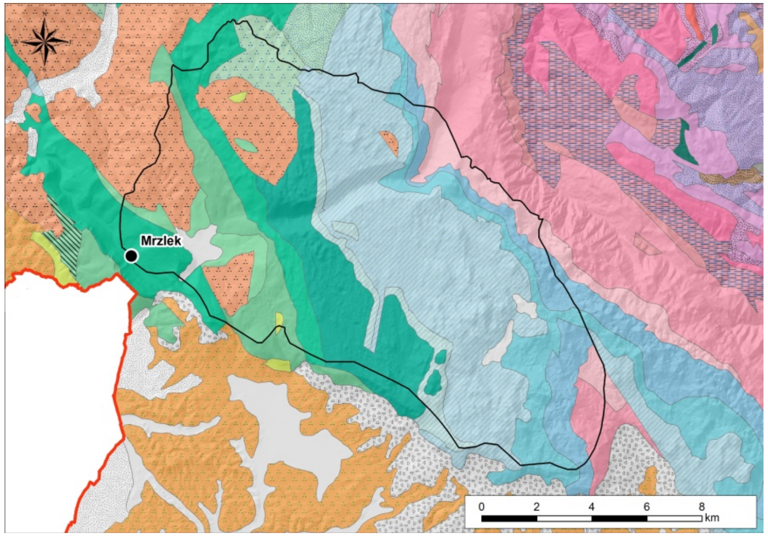

Sampling location Mrzlek (Geological classification)

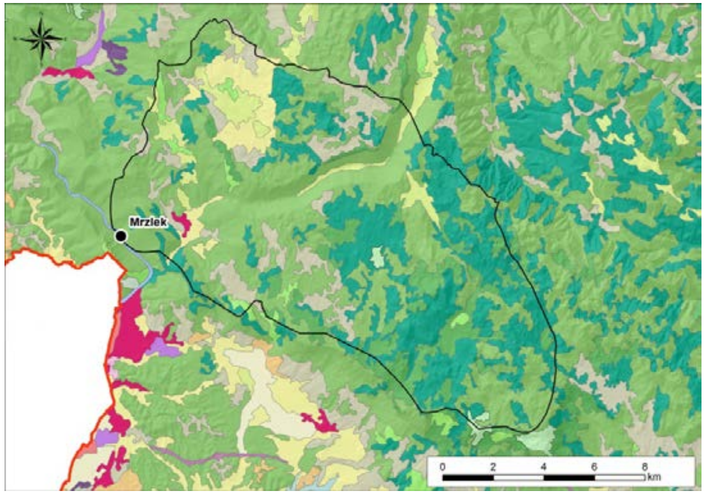

Sampling location Mrzlek (CLC classification)

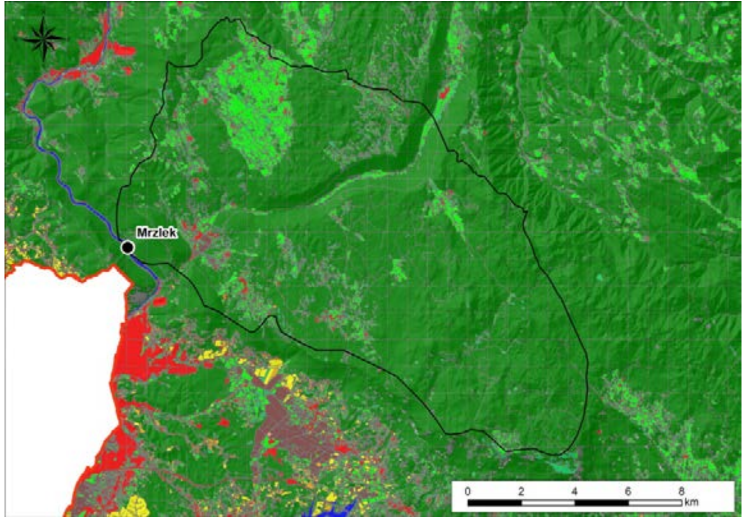

Sampling location Mrzlek (Land use classification)

NG-4

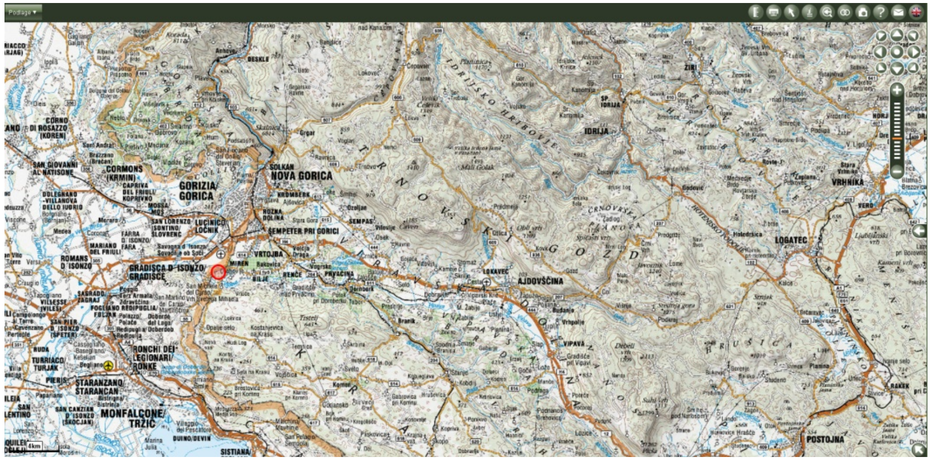

Sampling location NG-4

Sampling location NG-4

Sampling location NG-4

Sampling location NG-4

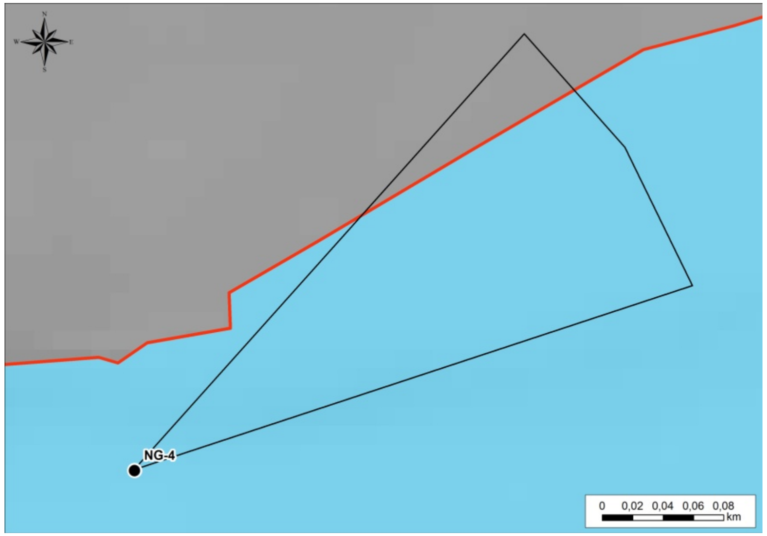

Sampling location NG-4 (IAH classification)

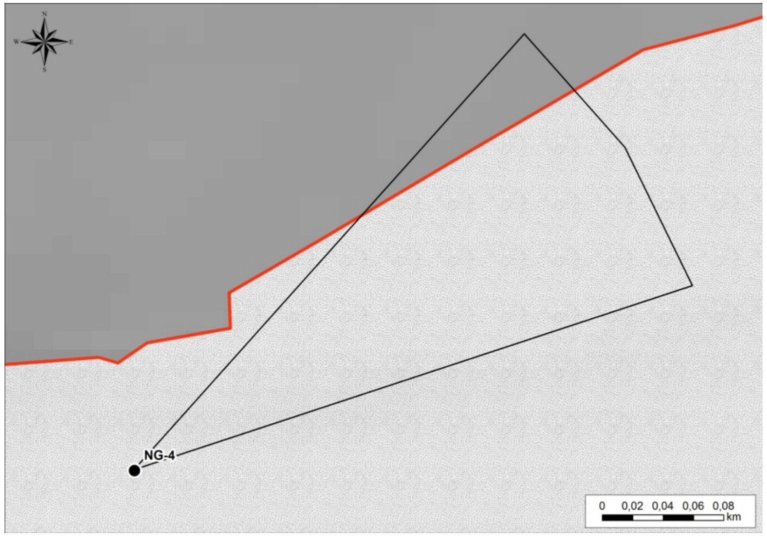

Sampling location NG-4 (Geological classification)

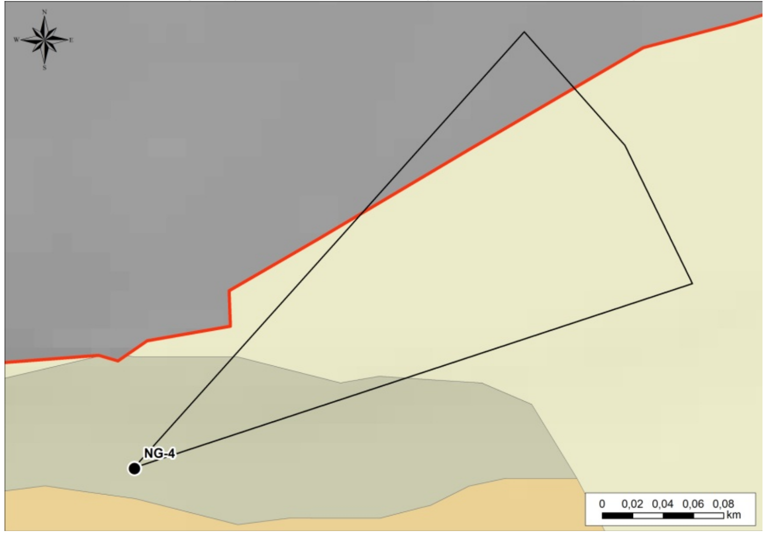

Sampling location NG-4 (CLC classification)

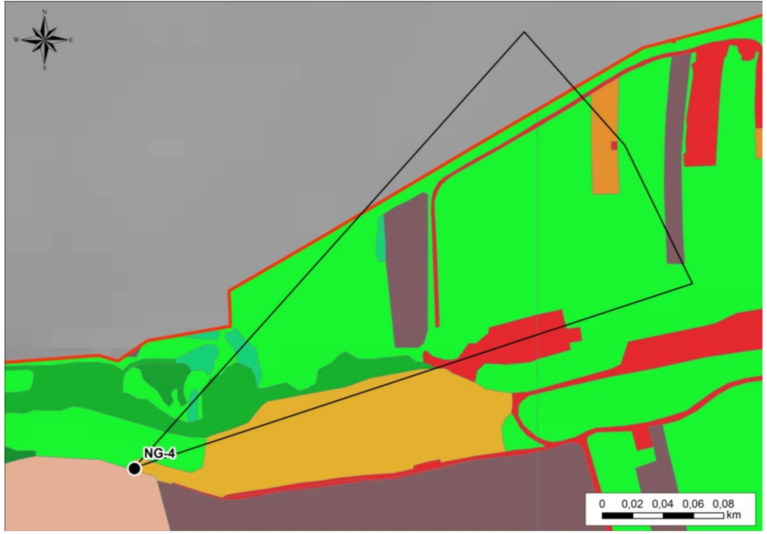

Sampling location NG-4 (Land use classification)

Obrh Rinža

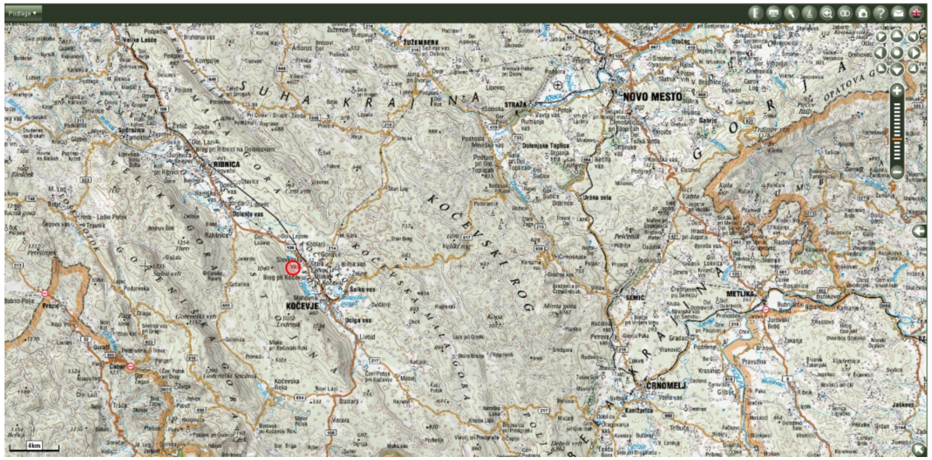

Sampling location Obrh Rinža

Sampling location Obrh Rinža

Sampling location Obrh Rinža

Sampling location Obrh Rinža

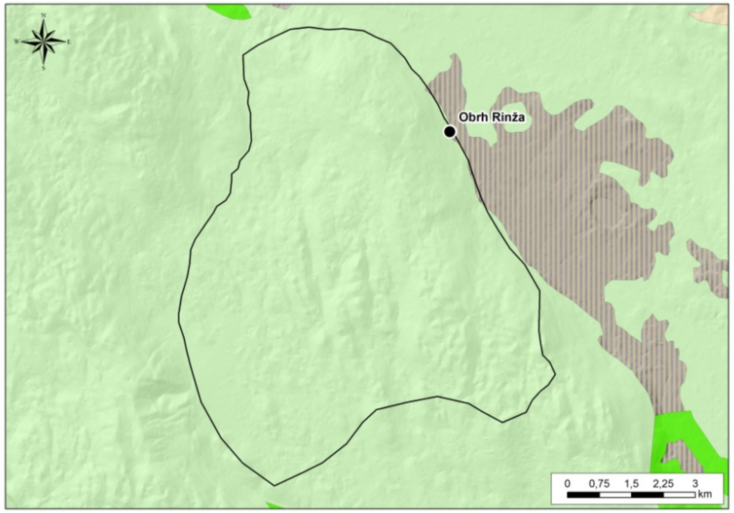

Sampling location Obrh Rinža (IAH classification)

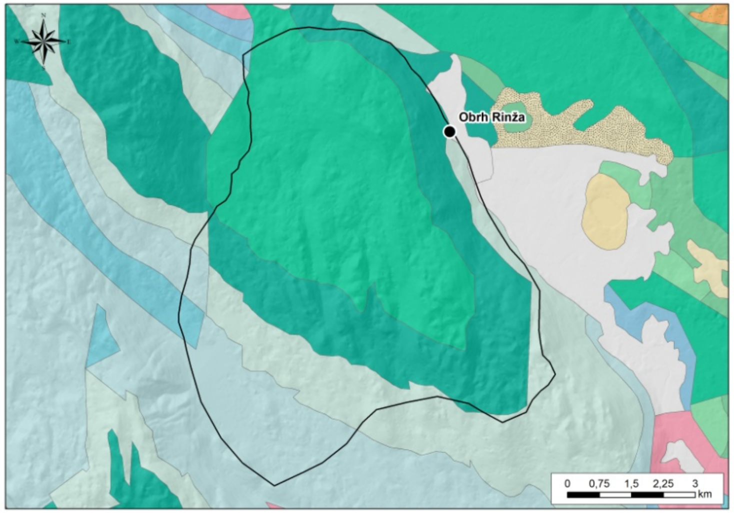

Sampling location Obrh Rinža (Geological classification)

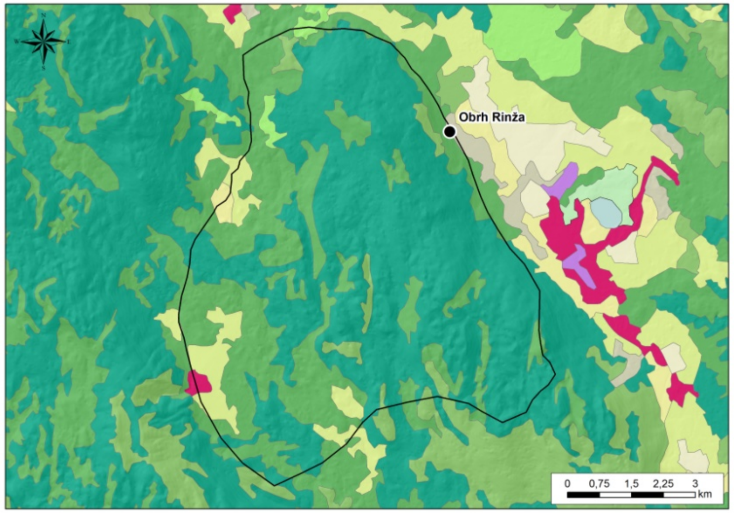

Sampling location Obrh Rinža (CLC classification)

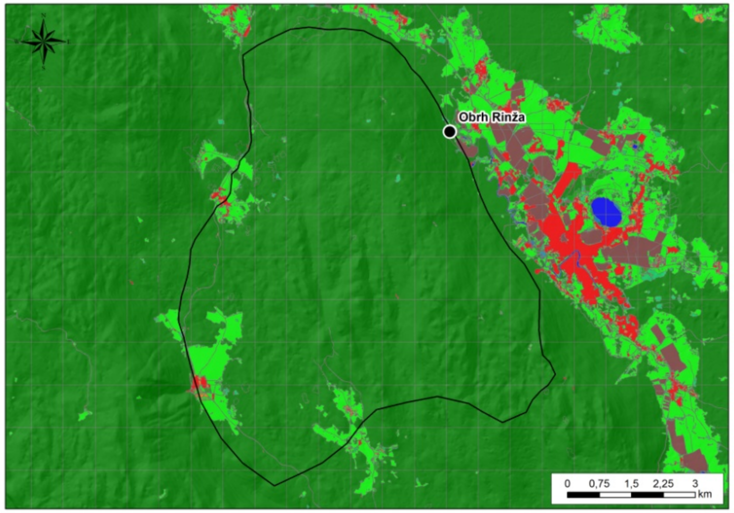

Sampling location Obrh Rinža (Land use classification)

Odolina

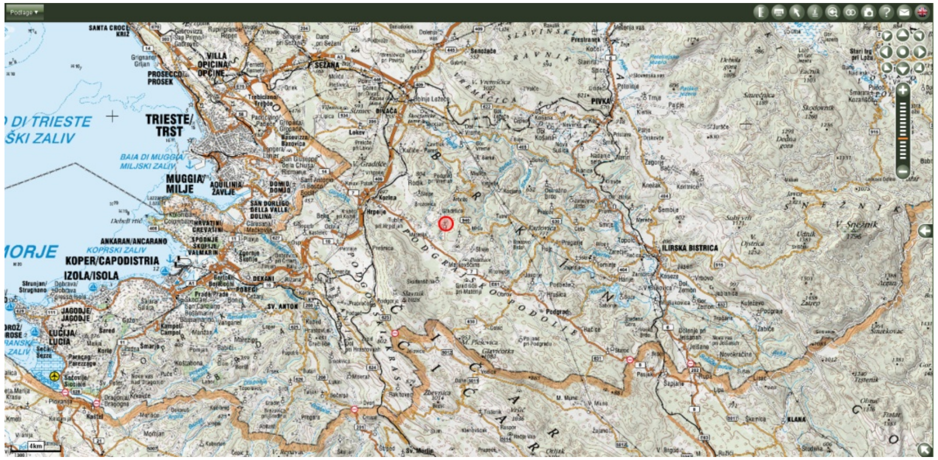

Sampling location Odolina

Sampling location Odolina

Sampling location Odolina

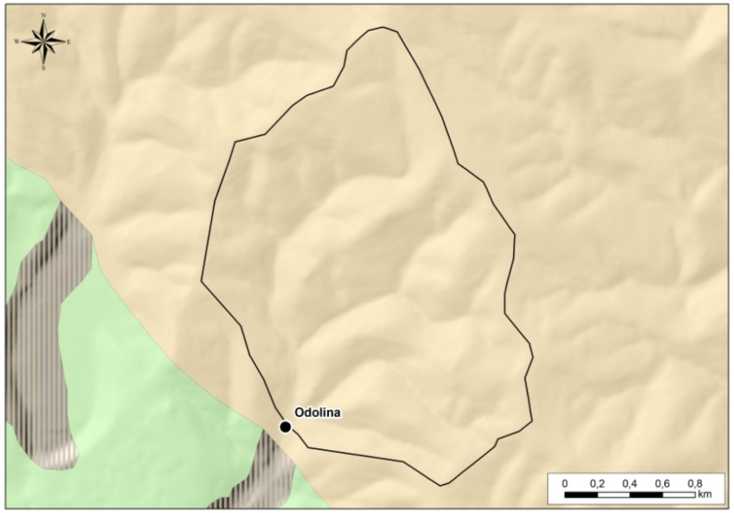

Sampling location Odolina (IAH classification)

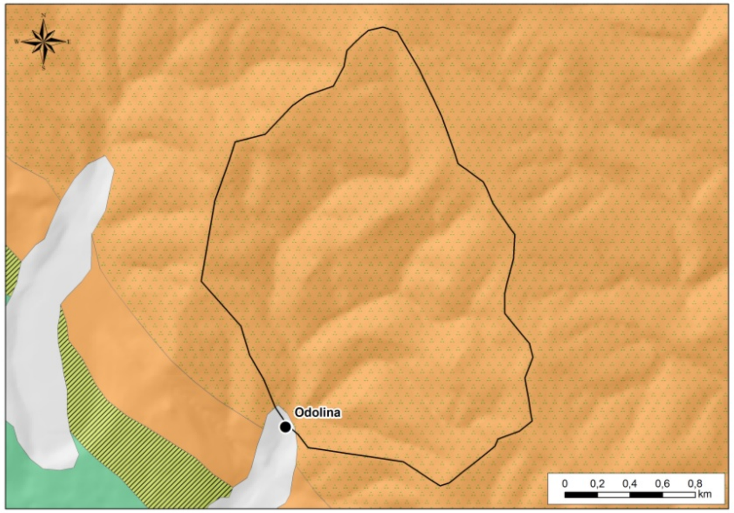

Sampling location Odolina (Geological classification)

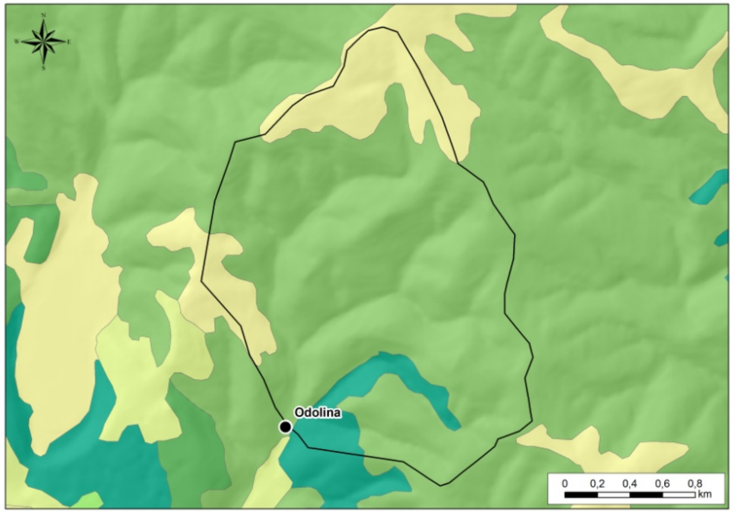

Sampling location Odolina (CLC classification)

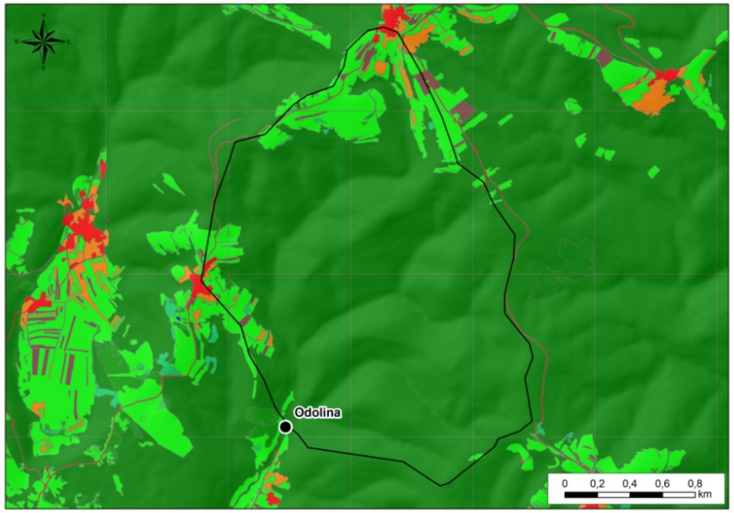

Sampling location Odolina (Land use classification)

OV-29, Brunšvik

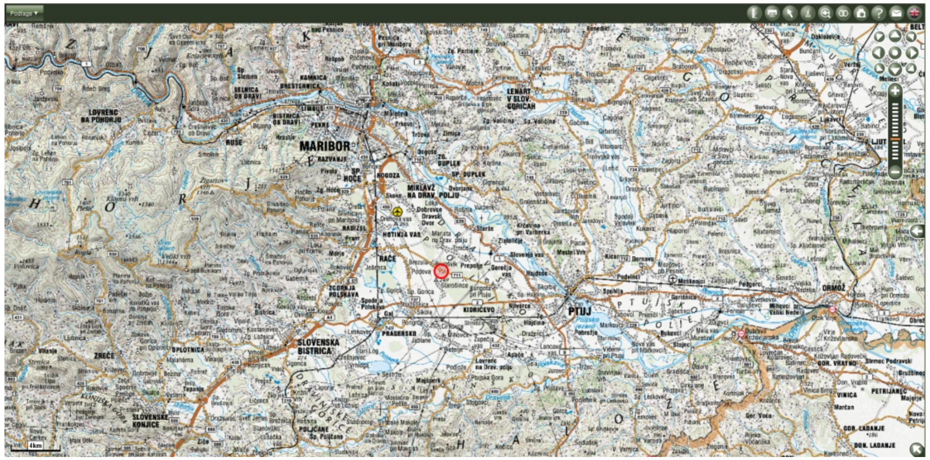

Sampling location OV-29, Brunšvik

Sampling location OV-29, Brunšvik

Sampling location OV-29, Brunšvik

Sampling location OV-29, Brunšvik

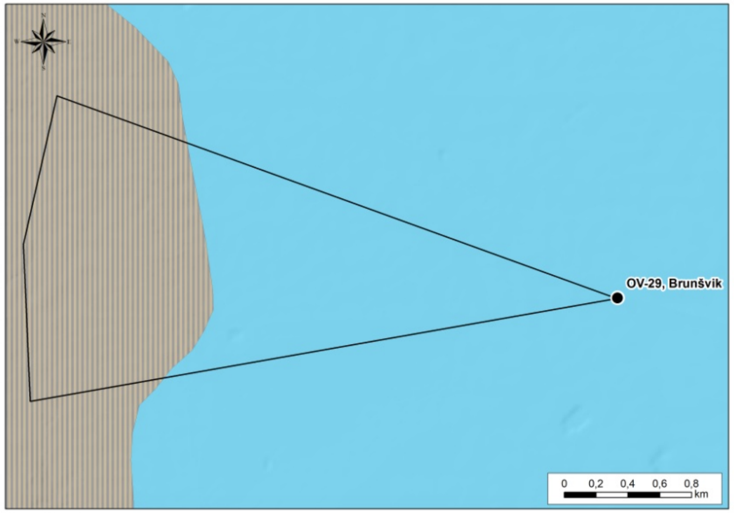

Sampling location OV-29, Brunšvik (IAH classification)

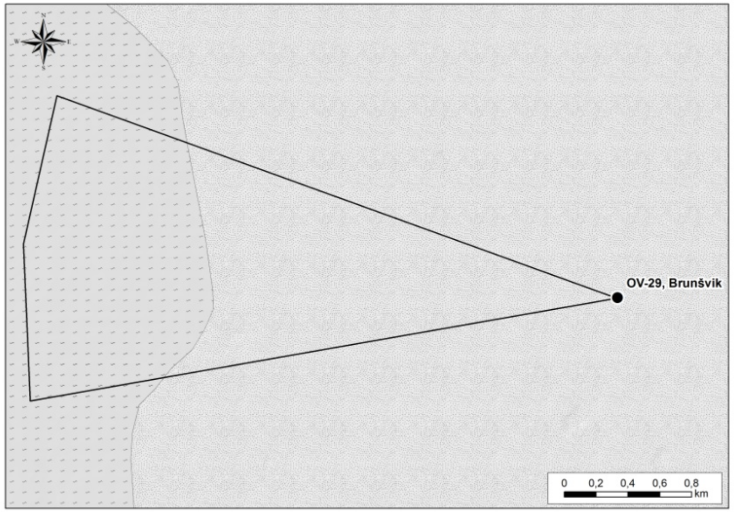

Sampling location OV-29, Brunšvik (Geological classification)

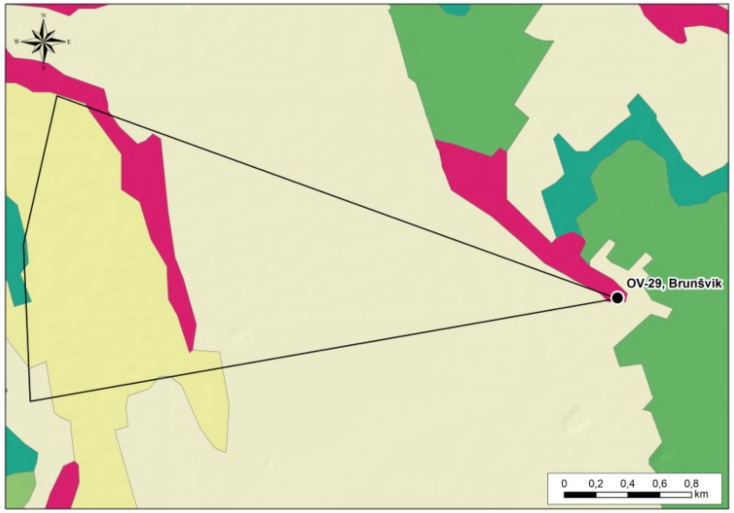

Sampling location OV-29, Brunšvik (CLC classification)

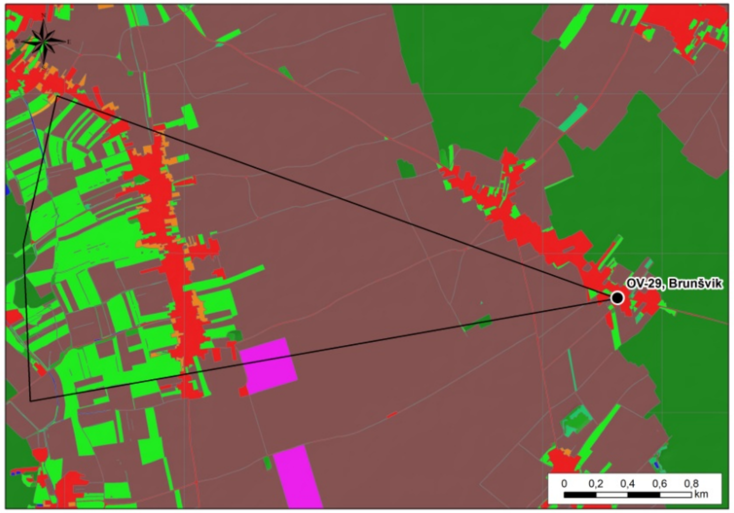

Sampling location OV-29, Brunšvik (Land use classification)

P-1, Pliskovica

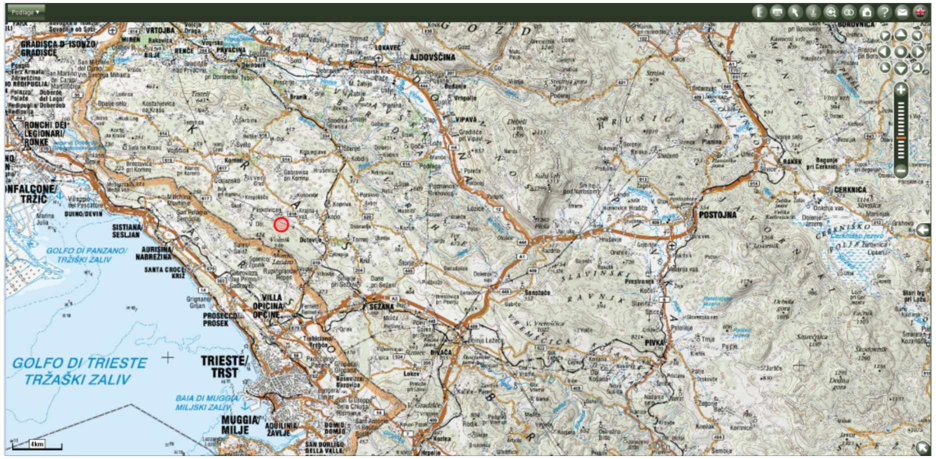

Sampling location P-1, Pliskovica

Sampling location P-1, Pliskovica

Sampling location P-1, Pliskovica

Padiščak

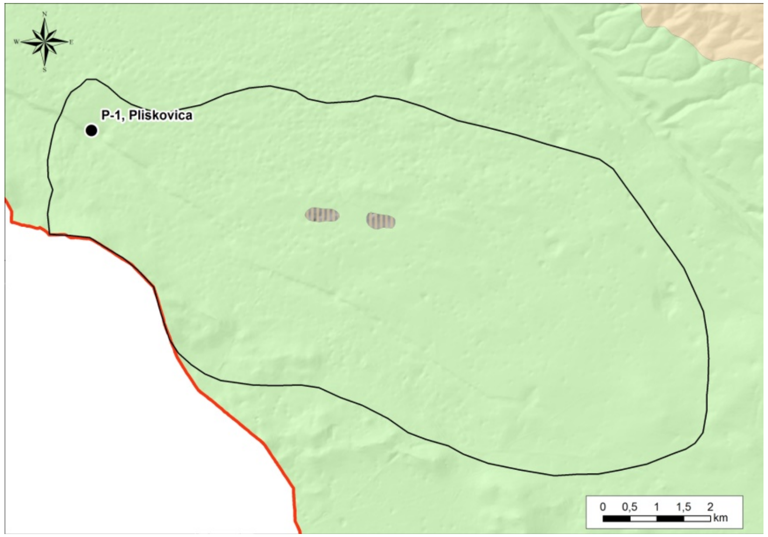

Sampling location P-1, Pliskovica (IAH classification)

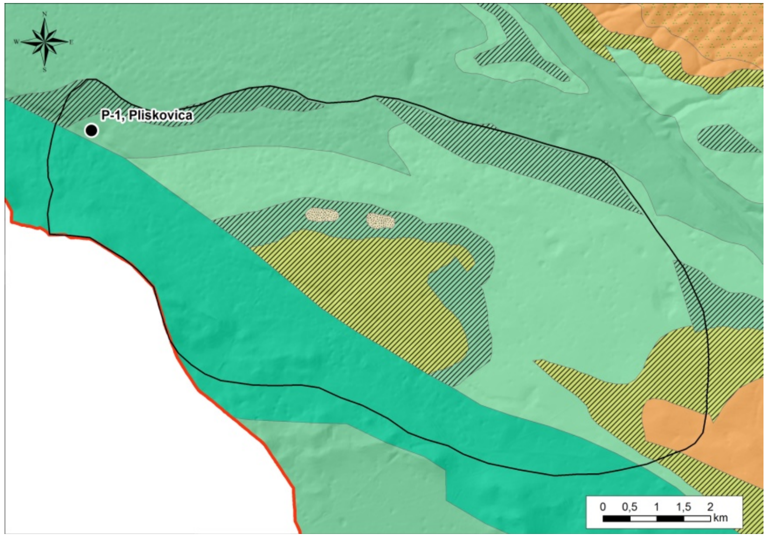

Sampling location P-1, Pliskovica (Geological classification)

Rakit

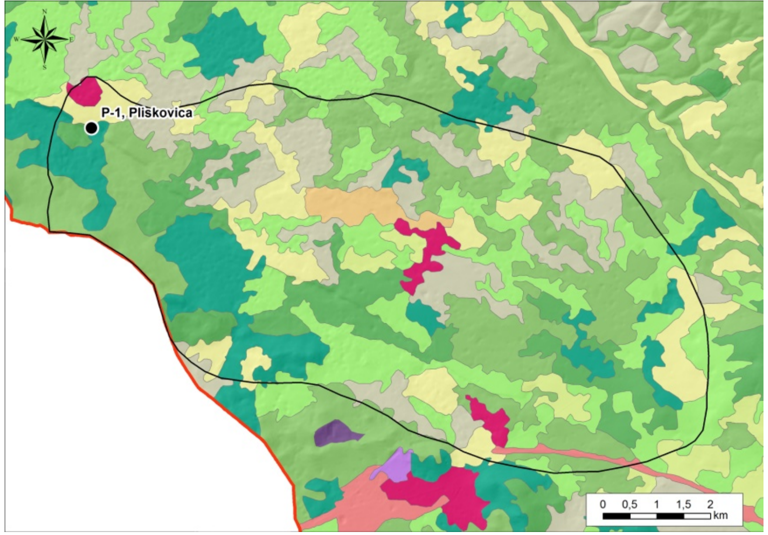

Sampling location P-1, Pliskovica (CLC classification)

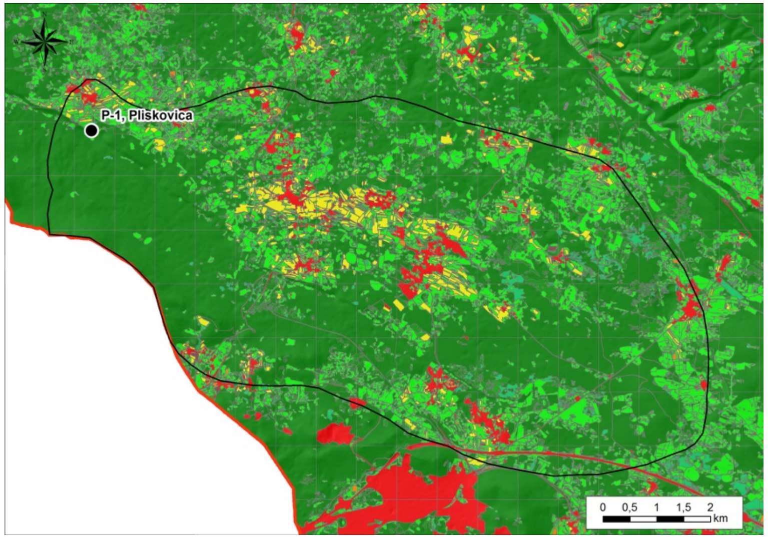

Sampling location P-1, Pliskovica (Land use classification)

Padiščak

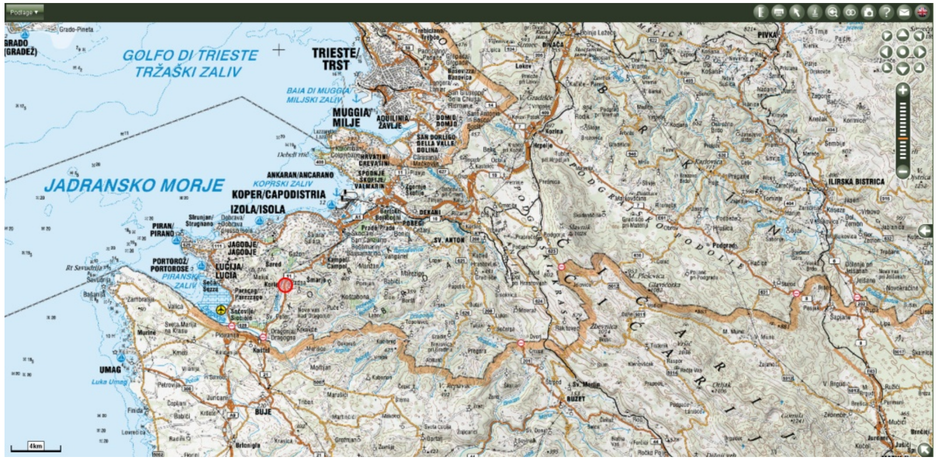
Sampling location Padiščak


Sampling location Padiščak


Sampling location Padiščak


Sampling location Padiščak

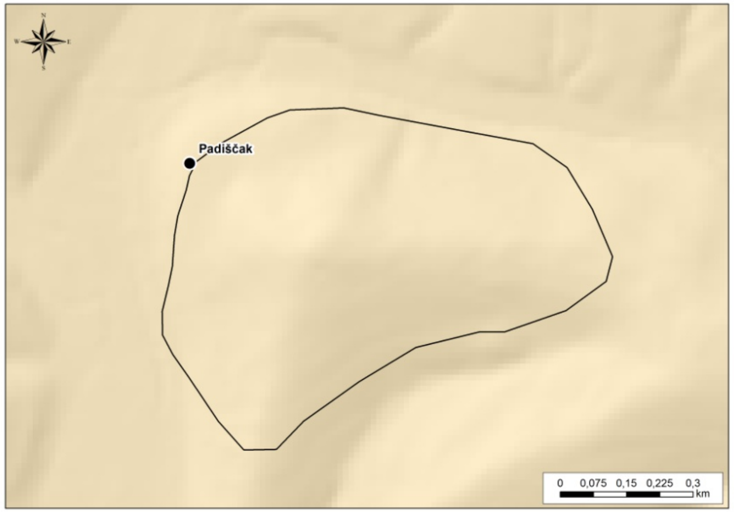

Sampling location Padiščak (IAH classification)

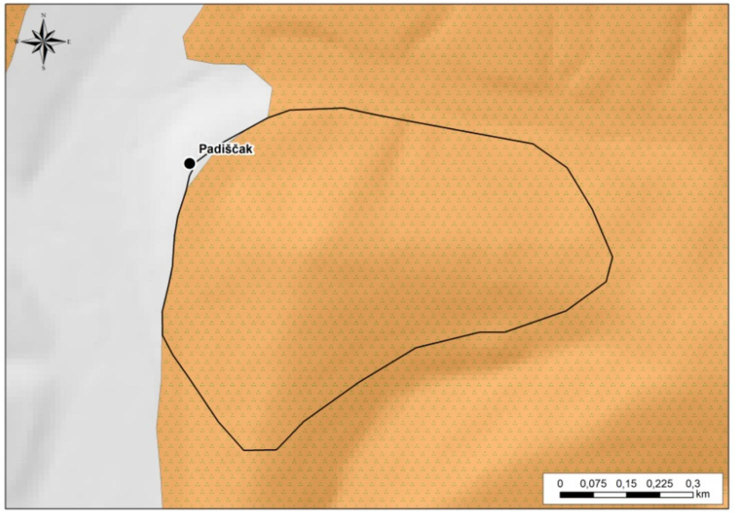

Sampling location Padiščak (Geological classification)

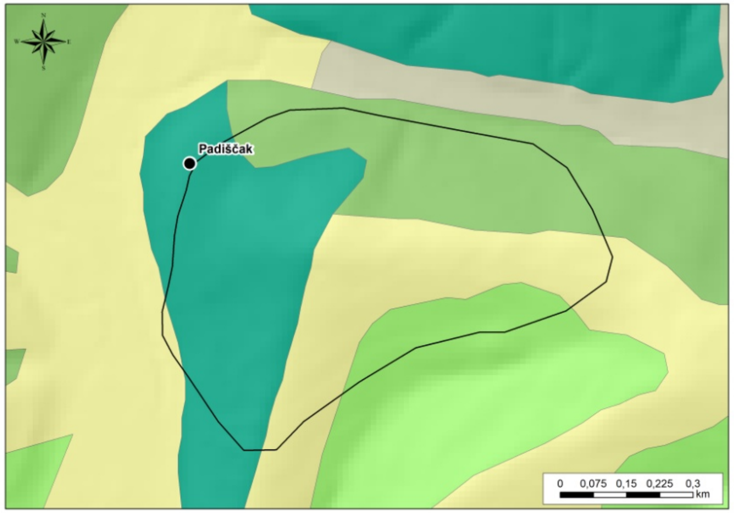

Sampling location Padiščak (CLC classification)

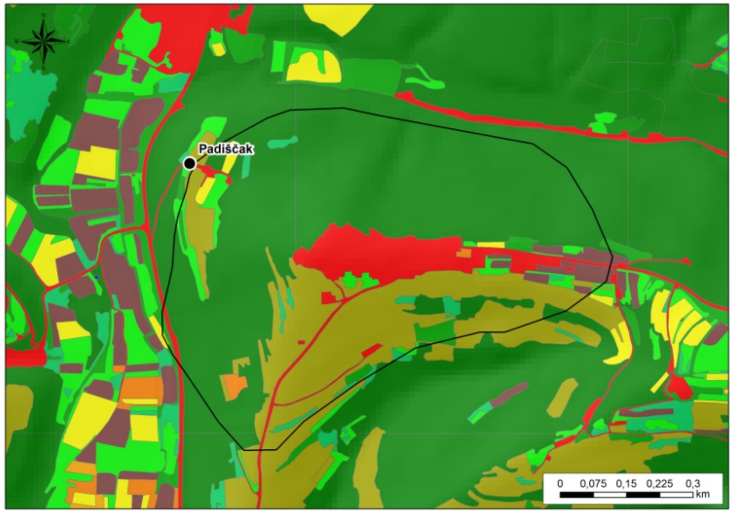

Sampling location Padiščak (Land use classification)

Pasji rep

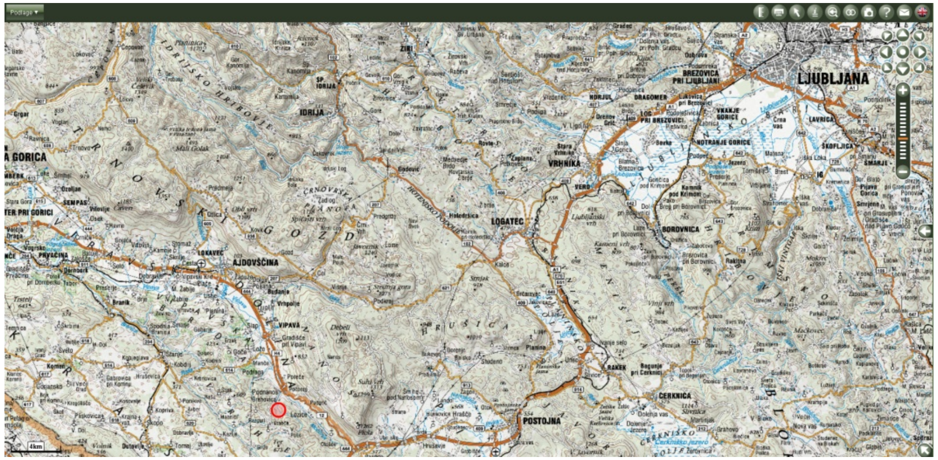

Sampling location Pasji rep

Sampling location Pasji rep

Sampling location Pasji rep

Sampling location Pasji rep

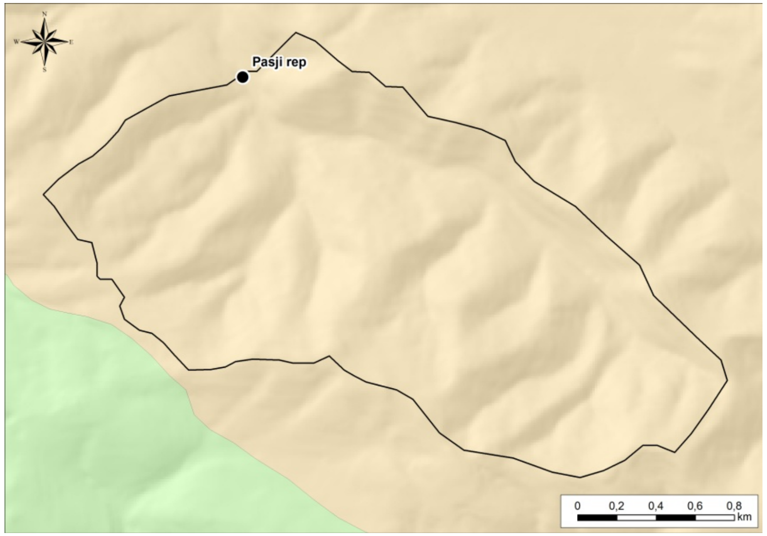

Sampling location Pasji rep (IAH classification)

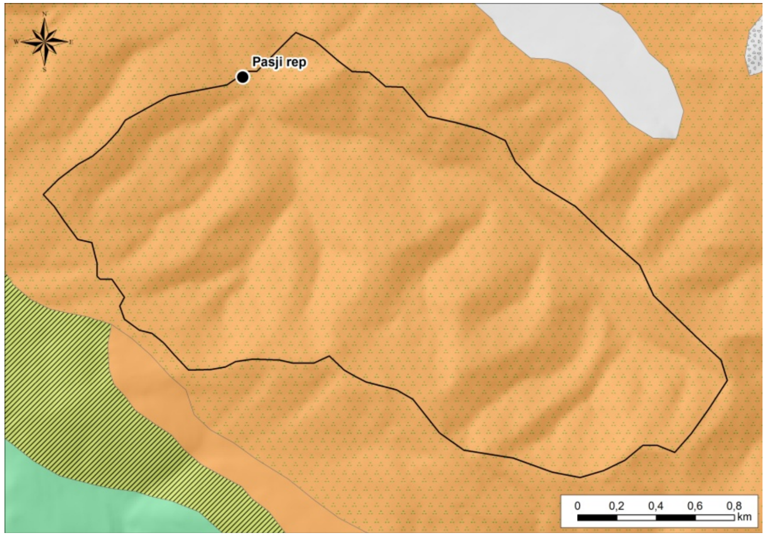

Sampling location Pasji rep (Geological classification)

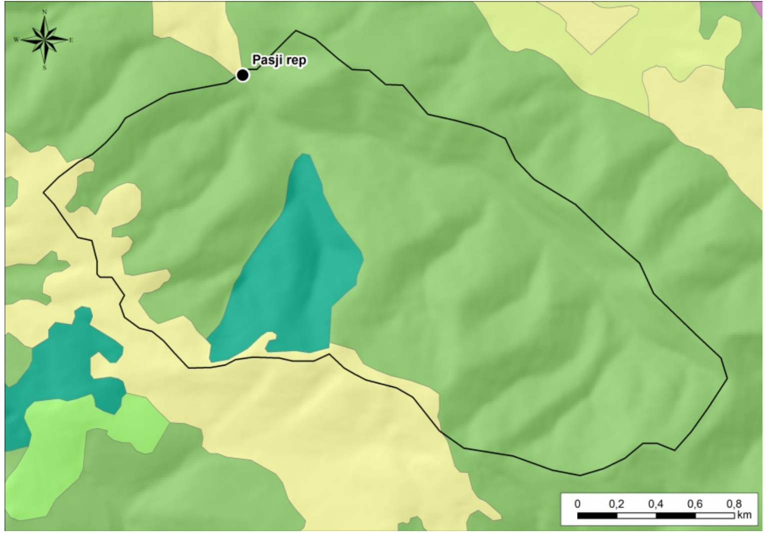

Sampling location Pasji rep (CLC classification)

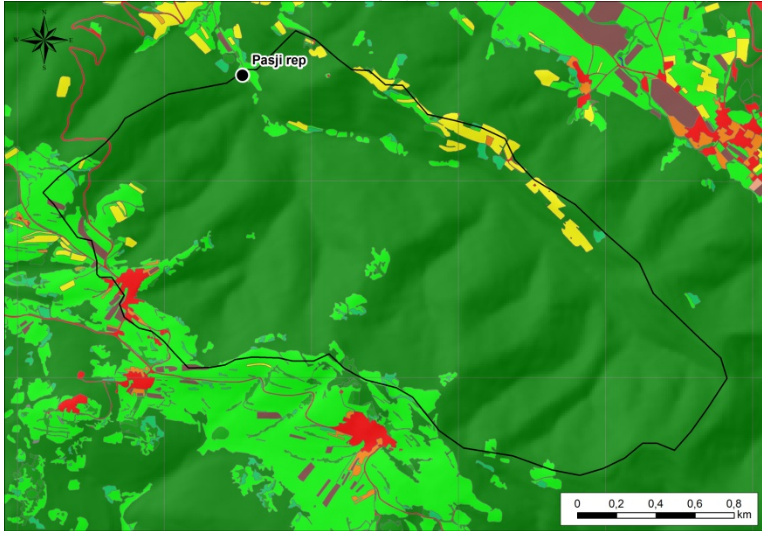

Sampling location Pasji rep (Land use classification)

Pevčevo

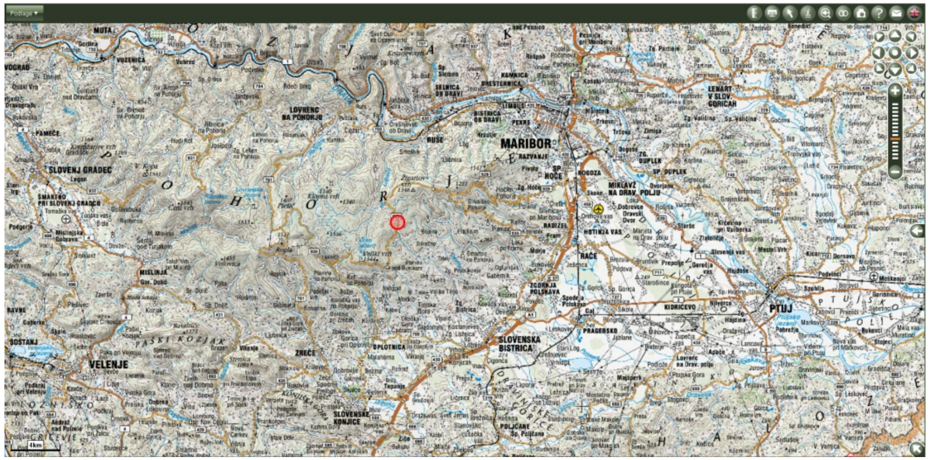

Sampling location Pevčevo

Sampling location Pevčevo

Sampling location Pevčevo

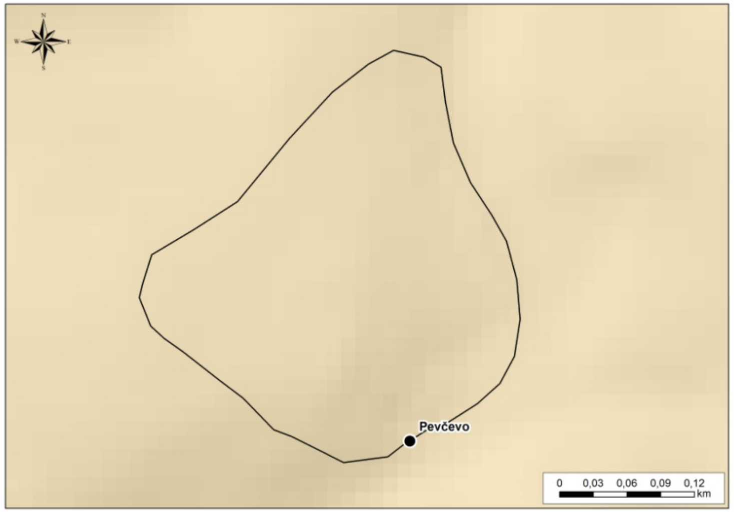

Sampling location Pevčevo (IAH classification)

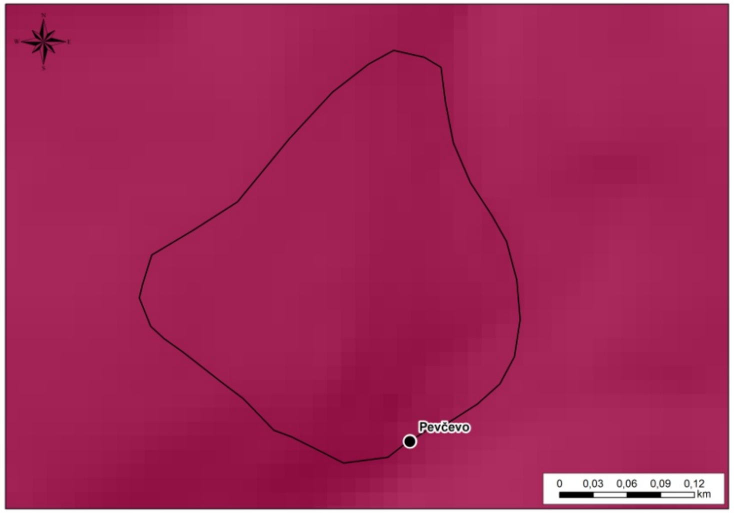

Sampling location Pevčevo (Geological classification)

Sampling location Pevčevo (CLC classification)

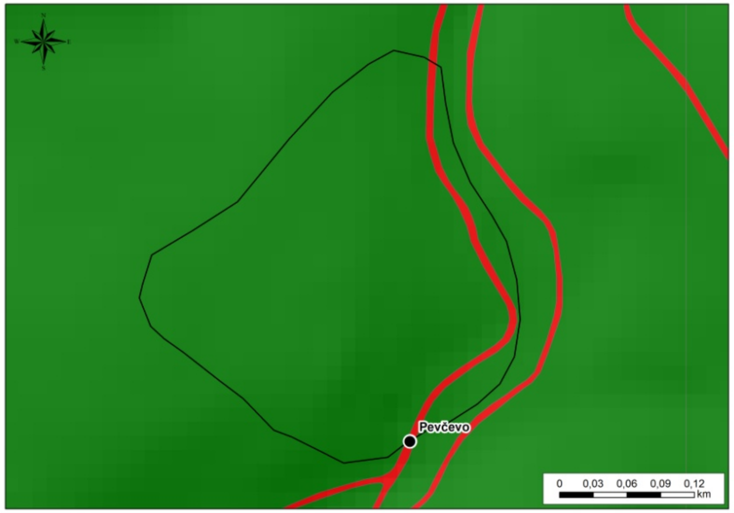

Sampling location Pevčevo (Land use classification)

Podroteja

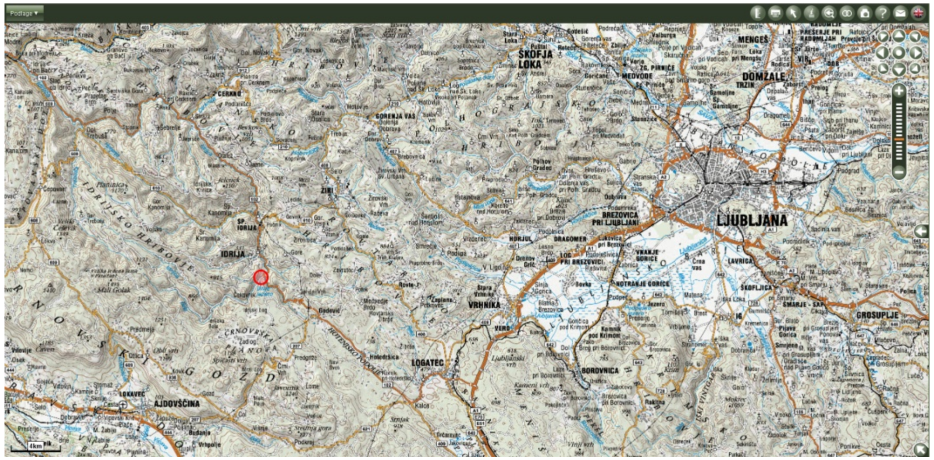

Sampling location Podroteja

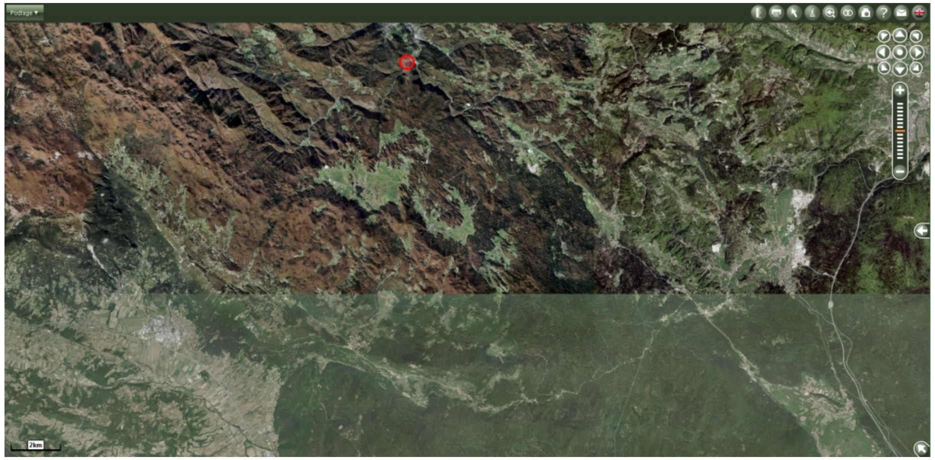

Sampling location Podroteja

Sampling location Podroteja

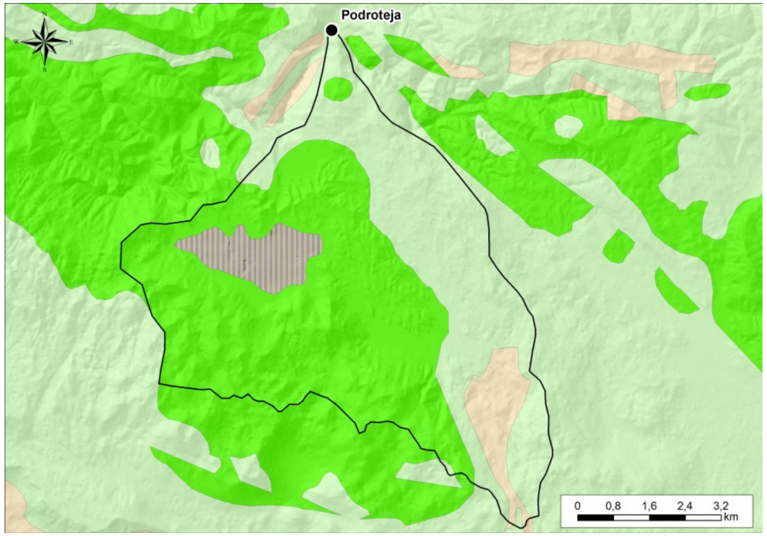

Sampling location Podroteja(IAH classification)

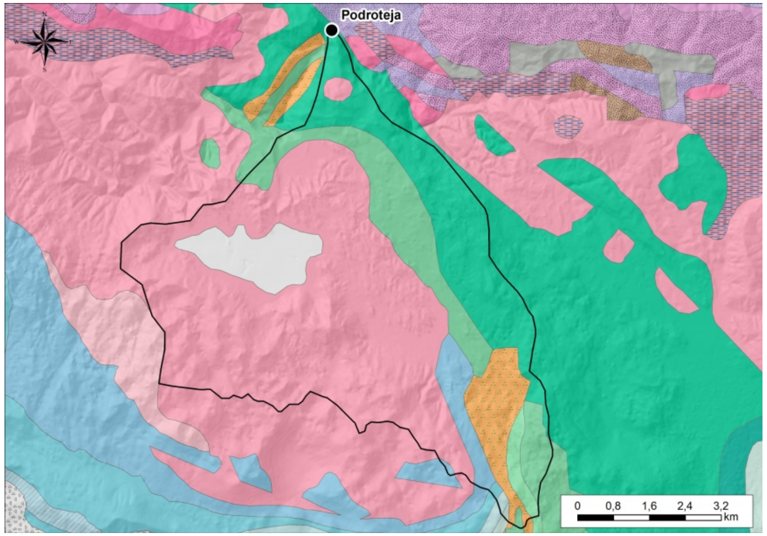

Sampling location Podroteja (Geological classification)

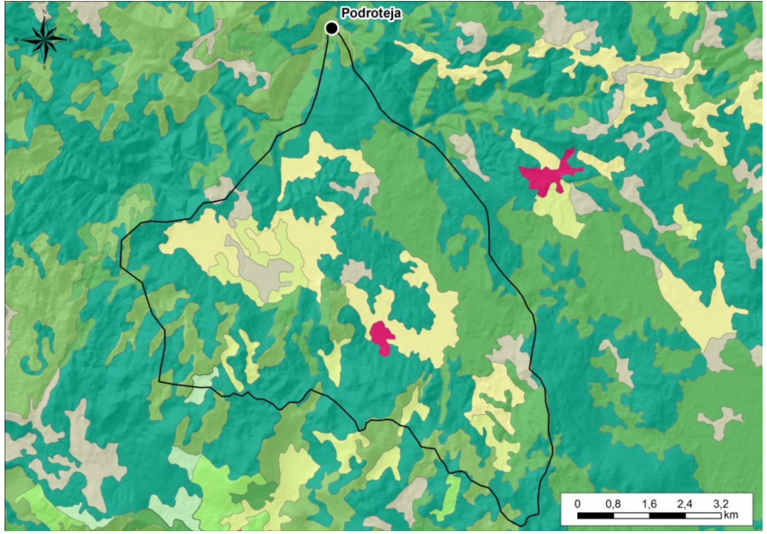

Sampling location Podroteja (CLC classification)

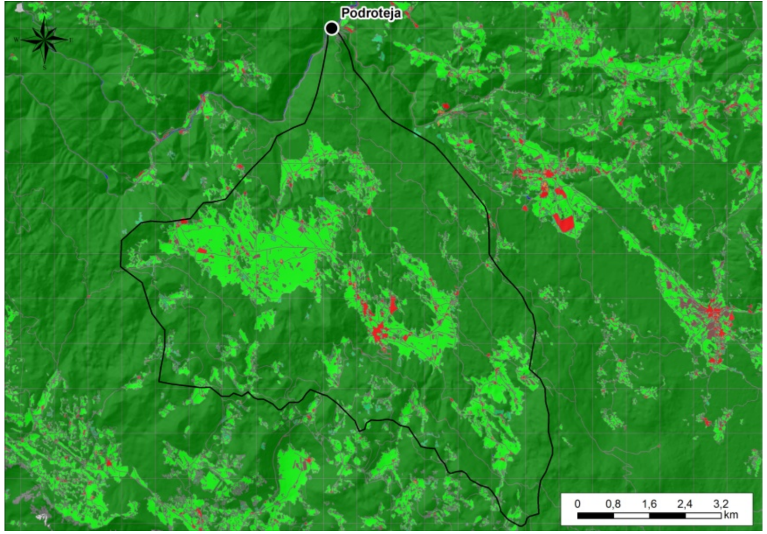

Sampling location Podroteja (Land use classification)

Potok pri dvorcu Visoko

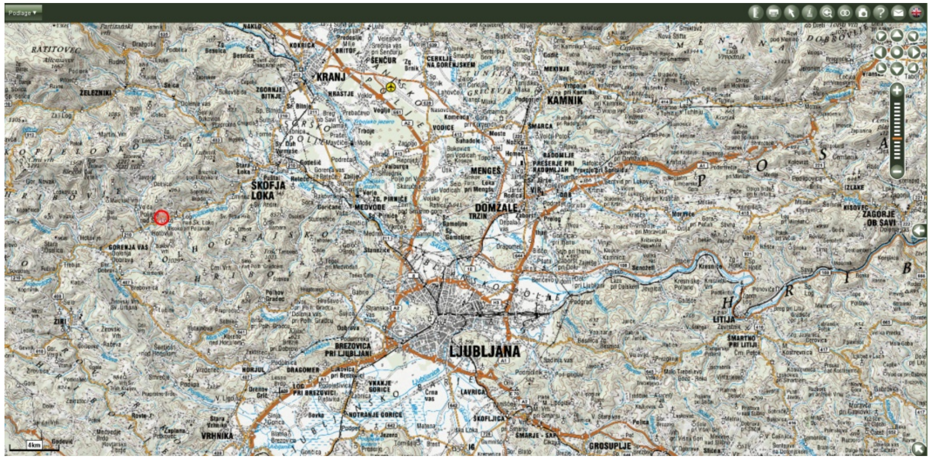

Sampling location Potok pri dvorcu Visoko

Sampling location Potok pri dvorcu Visoko

Sampling location Potok pri dvorcu Visoko

Sampling location Potok pri dvorcu Visoko

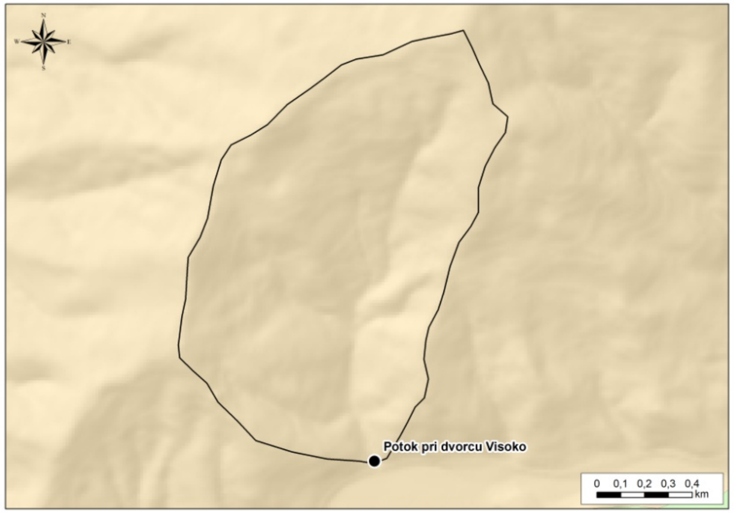

Sampling location Potok pri dvorcu Visoko (IAH classification)

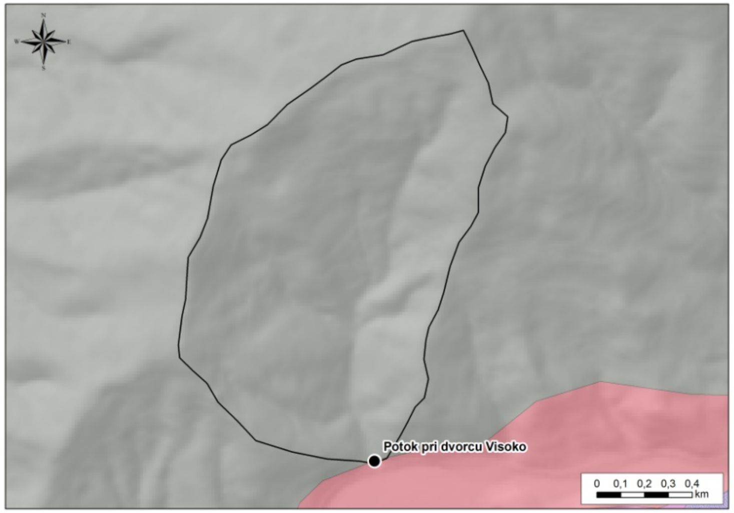

Sampling location Potok pri dvorcu Visoko (Geological classification)

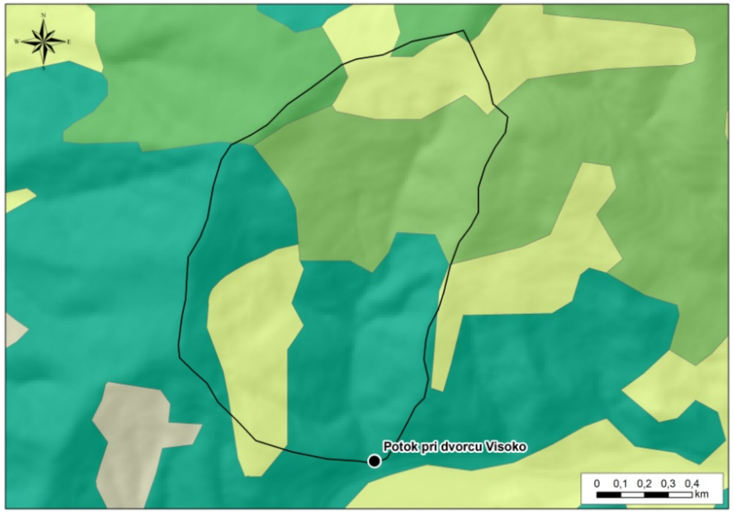

Sampling location Potok pri dvorcu Visoko (CLC classification)

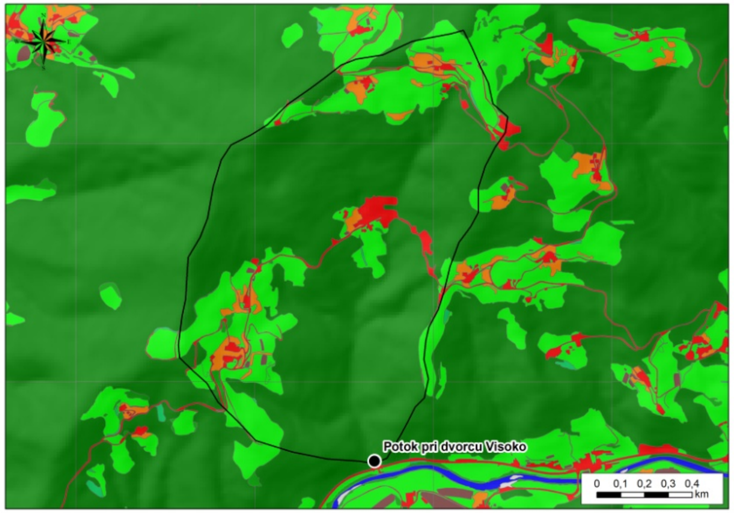

Sampling location Potok pri dvorcu Visoko (Land use classification)

Pšata

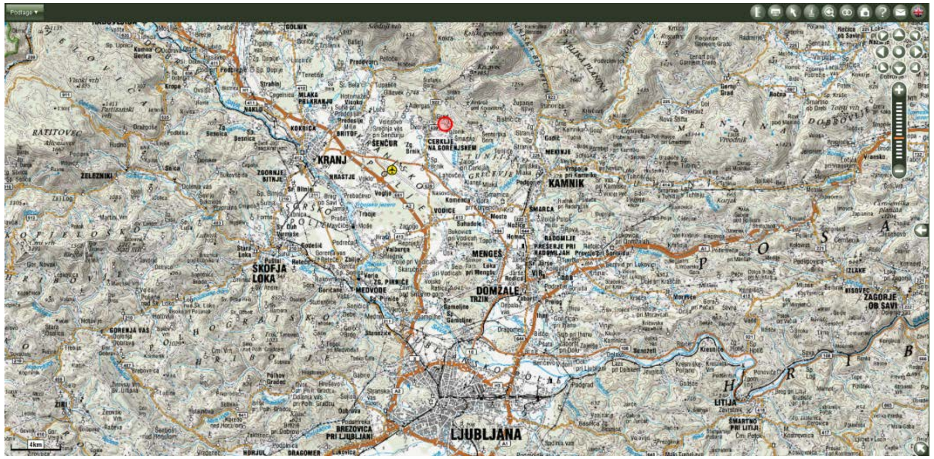

Sampling location Pšata

Sampling location Pšata

Sampling location Pšata

Sampling location Pšata

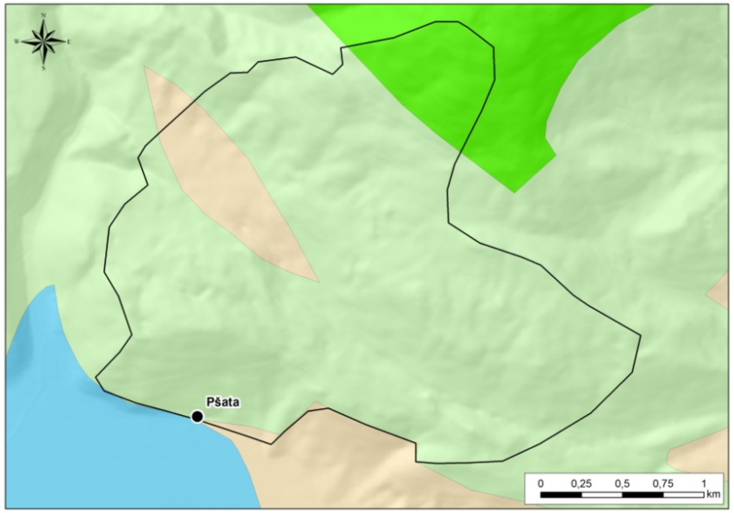

Sampling location Pšata (IAH classification)

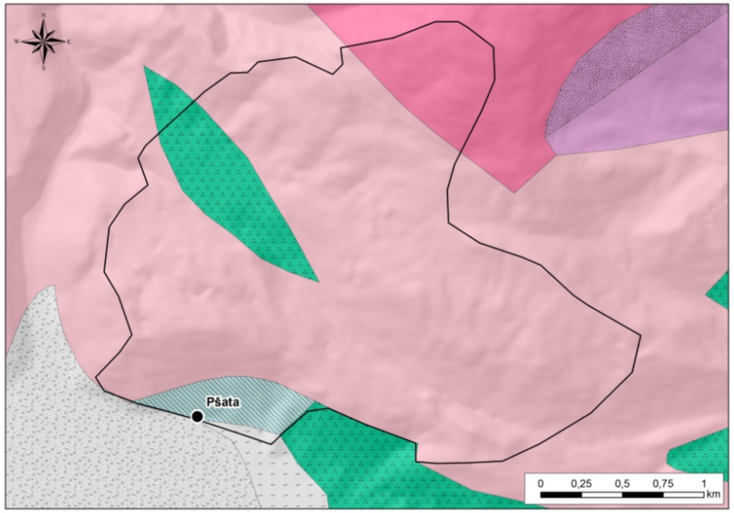

Sampling location Pšata (Geological classification)

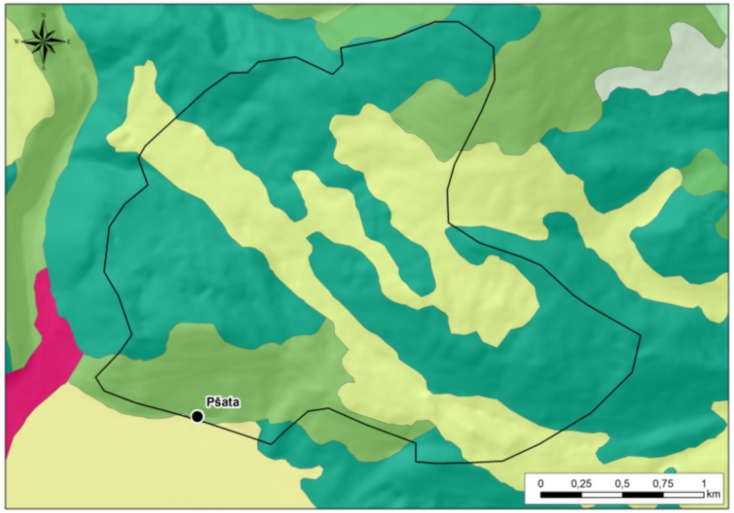

Sampling location Pšata (CLC classification)

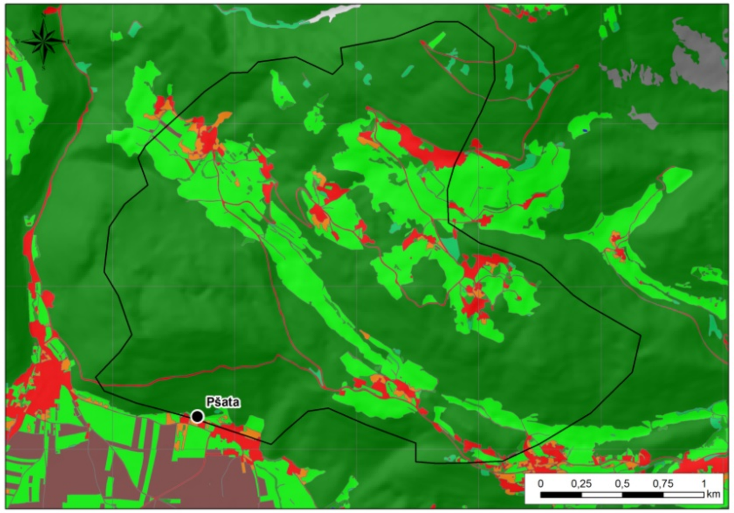

Sampling location Pšata (Land use classification)

Radešica

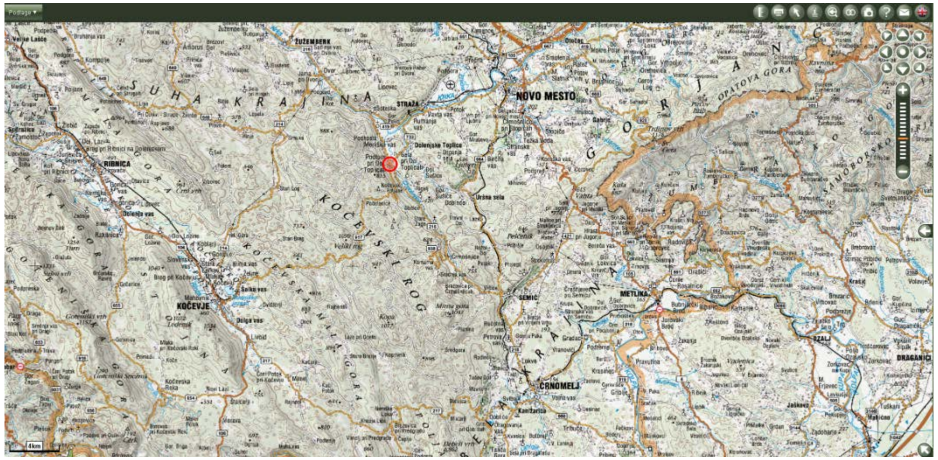

Sampling location Radeščica

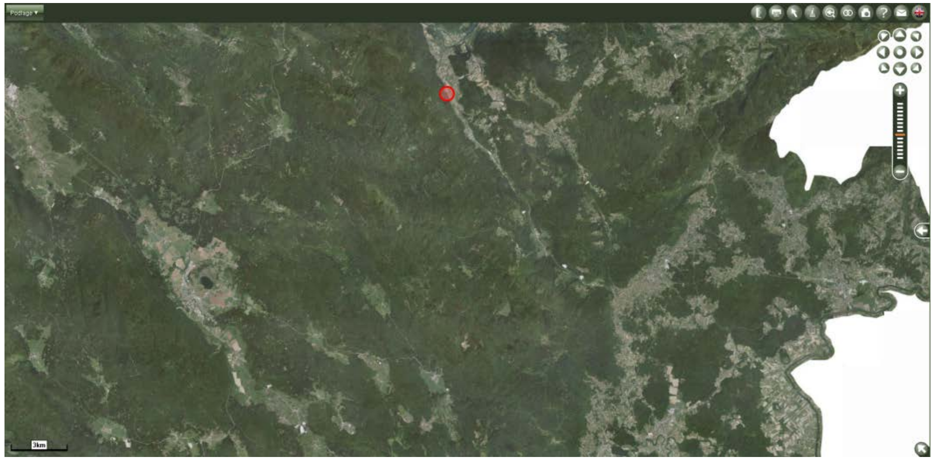

Sampling location Radeščica – PREVERI ZALEDJE ????

Sampling location Radeščica

Sampling location Radeščica

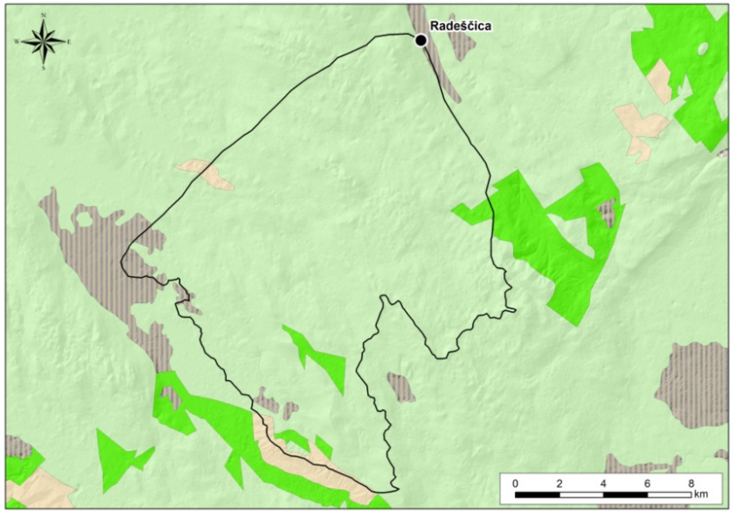

Sampling location Radeščica (IAH classification)

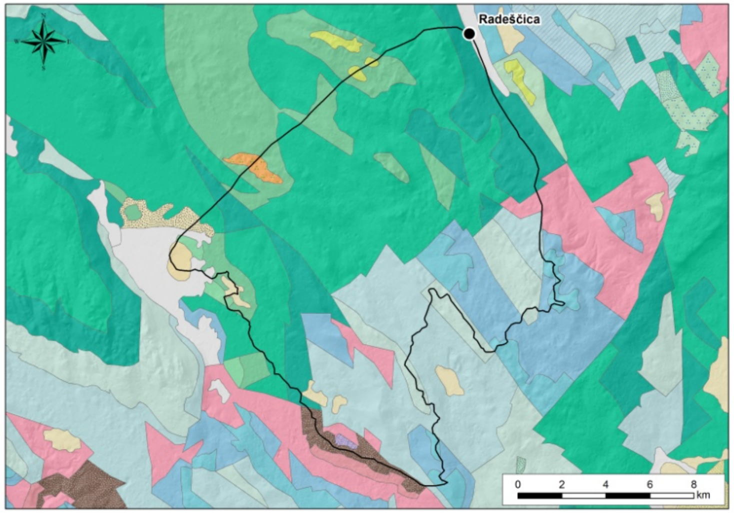

Sampling location Radeščica (Geological classification)

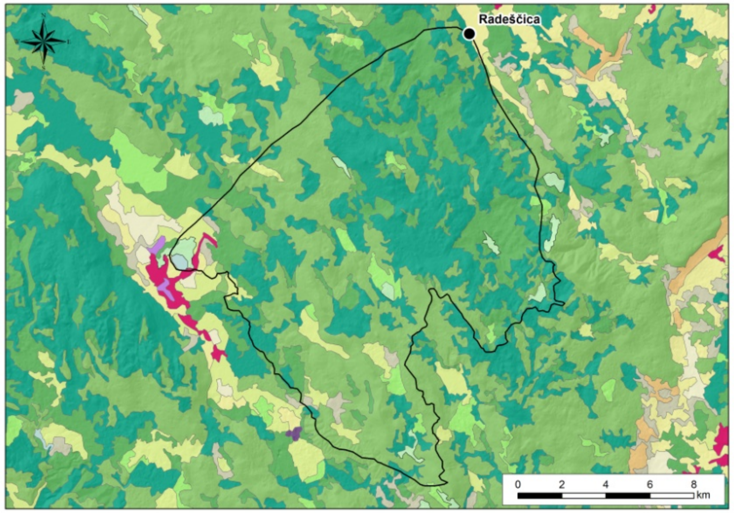

Sampling location Radeščica (CLC classification)

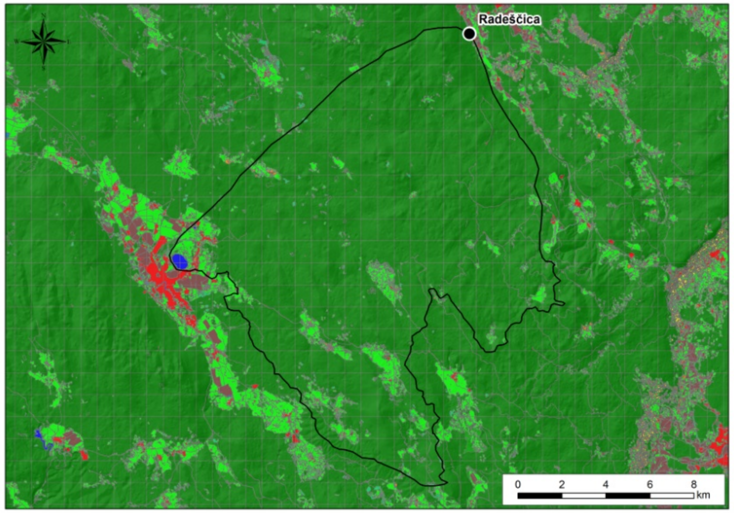

Sampling location Radeščica (Land use classification)

Rakitnica

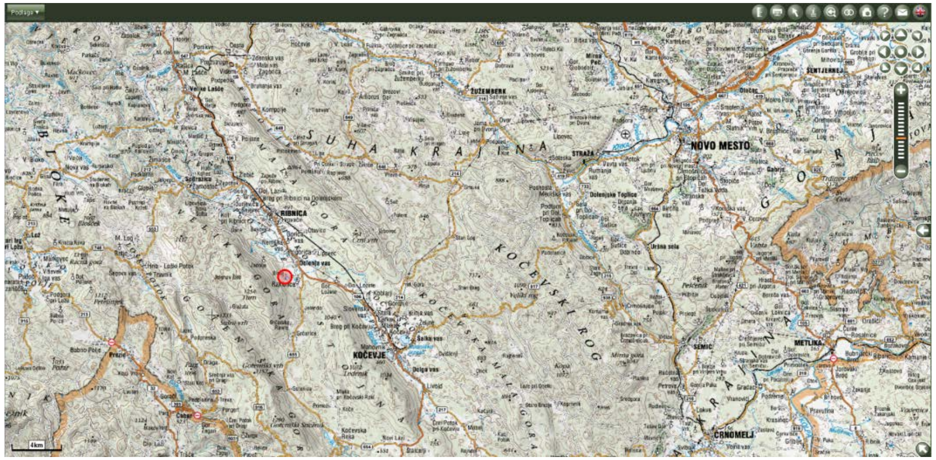

Sampling location Rakitnica

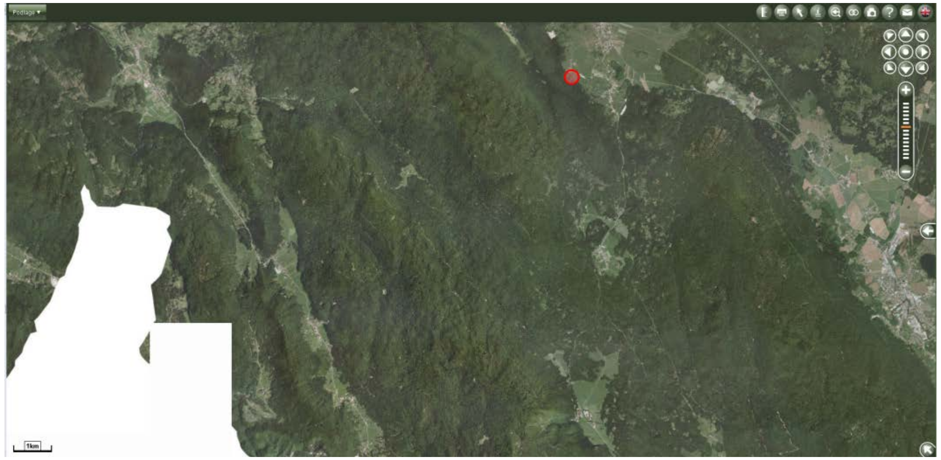

Sampling location Rakitnica

Sampling location Rakitnica

Sampling location Rakitnica

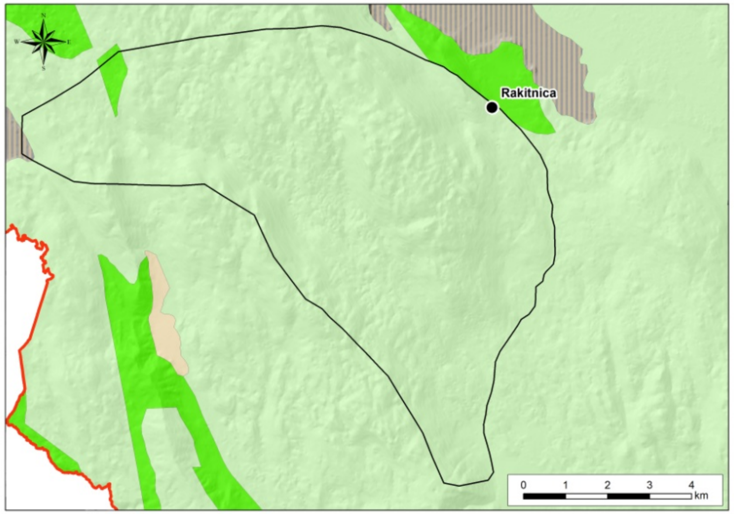

Sampling location Rakitnica (IAH classification)

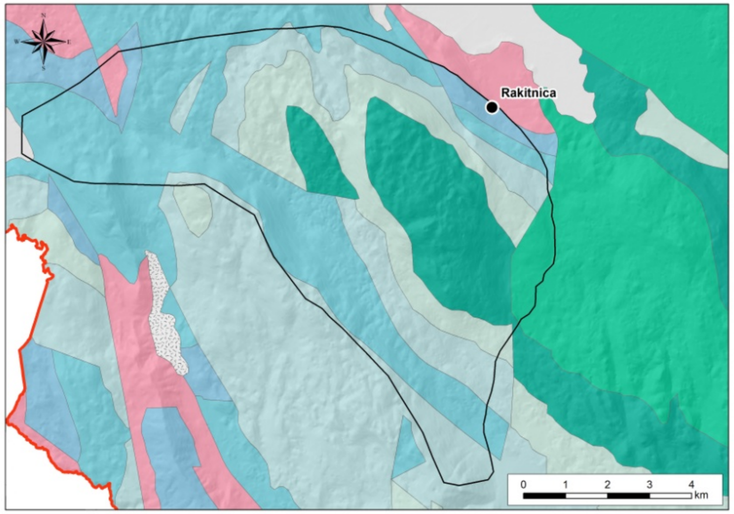

Sampling location Rakitnica (Geological classification)

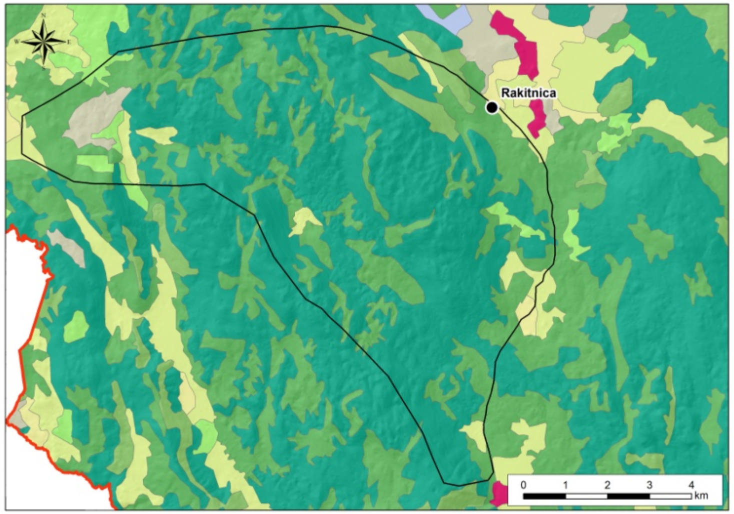

Sampling location Rakitnica (CLC classification)

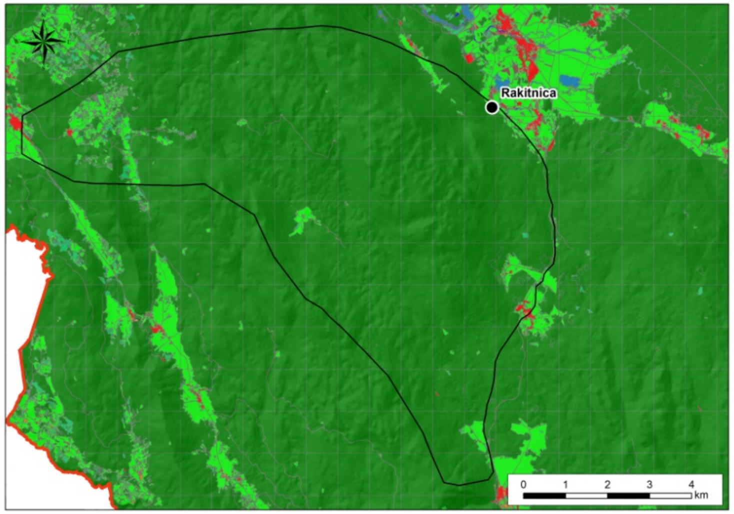

Sampling location Rakitnica (Land use classification)

Rižana

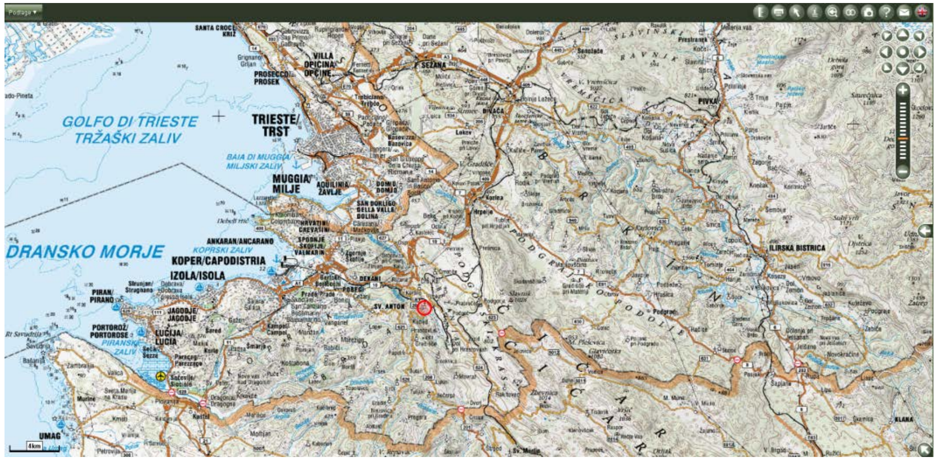

Sampling location Rižana

Sampling location Rižana

Sampling location Rižana

Sampling location Rižana

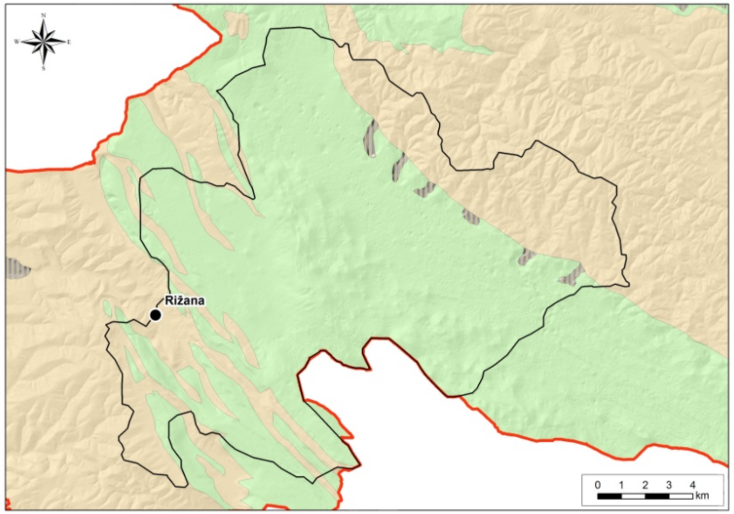

Sampling location Rižana (IAH classification)

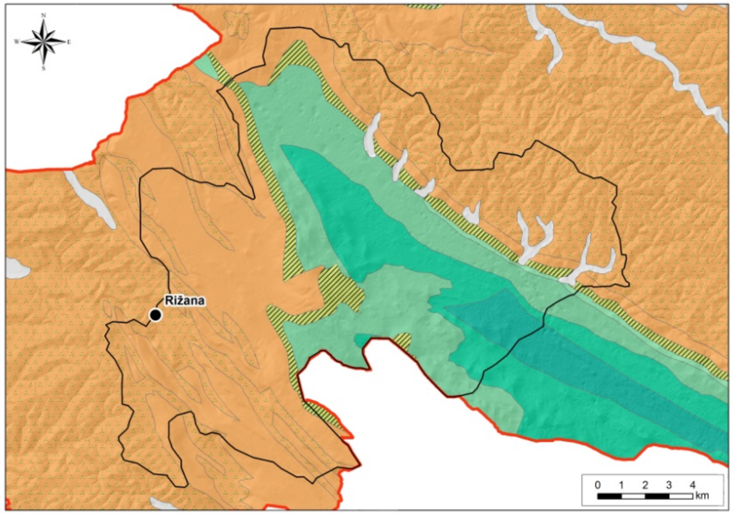

Sampling location Rižana (Geological classification)

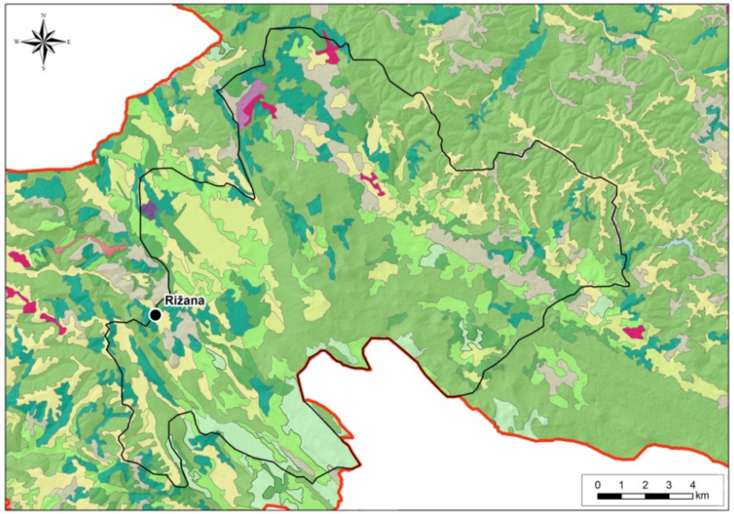

Sampling location Rižana (CLC classification)

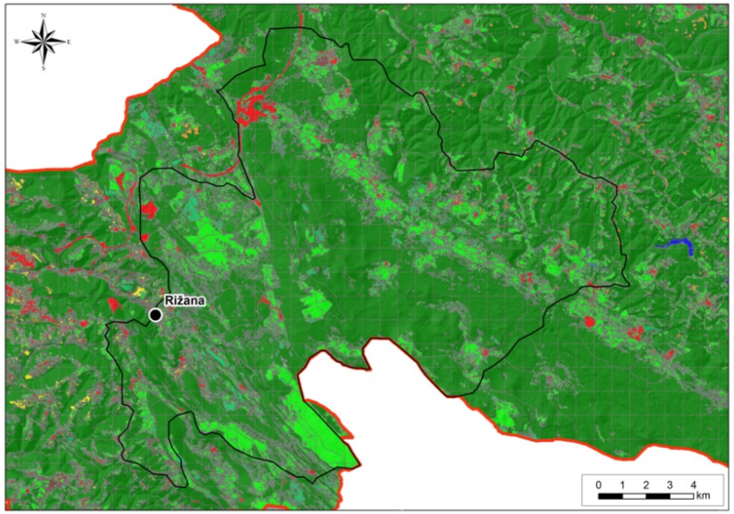

Sampling location Rižana (Land use classification)

Savica

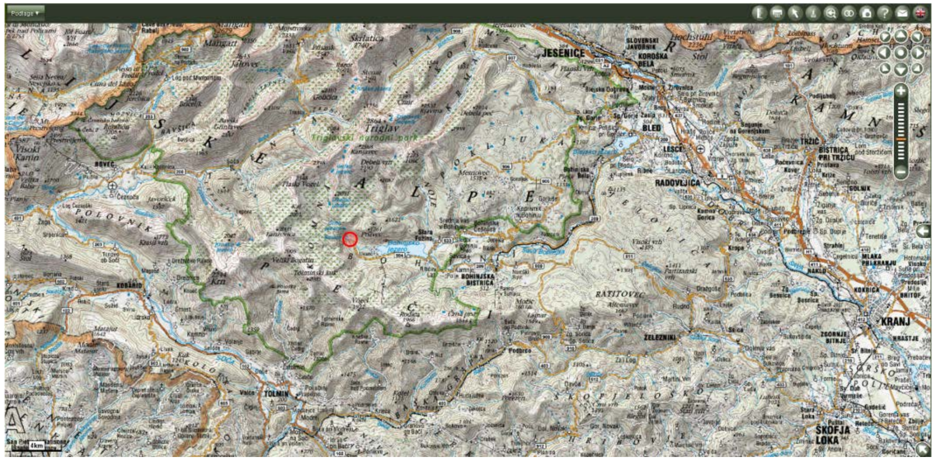

Sampling location Savica

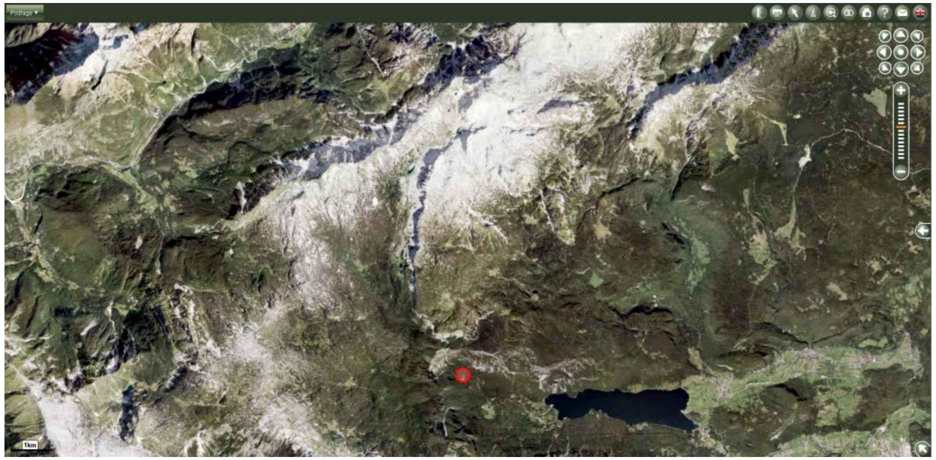

Sampling location Savica

Sampling location Savica

Sampling location Savica

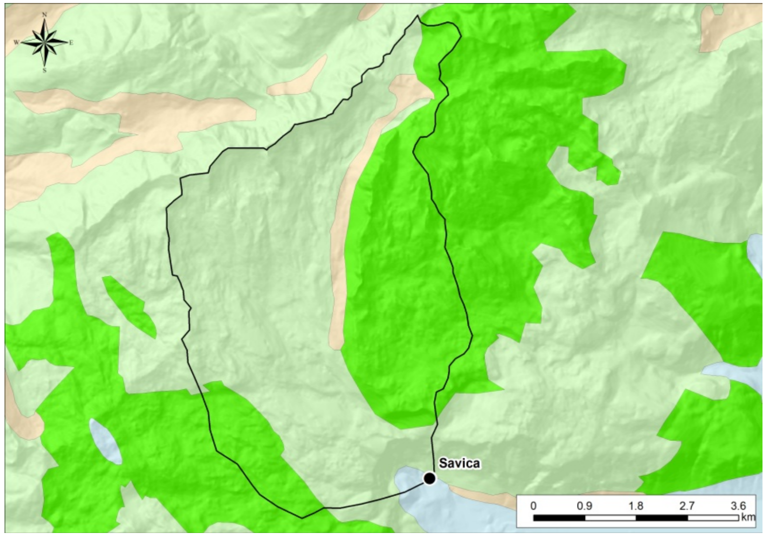

Sampling location Savica (IAH classification)

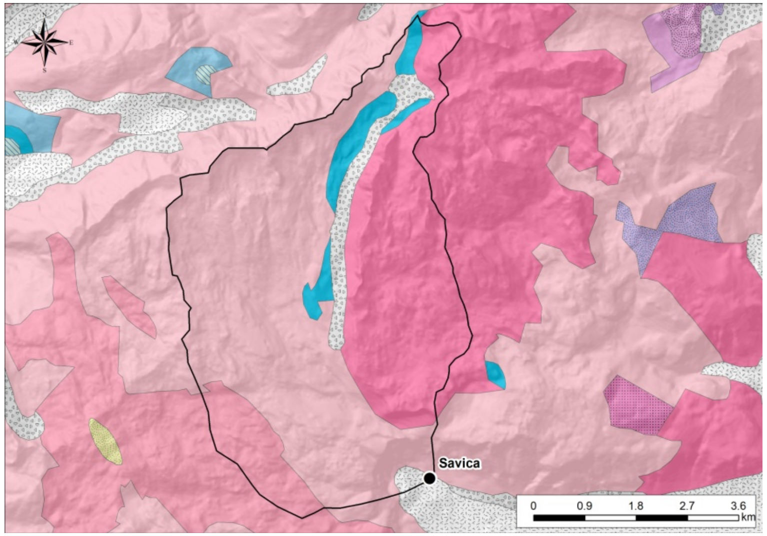

Sampling location Savica (Geological classification)

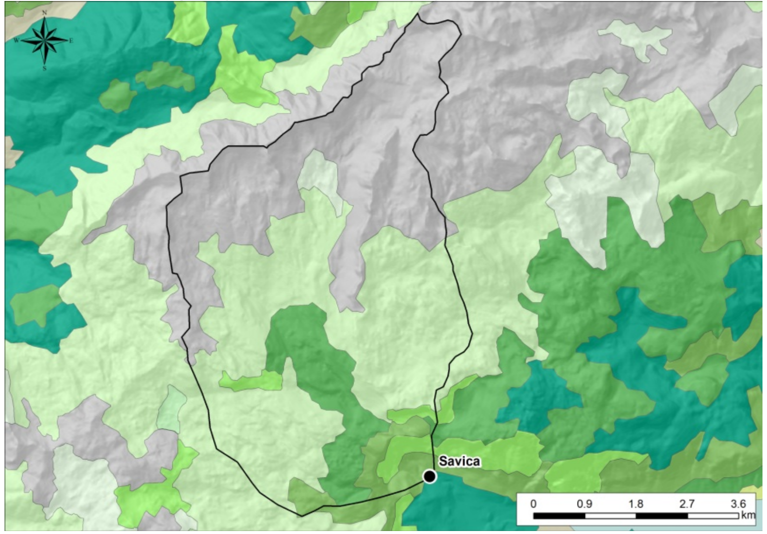

Sampling location Savica (CLC classification)

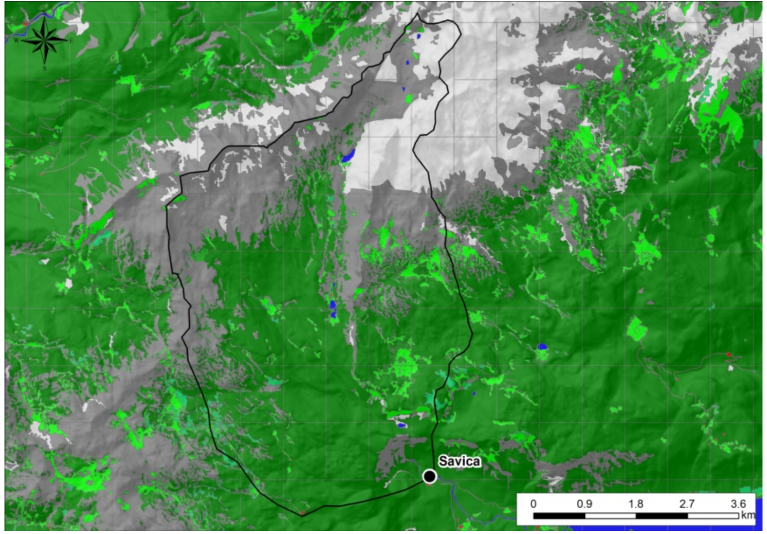

Sampling location Savica (Land use classification)

Sevšek

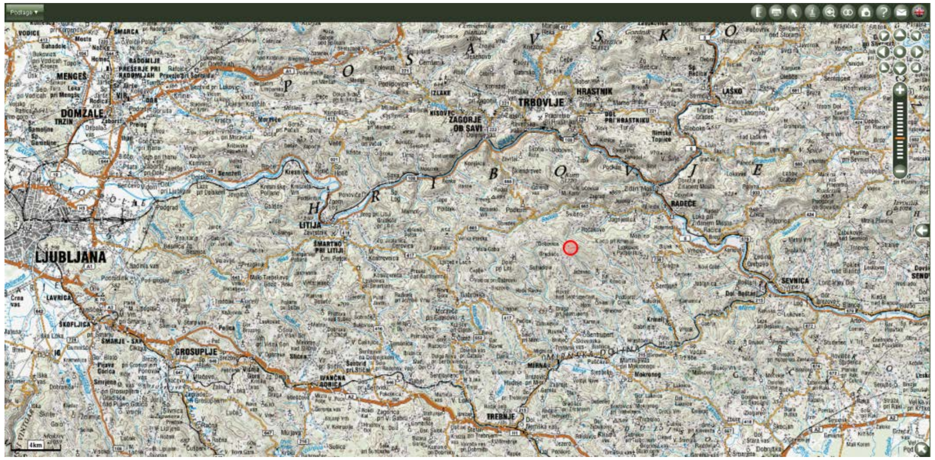

Sampling location Sevšek

Sampling location Sevšek

Sampling location Sevšek

Sampling location Sevšek

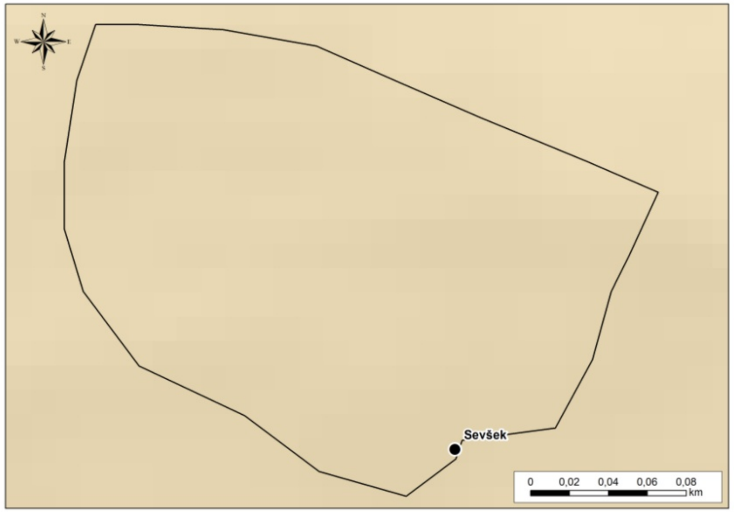

Sampling location Sevšek (IAH classification)

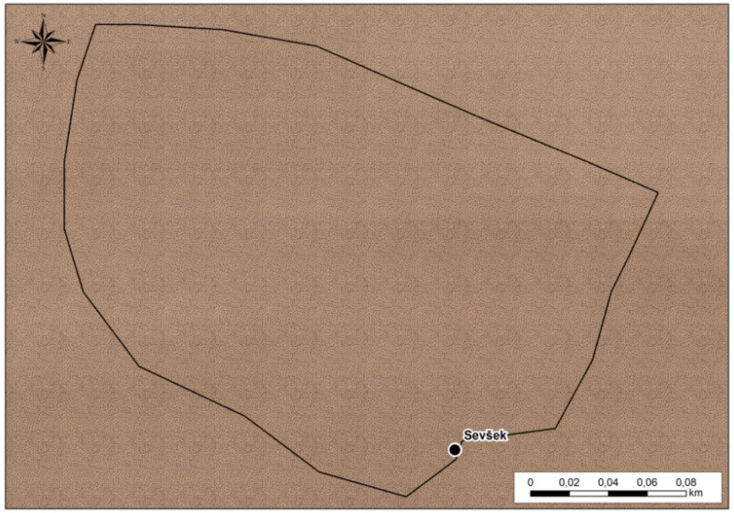

Sampling location Sevšek (Geological classification)

Sampling location Sevšek (CLC classification)

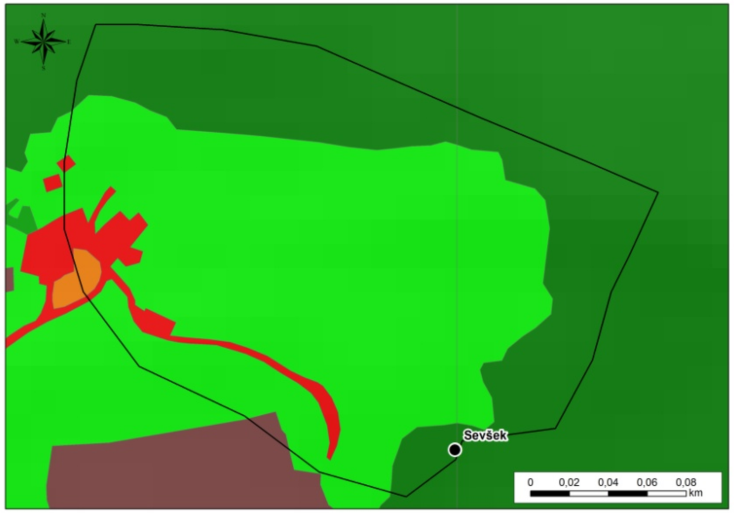

Sampling location Sevšek (Land use classification)

Soča

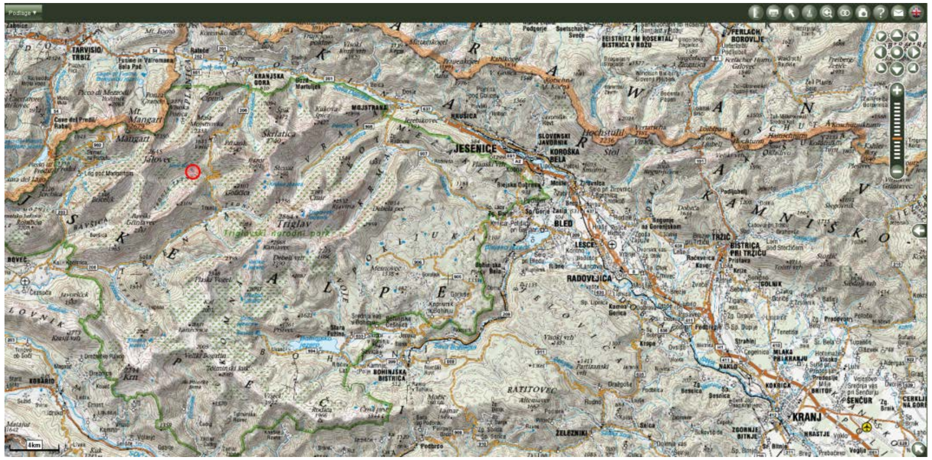

Sampling location Soča

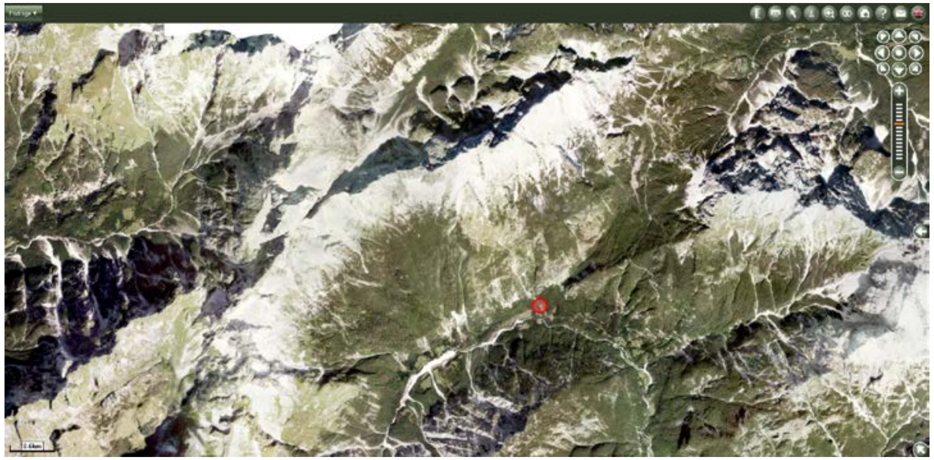

Sampling location Soča

Sampling location Soča

Sampling location Soča

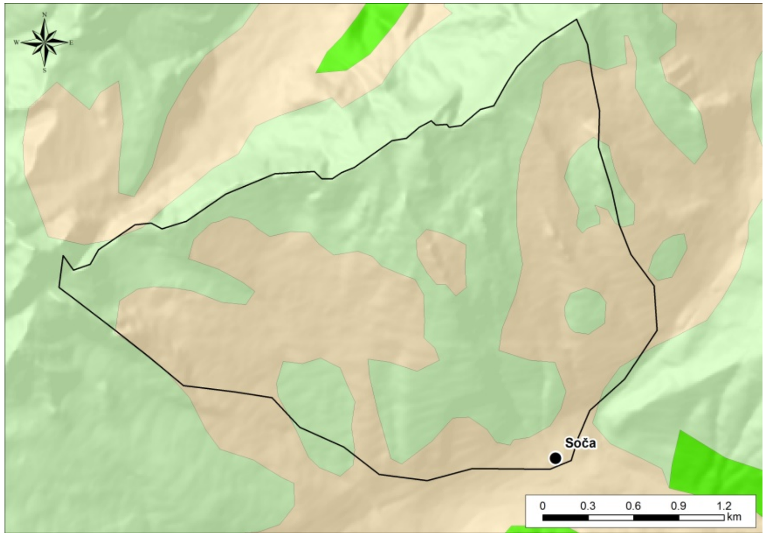

Sampling location Soča (IAH classification)

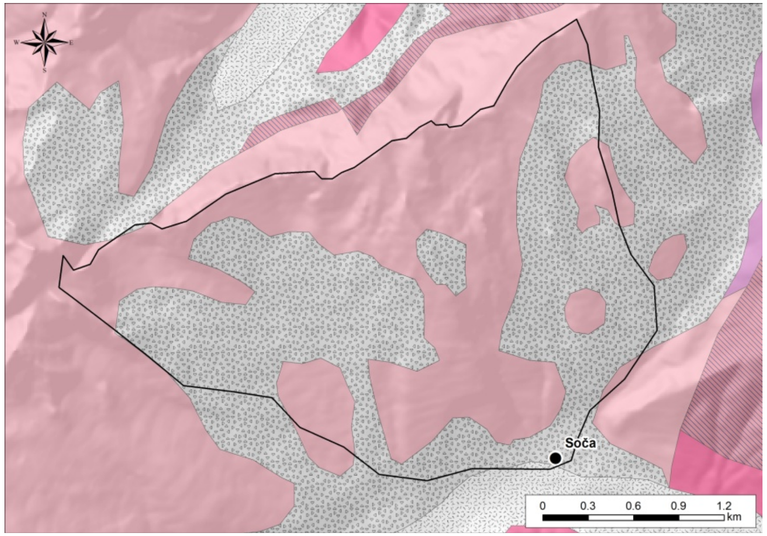

Sampling location Soča (Geological classification)

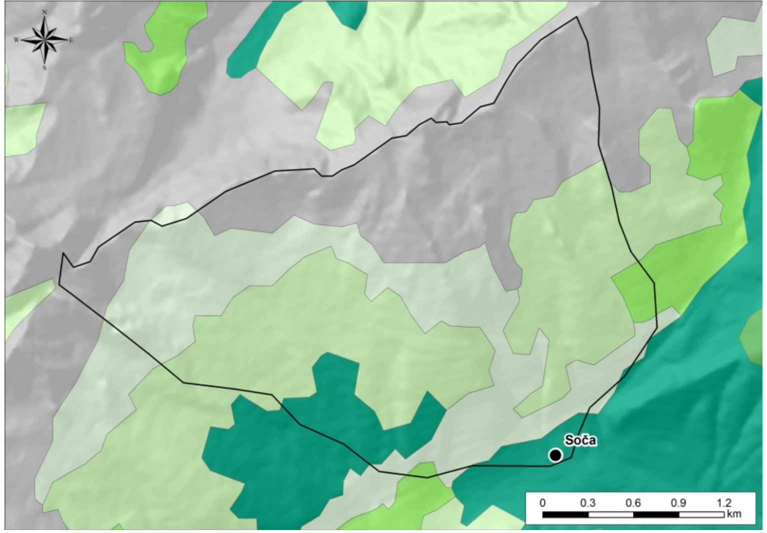

Sampling location Soča (CLC classification)

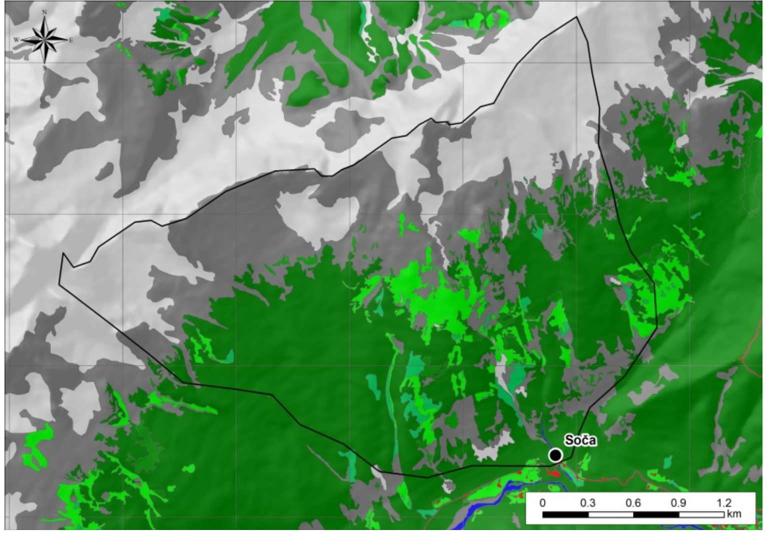

Sampling location Soča (Land use classification)

Strahinec

Sampling location Strahinec

Sampling location Strahinec

Sampling location Strahinec

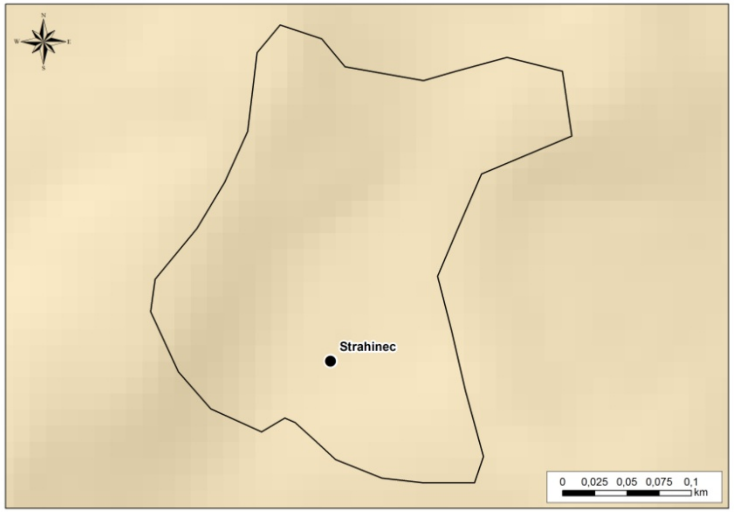

Sampling location Strahinec (IAH classification)

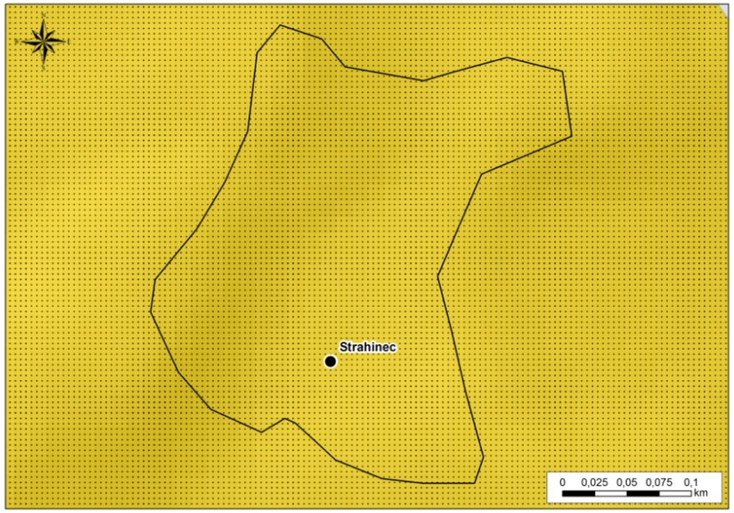

Sampling location Strahinec (Geological classification)

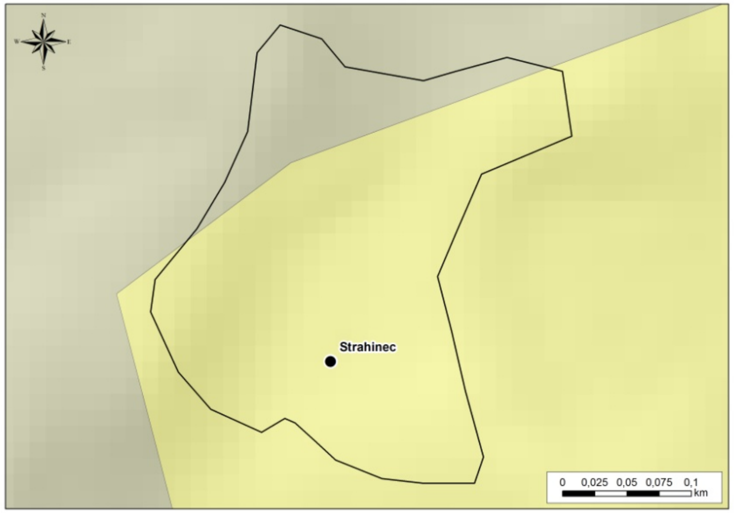

Sampling location Strahinec (CLC classification)

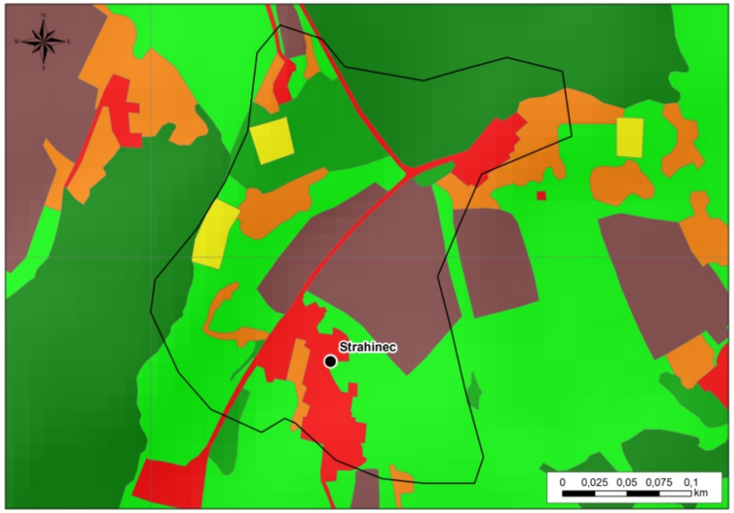

Sampling location Strahinec (Land use classification)

Ščetar

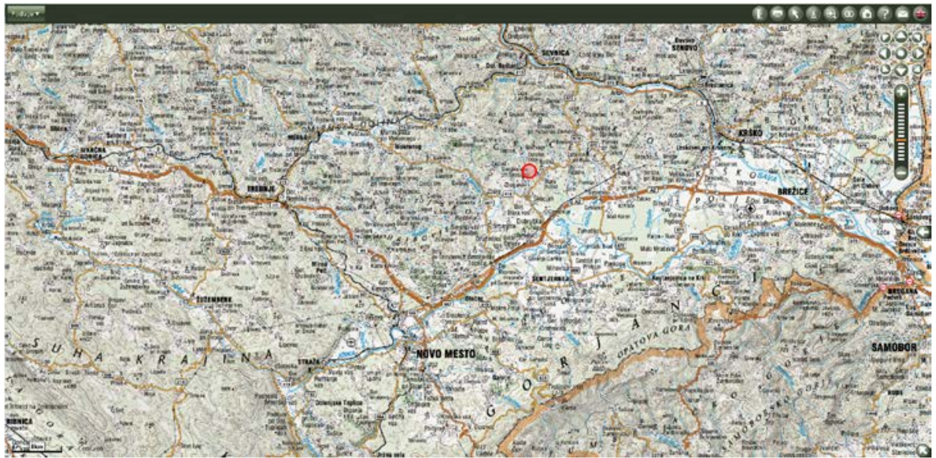

Sampling location Ščetar

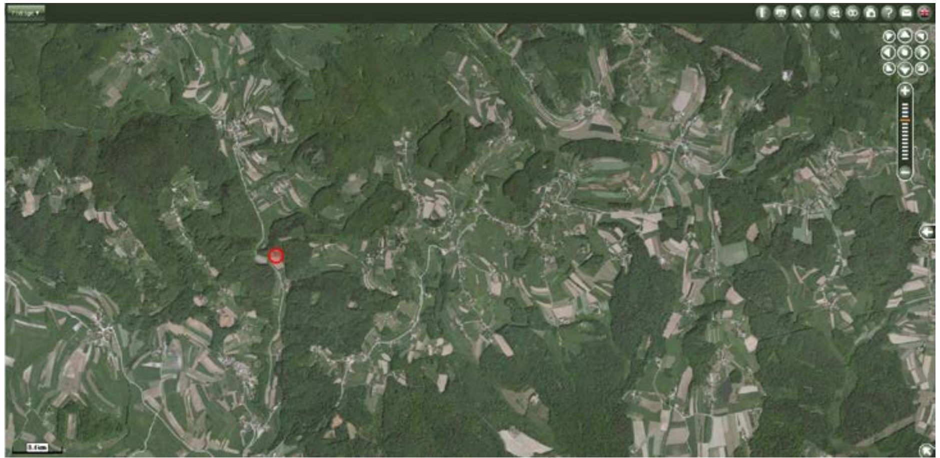

Sampling location Ščetar

Sampling location Ščetar

Sampling location Ščetar

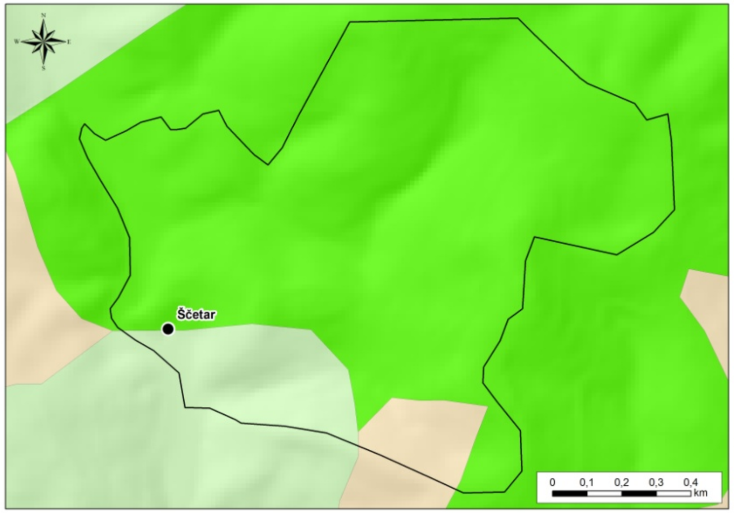

Sampling location Ščetar (IAH classification)

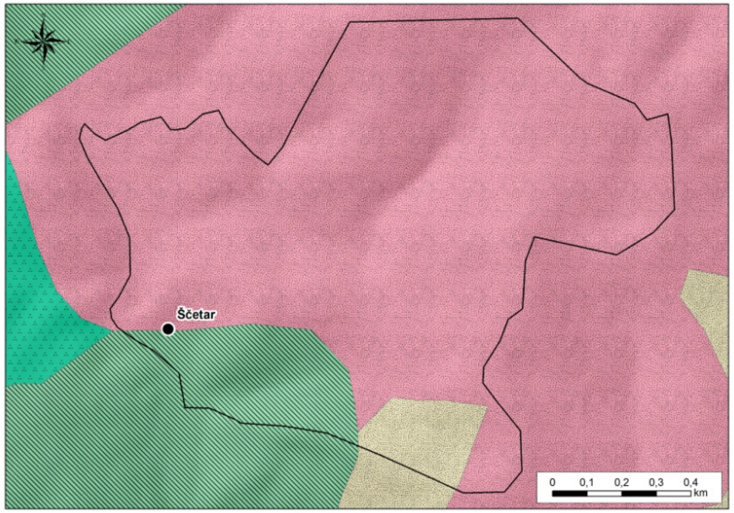

Sampling location Ščetar (Geological classification)

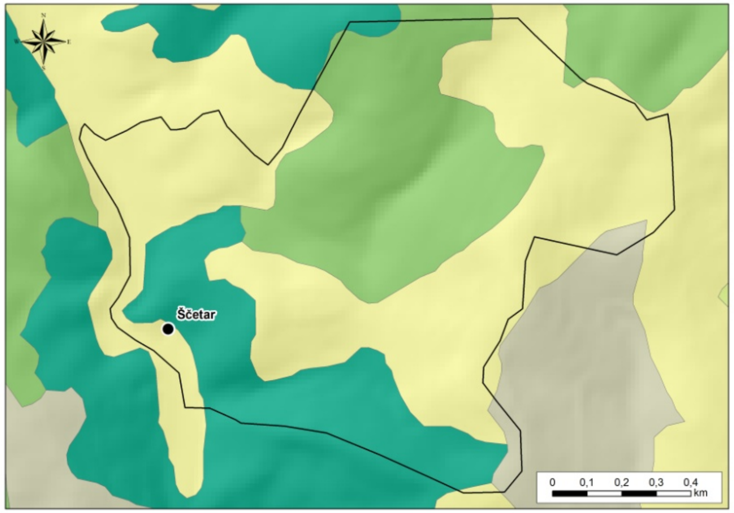

Sampling location Ščetar (CLC classification)

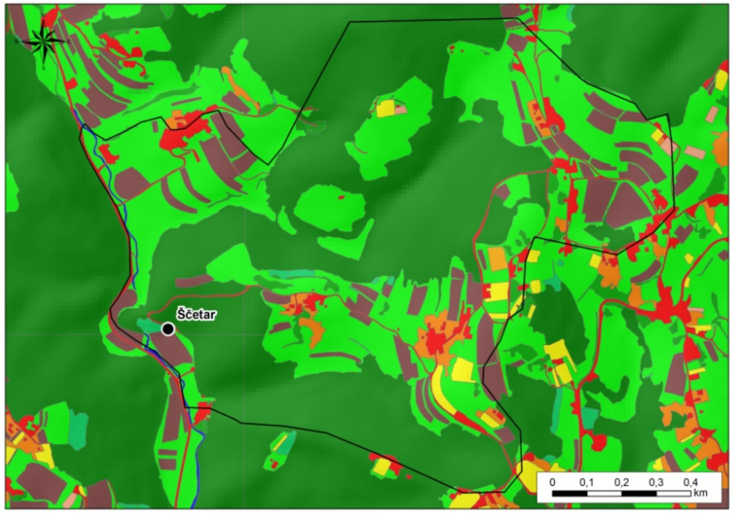

Sampling location Ščetar (Land use classification)

Šempeter 0840

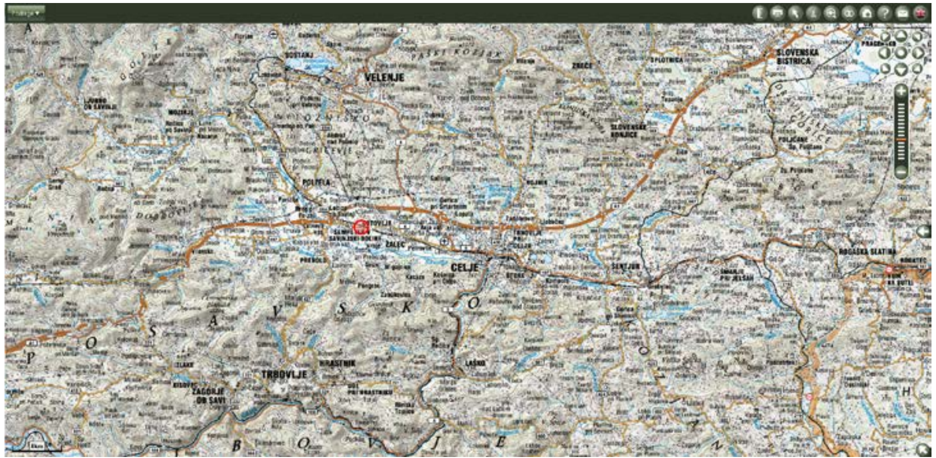

Sampling location Šempeter 0840

Sampling location Šempeter 0840

Sampling location Šempeter 0840

Sampling location Šempeter 0840

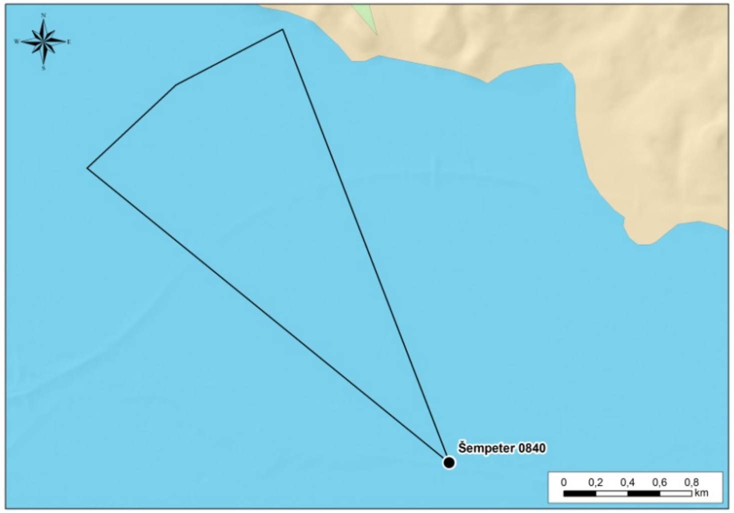

Sampling location Šempeter 0840 (IAH classification)

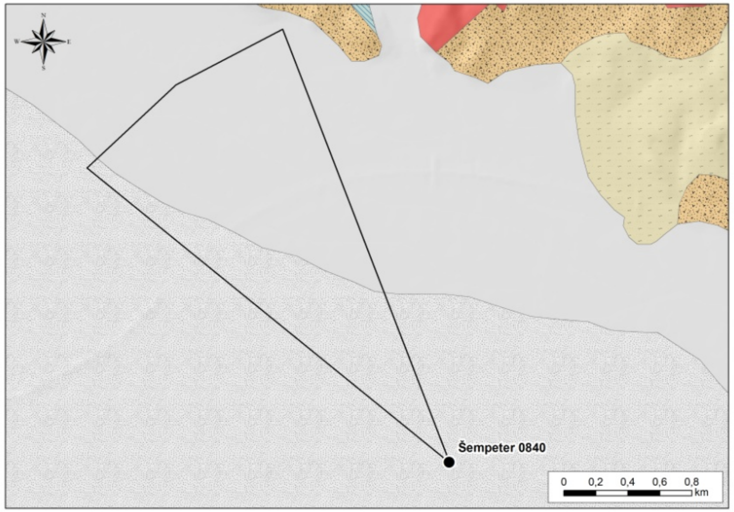

Sampling location Šempeter 0840 (Geological classification)

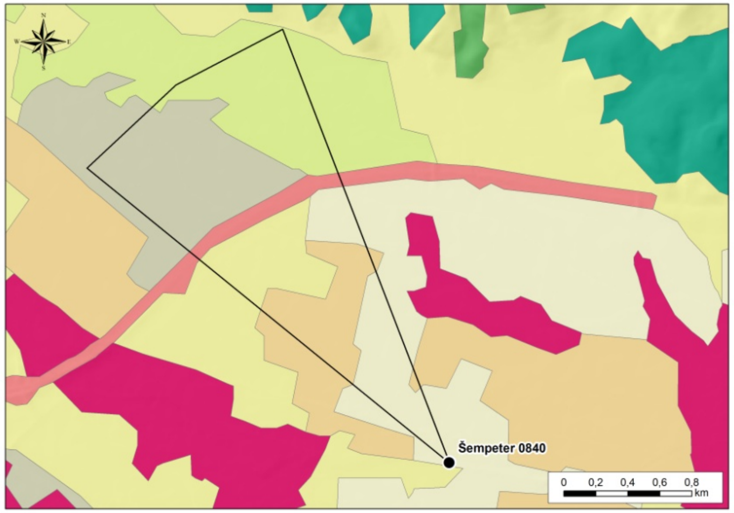

Sampling location Šempeter 0840 (CLC classification)

Sampling location Šempeter 0840 (Land use classification)

Šumec

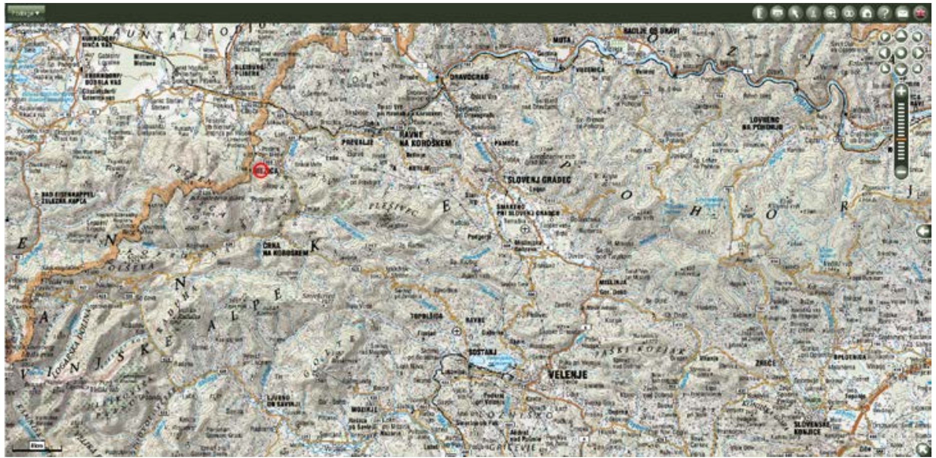

Sampling location Šumec

Sampling location Šumec

Sampling location Šumec

Sampling location Šumec

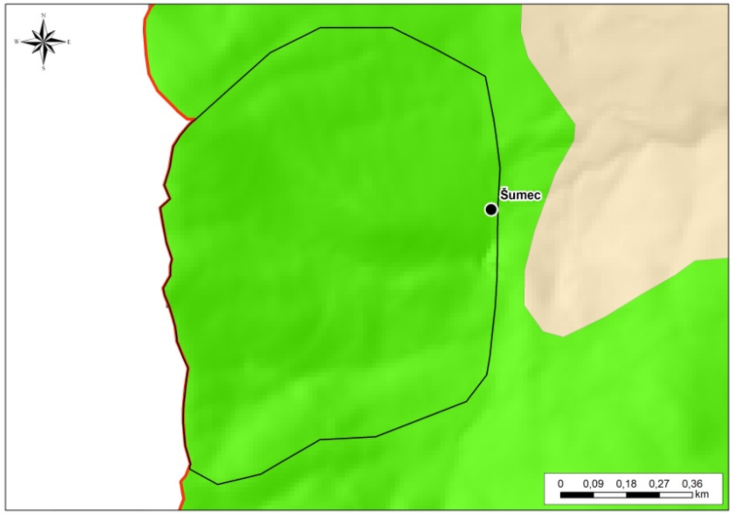

Sampling location Šumec (IAH classification)

Sampling location Šumec (Geological classification)

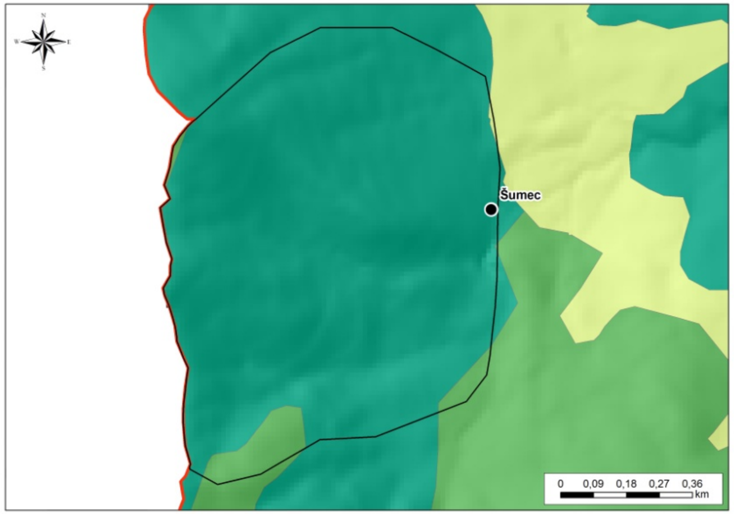

Sampling location Šumec (CLC classification)

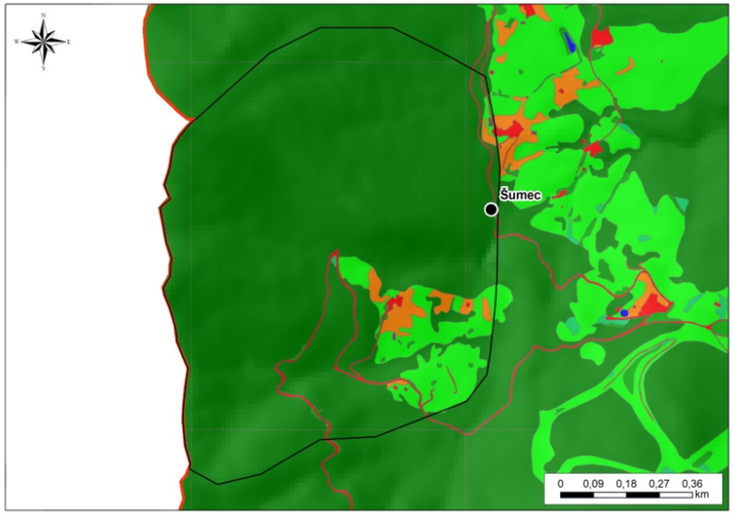

Sampling location Šumec (Land use classification)

Težka voda

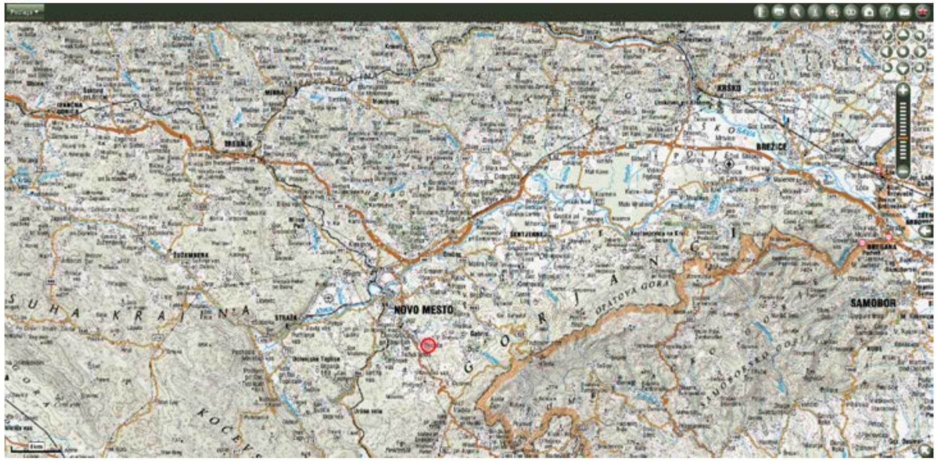

Sampling location Težka voda

Sampling location Težka voda

Sampling location Težka voda

Sampling location Težka voda

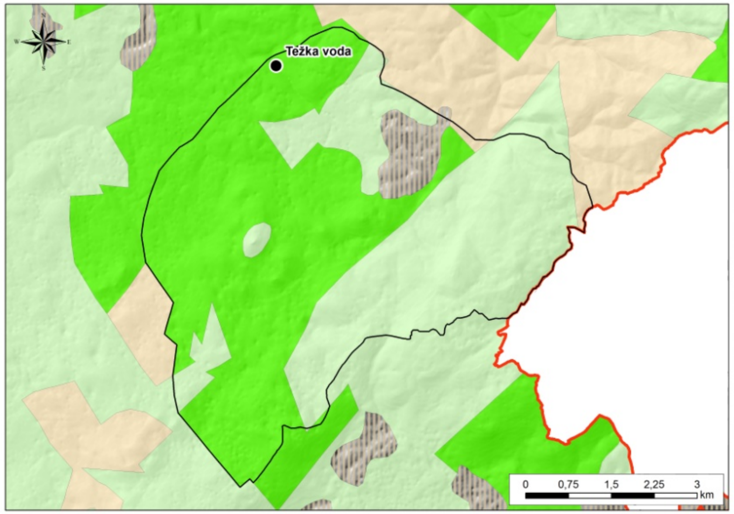

Sampling location Težka voda (IAH classification)

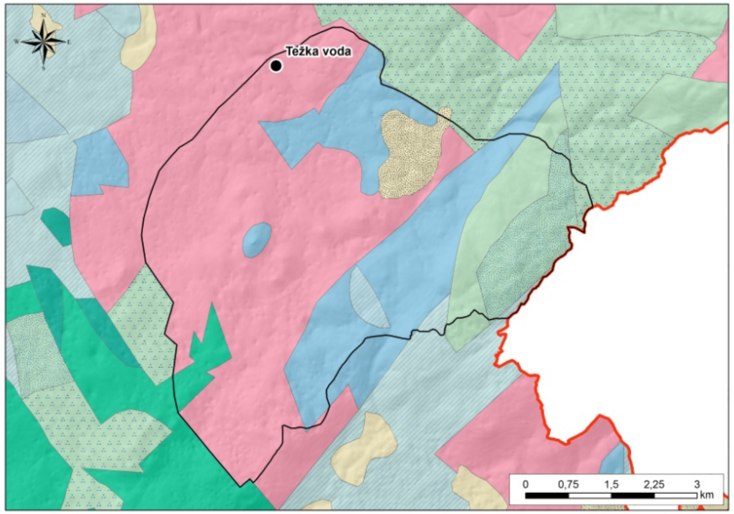

Sampling location Težka voda (Geological classification)

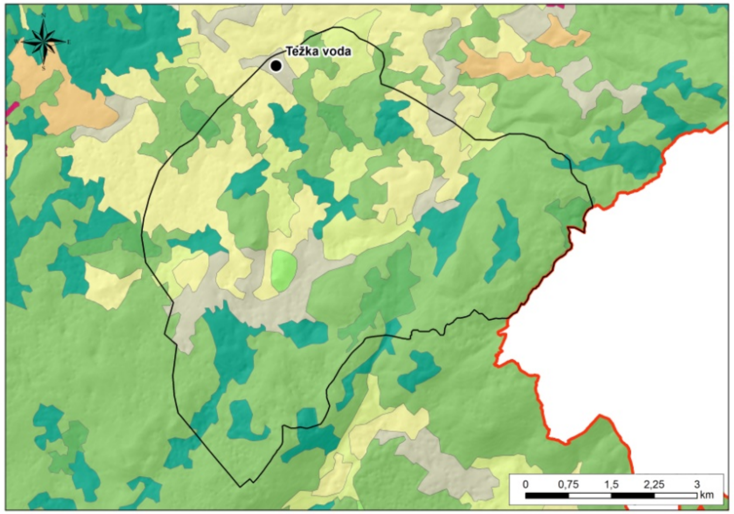

Sampling location Težka voda (CLC classification)

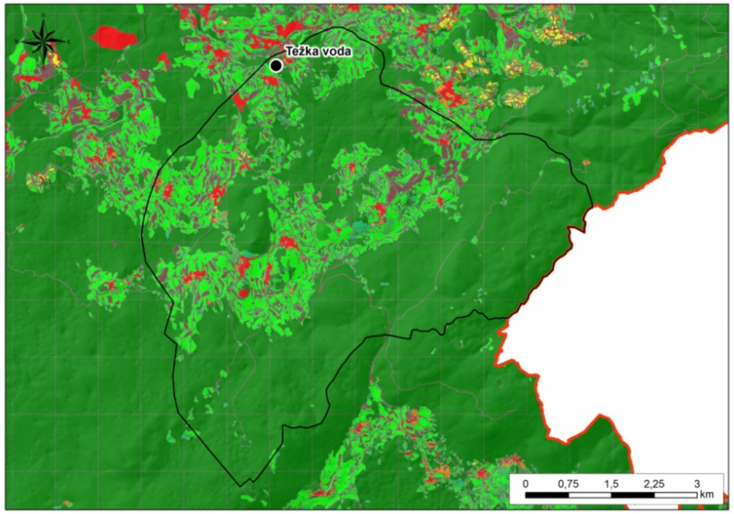

Sampling location Težka voda (Land use classification)

Tominčev Izvir

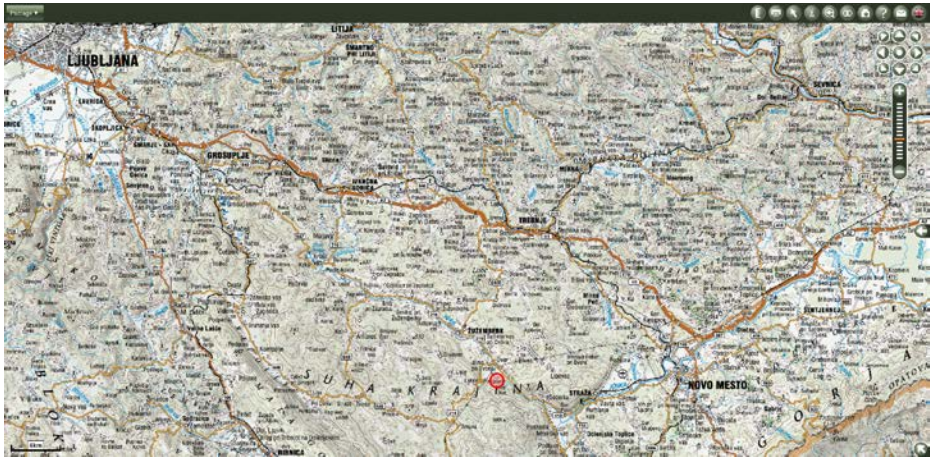

Sampling location Tominčev izvir

Sampling location Tominčev izvir

Sampling location Tominčev izvir

Sampling location Tominčev izvir

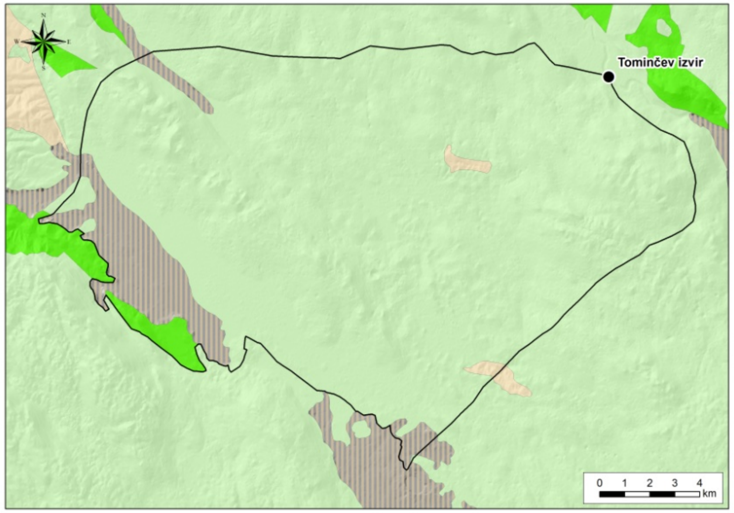

Sampling location Tominčev izvir (IAH classification)

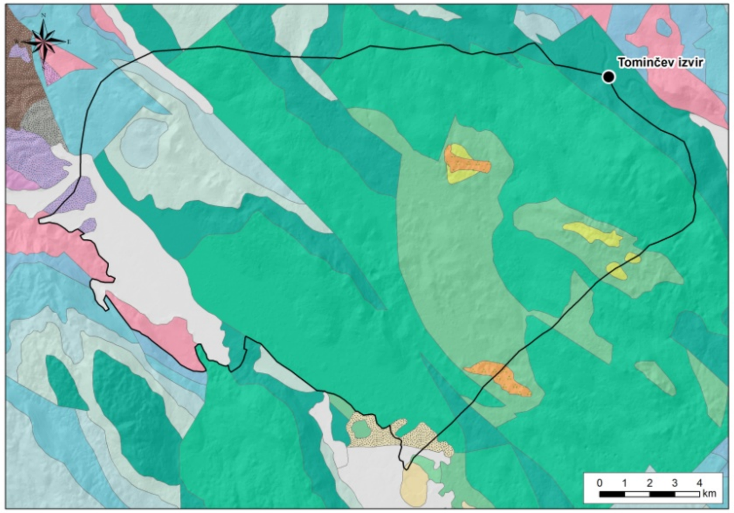

Sampling location Tominčev izvir (Geological classification)

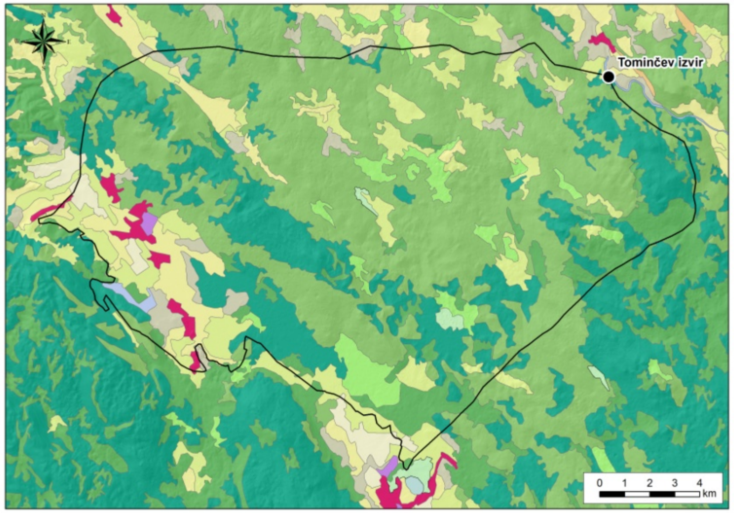

Sampling location Tominčev izvir (CLC classification)

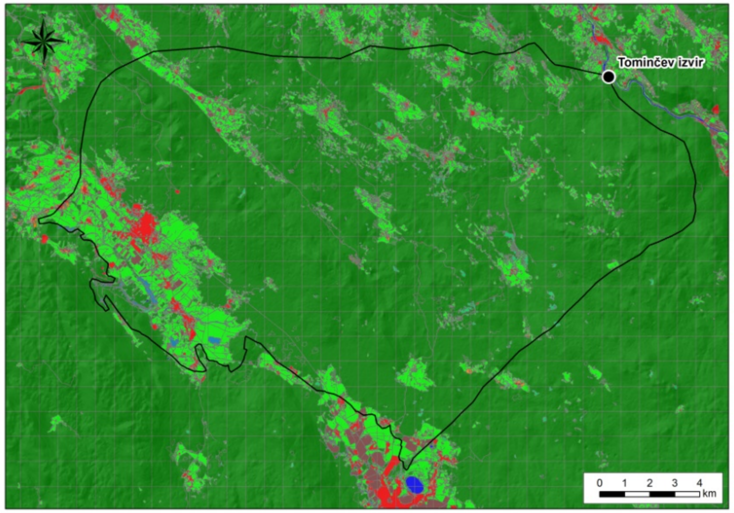

Sampling location Tominčev izvir (Land use classification)

TR-1/99, Trebelno

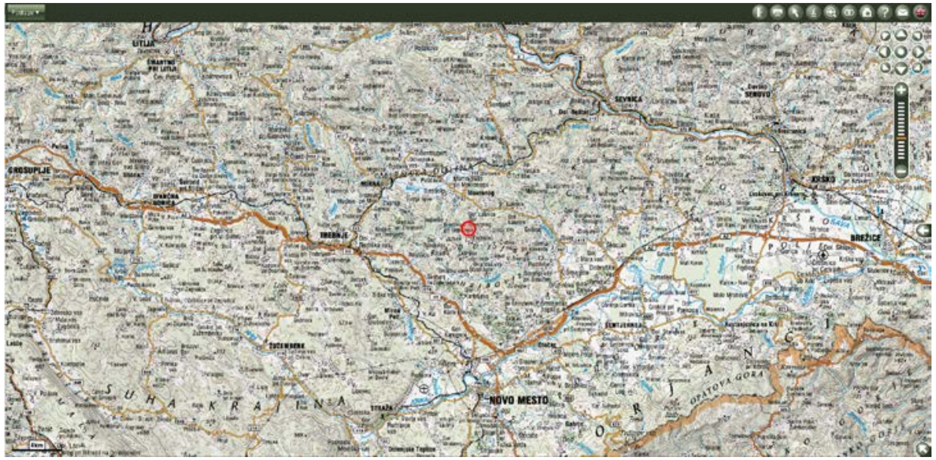

Sampling location TR-1/99, Trebelno

Sampling location TR-1/99, Trebelno

Sampling location TR-1/99, Trebelno

Sampling location TR-1/99, Trebelno

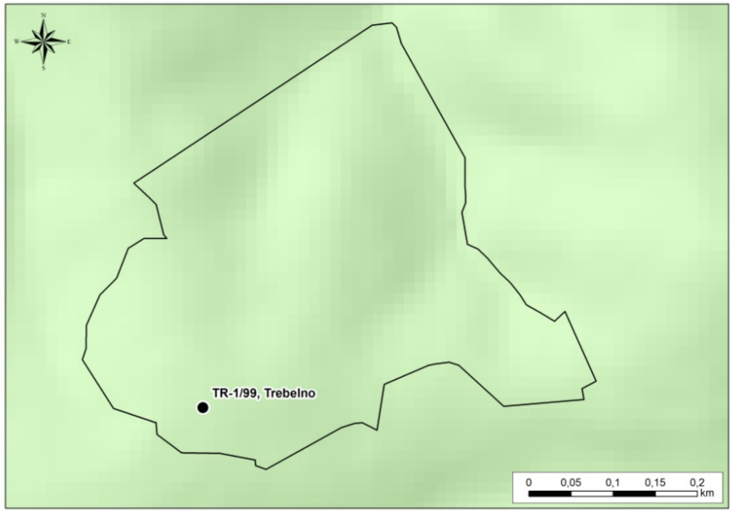

Sampling location TR-1/99, Trebelno (IAH classification)

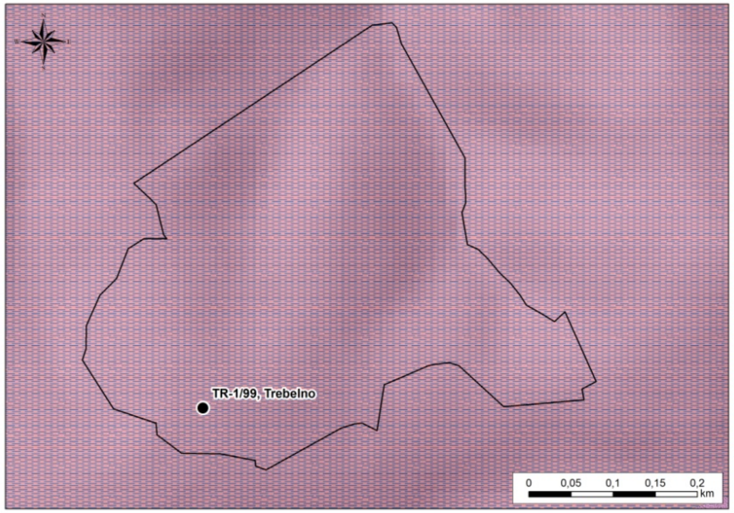

Sampling location TR-1/99, Trebelno (Geological classification)

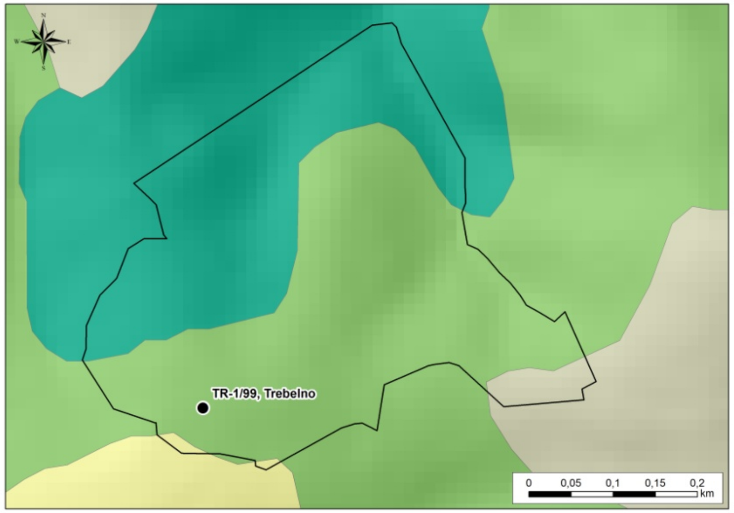

Sampling location TR-1/99, Trebelno (CLC classification)

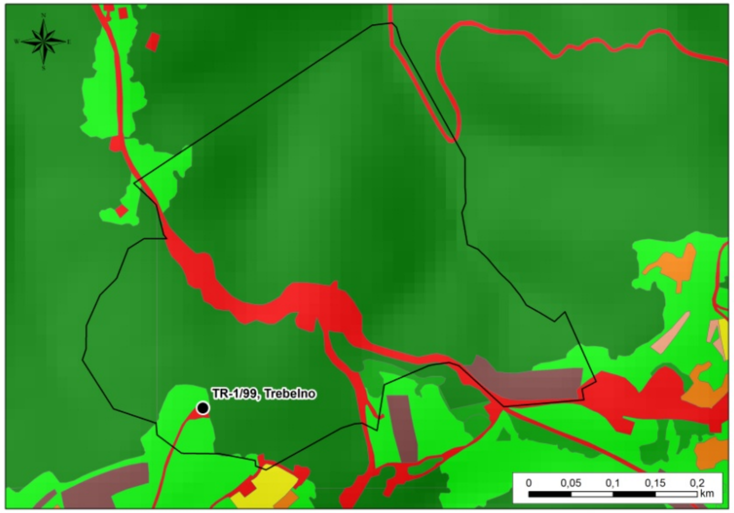

Sampling location TR-1/99, Trebelno (Land use classification)

Trate

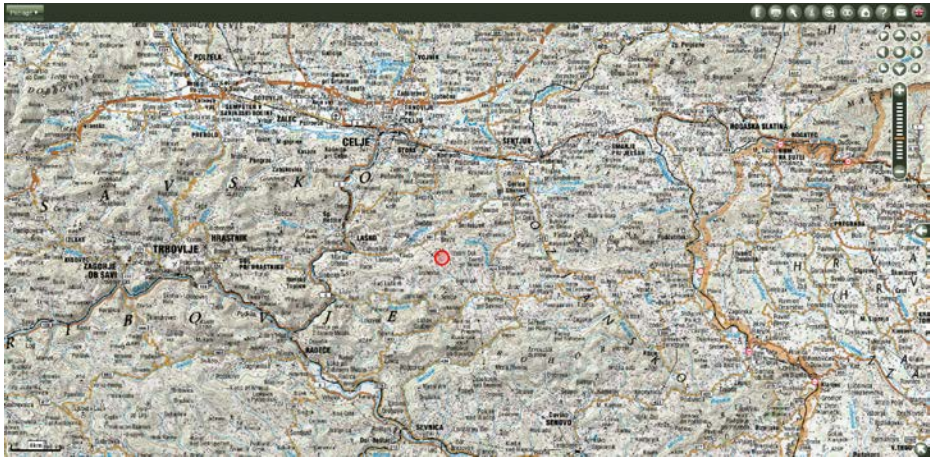

Sampling location Trate

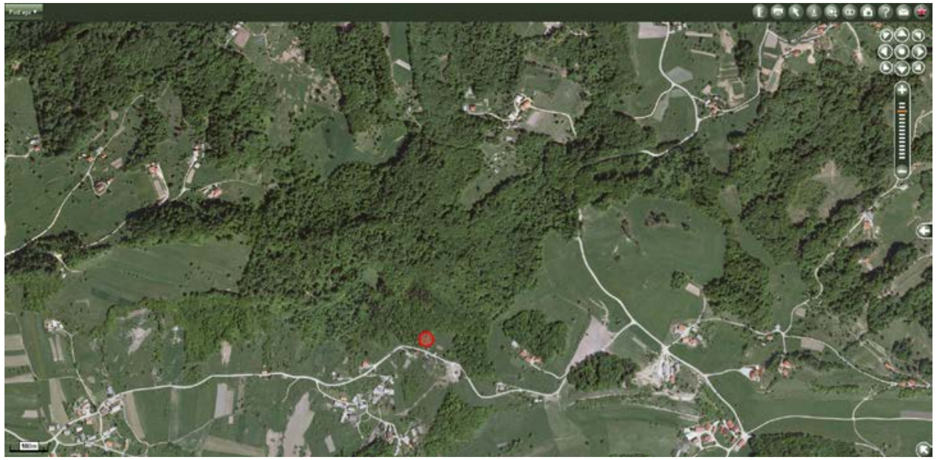

Sampling location Trate

Sampling location Trate

Sampling location Trate

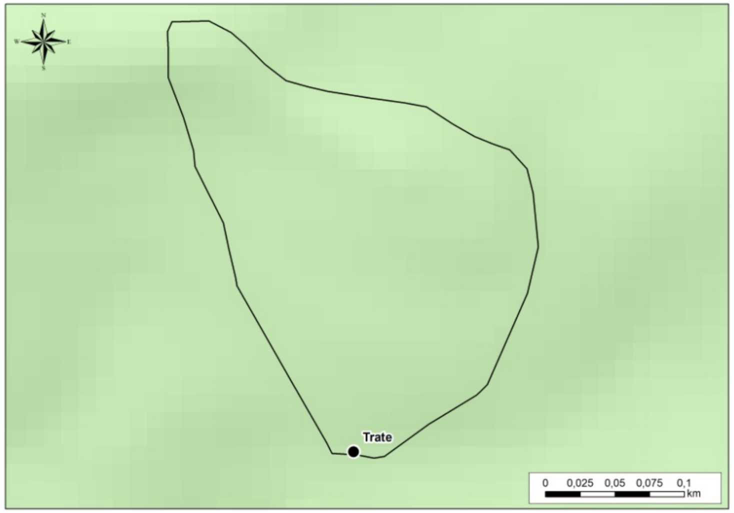

Sampling location Trate (IAH classification)

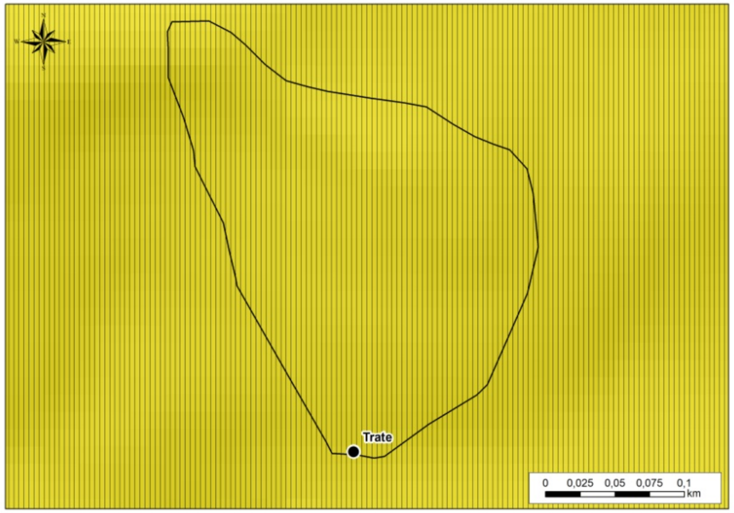

Sampling location Trate (Geological classification)

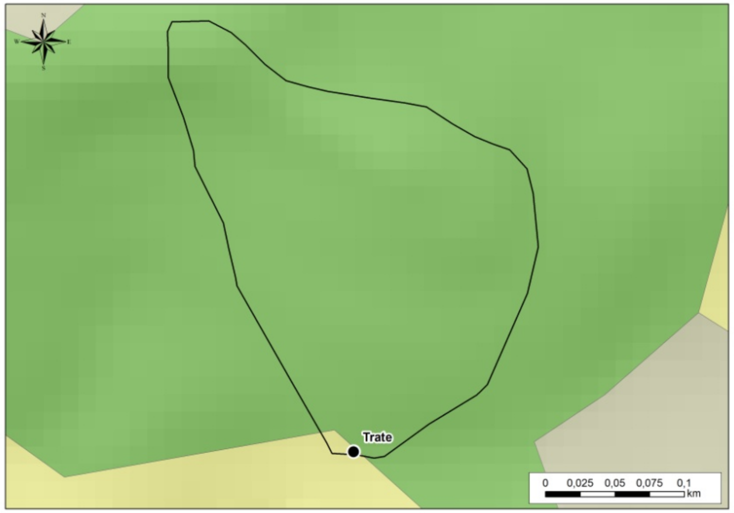

Sampling location Trate (CLC classification)

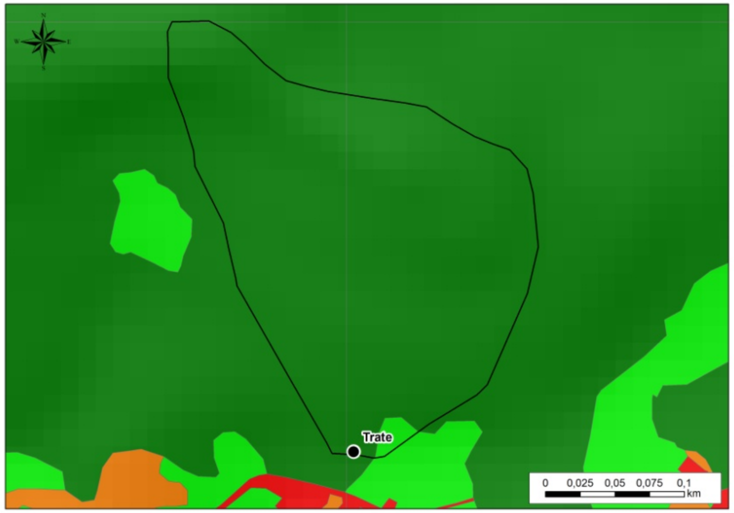

Sampling location Trate (Land use classification)

Trebija

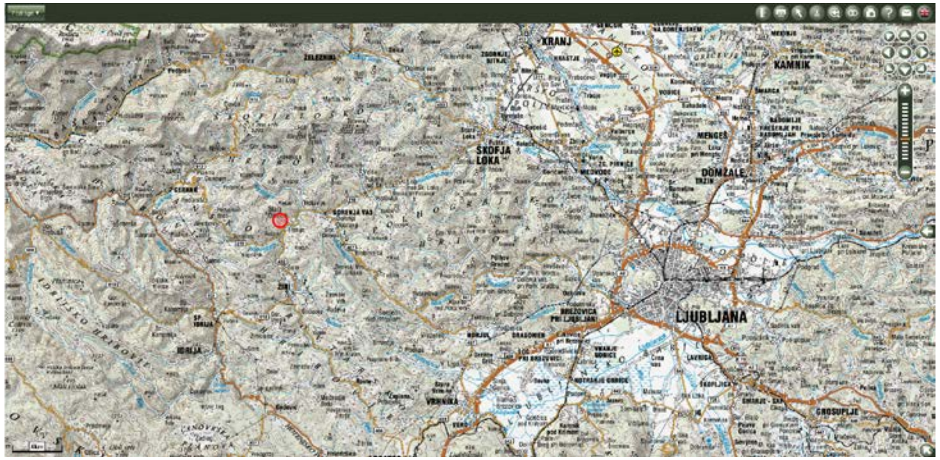

Sampling location Trebija

Sampling location Trebija

Sampling location Trebija

Sampling location Trebija

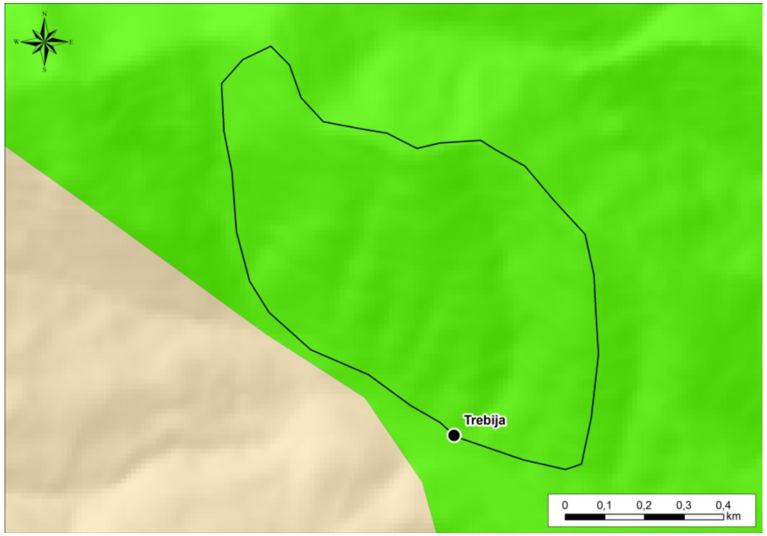

Sampling location Trebija (IAH classification)

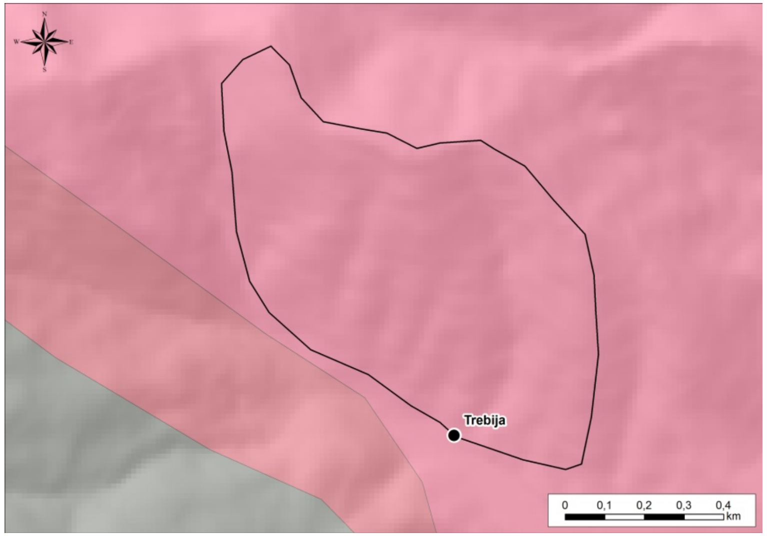

Sampling location Trebija (Geological classification)

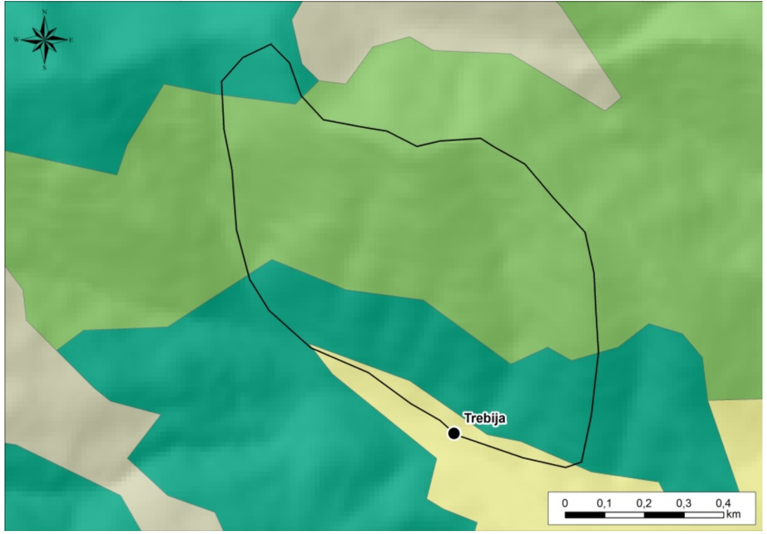

Sampling location Trebija (CLC classification)

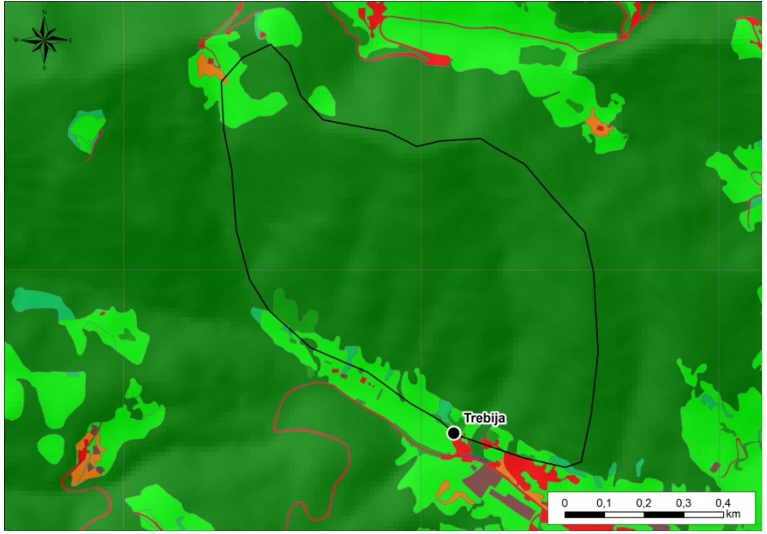

Sampling location Trebija (Land use classification)

Trgovina, Vurberk

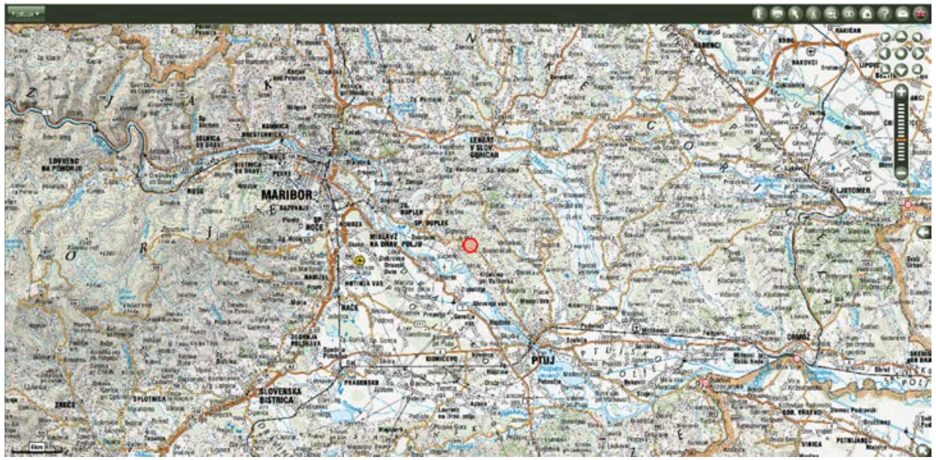

Sampling location Trgovina, Vurberk

Sampling location Trgovina, Vurberk

Sampling location Trgovina, Vurberk

Sampling location Trgovina, Vurberk

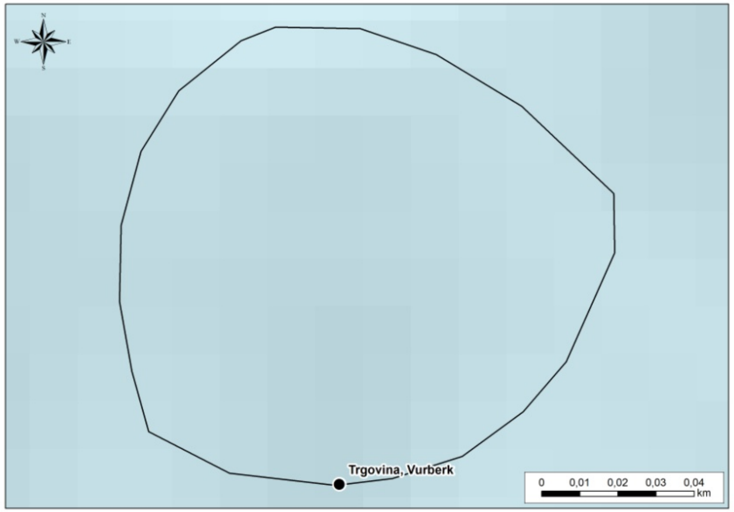

Sampling location Trgovina, Vurberk (IAH classification)

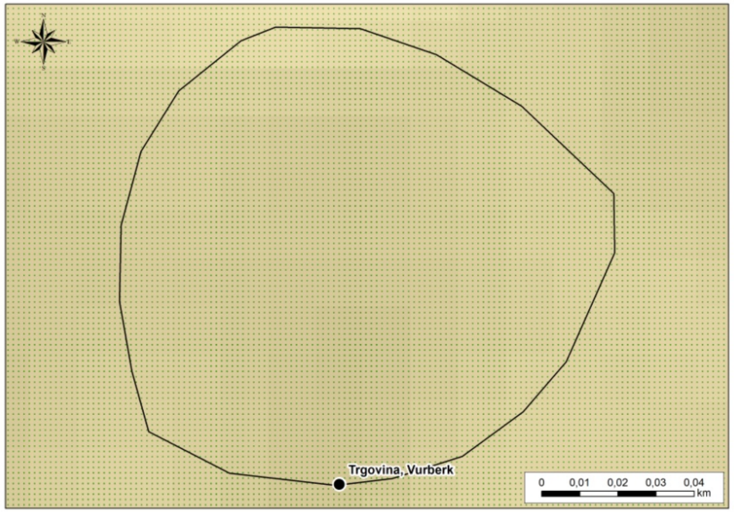

Sampling location Trgovina, Vurberk (Geological classification)

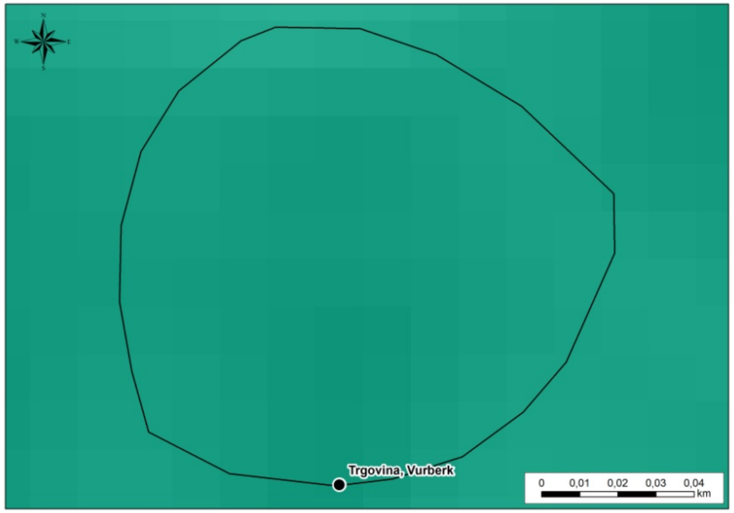

Sampling location Trgovina, Vurberk (CLC classification)

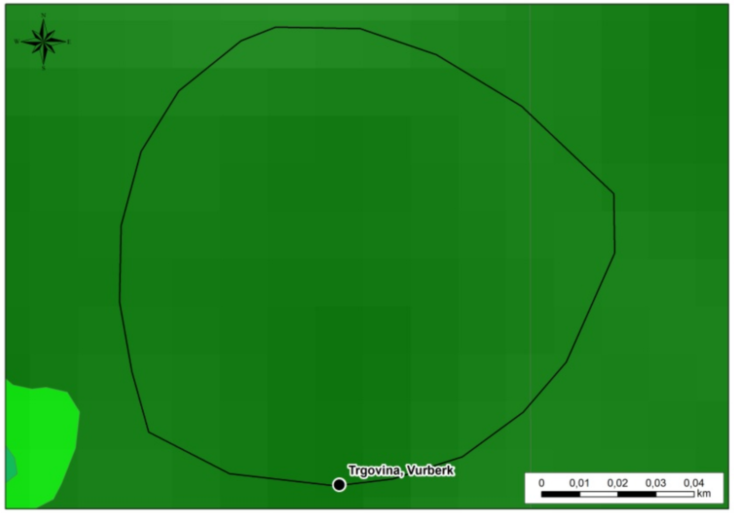

Sampling location Trgovina, Vurberk (Land use classification)

V-3A, Lukavci

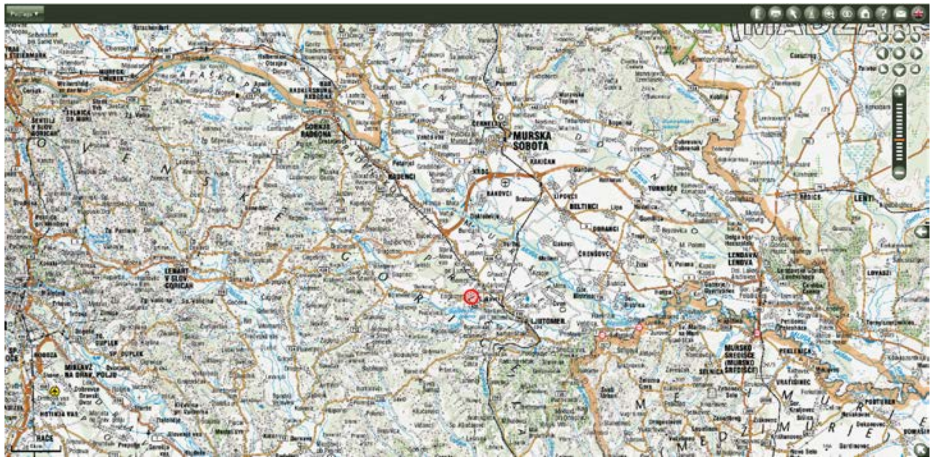

Sampling location V-3A, Lukavci

Sampling location V-3A, Lukavci

Sampling location V-3A, Lukavci

Sampling location V-3A, Lukavci

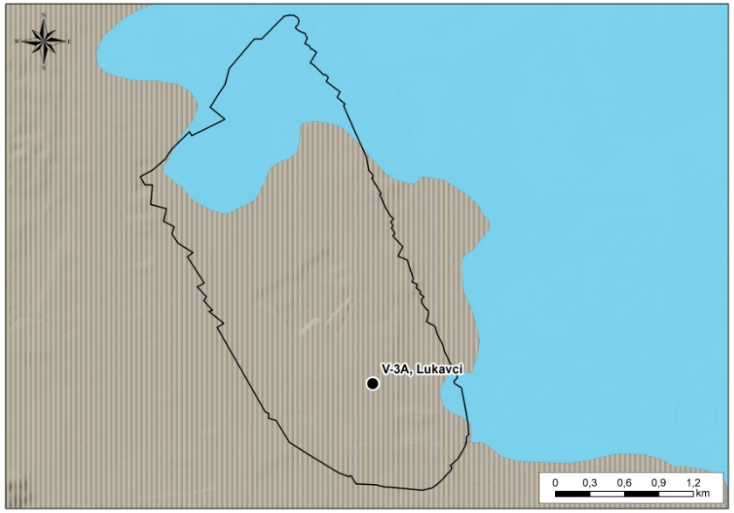

Sampling location V-3A, Lukavci (IAH classification)

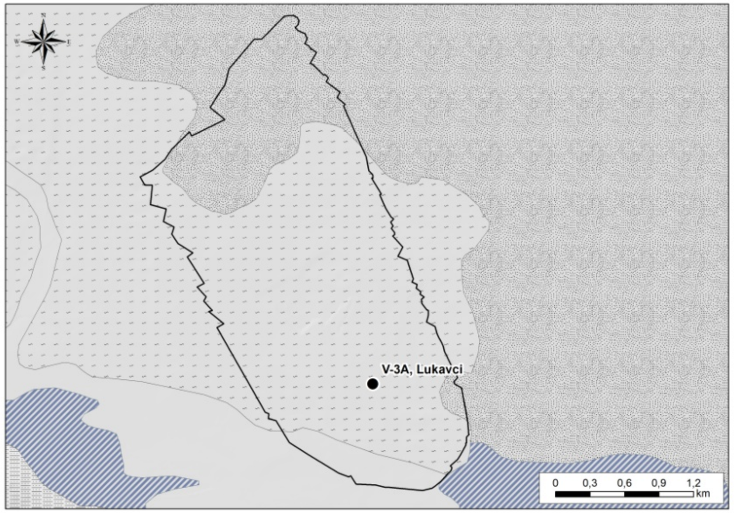

Sampling location V-3A, Lukavci (Geological classification)

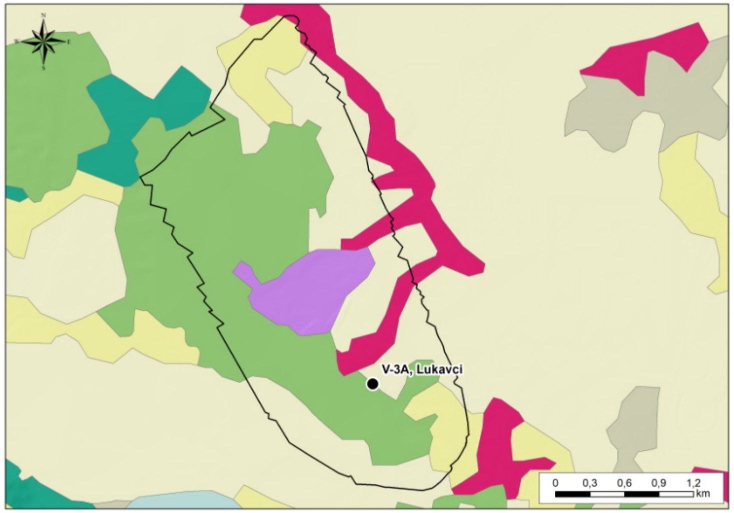

Sampling location V-3A, Lukavci (CLC classification)

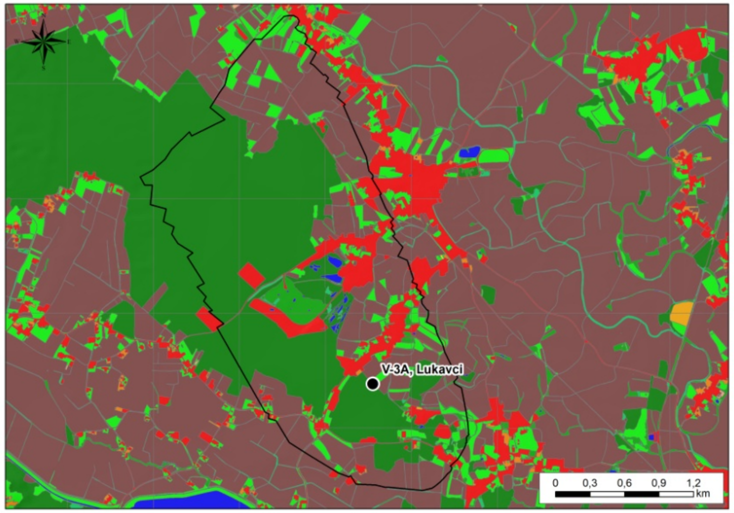

Sampling location V-3A, Lukavci (Land use classification)

V-6, Skorba

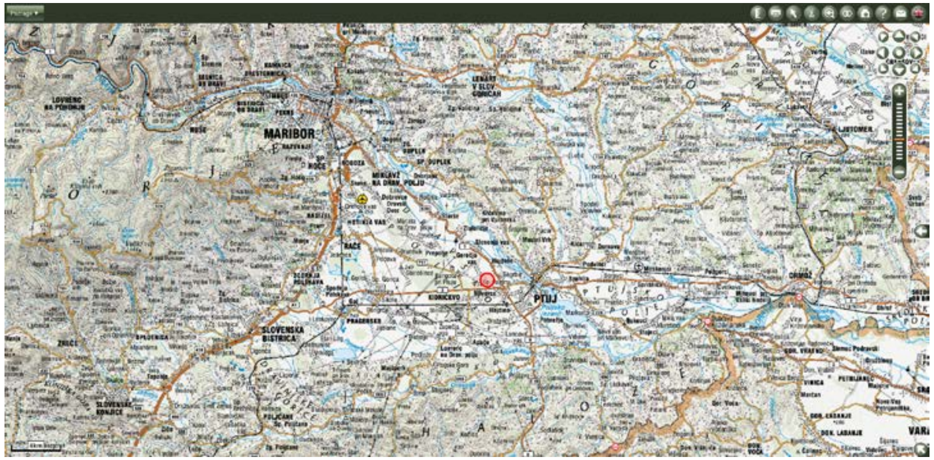

Sampling location V-6, Skorba

Sampling location V-6, Skorba

Sampling location V-6, Skorba

Sampling location V-6, Skorba

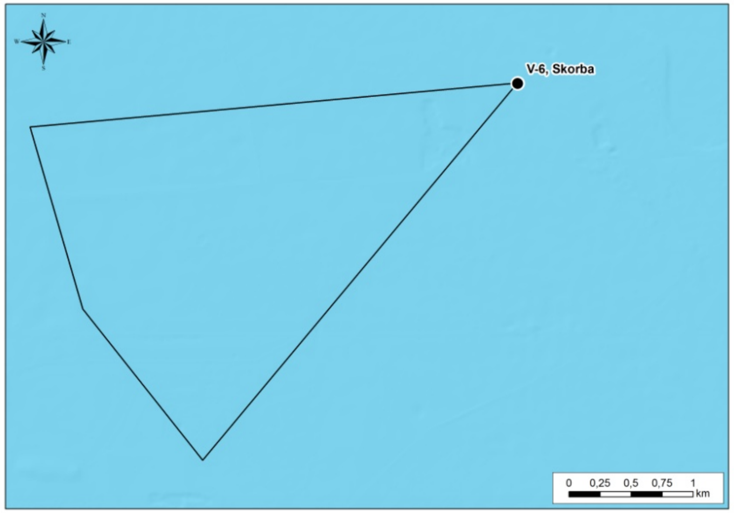

Sampling location V-6, Skorba (IAH classification)

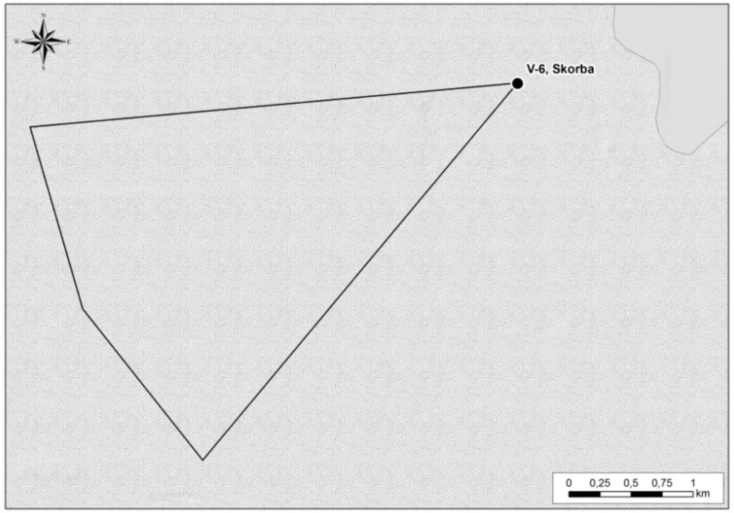

Sampling location V-6, Skorba (Geological classification)

Sampling location V-6, Skorba (CLC classification)

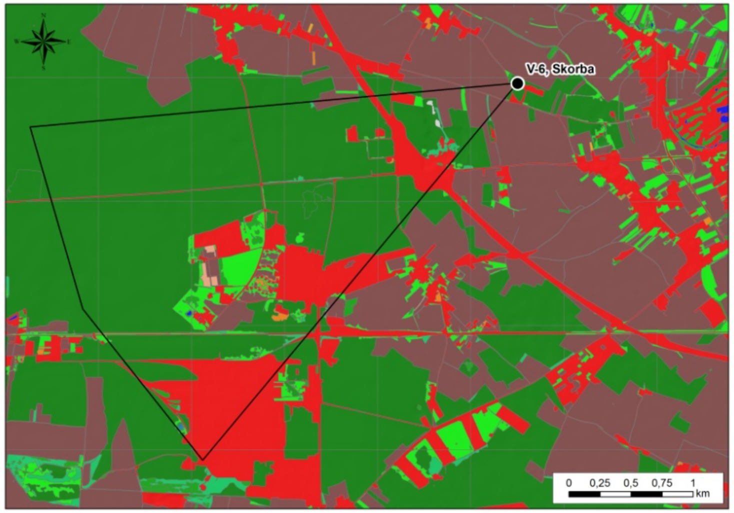

Sampling location V-6, Skorba (Land use classification)

Velika Toplica

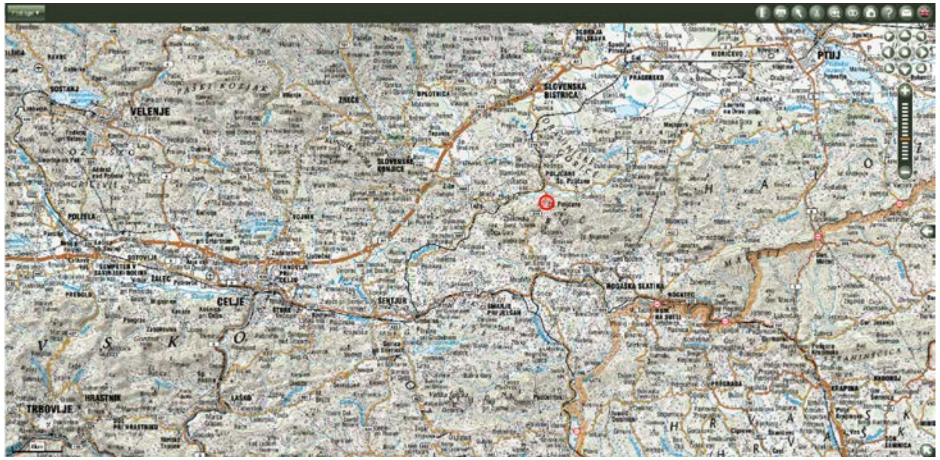

Sampling location Velika Toplica

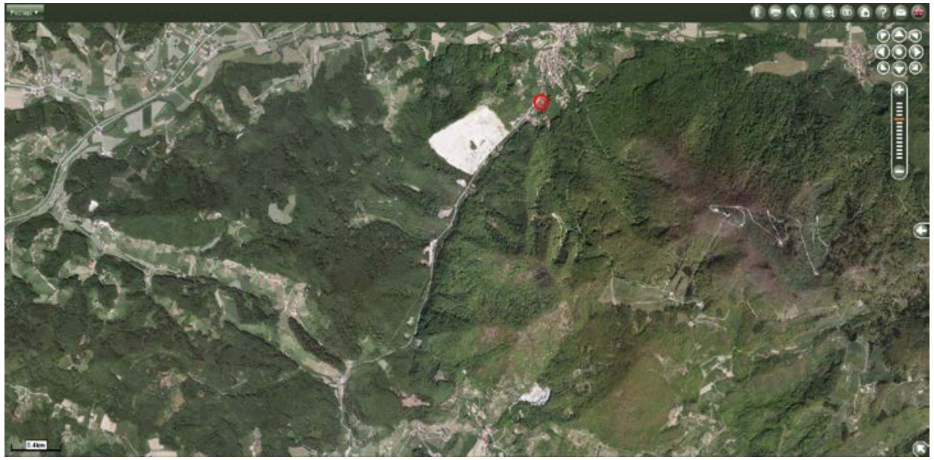

Sampling location Velika Toplica

Sampling location Velika Toplica

Sampling location Velika Toplica

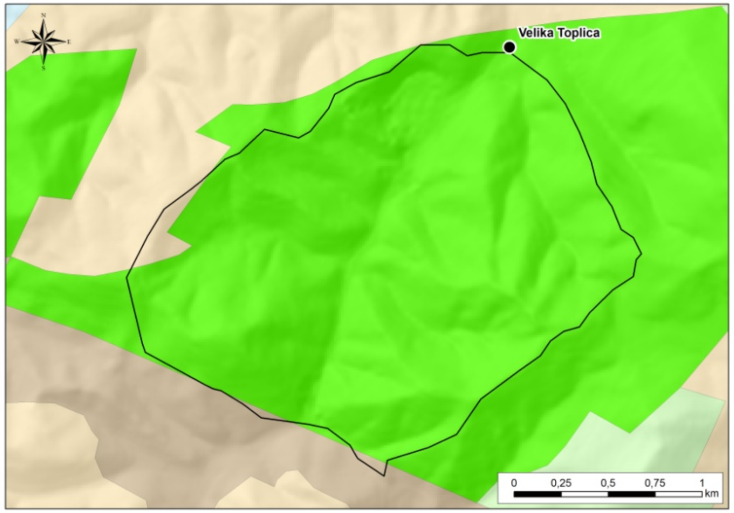

Sampling location Velika Toplica (IAH classification)

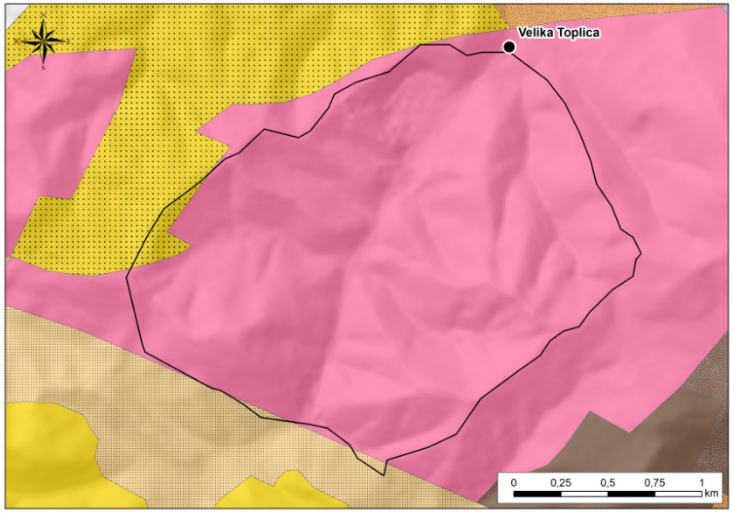

Sampling location Velika Toplica (Geological classification)

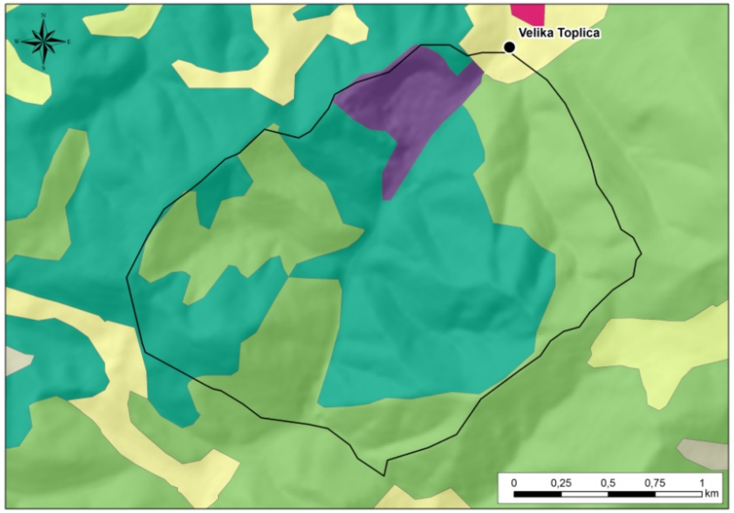

Sampling location Velika Toplica (CLC classification)

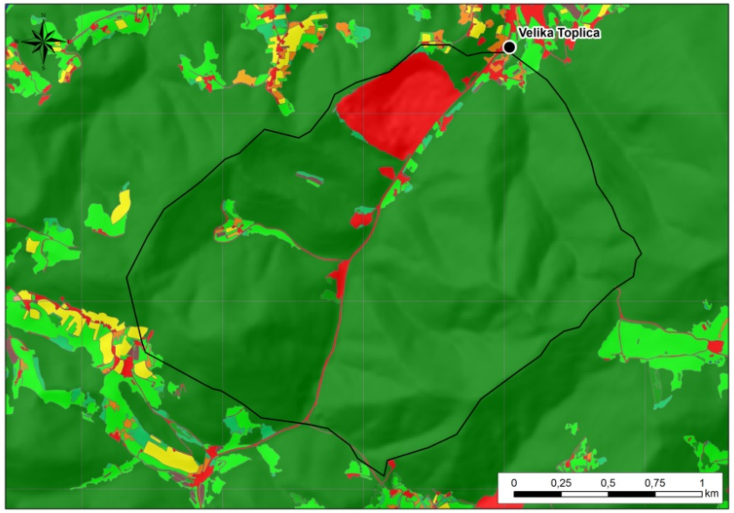

Sampling location Velika Toplica (Land use classification)

Veliki Vrh, Bloke

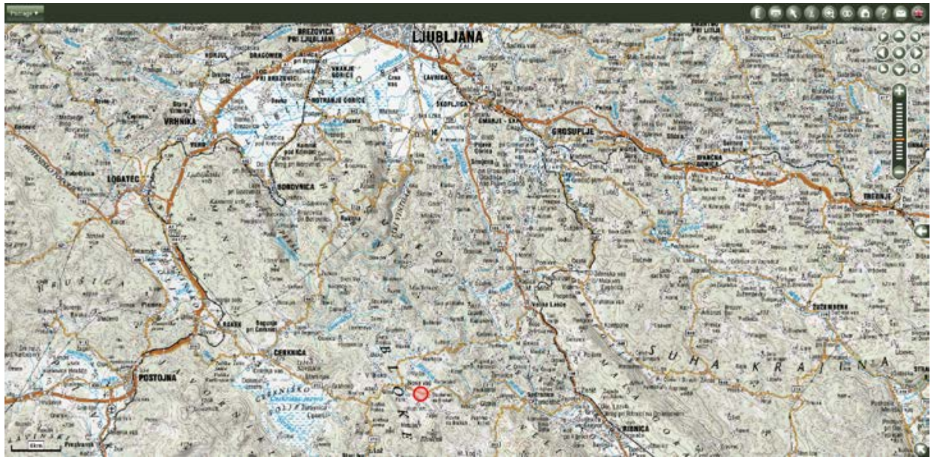

Sampling location Veliki Vrh, Bloke

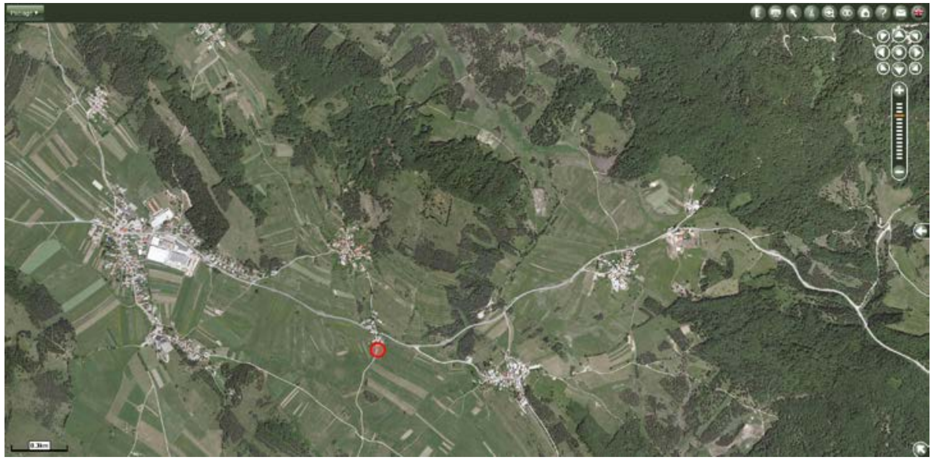

Sampling location Veliki Vrh, Bloke

Sampling location Veliki Vrh, Bloke

Sampling location Veliki Vrh, Bloke

Sampling location Veliki Vrh, Bloke (IAH classification)

Sampling location Veliki Vrh, Bloke (Geological classification)

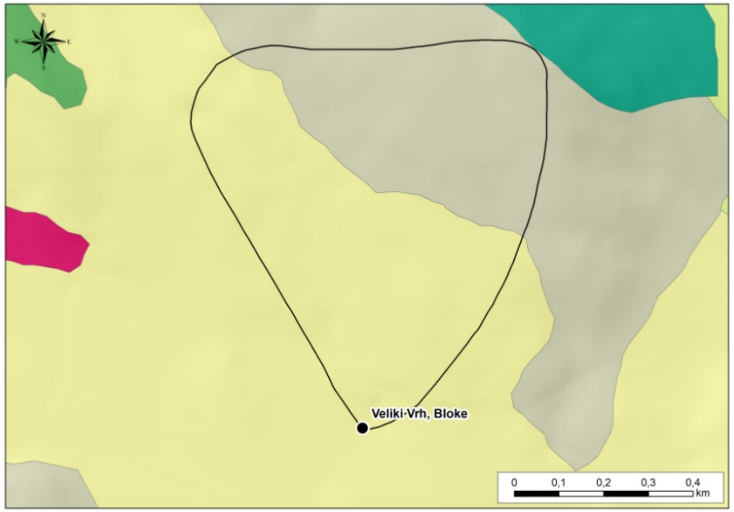

Sampling location Veliki Vrh, Bloke (CLC classification)

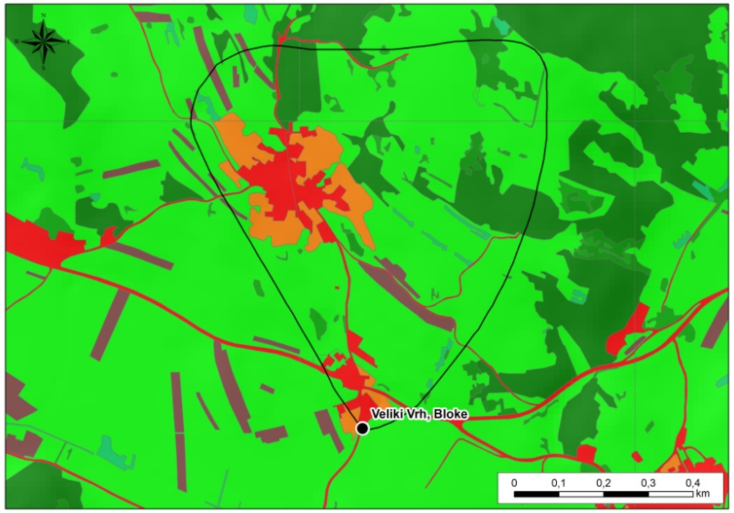

Sampling location Veliki Vrh, Bloke (Land use classification)

VG-10, Mala Goba

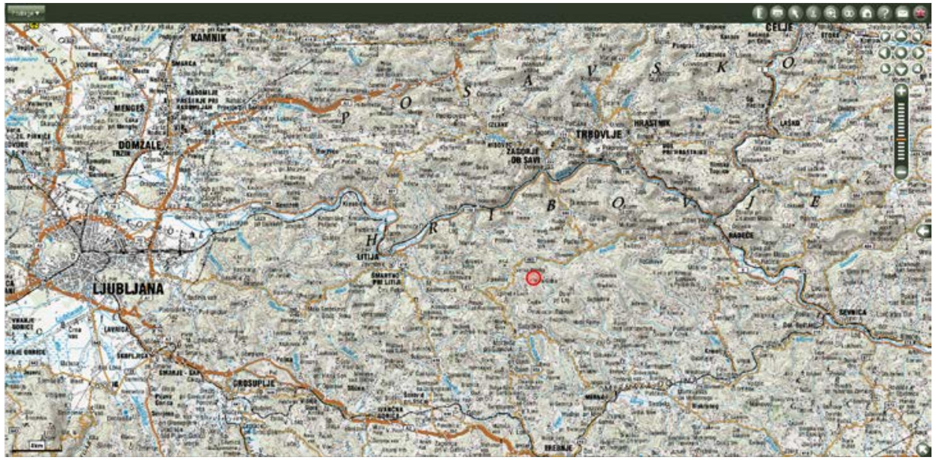

Sampling location VG-10, Mala Goba

Sampling location VG-10, Mala Goba

Sampling location VG-10, Mala Goba

Sampling location VG-10, Mala Goba

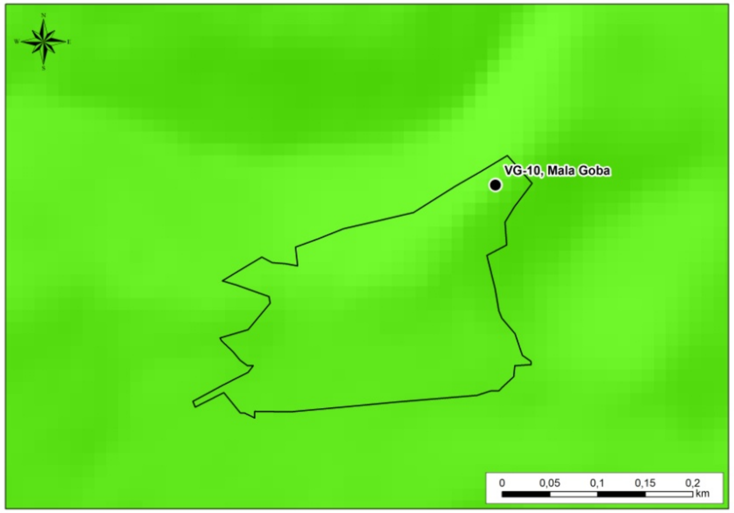

Sampling location VG-10, Mala Goba (IAH classification)

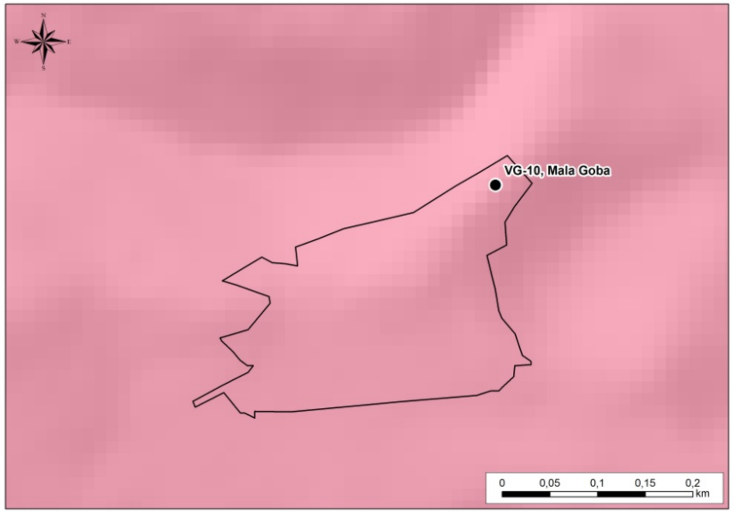

Sampling location VG-10, Mala Goba (Geological classification)

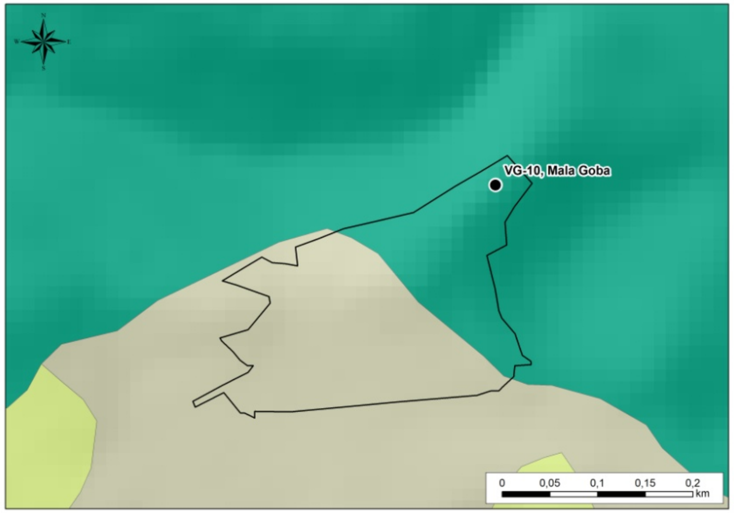

Sampling location VG-10, Mala Goba (CLC classification)

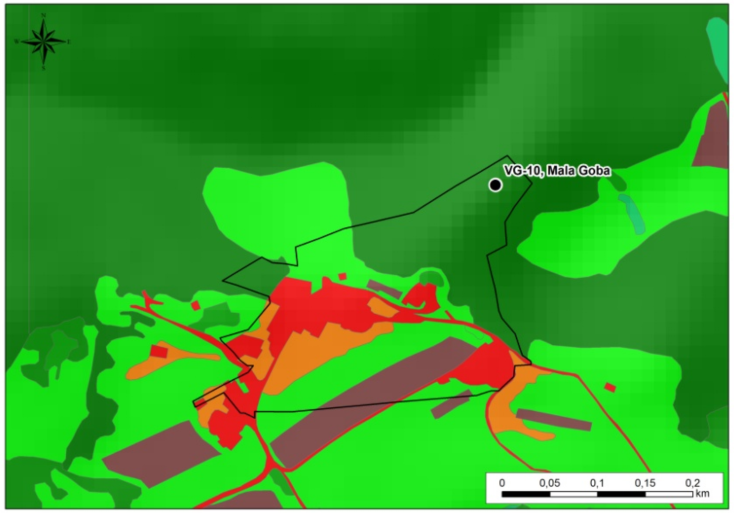

Sampling location VG-10, Mala Goba (Land use classification)

Vidovič

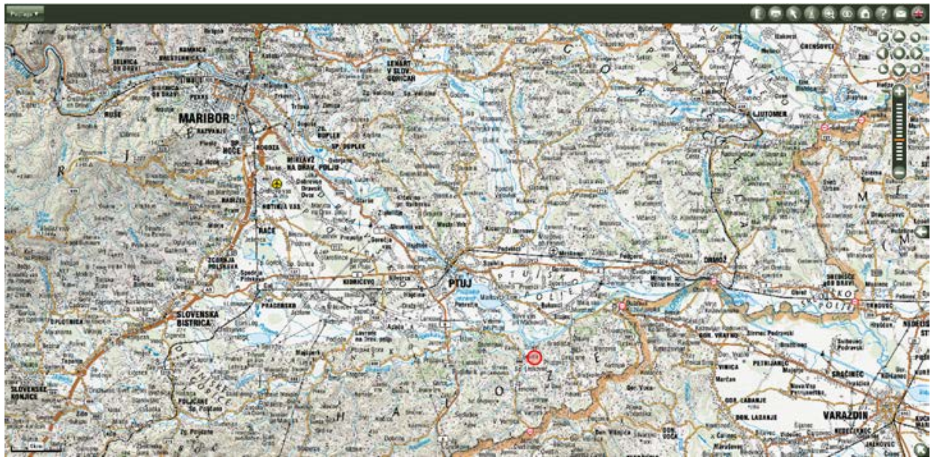

Sampling location Vidovič

Sampling location Vidovič

Sampling location Vidovič

Sampling location Vidovič

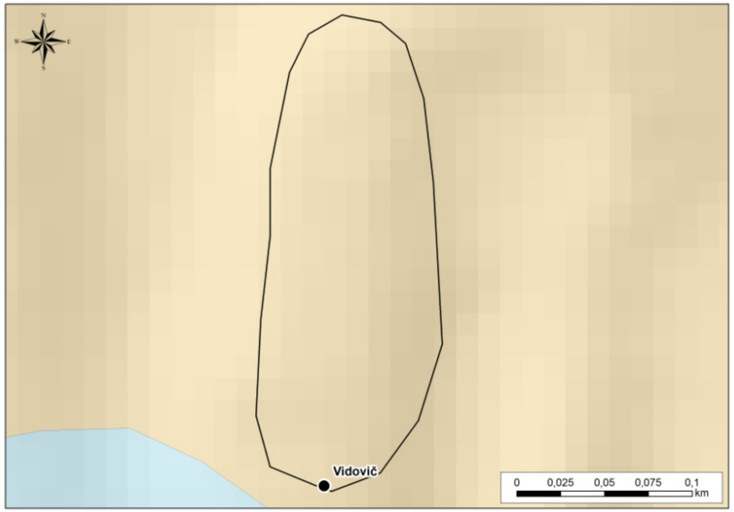

Sampling location Vidovič (IAH classification)

Sampling location Vidovič (Geological classification)

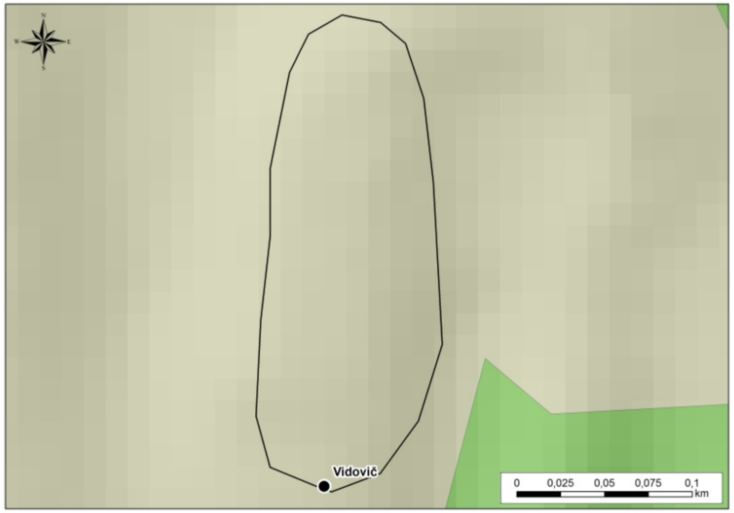

Sampling location Vidovič (CLC classification)

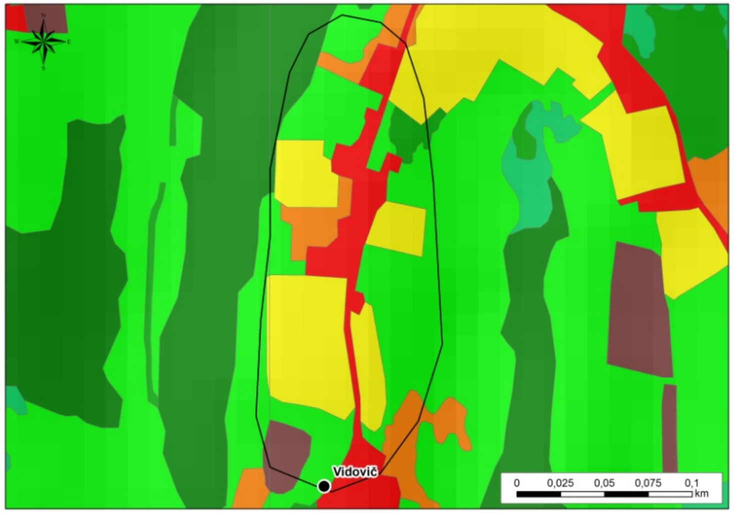

Sampling location Vidovič (Land use classification)

Vipava

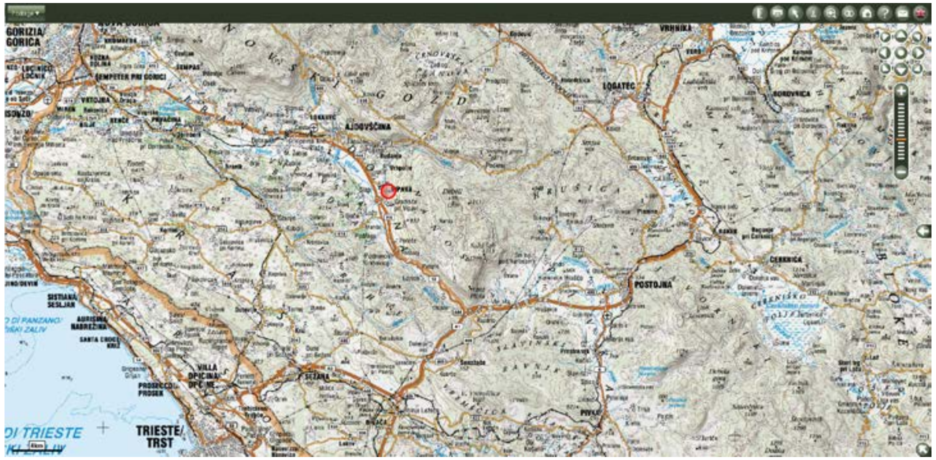

Sampling location Vipava

Sampling location Vipava

Sampling location Vipava

Sampling location Vipava

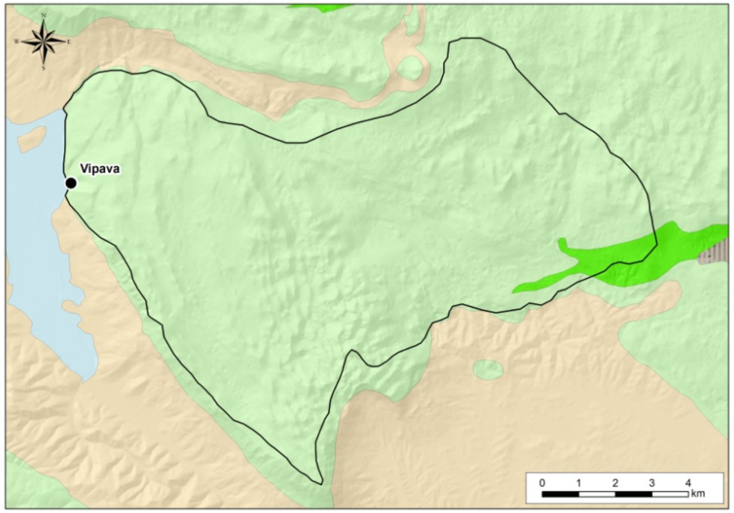

Sampling location Vipava (IAH classification)

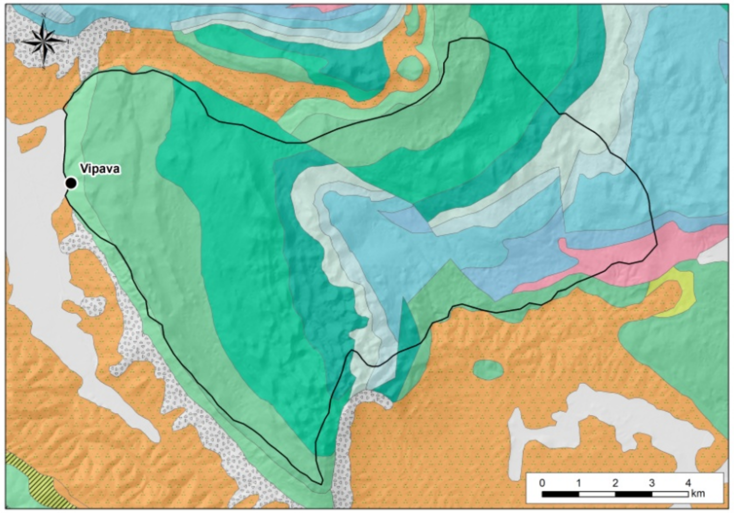

Sampling location Vipava (Geological classification)

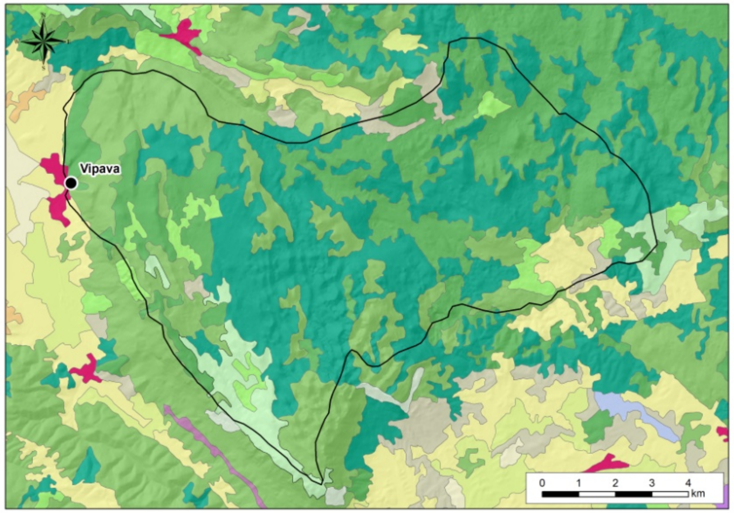

Sampling location Vipava (CLC classification)

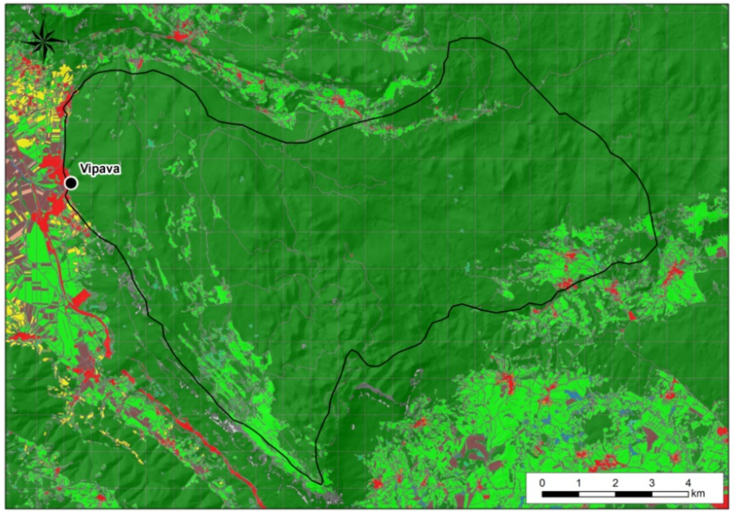

Sampling location Vipava (Land use classification)

Vo-1, Vodice

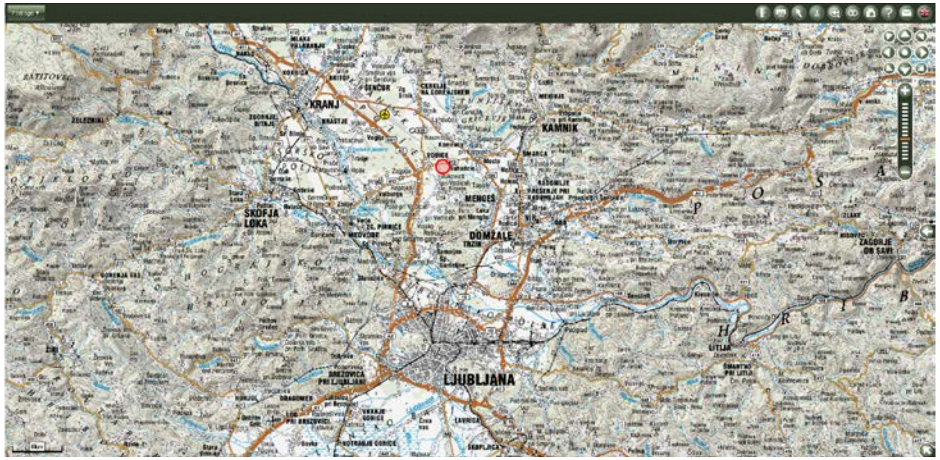

Sampling location Vo-1, Vodice

Sampling location Vo-1, Vodice

Sampling location Vo-1, Vodice

Sampling location Vo-1, Vodice

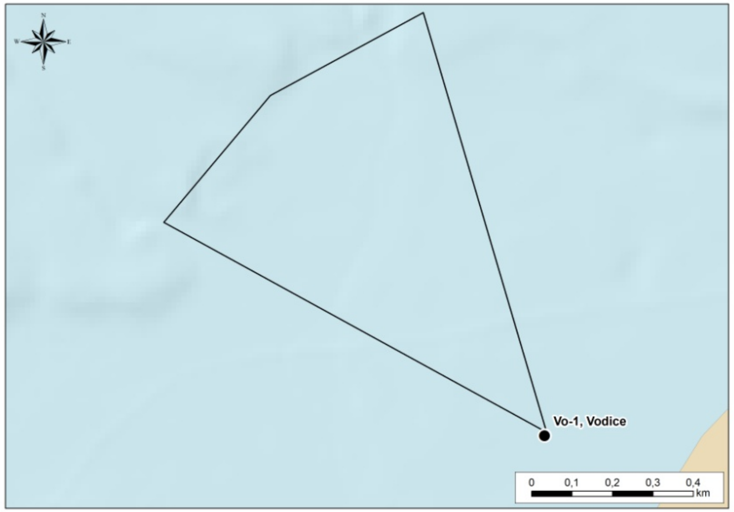

Sampling location Vo-1, Vodice (IAH classification)

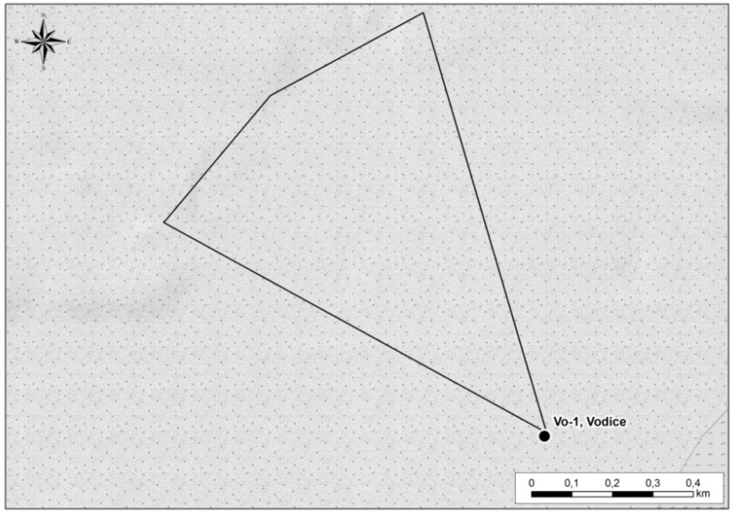

Sampling location Vo-1, Vodice (Geological classification)

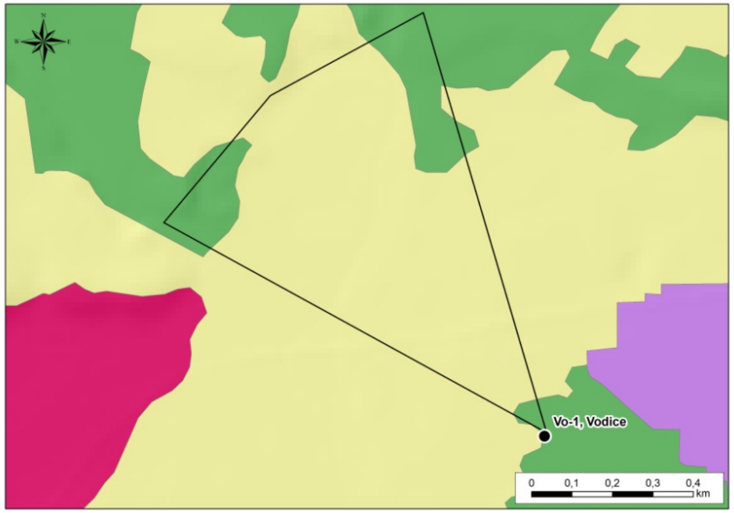

Sampling location Vo-1, Vodice (CLC classification)

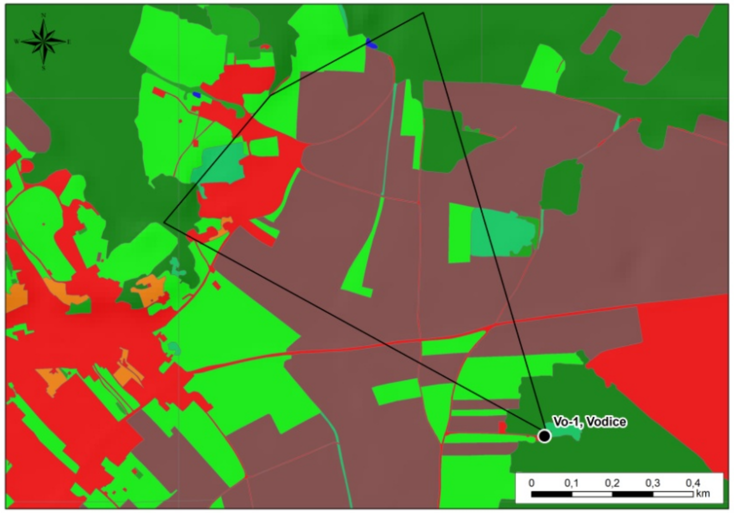

Sampling location Vo-1, Vodice (Land use classification)

VP-1, Prosenjakovci

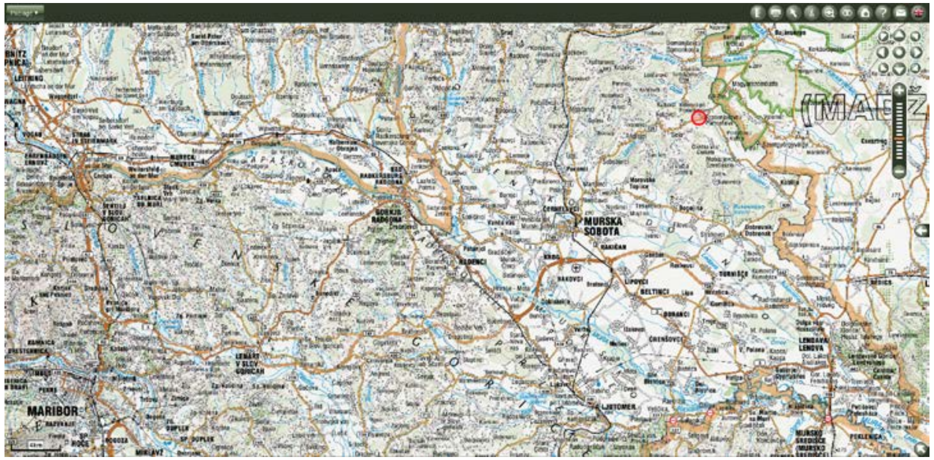

Sampling location VP-1, Prosenjakovci

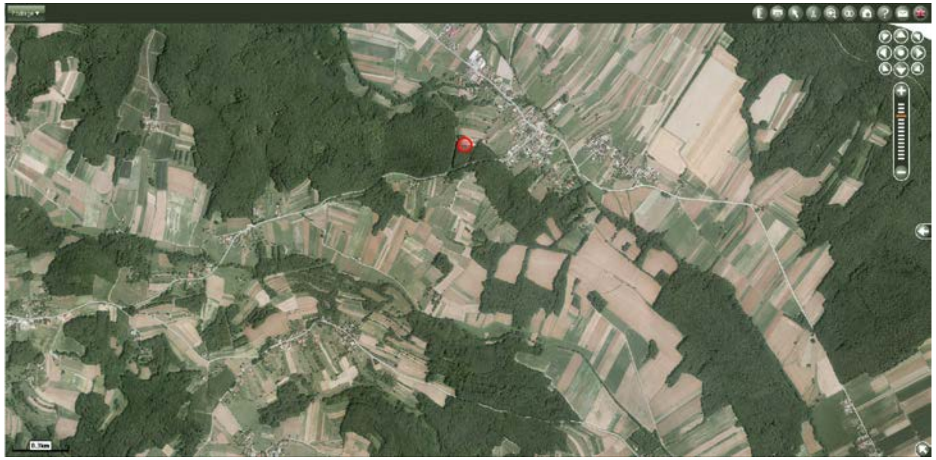

Sampling location VP-1, Prosenjakovci

Sampling location VP-1, Prosenjakovci

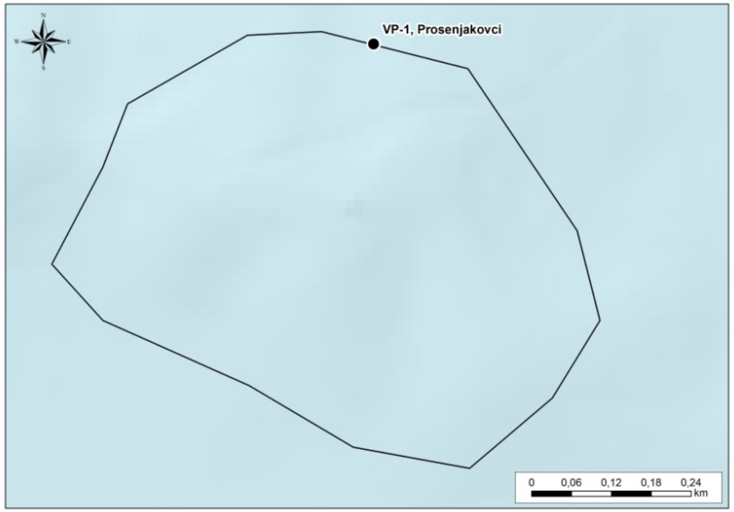

Sampling location VP-1, Prosenjakovci (IAH classification)

Sampling location VP-1, Prosenjakovci (Geological classification)

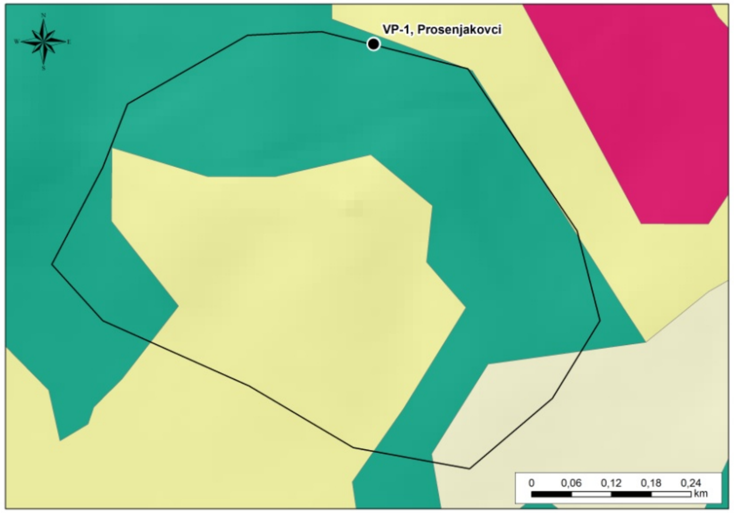

Sampling location VP-1, Prosenjakovci (CLC classification)

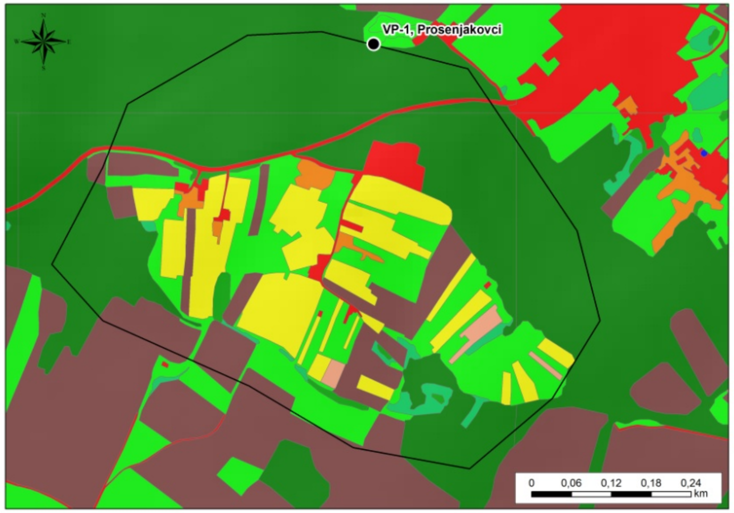

Sampling location VP-1, Prosenjakovci (Land use classification)

Vt-1, Tinsko

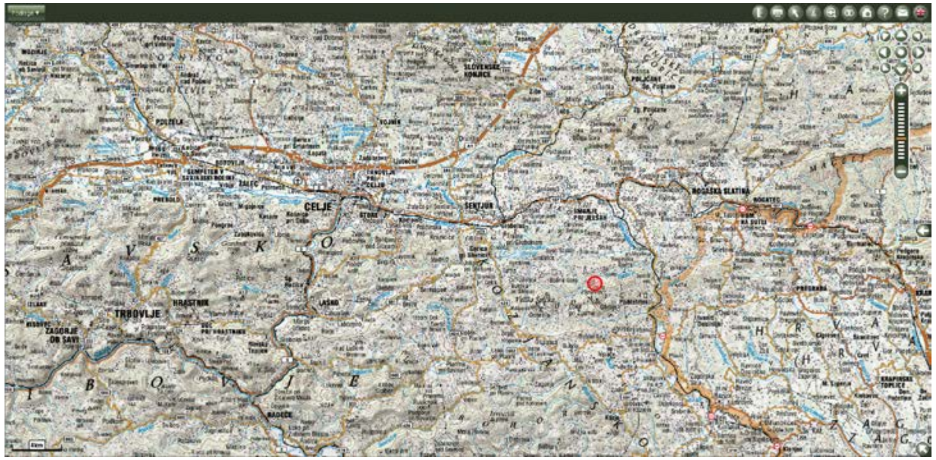

Sampling location Vt-1, Tinsko

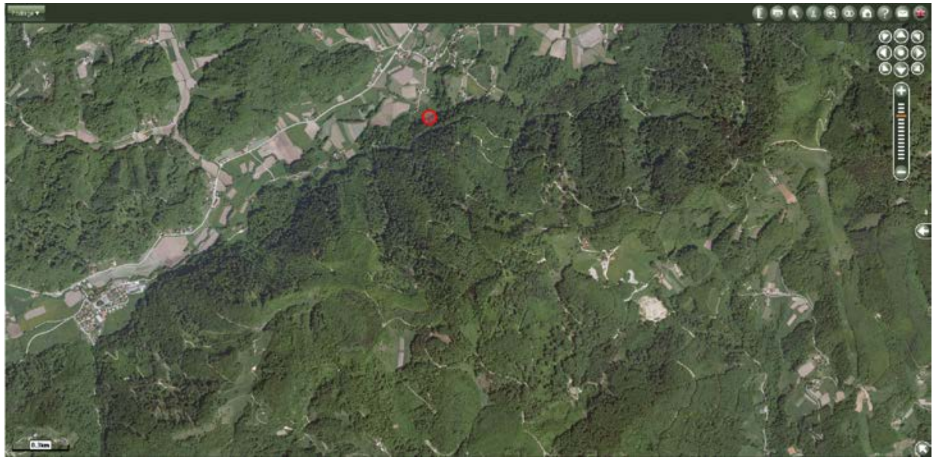

Sampling location Vt-1, Tinsko

Sampling location Vt-1, Tinsko

Sampling location Vt-1, Tinsko

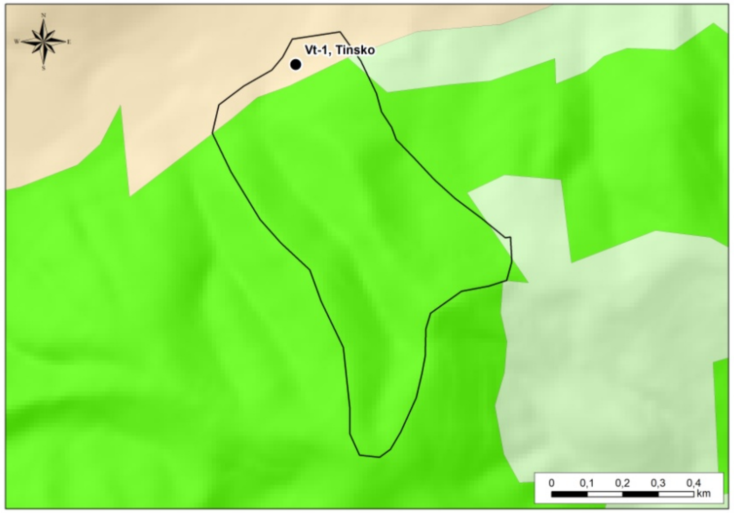

Sampling location Vt-1, Tinsko (IAH classification)

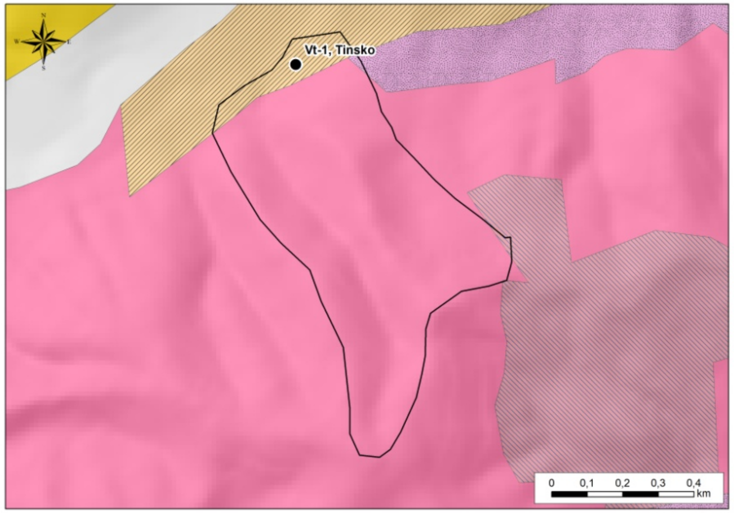

Sampling location Vt-1, Tinsko (Geological classification)

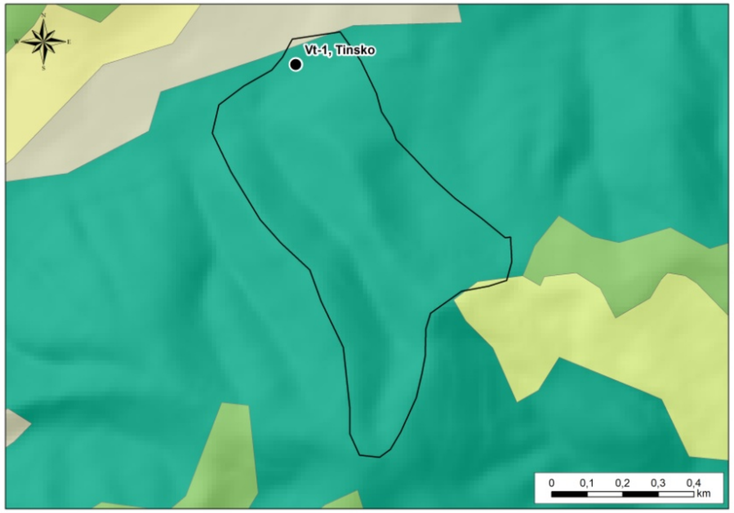

Sampling location Vt-1, Tinsko (CLC classification)

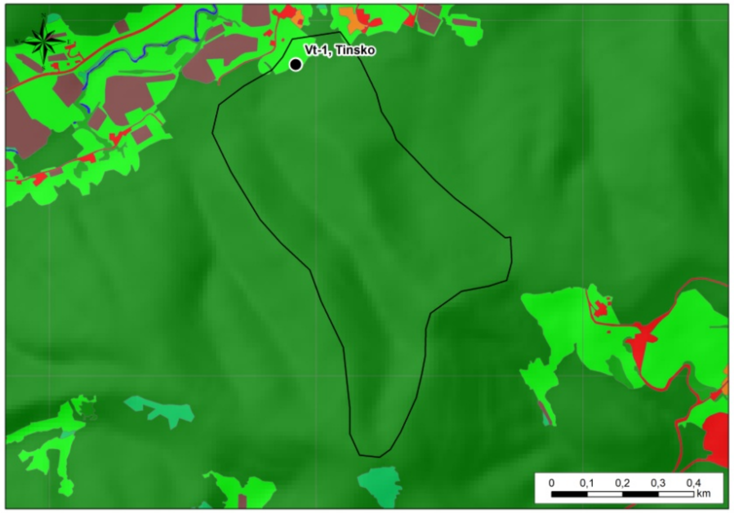

Sampling location Vt-1, Tinsko (Land use classification)

Zadlaščica

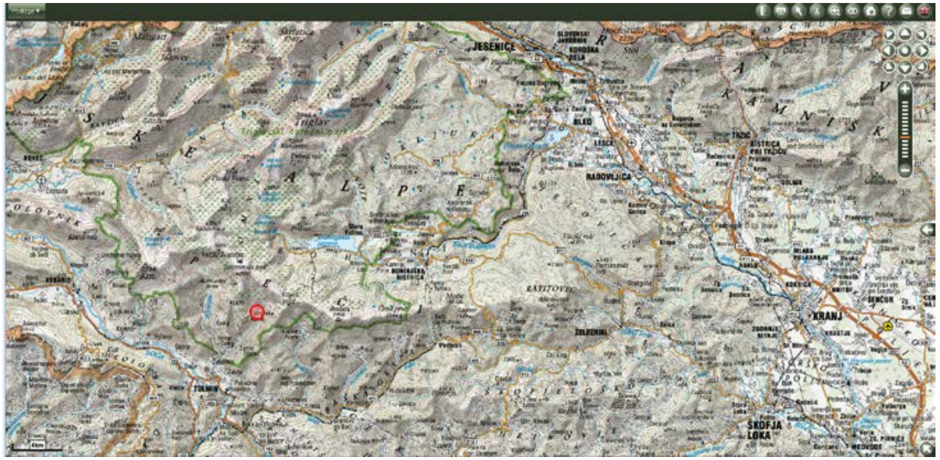

Sampling location Zadlaščica

Sampling location Zadlaščica

Sampling location Zadlaščica

Sampling location Zadlaščica

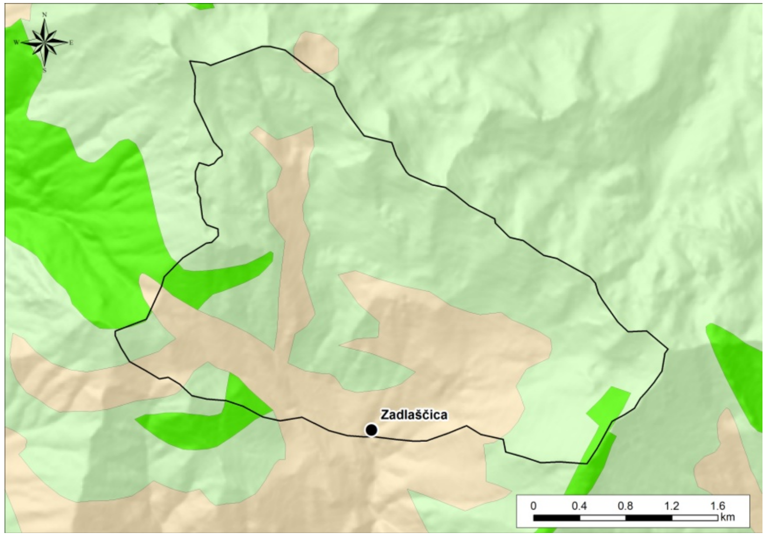

Sampling location Zadlaščica (IAH classification)

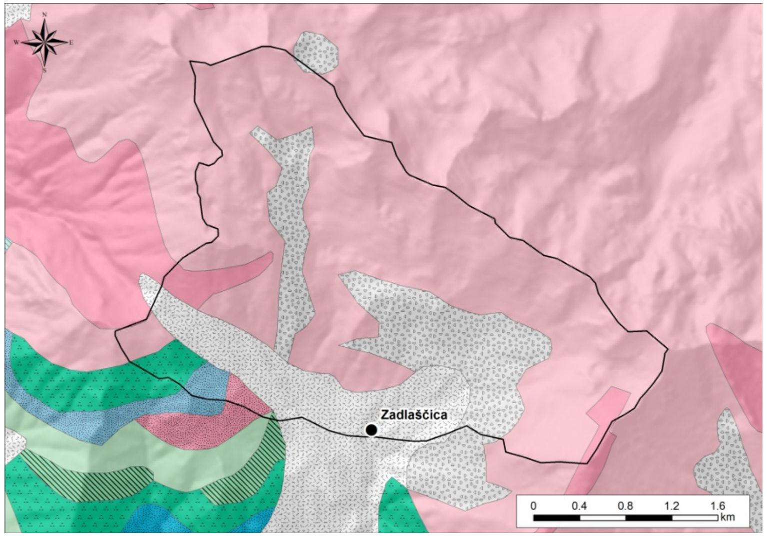

Sampling location Zadlaščica (Geological classification)

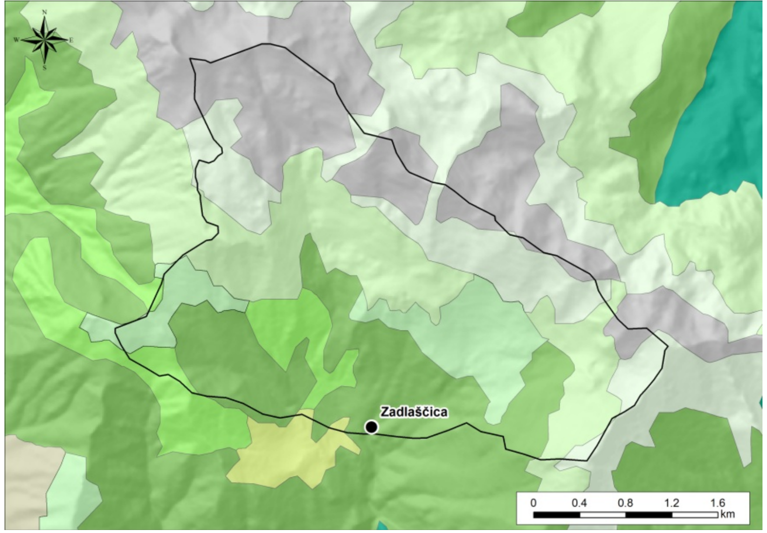

Sampling location Zadlaščica (CLC classification)

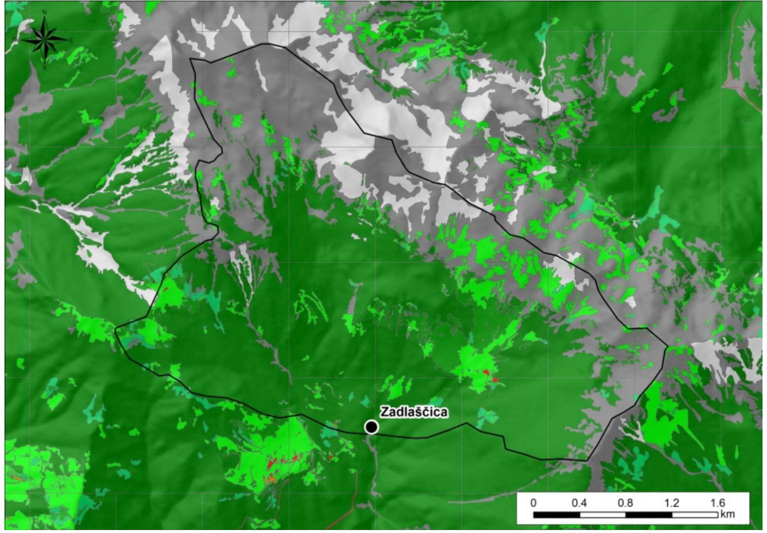

Sampling location Zadlaščica (Land use classification)

Žegnan studenec

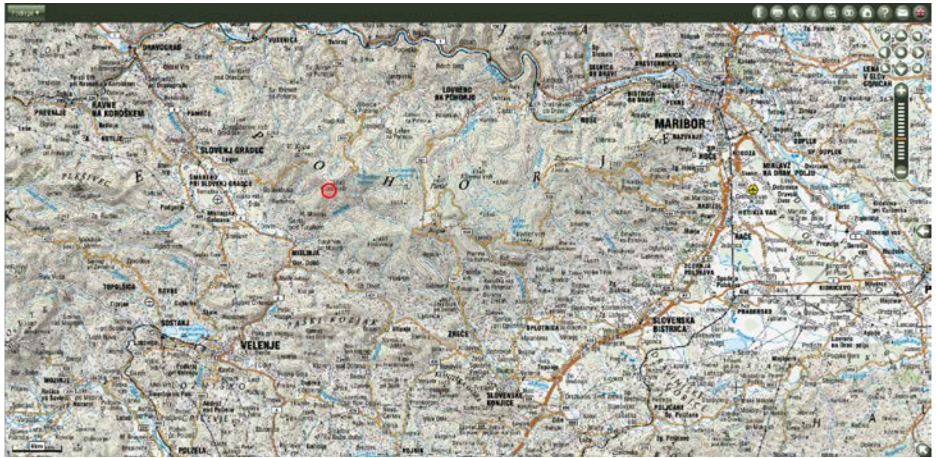

Sampling location Žegnan studenec

Sampling location Žegnan studenec

Sampling location Žegnan studenec

Sampling location Žegnan studenec

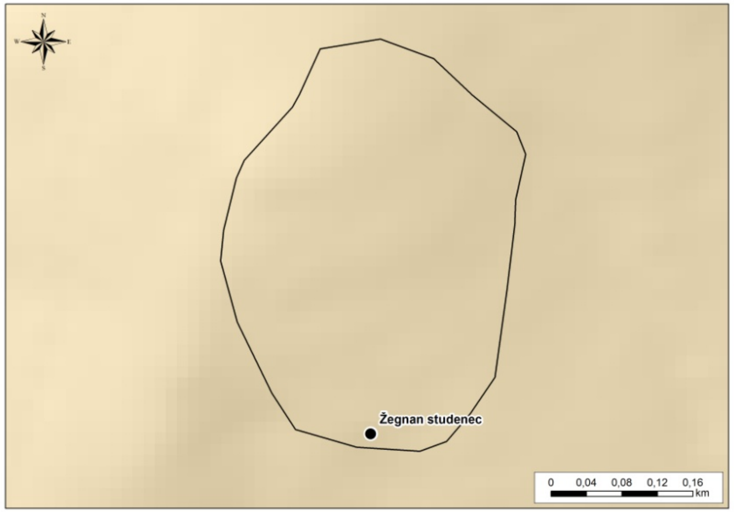

Sampling location Žegnan studenec (IAH classification)

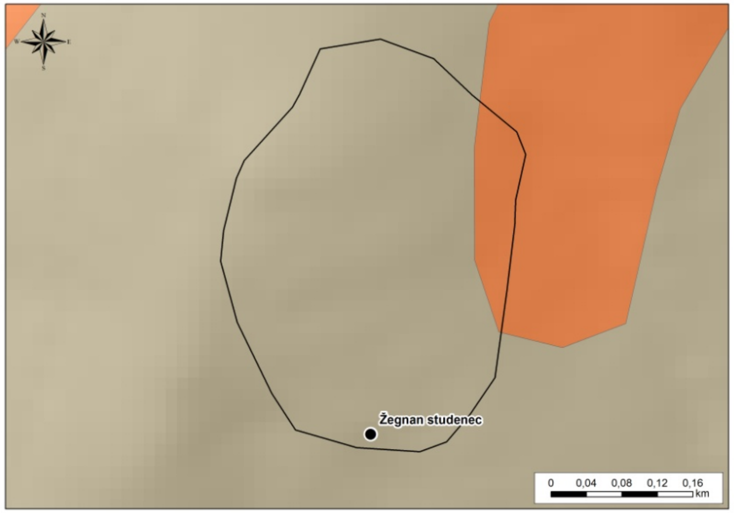

Sampling location Žegnan studenec (Geological classification)

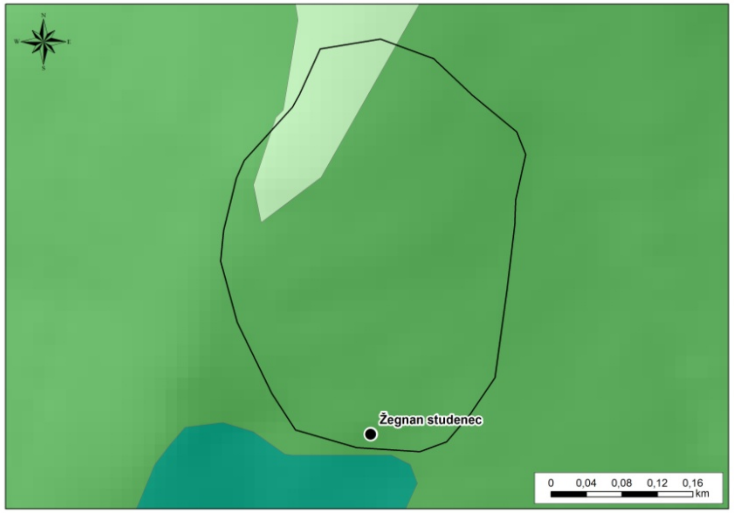

Sampling location Žegnan studenec (CLC classification)

Sampling location Žegnan studenec (Land use classification)

Appendix 11

Detailed information on sampling locations and groundwater chemical and isotopic composition

sampling location	X	Y	Z	mean altitude (m)	distance from the sea (km)	object type	groundwater body	aquifer porosity type	major rock type	lithological unit	lithostratigraphic unit	T GIS (°C) (1971-2000)	CORINE Land Cover classification	Actual agricultural and forest land usage classification	mean amount of precipitations (mm)	recharge area (km^2)	n	T (°C)		pH		EC (µS/cm)		δ^{18}O (‰)		δ^{2}H (‰)		d-*excess* (‰)		δ^{13}C-DIC (‰)		δ^{15}N$_{tot}$ (‰)		^{3}H (TU)		Ca^{2+} (mg/L)		Mg^{2+} (mg/L)		Na^{+} (mg/L)		K^{+} (mg/L)		NH$_4$+ (mg/L)		HCO$_3^-$ (mg/L)		Cl$^-$ (mg/L)		NO$_3^-$ (mg/L)		SO$_4^{2-}$ (mg/L)		Si (mg/L)		As (µg/L)		B (µg/L)		Br (µg/L)		Cr (µg/L)		Fe (µg/L)		Mn (µg/L)		SIcal		SIdol	
																		X	S	X	S	X	S	X	S	X	S	X	S	X	S	X	S	X	S	X	S	X	S	X	S	X	S	X	S	X	S	X	S	X	S	X	S	X	S	X	S	X	S	X	S	X	S	X	S	X	S	X	S	X	S
B-9, Brestovica	5075107	5392110	22	247.072	33.977	borehole	Obala in Kras z Brkini	karstic and fractured	carbonate rocks	limestone prevailing	Cretaceous carbonates	12.2	broad-leaved forest	forest	1565	83.8	2	15.0	0.1	7.45	0.03	450	1	-7.70	0.23	-48.4	1.0	13.2	0.9	-10.5	0.9	5.9	0.1	5.15	0.72	75	0	8.9	0.5	5.8	0.0	0.71	0.04	0.01	0.00	252	1	9.00	0.06	8.75	0.72	10.05	0.07	1.94	0.14	0.25	0.00	11.50	4.95	29.00	2.83	0.95	0.07	73.50	82.73	1.89	1.48	0.20	0.03	-0.25	0.03
Berglez	5135661	5485962	682	796.549	134.216	spring capture	Kamniško-Savinjske Alpe	fractured	igneous and metamorphic rocks	igneous rocks	Oligocene igneous rocks	7.0	coniferous forest	forest	1700	0.29	2	13.8	1.4	8.00	0.00	145	11	-8.90	0.02	-60.3	0.2	10.9	0.0	-13.3	0.5			5.61	0.33	24	2	2.7	0.3	4.8	0.4	0.50	0.00	0.01	0.00	82	11	1.52	0.05	3.61	0.28	10.28	0.60	5.21	0.39	0.25	0.00	5.50	0.71	4.75	3.18	0.25	0.00	5.00	0.00	0.48	0.13	-0.17	0.09	-1.00	0.19
BLP-2, Nedelica	5162986	5602609	167	170.207	244.489	borehole	Murska kotlina	intergranular	clastic sedimentary rocks	gravel and sand	Quaternary clastics (medium- and coarse-grained)	9.6	non-irrigated arable land	areas of intense use of nutrients and plant protection products	850	2.43	2	12.1	0.2	6.47	0.08	438	18	-9.04	0.17	-63.3	0.6	9.1	2.0	-18.0	0.0	9.6	2.3	9.00	0.43	56	1	14.0	0.0	8.1	0.4	1.35	0.07	0.01	0.00	101	6	26.70	2.26	72.38	4.07	38.85	0.92	9.70	1.20	0.25	0.00	4.75	3.18	38.00	0.00	0.25	0.00	17.50	17.68	1.71	1.31	-1.31	0.05	-2.95	0.11
Bohinjska Bistrica	5124083	5417338	614	1297.67	87.107	surface water	Julijske Alpe v porečju Save	karstic and fractured	carbonate rocks	limestone prevailing	Triassic carbonates	5.0	coniferous forest	forest	2856	8.8	2	5.9		8.17	0.04	179	10	-9.34	0.73	-61.3	5.2	13.4	0.6	-4.2	1.4	-1.6	1.8	5.90		30	2	7.3	0.4	0.3	0.0	0.13	0.00	0.01	0.00	123	5	0.38	0.00	2.46	0.09	1.17	0.59	0.31	0.07	0.25	0.00	2.50	0.00	2.50	0.00	0.38	0.18	12.50	10.61	0.16	0.06	0.25	0.08	0.18	0.15
Brekovice	5098066	5432416	527	556.913	70.565	spring	Cerkljansko, Škofjeloško in Polhograjsko hribovje	mixed (karstic, fractured, intergranular)	carbonate rocks	carbonates with clastics	Triassic carbonates	9.0	coniferous forest	forest	1900	0.03	2	9.4	0.6	7.85	0.07	238	7	-8.93	0.08	-58.8	1.0	12.6	0.4	-13.5	0.5			5.32	0.77	48	1	3.1	0.4	1.7	0.1	0.69	0.08	0.01	0.00	166	5	1.66	0.00	4.09	0.66	4.26	0.33	2.96	0.12	0.25	0.00	2.50	0.00	11.00	5.66	0.25	0.00	5.00	0.00	0.13	0.07	0.26	0.07	-0.38	0.17
C-4, Domžale	5111465	5467594	304	313.52	104.23	pumping station	Savska kotlina in Ljubljansko barje	intergranular	clastic sedimentary rocks	gravel and sand	Quaternary clastics (medium- and coarse-grained)	9.0	non-irrigated arable land	areas of intense use of nutrients and plant protection products	1450	1.38	2	12.3	0.1	7.41	0.04	532	23	-8.26	0.41	-56.5	0.9	9.7	2.3	-14.6	3.4	10.7	5.0	5.29	1.22	86	3	20.0	0.0	3.7	0.4	1.05	0.07	0.01	0.00	315	12	9.27	0.42	23.47	1.38	8.86	0.38	3.87	0.07	0.25	0.00	18.00	1.41	20.00	1.41	3.70	0.42	13.00	11.31	0.03	0.00	0.28	0.01	0.22	0.03
Čemažarjev izvir	5122072	5441604	848	904.37	95.633	spring capture	Cerkljansko, Škofjeloško in Polhograjsko hribovje	fractured	igneous and metamorphic rocks	igneous rocks	Ladinian igneous rocks	7.0	land principally occupied by agriculture, with significant areas of natural vegetation	areas of less intense use of nutrients and plant protection products	1900	0.11	2	9.9	0.3	7.75	0.07	170	13	-9.45	0.03	-62.5	0.1	13.2	0.3	-14.0	0.1			5.70	1.10	31	1	1.7	0.9	2.7	0.1	0.46	0.13	0.01	0.00	105	1	4.04	0.32	4.96	0.13	5.00	0.04	4.94	0.35	0.25	0.00	2.50	0.00	7.25	6.72	0.38	0.18	5.00	0.00	0.22	0.11	-0.20	0.07	-1.42	0.39
Čepovan-1/94	5102664	5407570	697	861.757	63.786	pumping station	Goriška Brda in Trnovsko-Banjška planota	fractured and karstic	carbonate rocks	dolomite prevailing	Triassic carbonates	9.0	broad-leaved forest	forest	2300	3.51	2	17.7	0.7	7.80	0.14	380	8	-8.25	0.02	-52.6	0.5	13.4	0.7	-12.6	0.8			3.94	0.94	49	3	26.5	0.7	2.6	0.1	0.46	0.04	0.01	0.00	277	16	6.10	0.37	3.96	0.03	5.10	0.91	0.73	0.19	0.25	0.00	2.50	0.00	7.25	6.72	0.80	0.00	23.50	26.16	0.25	0.09	0.40	0.18	0.82	0.33
Črna	5140583	5472327	744	1320.75	128.654	spring	Kamniško-Savinjske Alpe	fractured and karstic	carbonate rocks	dolomite prevailing	Triassic carbonates	4.5	broad-leaved forest	forest	2077	22.01	2	7.0	0.3	7.87	0.06	249	8	-9.82	0.07	-66.6	0.4	12.1	0.2	-9.2	0.1	1.6	1.6	5.61	0.45	40	1	11.0	0.0	0.3	0.0	0.13	0.00	0.01	0.00	169	3	0.38	0.00	2.37	0.22	4.09	0.37	0.59	0.05	0.25	0.00	5.00	0.00	3.75	1.77	0.25	0.00	5.00	0.00	0.17	0.11	0.21	0.04	0.14	0.10
DAC-3, Skopice	5085100	5541050	155	155.047	156.697	borehole	Krška kotlina	intergranular	clastic sedimentary rocks	gravel and sand	Quaternary clastics (medium- and coarse-grained)	11.0	complex cultivation patterns	areas of intense use of nutrients and plant protection products	1250	0.04	2	14.1	0.6	7.37	0.00	674	1	-8.90	0.29	-61.5	2.4	9.7	0.1	-12.8	0.7	12.1	9.3	8.02	0.15	97	1	25.0	0.0	9.9	1.6	1.90	0.14	0.01	0.00	355	4	23.10	0.14	23.62	2.10	10.85	0.35	4.77	0.62	0.25	0.00	12.50	0.71	20.00	4.24	0.65	0.21	5.00	0.00	0.27	0.11	0.33	0.00	0.36	0.01
Debevčev mlin	5123206	5472078	416	716.964	115.605	spring	Kamniško-Savinjske Alpe	karstic and fractured	carbonate rocks	limestone prevailing	Triassic carbonates	7.6	mixed forest	forest	1700	1.03	2	9.8	0.2	7.45	0.10	369	14	-8.80	0.00	-57.9	0.1	12.5	0.1	-13.8	0.8	3.4	1.4	5.32	0.14	81	4	3.9	0.1	1.2	0.1	0.29	0.02	0.01	0.00	243	9	2.10	0.08	6.09	0.16	7.44	0.49	1.19	0.08	0.25	0.00	2.50	0.00	7.50	0.71	0.48	0.32	5.00	0.00	0.15	0.00	0.22	0.06	-0.59	0.14
DEV-1, Desenci	5150900	5569790	240	240	210.122	pumping station	Zahodne Slovenske Gorice	intergranular	clastic sedimentary rocks	gravel, sand and clay	Pliocene clastics						2	15.2	0.6	7.27	0.16	577	19	-10.39	0.16	-71.0	1.4	12.1	0.1	-13.2	0.2	8.4	1.3	1.12	0.19	73	1	32.0	0.0	5.1	0.0	0.74	0.04	0.01	0.00	371	4	2.81	0.12	2.59	0.03	1.96	0.03	9.95	1.24	0.85	0.07	2.50	0.00	13.00	1.41	0.25	0.00	65.00	7.07	11.08	0.50	0.14	0.15	0.21	0.31
Dobličica	5045259	5511586	147	553.373	121.013	pumping station	Dolenjski kras	karstic and fractured	carbonate rocks	limestone prevailing	Cretaceous carbonates	8.8	broad-leaved forest	forest	1489	45.63	2	11.1	0.1	7.65	0.01	381	33	-10.46	0.95	-72.4	8.0	11.3	0.4	-14.7	0.7	5.3	0.8	8.22	0.99	81	15	7.4	0.1	1.1	0.1	0.13	0.00	0.01	0.00	285	59	1.23	0.27	1.86	1.06	4.35	0.10	1.45	0.17	0.25	0.00	2.50	0.00	7.50	2.12	0.43	0.25	8.50	4.95	0.10	0.01	0.47	0.14	0.20	0.21
Dobravca	5136639	5433382	466	505.802	104.6	spring	Savska kotlina in Ljubljansko barje	intergranular	clastic sedimentary rocks	gravel and sand	Quaternary clastics (medium- and coarse-grained)	7.0	complex cultivation patterns	areas of less intense use of nutrients and plant protection products	1714	0.88	2	10.6	0.2	7.49	0.04	515	19	-8.60	0.16	-58.4	1.1	10.4	0.3	-13.2	0.2	7.6	1.6	5.71	0.23	89	1	22.5	0.7	4.4	0.1	0.52	0.01	0.01	0.00	346	4	7.48	0.44	12.11	0.66	8.95	0.39	3.51	0.05	0.25	0.00	26.50	3.54	12.50	3.54	0.25	0.00	5.00	0.00	0.21	0.06	0.42	0.05	0.52	0.11
Dobrova	5100633	5535519	372	689.128	156.622	surface water	Posavsko hribovje do osrednje Sotle	karstic and fractured	carbonate rocks	limestone prevailing	Miocene Lithothamnium limestone	8.9	land principally occupied by agriculture, with significant areas of natural vegetation	forest	1320	1.84	2	10.3	0.2	7.77	0.05	459	16	-10.31	0.02	-69.4	0.4	13.1	0.1	-12.7	0.4	6.0	3.1	6.23	1.35	70	3	18.0	1.4	1.5	0.1	0.71	0.06	0.01	0.00	279	5	2.70	0.30	6.33	0.38	10.40	0.42	1.98	0.23	0.25	0.00	4.75	3.18	9.50	0.71	0.25	0.00	5.00	0.00	0.14	0.09	0.52	0.06	0.73	0.07
Framski slap	5150824	5542540	993	1098.99	187.361	spring capture	Vzhodne Alpe	fractured	igneous and metamorphic rocks	metamorphic rocks	old Paleozoic rocks	7.0	mixed forest	forest	1550	0.51	2	7.2	0.3	6.70	0.07	38	2	-10.65	0.01	-71.1	0.0	14.1	0.1	-20.2	0.5	0.2	0.6	6.54	0.21	2	0	1.0	0.0	2.4	0.1	0.51	0.02	0.01	0.00	25	2	0.38	0.00	2.26	0.00	2.13	0.02	8.94	0.00	0.25	0.00	2.50	0.00	11.50	0.71	1.10	0.14	5.00	0.00	0.10	0.10	-2.98	0.04	-5.97	0.09
GI-1, Gornji Ig	5086419	5461014	640	806.566	83.665	pumping station	Kraška Ljubljanica	fractured and karstic	carbonate rocks	dolomite prevailing	Triassic carbonates	7.2	mixed forest	forest	1734	5.93	2	11.2	0.3	7.66	0.04	436	3	-9.69	0.01	-65.0	0.4	12.5	0.4	-12.9	0.3	9.6	2.1	6.89	1.07	54	0	31.5	0.7	2.0	0.3	1.50	0.14	0.01	0.00	354	23	5.07	0.35	10.69	0.41	1.82	0.18	1.26	0.01	0.25	0.00	2.50	0.00	11.00	0.00	0.58	0.46	9.00	5.66	0.41	0.31	0.39	0.07	0.84	0.14
Gljun	5133418	5385668	436	1541.46	92.39	surface water	Julijske Alpe v porečju Soče	karstic and fractured	carbonate rocks	limestone prevailing	Triassic carbonates	4.1	bare rocks	forest	3286	18.53	2	5.9	0.3	8.04	0.11	168	16	-9.44	1.21	-61.7	10.7	13.8	1.1	-2.6	0.3	-1.5	1.1	6.39	0.63	28	3	3.7	0.0	0.2	0.1	0.08	0.06	0.01	0.00	111	2	0.25	0.18	1.17	0.09	0.77	0.02	0.20	0.04	0.25	0.00	2.50	0.00	3.75	1.77	0.25	0.00	5.00	0.00	0.14	0.04	0.08	0.08	-0.44	0.20
Godec	5144027	5489835	942	987.301	142.902	spring capture	Kamniško-Savinjske Alpe	fractured	igneous and metamorphic rocks	igneous rocks	Oligocene igneous rocks	6.1	coniferous forest	forest	1550	0.07	2	14.6	1.4	7.80	0.42	65	1	-9.76	0.22	-64.1	0.4	14.0	1.4	-19.0	0.4			5.82	0.04	9	0	1.0	0.0	2.4	0.1	0.73	0.01	0.01	0.00	38	1	0.38	0.00	1.11	0.00	5.88	0.10	7.80	0.26	0.25	0.00	2.50	0.00	5.25	3.89	0.25	0.00	5.00	0.00	0.23	0.18	-1.09	0.44	-2.84	0.88
Grad-1, Grad	5184942	5583431	271	301.579	240.495	pumping station	Goričko	intergranular	clastic sedimentary rocks	gravel, sand and clay	Pliocene clastics	9.0	mixed forest	forest	895	0.7	2	12.4	0.3	6.99	0.03	335	25	-9.87	0.30	-69.6	1.3	9.4	1.1	-15.1	2.7	7.2		1.10	0.48	40	0	17.0	0.0	6.1	0.0	0.99	0.01	0.01	0.00	206	2	4.93	0.08	1.17	0.09	3.51	0.06	12.82	0.88	0.25	0.00	3.75	1.77	18.50	2.12	1.35	0.07	62.00	28.28	18.82	4.66	-0.59	0.03	-1.27	0.06
Gradišče	5167493	5585013	193	196.389	231.788	pumping station	Murska kotlina	intergranular	clastic sedimentary rocks	gravel and sand	Quaternary clastics (medium- and coarse-grained)	9.0	non-irrigated arable land	areas of intense use of nutrients and plant protection products	874	6.01	2	13.7	0.9	6.63	0.01	449	21	-8.80	0.13	-60.2	1.7	10.2	0.6	-16.0	0.1	13.9	0.1	8.76	1.59	57	4	11.5	0.7	23.0	1.4	9.55	0.64	0.01	0.00	175	14	34.70	2.83	25.19	2.95	39.55	3.61	8.52	0.08	0.25	0.00	77.50	3.54	42.50	0.71	0.43	0.25	5.00	0.00	0.45	0.25	-0.91	0.04	-2.23	0.08
Grajsko zajetje	5102756	5446784	411	558.675	83.365	spring capture	Cerkljansko, Škofjeloško in Polhograjsko hribovje	fractured and karstic	carbonate rocks	dolomite prevailing	Triassic carbonates	9.0	broad-leaved forest	forest	1700	0.44	2	10.9	0.7	7.68	0.04	457	2	-8.89	0.08	-59.5	0.4	11.6	0.3	-13.3	0.2	6.7	8.3	5.52	1.93	57	0	33.5	0.7	0.7	0.1	0.13	0.00	0.01	0.00	345	33	1.30	0.10	3.87	0.09	9.61	0.56	0.77	0.00	0.25	0.00	2.50	0.00	8.50	0.71	0.48	0.32	5.00	0.00	0.04	0.02	0.42	0.07	0.89	0.14
Grešnikov hrib	5099163	5473153	392	462.161	100.833	spring	Posavsko hribovje do osrednje Sotle	fractured	clastic sedimentary rocks	shale and sandstone	Carboniferous-Permian beds	9.0	mixed forest	forest	1350	0.04	2	10.2	5.2	7.78	0.21	116	12	-8.87	0.11	-59.3	0.1	11.6	0.7	-9.8	0.1	6.6	2.5	6.47	0.96	16	1	2.2	0.1	2.0	0.1	0.39	0.08	0.01	0.00	53	10	1.03	0.05	0.72	0.55	11.80	1.84	5.00	0.65	0.38	0.18	2.50	0.00	14.50	3.54	0.25	0.00	5.00	0.00	0.84	0.08	-0.72	0.32	-2.02	0.63
Hotešk	5110130	5406520	206	826.344	70.761	surface water	Goriška Brda in Trnovsko-Banjška planota	karstic and fractured	carbonate rocks	limestone prevailing	Triassic carbonates	8.1	broad-leaved forest	forest	2373	46.54	2	9.6	0.4	8.16	0.04	269	18	-8.46	0.77	-53.1	3.4	14.6	2.8	-10.2	0.9	4.8		5.82	1.28	48	4	4.4	0.5	0.9	0.1	0.16	0.05	0.01	0.00	159	13	1.50	0.23	4.50	0.59	3.35	0.14	1.07	0.03	0.25	0.00	2.50	0.00	5.25	3.89	0.60	0.00	16.50	16.26	0.22	0.07	0.54	0.10	0.32	0.11
Hubelj	5085023	5416044	229	1006.48	50.697	spring	Goriška Brda in Trnovsko-Banjška planota	karstic and fractured	carbonate rocks	limestone prevailing	Jurassic carbonates	6.9	broad-leaved forest	forest	2483	52.16	2	8.5	0.4	8.02	0.04	244	0	-8.78	0.30	-52.6	2.9	17.7	5.3	-7.7	0.0	1.7	2.1	6.52	1.36	39	1	6.6	1.1	0.9	0.0	0.15	0.04	0.01	0.00	140	0	1.68	0.04	5.34	0.47	3.27	0.12	0.55	0.04	0.25	0.00	2.50	0.00	6.25	5.30	0.25	0.00	11.00	8.49	0.09	0.01	0.27	0.05	0.06	0.02
Ilirska Bistrica	5047352	5442029	424	777.595	51.771	spring capture	Obala in Kras z Brkini	karstic and fractured	carbonate rocks	limestone prevailing	Cretaceous carbonates	7.7	natural grasslands	forest	1954	19.22	2	9.7	0.2	7.66	0.19	351	20	-8.05	0.04	-49.9	0.8	14.5	0.6	-11.5	1.0	0.2	0.3	3.39	1.67	61	3	8.8	0.3	1.3	0.0	0.13	0.00	0.01	0.00	234	23	2.35	0.01	3.76	0.19	3.96	0.29	1.09	0.07	0.25	0.00	2.50	0.00	10.50	3.54	0.25	0.00	21.50	23.33	0.38	0.26	0.30	0.21	0.04	0.42
Iščica	5090599	5463736	293	685.777	88.267	spring	Savska kotlina in Ljubljansko barje	fractured and karstic	carbonate rocks	dolomite prevailing	Triassic carbonates	7.7	mixed forest	forest	1640	23.78	2	9.8	0.2	7.69	0.00	402	6	-9.43	0.35	-63.6	3.1	11.8	0.3	-12.8	0.5	4.7	1.5	6.09	0.23	61	5	23.5	0.7	1.6	0.1	0.62	0.03	0.01	0.00	341	58	2.97	0.28	5.84	0.38	5.10	0.70	1.17	0.04	0.25	0.00	5.50	0.71	8.00	0.00	0.53	0.39	5.00	0.00	0.15	0.12	0.46	0.03	0.79	0.11
Jelševa Loka	5136200	5522000	432	778.582	162.144	spring capture	Spodnji del Savinje do Sotle	fractured and karstic	carbonate rocks	dolomite prevailing	Triassic carbonates	7.4	mixed forest	forest	1352	2.41	2	9.1	0.1	7.60	0.09	423	13	-9.81	0.06	-65.7	0.1	12.9	0.5	-12.2	0.4	2.2	0.8	6.33	0.40	62	1	18.0	1.4	0.7	0.0	0.44	0.00	0.01	0.00	259	8	1.14	0.03	5.67	0.44	8.20	0.50	1.50	0.14	0.25	0.00	2.50	0.00	8.50	0.71	0.38	0.18	18.00	18.38	0.36	0.09	0.27	0.09	0.30	0.23
Jurčičev izvir	5111220	5454048	318	340.165	94.465	spring	Savska kotlina in Ljubljansko barje	intergranular porosity	clastic sedimentary rocks	gravel and sand	Quaternary clastics (medium- and coarse-grained)	9.0	complex cultivation patterns	areas of intense use of nutrients and plant protection products	1550	0.53	2	10.9	0.1	7.30	0.00	605	32	-8.56	0.48	-57.8	0.4	10.7	3.4	-12.9	0.7	6.4	0.8	5.60	0.90	101	4	22.0	0.0	6.4	0.1	0.71	0.06	0.01	0.00	356	8	13.10	0.99	21.47	0.75	13.75	0.21	3.04	0.09	0.38	0.18	14.50	0.71	18.50	2.12	0.75	0.07	12.50	10.61	0.25	0.08	0.28	0.02	0.19	0.03
Kamniška Bistrica	5131580	5468815	592	1534.13	119.502	spring	Kamniško-Savinjske Alpe	karstic and fractured	carbonate rocks	limestone prevailing	Triassic carbonates	3.7	bare rocks	forest	2208	22.12	2	5.7	0.1	8.02	0.12	171	5	-10.11	0.47	-67.0	2.7	13.9	1.1	-3.1	1.2	-1.0	0.1	6.65	0.92	27	0	4.1	0.6	0.2	0.1	0.08	0.06	0.01	0.00	122	23	0.25	0.18	1.28	0.25	1.46	0.28	0.22	0.02	0.25	0.00	2.50	0.00	2.50	0.00	0.25	0.00	5.00	0.00	0.17	0.01	0.07	0.04	-0.39	0.15
Korentan	5068310	5433092	537	644.7	50.39	spring	Kraška Ljubljanica	karstic and fractured	carbonate rocks	limestone prevailing	Cretaceous carbonates	9.0	broad-leaved forest	forest	1900	6.34	2	9.0	0.1	7.45	0.07	320	21	-8.09	0.05	-49.9	1.3	14.8	1.7	-14.1	0.5			5.50	0.96	72	6	1.0	0.0	2.1	0.1	0.71	0.19	0.01	0.00	224	5	2.71	0.42	5.18	0.88	4.69	0.44	1.22	0.24	0.25	0.00	2.50	0.00	8.50	3.54	0.38	0.18	14.00	1.41	0.52	0.23	0.15	0.03	-1.27	0.09
Krajcarica	5138489	5405965	706	1202.98	98.522	spring	Julijske Alpe v porečju Soče	karstic and fractured	carbonate rocks	limestone prevailing	Triassic carbonates	5.2	mixed forest	forest	2537	0.87	2	5.4	0.3	8.07	0.04	168	14	-10.33	0.88	-67.7	4.0	15.0	3.0	-6.6	5.0	-1.1	0.6	7.05	1.69	26	0	4.8	1.3	0.2	0.1	0.08	0.06	0.01	0.00	122	18	0.25	0.18	1.33	0.31	1.71	0.41	0.27	0.06	0.25	0.00	2.50	0.00	2.50	0.00	0.25	0.00	5.00	0.00	0.15	0.03	0.11	0.03	-0.25	0.07
Krka	5082860	5482630	272	493.167	100.996	spring	Dolenjski kras	karstic and fractured	carbonate rocks	limestone prevailing	Triassic carbonates	8.6	mixed forest	forest	1466	261.3	2	10.4	0.2	7.75	0.19	454	39	-9.20	0.25	-62.3	2.1	11.4	0.1	-13.2	1.0	7.5	0.9	6.27	0.97	63	4	20.0	1.4	4.2	0.6	0.88	0.31	0.01	0.00	310	81	7.02	0.34	6.29	1.32	7.03	0.91	1.81	0.08	0.25	0.00	8.00	4.24	12.00	2.83	0.25	0.00	5.00	0.00	0.39	0.09	0.49	0.31	0.76	0.63
Kropa	5127330	5488035	408	958.487	130.048	spring	Kamniško-Savinjske Alpe	karstic and fractured	carbonate rocks	limestone prevailing	Triassic carbonates	6.7	mixed forest	forest	1660	3.57	2	8.1	0.0	7.52	0.28	317	2	-9.68	0.16	-62.5	0.4	15.0	1.6	-11.9	1.3	0.1	0.6	6.22	0.02	55	3	6.7	1.1	0.5	0.0	0.16	0.05	0.01	0.00	201	24	0.76	0.04	4.40	0.47	3.90	0.20	0.77	0.02	0.25	0.00	2.50	0.00	6.50	0.71	0.43	0.25	15.50	14.85	0.60	0.75	0.07	0.35	-0.50	0.61
Krupa	5054543	5517284	139	369.141	127.336	spring	Dolenjski kras	karstic and fractured	carbonate rocks	limestone prevailing	Cretaceous carbonates	9.6	broad-leaved forest	forest	1347	85.69	2	12.7	0.8	7.67	0.22	414	52	-9.62	0.11	-64.6	1.8	12.4	0.8	-14.4	0.7	10.8	6.1	7.21	0.11	73	6	9.9	3.0	2.0	0.2	0.49	0.06	0.01	0.00	265	59	3.28	0.18	4.69	1.00	5.62	0.24	1.93	0.29	0.25	0.00	4.25	2.47	10.00	1.41	0.70	0.00	5.00	0.00	0.52	0.04	0.42	0.33	0.24	0.77
Lipnica	5131112	5435693	494	1100.68	100.603	spring	Julijske alpe v porečju Save	karstic and fractured	carbonate rocks	limestone prevailing	Triassic carbonates	5.2	coniferous forest	forest	2278	21.26	2	7.2	0.1	7.98	0.04	276	3	-8.85	0.15	-57.8	0.8	13.0	0.4	-10.5	0.6	-0.7	0.6	6.23	0.24	47	1	6.4	0.2	0.5	0.1	0.12	0.01	0.01	0.00	196	37	0.41	0.05	2.37	0.16	2.69	0.52	1.03	0.18	0.25	0.00	2.50	0.00	6.00	0.00	0.38	0.18	12.50	10.61	0.43	0.28	0.44	0.13	0.30	0.23
Lipnik	5138328	5425514	648	1244.87	103.214	spring	Julijske Alpe v porečju Save	fractured and karstic	carbonate rocks	dolomite prevailing	Triassic carbonates	4.8	coniferous forest	forest	2302	20.39	2	6.8	0.0	7.77	0.01	275	2	-9.38	0.18	-63.1	1.3	12.0	0.1	-11.0	0.8	3.7	3.0	6.28	0.69	54	4	4.5	0.3	1.9	0.4	0.20	0.11	0.01	0.00	207	30	3.91	1.05	1.79	0.97	3.07	0.40	1.60	0.15	0.25	0.00	2.50	0.00	6.50	0.71	0.58	0.46	5.00	0.00	0.22	0.00	0.31	0.02	-0.16	0.09
LMV-1, Ljubljana	5103755	5461973	305	306.885	94.883	pumping station	Savska kotlina in Ljubljansko barje	intergranular	clastic sedimentary rocks	gravel and sand	Quaternary clastics (medium- and coarse-grained)	9.0	industrial or commercial units	urban areas	1450	1.28	2	13.5	0.4	7.45	0.03	581	35	-8.59	0.33	-60.4	0.6	8.3	3.3	-12.7	1.3	8.3	1.1	6.58	0.51	88	9	22.5	0.7	9.5	9.2	0.96	0.62	0.01	0.00	313	33	22.20	14.14	24.42	0.53	24.10	0.85	2.84	0.06	0.48	0.32	23.00	19.80	28.00	4.24	35.30	9.48	10.50	7.78	2.73	3.29	0.32	0.11	0.33	0.16
Lučnica	5129977	5477111	595	1306.41	123.956	spring	Kamniško-Savinjske Alpe	fractured and karstic	carbonate rocks	dolomite prevailing	Triassic carbonates	5.1	mixed forest	forest	1881	10.82	2	7.6	0.2	7.97	0.01	248	1	-9.39	0.43	-62.0	2.6	13.1	0.8	-9.8	0.5	3.7	4.7	5.44	0.53	42	1	9.4	0.8	0.3	0.0	0.20	0.10	0.01	0.00	170	1	0.38	0.00	2.92	0.44	3.33	0.57	0.66	0.01	0.25	0.00	2.50	0.00	6.00	1.41	0.25	0.00	5.00	0.00	0.29	0.25	0.33	0.00	0.30	0.04
Malenščica	5075629	5442509	450	645.879	62.254	spring	Kraška Ljubljanica	karstic and fractured	carbonate rocks	limestone prevailing	Cretaceous carbonates	8.6	mixed forest	forest	1962	22.81	2	10.2	3.3	7.73	0.01	371	8	-8.86	0.19	-58.6	1.9	12.3	0.4	-12.4	0.7	4.1	2.8	5.71	0.18	65	2	8.0	1.0	1.6	0.1	0.23	0.15	0.01	0.00	224	1	2.65	0.19	3.81	0.75	4.39	0.59	0.93	0.31	0.25	0.00	2.50	0.00	9.00	1.41	0.25	0.00	5.00	0.00	0.28	0.08	0.37	0.02	0.12	0.03
Mali Obrh	5059874	5458907	605	898.215	70.809	spring	Kraška Ljubljanica	karstic and fractured	carbonate rocks	limestone prevailing	Cretaceous carbonates	6.7	mixed forest	forest	2014	9.99	2	8.0	0.1	7.49	0.06	396	31	-9.16	0.66	-61.9	6.7	11.4	1.4	-14.5	0.6	2.4	1.9	5.30	0.28	83	8	6.7	1.0	0.7	0.0	0.13	0.00	0.01	0.00	277	33	1.00	0.08	2.74	0.44	3.70	0.02	0.96	0.06	0.25	0.00	2.50	0.00	7.50	0.71	0.43	0.25	26.00	29.70	0.11	0.01	0.32	0.02	-0.17	0.06
Maver	5132462	5505693	386	425.588	146.865	spring capture	Spodnji del Savinje do Sotle	intergranular	clastic sedimentary rocks	clay	Oligocene clay "sivica"	9.0	complex cultivation patterns	areas of less intense use of nutrients and plant protection products	1350	0.11	2	12.3	4.5	7.85	0.07	317	18	-9.72	0.59	-63.3	0.7	14.4	5.4	-14.9	1.3			4.79	0.91	37	1	5.8	0.1	32.0	5.7	1.04	0.37	0.01	0.00	168	12	7.31	0.21	11.18	1.16	27.50	2.83	10.81	0.91	0.38	0.18	31.50	3.54	16.50	3.54	0.25	0.00	10.50	7.78	0.21	0.13	0.13	0.10	-0.26	0.19
Mazej	5141306	5500227	552	733.237	148.477	spring capture	Spodnji del Savinje do Sotle	mixed (karstic, fractured, intergranular)	carbonate rocks	carbonates with clastics	Triassic carbonates	7.0	mixed forest	forest	1376	0.86	2	11.2	0.0	7.67	0.01	296	19	-9.46	0.00	-65.4	1.2	10.4	1.2	-9.2	0.3	2.5	0.5	7.98	2.28	48	2	11.5	0.7	2.0	0.1	0.54	0.03	0.01	0.00	217	54	0.99	0.01	3.17	0.03	12.60	0.00	4.24	0.15	0.25	0.00	2.50	0.00	4.25	2.47	0.25	0.00	5.00	0.00	0.13	0.08	0.17	0.11	0.00	0.23
Metliški Obrh	5056517	5525151	152	314.589	135.38	spring	Dolenjski kras	karstic and fractured	carbonate rocks	limestone prevailing	Jurassic carbonates	9.6	complex cultivation patterns	forest	1277	23.05	2	11.0	0.4	7.40	0.01	399	3	-9.60	0.45	-66.0	4.1	10.8	0.4	-14.4	0.3	4.8	0.0	7.27	0.67	88	6	3.4	0.2	2.5	0.2	1.20	0.00	0.01	0.00	283	38	3.73	0.43	6.84	0.47	6.06	0.18	3.16	0.14	0.25	0.00	8.00	1.41	8.50	0.71	0.65	0.21	5.00	0.00	0.18	0.01	0.26	0.09	-0.60	0.18
Mitovšek	5108462	5502707	270	808.377	130.717	spring capture	Posavsko hribovje do osrednje Sotle	karstic and fractured	carbonate rocks	limestone prevailing	Triassic carbonates	7.8	mixed forest	forest	1406	4.64	2	9.2	0.3	7.79	0.04	366	8	-10.01	0.21	-66.0	0.3	14.1	1.3	-12.6	0.8	3.6	3.1	5.45	0.68	61	1	10.1	1.3	1.0	0.0	0.18	0.08	0.01	0.00	259	66	1.83	0.08	5.07	0.09	9.65	0.64	1.08	0.11	0.25	0.00	2.50	0.00	8.00	0.00	0.75	0.21	32.00	38.18	0.21	0.11	0.46	0.13	0.42	0.33
Močilnik	5090215	5445514	295	701.869	73.612	spring	Kraška Ljubljanica	karstic and fractured	carbonate rocks	limestone prevailing	Cretaceous carbonates	7.9	coniferous forest	forest	1941	1054	2	9.5	0.5	7.67	0.08	356	21	-8.62	0.51	-56.4	4.2	12.6	0.1	-13.0	1.0	3.3	0.5	5.98	0.43	59	6	8.7	1.9	2.8	0.1	0.46	0.04	0.01	0.00	212	8	4.17	0.09	5.85	0.38	5.03	0.89	1.06	0.24	0.25	0.00	5.25	3.89	10.00	2.83	0.55	0.07	19.00	1.41	0.29	0.06	0.25	0.14	-0.04	0.14
Mošenik	5142016	5444274	841	1265.46	114.222	spring	Karavanke	karstic and fractured	carbonate rocks	limestone prevailing	Triassic carbonates	4.3	bare rocks	forest	2178	2.11	2	8.4	0.2	7.97	0.00	268	19	-10.34	0.13	-69.2	0.6	13.5	0.4	-4.5	0.4	1.3	0.8	6.41	1.67	40	1	11.5	0.7	1.5	0.1	0.24	0.16	0.01	0.00	146	12	1.34	0.24	2.35	0.06	30.45	7.42	1.27	0.03	0.25	0.00	4.25	2.47	4.75	3.18	0.43	0.25	5.00	0.00	0.16	0.12	0.23	0.04	0.20	0.10
Mrzlek	5095431	5395038	77	824.729	54.45	spring capture	Goriška Brda in Trnovsko-Banjška planota	karstic and fractured	carbonate rocks	limestone prevailing	Jurassic carbonates	8.6	broad-leaved forest	forest	2300	155.5	2	10.1	1.1	7.86	0.05	210	60	-8.27	0.23	-54.5	3.9	11.7	2.1	-10.7	1.1	-0.8	0.7	5.19	0.73	48	4	4.2	0.4	1.1	0.1	0.13	0.00	0.01	0.00	166	11	1.50	0.16	3.54	0.44	3.59	0.16	0.80	0.03	0.25	0.00	2.50	0.00	7.00	0.00	0.43	0.25	5.00	0.00	0.39	0.45	0.27	0.06	-0.24	0.03
NG-4	5084377	5391735	42	51.9448	43.219	borehole	Goriška Brda in Trnovsko-Banjška planota	intergranular	clastic sedimentary rocks	gravel and sand	Quaternary clastics (medium- and coarse-grained)	13.0	non-irrigated arable land	areas of less intense use of nutrients and plant protection products	1550	0.04	2	15.7	0.8	7.35	0.07	468	10	-7.12	0.06	-44.7	0.9	12.3	0.4	-11.6	0.6			4.38	0.16	91	1	12.0	0.0	4.9	0.4	1.45	0.35	0.01	0.00	307	10	6.15	0.21	18.19	2.32	13.60	0.42	2.68	0.11	0.25	0.00	24.50	0.71	14.50	4.95	1.55	0.07	55.00	36.77	0.58	0.35	0.25	0.05	-0.10	0.11
Obrh Rinža	5057946	5486583	468	708.937	97.395	pumping station	Dolenjski kras	karstic and fractured	carbonate rocks	limestone prevailing	Cretaceous carbonates	7.5	mixed forest	forest	1717	61	2	9.0	0.8	7.56	0.11	361	37	-10.07	1.61	-68.2	13.8	12.4	0.9	-13.5	0.7	0.3	1.3	7.49	2.15	77	9	4.2	0.6	0.7	0.1	0.13	0.00	0.01	0.00	262	8	0.89	0.16	2.95	0.34	3.38	0.21	0.97	0.08	0.25	0.00	2.50	0.00	8.00	1.41	0.48	0.32	5.00	0.00	0.11	0.06	0.34	0.05	-0.29	0.10
Odolina	5050062	5423852	505	674.563	34.371	surface water	Obala in Kras z Brkini	fractured	clastic sedimentary rocks	flysch rocks	Eocene flysch rocks	9.0	broad-leaved forest	forest	1700	3.68	2	12.6	4.1	7.81	0.06	326	12	-8.01	0.18	-49.9	0.9	14.2	0.6	-11.6	0.5	2.3	0.3	5.63	1.26	54	1	5.3	0.2	5.3	0.0	0.75	0.04	0.01	0.00	212	42	3.56	0.21	1.17	0.09	10.65	0.64	4.47	0.71	0.25	0.00	5.75	4.60	10.50	2.12	0.25	0.00	5.00	0.00	8.14	5.76	0.36	0.15	-0.01	0.30
OV-29, Brunšvik	5143720	5556721	248	252.862	195.185	private well	Dravska kotlina	intergranular	clastic sedimentary rocks	gravel and sand	Quaternary clastics (medium- and coarse-grained)	11.0	non-irrigated arable land	areas of intense use of nutrients and plant protection products	1150	3.6	2	13.7	1.9	7.14	0.01	861	30	-9.38	0.40	-64.5	3.5	10.5	0.3	-12.2	1.9	7.7	0.1	7.23	0.80	120	3	23.5	0.7	23.5	0.7	10.95	1.48	0.01	0.00	372	1	29.00	2.55	91.23	1.88	28.85	2.76	6.85	1.05	0.25	0.00	140.50	10.61	31.50	0.71	0.70	0.14	5.00	0.00	0.38	0.20	0.18	0.01	-0.06	0.01
P-1, Pliskovica	5069843	5405820	202	316.743	32.436	borehole	Obala in Kras z Brkini	karstic and fractured	carbonate rocks	limestone prevailing	Cretaceous carbonates	11.0	broad-leaved forest	forest	1535	60.94	2	14.8	2.3	7.35	0.07	496	1	-6.96	0.11	-44.5	0.7	11.2	0.2	-12.4	0.3			7.13	1.75	81	1	26.5	0.7	1.5	0.1	0.13	0.00	0.01	0.00	375	13	2.17	0.05	1.11	0.00	7.04	0.06	2.19	0.14	0.25	0.00	2.50	0.00	9.00	4.24	0.50	0.00	35.00	32.53	1.00	0.49	0.27	0.05	0.35	0.12
Padiščak	5039609	5397011	88	147.768	6.537	spring capture	Obala in Kras z Brkini	fractured	clastic sedimentary rocks	flysch rocks	Eocene flysch rocks	13.0	mixed forest	forest	1138	0.51	2	13.7	0.3	7.50	0.29	717	3	-6.91	0.59	-40.9	0.4	14.4	5.1	-12.7	0.9	9.3	0.9	5.71	0.86	145	0	10.4	2.3	15.5	0.7	4.30	0.42	0.01	0.00	426	54	26.05	0.35	22.81	3.82	47.60	1.84	6.94	0.19	0.25	0.00	76.50	2.12	60.00	9.90	0.48	0.32	5.00	0.00	0.38	0.38	0.68	0.33	0.49	0.77
Pasji rep	5071540	5420149	227	425.213	42.34	surface water	Goriška Brda in Trnovsko-Banjška planota	fractured	clastic sedimentary rocks	flysch rocks	Eocene flysch rocks	10.3	broad-leaved forest	forest	1700	4.23	3	15.2	3.8	8.11	0.14	392	30	-7.17	0.06	-45.2	2.6	12.2	3.1	-10.9	0.8	5.0	0.1	5.16	0.51	72	2	6.2	0.3	5.9	0.6	1.33	0.06	0.01	0.00	244	29	3.76	0.44	4.34	0.70	16.93	1.53	4.07	0.24	0.25	0.00	15.50	4.95	5.75	4.60	0.38	0.18	5.00	0.00	1.40	0.29	0.81	0.09	0.85	0.18
Pevčevo	5147489	5536505	1054	1080.66	180.499	spring	Vzhodne Alpe	fractured	igneous and metamorphic rocks	igneous rocks	Oligocene igneous rocks	7.0	coniferous forest	forest	1550	0.08	2	7.3	0.5	6.80	0.57	29	1	-10.74	0.15	-73.1	0.1	12.8	1.1	-20.3	0.5			7.23	0.36	2	0	1.0	0.0	2.4	0.0	0.51	0.06	0.01	0.00	21	3	0.38	0.00	3.19	0.19	3.06	0.01	6.26	0.35	0.25	0.00	2.50	0.00	5.75	4.60	0.25	0.00	5.00	0.00	0.26	0.08	-2.96	0.62	-5.93	1.24
Podroteja	5094010	5425185	330	785.505	63.122	spring	Goriška Brda in Trnovsko-Banjška planota	fractured and karstic	carbonate rocks	dolomite prevailing	Triassic carbonates	8.2	mixed forest	forest	2300	51.05	2	8.8	0.1	7.85	0.09	325	6	-8.86	0.07	-57.0	0.1	14.0	0.6	-10.9	0.0	2.4	2.5	5.88	1.27	42	1	15.5	0.7	1.3	0.0	0.17	0.07	0.01	0.00	191	2	2.24	0.21	6.05	0.53	3.81	0.18	0.62	0.02	0.25	0.00	2.50	0.00	7.50	3.54	0.50	0.00	13.50	0.71	0.13	0.05	0.24	0.08	0.34	0.18
Potok pri dvorcu Visoko	5109667	5439003	384	636.793	83.873	surface water	Cerkljansko, Škofjeloško in Polhograjsko hribovje	fractured	clastic sedimentary rocks	shale and sandstone	Carboniferous-Permian beds	8.2	mixed forest	forest	1802	1.64	3	12.2	4.7	7.72	0.09	82	12	-8.75	0.13	-56.7	0.4	13.3	1.4	-7.8	0.5	6.2	3.7	5.11	0.26	7	1	3.2	0.4	2.9	0.2	0.59	0.05	0.01	0.00	35	3	2.17	0.21	3.01	0.85	7.02	0.65	3.94	0.44	0.25	0.00	5.25	3.89	12.00	1.41	0.25	0.00	5.00	0.00	0.86	0.25	-1.29	0.16	-2.64	0.32
Pšata	5124201	5462272	407	805.037	109.636	spring	Kamniško-Savinjske Alpe	karstic and fractured	carbonate rocks	limestone prevailing	Triassic carbonates	7.1	mixed forest	forest	1697	5.67	2	10.5	0.3	7.60	0.06	370	14	-8.74	0.01	-60.0	1.3	9.9	1.4	-13.6	0.7	6.7	2.5	6.71	1.08	69	3	9.5	0.1	4.1	0.7	0.49	0.06	0.01	0.00	289	22	8.10	1.44	4.52	0.06	4.79	0.01	1.73	0.12	0.25	0.00	5.50	0.71	8.50	0.71	1.00	0.57	5.00	0.00	0.19	0.06	0.37	0.08	0.16	0.16
Radeščica	5066427	5503442	176	678.37	115.604	spring	Dolenjski kras	karstic and fractured	carbonate rocks	limestone prevailing	Cretaceous carbonates	8.0	mixed forest	forest	1630	194.5	2	9.8	0.5	7.41	0.05	398	30	-10.18	0.73	-70.2	7.4	11.2	1.6	-14.1	0.6	10.6	8.9	6.47	1.04	82	7	7.3	2.5	1.9	0.4	0.44	0.01	0.01	0.00	273	33	2.66	0.52	4.74	0.94	5.52	0.02	1.26	0.10	0.25	0.00	3.75	1.77	9.00	1.41	0.48	0.32	5.00	0.00	0.10	0.03	0.23	0.03	-0.33	0.18
Rakitnica	5061215	5480413	486	867.883	92.019	pumping station	Dolenjski kras	karstic and fractured	carbonate rocks	limestone prevailing	Jurassic carbonates	6.9	mixed forest	forest	1842	65.65	2	8.9	0.6	7.90	0.01	329	31	-9.75	0.56	-65.1	6.2	12.9	1.8	-12.3	0.8	1.5	1.5	5.50	1.10	56	7	8.4	0.4	0.9	0.1	0.16	0.05	0.01	0.00	218	50	1.60	0.30	4.67	0.41	3.86	0.45	0.68	0.02	0.25	0.00	2.50	0.00	8.50	2.12	0.25	0.00	5.00	0.00	0.11	0.04	0.46	0.14	0.39	0.20
Rižana	5043199	5413318	74	555.765	22.751	spring capture	Obala in Kras z Brkini	karstic and fractured	carbonate rocks	limestone prevailing	Cretaceous carbonates	9.9	broad-leaved forest	forest	1606	226.2	2	11.3	0.2	7.62	0.20	404	23	-7.89	0.34	-50.4	3.8	12.7	1.1	-13.5	0.6	2.6	3.1	4.81	0.95	75	3	5.7	0.2	2.5	0.1	0.39	0.01	0.01	0.00	290	78	3.56	0.11	3.59	0.56	6.07	0.27	1.85	0.17	0.25	0.00	5.25	3.89	11.50	3.54	0.85	0.07	37.50	28.99	0.55	0.35	0.42	0.32	0.01	0.63
Savica	5128056	5408071	648	1784.8	88.61	surface water	Julijske Alpe v porečju Save	karstic and fractured	carbonate rocks	limestone prevailing	Triassic carbonates	2.6	bare rocks	forest	3477	30.28	2	6.5	1.1	7.97	0.01	170	18	-9.61	0.89	-61.8	7.3	15.1	0.1	-3.2	1.2	-0.6		6.16	0.27	29	2	3.4	0.8	0.2	0.0	0.08	0.06	0.01	0.00	91	26	0.25	0.18	1.22	0.16	1.22	0.44	0.26	0.05	0.25	0.00	2.50	0.00	2.50	0.00	0.25	0.00	8.50	4.95	0.33	0.19	-0.08	0.13	-0.80	0.34
Sevšek	5099488	5506749	801	825.396	129.932	spring capture	Posavsko hribovje do osrednje Sotle	fractured	clastic sedimentary rocks	shale and sandstone	Permian Val Gardena layers	7.0	broad-leaved forest	areas of less intense use of nutrients and plant protection products	1350	0.05	2	13.6	0.6	7.50	0.28	195	36	-9.82	0.09	-65.6	0.7	12.9	0.0	-16.5	1.2			6.52	0.70	26	5	10.8	1.8	2.7	0.4	0.23	0.15	0.01	0.00	130	22	1.50	0.40	2.15	1.47	6.35	0.02	5.12	0.36	0.25	0.00	6.00	0.00	10.00	2.83	0.25	0.00	5.00	0.00	0.53	0.09	-0.45	0.43	-1.00	0.84
Soča	5141410	5402362	890	1749.31	100.941	surface water	Julijske Alpe v porečju Soče	karstic and fractured	carbonate rocks	limestone prevailing	Triassic carbonates	2.5	moors and heathland	forest	2813	6.45	2	10.4		8.09	0.06	156	5	-10.50	0.86	-71.3	5.2	12.7	1.7	-1.0	0.4	-0.3	2.7	5.87	0.51	26	1	4.7	0.5	0.3	0.0	0.13	0.00	0.01	0.00	117	15	0.38	0.00	1.11	0.00	1.24	0.69	0.24	0.03	0.25	0.00	2.50	0.00	2.50	0.00	0.25	0.00	5.00	0.00	0.07	0.07	0.11	0.02	-0.24	0.07
Strahinec	5162919	5554140	283	295.531	203.881	private well	Zahodne Slovenske Gorice	intergranular	clastic sedimentary rocks	gravel, sand and clay	Miocene clastics	9.0	complex cultivation patterns	areas of less intense use of nutrients and plant protection products	1050	0.07	2	16.2	0.7	7.00	0.00	849	24	-9.07	0.08	-61.3	0.9	11.3	1.6	-12.7	0.5			6.62	0.13	144	4	41.0	1.4	14.5	3.5	1.90	0.42	0.01	0.00	555	29	9.07	3.15	5.29	2.35	64.70	3.82	4.53	0.32	0.25	0.00	107.50	7.78	25.00	2.83	0.48	0.32	49.50	62.93	0.60	0.24	0.27	0.03	0.28	0.06
Ščetar	5087015	5523032	186	265.888	140.109	spring capture	Dolenjski kras	fractured and karstic	carbonate rocks	dolomite prevailing	Triassic carbonates	9.8	complex cultivation patterns	forest	1250	1.4	2	13.1	0.8	7.46	0.22	588	6	-9.59	0.08	-65.4	0.4	11.3	1.1	-13.3	0.3	6.2	0.7	3.73	0.27	76	0	36.0	0.0	1.2	0.0	0.36	0.12	0.01	0.00	406	32	2.13	0.01	5.25	0.16	3.03	0.04	3.37	0.50	0.25	0.00	2.50	0.00	10.50	0.71	0.70	0.00	7.50	3.54	0.11	0.07	0.38	0.25	0.72	0.49
Šempeter 0840	5123490	5510688	267	275.096	145.572	private well	Savinjska kotlina	intergranular	clastic sedimentary rocks	gravel and sand	Quaternary clastics (medium- and coarse-grained)	9.9	land principally occupied by agriculture, with significant areas of natural vegetation	areas of intense use of nutrients and plant protection products	1250	2.19	2	14.1	0.2	7.77	0.76	751	14	-8.32	0.05	-56.9	0.0	9.6	0.4	-12.7	0.5	6.4	0.1	8.08	1.24	113	4	25.0	1.4	7.3	0.2	1.05	0.07	0.01	0.00	363	13	15.80	2.26	74.18	9.71	15.50	0.00	4.82	0.48	0.38	0.18	28.00	2.83	28.00	5.66	0.65	0.21	28.50	33.23	0.52	0.33	0.77	0.73	1.17	1.46
Šumec	5152600	5487320	667	900.678	147.528	spring capture	Karavanke	karstic and fractured	carbonate rocks	limestone prevailing	Triassic carbonates	6.4	mixed forest	forest	1450	0.91	2	6.6	0.0	7.96	0.13	232	0	-11.41	0.03	-77.9	1.0	13.4	0.8	-5.9	0.9	2.8	1.0	9.62	0.39	31	1	10.5	0.7	0.2	0.0	0.12	0.00	0.01	0.00	152	21	0.42	0.06	2.41	0.03	3.22	0.21	0.66	0.10	0.25	0.00	2.50	0.00	2.50	0.00	0.25	0.00	5.00	0.00	0.16	0.10	0.14	0.07	0.10	0.12
Težka voda	5069089	5516618	199	475.928	129.037	spring capture	Dolenjski kras	karstic and fractured	carbonate rocks	limestone prevailing	Triassic carbonates	9.1	broad-leaved forest	forest	1397	34.4	2	8.8	0.6	7.69	0.06	357	6	-10.22	0.25	-70.1	1.6	11.7	0.4	-13.7	0.2	1.8	0.8	7.61	0.11	73	3	8.4	1.2	1.1	0.2	0.33	0.04	0.01	0.00	255	21	1.71	0.18	4.29	0.25	4.87	0.18	2.20	0.06	0.25	0.00	2.50	0.00	7.50	0.71	0.70	0.28	5.00	0.00	0.07	0.02	0.44	0.10	0.21	0.25
Tominčev izvir	5072369	5498020	173	527.375	111.823	spring	Dolenjski kras	karstic and fractured	carbonate rocks	limestone prevailing	Cretaceous carbonates	8.6	broad-leaved forest	forest	1524	278.2	2	9.5	0.3	7.71	0.11	364	50	-9.74	0.76	-65.3	6.3	12.7	0.2	-13.3	0.9	2.5	0.8	6.35	0.90	62	8	8.7	1.2	1.7	0.1	0.26	0.04	0.01	0.00	228	52	2.85	0.13	4.58	0.66	4.57	0.77	1.05	0.04	0.25	0.00	3.75	1.77	8.50	2.12	0.25	0.00	7.50	3.54	0.21	0.14	0.34	0.25	0.10	0.50
TR-1/99, Trebelno	5086095	5512055	510	426.995	129.455	pumping station	Dolenjski kras	mixed (karstic, fractured, intergranular)	carbonate rocks	carbonates with clastics	Triassic carbonates	9.0	broad-leaved forest	forest	1250	0.18	2	11.5	0.7	7.45	0.07	516	4	-9.83	0.09	-67.1	0.7	11.5	0.0	-12.6	0.9			9.14	1.41	73	1	33.5	0.7	2.2	0.1	0.60	0.02	0.01	0.00	384	1	4.23	0.09	7.26	0.38	5.90	0.13	3.45	0.24	0.69	0.12	2.50	0.00	10.00	5.66	0.25	0.00	30.50	36.06	0.28	0.06	0.33	0.07	0.62	0.15
Trate	5110690	5526255	621	680.235	152.434	spring capture	Spodnji del Savinje do Sotle	karstic and fractured	carbonate rocks	limestone prevailing	Miocene Lithothamnium limestone	9.0	broad-leaved forest	forest	1350	0.05	2	11.0	0.8	7.60	0.00	406	11	-9.95	0.29	-65.2	0.1	14.4	2.2	-12.2	0.6			6.39	0.25	77	1	13.0	1.4	2.7	0.4	0.13	0.00	0.01	0.00	275	11	1.42	0.08	1.84	1.03	17.50	0.85	3.84	0.04	0.25	0.00	2.50	0.00	5.25	3.89	0.25	0.00	15.00	5.66	0.11	0.04	0.39	0.01	0.29	0.07
Trebija	5106590	5430333	458	657.371	76.527	spring	Cerkljansko, Škofjeloško in Polhograjsko hribovje	fractured and karstic	carbonate rocks	dolomite prevailing	Triassic carbonates	8.5	broad-leaved forest	forest	1900	0.6	2	10.2	0.6	7.63	0.13	367	1	-8.97	0.03	-58.3	0.4	13.5	0.2	-12.2	1.0	3.3		6.04	0.60	43	1	22.5	0.7	0.9	0.0	0.29	0.04	0.01	0.00	227	2	1.46	0.13	3.96	0.34	4.18	0.06	1.08	0.11	0.25	0.00	2.50	0.00	7.50	0.71	0.38	0.18	25.00	19.80	0.22	0.15	0.10	0.14	0.20	0.29
Trgovina, Vurberk	5149847	5562200	379	405.448	203.098	spring capture	Zahodne Slovenske Gorice	intergranular	clastic sedimentary rocks	gravel, sand and clay	Pliocene clastics	9.0	mixed forest	forest	1150	0.01	2	12.1	1.8	7.32	0.18	592	14	-10.32	0.09	-69.3	3.0	13.2	2.3	-13.2	0.3	1.6	1.5	10.88	1.25	96	1	22.5	0.7	1.9	0.0	0.51	0.12	0.01	0.00	352	4	2.56	0.10	6.37	0.13	29.45	0.35	4.90	0.41	0.25	0.00	2.50	0.00	19.50	0.71	0.60	0.00	5.00	0.00	0.19	0.01	0.28	0.16	0.21	0.35
V-3A, Lukavci	5156385	5587413	185	186.468	228.025	pumping station	Vzhodne Slovenske Gorice	intergranular	clastic sedimentary rocks	gravel and sand	Quaternary clastics (medium- and coarse-grained)	11.0	broad-leaved forest	forest	950	6.19	2	13.0	0.4	6.80	0.14	254	3	-9.31	0.21	-64.3	0.3	10.2	2.0	-17.5	0.3			4.33	0.09	29	1	12.0	0.0	12.0	0.0	0.42	0.05	0.01	0.00	138	4	11.20	0.28	15.54	0.63	4.01	0.13	10.47	0.49	0.25	0.00	8.00	1.41	23.00	7.07	0.25	0.00	32.00	4.24	0.36	0.07	-1.09	0.14	-2.26	0.29
V-6, Skorba	5141951	5563379	236	237.962	199.992	pumping station	Dravska kotlina	intergranular	clastic sedimentary rocks	gravel and sand	Quaternary clastics (medium- and coarse-grained)	9.9	coniferous forest	forest	1150	5.97	2	11.3	0.1	7.44	0.00	583	7	-9.23	0.04	-62.9	0.6	11.0	0.9	-12.7	0.3	6.2	0.8	6.35	0.22	102	1	22.0	0.0	5.5	0.1	0.84	0.01	0.01	0.00	351	45	11.50	0.71	45.32	1.67	24.95	0.35	5.72	0.12	0.25	0.00	16.00	0.00	22.00	2.83	0.70	0.28	5.00	0.00	0.17	0.12	0.41	0.05	0.44	0.10
Velika Toplica	5128352	5545029	284	445.749	177.304	pumping station	Haloze in Dravinjske Gorice	fractured and karstic	carbonate rocks	dolomite prevailing	Triassic carbonates	9.0	mixed forest	forest	1273	3.87	2	11.9	1.1	7.42	0.02	556	44	-10.20	0.21	-68.5	2.8	13.1	1.2	-13.0	0.1	5.1	4.2	6.23	1.04	71	1	32.0	2.8	0.9	0.1	0.23	0.14	0.01	0.00	344	19	1.57	0.08	6.24	0.06	15.30	1.70	1.58	0.37	0.25	0.00	2.50	0.00	9.50	0.71	0.25	0.00	38.50	47.38	0.23	0.02	0.25	0.01	0.43	0.04
Veliki Vrh, Bloke	5069312	5463391	723	793.203	78.045	spring capture	Kraška Ljubljanica	fractured and karstic	carbonate rocks	dolomite prevailing	Triassic carbonates	7.0	complex cultivation patterns	areas of less intense use of nutrients and plant protection products	1700	0.47	2	11.6	0.1	7.55	0.07	460	39	-10.11	0.01	-67.6	1.1	12.9	0.6	-13.5	0.3			5.02	0.09	61	4	31.5	2.1	2.9	2.0	1.86	2.46	0.01	0.00	340	1	5.29	3.51	6.68	3.38	4.88	0.74	0.90	0.22	0.25	0.00	4.75	3.18	7.00	2.83	0.25	0.00	33.00	39.60	0.43	0.37	0.31	0.09	0.63	0.18
VG-10, Mala Goba	5099600	5498990	697	715.022	123.098	pumping station	Posavsko hribovje do osrednje Sotle	fractured and karstic	carbonate rocks	dolomite prevailing	Triassic carbonates	9.0	land principally occupied by agriculture, with significant areas of natural vegetation	areas of less intense use of nutrients and plant protection products	1350	0.05	2	9.1	0.3	7.67	0.00	395	10	-9.46	0.11	-64.2	0.4	11.5	1.3	-13.2	0.2	8.1	0.2	6.50	1.36	52	1	25.5	0.7	1.6	0.1	2.85	0.35	0.01	0.00	314	11	2.57	0.21	5.71	0.50	10.05	0.64	1.48	0.04	0.25	0.00	5.50	0.71	9.00	1.41	0.53	0.39	5.00	0.00	0.64	0.12	0.34	0.02	0.66	0.05
Vidovič	5134270	5574281	267	276.849	205.924	private well	Haloze in Dravinjske Gorice	intergranular	clastic sedimentary rocks	gravel, sand and clay	Miocene clastics	11.0	land principally occupied by agriculture, with significant areas of natural vegetation	areas of less intense use of nutrients and plant protection products	1150	0.02	2	15.7	2.1	6.95	0.07	683	126	-8.89	0.13	-60.7	0.0	10.4	1.1	-14.3	0.6			6.62	1.61	135	24	17.5	6.4	6.2	2.5	1.15	0.07	0.03	0.03	391	105	13.35	8.85	44.98	25.92	38.85	15.63	6.98	0.08	0.25	0.00	24.50	0.71	21.00	5.66	0.25	0.00	39.50	48.79	3.52	2.40	0.06	0.24	-0.48	0.57
Vipava	5078341	5419948	103	824.073	47.376	spring	Goriška Brda in Trnovsko-Banjška planota	karstic and fractured	carbonate rocks	limestone prevailing	Cretaceous carbonates	7.9	mixed forest	forest	2276	100.9	2	10.7	1.1	7.83	0.00	308	6	-8.60	0.28	-53.8	1.7	15.0	0.6	-11.5	0.1	1.5	2.4	5.70	1.02	57	0	2.9	0.1	1.4	0.1	0.20	0.11	0.01	0.00	180	5	2.08	0.18	6.07	1.38	4.32	0.06	0.90	0.07	0.25	0.00	2.50	0.00	8.00	4.24	0.38	0.18	5.00	0.00	0.15	0.03	0.34	0.01	-0.32	0.04
Vo-1, Vodice	5116163	5462656	338	339.377	103.979	pumping station	Savska kotlina in Ljubljansko barje	intergranular	clastic sedimentary rocks	gravel and sand	Quaternary clastics (medium- and coarse-grained)	9.0	complex cultivation patterns	areas of intense use of nutrients and plant protection products	1450	0.45	2	12.0	0.9	7.64	0.00	419	23	-8.35	0.25	-56.9	1.4	9.9	0.6	-13.1	0.7	7.0		6.62	1.03	77	4	13.0	1.4	4.4	0.1	0.39	0.03	0.01	0.00	316	50	12.95	0.64	27.38	0.97	7.93	0.06	4.12	0.01	0.25	0.00	10.50	0.71	19.00	0.00	0.78	0.74	5.00	0.00	0.17	0.01	0.47	0.08	0.46	0.19
VP-1, Prosenjakovci	5178104	5600285	261	272.765	250.376	pumping station	Goričko	intergranular	clastic sedimentary rocks	gravel, sand and clay	Pliocene clastics	9.0	mixed forest	forest	850	0.37	2	12.2	0.8	6.84		188		-10.05	0.06	-69.9	0.7	10.5	0.3	-18.7		6.1		0.48		20		9.8		6.5		0.89		0.01		123		1.28		1.11		1.58		12.05	1.24	0.25	0.00	2.50	0.00	16.50	0.71	1.05	0.07	27.75	38.54	0.65	0.54	-1.22		-2.46	
Vt-1, Tinsko	5113876	5541943	271	463.508	167.857	pumping station	Spodnji del Savinje do Sotle	fractured and karstic	carbonate rocks	dolomite prevailing	Triassic carbonates	9.0	mixed forest	forest	1250	0.45	2	10.8	0.5	7.58	0.06	498	13	-9.39	0.04	-64.0	0.9	11.2	0.6	-13.8	0.0	1.6	0.2	9.27	0.67	65	1	36.0	0.0	0.8	0.0	0.44	0.04	0.01	0.00	429	60	1.41	0.01	6.80	0.10	21.70	0.28	2.17	0.01	0.25	0.00	2.50	0.00	8.50	0.71	0.58	0.46	5.00	0.00	0.41	0.16	0.45	0.11	0.93	0.22
Zadlaščica	5121573	5406218	813	1510.77	81.881	spring capture	Julijske Alpe v porečju Soče	karstic and fractured	carbonate rocks	limestone prevailing	Triassic carbonates	4.2	broad-leaved forest	forest	3474	9.28	2	5.6	0.1	8.16	0.09	208	49	-9.34	0.52	-60.8	4.4	14.0	0.2	-3.1	1.0	-1.0	1.4	4.99	0.12	27	2	6.5	0.4	0.3	0.0	0.13	0.00	0.01	0.00	116	4	0.38	0.00	2.26	0.00	1.19	0.62	0.33	0.06	0.25	0.00	2.50	0.00	3.75	1.77	0.38	0.18	5.00	0.00	0.06	0.05	0.18	0.11	0.03	0.20
Žegnani studenec	5148505	5518250	1403	1466.25	166.759	spring capture	Vzhodne Alpe	fractured	igneous and metamorphic rocks	metamorphic rocks	old Paleozoic rocks	5.0	coniferous forest	forest	1620	0.12	2	5.7	0.0	7.52	0.09	136	10	-10.89	0.01	-71.1	1.7	16.0	1.6	-16.3	0.8	-0.6		6.76	0.66	21	2	1.0	0.0	2.8	0.1	0.52	0.01	0.01	0.00	90	8	0.38	0.00	3.43	0.34	5.58	0.34	7.05	1.09	0.75	0.35	2.50	0.00	8.50	0.71	0.25	0.00	5.00	0.00	0.09	0.00	-0.65	0.10	-2.34	0.15

Appendix 12

Summary of statistical data analyses

n – number of observations; X – mean; X_G – geometric mean; Md – median; Min – minimum; Max – maximum; S – standard deviation; S_X – standard error of mean; VAR – variance; C_V – coefficient of variation; A – skewness; E – kurtosis; Dis. – distribution; N – Normal; Log – Log-normal; KS – Kolmogorov-Smirnov test; W – Shapiro-Wilk's test; $\chi 2$ – Chi-Square test.

Table: Descriptive statistics of raw data

Parameter	n	X	X_G	Md	Min	Max	$VAR=S^2$	S	A	E
T	174	10.7	10.3	10.6	5.2	18.2	8.7	2.9	0.26	-0.43
pH	175	7.60	7.59	7.64	6.40	8.30	0.14	0.37	-0.91	1.13
EC	175	368	319	366	28	882	29948	173	0.50	0.42
$\delta^{18}O$	174	-9.25		-9.23	-11.43	-6.49	0.88	0.94	0.25	0.15
$\delta^{2}H$	174	-61.6		-62.5	-78.6	-40.6	55.7	7.5	0.44	0.25
d-excess	174	12.4	12.2	12.4	6.0	21.4	4.1	2.0	0.53	2.33
$\delta^{13}C$-DIC	173	-12.1		-12.9	-20.6	-0.7	13.7	3.7	0.9	1.7
$\delta^{15}N_{tot}$	133	4.2		3.7	-2.8	18.6	17.2	4.1	0.8	0.9
^{3}H	172	6.14	5.80	6.01	0.48	11.77	2.85	1.69	-0.19	2.17
Ca^{2+}	175	60	49	58	2	152	886	30	0.52	0.65
Mg^{2+}	175	13.0	9.0	9.5	1.0	42.0	102.8	10.1	0.91	-0.19
Na^{+}	175	3.7	1.9	2.0	0.1	36.0	28.5	5.3	3.29	12.67
K^{+}	175	0.82	0.41	0.44	0.04	12.00	2.57	1.60	5.07	28.09
HCO_3^-	175	235	201	234	19	575	12060	110	0.16	-0.28
Cl^-	175	5.00	2.35	2.34	0.12	36.70	50.38	7.10	2.55	6.40
NO_3^-	175	9.56	4.94	4.47	0.33	92.56	251.73	15.87	3.51	12.96
SO_4^{2-}	175	10.06	6.37	5.66	0.75	67.40	132.02	11.49	2.50	6.96
Si	174	3.19	1.98	1.86	0.17	13.44	9.16	3.03	1.39	1.34
Mn	174	0.82	0.26	0.23	0.03	22.11	6.48	2.55	5.89	38.49

Table: Tests of normality for raw data

Parameter	n	max D	K-S (p)	Lilliefors (p)	W	p	X^2
T	174	0.06	p > .20	p > .20	0.98	0.0409	0.94
pH	175	0.09	p < ,10	p < ,01	0.95	0.0000	7.78
EC	175	0.07	p > .20	p < ,10	0.98	0.0043	1.80
$\delta^{18}O$	174	0.06	p > .20	p < ,10	0.99	0.2377	3.42
$\delta^{2}H$	174	0.07	p > .20	p < ,05	0.98	0.0159	4.80
d-excess	174	0.06	p > .20	p < ,10	0.97	0.0016	0.75
$\delta^{13}C$-DIC	173	0.15	p < ,01	p < ,01	0.90	0.0000	58.15
$\delta^{15}N_{tot}$	133	0.07	p > .20	p < ,10	0.95	0.0001	1.47
^{3}H	172	0.08	p > .20	p < ,01	0.95	0.0000	6.69
Ca^{2+}	175	0.07	p > .20	p < ,05	0.97	0.0020	2.76
Mg^{2+}	175	0.18	p < ,01	p < ,01	0.89	0.0000	28.08
Na^{+}	175	0.25	p < ,01	p < ,01	0.60	0.0000	210.99
K^{+}	175	0.31	p < ,01	p < ,01	0.41	0.0000	268.45
HCO_3^-	175	0.05	p > .20	p > .20	0.98	0.0483	1.11
Cl^-	175	0.27	p < ,01	p < ,01	0.64	0.0000	216.34
NO_3^-	175	0.34	p < ,01	p < ,01	0.51	0.0000	294.28
SO_4^{2-}	175	0.24	p < ,01	p < ,01	0.69	0.0000	103.61
Si	174	0.18	p < ,01	p < ,01	0.83	0.0000	10.87
Mn	174	0.39	p < ,01	p < ,01	0.29	0.0000	382.46

Table: Descriptive statistics of transformed data

Parameter	n	X	X_G	Md	Min	Max	$VAR=S^2$	S	A	E
T	174	2.0	2.0	2.0	2.0	2.1	0.0	0.0	0.20	-0.47
pH	175	2.03	2.03	2.03	2.03	2.03	0.00	0.00	-0.92	1.15
EC	175	3	3	3	2	3	0	0	-0.72	0.67
$\delta^{18}O$	174	1.96	1.96	1.96	1.95	1.97	0.00	0.00	0.22	0.13
$\delta^{2}H$	174	1.6	1.6	1.6	1.3	1.8	0.0	0.1	-0.18	0.32
d-excess	174	2.1	2.1	2.1	2.0	2.1	0.0	0.0	0.42	2.10
$\delta^{13}C$-DIC	173	1.9	1.9	1.9	1.9	2.0	0.0	0.0	0.7	1.5
$\delta^{15}Nt_{ot}$	131	2.0	2.0	2.0	2.0	2.1	0.0	0.0	0.7	0.5
^{3}H	172	2.03	2.03	2.03	2.00	2.05	0.00	0.01	-0.28	2.27
Ca^{2+}	175	2	2	2	2	2	0	0	-0.07	0.05
Mg^{2+}	175	2.1	2.1	2.0	2.0	2.2	0.0	0.0	0.79	-0.45
Na^{+}	175	2.0	2.0	2.0	2.0	2.1	0.0	0.0	3.05	10.71
K^{+}	175	2.00	2.00	2.00	2.00	2.05	0.00	0.01	4.97	27.17
HCO_3^-	175	2	2	3	2	3	0	0	-0.68	0.09
Cl^-	175	2.02	2.02	2.01	2.00	2.14	0.00	0.03	2.39	5.49
NO_3^-	175	2.04	2.04	2.02	2.00	2.28	0.00	0.05	3.09	9.96
SO_4^{2-}	175	2.04	2.04	2.02	2.00	2.22	0.00	0.04	2.17	4.93
Si	174	2.01	2.01	2.01	2.00	2.05	0.00	0.01	1.33	1.13
Mn	174	2.00	2.00	2.00	2.00	2.09	0.00	0.01	5.71	35.93

Table: Tests of normality for transformed data

Parameter	n	max D	K-S (p)	Lilliefors (p)	W	p	χ^2
T	174	0.05	p > .20	p > .20	0.99	0.0658	1.49
pH	175	0.09	p < ,10	p < ,01	0.95	0.0000	7.78
EC	175	0.10	p < ,05	p < ,01	0.96	0.0001	11.67
$\delta^{18}O$	174	0.06	p > .20	p < ,15	0.99	0.3008	3.42
$\delta^{2}H$	174	0.06	p > .20	p > .20	0.99	0.2044	3.61
d-excess	174	0.06	p > .20	p < ,10	0.98	0.0044	0.76
$\delta^{13}C$-DIC	173	0.15	p < ,01	p < ,01	0.91	0.0000	53.24
$\delta^{15}Nt_{ot}$	131	0.07	p > .20	p < ,20	0.96	0.0009	0.88
^{3}H	172	0.08	p < ,20	p < ,01	0.95	0.0000	6.37
Ca^{2+}	175	0.05	p > .20	p > .20	0.99	0.1060	6.37
Mg^{2+}	175	0.17	p < ,01	p < ,01	0.91	0.0000	28.08
Na^{+}	175	0.25	p < ,01	p < ,01	0.63	0.0000	112.47
K^{+}	175	0.31	p < ,01	p < ,01	0.42	0.0000	268.45
HCO_3^-	175	0.09	p < ,15	p < ,01	0.96	0.0000	6.37
Cl^-	175	0.26	p < ,01	p < ,01	0.67	0.0000	90.44
NO_3^-	175	0.33	p < ,01	p < ,01	0.57	0.0000	283.67
SO_4^{2-}	175	0.22	p < ,01	p < ,01	0.73	0.0000	86.73
Si	174	0.18	p < ,01	p < ,01	0.84	0.0000	12.53
Mn	174	0.39	p < ,01	p < ,01	0.30	0.0000	369.22

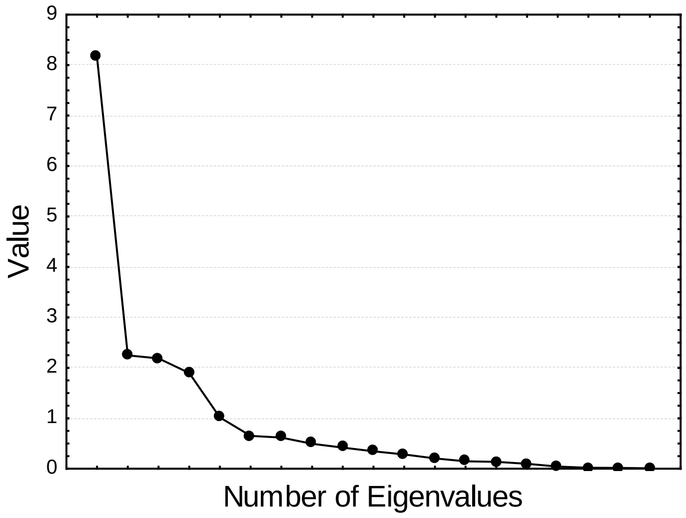

Figure: Number of factors versus the number of eigenvalues

Appendix 13

Detailed information on studied groundwater parameters

Oxygen isotopic composition in Slovenian groundwaters

Table: Groundwater $\delta^{18}O$ value according to major rock type

Major rock type class	n	X	Md	Min	Max	S
clastic sedimentary rocks	52	-8.85	-8.90	-10.50	-6.49	0.92
carbonate rocks	110	-9.35	-9.44	-11.43	-6.88	0.88
igneous and metamorphic rocks	12	-10.06	-10.27	-10.90	-8.88	0.78

Table: Groundwater $\delta^{18}O$ value according to prevailing lithological unit

Lithological class	n	X	Md	Min	Max	S
flysch rocks	6	-7.36	-7.27	-8.14	-6.49	0.59
clay	2	-9.72	-9.72	-10.13	-9.30	0.59
gravel and sand	26	-8.65	-8.71	-9.66	-7.07	0.61
gravel, sand and clay	12	-9.76	-10.05	-10.50	-8.79	0.62
shale and sandstone	6	-9.14	-8.89	-9.88	-8.65	0.53
limestone prevailing	74	-9.32	-9.32	-11.43	-6.88	1.02
dolomite prevailing	30	-9.41	-9.52	-10.34	-8.23	0.52
carbonates with clastics	6	-9.40	-9.46	-9.89	-8.87	0.41
igneous rocks	8	-9.71	-9.54	-10.84	-8.88	0.72
metamorphic rocks	4	-10.77	-10.77	-10.90	-10.64	0.14

Table: Groundwater $\delta^{18}O$ value according to prevailing lithostratigraphic unit

Lithostratigraphic class	n	X	Md	Min	Max	S
old Paleozoic rocks	4	-10.77	-10.77	-10.90	-10.64	0.14
Carboniferous-Permian beds	4	-8.81	-8.82	-8.94	-8.65	0.12
Permian Val Gardena layers	2	-9.82	-9.82	-9.88	-9.75	0.09
Ladinian igneous rocks	2	-9.45	-9.45	-9.47	-9.43	0.03
Triassic carbonates	70	-9.54	-9.56	-11.43	-7.91	0.70
Jurassic carbonates	8	-9.10	-9.14	-10.14	-8.10	0.72
Cretaceous carbonates	28	-8.85	-8.76	-11.20	-6.88	1.13
Eocene flysch rocks	6	-7.36	-7.27	-8.14	-6.49	0.59
Oligocene igneous rocks	6	-9.80	-9.76	-10.84	-8.88	0.83
Oligocene clay “sivica”	2	-9.72	-9.72	-10.13	-9.30	0.59
Miocene Lithothamnium limestone	4	-10.13	-10.22	-10.32	-9.74	0.27
Miocene clastics	4	-8.98	-9.00	-9.13	-8.79	0.14
Pliocene clastics	8	-10.15	-10.17	-10.50	-9.65	0.26
Quaternary clastics (medium- and coarse-grained)	26	-8.65	-8.71	-9.66	-7.07	0.61

Table: Groundwater $\delta^{18}O$ value according to prevailing aquifer porosity type

Aquifer porosity type	n	X	Md	Min	Max	S
intergranular porosity	40	-9.04	-9.00	-10.50	-7.07	0.80
fractured porosity	24	-9.16	-9.19	-10.90	-6.49	1.30
fractured and karstic porosity	30	-9.41	-9.52	-10.34	-8.23	0.52
karstic and fractured porosity	74	-9.32	-9.32	-11.43	-6.88	1.02
mixed porosity (karstic, fractured, intergranular)	6	-9.40	-9.46	-9.89	-8.87	0.41

Table: Groundwater δ^{18}O value according to sampling object type

Sampling object type	n	X	Md	Min	Max	S
pumping station	36	-9.44	-9.44	-11.20	-7.97	0.80
borehole	10	-7.94	-7.70	-9.16	-6.88	0.93
private well	8	-8.91	-9.00	-9.66	-8.28	0.44
spring capture	44	-9.52	-9.73	-11.43	-6.49	1.05
spring	58	-9.27	-9.01	-10.95	-8.05	0.70
surface water	18	-9.06	-8.91	-11.10	-7.13	1.16

Deuterium isotopic composition in Slovenian groundwaters

Table: Groundwater δ^2H value according to major rock type

Major rock type classification	n	X	Md	Min	Max	S
clastic sedimentary rocks	52	-59.6	-60.7	-72.0	-40.6	7.7
carbonate rocks	110	-62.0	-63.5	-78.6	-44.0	7.3
igneous and metamorphic rocks	12	-67.0	-67.1	-73.1	-60.1	5.2

Table: Groundwater δ^2H value according to prevailing lithological unit

Lithological class	n	X	Md	Min	Max	S
flysch rocks	6	-45.3	-45.2	-50.5	-40.6	4.2
clay	2	-63.3	-63.3	-63.8	-62.8	0.7
gravel and sand	26	-59.1	-59.5	-67.0	-44.0	5.2
gravel, sand and clay	12	-67.0	-69.0	-72.0	-60.6	4.6
shale and sandstone	6	-60.5	-59.3	-66.1	-56.4	4.1
limestone prevailing	74	-61.5	-61.6	-78.6	-44.0	8.3
dolomite prevailing	30	-62.8	-64.2	-70.5	-52.2	4.4
carbonates with clastics	6	-63.8	-65.4	-67.6	-58.1	4.0
igneous rocks	8	-65.0	-63.2	-73.1	-60.1	5.2
metamorphic rocks	4	-71.1	-71.1	-72.3	-69.9	1.0

Table: Groundwater δ^2H value according to prevailing lithostratigraphic unit

Lithostratigraphic class	n	X	Md	Min	Max	S
old Paleozoic rocks	4	-71.1	-71.1	-72.3	-69.9	1.0
Carboniferous-Permian beds	4	-58.0	-58.1	-59.4	-56.4	1.5
Permian Val Gardena layers	2	-65.6	-65.6	-66.1	-65.1	0.7
Ladinian igneous rocks	2	-62.5	-62.5	-62.5	-62.4	0.1
Triassic carbonates	70	-63.5	-64.5	-78.6	-50.7	5.5
Jurassic carbonates	8	-59.5	-59.0	-69.5	-50.5	7.3
Cretaceous carbonates	28	-58.2	-57.2	-78.0	-44.0	9.7
Eocene flysch rocks	6	-45.3	-45.2	-50.5	-40.6	4.2
Oligocene igneous rocks	6	-65.8	-64.1	-73.1	-60.1	5.9
Oligocene clay “sivica”	2	-63.3	-63.3	-63.8	-62.8	0.7
Miocene Lithothamnium limestone	4	-67.3	-67.2	-69.6	-65.1	2.4
Miocene clastics	4	-61.0	-60.7	-61.9	-60.6	0.6
Pliocene clastics	8	-69.9	-70.2	-72.0	-67.2	1.5
Quaternary clastics (medium- and coarse-grained)	26	-59.1	-59.5	-67.0	-44.0	5.2

Table: Groundwater δ^2H value according to prevailing aquifer porosity type

Aquifer porosity type	n	X	Md	Min	Max	S
intergranular porosity	40	-61.7	-61.7	-72.0	-44.0	6.0
fractured porosity	24	-60.0	-61.4	-73.1	-40.6	10.1
fractured and karstic porosity	30	-62.8	-64.2	-70.5	-52.2	4.4
karstic and fractured porosity	74	-61.5	-61.6	-78.6	-44.0	8.3
mixed porosity (karstic, fractured, intergranular)	6	-63.8	-65.4	-67.6	-58.1	4.0

Table: Groundwater δ^{2}H value according to sampling object type

Sampling object type	n	X	Md	Min	Max	S
pumping station	36	-64.4	-64.5	-78.0	-52.2	6.1
borehole	10	-52.5	-48.4	-63.7	-44.0	8.7
private well	8	-60.8	-60.7	-67.0	-56.9	3.2
spring capture	44	-63.0	-65.1	-78.6	-40.6	8.2
spring	58	-61.4	-60.5	-75.4	-49.0	5.7
surface water	18	-58.9	-56.8	-74.9	-43.3	9.2

Groundwater d-*excess*

Table: Groundwater d-excess value according to major rock type

Major rock type class	n	X	Md	Min	Max	S
clastic sedimentary rocks	52	11.20	10.65	6.00	18.24	2.27
carbonate rocks	110	12.82	12.70	8.90	21.40	1.69
igneous and metamorphic rocks	12	13.49	13.49	10.88	17.10	1.75

Table: Groundwater d-excess value according to prevailing lithological unit

Lithological class	n	X	Md	Min	Max	S
flysch rocks	6	13.60	14.10	10.00	18.00	2.89
clay	2	14.42	14.42	10.60	18.24	5.40
gravel and sand	26	10.10	10.30	6.00	13.10	1.54
gravel, sand and clay	12	11.14	10.92	8.60	14.80	1.62
shale and sandstone	6	12.61	12.60	11.10	14.30	1.07
limestone prevailing	74	13.09	13.00	8.90	21.40	1.86
dolomite prevailing	30	12.43	12.30	10.50	14.40	1.00
carbonates with clastics	6	11.48	11.50	9.50	12.86	1.15
igneous rocks	8	12.72	12.97	10.88	14.98	1.39
metamorphic rocks	4	15.03	14.50	14.00	17.10	1.44

Table: Groundwater d-excess value according to prevailing lithostratigraphic unit

Lithostratigraphic class	n	X	Md	Min	Max	S
old Paleozoic rocks	4	15.03	14.50	14.00	17.10	1.44
Carboniferous-Permian beds	4	12.45	12.20	11.10	14.30	1.34
Permian Val Gardena layers	2	12.92	12.92	12.90	12.94	0.03
Ladinian igneous rocks	2	13.15	13.15	12.94	13.36	0.30
Triassic carbonates	70	12.78	12.70	8.90	17.10	1.48
Jurassic carbonates	8	13.24	12.35	10.20	21.40	3.62
Cretaceous carbonates	28	12.68	12.50	10.10	15.96	1.43
Eocene flysch rocks	6	13.60	14.10	10.00	18.00	2.89
Oligocene igneous	6	12.58	12.52	10.88	14.98	1.61
Oligocene clay “sivica”	2	14.42	14.42	10.60	18.24	5.40
Miocene Lithothamnium limestone	4	13.73	13.10	12.82	15.90	1.45
Miocene clastics	4	10.85	10.66	9.62	12.44	1.23
Pliocene clastics	8	11.29	11.15	8.60	14.80	1.84
Quaternary clastics (medium- and coarse-grained)	26	10.10	10.30	6.00	13.10	1.54

Table: Groundwater d-excess value according to prevailing aquifer porosity type

Aquifer porosity type	n	X	Md	Min	Max	S
intergranular porosity	40	10.63	10.40	6.00	18.24	2.00
fractured porosity	24	13.30	13.18	10.00	18.00	1.93
fractured and karstic porosity	30	12.43	12.30	10.50	14.40	1.00
karstic and fractured porosity	74	13.09	13.00	8.90	21.40	1.86
mixed porosity (karstic, fractured, intergranular)	6	11.48	11.50	9.50	12.86	1.15

Table: Groundwater d-excess value according to sampling object type

Sampling object type	n	X	Md	Min	Max	S
pumping station	36	11.15	11.50	6.00	14.10	1.67
borehole	10	11.07	11.18	7.70	13.80	1.77
private well	8	10.45	10.24	9.30	12.44	0.99
spring capture	58	12.73	12.55	8.30	21.40	1.98
spring	44	13.10	12.97	9.50	18.24	1.95
surface water	18	13.59	13.80	10.00	16.50	1.48

pH in Slovenian groundwaters

Table: Groundwater pH value according to major rock type

Major rock type class	n	X	Md	Min	Max	S
clastic sedimentary rocks	53	7.37	7.38	6.41	8.30	0.43
carbonate rocks	110	7.73	7.72	7.30	8.22	0.23
igneous and metamorphic rocks	12	7.43	7.54	6.40	8.10	0.57

Table: Groundwater pH value according to prevailing lithological unit

Lithological unit	n	X	Md	Min	Max	S
flysch rocks	7	7.85	7.85	7.29	8.20	0.31
clay	2	7.85	7.85	7.80	7.90	0.07
gravel and sand	26	7.25	7.37	6.41	8.30	0.41
gravel, sand and clay	11	7.08	7.00	6.84	7.44	0.19
shale and sandstone	7	7.67	7.70	7.30	7.93	0.19
limestone prevailing	74	7.76	7.76	7.30	8.22	0.25
dolomite prevailing	30	7.68	7.68	7.30	7.98	0.16
carbonates with clastics	6	7.66	7.67	7.40	7.90	0.18
igneous rocks	8	7.59	7.75	6.40	8.10	0.56
metamorphic rocks	4	7.11	7.10	6.65	7.58	0.48

Table: Groundwater pH value according to prevailing lithostratigraphic unit

Lithostratigraphic unit	n	X	Md	Min	Max	S
old Paleozoic rocks	4	7.11	7.10	6.65	7.58	0.48
Carboniferous-Permian beds	5	7.74	7.72	7.63	7.93	0.13
Permian Val Gardena layers	2	7.50	7.50	7.30	7.70	0.28
Ladinian igneous rocks	2	7.75	7.75	7.70	7.80	0.07
Triassic carbonates	70	7.79	7.76	7.30	8.22	0.23
Jurassic carbonates	8	7.79	7.89	7.39	8.05	0.25
Cretaceous carbonates	28	7.59	7.57	7.30	7.83	0.16
Eocene flysch rocks	7	7.85	7.85	7.29	8.20	0.31
Oligocene igneous rocks	6	7.53	7.75	6.40	8.10	0.66
Oligocene clay “sivica”	2	7.85	7.85	7.80	7.90	0.07
Miocene Lithothamnium limestone	4	7.68	7.67	7.60	7.80	0.10
Miocene clastics	4	6.98	7.00	6.90	7.00	0.05
Pliocene clastics	7	7.14	7.15	6.84	7.44	0.22
Quaternary clastics (medium- and coarse-grained)	26	7.25	7.37	6.41	8.30	0.41

Table: Groundwater pH value according to prevailing aquifer porosity type

Aquifer porosity type	n	X	Md	Min	Max	S
intergranular porosity	39	7.23	7.30	6.41	8.30	0.38
fractured porosity	26	7.61	7.70	6.40	8.20	0.45
fractured and karstic porosity	30	7.68	7.68	7.30	7.98	0.16
karstic and fractured porosity	74	7.76	7.76	7.30	8.22	0.25
mixed porosity (karstic, fractured, intergranular	6	7.66	7.67	7.40	7.90	0.18

Table: Groundwater pH value according to the prevailing CORINE Land Cover type

CORINE Land Cover class	n	X	Md	Min	Max	S
bare rocks	8	8.00	7.97	7.93	8.12	0.07
moors and heathland	2	8.09	8.09	8.05	8.13	0.06
natural grasslands	2	7.66	7.66	7.52	7.79	0.19
coniferous forest	20	7.70	7.77	6.40	8.19	0.41
broad-leaved forest	45	7.69	7.70	6.70	8.22	0.32
mixed forest	56	7.60	7.65	6.65	8.09	0.31
non-irrigated arable land	10	7.00	7.14	6.41	7.43	0.40
complex cultivation patterns	18	7.45	7.44	7.00	7.90	0.24
land principally occupied by agriculture, with significant areas of natural vegetation	10	7.58	7.69	6.90	8.30	0.42
industrial or commercial units	2	7.45	7.45	7.43	7.47	0.03

Table: Groundwater pH value according to the prevailing Actual agricultural and forest land usage type

Actual agricultural and forest land usage class	n	X	Md	Min	Max	S
forest	137	7.67	7.70	6.40	8.22	0.33
areas of less intense use of nutrients and plant protection products	18	7.46	7.51	6.90	7.90	0.31
areas of intense use of nutrients and plant protection products	16	7.22	7.30	6.41	8.30	0.48
urban areas	2	7.45	7.45	7.43	7.47	0.03

Table: Groundwater pH value according to sampling object type

Sampling object type	n	X	Md	Min	Max	S
pumping station	35	7.41	7.47	6.62	7.90	0.35
borehole	10	7.20	7.37	6.41	7.47	0.39
private well	8	7.21	7.07	6.90	8.30	0.45
spring capture	44	7.64	7.67	6.65	8.22	0.31
spring	58	7.68	7.72	6.40	8.10	0.29
surface water	20	7.97	7.97	7.63	8.20	0.19

EC in Slovenian groundwaters

Table: Groundwater EC value according to the major rock type

Major rock type group	n	X	Md	Min	Max	S
clastic sedimentary rocks	53	477	475	75	882	215
carbonate rocks	110	346	361	152	592	105
igneous and metamorphic rocks	12	97	98	28	179	58

Table: Groundwater EC value according to prevailing lithological unit

Lithological unit	n	X	Md	Min	Max	S
flysch rocks	7	466	393	317	719	175
clay	2	317	317	304	330	18
gravel and sand	26	548	538	252	882	154
gravel, sand and clay	11	569	590	188	866	214
shale and sandstone	7	124	107	75	220	53
limestone prevailing	74	322	346	152	496	97
dolomite prevailing	30	404	404	243	592	101
carbonates with clastics	6	350	296	233	518	131
igneous rocks	8	102	102	28	179	62
metamorphic rocks	4	87	84	37	143	57

Table: Groundwater EC value according to prevailing lithostratigraphic unit

Lithostratigraphic unit	n	X	Md	Min	Max	S
Old Paleozoic rocks	4	87	84	37	143	57
Carboniferous-Permian beds	5	95	95	75	124	21
Permian Val Gardena layers	2	195	195	169	220	36
Ladinian igneous rocks	2	170	170	161	179	13
Triassic carbonates	70	331	325	152	592	119
Jurassic carbonates	8	295	280	167	401	83
Cretaceous carbonates	28	383	377	304	496	52
Eocene flysch rocks	7	466	393	317	719	175
Oligocene igneous rocks	6	79	65	28	152	53
Oligocene clay “sivica”	2	317	317	304	330	18
Miocene Lithothamnium limestone	4	433	431	398	470	33
Miocene clastics	4	766	802	594	866	121
Pliocene clastics	7	456	563	188	602	168
Quaternary clastics (medium- and coarse-grained)	26	548	538	252	882	154

Table: Groundwater EC value according to prevailing aquifer porosity type

Aquifer porosity type	n	X	Md	Min	Max	S
intergranular porosity	39	542	556	188	882	175
fractured porosity	26	203	140	28	719	190
fractured and karstic porosity	30	404	404	243	592	101
karstic and fractured porosity	74	322	346	152	496	97
mixed porosity	6	350	296	233	518	131

Table: Groundwater EC value according to prevailing CORINE Land Cover type

CORINE Land Cover class	n	X	Md	Min	Max	S
bare rocks	8	194	177	156	281	47
moors and heathland	2	156	156	152	159	5
natural grasslands	2	351	351	337	365	20
coniferous forest	20	228	210	28	588	156
broad-leaved forest	45	349	361	167	518	94
mixed forest	56	344	360	37	719	152
non-irrigated arable land	10	549	469	425	882	168
complex cultivation patterns	18	536	515	304	866	158
land principally occupied by agriculture, with significant areas of natural vegetation	10	492	459	161	772	224
industrial or commercial units	2	581	581	556	605	35

Table: Groundwater EC value according to prevailing Actual agricultural and forest land usage type

Actual agricultural and forest land usage class	n	X	Md	Min	Max	S
forest	137	325	337	28	719	141
areas of less intense use of nutrients and plant protection products	18	450	447	161	866	215
areas of intense use of nutrients and plant protection products	16	591	565	402	882	157
urban areas	2	581	581	556	605	35

Table: Groundwater EC value according to the sampling object type

Sampling object type	n	X	Md	Min	Max	S
pumping station	35	438	434	188	605	108
borehole	10	505	468	425	674	91
private well	8	786	802	594	882	93
spring capture	44	324	334	37	719	175
spring	58	322	329	28	627	117
surface water	20	244	185	75	470	126

Ca^{2+} in Slovenian groundwater

Table: Groundwater Ca^{2+} concentration according to major rock type

Major rock type	n	X	Md	Min	Max	S
clastic sedimentary rocks	53	75	79	6	152	39
carbonate rocks	110	57	57	25	92	18
igneous and metamorphic rocks	12	15	14	2	31	11

Table: Groundwater Ca^{2+} concentration according to prevailing lithological unit

Lithological unit	n	X	Md	Min	Max	S
flysch rocks	7	88	72	53	145	40
clay	2	37	37	36	37	1
gravel and sand	26	85	90	28	122	25
gravel, sand and clay	11	90	95	20	152	46
shale and sandstone	7	15	15	6	29	8
limestone prevailing	74	58	62	25	92	20
dolomite prevailing	30	55	55	39	76	11
carbonates with clastics	6	56	49	46	73	13
igneous rocks	8	16	15	2	31	12
metamorphic rocks	4	11	11	2	22	11

Table: Groundwater Ca^{2+} concentration according to prevailing lithostratigraphic unit

Lithostratigraphic unit	n	X	Md	Min	Max	S
old Paleozoic rocks	4	11	11	2	22	11
Carboniferous-Permian beds	5	11	8	6	17	5
Permian Val Gardena layers	2	26	26	22	29	5
Ladinian igneous rocks	2	31	31	30	31	1
Triassic carbonates	70	50	51	25	84	16
Jurassic carbonates	8	58	51	38	92	20
Cretaceous carbonates	28	71	72	54	91	10
Eocene flysch rocks	7	88	72	53	145	40
Oligocene igneous rocks	6	11	9	2	25	10
Oligocene clay “sivica”	2	37	37	36	37	1
Miocene Lithothamnium limestone	4	73	74	68	77	4
Miocene clastics	4	139	144	118	152	15
Pliocene clastics	7	62	72	20	97	30
Quaternary clastics (medium- and coarse-grained)	26	85	90	28	122	25

Table: Groundwater Ca^{2+} concentration according to prevailing aquifer porosity type

Aquifer porosity type	n	X	Md	Min	Max	S
intergranular porosity	39	84	89	20	152	33
fractured porosity	26	34	22	2	145	39
fractured and karstic porosity	30	55	55	39	76	11
karstic and fractured porosity	74	58	62	25	92	20
mixed porosity	6	56	49	46	73	13

Table: Groundwater Ca^{2+} concentrations according to prevailing CORINE Land Cover type

CORINE Land Cover class	n	X	Md	Min	Max	S
bare rocks	8	31	29	26	41	6
moors and heathland	2	26	26	25	27	1
natural grasslands	2	61	61	59	63	3
coniferous forest	20	39	39	2	102	28
broad-leaved forest	45	58	57	22	91	18
mixed forest	56	56	59	2	145	29
non-irrigated arable land	10	82	86	54	122	25
complex cultivation patterns	18	85	86	36	146	29
land principally occupied by agriculture, with significant areas of natural vegetation	10	80	70	30	152	42
industrial or commercial units	2	88	88	81	94	9

Table: Groundwater Ca^{2+} concentrations according to prevailing Actual agricultural and forest land usage type

Actual agricultural and forest land usage class	n	X	Md	Min	Max	S
forest	137	54	56	2	145	26
areas of less intense use of nutrients and plant protection products	18	74	61	22	152	43
areas of intense use of nutrients and plant protection products	16	88	92	54	122	23
urban areas	2	88	88	81	94	9

Table: Groundwater Ca^{2+} concentrations according to sampling object type

Sampling object type	n	X	Md	Min	Max	S
pumping station	35	65	70	20	102	20
borehole	10	80	81	55	97	15
private well	8	128	120	110	152	16
spring capture	44	52	54	2	145	32
spring	58	56	57	2	103	23
surface water	20	40	31	6	73	23

Mg^{2+} in Slovenian groundwaters

Table: Groundwater Mg^{2+} concentration according to major rock type

Major rock type	n	X	Md	Min	Max	S
clastic sedimentary rocks	53	16.2	14.0	2.1	42.0	9.4
carbonate rocks	110	12.7	8.8	1.0	36.0	10.1
igneous and metamorphic rocks	12	1.4	1.0	1.0	2.9	0.7

Table: Groundwater Mg^{2+} concentration according to prevailing lithological unit

Lithological unit	n	X	Md	Min	Max	S
flysch rocks	7	7.1	6.3	5.1	12.0	2.5
clay	2	5.8	5.8	5.7	5.9	0.1
gravel and sand	26	18.8	22.0	11.0	26.0	5.3
gravel, sand and clay	11	24.5	22.0	9.8	42.0	10.7
shale and sandstone	7	5.1	3.4	2.1	12.0	4.0
limestone prevailing	74	7.9	7.3	1.0	27.0	5.0
dolomite prevailing	30	23.8	25.5	4.3	36.0	10.0
carbonates with clastics	6	16.0	11.5	2.8	34.0	14.1
igneous rocks	8	1.6	1.0	1.0	2.9	0.8
metamorphic rocks	4	1.0	1.0	1.0	1.0	0.0

Table: Groundwater Mg^{2+} concentration according to prevailing lithostratigraphic unit

Lithostratigraphic unit	n	X	Md	Min	Max	S
old Paleozoic rocks	4	1.0	1.0	1.0	1.0	0.0
Carboniferous-Permian beds	5	2.8	2.8	2.1	3.5	0.6
Permian Val Gardena layers	2	10.8	10.8	9.5	12.0	1.8
Ladinian igneous rocks	2	1.7	1.7	1.0	2.3	0.9
Triassic carbonates	70	15.2	11.0	2.8	36.0	11.3
Jurassic carbonates	8	5.6	5.2	3.2	8.6	2.2
Cretaceous carbonates	28	8.2	7.5	1.0	27.0	5.8
Eocene flysch rocks	7	7.1	6.3	5.1	12.0	2.5
Oligocene igneous rocks	6	1.6	1.0	1.0	2.9	0.9
Oligocene clay “sivica”	2	5.8	5.8	5.7	5.9	0.1
Miocene Lithothamnium limestone	4	15.5	15.5	12.0	19.0	3.1
Miocene clastics	4	29.3	31.0	13.0	42.0	14.1
Pliocene clastics	7	21.8	22.0	9.8	32.0	8.2
Quaternary clastics (medium- and coarse-grained)	26	18.8	22.0	11.0	26.0	5.3

Table: Groundwater Mg^{2+} concentration according to prevailing aquifer porosity type

Aquifer porosity type	n	X	Md	Min	Max	S
intergranular porosity	39	19.8	22.0	5.7	42.0	8.1
fractured porosity	26	3.9	2.7	1.0	12.0	3.4
fractured and karstic porosity	30	23.8	25.5	4.3	36.0	10.0
karstic and fractured porosity	74	7.9	7.3	1.0	27.0	5.0
mixed porosity (karstic, fractured, intergranular)	6	16.0	11.5	2.8	34.0	14.1

Table: Groundwater Mg^{2+} concentration according to prevailing CORINE Land Cover type

CLC class	n	X	Md	Min	Max	S
bare rocks	8	5.7	3.8	2.8	12.0	3.7
moors and heathland	2	4.7	4.7	4.3	5.0	0.5
natural grasslands	2	8.8	8.8	8.6	9.0	0.3
coniferous forest	20	5.8	3.8	1.0	22.0	6.2
broad-leaved forest	45	12.2	8.5	1.0	34.0	9.5
mixed forest	56	12.2	9.3	1.0	36.0	9.5
non-irrigated arable land	10	16.2	14.0	11.0	24.0	5.0
complex cultivation patterns	18	22.2	22.5	3.2	42.0	12.6
land principally occupied by agriculture, with significant areas of natural vegetation	10	17.5	20.5	1.0	26.0	9.4
industrial or commercial units	2	22.5	22.5	22.0	23.0	0.7

Table: Groundwater Mg^{2+} concentration according to prevailing Actual agricultural and forest land usage type

Actual agricultural and forest land usage class	n	X	Md	Min	Max	S
forest	137	11.1	7.7	1.0	36.0	9.5
areas of less intense use of nutrients and plant protection products	18	18.7	17.5	1.0	42.0	12.4
areas of intense use of nutrients and plant protection products	16	19.3	21.0	11.0	26.0	5.4
urban areas	2	22.5	22.5	22.0	23.0	0.7

Table: Groundwater Mg^{2+} concentration according to sampling object type

Sampling object type	n	X	Md	Min	Max	S
pumping station	35	20.6	22.0	3.8	36.0	10.1
borehole	10	17.3	14.0	8.5	27.0	7.5
private well	8	26.8	24.0	13.0	42.0	9.6
spring capture	44	11.6	9.1	1.0	36.0	10.4
spring	58	9.2	7.4	1.0	24.0	6.8
surface water	20	6.1	4.9	2.8	19.0	4.3

Ca^{2+}/Mg^{2+} molar ratio in Slovenian groundwaters

Table: Groundwater Ca^{2+}/Mg^{2+} molar ratio according to major rock type

Major rock type	n	X	Md	Min	Max	S
clastic sedimentary rocks	53	3.3	2.7	1.2	10.1	1.9
carbonate rocks	108	4.3	3.6	1.0	15.9	3.3
igneous and metamorphic rocks	3	6.2	5.3	5.2	8.2	1.7

Table: Groundwater Ca^{2+}/Mg^{2+} molar ratio according to prevailing lithological unit

Major lithological units	n	X	Md	Min	Max	S
flysch rocks	7	7.3	7.0	6.2	10.1	1.3
clay	2	3.8	3.8	3.7	3.9	0.2
gravel and sand	26	2.8	2.7	1.4	4.6	0.7
gravel, sand and clay	11	2.4	2.1	1.2	5.5	1.4
shale and sandstone	7	2.3	1.4	1.3	4.5	1.5
imestone prevailing	72	5.3	4.4	1.7	15.9	3.2
dolomite prevailing	30	1.9	1.3	1.0	7.9	1.6
carbonates with clastics	6	4.5	2.5	1.3	10.2	4.0
igneous rocks	3	6.2	5.3	5.2	8.2	1.7
metamorphic rocks	**0**					

Table: Groundwater Ca^{2+}/Mg^{2+} molar ratio according to prevailing lithostratigraphic units

Lithostratigraphic unit	n	X	Md	Min	Max	S
old Paleozoic rocks	**0**					
Carboniferous-Permian beds	5	2.6	1.4	1.3	4.5	1.7
Permian Val Gardena layers	2	1.4	1.4	1.4	1.5	0.0
Ladinian igneous rocks	1	8.2	8.2	8.2	8.2	
Triassic carbonates	70	3.3	2.4	1.0	13.1	2.6
Jurassic carbonates	8	7.7	5.3	3.2	15.9	5.3
Cretaceous carbonates	26	6.3	5.5	1.8	12.3	2.9
Eocene flysch rocks	7	7.3	7.0	6.2	10.1	1.3
Oligocene igneous rocks	2	5.3	5.3	5.2	5.3	0.1
Oligocene clay ˝sivica˝	2	3.8	3.8	3.7	3.9	0.2
Miocene Lithothamnium limestone	4	3.0	2.9	2.2	3.9	0.8
Miocene clastics	4	3.5	3.2	2.1	5.5	1.7
Pliocene clastics	7	1.7	1.4	1.2	2.7	0.6
Quaternary clastics (medium- and coarse-grained)	26	2.8	2.7	1.4	4.6	0.7

HCO_3^- in Slovenian groundwaters

Table: Groundwater HCO_3^- concentration according to major rock type

Major rock type	n	X	Md	Min	Max	S
clastic sedimentary rocks	53	270	306	32	575	130
carbonate rocks	110	238	235	72	471	85
igneous and metamorphic rocks	12	60	57	19	106	35

Table: Groundwater HCO_3^- concentration according to prevailing lithological unit

Lithological class	n	X	Md	Min	Max	S
flysch rocks	7	287	242	182	464	101
clay	2	168	168	159	176	12
gravel and sand	26	293	330	97	383	92
gravel, sand and clay	11	352	355	123	575	139
shale and sandstone	7	67	46	32	145	44
limestone prevailing	74	215	223	72	384	73
dolomite prevailing	30	291	303	167	471	85
carbonates with clastics	6	255	217	162	384	105
igneous rocks	8	61	57	19	106	36
metamorphic rocks	4	58	55	24	96	38

Table: Groundwater HCO_3^- concentration according to prevailing lithostratigraphic unit

Lithostratigraphic class	n	X	Md	Min	Max	S
old Paleozoic rocks	4	58	55	24	96	38
Carboniferous-Permian beds	5	43	38	32	60	11
Permian Val Gardena layers	2	130	130	114	145	22
Ladinian igneous rocks	2	105	105	104	106	1
Triassic carbonates	70	233	224	72	471	97
Jurassic carbonates	8	202	178	140	310	63
Cretaceous carbonates	28	256	250	176	384	53
Eocene flysch rocks	7	287	242	182	464	101
Oligocene igneous rocks	6	47	38	19	89	28
Oligocene clay ˝sivica˝	2	168	168	159	176	12
Miocene Lithothamnium limestone	4	277	279	267	282	7
Miocene clastics	4	473	500	317	575	113
Pliocene clastics	7	283	349	123	373	102
Quaternary clastics (medium- and coarse-grained)	26	293	330	97	383	92

Table: Groundwater HCO_3^- concentration according to prevailing aquifer porosity type

Aquifer porosity type	n	X	Md	Min	Max	S
intergranular porosity	39	303	336	97	575	111
fractured porosity	26	123	87	19	464	117
fractured and karstic porosity	30	291	303	167	471	85
karstic and fractured porosity	74	215	223	72	384	73
mixed porosity (karstic, fractured, intergranular)	6	255	217	162	384	105

Table: Groundwater HCO_3^- concentration according to prevailing CORINE Land Cover type

CLC class	n	X	Md	Min	Max	S
bare rocks	8	117	111	72	154	25
moors and heathland	2	117	117	106	127	15
natural grasslands	2	234	234	218	250	23
coniferous forest	20	148	144	19	383	97
broad-leaved forest	45	234	234	113	384	78
mixed forest	56	232	243	24	471	109
non-irrigated arable land	10	254	303	97	373	106
complex cultivation patterns	18	347	350	159	575	101
land principally occupied by agriculture, with significant areas of natural vegetation	10	290	312	104	465	112
industrial or commercial units	2	313	313	289	336	33

Table: Groundwater HCO_3^- concentration according to prevailing Actual agricultural and forest land usage type

Land use type class	n	X	Md	Min	Max	S
forest	137	217	222	19	471	102
areas of less intense use of nutrients and plant protection products	18	295	316	104	575	140
areas of intense use of nutrients and plant protection products	16	294	351	97	373	98
urban areas	2	313	313	289	336	33

Table: Groundwater HCO_3^- concentration according to sampling object type

Sampling object type	n	X	Md	Min	Max	S
pumping station	35	292	306	123	471	84
borehole	10	278	307	97	384	104
private well	8	420	373	317	575	93
spring capture	44	215	215	24	464	117
spring	58	213	219	19	382	83
surface water	20	151	127	32	282	81

$CaCO_3$ in Slovenian groundwaters

Table: Groundwater $CaCO_3$ (mmol/L) concentration according to major rock type

Main rock type	n	X	Md	Min	Max	S
clastic sedimentary rocks	53	2.5	2.8	0.3	5.4	1.3
carbonate rocks	110	1.9	1.9	0.8	3.4	0.7
igneous and metamorphic rocks	12	0.4	0.4	0.1	0.9	0.3

Table: Groundwater $CaCO_3$ (mmol/L) concentration according to prevailing lithological unit

Lithological unit	n	X	Md	Min	Max	S
flysch rocks	7	2.5	2.1	1.5	4.1	1.1
clay	2	1.1	1.1	1.1	1.2	0
gravel and sand	26	2.9	3.1	1.2	4	0.8
gravel, sand and clay	11	3.3	3.3	0.9	5.4	1.4
shale and sandstone	7	0.6	0.5	0.3	1.2	0.4
limestone prevailing	74	1.8	1.9	0.8	3.1	0.6
dolomite prevailing	30	2.4	2.4	1.4	3.4	0.6
carbonates with clastics	6	2.1	1.7	1.3	3.2	0.9
igneous rocks	8	0.5	0.5	0.1	0.9	0.3
metamorphic rocks	4	0.3	0.3	0.1	0.6	0.3

Table: Groundwater $CaCO_3$ (mmol/L) concentrations according to prevailing lithostratigraphic unit

Lithostratigraphic units	n	X	Md	Min	Max	S
old Paleozoic rocks	4	0.3	0.3	0.1	0.6	0.3
Carboniferous-Permian beds	5	0.4	0.3	0.3	0.5	0.1
Permian Val Gardena layers	2	1.1	1.1	0.9	1.2	0.2
Ladinian igneous rocks	2	0.8	0.8	0.8	0.9	0.1
Triassic carbonates	70	1.9	1.7	0.8	3.4	0.8
Jurassic carbonates	8	1.7	1.5	1.2	2.4	0.5
Cretaceous carbonates	28	2.1	2.0	1.5	3.1	0.4
Eocene flysch rocks	7	2.5	2.1	1.5	4.1	1.1
Oligocene igneous rocks	6	0.3	0.3	0.1	0.7	0.3
Oligocene clay ˝sivica˝	2	1.1	1.1	1.1	1.2	0.0
Miocene Lithothamnium limestone	4	2.5	2.5	2.4	2.5	0.0
Miocene clastics	4	4.7	4.9	3.5	5.4	0.8
Pliocene clastics	7	2.5	3.1	0.9	3.3	1.0
Quaternary clastics (medium- and coarse-grained)	26	2.9	3.1	1.2	4.0	0.8

Table: Groundwater $CaCO_3$ (mmol/L) concentration according to prevailing aquifer porosity type

Porosity type	n	X	Md	Min	Max	S
intergranular porosity	39	2.9	3.1	0.9	5.4	1.1
fractured porosity	26	1.0	0.6	0.1	4.1	1.2
fractured and karstic porosity	30	2.4	2.4	1.4	3.4	0.6
karstic and fractured porosity	74	1.8	1.9	0.8	3.1	0.6
mixed porosity (karstic, fractured, intergranular)	6	2.1	1.7	1.3	3.2	0.9

Table: Groundwater $CaCO_3$ (mmol/L) concentration according to prevailing CORINE Land Cover type

CORINE Land Cover class	n	X	Md	Min	Max	S
bare rocks	8	1.0	0.9	0.8	1.5	0.3
moors and heathland	2	0.8	0.8	0.8	0.9	0.1
natural grasslands	2	1.9	1.9	1.8	1.9	0.1
coniferous forest	20	1.2	1.2	0.1	3.4	0.9
broad-leaved forest	45	1.9	2.0	0.9	3.2	0.6
mixed forest	56	1.9	1.9	0.1	4.1	0.9
non-irrigated arable land	10	2.7	2.8	1.8	4.0	0.8
complex cultivation patterns	18	3.0	3.1	1.1	5.4	1.1
land principally occupied by agriculture, with significant areas of natural vegetation	10	2.7	2.5	0.8	4.7	1.3
industrial or commercial units	2	3.1	3.1	3.0	3.2	0.2

Table: Groundwater $CaCO_3$ (mmol/L) concentration according to prevailing Actual agricultural and forest land usage type

Actual agricultural and forest land usage class	n	X	Md	Min	Max	S
forest	137	1.8	1.8	0.1	4.1	0.9
areas of less intense use of nutrients and plant protection products	18	2.6	2.7	0.8	5.4	1.4
areas of intense use of nutrients and plant protection products	16	3.0	3.2	1.8	4.0	0.8
urban areas	2	3.1	3.1	3.0	3.2	0.2

13K

Initial soil CO_2 partial pressure in Slovenian groundwaters

Open system:

```
TITLE Open system (wateqf4.dat)
SOLUTION 1
pH 7.0
temp 10.0
equilibrium_phases 1
CO2(g) -1.456 #I was changing those values from -4.00 to -0.70
calcite 0.0 10.0
save solution 1
end
```

Closed system:

```
TITLE Closed system (wateqf4.dat)
SOLUTION 1
pH 7.0
temp 10
equilibrium_phases 1
CO2(g) -1.824 #changing those values from -4.00 to -0.70
save solution 1
end
```

δ^{13}C-DIC in Slovenian groundwater

Table: Groundwater δ^{13}C-DIC value according to major rock type

Major rock type	n	X	Md	Min	Max	S
clastic sedimentary rocks	51	-13.4	-13.1	-18.7	-7.5	2.5
carbonate rocks	110	-11.0	-12.5	-15.2	-0.7	3.6
igneous and metamorphic rocks	12	-17.1	-17.8	-20.6	-12.9	3.0

Table: Groundwater δ^{13}C-DIC value according to prevailing lithological unit

Lithological unit	n	X	Md	Min	Max	S
flysch rocks	6	-11.7	-11.7	-13.3	-10.3	1.0
clay	2	-14.9	-14.9	-15.8	-14.0	1.3
gravel and sand	26	-13.8	-13.2	-18.0	-10.8	2.2
gravel, sand and clay	11	-14.1	-13.3	-18.7	-12.3	2.0
shale and sandstone	6	-11.4	-9.8	-17.3	-7.5	4.1
limestone prevailing	74	-10.5	-12.2	-15.2	-0.7	4.2
dolomite prevailing	30	-12.2	-12.9	-13.8	-9.2	1.4
carbonates with clastics	6	-11.7	-12.5	-13.8	-9.0	2.1
igneous rocks	8	-16.6	-16.4	-20.6	-12.9	3.3
metamorphic rocks	4	-18.2	-18.4	-20.5	-15.7	2.3

Table: Groundwater δ^{13}-DIC value according to prevailing lithostratigraphic unit

Lithostratigraphic unit	n	X	Md	Min	Max	S
old Paleozoic rocks	4	-18.2	-18.4	-20.5	-15.7	2.3
Carboniferous-Permian beds	4	-8.8	-8.9	-9.8	-7.5	1.1
Permian Val Gardena layers	2	-16.5	-16.5	-17.3	-15.7	1.2
Ladinian igneous rocks	2	-14.0	-14.0	-14.0	-13.9	0.1
Triassic carbonates	70	-10.1	-11.9	-14.3	-0.7	4.1
Jurassic carbonates	8	-11.3	-11.6	-14.6	-7.7	2.7
Cretaceous carbonates	28	-13.1	-13.4	-15.2	-9.9	1.4
Eocene flysch rocks	6	-11.7	-11.7	-13.3	-10.3	1.0
Oligocene igneous rocks	6	-17.5	-19.0	-20.6	-12.9	3.4
Oligocene clay ˝sivica˝	2	-14.9	-14.9	-15.8	-14.0	1.3
Miocene Lithothamnium limestone	4	-12.5	-12.5	-13.0	-11.8	0.5
Miocene clastics	4	-13.5	-13.4	-14.7	-12.3	1.0
Pliocene clastics	7	-14.5	-13.3	-18.7	-13.0	2.3
Quaternary clastics (medium- and coarse-grained)	26	-13.8	-13.2	-18.0	-10.8	2.2

Table: Groundwater δ^{13}-DIC value according to prevailing aquifer porosity type

Aquifer porosity type	n	X	Md	Min	Max	S
intergranular porosity	39	-14.0	-13.3	-18.7	-10.8	2.1
fractured porosity	24	-14.3	-13.8	-20.6	-7.5	4.0
fractured and karstic porosity	30	-12.2	-12.9	-13.8	-9.2	1.4
karstic and fractured porosity	74	-10.5	-12.2	-15.2	-0.7	4.2
mixed porosity	6	-11.7	-12.5	-13.8	-9.0	2.1

Table: Groundwater δ^{13}C-DIC value according to prevailing CORINE Land Cover type

CORINE Land Cover class	n	X	Md	Min	Max	S
bare rocks	8	-3.4	-3.4	-4.8	-2.2	1.0
moors and heathland	2	-1.0	-1.0	-1.3	-0.7	0.4
natural grasslands	2	-11.5	-11.5	-12.3	-10.8	1.0
coniferous forest	20	-13.4	-13.0	-20.6	-3.2	4.5
broad-leaved forest	44	-12.1	-12.6	-17.7	-2.4	3.0
mixed forest	55	-12.3	-12.9	-20.5	-3.1	3.0
non-irrigated arable land	10	-14.5	-14.7	-18.0	-10.8	2.8
complex cultivation patterns	18	-13.4	-13.3	-15.8	-12.3	0.9
land principally occupied by agriculture, with significant areas of natural vegetation	10	-13.4	-13.2	-14.7	-12.4	0.7
industrial or commercial units	2	-12.7	-12.7	-13.6	-11.7	1.3

Table: Groundwater δ^{13}C-DIC value according to prevailing Actual agricultural and forest land usage type

Actual agricultural and forest land usage class	n	X	Md	Min	Max	S
forest	135	-11.7	-12.6	-20.6	-0.7	4.0
areas of less intense use of nutrients and plant protection products	18	-13.7	-13.5	-17.3	-11.1	1.5
areas of intense use of nutrients and plant protection products	16	-14.0	-13.4	-18.0	-10.8	2.2
urban areas	2	-12.7	-12.7	-13.6	-11.7	1.3

Table: Groundwater δ^{13}C-DIC according to sampling object type

Sampling object type	n	X	Md	Min	Max	S
pumping station	35	-13.9	-13.2	-18.7	-11.7	1.8
borehole	10	-13.1	-12.3	-18.0	-9.9	2.8
private well	8	-13.0	-13.0	-14.7	-10.8	1.2
spring capture	44	-12.9	-13.2	-20.5	-2.4	3.7
spring	58	-11.8	-12.6	-20.6	-2.2	3.4
surface water	18	-7.1	-7.8	-13.0	-0.7	4.3

Si in Slovenian groundwaters

Table: Groundwater Si concentration according to major rock type

Major rock type	n	X	Md	Min	Max	S
clastic sedimentary rocks	52	6.25	5.18	2.60	13.44	3.00
carbonate rocks	110	1.36	1.14	0.17	4.34	0.94
igneous and metamorphic rocks	12	6.70	6.39	4.70	8.94	1.52

Table: Groundwater Si concentration according to prevailing lithological unit

Lithological unit	n	X	Md	Min	Max	S
flysch rocks	6	5.16	4.60	3.90	7.08	1.44
clay	2	10.81	10.81	10.17	11.46	0.91
gravel and sand	26	5.45	4.41	2.60	10.81	2.62
gravel, sand and clay	12	8.54	8.05	4.31	13.44	3.48
shale and sandstone	6	4.69	4.70	3.63	5.46	0.70
limestone prevailing	74	1.20	1.05	0.17	3.86	0.81
dolomite prevailing	30	1.30	1.18	0.56	3.72	0.73
carbonates with clastics	6	3.55	3.45	2.88	4.34	0.59
igneous rocks	8	6.05	5.75	4.70	7.98	1.23
metamorphic rocks	4	7.99	8.38	6.28	8.94	1.26

Table: Groundwater Si concentration according to prevailing lithostratigraphic unit

Lithostratigraphic unit	n	X	Md	Min	Max	S
old Paleozoic rocks	4	7.99	8.38	6.28	8.94	1.26
Carboniferous-Permian beds	4	4.47	4.40	3.63	5.46	0.76
Permian Val Gardena layers	2	5.12	5.12	4.86	5.38	0.36
Ladinian igneous rocks	2	4.94	4.94	4.70	5.19	0.35
Triassic carbonates	70	1.28	1.11	0.17	4.34	0.99
Jurassic carbonates	8	1.30	0.74	0.52	3.25	1.15
Cretaceous carbonates	28	1.34	1.17	0.72	2.29	0.46
Eocene flysch rocks	6	5.16	4.60	3.90	7.08	1.44
Oligocene igneous rocks	6	6.42	6.26	4.93	7.98	1.19
Oligocene clay ˝sivica˝	2	10.81	10.81	10.17	11.46	0.91
Miocene Lithothamnium limestone	4	2.91	2.98	1.82	3.86	1.08
Miocene clastics	4	5.76	5.84	4.31	7.04	1.42
Pliocene clastics	8	9.93	11.00	4.61	13.44	3.39
Quaternary clastics (medium- and coarse-grained)	26	5.45	4.41	2.60	10.81	2.62

Table: Groundwater Si concentration according to prevailing aquifer porosity type

Aquifer porosity type	n	X	Md	Min	Max	S
intergranular porosity	40	6.65	5.42	2.60	13.44	3.28
fractured porosity	24	5.81	5.42	3.63	8.94	1.58
fractured and karstic porosity	30	1.30	1.18	0.56	3.72	0.73
karstic and fractured porosity	74	1.20	1.05	0.17	3.86	0.81
mixed porosity	6	3.55	3.45	2.88	4.34	0.59

Dissolution of SiO_2

```
TITLE SiO2 solubility (wateqf4.dat)

SOLUTION 1
pH 7
temp 10.0

EQUILIBRIUM_PHASES 1
quartz 0.0 10.0
CO2(g) -3.456 #0.035 Vol.%

End
```

Table: Groundwater Si concentration according to prevailing CORINE Land Cover type

CORINE Land Cover class	n	X	Md	Min	Max	S
bare rocks	8	0.49	0.23	0.17	1.29	0.48
moors and heathland	2	0.24	0.24	0.23	0.26	0.03
natural grasslands	2	1.09	1.09	1.04	1.14	0.07
coniferous forest	2	3.90	3.99	0.26	7.98	2.75
broad-leaved forest	44	2.33	1.65	0.29	10.81	2.27
mixed forest	56	2.89	1.26	0.23	13.44	3.39
non-irrigated arable land	10	6.32	6.85	2.60	10.55	2.87
complex cultivation patterns	18	4.25	3.63	0.75	11.46	2.64
land principally occupied by agriculture, with significant areas of natural vegetation	10	4.04	4.59	1.45	7.04	2.16
industrial or commercial units	2	2.84	2.84	2.80	2.88	0.06

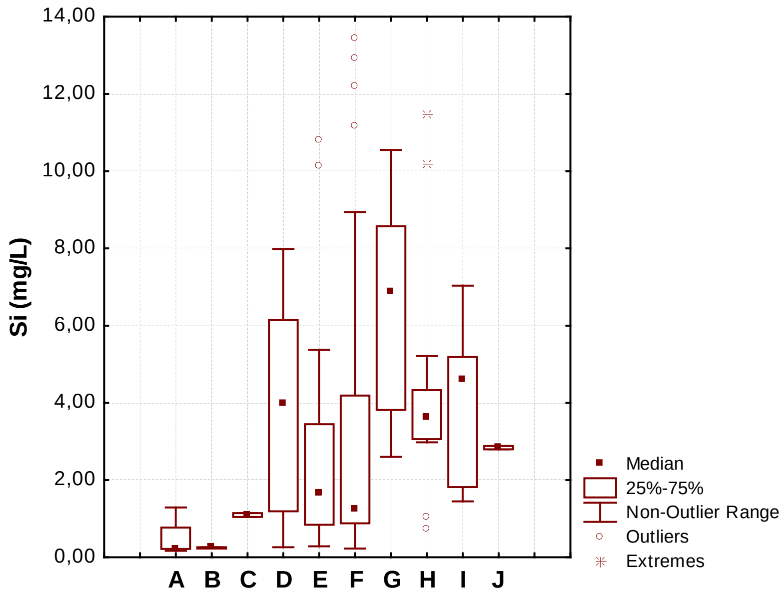

A = bare rocks (n=8)
B = moors and heathland (n=2)
C= natural grasslands (n=2)
D = coniferous forest (n=20)
E = broad-leaved forest (n=45)
F = mixed forest (n=51)
G = non-irrigated arable land (n=10)
H = complex cultivation patterns (n=18)
I = land principally occupied by agriculture, with significant areas of natural vegetation (n=10)
J = industrial or commercial units (n=2)

Figure: Box and whisker plot for groundwater Si concentration according to prevailing CORINE Land Cover type

Table: Groundwater Si concentration according to prevailing Actual agricultural and forest land usage type

Actual agricultural and forest land usage class	n	X	Md	Min	Max	S
forest	136	2.62	1.33	0.17	13.44	2.83
areas of less intense use of nutrients and plant protection products	18	4.55	4.50	0.75	11.46	2.94
areas of intense use of nutrients and plant protection products	16	5.71	4.82	2.98	10.55	2.35
urban areas	2	2.84	2.84	2.80	2.88	0.06

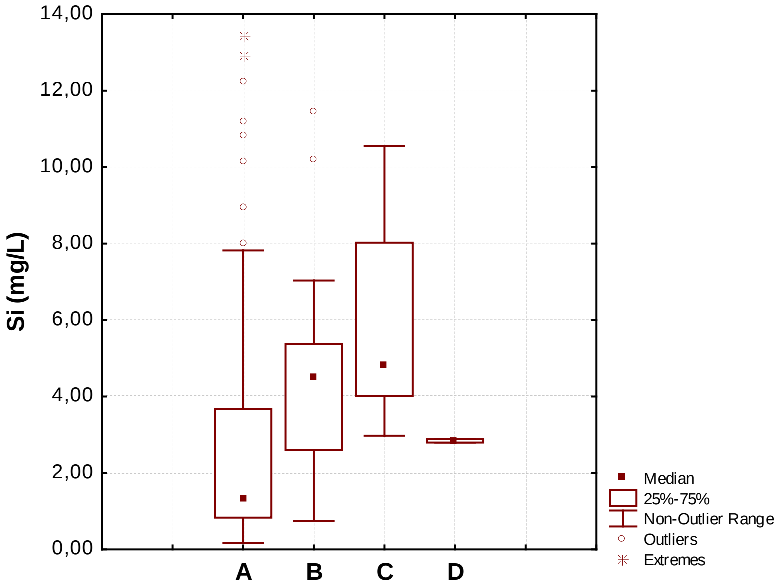

A = forest (n=136)
B = areas of less intense use of nutrients and plant protection products (n=18)
C = areas of intense use of nutrients and plant protection products (n=16)
D = urban areas (n=2)

Figure: Box and whisker plot for groundwater Si concentration according to prevailing Actual agricultural and forest land usage type

Table: Groundwater Si concentration according to sampling object type

Sampling object type	n	X	Md	Min	Max	S
pumping station	36	4.672	3.079	0.602	13.439	4.136
borehole	10	4.255	2.682	1.837	10.548	3.090
private well	8	5.796	5.635	4.305	7.588	1.283
spring capture	44	3.833	3.767	0.287	11.458	3.012
spring	58	1.649	1.157	0.205	6.500	1.395
surface water	18	1.839	1.070	0.170	4.969	1.794

Na^+ in Slovenian groundwaters

Table: Groundwater Na^+ concentration according to major rock

Major rock type class	n	X	Md	Min	Max	S
clastic sedimentary rocks	53	8.7	6.1	1.9	36.0	7.5
carbonate rocks	110	1.4	1.2	0.1	5.8	1.1
igneous and metamorphic rocks	12	2.9	2.5	2.3	5.0	0.9

Table: Groundwater Na^+ concentration according to prevailing lithological unit

Lithological class	n	X	Md	Min	Max	S
flysch rocks	7	8.5	6.2	5.2	16.0	4.8
clay	2	32.0	32.0	28.0	36.0	5.7
gravel and sand	26	9.4	6.8	3.0	24.0	6.7
gravel, sand and clay	11	6.7	6.1	1.9	17.0	4.4
shale and sandstone	7	2.6	2.8	1.9	3.1	0.5
limestone prevailing	74	1.4	1.1	0.1	5.8	1.2
dolomite prevailing	30	1.3	1.2	0.3	4.3	0.9
carbonates with clastics	6	1.9	2.0	1.6	2.2	0.2
igneous rocks	8	3.0	2.5	2.3	5.0	1.1
metamorphic rocks	4	2.6	2.6	2.3	2.9	0.3

Table: Groundwater Na^+ concentration according to prevailing lithostratigraphic unit

Lithostratigraphic class	n	X	Md	Min	Max	S
old Paleozoic rocks	4	2.6	2.6	2.3	2.9	0.3
Carboniferous-Permian beds	5	2.5	2.8	1.9	3.1	0.6
Permian Val Gardena layers	2	2.7	2.7	2.4	2.9	0.4
Ladinian igneous rocks	2	2.7	2.7	2.6	2.7	0.1
Triassic carbonates	70	1.2	0.9	0.1	4.6	1.1
Jurassic carbonates	8	1.3	1.0	0.9	2.6	0.7
Cretaceous carbonates	28	1.9	1.6	0.7	5.8	1.2
Eocene flysch rocks	7	8.5	6.2	5.2	16.0	4.8
Oligocene igneous rocks	6	3.2	2.4	2.3	5.0	1.2
Oligocene clay ˝sivica˝	2	32.0	32.0	28.0	36.0	5.7
Miocene Lithothamnium limestone	4	2.1	2.0	1.4	2.9	0.7
Miocene clastics	4	10.3	10.0	4.4	17.0	5.4
Pliocene clastics	7	4.7	5.1	1.9	6.5	2.0
Quaternary clastics (medium- and coarse-grained)	26	9.4	6.8	3.0	24.0	6.7

Table: Groundwater Na^+ concentration according to prevailing aquifer porosity type

Aquifer porosity type	n	X	Md	Min	Max	S
intergranular porosity	39	9.8	6.5	1.9	36.0	8.0
fractured porosity	26	4.3	2.9	1.9	16.0	3.6
fractured and karstic porosity	30	1.3	1.2	0.3	4.3	0.9
karstic and fractured porosity	74	1.4	1.1	0.1	5.8	1.2
mixed porosity (karstic, fractured, intergranular)	6	1.9	2.0	1.6	2.2	0.2

Table: Groundwater Na$^+$ concentration according to prevailing CORINE Land Cover type

CLC class	n	X	Md	Min	Max	S
bare rocks	8	0.5	0.3	0.2	1.6	0.6
moors and heathland	2	0.3	0.3	0.3	0.3	0.0
natural grasslands	2	1.3	1.3	1.3	1.3	0.0
coniferous forest	20	2.5	2.4	0.3	5.6	1.6
broad-leaved forest	45	2.6	1.8	0.3	12.0	2.7
mixed forest	56	2.3	1.5	0.1	16.0	3.0
non-irrigated arable land	10	12.6	8.1	3.4	24.0	9.3
complex cultivation patterns	18	8.7	4.5	1.2	36.0	9.5
land principally occupied by agriculture, with significant areas of natural vegetation	10	3.8	2.7	1.4	7.9	2.7
industrial or commercial units	2	9.5	9.5	3.0	16.0	9.2

Table: Groundwater Na$^+$ concentration according to prevailing Actual agricultural and forest land usage type

Land use type class	n	X	Md	Min	Max	S
forest	137	2.2	1.5	0.1	16.0	2.6
areas of less intense use of nutrients and plant protection products	18	8.0	4.4	1.5	36.0	9.7
areas of intense use of nutrients and plant protection products	16	10.8	7.6	3.4	24.0	7.7
urban areas	2	9.5	9.5	3.0	16.0	9.2

Table: Groundwater Na$^+$ concentration according to sampling object type

Sampling object type	n	X	Md	Min	Max	S
pumping station	35	4.9	2.7	0.7	24.0	5.7
borehole	10	6.0	5.8	1.4	11.0	3.1
private well	8	12.9	10.0	4.4	24.0	7.6
spring capture	44	3.8	2.0	0.2	36.0	7.0
spring	58	1.8	1.6	0.1	6.5	1.4
surface water	20	2.2	1.2	0.2	6.2	2.3

Cl^- in Slovenian groundwaters

Table: Groundwater Cl^- concentration according to major rock type

Major rock type	n	X	Md	Min	Max	S
clastic sedimentary rocks	53	11.50	7.79	0.99	36.70	9.88
carbonate rocks	110	2.28	1.69	0.12	9.12	2.00
igneous and metamorphic rocks	12	1.18	0.38	0.38	4.26	1.41

Table: Groundwater Cl^- concentration according to prevailing lithological unit

Lithological unit	n	X	Md	Min	Max	S
flysch rocks	7	10.07	3.70	3.39	26.30	10.92
clay	2	7.31	7.31	7.16	7.45	0.21
gravel and sand	26	17.17	12.95	6.00	36.70	9.36
gravel, sand and clay	11	6.06	4.87	1.28	19.60	5.33
shale and sandstone	7	1.65	1.78	0.99	2.38	0.56
limestone prevailing	74	2.17	1.69	0.12	9.12	2.08
dolomite prevailing	30	2.52	2.11	0.38	7.77	1.90
carbonates with clastics	6	2.29	1.66	0.98	4.29	1.53
igneous rocks	8	1.58	0.93	0.38	4.26	1.60
metamorphic rocks	4	0.38	0.38	0.38	0.38	0.00

Table: Groundwater Cl^- concentration according to prevailing lithostratigraphic unit

Lithostratigraphic unit	n	X	Md	Min	Max	S
old Paleozoic rocks	4	0.38	0.38	0.38	0.38	0.00
Carboniferous-Permian beds	5	1.71	1.96	0.99	2.38	0.65
Permian Val Gardena layers	2	1.50	1.50	1.22	1.78	0.40
Ladinian igneous rocks	2	4.04	4.04	3.81	4.26	0.32
Triassic carbonates	70	2.06	1.46	0.12	9.12	2.11
Jurassic carbonates	8	2.13	1.68	1.38	4.03	1.01
Cretaceous carbonates	28	2.90	2.46	0.78	9.04	1.96
Eocene flysch rocks	7	10.07	3.70	3.39	26.30	10.92
Oligocene igneous rocks	6	0.76	0.38	0.38	1.55	0.59
Oligocene clay ˝sivica˝	2	7.31	7.31	7.16	7.45	0.21
Miocene Lithothamnium limestone	4	2.06	1.98	1.36	2.91	0.76
Miocene clastics	4	11.21	9.20	6.84	19.60	5.96
Pliocene clastics	7	3.12	2.72	1.28	4.99	1.34
Quaternary clastics (medium- and coarse-grained)	26	17.17	12.95	6.00	36.70	9.36

Table: Groundwater Cl^- concentration according to prevailing aquifer porosity type

Aquifer porosity type	n	X	Md	Min	Max	S
intergranular porosity	39	13.53	11.30	1.28	36.70	9.61
fractured porosity	26	3.70	1.67	0.38	26.30	6.72
fractured and karstic porosity	30	2.52	2.11	0.38	7.77	1.90
karstic and fractured porosity	74	2.17	1.69	0.12	9.12	2.08
mixed porosity (karstic, fractured, intergranular)	6	2.29	1.66	0.98	4.29	1.53

Table: Groundwater Cl^- concentration according to prevailing CORINE Land Cover type

CORINE Land Cover class	n	X	Md	Min	Max	S
bare rocks	8	0.52	0.38	0.12	1.51	0.53
moors and heathland	2	0.38	0.38	0.38	0.38	0.00
natural grasslands	2	2.35	2.35	2.34	2.35	0.01
coniferous forest	20	2.47	0.96	0.38	12.00	3.41
broad-leaved forest	45	3.04	2.13	0.38	11.40	2.63
mixed forest	56	3.07	1.85	0.12	26.30	4.86
non-irrigated arable land	10	21.16	26.15	6.00	36.70	12.04
complex cultivation patterns	18	9.35	7.61	2.12	23.20	6.29
land principally occupied by agriculture, with significant areas of natural vegetation	10	7.69	4.04	2.42	19.60	6.74
industrial or commercial units	2	22.20	22.20	12.20	32.20	14.14

Table: Groundwater Cl^- concentration according to prevailing Actual agricultural and forest land usage type

Actual agricultural and forest land usage class	n	X	Md	Min	Max	S
forest	137	2.78	1.71	0.12	26.3	3.73
areas of less intense use of nutrients and plant protection products	18	6.3	6.57	1.22	19.6	4.25
areas of intense use of nutrients and plant protection products	16	20.58	20.2	8.97	36.7	8.89
urban areas	2	22.2	22.2	12.2	32.2	14.14

Table: Groundwater Cl^- concentration according to sampling object type

Sampling object type	n	X	Md	Min	Max	S
pumping station	35	7.71	4.82	0.78	36.70	9.09
borehole	10	13.42	9.00	2.13	28.30	10.24
private well	8	16.80	15.80	6.84	30.80	8.81
spring capture	44	3.09	1.57	0.38	26.30	5.37
spring	58	2.83	2.13	0.12	13.80	2.88
surface water	20	1.79	1.81	0.12	4.24	1.42

NO_3^- in Slovenian groundwaters

Table: Groundwater NO_3^- concentration according to major rock type

Major rock type class	n	X	Md	Min	Max	S
clastic sedimentary rocks	53	22.06	15.98	0.33	92.56	24.58
carbonate rocks	110	4.25	4.10	1.11	10.98	2.11
igneous and metamorphic rocks	12	3.09	3.25	1.11	5.05	1.25

Table: Groundwater NO_3^- concentration according to prevailing lithological unit

Lithological class	n	X	Md	Min	Max	S
flysch rocks	7	8.71	4.65	1.11	25.51	9.87
clay	2	11.18	11.18	10.36	12.00	1.16
gravel and sand	26	36.50	24.62	11.64	92.56	25.52
gravel, sand and clay	11	11.08	3.63	1.11	63.30	18.78
shale and sandstone	7	2.11	2.43	0.33	3.98	1.30
limestone prevailing	74	3.82	3.99	1.11	9.26	1.95
dolomite prevailing	30	5.19	5.36	1.11	10.98	2.26
carbonates with clastics	6	4.84	4.09	3.14	7.53	1.95
igneous rocks	8	3.21	3.36	1.11	5.05	1.48
metamorphic rocks	4	2.84	2.72	2.26	3.67	0.71

Table: Groundwater NO_3^- concentration according to prevailing lithostratigraphic unit

Lithostratigraphic unit	n	X	Md	Min	Max	S
old Paleozoic rocks	4	2.84	2.72	2.26	3.67	0.71
Carboniferous-Permian beds	5	2.09	2.43	0.33	3.98	1.42
Permian Val Gardena layers	2	2.15	2.15	1.11	3.19	1.47
Ladinian igneous rocks	2	4.96	4.96	4.87	5.05	0.13
Triassic carbonates	70	4.16	4.07	1.11	10.98	2.23
Jurassic carbonates	8	5.10	4.98	3.23	7.17	1.32
Cretaceous carbonates	28	4.26	4.03	1.11	9.26	1.96
Eocene flysch rocks	7	8.71	4.65	1.11	25.51	9.87
Oligocene igneous rocks	6	2.63	3.19	1.11	3.81	1.21
Oligocene clay ˝sivica˝	2	11.18	11.18	10.36	12.00	1.16
Miocene Lithothamnium limestone	4	4.09	4.32	1.11	6.60	2.67
Miocene clastics	4	25.13	16.80	3.63	63.30	27.40
Pliocene clastics	7	3.05	2.57	1.11	6.46	2.36
Quaternary clastics (medium- and coarse-grained)	26	36.50	24.62	11.64	92.56	25.52

Table: Groundwater NO_3^- concentration according to prevailing aquifer porosity type

Aquifer porosity type	n	X	Md	Min	Max	S
intergranular porosity	39	28.03	22.13	1.11	92.56	25.85
fractured porosity	26	4.34	3.19	0.33	25.51	5.65
fractured and karstic porosity	30	5.19	5.36	1.11	10.98	2.26
karstic and fractured porosity	74	3.82	3.99	1.11	9.26	1.95
mixed porosity (karstic, fractured, intergranular)	6	4.84	4.09	3.14	7.53	1.95

Table: Groundwater NO_3^- concentration according to prevailing CORINE Land Cover type

CORINE Land Cover class	n	X	Md	Min	Max	S
bare rocks	8	1.51	1.28	1.11	2.39	0.53
moors and heathland	2	1.11	1.11	1.11	1.11	0.00
natural grasslands	2	3.76	3.76	3.63	3.90	0.19
coniferous forest	20	7.32	3.25	1.11	46.50	13.07
broad-leaved forest	45	4.37	3.98	1.11	15.98	3.07
mixed forest	56	5.03	4.52	0.33	25.51	4.12
non-irrigated arable land	10	46.09	25.86	16.56	92.56	31.53
Complex cultivation patterns	18	13.31	11.00	3.63	28.07	8.43
land principally occupied by agriculture, with significant areas of natural vegetation	10	27.23	6.33	4.87	81.04	30.91
industrial or commercial units	2	24.42	24.42	24.05	24.80	0.53

Table: Groundwater NO_3^- concentration according to prevailing Actual agricultural and forest land usage type

Actual agricultural and forest land usage class	n	X	Md	Min	Max	S
forest	137	4.96	3.94	0.33	46.50	5.97
areas of less intense use of nutrients and plant protection products	18	12.36	8.01	1.11	63.30	14.28
areas of intense use of nutrients and plant protection products	16	44.86	26.99	20.94	92.56	28.24
urban areas	2	24.42	24.42	24.05	24.80	0.53

Table: Groundwater NO_3^- concentration according to sampling object type

Sampling object type	n	X	Md	Min	Max	S
pumping station	35	12.33	6.73	1.11	46.50	12.17
borehole	10	24.81	18.19	1.11	75.26	26.42
private well	8	53.92	65.31	3.63	92.56	36.39
spring capture	44	4.97	3.83	1.11	25.51	4.56
spring	58	4.93	4.41	0.33	22.00	3.89
surface water	20	2.90	2.48	1.11	6.60	1.81

$\delta^{15}N_{tot}$ in Slovenian groundwaters

Table: Groundwater $\delta^{15}N_{tot}$ values according to prevailing CORINE Land Cover type

CORINE Land Cover class	n	X	Md	Min	Max	S
bare rocks	7	-0.41	-0.70	-2.30	1.90	1.34
moors and heathland	2	-0.30	-0.30	-2.20	1.60	2.69
natural grasslands	2	0.20	0.20	0.00	0.40	0.28
coniferous forest	11	1.93	1.60	-2.80	6.70	3.20
broad-leaved forest	28	3.44	2.90	-2.04	15.10	3.76
mixed forest	54	3.90	3.00	-1.50	16.90	3.62
non-irrigated arable land	8	10.45	9.55	7.10	14.20	3.19
complex cultivation patterns	11	7.37	6.50	4.80	18.60	3.89
land principally occupied by agriculture, with significant areas of natural vegetation	6	6.80	7.15	3.80	8.20	1.71
industrial or commercial units	2	8.25	8.25	7.50	9.00	1.06

Table: Groundwater $\delta^{15}N_{tot}$ values according to prevailing Actual agricultural and forest land usage type

Land cover class	n	µ	Md	Min	Max	s
forest	110	3.26	2.65	-2.80	16.90	3.61
areas of less intense use of nutrients and plant protection products	4	7.83	8.05	6.50	8.70	0.94
areas of intense use of nutrients and plant protection products	15	9.35	7.60	5.50	18.60	3.99
urban areas	2	8.25	8.25	7.50	9.00	1.06

K^+ in Slovenian groundwaters

Table: Groundwater K^+ concentration according to major rock type

Major rock type	n	X	Md	Min	Max	S
clastic sedimentary rocks	53	1.75	0.98	0.13	12.00	2.59
carbonate rocks	110	0.41	0.24	0.04	3.60	0.54
igneous and metamorphic rocks	12	0.54	0.52	0.37	0.73	0.10

Table: Groundwater K^+ concentration according to prevailing lithological unit

Lithological class	n	X	Md	Min	Max	S
flysch rocks	7	2.01	1.30	0.72	4.60	1.59
clay	2	1.04	1.04	0.78	1.30	0.37
gravel and sand	26	2.39	1.05	0.37	12.00	3.47
gravel, sand and clay	11	1.04	0.98	0.42	2.20	0.50
shale and sandstone	7	0.43	0.44	0.13	0.63	0.18
limestone prevailing	74	0.29	0.13	0.04	1.20	0.26
dolomite prevailing	30	0.66	0.32	0.13	3.60	0.90
carbonates with clastics	6	0.61	0.60	0.52	0.75	0.08
igneous rocks	8	0.55	0.53	0.37	0.73	0.12
metamorphic rocks	4	0.51	0.52	0.49	0.52	0.01

Table: Groundwater K^+ concentration according to prevailing lithostratigraphic unit

Lithostratigraphic class	n	X	Md	Min	Max	S
Old Paleozoic rocks	4	0.51	0.52	0.49	0.52	0.01
Carboniferous-Permian beds	5	0.51	0.54	0.33	0.63	0.12
Permian Val Gardena layers	2	0.23	0.23	0.13	0.34	0.15
Ladinian igneous rocks	2	0.46	0.46	0.37	0.55	0.13
Triassic carbonates	70	0.44	0.25	0.04	3.60	0.64
Jurassic carbonates	8	0.41	0.15	0.13	1.20	0.49
Cretaceous carbonates	28	0.32	0.28	0.13	0.84	0.21
Eocene flysch rocks	7	2.01	1.30	0.72	4.60	1.59
Oligocene igneous rocks	6	0.58	0.53	0.47	0.73	0.12
Oligocene clay ˝sivica˝	2	1.04	1.04	0.78	1.30	0.37
Miocene Lithothamnium limestone	4	0.42	0.39	0.13	0.75	0.34
Miocene clastics	4	1.53	1.40	1.10	2.20	0.50
Pliocene clastics	7	0.76	0.76	0.42	1.00	0.21
Quaternary clastics (medium- and coarse-grained)	26	2.39	1.05	0.37	12.00	3.47

Table: Groundwater K^+ concentration according to prevailing aquifer porosity type

Aquifer porosity type	n	X	Md	Min	Max	S
intergranular porosity	39	1.94	1.00	0.37	12.00	2.90
fractured porosity	26	0.90	0.55	0.13	4.60	1.05
fractured and karstic porosity	30	0.66	0.32	0.13	3.60	0.90
karstic and fractured porosity	74	0.29	0.13	0.04	1.20	0.26
mixed porosity (karstic, fractured, intergranular)	6	0.61	0.60	0.52	0.75	0.08

Table: Groundwater K^+ concentration according to prevailing CORINE Land Cover type

CLC class	n	X	Md	Min	Max	S
bare rocks	8	0.12	0.13	0.04	0.35	0.10
moors and heathland	2	0.13	0.13	0.13	0.13	0.00
natural grasslands	2	0.13	0.13	0.13	0.13	0.00
coniferous forest	20	0.47	0.50	0.11	0.84	0.25
broad-leaved forest	45	0.39	0.30	0.13	1.40	0.33
mixed forest	56	0.56	0.42	0.04	4.60	0.80
non-irrigated arable land	10	4.87	1.55	1.00	12.00	4.69
complex cultivation patterns	18	1.10	0.77	0.13	3.60	0.88
land principally occupied by agriculture, with significant areas of natural vegetation	10	1.24	1.05	0.37	3.10	0.90
industrial or commercial units	2	0.96	0.96	0.52	1.40	0.62

Table: Groundwater K^+ concentration according to prevailing Actual agricultural and forest land usage type

land use type class	n	X	Md	Min	Max	S
forest	137	0.47	0.35	0.04	4.60	0.57
areas of less intense use of nutrients and plant protection products	18	1.27	1.15	0.13	3.60	1.03
areas of intense use of nutrients and plant protection products	16	3.37	1.20	0.37	12.00	4.16
urban areas	2	0.96	0.96	0.52	1.40	0.62

Table: Groundwater K^+ concentration according to sampling object type

Sampling object type	n	X	Md	Min	Max	S
pumping station	35	1.25	0.58	0.13	10.00	2.18
borehole	10	1.11	1.25	0.13	2.00	0.67
private well	8	3.76	1.40	1.00	12.00	4.49
spring capture	44	0.62	0.39	0.12	4.60	0.98
spring	58	0.38	0.31	0.04	1.20	0.28
surface water	20	0.49	0.37	0.04	1.40	0.45

SO_4^{2-} in Slovenian groundwaters

Table: Groundwater SO_4^{2-} concentration according to major rock type

Major rock type	n	X	Md	Min	Max	S
clastic sedimentary rocks	53	19.57	13.90	1.58	67.	15.77
carbonate rocks	110	5.98	4.37	0.75	35.70	5.29
igneous and metamorphic rocks	12	5.31	5.18	2.11	10.70	2.71

Table: Groundwater SO_4^{2-} concentration according to prevailing lithological unit

Rock type	n	X	**Md**	**Min**	**Max**	**S**
flysch rocks	7	23.90	17.50	10.20	48.90	16.47
clay	2	27.50	27.50	25.50	29.50	2.82
gravel and sand	26	18.44	19.90	3.91	42.10	11.55
gravel, sand and clay	11	25.31	27.80	1.58	67.40	25.23
shale and sandstone	7	8.19	7.15	6.31	13.10	2.62
limestone prevailing	74	5.49	4.28	0.75	35.70	5.34
dolomite prevailing	30	6.88	4.41	1.69	21.9	5.35
carbonates with clastics	6	7.58	5.90	4.03	12.60	3.95
igneous rocks	8	6.05	5.41	3.05	10.70	2.83
metamorphic rocks	4	3.85	3.74	2.11	5.82	2.00

Table: Groundwater SO_4^{2-} concentration according to prevailing lithostratigraphic unit

Lithostratigraphic unit	n	X	**Md**	**Min**	**Max**	**S**
old Paleozoic rocks	4	3.85	3.74	2.11	5.82	2.00
Carboniferous-Permian beds	5	8.93	7.59	6.31	13.1	2.81
Permian Val Gardena layers	2	6.34	6.34	6.33	6.36	0.02
Ladinian igneous rocks	2	4.99	4.99	4.97	5.02	0.03
Triassic carbonates	70	6.06	4.17	0.75	35.70	6.15
Jurassic carbonates	8	4.19	3.62	3.18	6.18	1.18
Cretaceous carbonates	28	5.19	4.61	3.23	10.10	1.96
Eocene flysch rocks	7	23.90	17.50	10.20	48.90	16.47
Oligocene igneous rocks	6	6.40	5.88	3.05	10.70	3.26
Oligocene clay ˝sivica˝	2	27.50	27.50	25.50	29.50	2.82
Miocene Lithothamnium limestone	4	13.95	13.80	10.10	18.10	4.13
Miocene clastics	4	51.77	55.95	27.80	67.40	17.57
Pliocene clastics	7	10.20	3.46	1.58	29.70	13.17
Quaternary clastics (medium- and coarse-grained)	26	18.44	13.90	3.91	42.10	11.55

Table: Groundwater SO_4^{2-} concentration according to prevailing aquifer porosity type

Aquifer porosity type	n	X	Md	Min	Max	S
intergranular porosity	39	20.85	15.50	1.58	67.40	16.36
fractured porosity	26	11.09	6.76	2.11	48.90	11.59
fractured and karstic porosity	30	6.88	4.41	1.69	21.90	5.35
karstic and fractured porosity	74	5.50	4.28	0.75	35.70	5.35
mixed porosity (karstic, fractured, intergranular)	6	7.59	5.90	4.03	12.60	3.96

Table: Groundwater SO_4^{2-} concentration according to prevailing CORINE Land Cover type

CORINE Land Cover class	n	X	Md	Min	Max	S
bare rocks	8	8.47	1.39	0.75	35.70	13.85
moors and heathland	2	1.23	1.23	0.75	1.72	0.68
natural grasslands	2	3.95	3.95	3.75	4.16	0.28
coniferous forest	20	6.59	4.44	0.75	25.20	6.73
broad-leaved forest	45	6.72	5.11	0.75	18.10	4.36
mixed forest	56	8.58	4.79	1.42	48.90	9.81
non-irrigated arable land	10	25.94	28.85	8.59	42.10	13.45
complex cultivation patterns	18	16.40	8.94	3.00	67.40	18.94
land principally occupied by agriculture, with significant areas of natural vegetation	10	15.95	10.60	4.97	49.90	13.60
industrial or commercial units	2	24.10	24.10	23.50	24.70	0.84

Table: Groundwater SO_4^{2-} concentration according to prevailing Actual agricultural and forest land usage type

Actual agricultural and forest land usage class	n	X	Md	Min	Max	S
forest	137	7.44	4.60	0.75	48.90	7.96
areas of less intense use of nutrients and plant protection products	18	19.98	10.04	4.36	67.40	20.13
areas of intense use of nutrients and plant protection product	16	20.51	14.70	7.88	42.10	12.84
urban areas	2	24.10	24.10	23.50	24.70	0.84

Table: Groundwater **SO_4^{2-}** ***concentration according to sampling object type***

Sampling object type	n	X	Md	Min	Max	S
pumping station	35	10.69	5.81	1.58	42.10	10.48
borehole	10	16.08	10.85	6.99	39.50	12.21
private well	8	36.98	29.30	15.50	67.40	20.23
spring capture	44	10.37	5.92	0.75	48.90	11.05
spring	58	5.93	4.37	1.26	35.70	5.47
surface water	20	6.47	4.88	0.75	18.10	5.86

Appendix 14

Comparison of typical groundwater values according to lithological, lithostratigraphic, CORINE Land Cover, and Actual agricultural and forest land usage classification

- 14A: Typical groundwater geochemistry according to lithological and lithostratigraphic classification
- 14B: Typical groundwater geochemistry according to CORINE Land Cover and Actual agricultural and forest land usage classification

14A

Table: Typical groundwater values according to lithological classification

	n	T (°C)		pH		EC (µS/cm)		δ^{18}O (‰)		δ^{2}H (‰)		d-excess (‰)		δ^{13}C-DIC (‰)		$\delta^{15}N_{tot}$ (‰)		^{3}H (TU)		Ca^{2+} (mg/L)		Mg^{2+} (mg/L)		Na^{+} (mg/L)		K^{+} (mg/L)		NH$_4^+$ (mg/L)		HCO$_3^-$ (mg/L)		Cl$^-$ (mg/L)		NO$_3^-$ (mg/L)		SO$_4^{2-}$ (mg/L)		Si (mg/L)		As (µg/L)		B (µg/L)		Br (µg/L)		Cr (µg/L)		Fe (µg/L)		Mn (µg/L)	
Lithological unit		X	S	X	S	X	EC	X	S	X	S	X	S	X	S	X	S	X	S	X	S	X	S	X	S	X	S	X	S	X	S	X	S	X	S	X	S	X	S	X	S	X	S	X	S	X	S	X	S	X	S
flysch rocks	7	14.0	3.0	7.85	0.31	466	175	-7.36	0.59	-45.3	4.2	13.6	2.9	-11.7	1.0	5.5	3.2	5.50	0.77	88	40	7.1	2.5	8.5	4.8	2.01	1.59	0.01	0.00	287	101	10.07	10.92	8.71	9.87	23.90	16.48	5.16	1.44	0.25	0.00	32.58	34.44	25.42	27.33	0.37	0.19	5.00	0.00	3.31	4.57
clay	2	12.3	4.5	7.85	0.07	317	18	-9.72	0.59	-63.3	0.7	14.4	5.4	-14.9	1.3			4.79	0.91	37	1	5.8	0.1	32.0	5.7	1.04	0.37	0.01	0.00	168	12	7.31	0.21	11.18	1.16	27.50	2.83	10.81	0.91	0.38	0.18	31.50	3.54	16.50	3.54	0.25	0.00	10.50	7.78	0.21	0.13
gravel and sand	26	12.8	1.5	7.25	0.41	548	154	-8.65	0.61	-59.1	5.2	10.1	1.5	-13.8	2.2	8.8	3.5	6.61	1.63	85	25	18.8	5.3	9.4	6.7	2.39	3.47	0.01	0.00	293	92	17.17	9.36	36.50	25.52	18.44	11.56	5.45	2.62	0.29	0.11	31.10	37.11	24.42	9.05	3.53	9.59	15.31	18.44	0.60	1.04
gravel, sand and clay	12	14.0	2.1	7.08	0.19	569	214	-9.76	0.62	-67.0	4.6	11.1	1.6	-14.1	2.0	5.5	3.3	4.83	4.06	90	46	24.5	10.7	6.7	4.4	1.04	0.50	0.02	0.01	352	139	6.06	5.33	11.08	18.78	25.32	25.23	8.54	3.48	0.35	0.23	23.88	40.00	18.92	4.40	0.66	0.44	41.46	35.42	5.81	7.40
shale and sandstone	7	12.0	3.7	7.67	0.19	124	53	-9.14	0.53	-60.5	4.1	12.6	1.1	-11.4	4.1	6.4	2.6	6.03	0.90	15	8	5.1	4.0	2.6	0.5	0.43	0.18	0.01	0.00	67	44	1.65	0.56	2.11	1.30	8.19	2.62	4.69	0.70	0.29	0.10	4.58	2.40	12.17	2.93	0.25	0.00	5.00	0.00	0.74	0.21
limestone prevailing	74	9.3	2.3	7.76	0.25	322	97	-9.32	1.02	-61.5	8.3	13.1	1.9	-10.5	4.2	2.6	3.7	6.22	1.28	58	20	7.9	5.0	1.4	1.2	0.29	0.26	0.01	0.00	215	73	2.17	2.08	3.82	1.95	5.50	5.35	1.20	0.81	0.25	0.00	3.49	2.31	7.55	4.79	0.44	0.25	12.59	18.88	0.29	0.40
dolomite prevailing	30	10.4	2.7	7.68	0.16	404	101	-9.41	0.52	-62.8	4.4	12.4	1.0	-12.2	1.4	4.6	3.4	5.92	1.42	55	11	23.8	10.0	1.3	0.9	0.66	0.90	0.01	0.00	291	85	2.52	1.90	5.19	2.26	6.88	5.35	1.30	0.73	0.25	0.00	3.05	1.29	7.93	2.40	0.47	0.26	13.53	17.53	0.27	0.19
carbonates with clastics	6	10.7	1.1	7.66	0.18	350	131	-9.40	0.41	-63.8	4.0	11.5	1.2	-11.7	2.1	2.5	0.5	7.48	2.15	56	13	16.0	14.1	1.9	0.2	0.61	0.08	0.01	0.00	255	105	2.29	1.53	4.84	1.95	7.59	3.96	3.55	0.59	0.40	0.23	2.50	0.00	8.42	4.96	0.25	0.00	13.50	20.82	0.18	0.10
igneous rocks	8	11.4	3.3	7.59	0.56	102	62	-9.71	0.72	-65.0	5.2	12.7	1.4	-16.6	3.3			6.09	0.84	16	12	1.6	0.8	3.0	1.1	0.55	0.12	0.01	0.00	61	36	1.58	1.60	3.21	1.48	6.05	2.84	6.05	1.23	0.25	0.00	3.25	1.41	5.75	3.75	0.28	0.09	5.00	0.00	0.29	0.15
metamorphic rocks	4	6.5	0.9	7.11	0.48	87	57	-10.77	0.14	-71.1	1.0	15.0	1.4	-18.2	2.3	-0.1	0.6	6.65	0.42	11	11	1.0	0.0	2.6	0.3	0.51	0.01	0.01	0.00	58	38	0.38	0.00	2.84	0.71	3.85	2.00	7.99	1.26	0.50	0.35	2.50	0.00	10.00	1.83	0.68	0.50	5.00	0.00	0.09	0.06

Table: Typical groundwater values according to lithostratigraphic classification

Lithostratigraphic unit	n	T (°C)		pH		EC (µS/cm)		δ^{18}O (‰)		δ^{2}H (‰)		d-excess (‰)		δ^{13}C-DIC (‰)		$\delta^{15}N_{tot}$ (‰)		^{3}H (TU)		Ca^{2+} (mg/L)		Mg^{2+} (mg/L)		Na^{+} (mg/L)		K^{+} (mg/L)		NH$_4^+$ (mg/L)		HCO$_3^-$ (mg/L)		Cl$^-$ (mg/L)		NO$_3^-$ (mg/L)		SO$_4^{2-}$ (mg/L)		Si (mg/L)		As (µg/L)		B (µg/L)		Br (µg/L)		Cr (µg/L)		Fe (µg/L)		Mn (µg/L)	
		X	S	X	S	X	EC	X	S	X	S	X	S	X	S	X	S	X	S	X	S	X	S	X	S	X	S	X	S	X	S	X	S	X	S	X	S	X	S	X	S	X	S	X	S	X	S	X	S	X	S
old Paleozoic rocks	4	6.5	0.9	7.11	0.48	87	57	-10.77	0.14	-71.1	1.0	15.0	1.4	-18.2	2.3	-0.1	0.6	6.65	0.42	11	11	1.0	0.0	2.6	0.3	0.51	0.01	0.01	0.00	58	38	0.38	0.00	2.84	0.71	3.85	2.00	7.99	1.26	0.50	0.35	2.50	0.00	10.00	1.83	0.68	0.50	5.00	0.00	0.09	0.06
Carboniferous-Permian beds	5	11.4	4.4	7.74	0.13	95	21	-8.81	0.12	-58.0	1.5	12.5	1.3	-8.8	1.1	6.4	2.6	5.79	0.97	11	5	2.8	0.6	2.5	0.6	0.51	0.12	0.01	0.00	43	11	1.71	0.65	2.09	1.42	8.93	2.81	4.47	0.76	0.31	0.13	3.88	2.75	13.25	2.63	0.25	0.00	5.00	0.00	0.85	0.15
Permian Val Gardena layers	2	13.6	0.6	7.50	0.28	195	36	-9.82	0.09	-65.6	0.7	12.9	0.0	-16.5	1.2			6.52	0.70	26	5	10.8	1.8	2.7	0.4	0.23	0.15	0.01	0.00	130	22	1.50	0.40	2.15	1.47	6.35	0.02	5.12	0.36	0.25	0.00	6.00	0.00	10.00	2.83	0.25	0.00	5.00	0.00	0.53	0.09
Ladinian igneous rocks	2	9.9	0.3	7.75	0.07	170	13	-9.45	0.03	-62.5	0.1	13.2	0.3	-14.0	0.1			5.70	1.10	31	1	1.7	0.9	2.7	0.1	0.46	0.13	0.01	0.00	105	1	4.04	0.32	4.96	0.13	5.00	0.04	4.94	0.35	0.25	0.00	2.50	0.00	7.25	6.72	0.38	0.18	5.00	0.00	0.22	0.11
Triassic carbonates	70	9.2	2.6	7.79	0.23	331	119	-9.54	0.70	-63.5	5.5	12.8	1.5	-10.1	4.1	2.8	3.5	6.29	1.44	50	16	15.2	11.3	1.2	1.1	0.44	0.64	0.01	0.00	233	97	2.06	2.11	4.16	2.23	6.06	6.16	1.28	0.99	0.26	0.07	3.03	1.46	6.65	3.24	0.43	0.25	11.31	14.89	0.23	0.19
Jurassic carbonates	8	9.6	1.2	7.79	0.25	295	83	-9.10	0.72	-59.5	7.3	13.2	3.6	-11.3	2.7	1.8	2.4	6.12	1.17	58	20	5.6	2.2	1.3	0.7	0.41	0.49	0.01	0.00	202	63	2.13	1.01	5.10	1.32	4.19	1.19	1.30	1.15	0.25	0.00	3.88	2.60	7.56	2.41	0.39	0.21	6.50	4.24	0.19	0.21
Cretaceous carbonates	28	10.7	2.2	7.59	0.16	383	52	-8.85	1.13	-58.2	9.7	12.7	1.4	-13.1	1.4	4.1	4.3	6.03	1.46	71	10	8.2	5.8	1.9	1.2	0.32	0.21	0.01	0.00	256	53	2.90	1.96	4.26	1.96	5.19	1.70	1.34	0.46	0.25	0.00	3.84	2.86	10.43	5.72	0.49	0.24	19.11	27.18	0.44	0.57
Eocene flysch rocks	7	14.0	3.0	7.85	0.31	466	175	-7.36	0.59	-45.3	4.2	13.6	2.9	-11.7	1.0	5.5	3.2	5.50	0.77	88	40	7.1	2.5	8.5	4.8	2.01	1.59	0.01	0.00	287	101	10.07	10.92	8.71	9.87	23.90	16.48	5.16	1.44	0.25	0.00	32.58	34.44	25.42	27.33	0.37	0.19	5.00	0.00	3.31	4.57
Oligocene igneous rocks	6	11.9	3.7	7.53	0.66	79	53	-9.80	0.83	-65.8	5.9	12.6	1.6	-17.5	3.4			6.22	0.82	11	10	1.6	0.9	3.2	1.2	0.58	0.12	0.01	0.00	47	28	0.76	0.59	2.63	1.21	6.40	3.27	6.42	1.19	0.25	0.00	3.50	1.58	5.25	3.08	0.25	0.00	5.00	0.00	0.32	0.16
Oligocene clay "sivica"	2	12.3	4.5	7.85	0.07	317	18	-9.72	0.59	-63.3	0.7	14.4	5.4	-14.9	1.3			4.79	0.91	37	1	5.8	0.1	32.0	5.7	1.04	0.37	0.01	0.00	168	12	7.31	0.21	11.18	1.16	27.50	2.83	10.81	0.91	0.38	0.18	31.50	3.54	16.50	3.54	0.25	0.00	10.50	7.78	0.21	0.13
Miocene Lithothamnium limestone	4	10.6	0.7	7.68	0.10	433	33	-10.13	0.27	-67.3	2.4	13.7	1.5	-12.5	0.5	6.0	3.1	6.31	0.80	73	4	15.5	3.1	2.1	0.7	0.42	0.34	0.01	0.00	277	7	2.06	0.76	4.09	2.67	13.95	4.14	2.91	1.08	0.25	0.00	3.63	2.25	7.38	3.35	0.25	0.00	10.00	6.63	0.12	0.06
Miocene clastics	4	16.0	1.3	6.98	0.05	766	121	-8.98	0.14	-61.0	0.6	10.8	1.2	-13.5	1.0			6.62	0.93	139	15	29.3	14.1	10.3	5.4	1.53	0.50	0.02	0.02	473	113	11.21	5.96	25.13	27.40	51.78	17.58	5.76	1.42	0.25	0.00	66.00	48.13	23.00	4.32	0.36	0.23	44.50	46.34	2.06	2.18
Pliocene clastics	8	13.0	1.6	7.14	0.22	456	168	-10.15	0.26	-69.9	1.5	11.3	1.8	-14.5	2.3	5.5	3.3	3.81	4.87	62	30	21.8	8.2	4.7	2.0	0.76	0.21	0.01	0.00	283	102	3.12	1.34	3.05	2.36	10.20	13.17	9.93	3.39	0.40	0.28	2.81	0.88	16.88	2.85	0.81	0.45	39.94	32.30	7.68	8.49
Quaternary clastics (medium- and coarse-grained)	26	12.8	1.5	7.25	0.41	548	154	-8.65	0.61	-59.1	5.2	10.1	1.5	-13.8	2.2	8.8	3.5	6.61	1.63	85	25	18.8	5.3	9.4	6.7	2.39	3.47	0.01	0.00	293	92	17.17	9.36	36.50	25.52	18.44	11.56	5.45	2.62	0.29	0.11	31.10	37.11	24.42	9.05	3.53	9.59	15.31	18.44	0.60	1.04

Table: Typical groundwater values according to CORINE Land cover classification

	n	T (°C)		pH		EC (µS/cm)		δ^{18}O (‰)		δ^{2}H (‰)		d-excess (‰)		δ^{13}C-DIC (‰)		$\delta^{15}N_{tot}$ (‰)		^{3}H (TU)		Ca^{2+} (mg/L)		Mg^{2+} (mg/L)		Na^{+} (mg/L)		K^{+} (mg/L)		NH$_4^{+}$ (mg/L)		HCO$_3^{-}$ (mg/L)		Cl^{-} (mg/L)		NO$_3^{-}$ (mg/L)		SO$_4^{2-}$ (mg/L)		Si (mg/L)		As (µg/L)		B (µg/L)		Br (µg/L)		Cr (µg/L)		Fe (µg/L)		Mn (µg/L)	
		X	S	X	S	X	EC	X	S	X	S	X	S	X	S	X	S	X	S	X	S	X	S	X	S	X	S	X	S	X	S	X	S	X	S	X	S	X	S	X	S	X	S	X	S	X	S	X	S
bare rocks	8	6.6	1.2	8.00	0.07	194	47	-9.87	0.71	-64.9	6.1	14.1	0.9	-3.4	1.0	-0.4	1.3	6.40	0.79	31	6	5.7	3.7	0.5	0.6	0.12	0.10	0.01	0.00	117	25	0.52	0.53	1.51	0.53	8.47	13.86	0.49	0.48	0.25	0.00	2.94	1.24	3.38	1.71	0.29	0.12	5.88	2.47	0.20	0.12
moors and heathland	2	10.4		8.09	0.06	156	5	-10.50	0.86	-71.3	5.2	12.7	1.7	-1.0	0.4	-0.3	2.7	5.87	0.51	26	1	4.7	0.5	0.3	0.0	0.13	0.00	0.01	0.00	117	15	0.38	0.00	1.11	0.00	1.24	0.69	0.24	0.03	0.25	0.00	2.50	0.00	2.50	0.00	0.25	0.00	5.00	0.00	0.07	0.07
natural grasslands	2	9.7	0.2	7.66	0.19	351	20	-8.05	0.04	-49.9	0.8	14.5	0.6	-11.5	1.0	0.2	0.3	3.39	1.67	61	3	8.8	0.3	1.3	0.0	0.13	0.00	0.01	0.00	234	23	2.35	0.01	3.76	0.19	3.96	0.29	1.09	0.07	0.25	0.00	2.50	0.00	10.50	3.54	0.25	0.00	21.50	23.33	0.38	0.26
coniferous forest	20	9.3	3.1	7.70	0.41	228	156	-9.46	0.79	-62.9	5.6	12.8	1.6	-13.4	4.5	1.9	3.2	6.16	0.65	39	28	5.8	6.2	2.5	1.6	0.47	0.25	0.01	0.00	148	97	2.47	3.41	7.32	13.07	6.60	6.73	3.90	2.75	0.30	0.17	4.43	4.22	8.23	5.77	0.38	0.21	7.90	5.96	0.24	0.15
broad-leaved forest	20	11.4	3.1	7.69	0.32	349	94	-8.89	1.02	-58.2	8.6	12.9	2.0	-12.1	3.0	3.4	3.8	6.03	1.43	58	18	12.2	9.5	2.6	2.7	0.39	0.33	0.01	0.00	234	78	3.04	2.63	4.37	3.07	6.73	4.37	2.33	2.27	0.27	0.09	4.32	3.68	9.33	6.34	0.45	0.24	17.02	23.36	0.78	1.92
mixed forest	57	9.9	2.3	7.60	0.31	344	152	-9.51	0.89	-63.6	7.4	12.5	1.9	-12.3	3.0	3.9	3.6	6.29	2.02	56	29	12.2	9.5	2.3	3.0	0.56	0.80	0.01	0.00	232	109	3.07	4.86	5.03	4.12	8.59	9.81	2.89	3.39	0.25	0.03	5.74	13.83	11.19	10.46	0.50	0.34	12.04	17.86	0.95	3.54
non-irrigated arable land	10	13.5	1.5	7.00	0.40	549	168	-8.52	0.86	-57.8	7.7	10.3	1.5	-14.5	2.8	10.5	3.2	6.93	2.08	82	25	16.2	5.0	12.6	9.3	4.87	4.69	0.01	0.00	254	106	21.16	12.04	46.09	31.53	25.94	13.46	6.32	2.87	0.25	0.00	53.05	53.10	29.30	11.29	1.33	1.35	19.10	24.14	0.63	0.76
complex cultivation patterns	18	12.4	2.1	7.45	0.24	536	158	-9.16	0.64	-62.0	4.0	11.3	2.2	-13.4	0.9	7.4	3.9	5.93	1.37	85	29	22.2	12.6	8.7	9.5	1.10	0.88	0.01	0.00	347	101	9.35	6.29	13.31	8.43	16.40	18.95	4.25	2.64	0.28	0.08	24.25	31.77	15.28	6.13	0.53	0.30	14.78	23.90	0.27	0.19
land principally occupied by agriculture, with significant areas of natural vegetation	10	11.8	2.8	7.58	0.42	492	224	-9.28	0.70	-62.7	4.3	11.5	1.6	-13.4	0.7	6.8	1.7	6.63	1.31	80	42	17.5	9.4	3.8	2.7	1.24	0.90	0.02	0.01	290	112	7.69	6.74	27.23	30.91	15.96	13.60	4.04	2.16	0.28	0.08	13.05	11.56	14.95	9.27	0.41	0.23	16.60	25.00	1.00	1.56
industrial or commercial units	2	13.5	0.4	7.45	0.03	581	35	-8.59	0.33	-60.4	0.6	8.3	3.3	-12.7	1.3	8.3	1.1	6.58	0.51	88	9	22.5	0.7	9.5	9.2	0.96	0.62	0.01	0.00	313	33	22.20	14.14	24.42	0.53	24.10	0.85	2.84	0.06	0.48	0.32	23.00	19.80	28.00	4.24	35.30	9.48	10.50	7.78	2.73	3.29

Table: Typical groundwater values according to Actual agricultural and forest land usage classification

Land use	n	T (°C)		pH		EC (µS/cm)		δ^{18}O (‰)		δ^{2}H (‰)		d-excess (‰)		δ^{13}C-DIC (‰)		$\delta^{15}N_{tot}$ (‰)		^{3}H (TU)		Ca^{2+} (mg/L)		Mg^{2+} (mg/L)		Na^{+} (mg/L)		K^{+} (mg/L)		NH$_4^{+}$ (mg/L)		HCO$_3^{-}$ (mg/L)		Cl^{-} (mg/L)		NO$_3^{-}$ (mg/L)		SO$_4^{2-}$ (mg/L)		Si (mg/L)		As (µg/L)		B (µg/L)		Br (µg/L)		Cr (µg/L)		Fe (µg/L)		Mn (µg/L)	
		X	S	X	S	X	EC	X	S	X	S	X	S	X	S	X	S	X	S	X	S	X	S	X	S	X	S	X	S	X	S	X	S	X	S	X	S	X	S	X	S	X	S	X	S	X	S	X	S
forest	138	10.1	2.8	7.67	0.33	325	141	-9.33	0.97	-61.8	7.9	12.8	1.8	-11.7	4.0	3.3	3.6	6.12	1.64	54	26	11.1	9.5	2.2	2.6	0.47	0.57	0.013	0.000	217	102	2.78	3.73	4.96	5.97	7.45	7.96	2.62	2.83	0.27	0.09	4.79	9.27	9.50	8.16	0.45	0.28	12.55	18.13	0.69	2.52
areas of less intense use of nutrients and plant protection products	18	12.7	2.9	7.46	0.31	450	215	-9.13	0.88	-60.9	6.5	12.1	1.9	-13.7	1.5	7.8	0.9	5.76	1.06	74	43	18.7	12.4	8.0	9.7	1.27	1.03	0.015	0.009	295	140	6.30	4.25	12.36	14.28	19.98	20.14	4.55	2.94	0.26	0.06	25.92	31.72	13.64	6.77	0.46	0.43	23.06	31.08	0.77	1.18
areas ofintense use of nutrients and plant protection products	16	12.8	1.3	7.22	0.48	591	157	-8.70	0.44	-59.7	3.3	9.9	1.3	-14.0	2.2	9.3	4.0	7.33	1.54	88	23	19.3	5.4	10.8	7.7	3.37	4.16	0.013	0.000	294	98	20.58	8.89	44.86	28.24	20.52	12.85	5.71	2.35	0.28	0.09	38.28	45.76	27.19	9.28	0.99	1.10	11.44	13.30	0.47	0.62
urban areas	2	13.5	0.4	7.45	0.03	581	35	-8.59	0.33	-60.4	0.6	8.3	3.3	-12.7	1.3	8.3	1.1	6.58	0.51	88	9	22.5	0.7	9.5	9.2	0.96	0.62	0.013	0.000	313	33	22.20	14.14	24.42	0.53	24.10	0.85	2.84	0.06	0.48	0.32	23.00	19.80	28.00	4.24	35.30	9.48	10.50	7.78	2.73	3.29